AD620959

FDL-TDR-64-124

PRESSURE MEASUREMENTS AT MACH 8 ON AN AERODYNAMICALLY CONTROLLABLE WINGED RE-ENTRY CONFIGURATION

PART OF AN INVESTIGATION OF HYPERSONIC FLOW SEPARATION AND CONTROL CHARACTERISTICS

TECHNICAL DOCUMENTARY REPORT FDL-TDR-64-124

JUNE 1965

AF FLIGHT DYNAMICS LABORATORY
RESEARCH AND TECHNOLOGY DIVISION
AIR FORCE SYSTEMS COMMAND
WRIGHT-PATTERSON AIR FORCE BASE, OHIO

Project No. 8219, Task No. 821902

(Prepared under Contract No. AF 33(616)-8130 by the Research Department, Grumman Aircraft Engineering Corporation, Bethpage, New York; Author: Lawrence Meckler)

NOTICES

When Government drawings, specifications, or other data are used for any purpose other than in connection with a definitely related Government procurement operation, the United States Government thereby incurs no responsibility nor any obligation whatsoever; and the fact that the Government may have formulated, furnished, or in any way supplied the said drawings, specifications, or other data, is not to be regarded by implication or otherwise as in any manner licensing the holder or any other person or corporation, or conveying any rights or permission to manufacture, use, or sell any patented invention that may in any way be related thereto.

Copies of this report should not be returned to the Research and Technology Division unless return is required by security considerations, contractual obligations, or notice on a specific document.

500 - August 1965 - AF33(615)773-4-53

FOREWORD

This report presents the results of one segment of an experimental program for the investigation of hypersonic flow separation and control characteristics being conducted by the Research Department of Grumman Aircraft Engineering Corporation, Bethpage, N. Y. Mr. Donald E. Hoak of the Flight Dynamics Laboratory, Research and Technology Division, located at Wright-Patterson Air Force Base, Ohio, is the Air Force Project Engineer for the program, which is being supported primarily under Contract AF 33(616)-8130, Air Force Task 821902.

The experimental data to be obtained, pressure distributions, heat transfer, and six component aerodynamic force data, are extensive and must be presented in a series of reports, of which this is one. These data reports are presented without analysis for the purpose of disseminating experimental information as rapidly as possible. Analyses of the data will be presented in the final report for the subject contract.

The author wishes to express his appreciation to the staff of the von Karman Facility, ARO Inc., for their helpfulness in conducting the tests and particularly to Messrs. Burchfield and Deitering for providing the machine plotted graphs of the experimental data included in this report. The tabulated data, not included herein, are available to qualified Air Force requestors as an appendix to this report. The appendix can be obtained on loan from the Flight Dynamics Laboratory, Research and Technology Division, Air Force Systems Command, Wright-Patterson Air Force Base, Ohio.

ABSTRACT

Pressure data were obtained at Mach 8 for a winged re-entry configuration having aerodynamic controls. The basic model consisted of a clipped delta wing with an overslung cone-cylinder body. The main controls tested were partial span trailing edge flaps. Data were also obtained on the effect of tip fins, hemisphere-cylinder body and a trailing edge spoiler. The data were obtained over an angle of attack range of -50° to +50°. Due to load limitations on the controls the unit test section Reynolds number varied from 3.3×10^6 at low angle of attack to 2.5×10^6 at high angle of attack.

This report has been reviewed and is approved.

C L Bryan

for W. A. Sloan, Jr.
Colonel USAF
Chief, Flight Control Division
AF Flight Dynamics Laboratory

TABLE OF CONTENTS

LIST OF ILLUSTRATIONS

LIST OF TABLES

LIST OF SYMBOLS

b	Wing semi-span ~ inches
C_p	pressure coefficient $= \dfrac{P - P_\infty}{q_\infty}$
c_{root} (virtual)	virtual root chord of Wing ~ inches
M_∞	free stream Mach number
P	static pressure measured at pressure tap ~ psia
P_∞	free stream static pressure ~ psia
q_∞	free stream dynamic pressure $= \dfrac{\gamma}{2} P_\infty M_\infty^{\ 2}$ ~ psia
Re_∞/ft	free stream unit Reynolds number $= \dfrac{\rho_\infty V_\infty}{\mu_\infty}$
V_∞	free stream velocity ~ ft/sec
x	chordwise distance measured from virtual apex of wing ~ inches
X'	non-dimensional chordwise coordinate (measured from virtual apex of wing) $= \dfrac{x}{c_{root\,(virtual)}}$
y	spanwise distance measured from centerplane of model ~ inches
Y'	non-dimensional spanwise coordinate (measured from vertical centerplane of model) $= \dfrac{y}{b}$
α	angle of attack ~ degrees

γ	ratio of specific heats = 1.4
δ_2, δ_3	flap defection angles ~ degrees (δ_2 ~ left flap; δ_3 ~ right flap)
μ_∞	free stream viscosity ~ $\frac{\text{slugs}}{\text{ft sec}}$
ρ_∞	free stream density ~ $\frac{\text{slugs}}{\text{ft}^3}$

INTRODUCTION

The Fluid Mechanics Section of the Grumman Research Department is currently engaged in a research program directed at determining flow separation phenomena and the effectiveness of aerodynamic controls on hypersonic flight vehicles. The program consists of theoretical and experimental research on "basic" configurations, flat plates with wedge-shaped flaps and fins, and "typical" hypersonic glide vehicles, a clipped delta wing-body combination, and a pyramidal body. The configurations under investigation in the over-all program are shown in Fig. 1a.

This report presents the results of one segment of the experimental program. It treats a winged hypersonic glider configuration consisting, in basic form, of a clipped delta wing with an overslung cone-cylinder body. This configuration was used for obtaining pressure and heat transfer data on various aerodynamic controls at hypersonic Mach numbers. The pressure data results are presented herein and the heat transfer results will be presented in a subsequent report (Ref. 1). The controls investigated were partial span trailing edge flaps, with deflection ranges of -39° to +39°, a full span plug-type trailing edge spoiler and tip fins. An overslung hemisphere-cylinder body was also tested.

The experimental work was done at the AEDC 50-inch Mach 8 Hypersonic Wind Tunnel during July and August of 1963. Descriptions of these test facilities can be found in Ref. 2. Pressure data were obtained at a unit Reynolds number varying from 3.3×10^6 to 2.5×10^6, depending on the angle of attack range, with selected points at a Reynolds number of 1.1×10^6. The same model was used to obtain heat transfer data in the AEDC 50-inch Hypersonic Tunnel at $M_\infty = 8.0$ and pressure data in the AEDC 40" x 40" Supersonic Tunnel at $M_\infty = 5.0$ (Ref. 3). A geometrically similar model, instrumented to obtain force and moment data, was tested in both the 40" and 50" tunnels at an earlier date (Ref. 4). Another geometrically similar model, with limited pressure instrumentation, was tested in the AEDC Hotshot 2 Hypervelocity Tunnel (Ref. 5).

Manuscript released by the author May 1964 for publication as an RTD Technical Documentary Report.

DESCRIPTION OF MODELS

Four test configurations were built up from a basic model that consisted of a clipped delta wing with an overslung body. The clipped delta wing had a spherically blunted apex, cylindrically blunted leading edges and a blunt base. Of the control surfaces to be tested, three partial span trailing edge flaps were built into the wing and attachments provided for mounting a full span spoiler. Only the outboard flaps were used in these tests. The flap-type control surfaces were remotely actuated from outside the tunnel. Three-view drawings of the four test configurations are presented in Fig. 1b through e. The dimensions of the basic configurations are shown in Fig. 1b and are the same for all other configurations. The other configuration drawings show dimensions only for the components added to the basic configuration. A summary of the geometric properties of the various model components is presented in Table 2.

The first major configuration consisted of a clipped delta wing with an overslung body. The body was composed of a half-cylindrical after-section and a half-hemispherical fore-section. A conical fairing, uninstrumented, was attached over the fore-section of the body to provide a body shape that was geometrically similar to that used in the force tests (Ref. 4). The half-conical foresection and half-cylindrical aftersection were joined together at the shoulder by a spherical fairing, this wing-body combination is referred to as Configuration I. The second major configuration was obtained by adding a set of tip fins to Configuration I and is referred to as Configuration IV. The tip fins were clipped deltas in elevation and were attached in such a way as not to alter the aspect ratio of the basic configuration. Configurations I and IV provided the pressure data needed to evaluate the force data previously obtained.

The conical forebody of the overslung body generates a weak shock wave on the upper surface. It was also desired to determine the effects of a strong shock generator on the pressure coefficients. With the conical forebody removed the basic, hemispherical-cylindrical overslung body remaining can be considered as a strong shock generator. It was also desired to compare the flow separation characteristics of the partial span trailing edge flaps with those of a trailing edge control that would be expected to induce strong separation effects. Thus, as for the force tests, it was decided to test a full span spoiler and compare the resulting pressure

distributions to those due to the partial span flaps deflected +20 degrees. The design condition for the full span, plug type, trailing edge spoiler was, therefore, that its height be equal to the vertical displacement of the trailing edge flaps when they are deflected +20 degrees. This spoiler was attached to the lower, flat plate surface at the trailing edge.

It was assumed that the effects of the blunt body and spoiler would be uncoupled because of their locations on opposite surfaces of the wing. Therefore, the hemispherical overslung body and the trailing edge spoiler were tested at the same time and referred to as Configuration VII.* Configuration VIII was obtained by adding the tip fins to Configuration VII.

The sign convention for denoting the angle of attack and the control deflection angle can be obtained from the basic model; namely, a flat plate clipped delta wing with an overslung body. This definition fixes the flat plate surface of the wing as the lower surface. Thus, the angle of attack is positive when the flat plate surface is the windward surface of the model. The control deflection angles are also defined with respect to the lower (flat-plate) surface of the model. If we consider our model at zero angle of attack (flow parallel to the lower flat-plate surface), then positive trailing edge flap deflections are obtained by deflecting the trailing edge down. The outboard partial span trailing edge flaps, designed to operate independently of each other, had a maximum travel angle of ±40 degrees and could be calibrated to yield any deflection angle in this range.

Each flap-type control was driven by a 28 volt dc, gear reduced, electrical motor through a 1/2 inch-10 acme thread drive screw which was connected to the flap bell cranks by push-pull rods. Control deflection read-outs were obtained through calibrated linear potentiometers. The three motors with their attendant potentiometers and drive screws were located in a water-cooled housing immediately behind the model. The drive screws were connected to the flap bell cranks by push-pull rods that passed through the front of the actuator housing and into the base of the model. This type of actuation system produced a deflection rate of 1 degree/sec. The control surfaces were calibrated cold, that is, when the model was installed in the tunnel, and checked regularly. The calibrating was done with precut templates varying, in 5-degree increments, from 0 degrees to

*In the force tests a full span trailing edge flap and a full span spoiler were tested with the conical overslung body, with and without tip fins, and referred to as Configurations II, III, V, and VI.

40 degrees. The potentiometer outputs were recorded visually from Leeds and Northrup Midget Model D indicators for use in setting flap angles during the test. This calibration was also recorded into the digital computing equipment at AEDC for use of the computer during the print-out procedure. The design provided for the independent operation of each control surface. We were thus capable of testing asymmetric, as well as symmetric, control configurations.

The wing of the model was fabricated of an internal stainless steel frame which served as the basic load supporting structure and instrumented surface panels which served as the data gathering units. The flaps were also fabricated the same way; i.e., an internal frame with attached, instrumented, panels. The flaps were connected to the wing structure by hinges and actuated from the actuator housing by a system of bell cranks and push-pull rods. All internal framework was made of 416 stainless steel and the surface panels were pressure relieved, silver braised honeycomb sections where the face sheets, core and frame were of 321 stainless steel. The body and the conical fairing were fabricated of 321 stainless steel sheet. The fins and spoiler were made of solid 321 stainless steel. The actuator housing which served as the connection between the model and the sting, as well as the housing for the actuation motors, was made of 17-4PH stainless steel.

The model was instrumented with 56 pressure taps distributed on the upper and lower surface of the wing and on the half-hemisphere cylinder body. The location of each pressure tap is listed in Table 3 and shown in Fig. 1f. When the conical fore-body fairing was installed, seven pressure taps (178-184) were lost and when the spoiler was installed four pressure taps (28, 38, 48, 88) were lost. Installation of the fins did not block any instrumentation.

DESCRIPTION OF WIND TUNNELS AND EQUIPMENT

This segment of the over-all experimental program described in the Introduction was conducted in the 50 in. Mach 8 Hypersonic Wind Tunnel located at Arnold Engineering Development Center's von Karman Facility. A complete description of the wind tunnels and their associated measuring, recording, and tabulating equipment is given in Ref. 2.

The angle of attack range was obtained by using two different pre-bend angles on the water-cooled split sting that is standard tunnel equipment. The two pre-bend angles used were 12 degrees and 39 degrees and between them provided an angle of attack range of 0 degrees to +50 degrees. The negative angles of attack were obtained by inverting the model.

TEST CONDITIONS

The test program was conducted at a nominal test section Mach number of 8.0 and test section unit Reynolds numbers ranging from 3.3×10^6 per foot to 1.1×10^6 per foot. Only selected data, to be used for comparative purposes, were obtained at the lowest unit Reynolds number. Most of the program was conducted at unit Reynolds numbers ranging from 3.3×10^6 per foot to 2.5×10^6 per foot. This variation in test section unit Reynolds number was caused by the necessity to reduce the free stream dynamic pressure in order to prevent overloading the control system. Thus the free stream unit Reynolds numbers and dynamic pressures were reduced as the magnitude of the angle of attack increased.

Due to tunnel operating conditions the actual test section Mach number ranged between 8.08 and 8.09. The nominal values of the free stream unit Reynolds number at which data were acquired were 3.3×10^6, 2.9×10^6, 2.5×10^6, and 1.1×10^6. The variation in Reynolds number, due to tunnel operating conditions, was ± 3% maximum with most of the variations being within ± 2% of the nominal values.

The two main configurations (I and IV) were tested most extensively while the tests on the other configurations were restricted and are used only to provide comparison data with the main configurations. Configurations I and IV were tested through an angle of attack range from -50 degrees to +50 degrees, for symmetric, partial span, flap deflections of -39 degrees to +39 degrees. Configurations VII and VIII were tested through an angle of attack range of -20 degrees to 0 degrees and provide information on the effect of a strong shock generator and plug type trailing edge spoiler on the pressure distributions and flow field about the delta wing.

A complete tabulation of the test program showing the angle of attack range, control deflection and flow conditions, is presented in Table 1.

DATA REDUCTION AND ACCURACY

All the pressure data were reduced to standard coefficient form using the equation $C_p = \frac{p - p_\infty}{q_\infty}$. The inaccuracy in the measured pressure data varied from ± 0.003 psia, for pressures below 0.40 psia, to 0.26 psia for pressures above 15 psia. Because of this, pressure coefficient uncertainties varied from 0.004 for $C_p<0.3$ and Re_∞/ft = 1.1 million to 0.13 for C_p = 2.0 and Re_∞/ft = 3.3 million.

The automatic plotting machines, used in presenting the data herein, introduce additional errors. The discrepancies in the plotted pressure coefficients due to these machine errors should not exceed ± 0.01. Nevertheless, there is always the possibility that a point will be completely misplotted. Each graph has been inspected and any questionable points were checked with the tabulated pressure coefficients.

RESULTS AND DISCUSSION

This portion of the over-all test program was designed to provide the pressure data needed to fully exploit the controls information previously obtained (Refs. 1 and 4) on a basic type of hypersonic flight vehicle and to assess the importance of separated flow effects. Data are presented at positive and negative angles of attack for the case of an overslung body mounted on a clipped delta wing.

The model was tested with tip fins on and off, with partial span trailing edge flaps, with a full span trailing edge spoiler, and with a blunt instrumented body as well as the conical body used in the force tests. The experiments were conducted at a nominal Mach number of 8 and with limited Reynolds number comparisons.

The basic wing-body combination was designed to provide pressure data for configurations having either overslung or underslung bodies. For convenience we have chosen the overslung body configuration as our reference, and we have defined the coordinate system and control deflection angles with reference to this basic configuration. Thus the positive angle of attack regime for the overslung body provides the aerodynamic data for the underslung

body at negative angles of attack. The sign of the flap deflection angles, for the underslung body case, must be reversed in order that both cases be viewed in the same reference system.

The data are presented in the form of pressure coefficients plotted as functions of nondimensionalized chordwise (streamwise), and spanwise, coordinates. The chordwise coordinate is measured from the virtual apex of the model and the spanwise coordinate from the vertical centerplane of the model. The data obtained on the upper and lower surfaces of the test configuration are presented separately for each set. Thus, for each test configuration, all the data are presented in four graphs (two graphs for the chordwise plots and two graphs for the spanwise plots).

The data for Configuration I are presented in Figs. 3 to 28; for Configuration IV in Figs. 29 to 49; for Configuration VII in Fig. 50 and for Configuration VIII in Fig. 51. The complete test program is tabulated in Table 1 and the specific conditions presented in each figure are noted in the list of illustrations on page VIII.

REFERENCES

1. Meckler, Lawrence, Heat Transfer Measurements at Mach 8 on an Aerodynamically Controllable Winged Re-entry Configuration, to be published.

2. Arnold Center Test Facilities Handbook, AEDC, Arnold Air Force Station, Tennessee, January 1961.

3. Kaufman, Louis II, Pressure Measurements for Mach 5 Flows Over a Winged Re-entry Configuration with Aerodynamic Controls, Part I: Blunt Cabin, Part II: Conical Cabin, RTD-TDR-63-4179, February 1964.

4. Meckler, Lawrence, Static Aerodynamic Characteristics at Mach 5 and 8 of an Aerodynamically Controllable Winged Re-entry Configuration, FDL-TDR-64-10, to be published.

5. Hartofilis, Stavros A., Pressure Measurements at Mach 19 for a Winged Re-entry Configuration, ASD-TDR-63-319, March 1963.

TABLE I
TEST PROGRAM
50" HYPERSONIC WIND TUNNEL
MACH 8.08

CONFIGURATION	TRAILING EDGE CONTROL			FOREBODY SHAPE	α RANGE ~ DEGREES	$Re_\infty/ft \times 10^{-6}$
	PARTIAL SPAN FLAPS		SPOILER			
	δ_2	δ_3				
I	0	0	OFF	CONICAL	-50 → +20	3.3
					+30 → +50	2.5
	+10	+10			-20 → +20	3.3
					+30 → +50	2.5
	+20	+20			-50 → -30	2.875
					-20 → +20	3.3
					+30 → +50	2.5
	+30	+30			-50 → -30	2.875
					-20 → +20	3.3
					+30 → +40	2.5
	+39	+39			-50 → -30	2.875
					-20 → +20	3.3
					+30 → +50	2.5
	-10	-10			-50 → -30	2.875
					-20 → +20	3.3
	-20	-20			-50 → -30	2.875
					-20 → +20	3.3
					+30 → +50	2.5
	-30	-30			-50 → -30	2.875
					-20 → +20	3.3
	-39	-39			-50 → -30	2.875
					-20 → +20	3.3
					+30 → +50	2.5
IV	0	0	OFF	CONICAL	-50 → +20	3.3
					+30 → +50	2.5
	+10	+10			-20 → +20	3.3
					+30 → +40	2.5
	+20	+20			-50 → -30	2.375
					-20 → +20	3.3
					+30 → +50	2.5
	+39	+39			-50 → -30	2.875
					-20 → +20	3.3
					+30 → +50	2.5

TABLE I (CONT'D)
TEST PROGRAM
50" HYPERSONIC WIND TUNNEL
MACH 8.08

CONFIGURATION	TRAILING EDGE CONTROL			FOREBODY SHAPE	α RANGE ~ DEGREES	$Re_\infty/ft \times 10^{-6}$
	PARTIAL SPAN FLAPS		SPOILER			
	δ_2	δ_3				
IV	-10	-10	OFF	CONICAL	-50 → -30	2.875
					-20 → +20	3.3
	-20	-20			-50 → -30	2.875
					-20 → +20	3.3
					+30 → +50	2.5
	-30	-30			-50 → -30	2.875
					-20 → +20	3.3
	-39	-39			-50 → -30	2.875
					-20 → +20	3.3
					+30 → +50	2.5
VII	0	0	ON	BLUNT	-20 → 0	3.3
					0	1.1
VIII	0	0	ON	BLUNT	-20 → 0	3.3

TABLE II

GEOMETRIC CHARACTERISTICS OF MODELS

Wing:

Clipped Delta Wing with Blunt Apex, Leading Edges, and Base

Root Chord	12.350 13.00	inches actual inches virtual
Tip Chord	2.608	inches
Span	12.00	inches
Apex Radius	0.650	inches
Leading Edge Sweep	60	degrees
Leading Edge Radius	0.650	inches
Wing Thickness (Constant)	1.30	inches
Planform Area	93.3 97.6	$inches^2$ actual, $inches^2$ virtual
Aspect Ratio	1.542	
Taper Ratio	0.211	
Thickness Ratio (Root)	0.1052	
Control Area - Partial Span Flaps	12.75	$inches^2$

Body:

Half Cone - Cylinder (Base Mounted Flush with Wing Trailing Edge)

Cone Angle	13	degrees
Cone Length	5.49	inches
Cone Radius (Maximum at Tangency Point)	1.269	inches
Cylinder Length	4.415	inches
Cylinder Radius	1.30	inches
Fairing (Cone to Cylinder)		
Length	0.292	inches
Radius	1.30	inches
Included Angle	13	degrees
Total Body Length (Half-Cone Cylinder)	10.20	inches
Planform Area (Half-Cone Cylinder)	17.81	$inches^2$
Hemisphere Radius	1.30	inches
Total Body Length (Half-Hemisphere Cylinder)	5.715	inches
Planform Area (Half-Hemisphere Cylinder)	14.145	$inches^2$

Tip Fin:

Clipped Delta Wing with Blunt Leading Edge

Root Chord	3.275	inches

TABLE II

GEOMETRIC CHARACTERISTICS OF MODELS

Tip Chord	0.990	inches
Span	4.160	inches
Leading Edge Sweep	50	degrees
Leading Edge Radius	0.325	inches
Thickness (Constant)	0.650	inches
Area	9.27	$inches^2$
Aspect Ratio	1.862	
Taper Ratio	0.3025	
Thickness Ratio (Fin Root-Wing Center Plane)	0.199	

<u>Spoiler</u>:

Full Span, Plug Type with Cylindrical Lower Edge

Chord (Constant)	0.650	inches
Span	10.70	inches
Height	0.611	inches
Planform Area	6.96	$inches^2$
Bottom Cylinder Radius	0.325	inches

TABLE III

PRESSURE TAP LOCATION

TAP NUMBER	X'	Y'
78	0.050	0
79	0.10	
80	0.2596	
81	0.4038	
82	0.5481	
84	0.6923	↓
86	0.8077	0
87	0.9173	0.0313
88	0.9750	0.0313
42	0.5481	0.3125
43	0.6347	
44	0.6923	
45	0.7500	
46	0.8077	
47	0.9173	↓
48	0.9750	0.3125
31	0.4423	0.5625
32	0.5481	
33	0.6347	
34	0.6923	
35	0.7500	
36	0.8077	
37	0.9173	↓
38	0.9750	0.5625
26	0.8077	0.8020
27	0.9173	↓
28	0.9750	0.8020

TAP NUMBER	X'	Y'
177	0.1000	0
178	0.2654	
179	0.3346	
180	0.4038	
181	0.4731	
182	0.5481	
183	0.5851	↓
184	0.6274	0
164	0.6923	0.1083
166	0.7846	0.1083
167	0.9173	0.1083
154	0.6923	0.1877
156	0.7846	0.1877
157	0.9173	0.1877
141	0.4904	0.3125
142	0.5481	0.4375
143	0.6058	0.3125
146	0.7846	
147	0.9173	↓
148	0.9750	0.3125
131	0.4423	0.5625
132	0.5481	
134	0.6923	
136	0.7846	
137	0.9173	↓
138	0.9750	0.5625
126	0.7846	0.8020
127	0.9173	0.8020
128	0.9750	0.8020

All pressure taps are located with respect to the virtual apex, and the vertical center plane, of the model. Pressure taps 26 — 88 are on the lower (flat-plate) surface and taps 126 — 184 are on the upper surface of the model.

TABLE IV

DESCRIPTION OF TEST CONFIGURATIONS

CONFIGURATION	DESCRIPTION
I	Basic Configuration (Wing-Body) Wing - Clipped delta wing, spherically blunted apex, cylindrically blunted leading edges, blunt base + Body - Overslung, half conical forebody and half-cylindrical afterbody
IV	Basic + Tip Fins (I)
VII	Wing - Clipped delta wing, spherically blunted apex, cylindrically blunted leading edges, blunt base + Body - Overslung, half-hemispherical forebody and half-cylindrical afterbody + Spoiler - Plug type, trailing edge spoiler
VIII	VII + Tip Fins

A

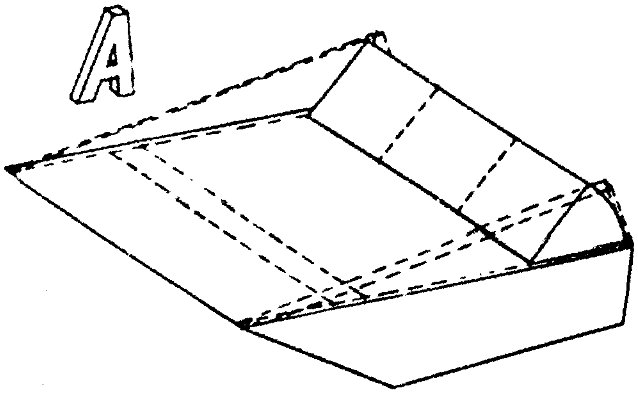

Separated Flows ahead of a Ramp
Fore and aft flaps, end plates
3 separate models:

1) Pressure and heat transfer, AEDC Tunnels A & B, M = 5 & 8

2) Controlled wall temperature, pressure, AEDC Tunnel B, M = 8

3) Pressure and heat transfer, Grumman Shock Tunnel, M $\simeq$ 13 & 19

B

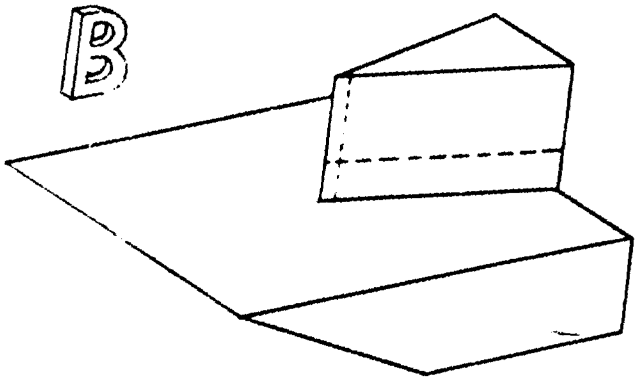

Wedge - Plate Interaction
Small and large fins with sharp and blunt leading edges
2 separate models:

1) Pressure and heat transfer, AEDC Tunnels A & B, M = 5 & 8

2) Pressure and heat transfer, Grumman Shock Tunnel, M $\approx$ 13 & 19

C

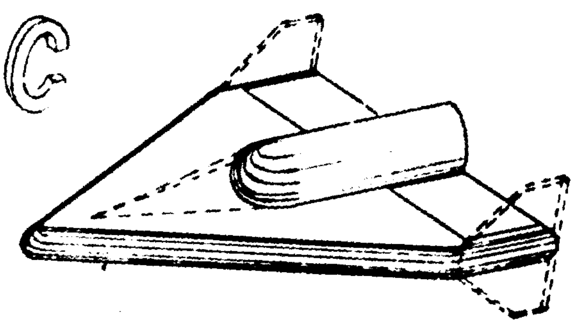

Clipped Delta, Blunt L.E.
Center body, T.E. flaps, drooped nose, spoiler, tip fins
3 separate models:

1) Pressure and heat transfer, AEDC Tunnels A & B, M = 5 & 8

2) Pressure, AEDC Hotshot 2, M $\approx$ 19

3) Six component force, AEDC Tunnels A & B, M = 5 & 8

D

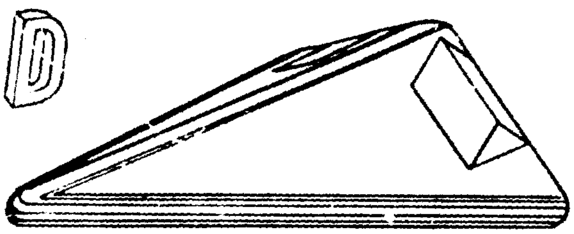

Delta, Blunt L.E., Dihedral
T.E. flaps, canard, ventral fin
3 separate models:

1) Pressure and heat transfer, AEDC Tunnels A & B, M = 5 & 8

2) Pressure and heat transfer, Grumman Shock Tunnel, M $\approx$ 19

3) Six component force, AEDC Tunnels A & B, M = 5 & 8

Fig. 1a General Outline of Models and Remarks for Over-all Program

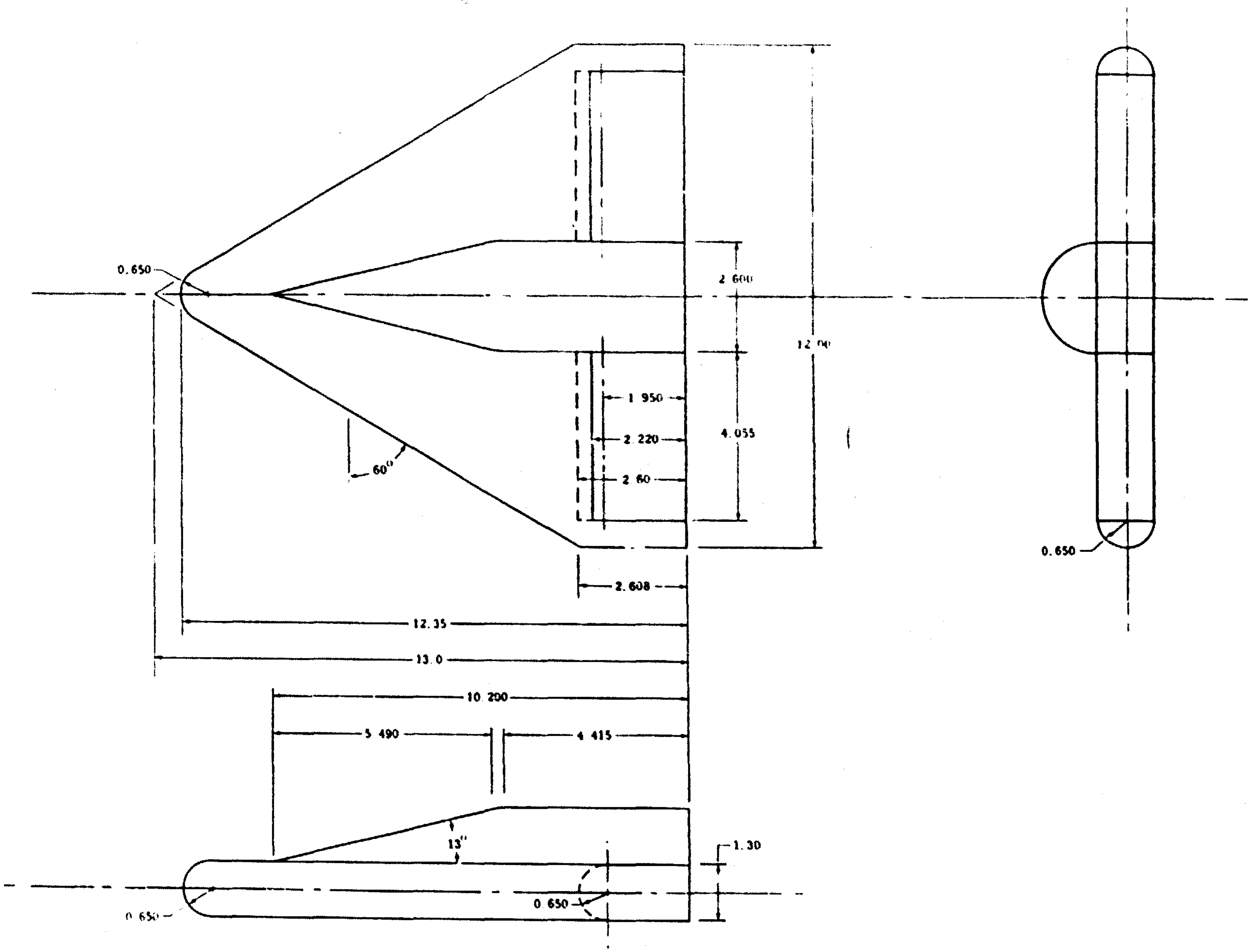

Fig. 1b Configuration I - Basic Wing-Body

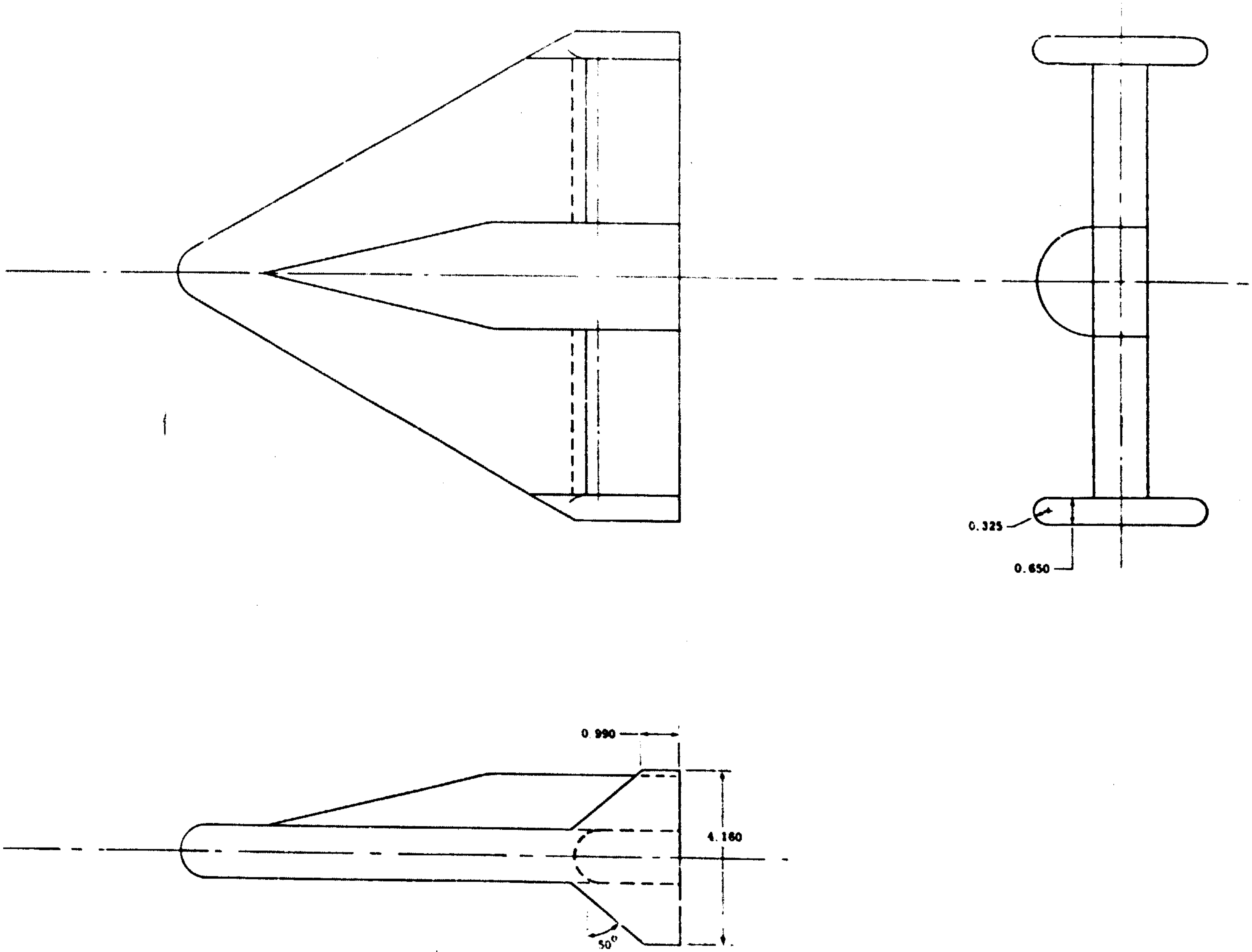

Fig. 1c Configuration IV - Basic Wing-Body + Tip Fins
(for dimensions see Figure 1b)

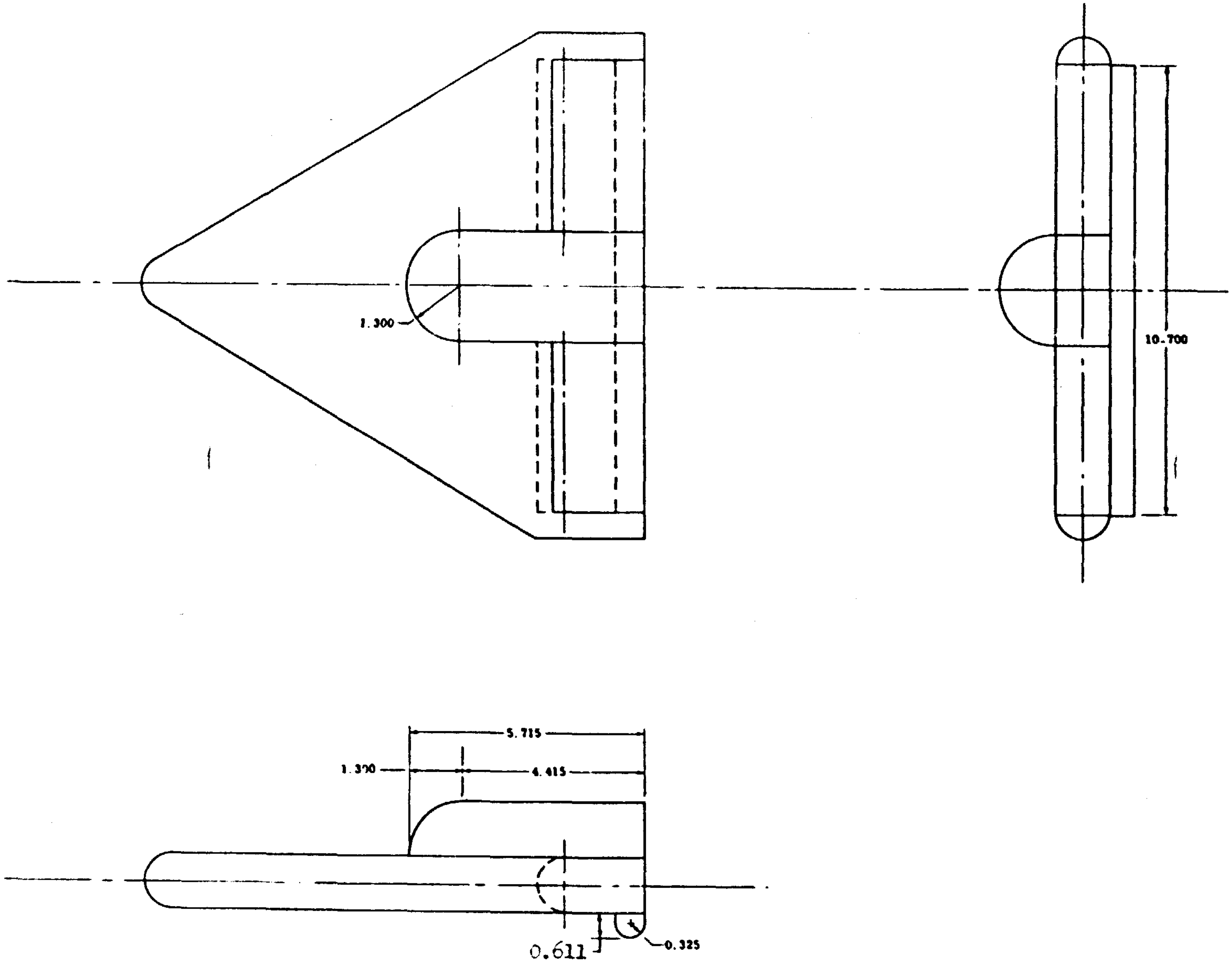

Fig. 1d Configuration VII - Wing - Blunt Body + Full Span Plug Spoiler
(for dimensions see Figure 1b)

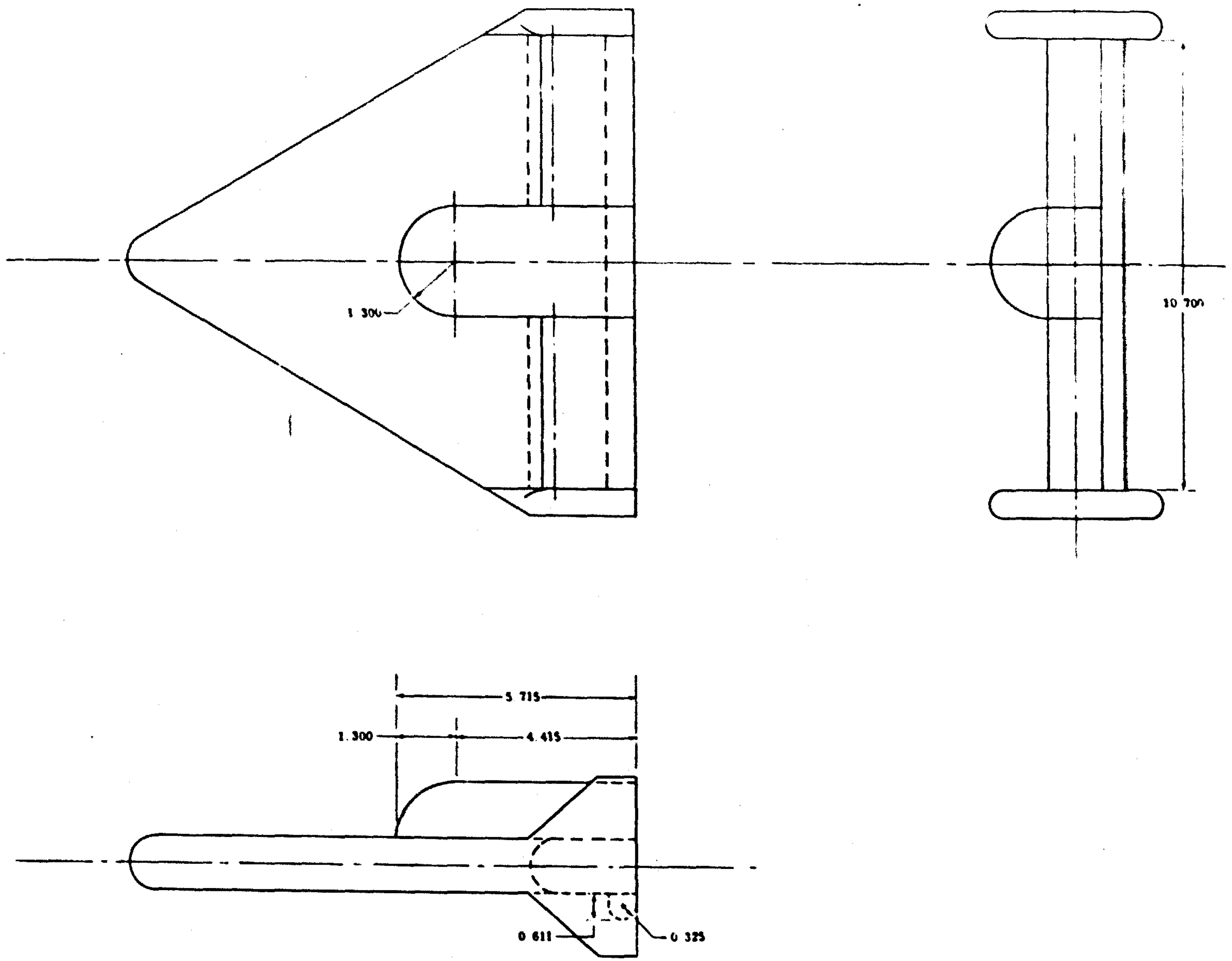

Fig. 1e Configuration VIII - Wing - Blunt Body + Full Span Plug Spoiler + Tip Fins (for dimensions see Figures 1b, 1c, 1d)

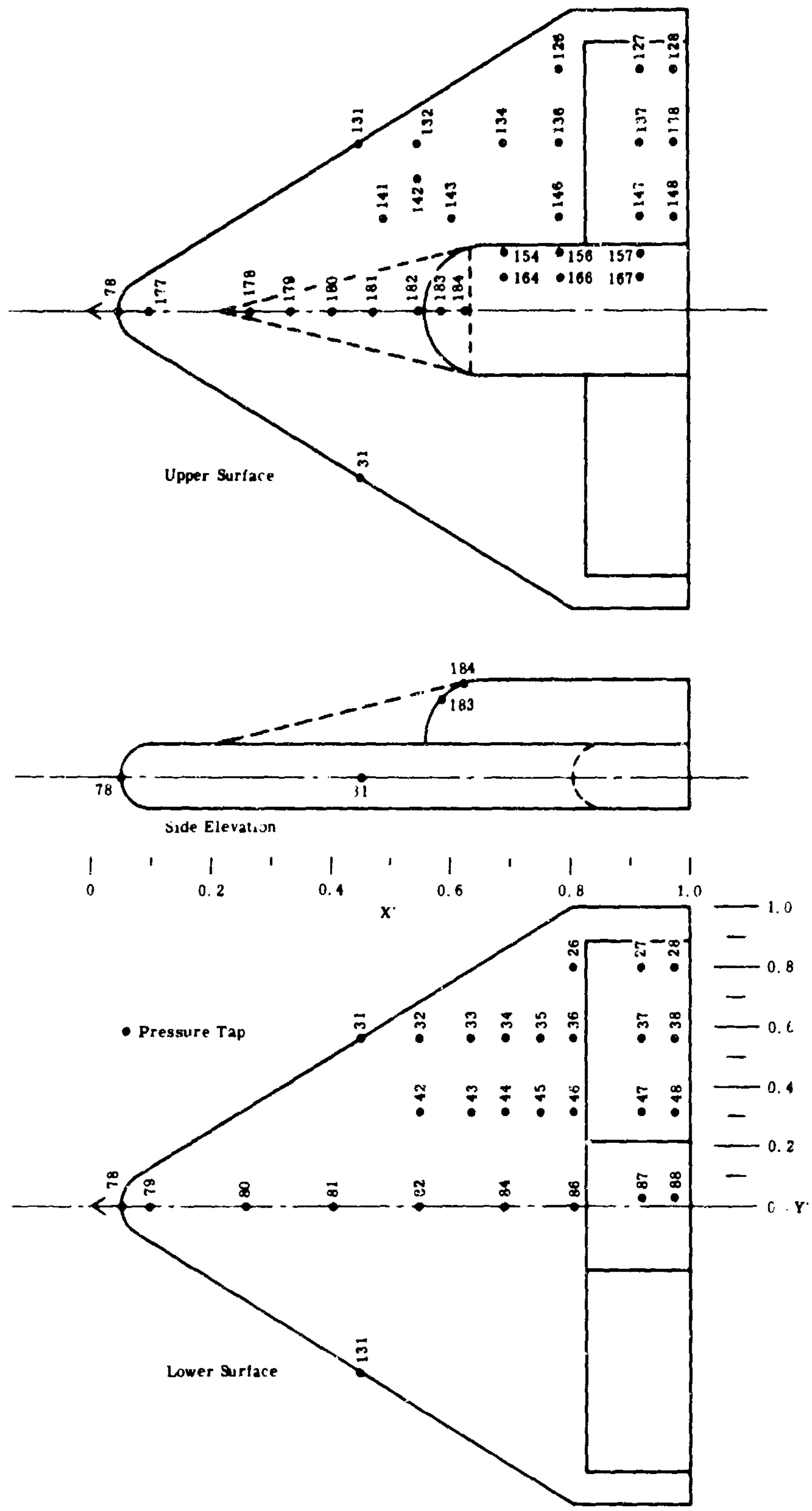

Fig. 1f Pressure Tap Location and Model Coordinate System

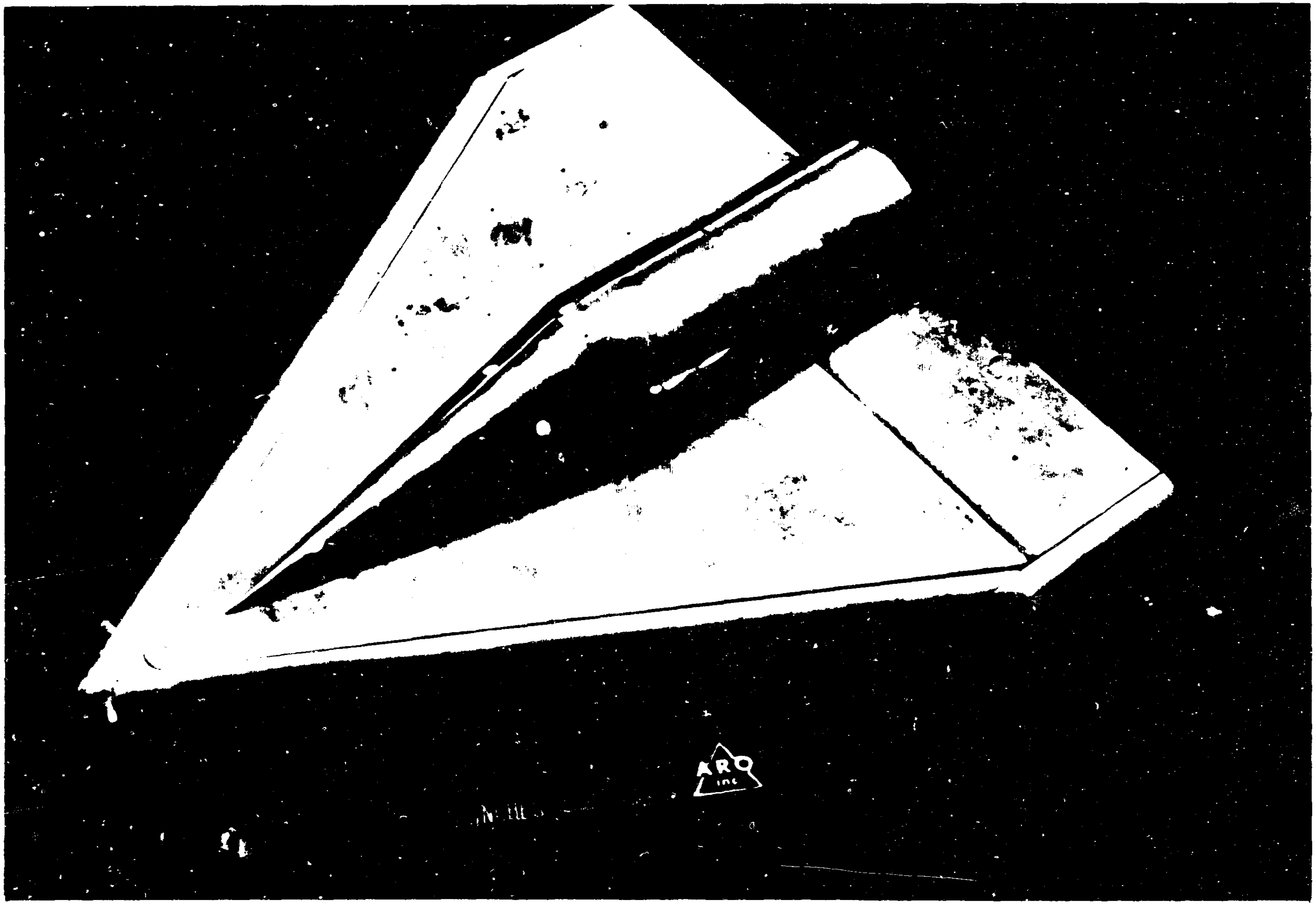

Figure 1g   Top View Photograph - Configuration I

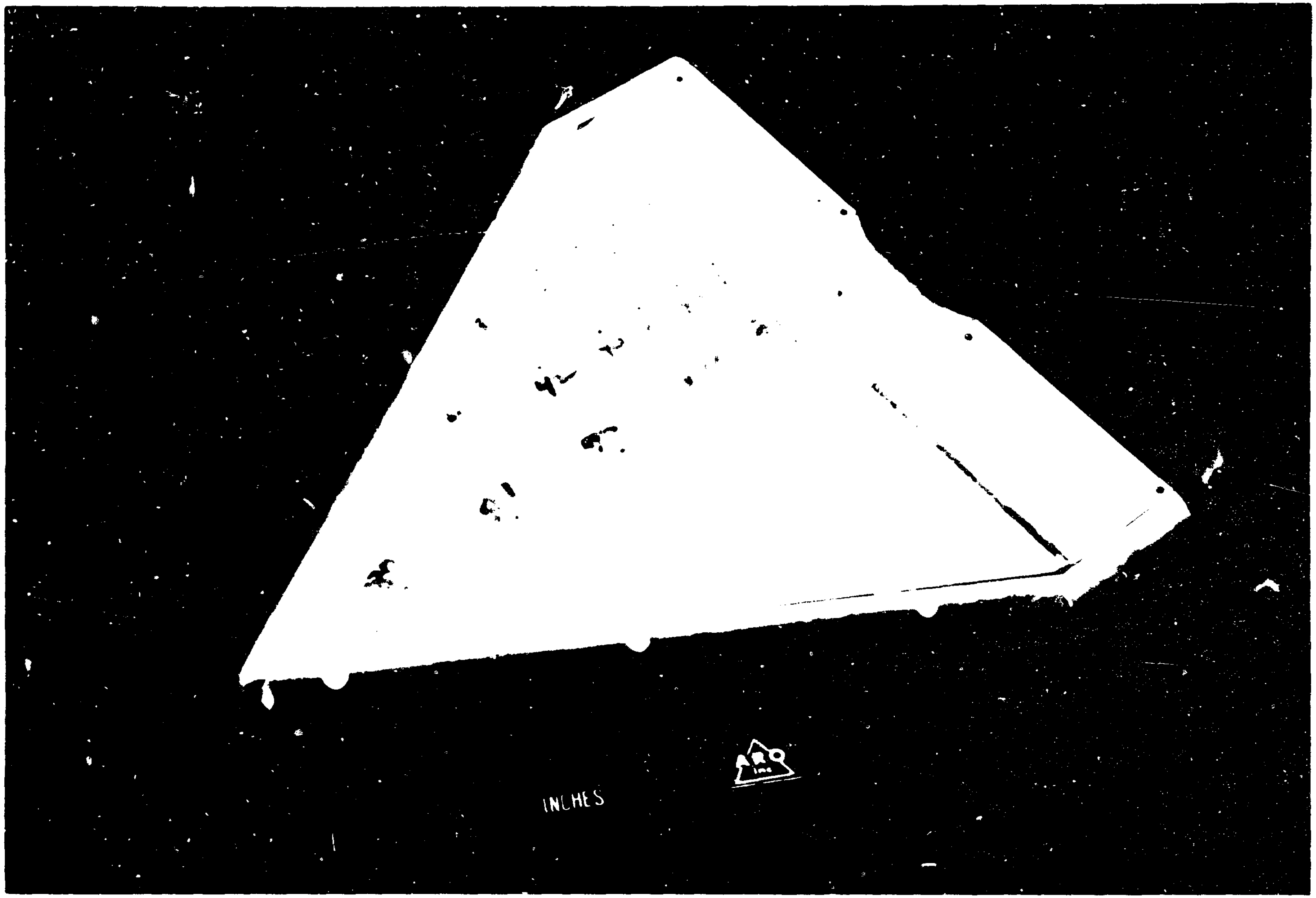

Figure 1h   Bottom View Photograph - Configuration I

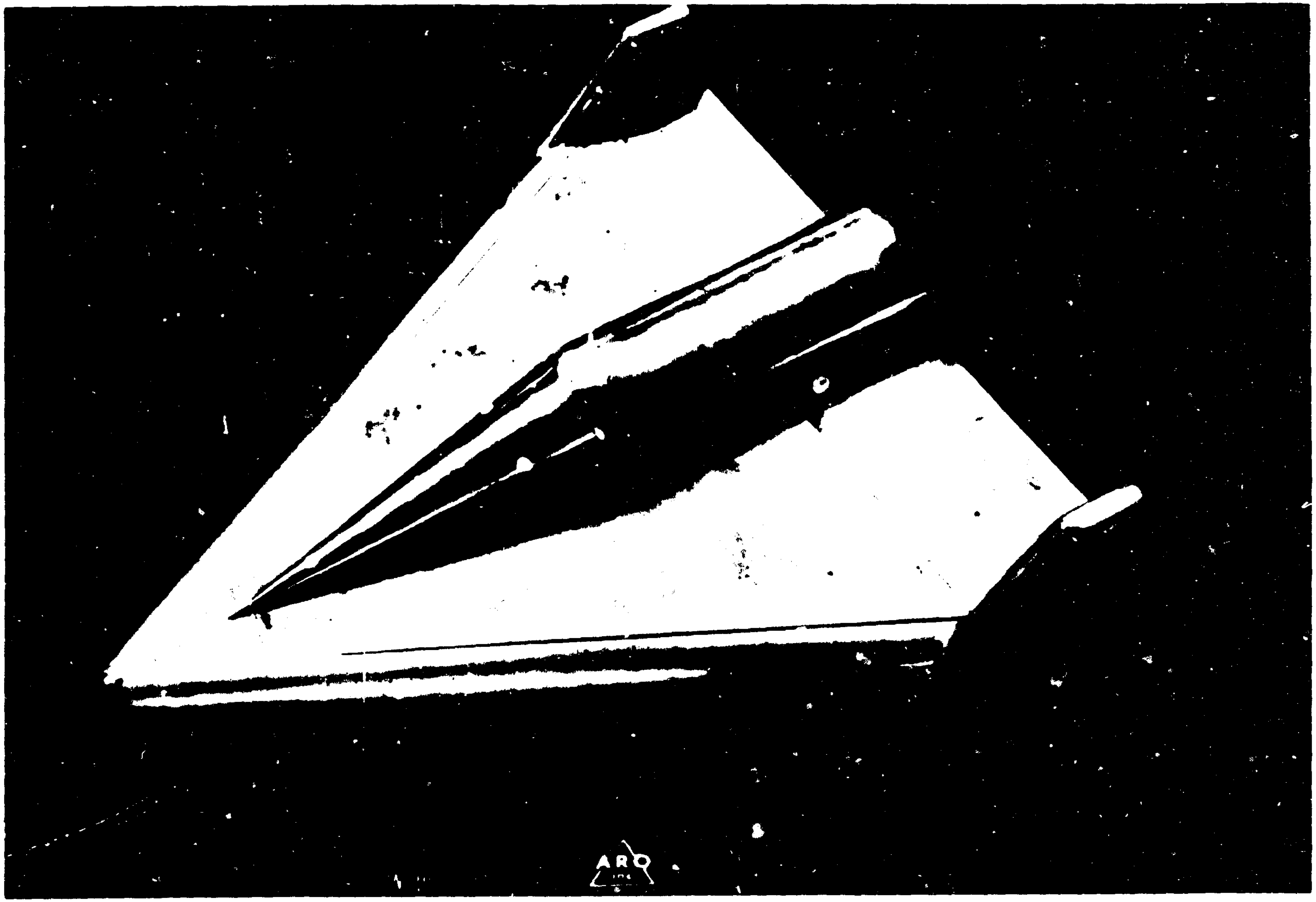

Figure 11 Top View Photograph - Configuration IV

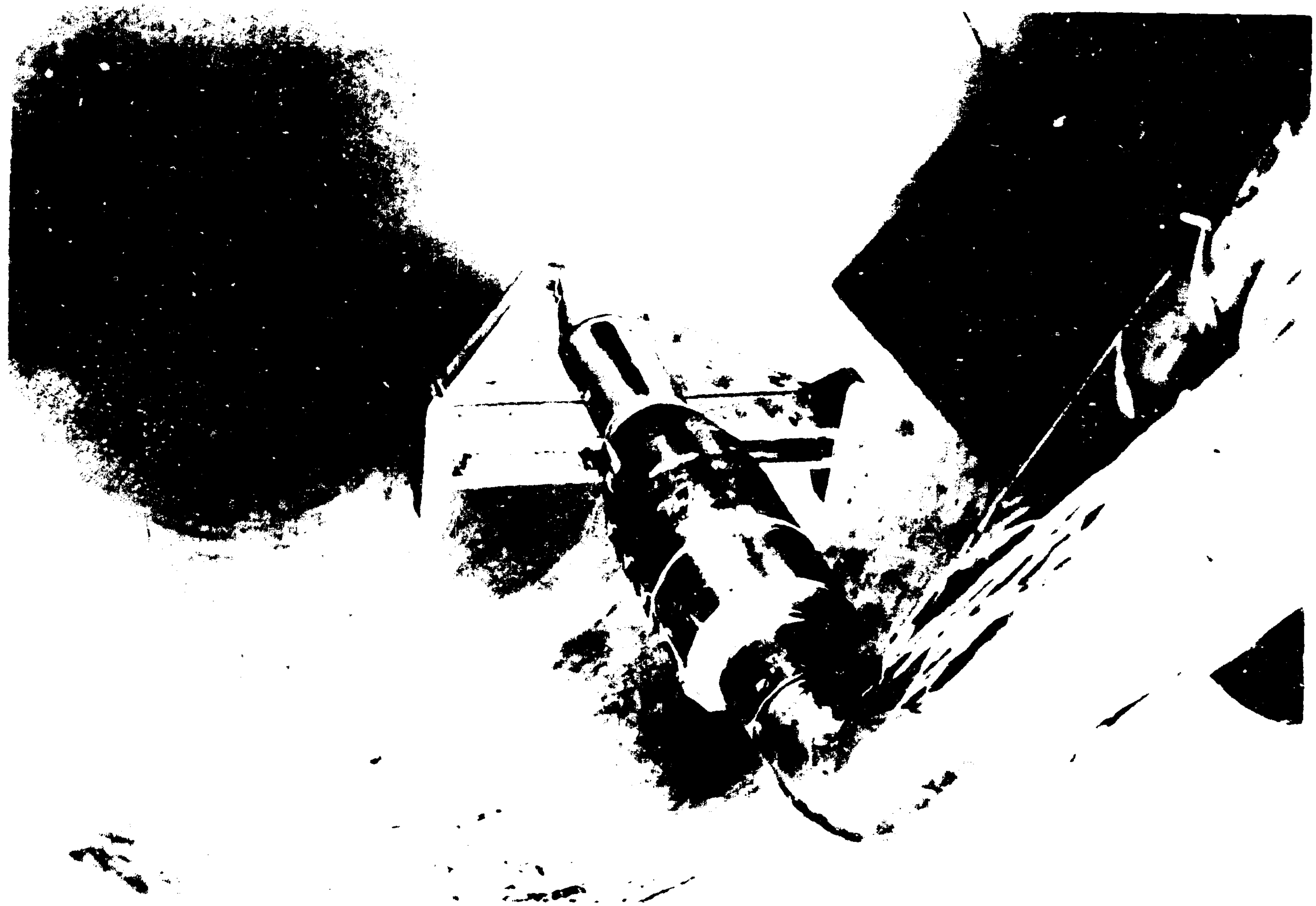

Figure 1j Photograph - Configuration IV, Mounted on Actuator Housing in the 50" Hypersonic Mach 8 Wind Tunnel

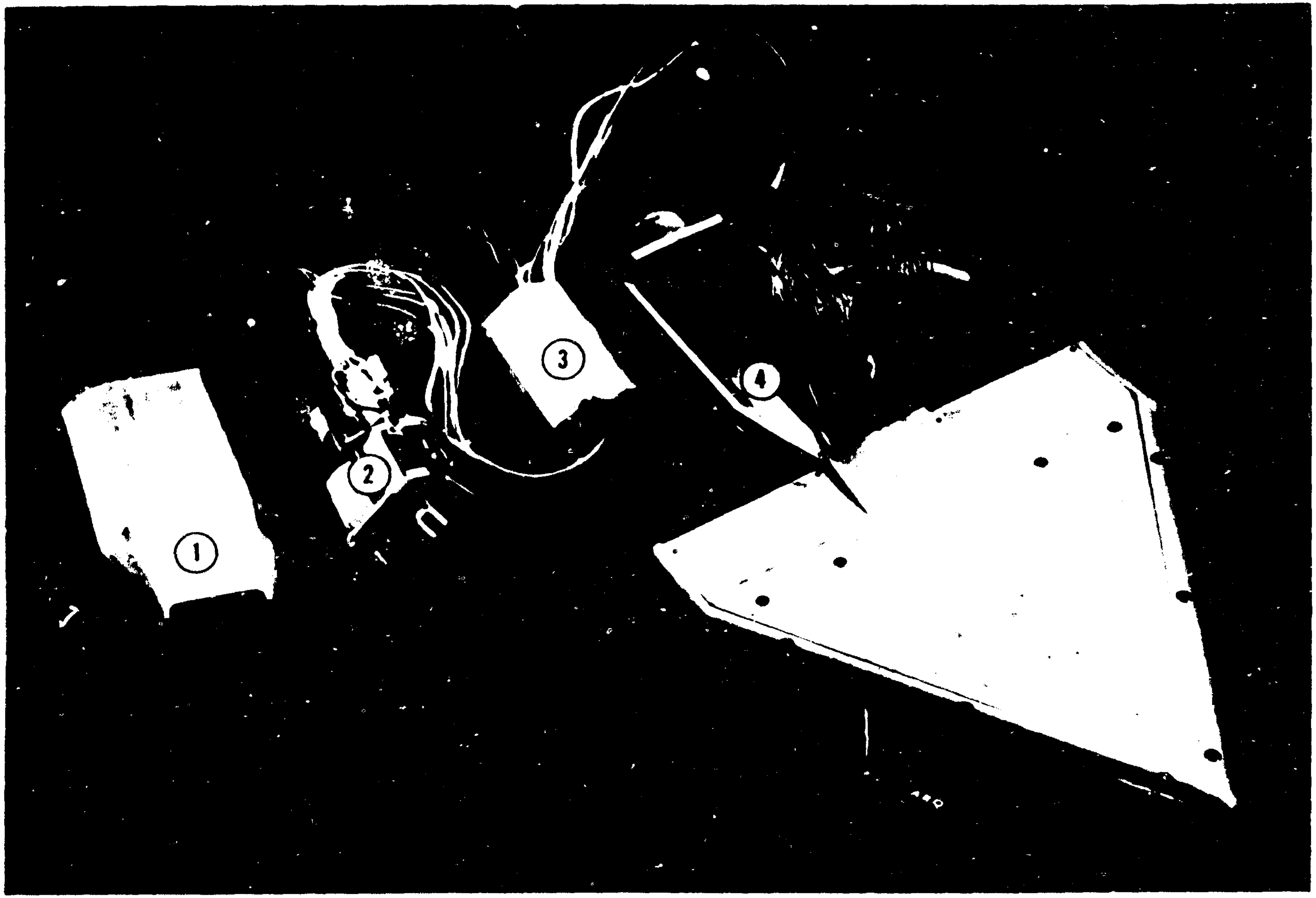

Figure 1k Photograph - Actuator Housing Components
(1) Actuator Housing Cover, (2) Actuator Assembly,
(3) Water Jacket, (4) Actuator Housing

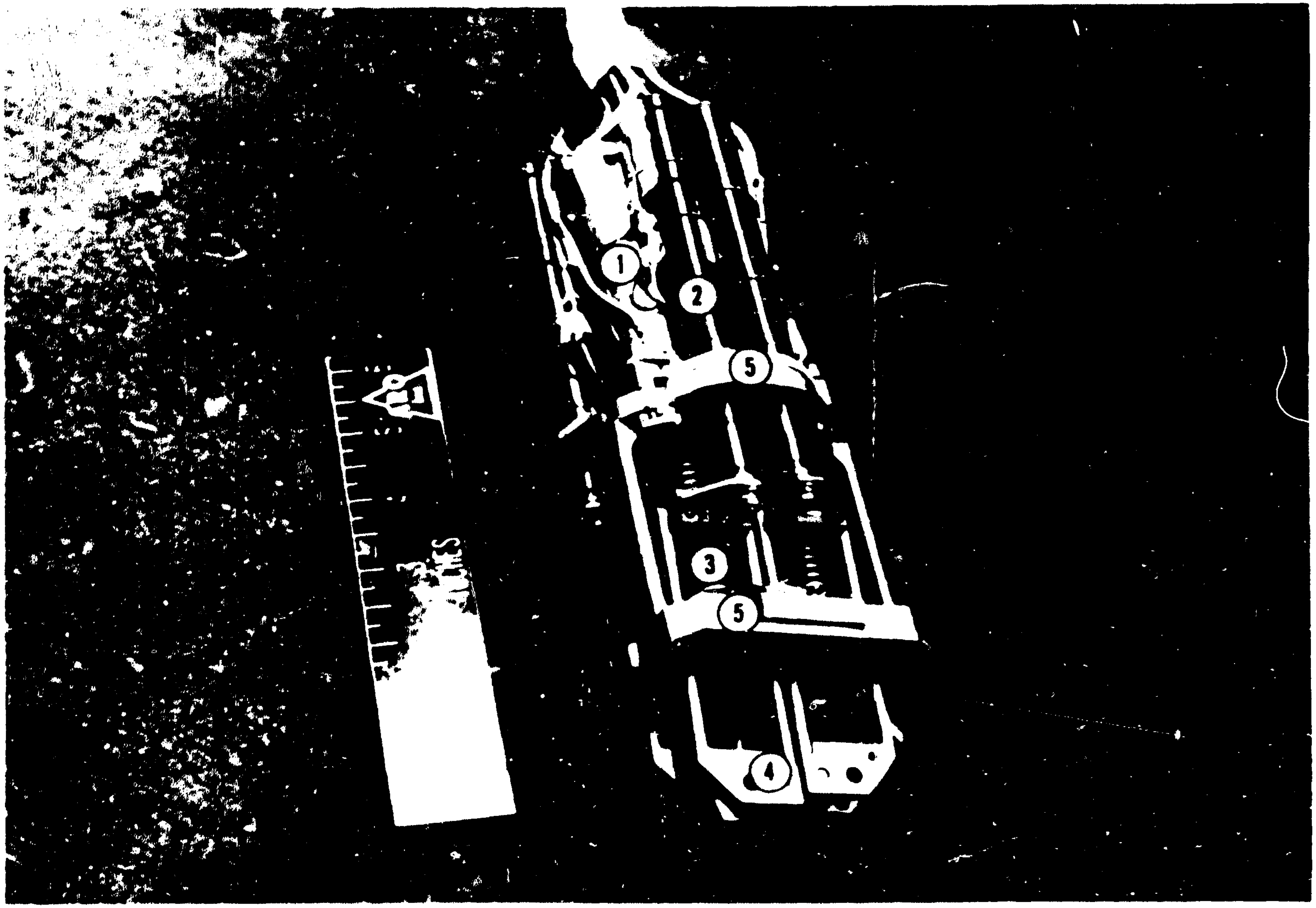

Figure 17 Photograph - Actuator Assembly
(1) Electric Motors, (2) Potentiometers,
(3) Lead Screws, (4) Control Rods
(5) Water Cooled Bulkheads

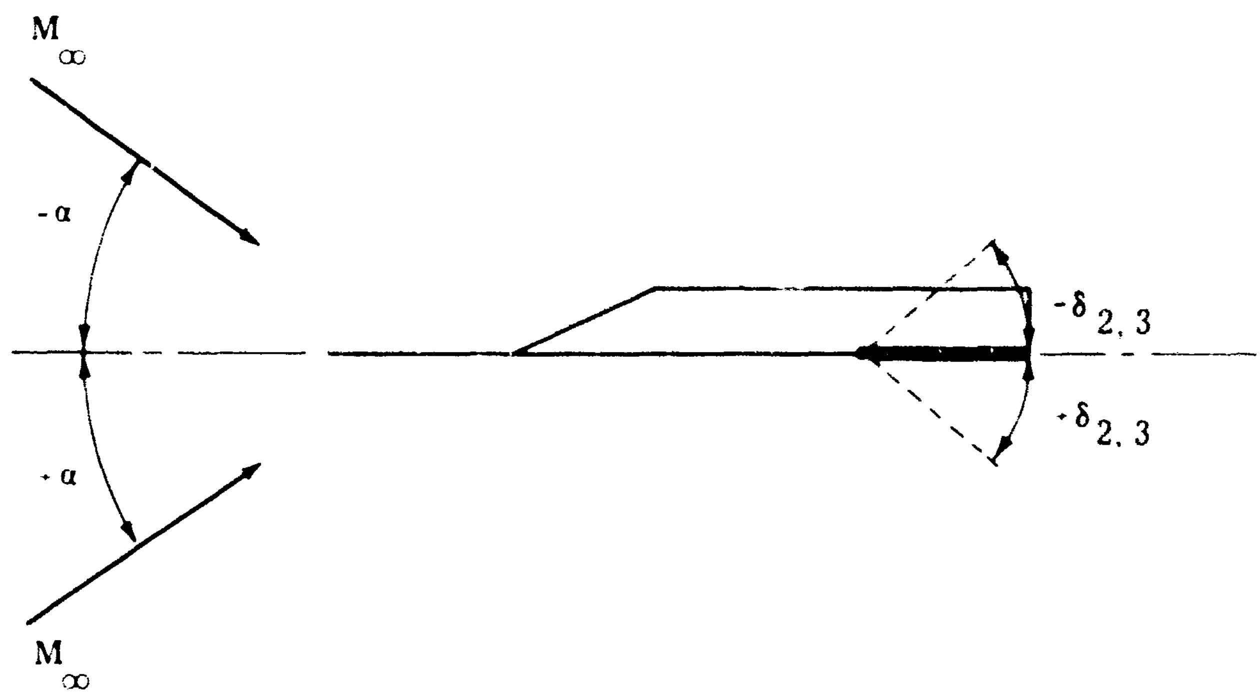

Fig. 2 Sign Convention for Model Angles and Control Deflection Angles

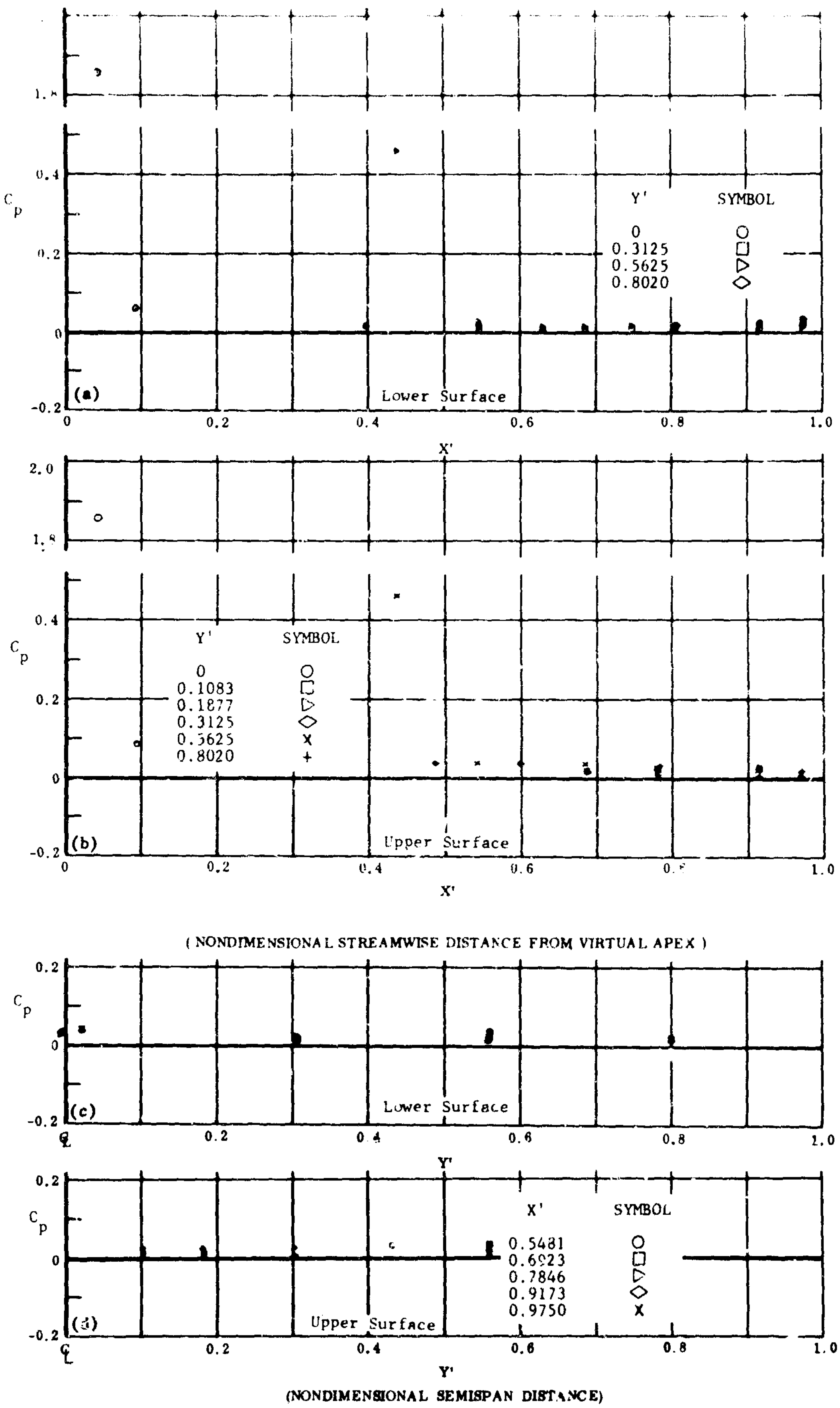

Fig. 3 Configuration I, $\alpha = 0$, $\delta_2 = \delta_3 = 0$

a) C_p vs. X', lower surface

b) C_p vs. X', upper surface

c) C_p vs. Y', lower surface

d) C_p vs. Y', upper surface

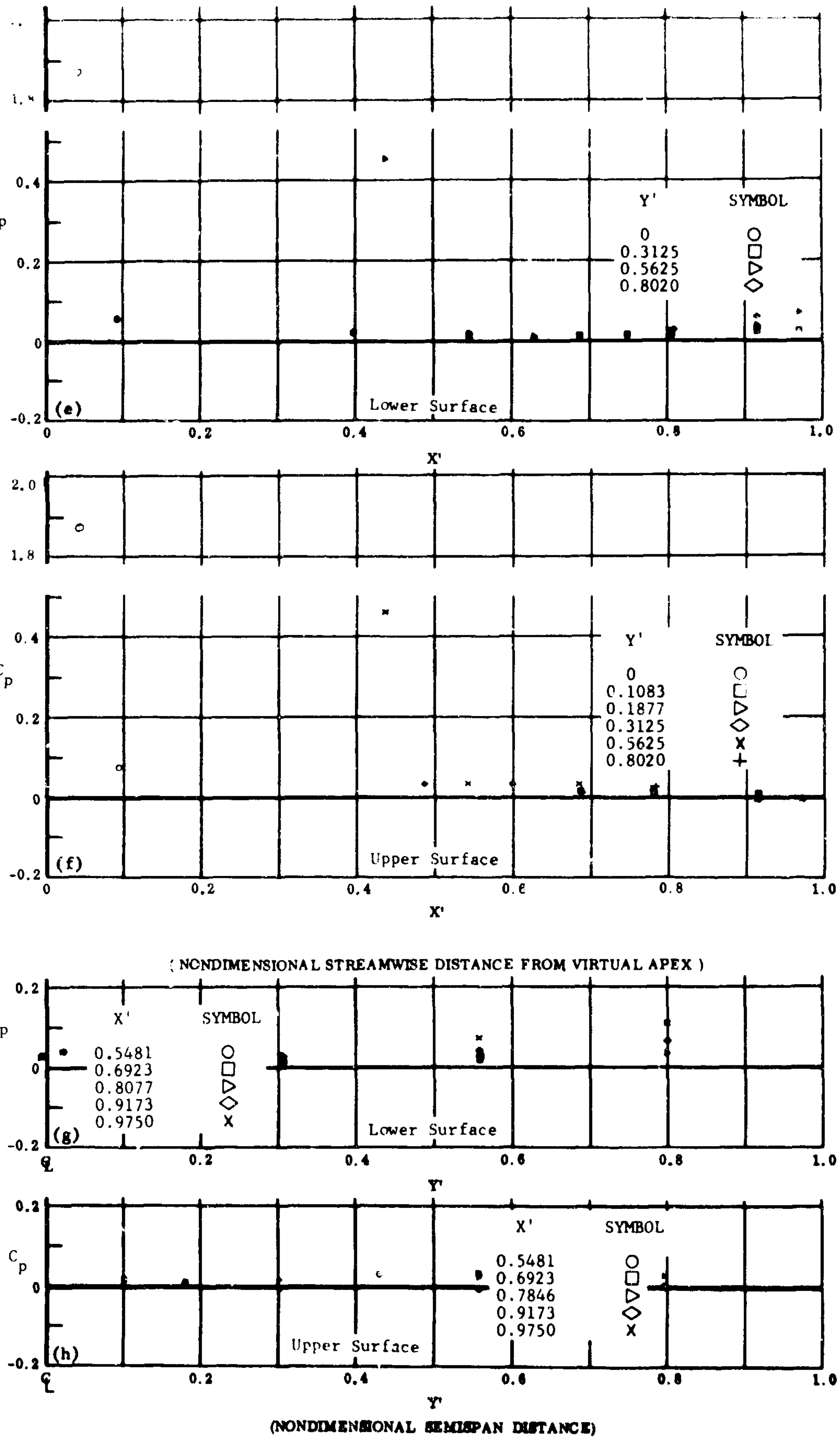

Fig. 3 Configuration I, $\alpha = 0$, $\delta_2 = \delta_3 = +10$

e) C_p vs. X', lower surface

f) C_p vs. X', upper surface

g) C_p vs. Y', lower surface

h) C_p vs. Y', upper surface

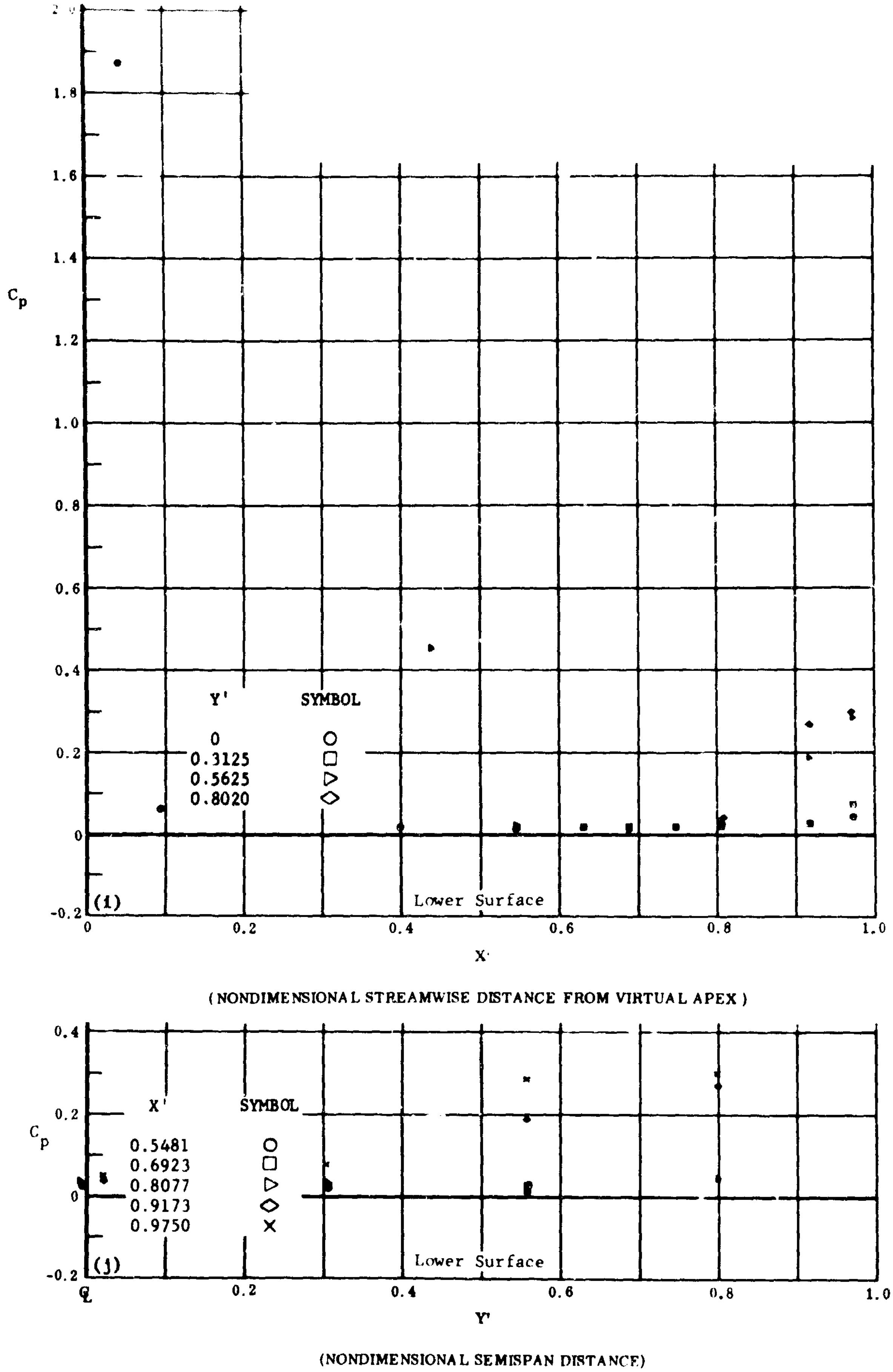

Fig. 3 Configuration I, $\alpha = 0$, $\delta_2 = \delta_3 = +20$

i) C_p vs. X', lower surface

j) C_p vs. Y', lower surface

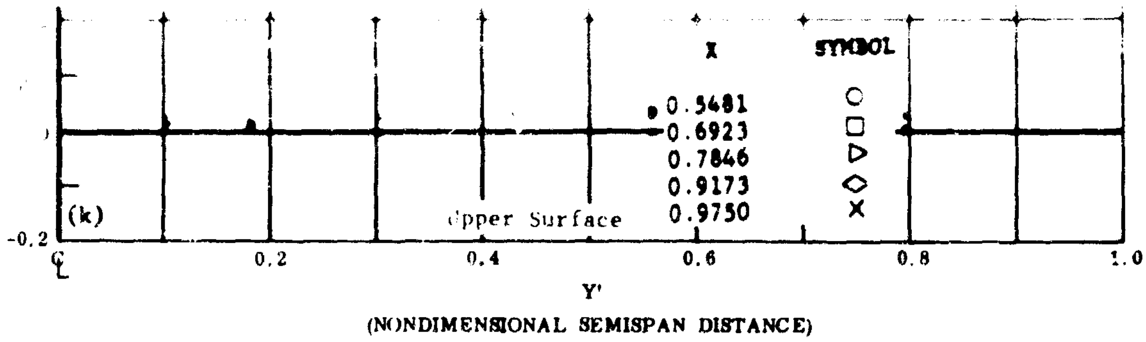

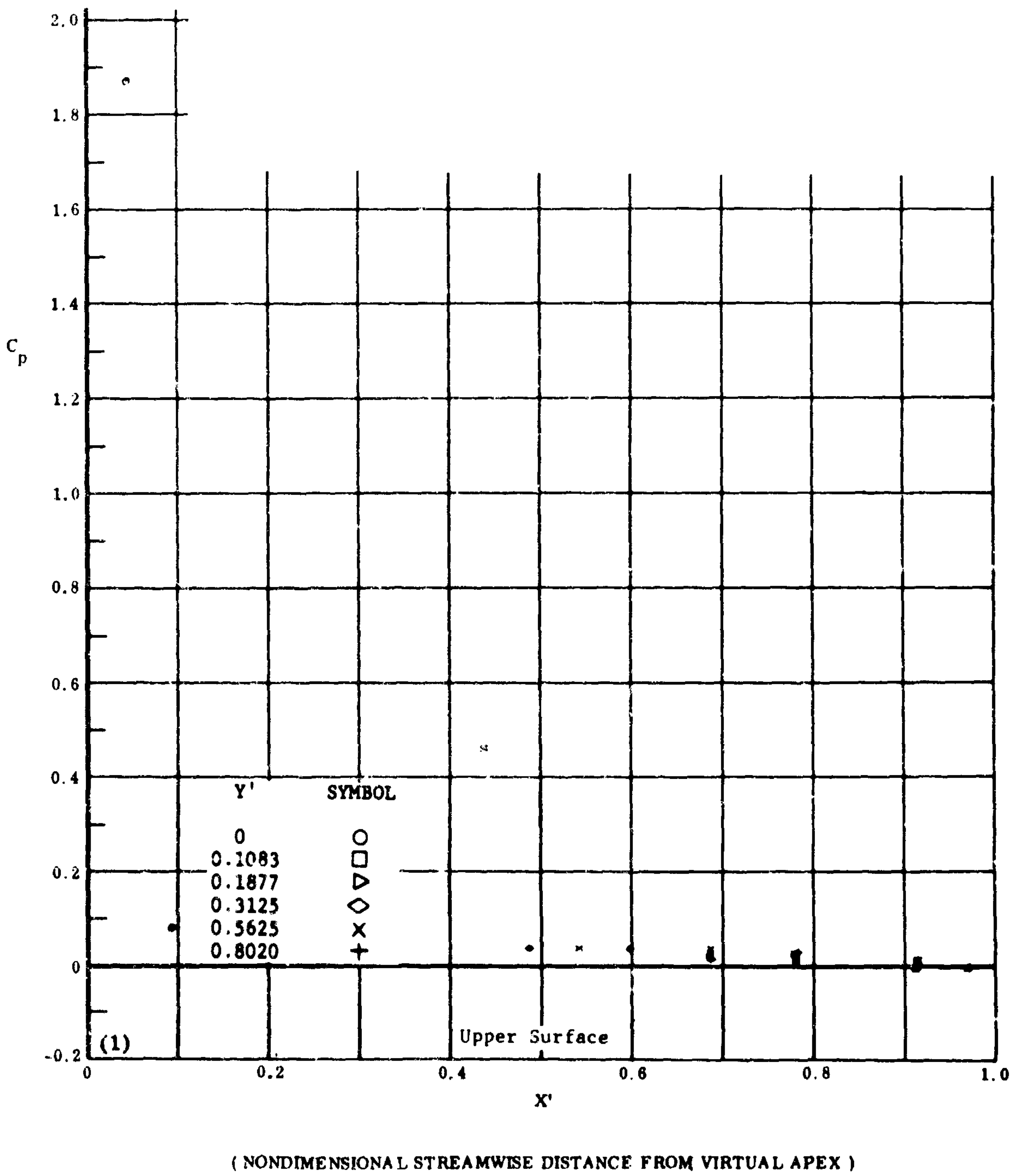

Fig. 3 Configuration I, $\alpha = 0$, $\delta_2 = \delta_3 = +20$

k) C_p vs. Y', upper surface

l) C_p vs. X', upper surface

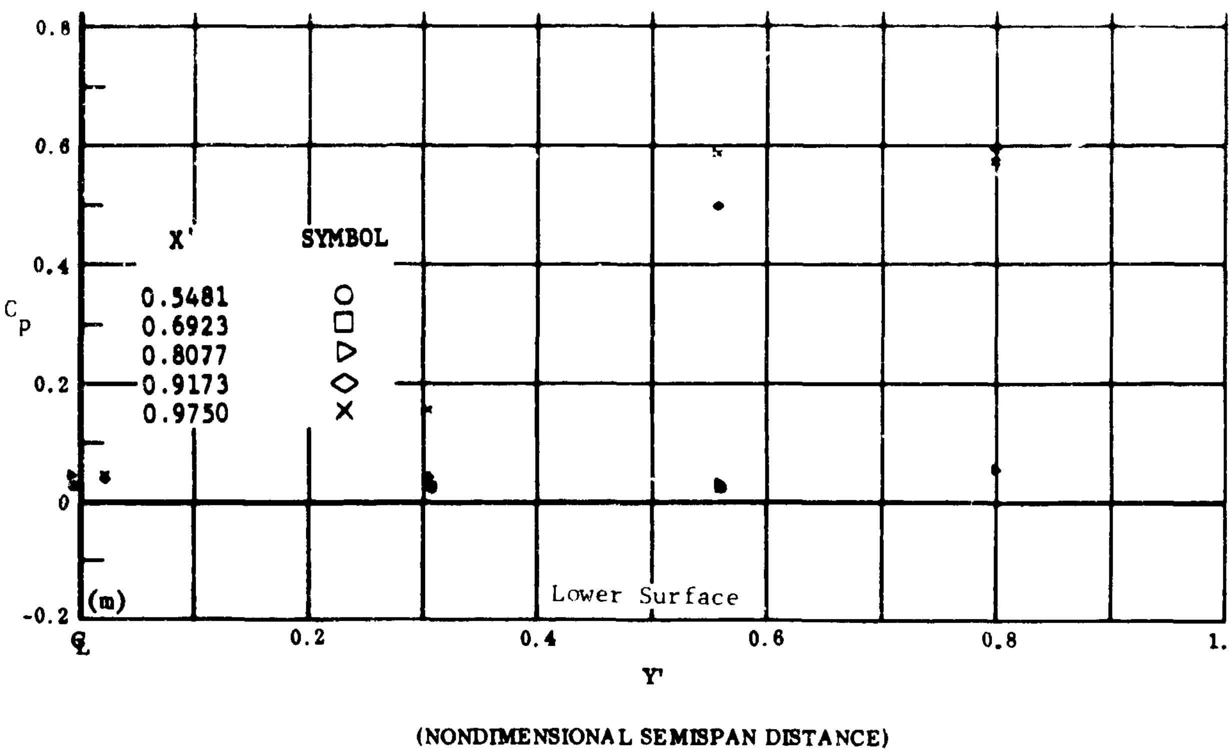

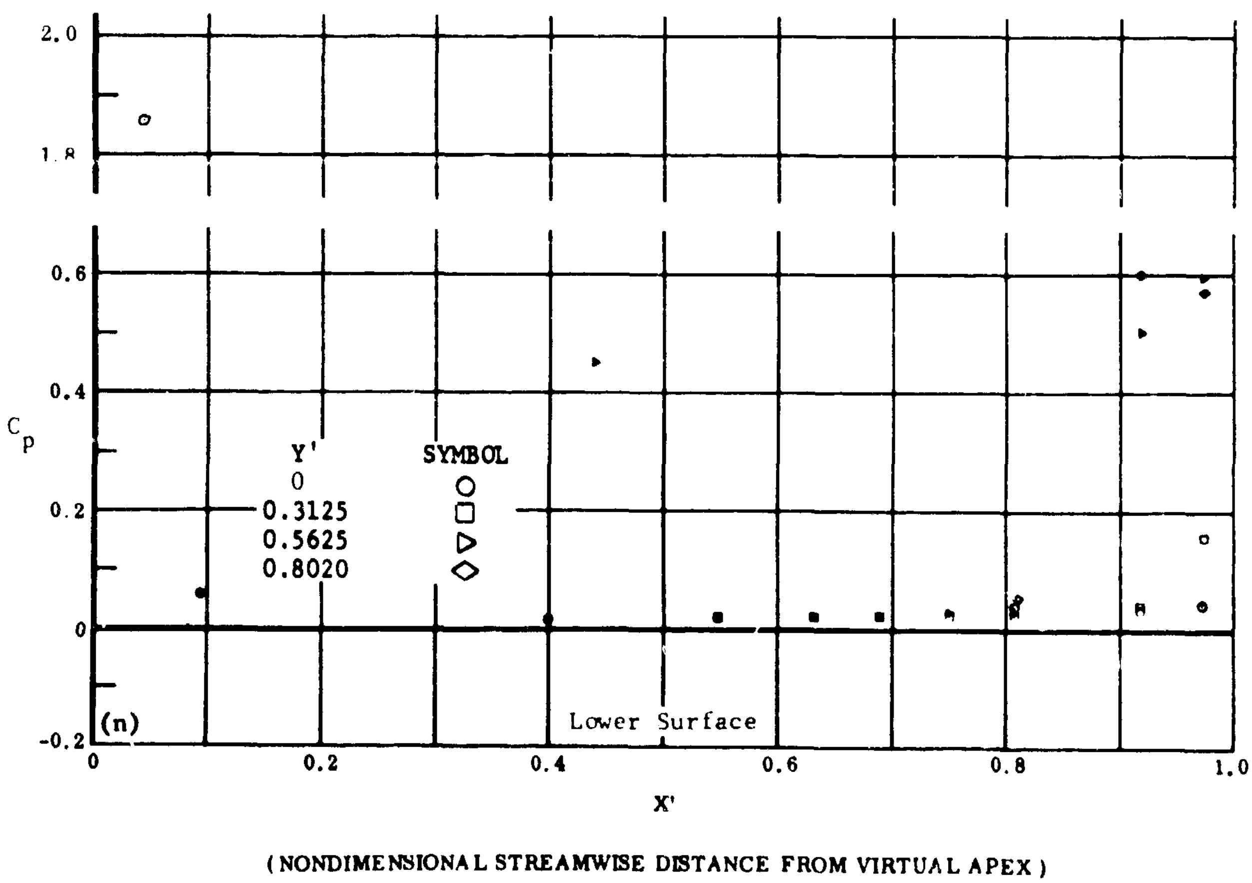

Fig. 3 Configuration I, $\alpha = 0$, $\delta_2 = \delta_3 = +30$

m) C_p vs. Y', lower surface

n) C_p vs. X', lower surface

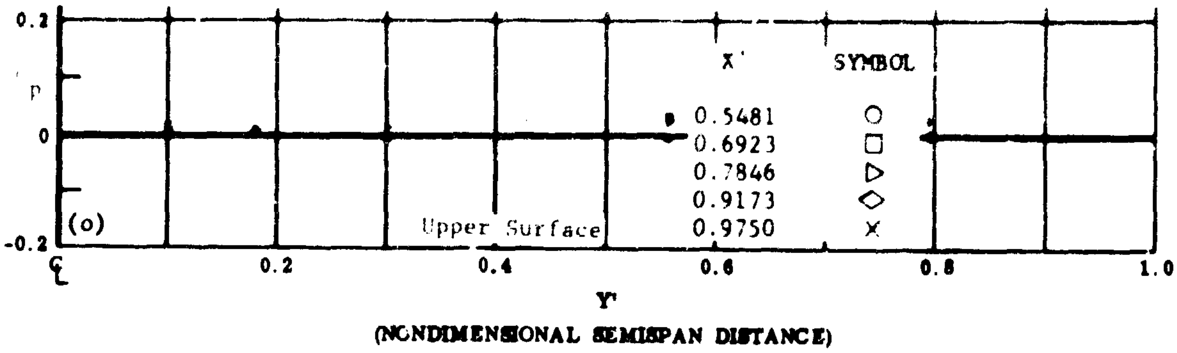

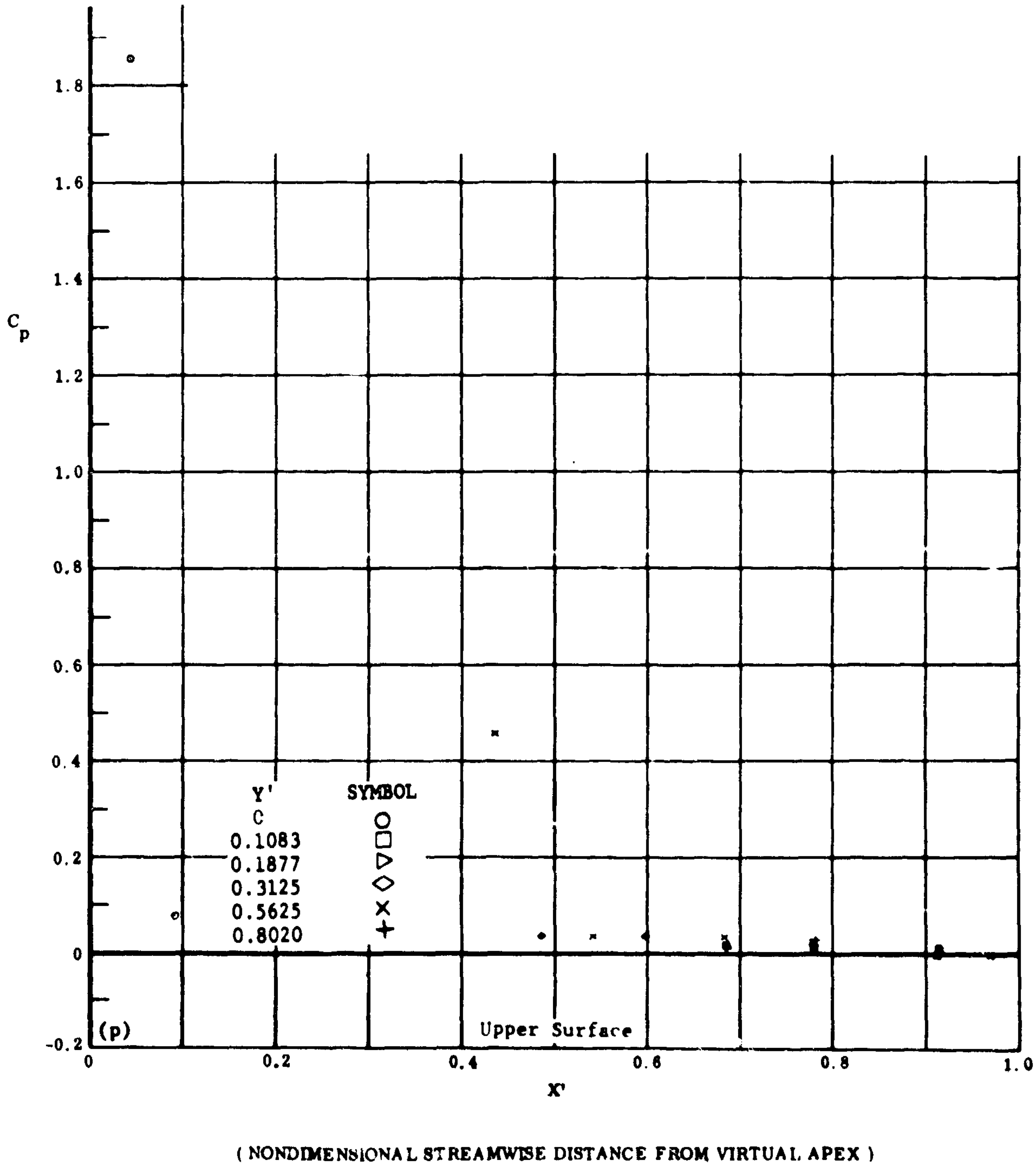

Fig. 3 Configuration I, $\alpha = 0$, $\delta_2 = \delta_3 = +30$

o) C_p vs. Y', upper surface

p) C_p vs. X', upper surface

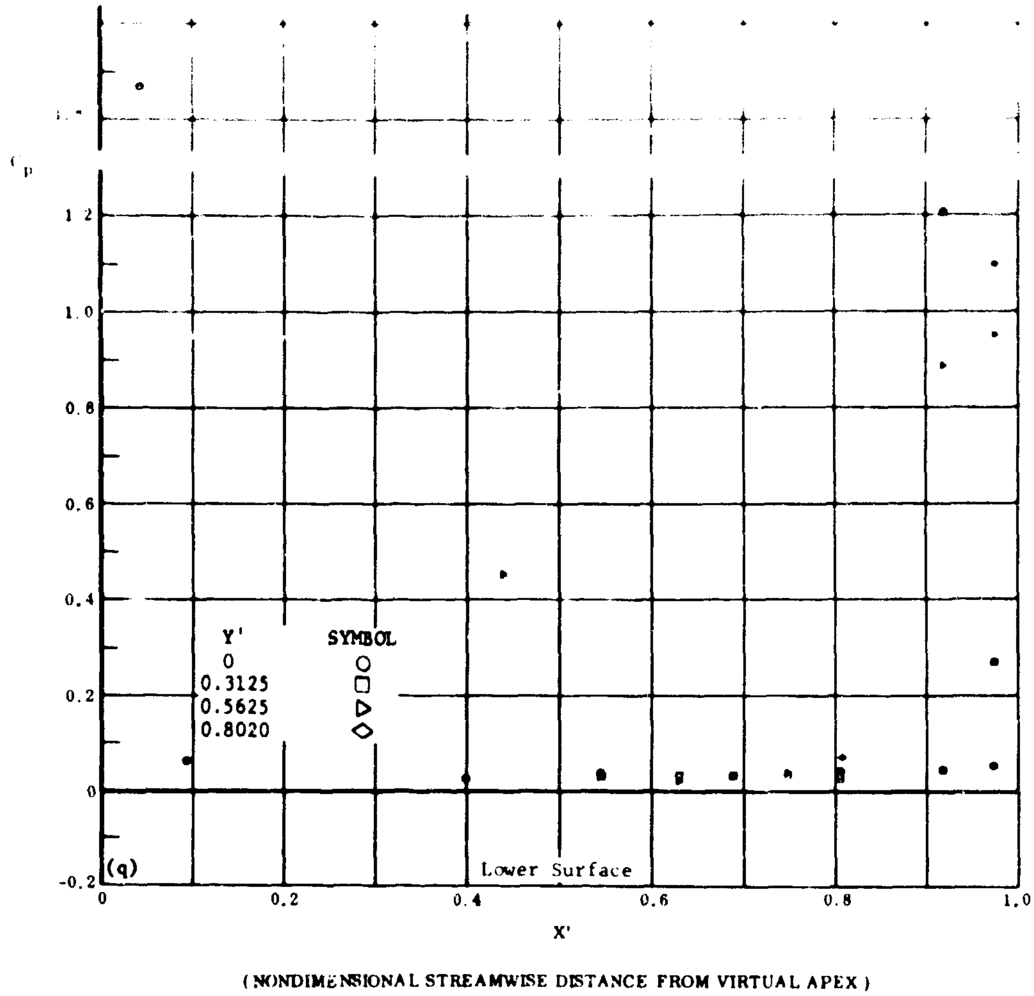

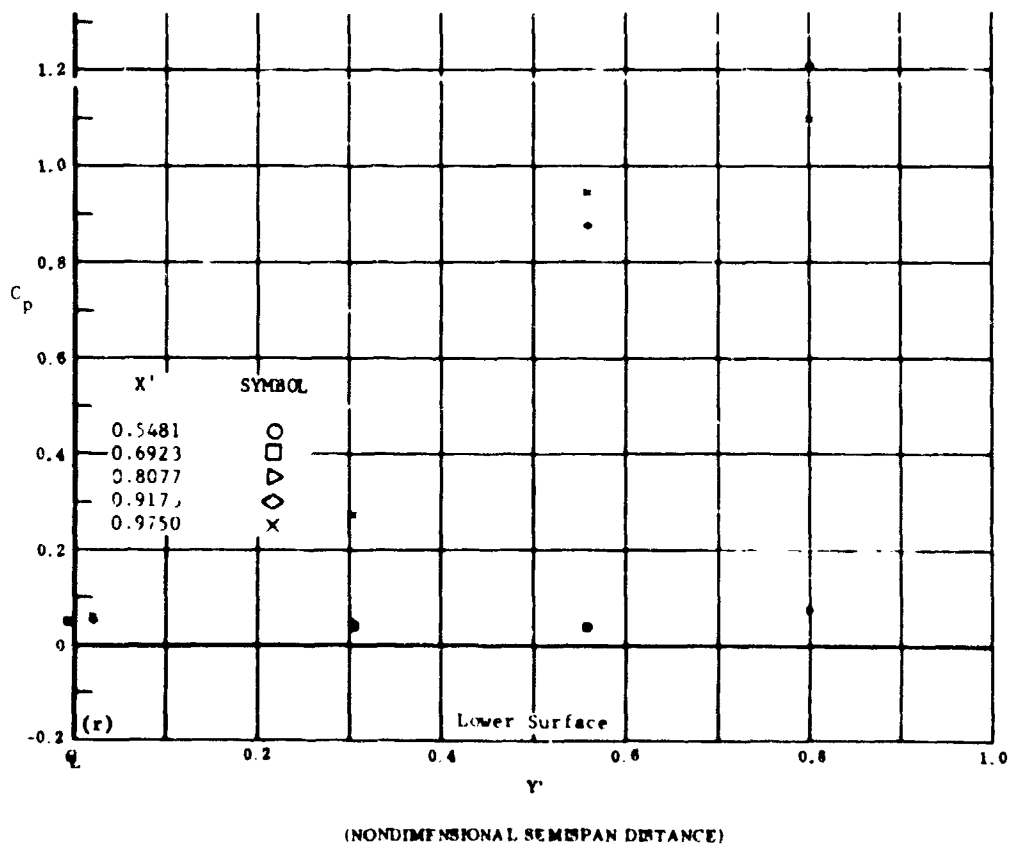

Fig. 3 Configuration I, $\alpha = 0$, $\delta_2 = \delta_3 = +39$

q) C_p vs. X', lower surface

r) C_p vs. Y', lower surface

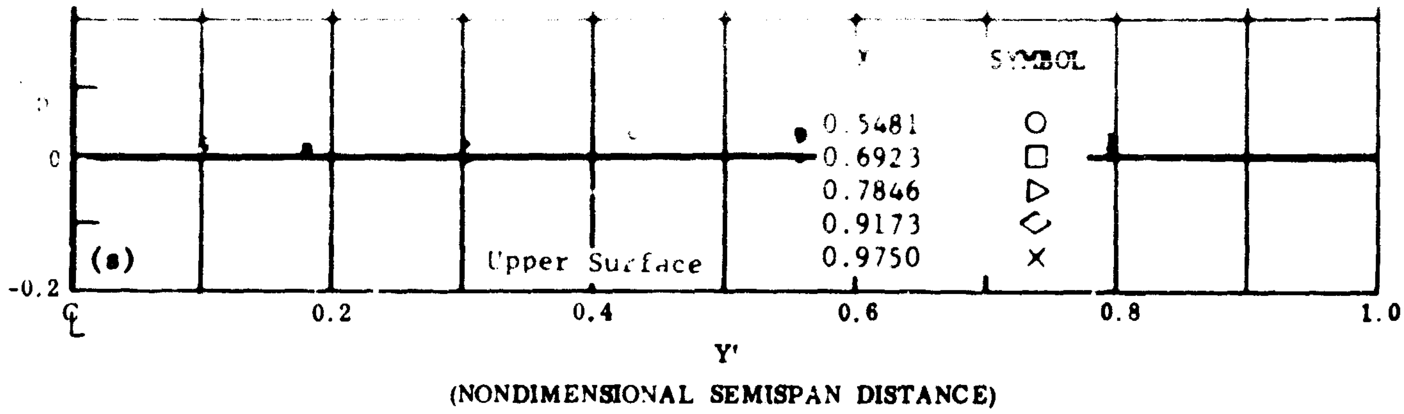

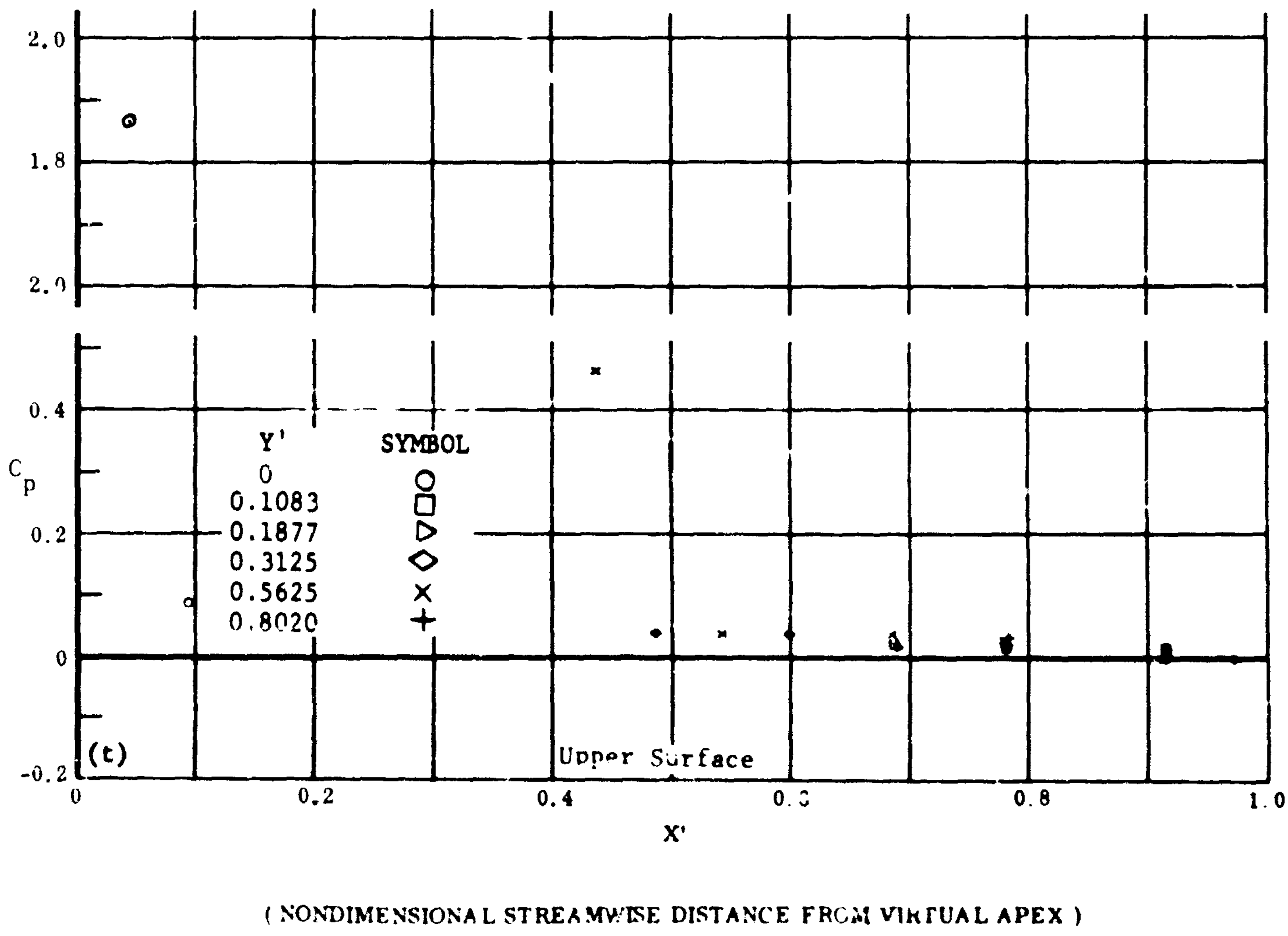

Fig. 3 Configuration I, $\alpha = 0$, $\delta_2 = \delta_3 = +39$

s) C_p vs. Y', upper surface

t) C_p vs. X', upper surface

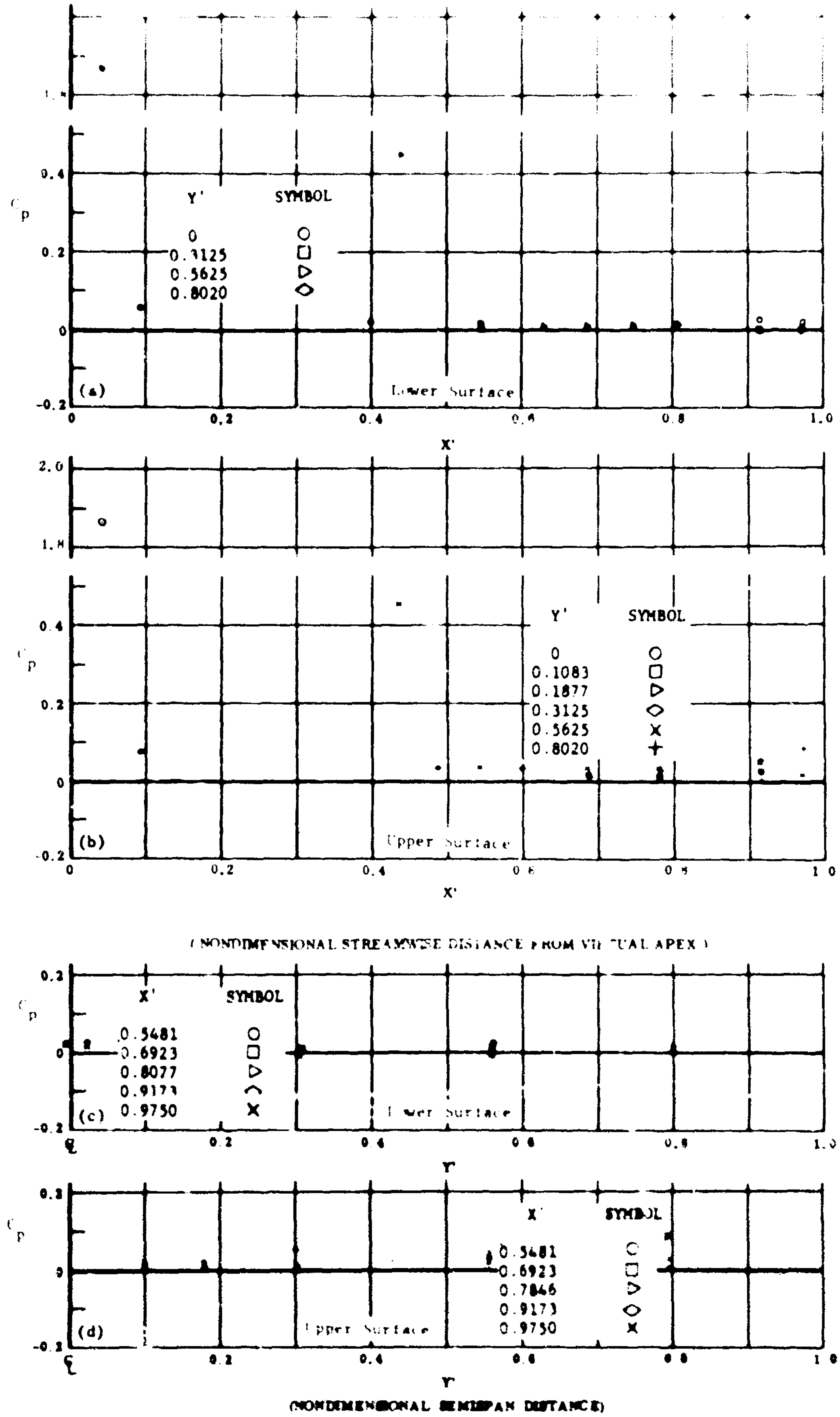

Fig. 4 Configuration I, = 0, = = -1)

a) C_p vs. X', lower surface

b) C_p vs. X', upper surface

c) C_p vs. Y', lower surface

d) C_p vs. Y', upper surface

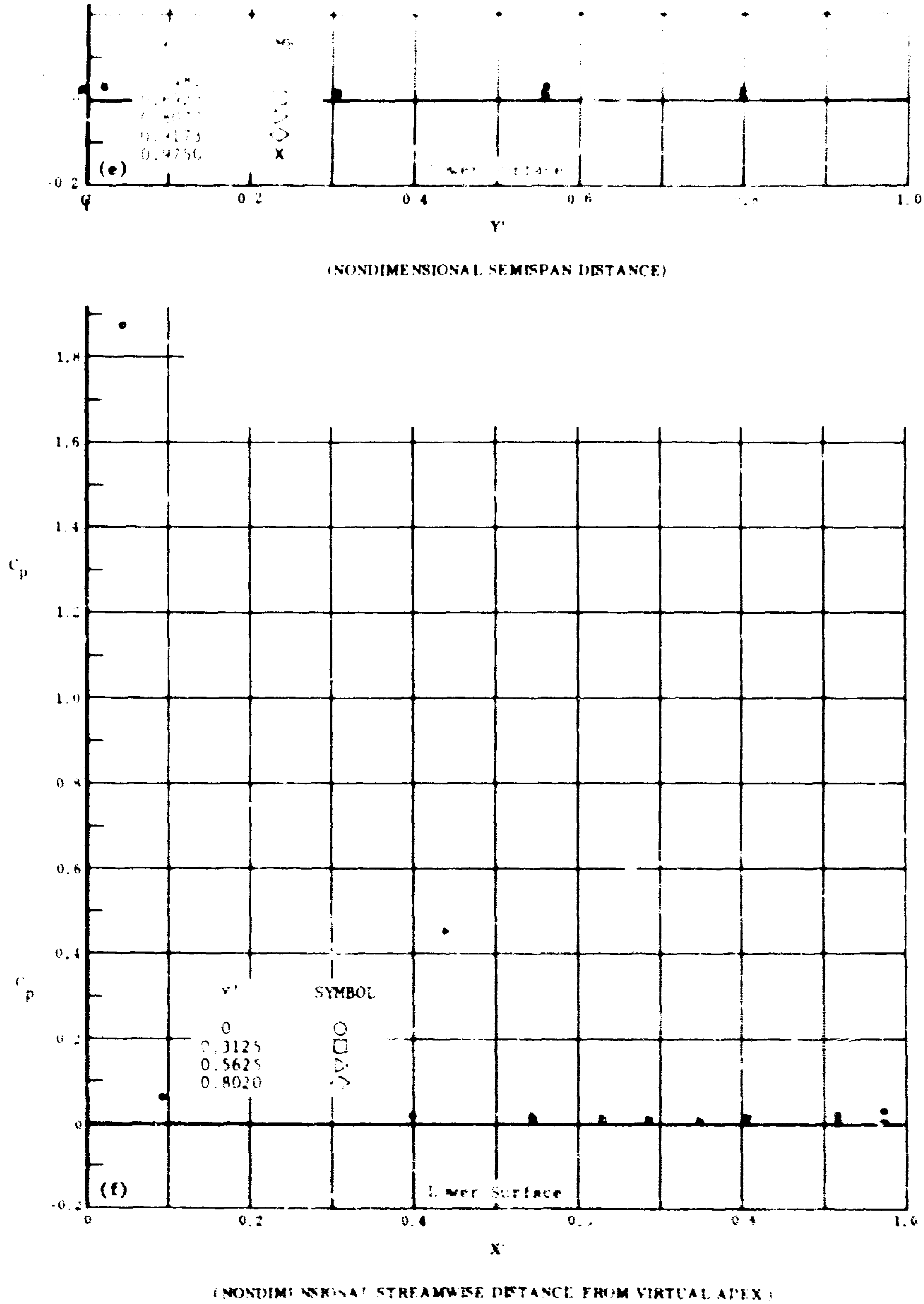

Fig. 4 Configuration I, $\alpha = 0$, $\delta_2 = \delta_3 = -20$

e) C_p vs. Y', lower surface

f) C_p vs. X', lower surface

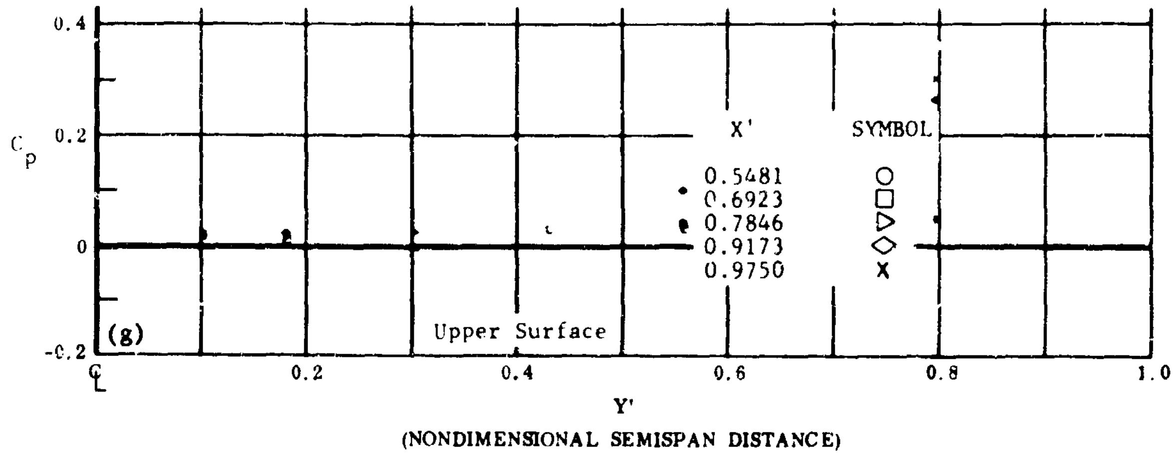

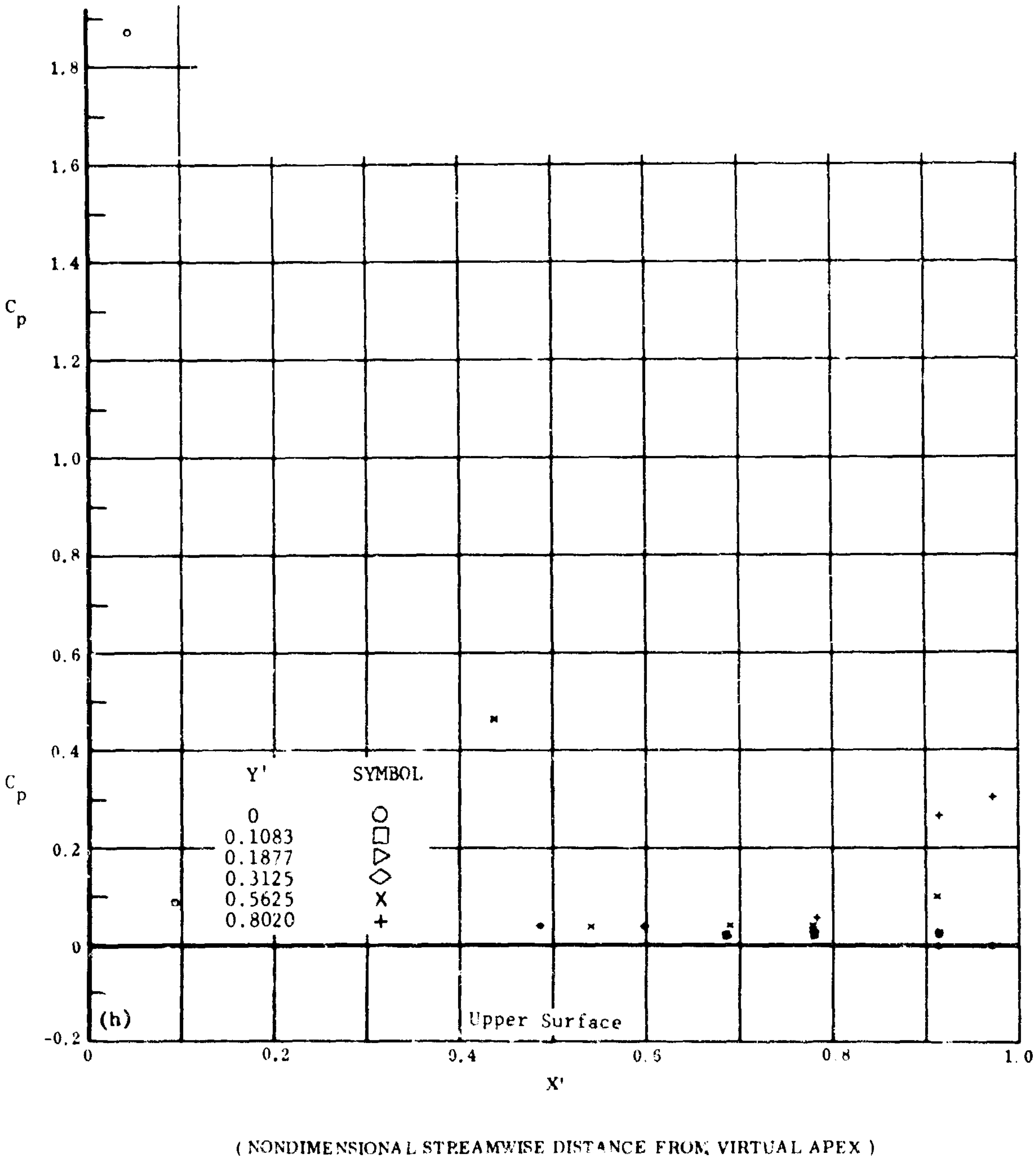

Fig. 4 Configuration I, $\alpha = 0$, $\delta_2 = \delta_3 = -20$

g) C_p vs. Y', upper surface

h) C_p vs. X', upper surface

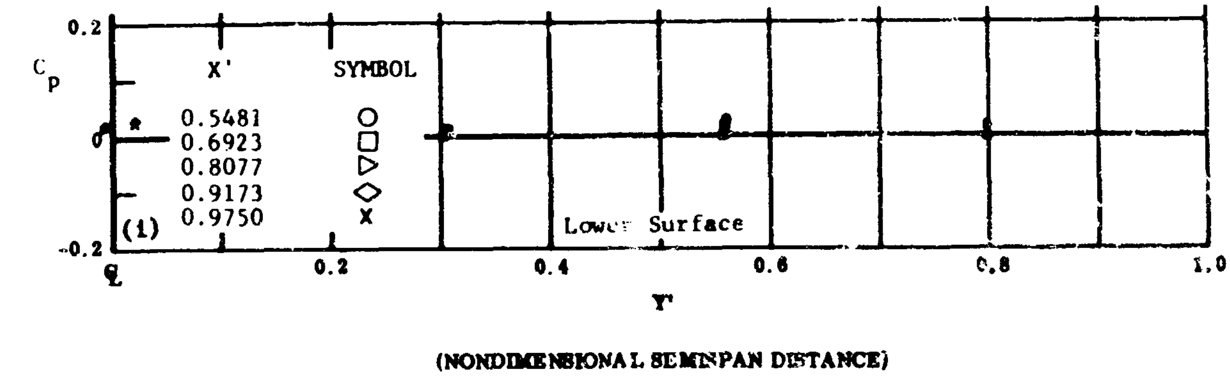

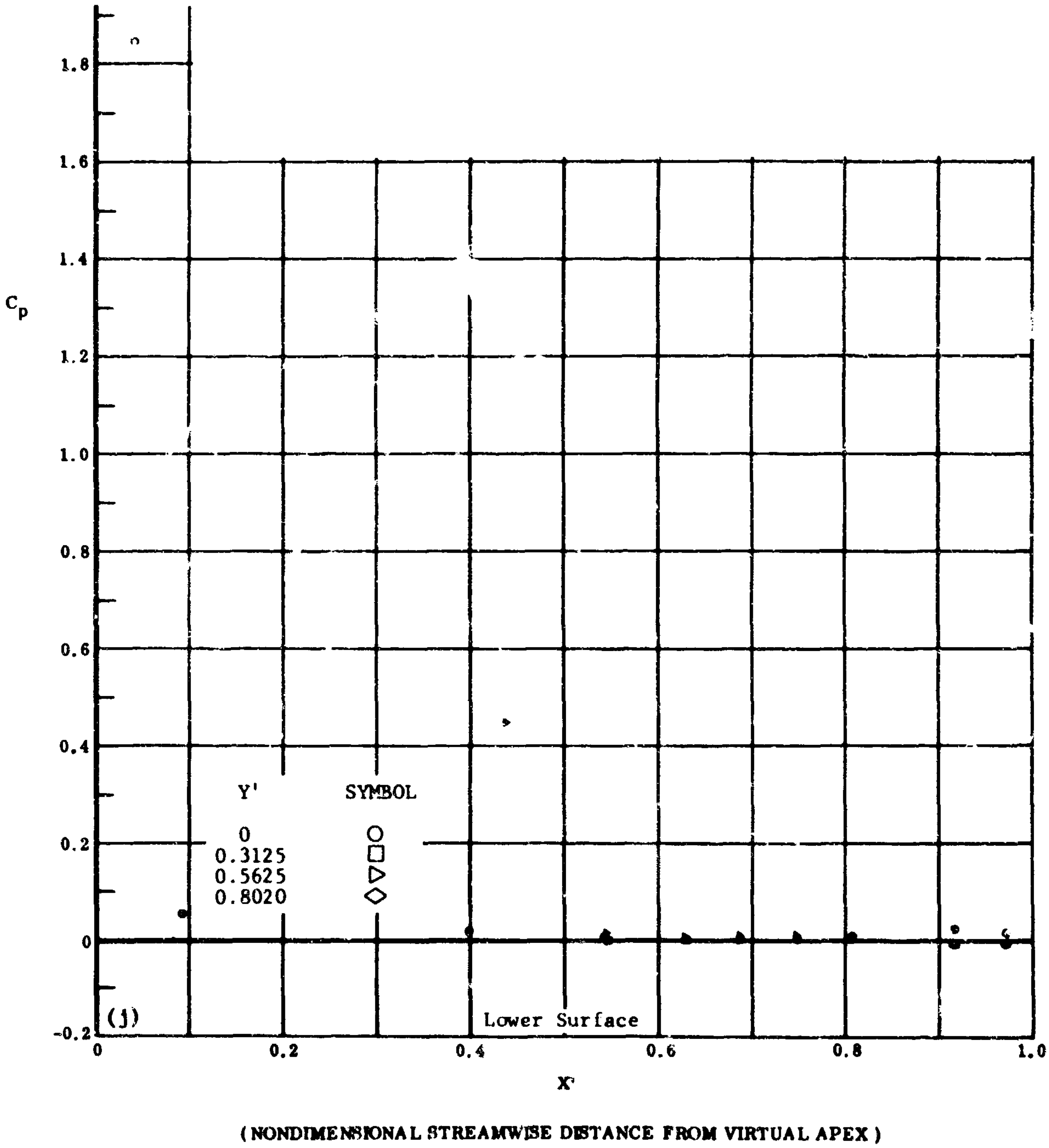

Fig. 4 Configuration I, $\alpha = 0$, $\delta_2 = \delta_3 = -30$

i) C_p vs. Y', lower surface

j) C_p vs. X', lower surface

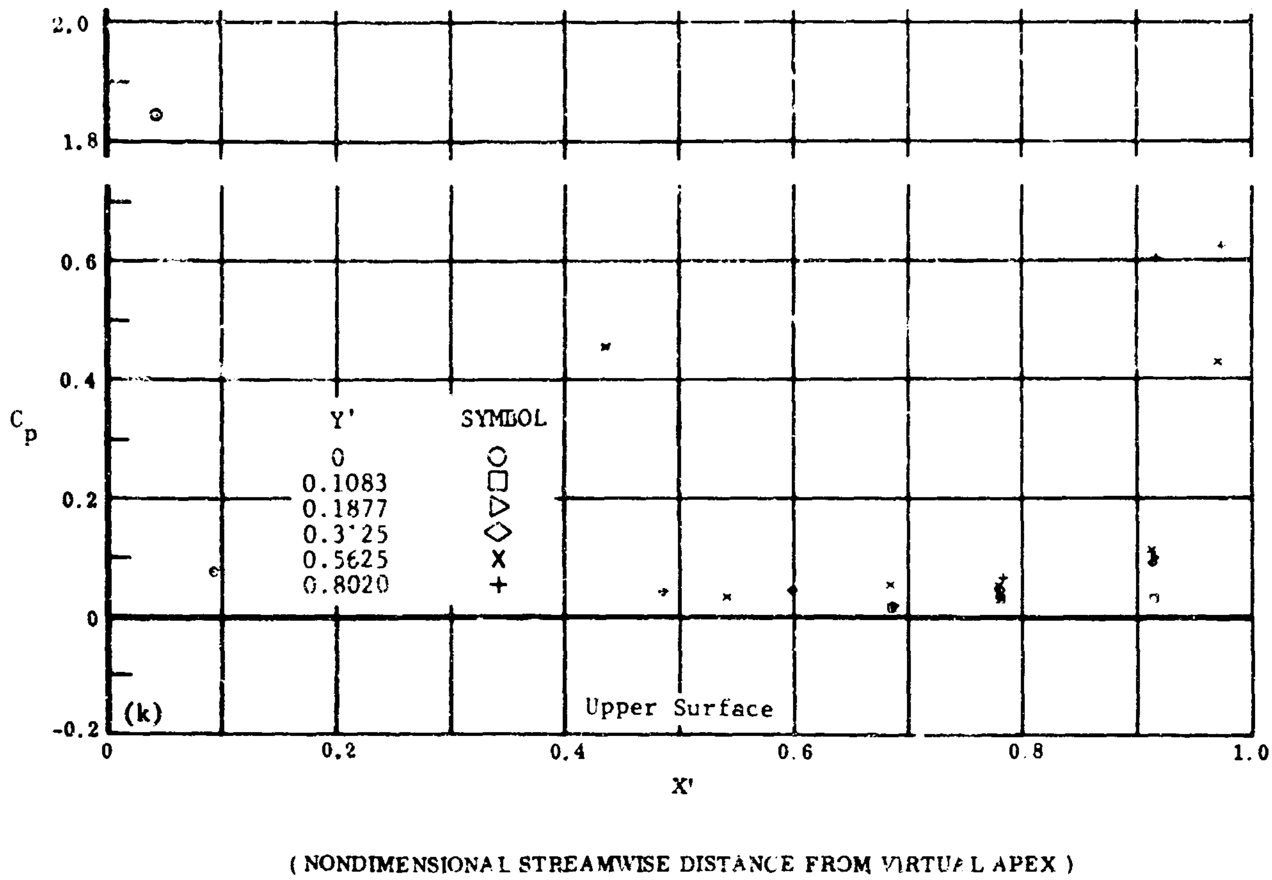

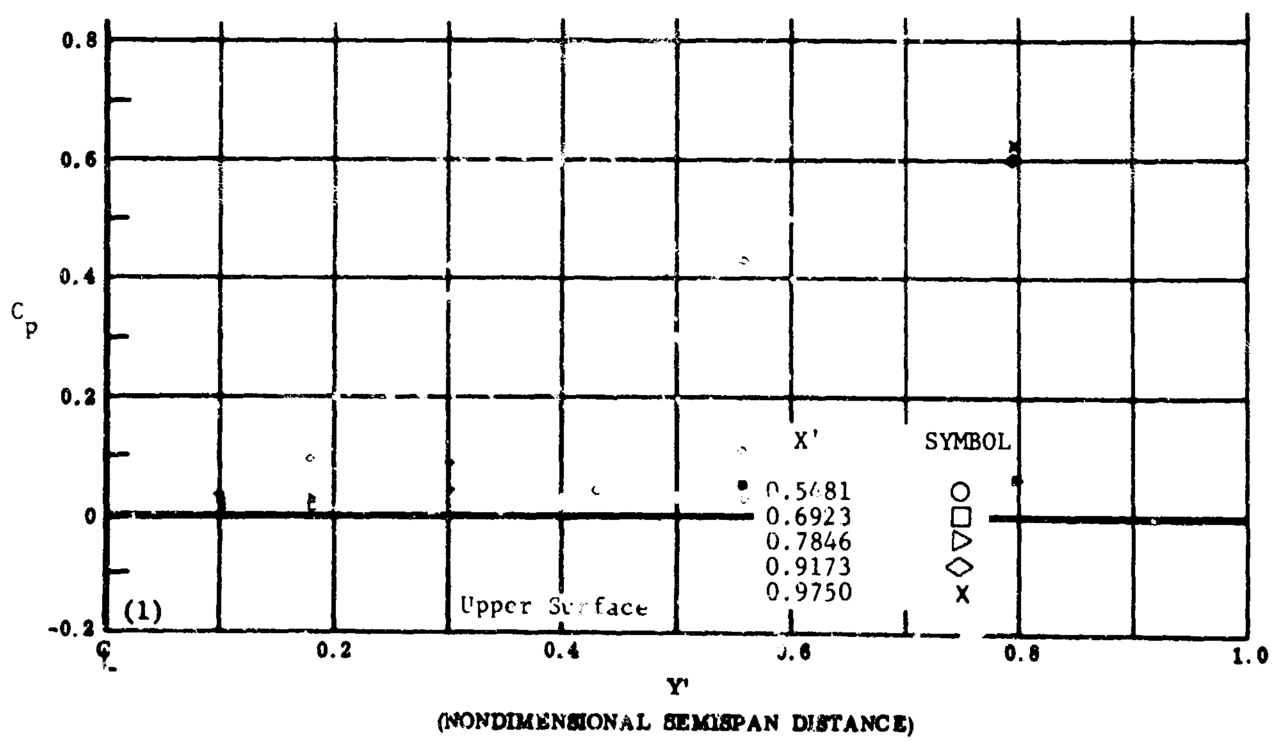

Fig. 4 Configuration I, $\alpha = 0$, $\delta_2 = \delta_3 = -30$

k) C_p vs. X', upper surface

l) C_p vs. Y', upper surface

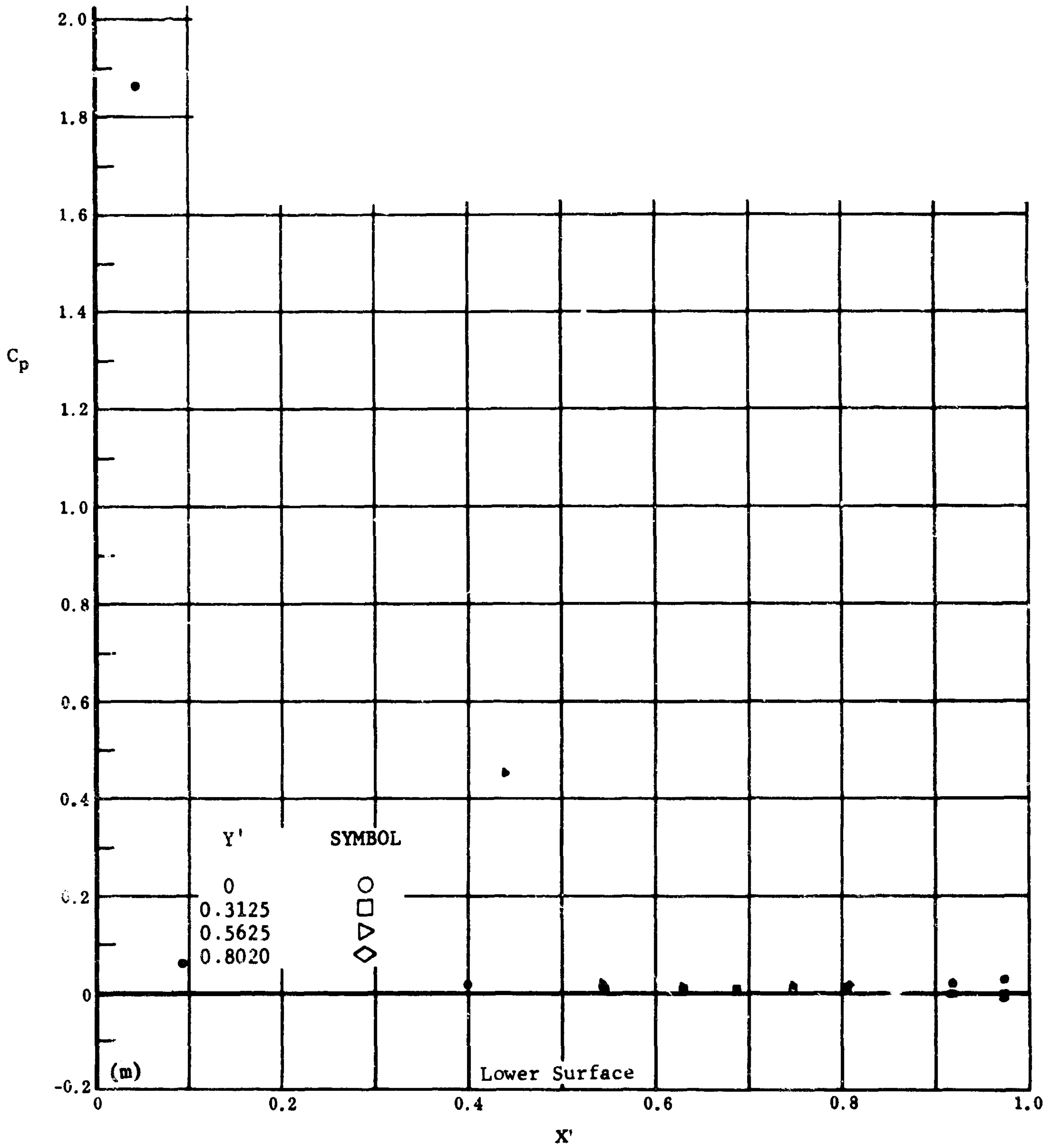

(NONDIMENSIONAL STREAMWISE DISTANCE FROM VIRTUAL APEX)

Fig. 4m Configuration I, $\alpha = 0$, $\delta_2 = \delta_3 = -39$

C_p vs. X', lower surface

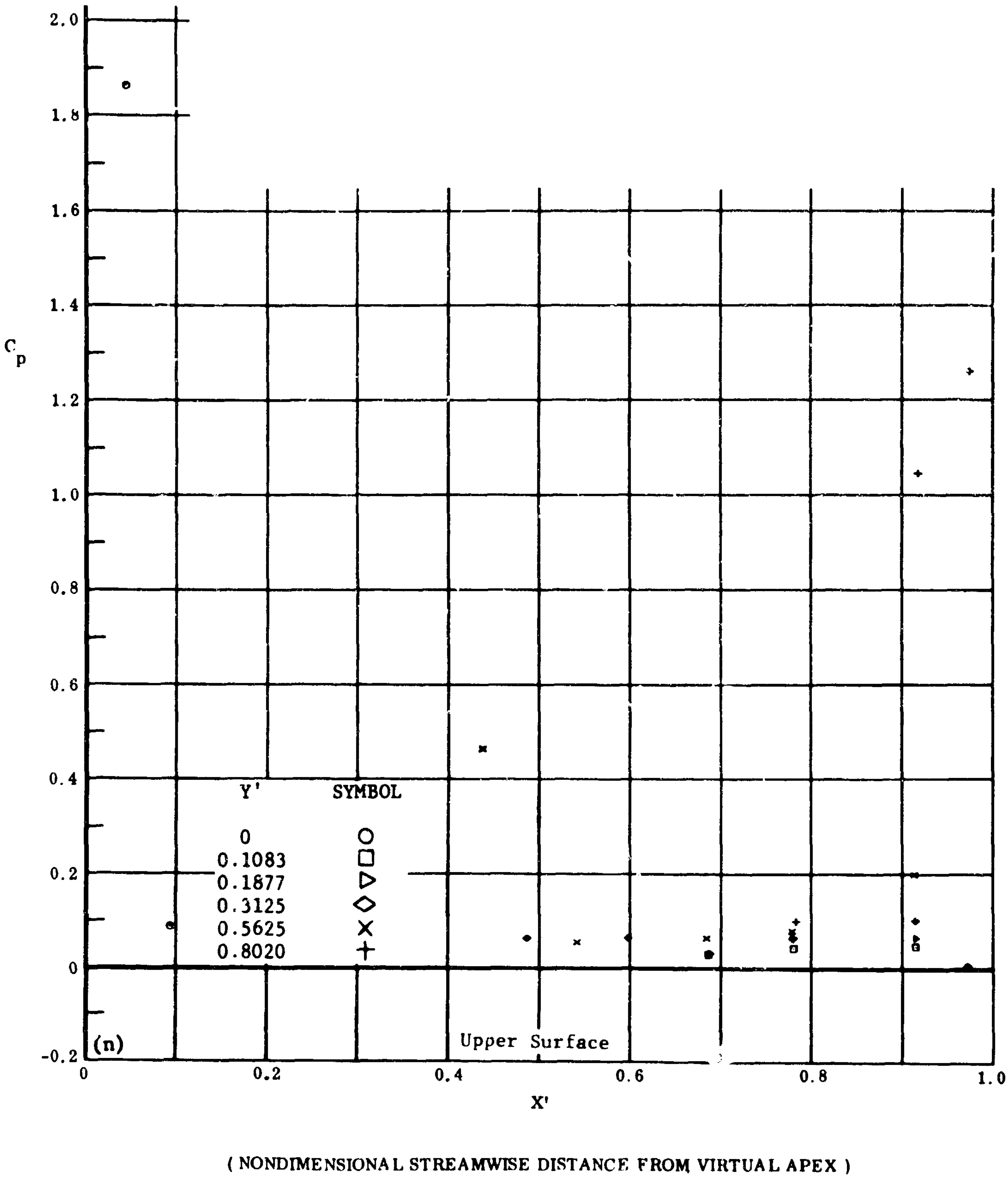

Fig. 4n Configuration I, a = 0 , $\delta_2 = \delta_3 = -39$

C_p vs. X', upper surface

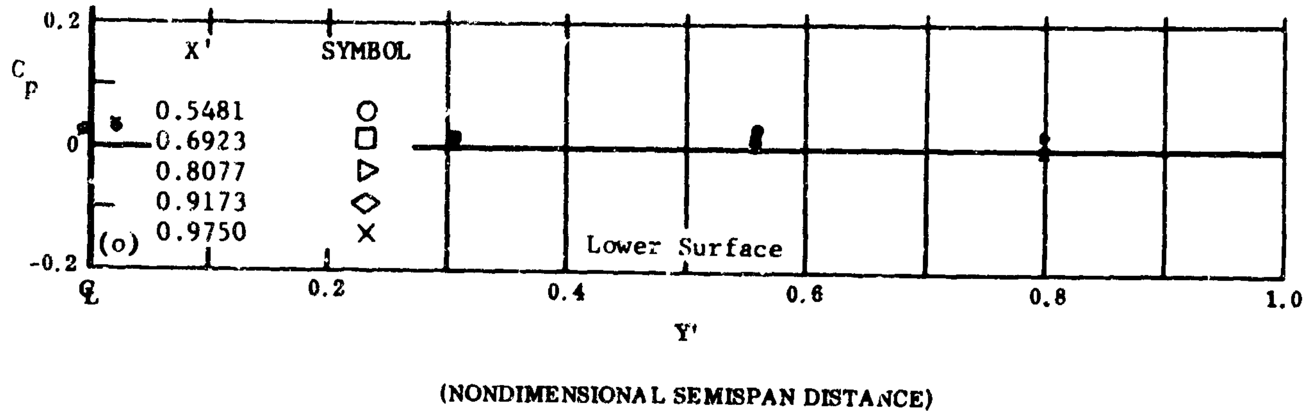

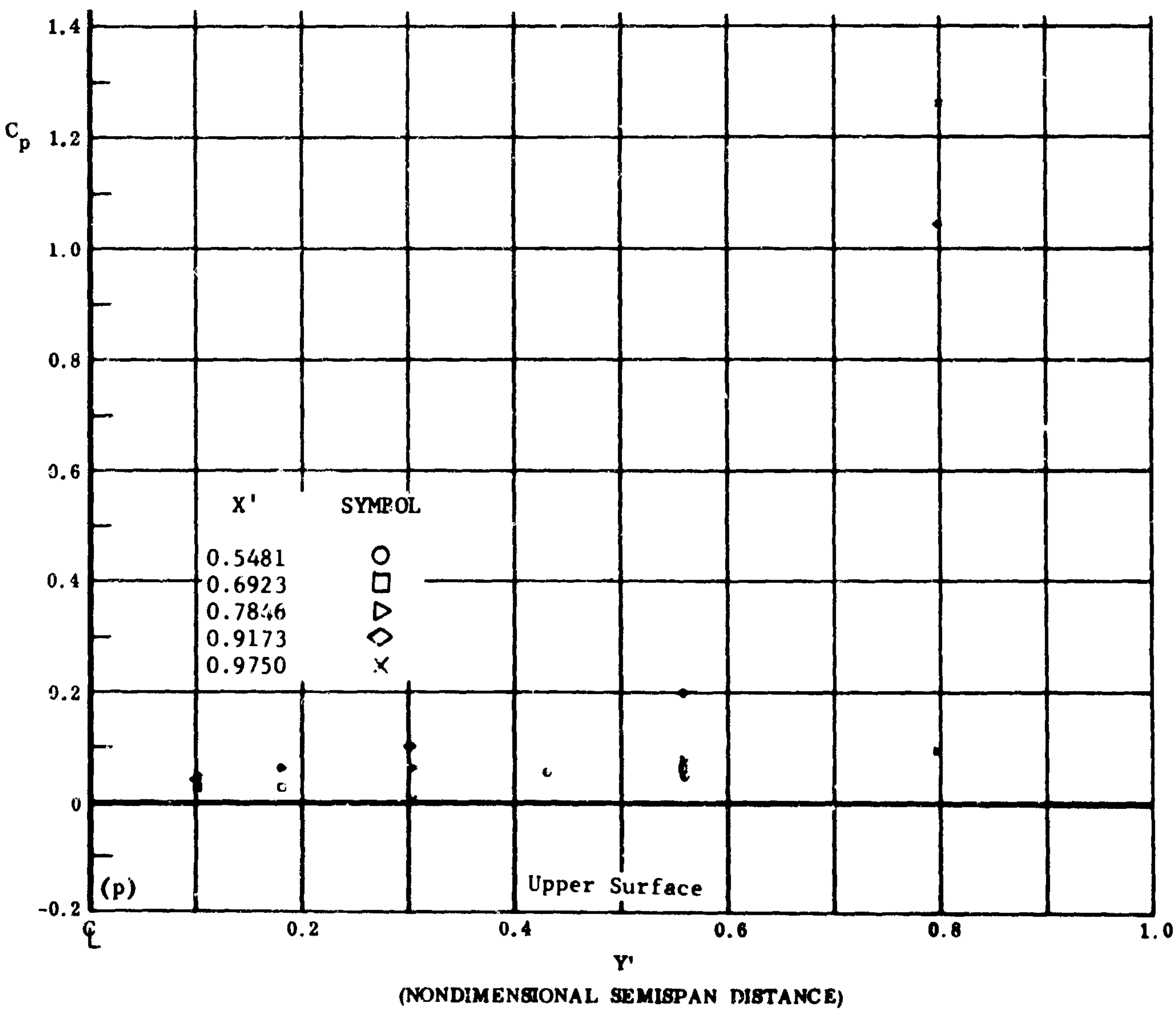

Fig. 4 Configuration I, $\alpha = 0$, $\delta_2 = \delta_3 = -39$

o) C_p vs. Y', lower surface

p) C_p vs. Y', upper surface

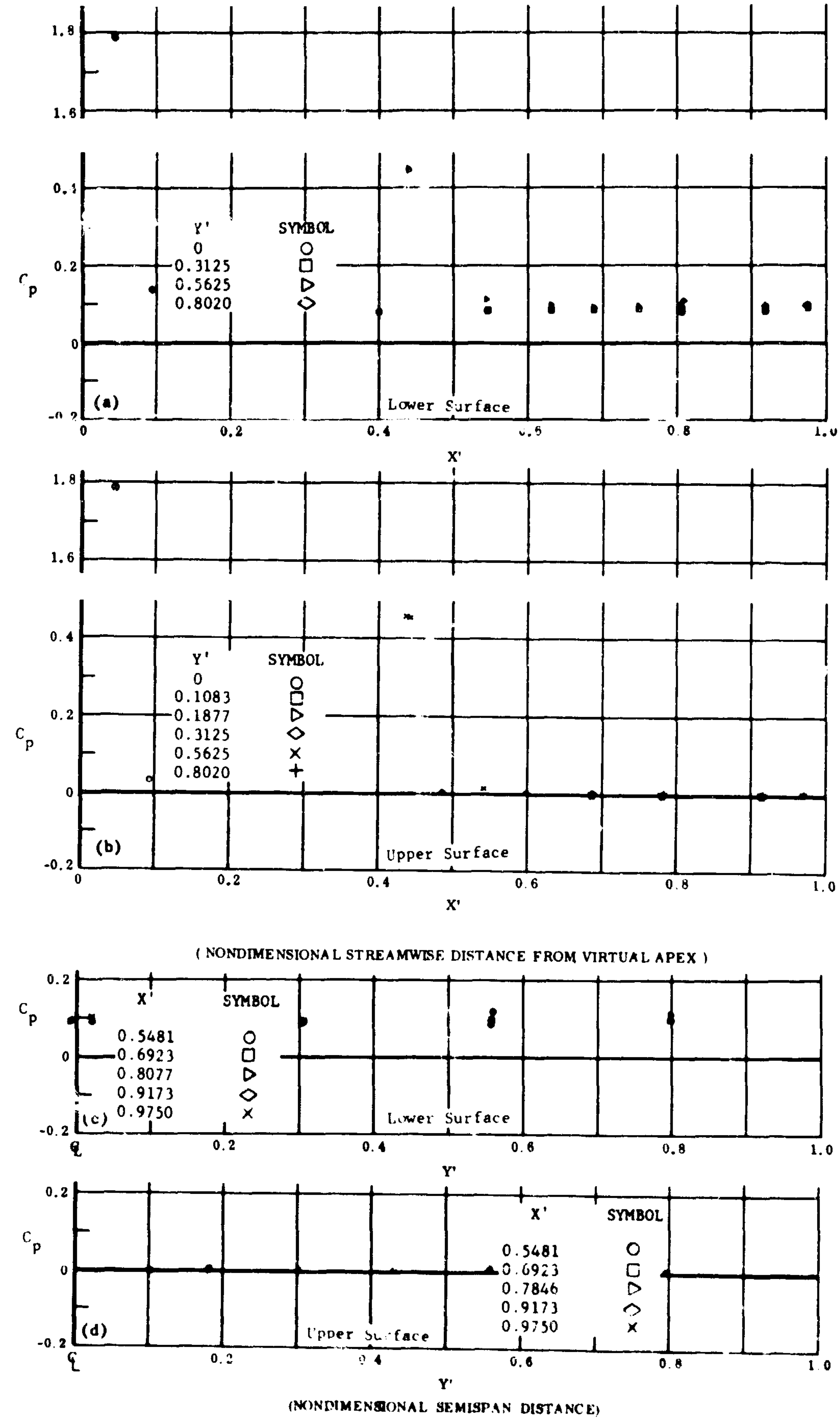

Fig. 5 Configuration I, $\iota_1 = +10$, $\iota_2 = \iota_3 = 0$

a) C_p vs. X', lower surface

b) C_p vs. X', upper surface

c) C_p vs. Y', lower surface

d) C_p vs. Y', upper surface

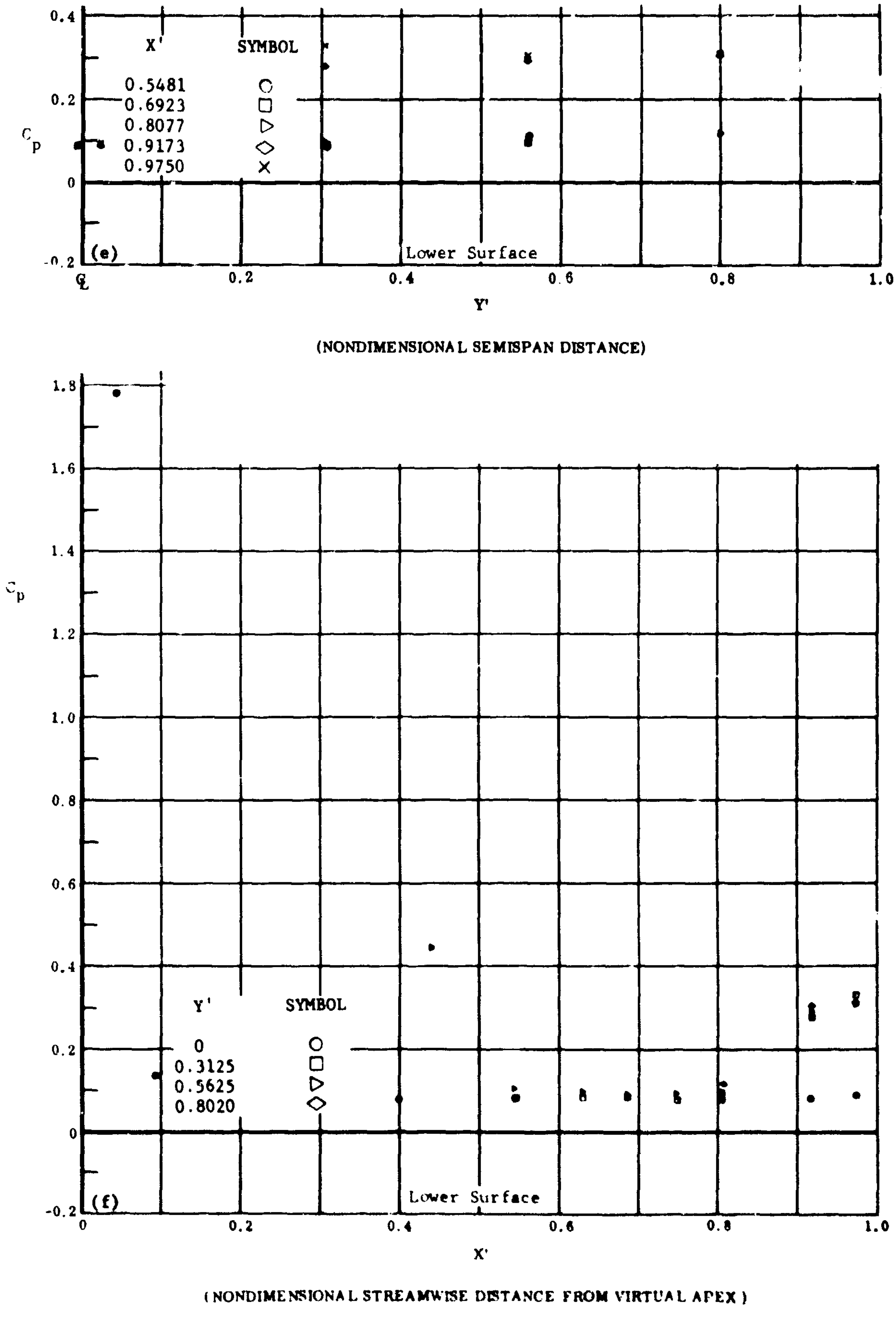

Fig. 5 Configuration I, $\alpha = +10$, $\delta_2 = \delta_3 = +10$

e) C_p vs. Y', lower surface

f) C_p vs. X', lower surface

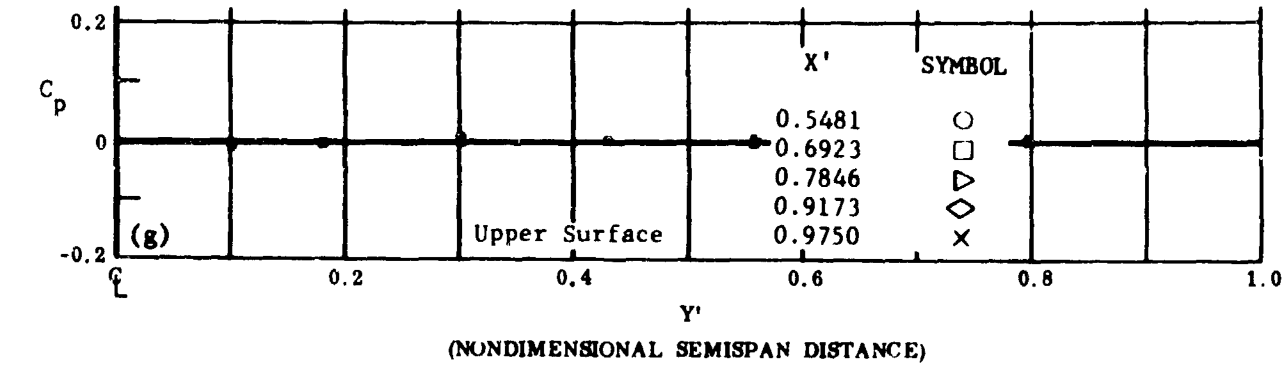

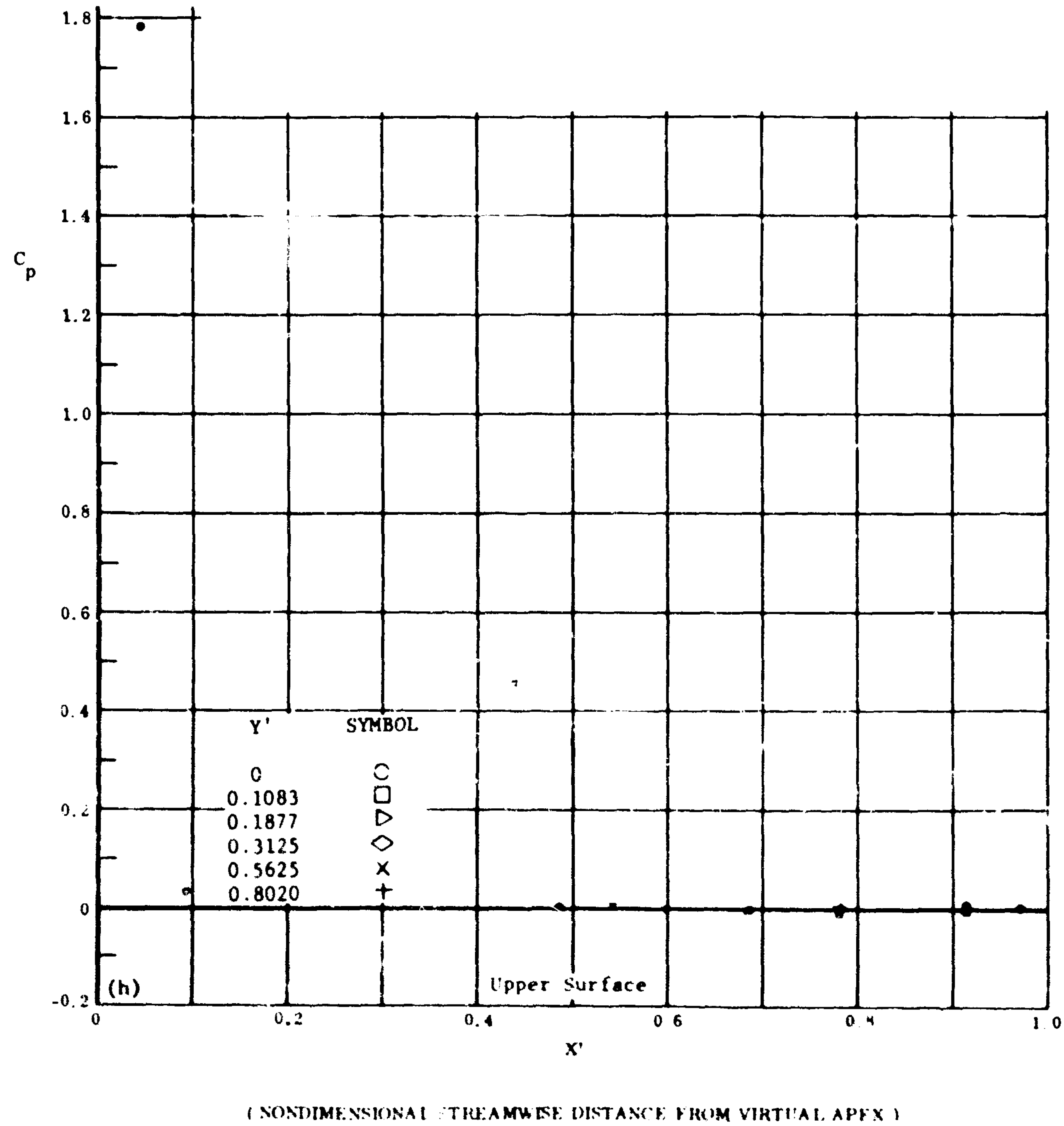

Fig. 5 Configuration I, $\alpha = +10$, $\delta_2 = \delta_3 = +10$

g) C_p vs. Y', upper surface

h) C_p vs. X', upper surface

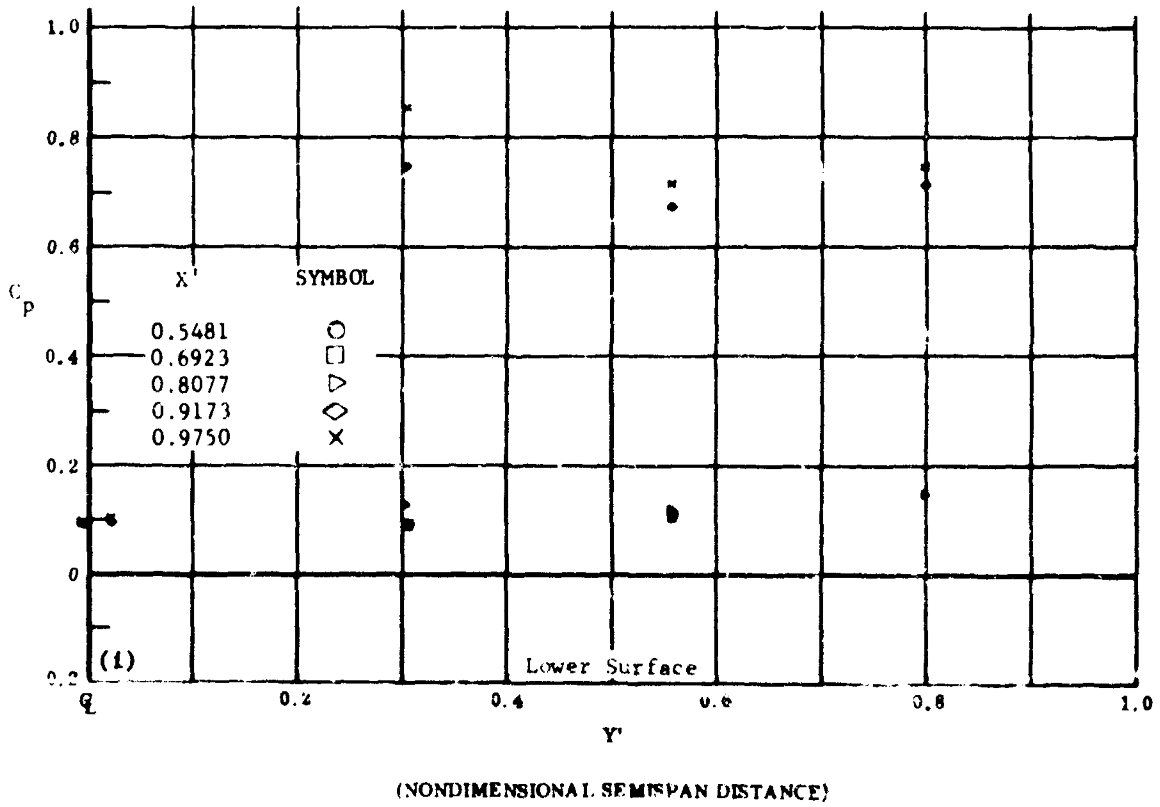

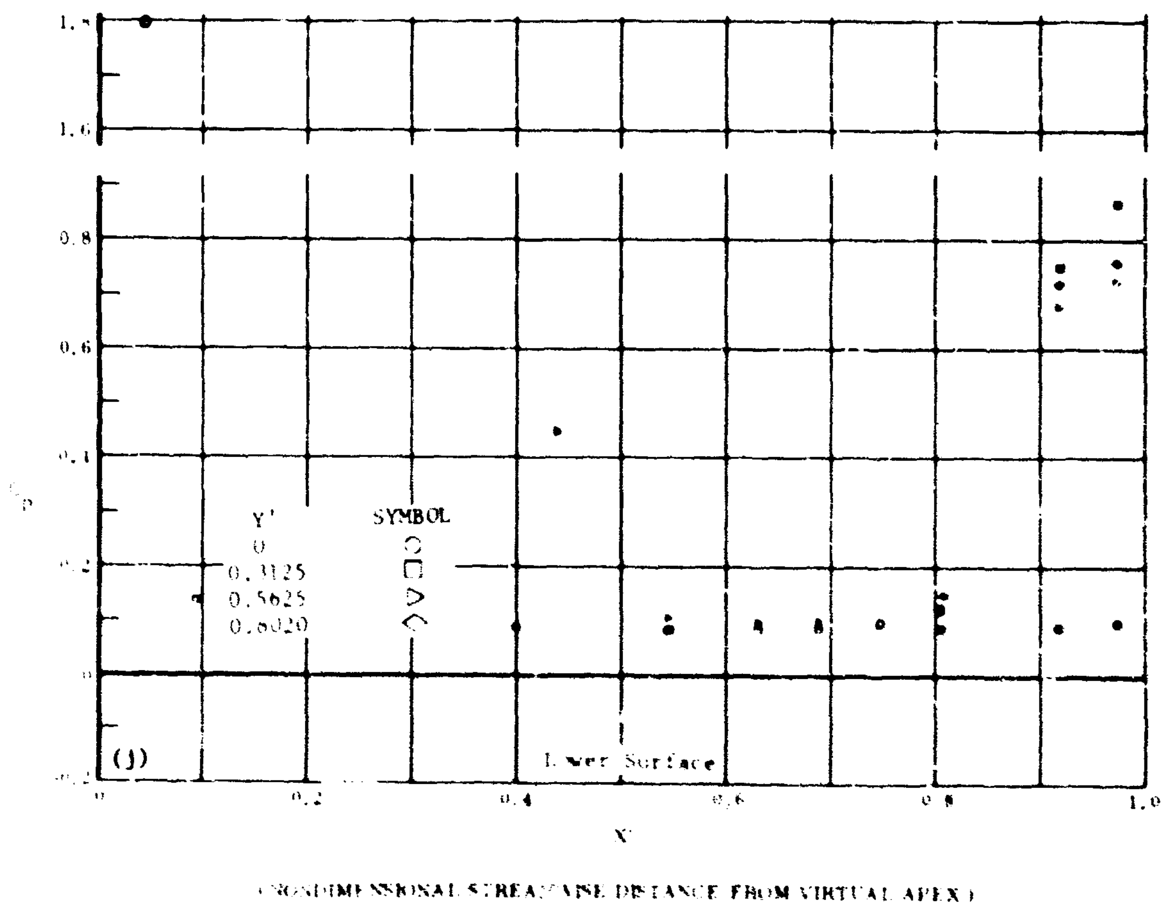

Fig. 5 Configuration I, [illegible] = +10, [illegible]$_2$ = [illegible]$_3$ = +20

(i) C_p vs. Y', lower surface

(j) C_p vs. X', lower surface

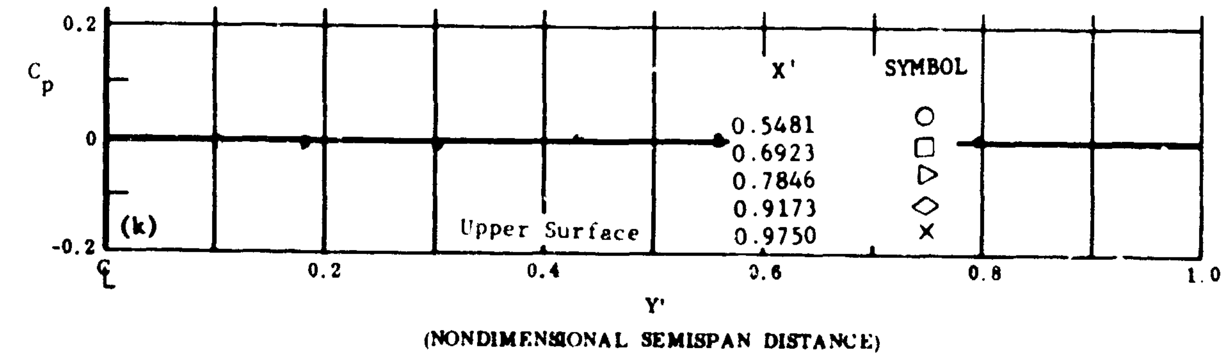

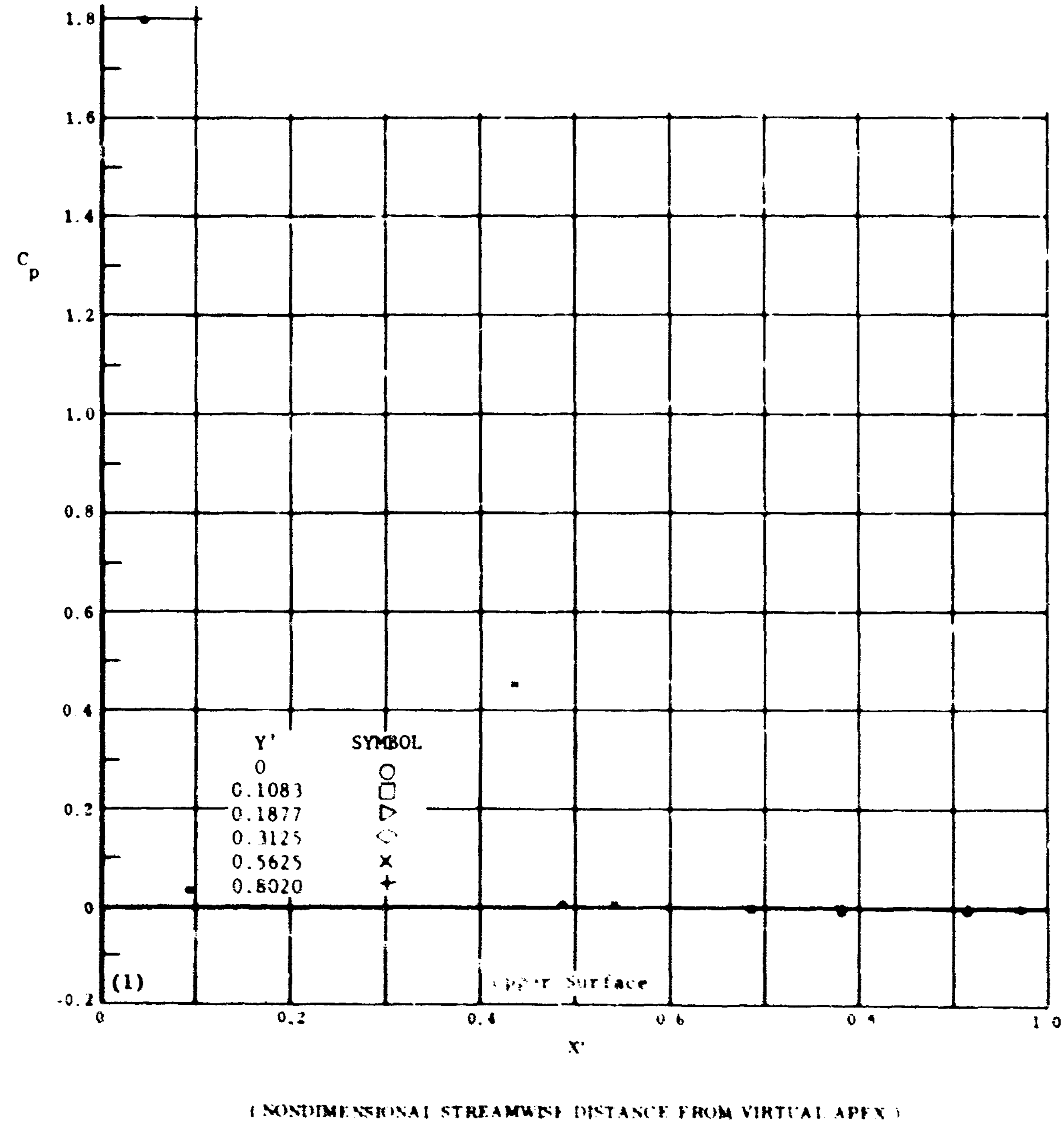

Fig. 5 Configuration I, ${}_1 = +10$, ${}_2 = {}_3 = +20$

k) C_p vs. Y', upper surface

l) C_p vs. X', upper surface

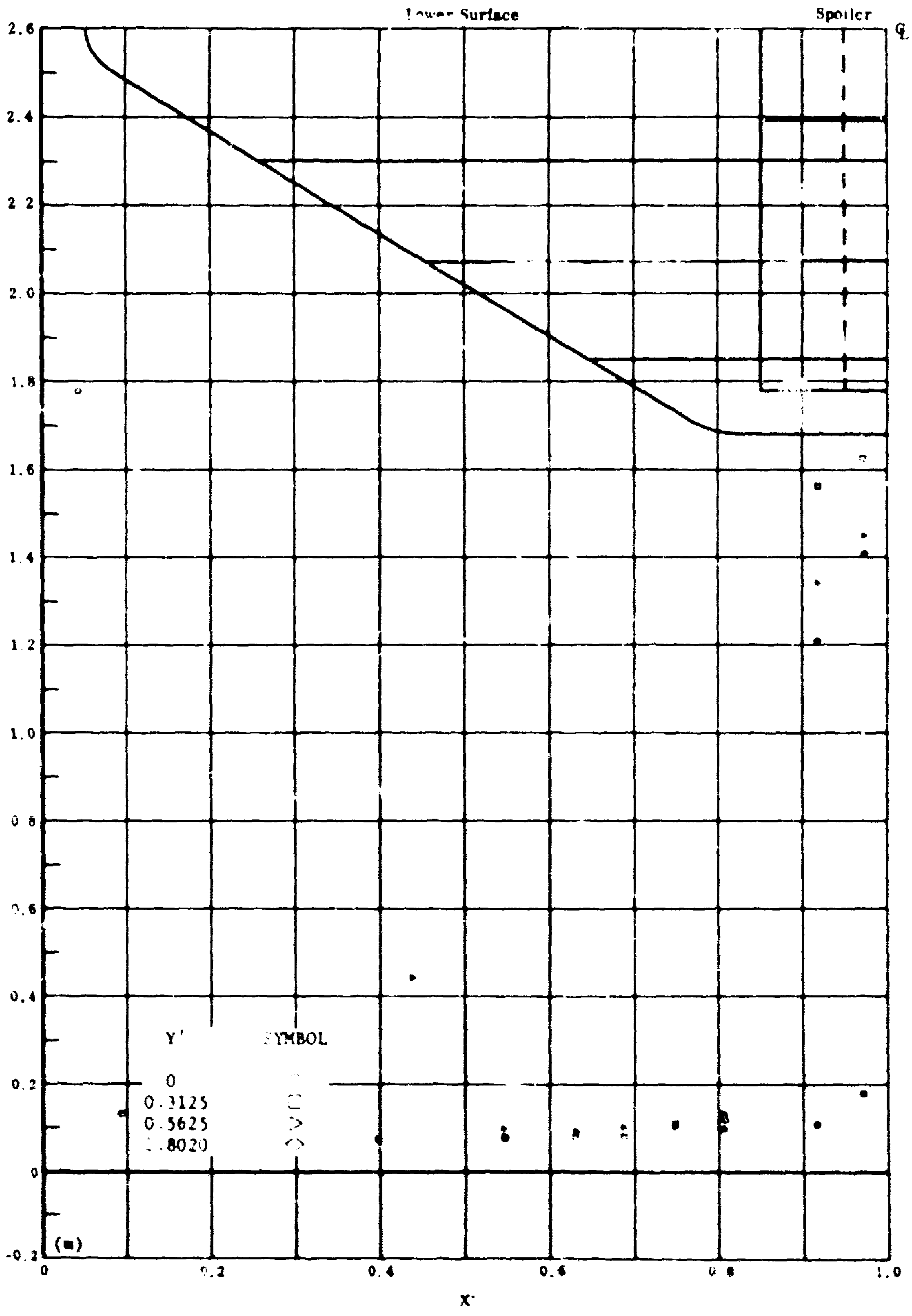

Fig. 5m Configuration I, $\delta = +10$, $\delta_2 = \delta_3 = +30$

C_p vs X', lower surface

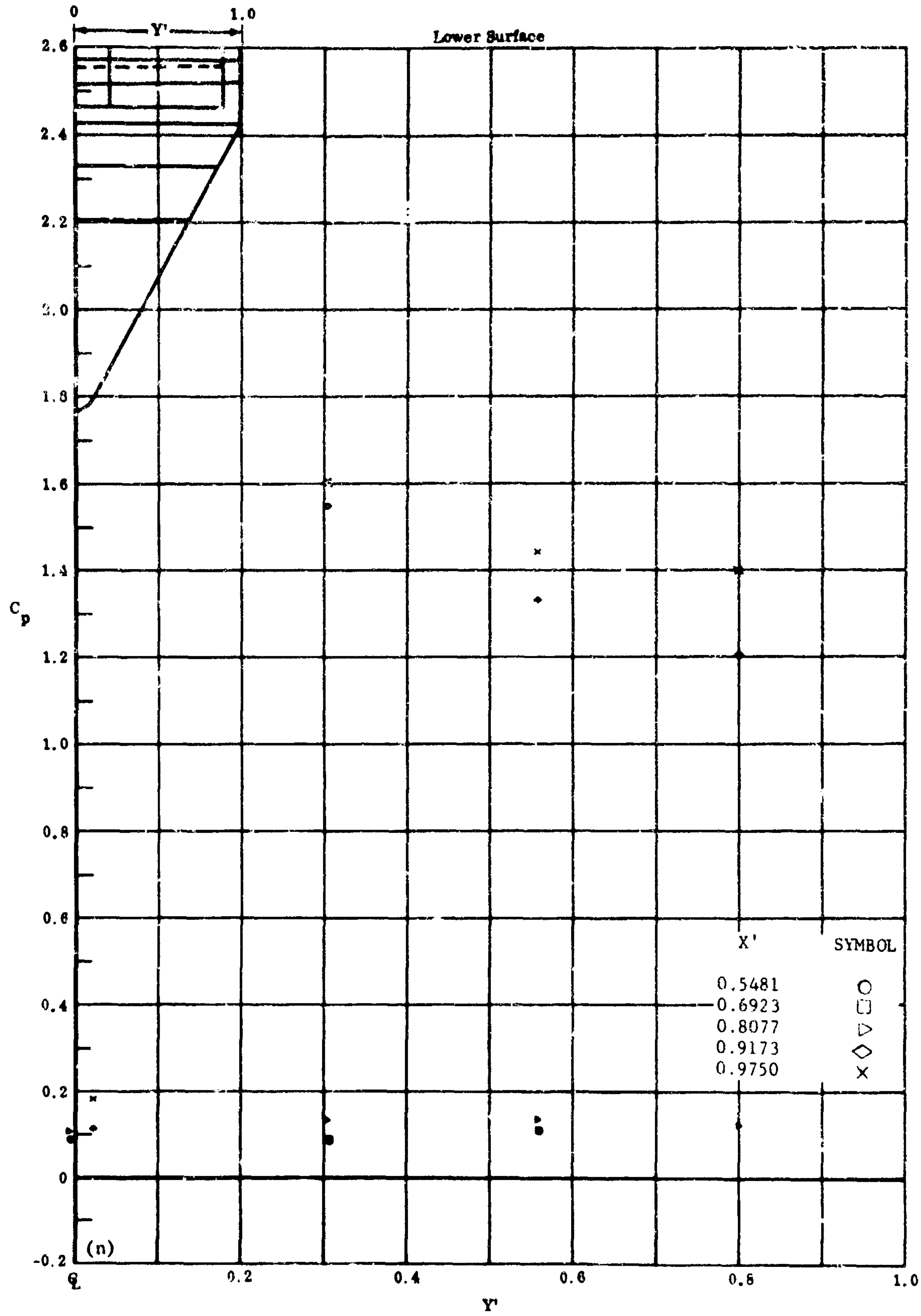

Fig. 5n Configuration I, α = +10 , $\delta_2 = \delta_3$ = +30

C_p vs. Y', lower surface

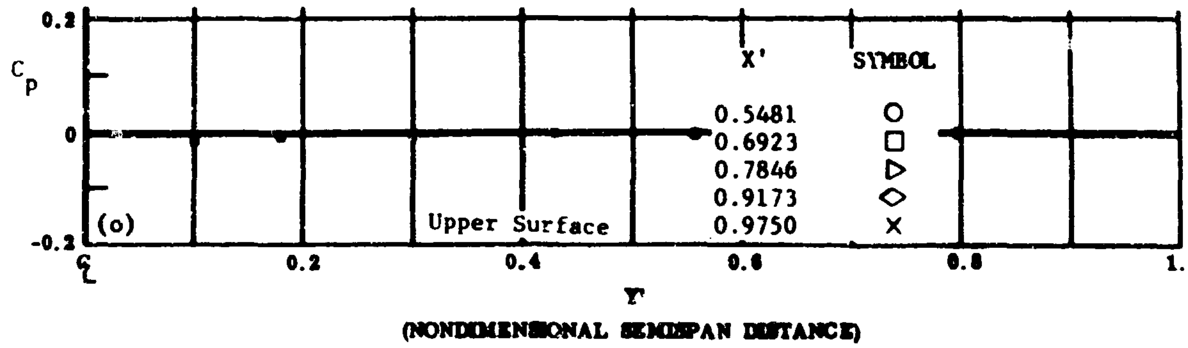

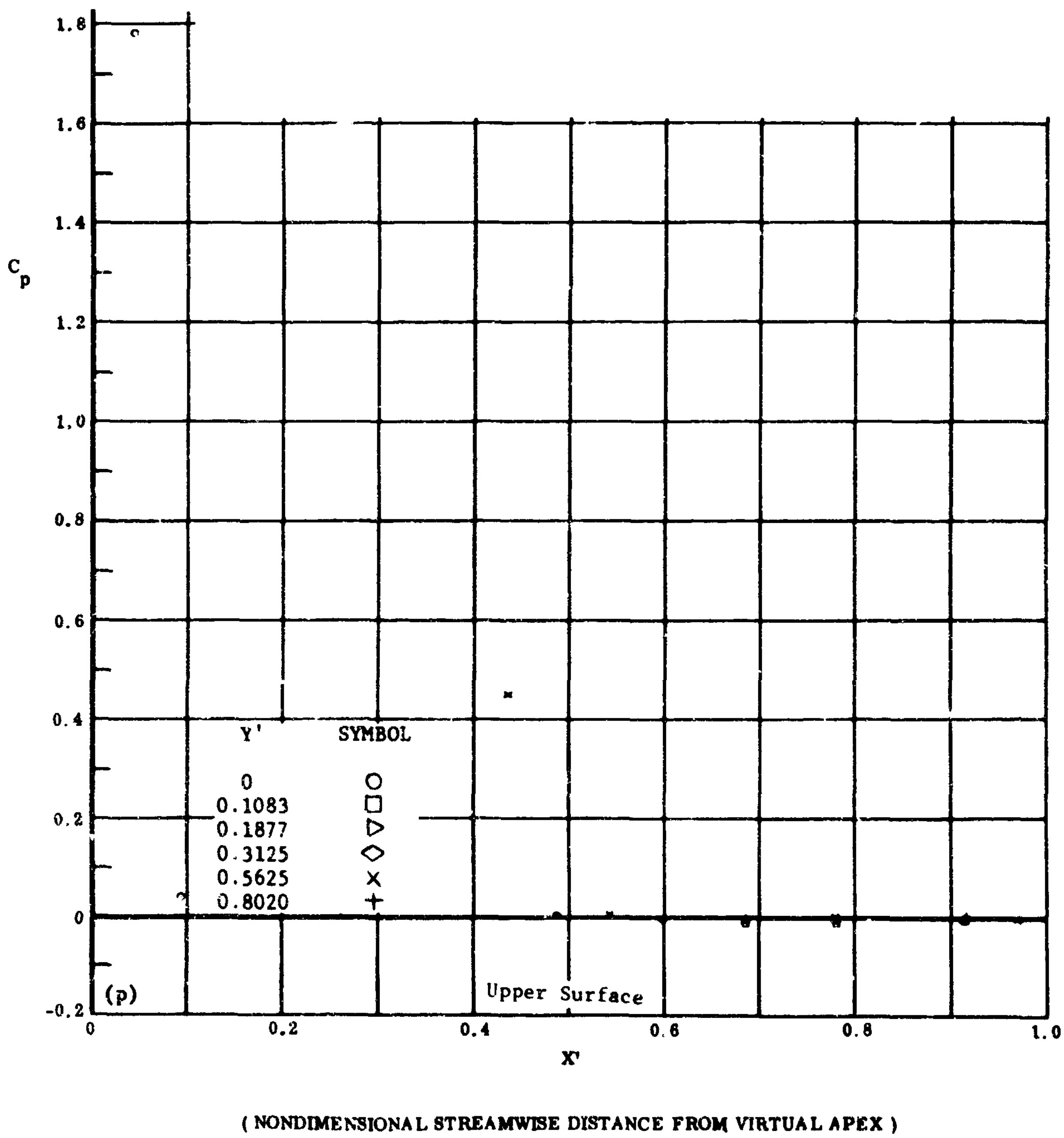

Fig. 5 Configuration I, $\alpha = +10$, $\delta_2 = \delta_3 = +30$

o) C_p vs. Y', upper surface

p) C_p vs. X', upper surface

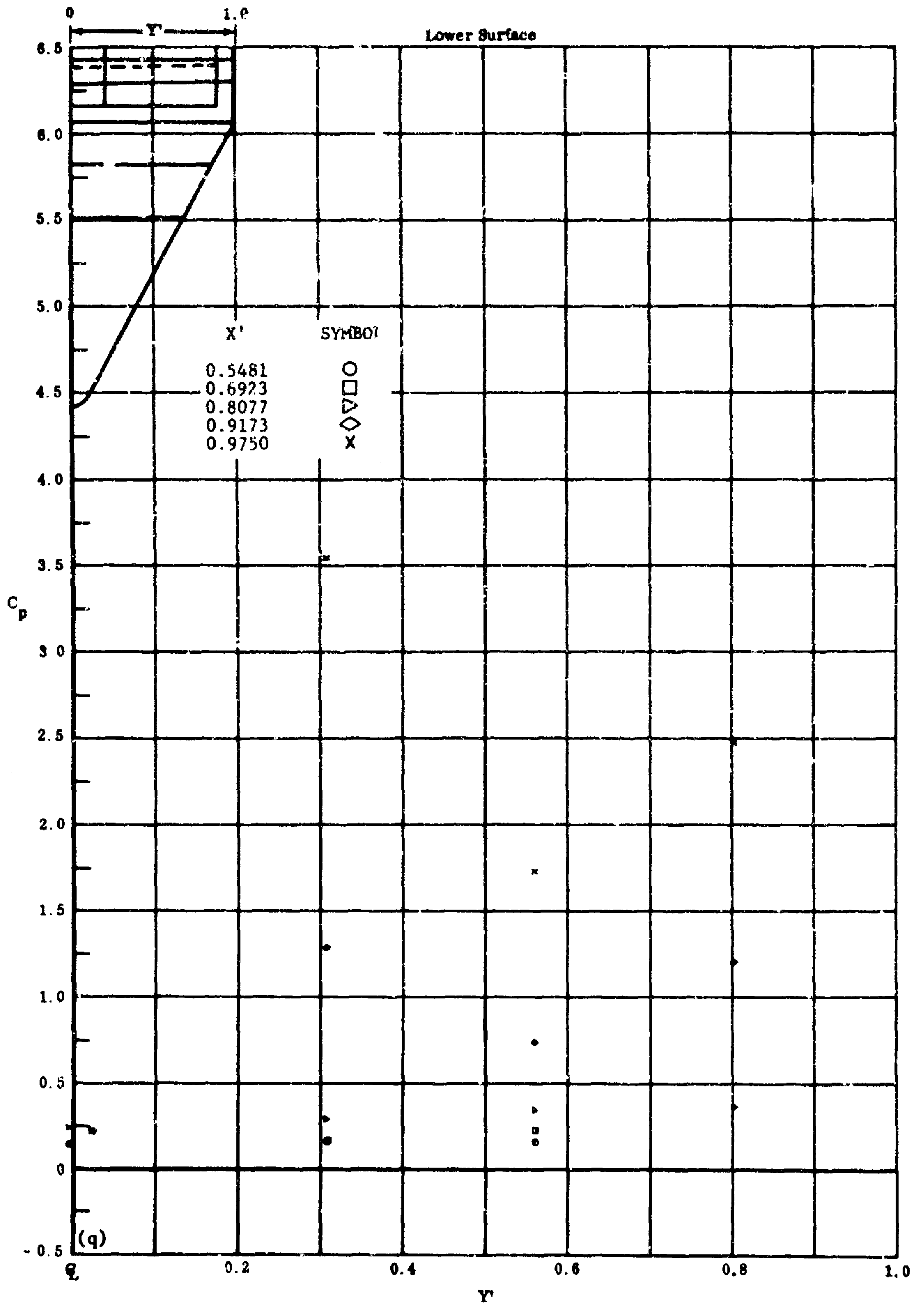

Fig. 5q Configuration I, $\alpha = +10$, $\delta_2 = \delta_3 = +39$

C_p vs. Y', lower surface

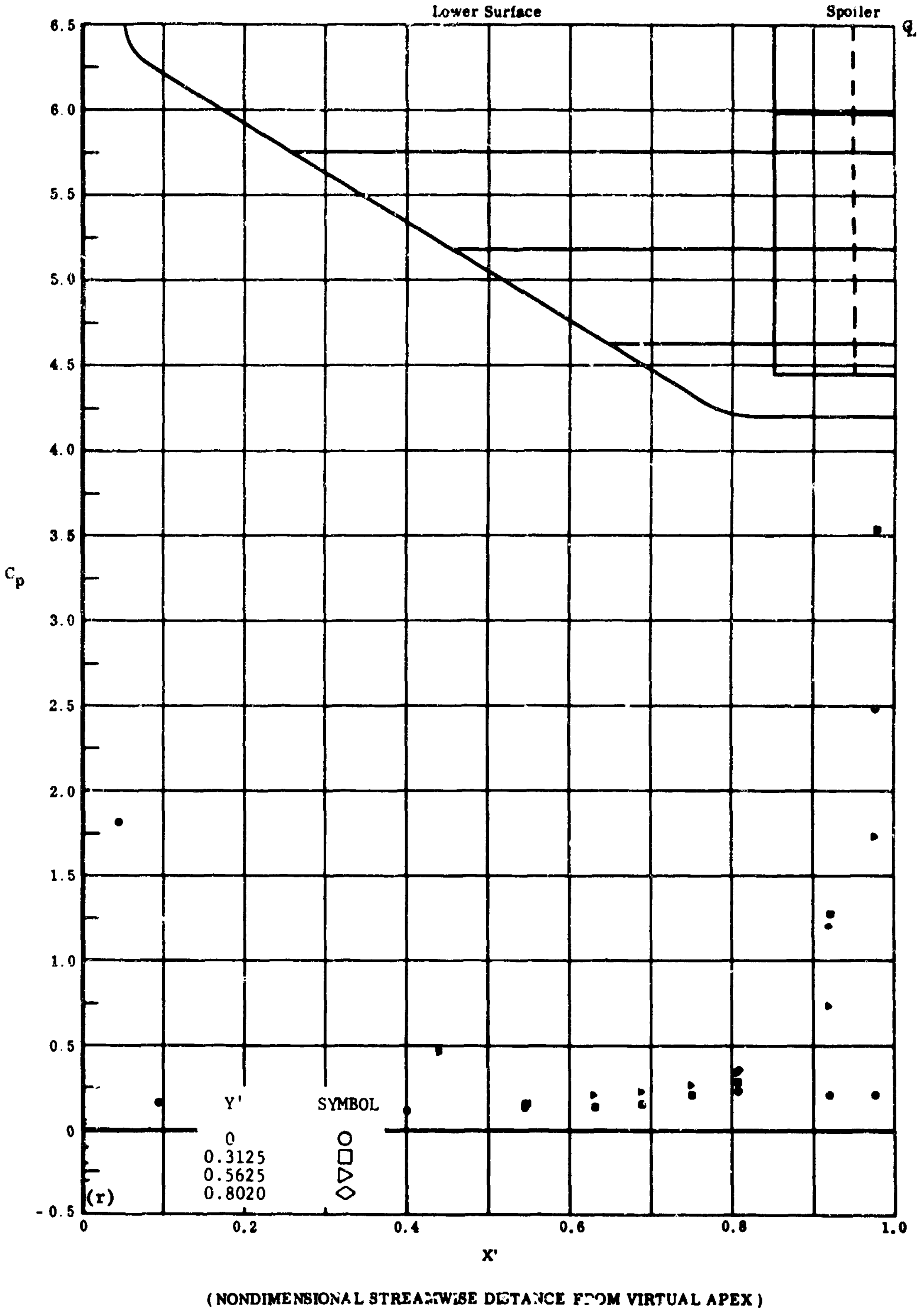

Fig. 5r Configuration I, $\alpha = +10$, $\delta_2 = \delta_3 = +39$

C_p vs. X', lower surface

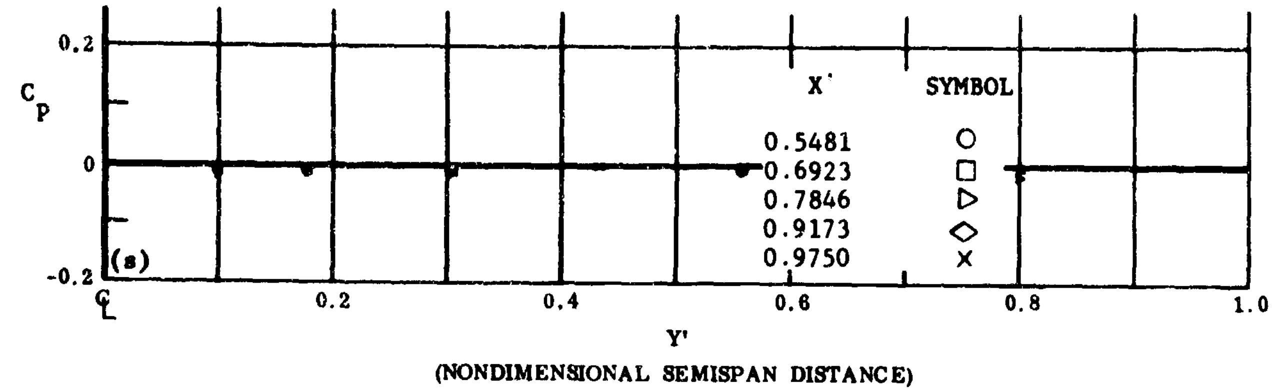

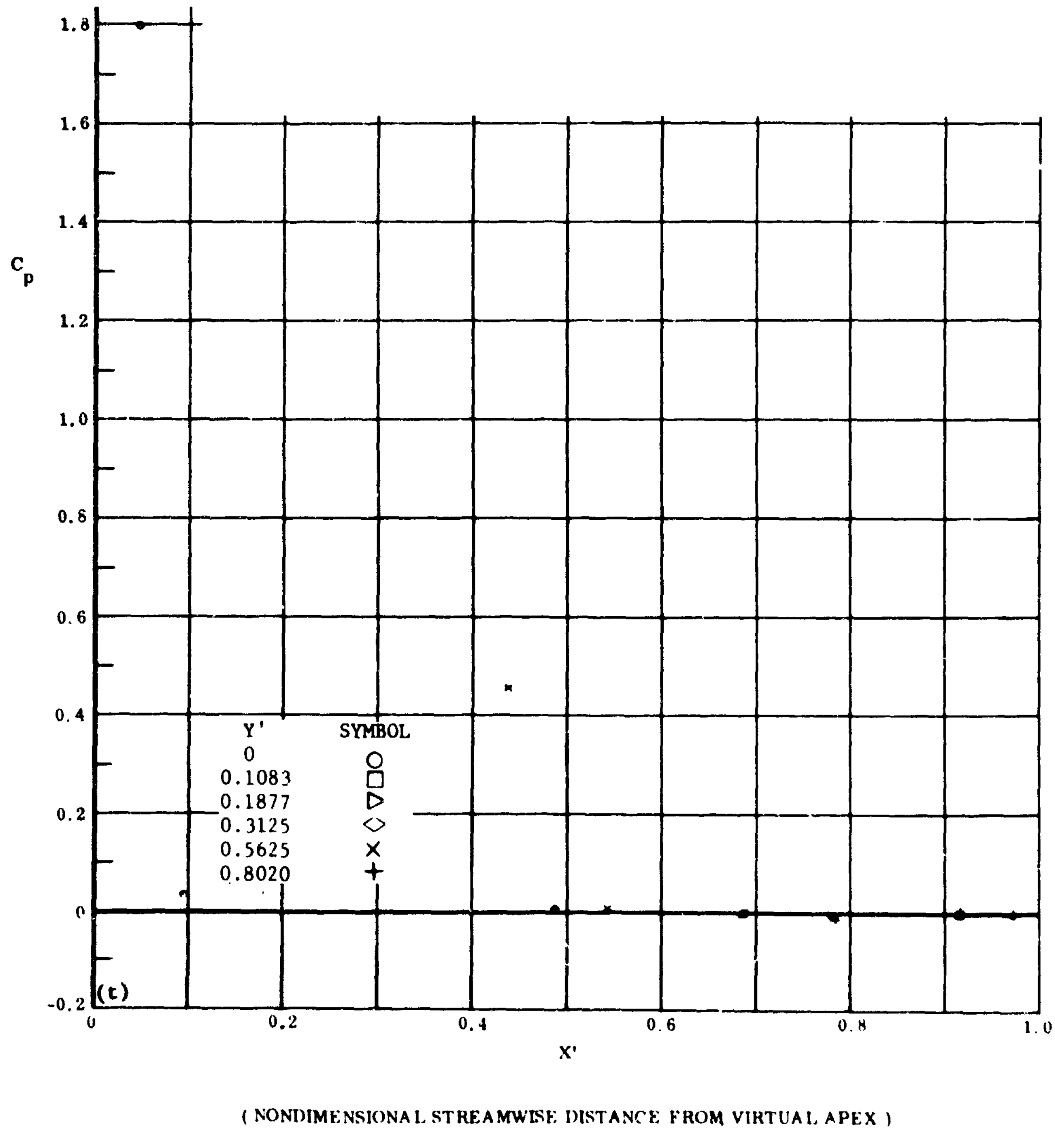

Fig. 5 Configuration I, α = +10 , δ_2 = δ_3 = +39

s) C_p vs. Y', upper surface

t) C_p vs. X', upper surface

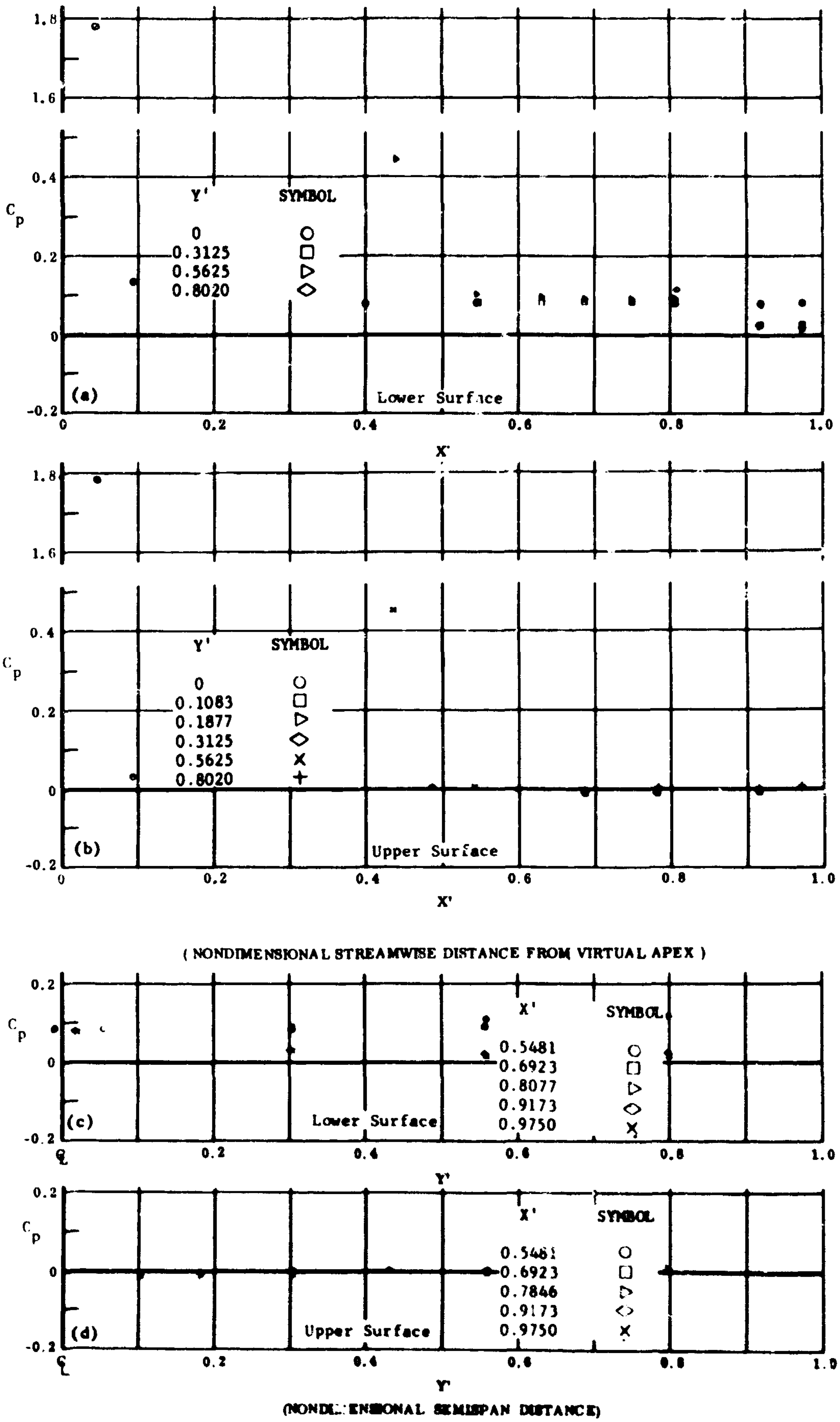

Fig. 6 Configuration I, $\alpha = +10$, $\delta_2 = \delta_3 = -10$

a) C_p vs. X', lower surface

b) C_p vs. X', upper surface

c) C_p vs. Y', lower surface

d) C_p vs. Y', upper surface

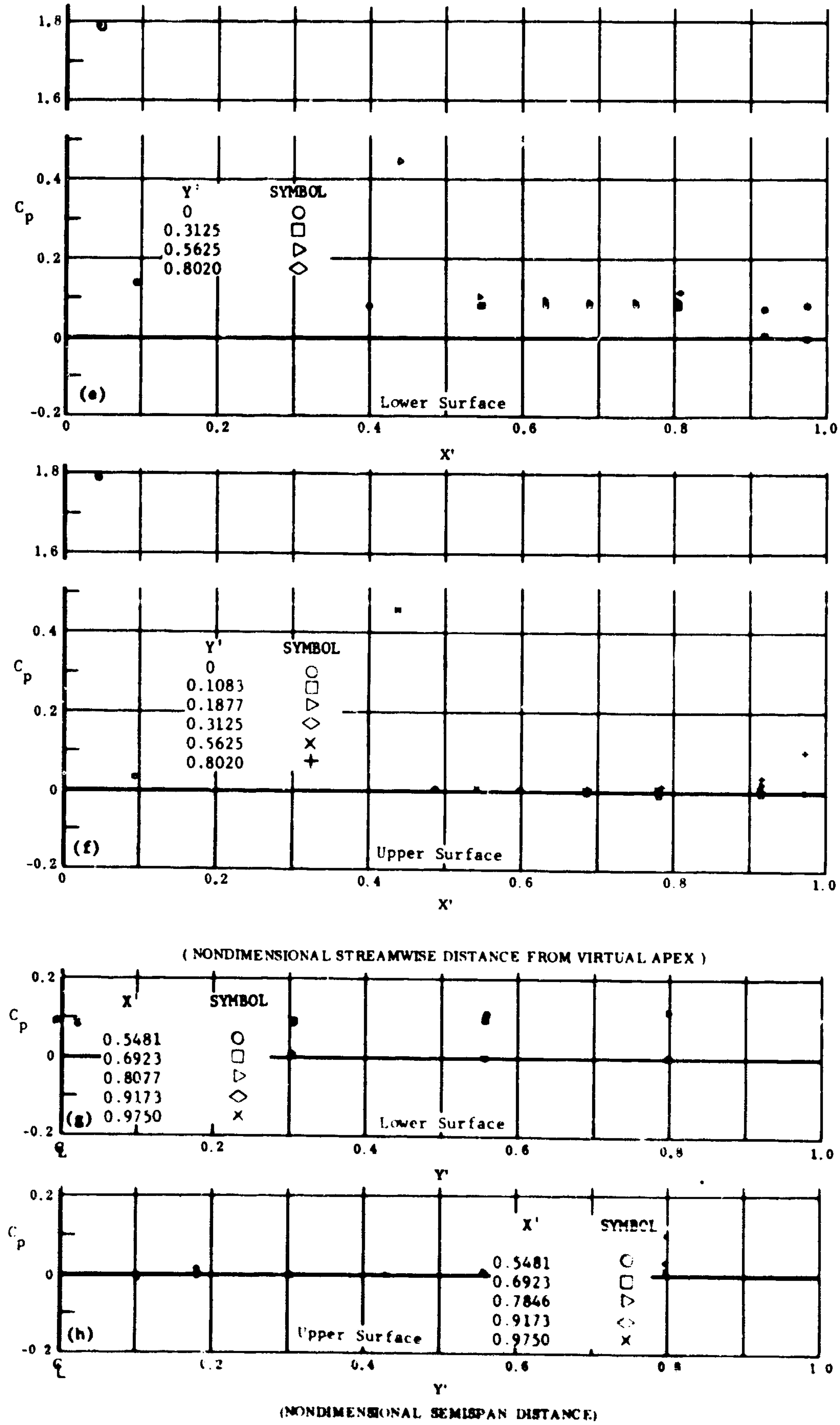

Fig. 6 Configuration I, ι = +10 , $\iota_2 = \iota_3$ = -20

e) C_p vs. X', lower surface

f) C_p vs. X', upper surface

g) C_p vs. Y', lower surface

h) C_p vs. Y', upper surface

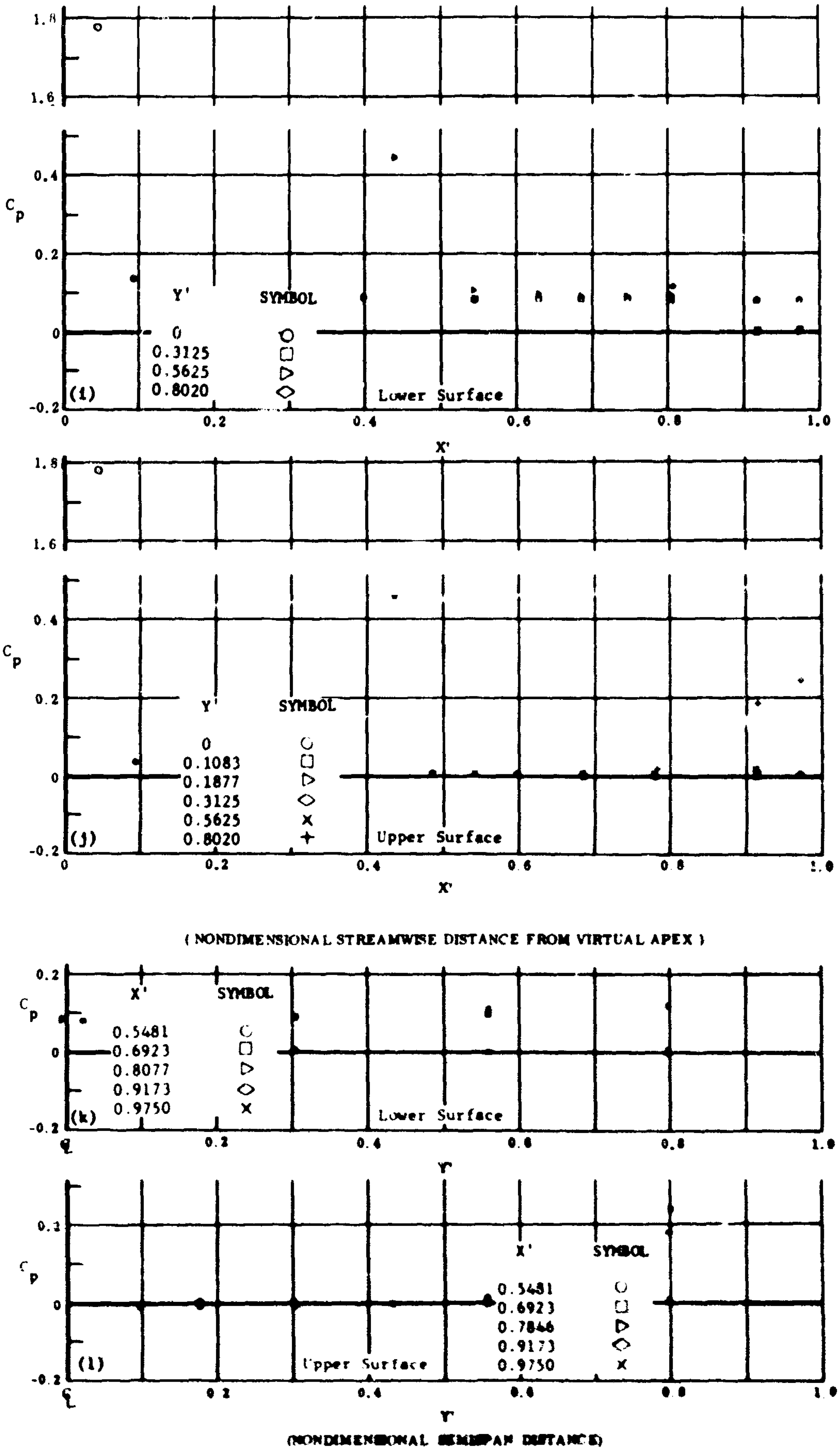

Fig. 6 Configuration I, $\alpha = +10$, $\delta_2 = \delta_3 = -30$

i) C_p vs. X', lower surface

j) C_p vs. X', upper surface

k) C_p vs. Y', lower surface

l) C_p vs. Y', upper surface

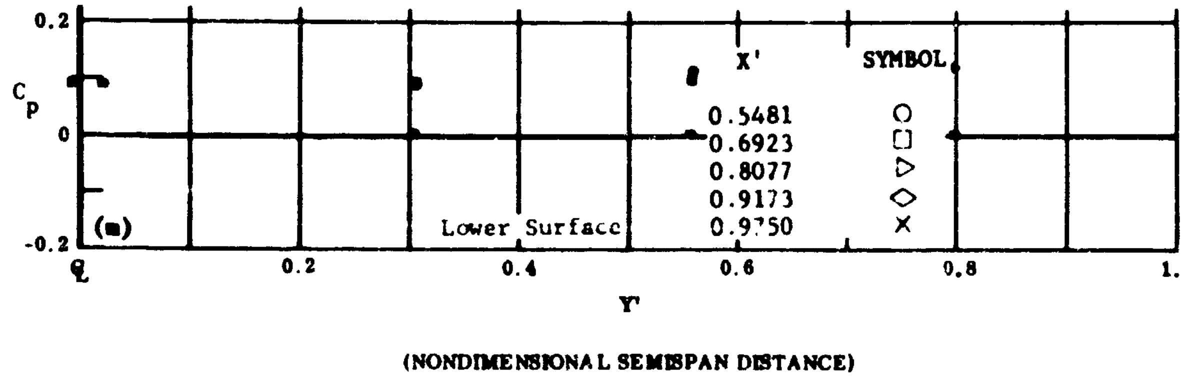

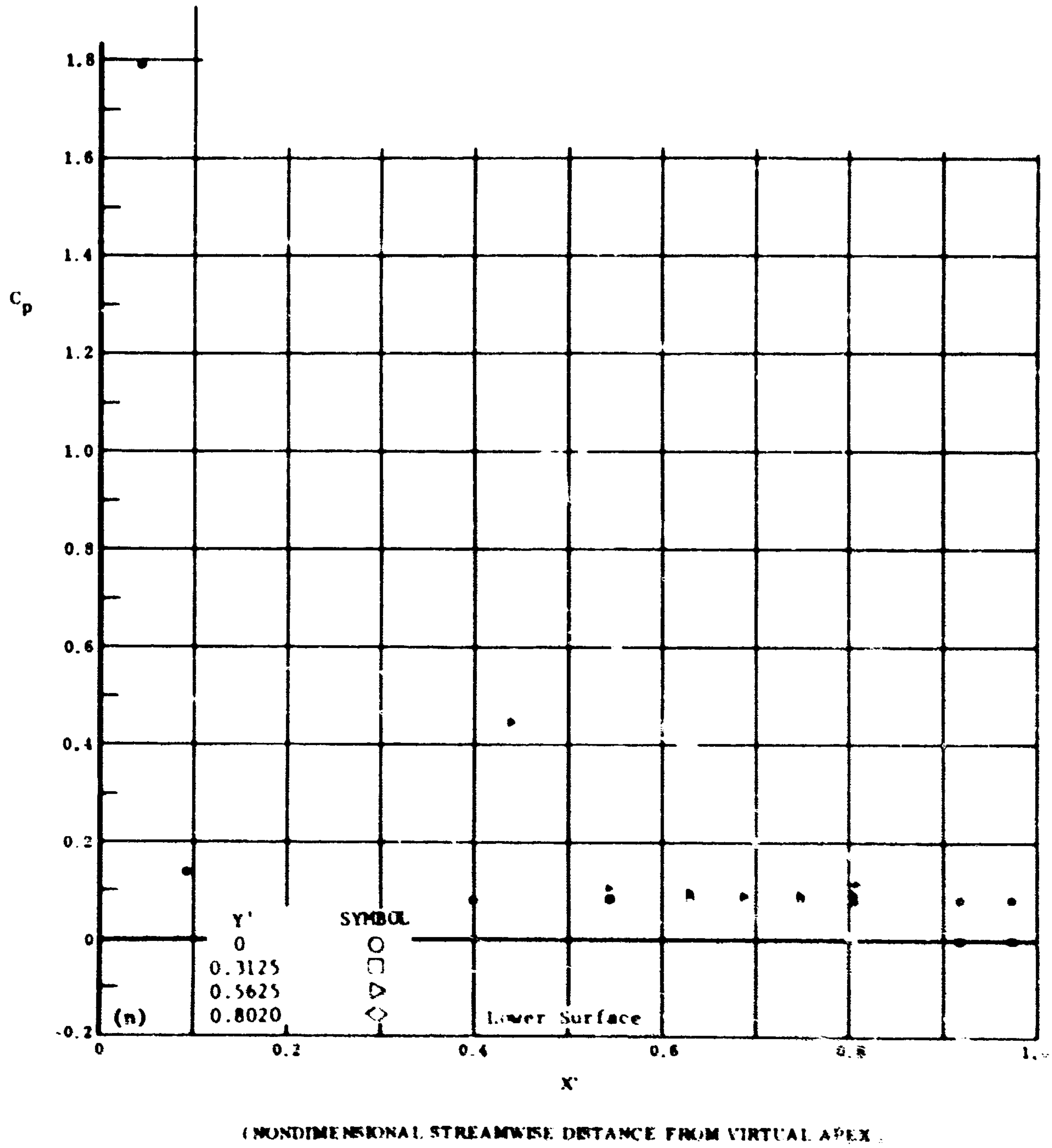

Fig. 8 Configuration I, α = +10, $\delta_2 = \delta_3$ = -39

m) C_p vs. Y', lower surface

n) C_p vs. X', lower surface

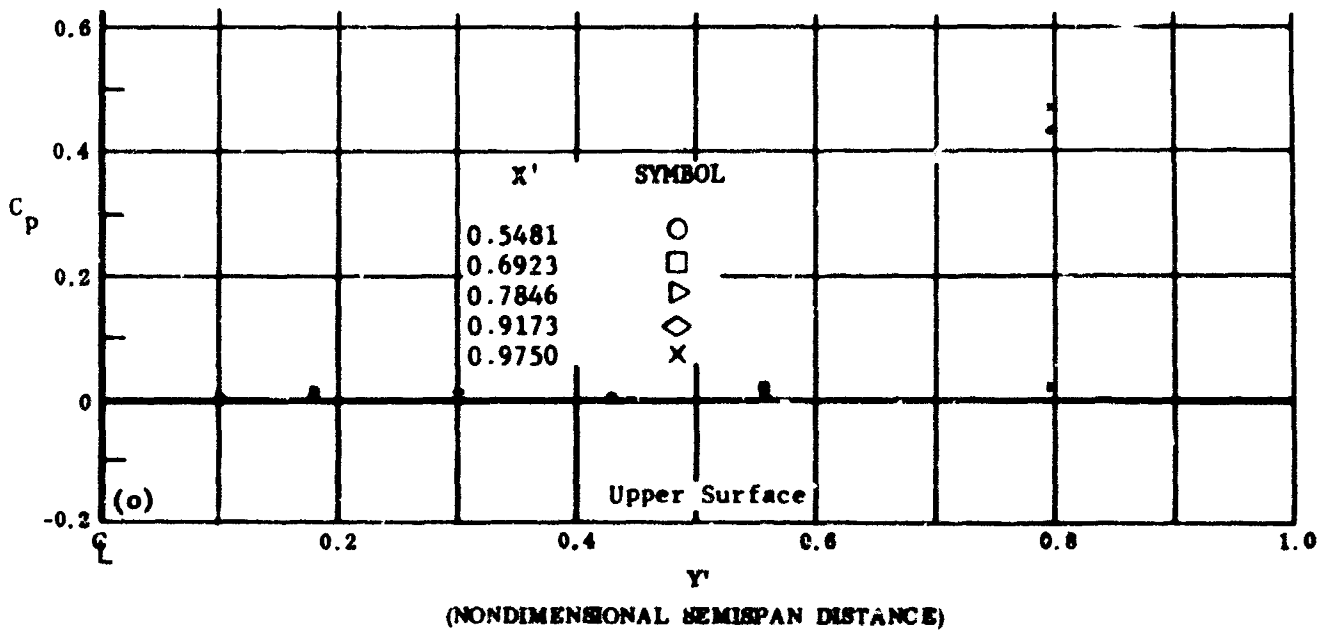

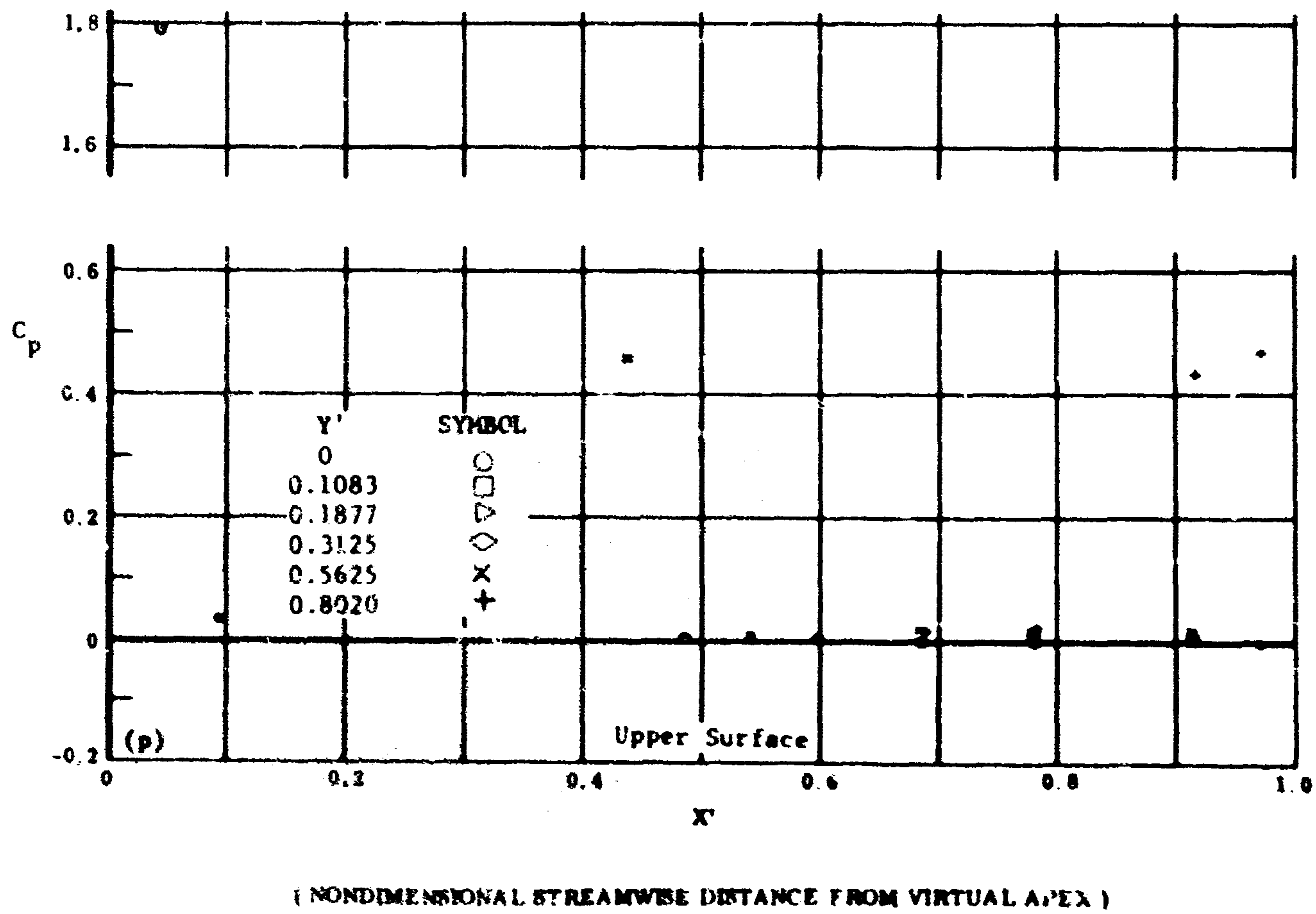

Fig. 6 Configuration I, α = +10 , $\delta_2 = \delta_3$ = -39

o) C_p vs. Y', upper surface

p) C_p vs. X', upper surface

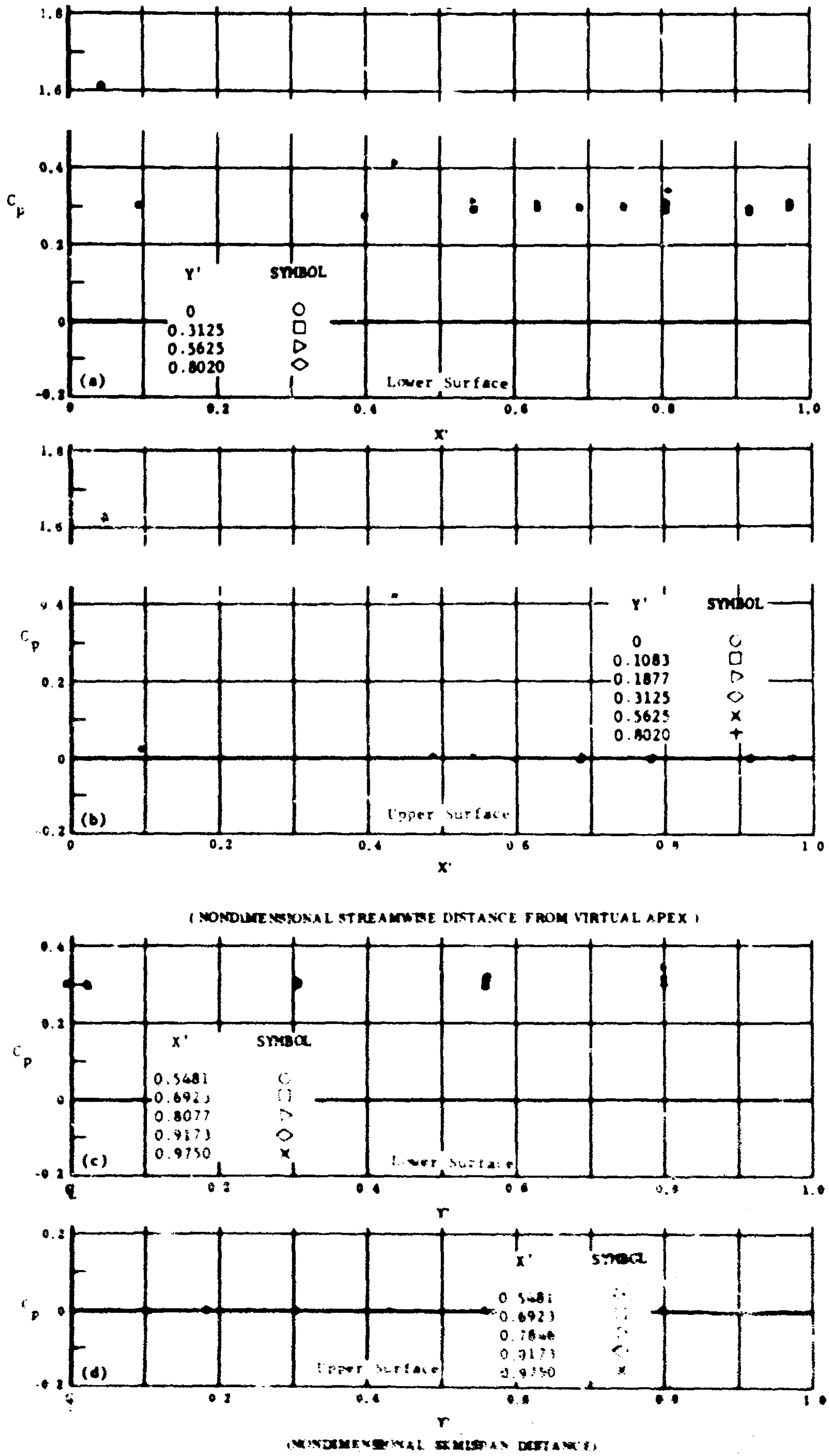

Fig. 7 Configuration I, $\alpha = 42^{\circ}$, $\delta_2 = \delta_3 = 0$

a) C_p vs. X', lower surface

b) C_p vs. X', upper surface

c) C_p vs. Y', lower surface

d) C_p vs. Y', upper surface

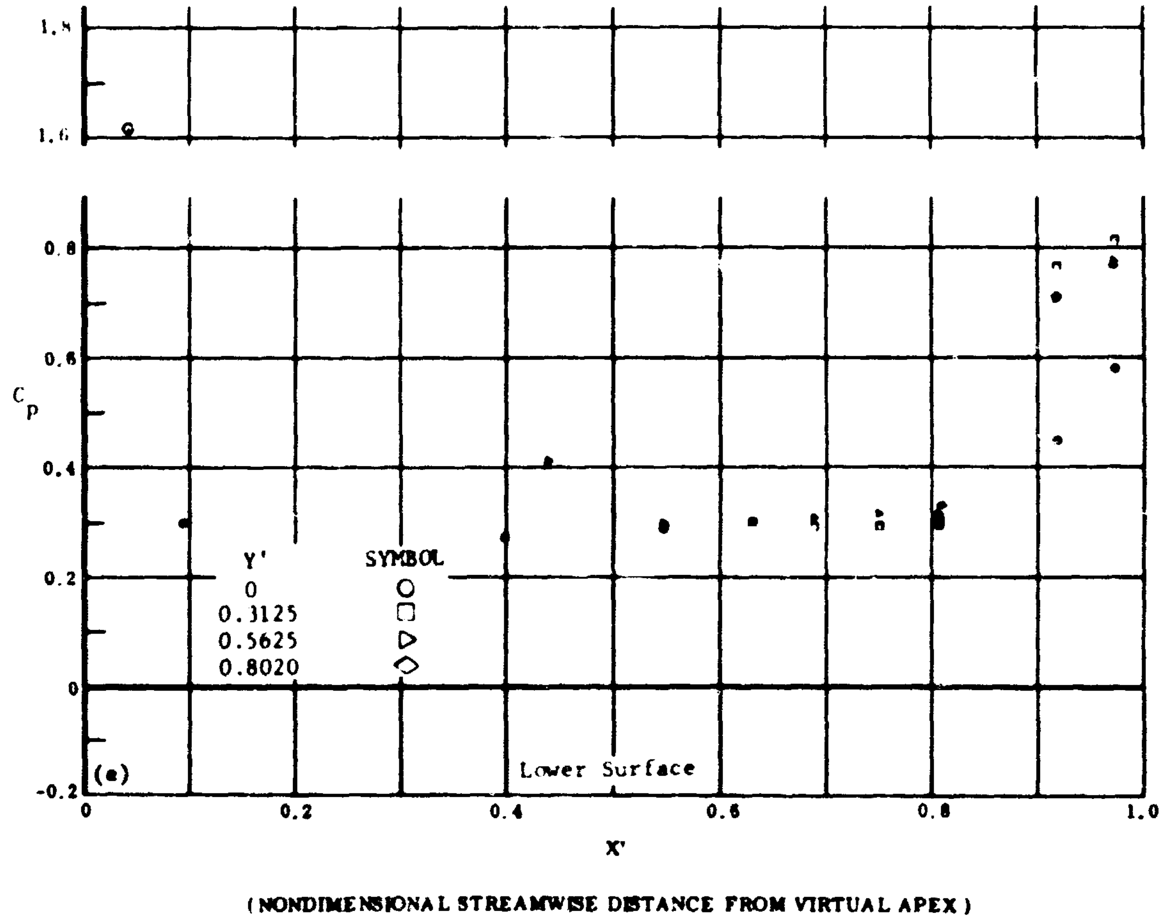

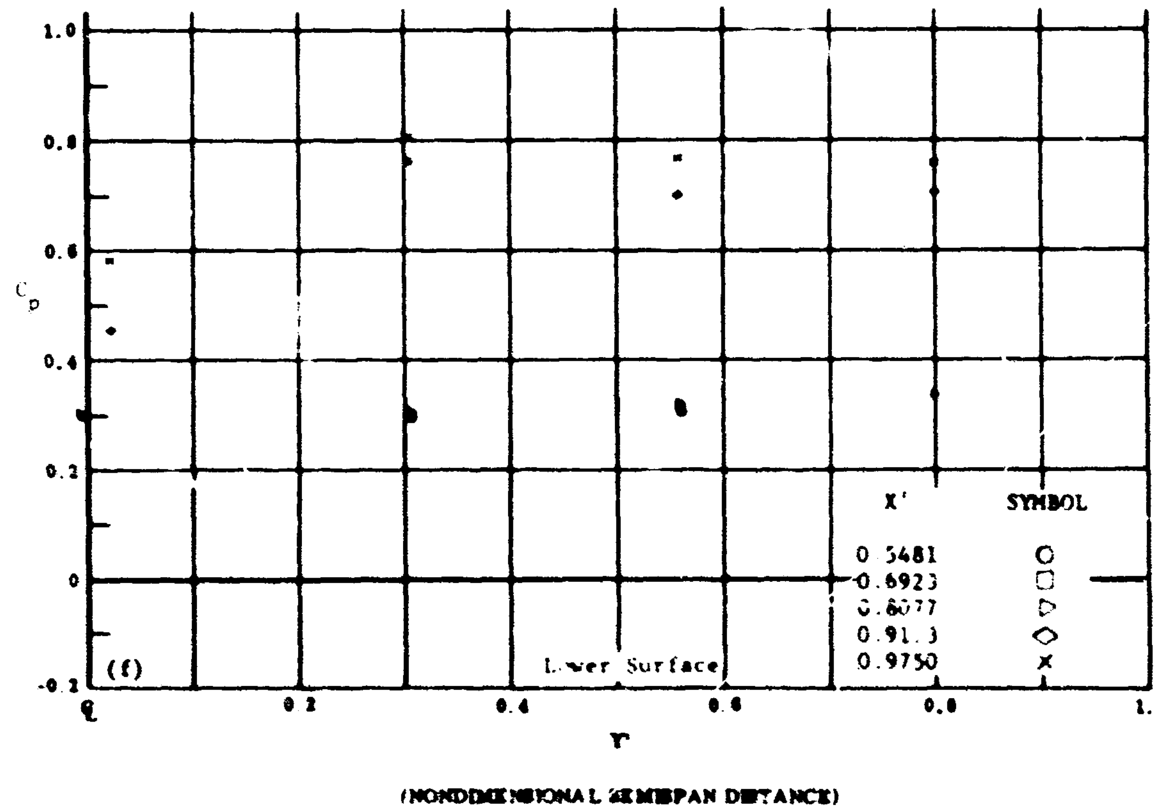

Fig. 7 Configuration I, α = +20 , δ_2 = δ_3 = +10

e) C_p vs. X', lower surface

f) C_p vs. Y', lower surface

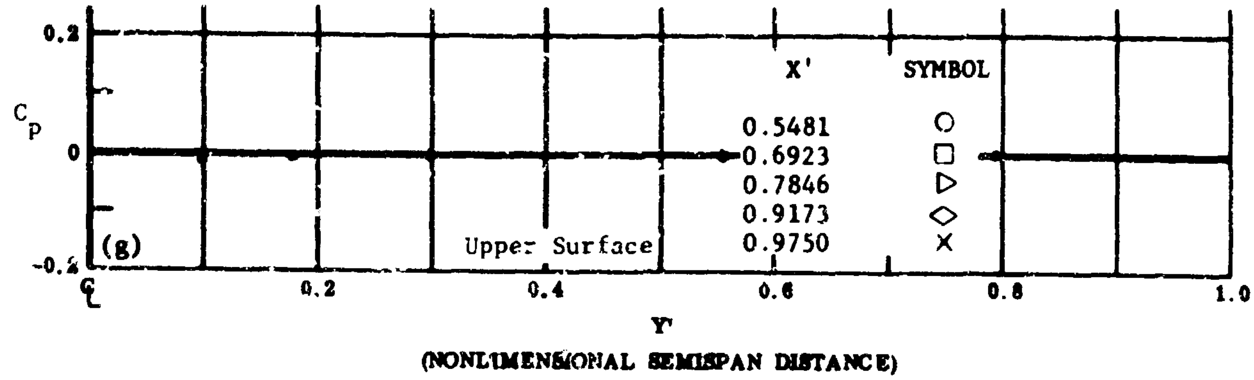

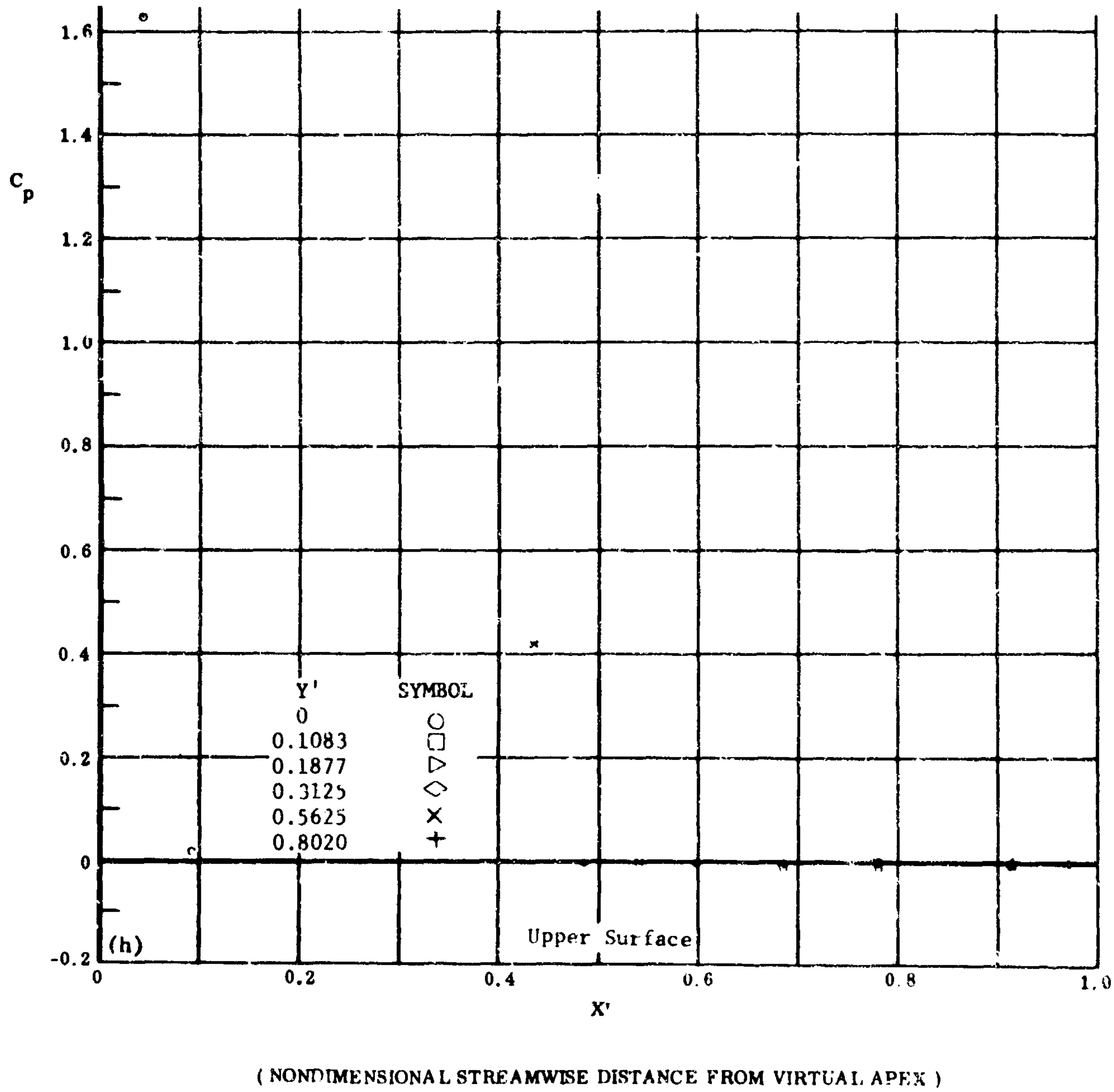

Fig. 7 Configuration I, α = +20 , $\delta_2 = \delta_3$ = +10

g) C_p vs. Y', upper surface

h) C_p vs. X', upper surface

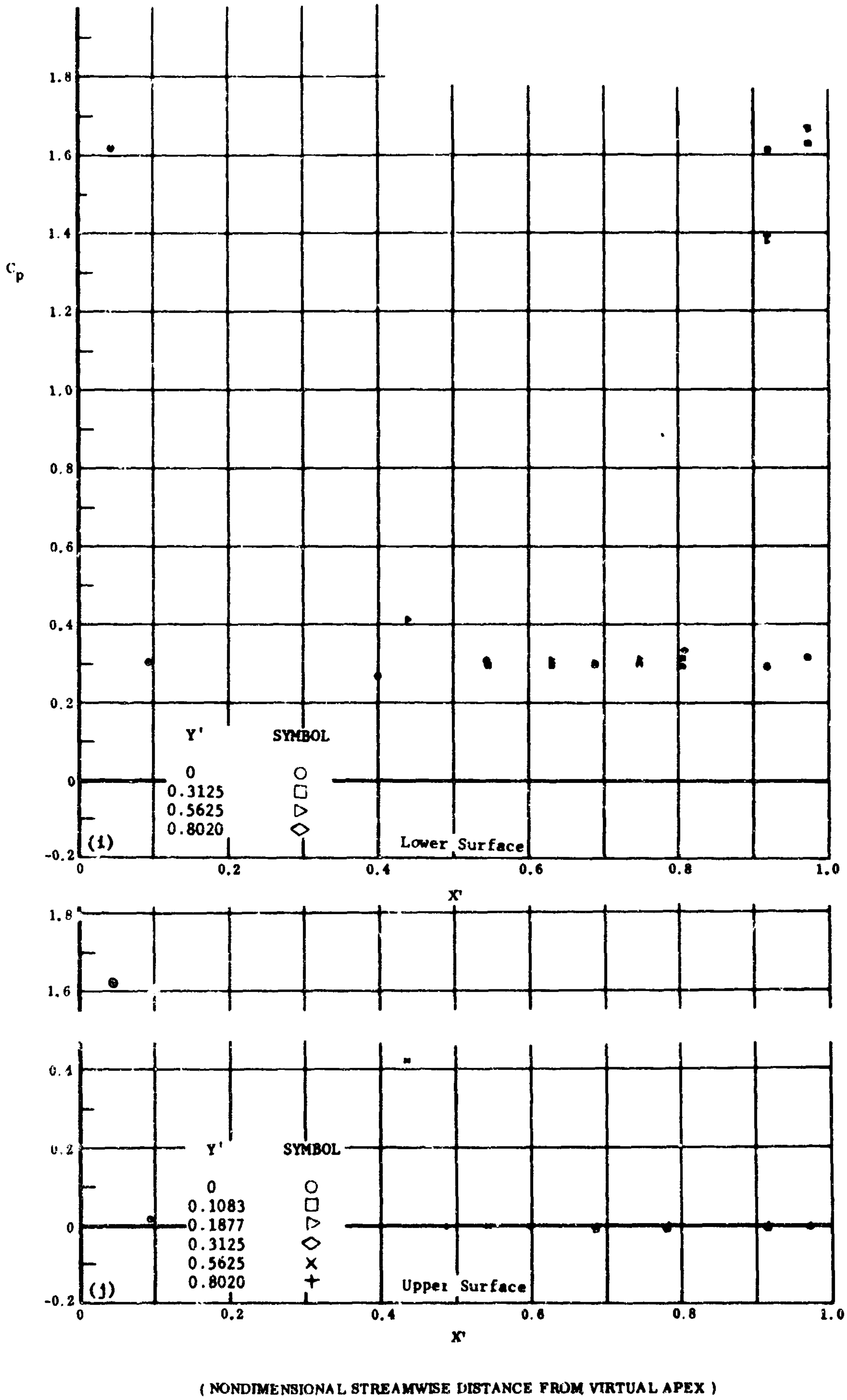

Fig. 7 Configuration I, α = +20 , δ_2 = δ_3 = +20

i) C_p vs. X', lower surface

j) C_p vs. X', upper surface

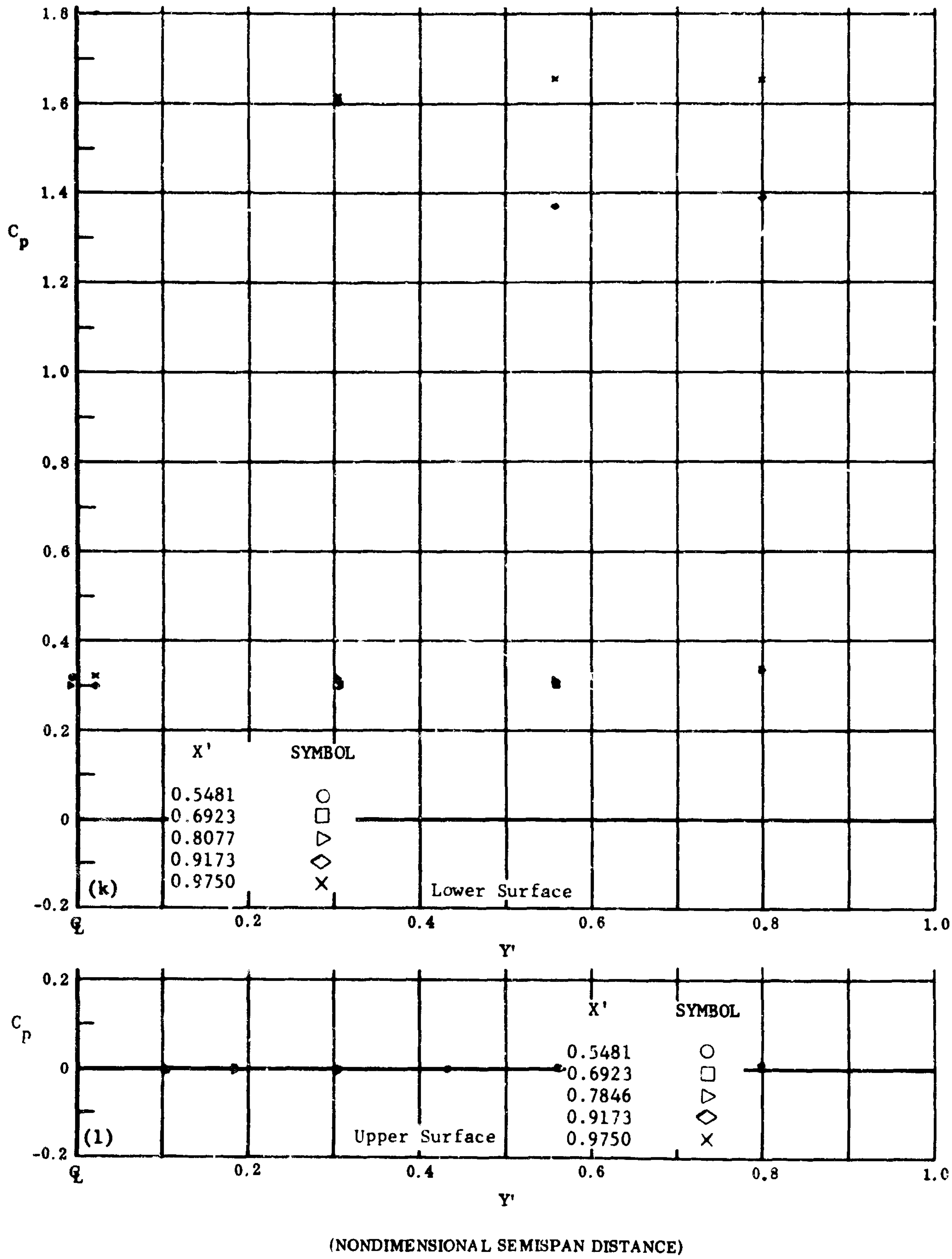

Fig. 7 Configuration I, $\alpha = +20$, $\delta_2 = \delta_3 = +20$

k) C_p vs. Y', lower surface

1) C_p vs. Y', upper surface

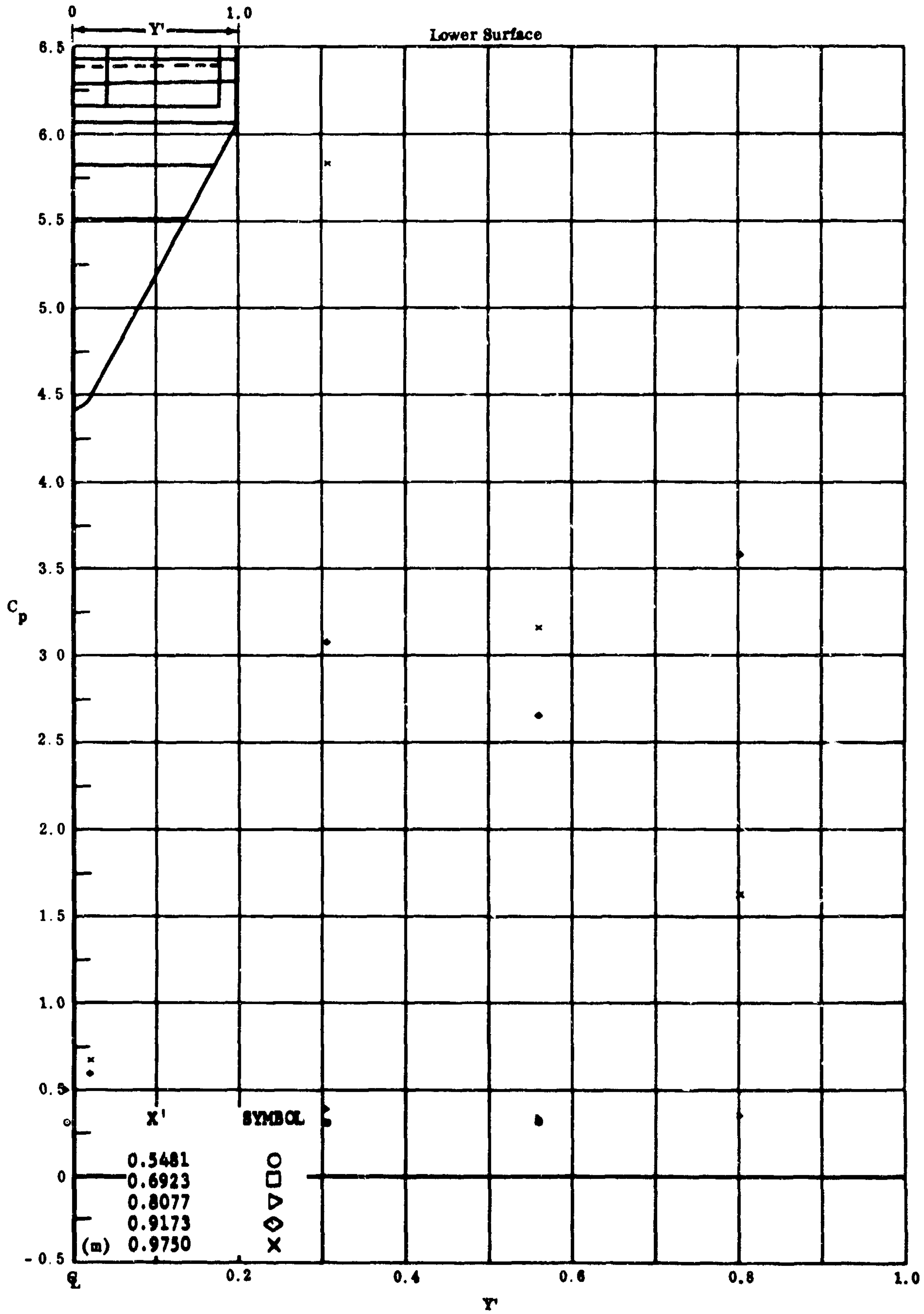

Fig. 7m Configuration X, $\alpha = +20$, $\delta_2 = \delta_3 = +30$

C_p vs. Y', lower surface

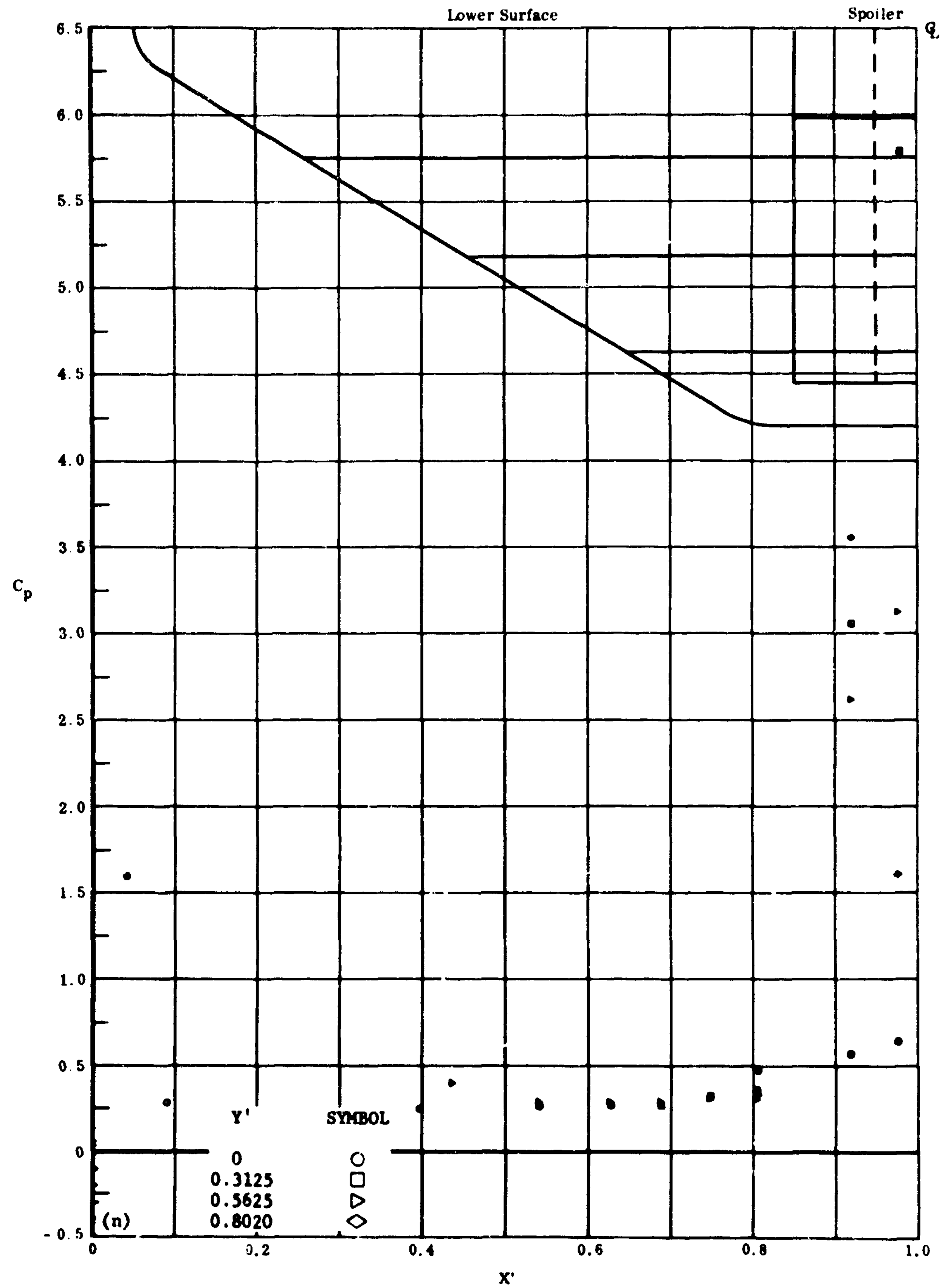

Fig. 7n Configuration I, α = +20 , $\delta_2 = \delta_3$ = +30

C_p vs. X', lower surface

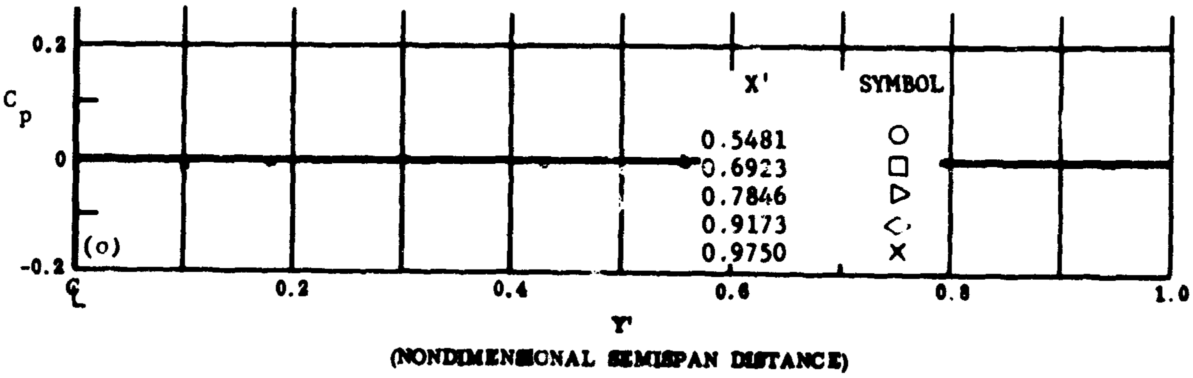

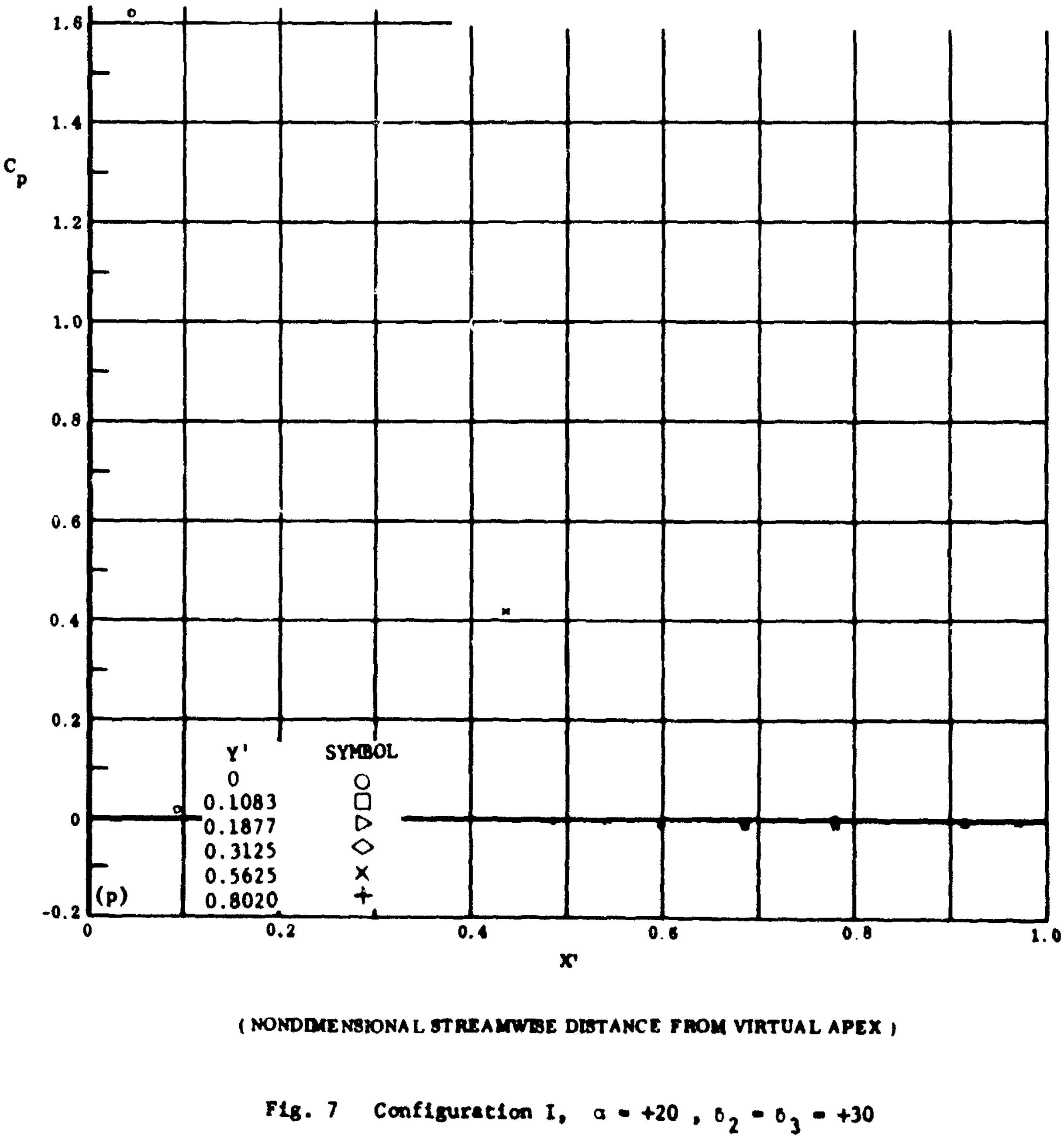

Fig. 7 Configuration I, $\alpha = +20$, $\delta_2 = \delta_3 = +30$

o) C_p vs. Y', upper surface

p) C_p vs. X', upper surface

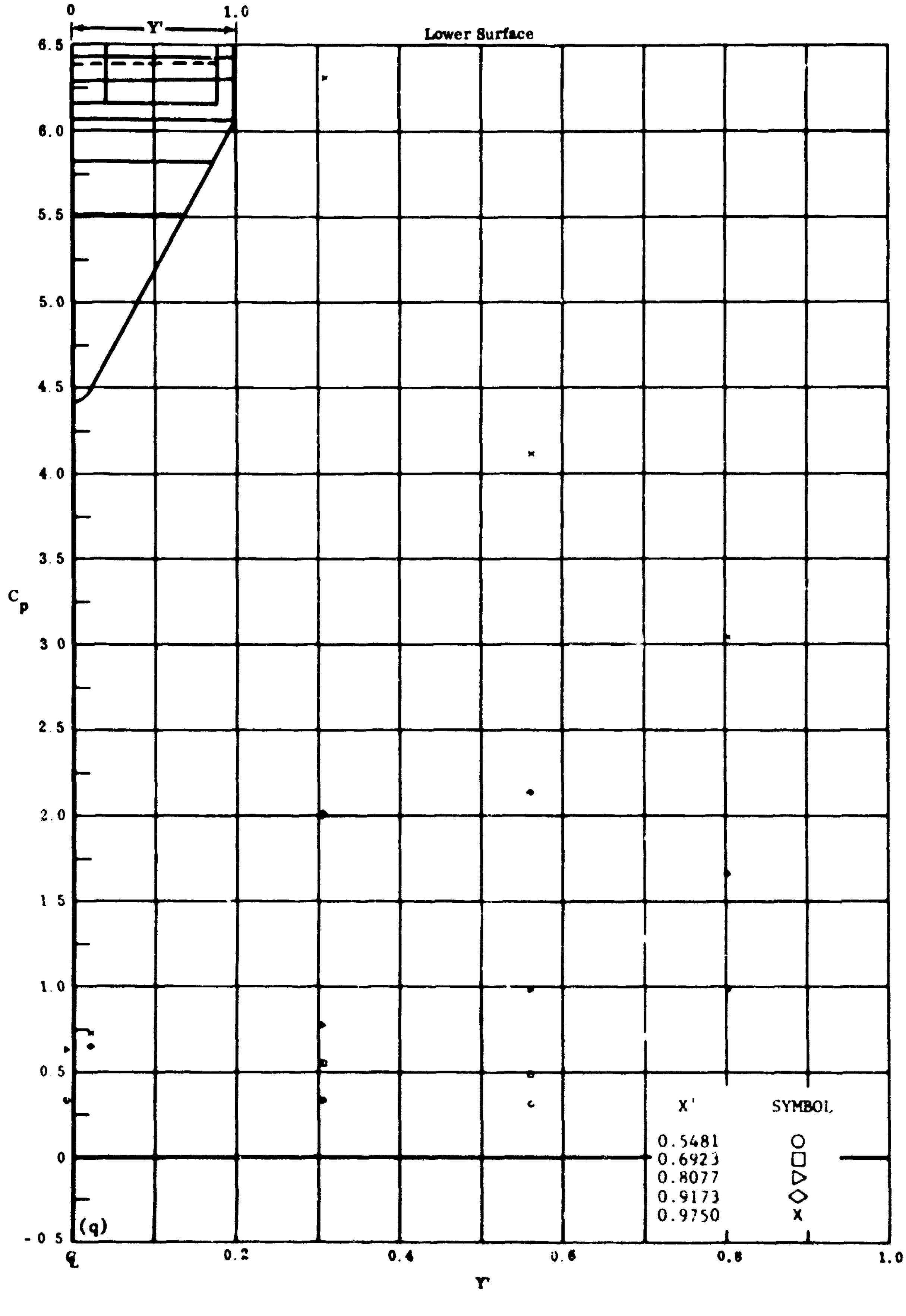

Fig. 7q Configuration I, ι = +20 , $\delta_2 = \delta_3$ = +39

C_p vs. Y', lower surface

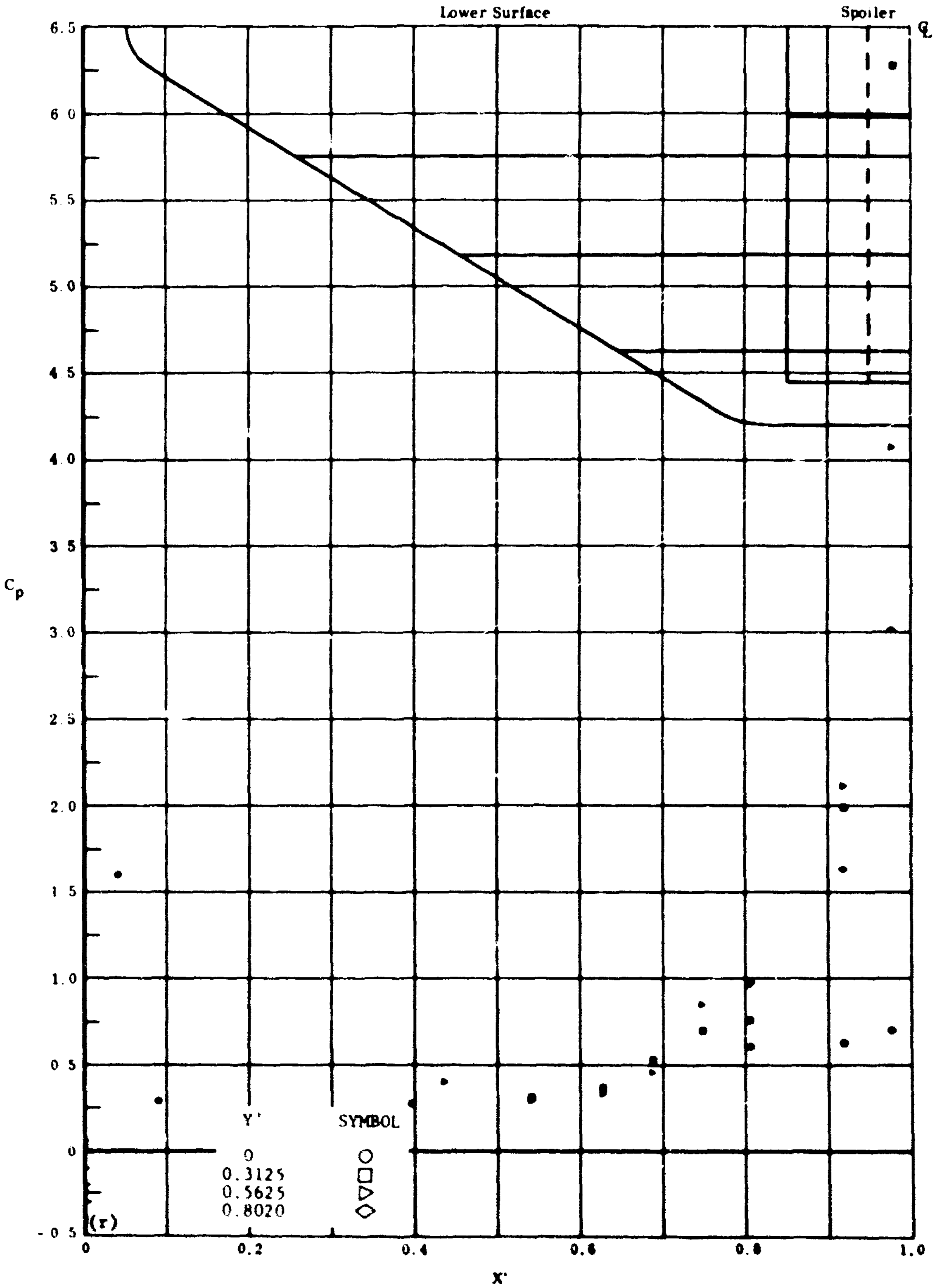

(NONDIMENSIONAL STREAMWISE DISTANCE FROM VIRTUAL APEX)

Fig. 7r Configuration I, $\alpha = +20$, $\delta_2 = \delta_3 = +39$

C_p vs. X', lower surface

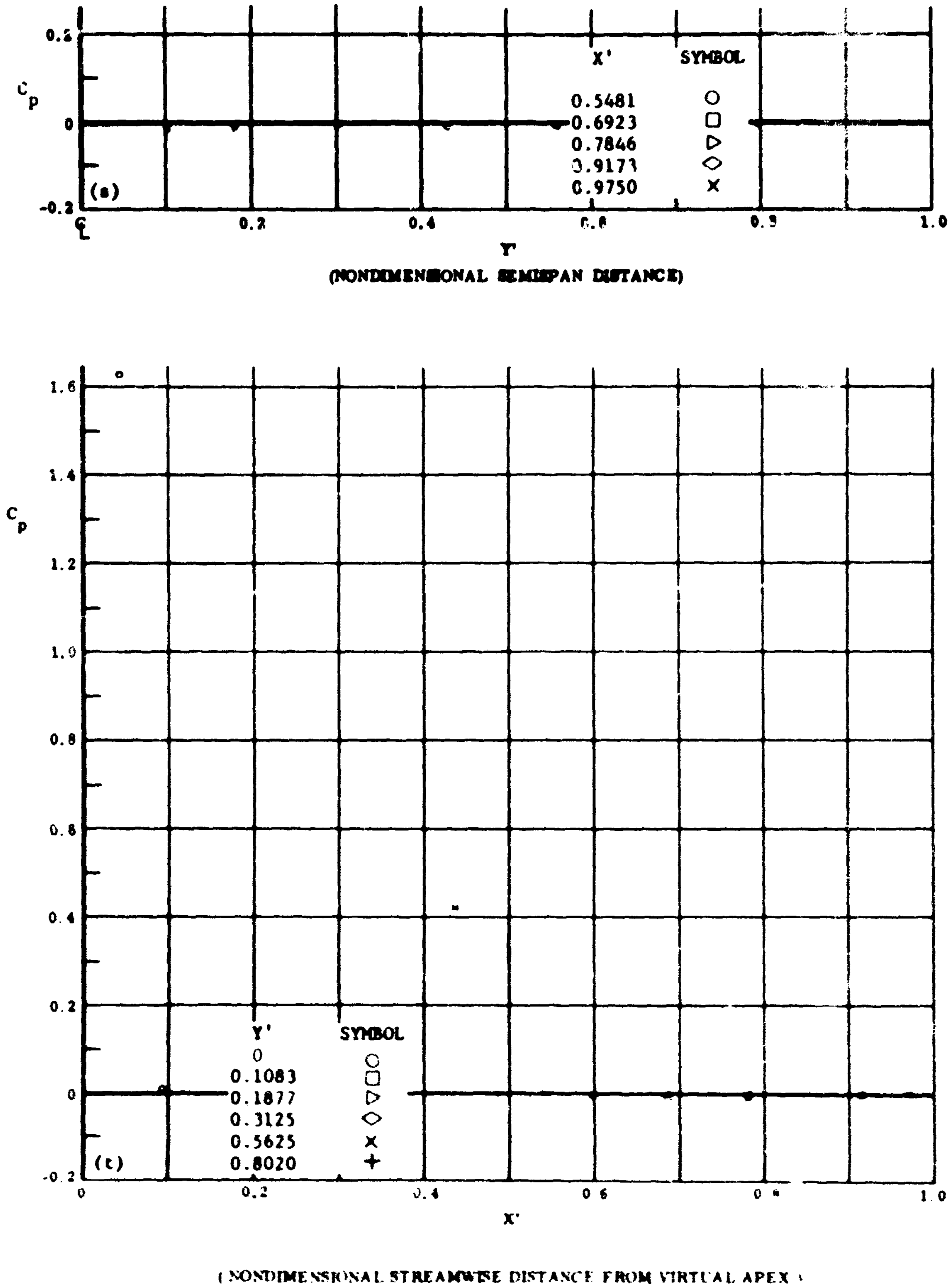

Fig. 7 Configuration I, = +20 , $_2$ = $_3$ = +39

s) C_p vs. Y', upper surface

t) C_p vs. X', upper surface

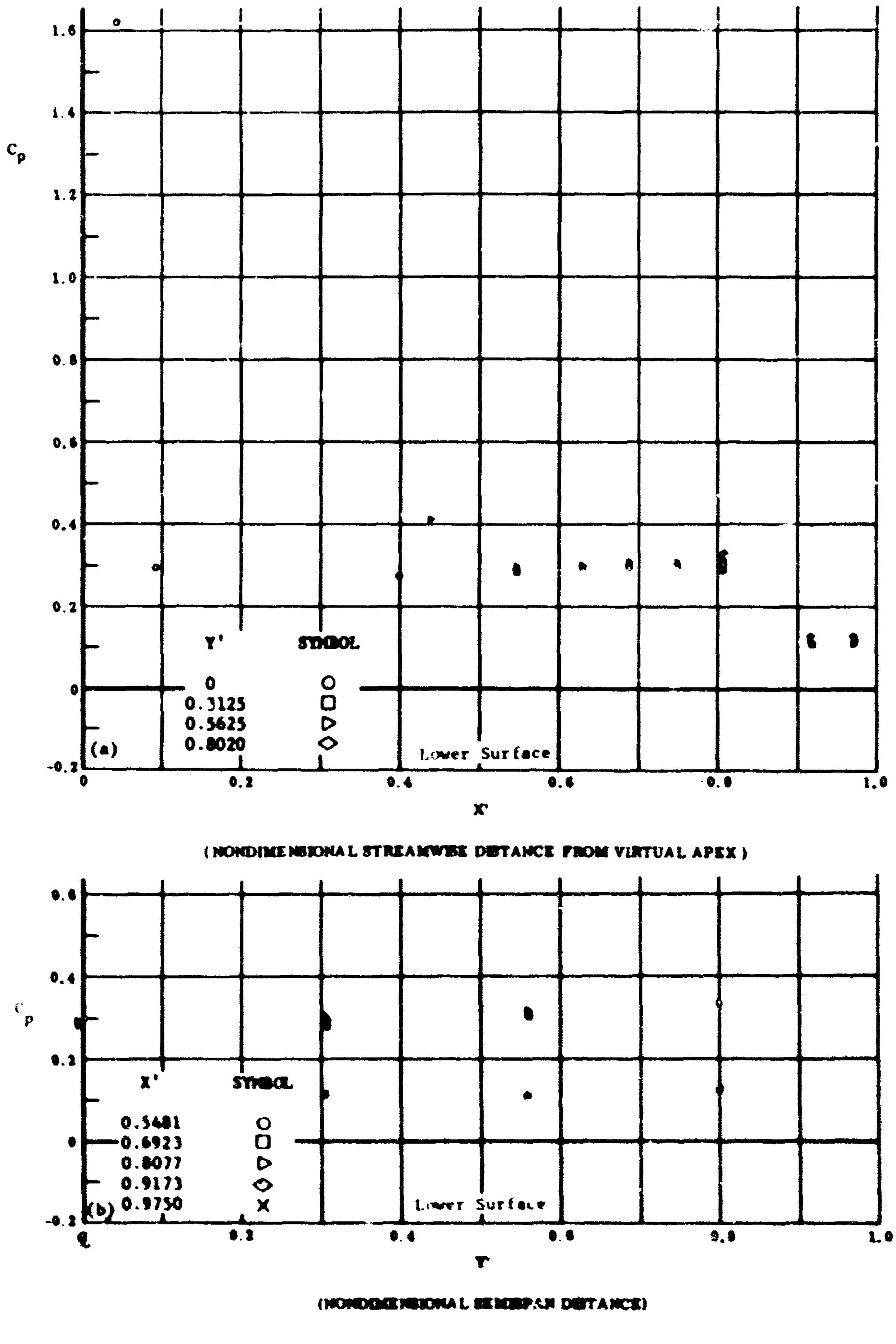

Fig. 8 Configuration I, $\alpha = +20$, $\delta_2 = \delta_3 = -10$

a) C_p vs. X', lower surface

b) C_p vs. Y', lower surface

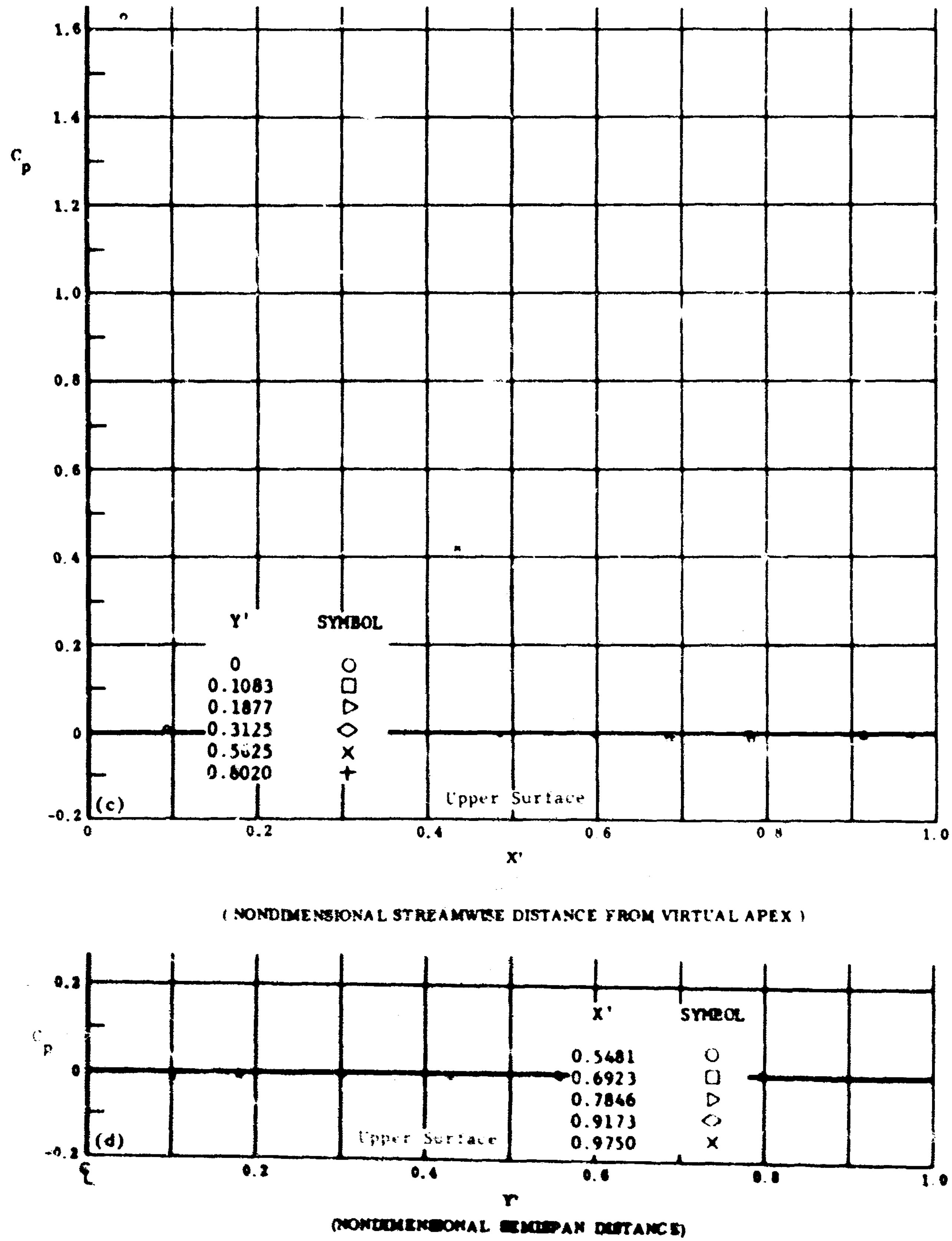

Fig. 8 Configuration I, $\epsilon_1 = +20$, $\epsilon_2 = \epsilon_3 = -10$

c) C_p vs. X', upper surface

d) C_p vs. Y', upper surface

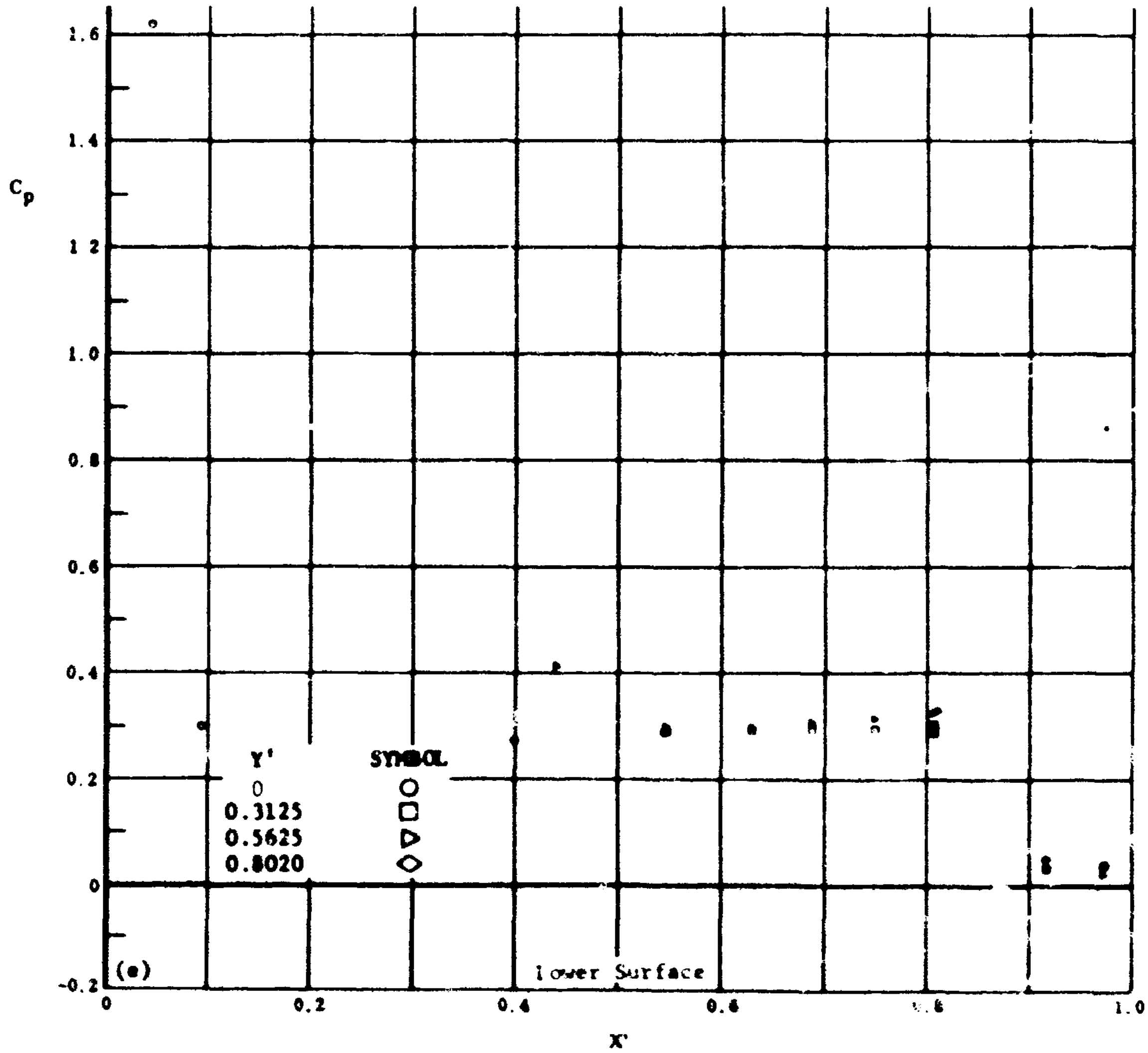

(NONDIMENSIONAL STREAMWISE DISTANCE FROM VIRTUAL APEX)

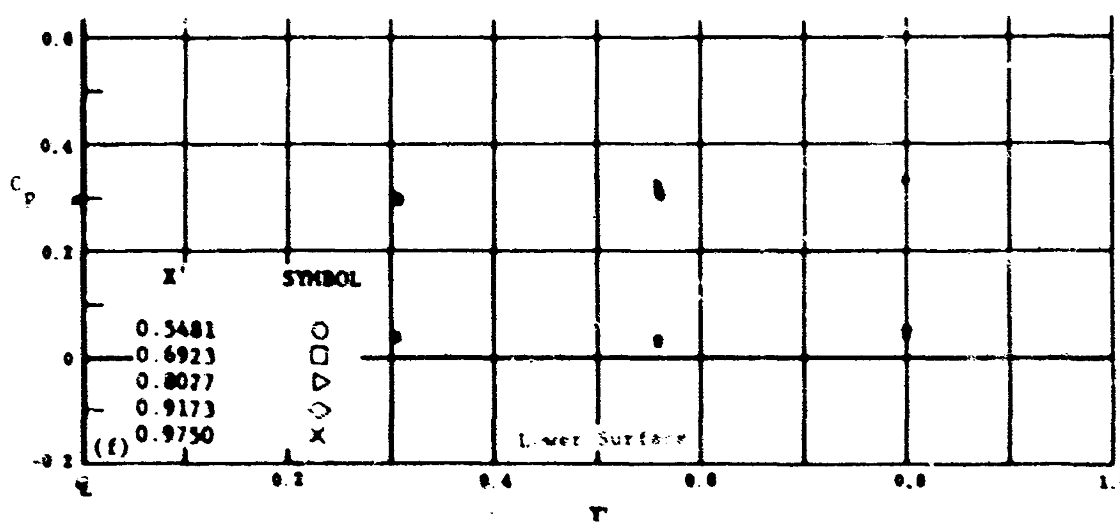

(NONDIMENSIONAL SEMISPAN DISTANCE)

Fig. 8 Configuration I, $\delta_1 = +20$, $\delta_2 = \delta_3 = -20$

e) C_p vs. X', lower surface

f) C_p vs. Y', lower surface

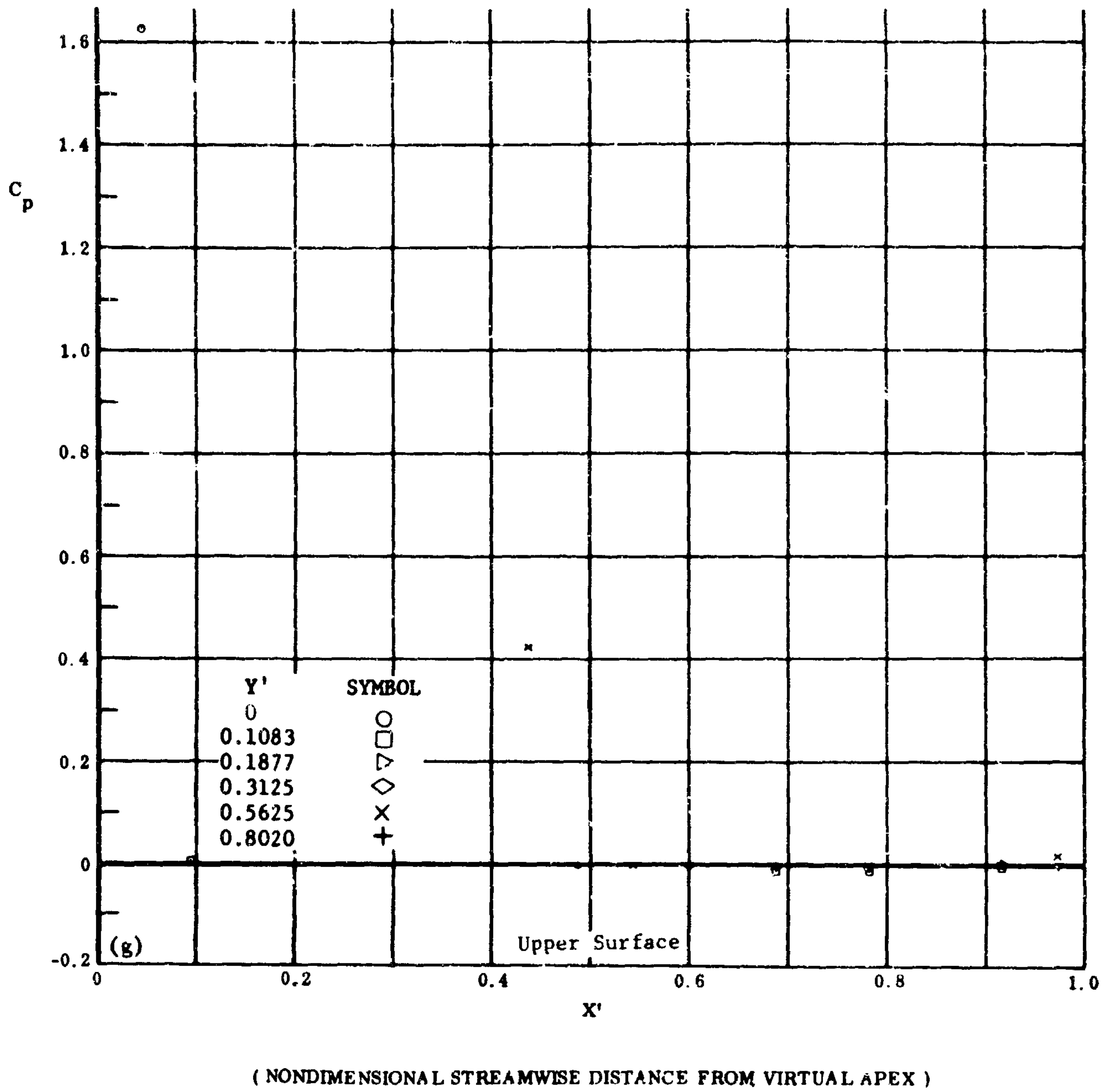

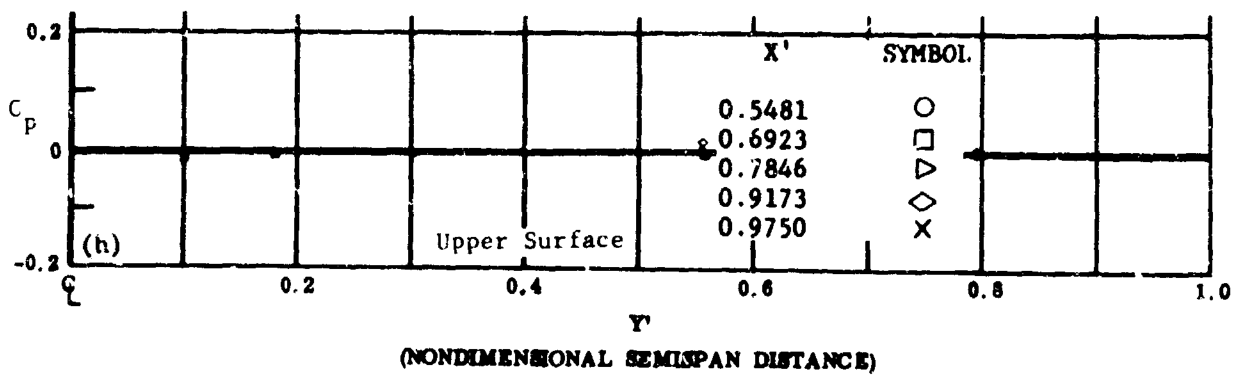

Fig. 8 Configuration I, $\alpha = +20$, $\delta_2 = \delta_3 = -20$

g) C_p vs. X', upper surface

h) C_p vs. Y', upper surface

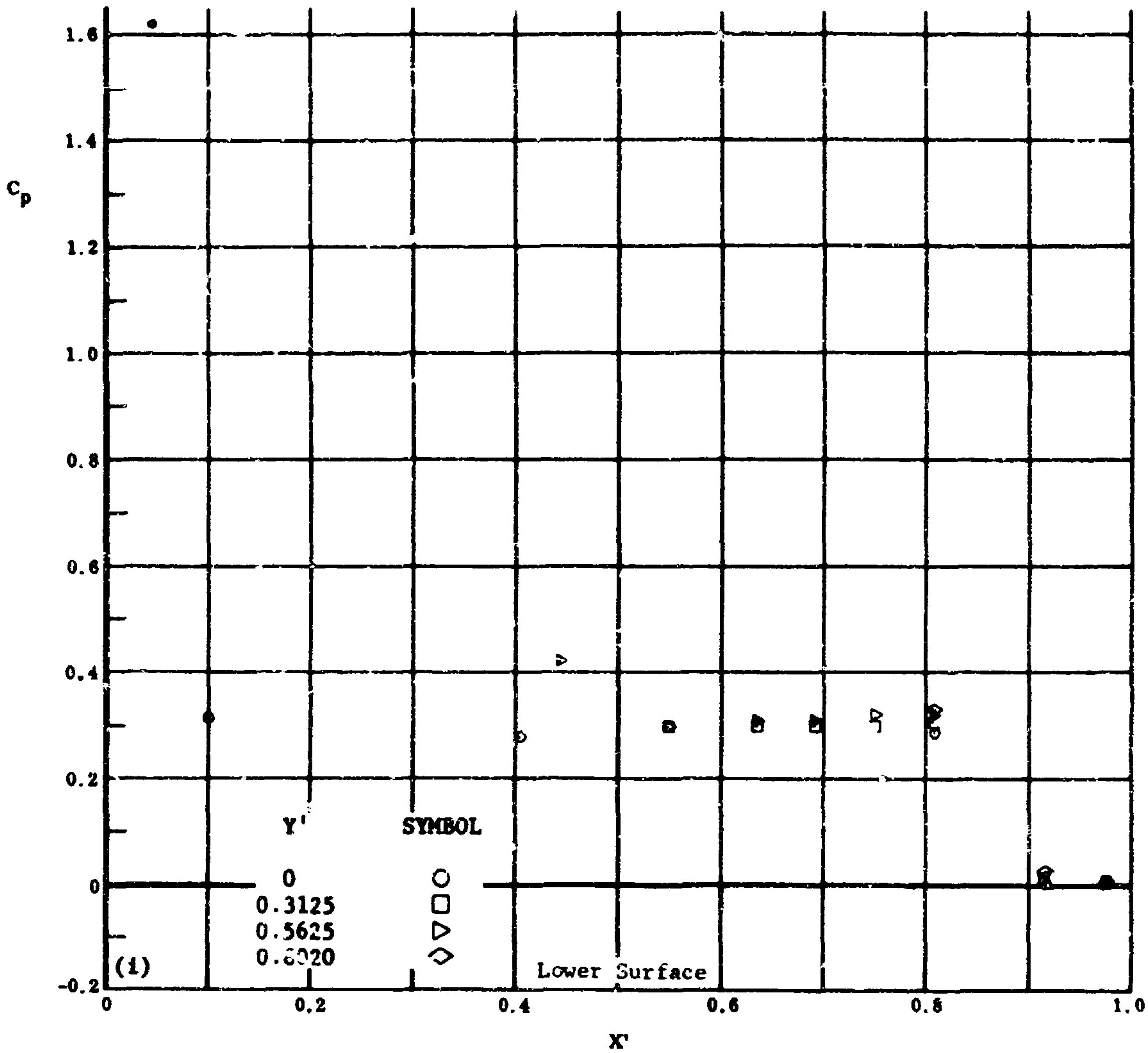

(NONDIMENSIONAL STREAMWISE DISTANCE FROM VIRTUAL APEX)

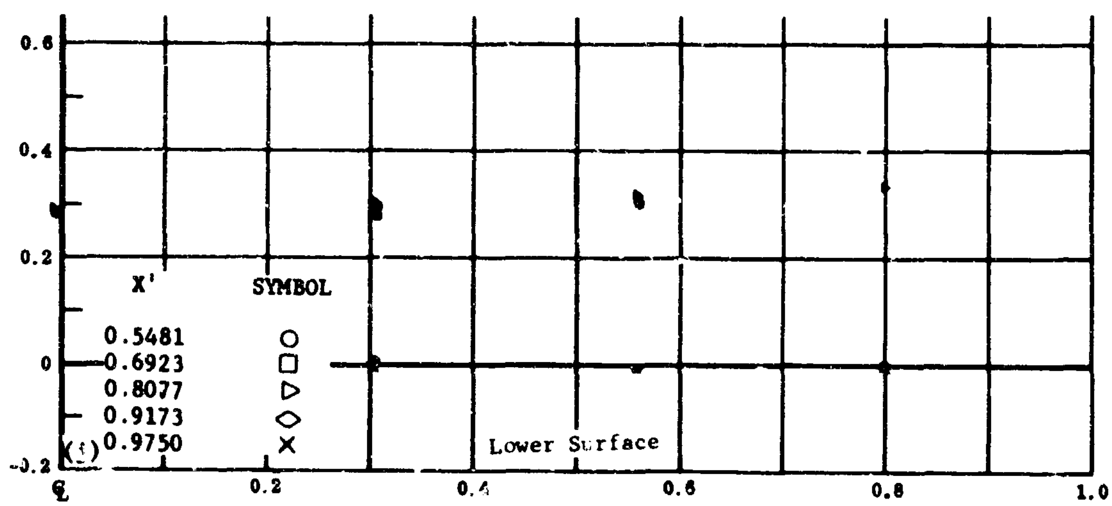

(NONDIMENSIONAL SEMISPAN DISTANCE)

Fig. 8 Configuration I, $\alpha = +20$, $\delta_2 = \delta_3 = -30$

i) C_p vs. X', lower surface

j) C_p vs. Y', lower surface

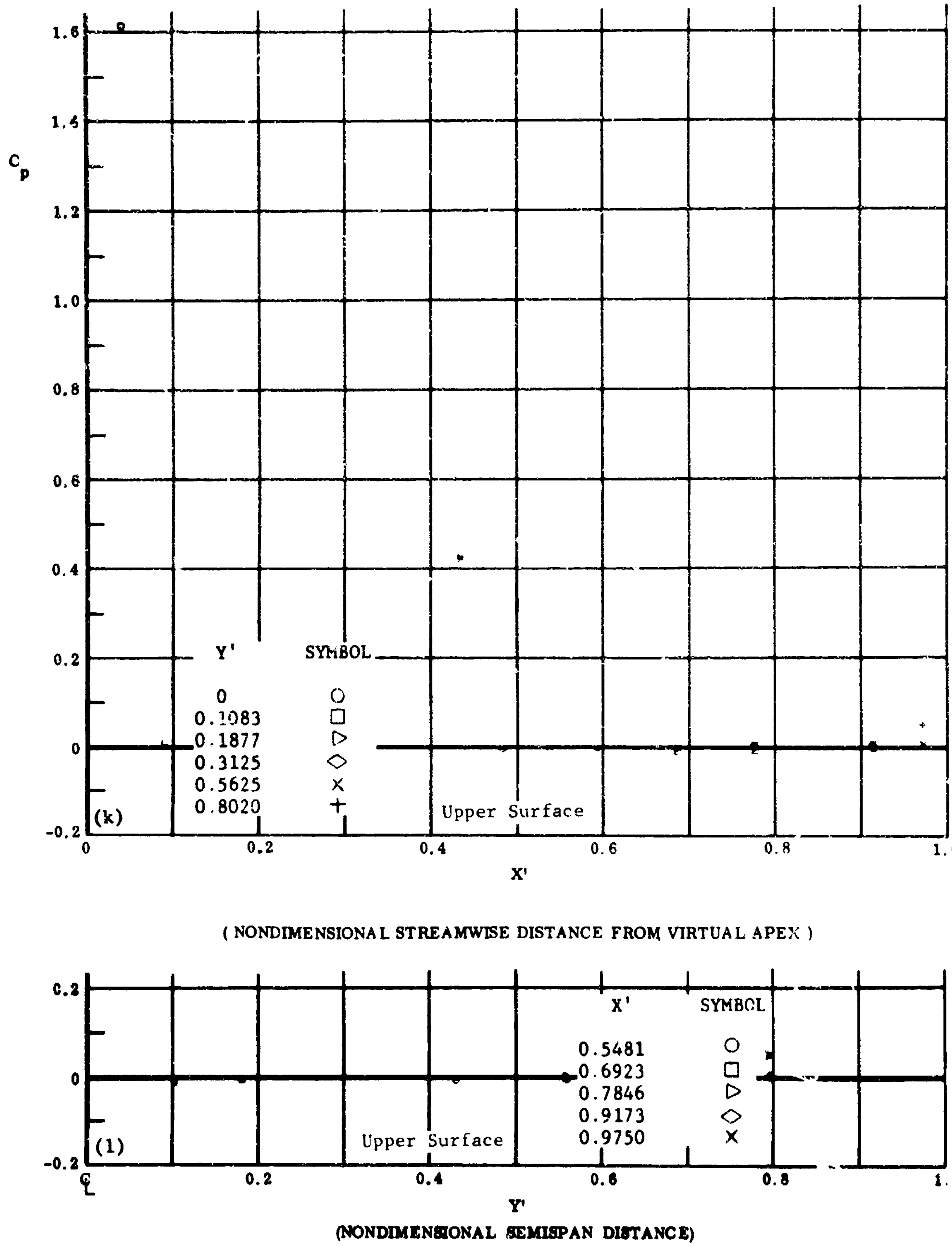

Fig. 8 Configuration I, $\alpha = +20$, $\delta_2 = \delta_3 = -30$

k) C_p vs. X', upper surface

1) C_p vs. Y', upper surface

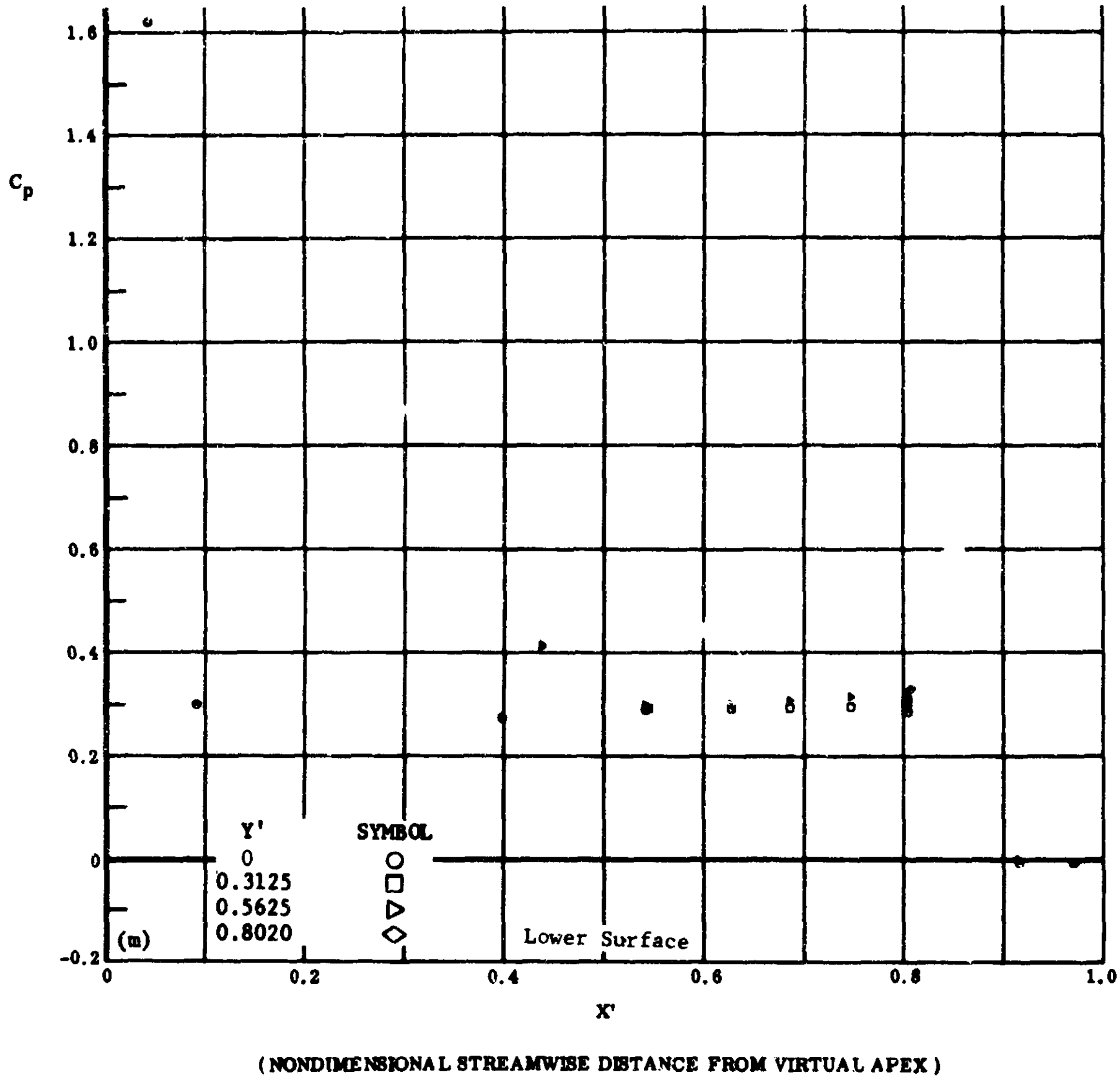

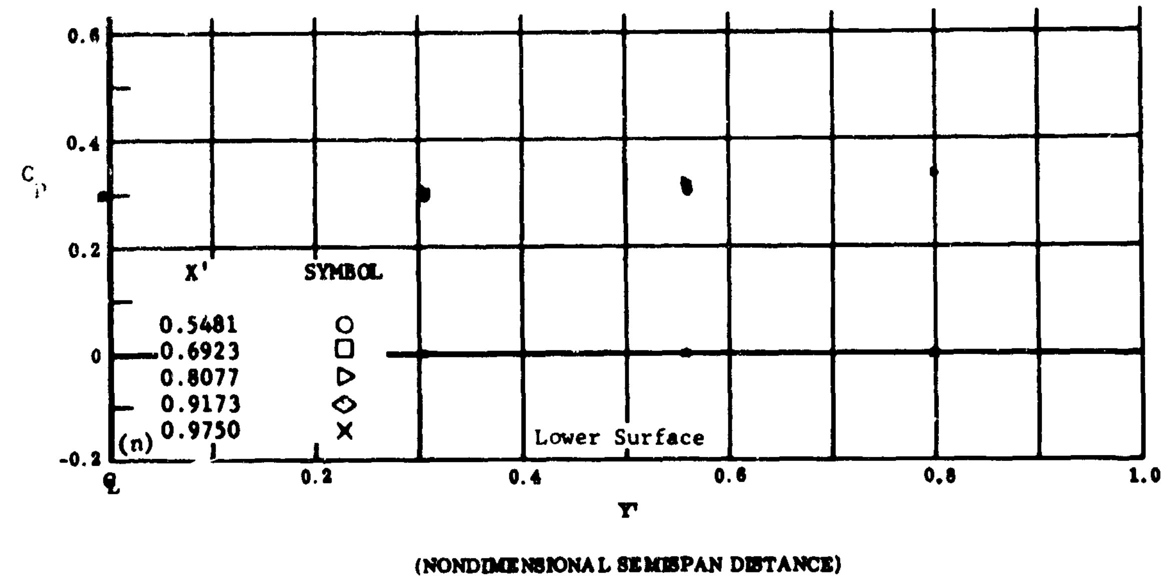

Fig. 8 Configuration I, $\alpha = +20$, $\delta_2 = \delta_3 = -39$

m) C_p vs. X', lower surface

n) C_p vs. Y', lower surface

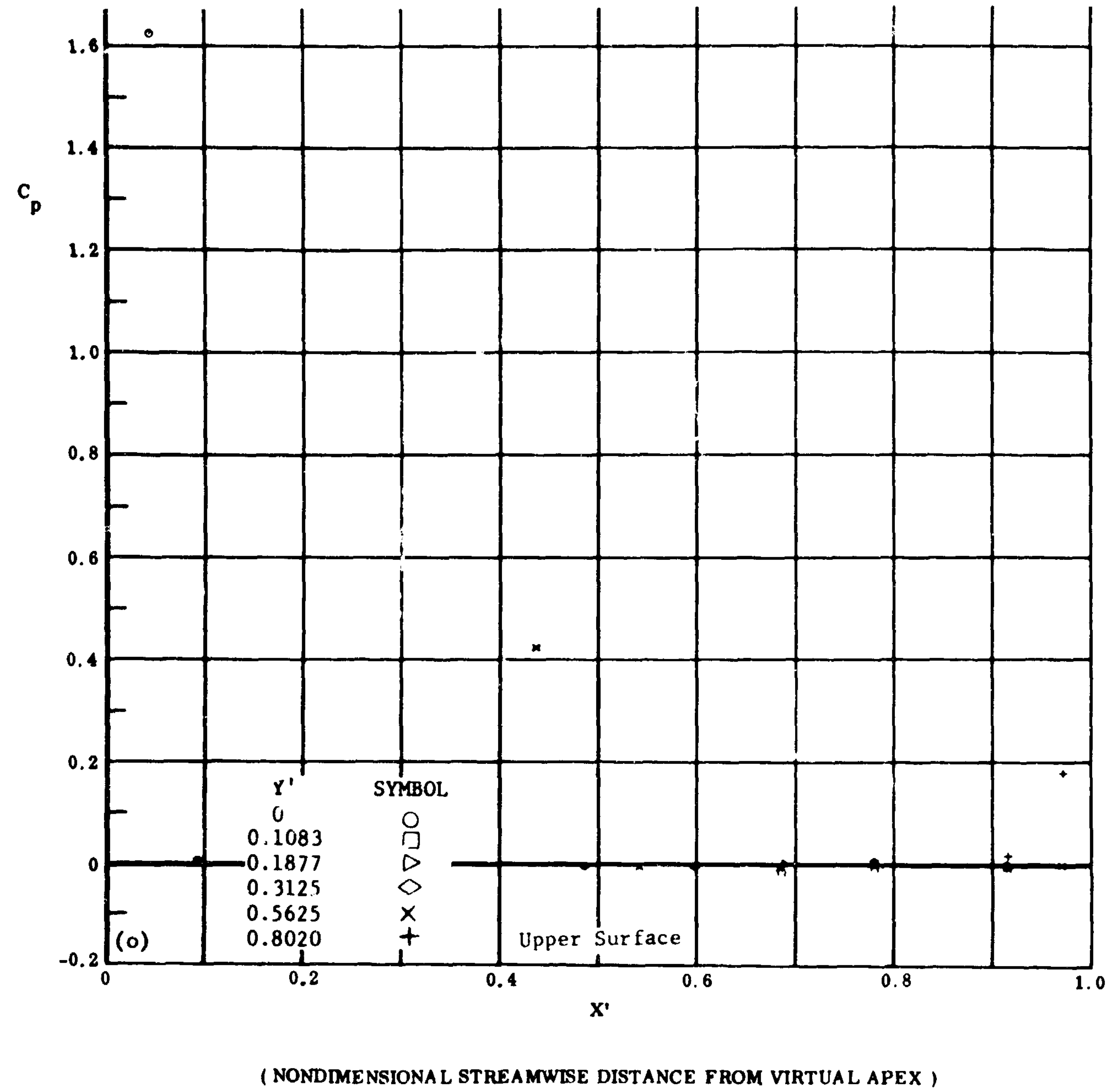

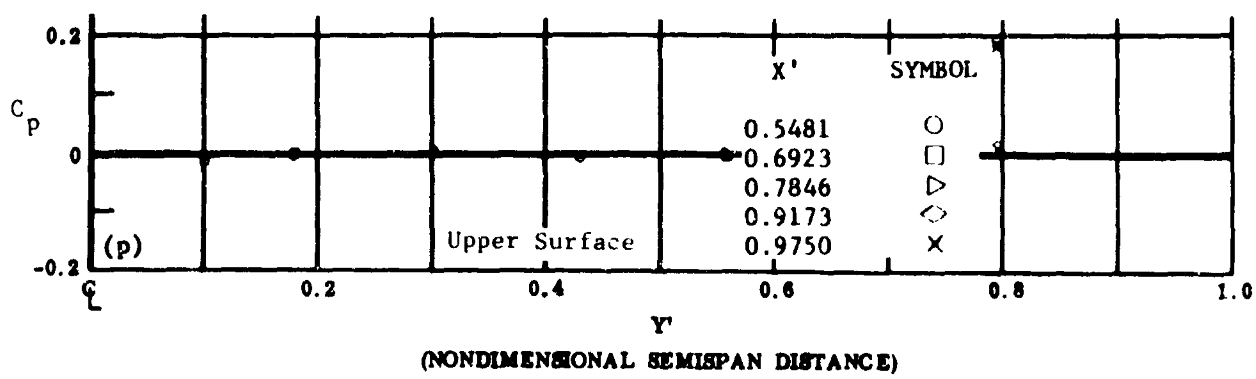

Fig. 8 Configuration I, $\alpha = +20$, $\delta_2 = \delta_3 = -39$

o) C_p vs. X', upper surface

p) C_p vs. Y', upper surface

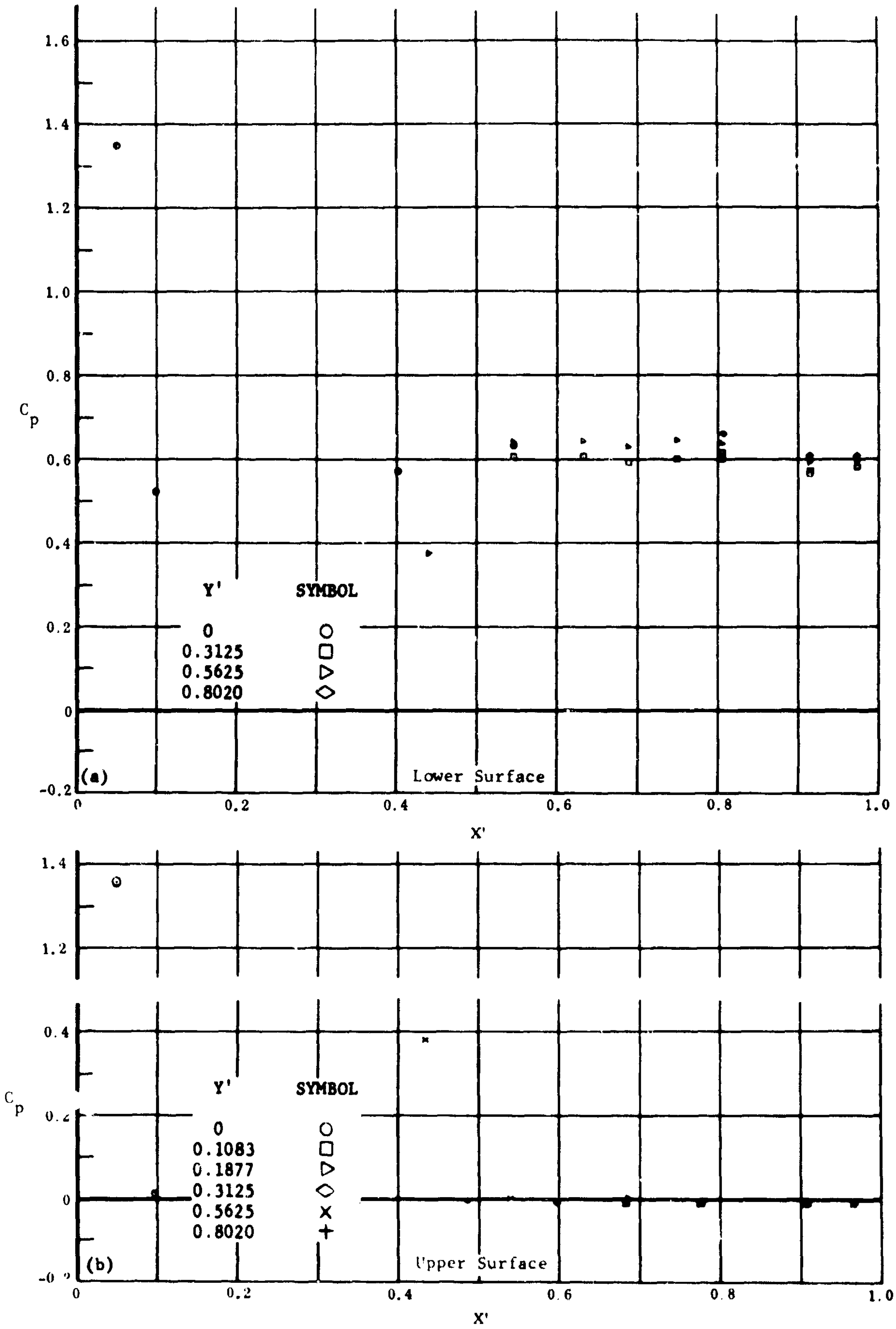

(NONDIMENSIONAL STREAMWISE DISTANCE FROM VIRTUAL APEX)

Fig. 9 Configuration I, $\alpha = +30$, $\delta_2 = \delta_3 = 0$

a) C_p vs. X', lower surface

b) C_p vs. X', upper surface

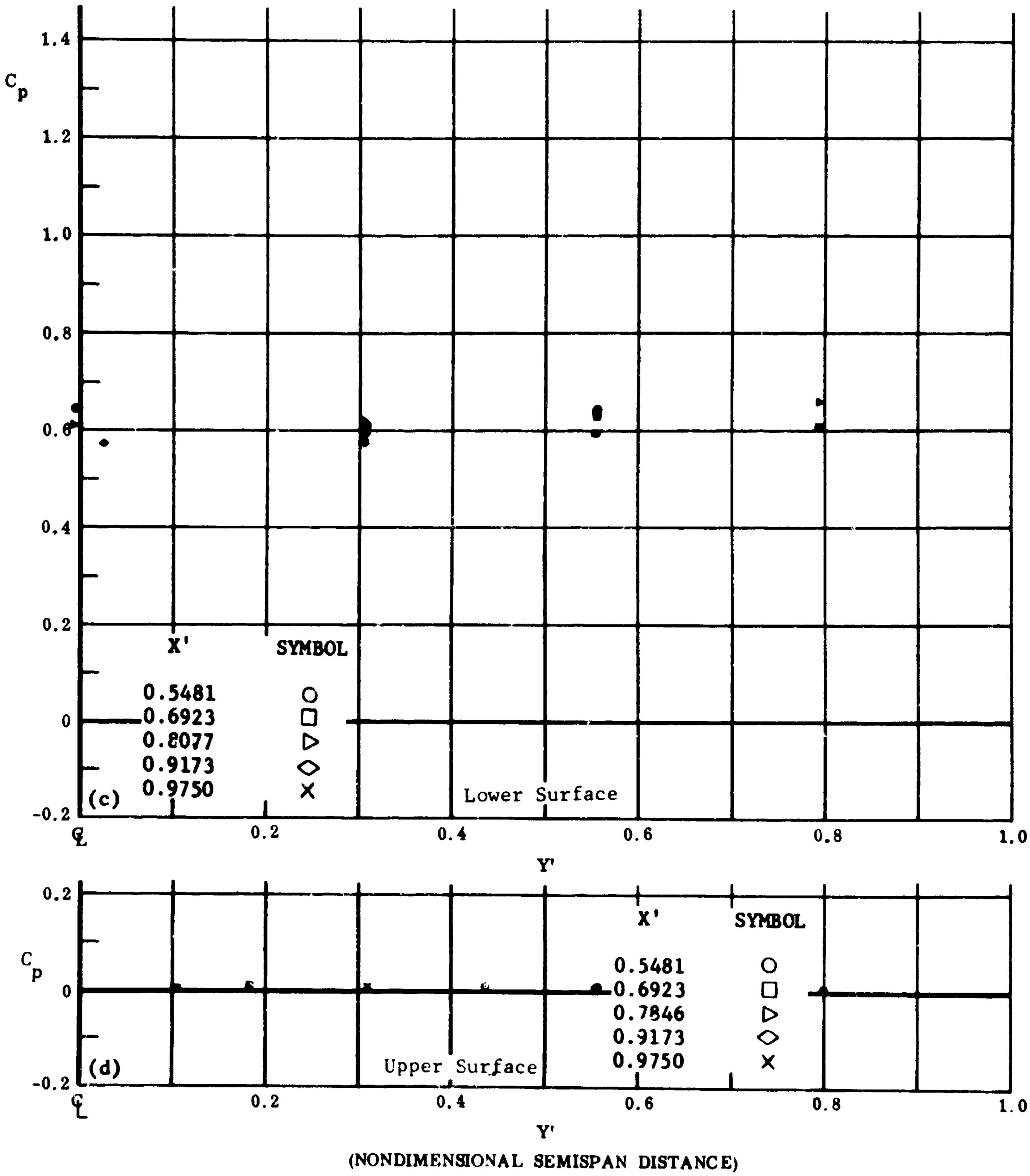

Fig. 9 Configuration I, $\alpha = +30$, $\delta_2 = \delta_3 = 0$

c) C_p vs. Y', lower surface

d) C_p vs. Y', upper surface

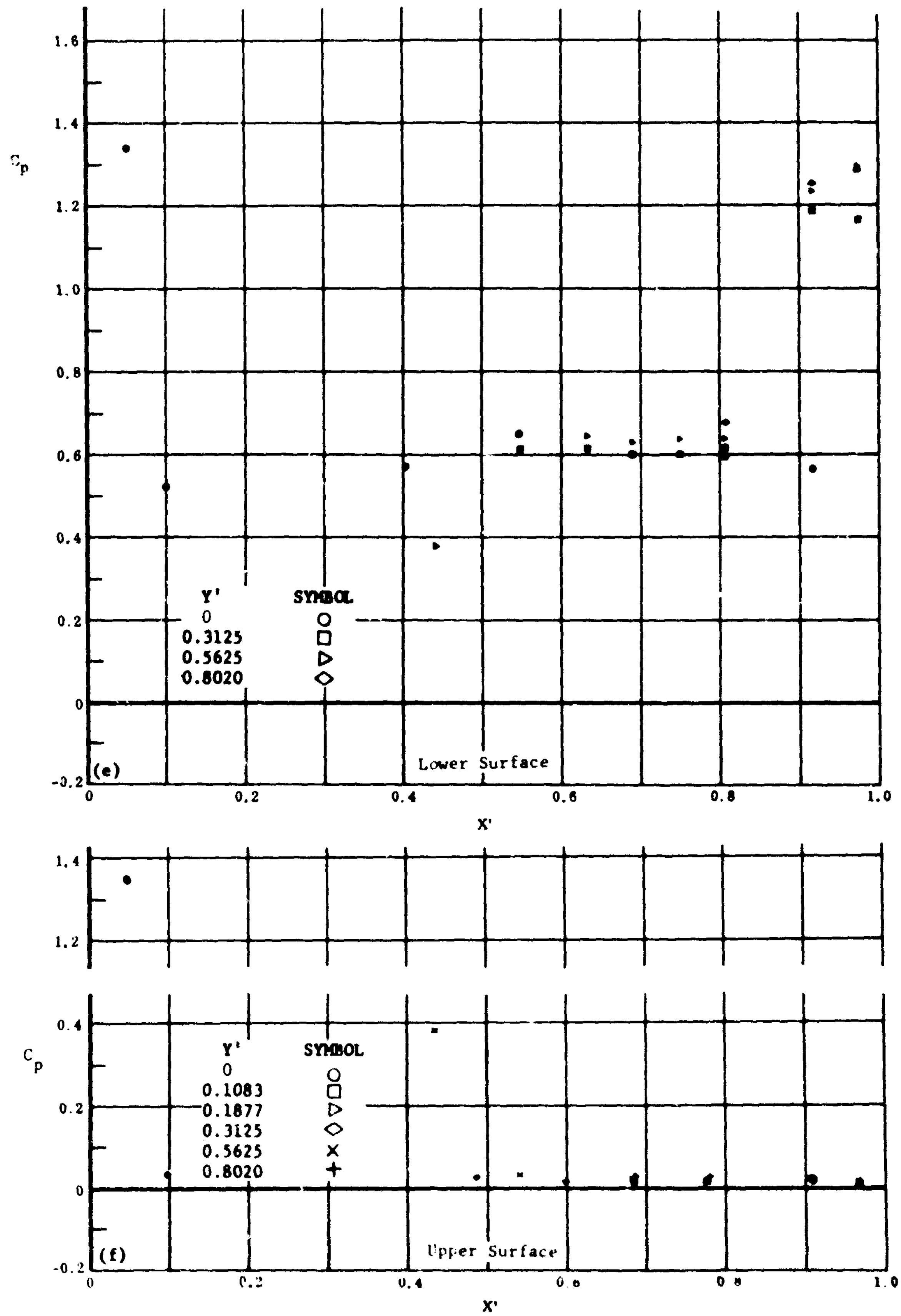

(NONDIMENSIONAL STREAMWISE DISTANCE FROM VIRTUAL APEX)

Fig. 9 Configuration I, $\alpha = +30$, $\delta_2 = \delta_3 = +10$

e) C_p vs. X', lower surface

f) C_p vs. X', upper surface

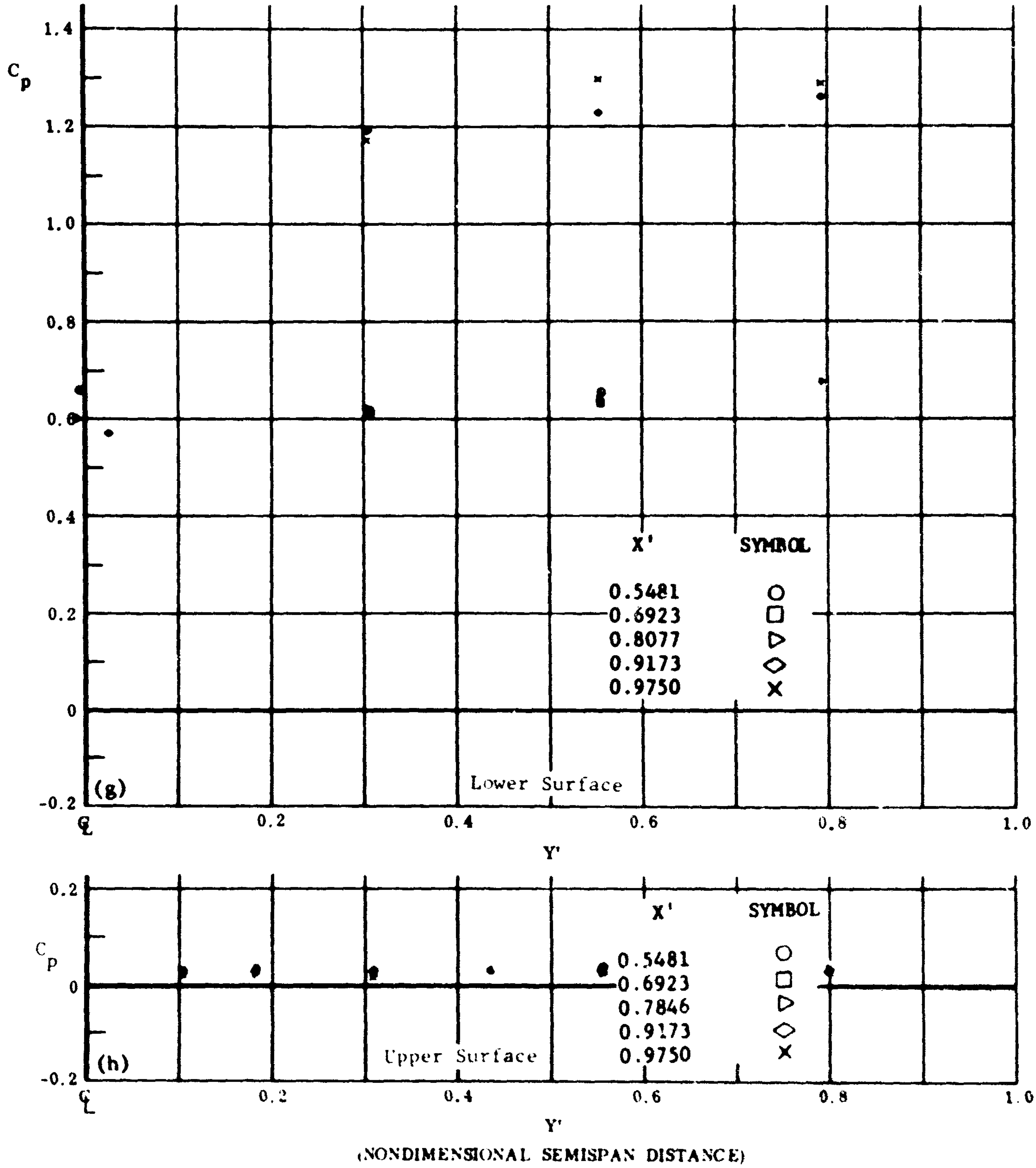

Fig. 9 Configuration I, $\delta = +30$, $\delta_2 = \delta_3 = +10$

g) C_p vs. Y', lower surface

h) C_p vs. Y', upper surface

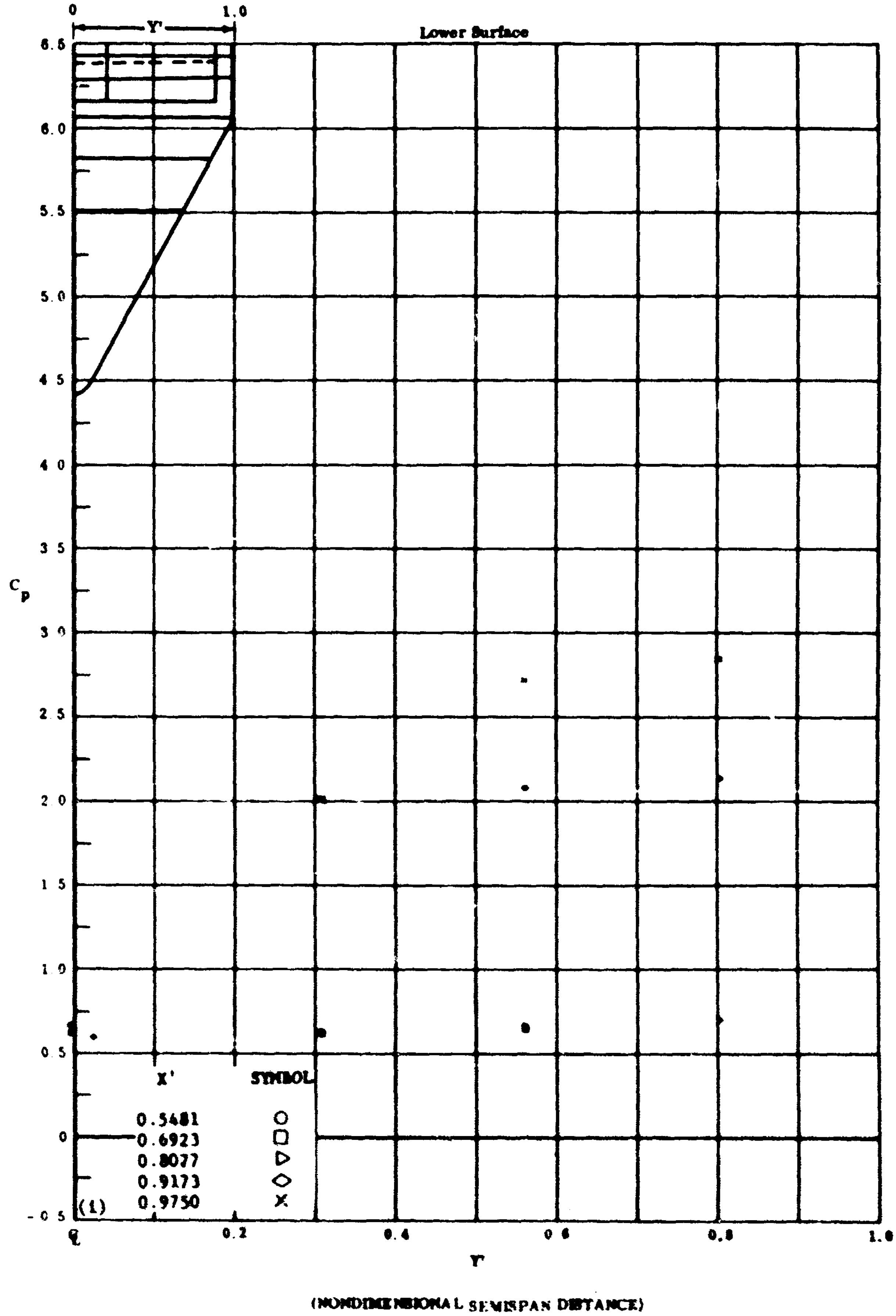

Fig. 91 Configuration I, $\alpha = +30$, $\delta_2 = \delta_3 = +20$

C_p vs. Y', lower surface

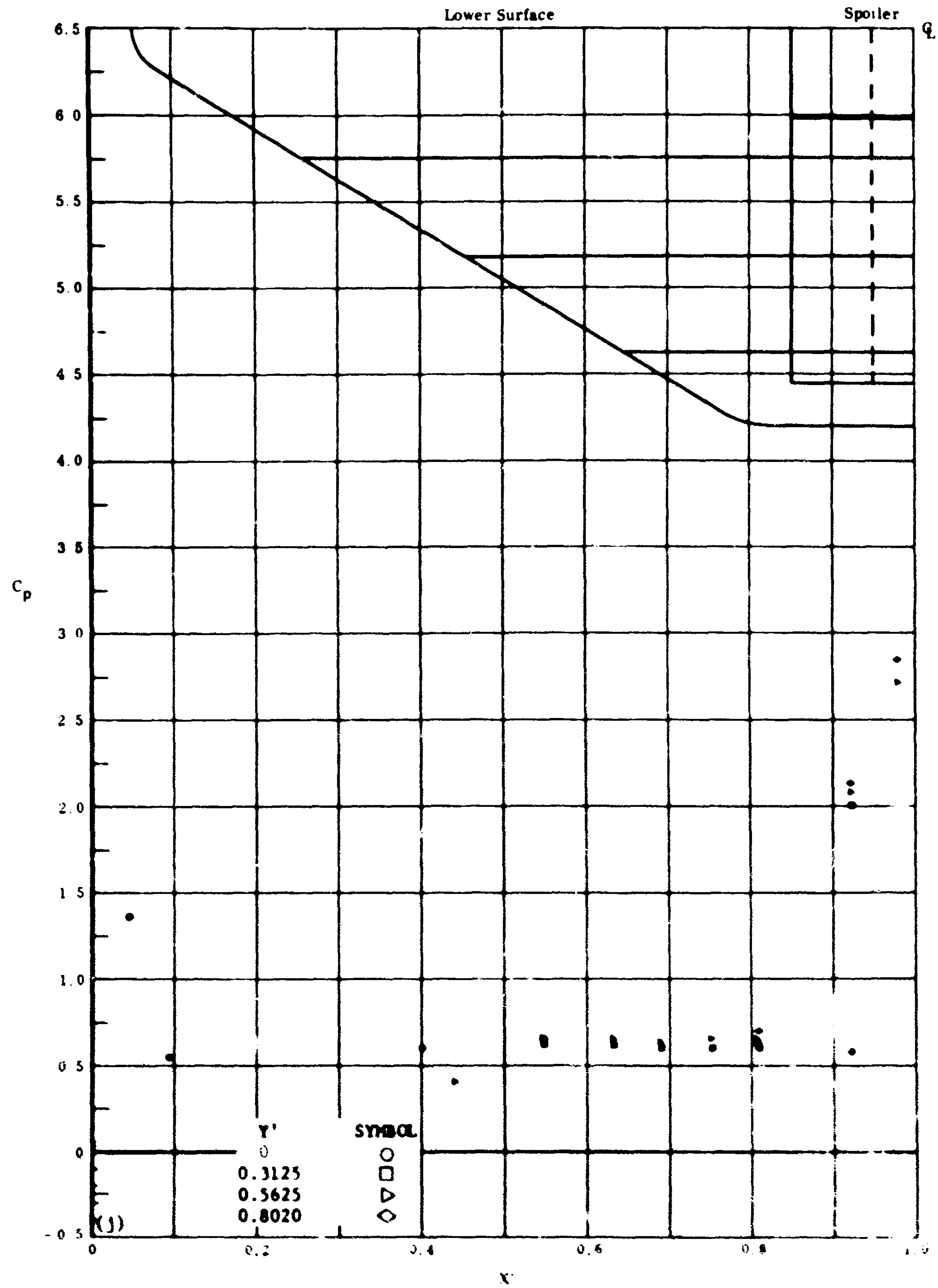

(NONDIMENSIONAL STREAMWISE DISTANCE FROM VIRTUAL APEX)

Fig. 9j Configuration I, α = +30 , $\delta_2 = \delta_3$ = +20

C_p vs X', lower surface

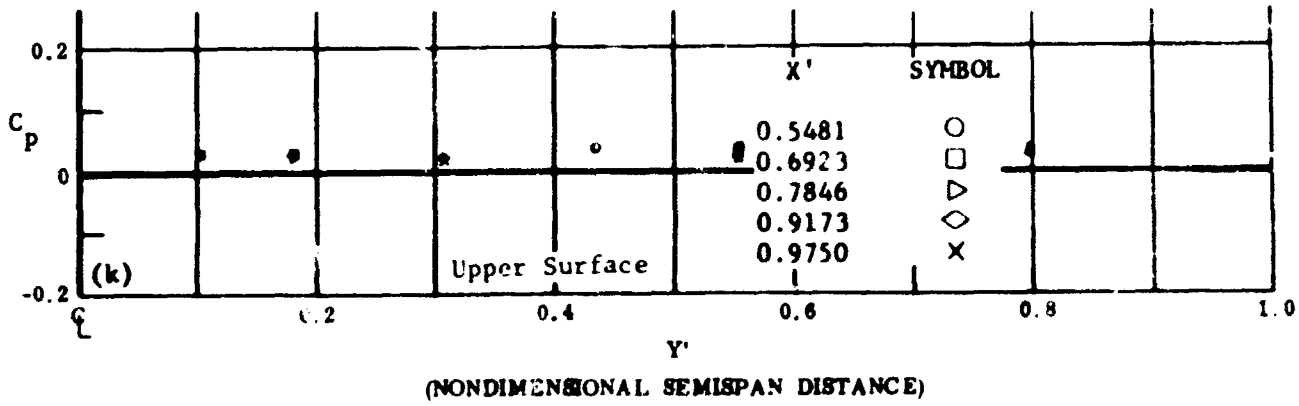

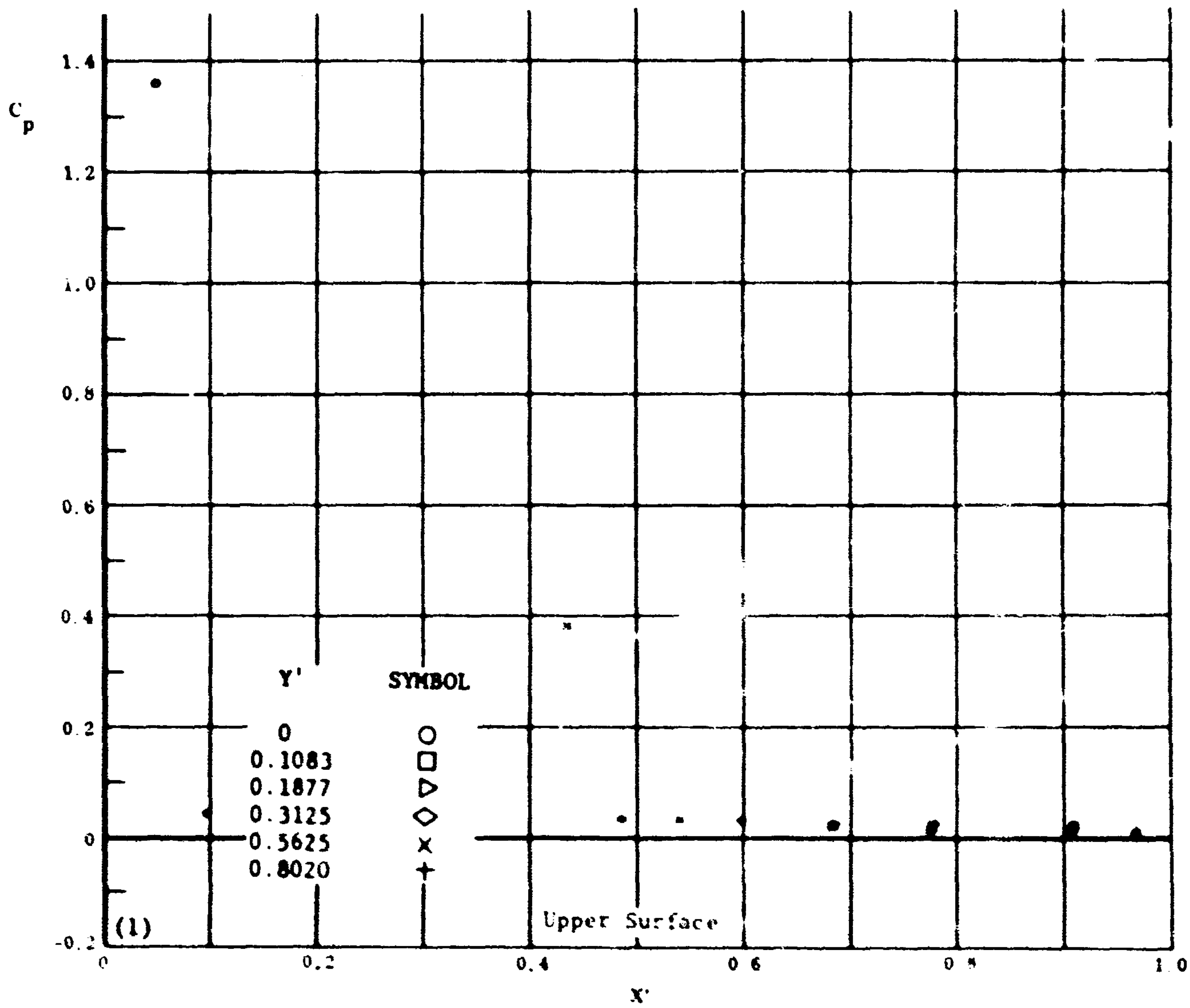

(NONDIMENSIONAL STREAMWISE DISTANCE FROM VIRTUAL APEX)

Fig. 9 Configuration I, $_1$ = +30 , $_2$ = $_3$ = +20

k) C_p vs. Y', upper surface

l) C_p vs. X', upper surface

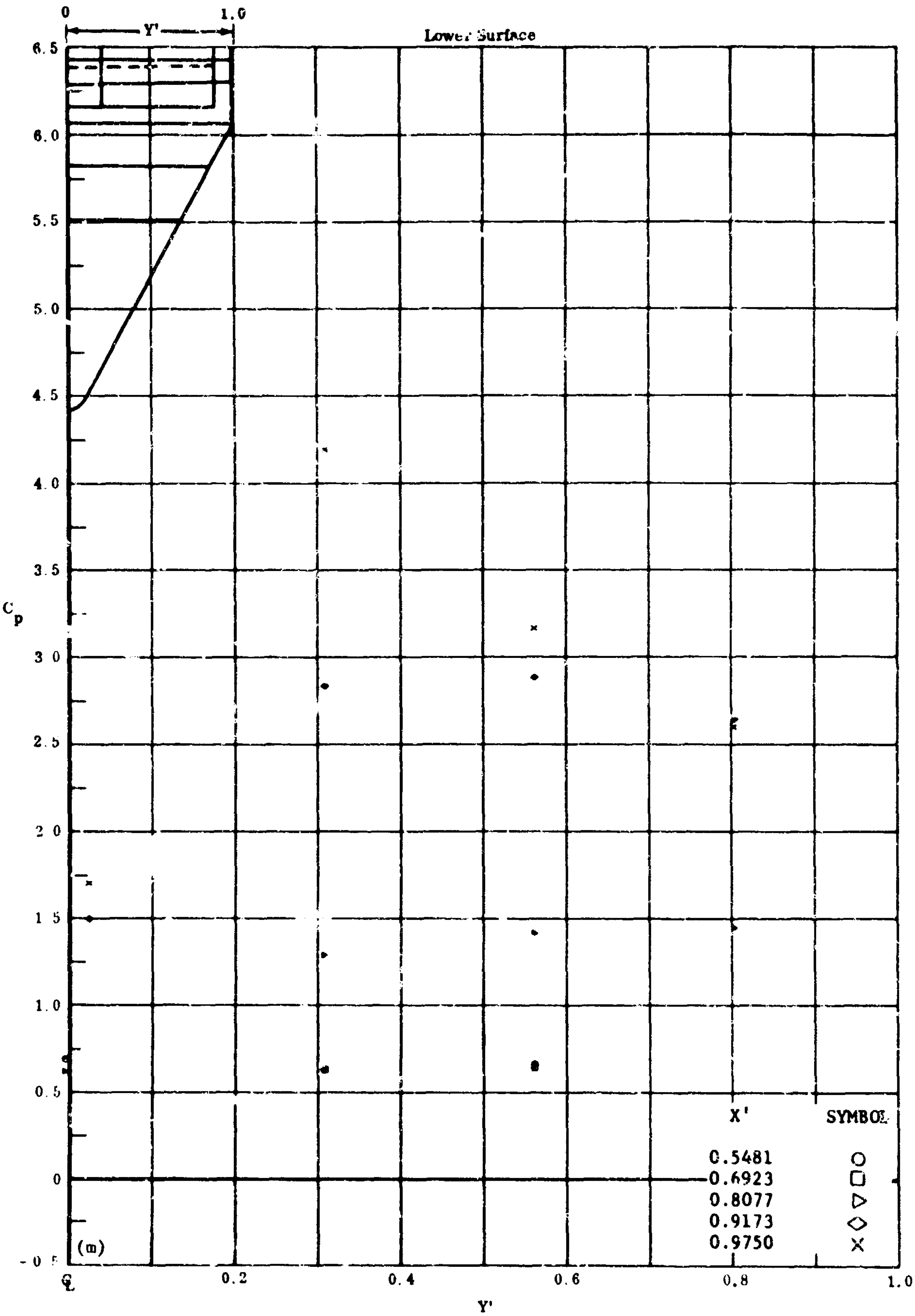

(NONDIMENSIONAL SEMISPAN DISTANCE)

Fig. 9m Configuration I, $\alpha = +30$, $\delta_2 = \delta_3 = +30$

C_p vs. Y', lower surface

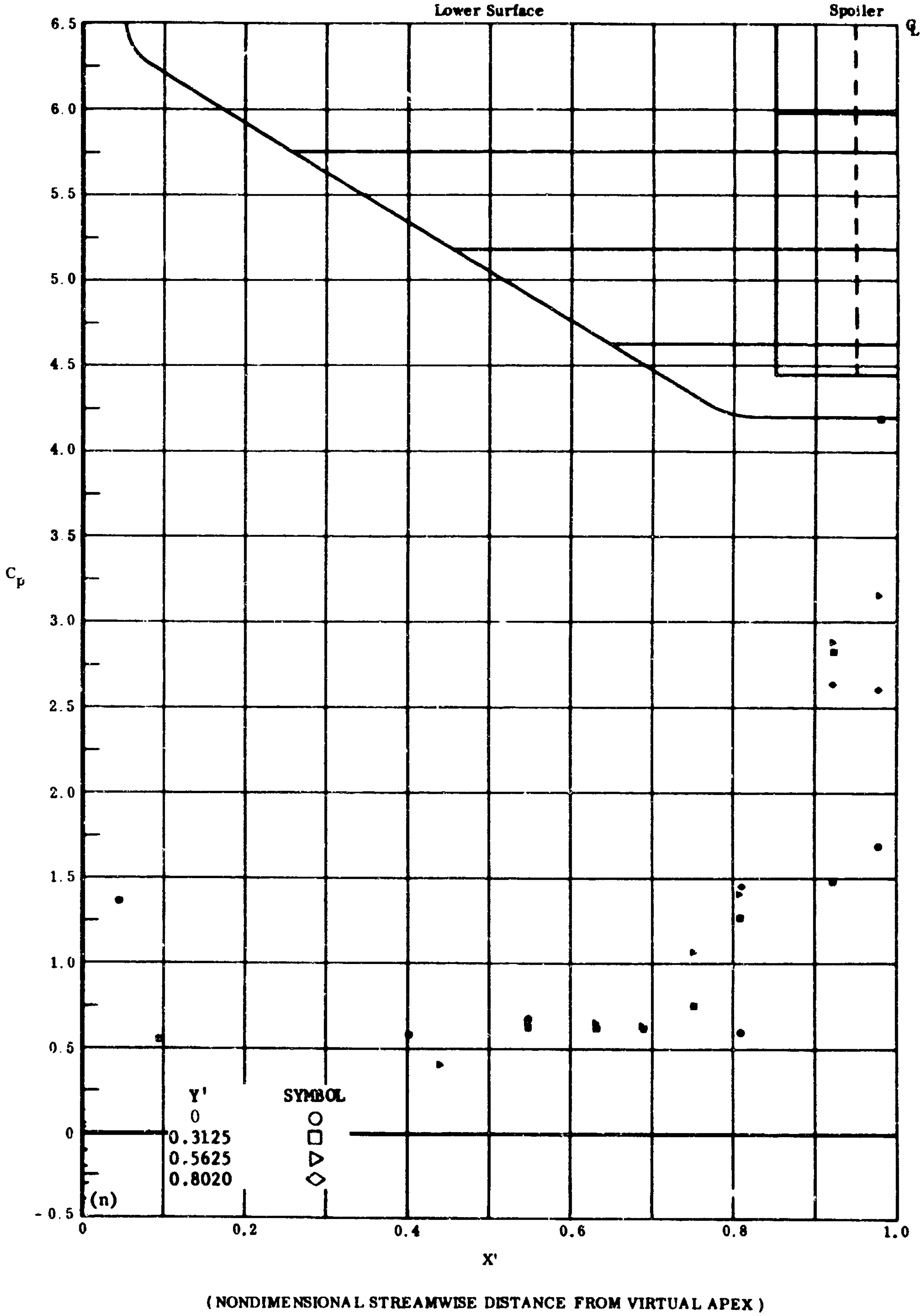

Fig. 9n Configuration I, α = +30 , δ_2 = δ_3 = +30
C_p vs. X', lower surface

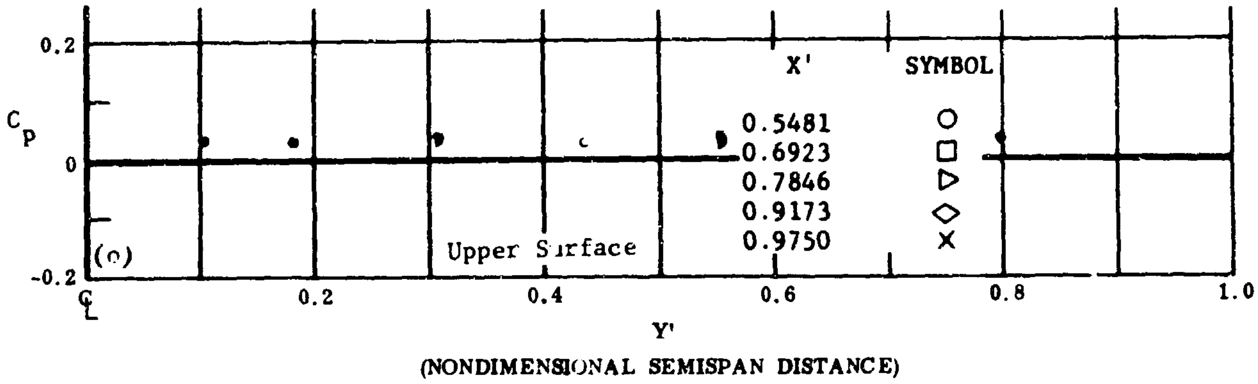

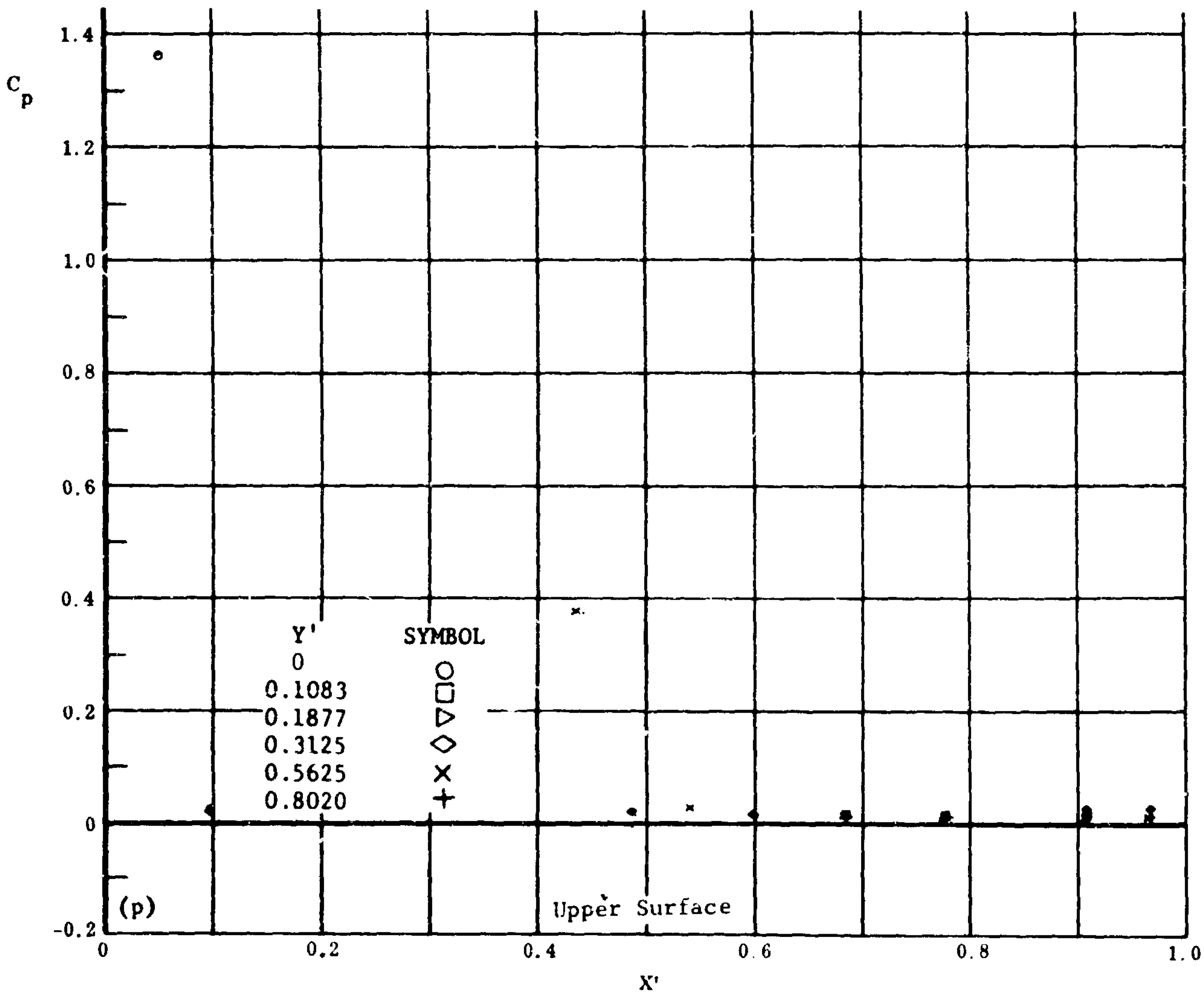

(NONDIMENSIONAL STREAMWISE DISTANCE FROM VIRTUAL APEX)

Fig. 9 Configuration I, $\alpha = +30$, $\delta_2 = \delta_3 = +30$

o) C_p vs. Y', upper surface

p) C_p vs. X', upper surface

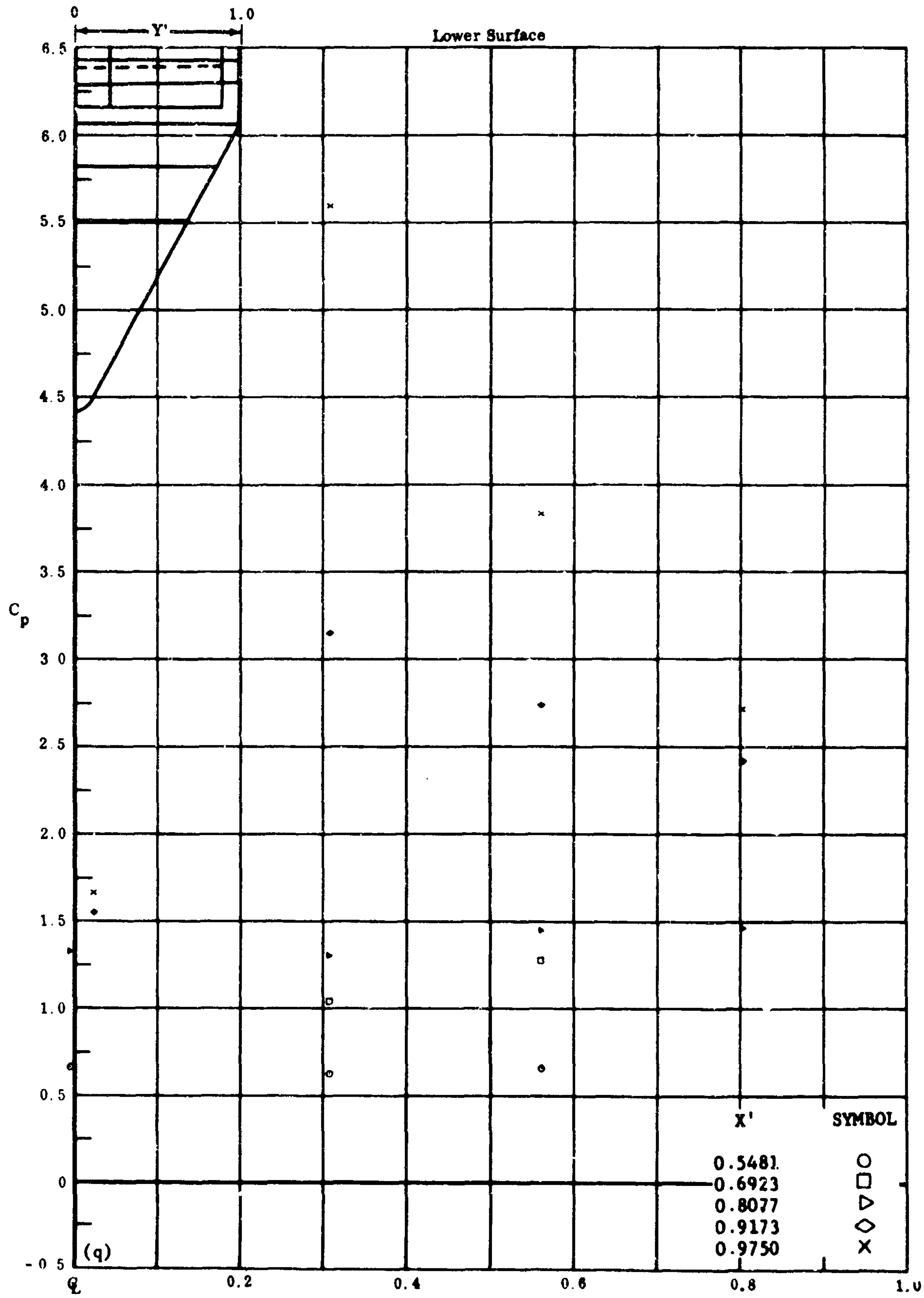

(NONDIMENSIONAL SEMISPAN DISTANCE)

Fig. 9q Configuration I, α = +30, $\delta_2 = \delta_3$ = +39

C_p vs. Y', lower surface

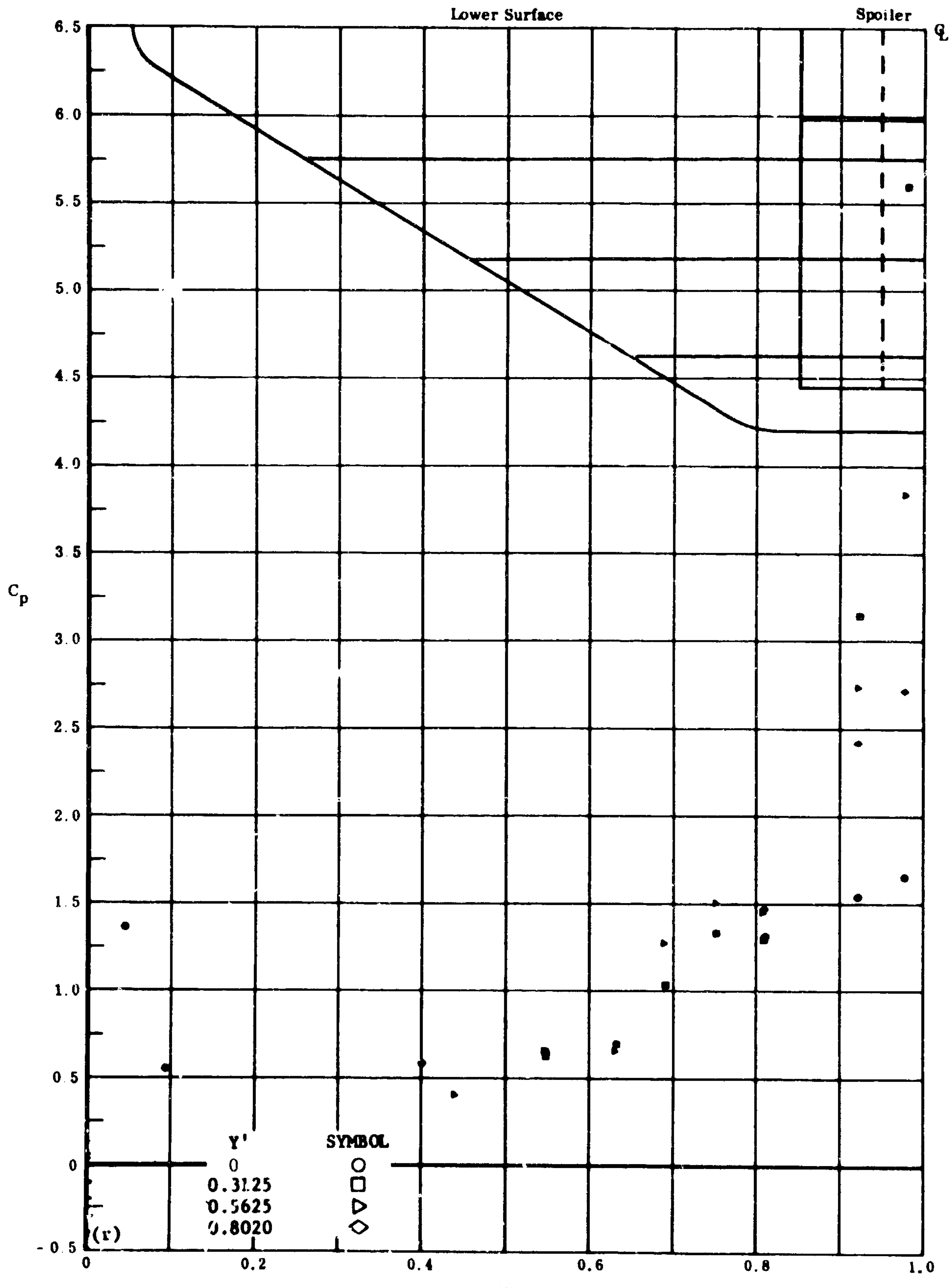

(NONDIMENSIONAL STREAMWISE DISTANCE FROM VIRTUAL APEX)

Fig 9r Configuration I, α = +30 , $\delta_2 = \delta_3$ = +39

C_p vs. X', lower surface

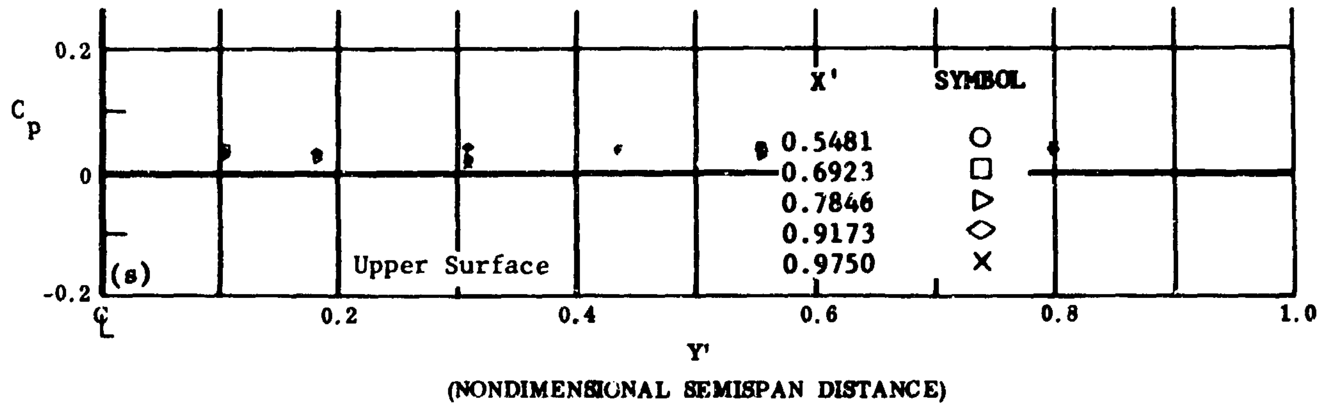

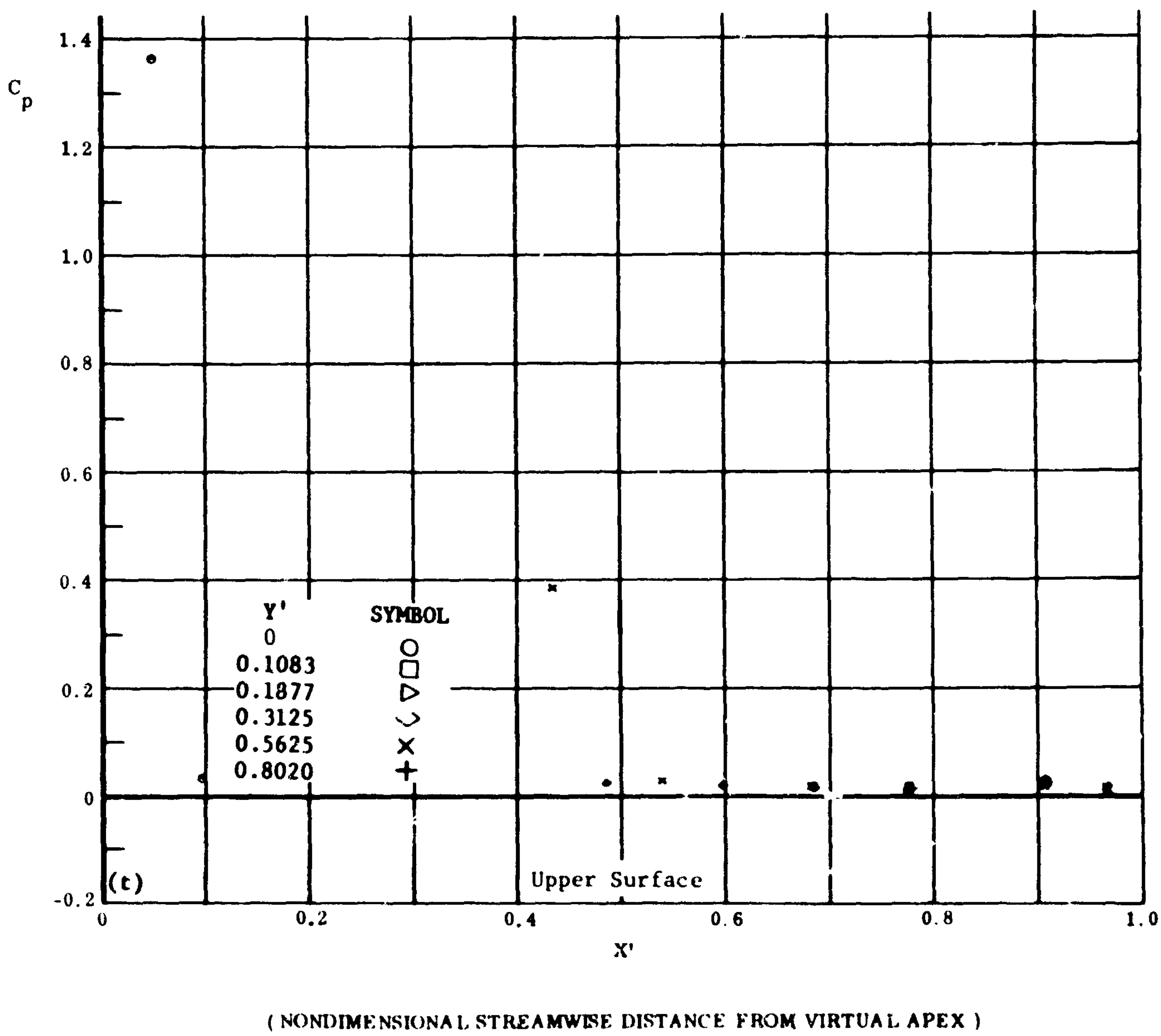

Fig. 9 Configuration I, α = +30 , $\delta_2 = \delta_3$ = +39

s) C_p vs. Y', upper surface

t) C_p vs. X', upper surface

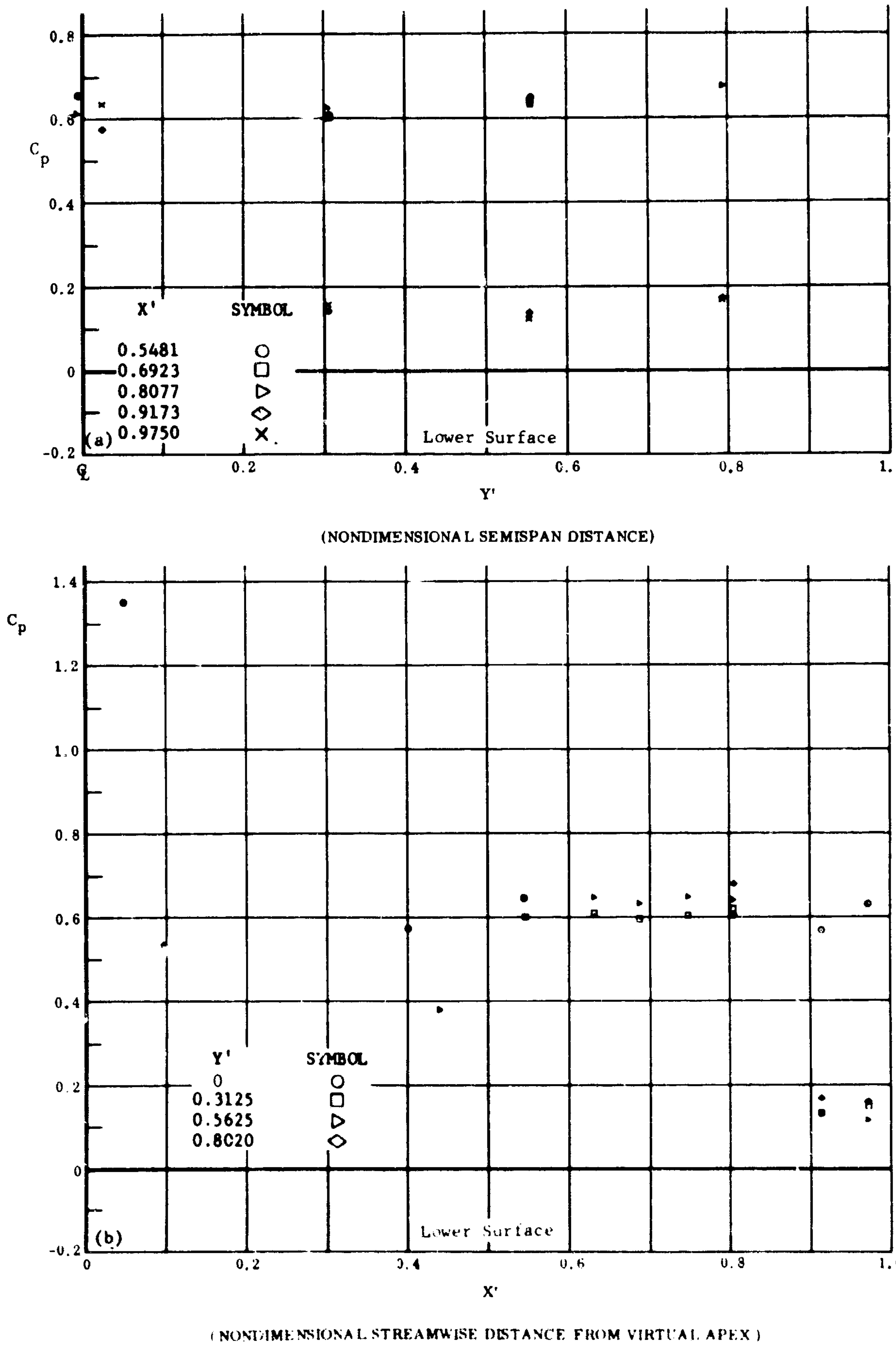

Fig. 10 Configuration I, δ_1 = +30 , $\delta_2 = \delta_3$ = -20

a) C_p vs. Y', lower surface

b) C_p vs. X', lower surface

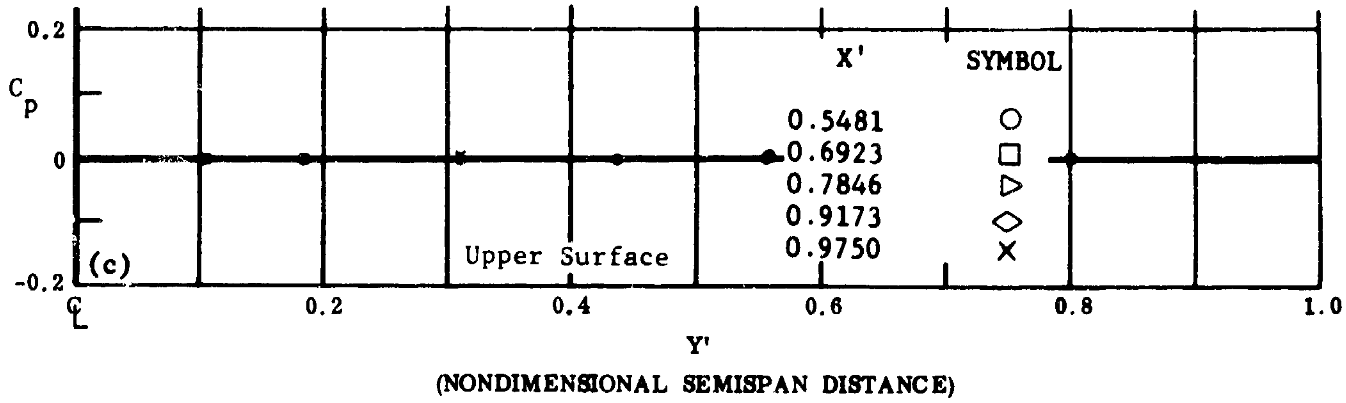

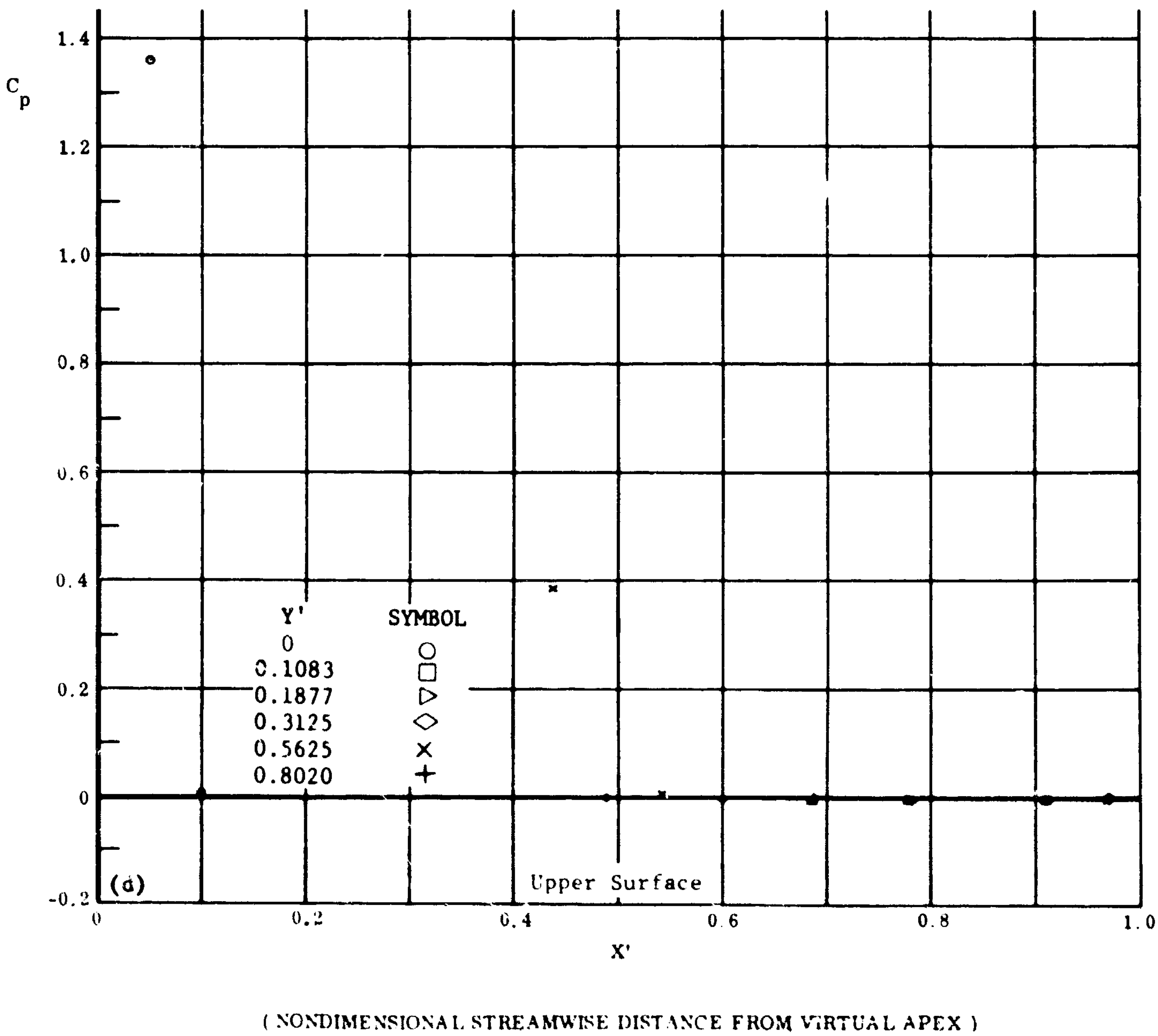

Fig. 10 Configuration I, $\alpha = +30$, $\delta_2 = \delta_3 = -20$

c) C_p vs. Y', upper surface

d) C_p vs. X', upper surface

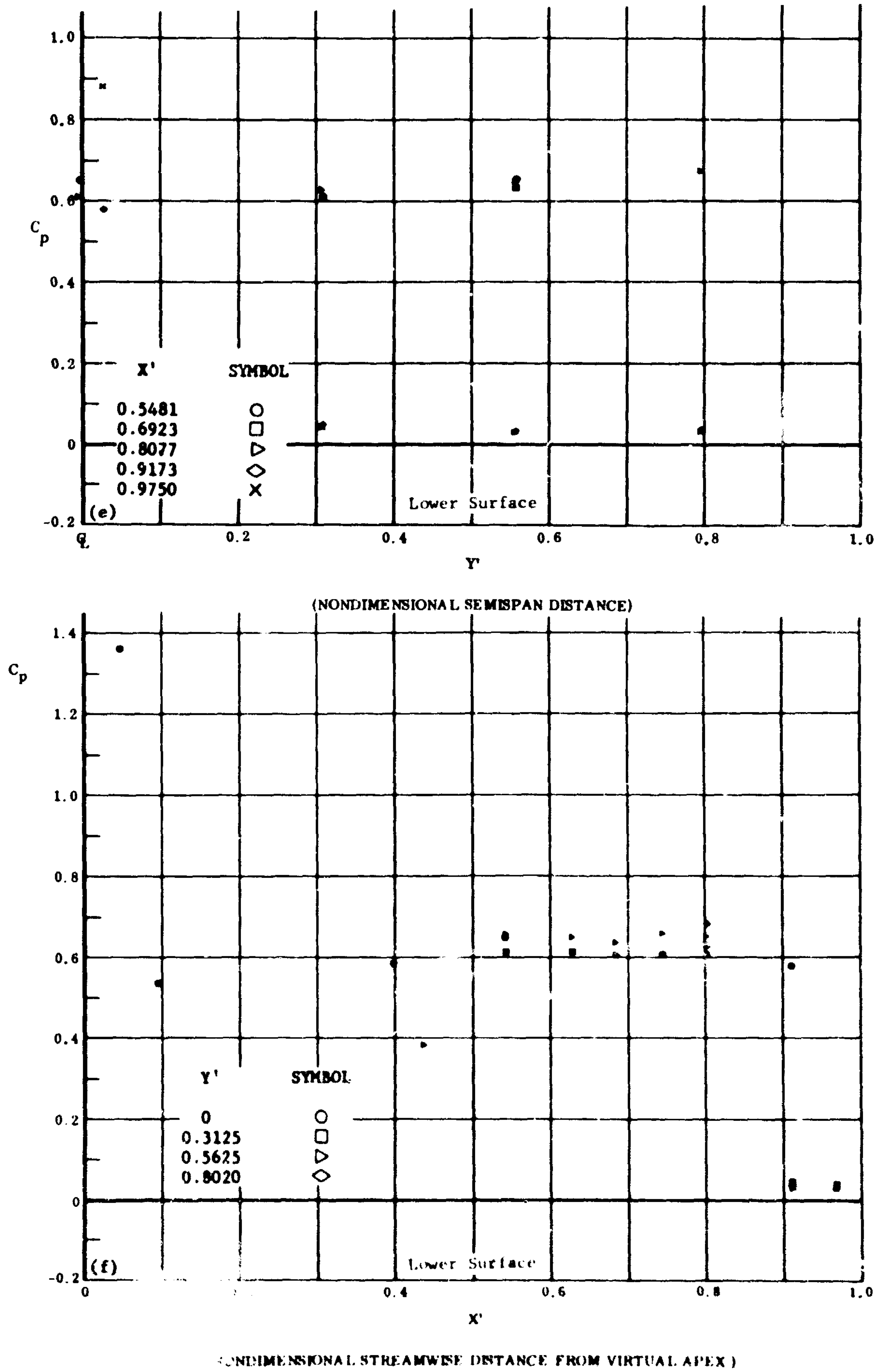

Fig. 10 Configuration I, α = +30 , δ_2 = δ_3 = -39

e) C_p vs. Y', lower surface

f) C_p vs. X', lower surface

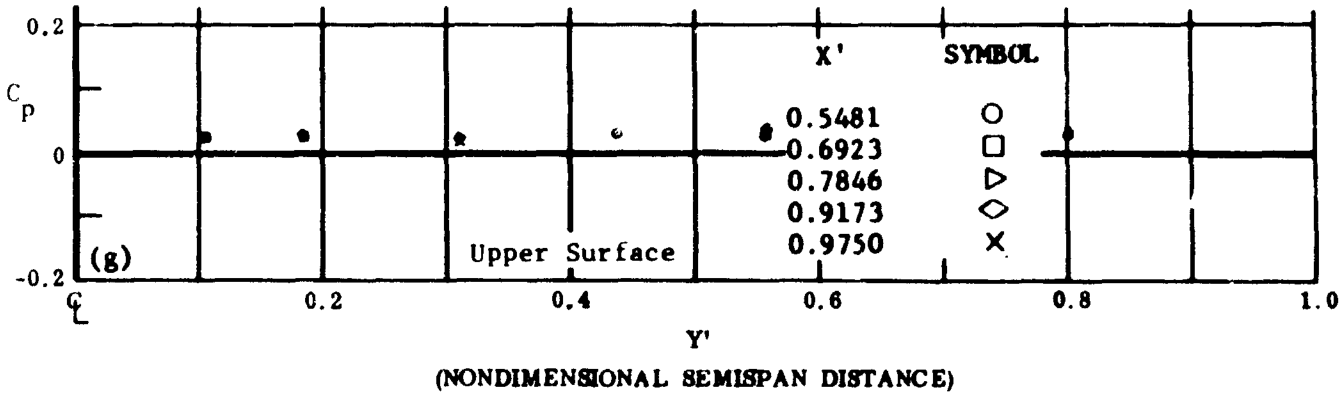

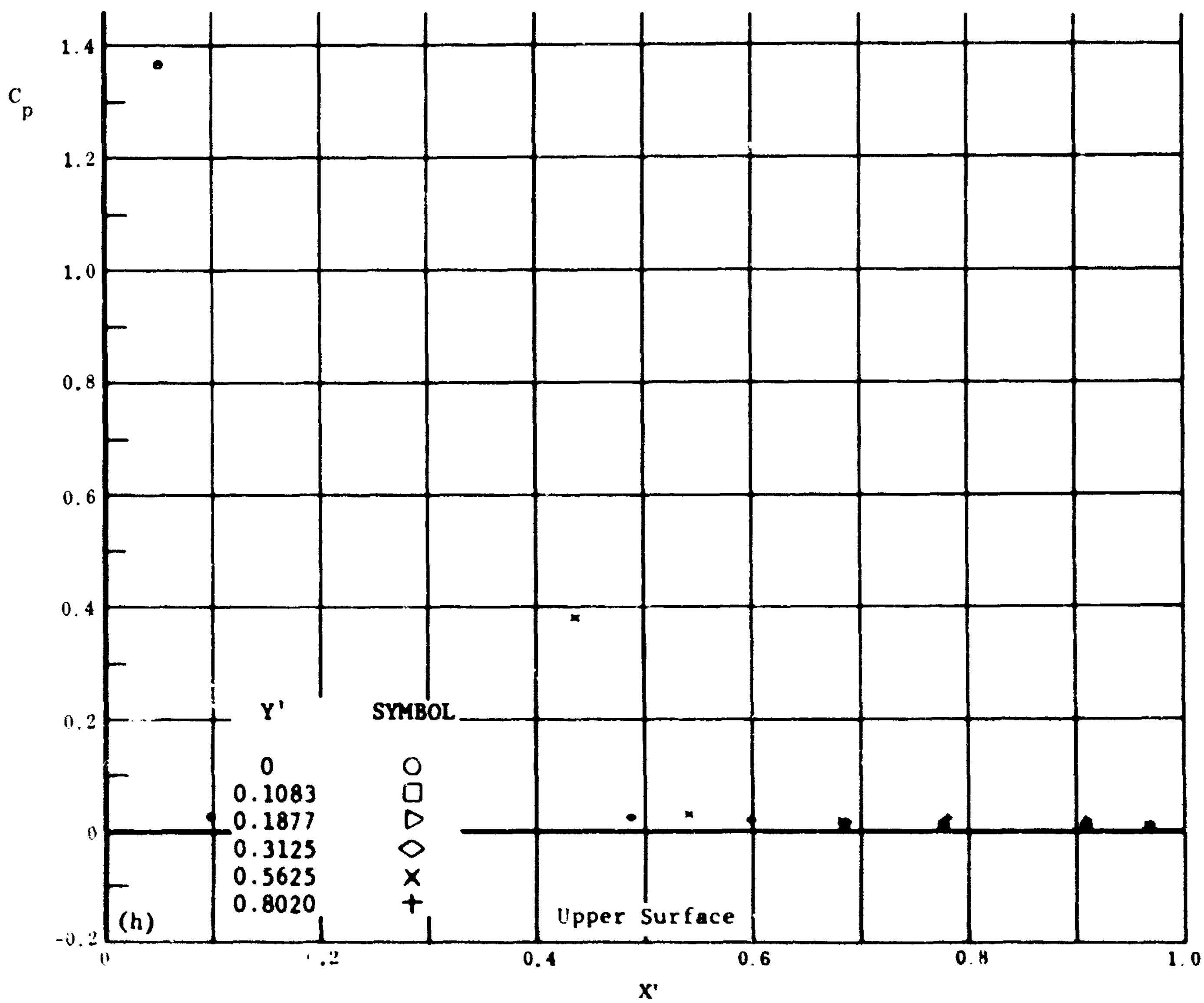

Fig. 10 Configuration I, $\alpha = +30$, $\delta_2 = \delta_3 = -39$

g) C_p vs. Y', upper surface

h) C_p vs. X', upper surface

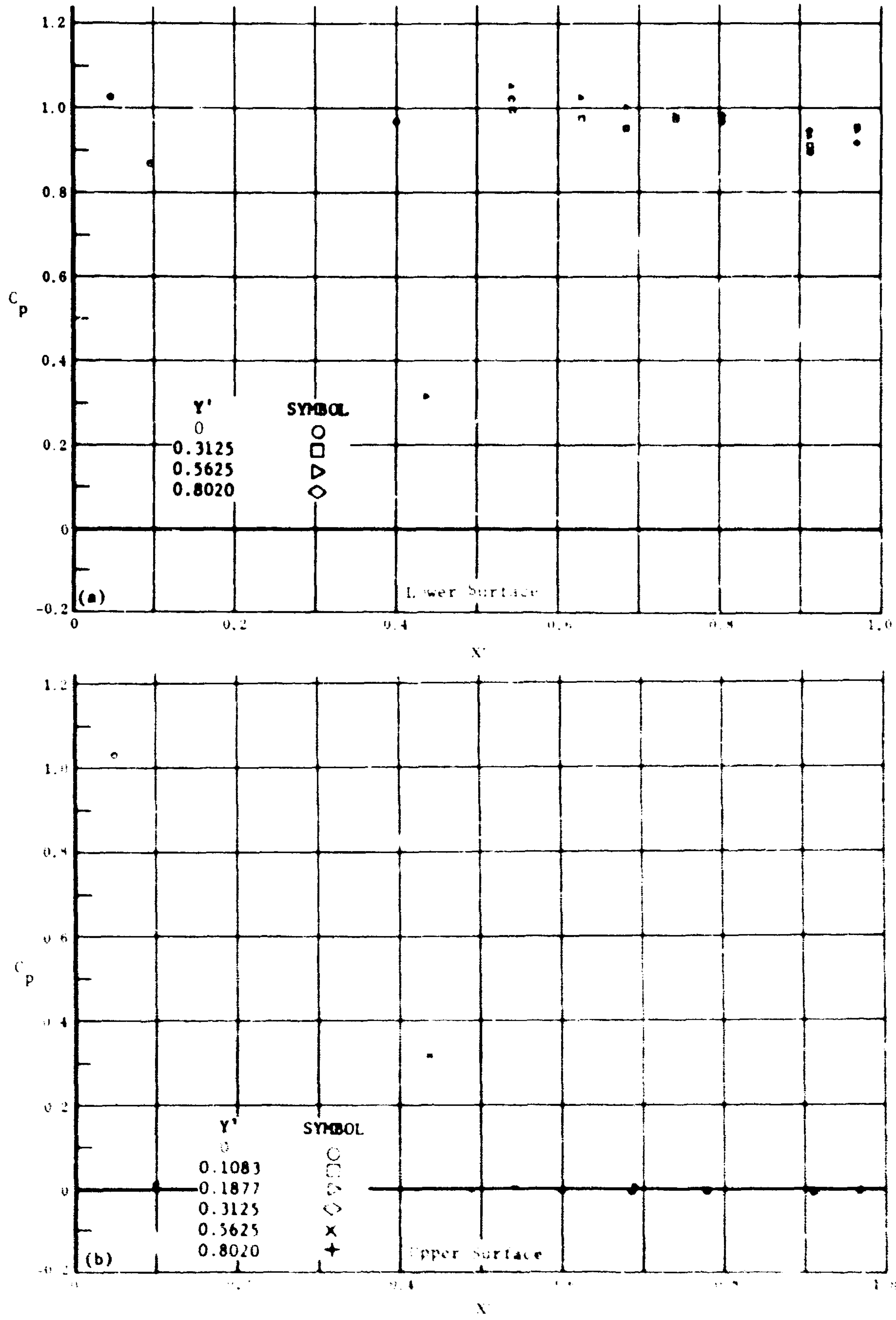

NONDIMENSIONAL STREAMWISE DISTANCE FROM VIRTUAL APEX

Fig. 11 Configuration I, [illegible] = 40 , [illegible] = [illegible] = 0

(a) C_p vs. X', lower surface

(b) C_p vs. X', upper surface

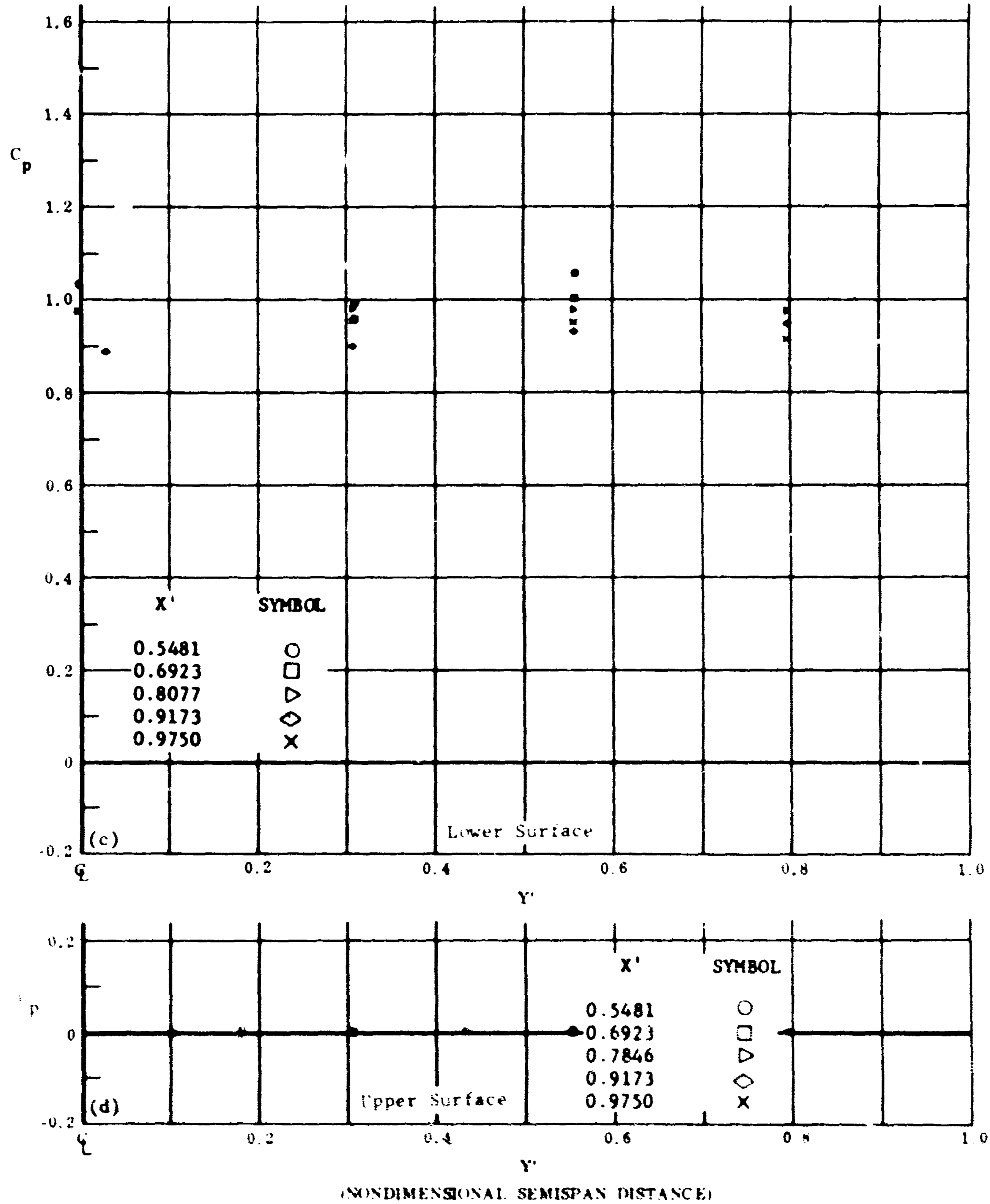

Fig. 11 Configuration I, $\delta = +40$, $\delta_2 = \delta_3 = 0$

c) C_p vs. Y', lower surface

d) C_p vs. Y', upper surface

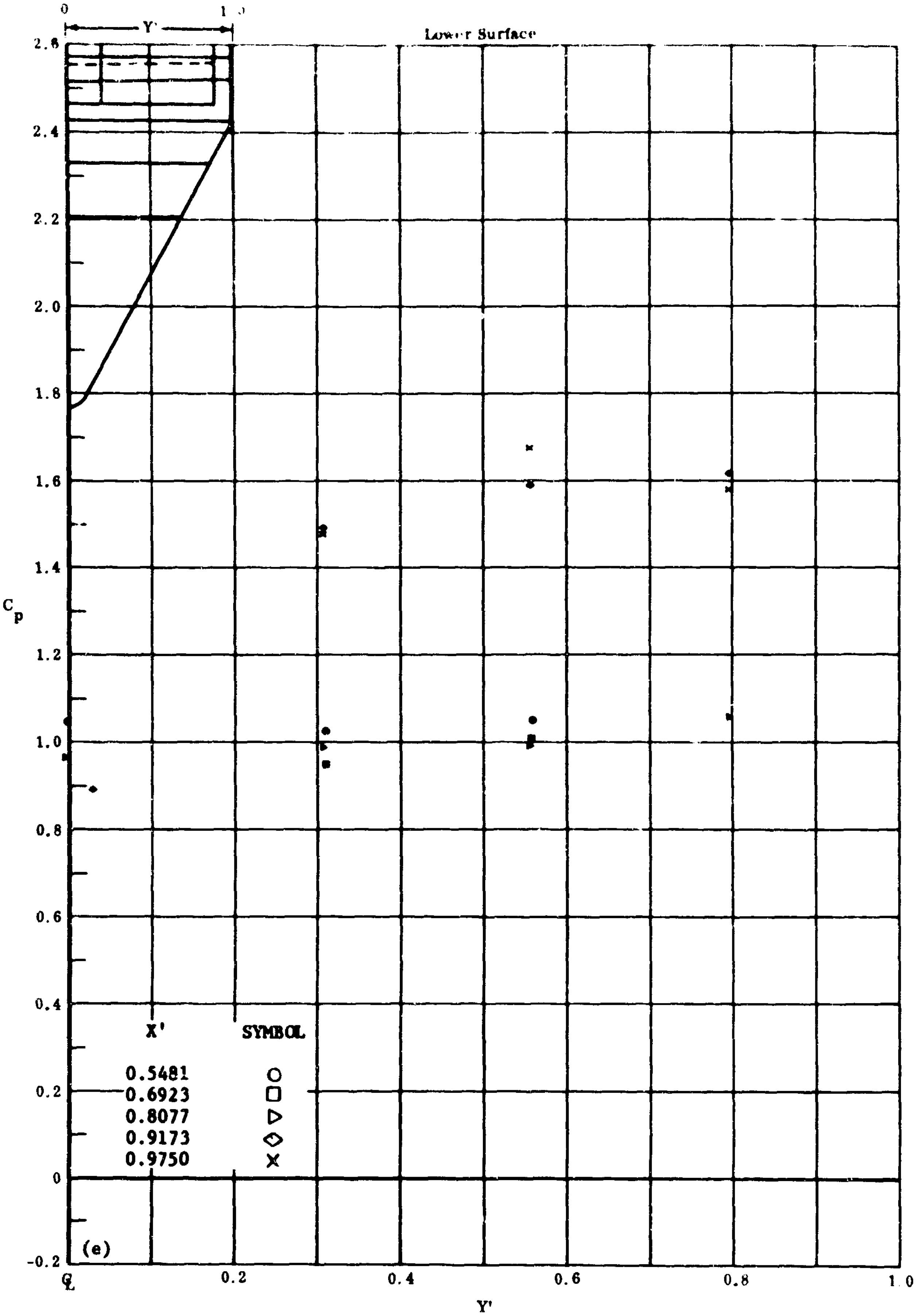

(NONDIMENSIONAL SEMISPAN DISTANCE)

Fig. 11e Configuration I, $\alpha = +40$, $\delta_2 = \delta_3 = +10$

C_p vs. Y', lower surface

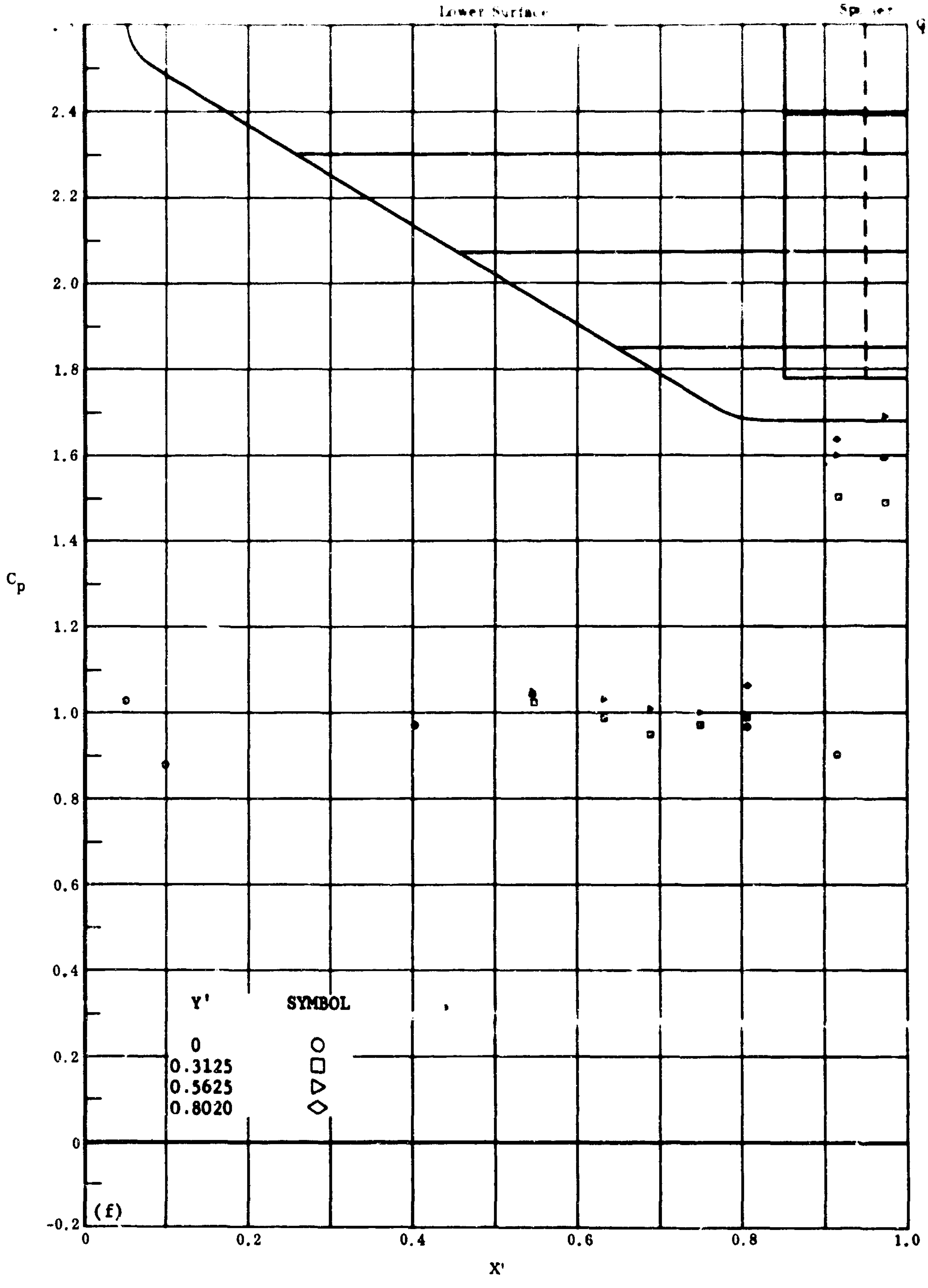

Fig. 11f Configuration I, $\alpha = +40$, $\delta_2 = \delta_3 = +10$

C_p vs. X', lower surface

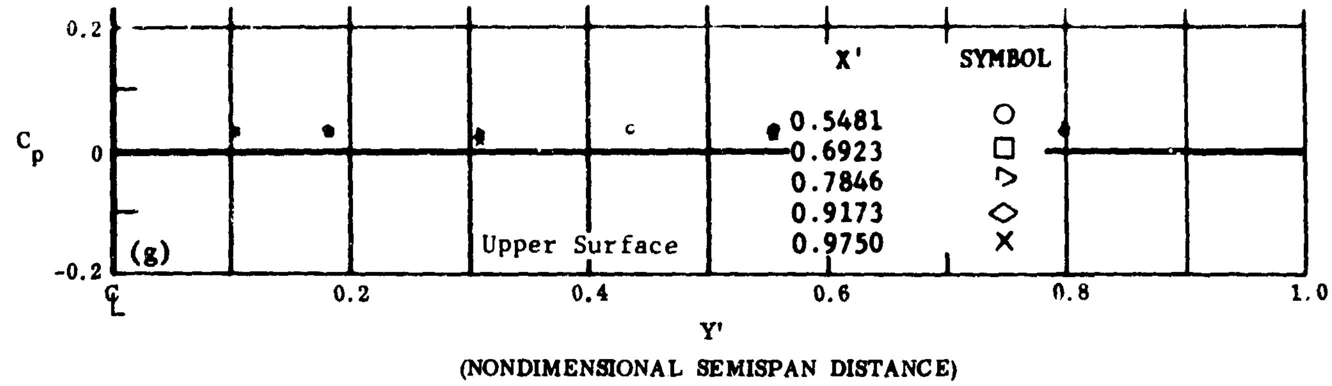

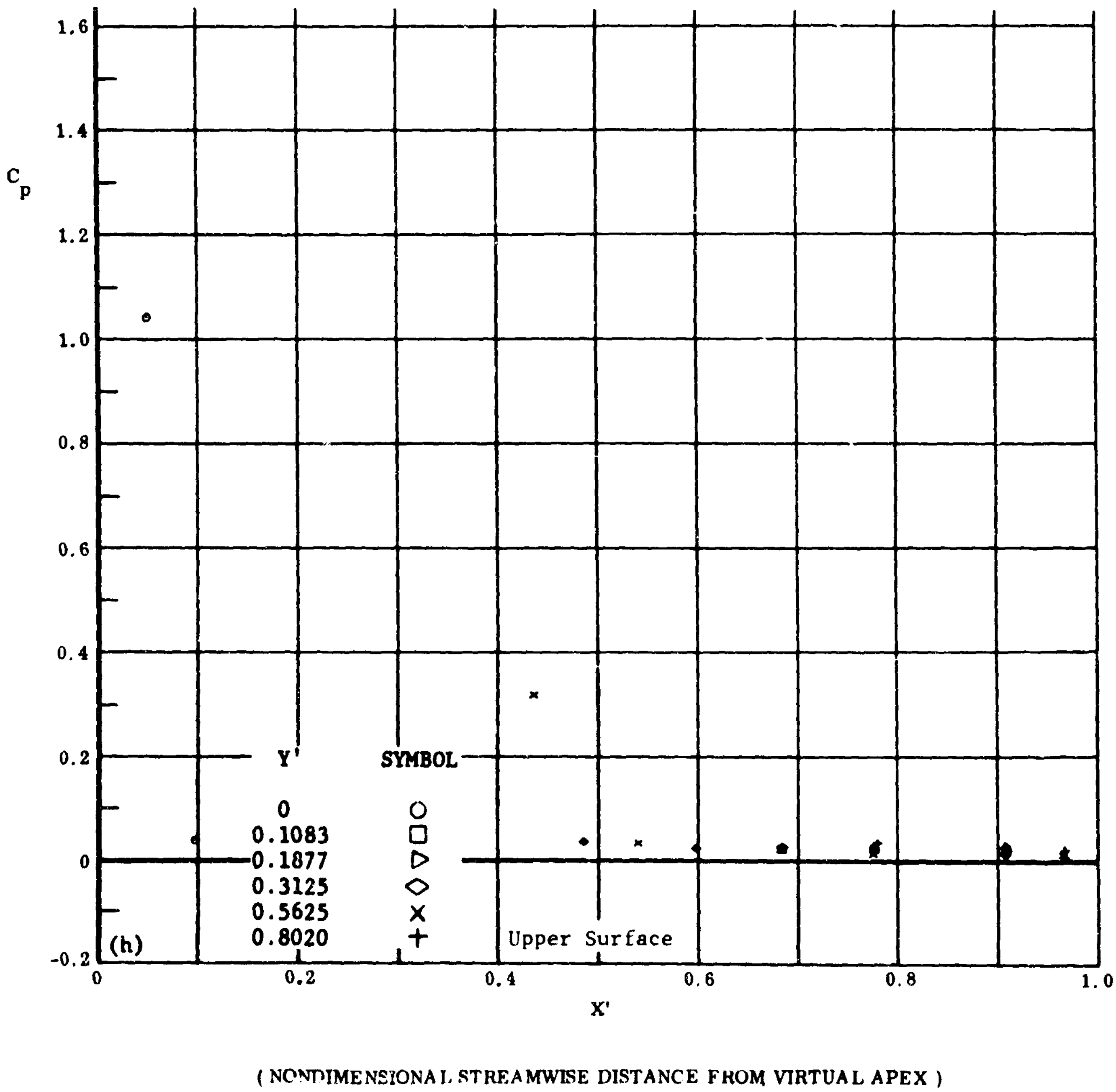

Fig. 11 Configuration I, $\alpha = +40$, $\delta_2 = \delta_3 = +10$

g) C_p vs. Y', upper surface

h) C_p vs. X', upper surface

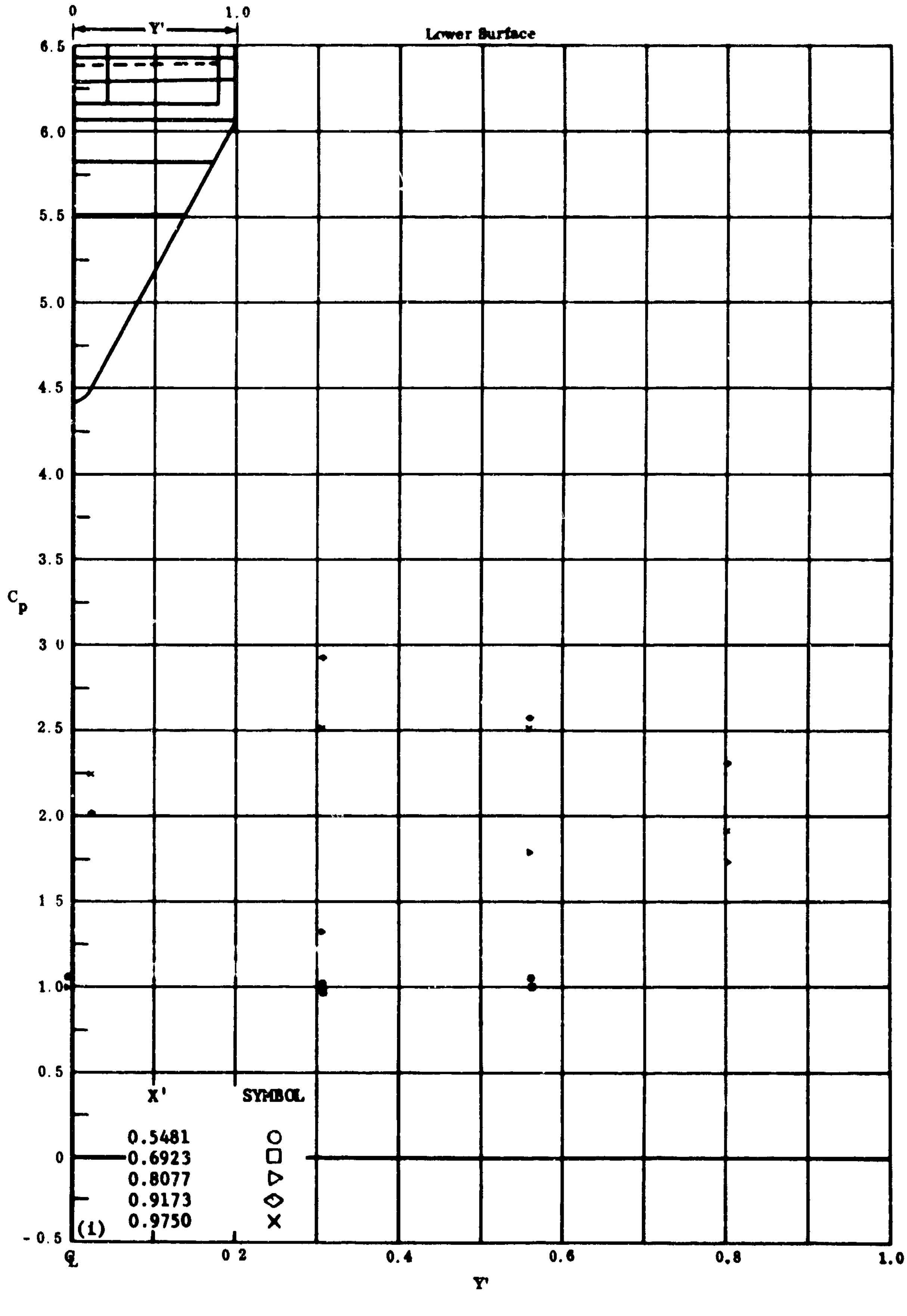

Fig. 11i Configuration I, $\alpha = +40^{\circ}$, $\delta_2 = \delta_3 = +20$

C_p vs. Y', lower surface

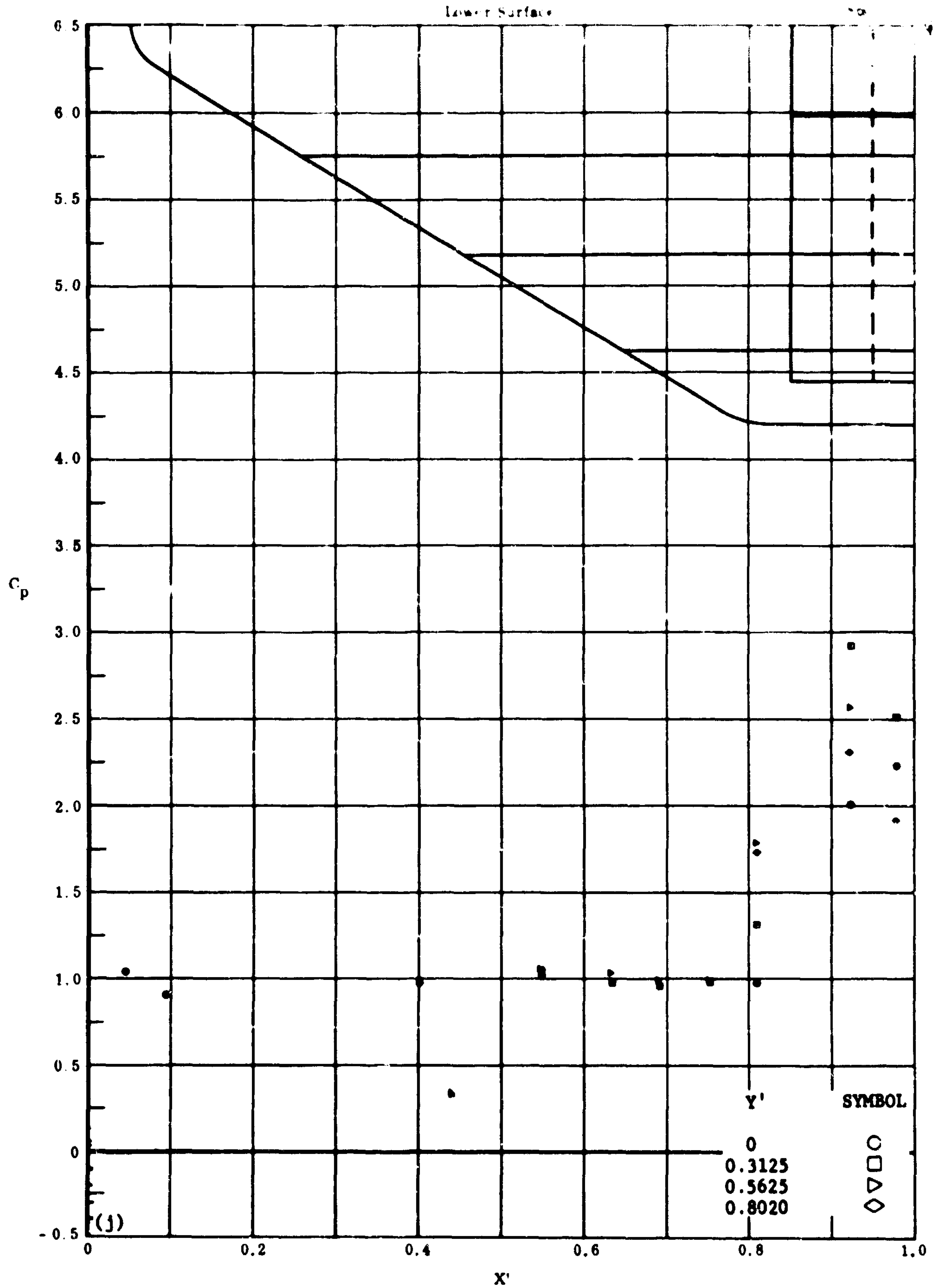

(NONDIMENSIONAL STREAMWISE DISTANCE FROM VIRTUAL APEX)

Fig 11j Configuration I, $\alpha = +40$, $\delta_2 = \delta_3 = +20$

C_p vs. X', lower surface

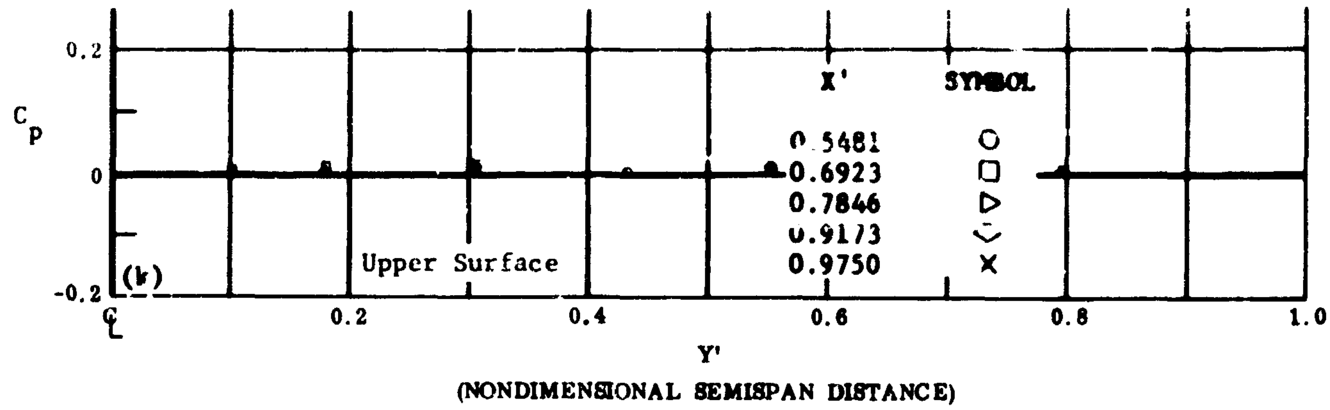

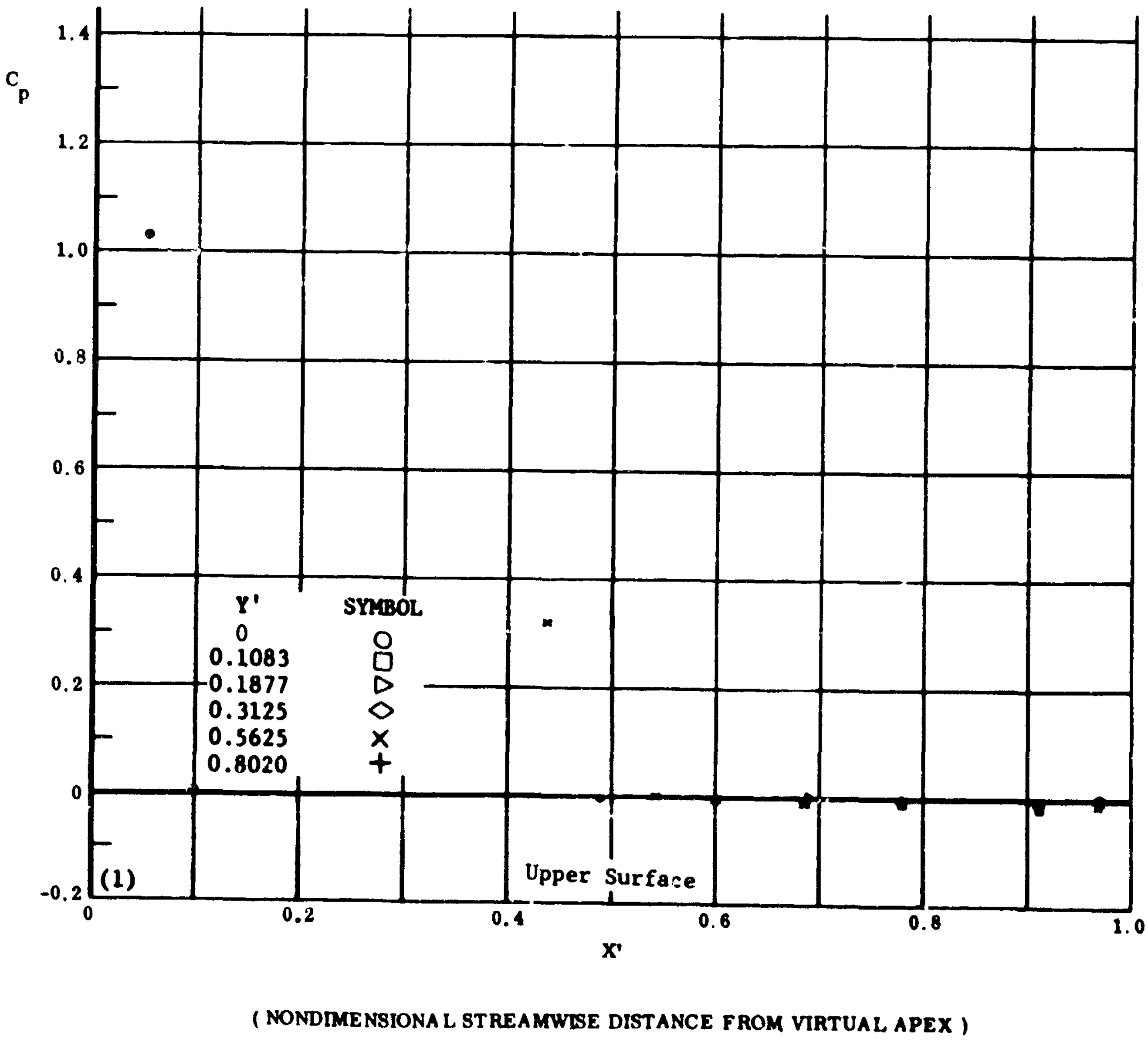

Fig. 11 Configuration I, $\alpha = +40$, $\delta_2 = \delta_3 = +20$

k) C_p vs. Y', upper surface

1) C_p vs. X', upper surface

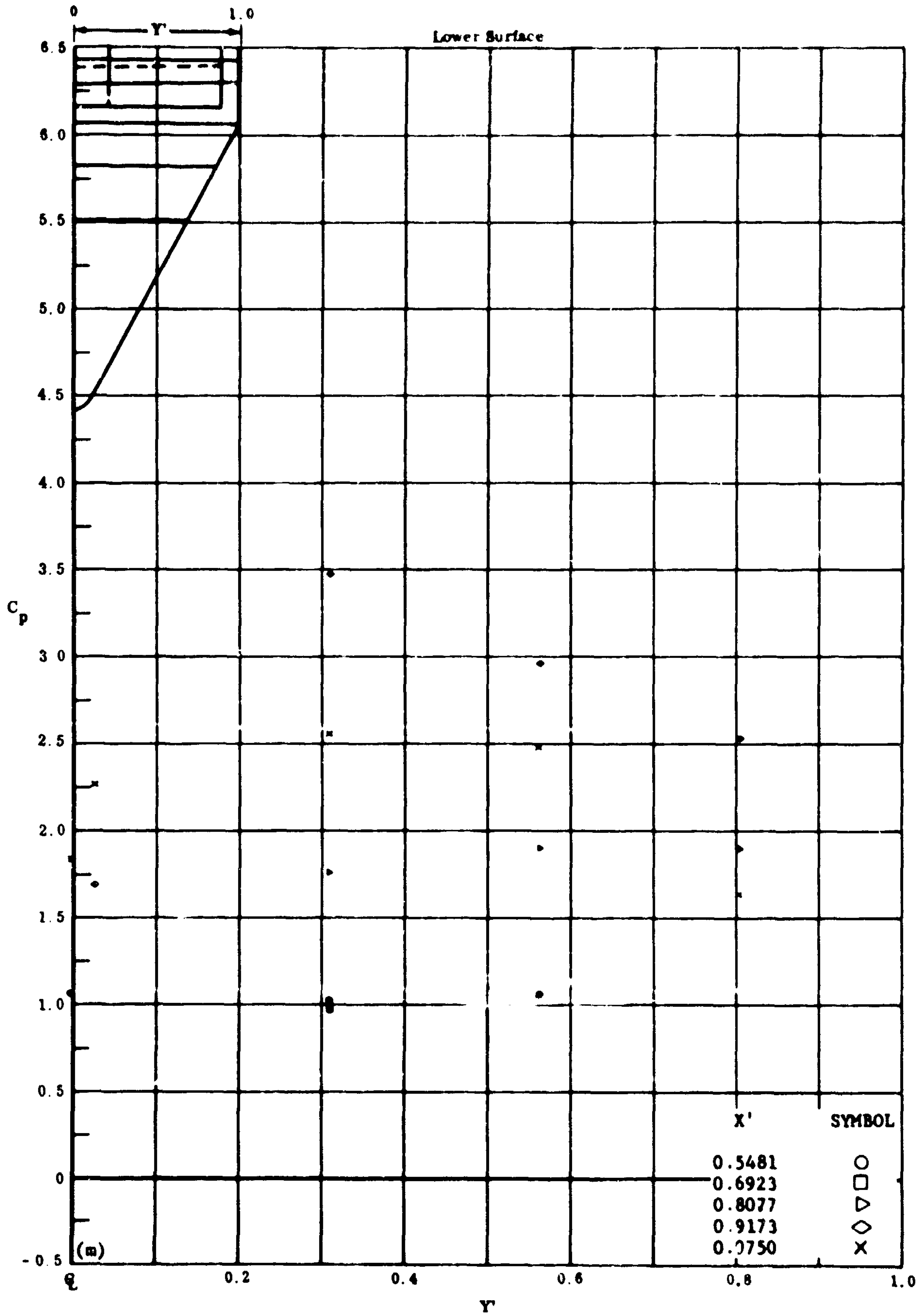

(NONDIMENSIONAL SEMISPAN DISTANCE)

Fig. 11m Configuration I, $\alpha = +40$, $\delta_2 = \delta_3 = +30$

C_p vs. Y', lower surface

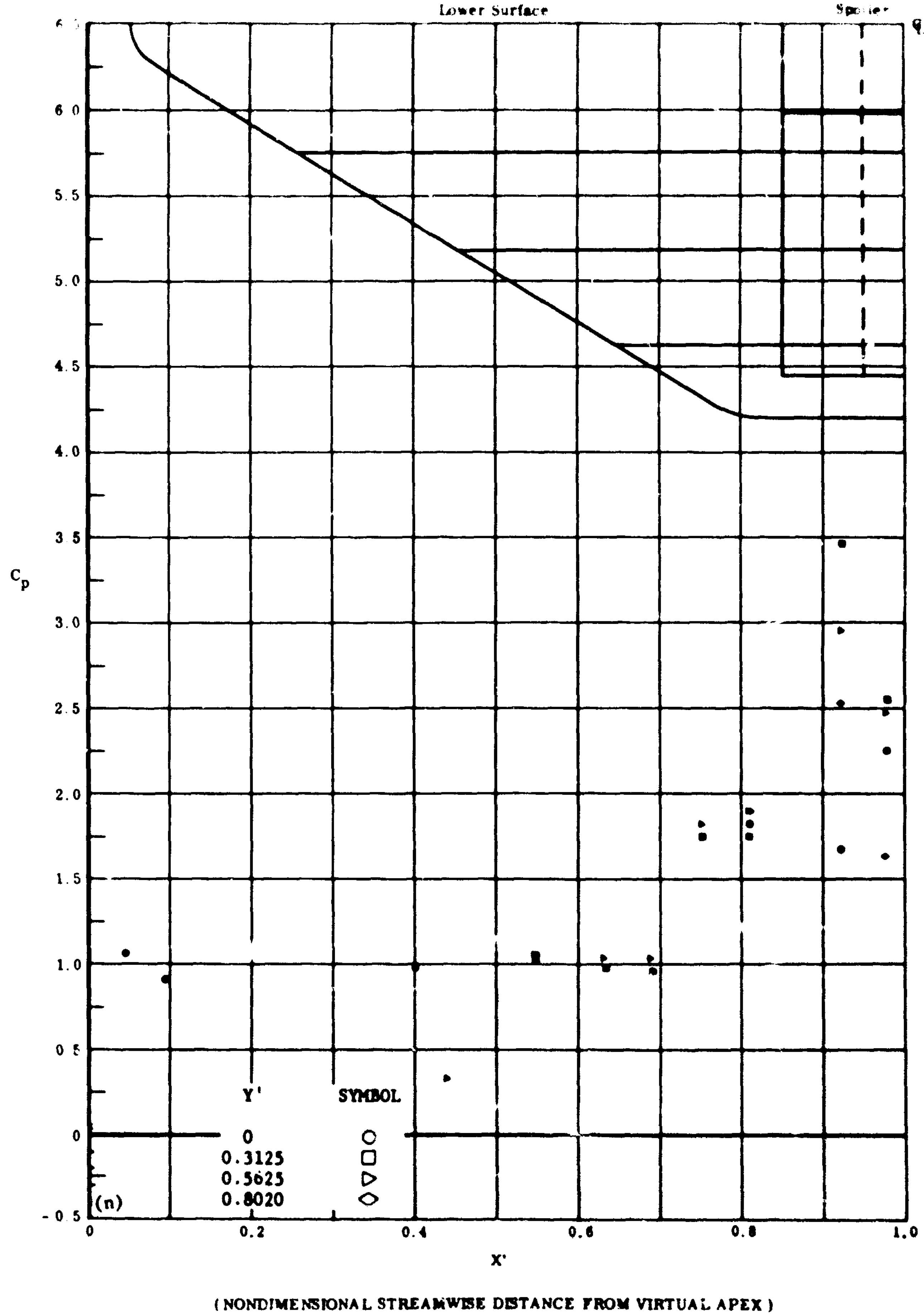

Fig. 11n Configuration I, $\alpha = +40$, $\delta_2 = \delta_3 = +30$

C_p vs. X', lower surface

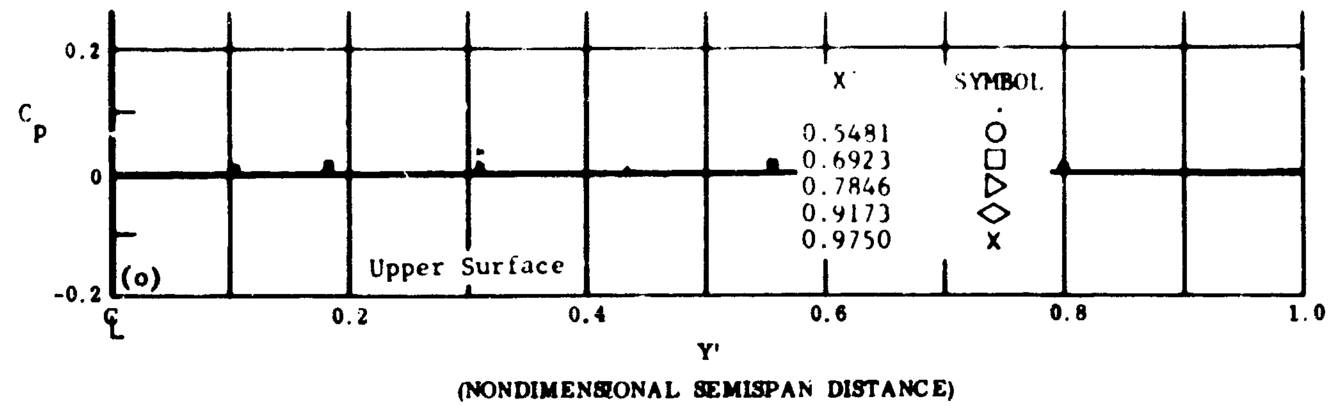

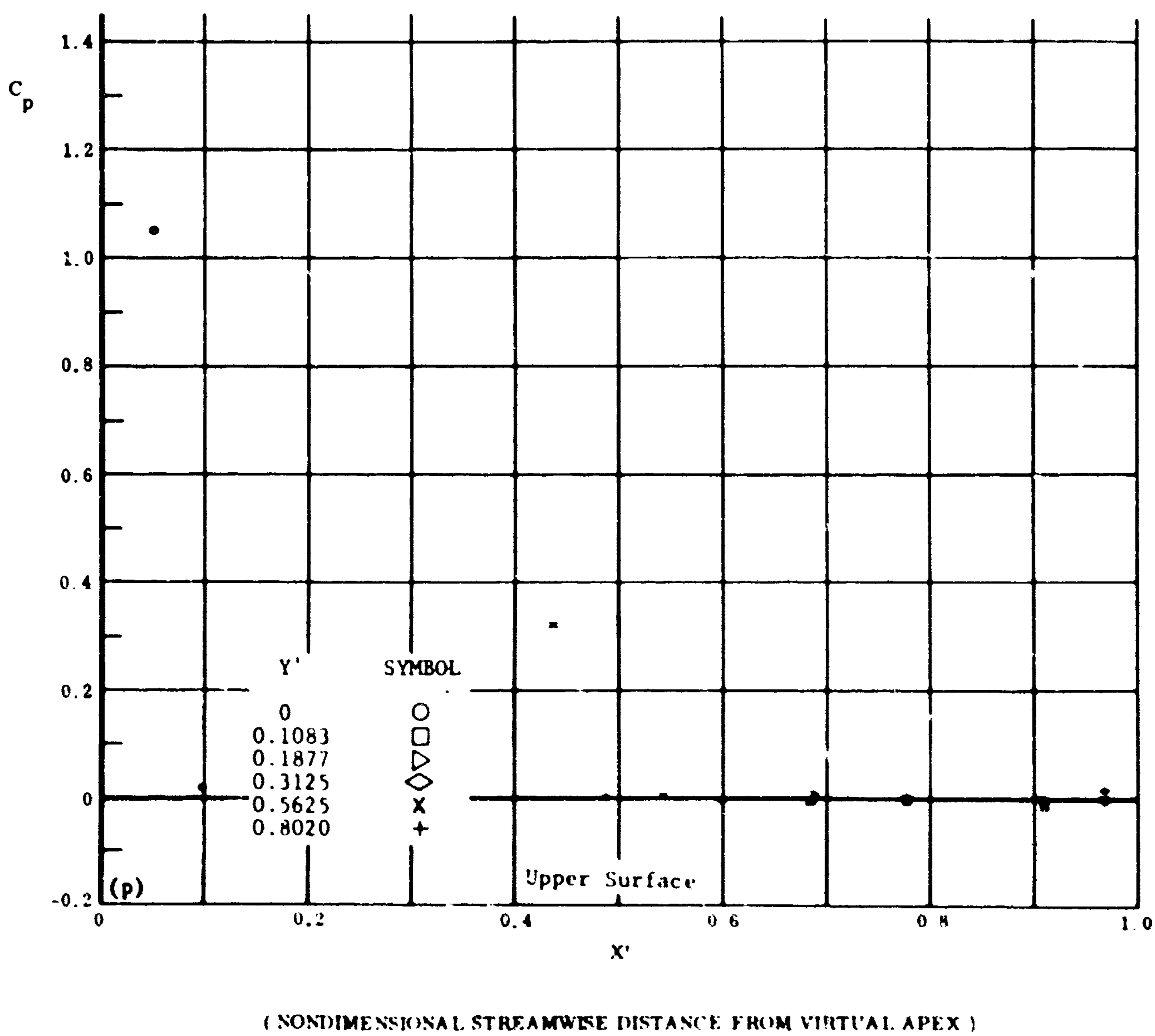

Fig. 11 Configuration I $\iota = +40$, $\delta_2 = \delta_3 = +30$

o) C_p vs. Y', upper surface

p) C_p vs. X', upper surface

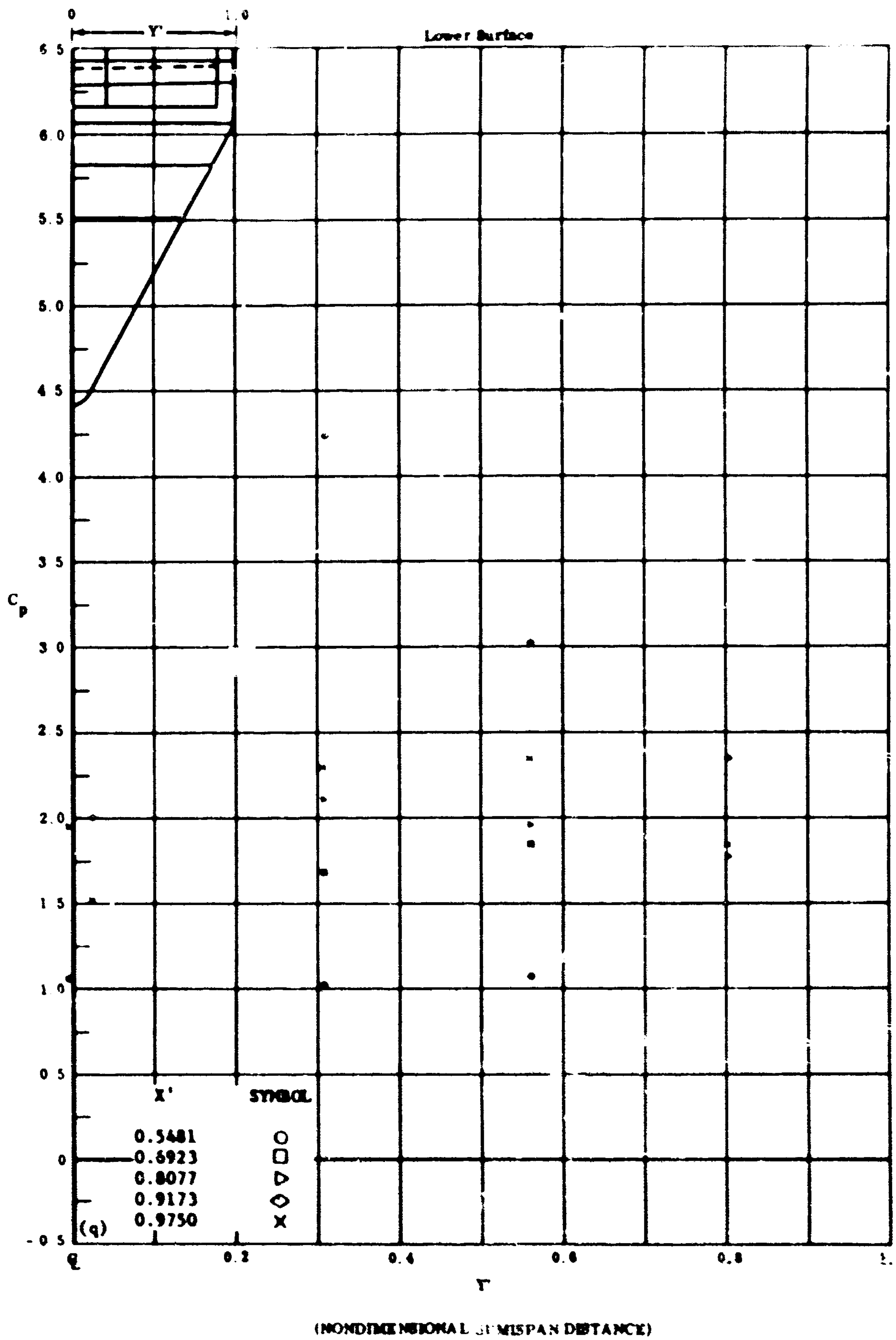

Fig. 11q Configuration I, $\alpha = +40$, $\delta_2 = \delta_3 = +39$

C_p vs. Y', lower surface

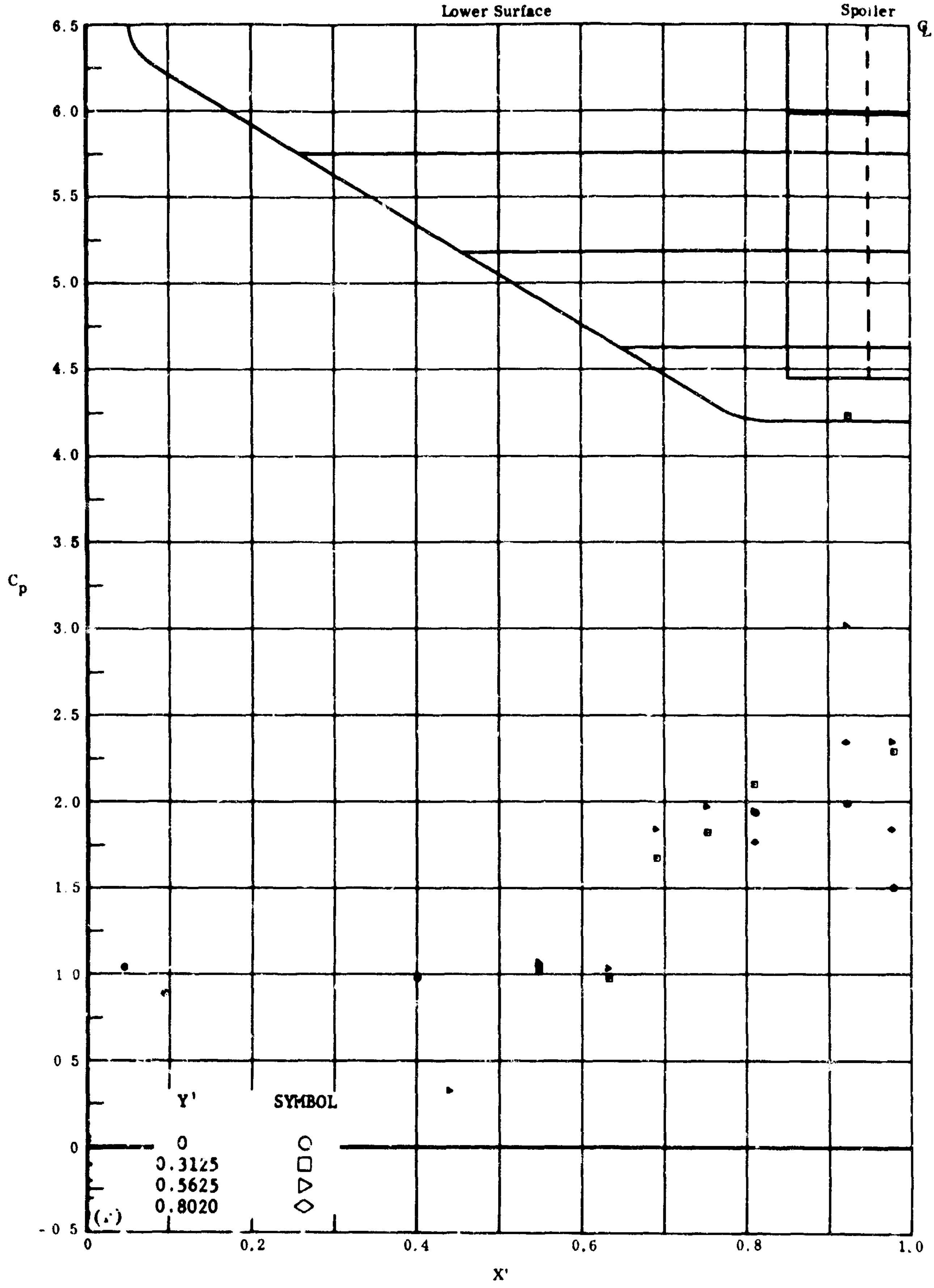

(NONDIMENSIONAL STREAMWISE DISTANCE FROM VIRTUAL APEX)

Fig. 11r Configuration I, ι = +40 , $\delta_2 = \delta_3$ = +39

C_p vs. X', lower surface

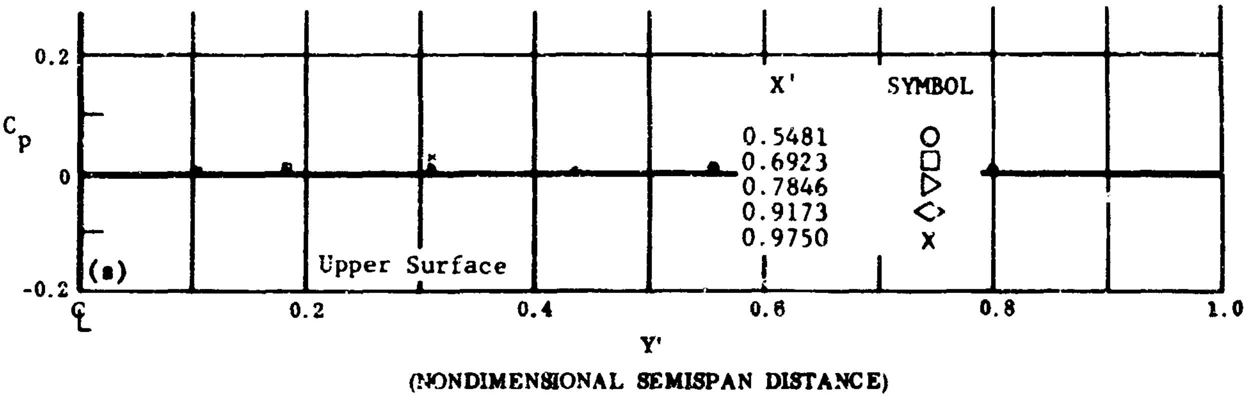

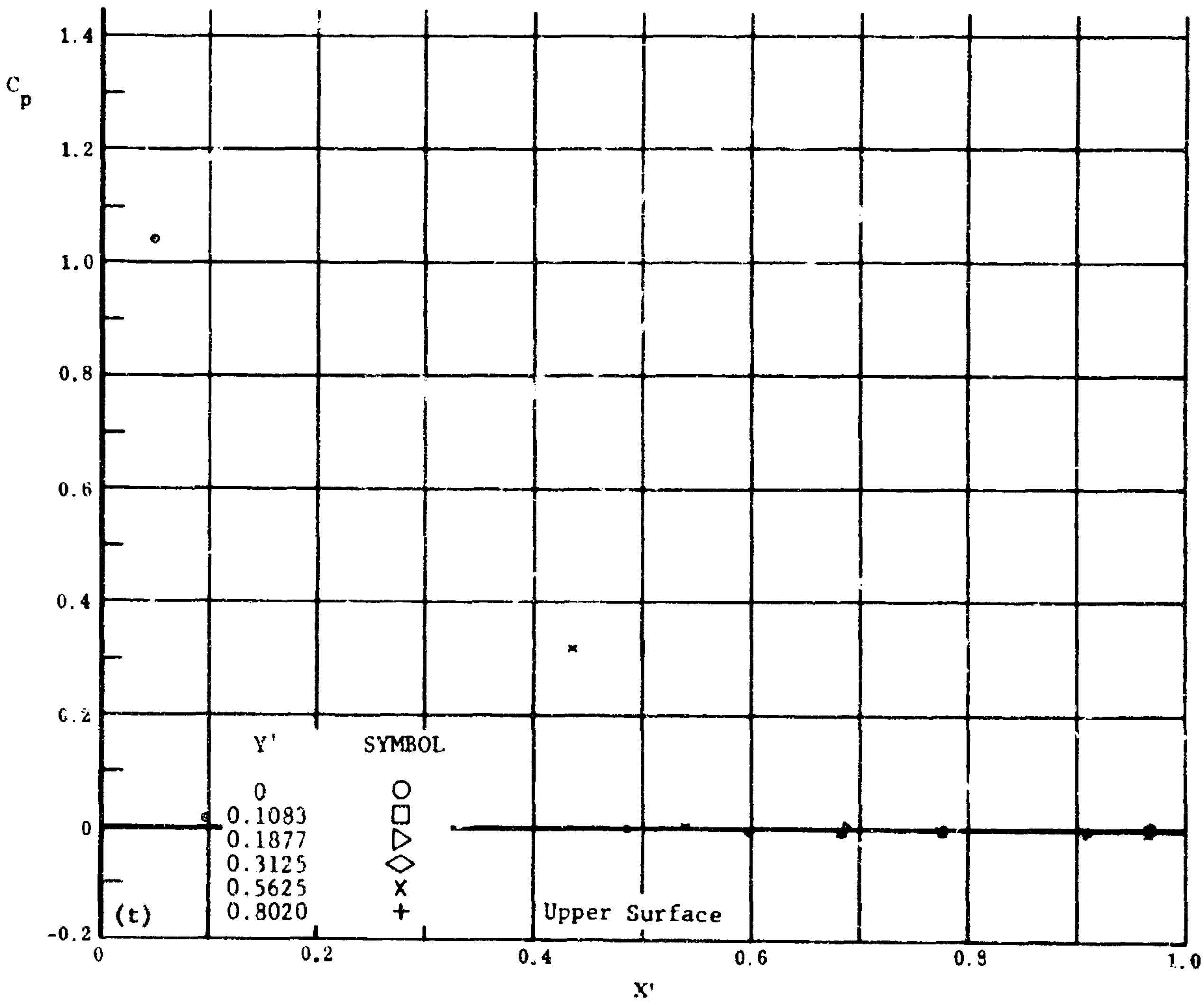

(NONDIMENSIONAL STREAMWISE DISTANCE FROM VIRTUAL APEX)

Fig. 11 Configuration I, $\alpha = +40$, $\delta_2 = \delta_3 = +39$

s) C_p vs. Y', upper surface

t) C_p vs. X', upper surface

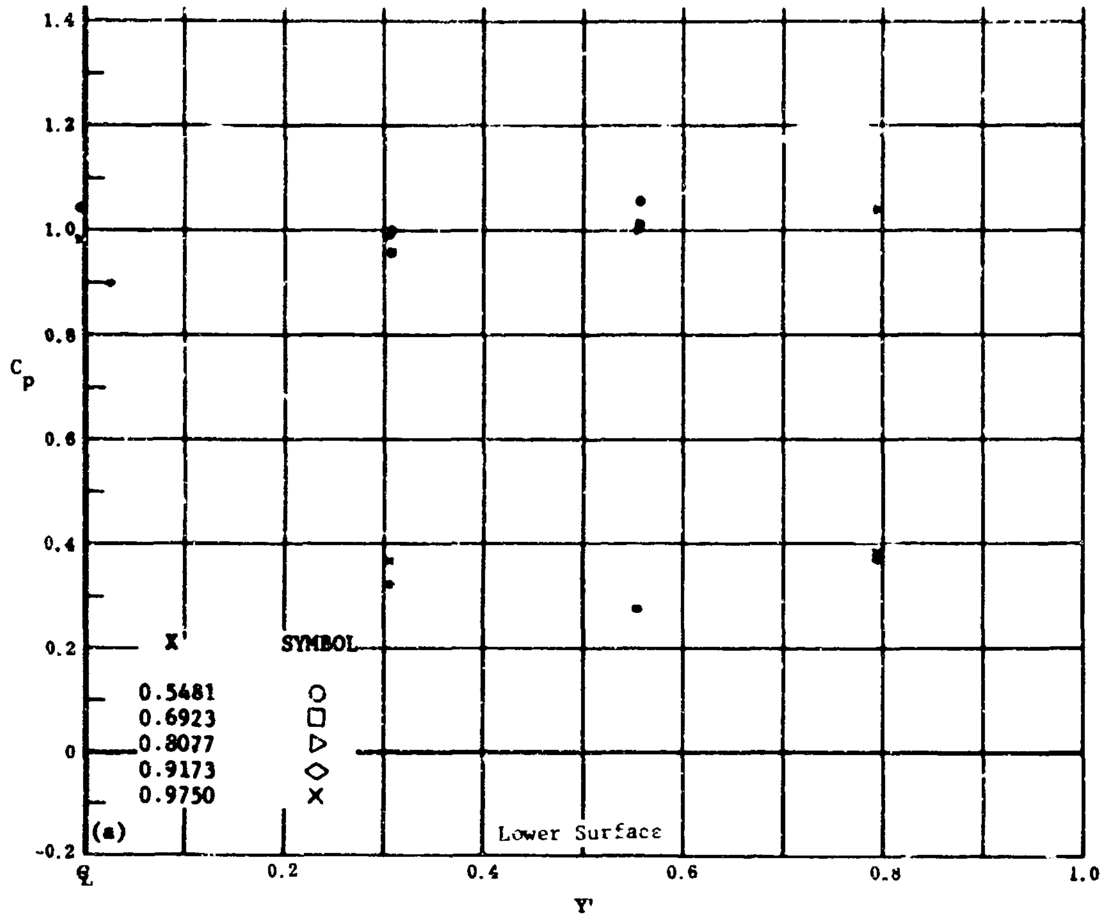

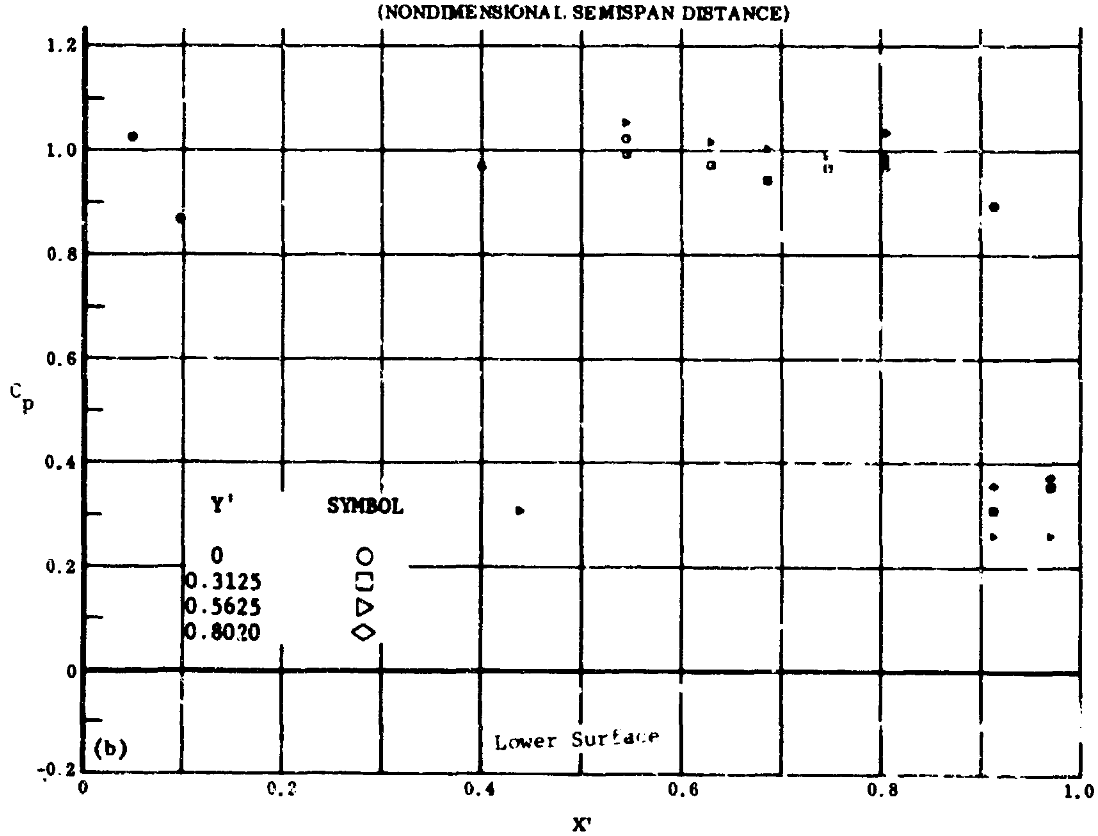

Fig. 12 Configuration I, $\alpha = +40$, $\delta_2 = \delta_3 = -20$

a) C_p vs. Y', lower surface

b) C_p vs. X', lower surface

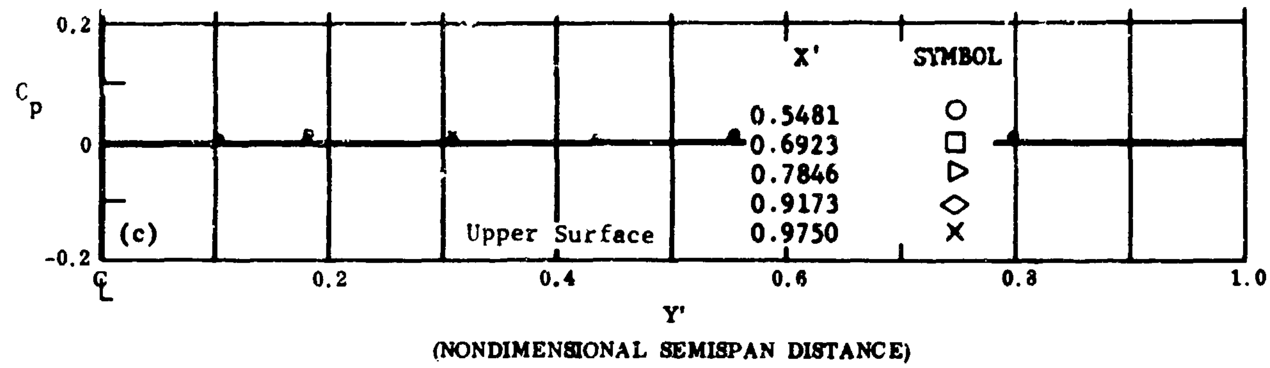

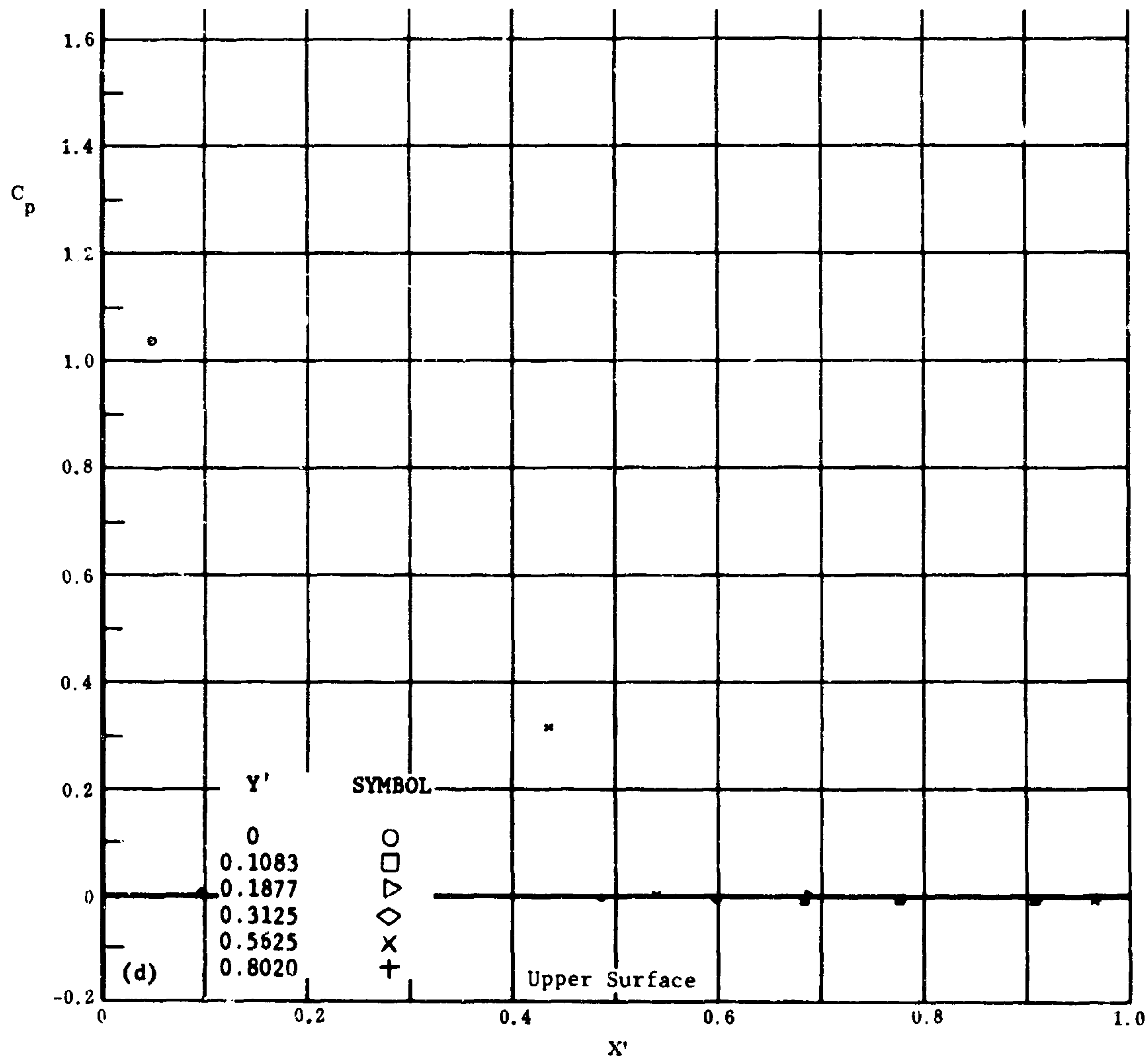

(NONDIMENSIONAL STREAMWISE DISTANCE FROM VIRTUAL APEX)

Fig. 12 Configuration I, $\alpha = +40$, $\delta_2 = \delta_3 = -20$

c) C_p vs. Y', upper surface

d) C_p vs. X', upper surface

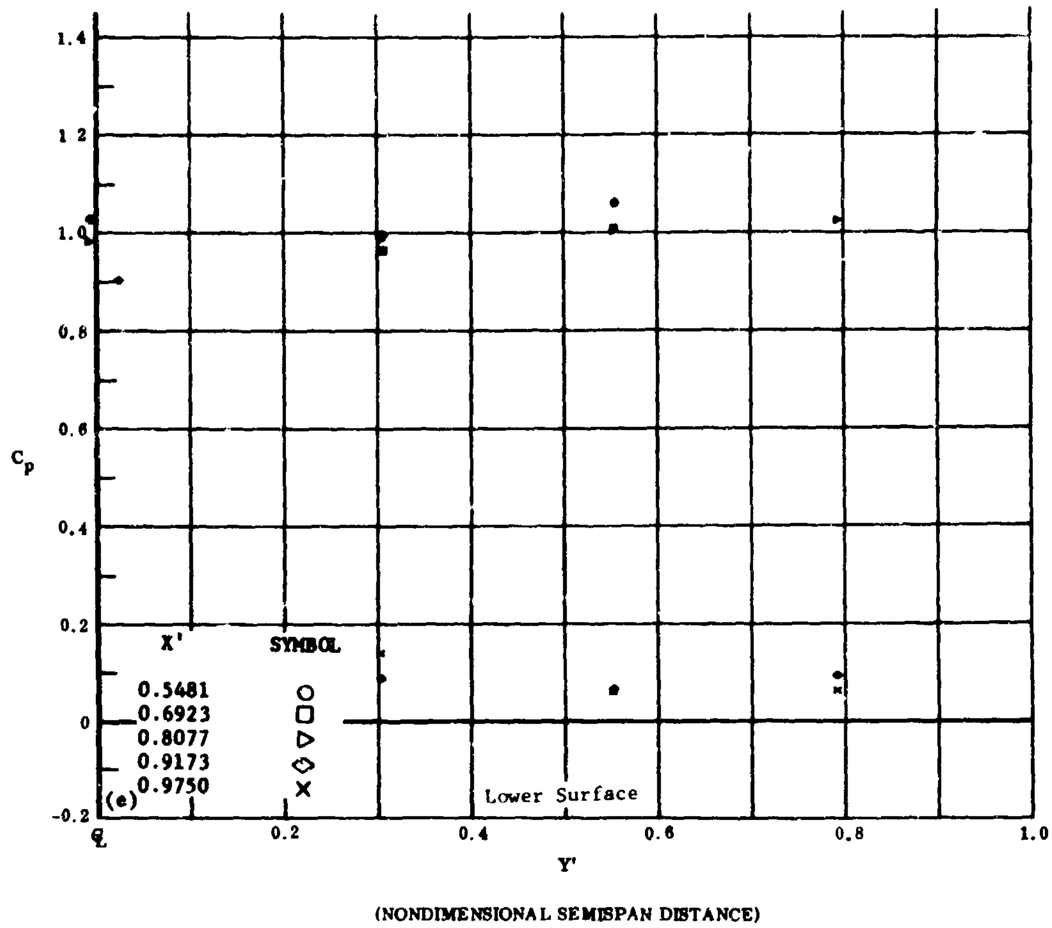

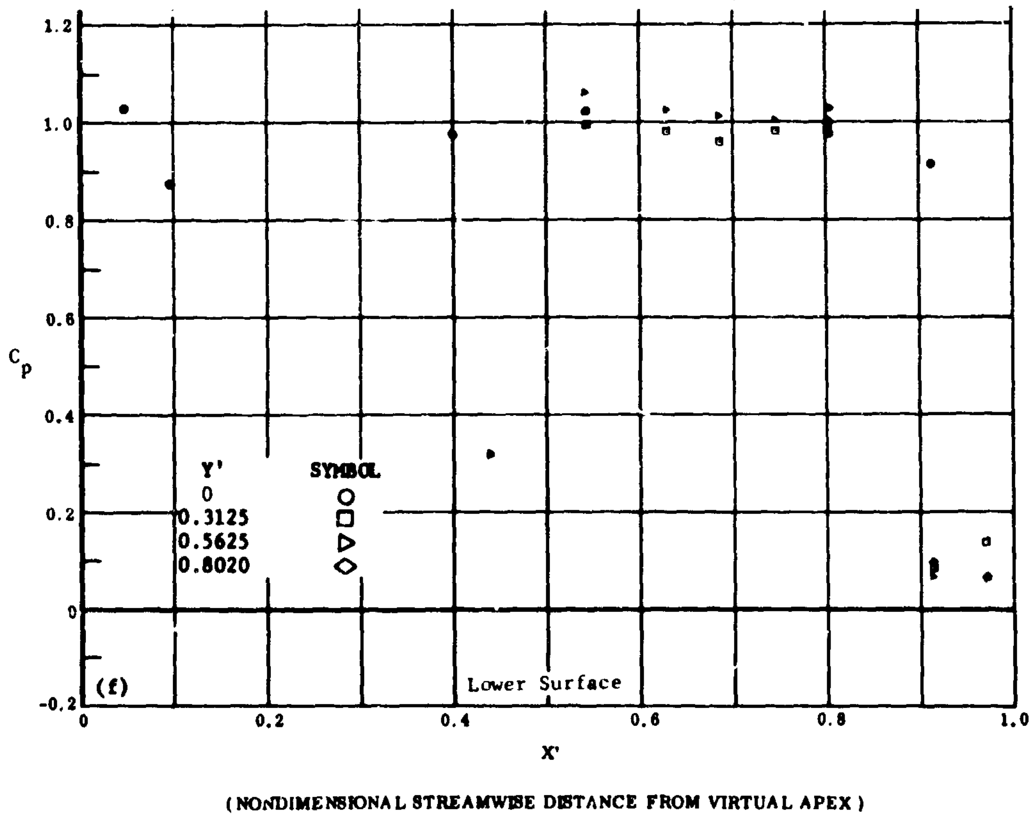

Fig. 12 Configuration I, α = +40 , $\delta_2 = \delta_3 = -39$

e) C_p vs. Y', lower surface

f) C_p vs. X', lower surface

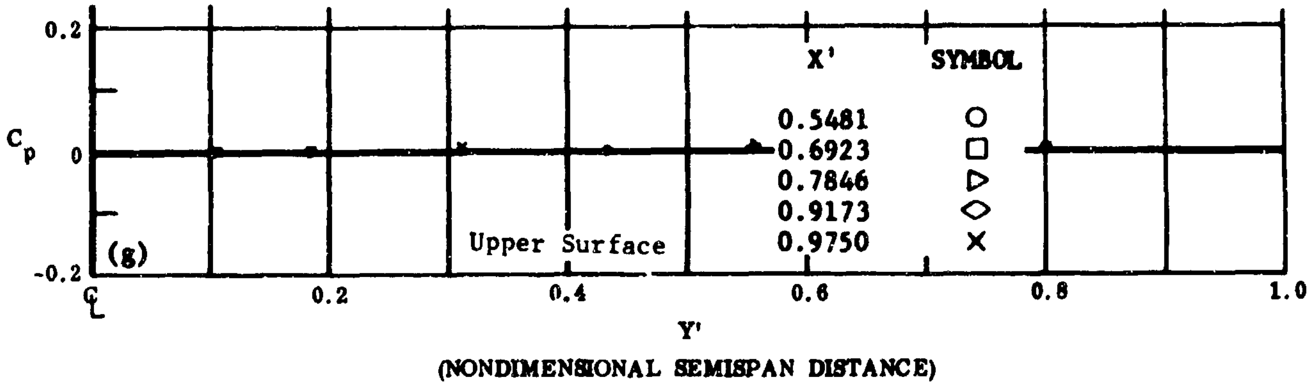

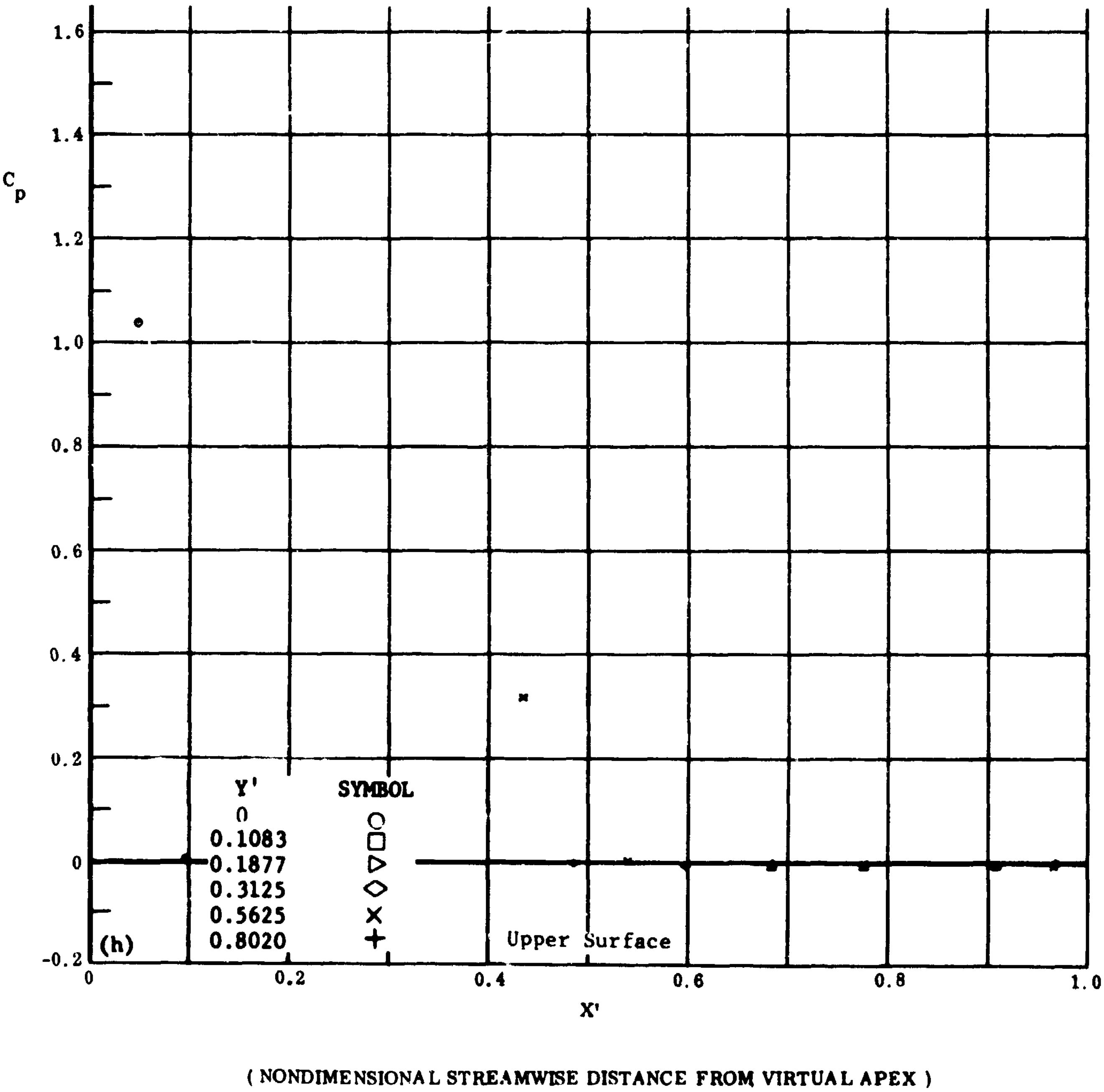

Fig. 12 Configuration I, $\alpha = +40$, $\delta_2 = \delta_3 = -39$

g) C_p vs. Y', upper surface

h) C_p vs. X', upper surface

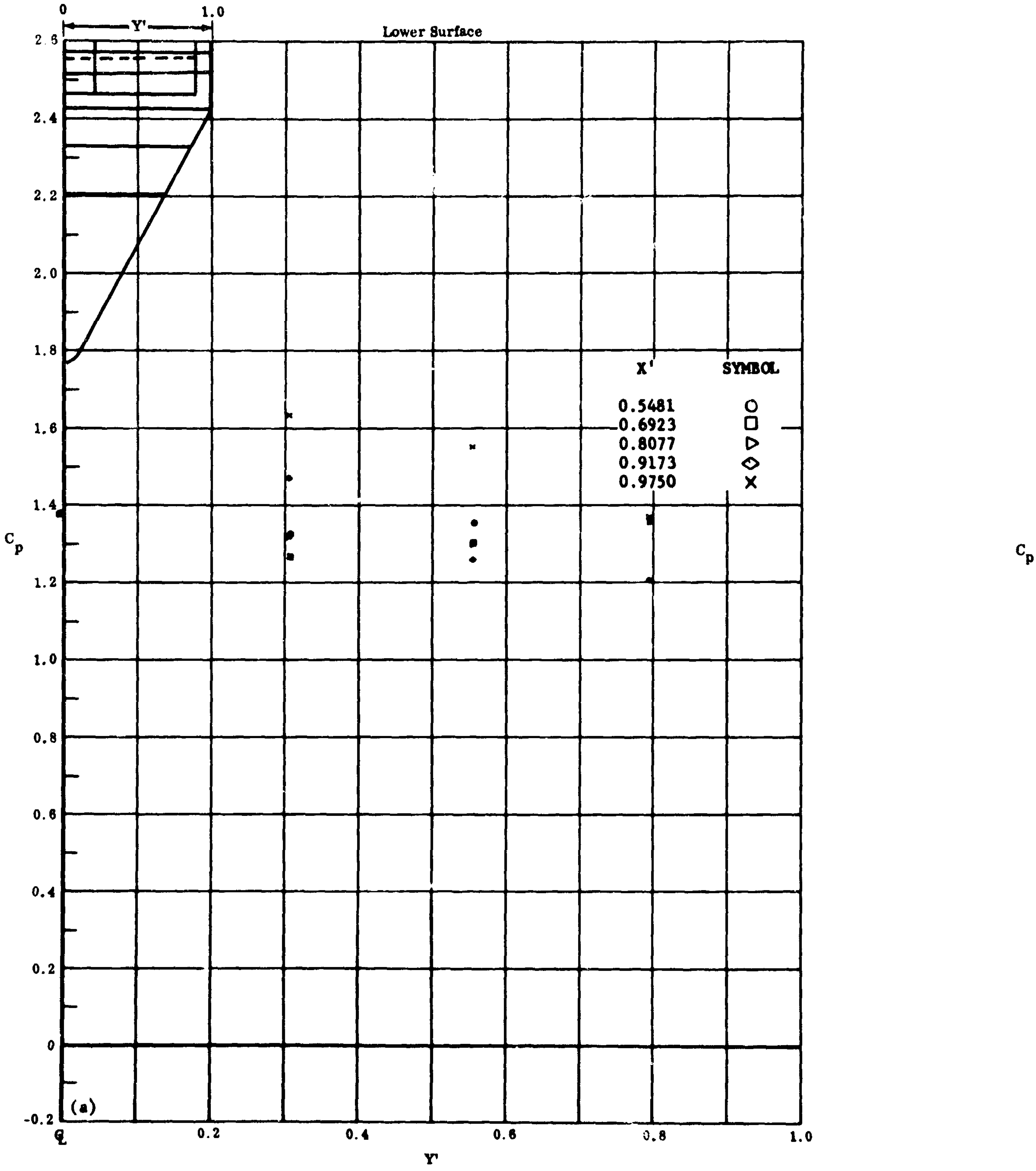

(NONDIMENSIONAL SEMISPAN DISTANCE)

Fig. 13a Configuration I, α = +50 , $\delta_2 = \delta_3 = 0$

C_p vs. Y', lower surface

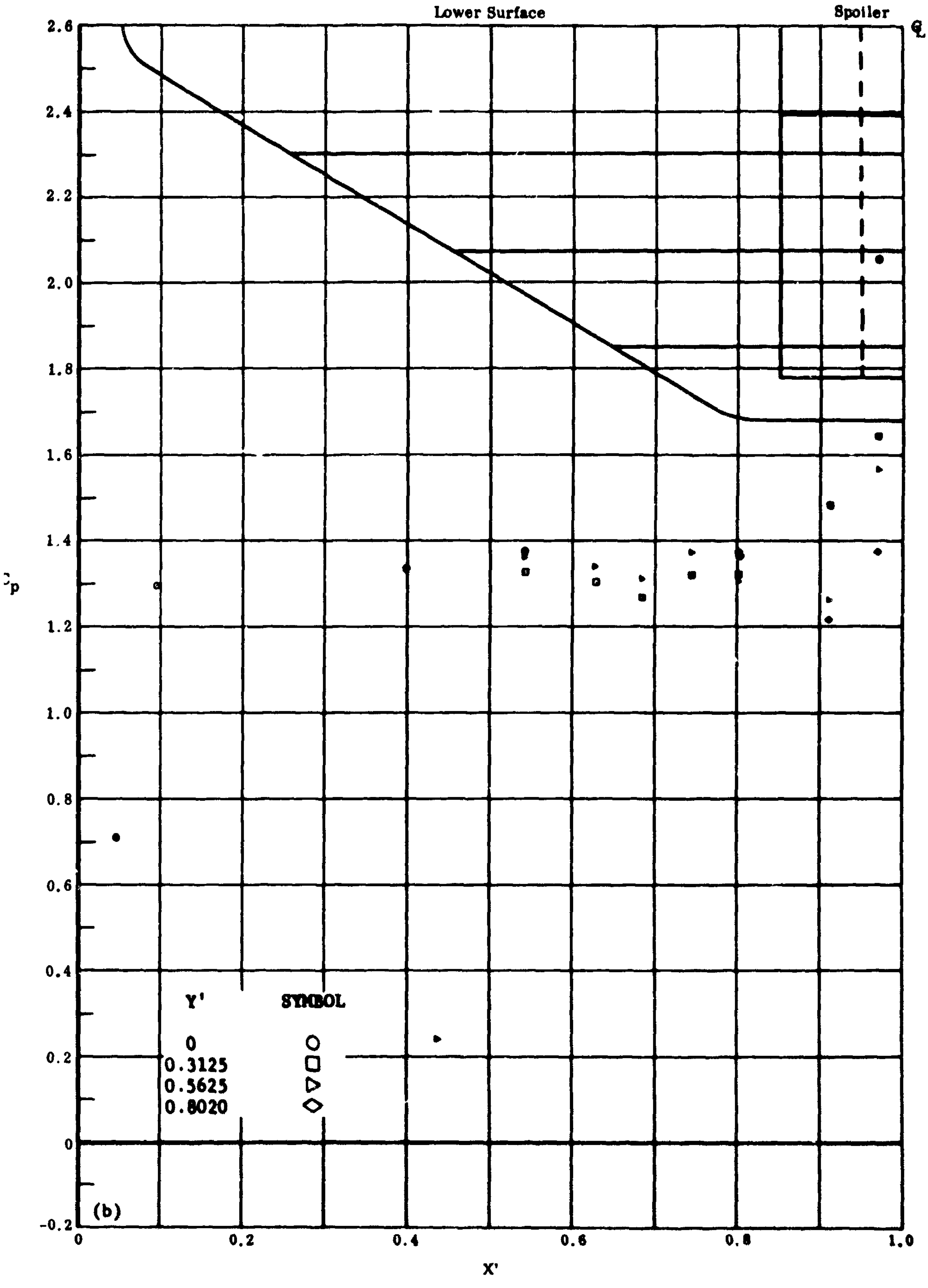

Fig. 13b Configuration I, $\alpha = +50$, $\delta_2 = \delta_3 = 0$

C_p vs. X', lower surface

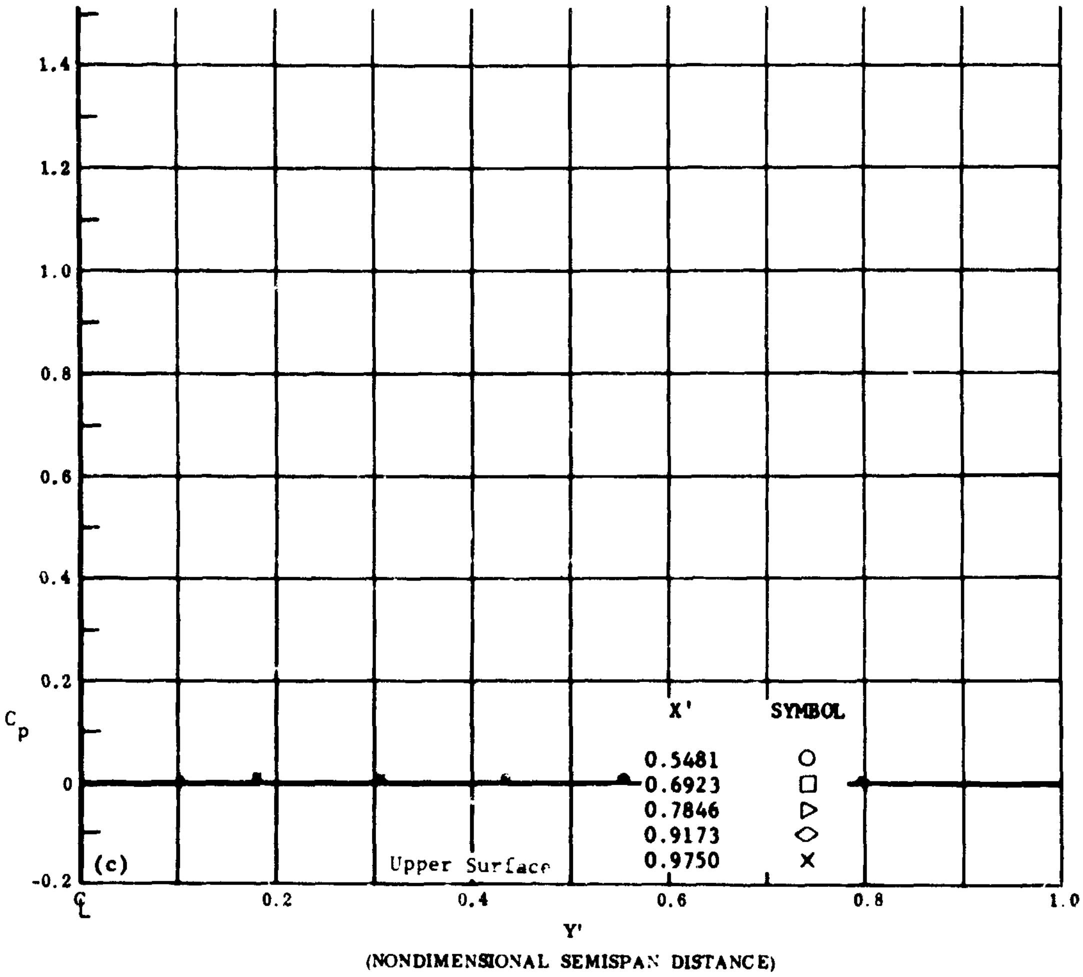

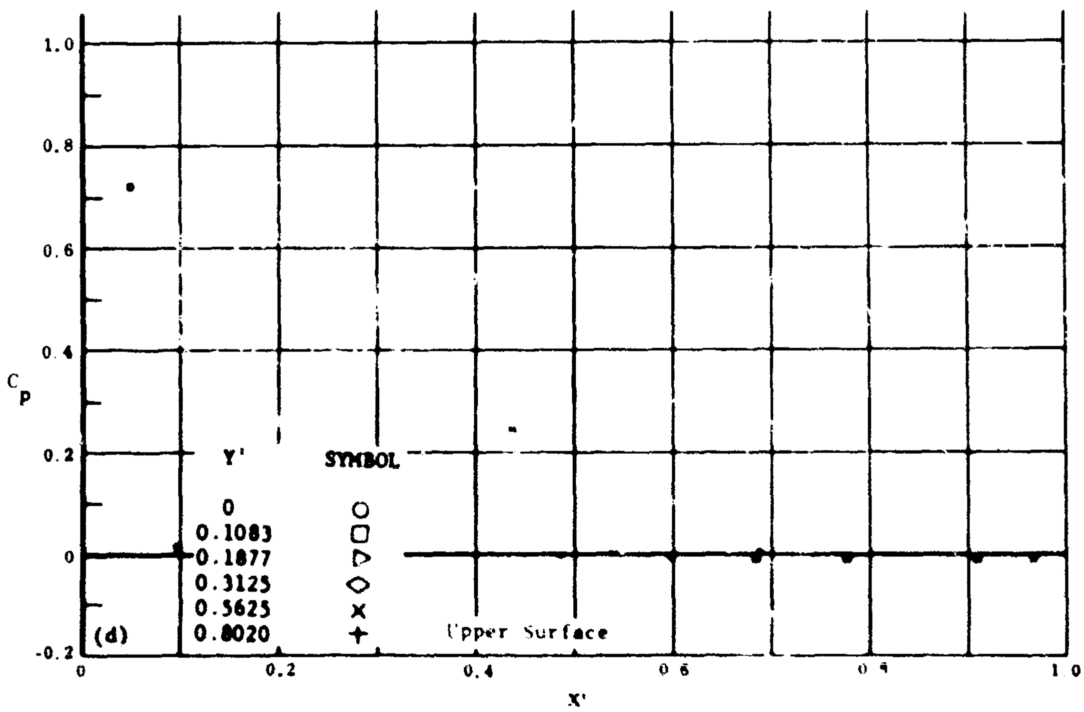

(NONDIMENSIONAL STREAMWISE [illegible] FROM VIRTUAL APEX)

Fig. 13 Configur[illegible] = +50 , [illegible]$_2$ = [illegible]$_3$ = 0

c) C_p vs. Y', upper surface

d) C_p vs. X', upper surface

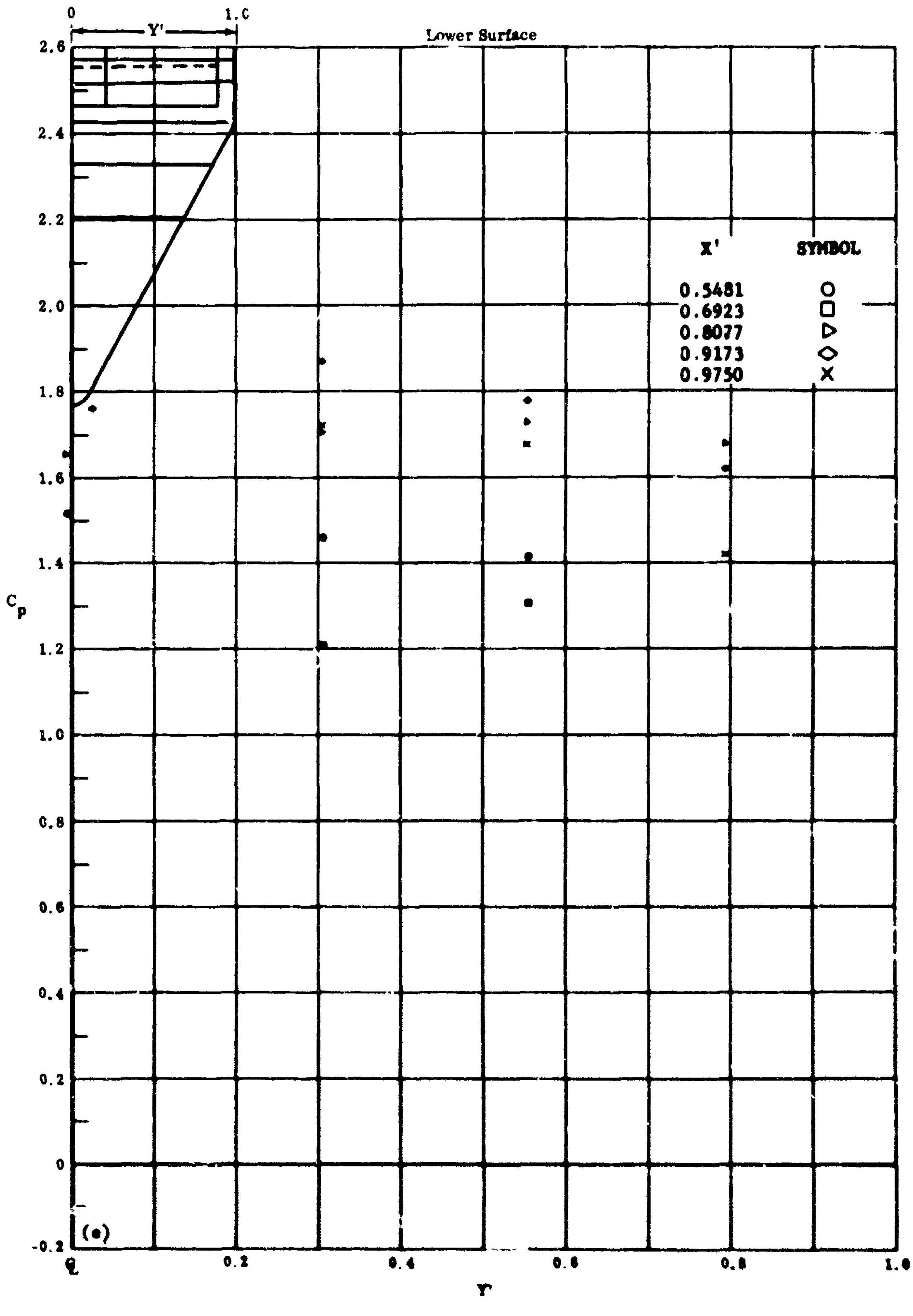

Fig. 13e Configuration I, α = +50 , $\delta_2 = \delta_3$ = +10

C_p vs. Y', lower surface

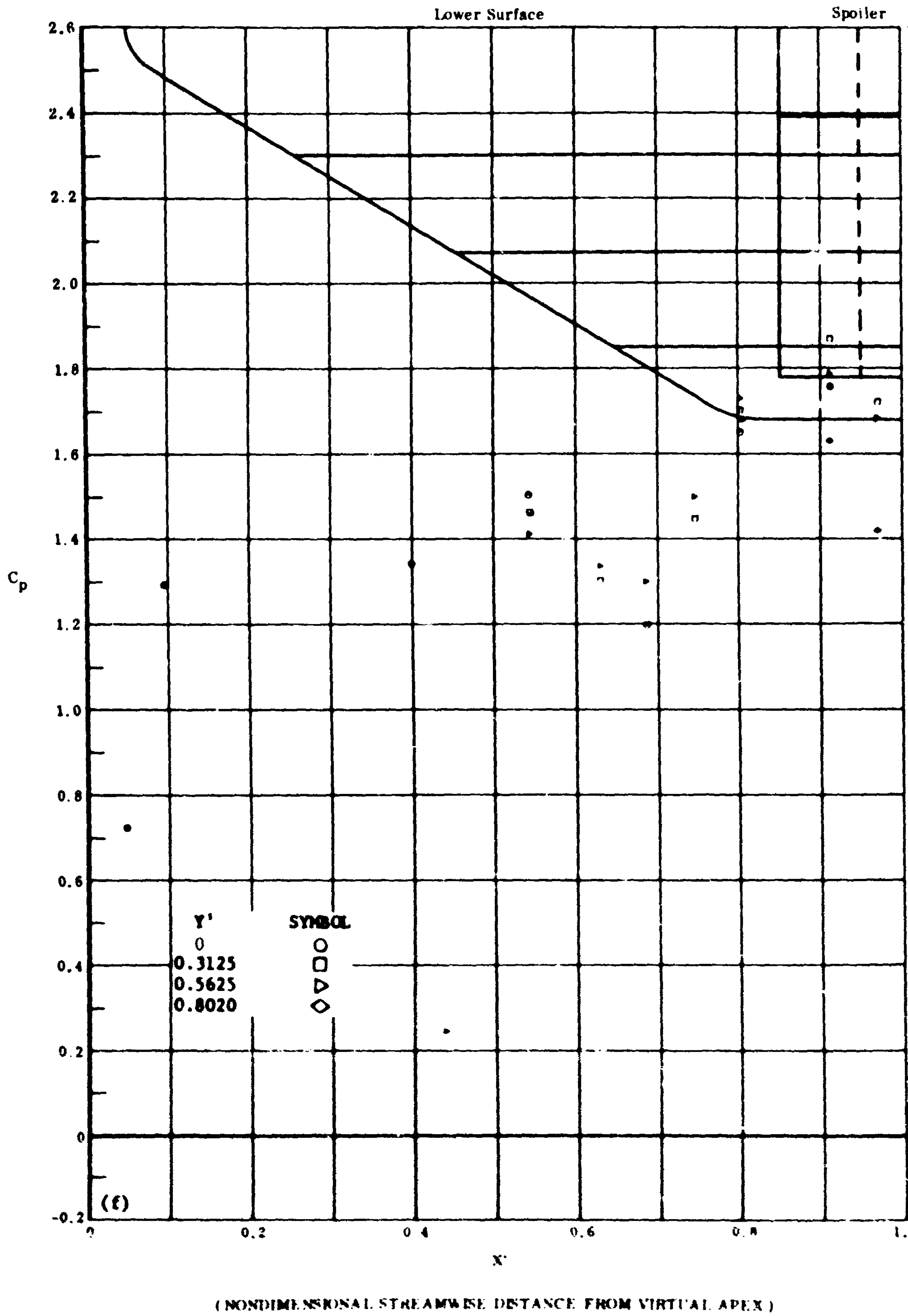

Fig. 13f Configuration I, $\delta_1 = +50$, $\delta_2 = \delta_3 = +10$

C_p vs. X', lower surface

C_l

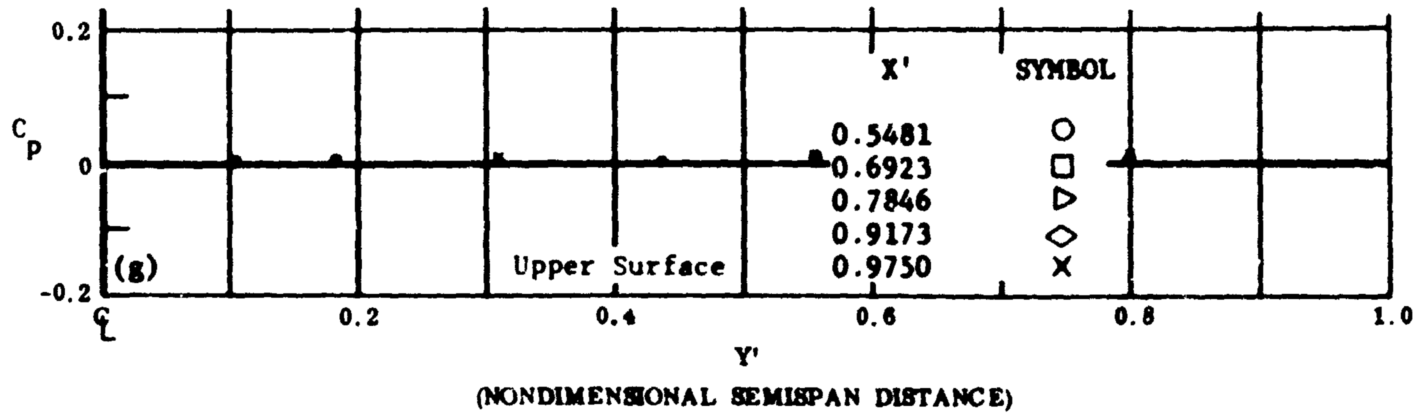

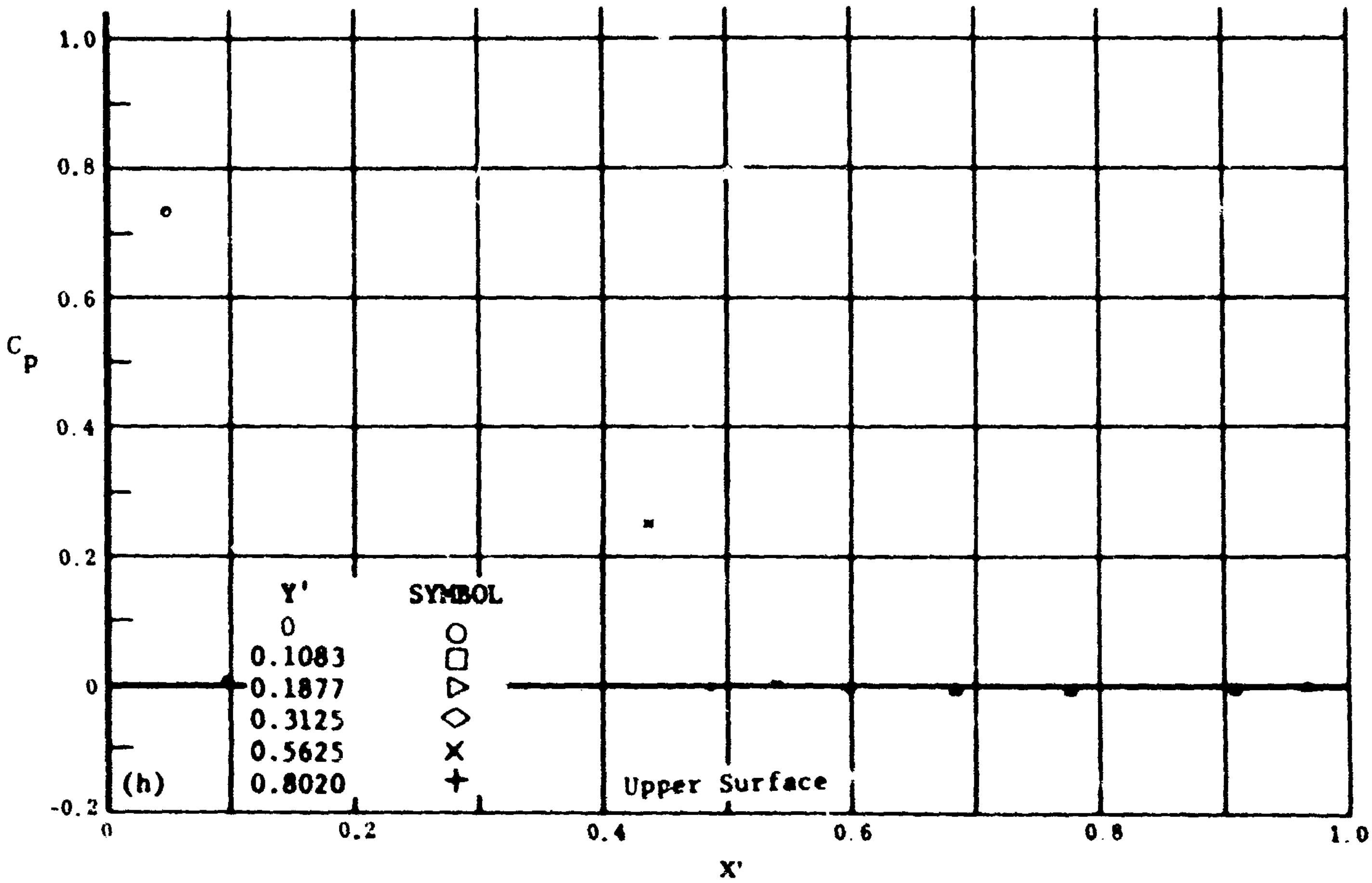

(NONDIMENSIONAL STREAMWISE DISTANCE FROM VIRTUAL APEX)

Fig. 13 Configuration I, α = +50 , $\delta_2 = \delta_3$ = +10

g) C_p vs. Y', upper surface

h) C_p vs. X', upper surface

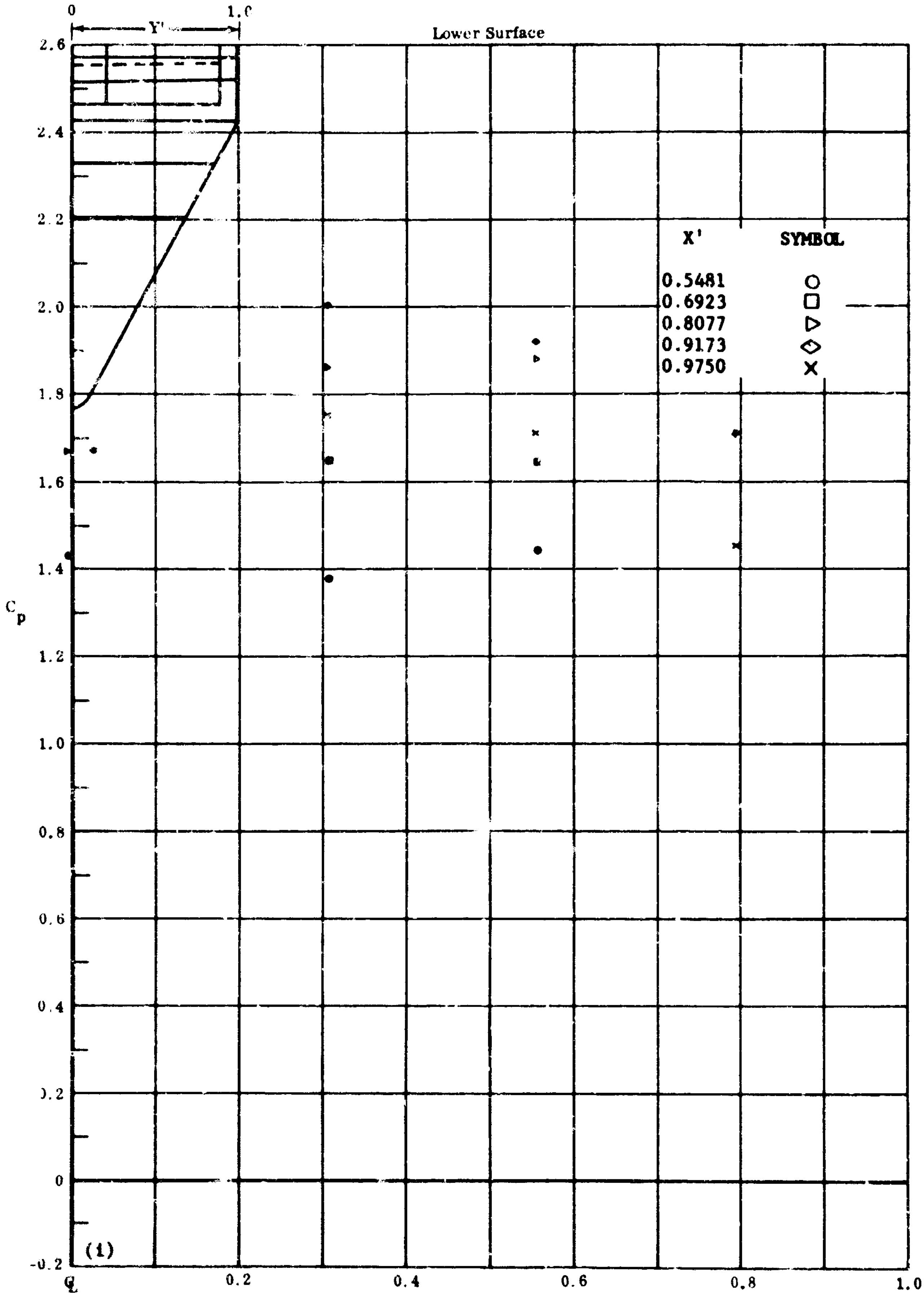

(NONDIMENSIONAL SEMISPAN DISTANCE)

Fig. 131 Configuration I, α = +50 , $\delta_2 = \delta_3$ = +20

C_p vs. Y', lower surface

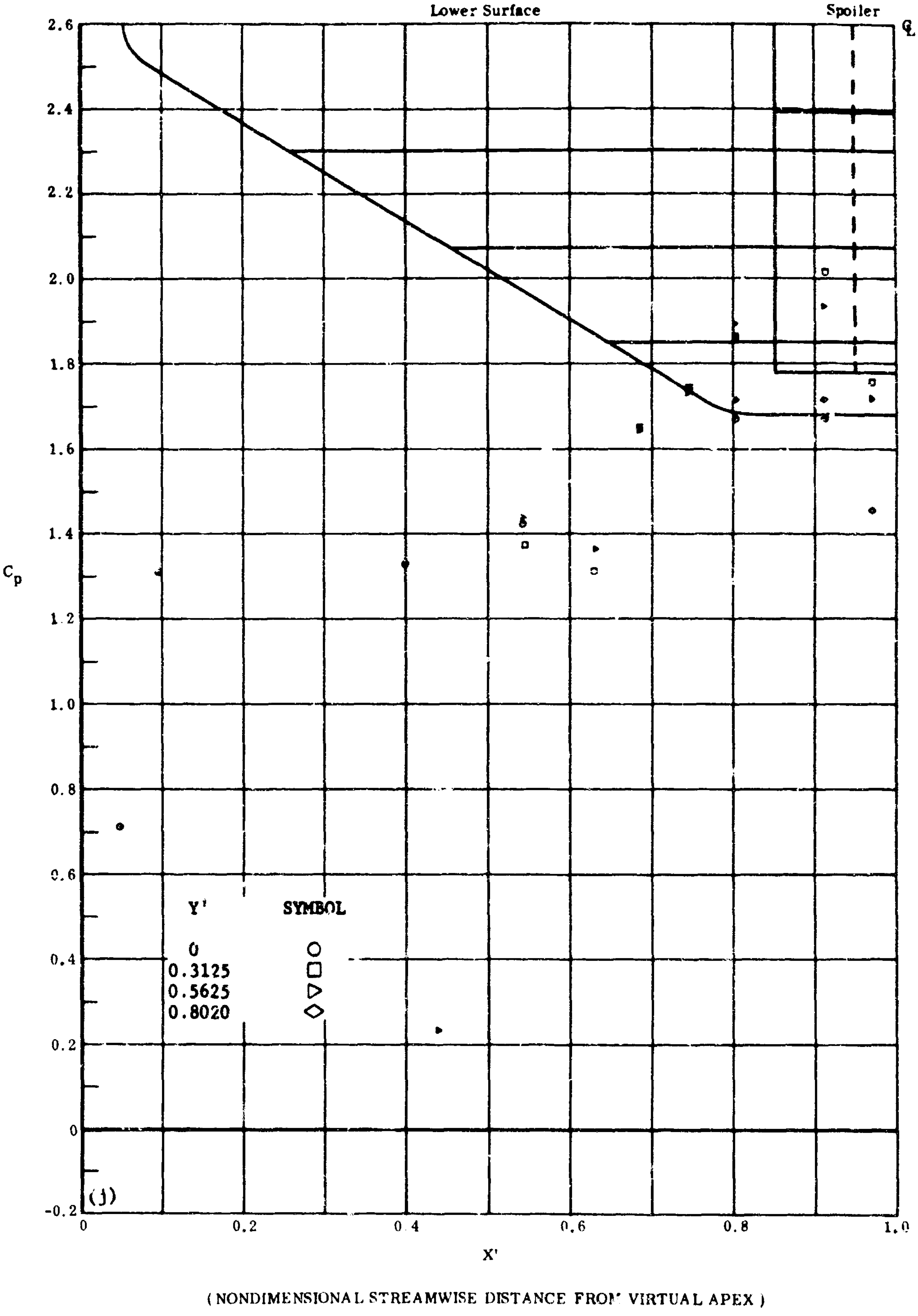

Fig. 13j Configuration I, α = +50 , $\delta_2 = \delta_3$ = +20

C_p vs. X', lower surface

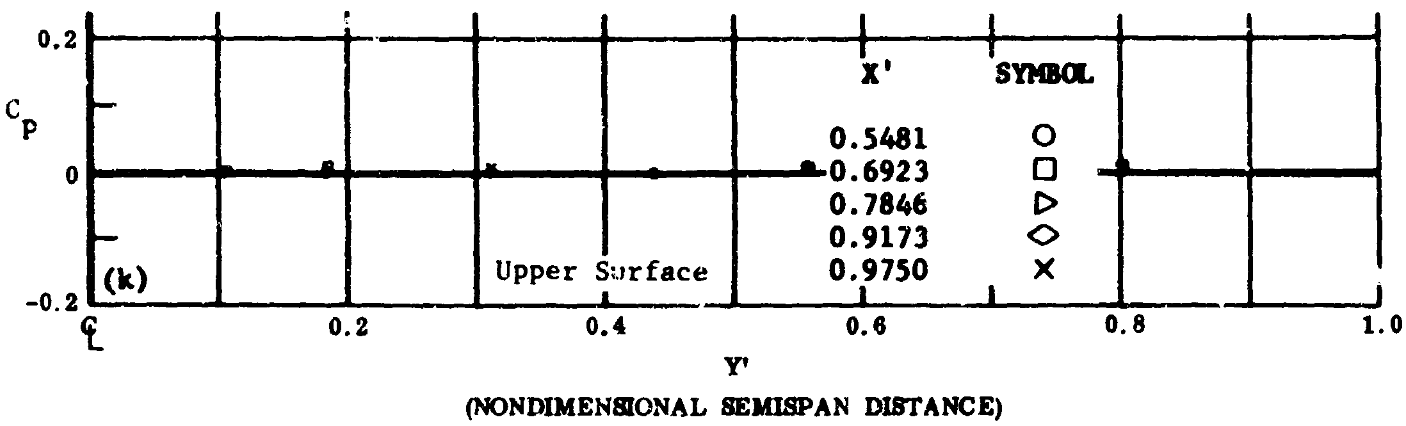

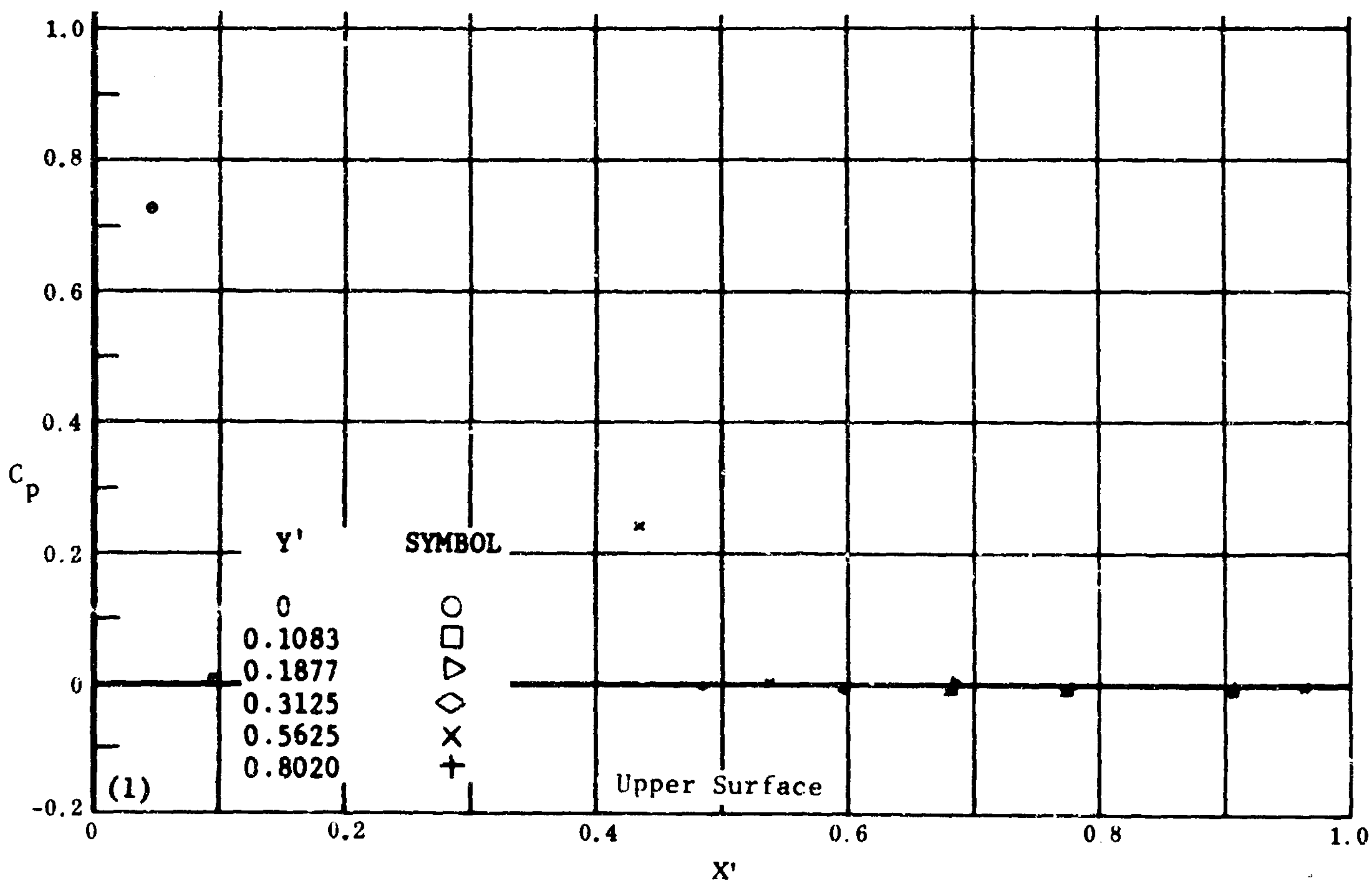

Fig. 13 Configuration I, α = +50 , $\delta_2 = \delta_3$ = +20

k) C_p vs. Y', upper surface

l) C_p vs. X', upper surface

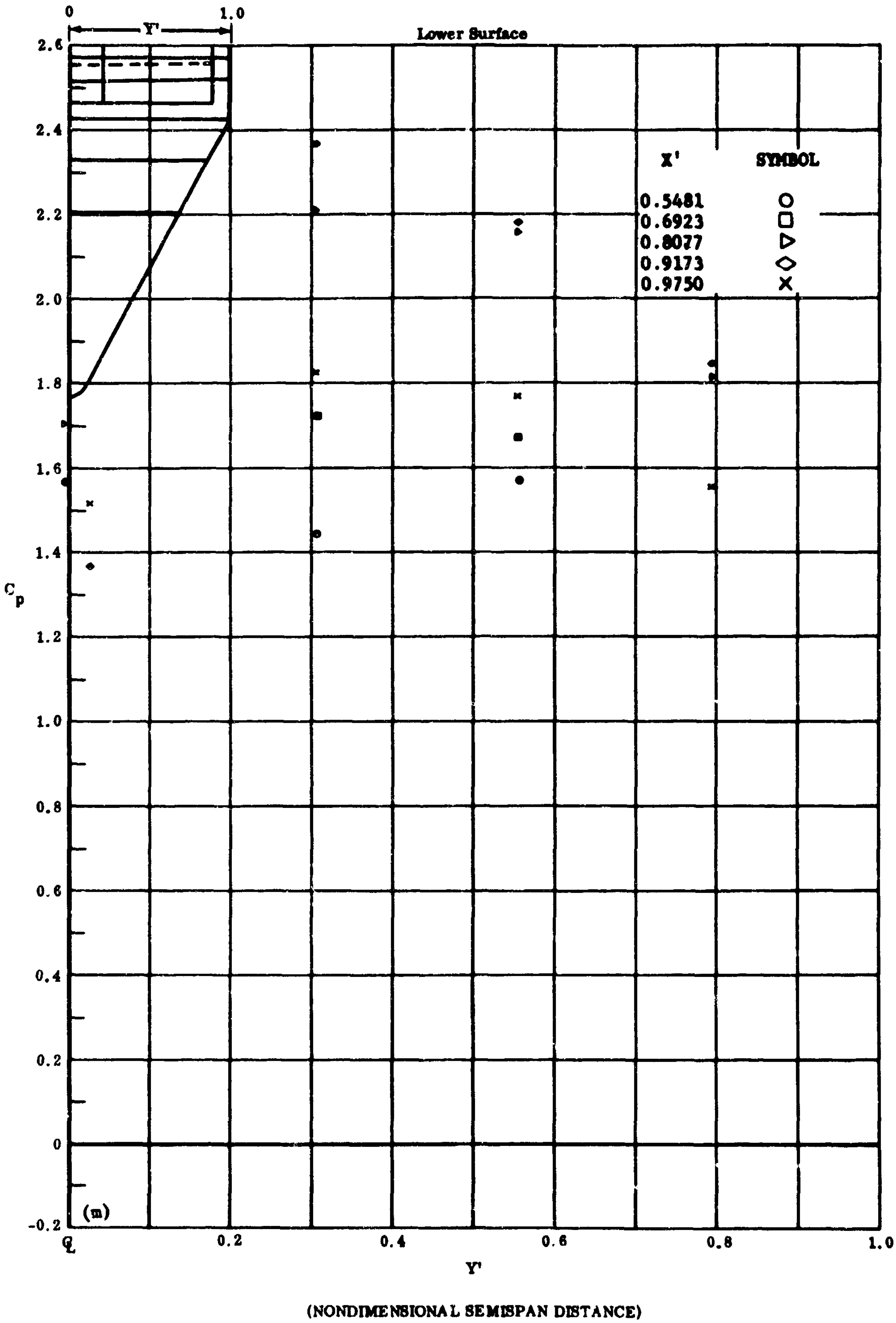

Fig. 13m Configuration I, $\alpha = +50$, $\delta_2 = \delta_3 = +39$

C_p vs. Y', lower surface

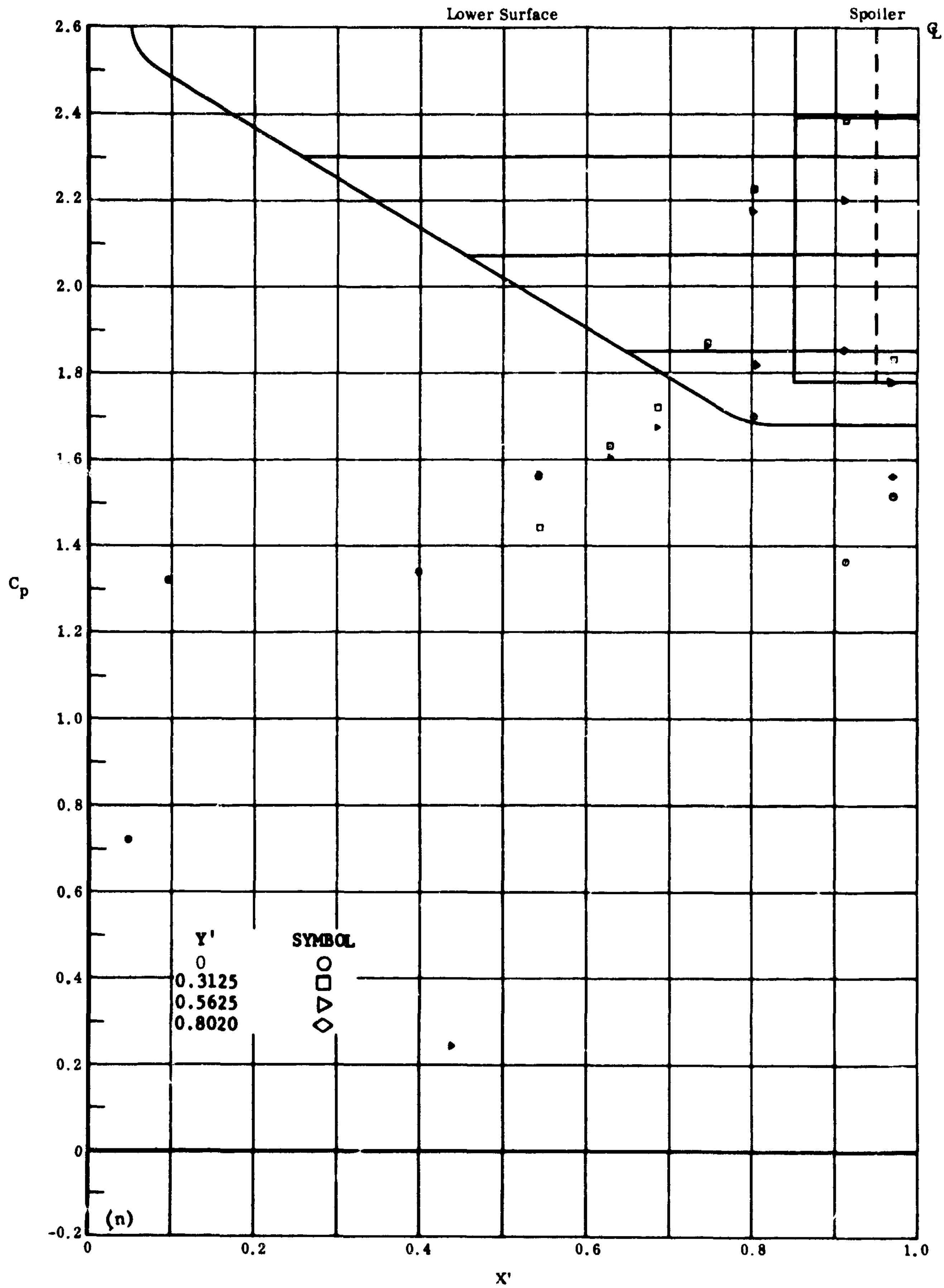

Fig. 13n Configuration I, α = +50 , $\delta_2 = \delta_2$ = +39

C_p vs. X', lower surface

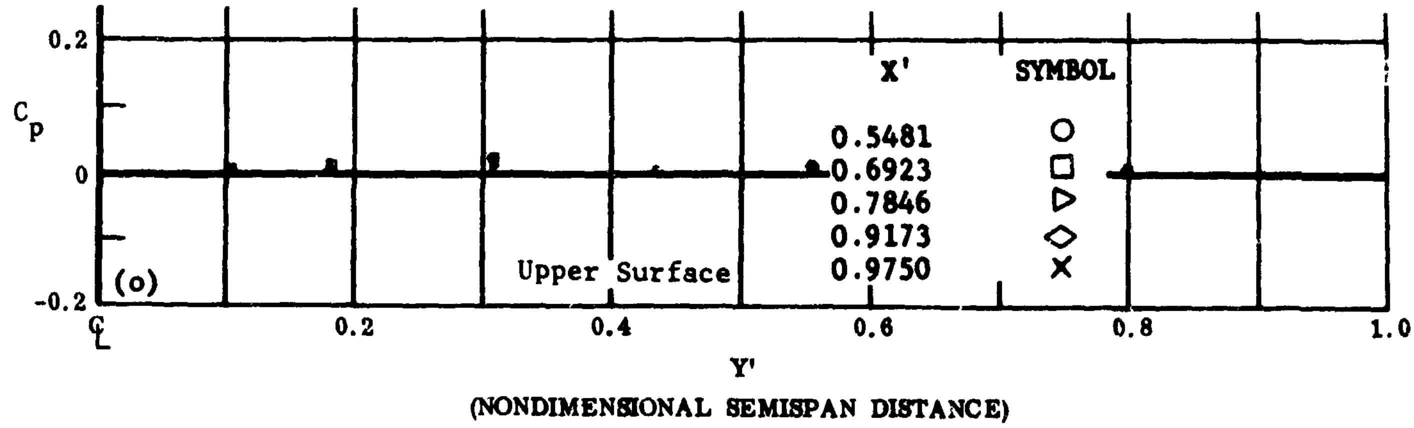

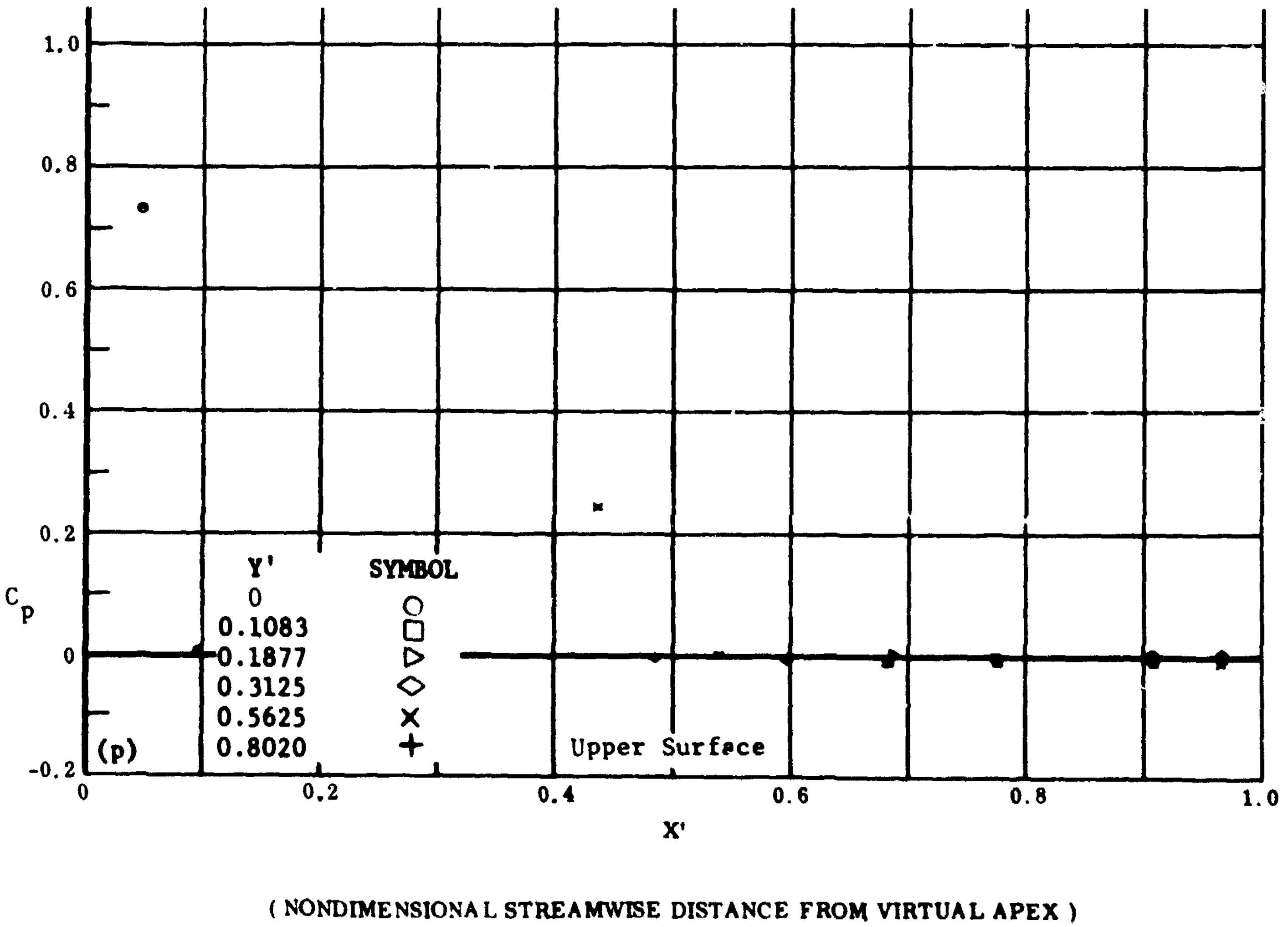

Fig. 13 Configuration I, $\alpha = +50$, $\delta_2 = \delta_3 = +39$

o) C_p vs. Y', upper surface

p) C_p vs. X', upper surface

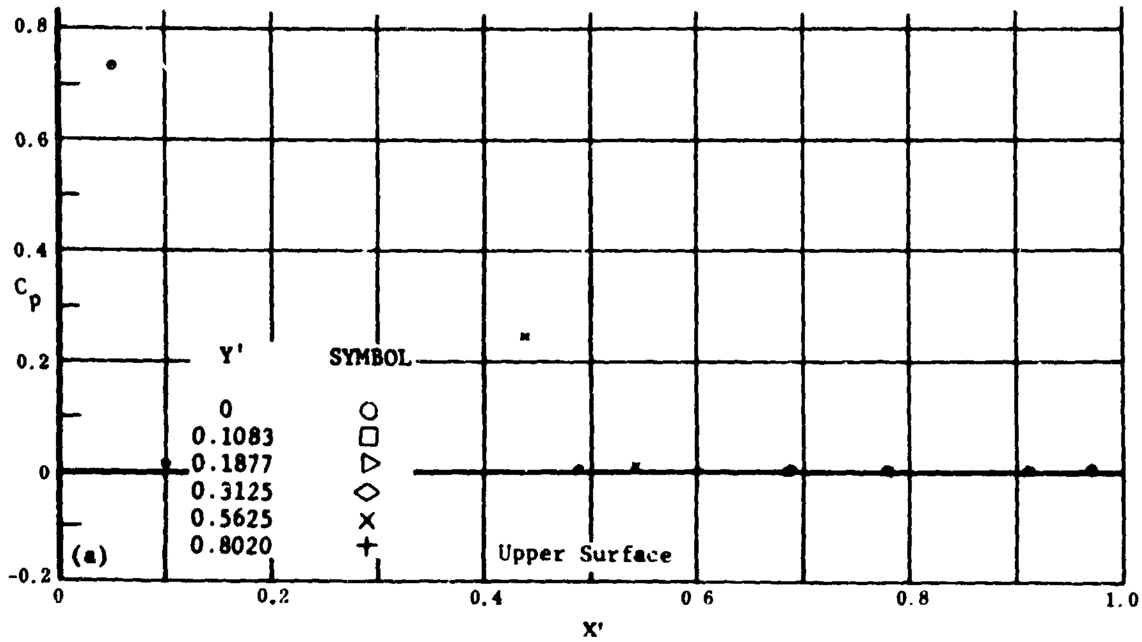

(NONDIMENSIONAL STREAMWISE DISTANCE FROM VIRTUAL APEX)

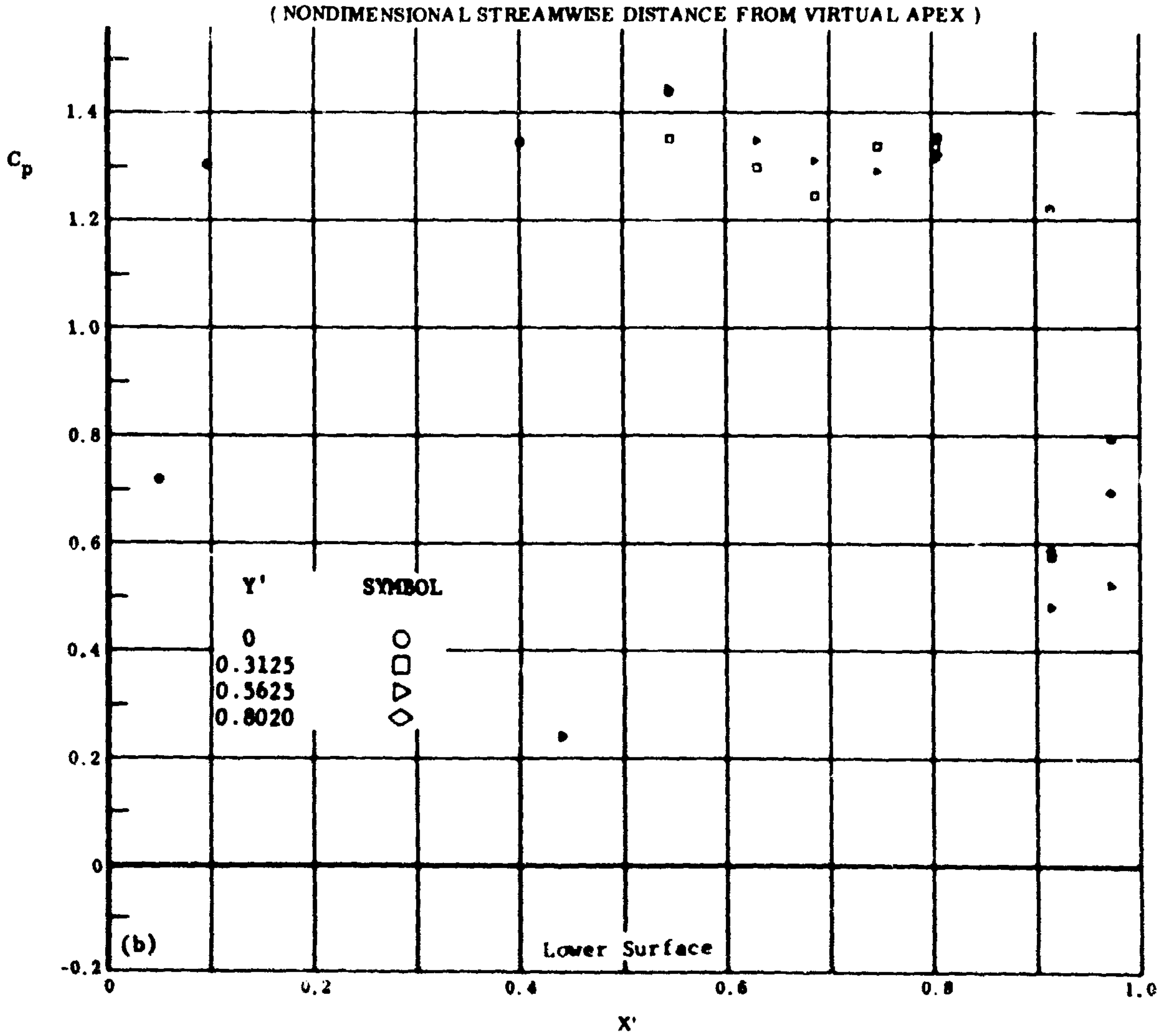

(NONDIMENSIONAL STREAMWISE DISTANCE FROM VIRTUAL APEX)

Fig. 14 Configuration I, $\alpha = +50$, $\delta_2 = \delta_3 = -20$

a) C_p vs. X', upper surface

b) C_p vs. X', lower surface

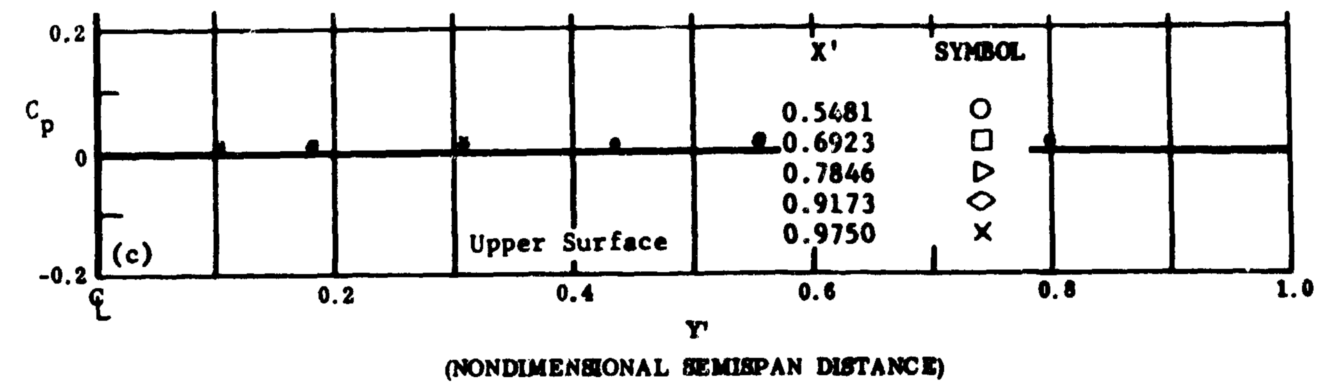

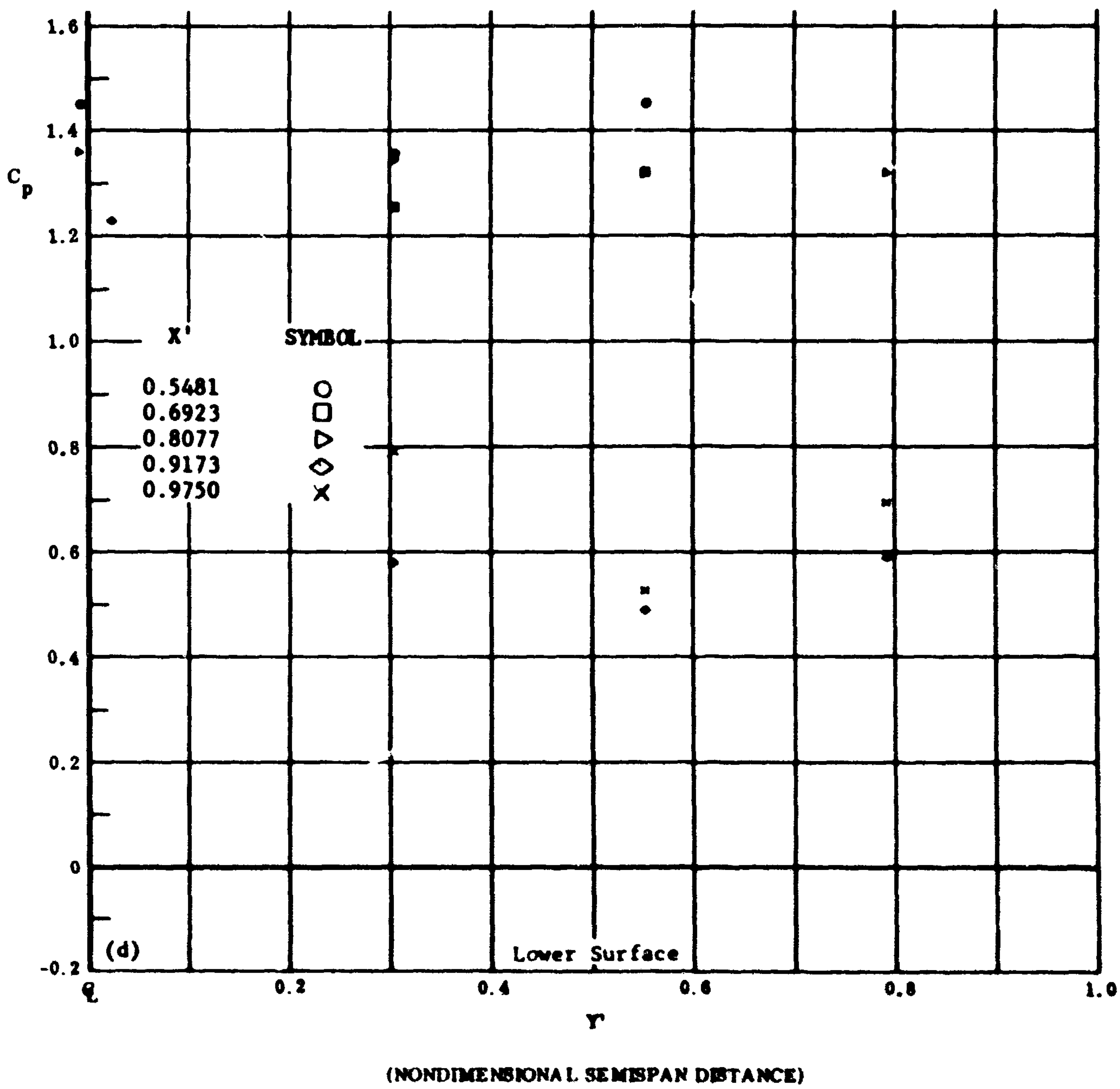

Fig. 14 Configuration I, $\alpha = +50$, $\delta_2 = \delta_3 = -20$

c) C_p vs. Y', upper surface

d) C_p vs. Y', lower surface

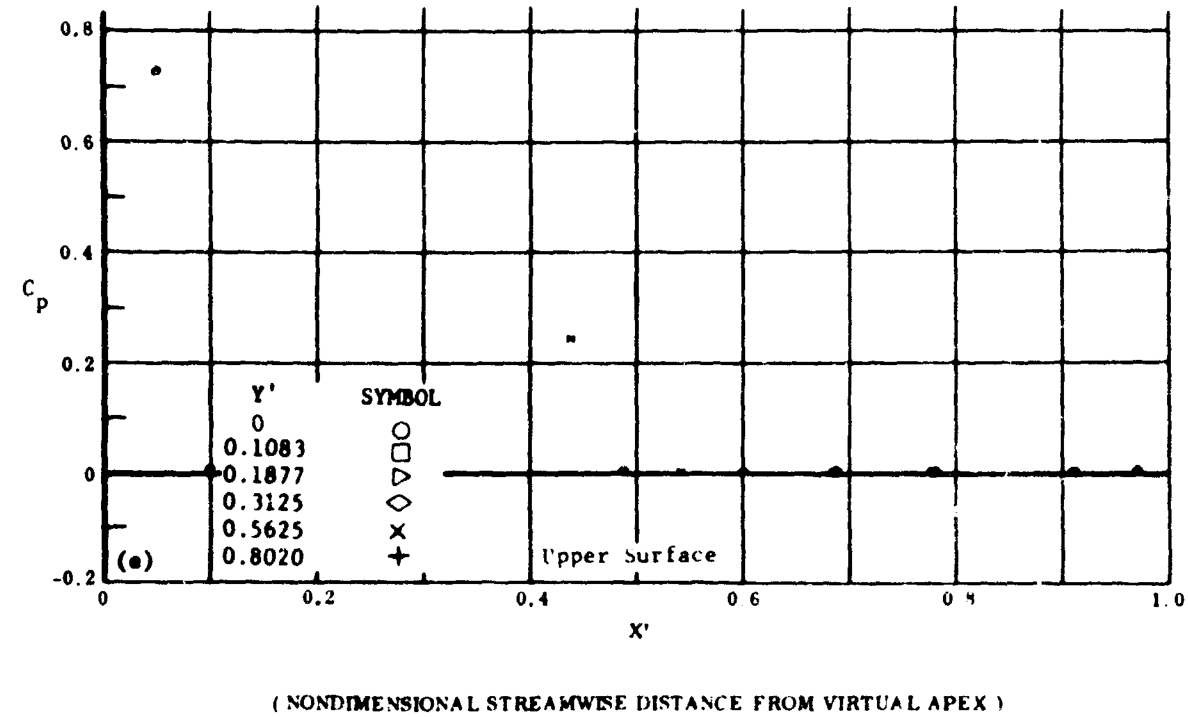

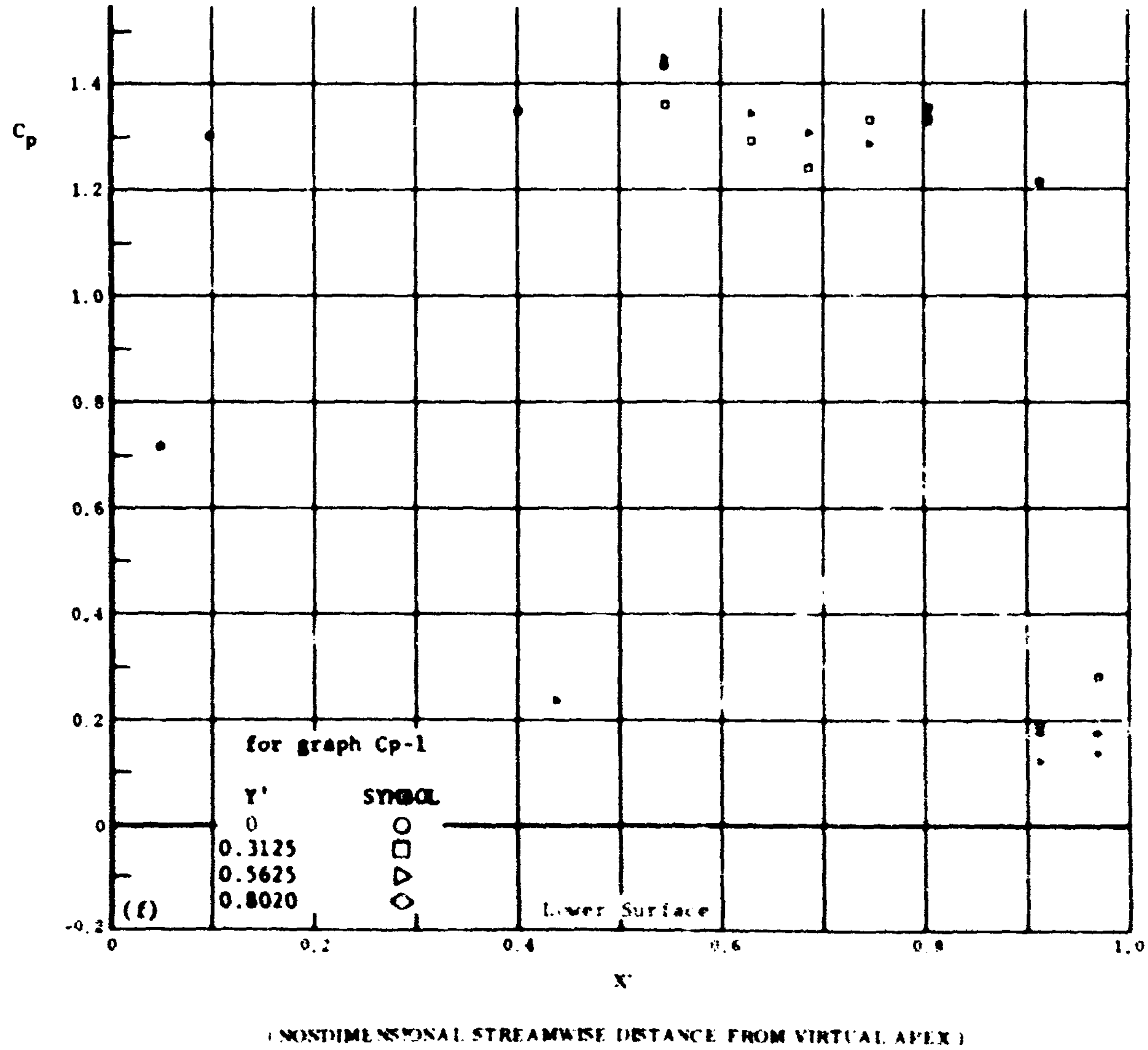

Fig. 14 Configuration I, ι = +50, $'_2$ = $'_3$ = -39

e) C_p vs. X', upper surface

f) C_p vs. X', lower surface

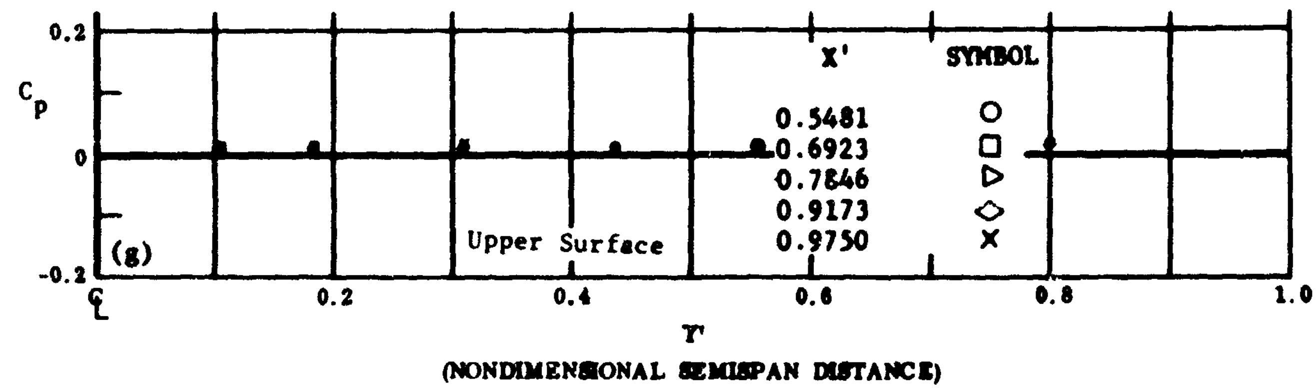

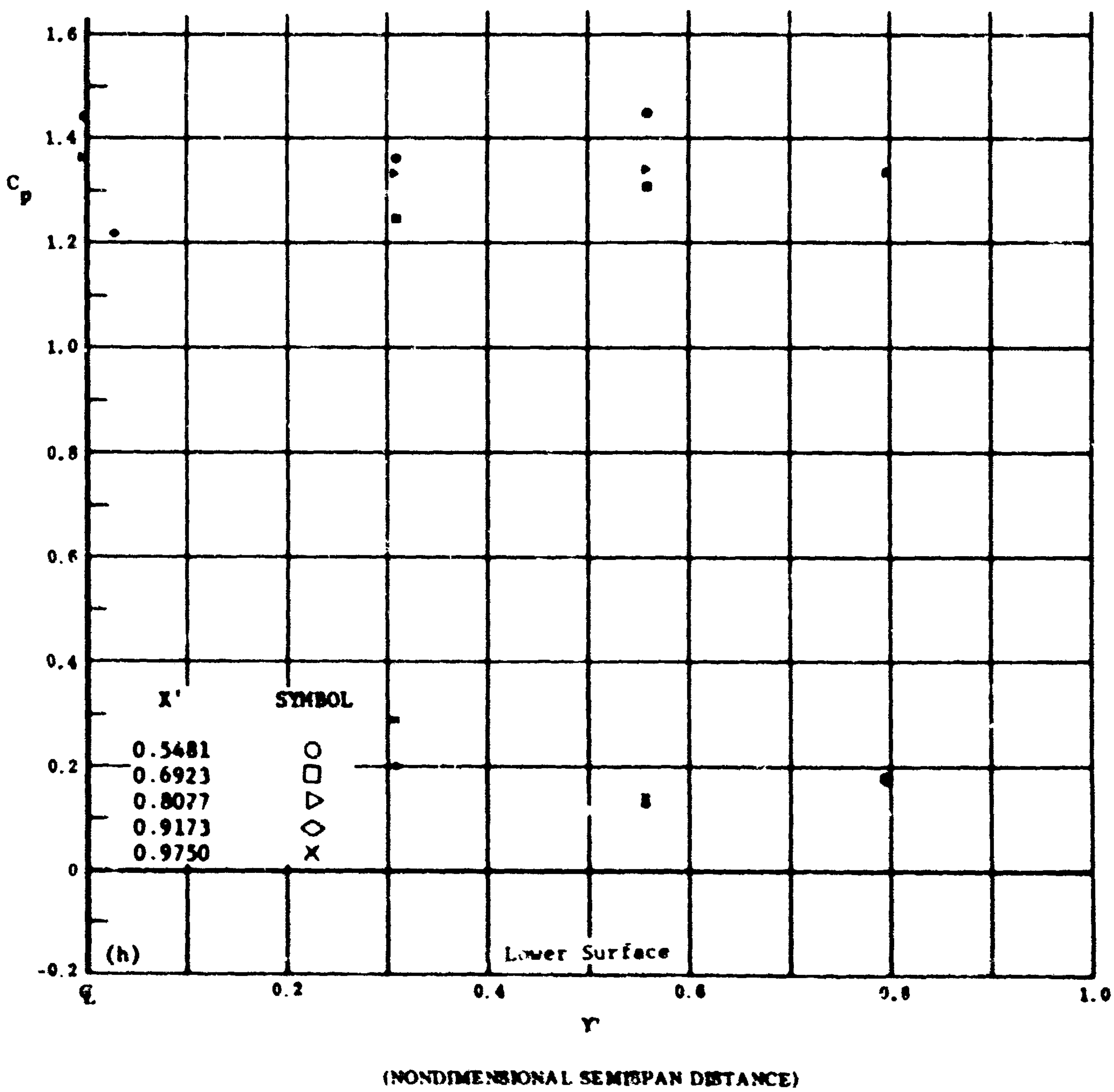

Fig. 14 Configuration I, $\alpha = +50$, $\delta_2 = \delta_3 = -39$

g) C_p vs. Y', upper surface

h) C_p vs. Y', lower surface

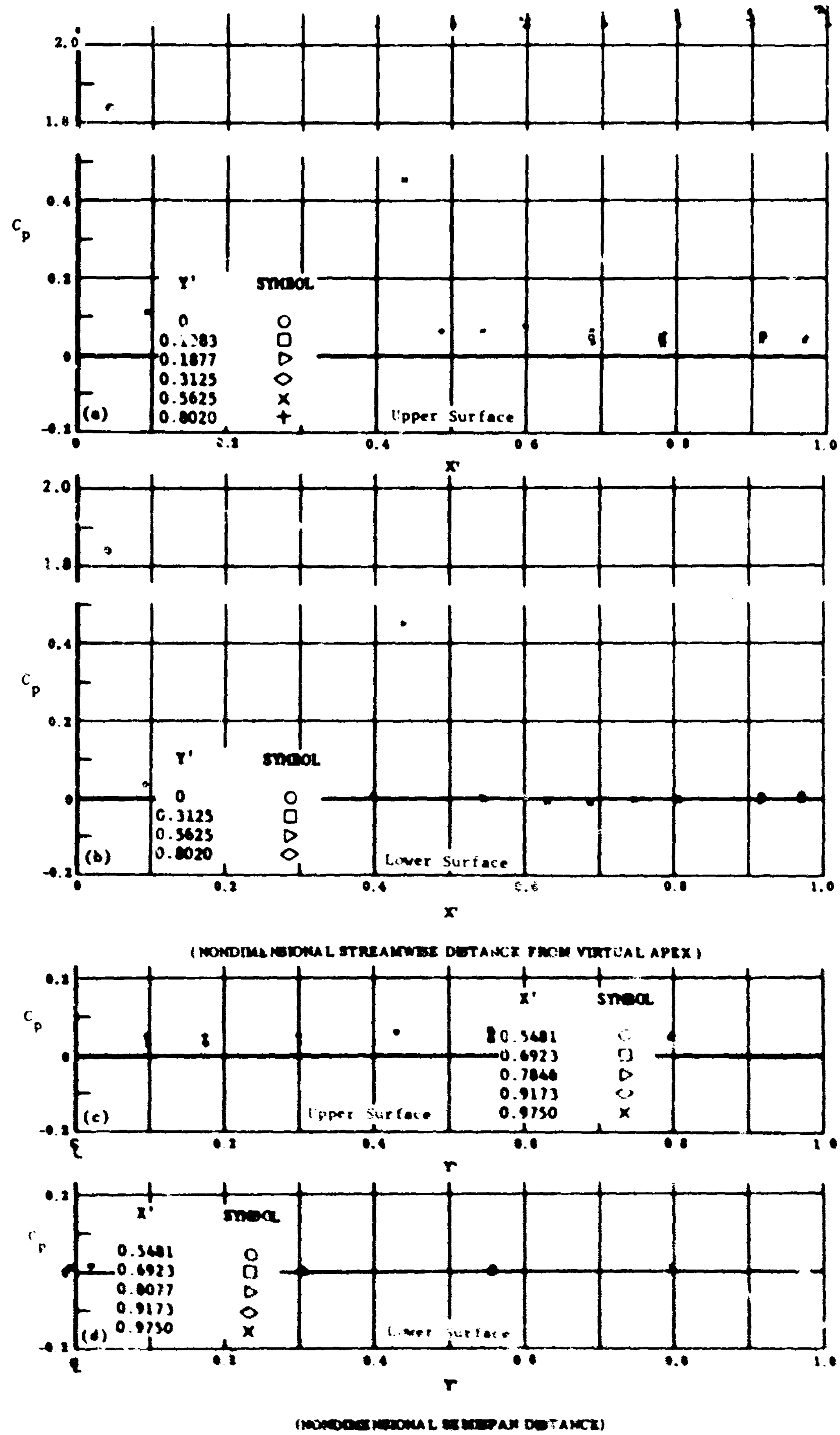

Fig. 15 Configuration I, $\alpha = -5$, $\delta_2 = \delta_3 = 0$

a) C_p vs. X', upper surface

b) C_p vs. X', lower surface

c) C_p vs. Y', upper surface

d) C_p vs. Y', lower surface

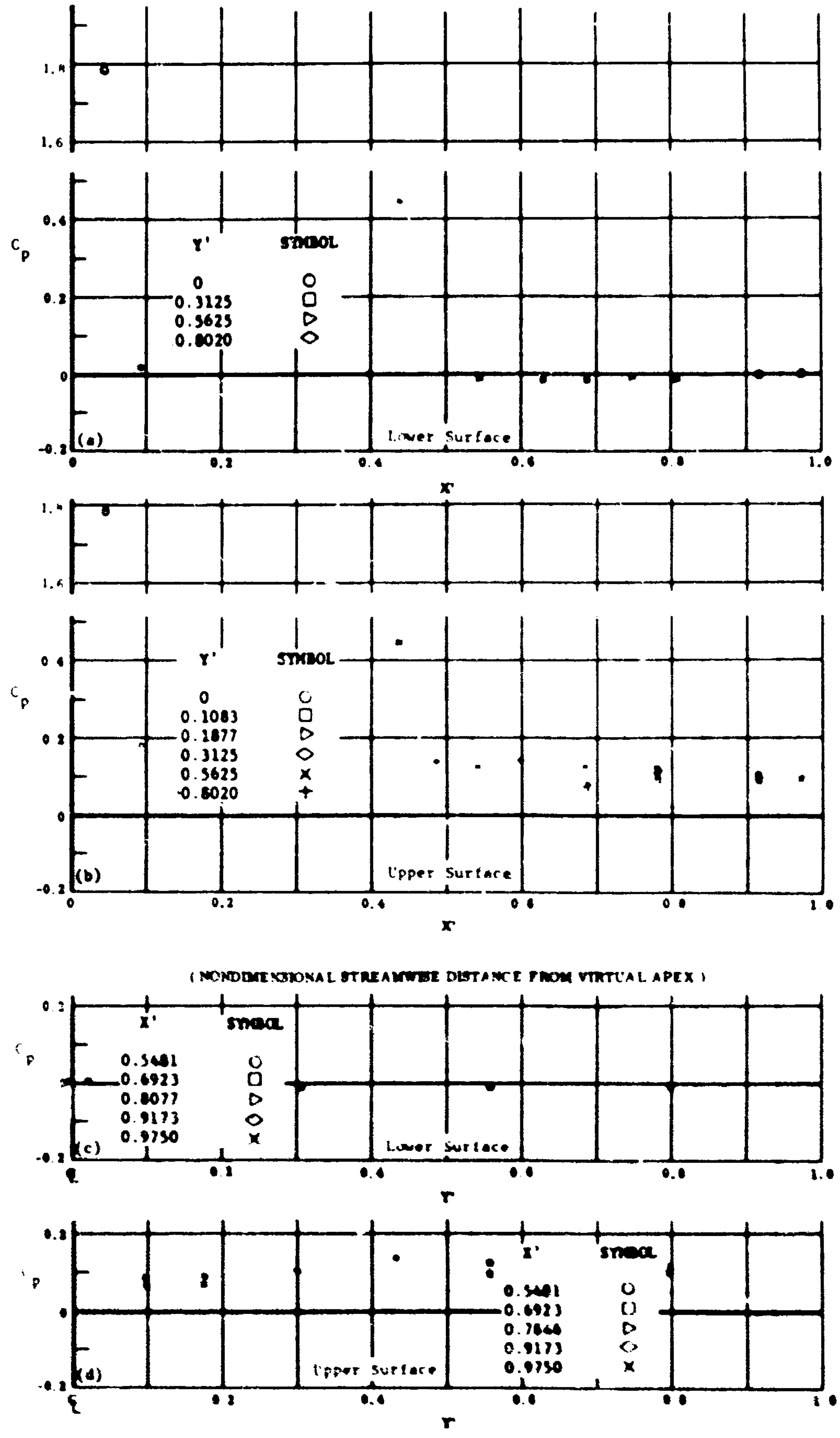

Fig. 16 Configuration I, $\alpha = -10$, $\delta_2 = \delta_3 = 0$

a) C_p vs. X', lower surface

b) C_p vs. X', upper surface

c) C_p vs. Y', lower surface

d) C_p vs. Y', upper surface

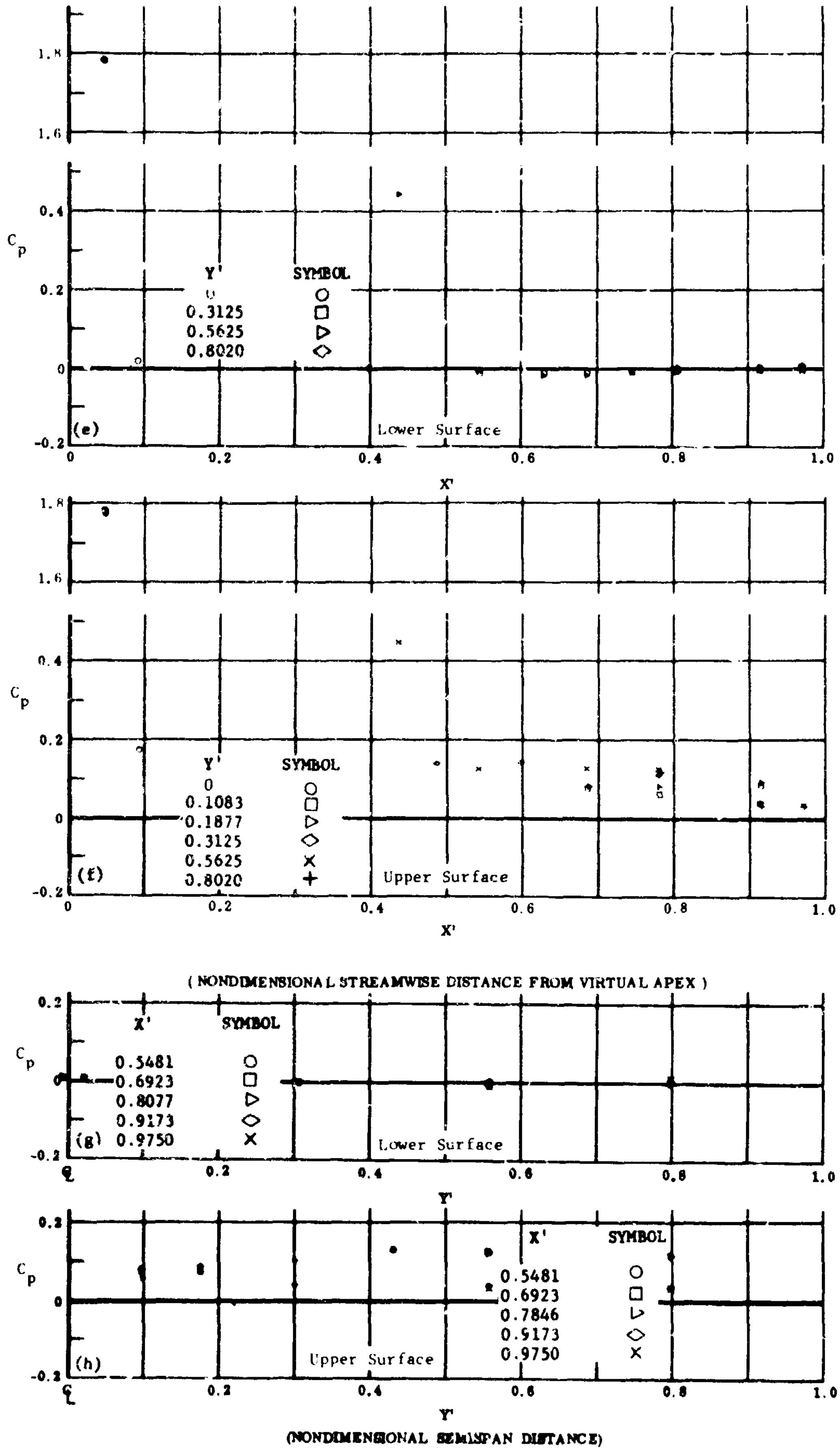

Fig. 16 Configuration I, $\alpha = -10$, $\delta_2 = \delta_3 = +10$

e) C_p vs. X', lower surface

f) C_p vs. X', upper surface

g) C_p vs. Y', lower surface

h) C_p vs. Y', upper surface

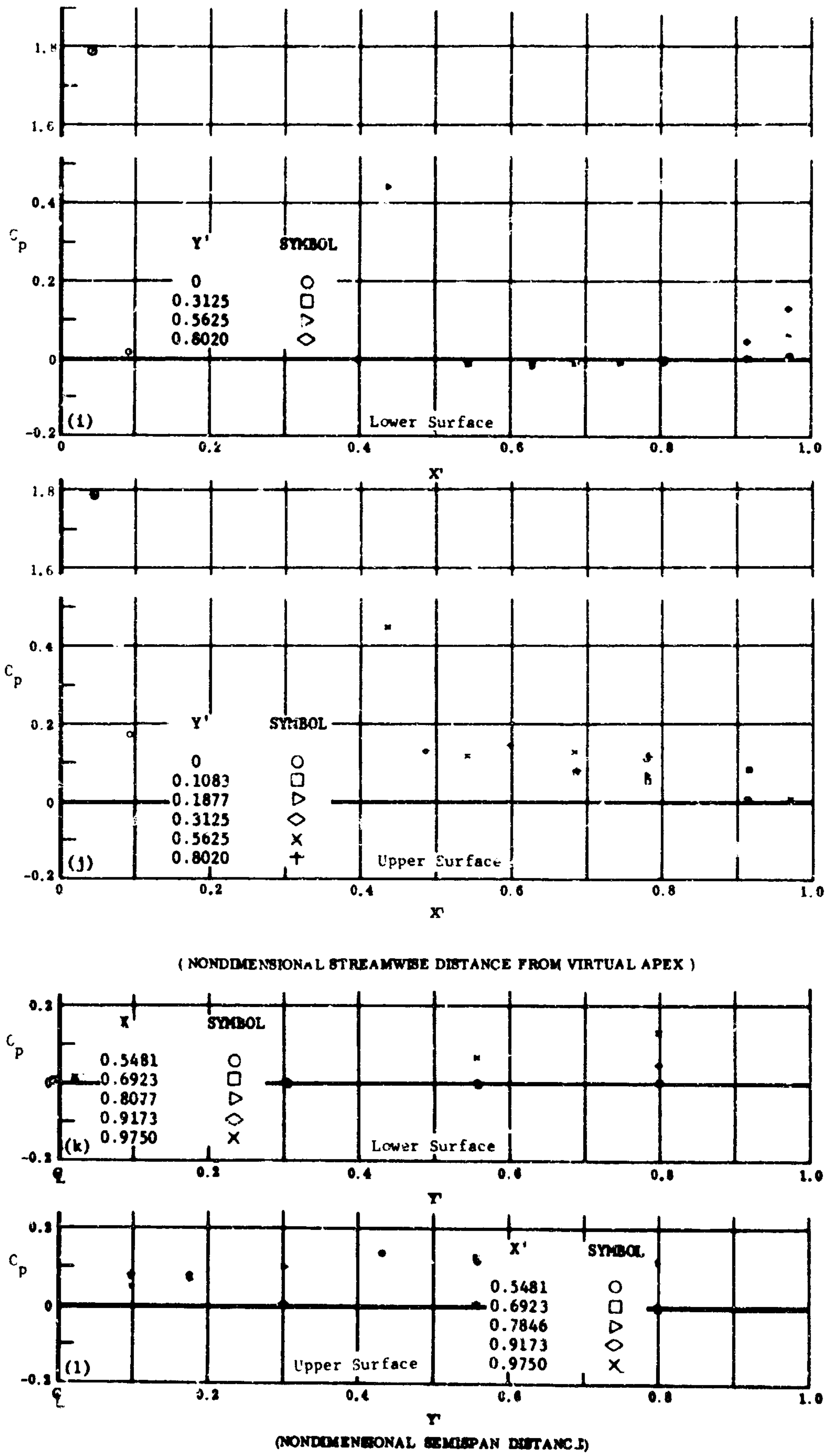

Fig. 16 Configuration I, $\alpha = -10$, $\delta_2 = \delta_3 = +20$

i) C_p vs. X', lower surface

j) C_p vs. X', upper surface

k) C_p vs. Y', lower surface

l) C_p vs. Y', upper surface

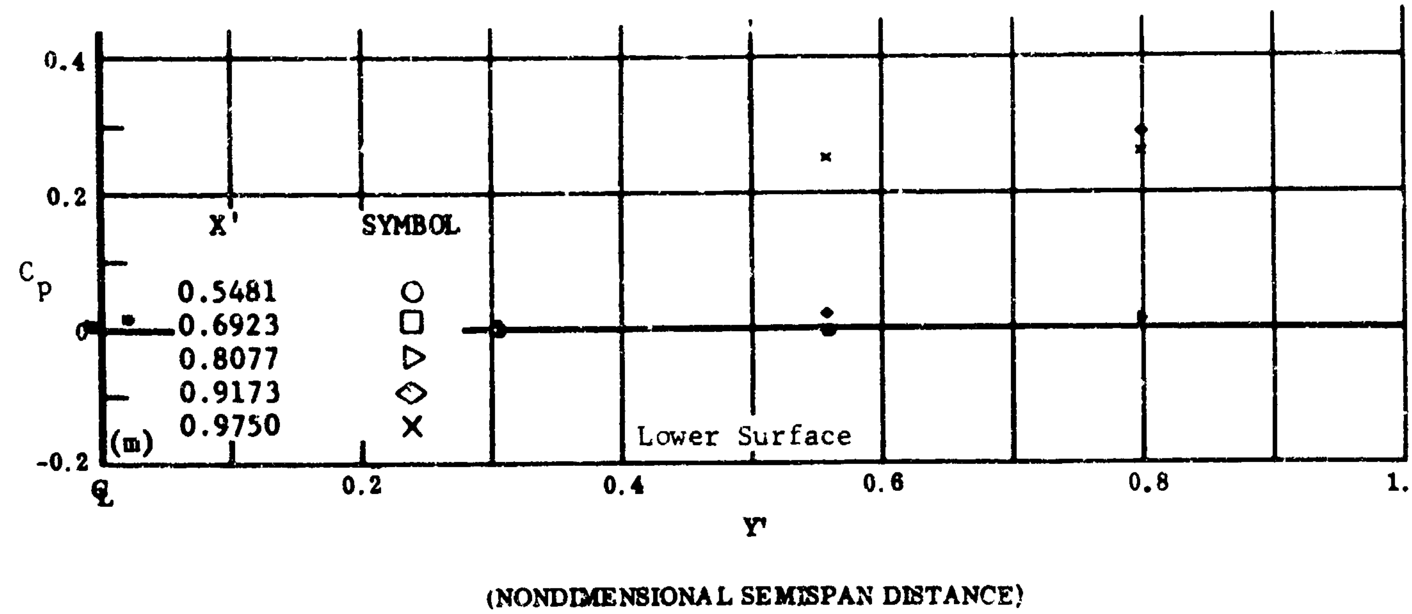

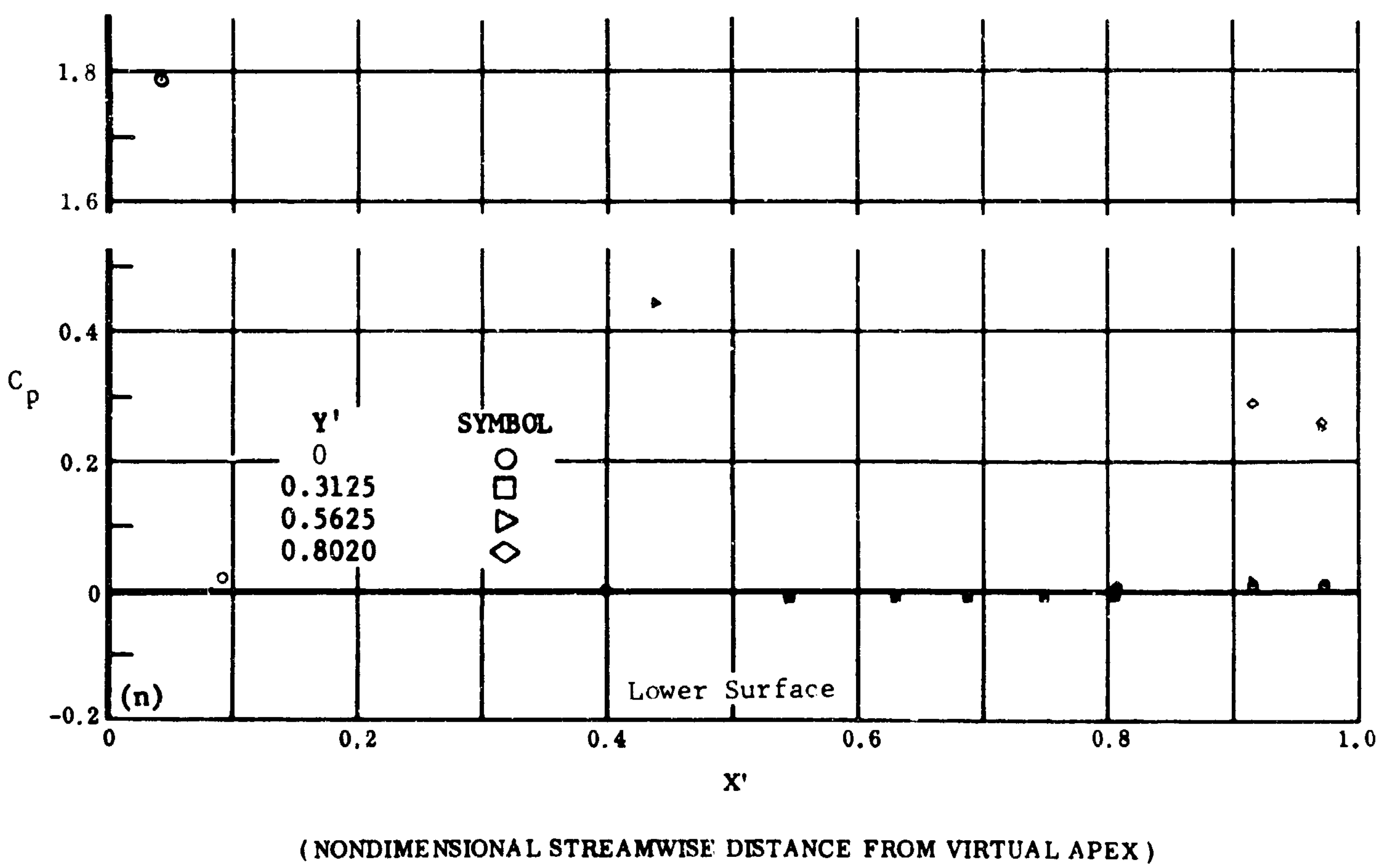

Fig. 16 Configuration I, $\alpha = -10$, $\delta_2 = \delta_3 = +30$

m) C_p vs. Y', lower surface

n) C_p vs. X', lower surface

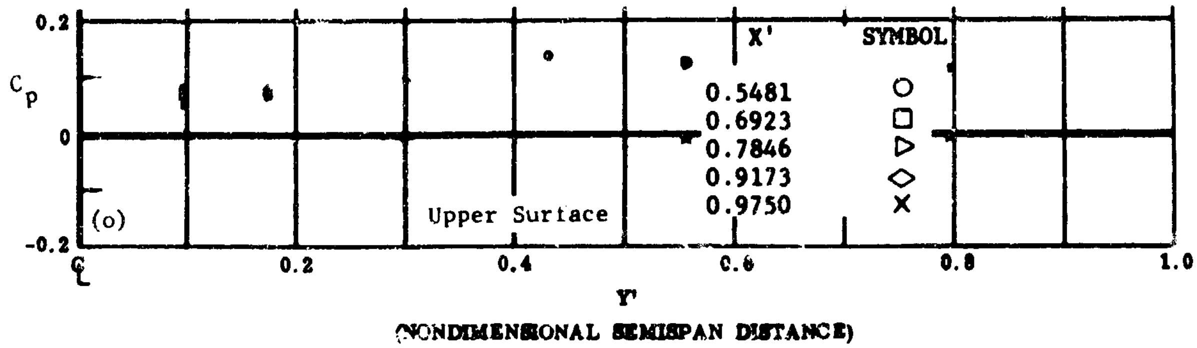

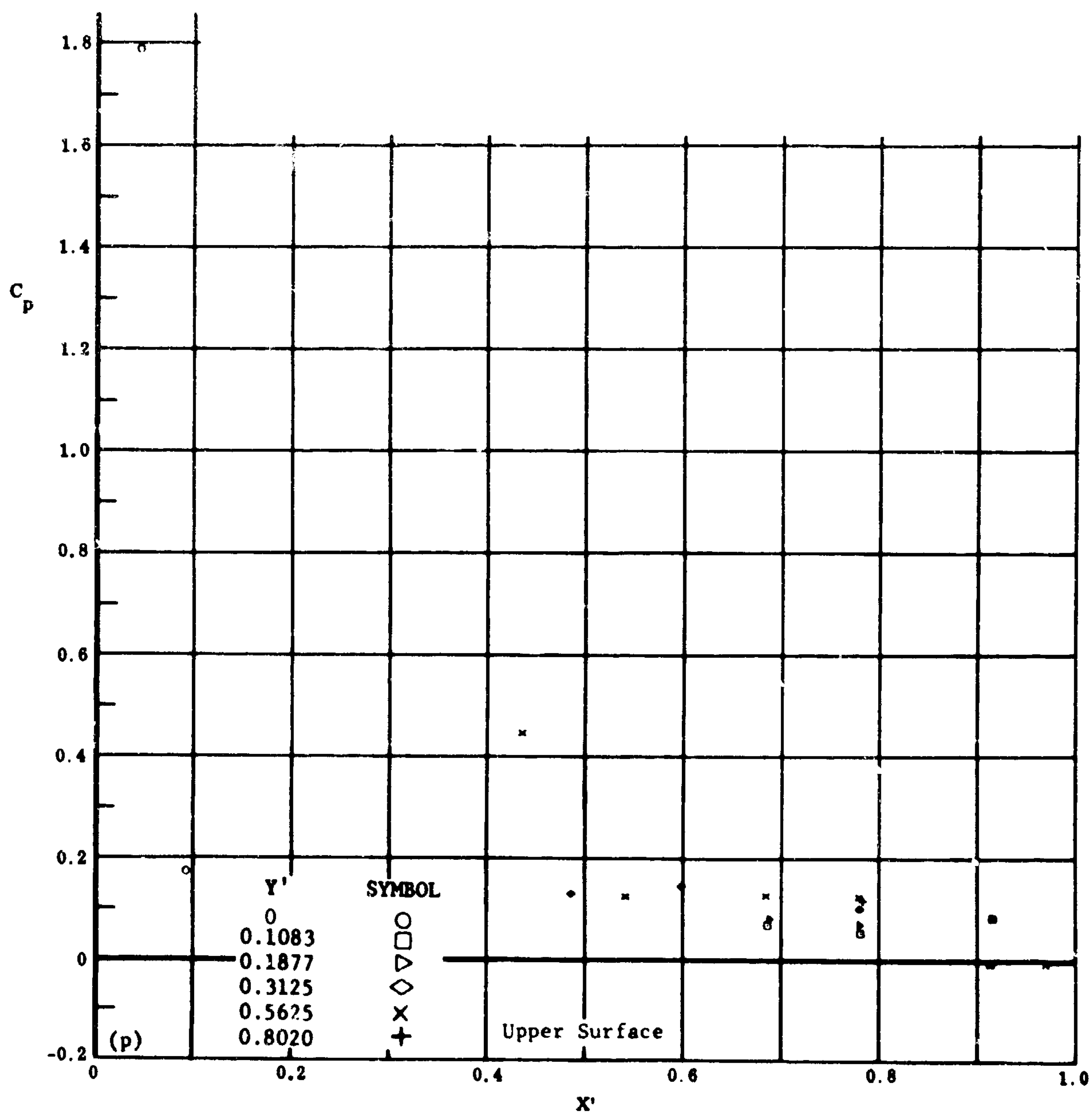

Fig. 16 Configuration I, $\alpha = -10$, $\delta_2 = \delta_3 = +30$

o) C_p vs. Y', upper surface

p) C_p vs. X', upper surface

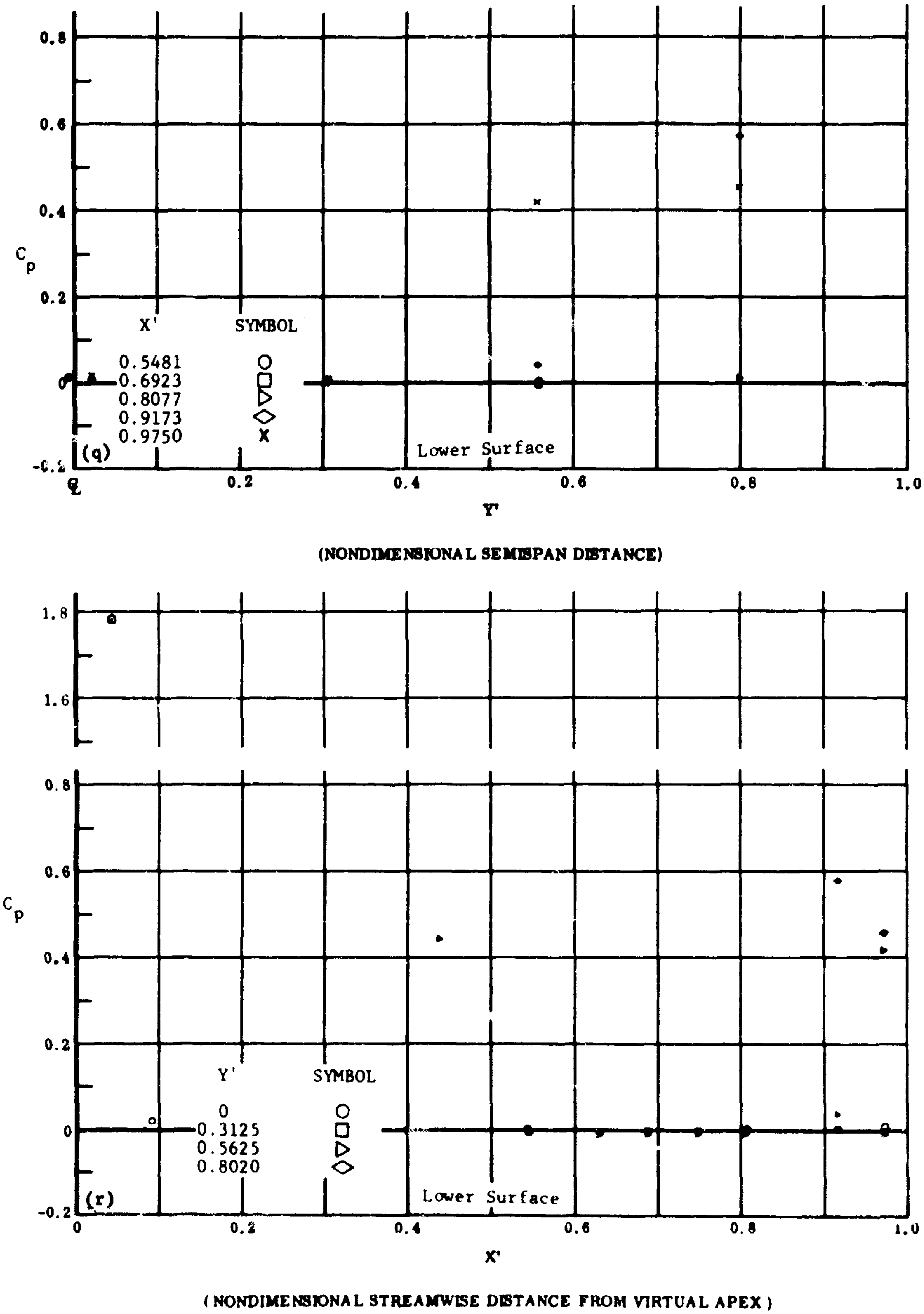

Fig. 16 Configuration I, $\alpha = -10$, $\delta_2 = \delta_3 = +39$

q) C_p vs. Y', lower surface

r) C_p vs. X', lower surface

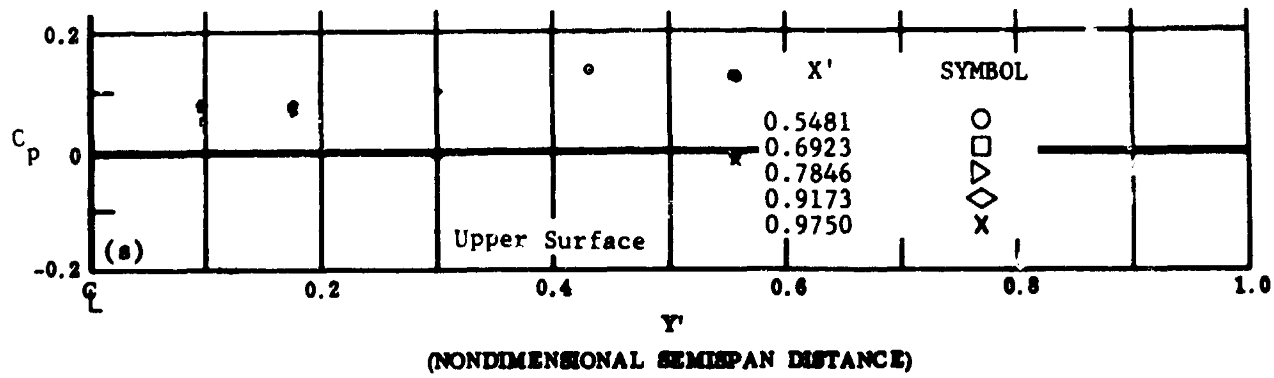

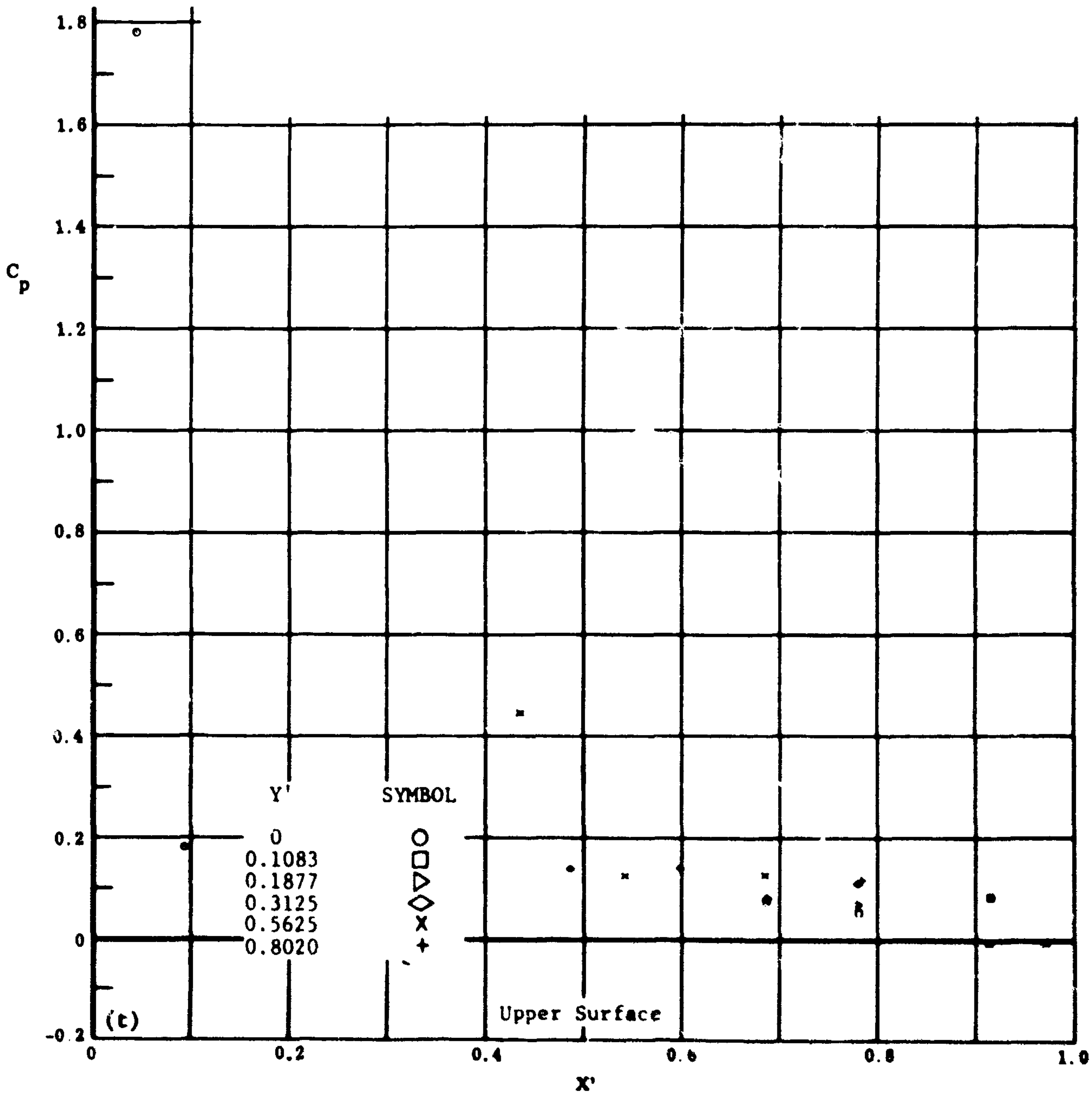

Fig. 16 Configuration I, $\alpha = -10$, $\delta_2 = \delta_3 = +39$

s) C_p vs. Y', upper surface

t) C_p vs. X', upper surface

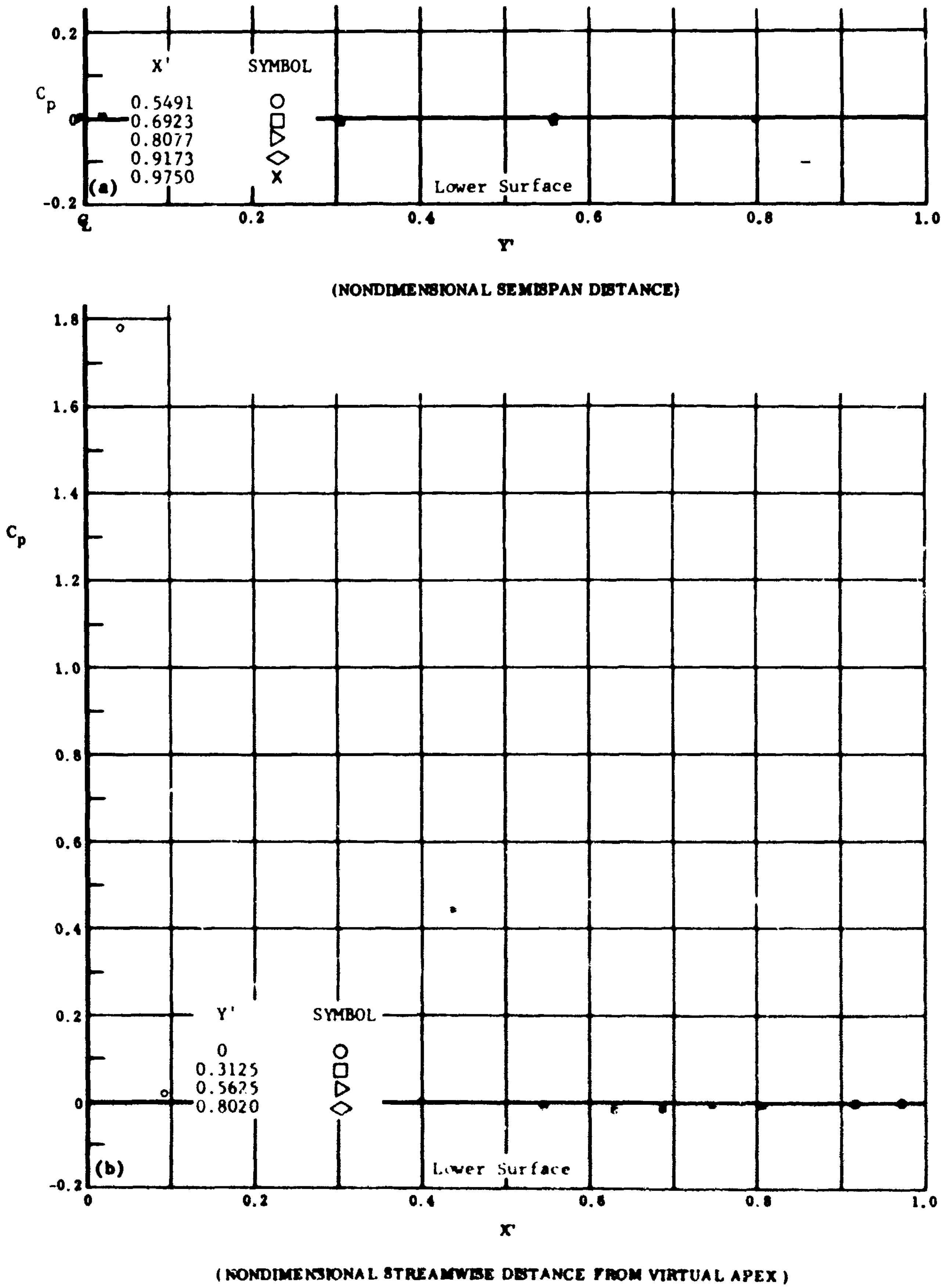

Fig. 17 Configuration I, $\alpha = -10$, $\delta_2 = \delta_3 = -10$

a) C_p vs. Y', lower surface

b) C_p vs. X', lower surface

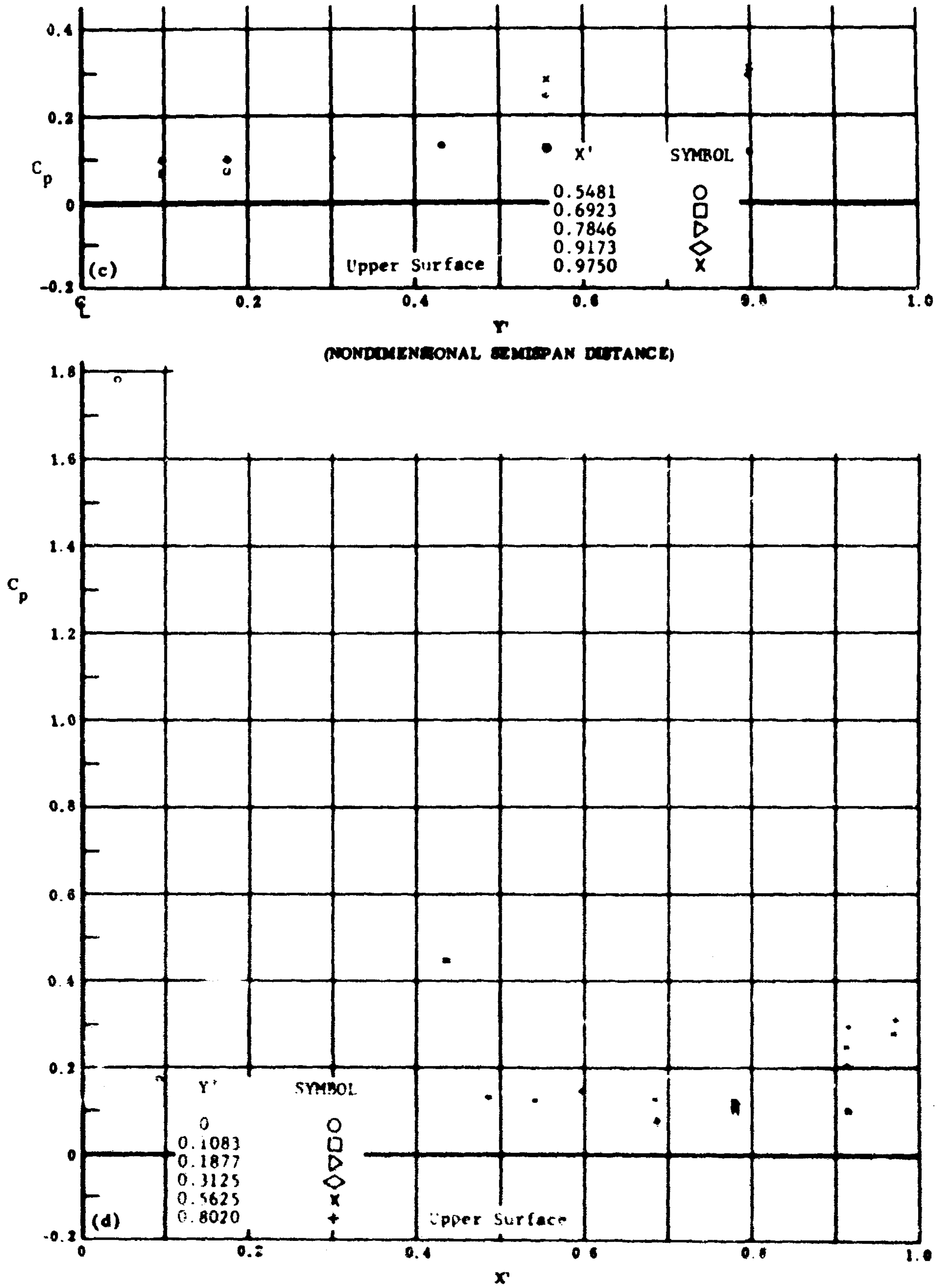

(NONDIMENSIONAL STREAMWISE DISTANCE FROM VIRTUAL APEX)

Fig. 17 Configuration I, $\delta_1 = -10$, $\delta_2 = \delta_3 = -10$

c) C_p vs. Y', upper surface

d) C_p vs. X', upper surface

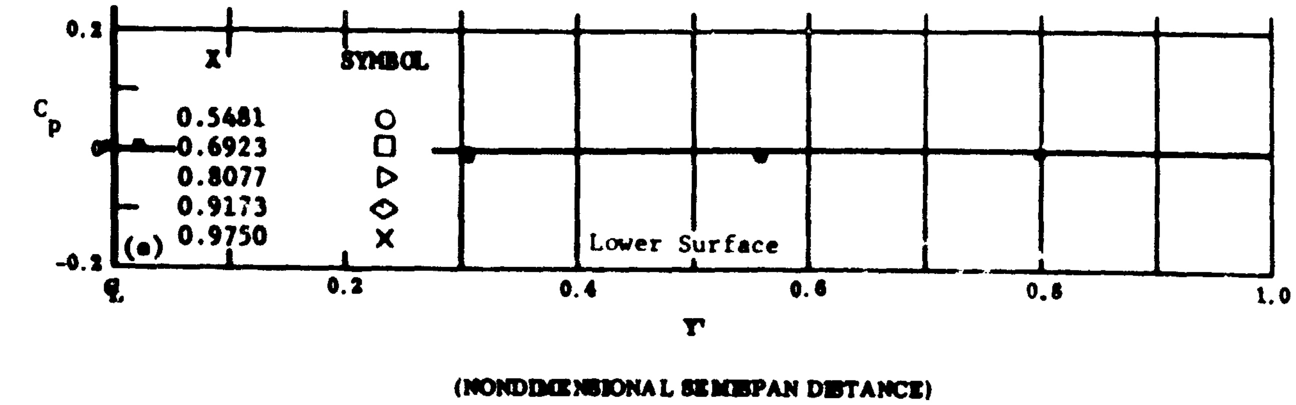

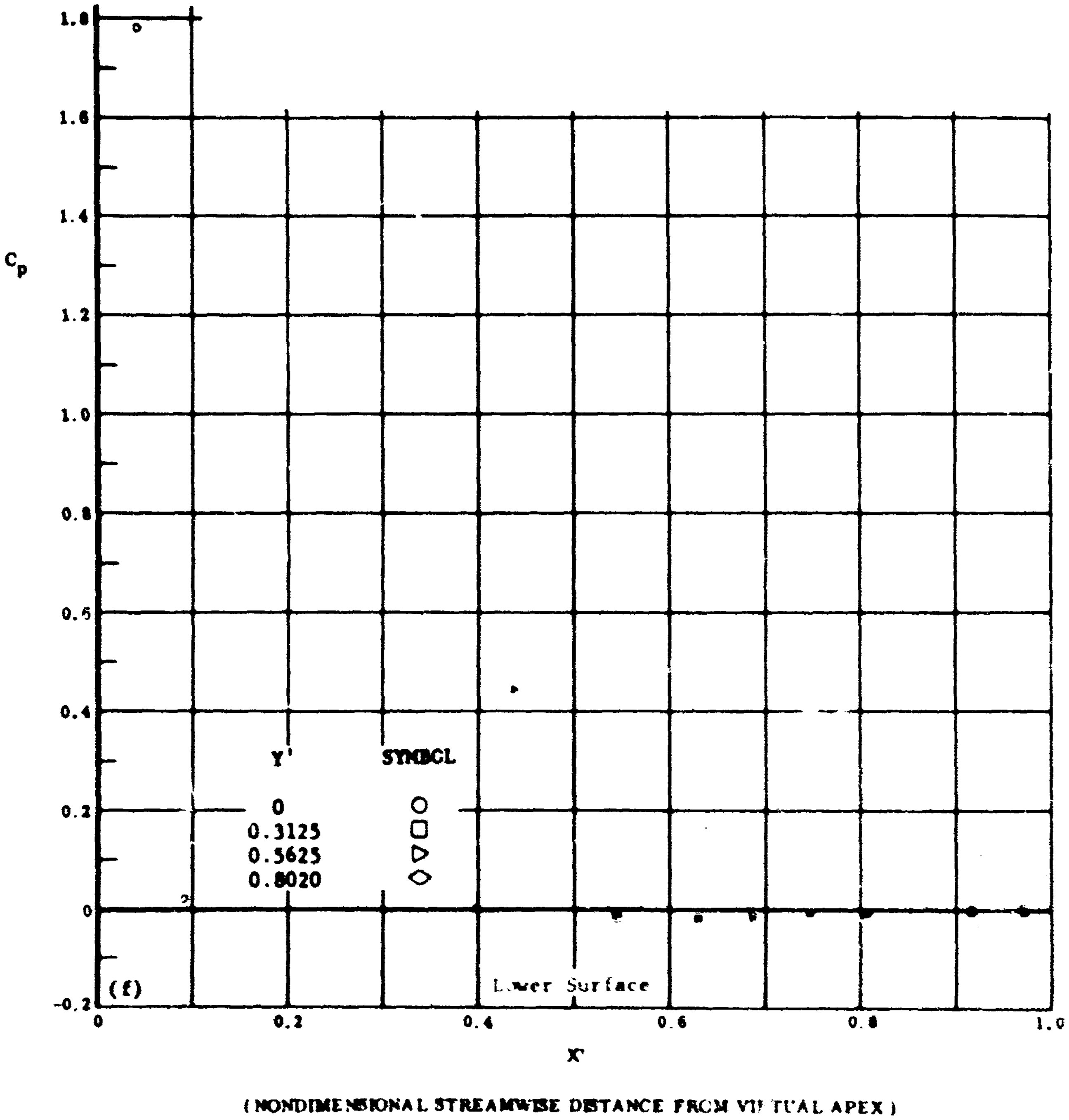

Fig. 17 Configuration I, $_1$ = -10 , $_2$ = $_3$ = -20

e) C_p vs. Y', lower surface

f) C_p vs. X', lower surface

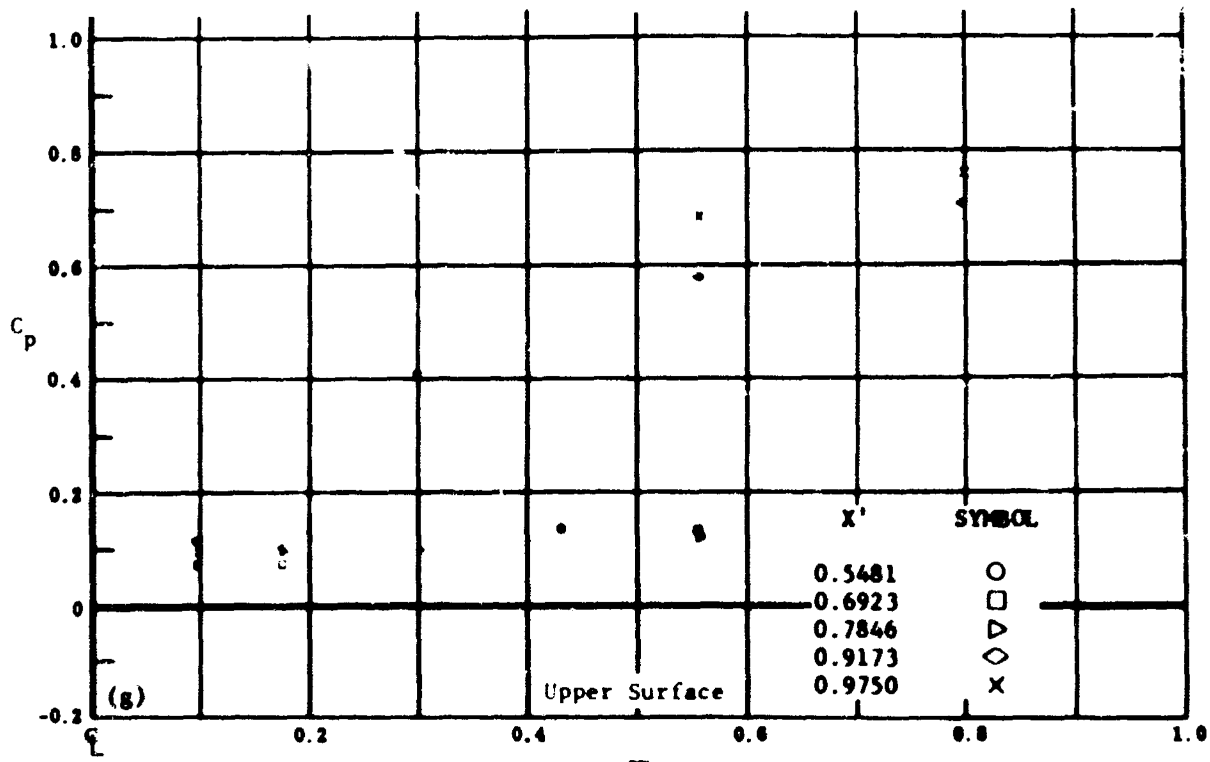

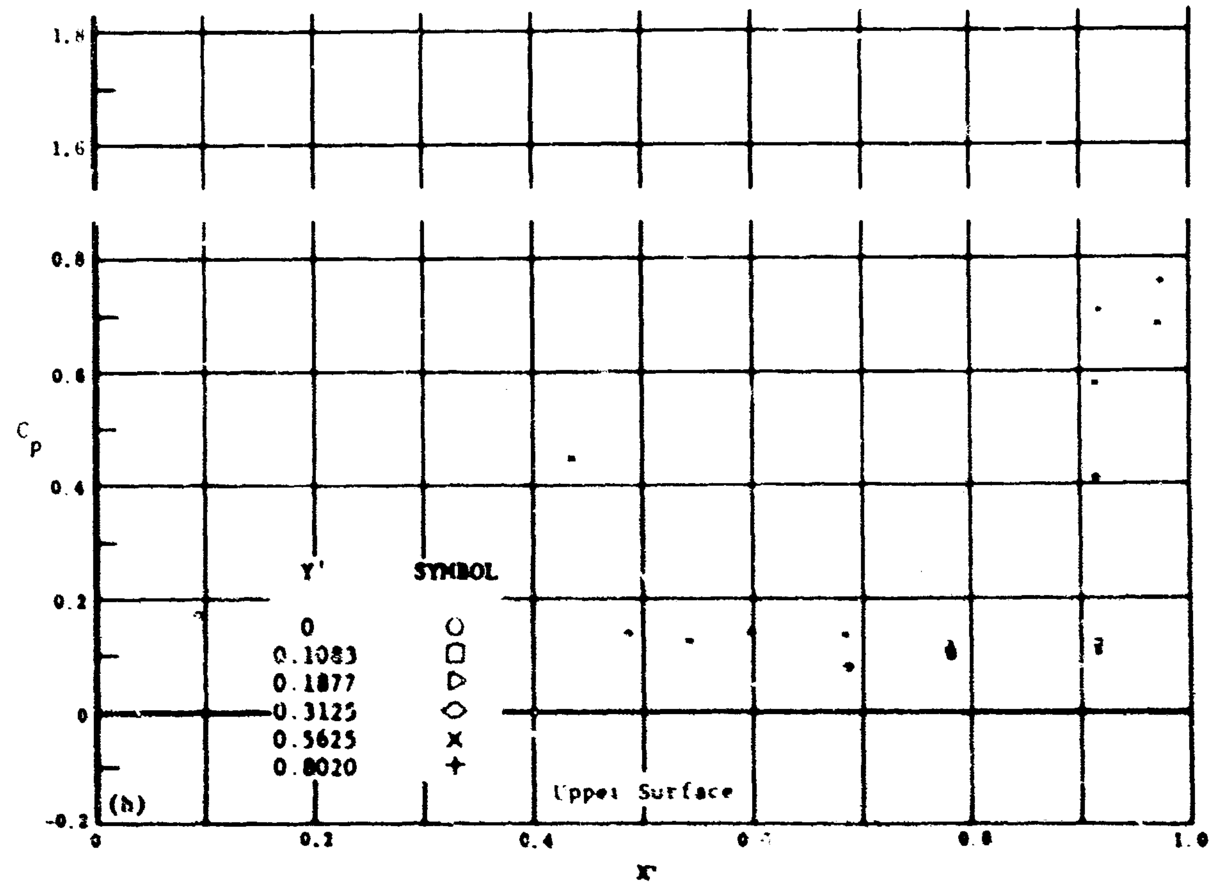

(NONDIMENSIONAL STREAMWISE DISTANCE FROM VIRTUAL APEX)

Fig. 17 Configuration I, α = -10 , $\delta_2 = \delta_3$ = -20

g) C_p vs. Y', upper surface

h) C_p vs. X', upper surface

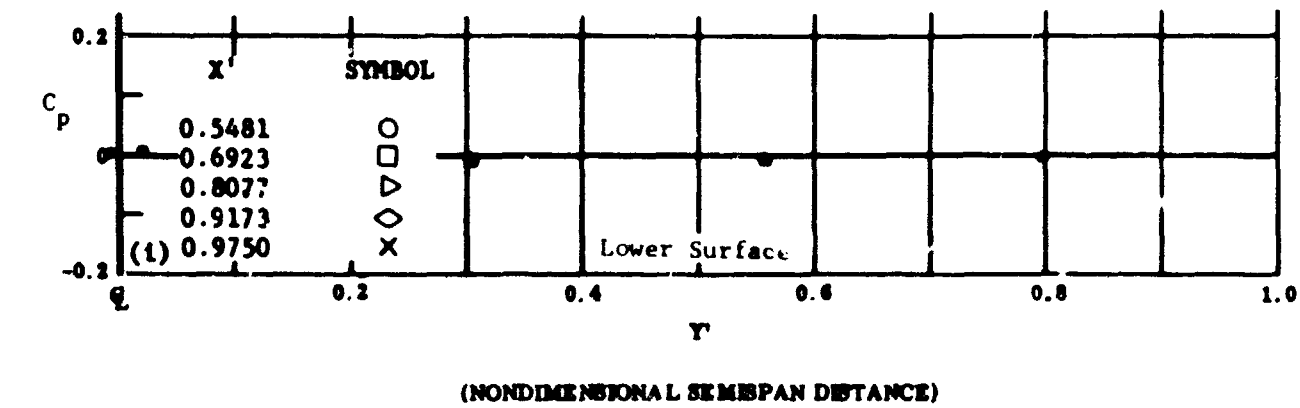

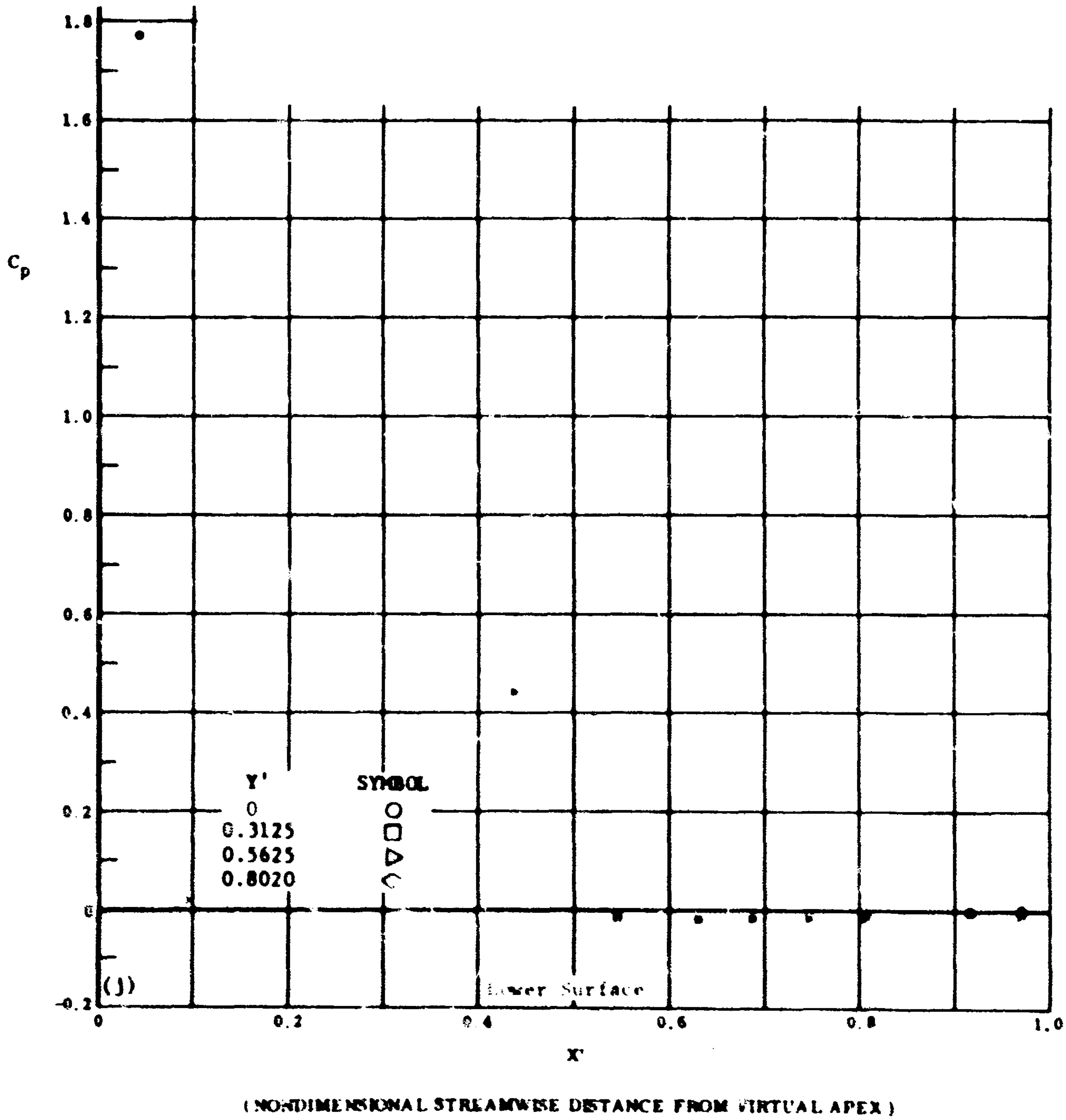

Fig. 17 Configuration I, [illegible] = -10, [illegible]$_2$ = [illegible]$_3$ = -30

i) C_p vs. Y', lower surface

j) C_p vs. X', lower surface

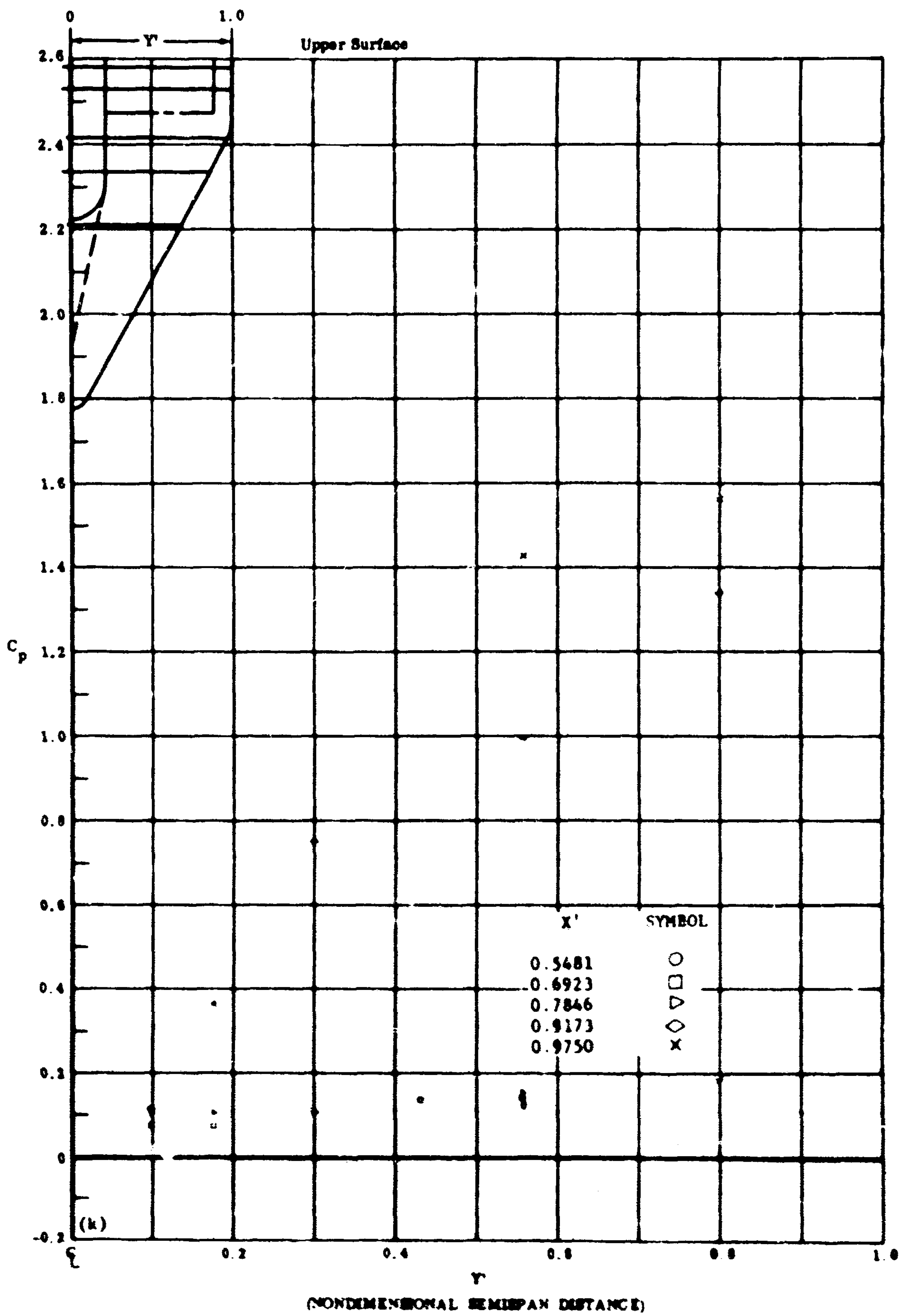

Fig. 17k Configuration I, δ_1 = -10 , $\delta_2 = \delta_3$ = -30

C_p vs. Y', upper surface

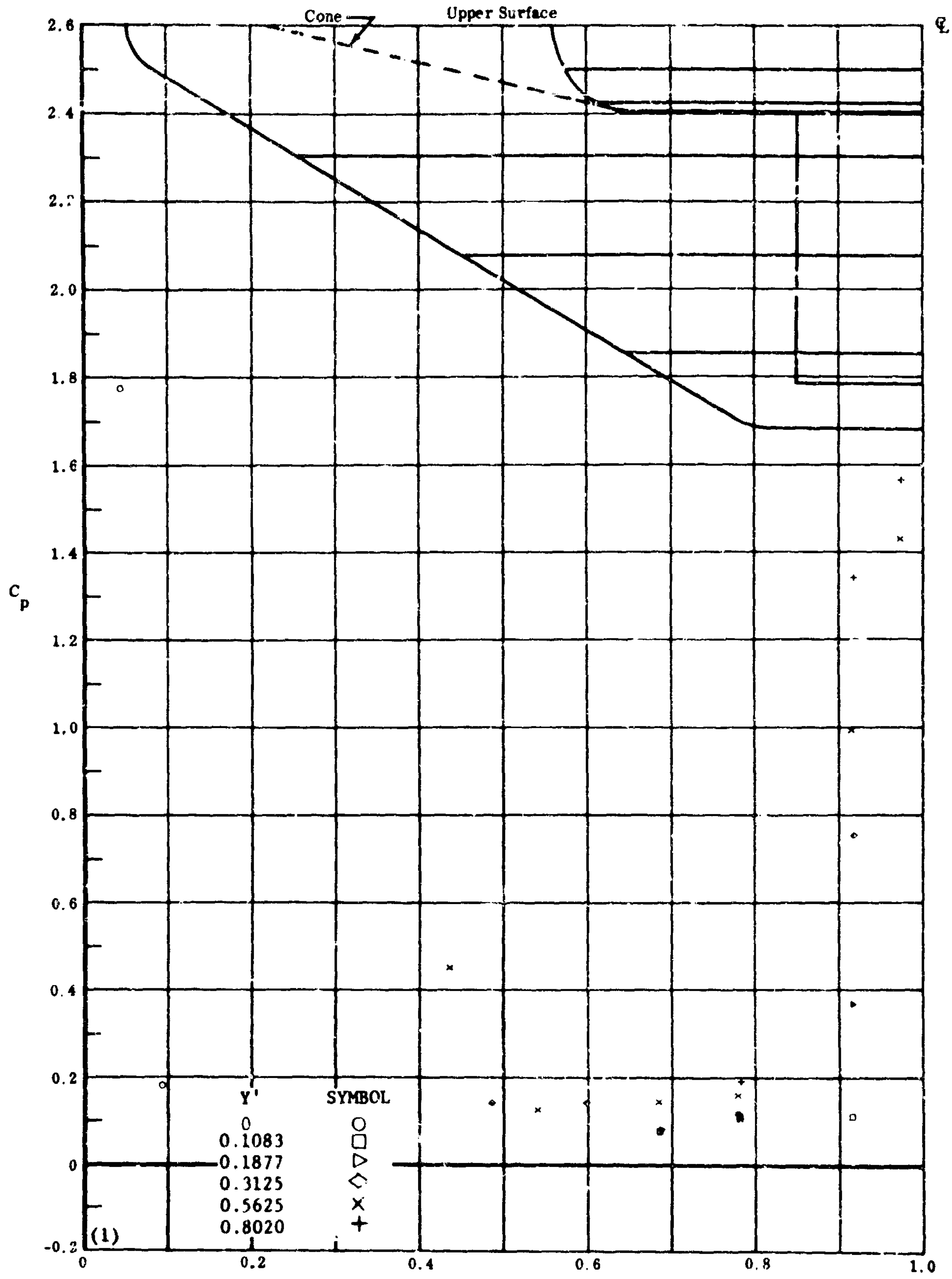

(NONDIMENSIONAL STREAMWISE DISTANCE FROM VIRTUAL APEX)

Fig. 171 Configuration I, α = -10 , δ_2 = δ_3 = -30

C_p vs. X', upper surface

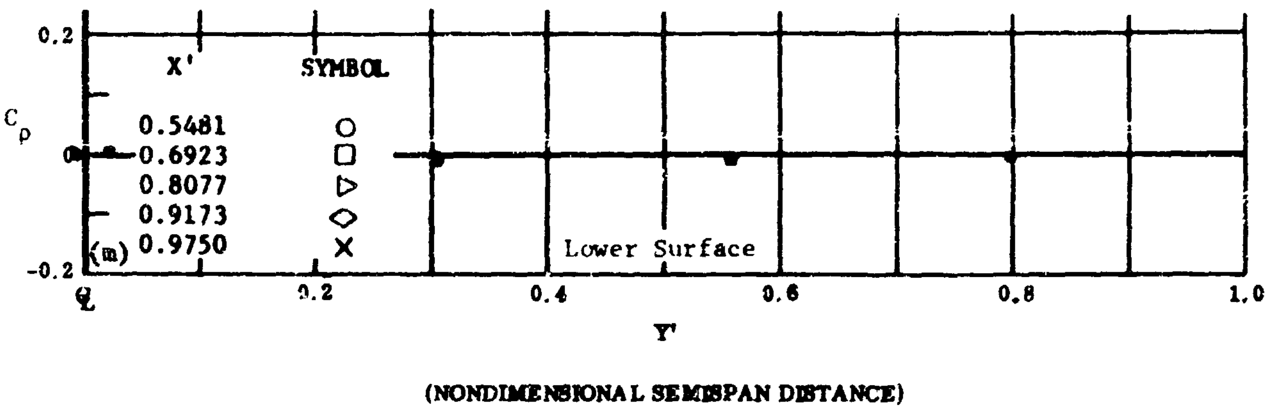

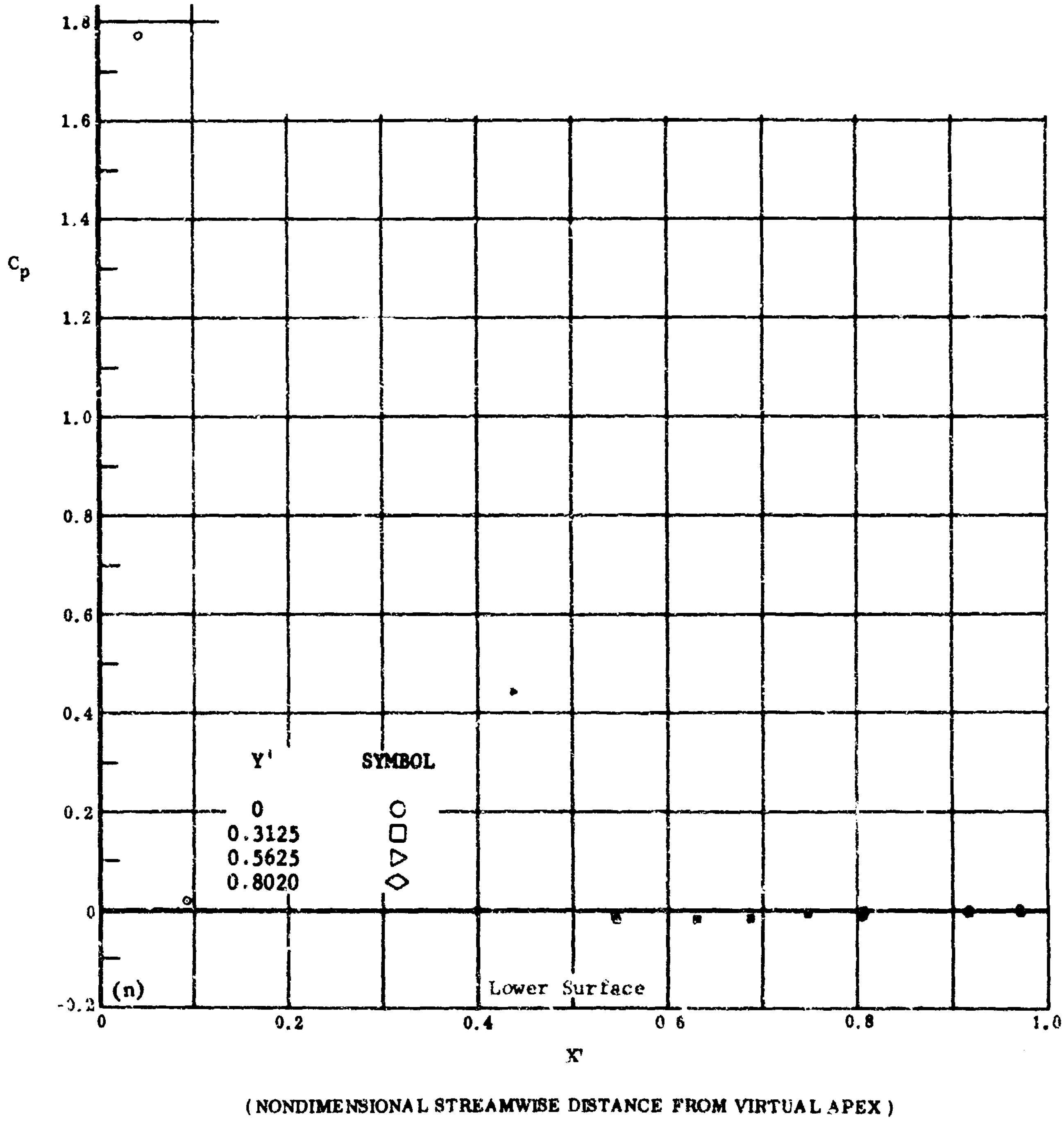

Fig. 17 Configuration I, $\alpha = -10$, $\delta_2 = \delta_3 = -39$

m) C_p vs. Y', lower surface

n) C_p vs. X', lower surface

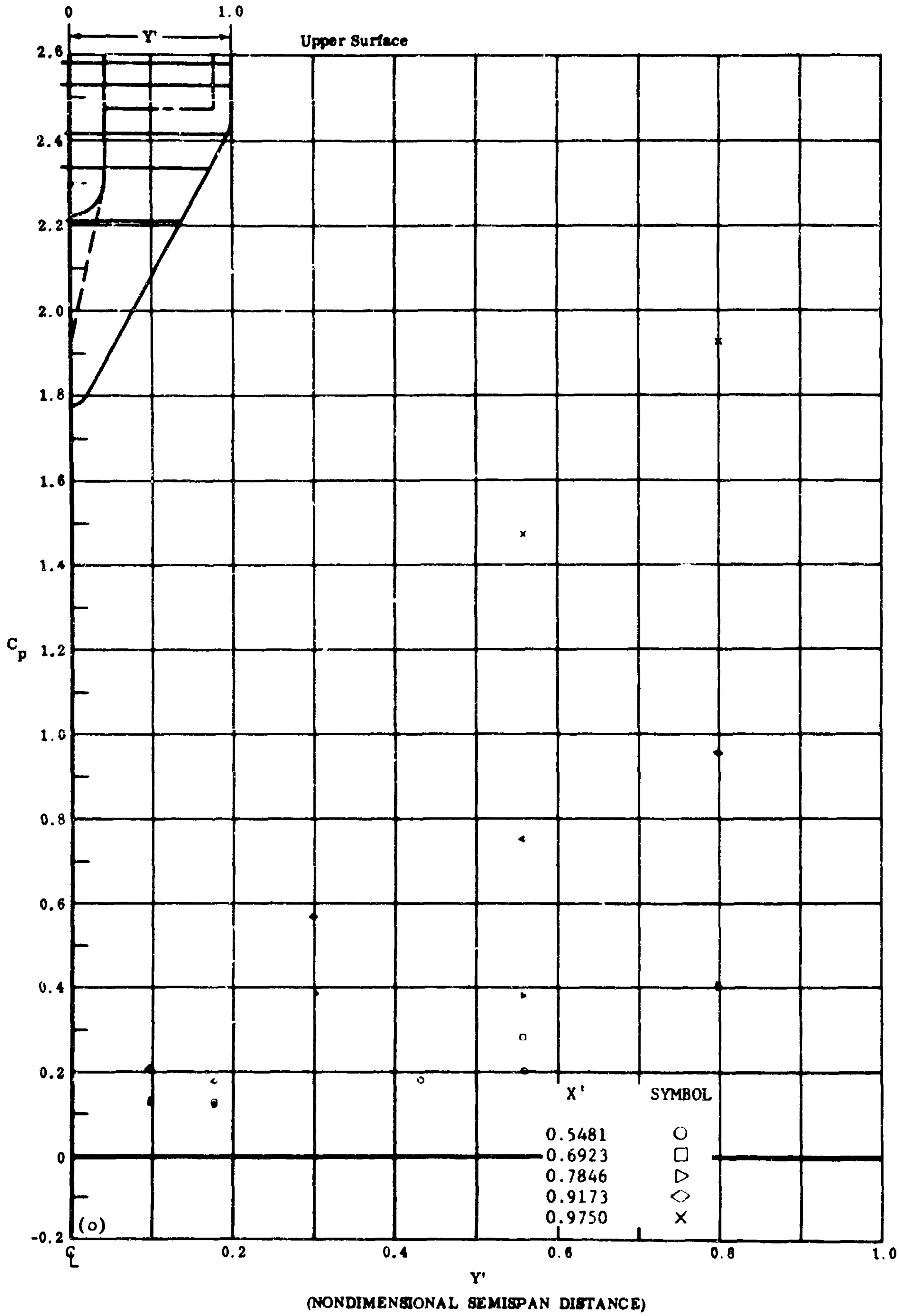

Fig. 17o Configuration I, α = -10 , $\delta_2 = \delta_3$ = -39

C_p vs. Y', upper surface

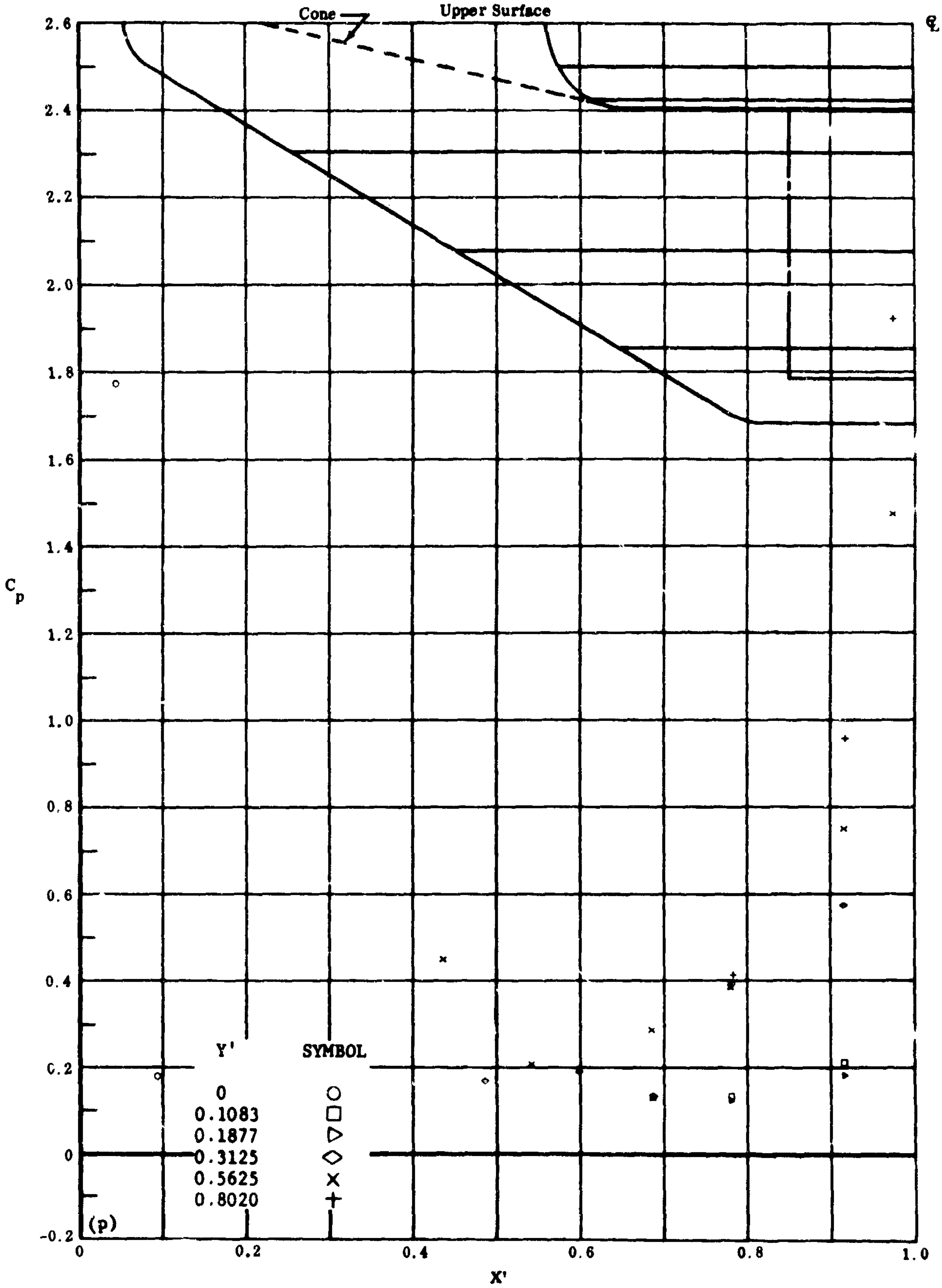

(NONDIMENSIONAL STREAMWISE DISTANCE FROM VIRTUAL APEX)

Fig. 17p Configuration I, $\alpha = -10$, $\delta_2 = \delta_3 = -39$

C_p vs. X', upper surface

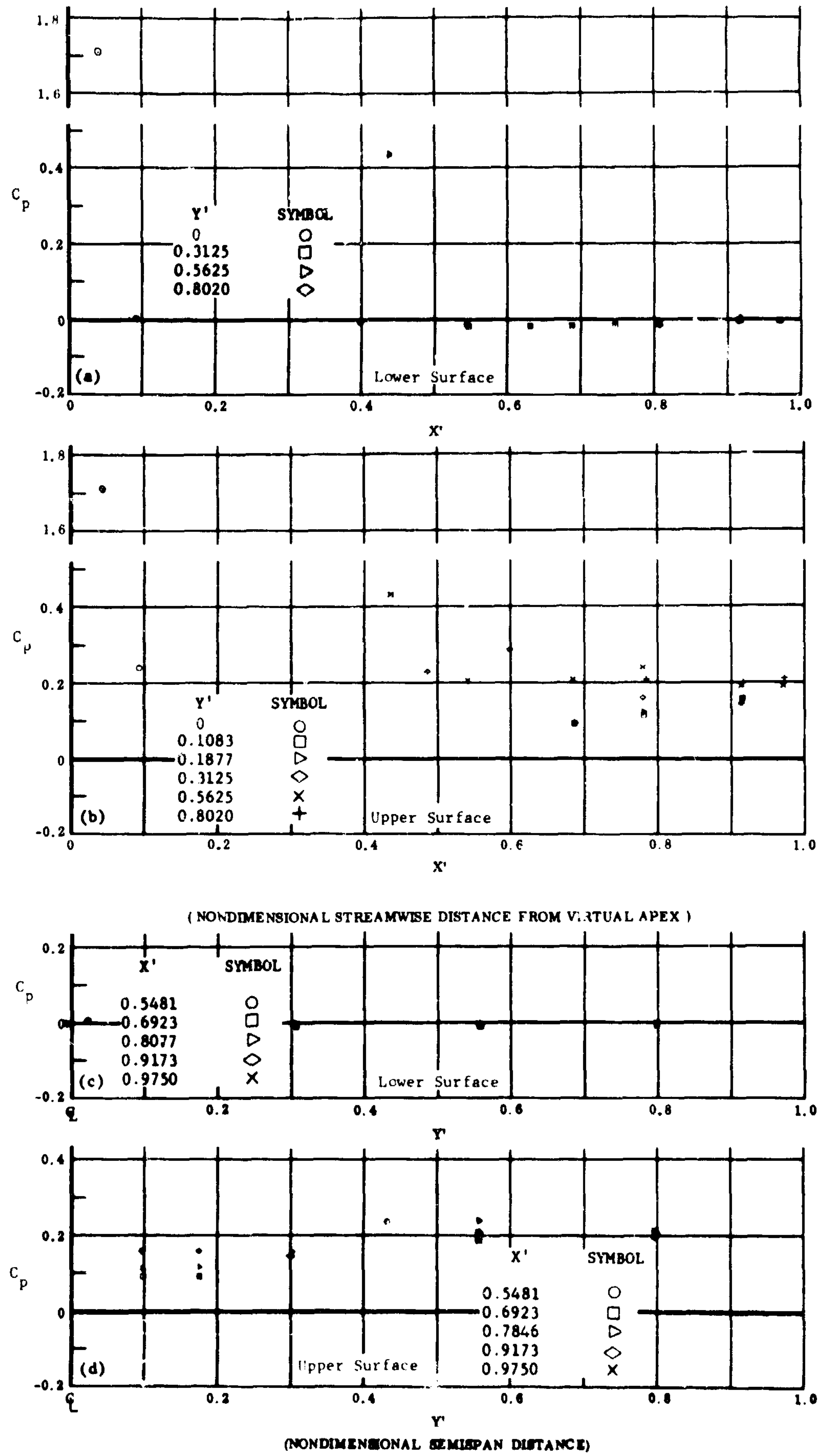

Fig. 18 Configuration I, $\alpha = -15$, $\delta_2 = \delta_3 = 0$

a) C_p vs. X', lower surface

b) C_p vs. X', upper surface

c) C_p vs. Y', lower surface

d) C_p vs. Y', upper surface

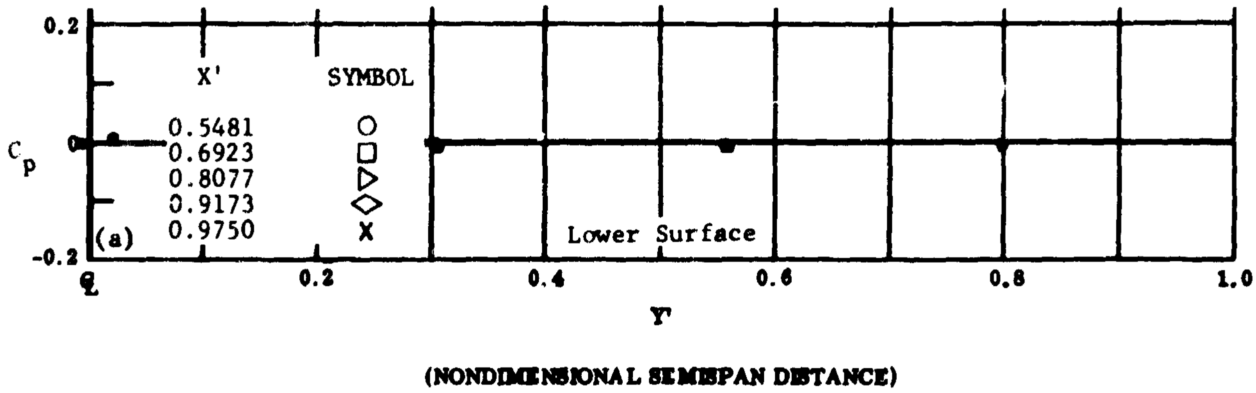

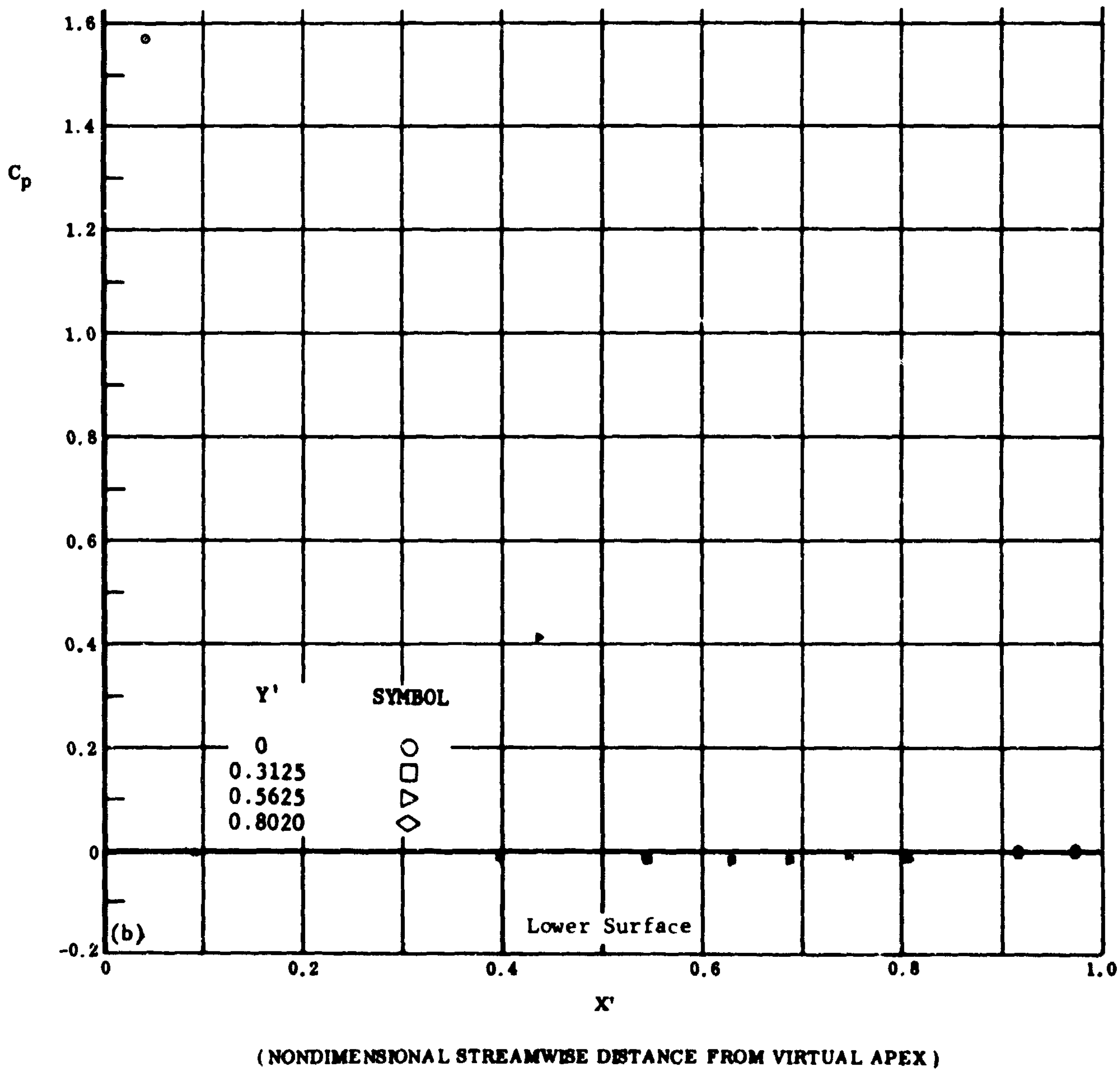

Fig. 19 Configuration I, $\alpha = -20$, $\delta_2 = \delta_3 = 0$

a) C_p vs. Y', lower surface

b) C_p vs. X', lower surface

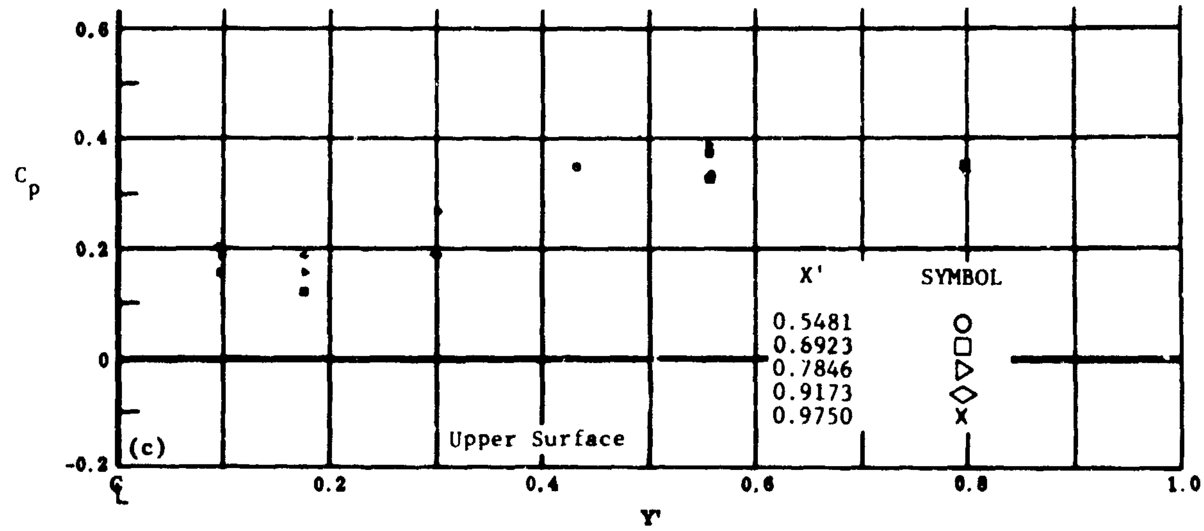

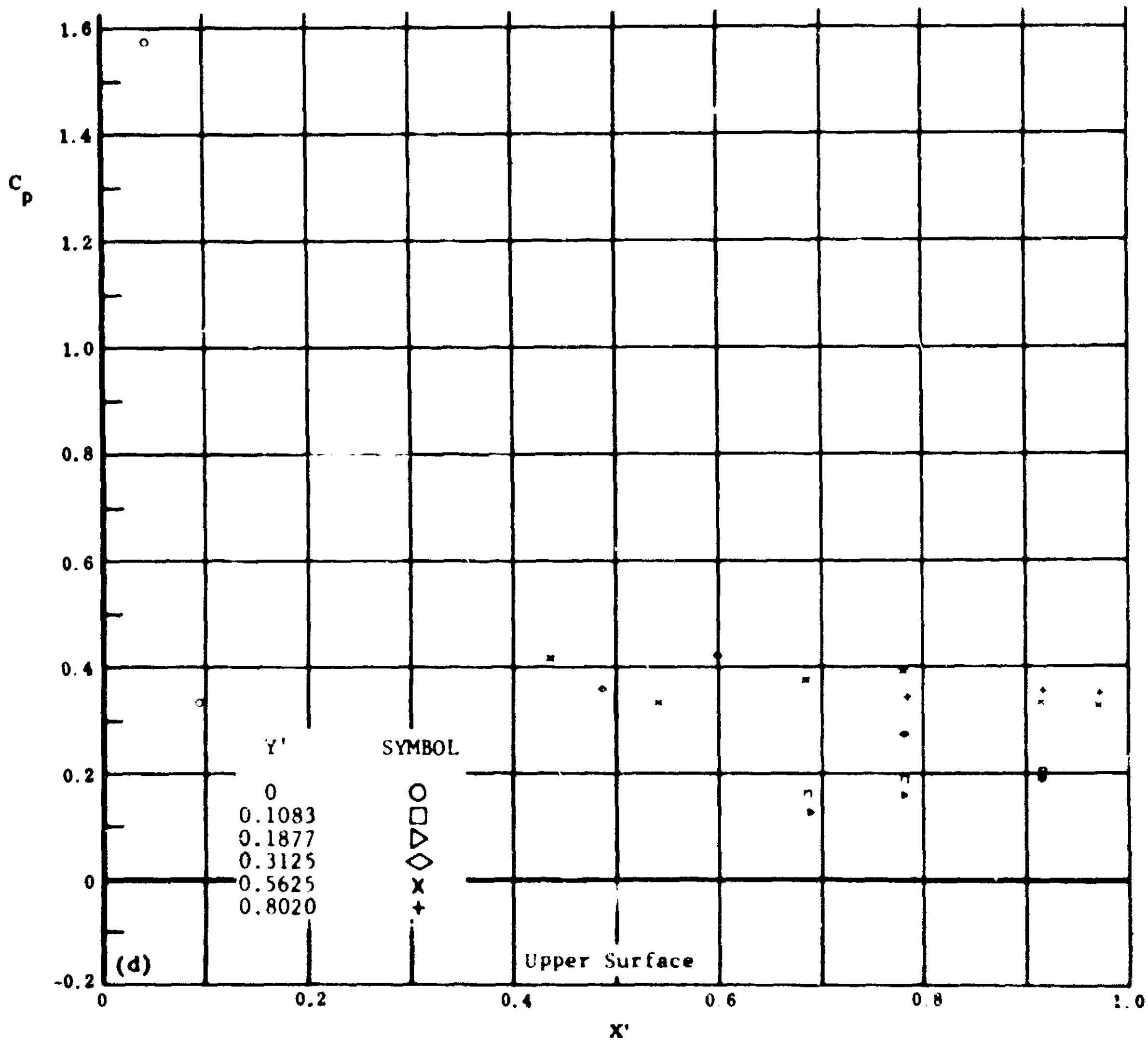

(NONDIMENSIONAL STREAMWISE DISTANCE FROM VIRTUAL APEX)

Fig. 19 Configuration I, $\iota = -20$, $\delta_2 = \delta_3 = 0$

c) C_p vs. Y', upper surface

d) C_p vs. X', upper surface

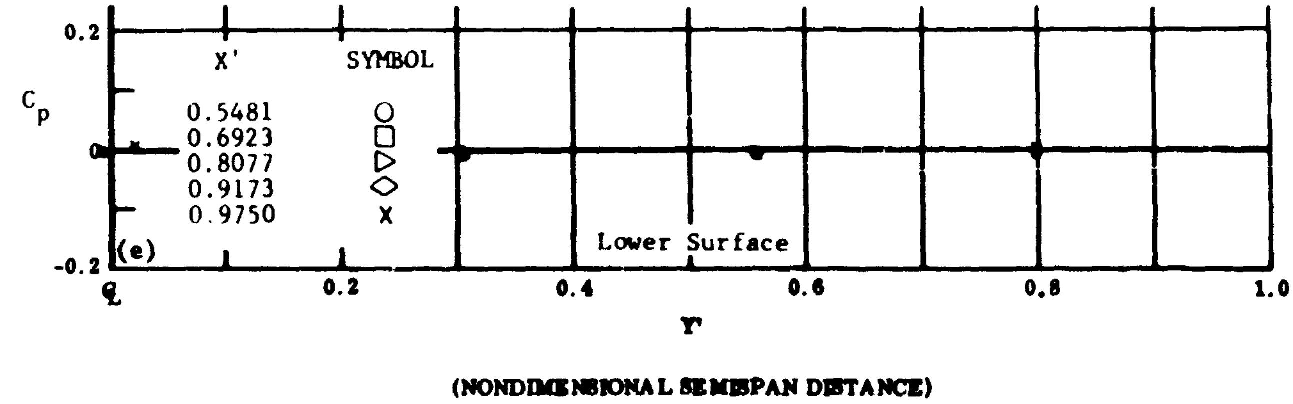

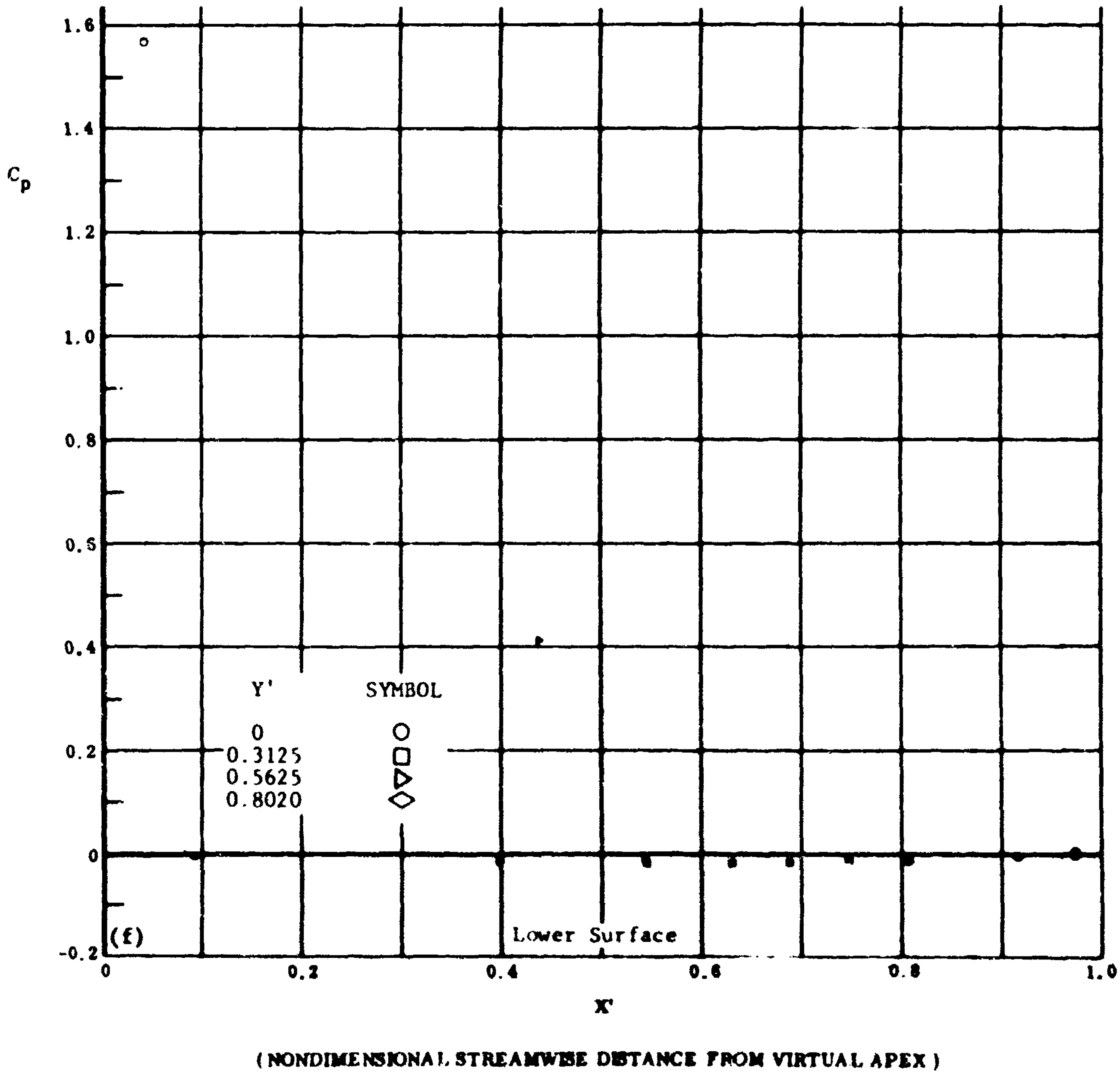

Fig. 19 Configuration I, $\alpha = -20$, $\delta_2 = \delta_3 = +10$

e) C_p vs. Y', lower surface

f) C_p vs. X', lower surface

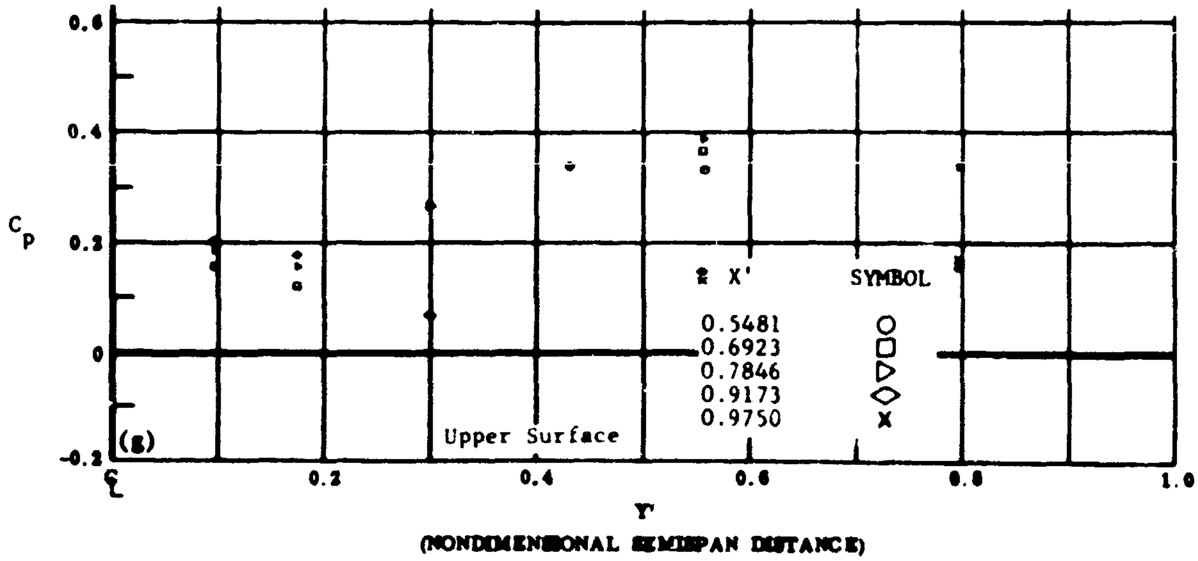

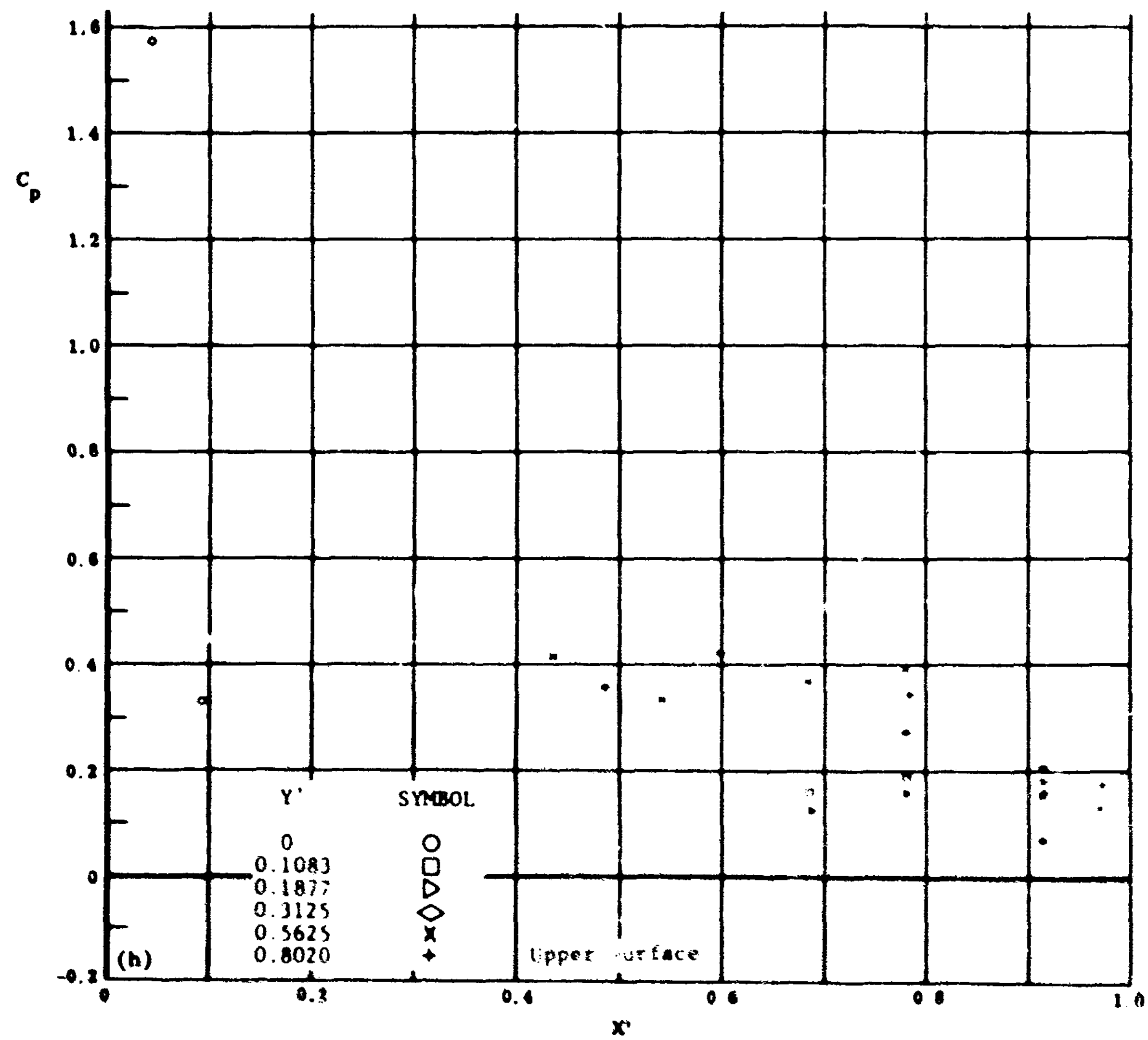

(NONDIMENSIONAL STREAMWISE DISTANCE FROM VIRTUAL APEX)

Fig. 19 Configuration I, $\alpha = -20$, $\delta_2 = \delta_3 = +10$

g) C_p vs. Y', upper surface

h) C_p vs. X', upper surface

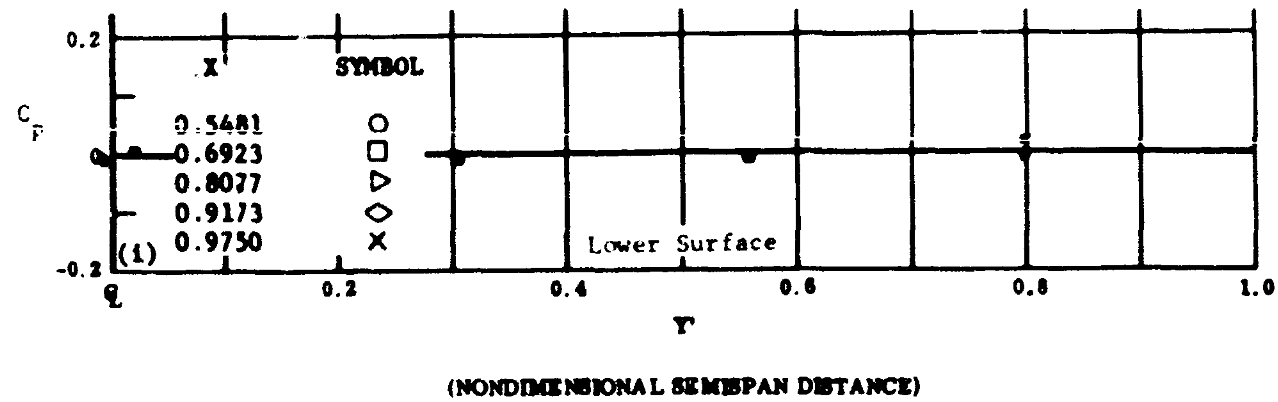

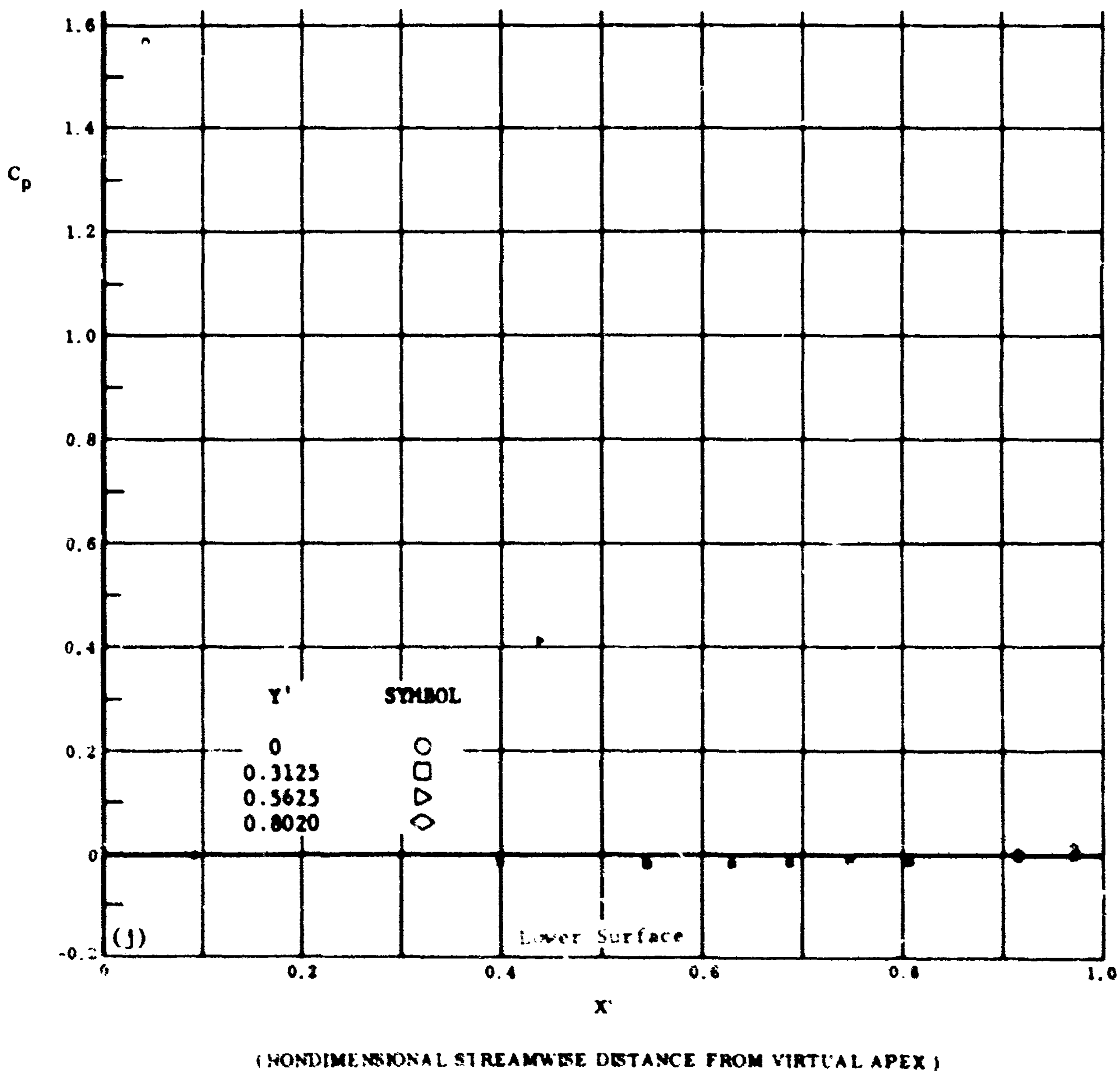

Fig. 19 Configuration I, $\delta_1 = -20$, $\delta_2 = \delta_3 = +20$

i) C_p vs. Y', lower surface

j) C_p vs. X', lower surface

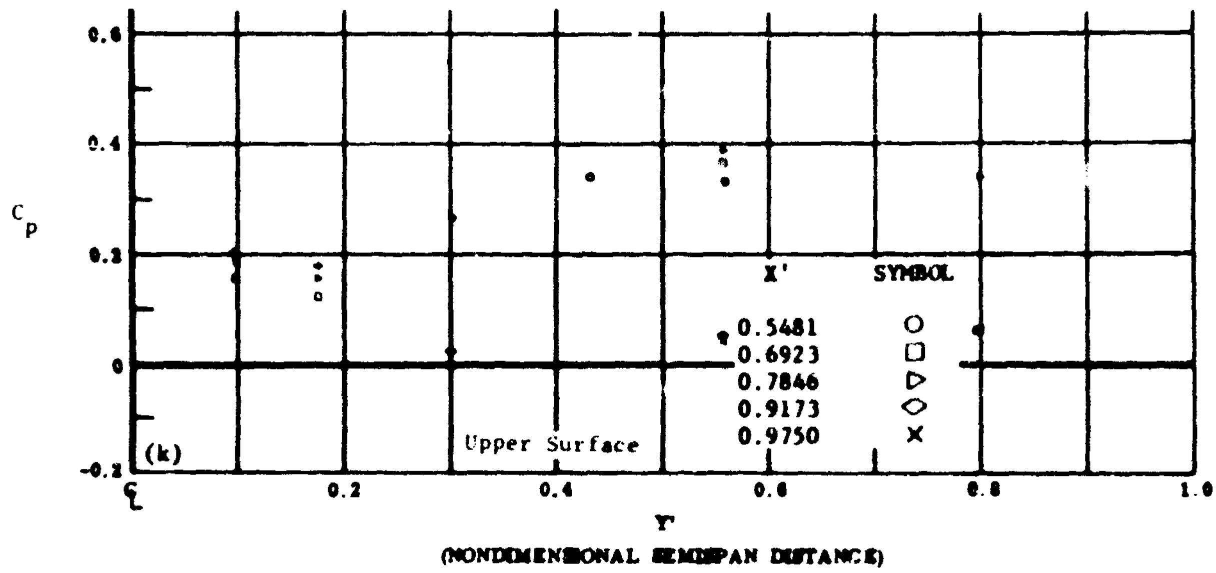

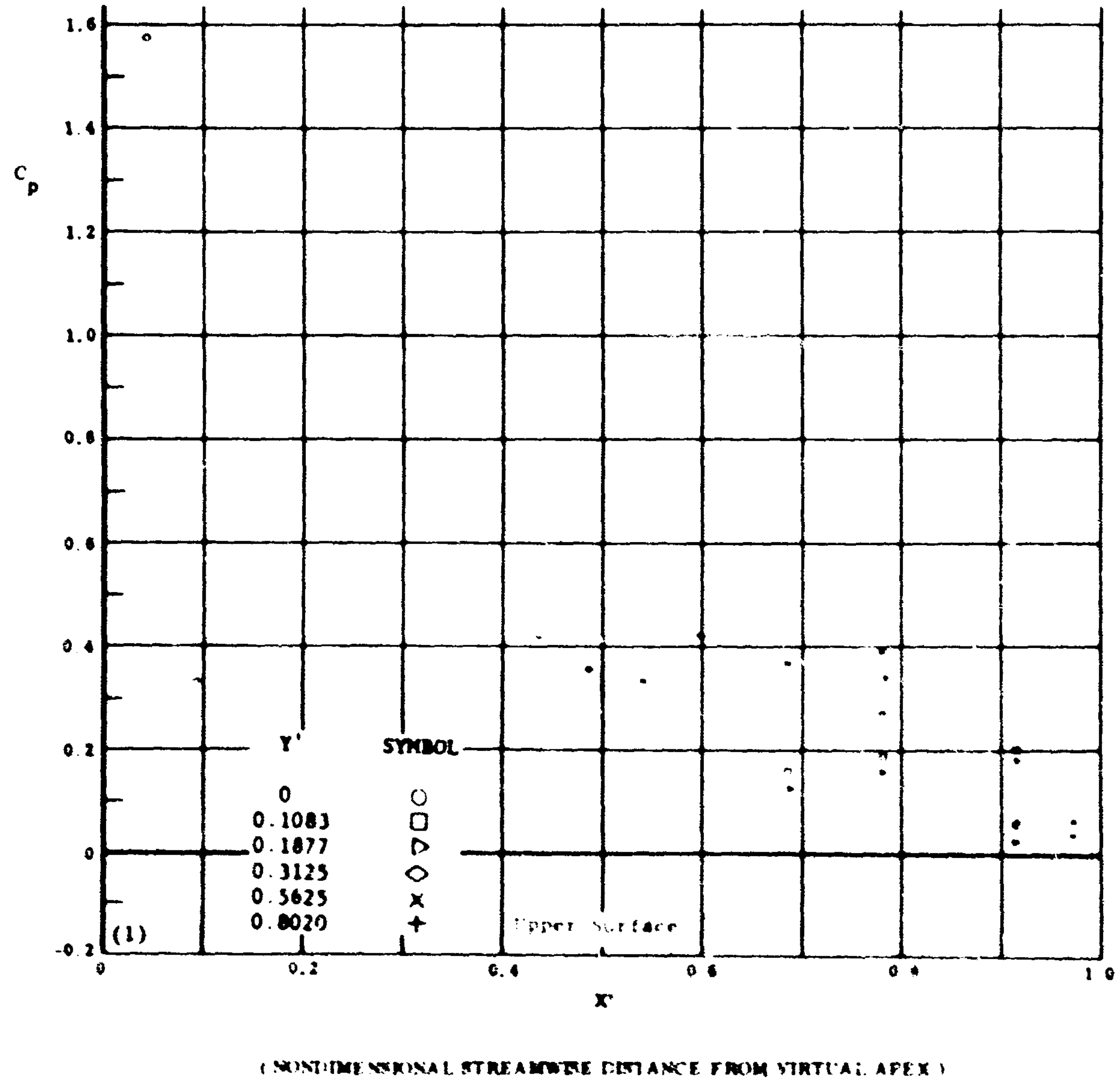

Fig. 19 Configuration I, $\delta_1 = -20$, $\delta_2 = \delta_3 = +20$

k) C_p vs. Y', upper surface

l) C_p vs. X', upper surface

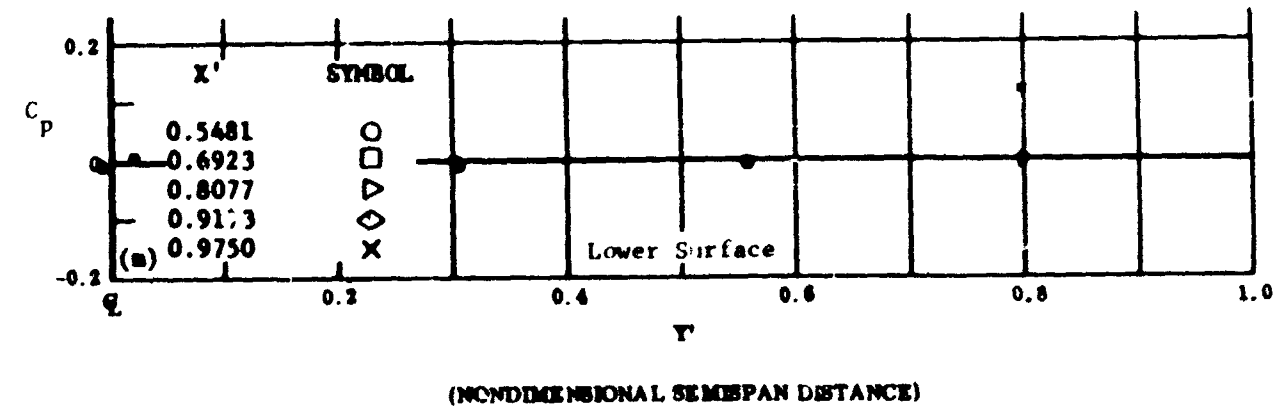

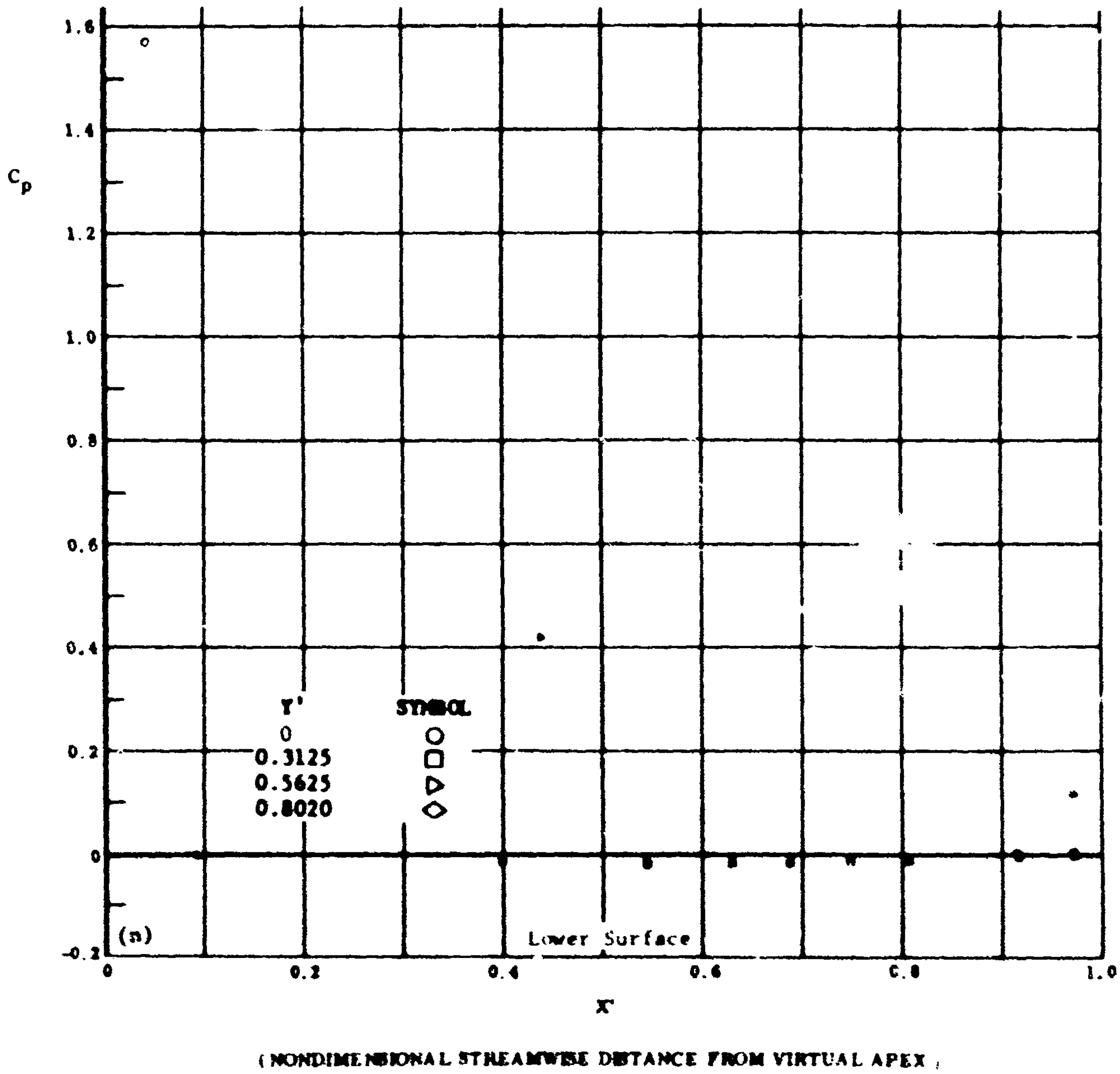

Fig. 19 Configuration I, $\delta_1 = -20$, $\delta_2 = \delta_3 = +30$

m) C_p vs. Y', lower surface

n) C_p vs. X', lower surface

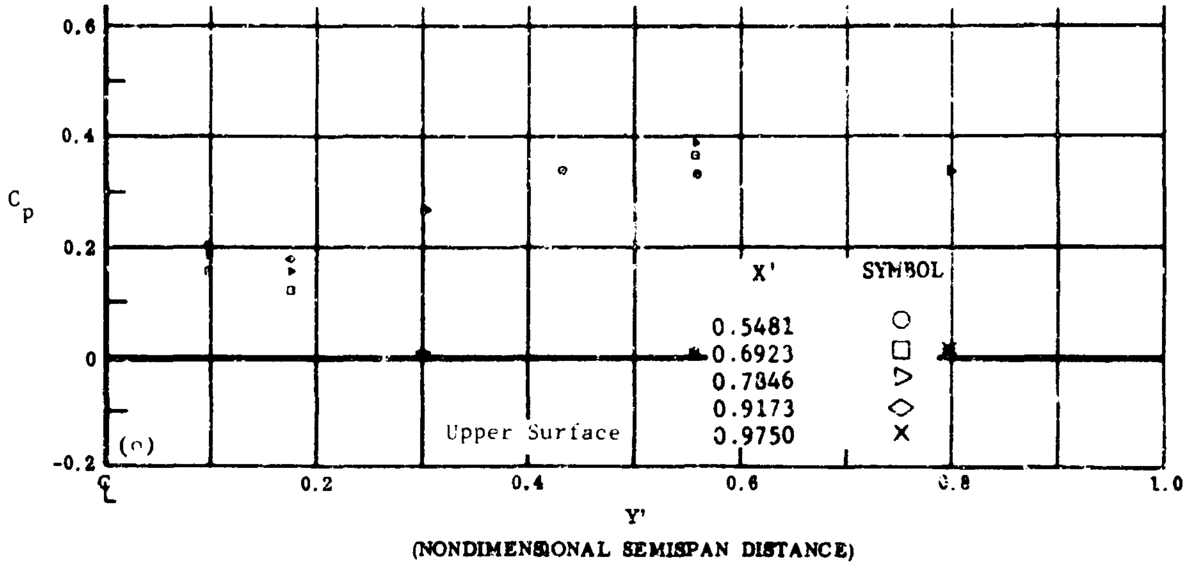

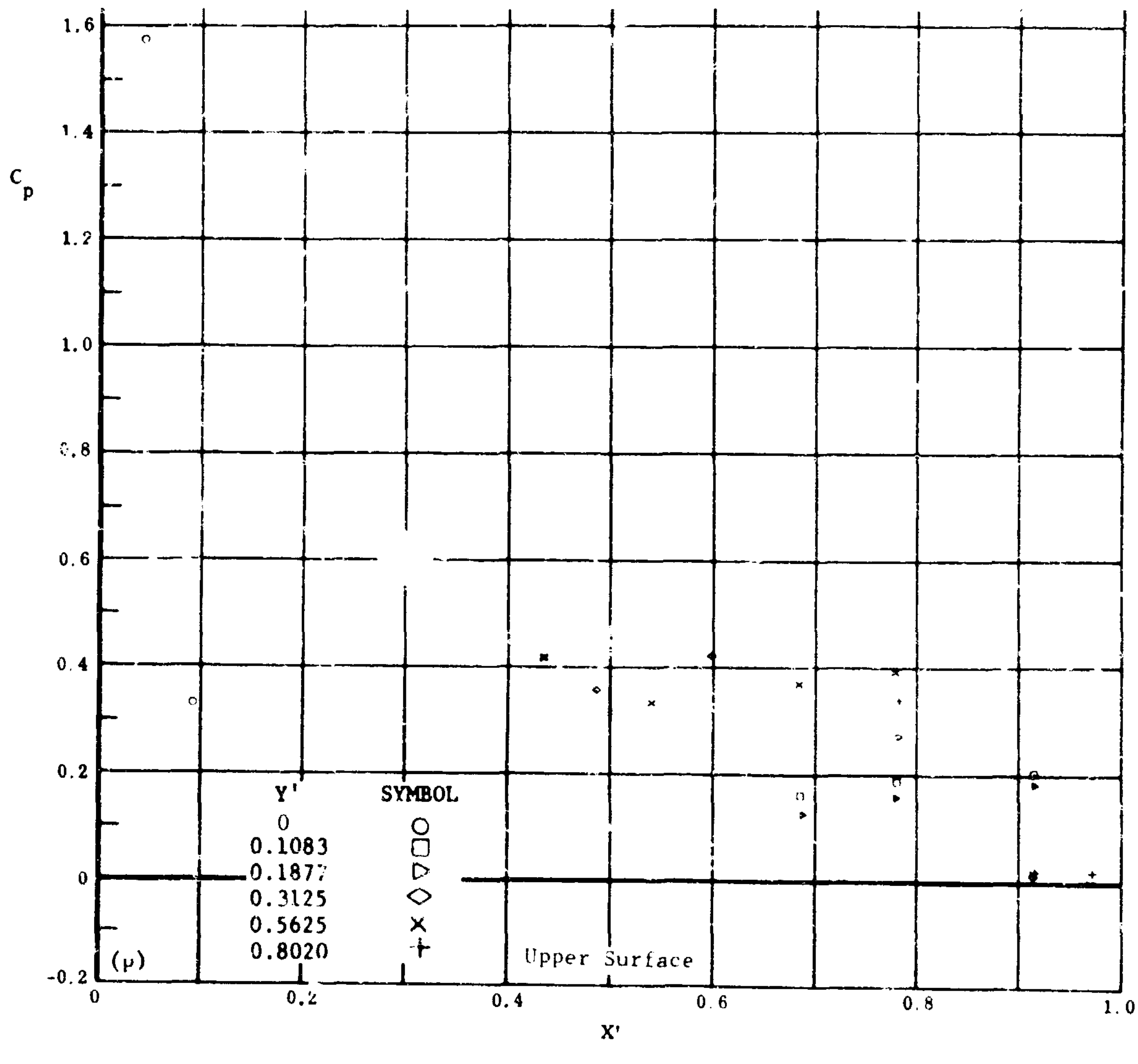

(NONDIMENSIONAL STREAMWISE DISTANCE FROM VIRTUAL APEX)

Fig. 19 Configuration I, α = -20 , $\delta_2 = \delta_3$ = +30

o) C_p vs. Y', upper surface

p) C_p vs. X', upper surface

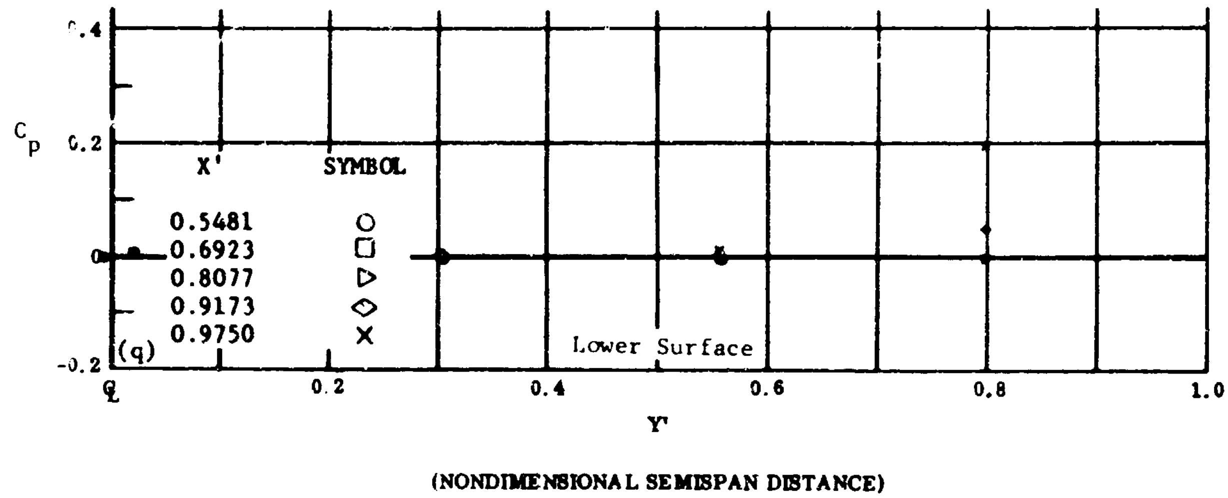

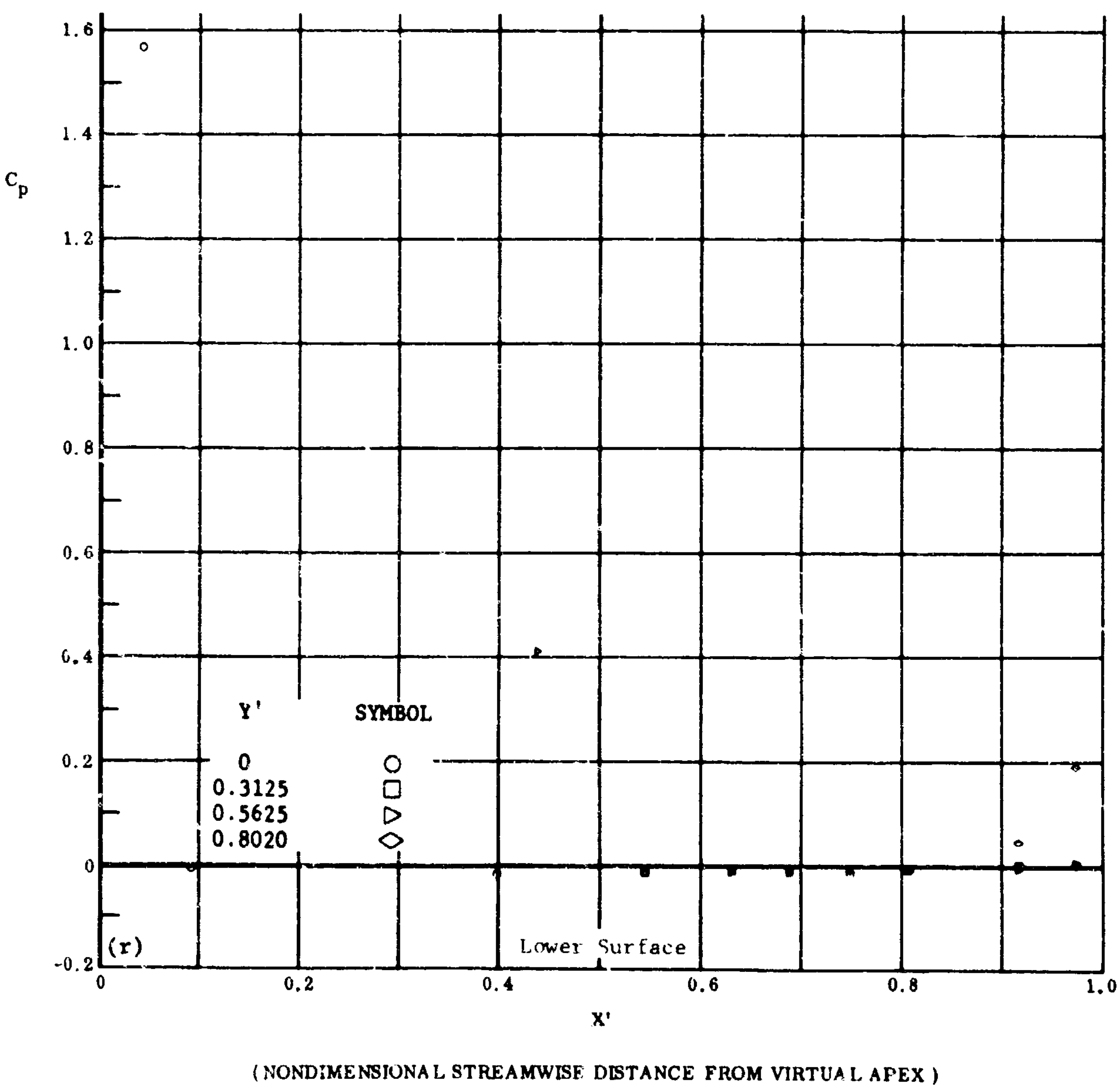

Fig. 19 Configuration I, $\alpha = -20$, $\delta_2 = \delta_3 = +39$

q) C_p vs. Y', lower surface

r) C_p vs. X', lower surface

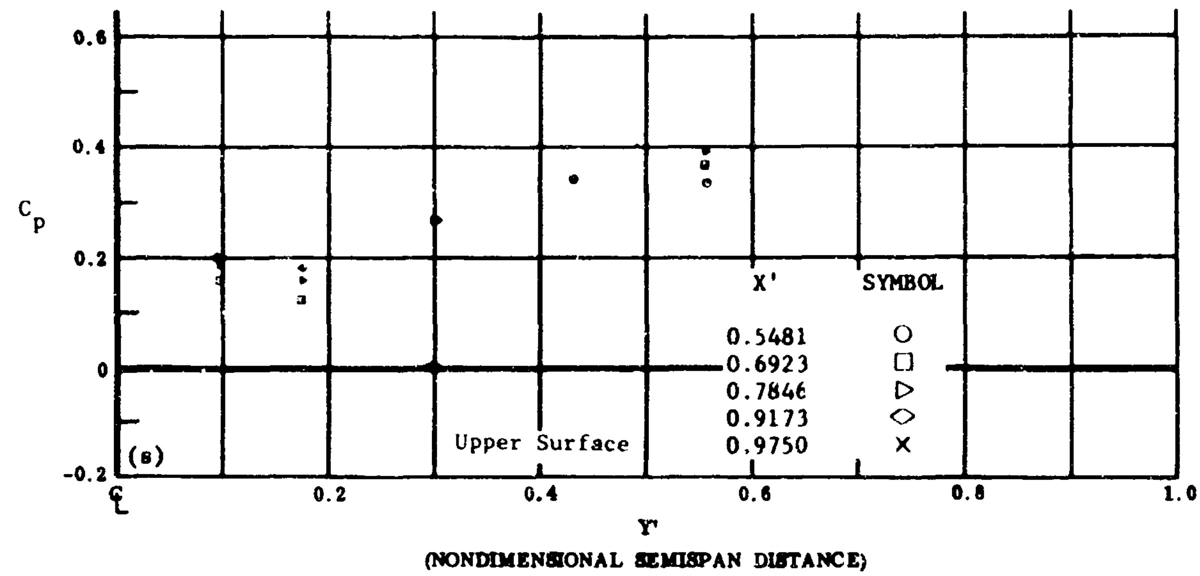

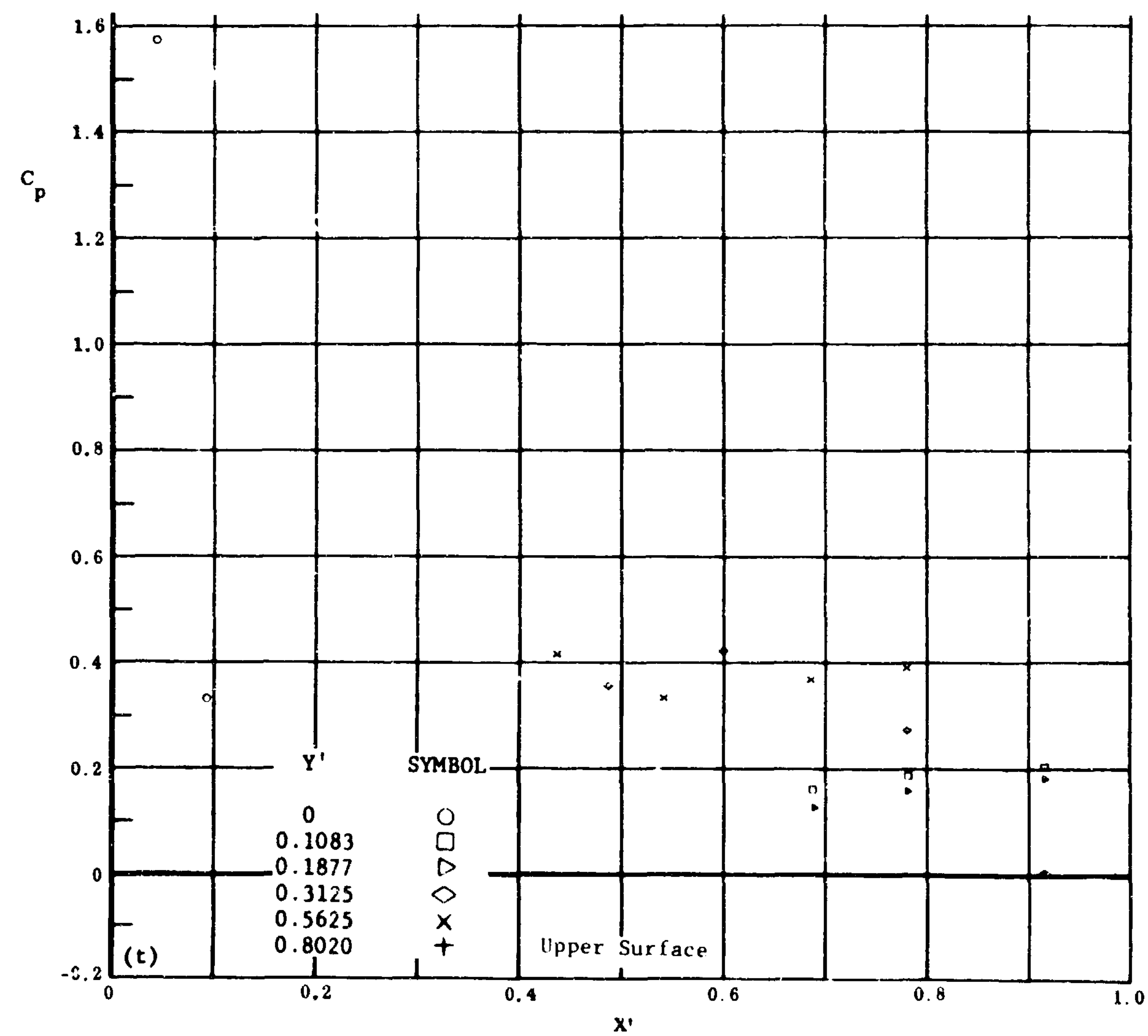

(NONDIMENSIONAL STREAMWISE DISTANCE FROM VIRTUAL APEX)

Fig. 19 Configuration I, α = -20 , $\delta_2 = \delta_3$ = +39

s) C_p vs. Y', upper surface

t) C_p vs. X', upper surface

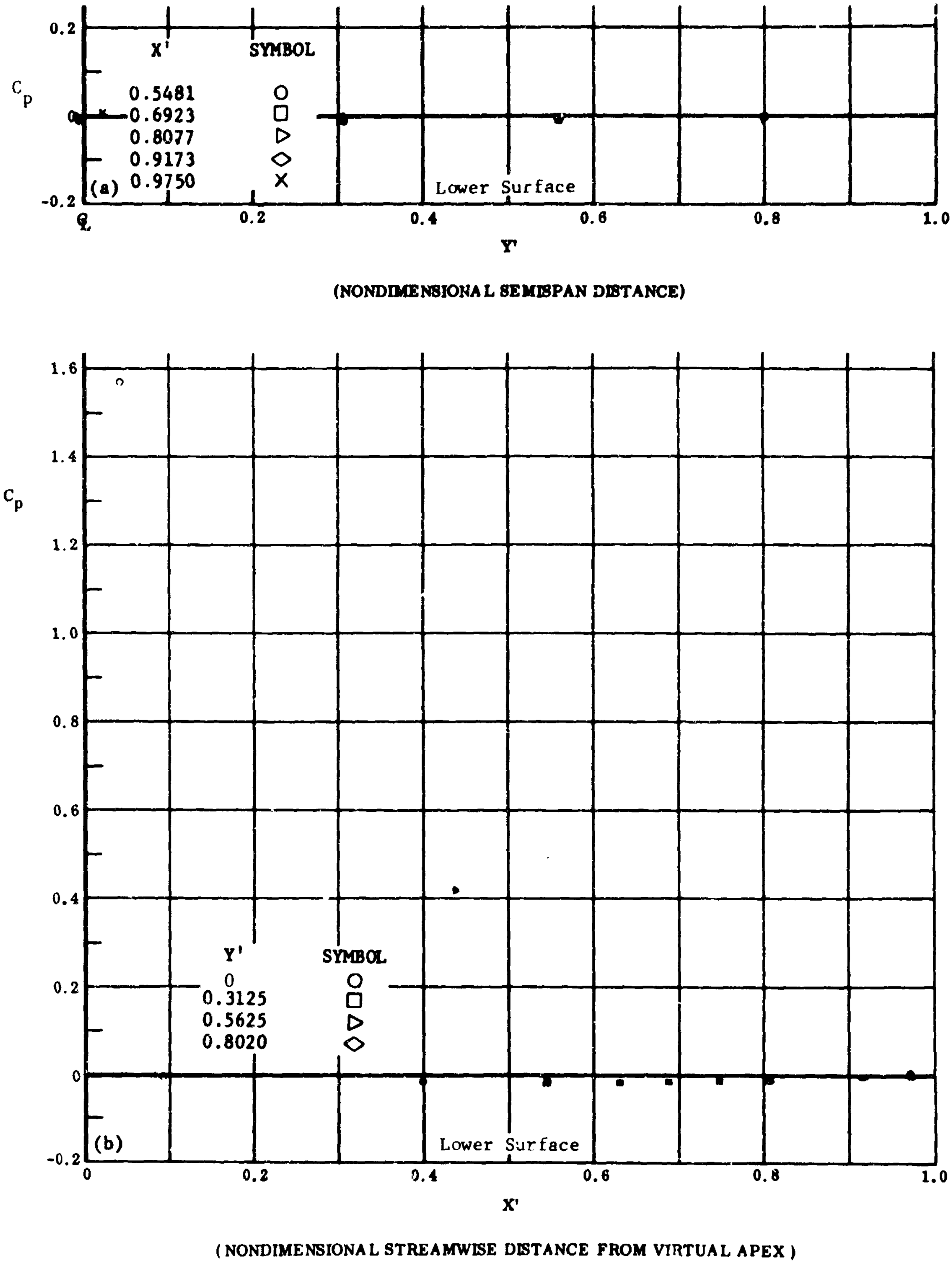

Fig. 20 Configuration I, $\alpha = -20$, $\delta_2 = \delta_3 = -10$

a) C_p vs. Y', lower surface

b) C_p vs. X', lower surface

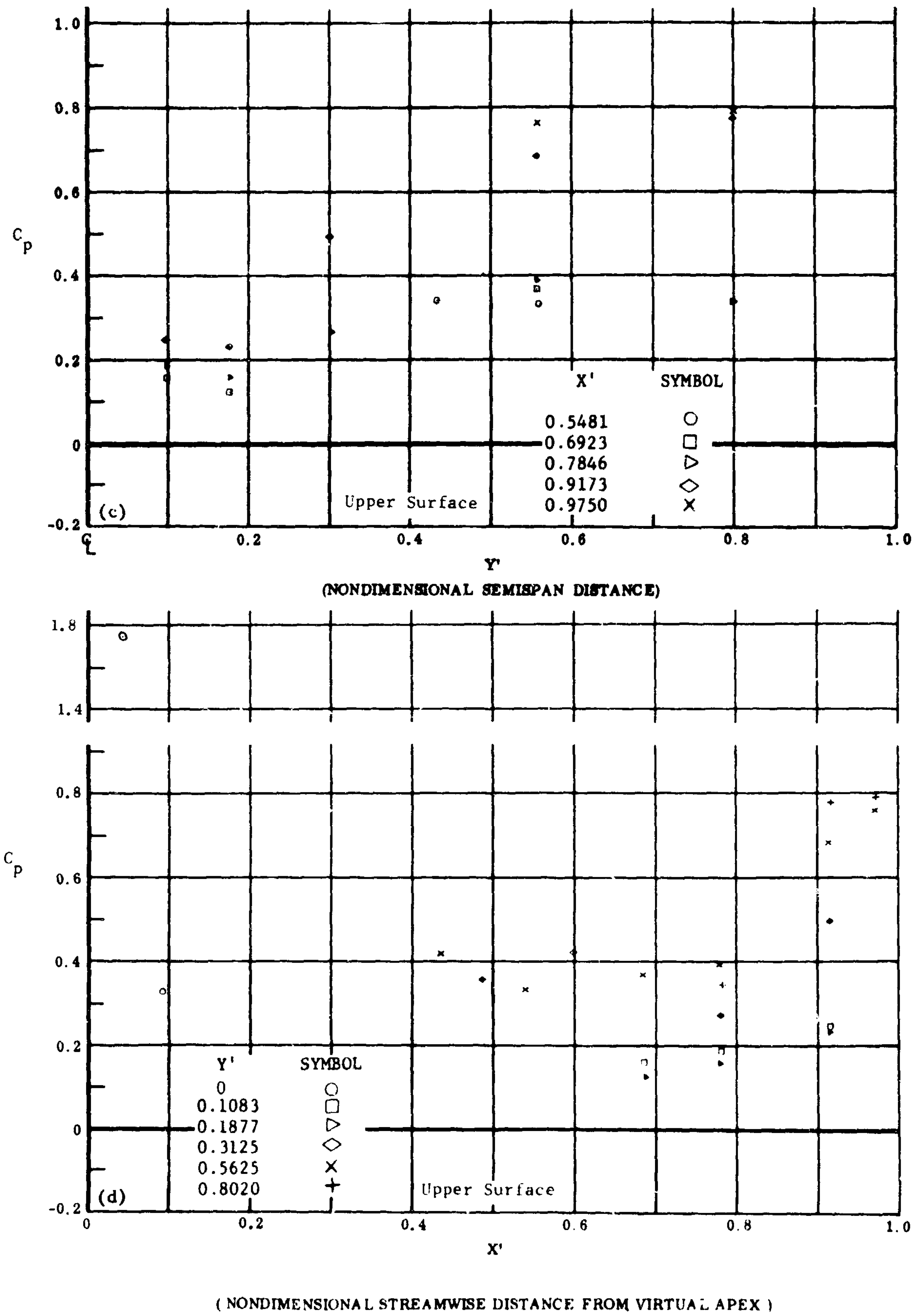

Fig. 20 Configuration I, $\alpha = -20$, $\delta_2 = \delta_3 = -10$

c) C_p vs. Y', upper surface

d) C_p vs. X', upper surface

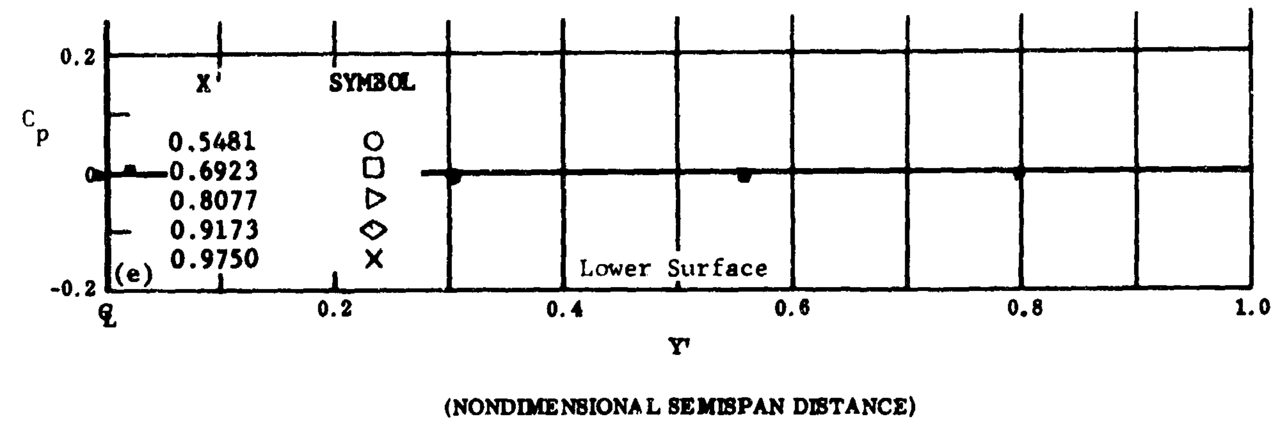

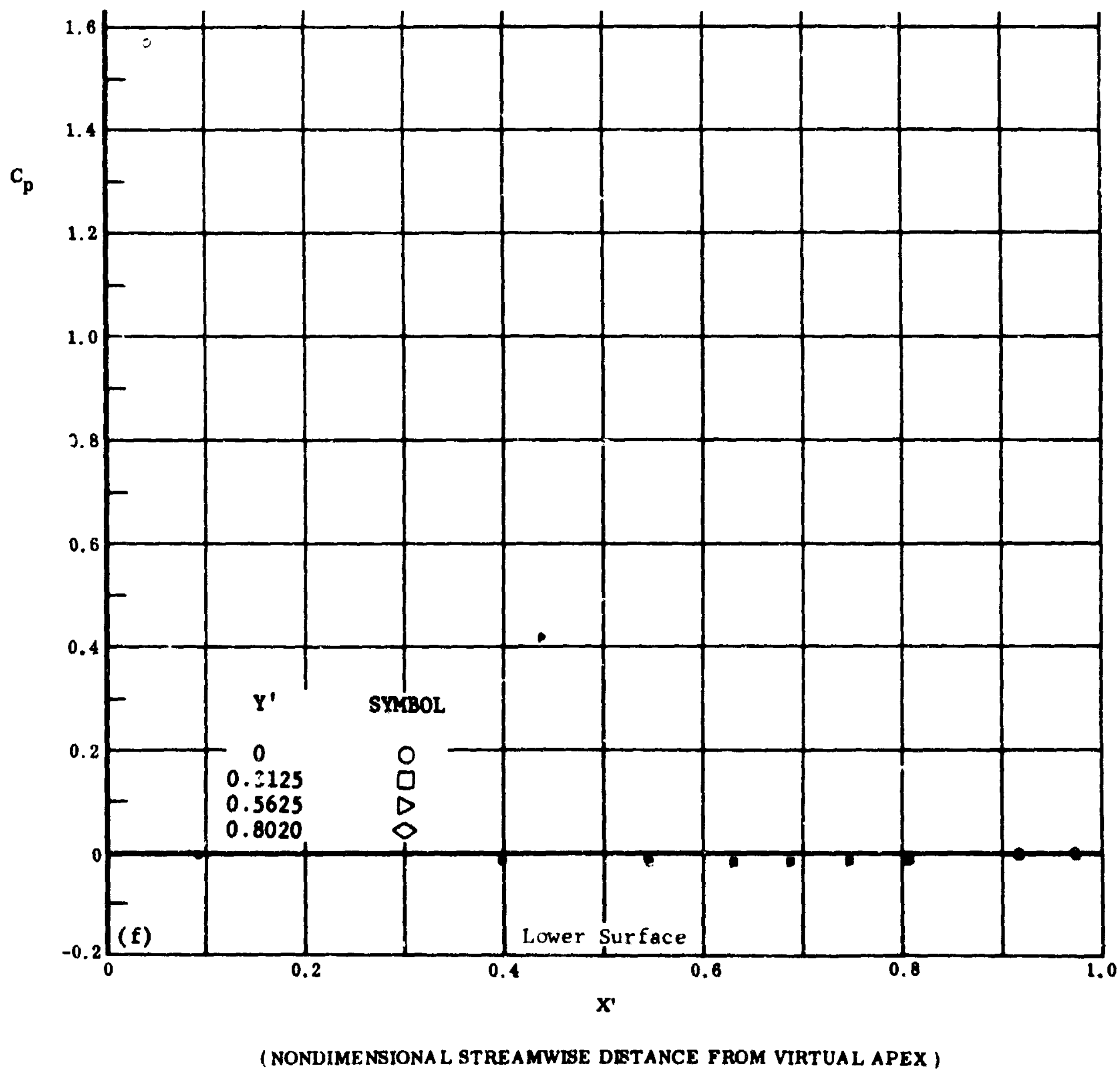

Fig. 20 Configuration I, $\alpha = -20$, $\delta_2 = \delta_3 = -20$

e) C_p vs. Y', lower surface

f) C_p vs. X', lower surface

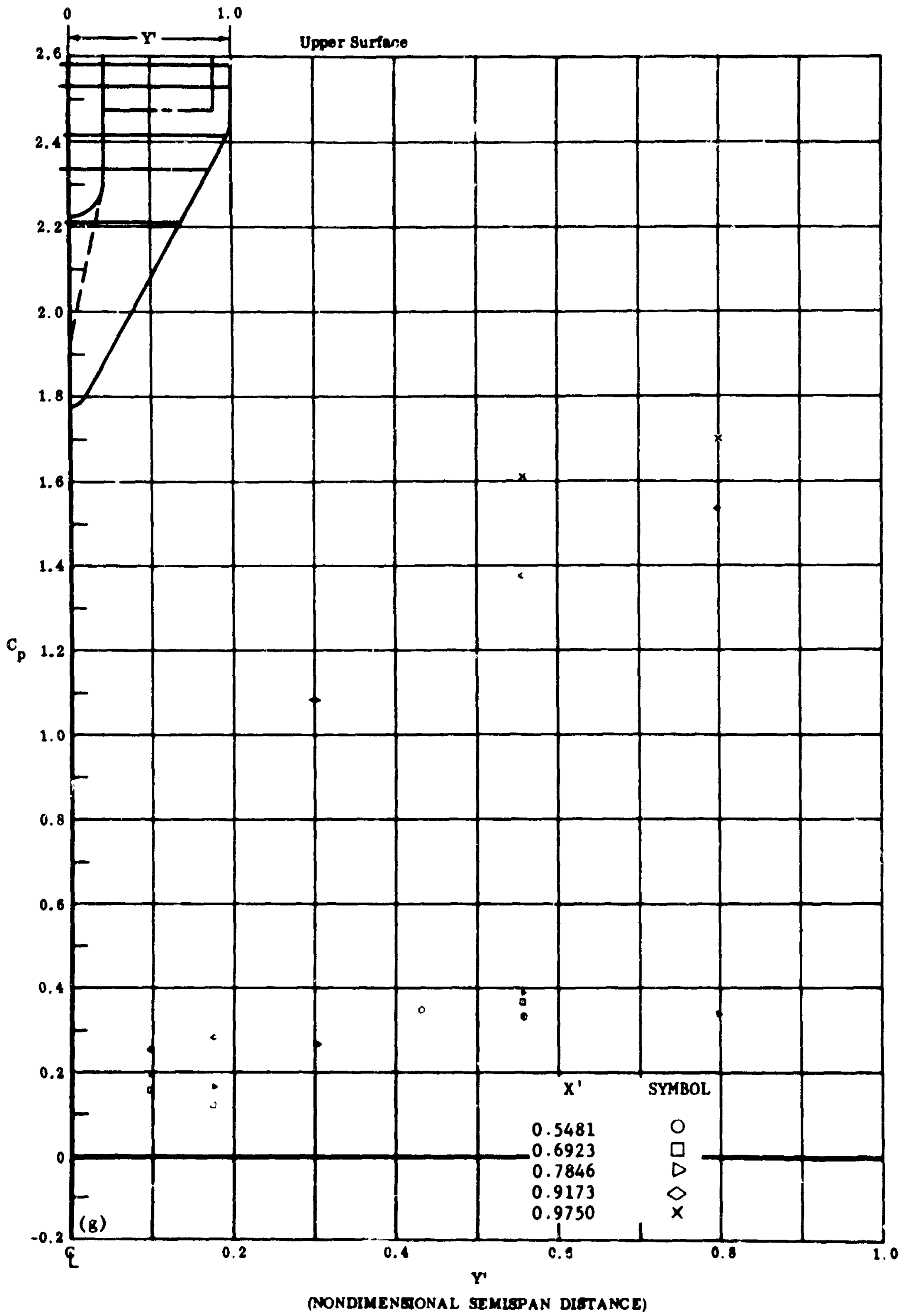

Fig. 20g Configuration I, α = -20 , $\delta_2 = \delta_3$ = -20

C_p vs. Y', upper surface

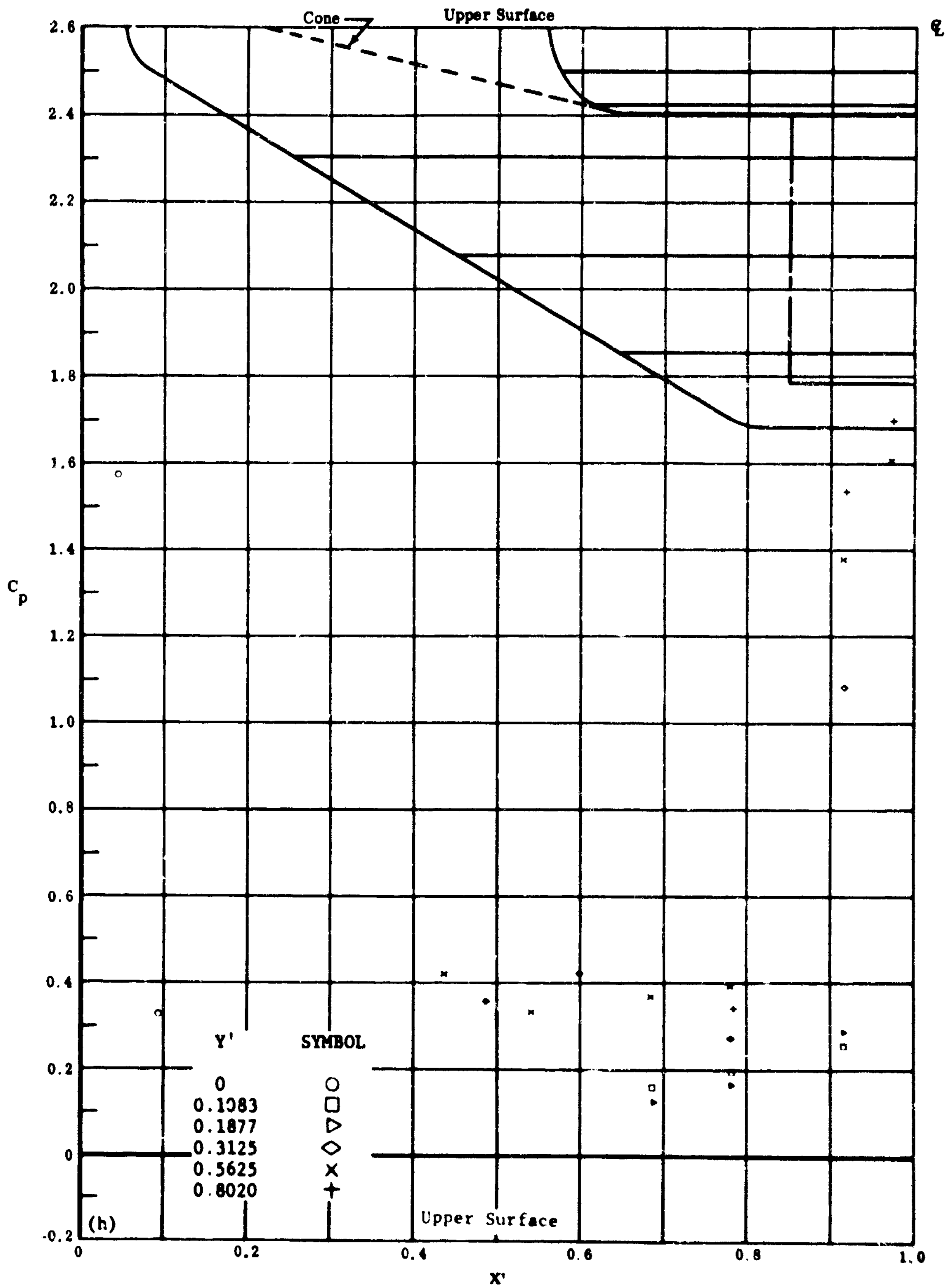

(NONDIMENSIONAL STREAMWISE DISTANCE FROM VIRTUAL APEX)

Fig. 20h Configuration I, $\alpha = -20$, $\delta_2 = \delta_3 = -20$

C_p vs. X', upper surface

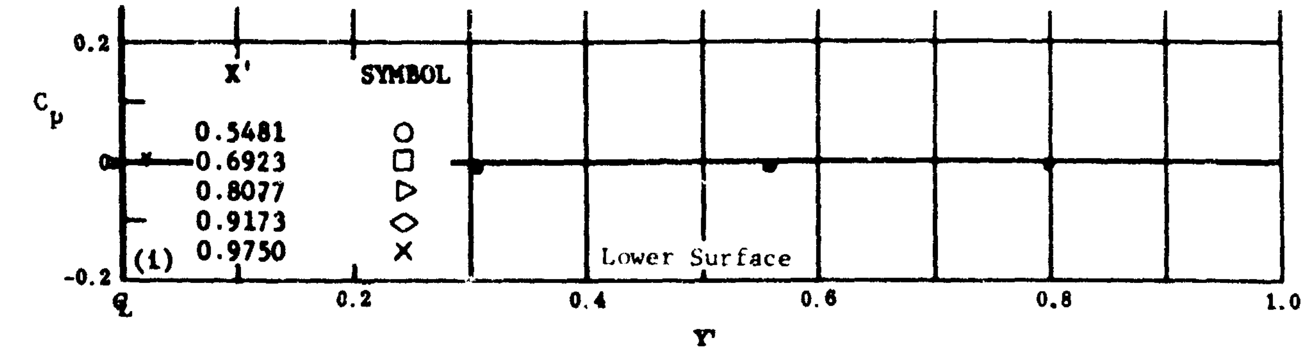

(NONDIMENSIONAL SEMISPAN DISTANCE)

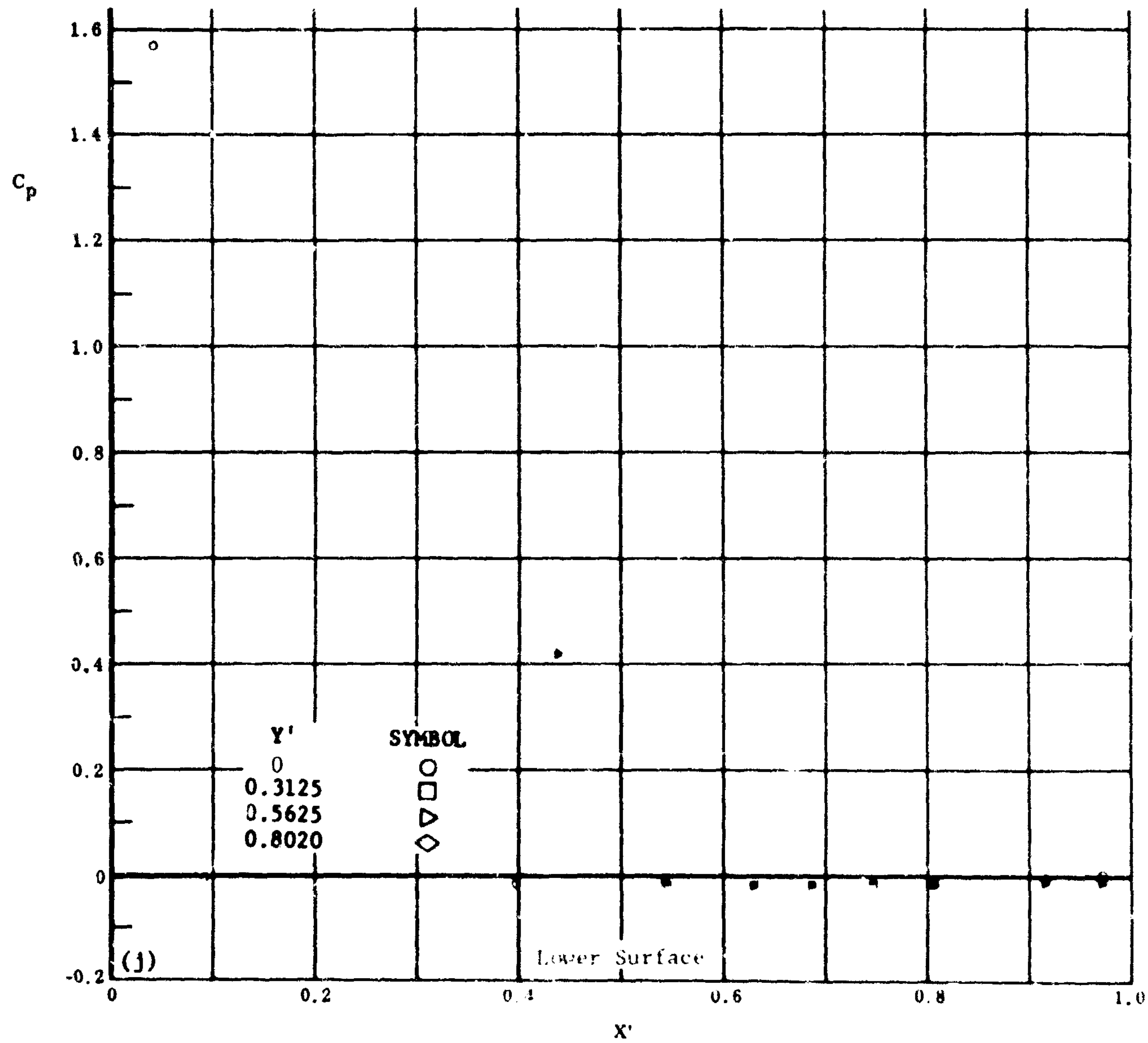

(NONDIMENSIONAL ... ISE DISTANCE FROM VIRTUAL APEX)

Fig. 20 ... ation I, ... = -20, $\ldots_2$ = $\ldots_3$ = -30

i) ..., lower surface

j) ... X', lower surface

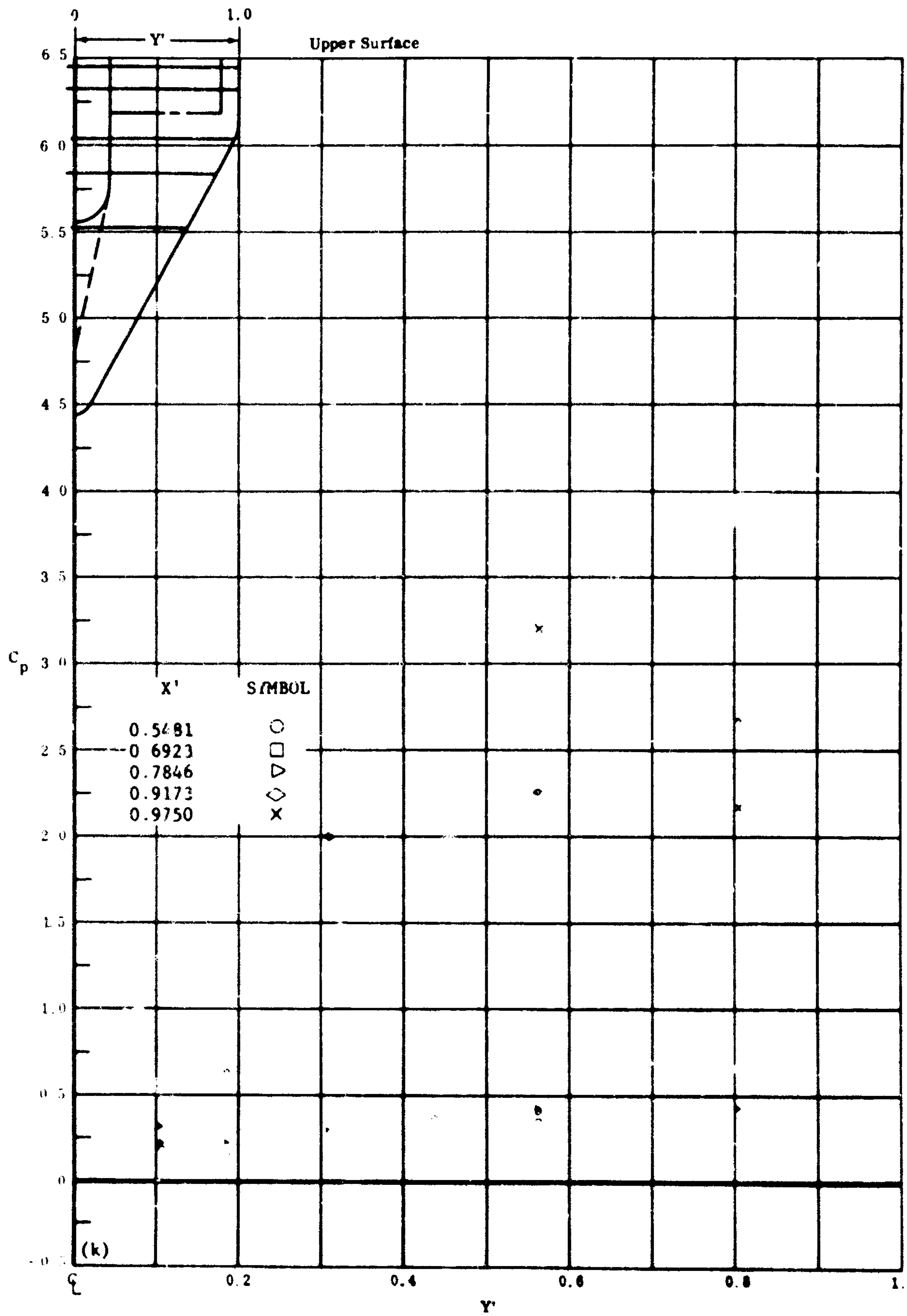

Fig. 20k Configuration I, $= -20$, $_2 = _3 = -30$

C_p vs. Y', upper surface

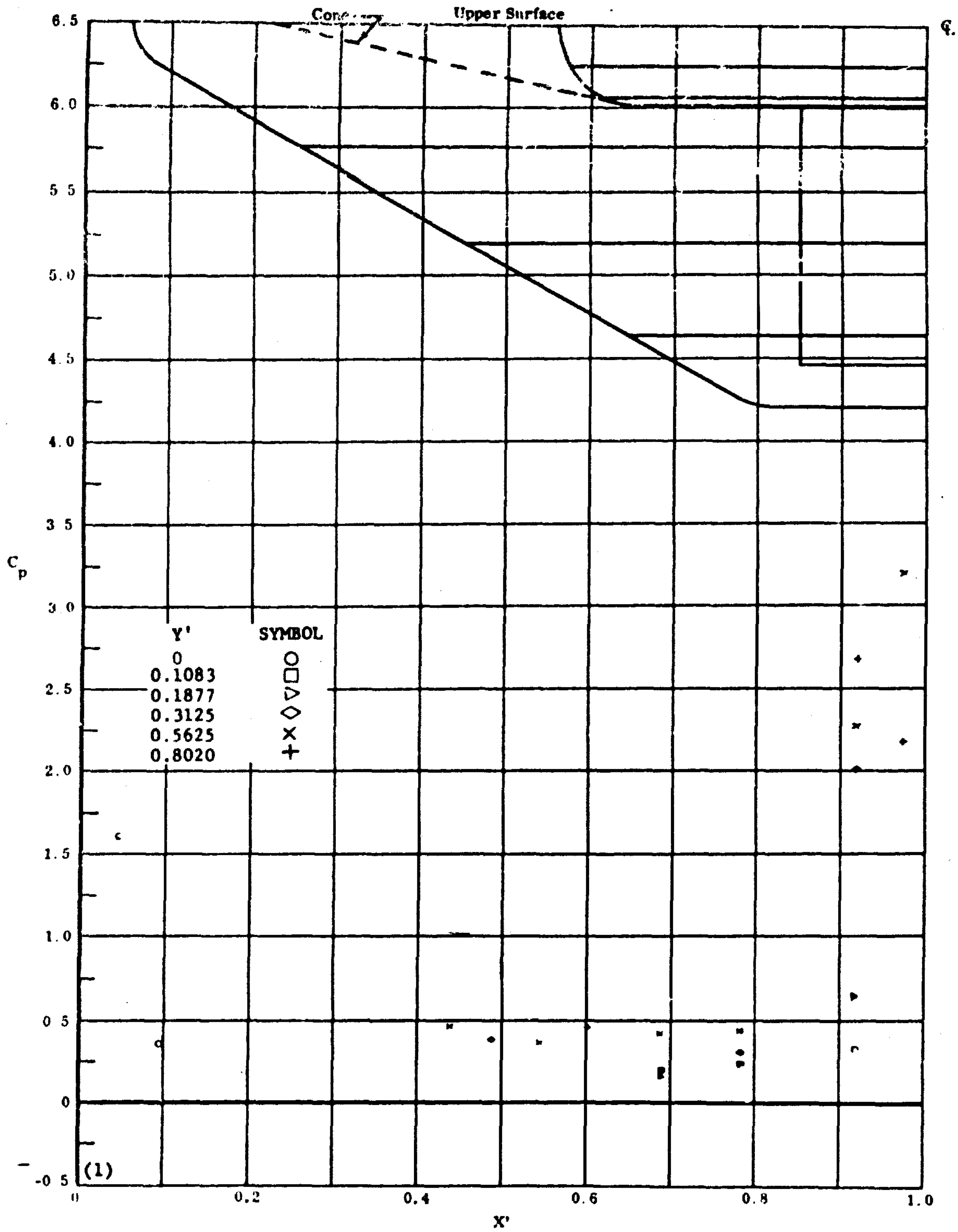

(NONDIMENSIONAL STREAMWISE DISTANCE FROM VIRTUAL APEX)

Fig. 201 Configuration I, $\alpha = -20$, $\delta_2 = \delta_3 = -30$

C_p vs. X', upper surface

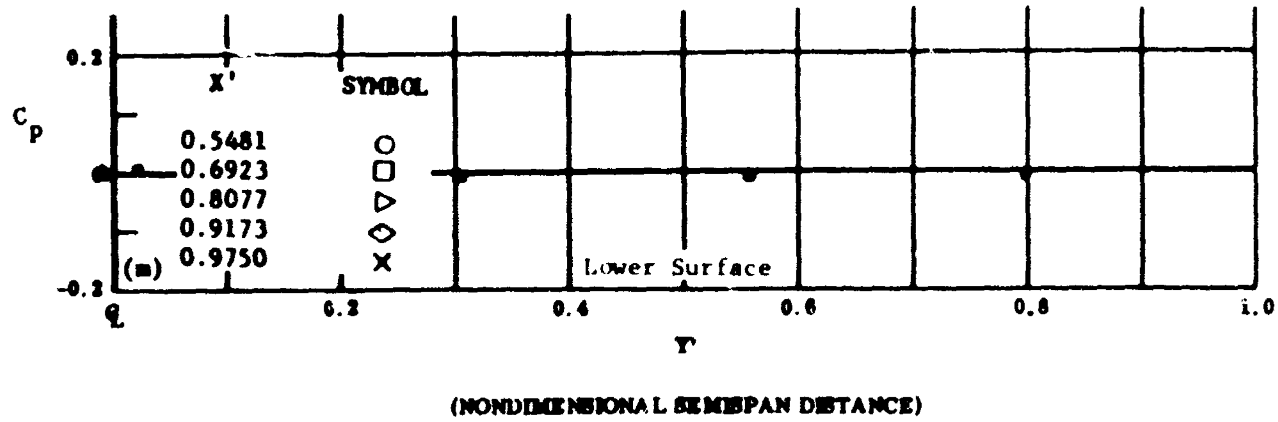

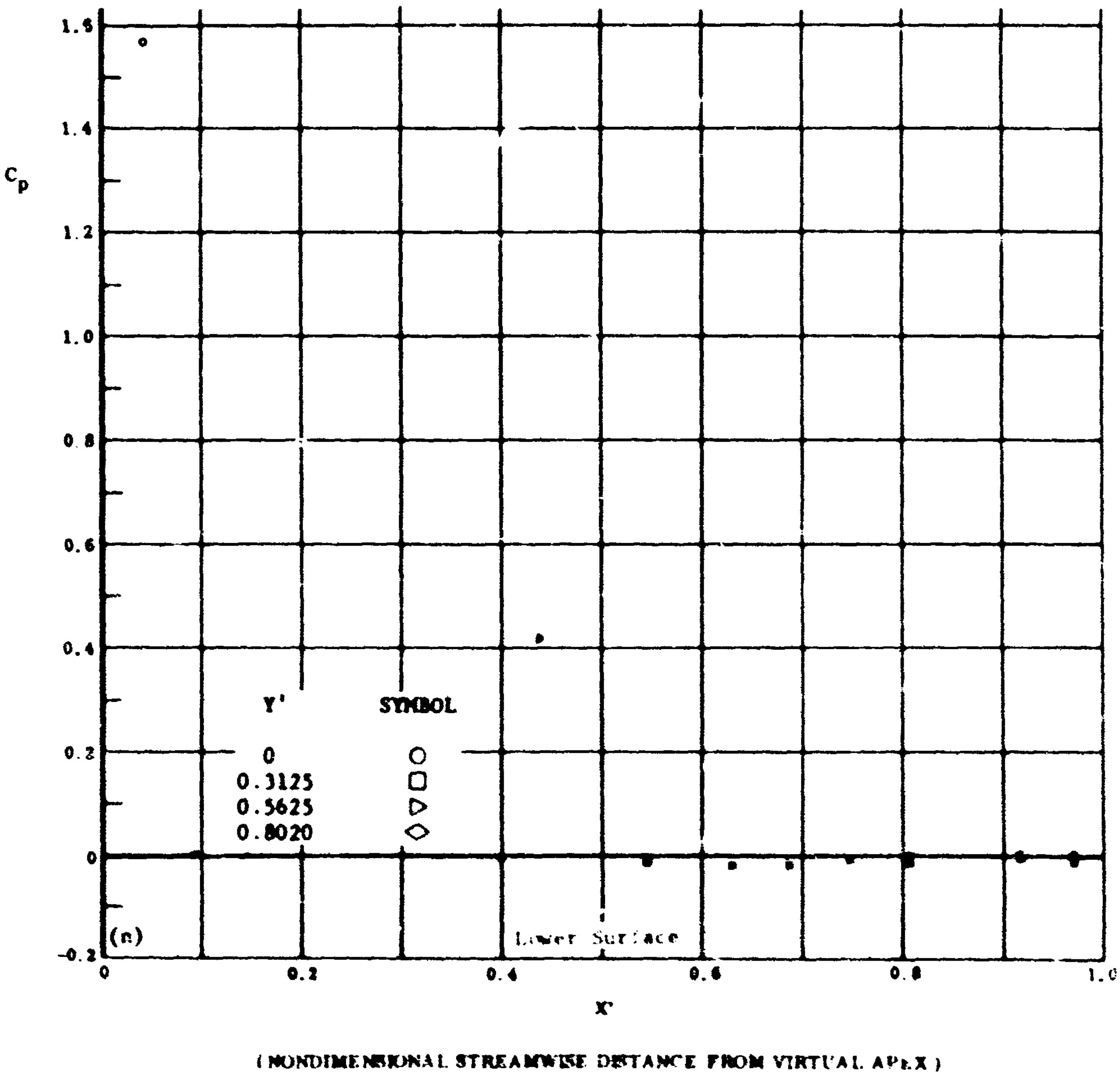

Fig. 20 Configuration I, $_1$ = -20, $_2$ = $_3$ = -39

m) C_p vs. Y', lower surface

n) C_p vs. X', lower surface

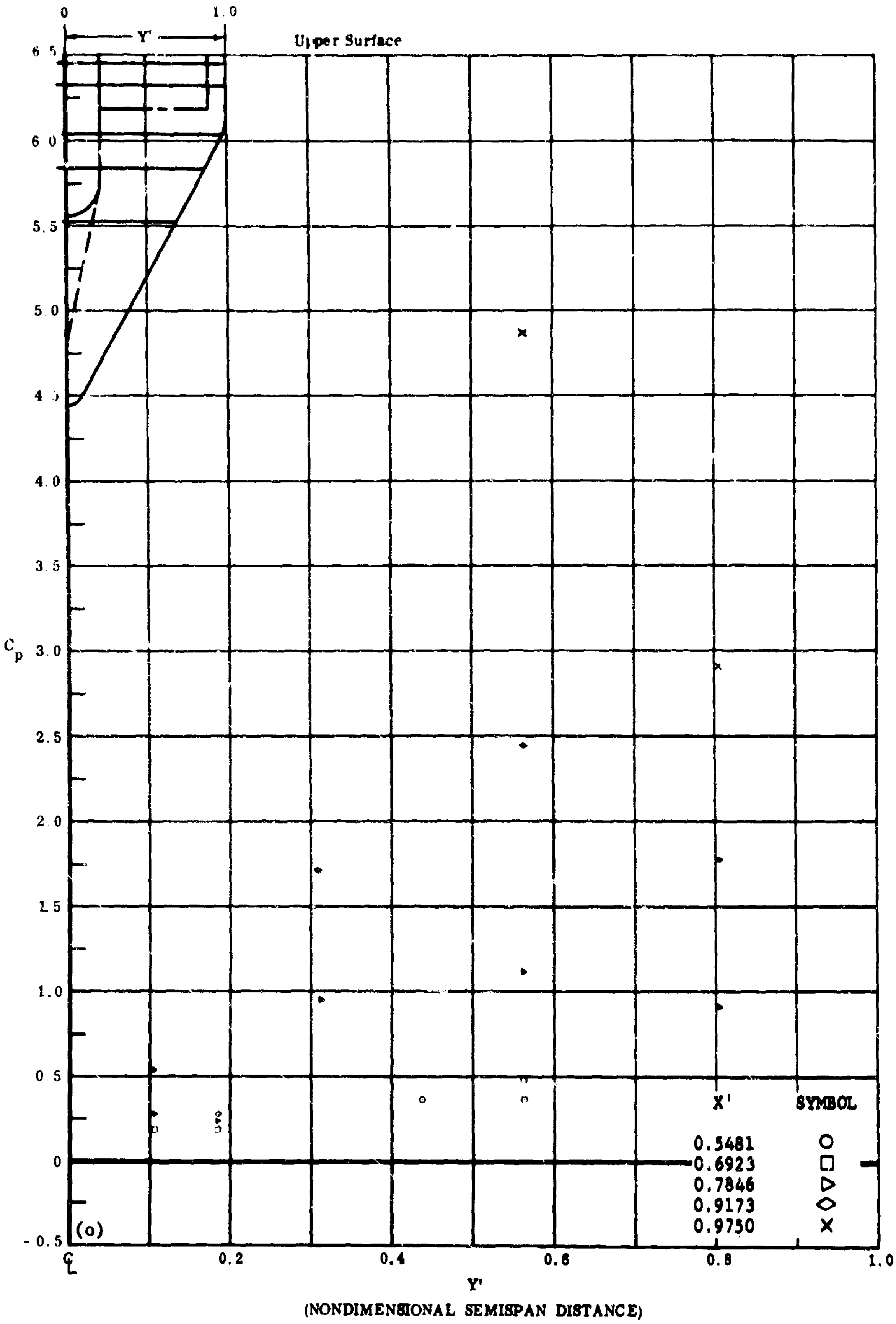

Fig. 20o Configuration I, α = -20 , $\delta_2 = \delta_3$ = -39
C_p vs. Y', upper surface

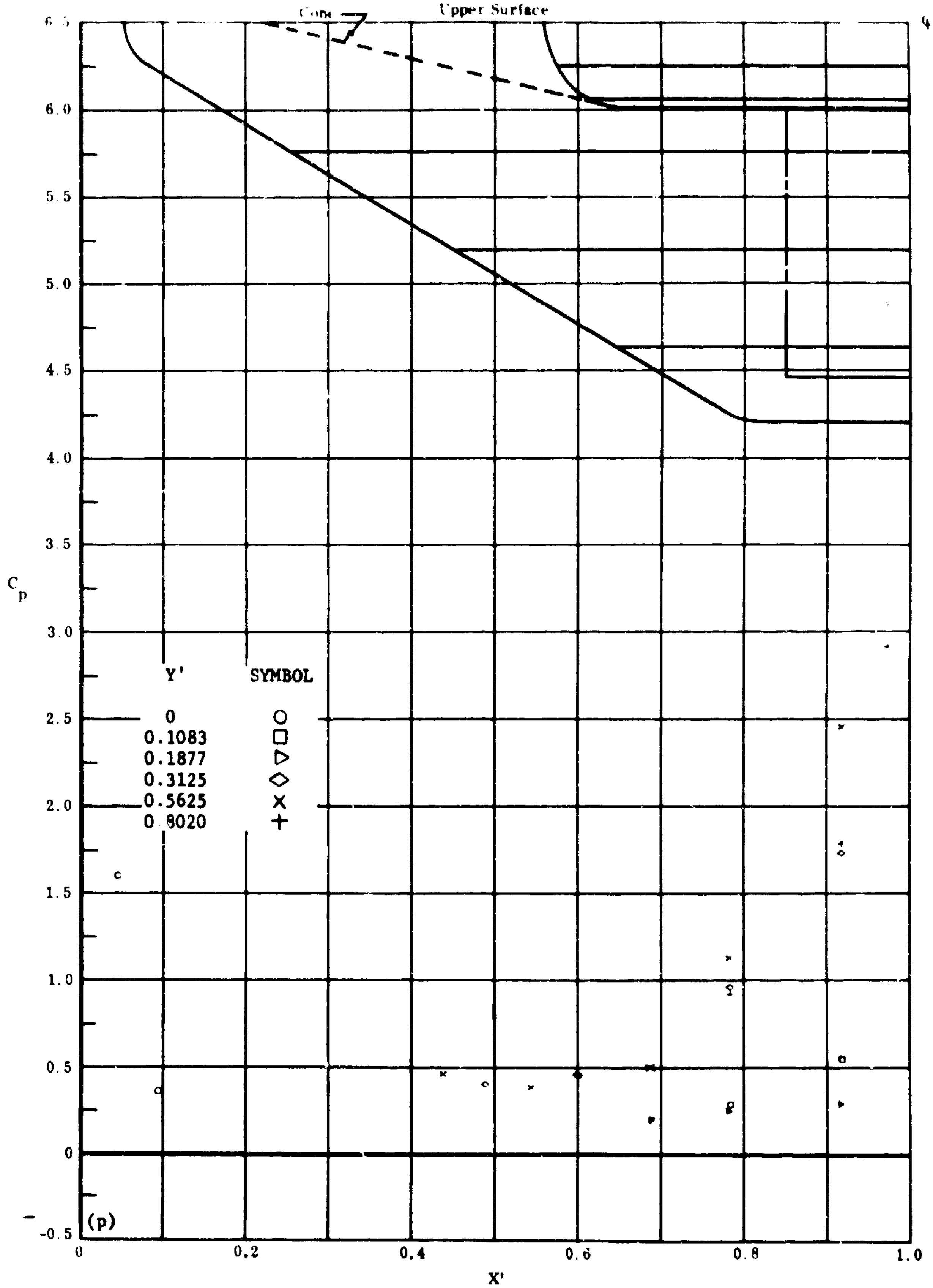

(NONDIMENSIONAL STREAMWISE DISTANCE FROM VIRTUAL APEX)

Fig. 20p Configuration I, $\alpha = -20$, $\delta_2 = \delta_3 = -39$

C_p vs. X', upper surface

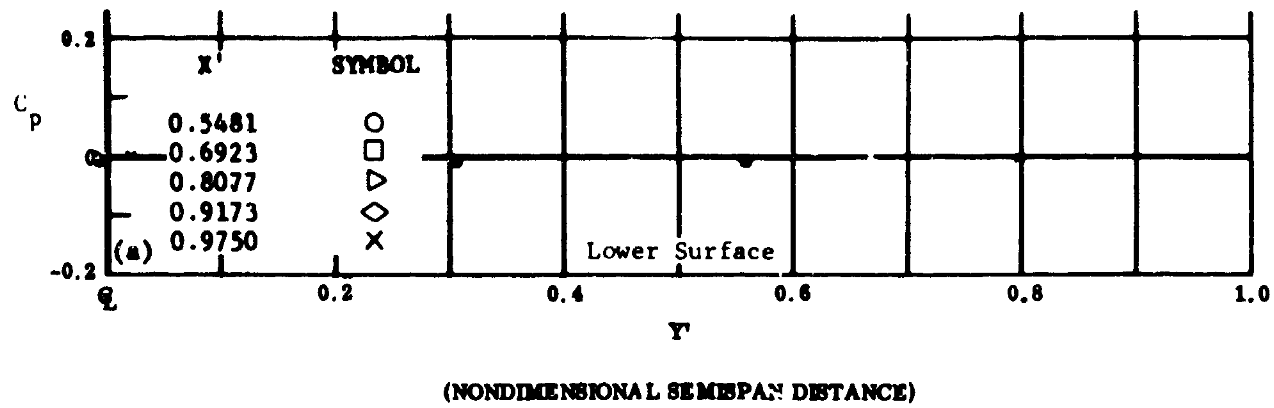

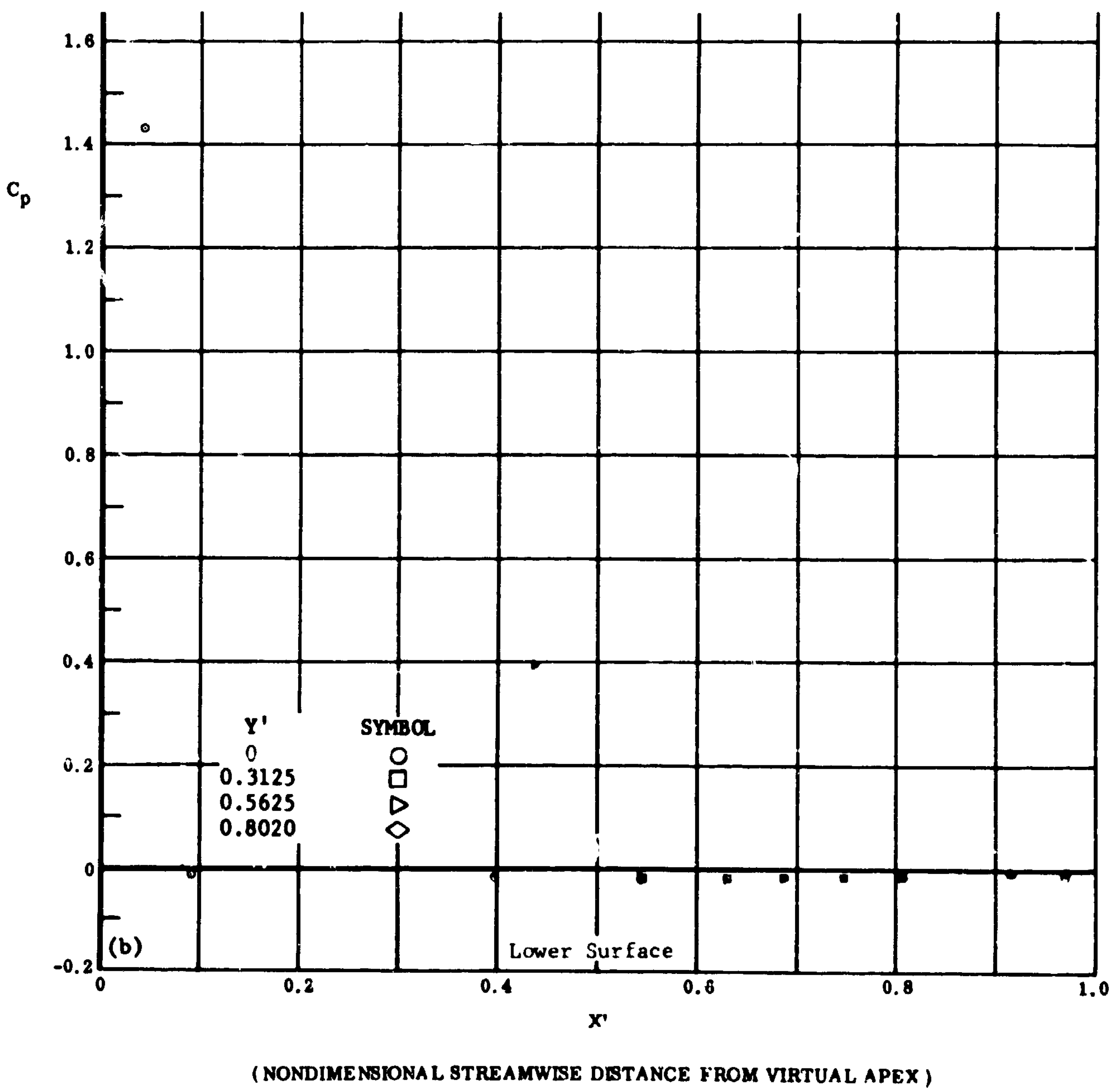

Fig. 21 Configuration I, $\alpha = -25$, $\delta_2 = \delta_3 = 0$

a) C_p vs. Y', lower surface

b) C_p vs. X', lower surface

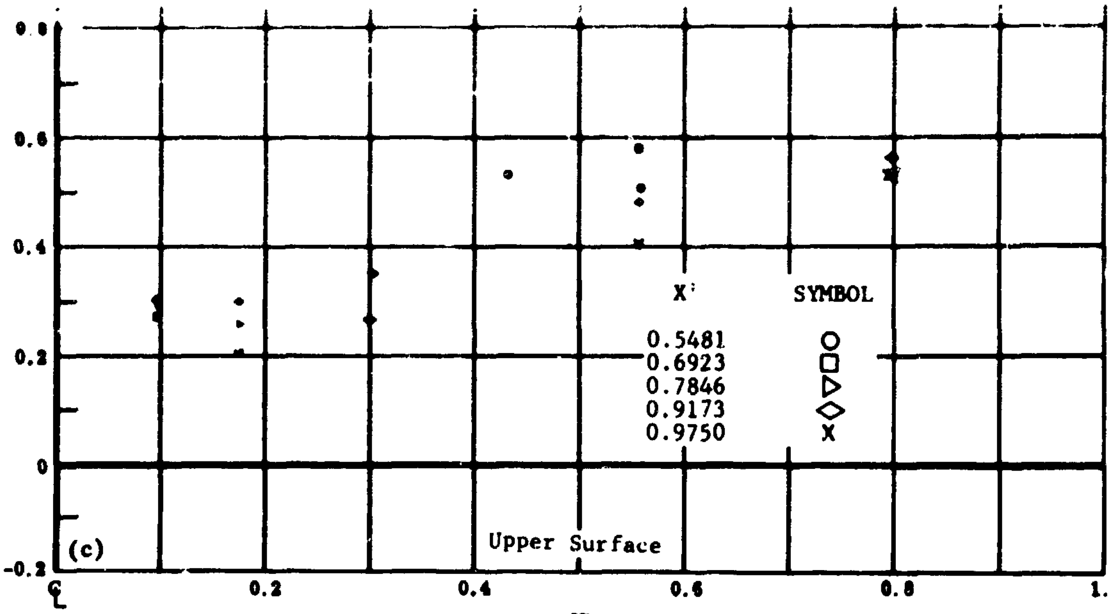

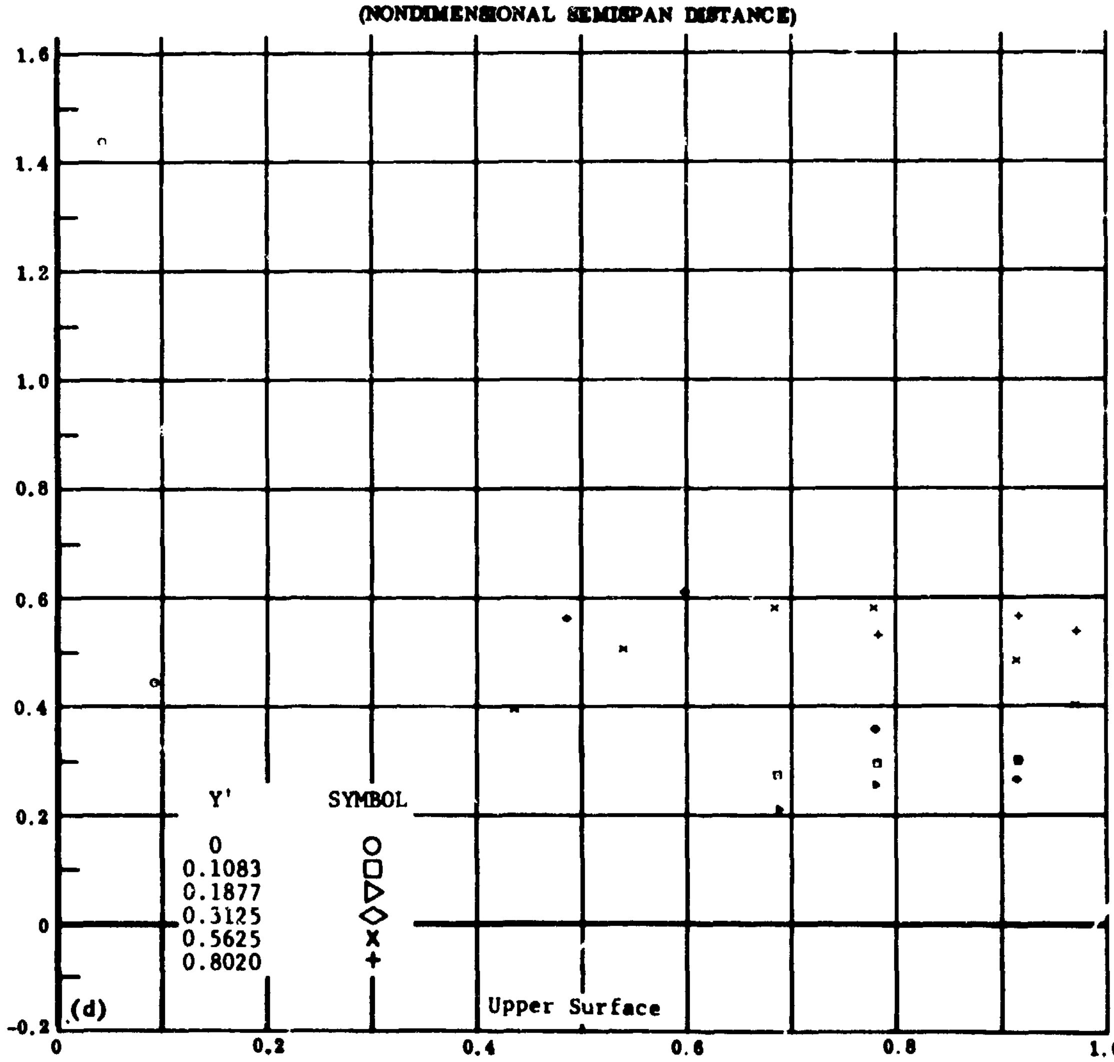

(NONDIMENSIONAL STREAMWISE DISTANCE FROM VIRTUAL APEX)

Fig. 21 Configuration I, $\alpha = -25$, $\delta_2 = \delta_3 = 0$

c) C_p vs. Y', upper surface

d) C_p vs. X', upper surface

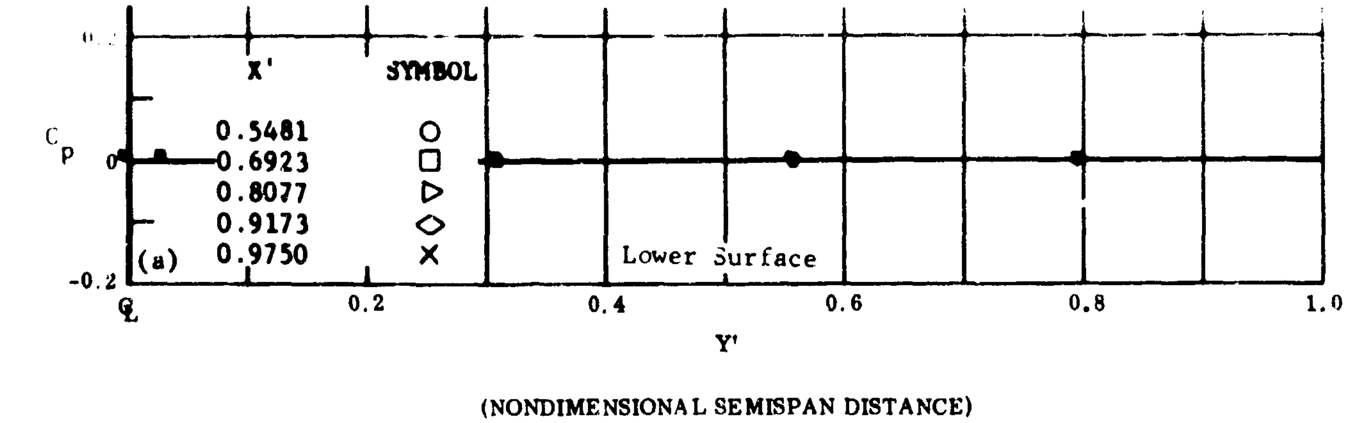

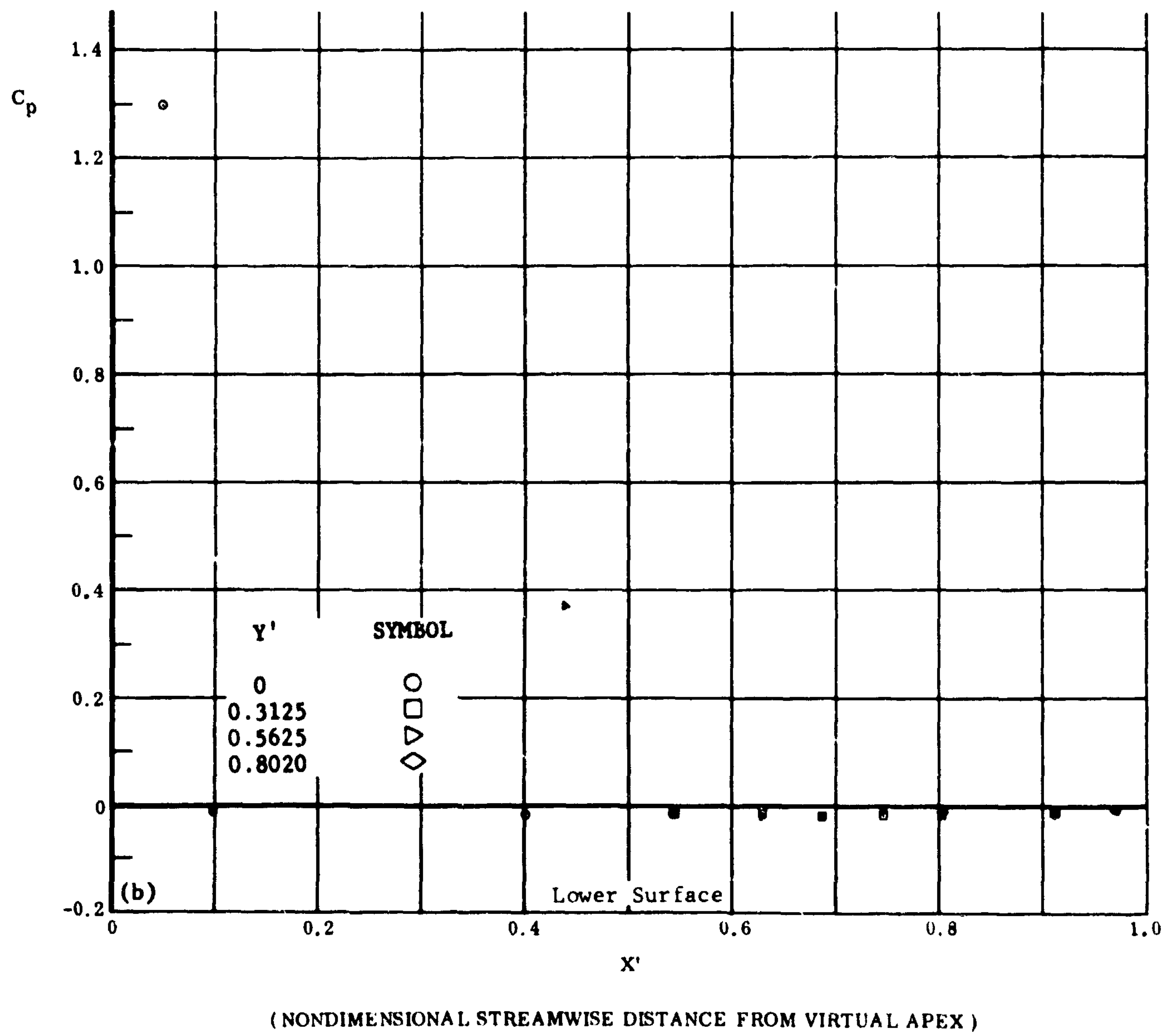

Fig. 22 Configuration I, $\alpha = -30$, $\delta_2 = \delta_3 = 0$

a) C_p vs. Y', lower surface

b) C_p vs. X', lower surface

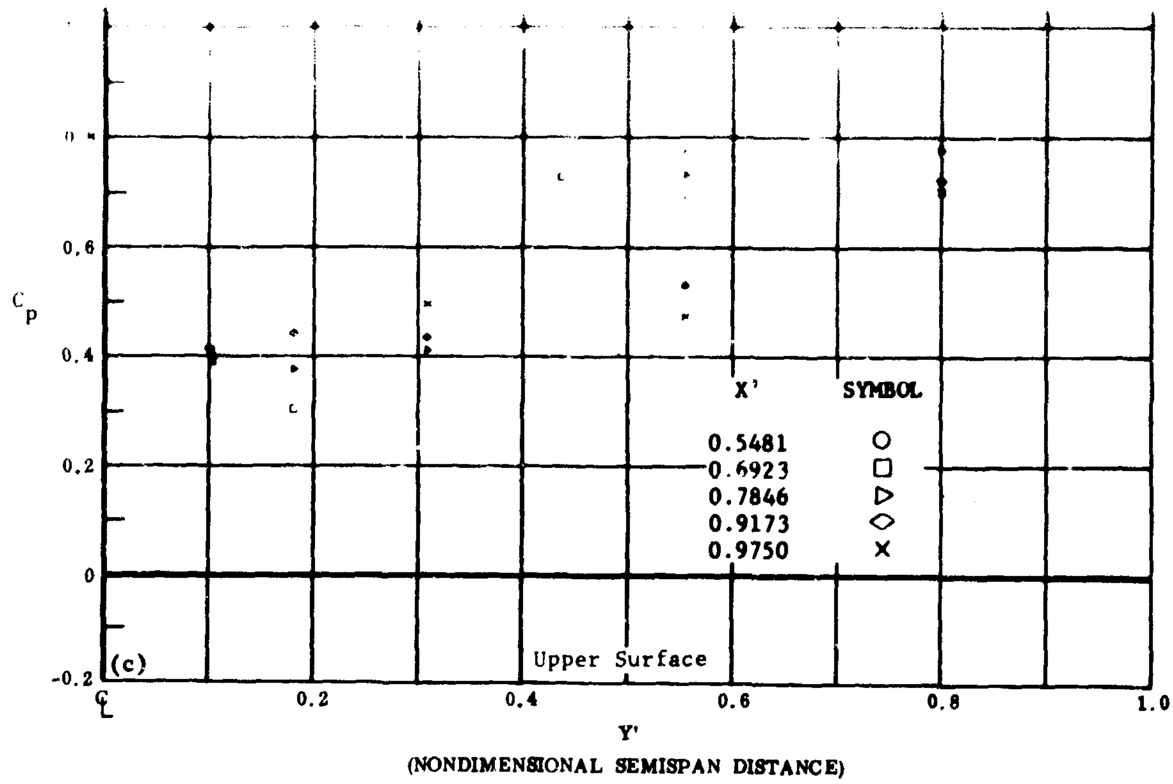

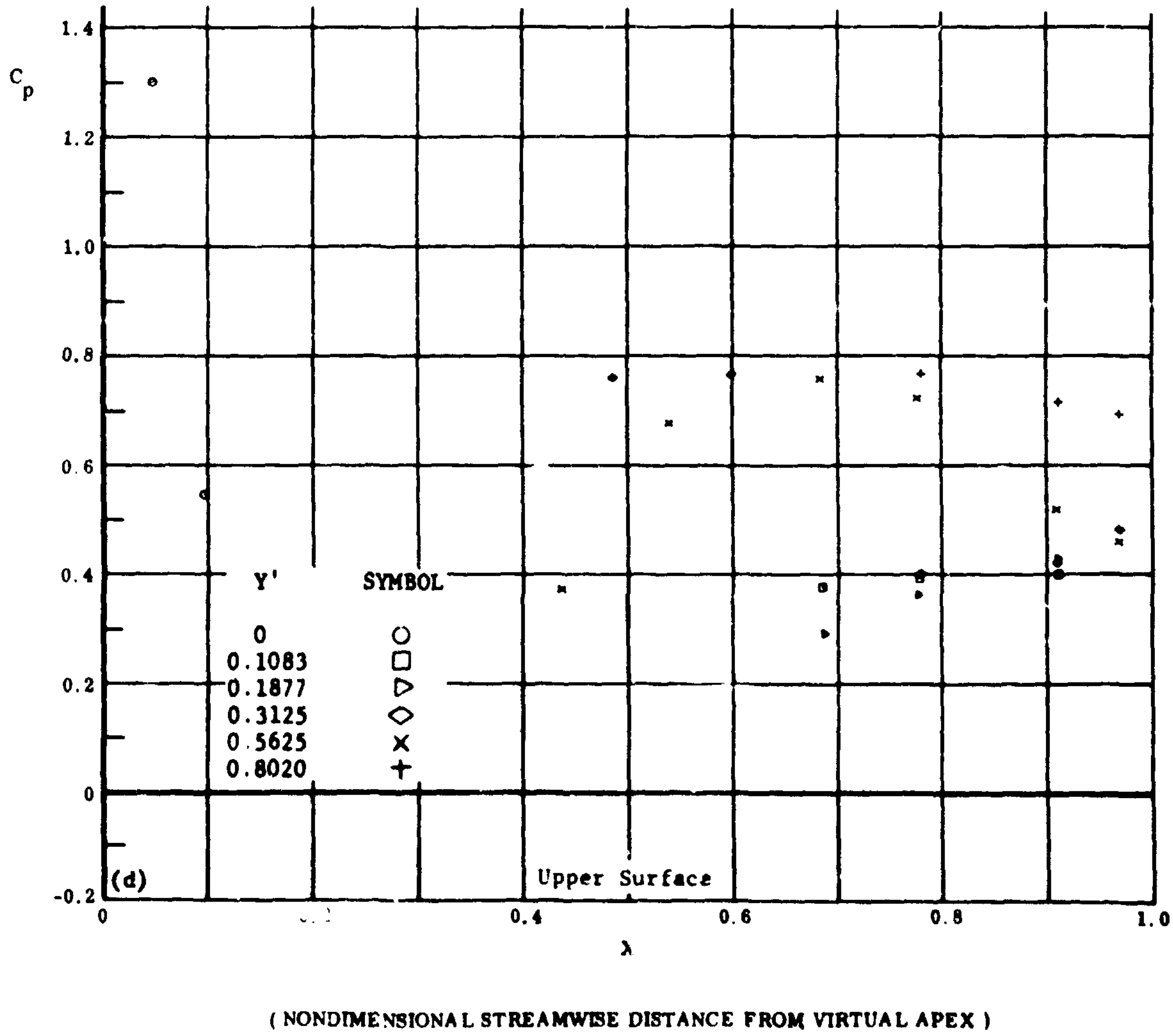

Fig. 22 Configuration I, $\alpha = -30$, $\delta_2 = \delta_3 = 0$

c) C_p vs. Y', upper surface

d) C_p vs. X', upper surface

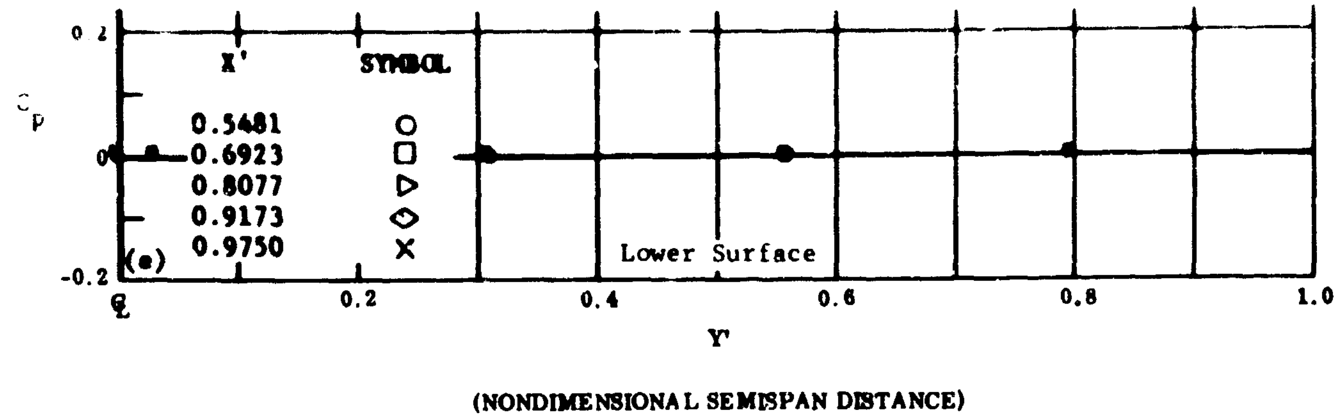

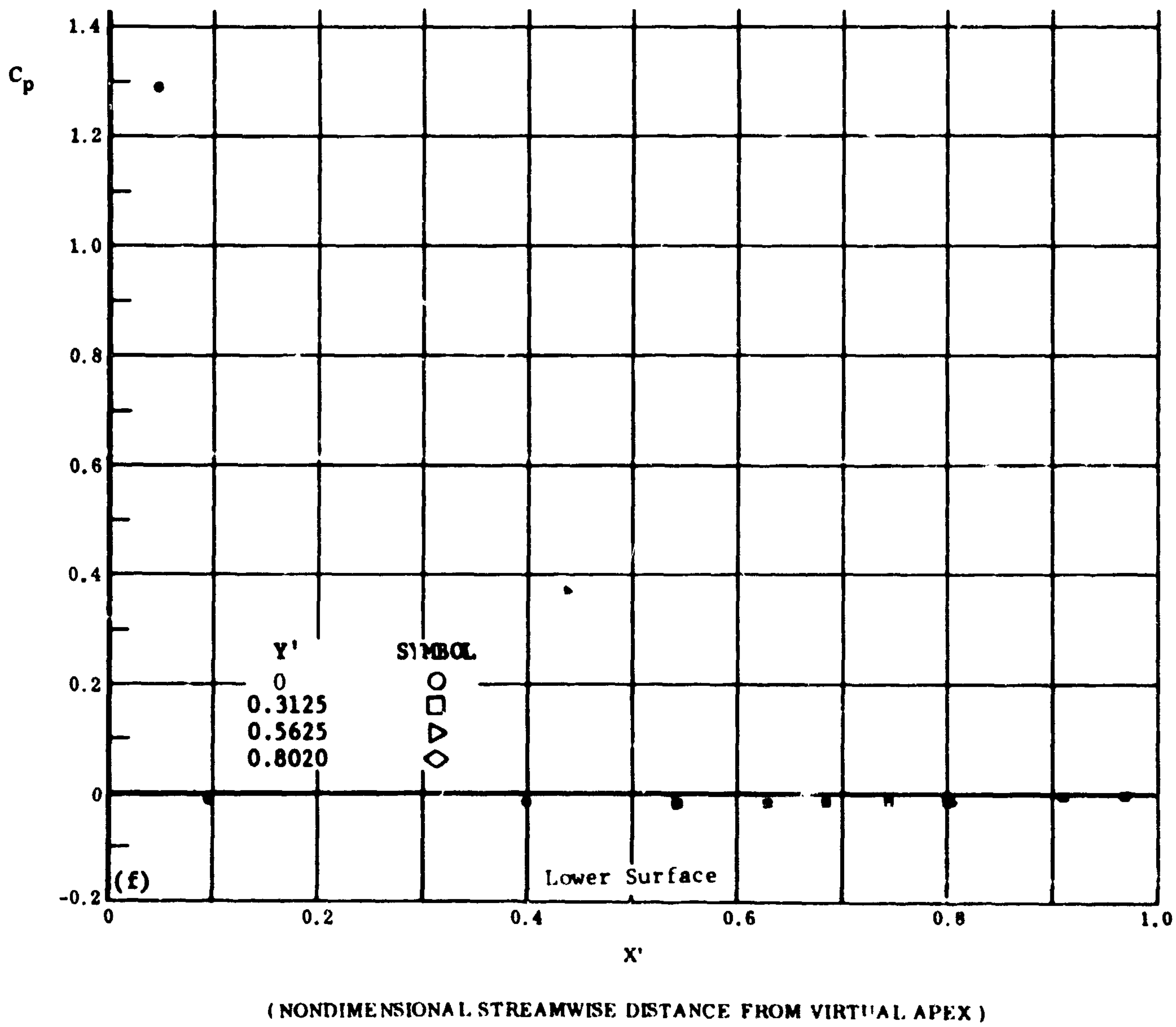

Fig. 22 Configuration I, $\alpha = -30$, $\delta_2 = \delta_3 = +20$

e) C_p vs. Y', lower surface

f) C_p vs. X', lower surface

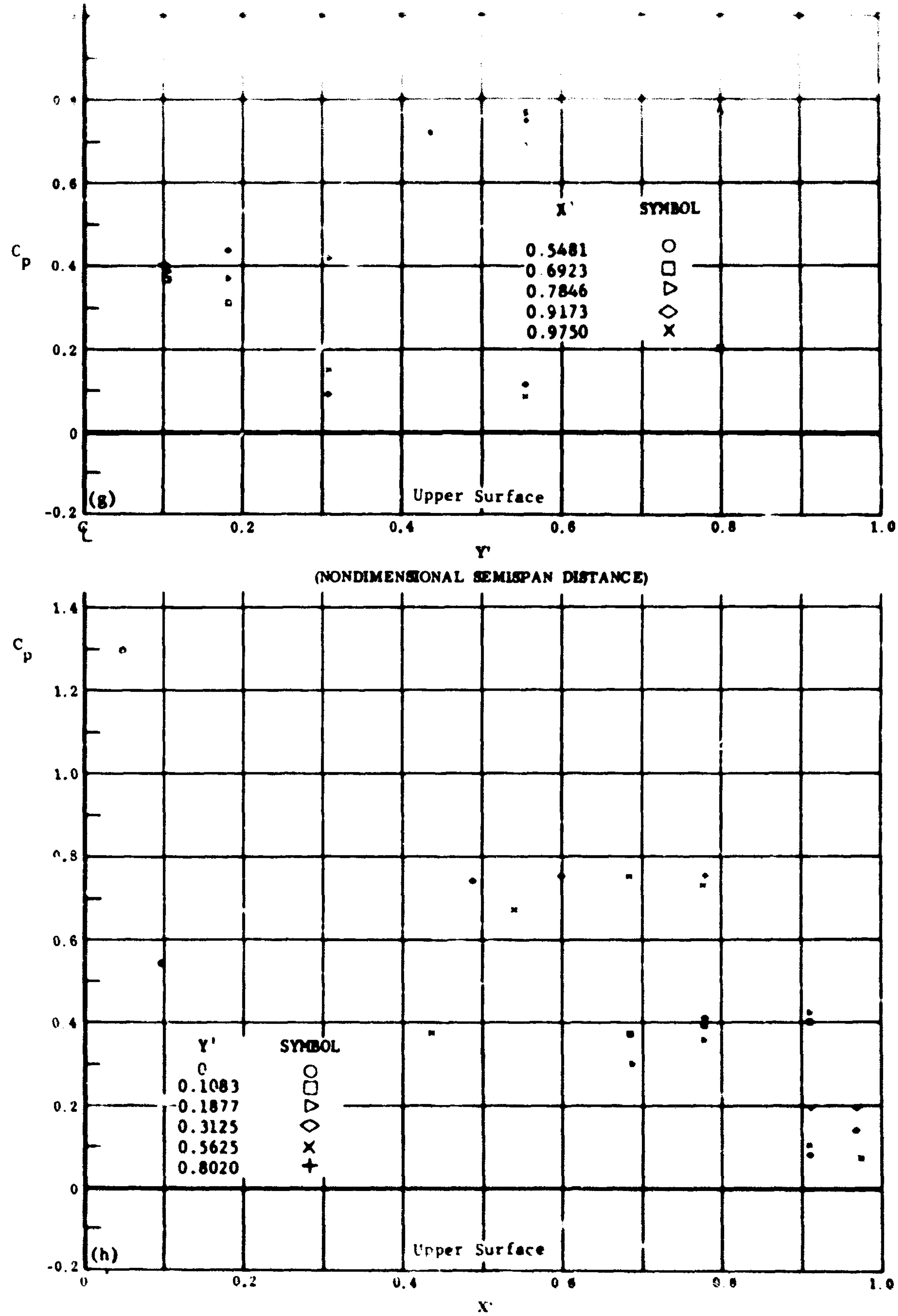

(NONDIMENSIONAL STREAMWISE DISTANCE FROM VIRTUAL APEX)

Fig. 22 Configuration I, $\delta_1 = -30$, $\delta_2 = \delta_3 = +20$

g) C_p vs. Y', upper surface

h) C_p vs. X', upper surface

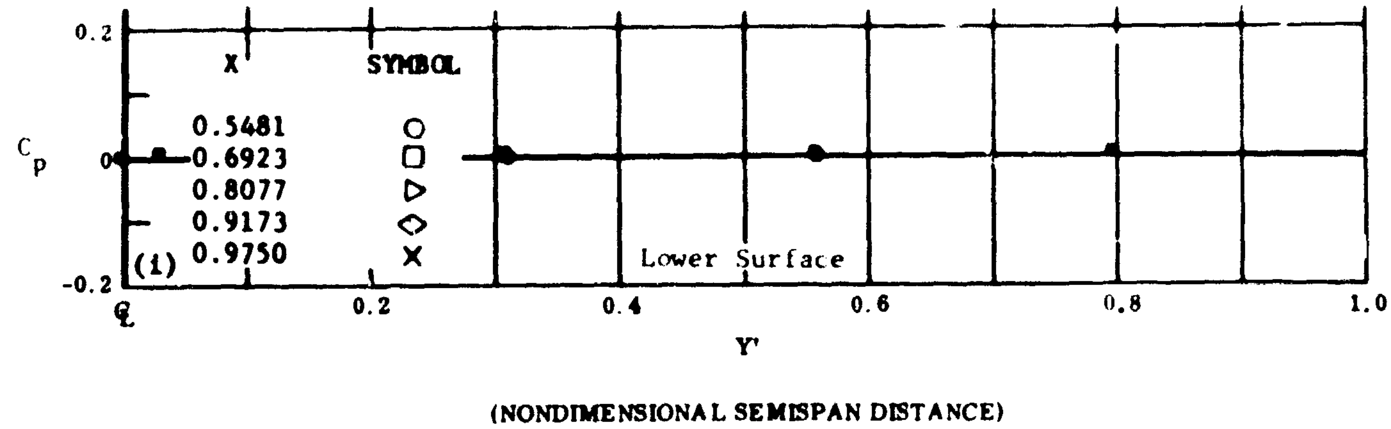

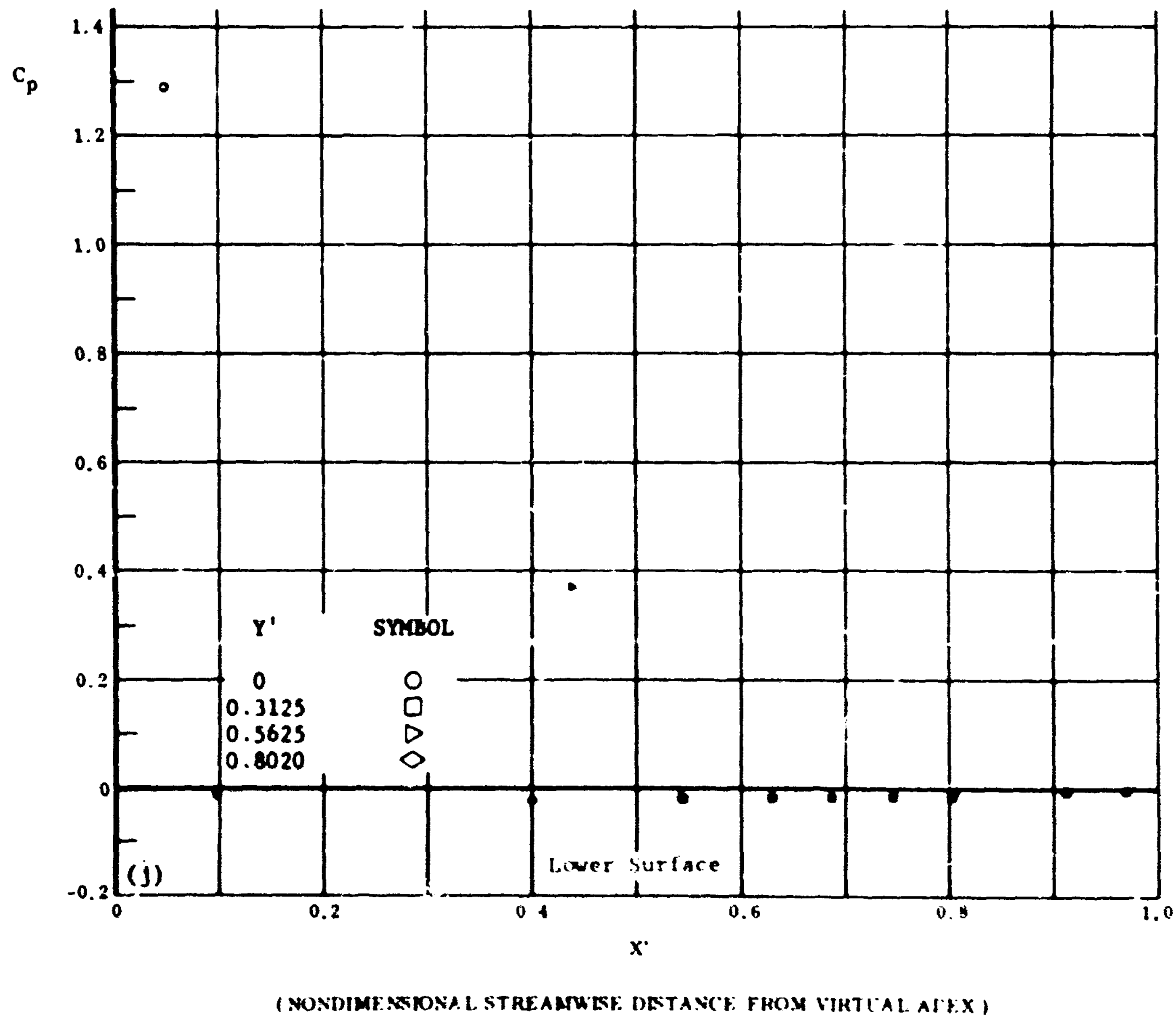

Fig. 22 Configuration I, $\delta_1 = -30$, $\delta_2 = \delta_3 = +30$

i) C_p vs. Y', lower surface

j) C_p vs. X', lower surface

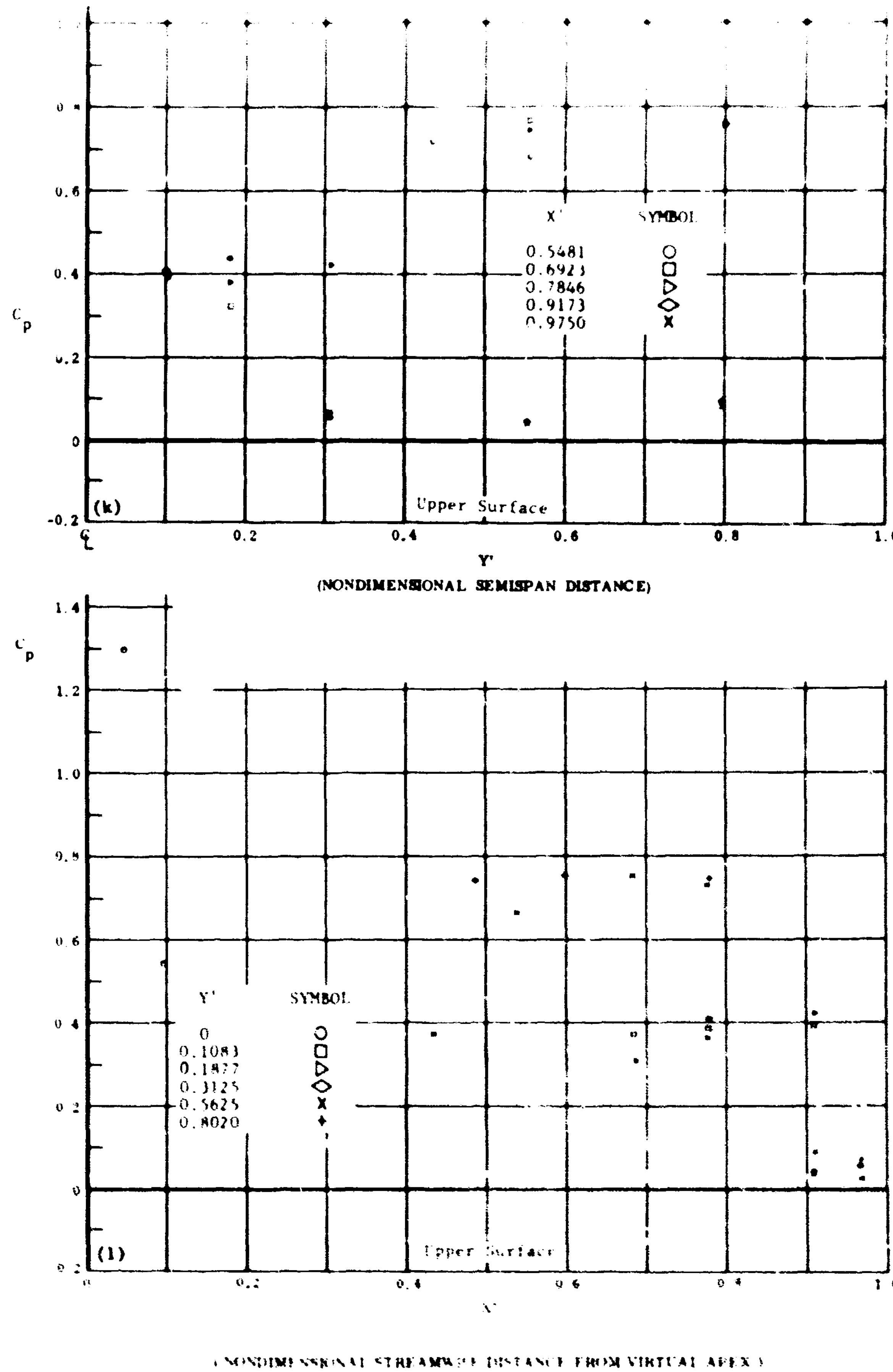

Fig. 22 Configuration I, [illegible] = -30, [illegible]$_2$ = [illegible]$_3$ = +30

k) C_p vs. Y', upper surface

l) C_p vs. X', upper surface

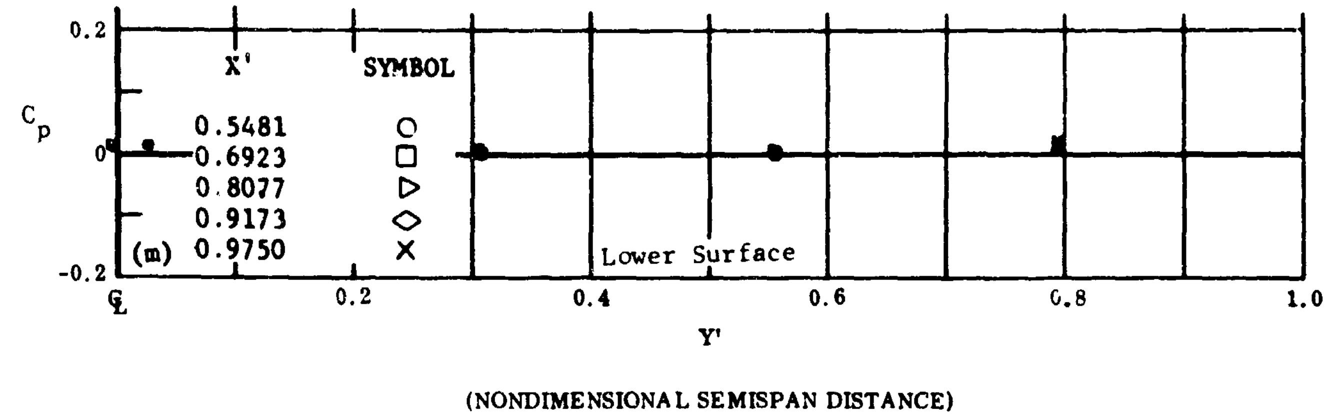

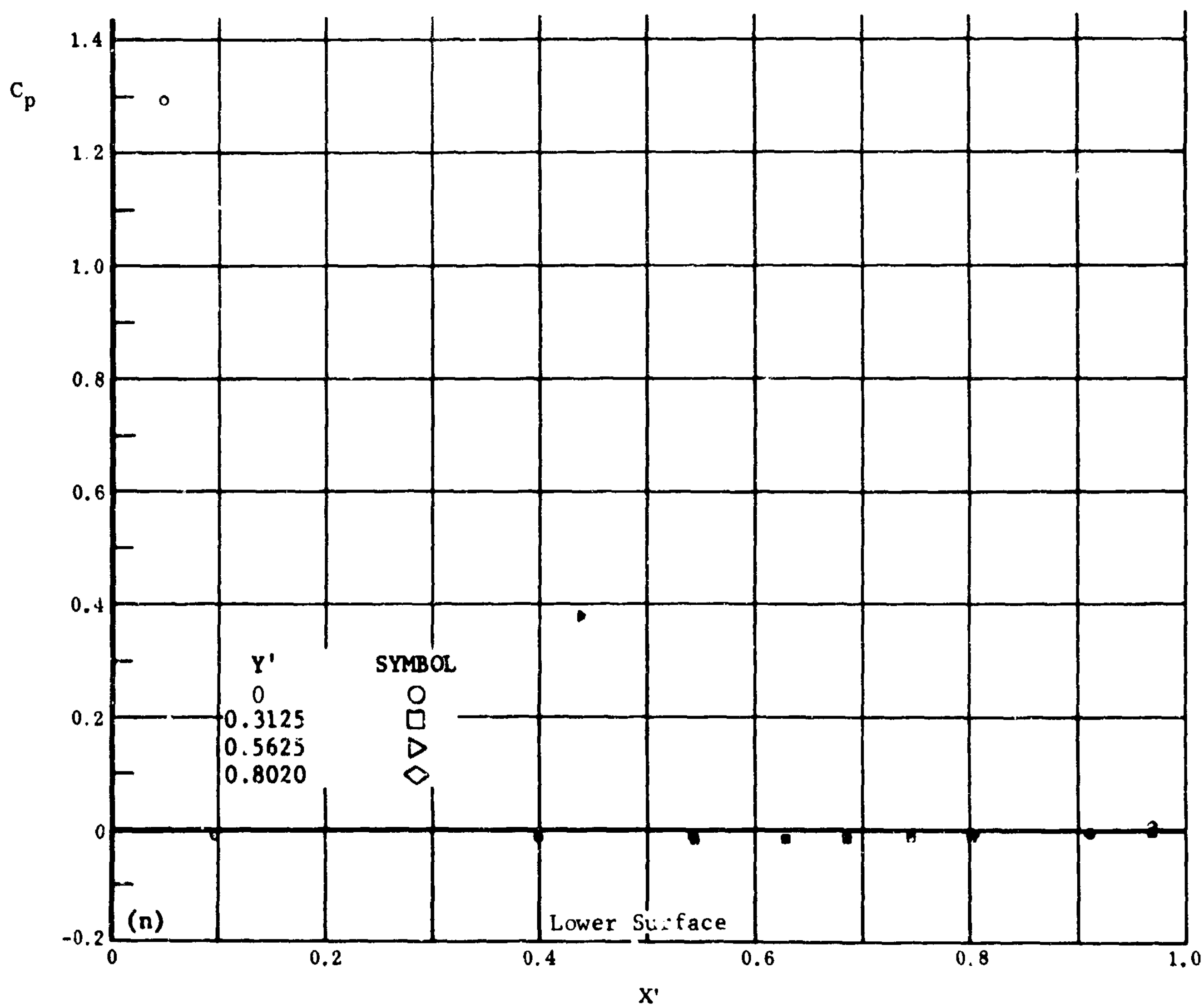

Fig. 22 Configuration I, α = -30 , $\delta_2 = \delta_3$ = +39

m) C_p vs. Y', lower surface

n) C_p vs. X', lower surface

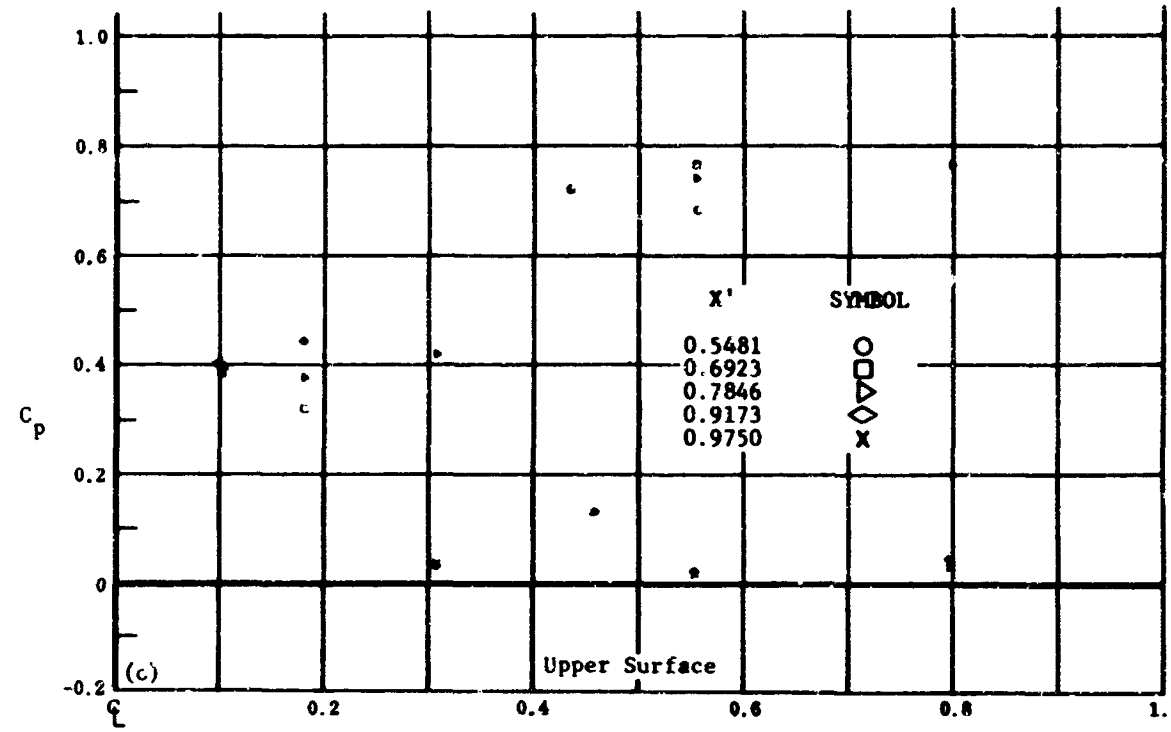

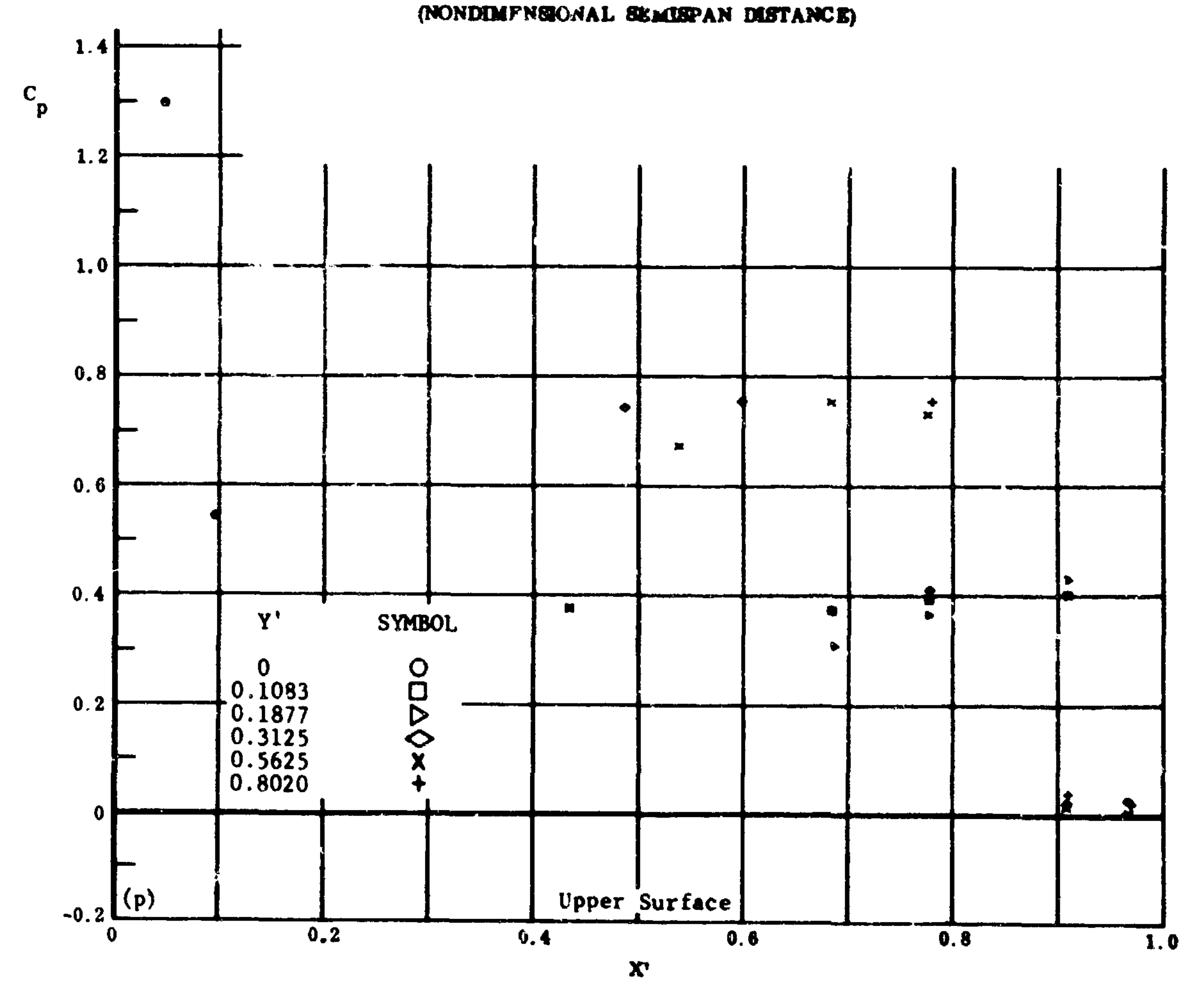

(NONDIMENSIONAL STREAMWISE DISTANCE FROM VIRTUAL APEX)

Fig. 22 Configuration I, $\alpha = -30$, $\delta_2 = \delta_3 = +39$

o) C_p vs. Y', upper surface

p) C_p vs. X', upper surface

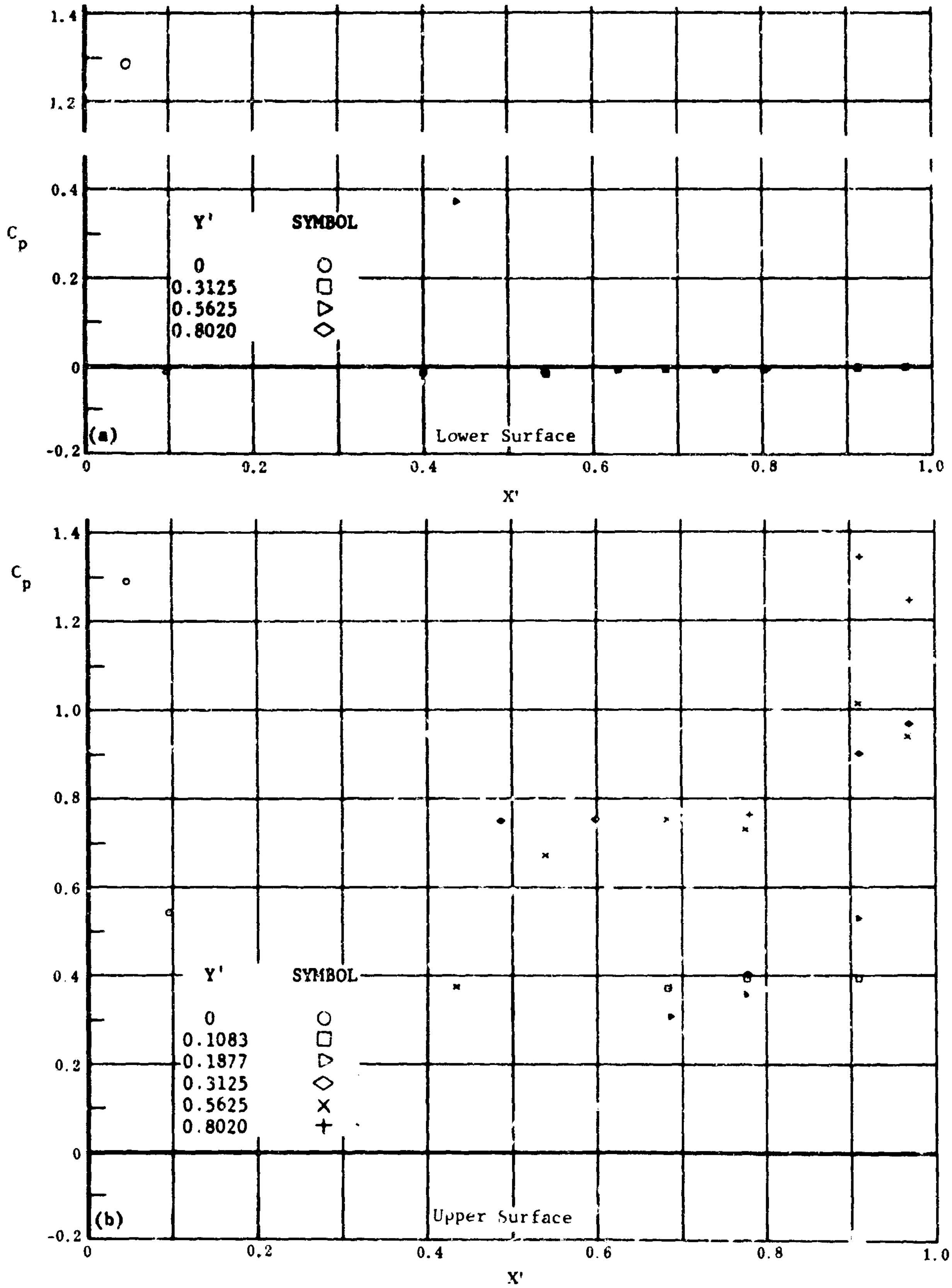

(NONDIMENSIONAL STREAMWISE DISTANCE FROM VIRTUAL APEX)

Fig. 23 Configuration I, $\alpha = -30$, $\delta_2 = \delta_3 = -10$

a) C_p vs. X', lower surface

b) C_p vs. X', upper surface

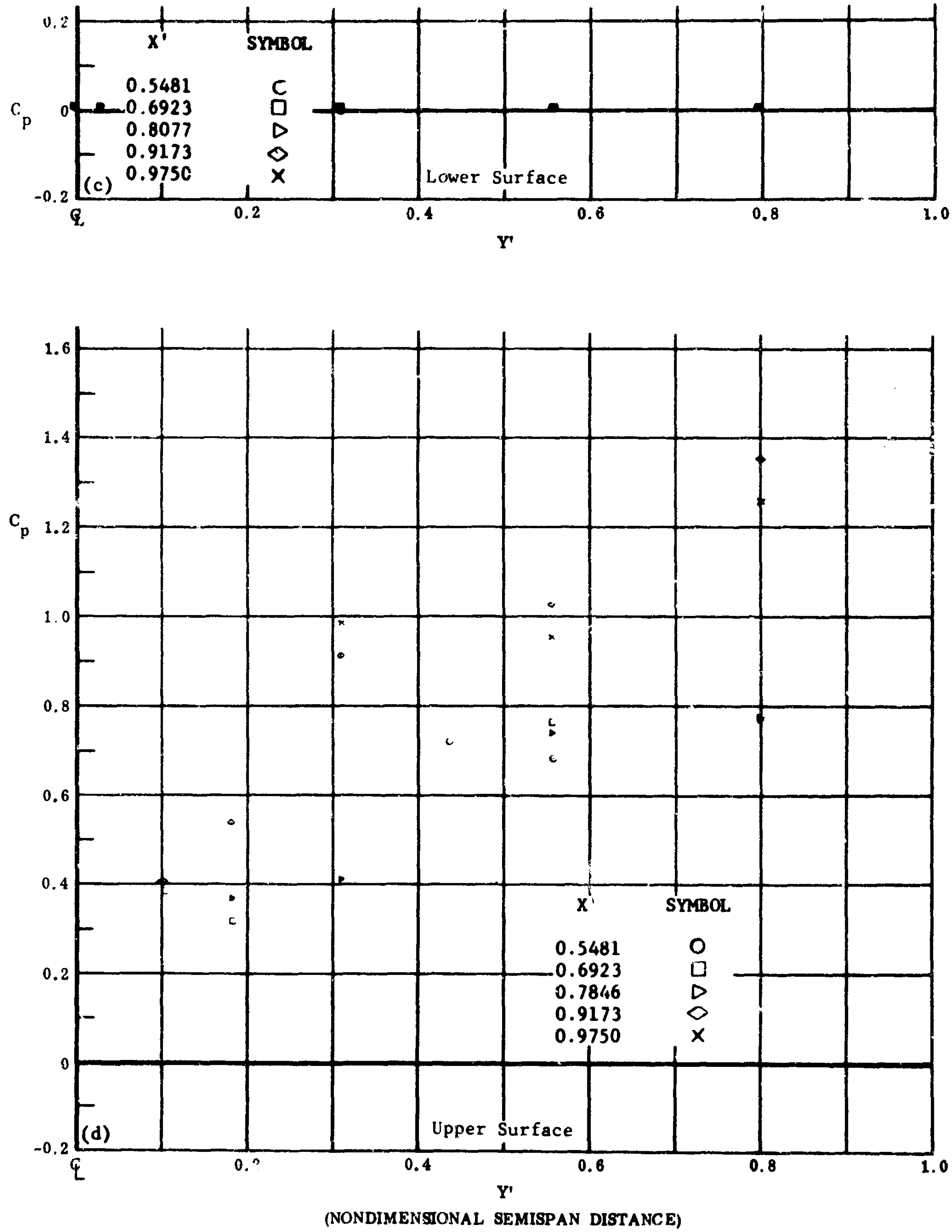

Fig. 23 Configuration I, α = -30 , $\delta_2 = \delta_3$ = -10

c) C_p vs. Y', lower surface

d) C_p vs. Y', upper surface

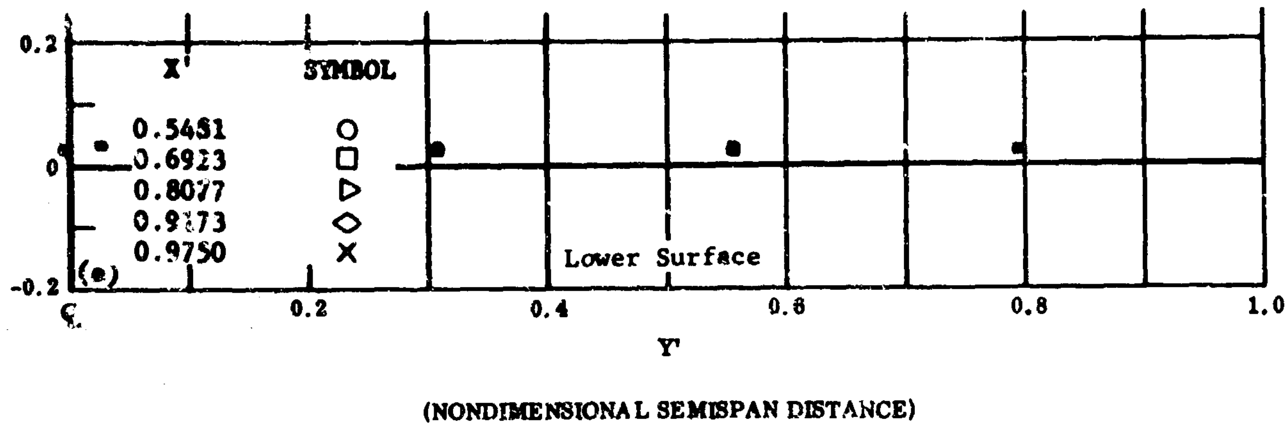

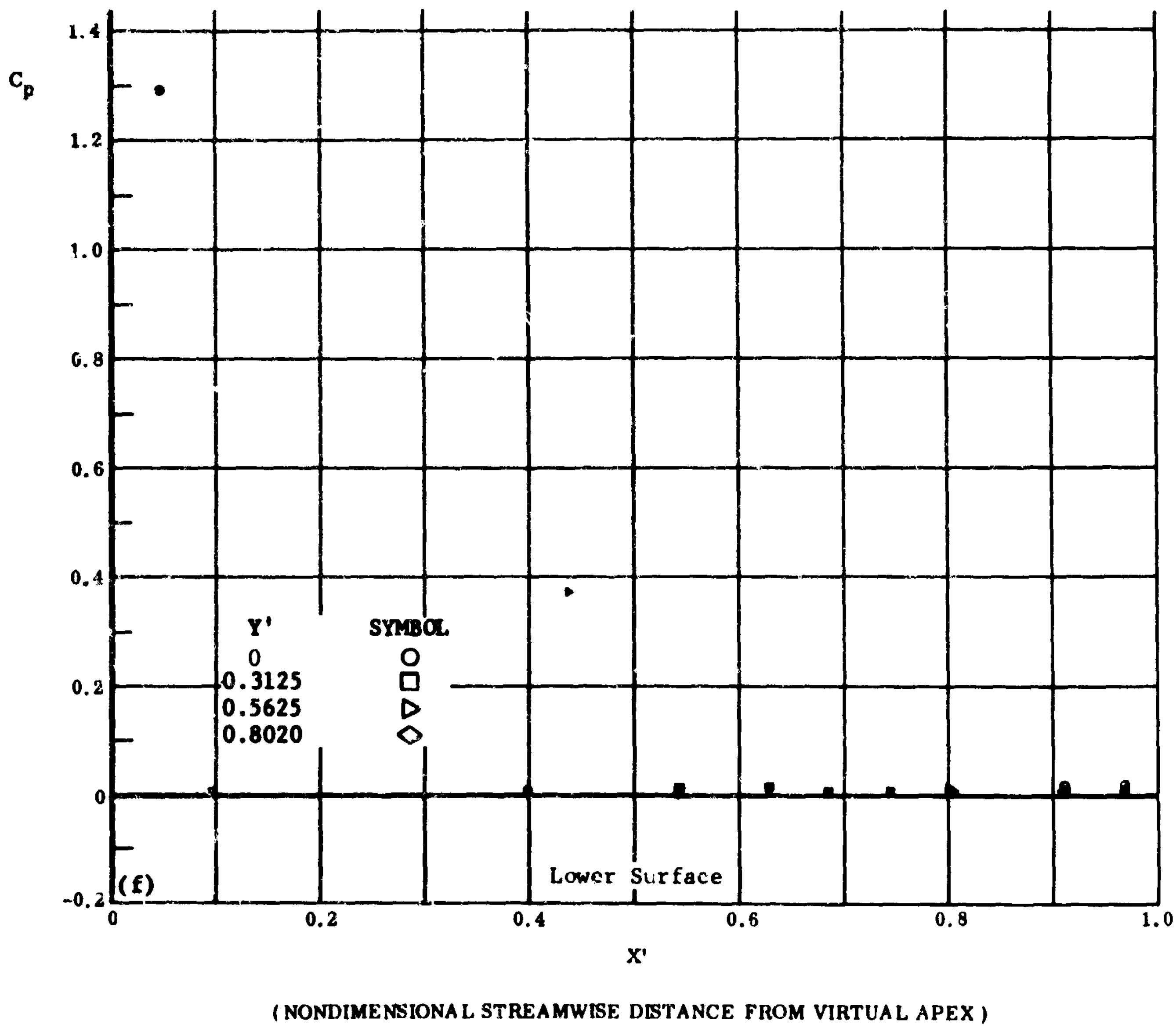

Fig. 23 Configuration I, $\alpha = -30$, $\delta_2 = \delta_3 = -20$

e) C_p vs. Y', lower surface

f) C_p vs. X', lower surface

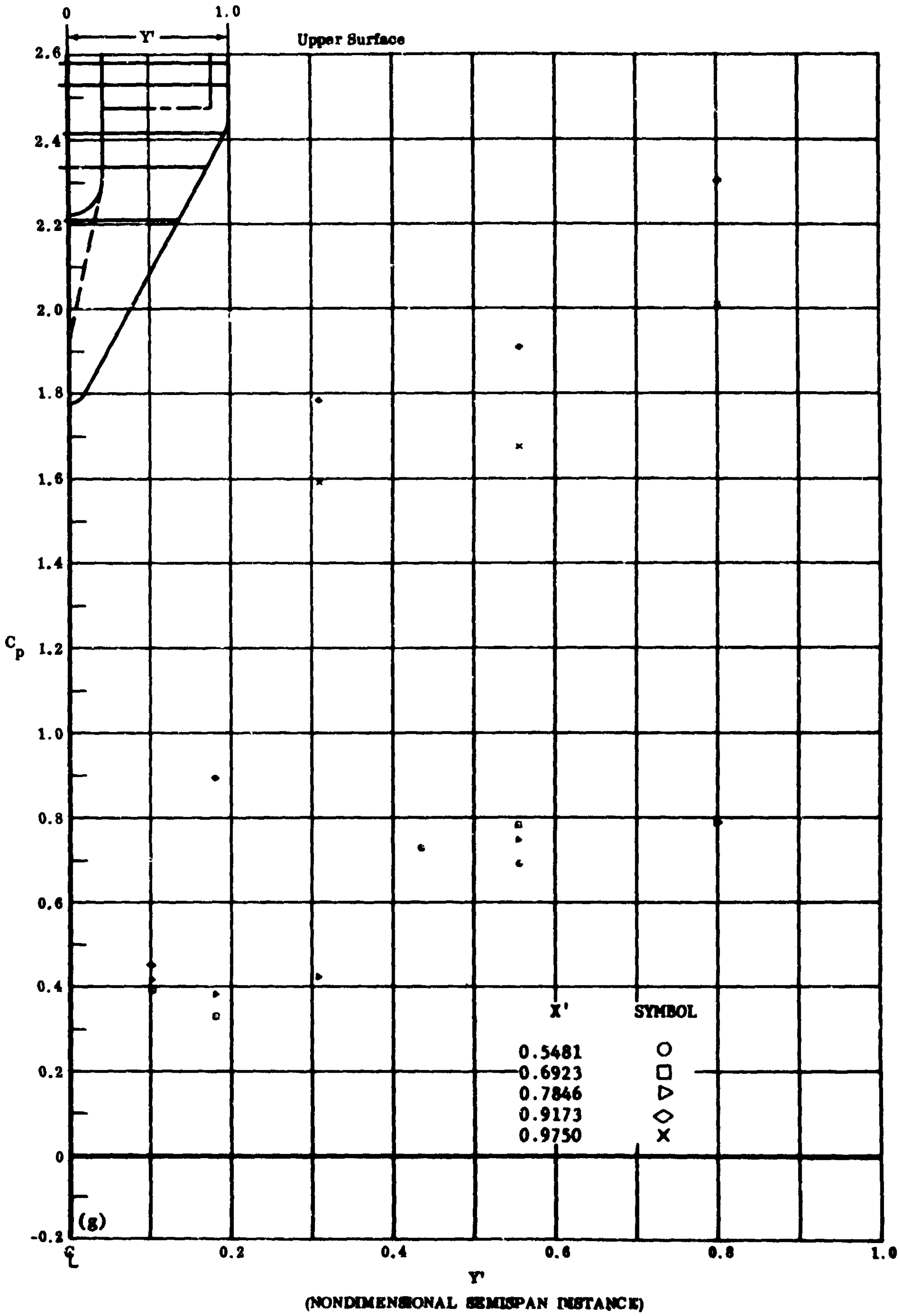

Fig. 23g Configuration I, $\alpha = -30$, $\delta_2 = \delta_3 = -20$

C_p vs. Y', upper surface

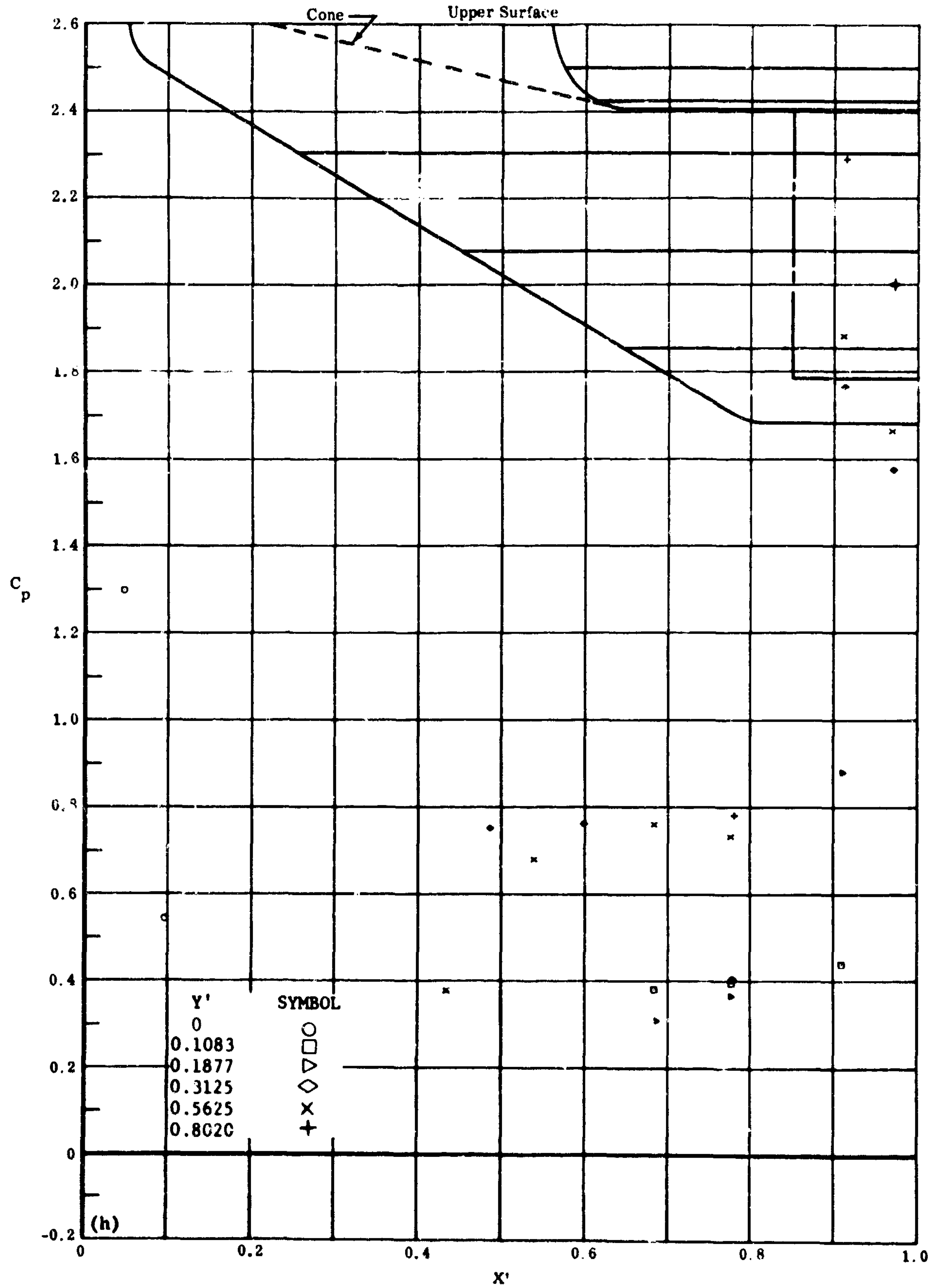

(NONDIMENSIONAL STREAMWISE DISTANCE FROM VIRTUAL APEX)

Fig. 23h Configuration I, $\alpha = -30$, $\delta_2 = \delta_3 = -20$

C_p vs. X', upper surface

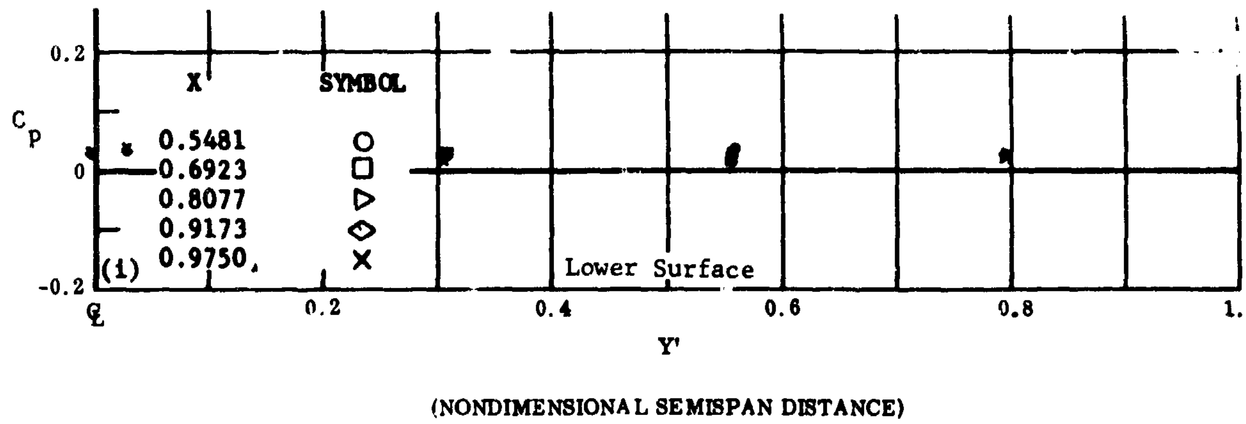

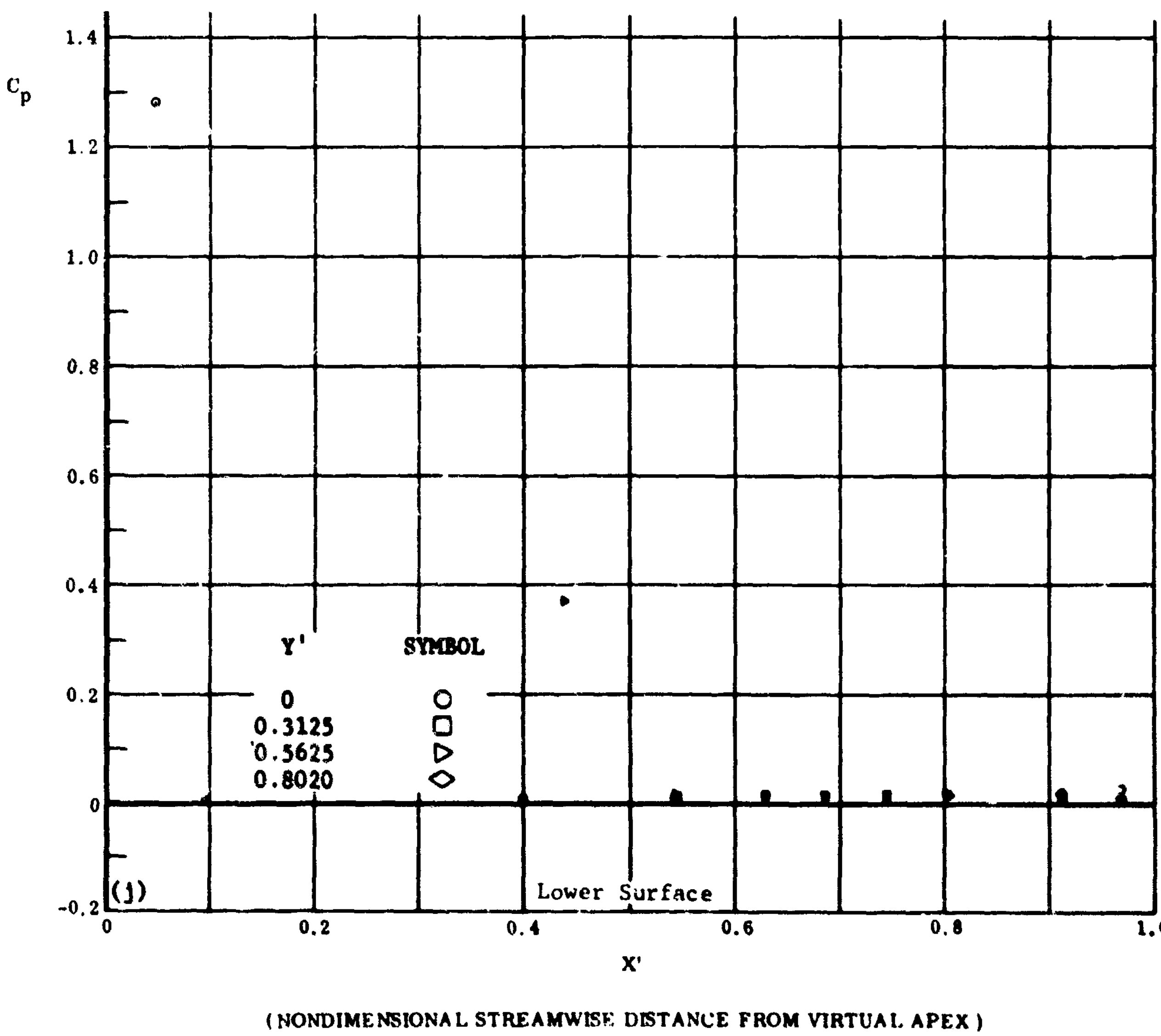

Fig. 23 Configuration I, $\alpha = -30$, $\delta_2 = \delta_3 = -30$

i) C_p vs. Y', lower surface

j) C_p vs. X', lower surface

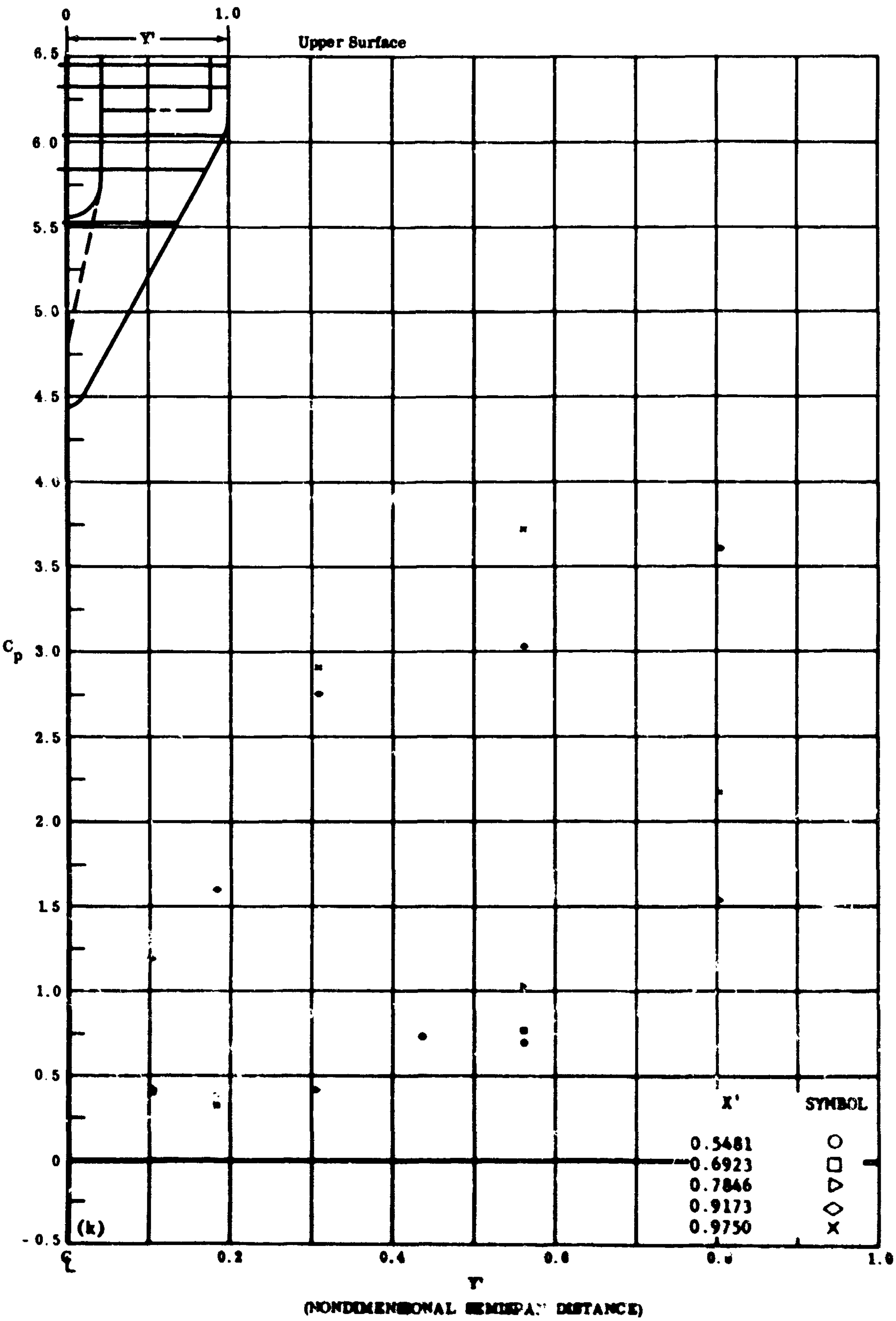

Fig. 23k Configuration I, α = -30 , $\delta_2 = \delta_3$ = -30

C_p vs Y' upper surface

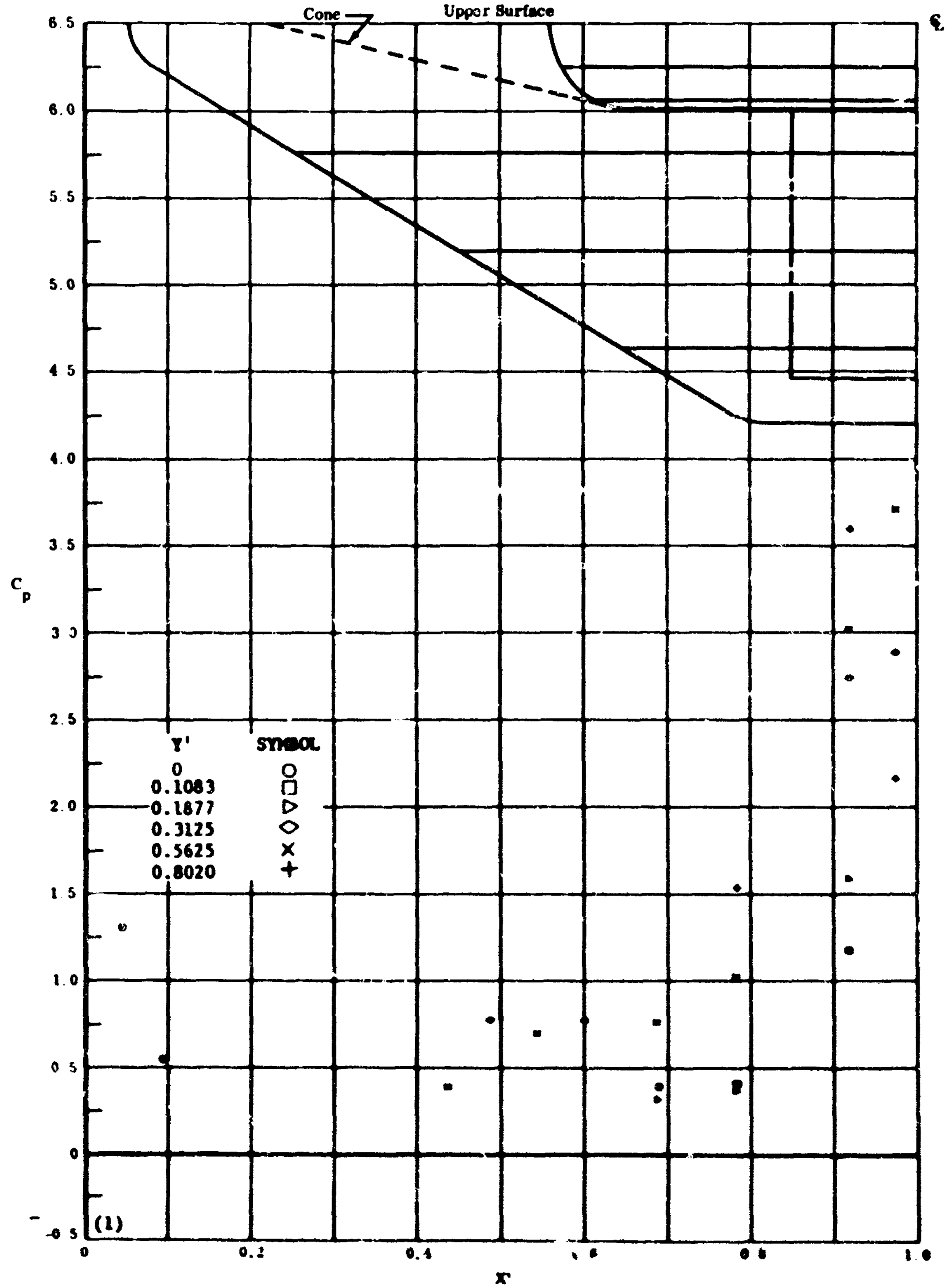

(NONDIMENSIONAL STREAMWISE DISTANCE FROM VIRTUAL APEX)

Fig. 231 Configuration I, $\alpha = -30$, $\delta_2 = \delta_3 = -10$

C_p vs. X', upper surface

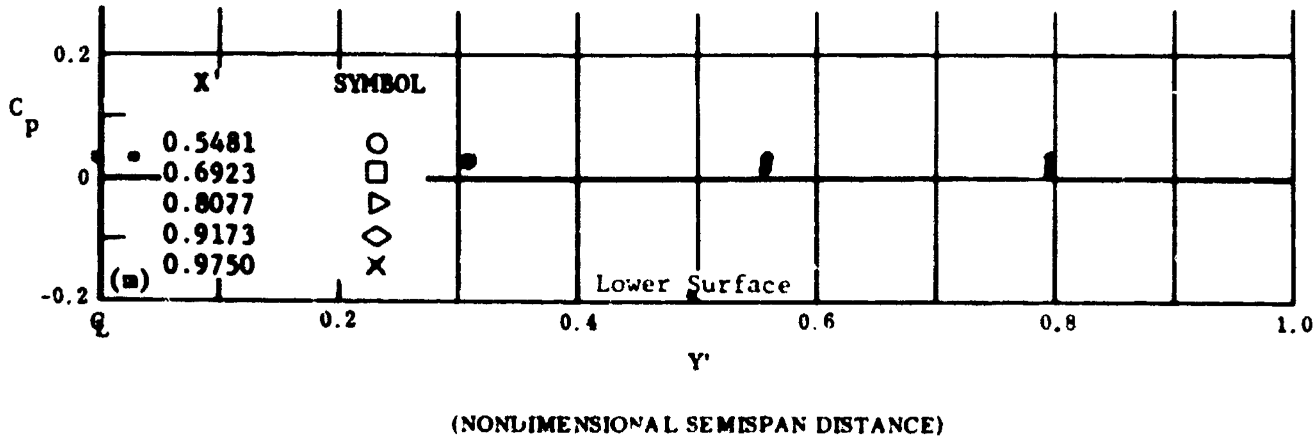

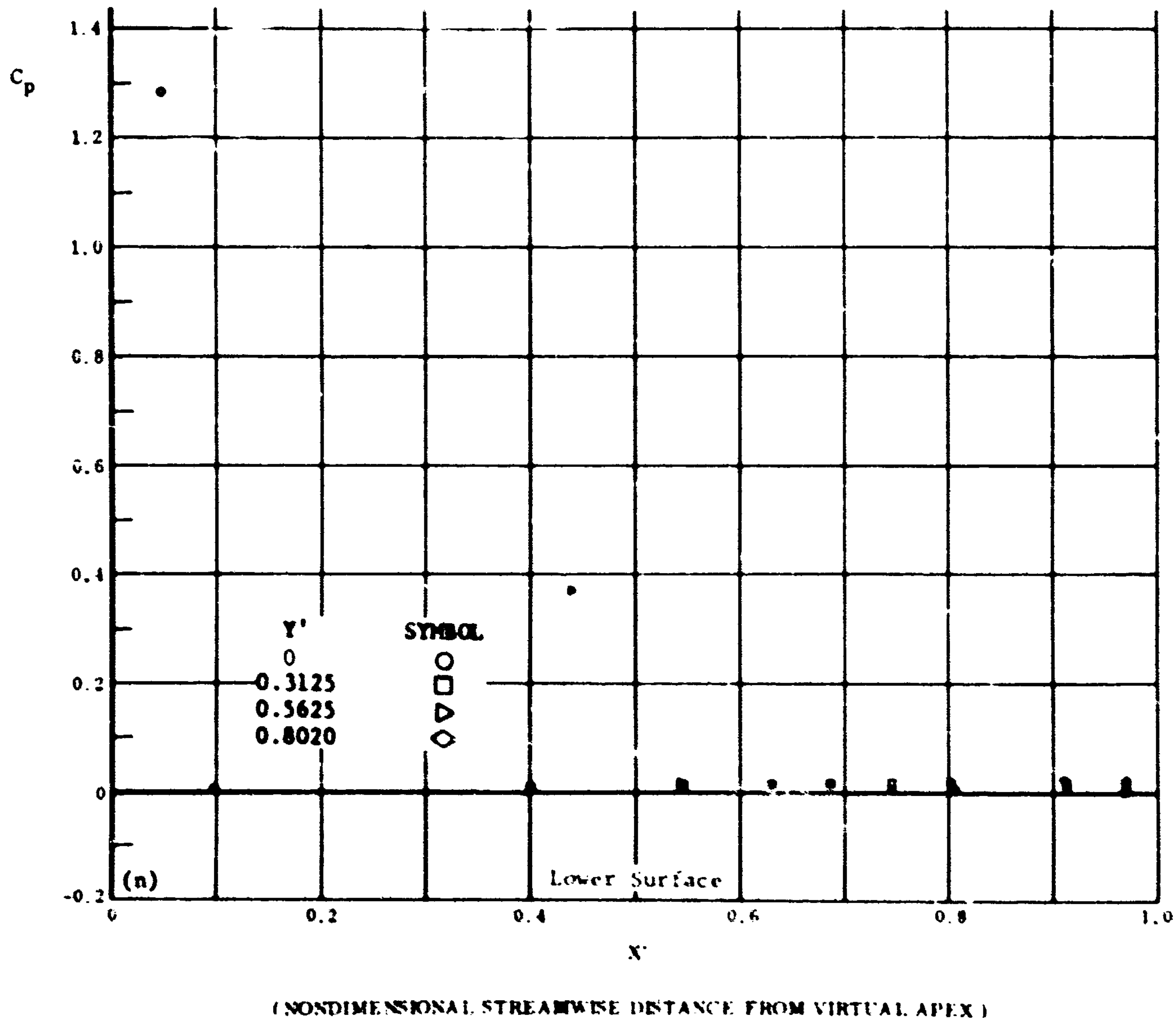

Fig. 23 Configuration I, : = -30 , $_2$ = $_3$ = -39

m) C_p vs. Y', lower surface

n) C_p vs. X', lower surface

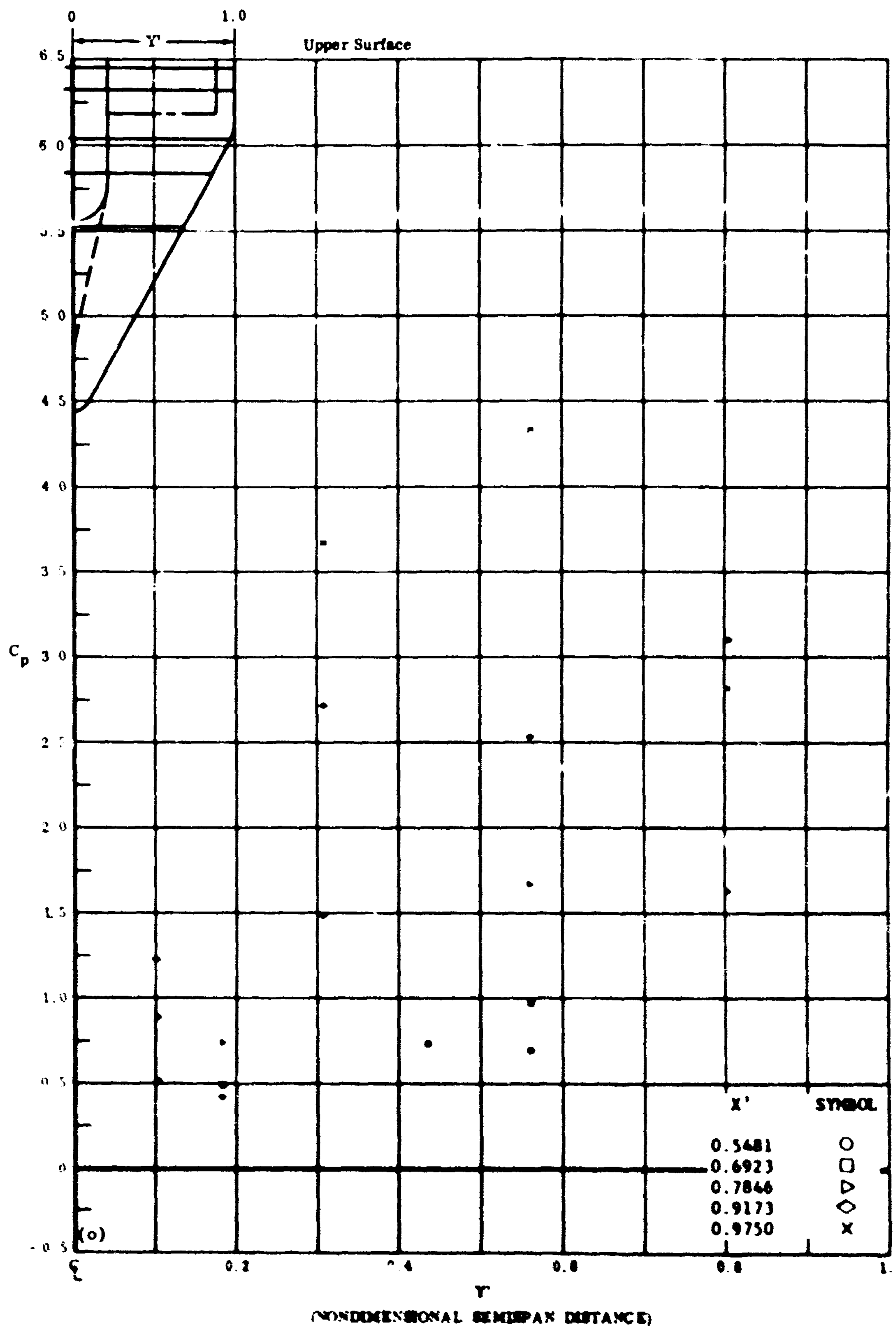

Fig. 23o Configuration I, δ_1 = -30 , $\delta_2 = \delta_3$ = -39

C_p vs. Y', upper surface

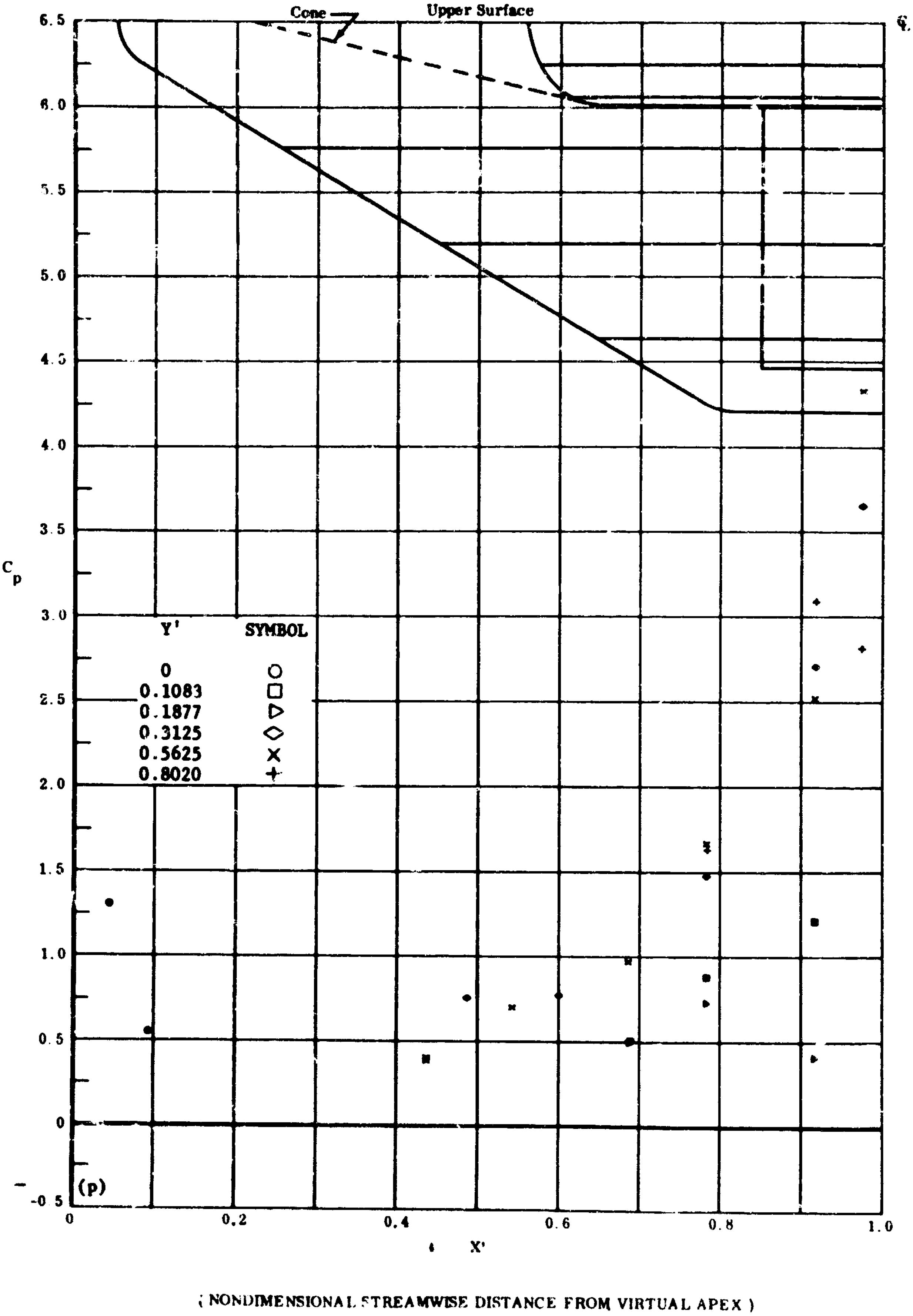

Fig. 23p Configuration I, $\alpha = -30$, $\delta_2 = \delta_3 = -39$

C_p vs. X', upper surface

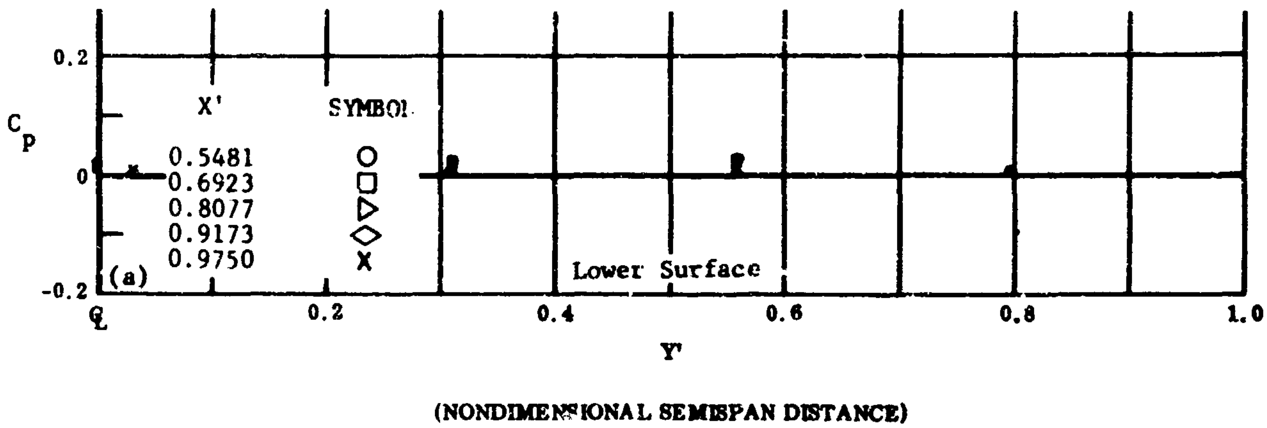

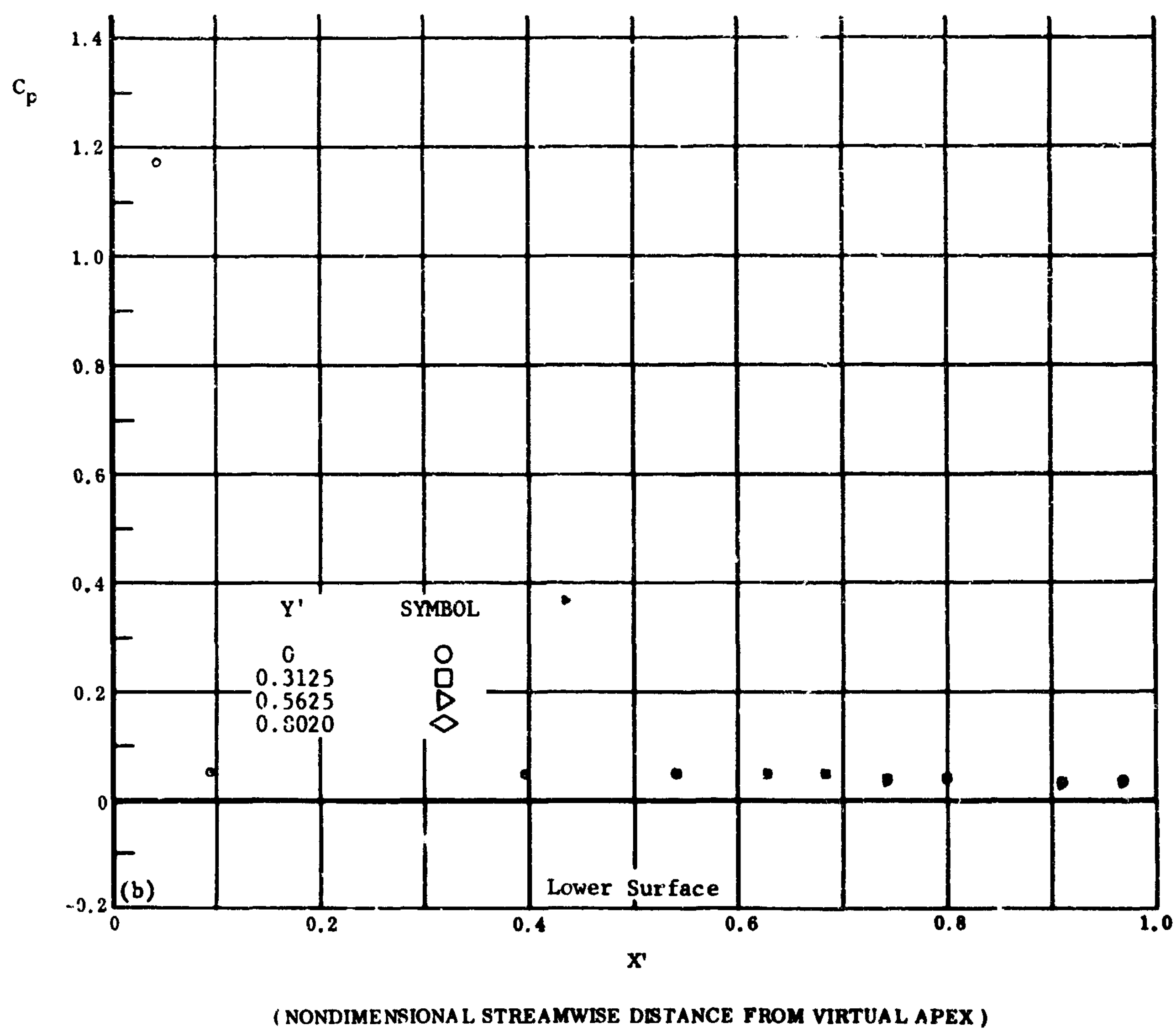

Fig. 24 Configuration I, $\alpha = -35$, $\delta_2 = \delta_3 = -30$

a) C_p vs. Y', lower surface

b) C_p vs. X', lower surface

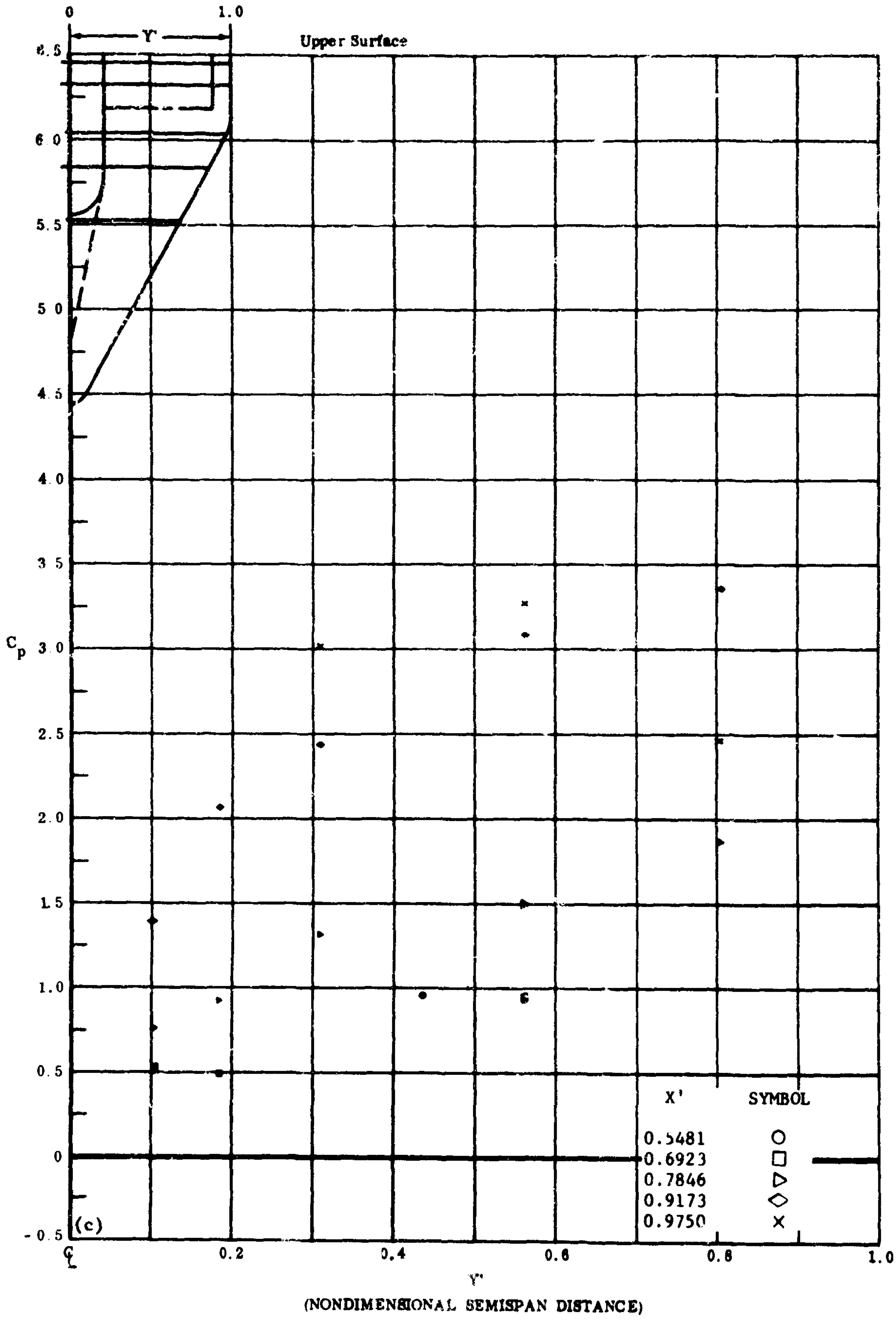

Fig. 24c Configuration I, α = -35 , $\delta_2 = \delta_3$ = -30

C_p vs. Y', upper surface

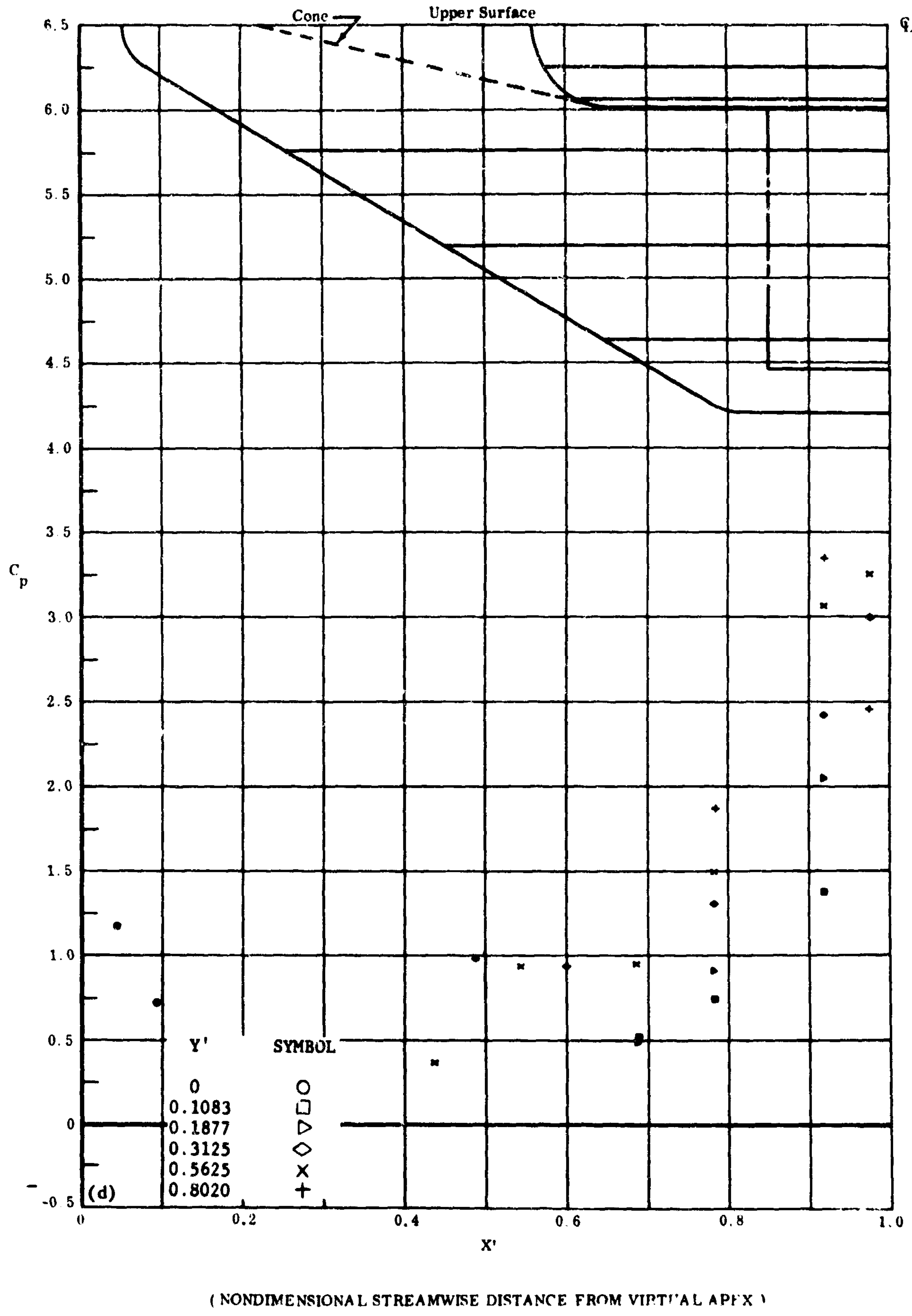

Fig. 24d Configuration I, α = -35 , $\delta_2 = \delta_3$ = -30

C_p vs. X', upper surface

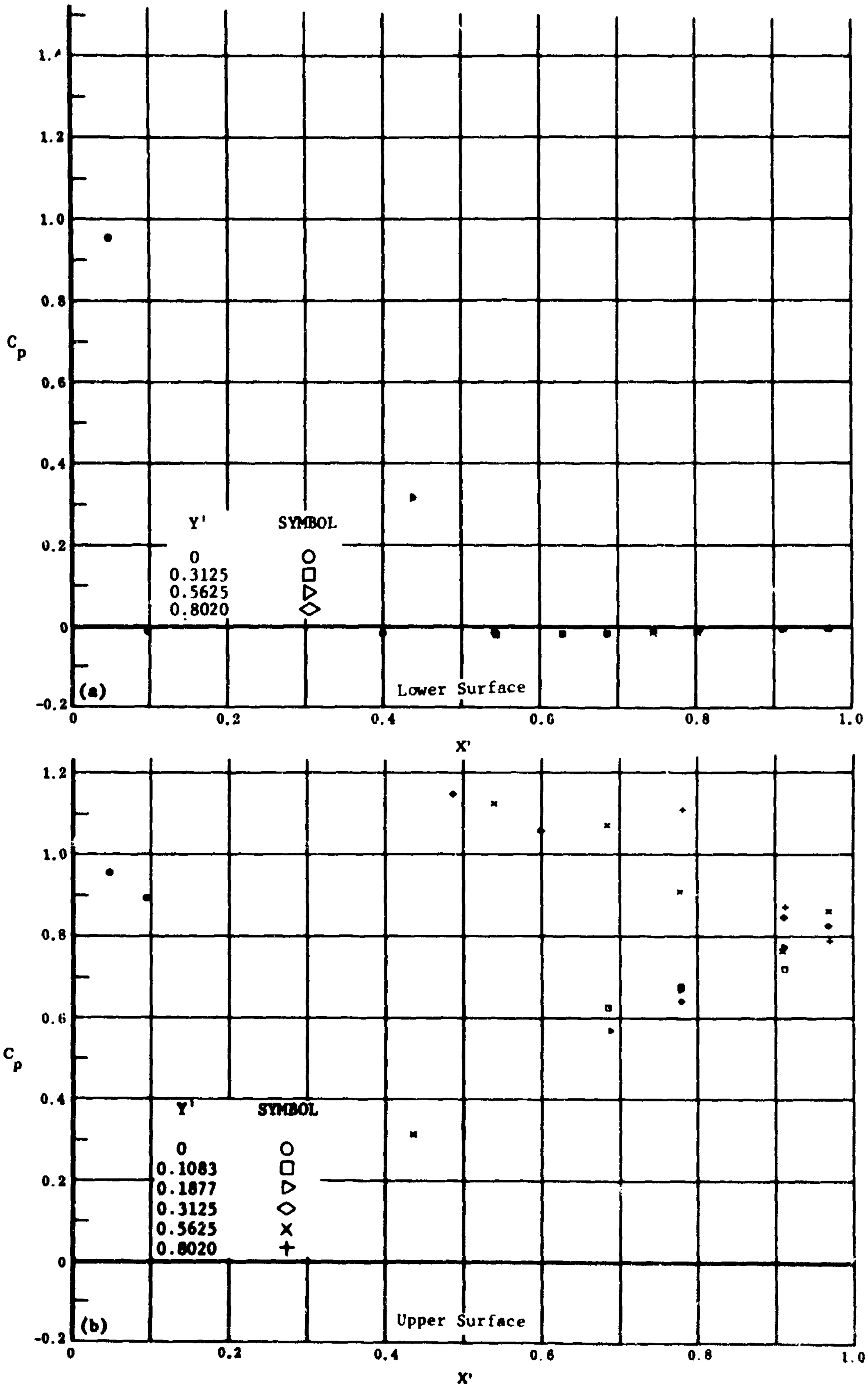

(NONDIMENSIONAL STREAMWISE DISTANCE FROM VIRTUAL APEX)

Fig. 25 Configuration I, $\alpha = -40$, $\delta_2 = \delta_3 = 0$

a) C_p vs. X', lower surface

b) C_p vs. X', upper surface

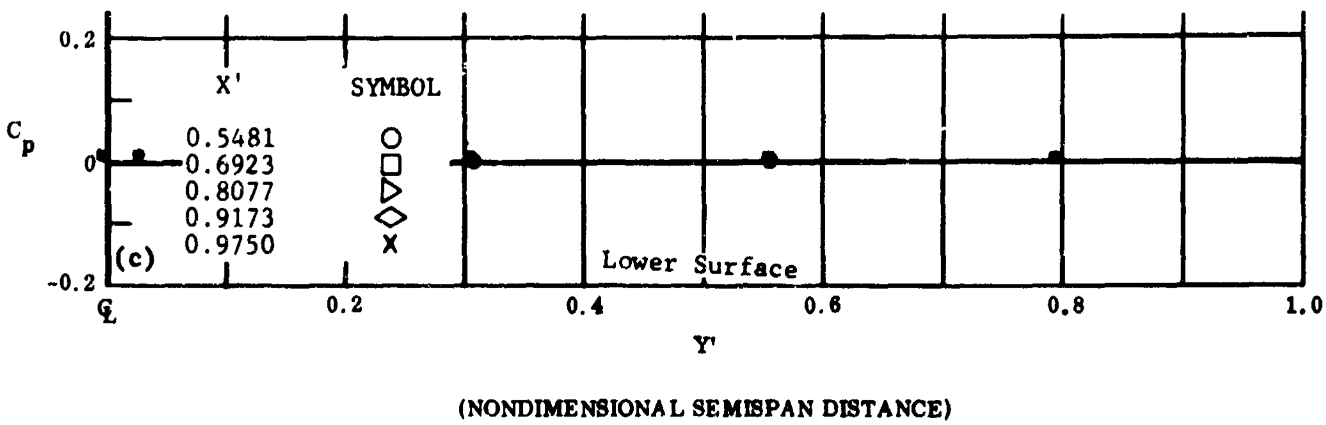

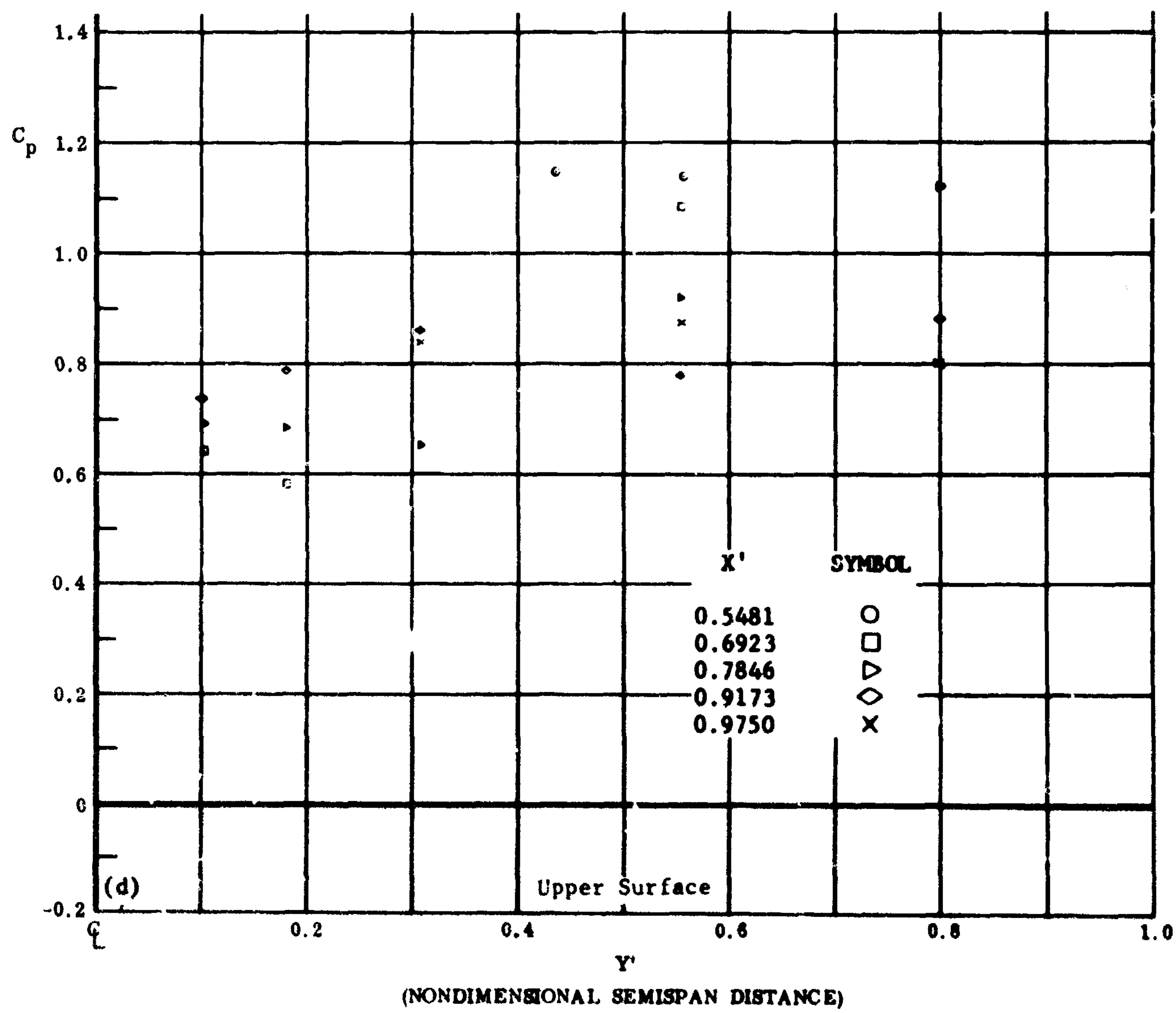

Fig. 25 Configuration I, $\alpha = -40$, $\delta_2 = \delta_3 = 0$

c) C_p vs. Y', lower surface

d) C_p vs. Y', upper surface

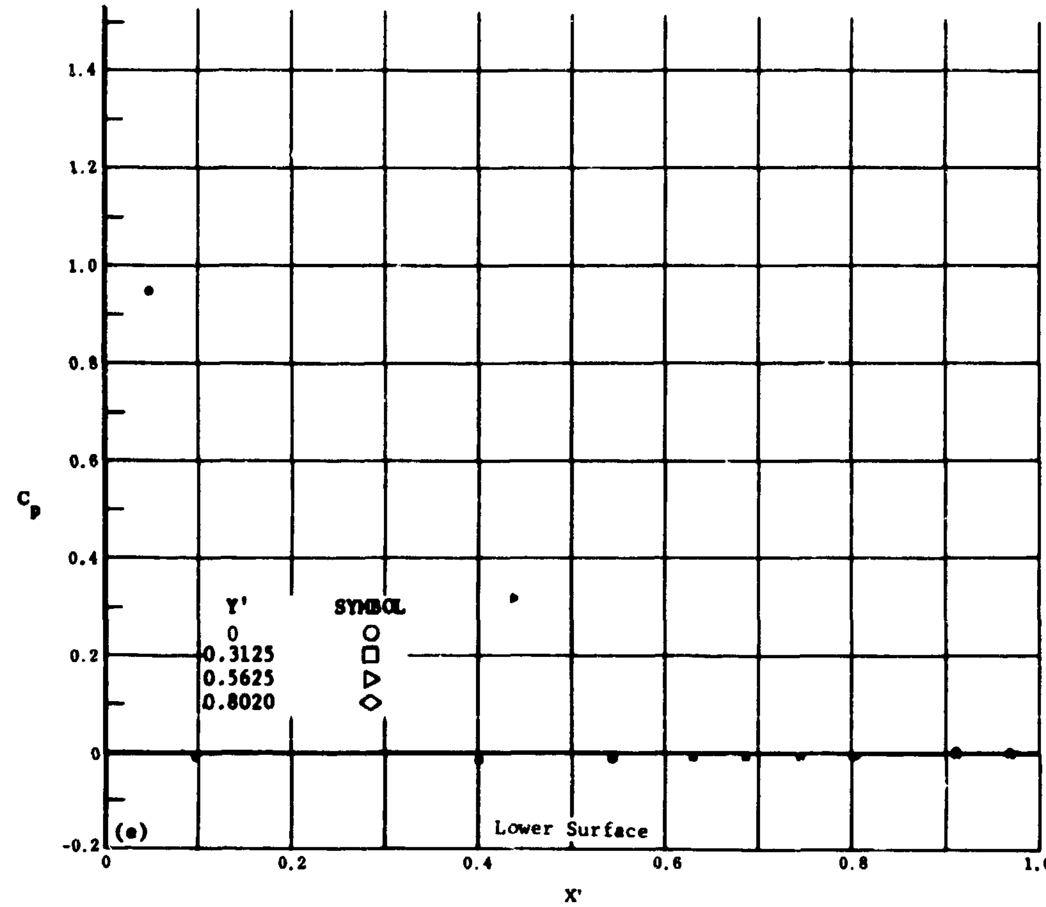

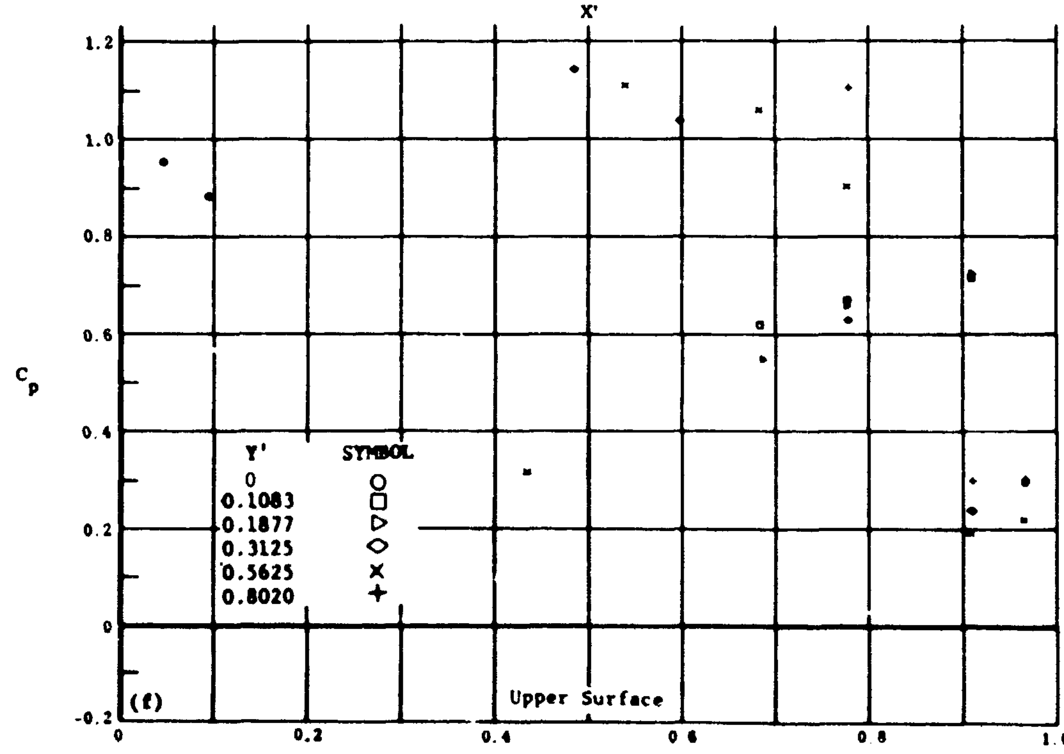

(NONDIMENSIONAL STREAMWISE DISTANCE FROM VIRTUAL APEX)

Fig. 25 Configuration I, $\alpha = -40$, $\delta_2 = \delta_3 = +20$

e) C_p vs. X', lower surface

f) C_p vs. X', upper surface

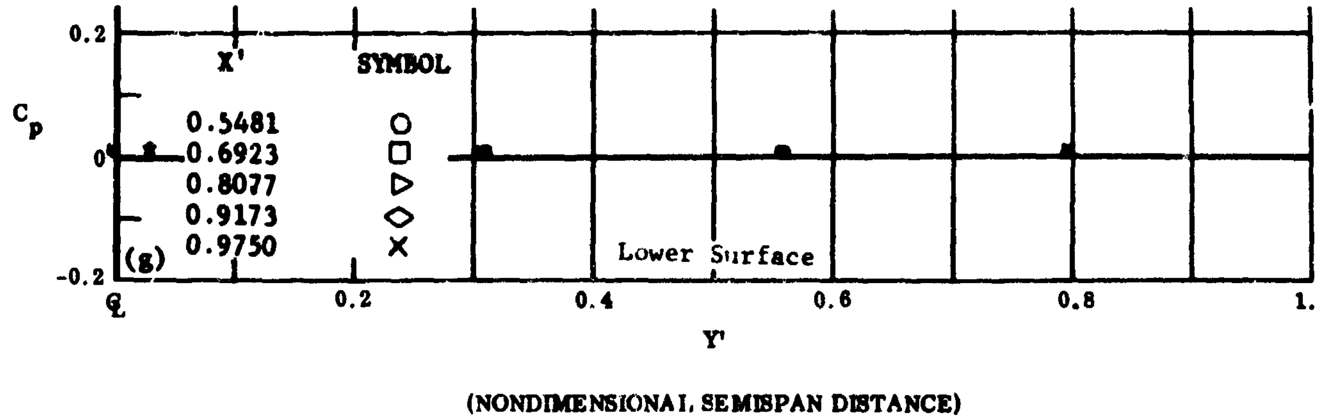

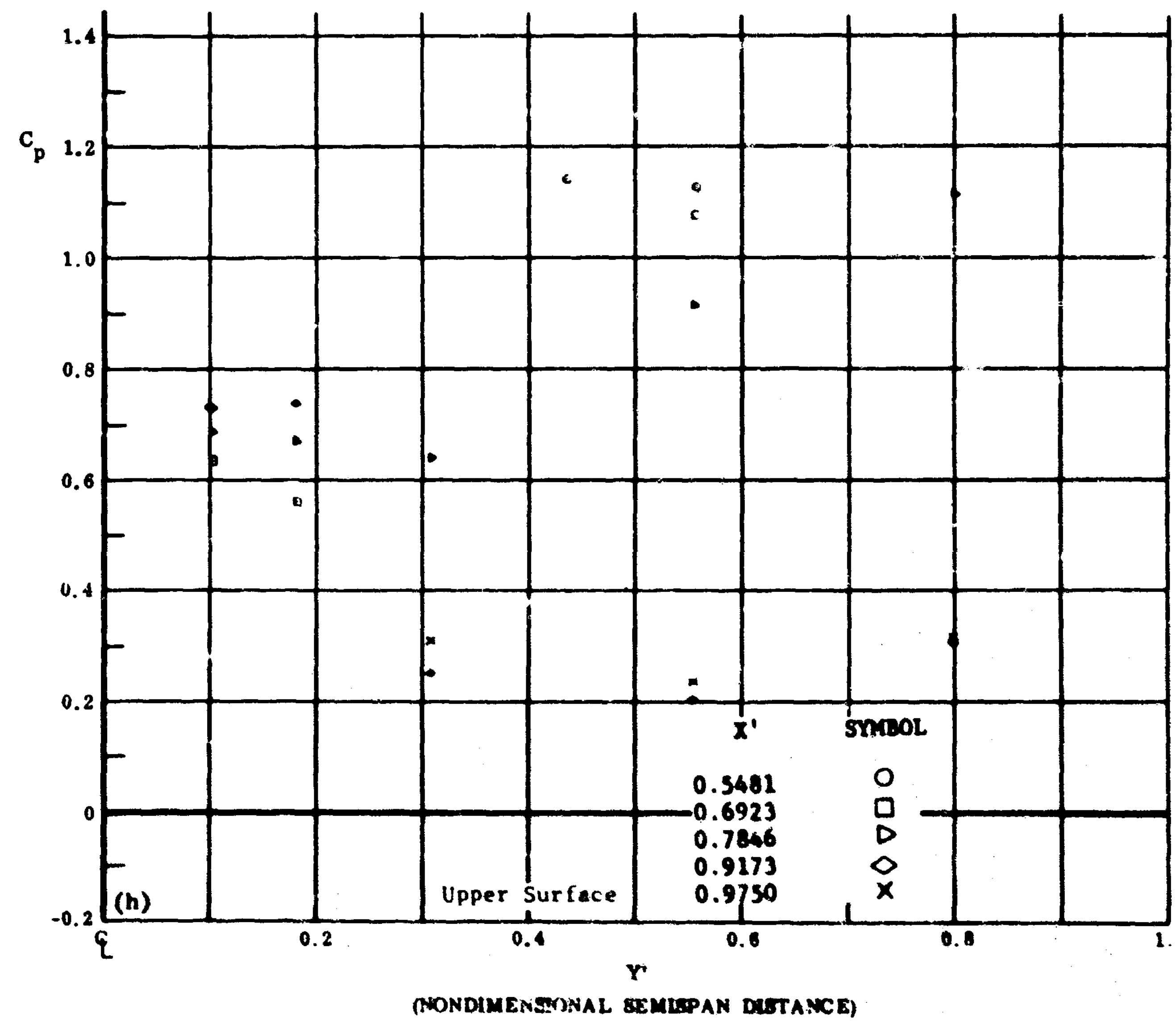

Fig. 25 Configuration I, α = -40 , $\delta_2 = \delta_3$ = +20

g) C_p vs. Y', lower surface

h) C_p vs. Y', upper surface

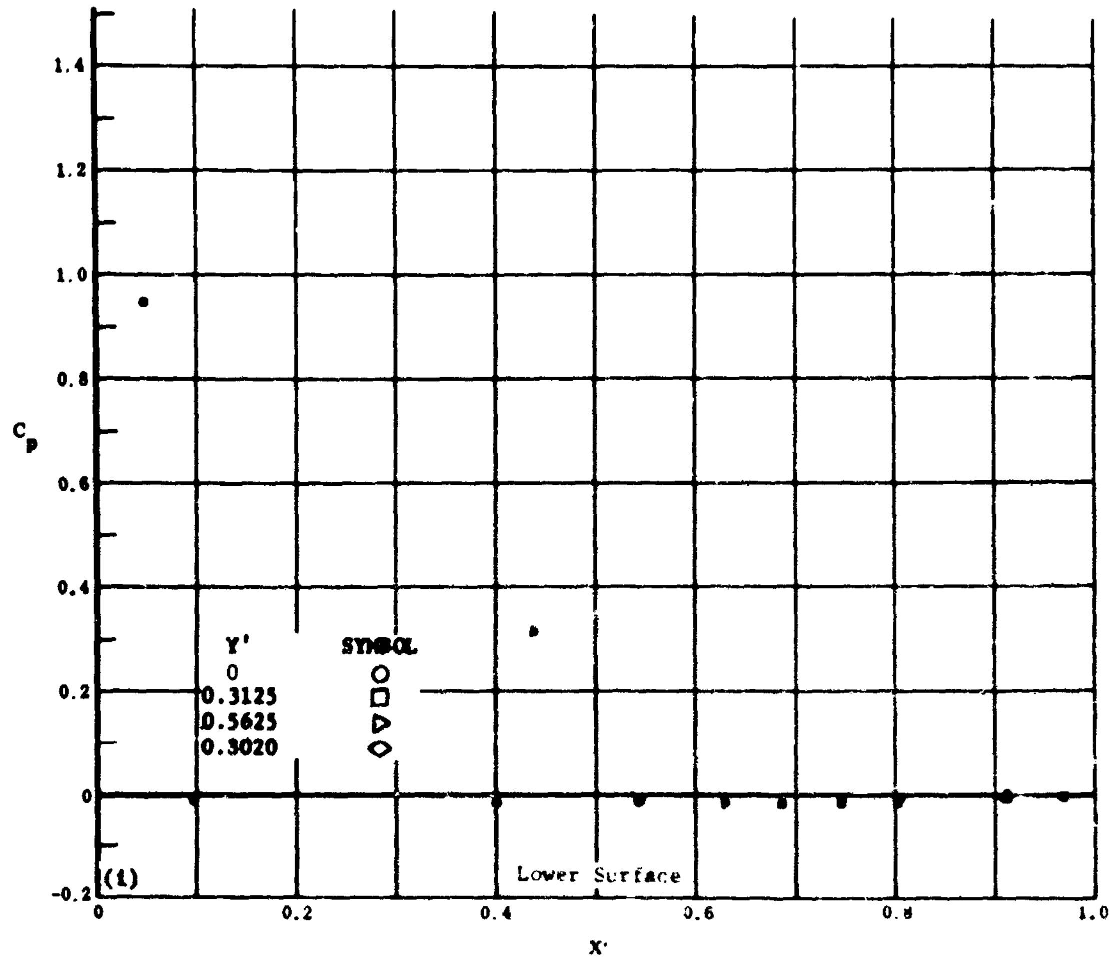

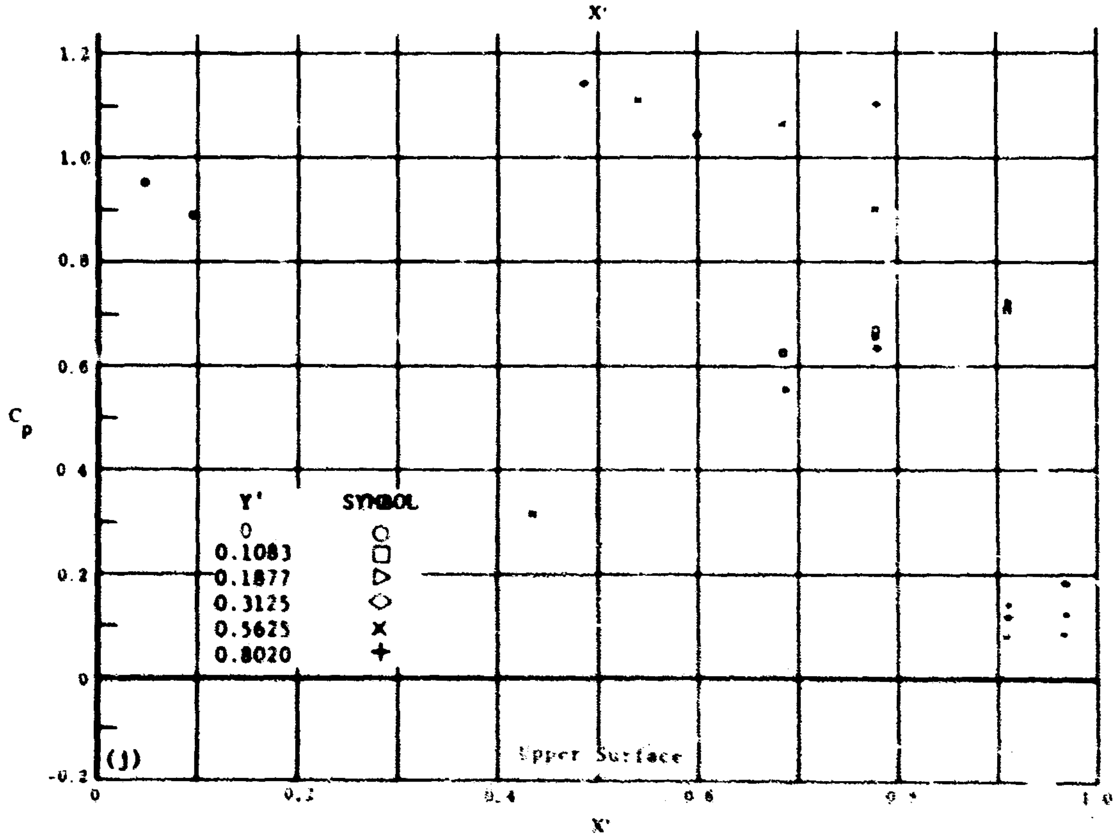

Fig. 25 Configuration I, $\alpha = +40$, $\delta_2 = \delta_3 = +40$

i) C_p vs. X', lower surface

j) C_p vs. X', upper surface

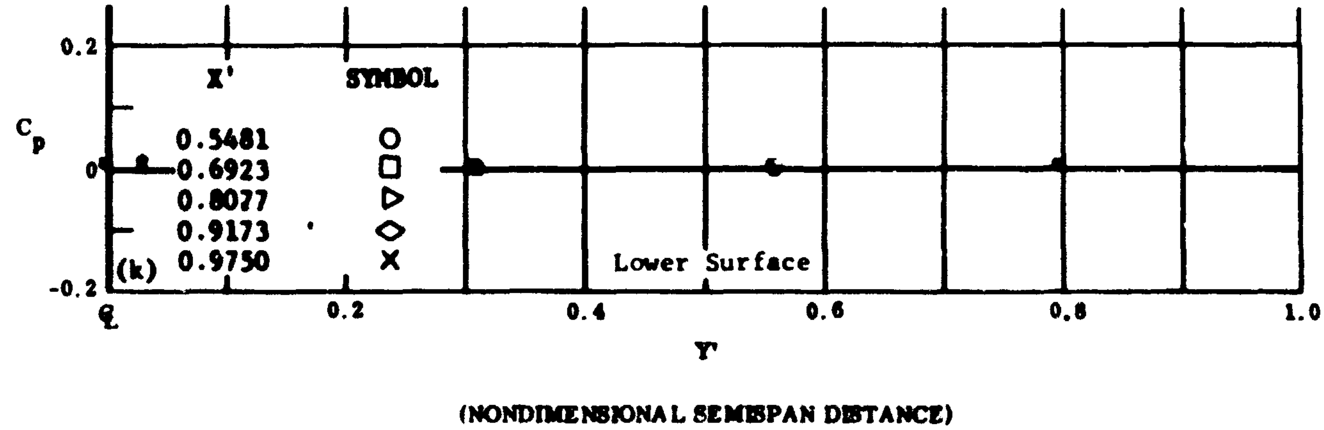

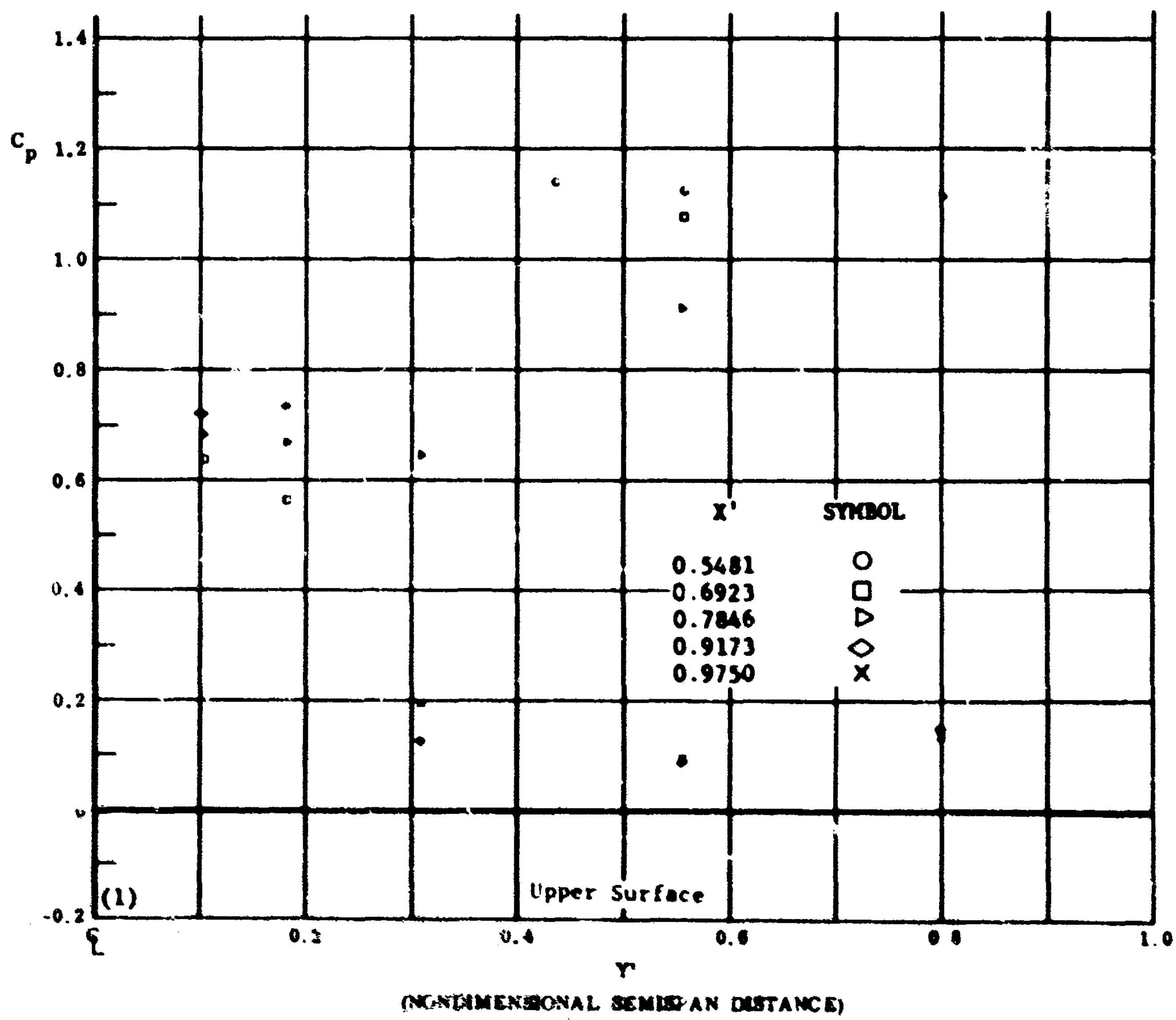

Fig. 25 Configuration I, α = -40 , $\delta_2 = \delta_3$ = +30

k) C_p vs. Y', lower surface

l) C_p vs. Y', upper surface

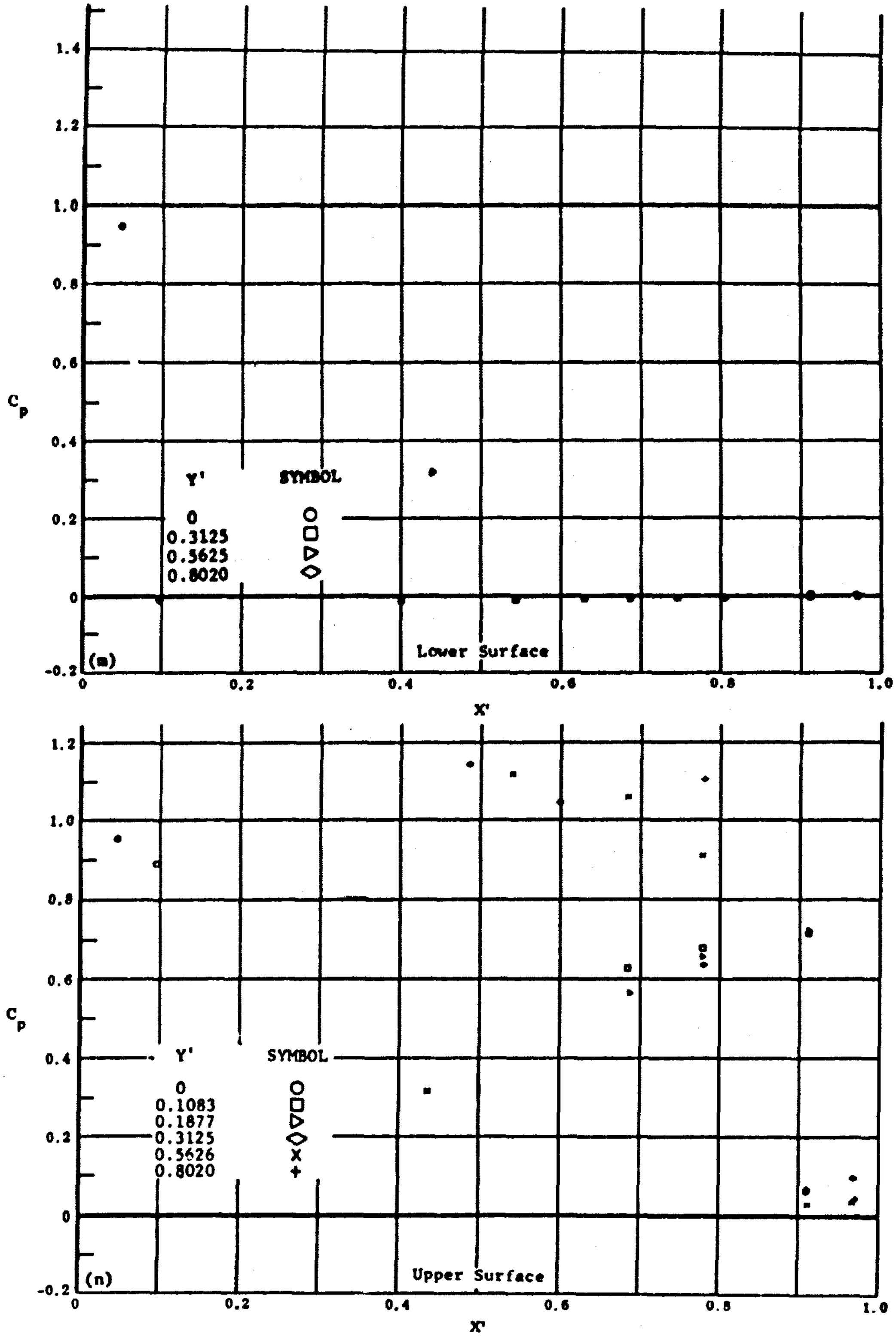

(NONDIMENSIONAL STREAMWISE DISTANCE FROM VIRTUAL APEX)

Fig. 25 Configuration I, $\alpha = -40$, $\delta_2 = \delta_3 = +39$

m) C_p vs. X', lower surface

n) C_p vs. X', upper surface

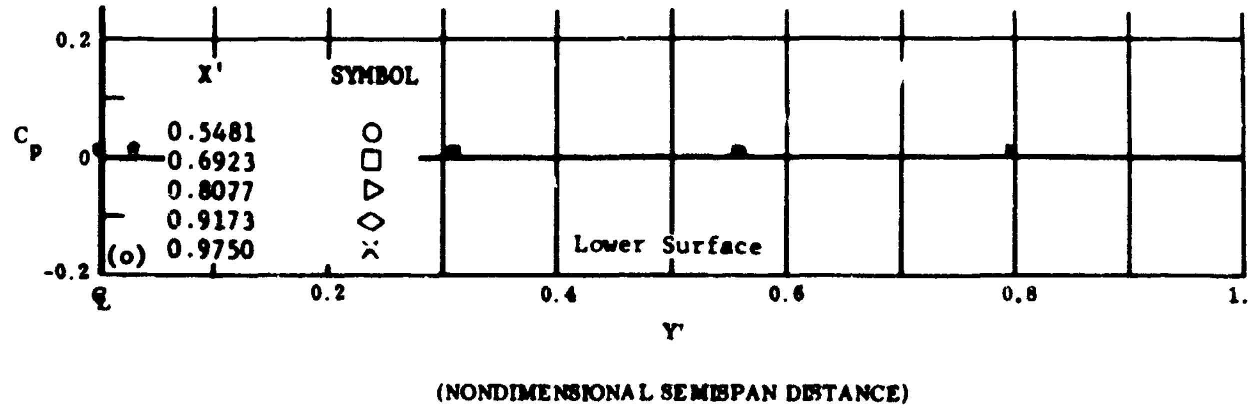

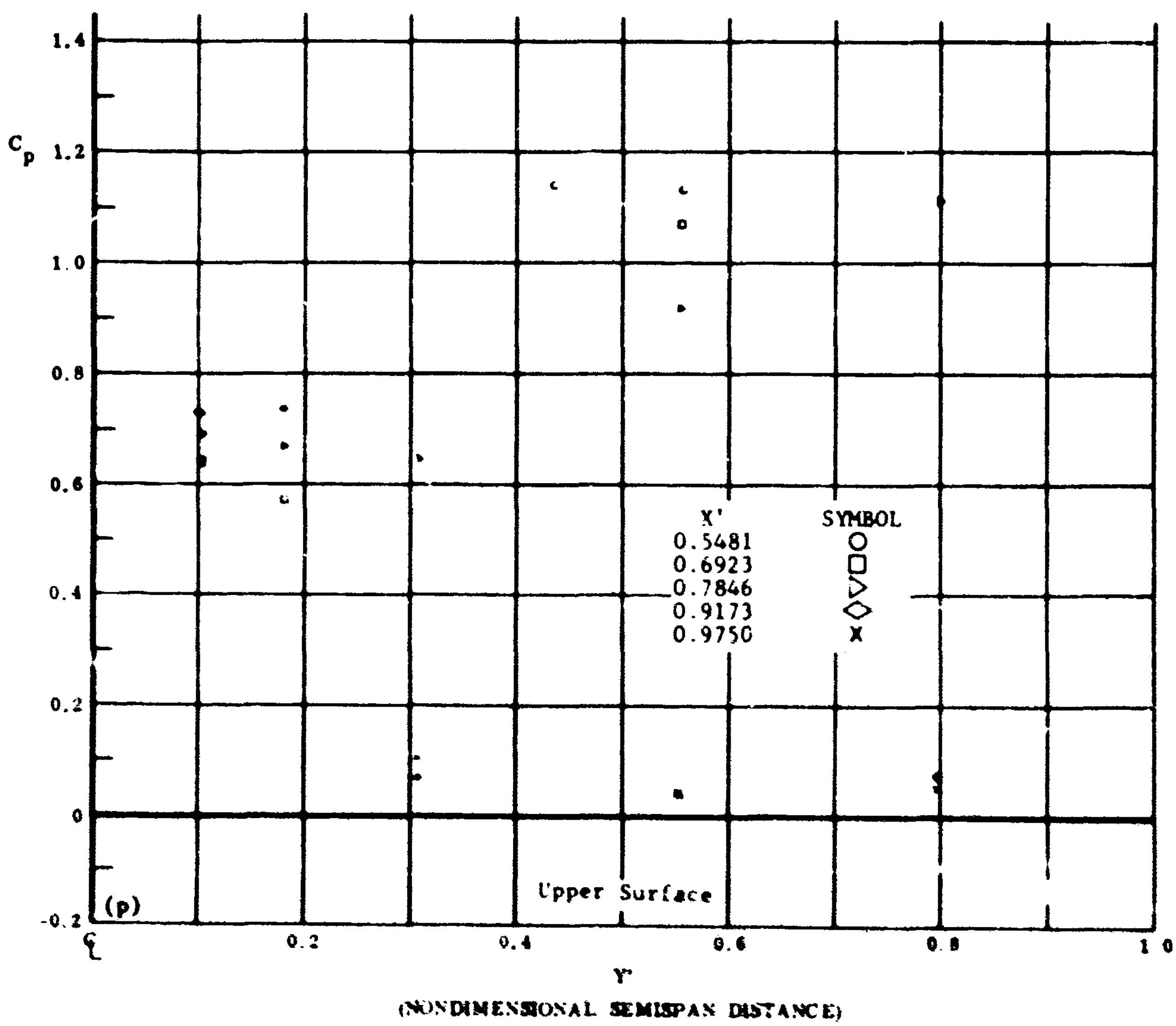

Fig. 25 Configuration I, δ_1 = -40 , $\delta_2 = \delta_3$ = +39

o) C_p vs. Y', lower surface

p) C_p vs. Y', upper surface

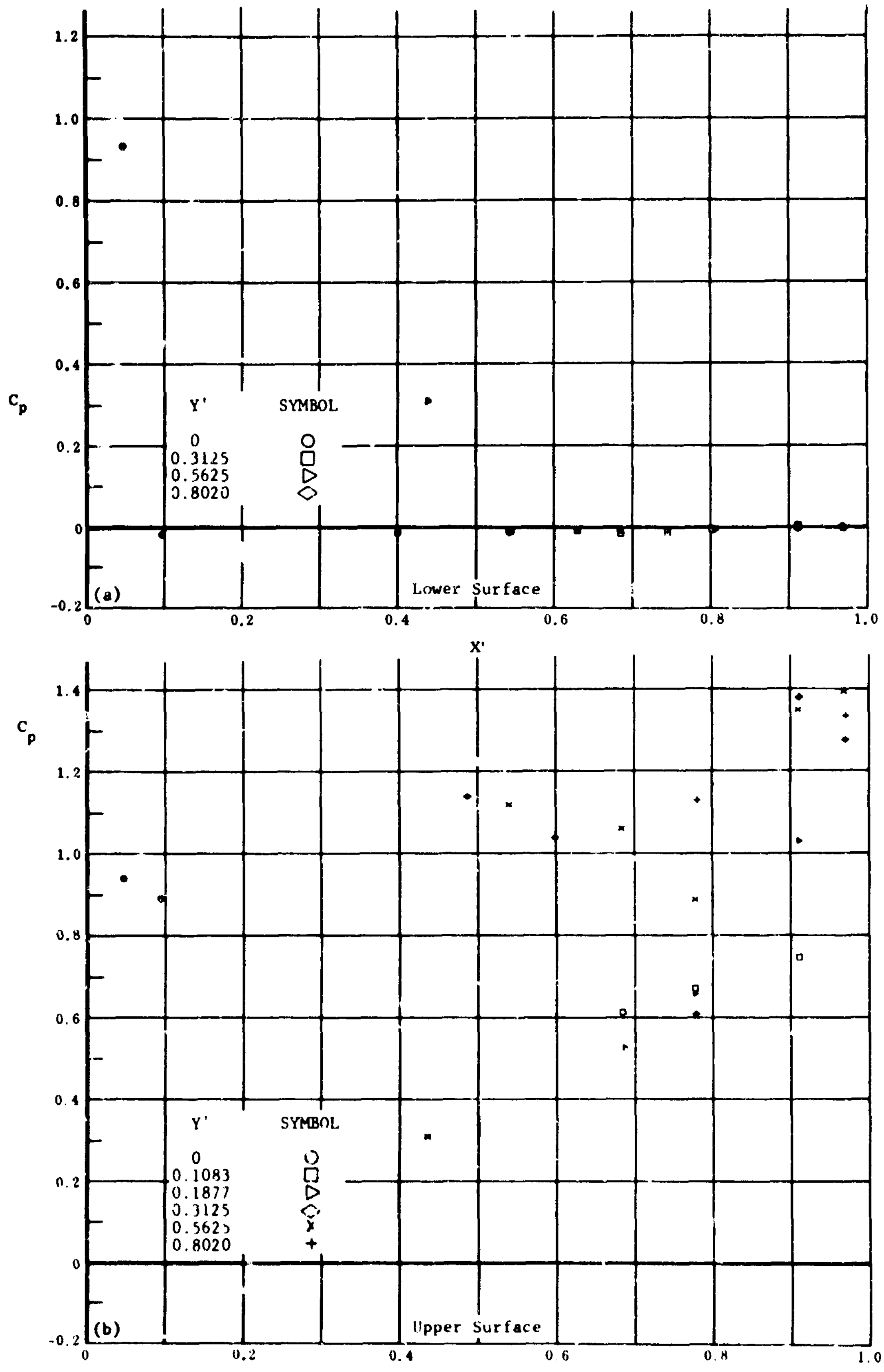

(NONDIMENSIONAL STREAMWISE DISTANCE FROM VIRTUAL APEX)

Fig. 26 Configuration I, α = -40 , δ_2 = δ_3 = -10

a) C_p vs. X', lower surface

b) C_p vs. X', upper surface

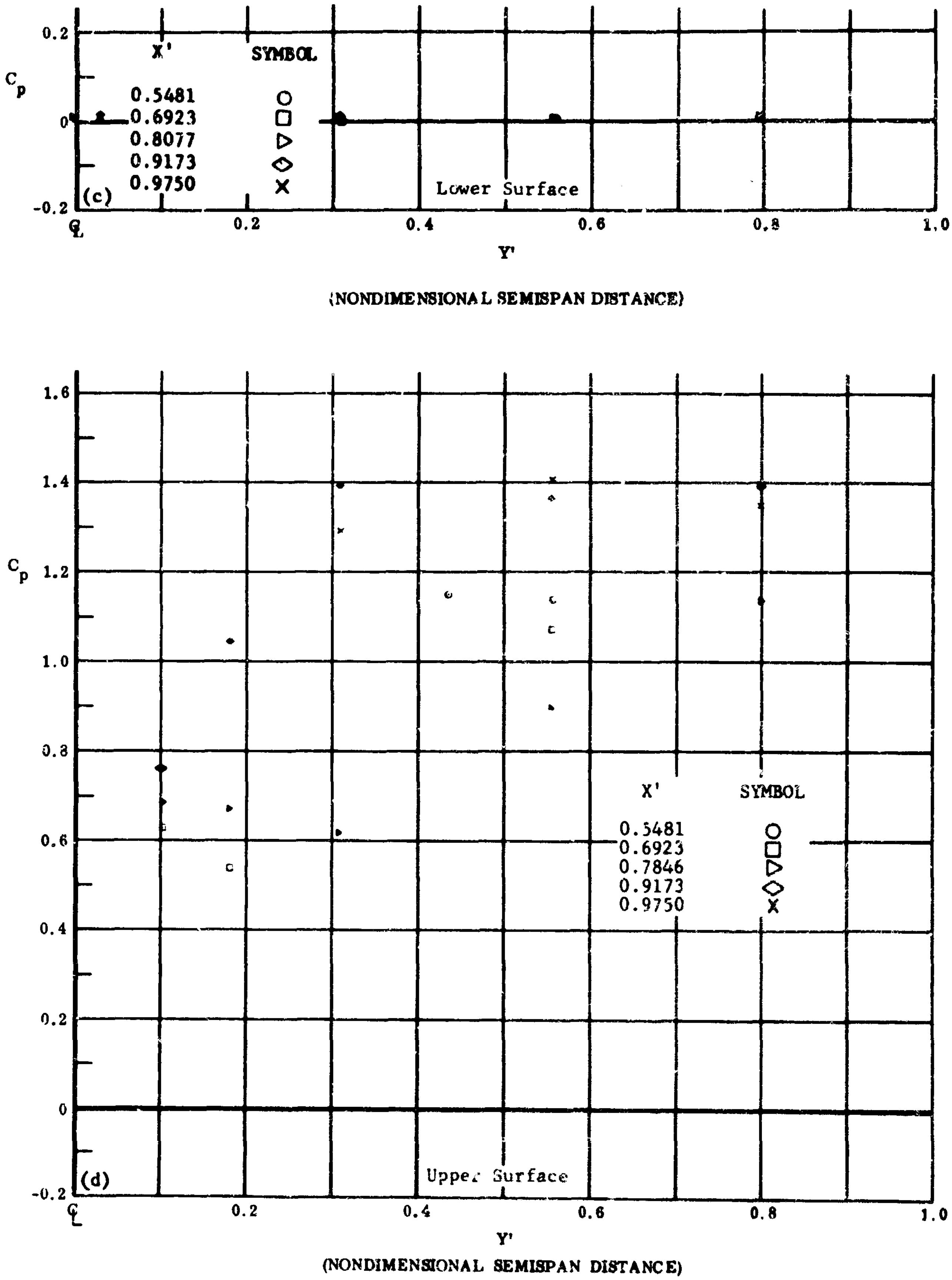

Fig. 26 Configuration I, $\alpha = -40$, $\delta_2 = \delta_3 = -10$

c) C_p vs. Y', lower surface

d) C_p vs. Y', upper surface

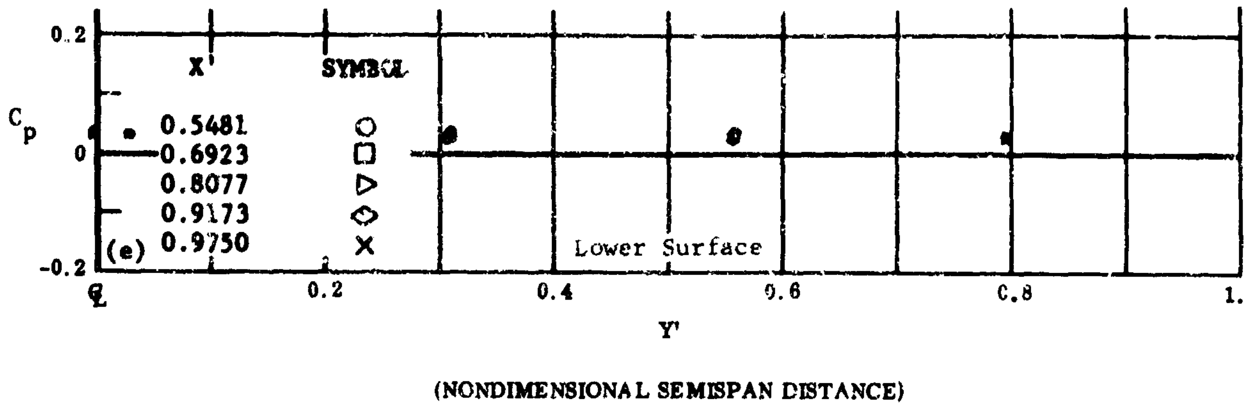

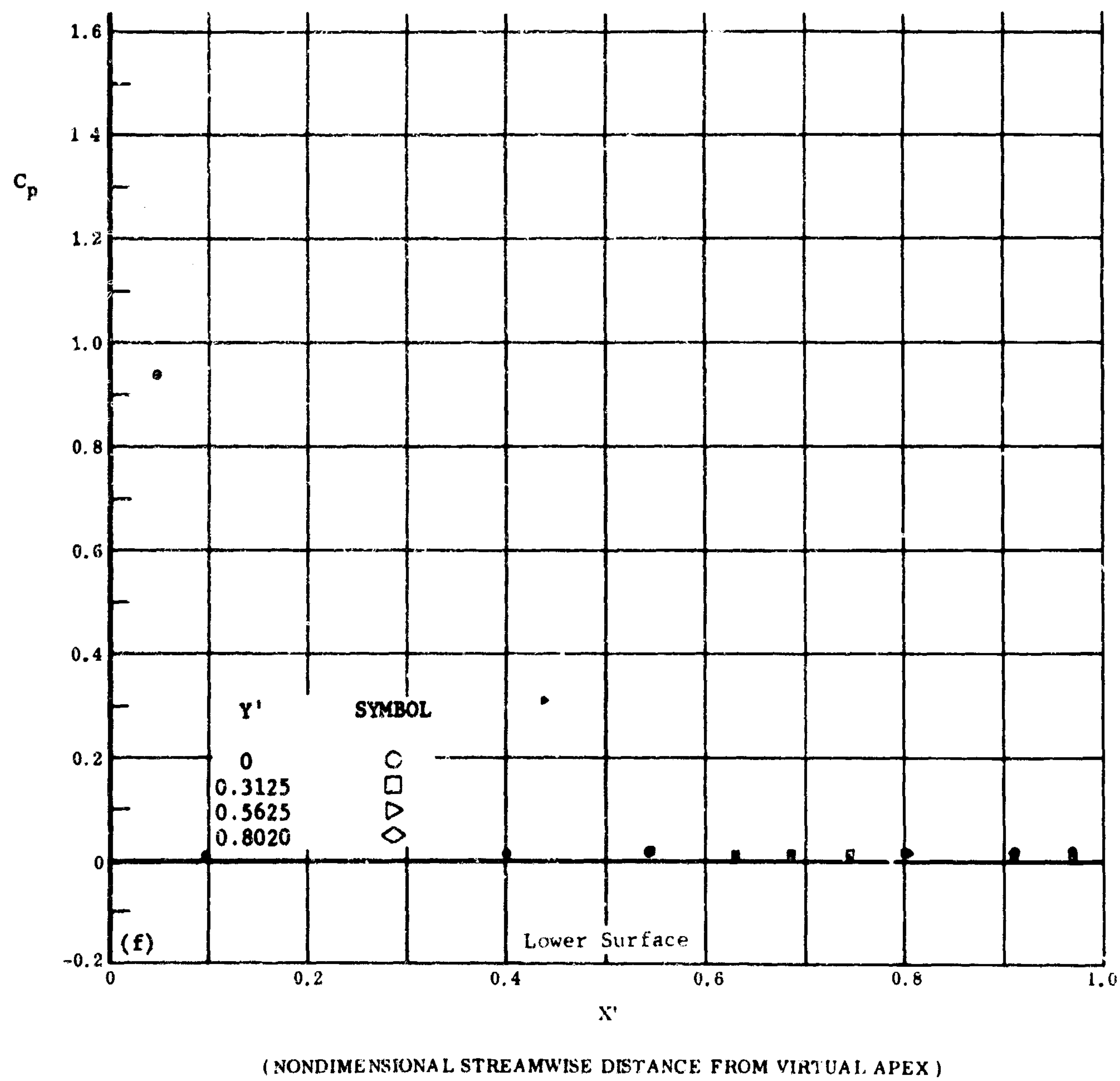

Fig. 26 Configuration I, $\alpha = -40$, $\delta_2 = \delta_3 = -20$

e) C_p vs. Y', lower surface

f) C_p vs. X', lower surface

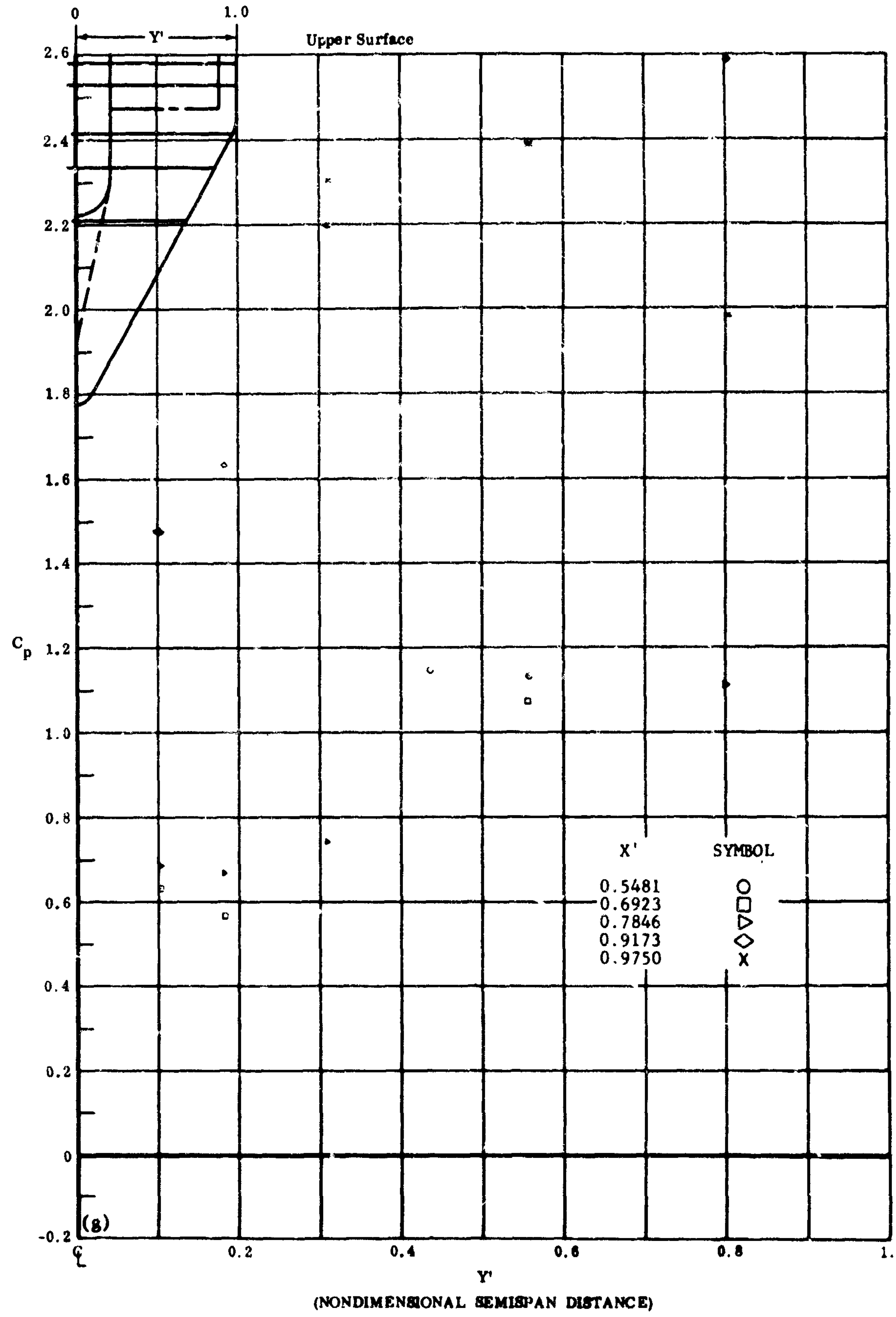

Fig. 26g Configuration I, α = -40 , δ_2 = δ_3 = -20

C_p vs. Y', upper surface

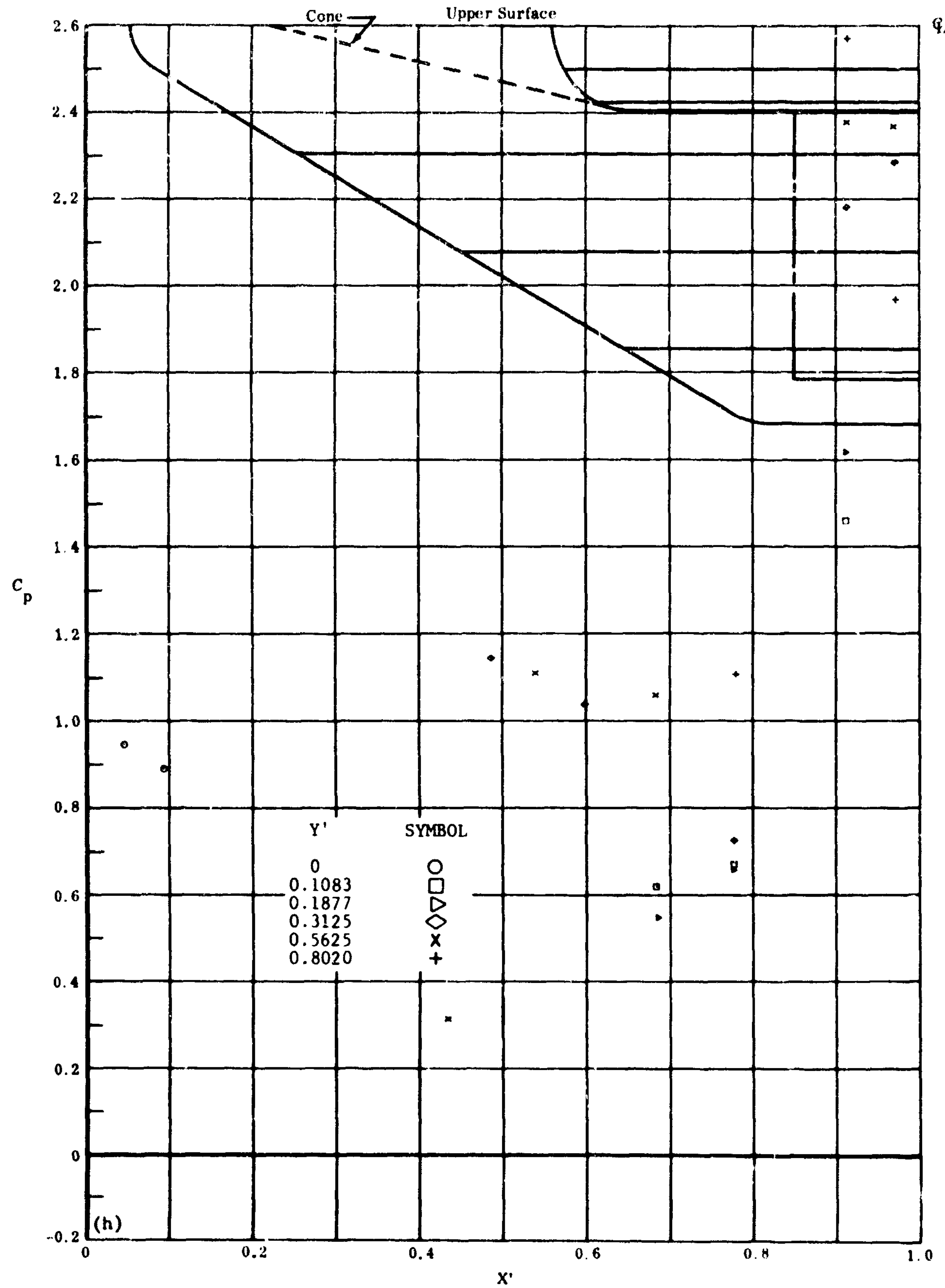

(NONDIMENSIONAL STREAMWISE DISTANCE FROM VIRTUAL APEX)

Fig. 26h Configuration I, α = -40 , $\delta_2 = \delta_3$ = -20

C_p vs. X', upper surface

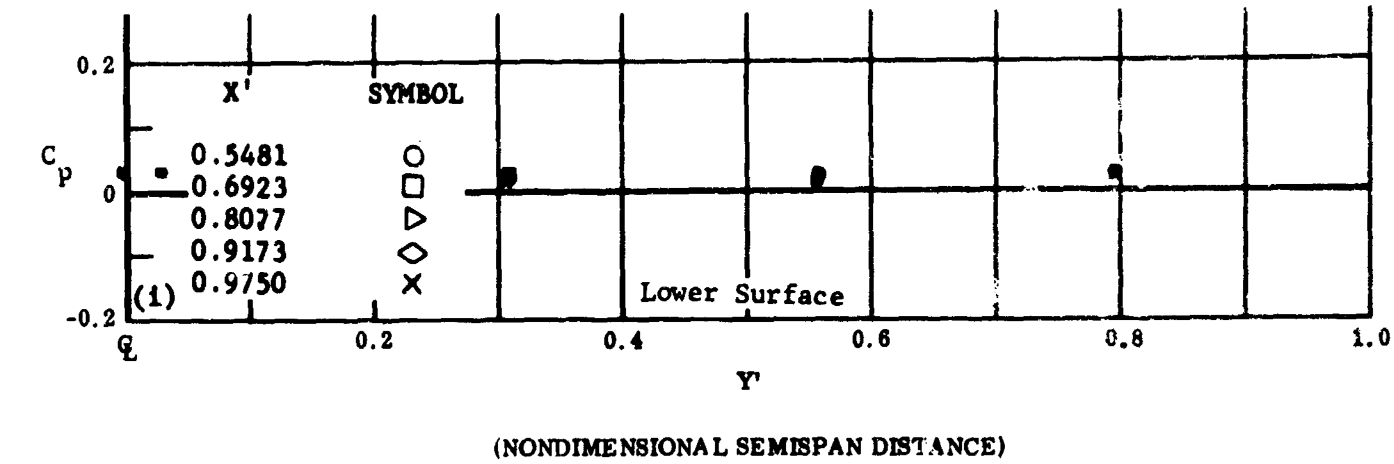

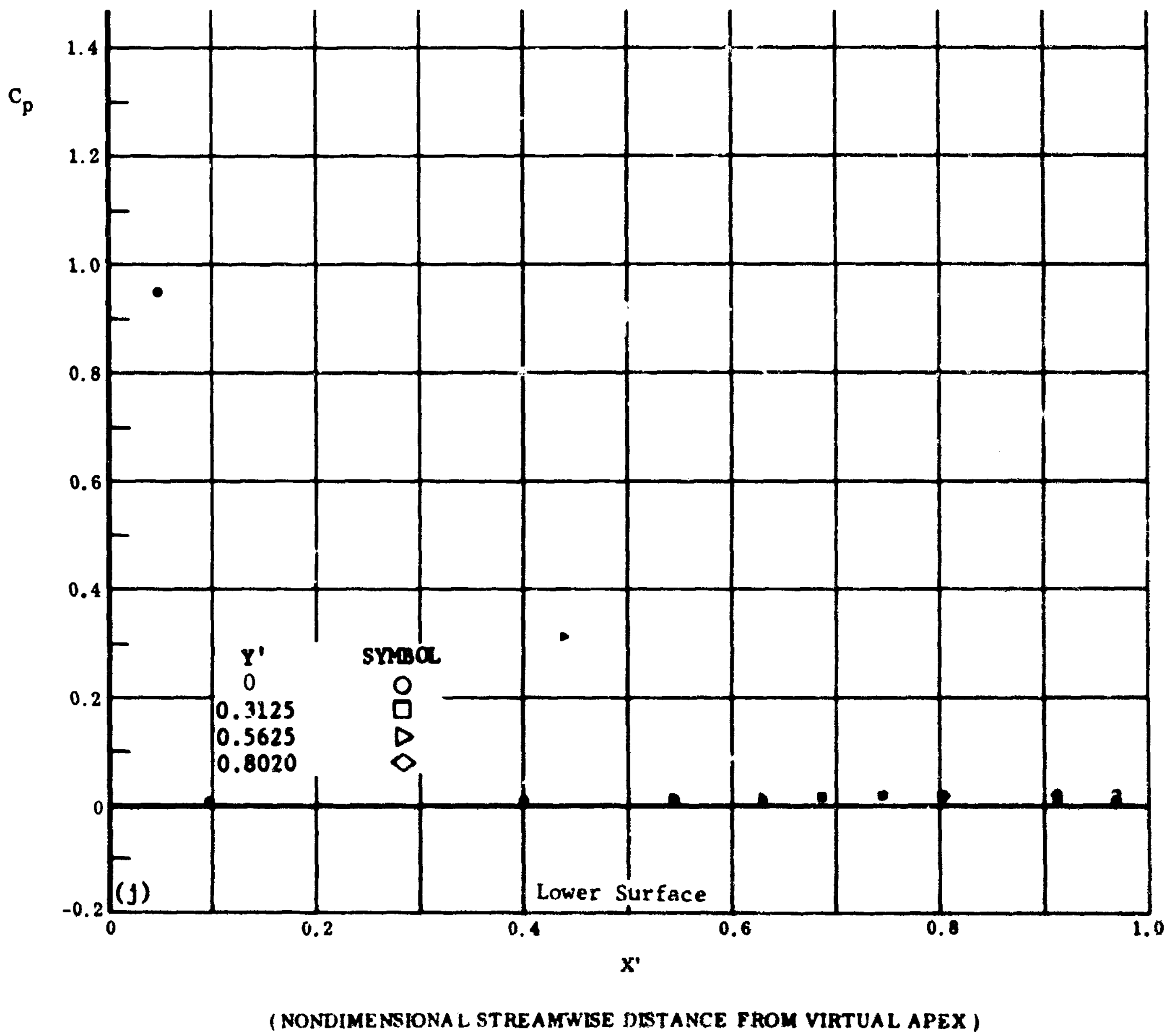

Fig. 26 Configuration I, $\alpha = -40$, $\delta_2 = \delta_3 = -30$

i) C_p vs. Y', lower surface

j) C_p vs. X', lower surface

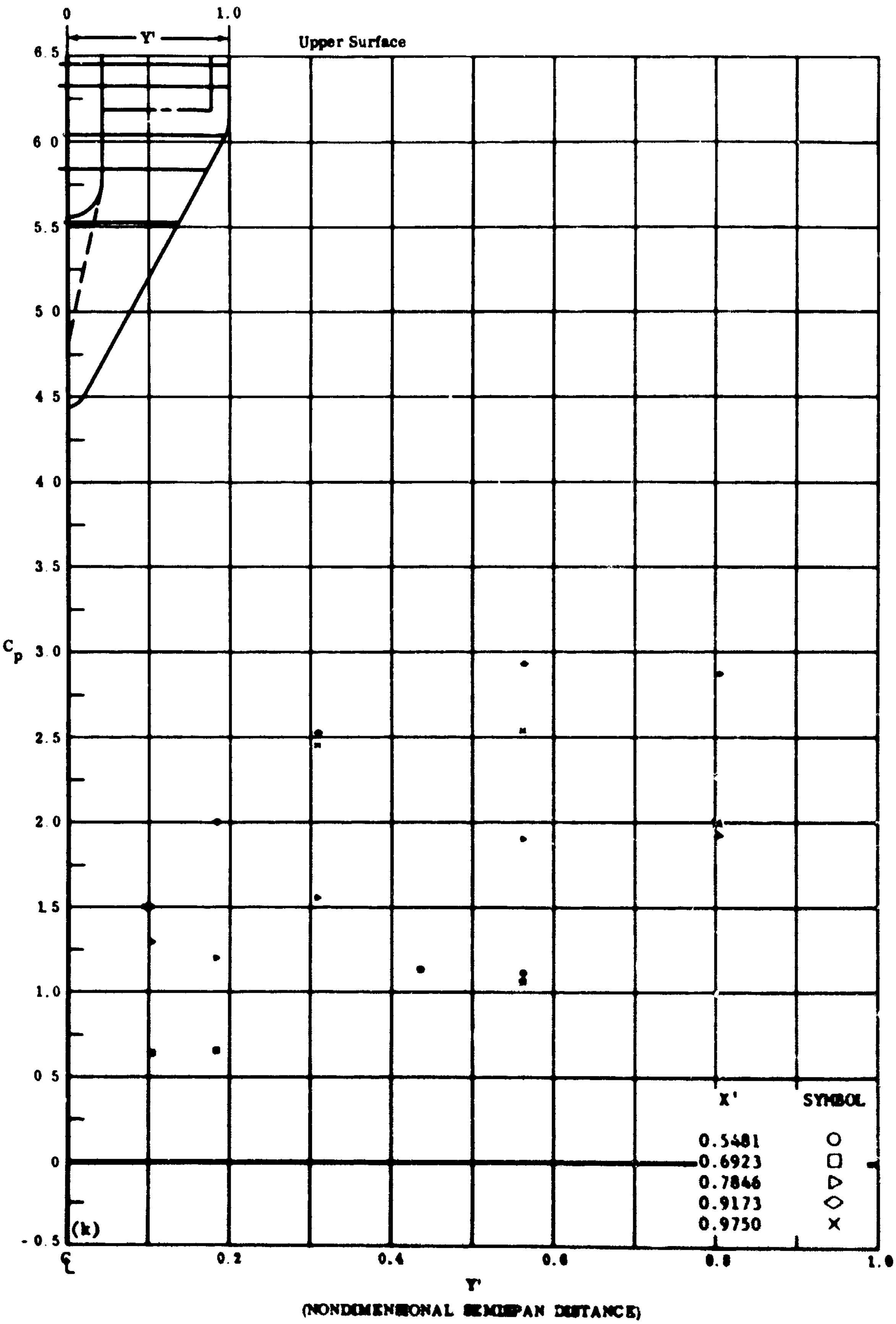

Fig. 26k Configuration I, $\alpha = -40$, $\delta_2 = \delta_3 = -30$

C_p vs. Y', upper surface

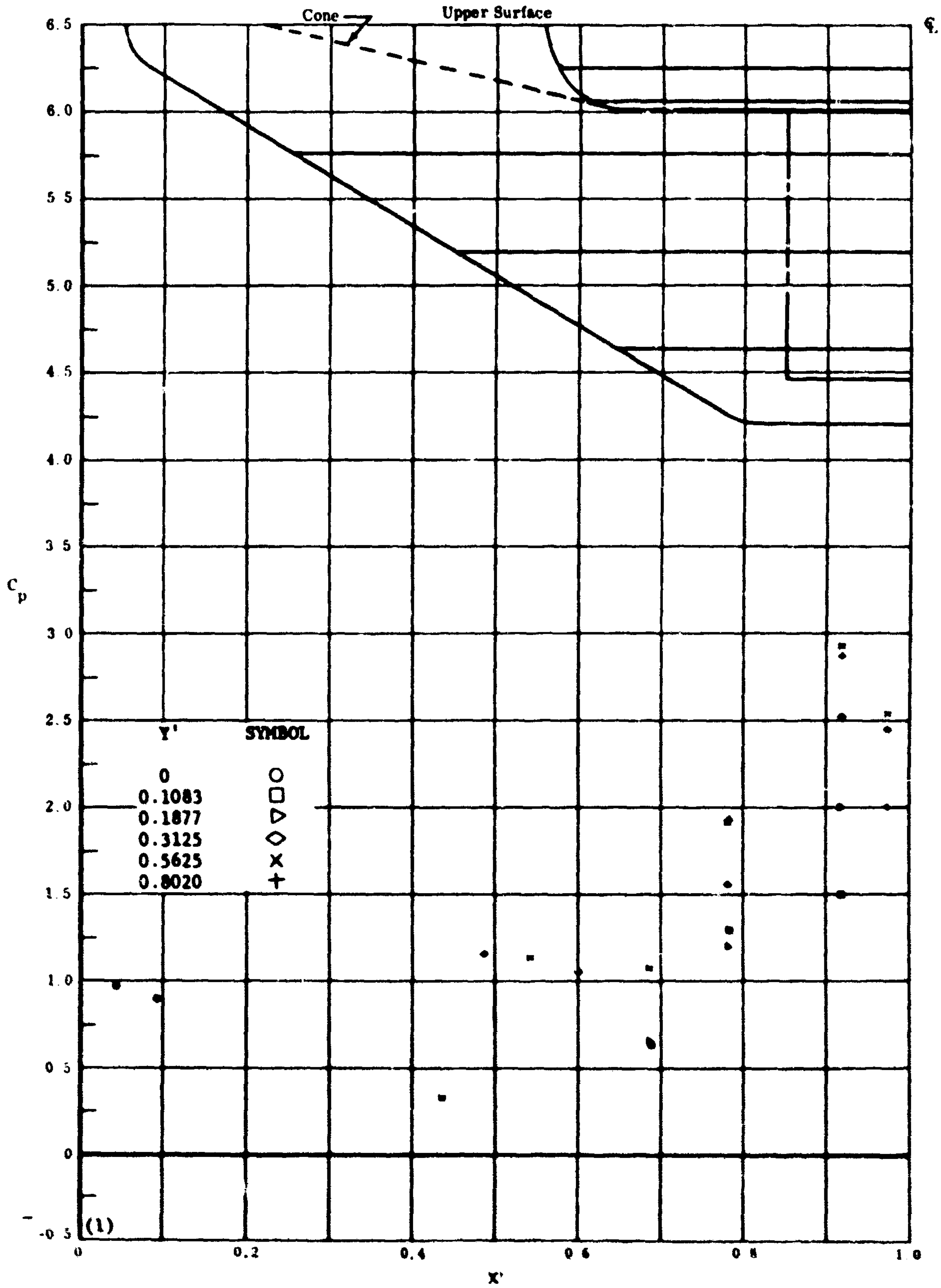

(NONDIMENSIONAL STREAMWISE DISTANCE FROM VIRTUAL APEX)

Fig. 261 Configuration I, α = -40 , δ_2 = δ_3 = -30

C_p vs. X', upper surface

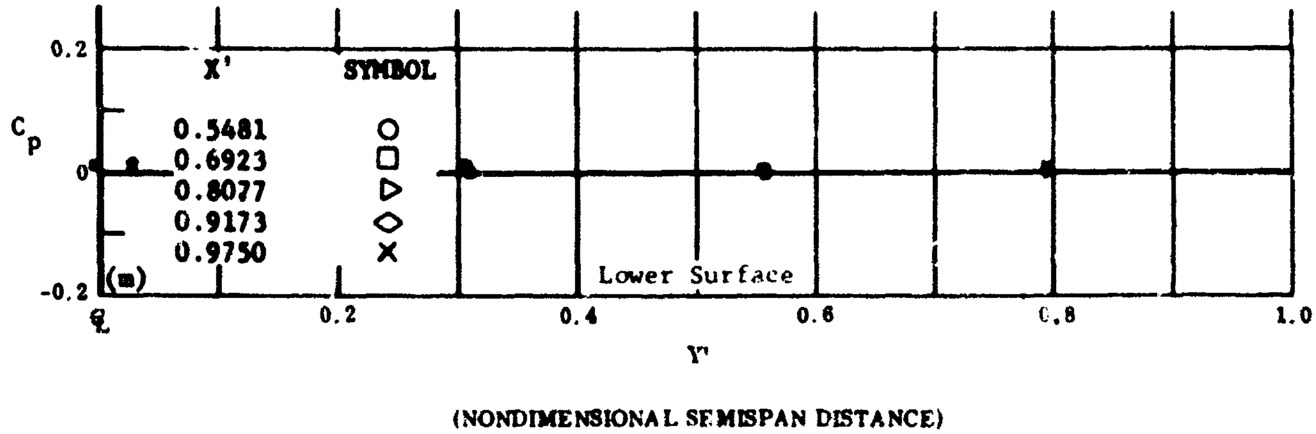

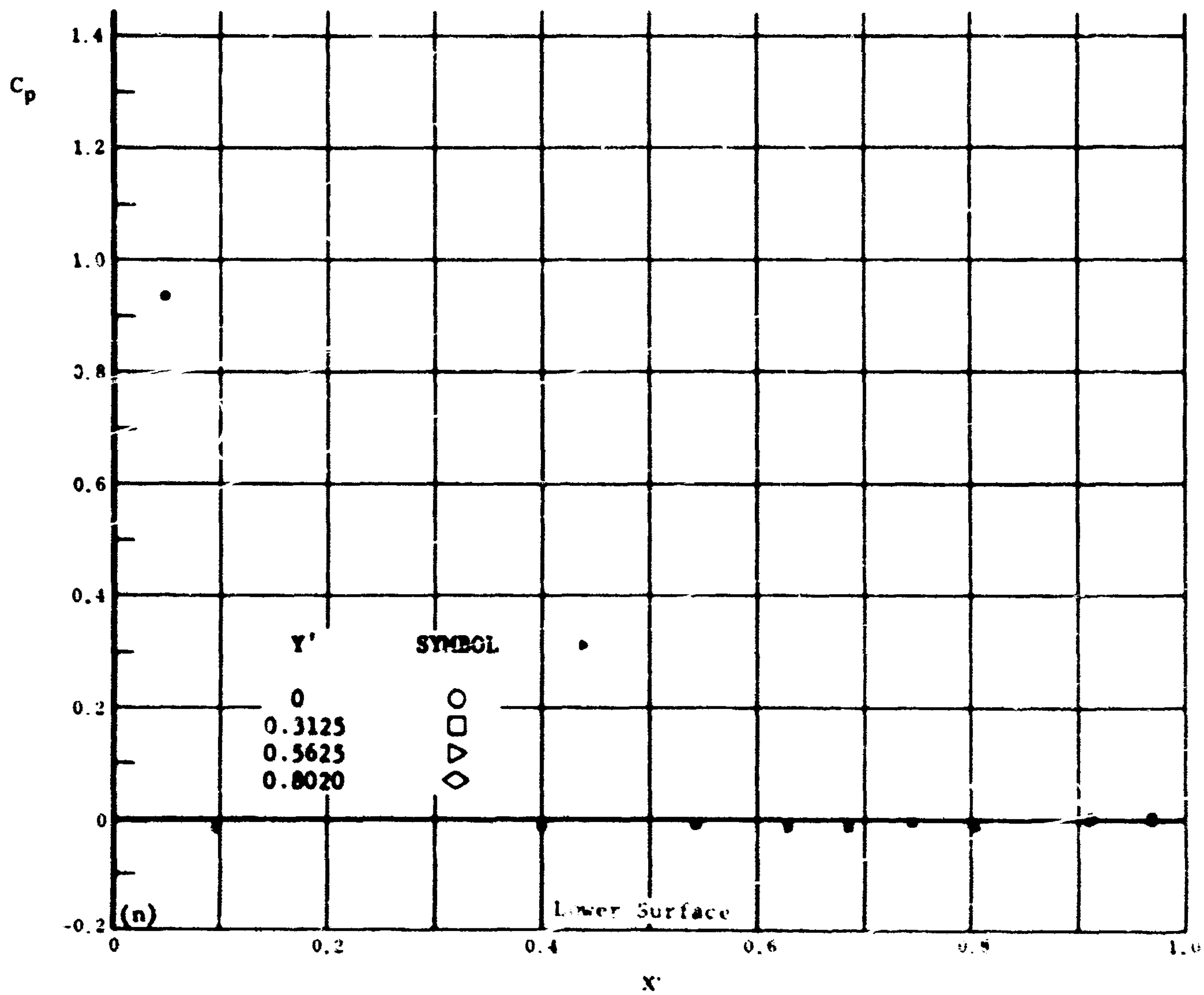

Fig. 26 Configuration I, ; = -40 , $'_2 = '_3$ · -39

m) C_p vs. Y', lower surface

n) C_p vs. X', lower surface

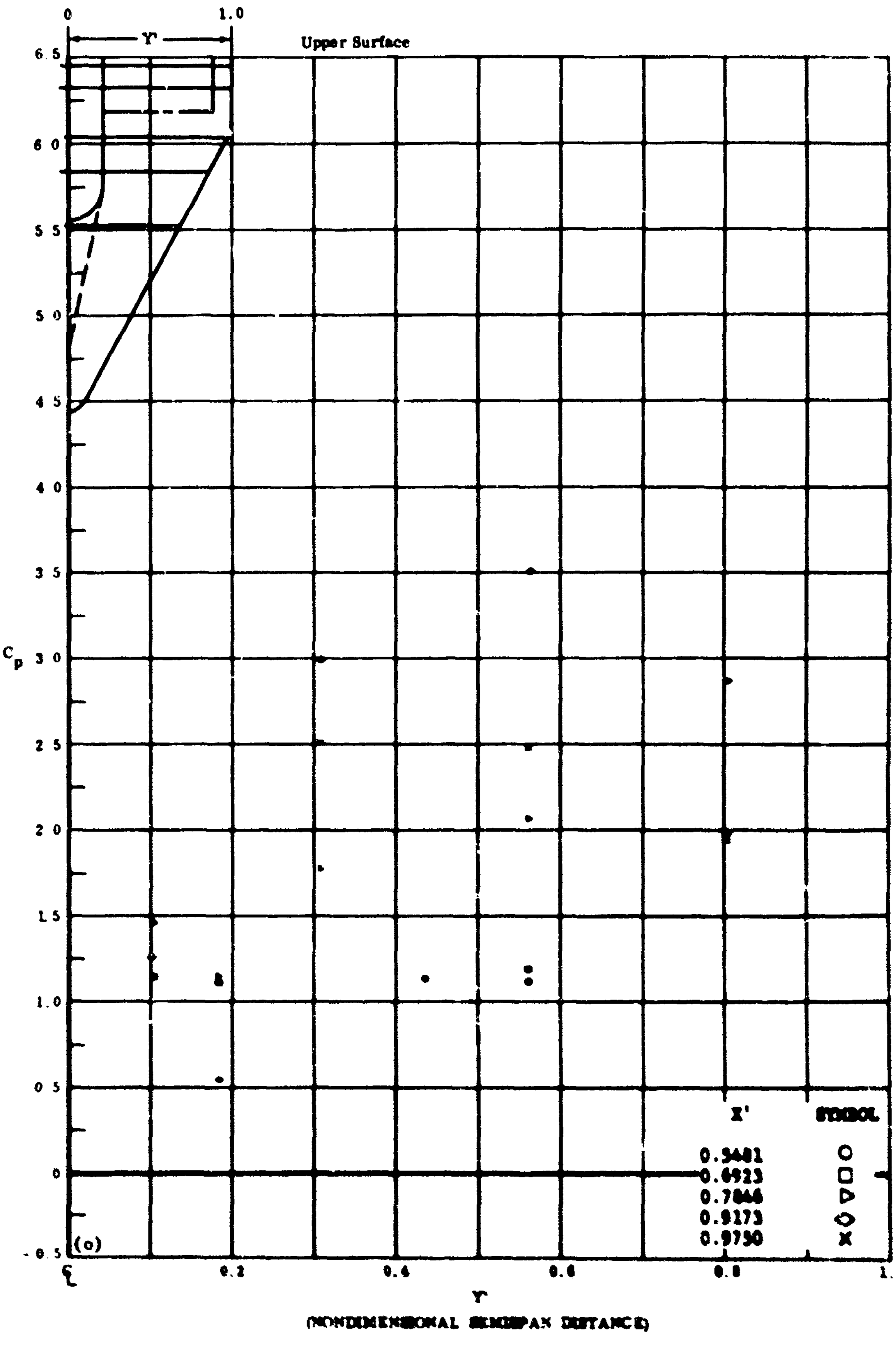

Fig. 26o Configuration I, α = -40 , $\delta_2 = \delta_3$ = -39

C_p vs. Y', upper surface

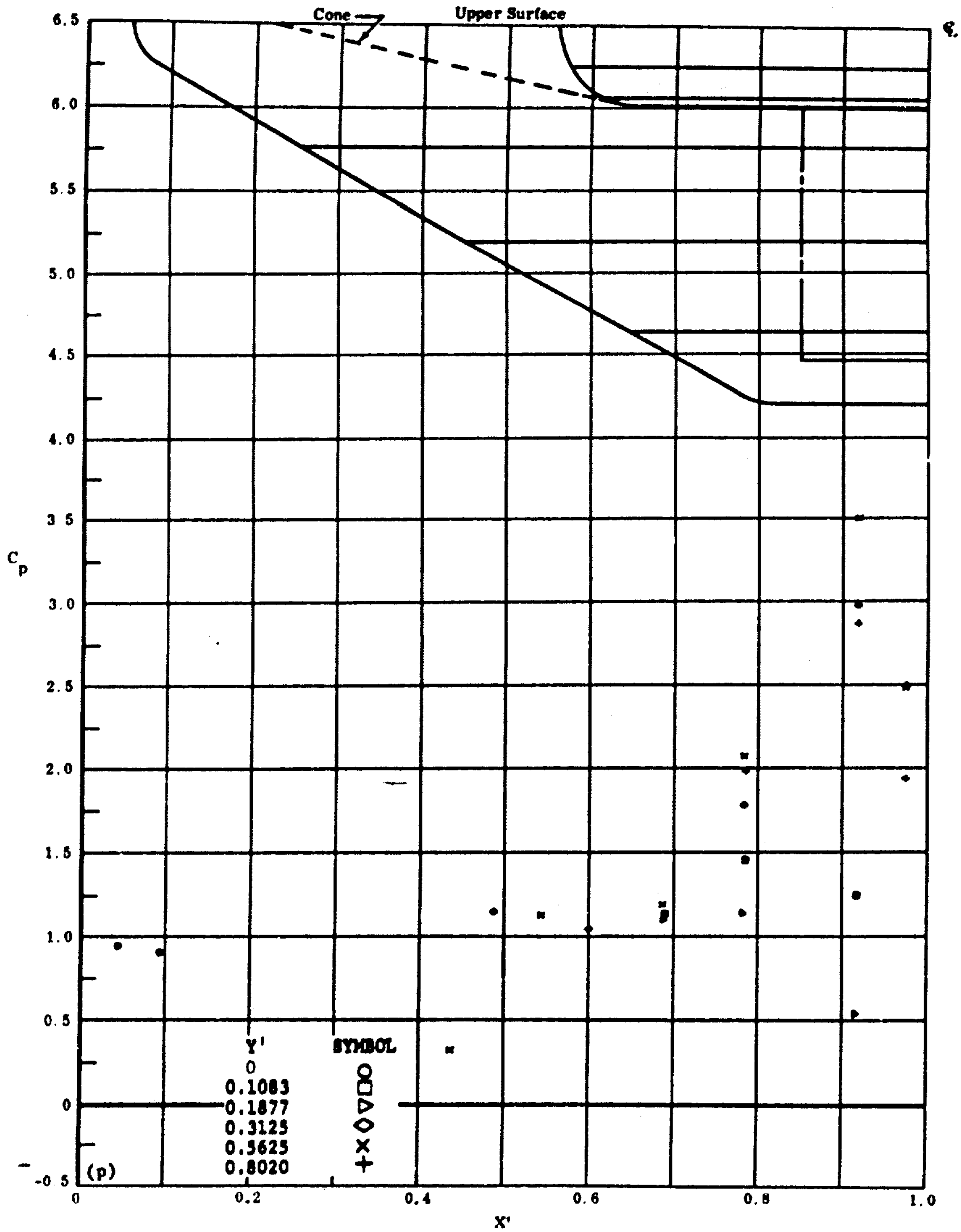

(NONDIMENSIONAL STREAMWISE DISTANCE FROM VIRTUAL APEX)

Fig. 26p Configuration I, $\alpha = -40$, $\delta_2 = \delta_3 = -39$

C_p vs. X', upper surface

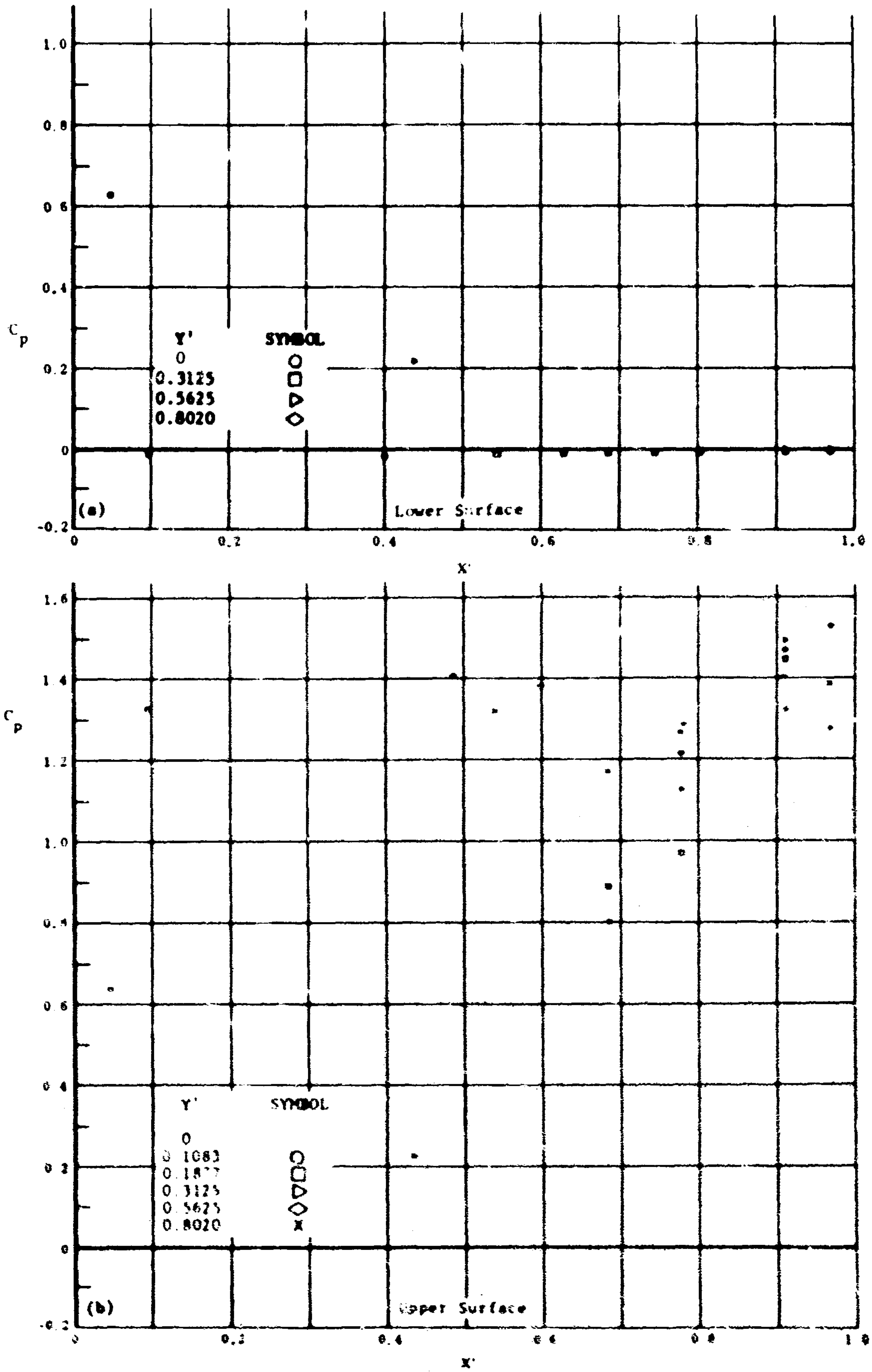

(NONDIMENSIONAL STREAMWISE DISTANCE FROM VIRTUAL APEX)

Fig. 27 Configuration [illegible], $\alpha = -5^{\circ}$, $\delta_2 = \delta_3 = 0$

a) C_p vs. X', lower surface

b) C_p vs. X', upper surface

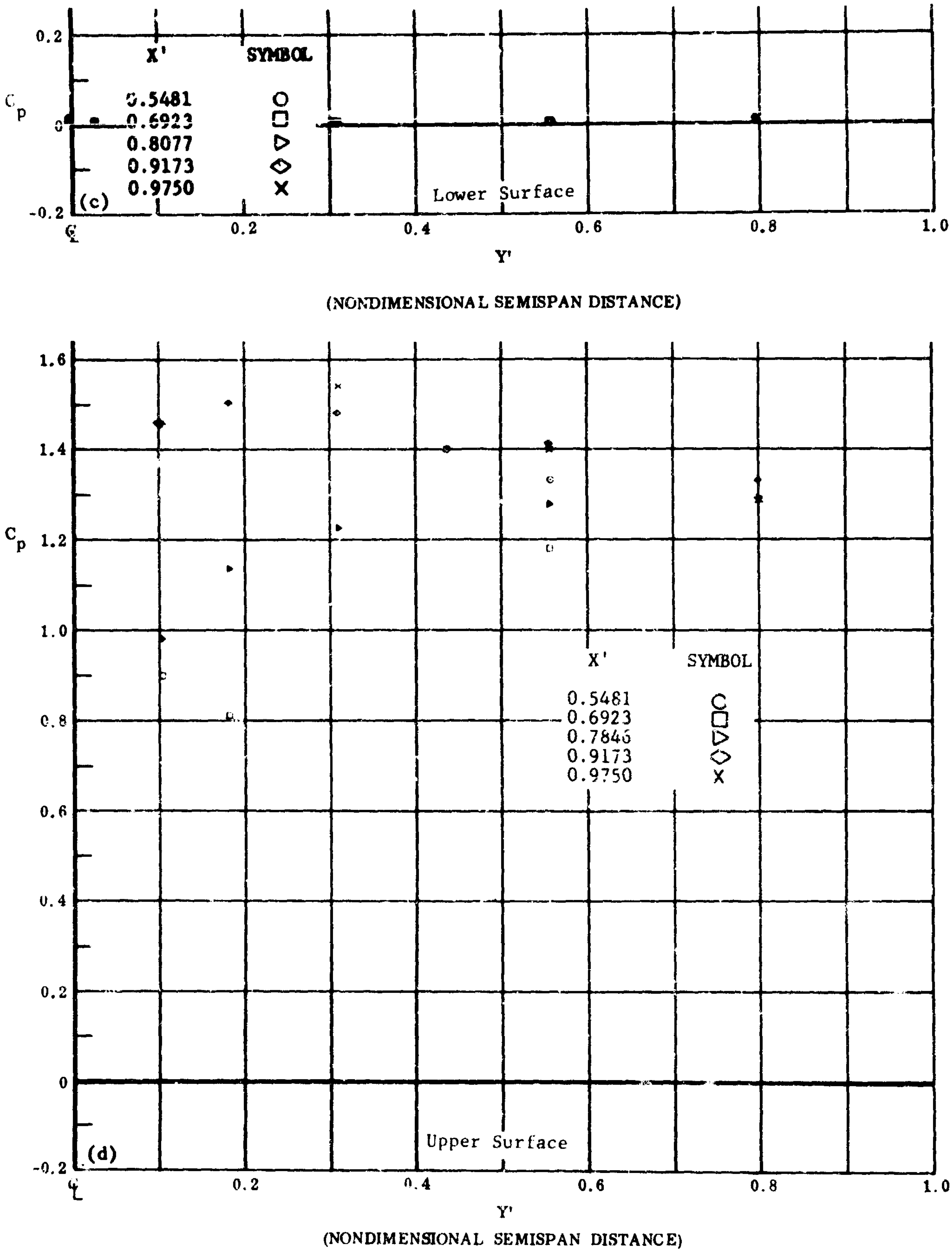

Fig. 27 Configuration I, α = -50 , $\delta_2 = \delta_3 = 0$

c) C_p vs. Y', lower surface

d) C_p vs. Y', upper surface

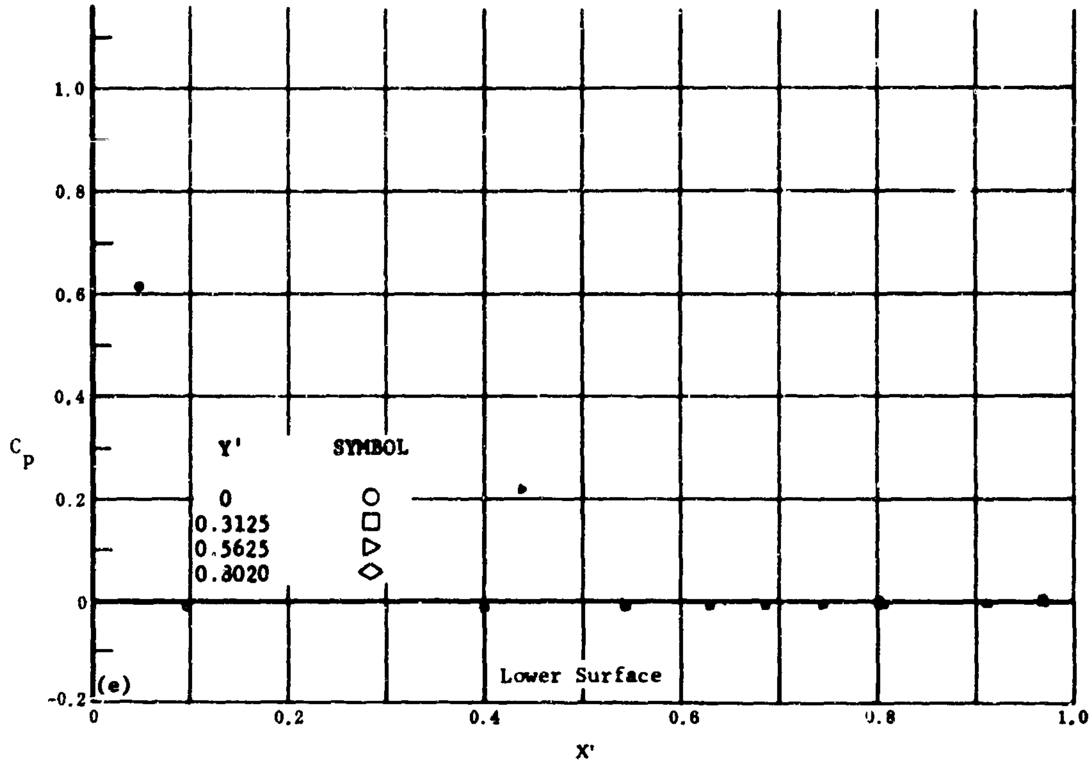

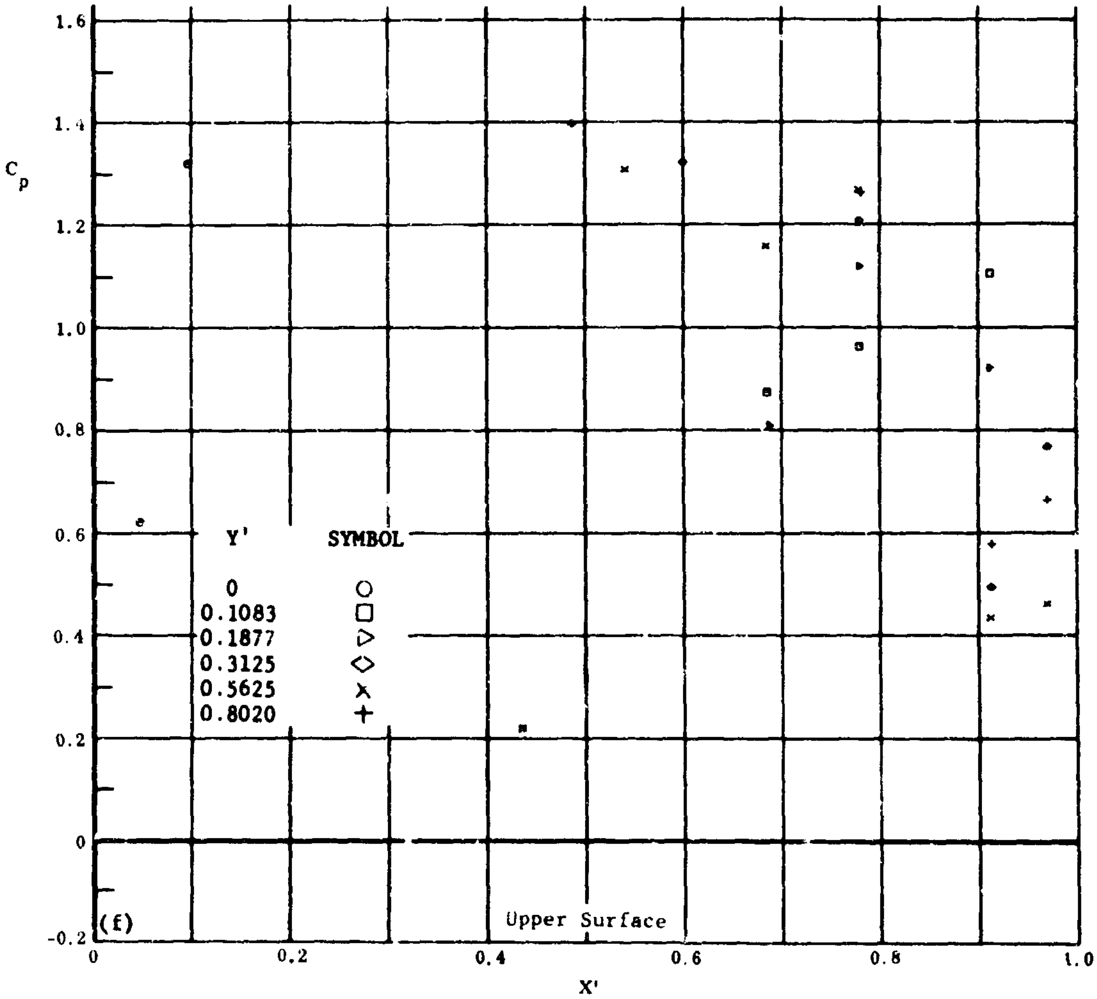

(NONDIMENSIONAL STREAMWISE DISTANCE FROM VIRTUAL APEX)

Fig. 27 Configuration I, α = -50 , $\delta_2 = \delta_3$ = +20

e) C_p vs. X', lower surface

f) C_p vs. X', upper surface

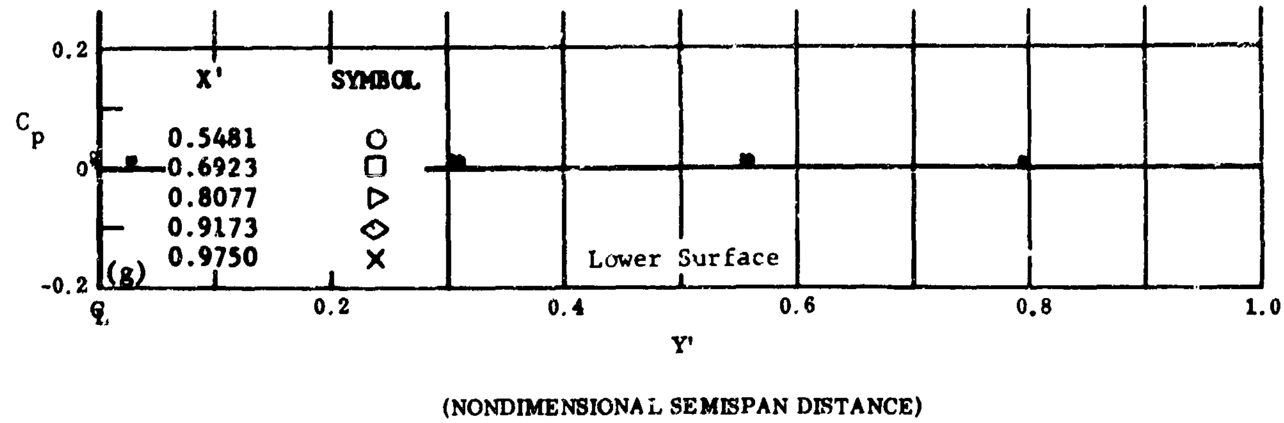

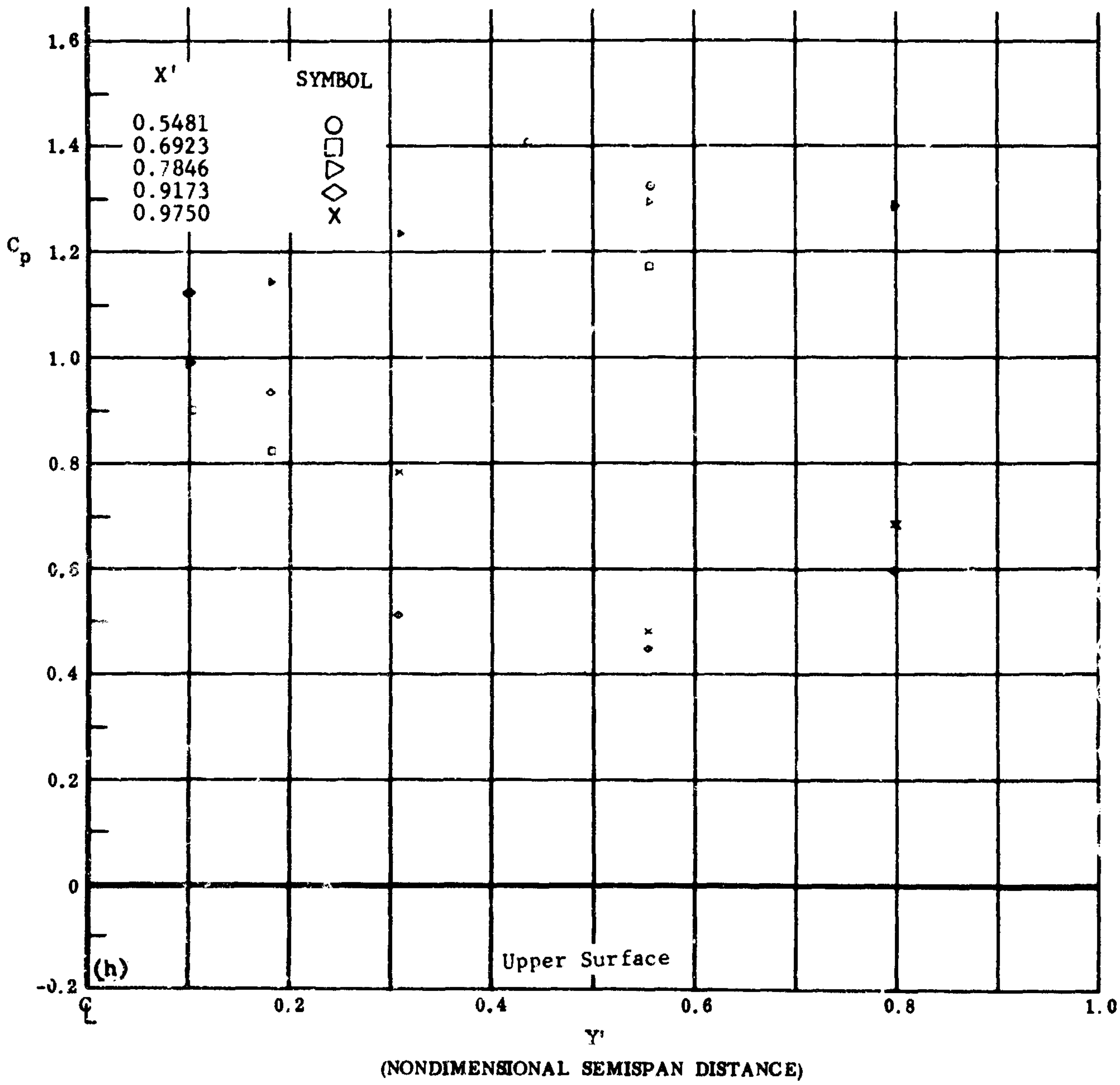

Fig. 27 Configuration I, α = -50 , $\delta_2 = \delta_3$ = +20

g) C_p vs. Y', lower surface

h) C_p vs. Y', upper surface

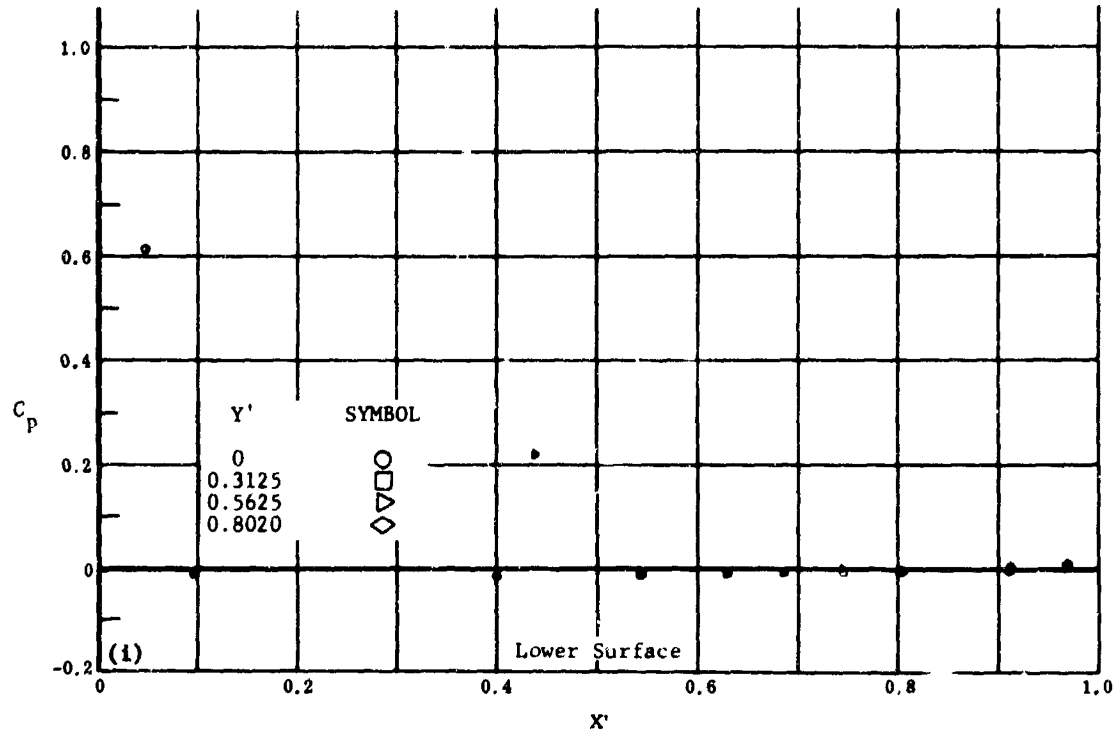

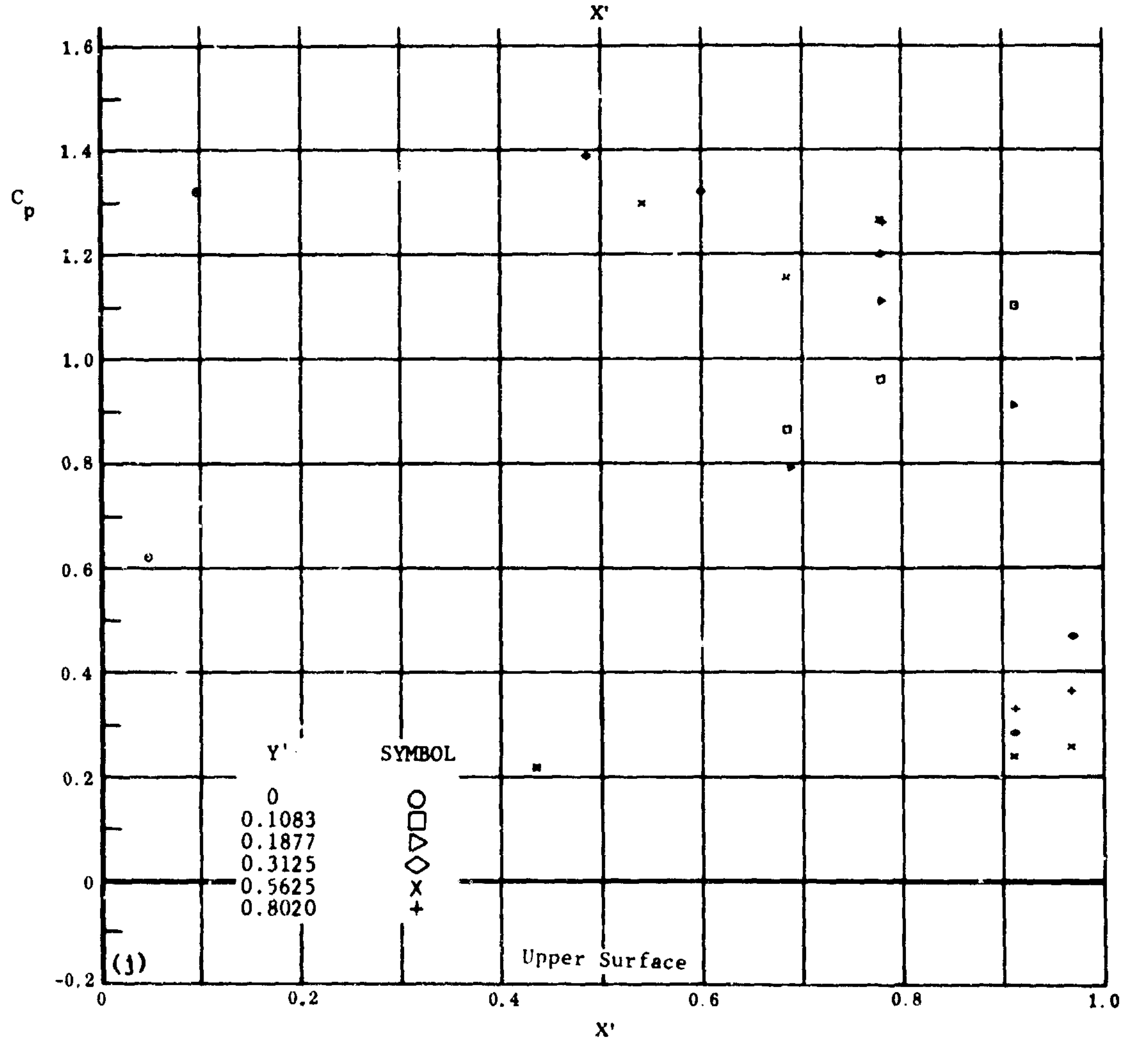

(NONDIMENSIONAL STREAMWISE DISTANCE FROM VIRTUAL APEX)

Fig. 27 Configuration I, α = -50 , $\delta_2 = \delta_3$ = +30

i) C_p vs. X', lower surface

j) C_p vs. X', upper surface

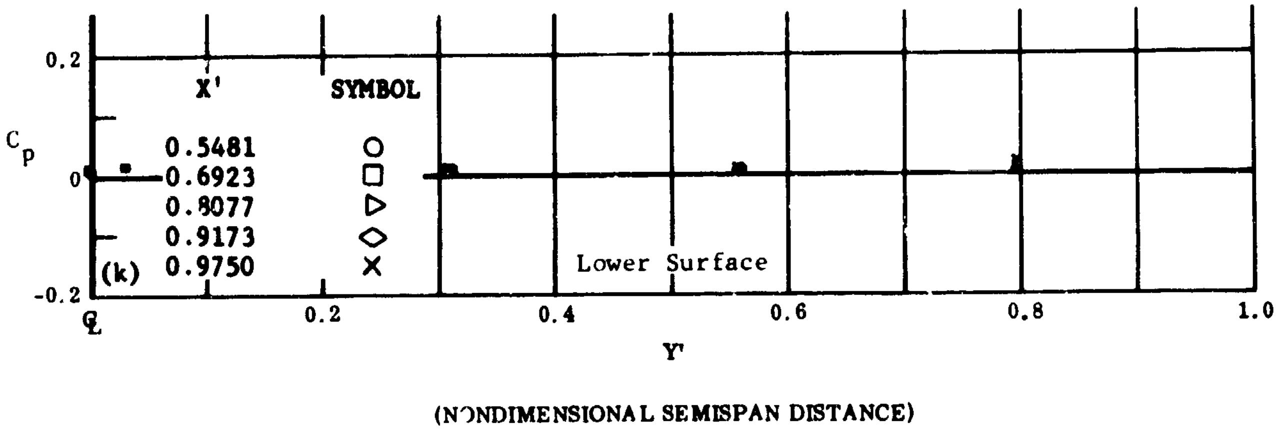

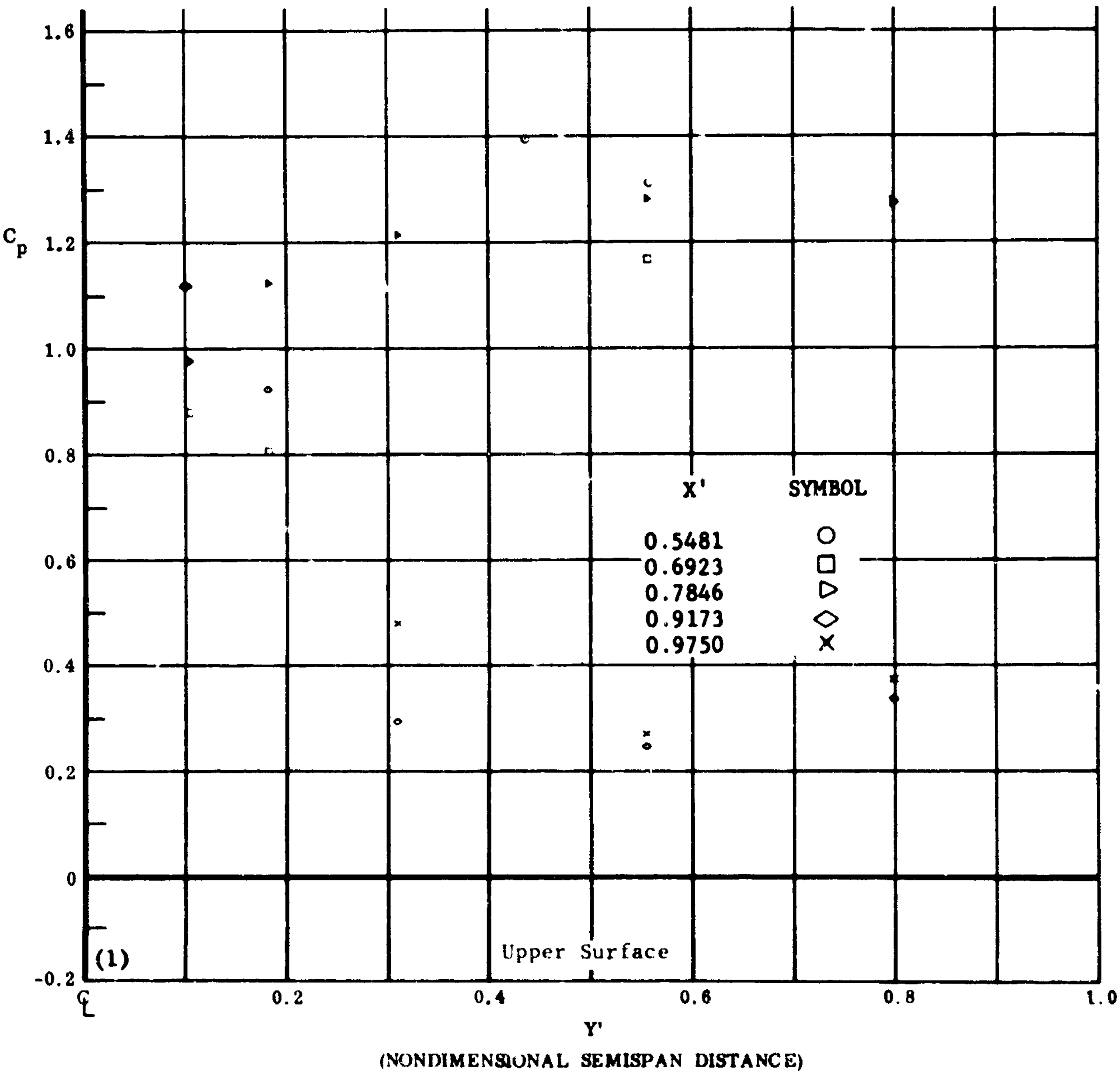

Fig. 27 Configuration I, α = -50 , $\delta_2 = \delta_3$ = +30

k) C_p vs. Y', lower surface

l) C_p vs. Y', upper surface

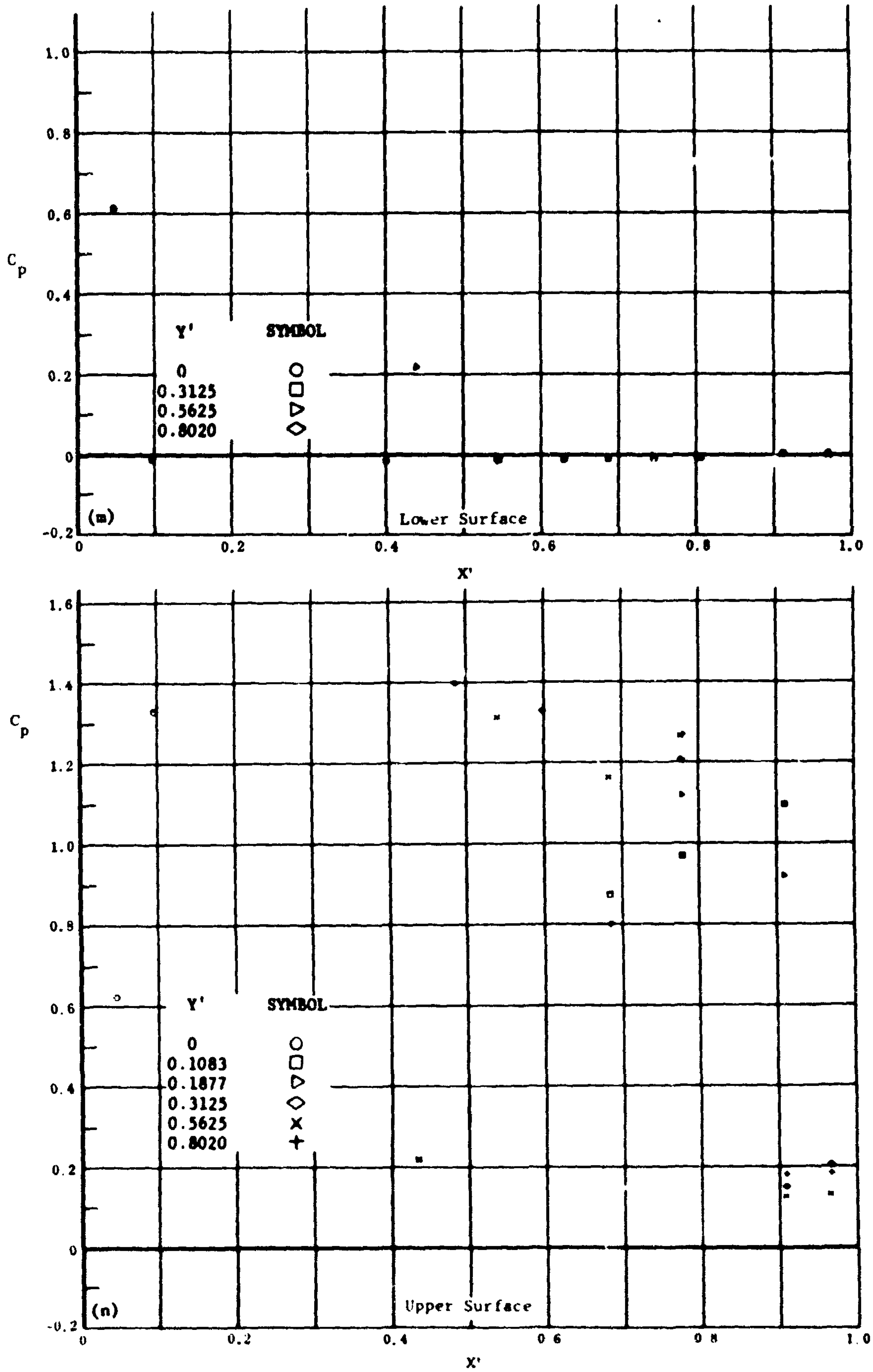

(NONDIMENSIONAL STREAMWISE DISTANCE FROM VIRTUAL APEX)

Fig. 27 Configuration I, $\alpha = -50$, $\delta_2 = \delta_3 = +39$

m) C_p vs. X', lower surface

n) C_p vs. X', upper surface

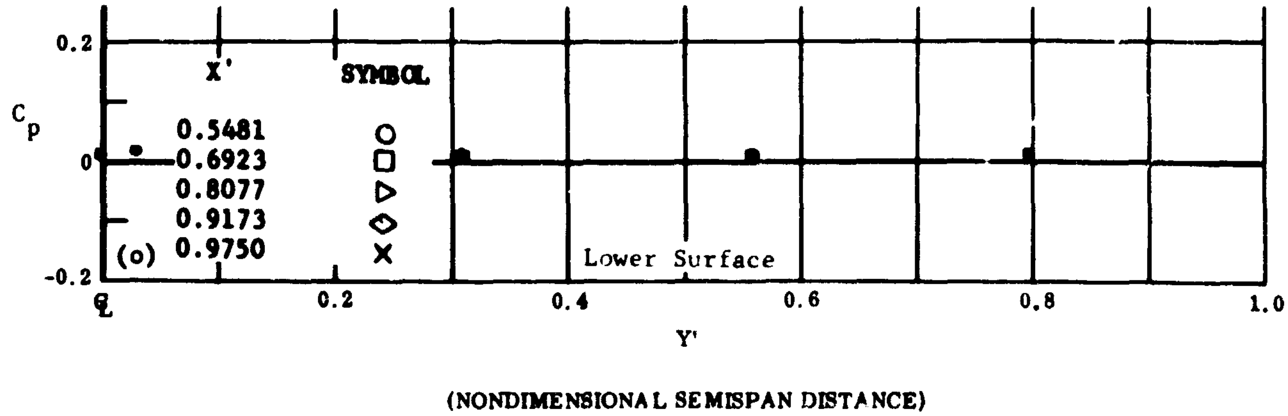

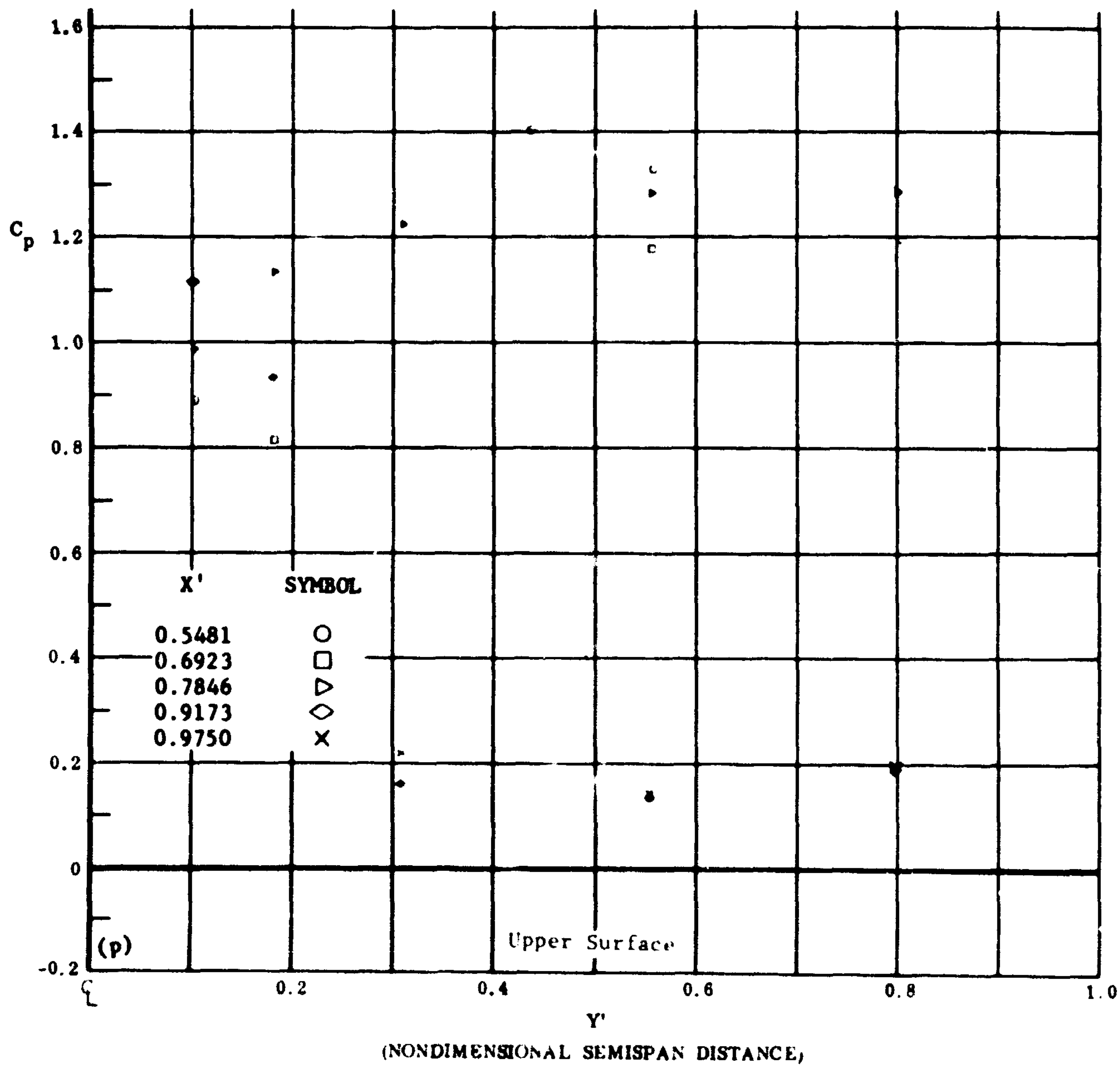

Fig. 27 Configuration I, ι = -50 , $\delta_2 = \delta_3$ = +39

o) C_p vs. Y', lower surface

p) C_p vs. Y', upper surface

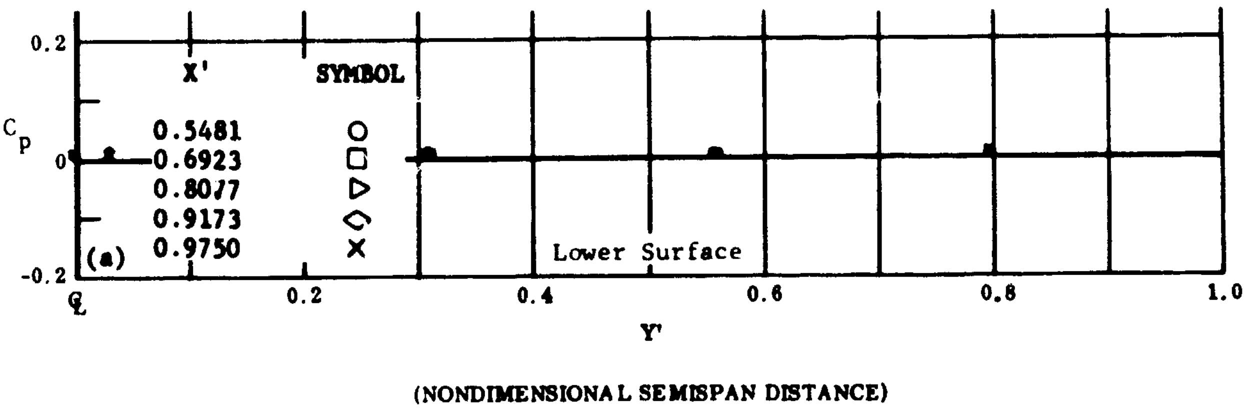

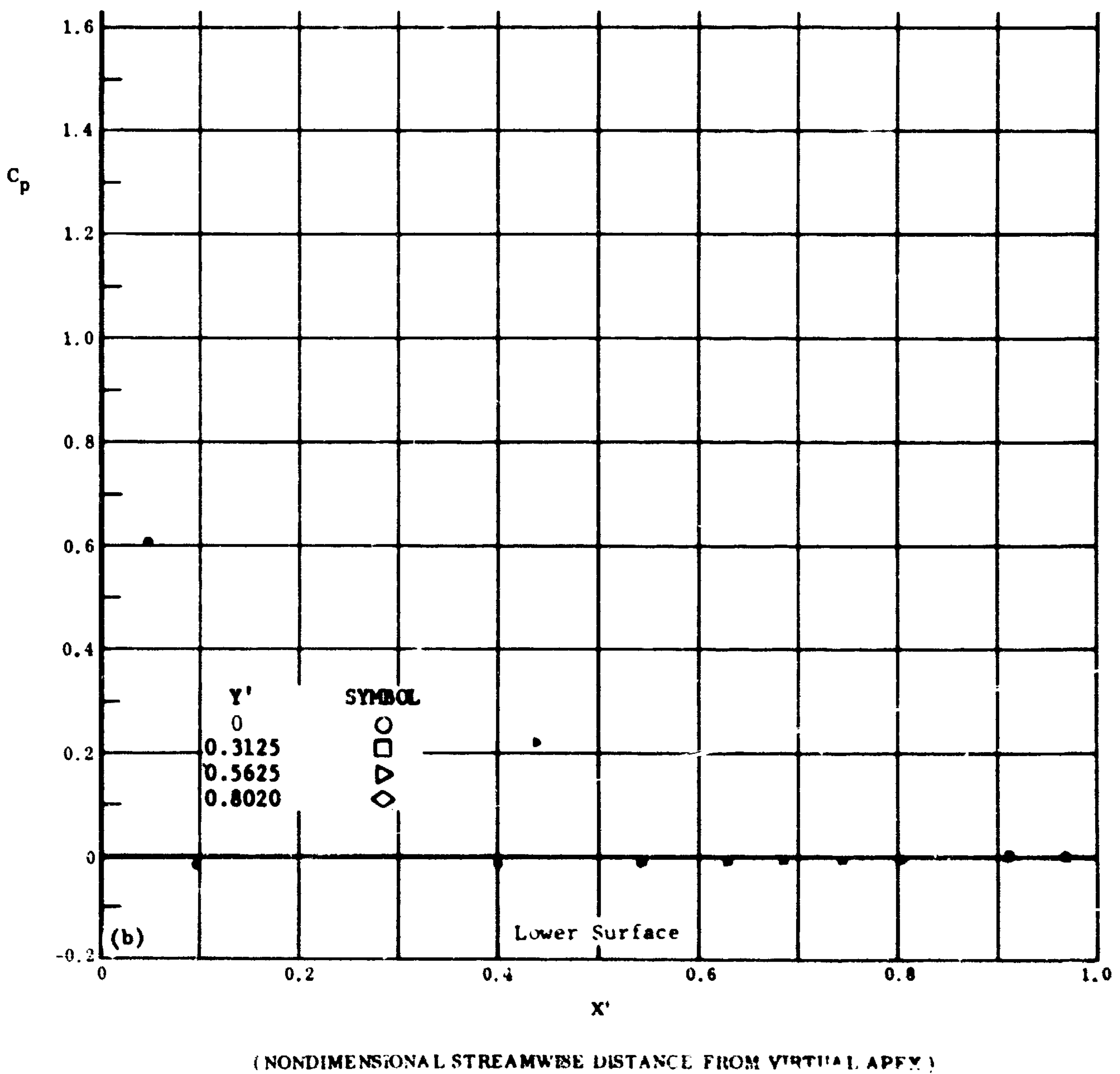

Fig. 28 Configuration I, α = -50 , $\delta_2 = \delta_3$ = -10

a) C_p vs. Y', lower surface

b) C_p vs. X', lower surface

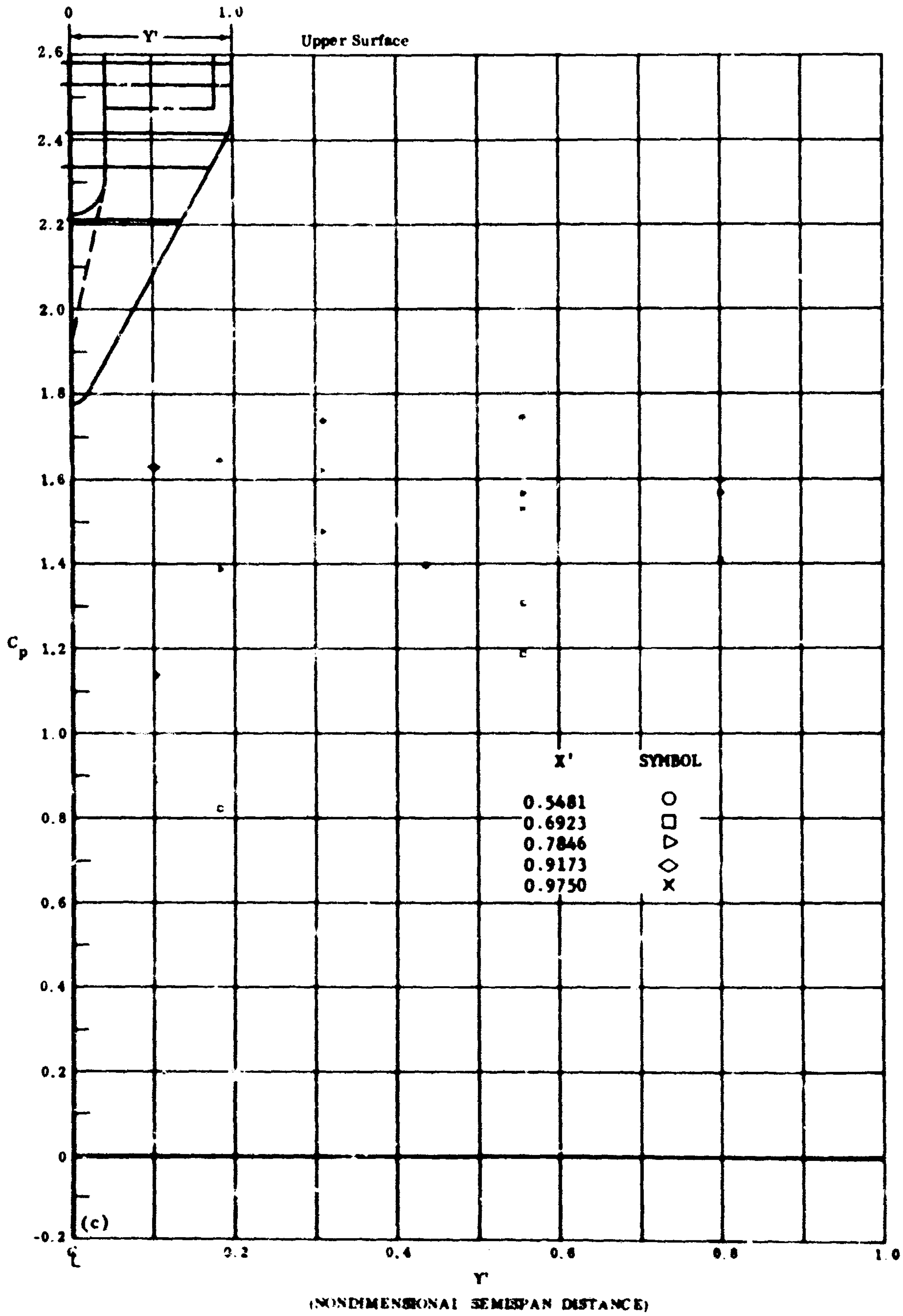

Fig. 28c Configuration I, δ_1 = -50 , δ_2 = δ_3 = -10
C_p vs. Y', upper surface

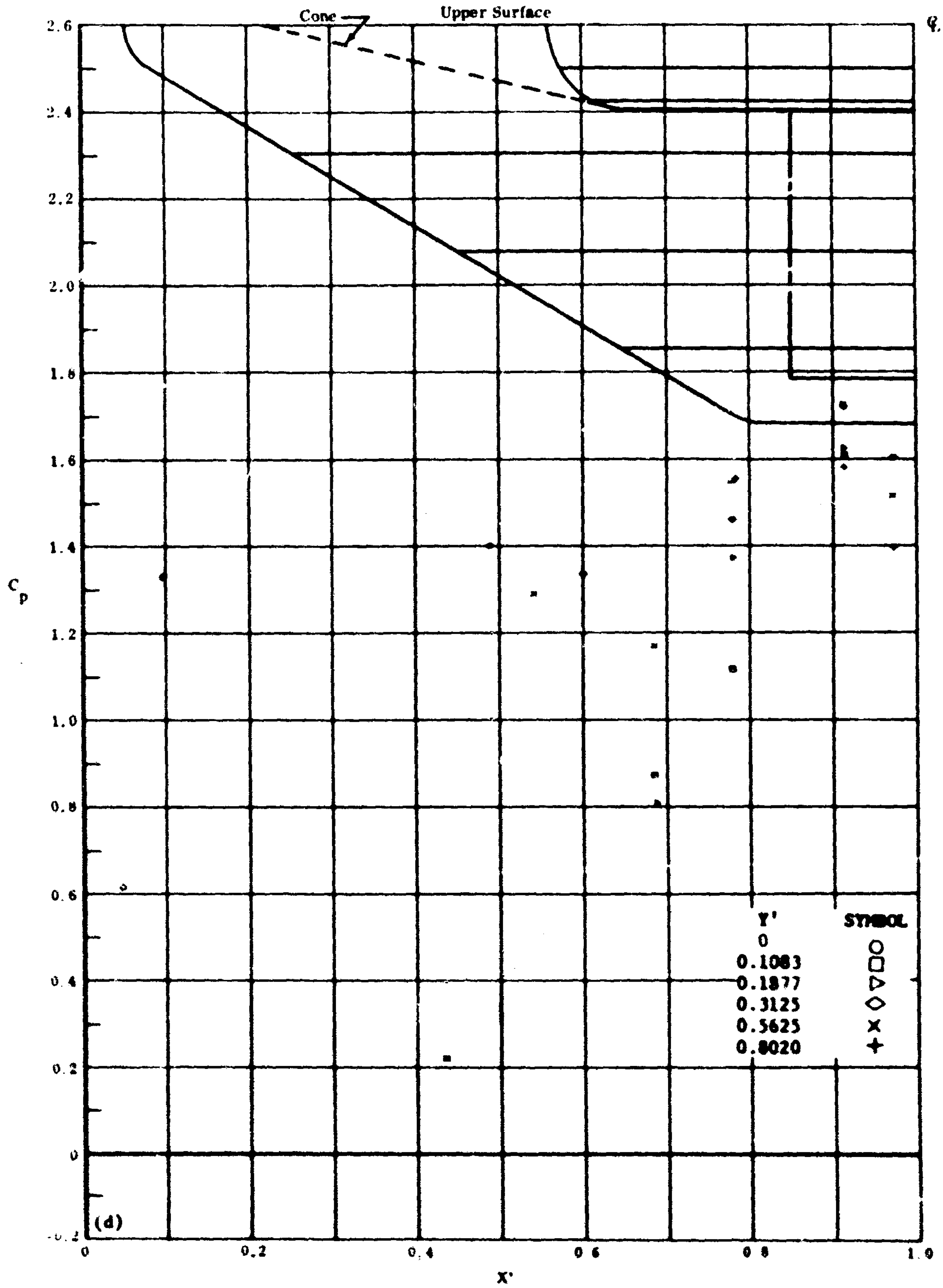

(NONDIMENSIONAL STREAMWISE DISTANCE FROM VIRTUAL APEX)

Fig. 28d Configuration I, α = -50 , $\delta_2 = \delta_3$ = -10

C_p vs. X', upper surface

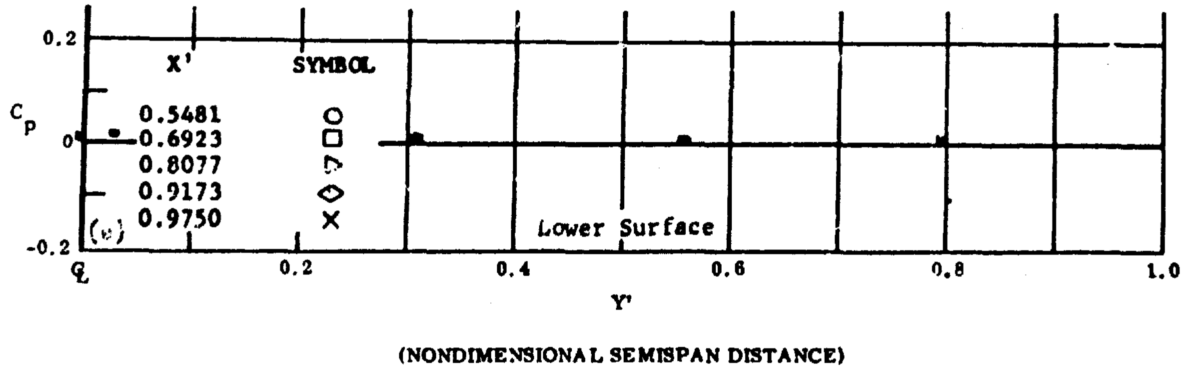

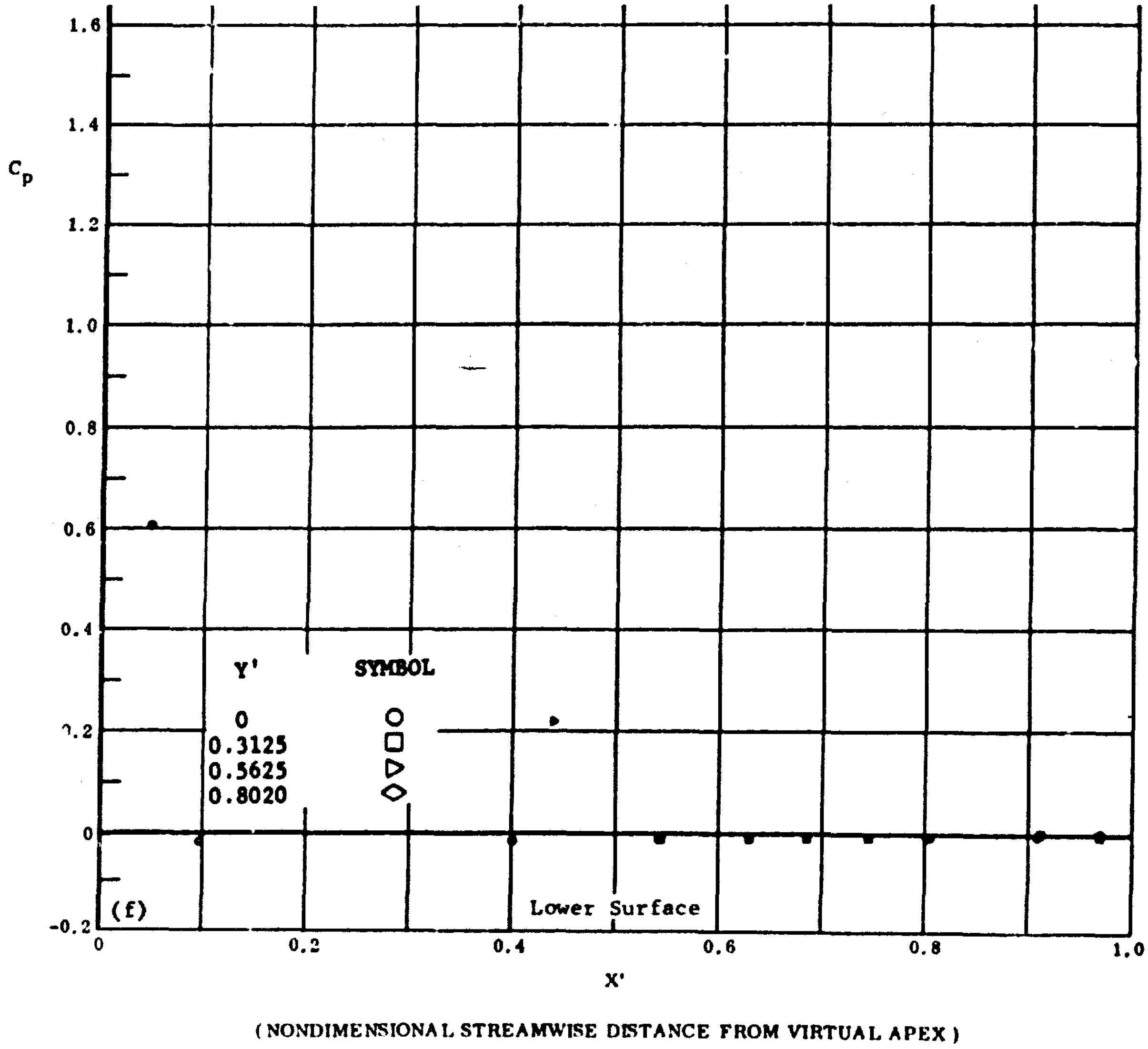

Fig. 28 Configuration I, $\alpha = -50$, $\delta_2 = \delta_3 = -20$

e) C_p vs. Y', lower surface

f) C_p vs. X', lower surface

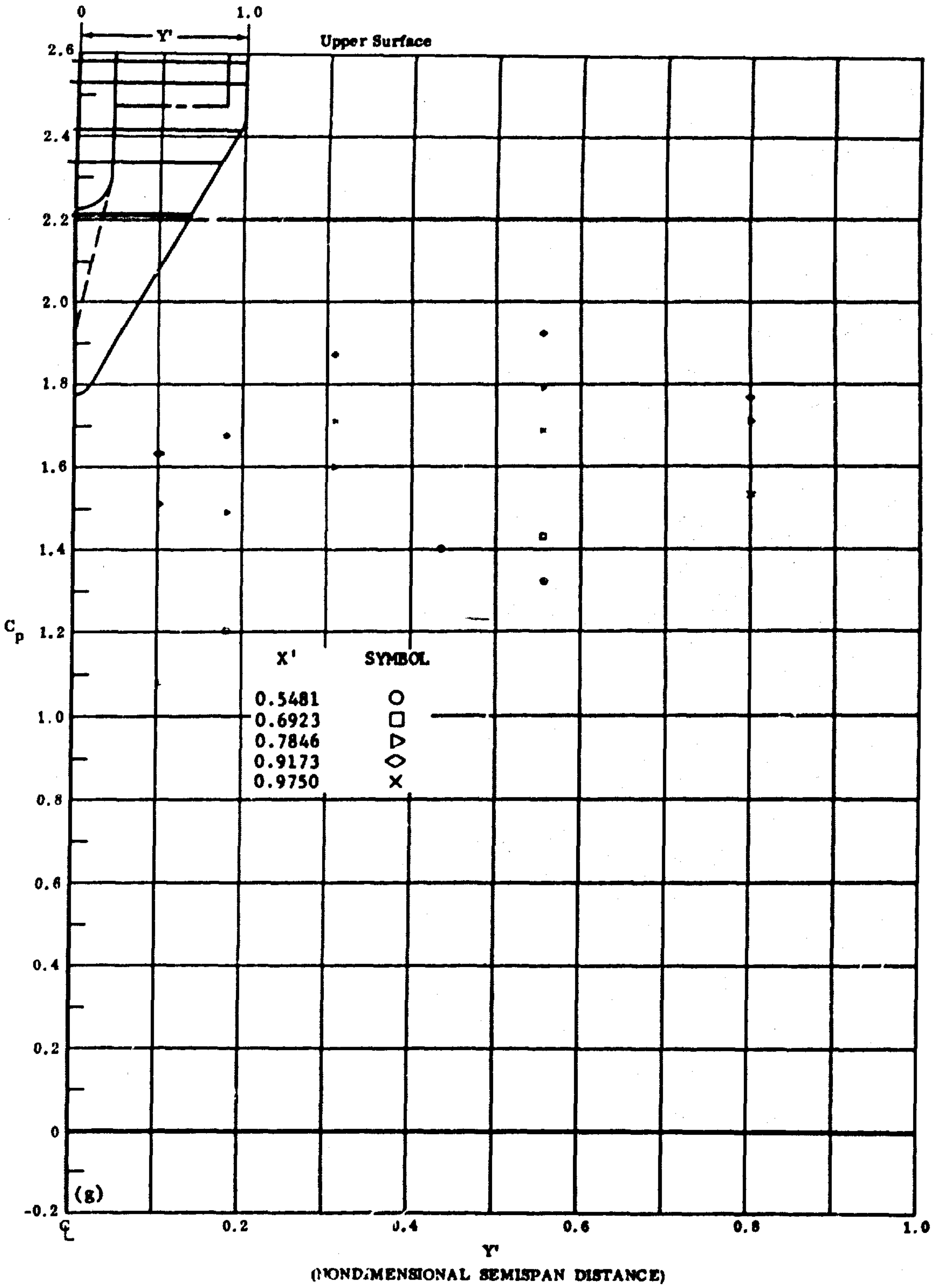

Fig. 28g Configuration I, α = -50 , $\delta_2 = \delta_3$ = -20

C_p vs. Y', upper surface

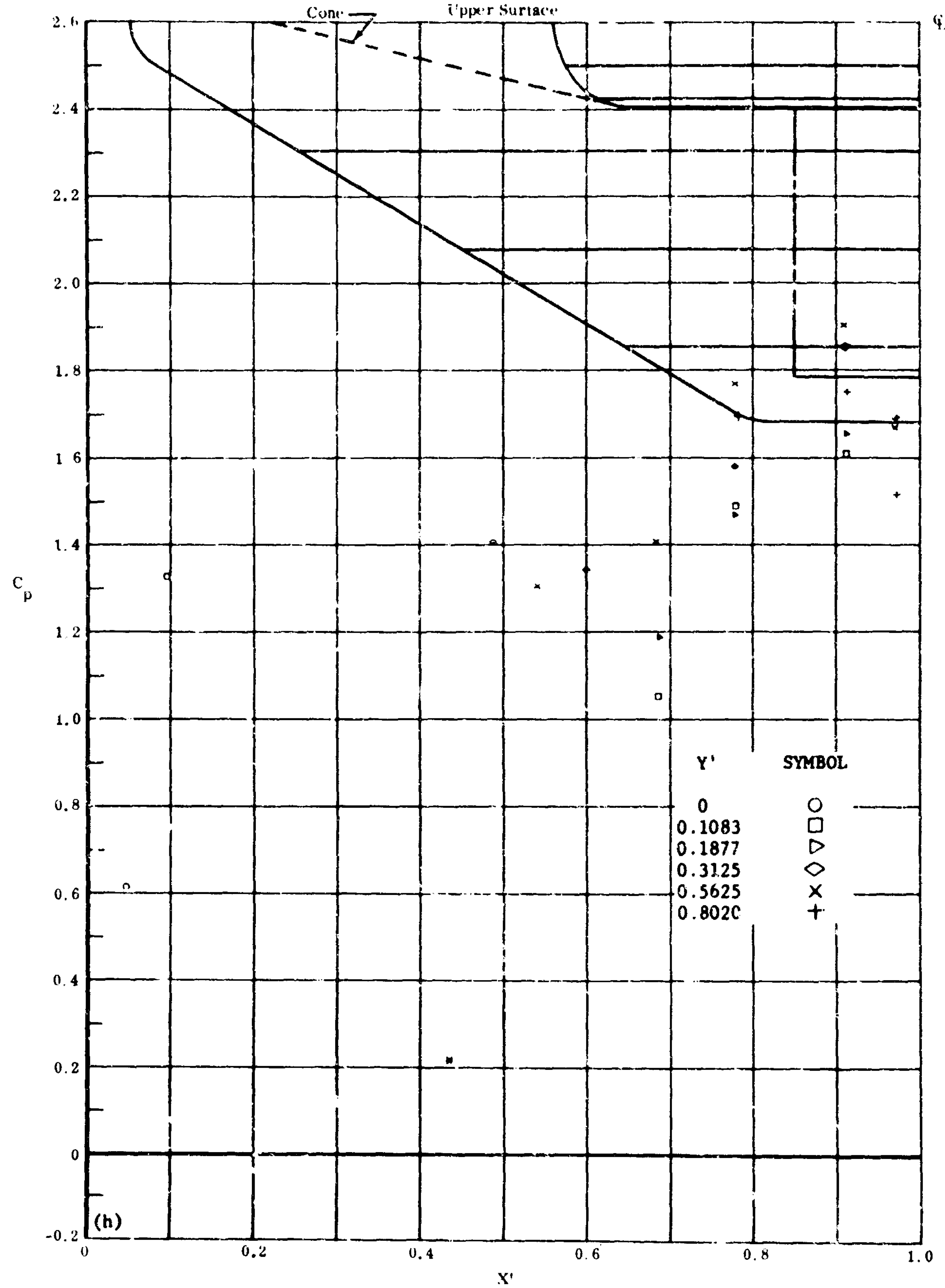

(NONDIMENSIONAL STREAMWISE DISTANCE FROM VIRTUAL APEX)

Fig. 28h Configuration I, $\alpha = -50$, $\delta_2 = \delta_3 = -20$

C_p vs. X', upper surface

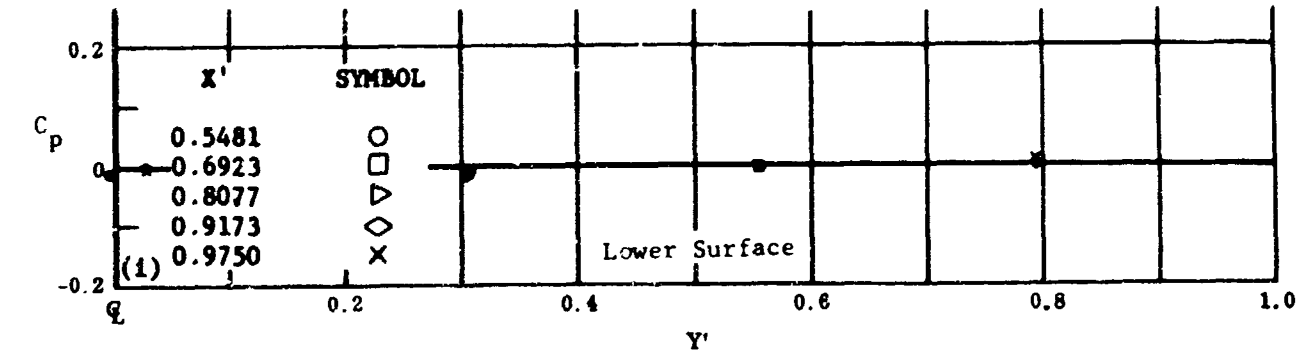

(NONDIMENSIONAL SEMISPAN DISTANCE)

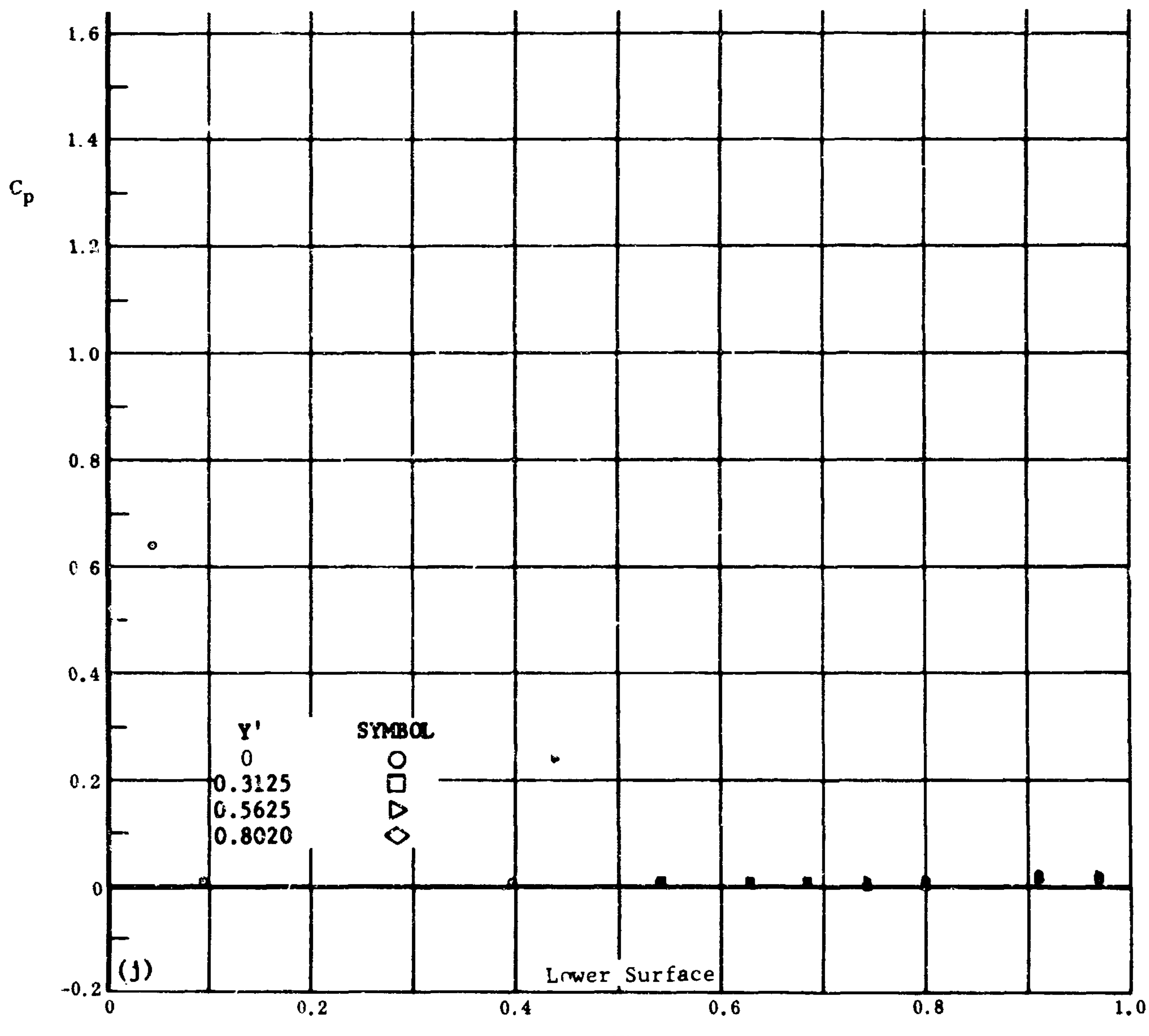

(NONDIMENSIONAL STREAMWISE DISTANCE FROM VIRTUAL APEX)

Fig. 28 Configuration I, $\alpha = -50$, $\delta_2 = \delta_3 = -30$

i) C_p vs. Y', lower surface

j) C_p vs. X', lower surface

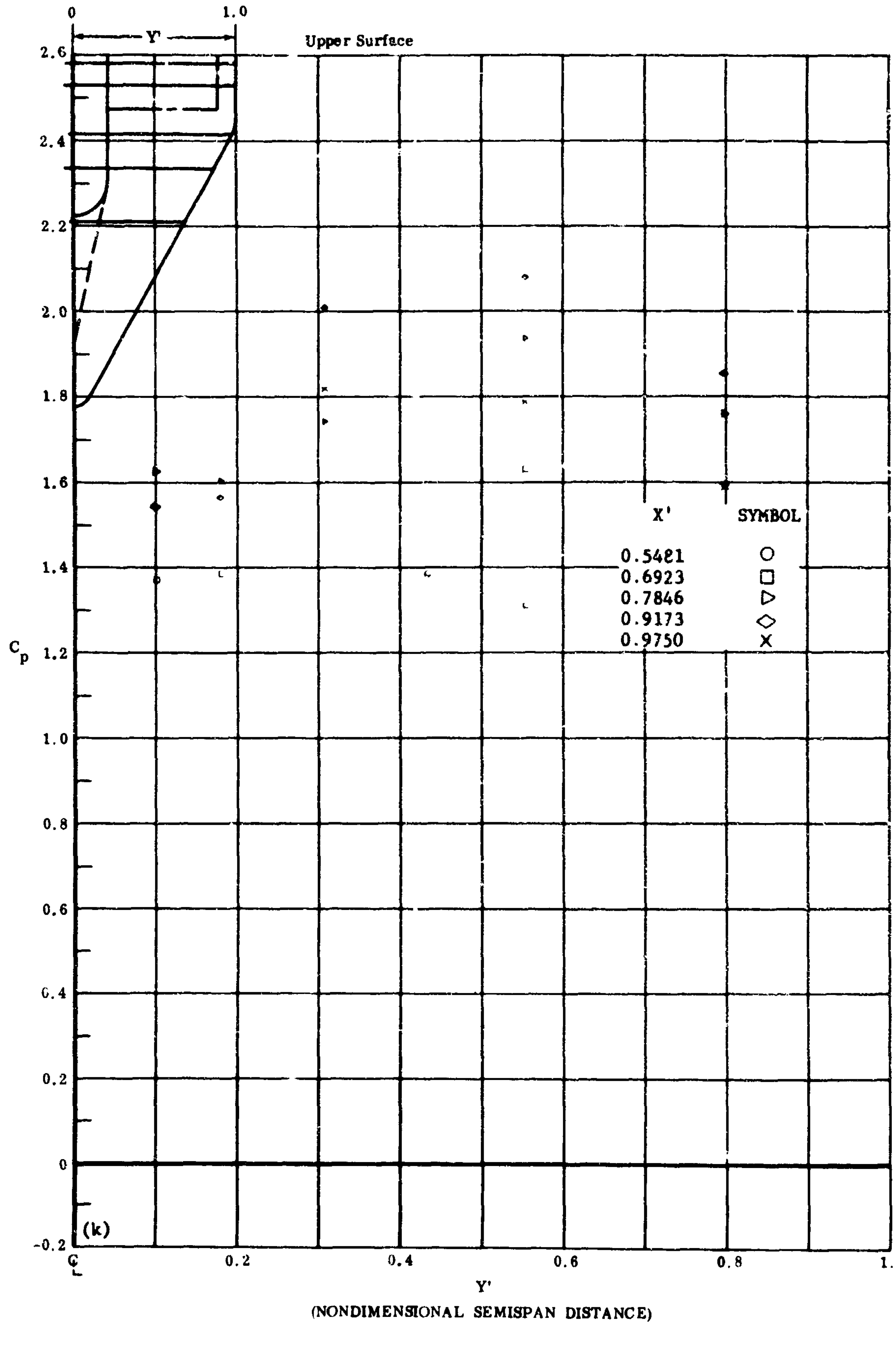

Fig. 28k Configuration I, $\alpha = -50$, $\delta_2 = \delta_3 = -30$

C_p vs. Y', upper surface

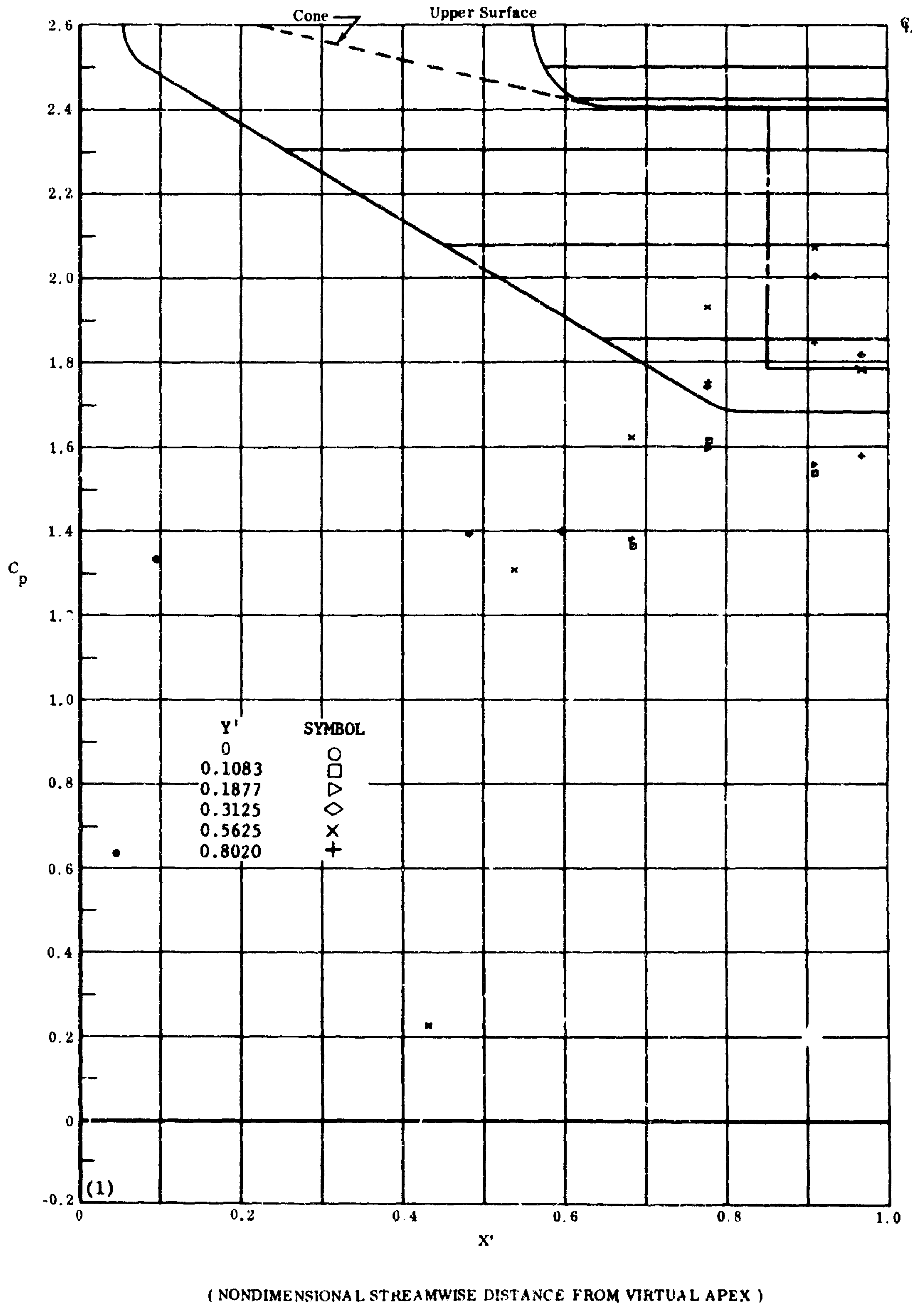

Fig. 281 Configuration I, α = -30 , $\delta_2 = \delta_3$ = -30

C_p vs. X', upper surface

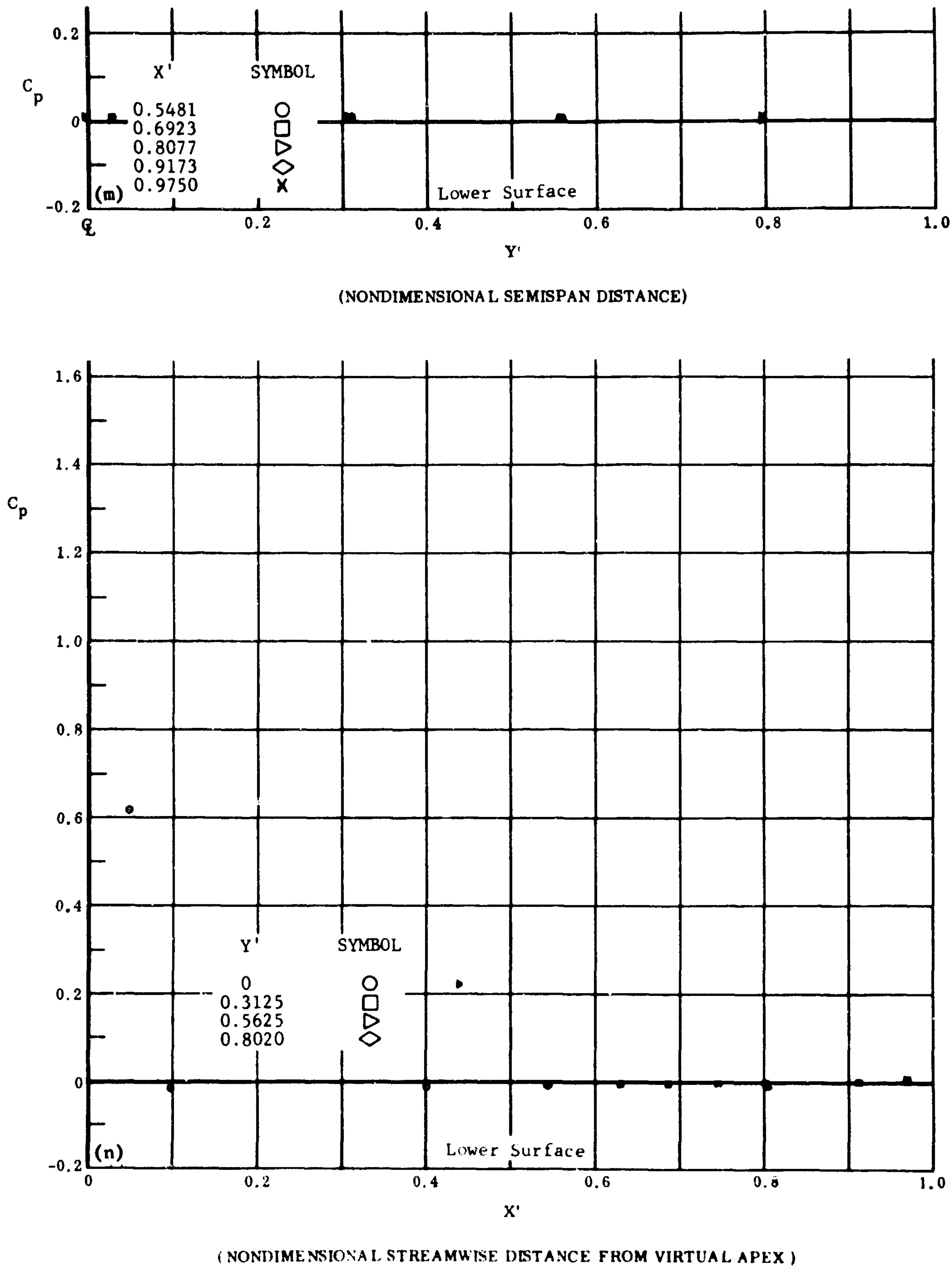

Fig. 28 Configuration I, α = -50 , $\delta_2 = \delta_3$ = -39

m) C_p vs. Y', lower surface

n) C_p vs. X', lower surface

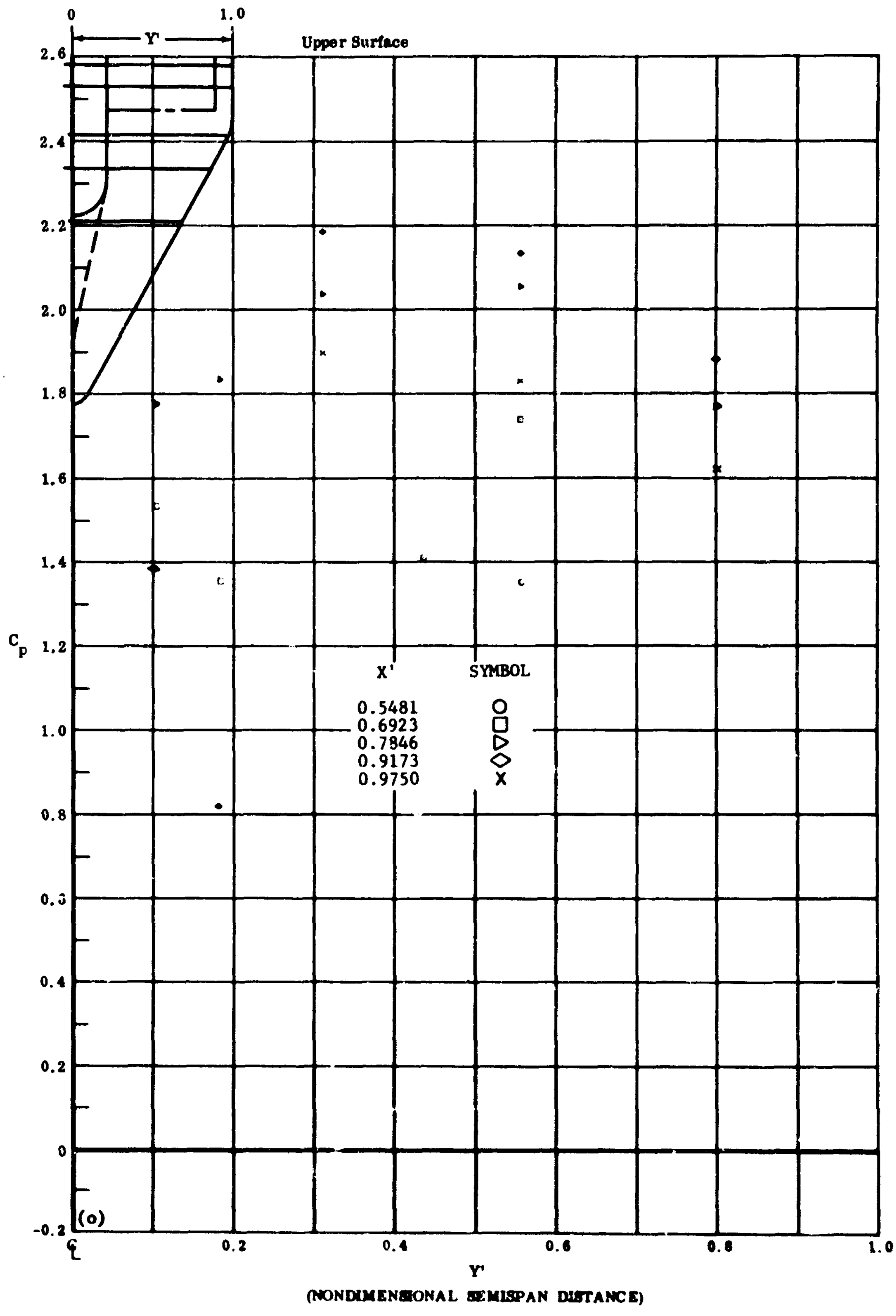

Fig. 28o Configuration I, $\alpha = -50$, $\delta_2 = \delta_3 = -39$

C_p vs. Y', upper surface

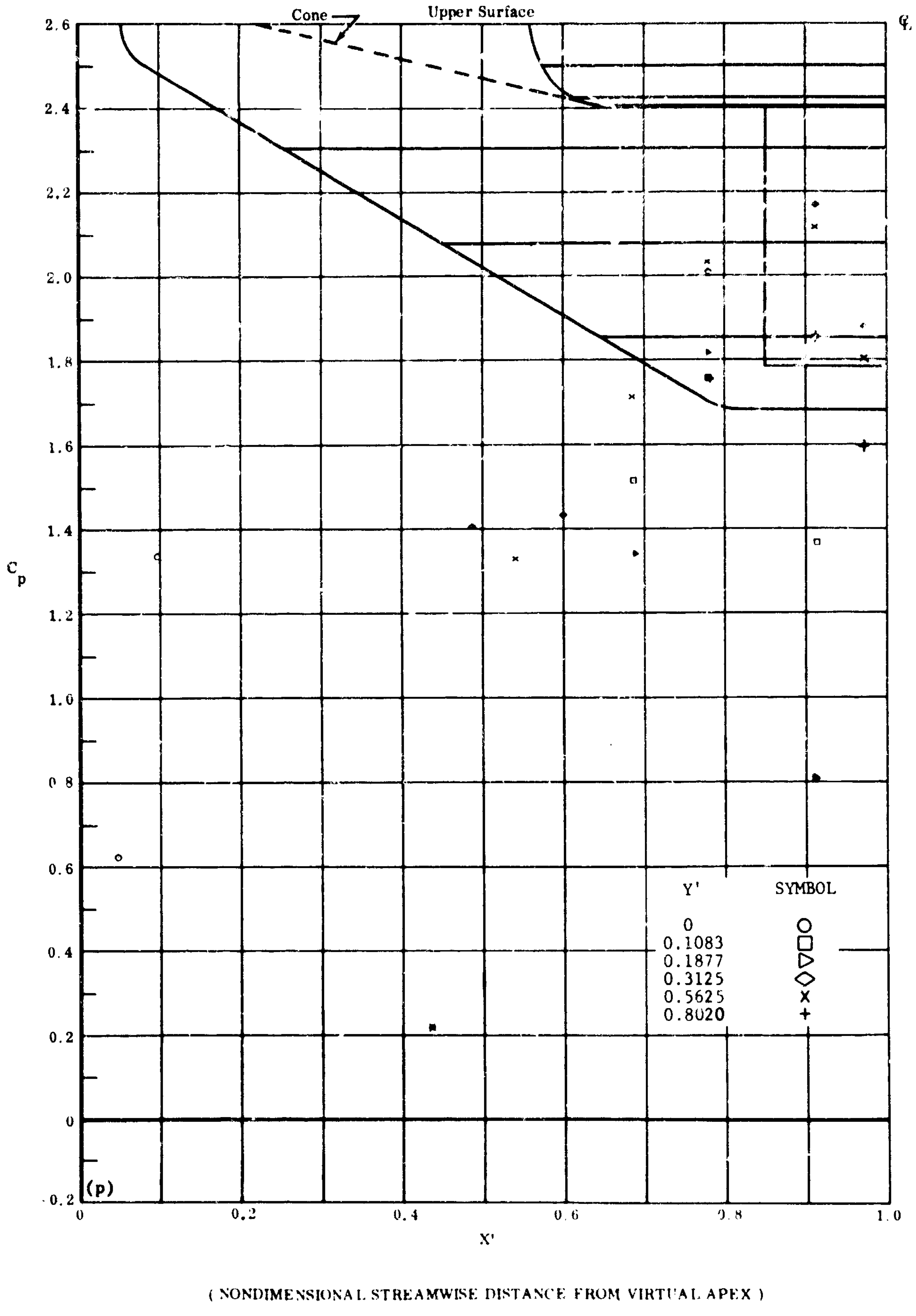

(NONDIMENSIONAL STREAMWISE DISTANCE FROM VIRTUAL APEX)

Fig. 28p Configuration I, α = -50 , $\delta_2 = \delta_3$ = -39

C_p vs. X', upper surface

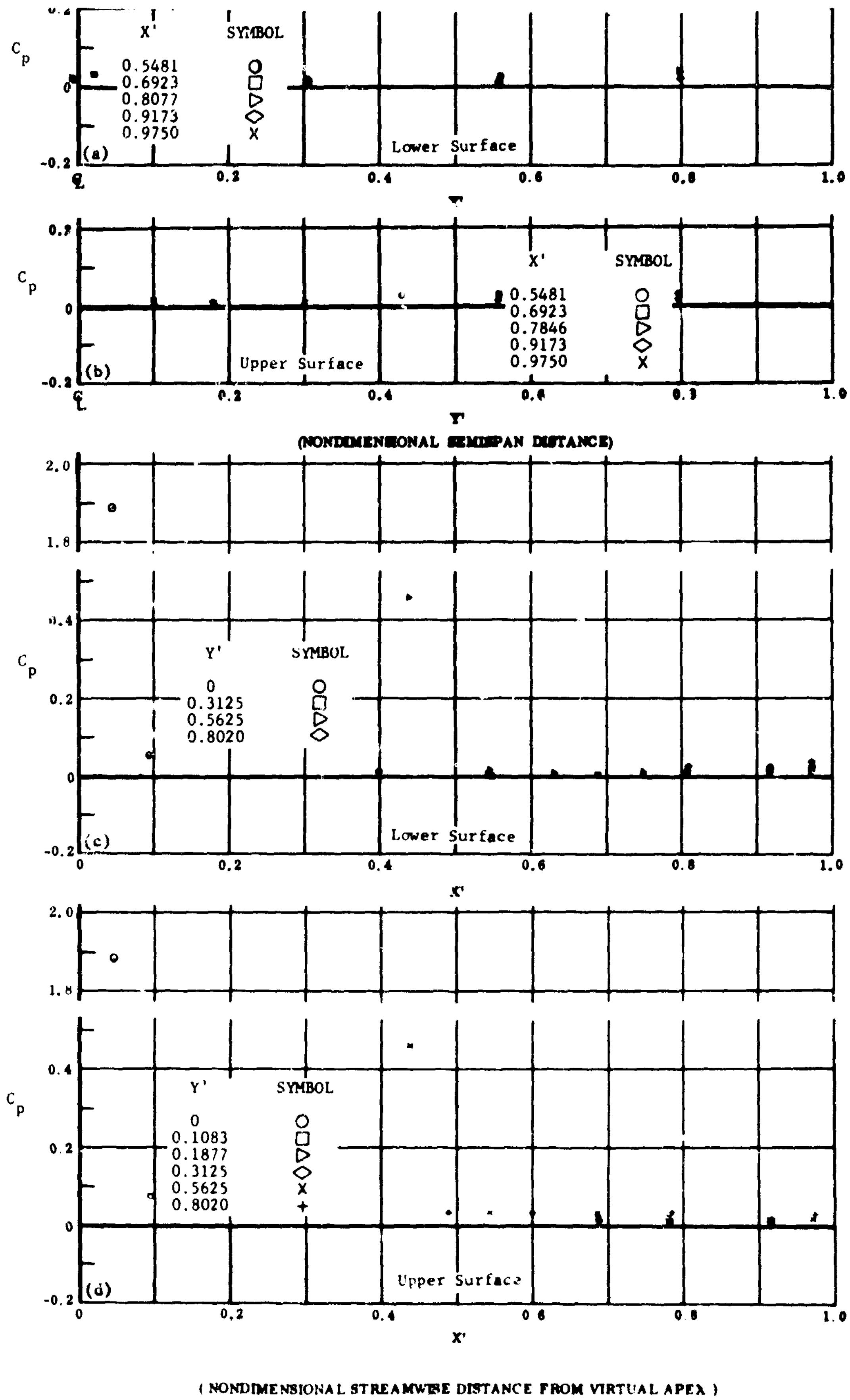

Fig. 29 Configuration IV, $\alpha = 0$, $\delta_2 = \delta_3 = 0$

a) C_p vs. Y', lower surface

b) C_p vs. Y', upper surface

c) C_p vs. X', lower surface

d) C_p vs. X', upper surface

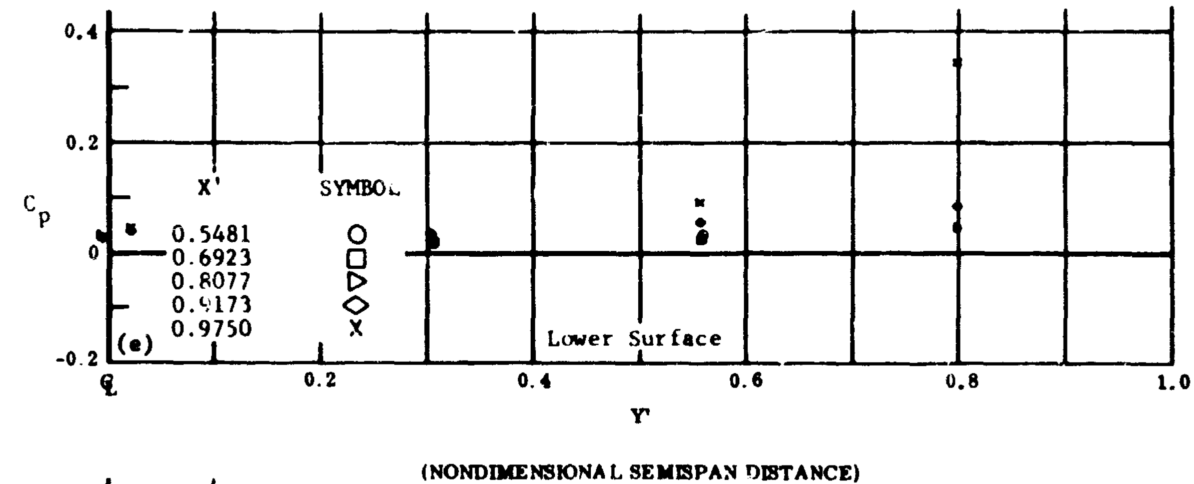

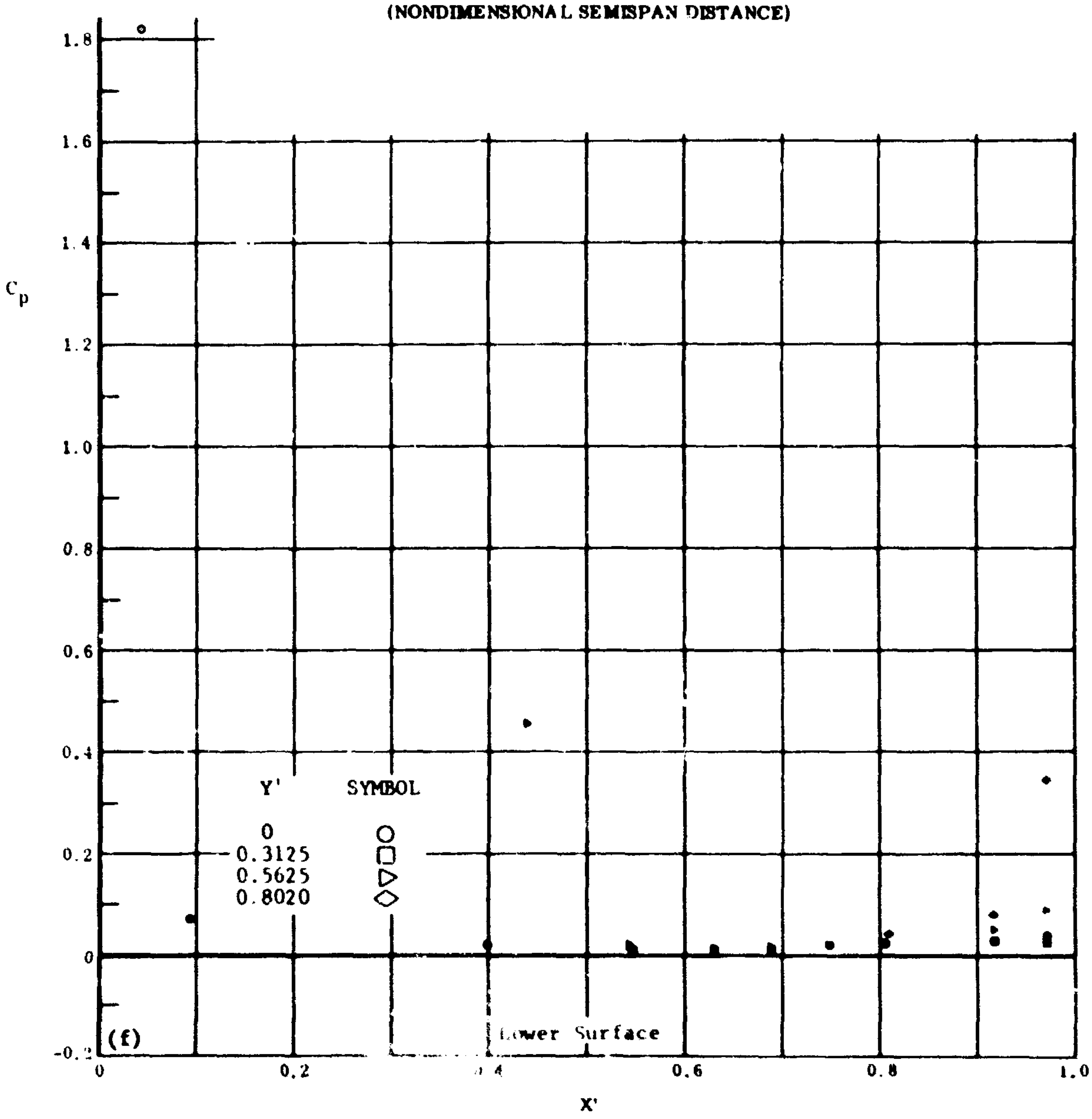

(NONDI... STREAMWISE DISTANCE FROM VIRTUAL APEX)

Fig. ...figuration IV, $\alpha = 0$, $\delta_2 = \delta_3 = +10$

...$_p$ vs. Y', lower surface

f) C_p vs. X', lower surface

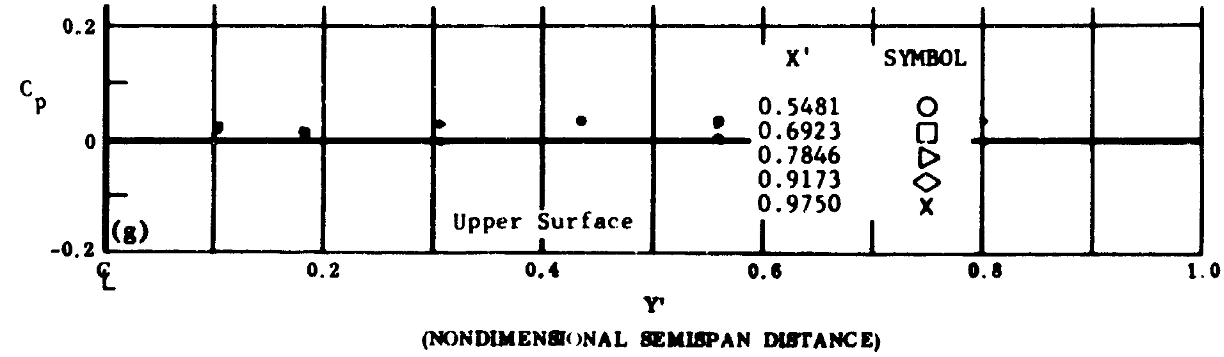

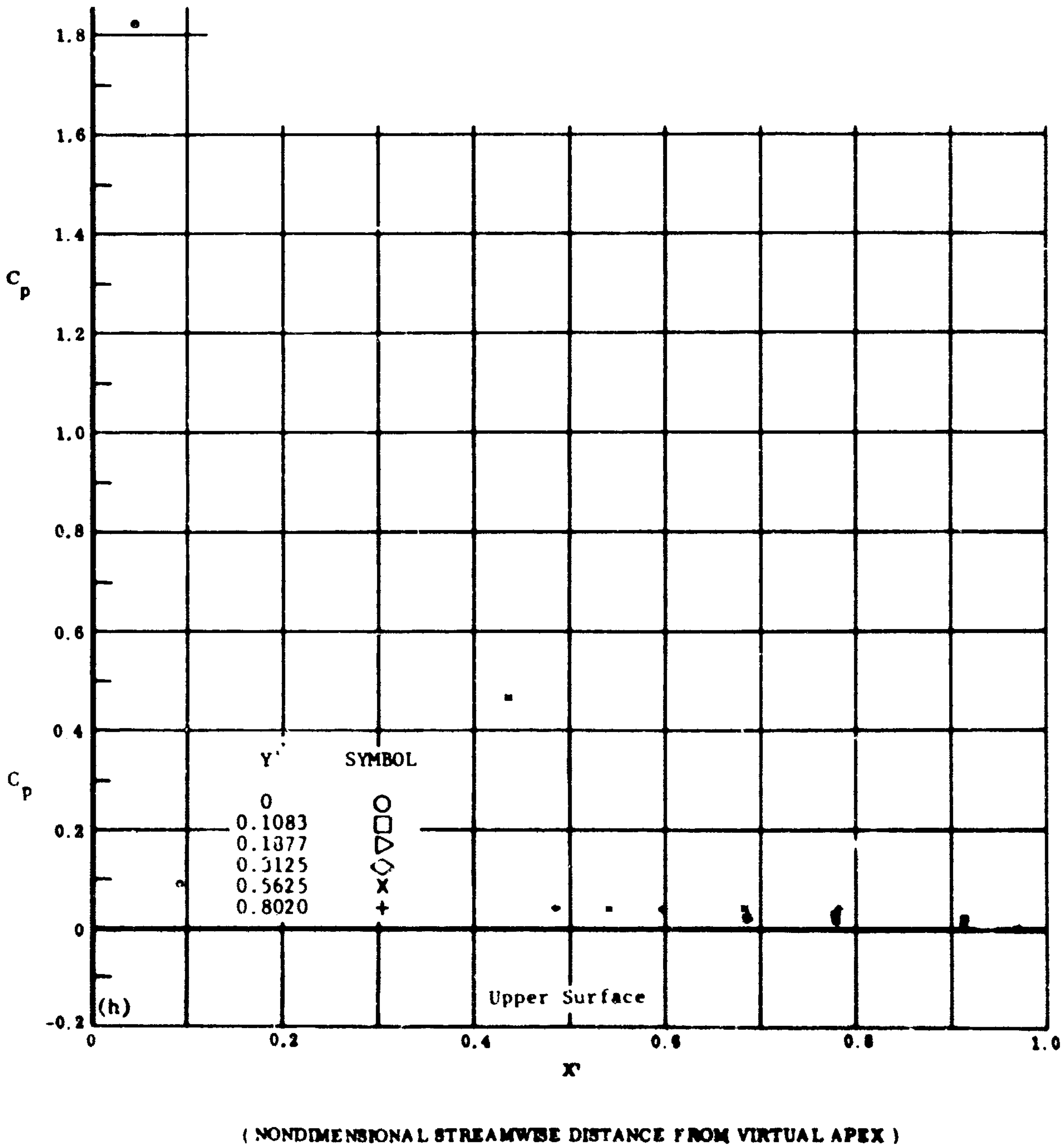

Fig. 29 Configuration IV, $\alpha = 0$, $\delta_2 = \delta_3 = +10$

g) C_p vs. Y', upper surface

h) C_p vs. X', upper surface

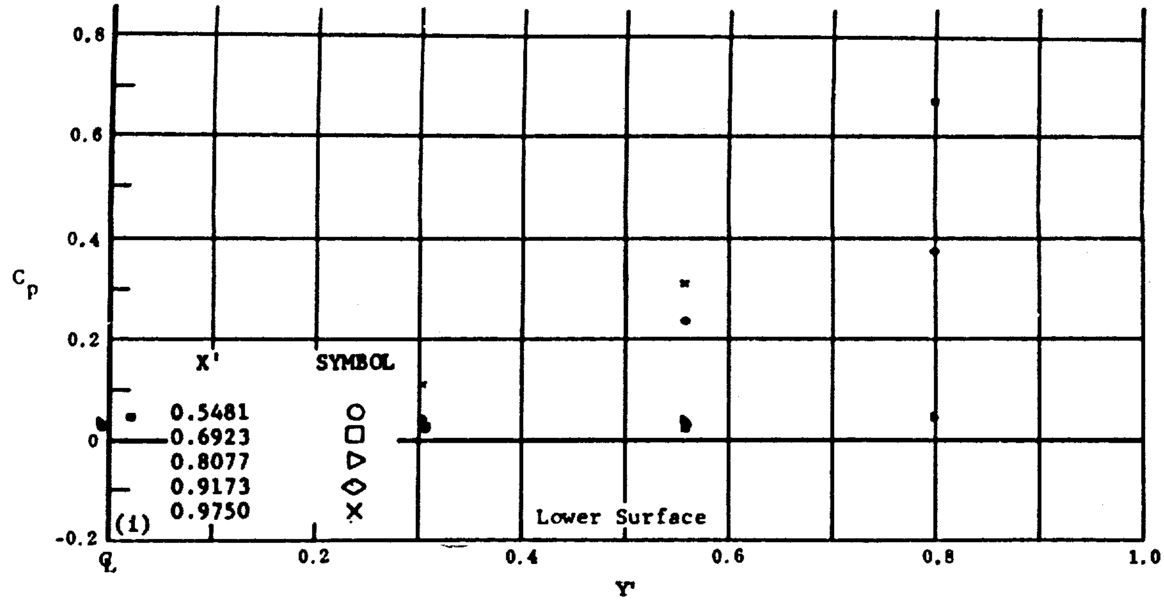

(NONDIMENSIONAL SEMISPAN DISTANCE)

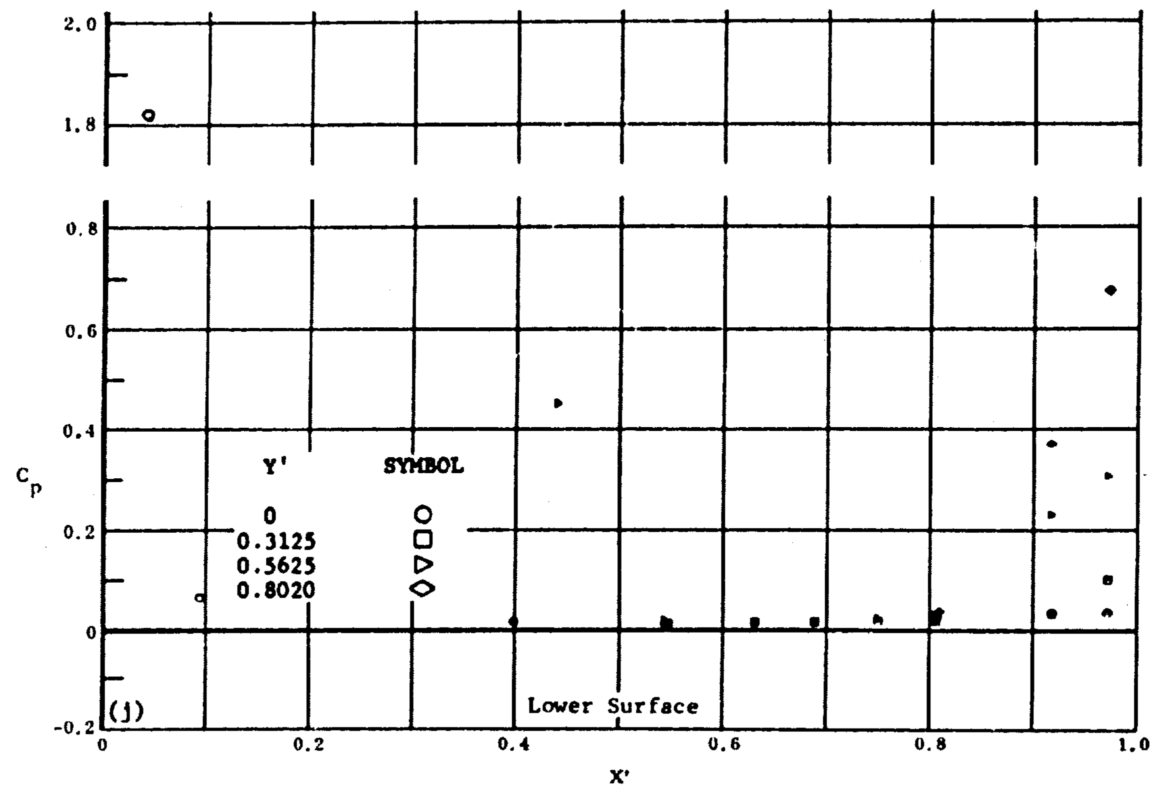

(NONDIMENSIONAL STREAMWISE DISTANCE FROM VIRTUAL APEX)

Fig. 29 Configuration IV, $\alpha = 0$, $\delta_2 = \delta_3 = +20$

i) C_p vs. Y', lower surface

j) C_p vs. X', lower surface

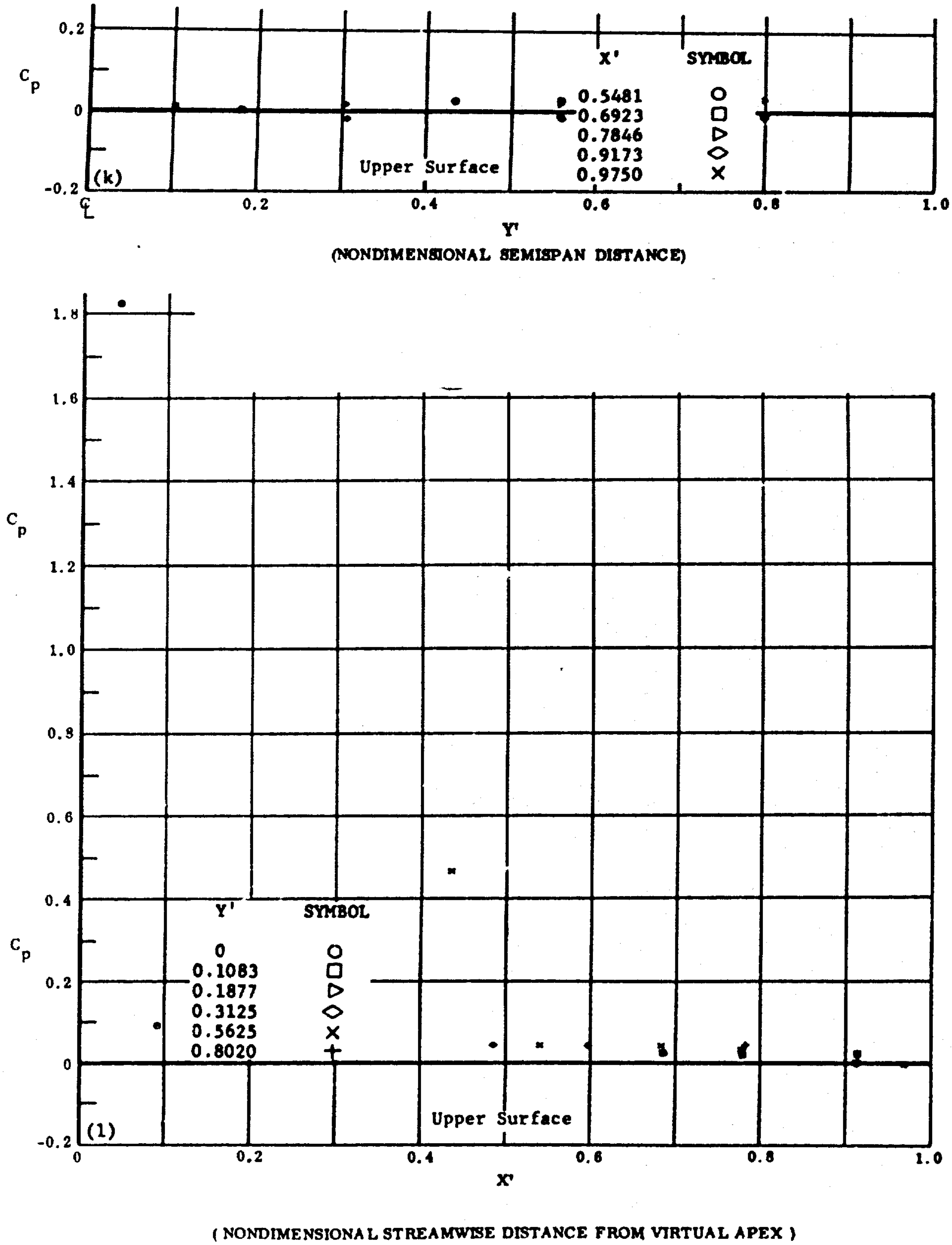

Fig. 29 Configuration IV, $\alpha = 0$, $\delta_2 = \delta_3 = +20$

k) C_p vs. Y', upper surface

l) C_p vs. X', upper surface

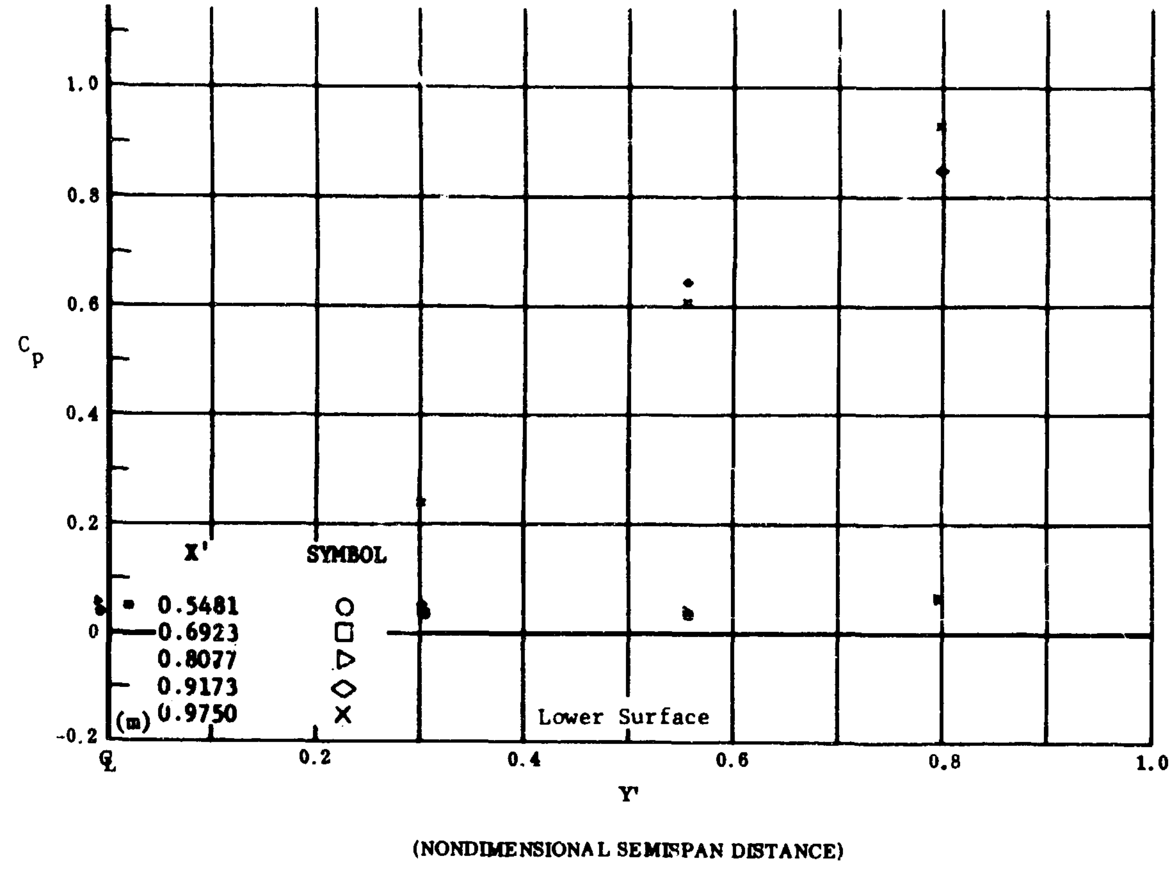

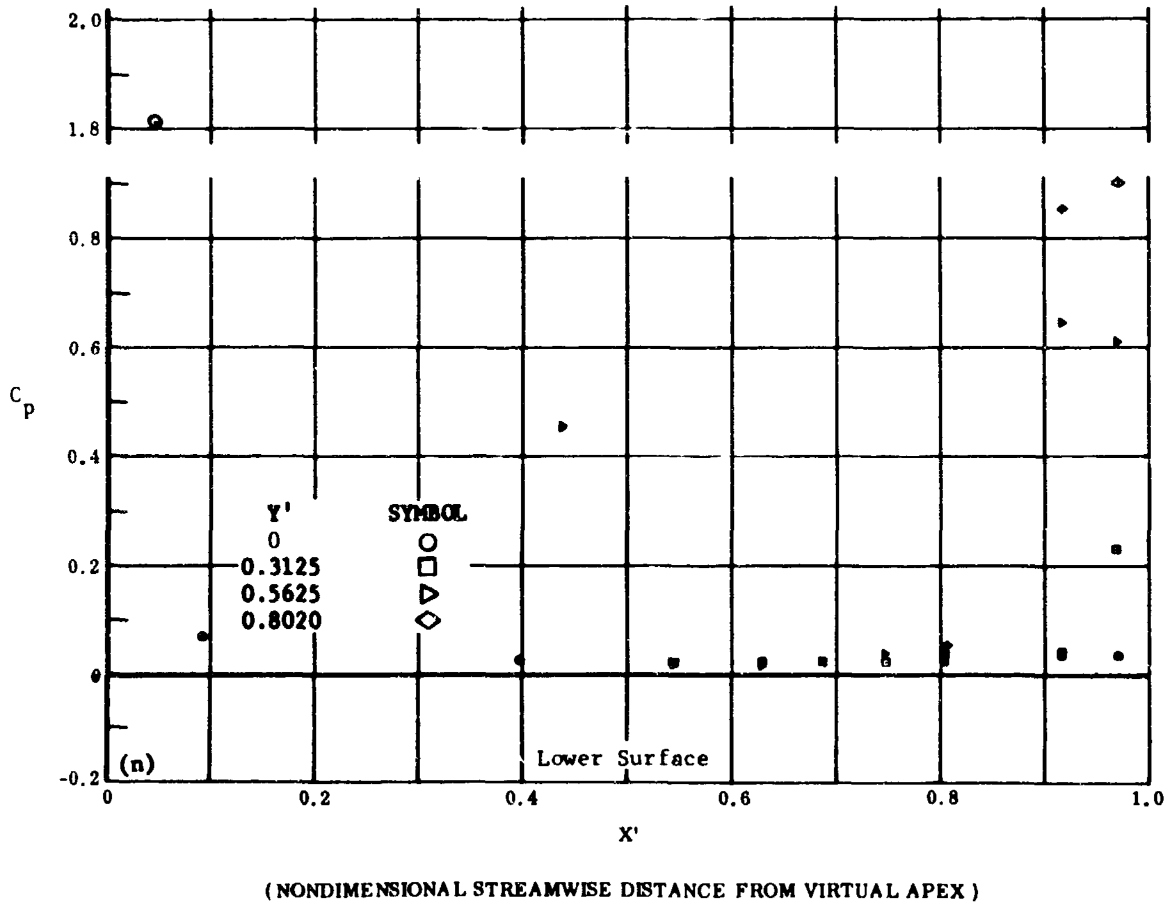

Fig. 29 Configuration IV, $\alpha = 0$, $\delta_2 = \delta_3 = +30$

m) C_p vs. Y', lower surface

n) C_p vs. X', lower surface

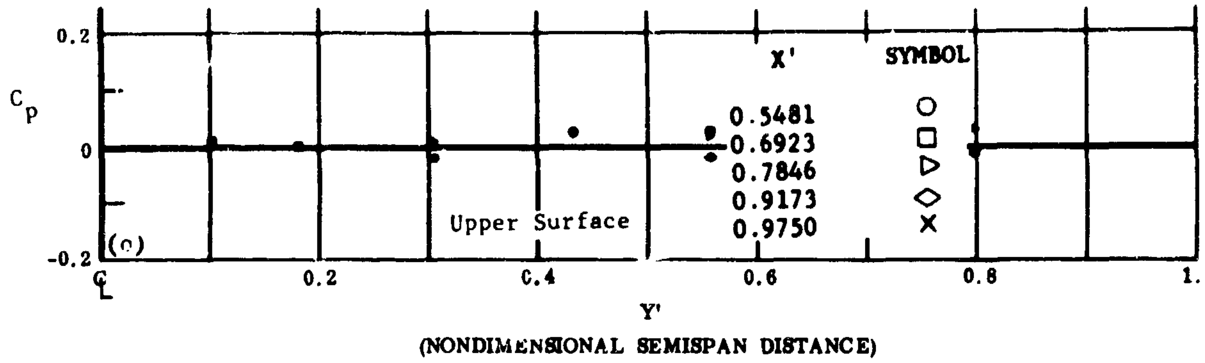

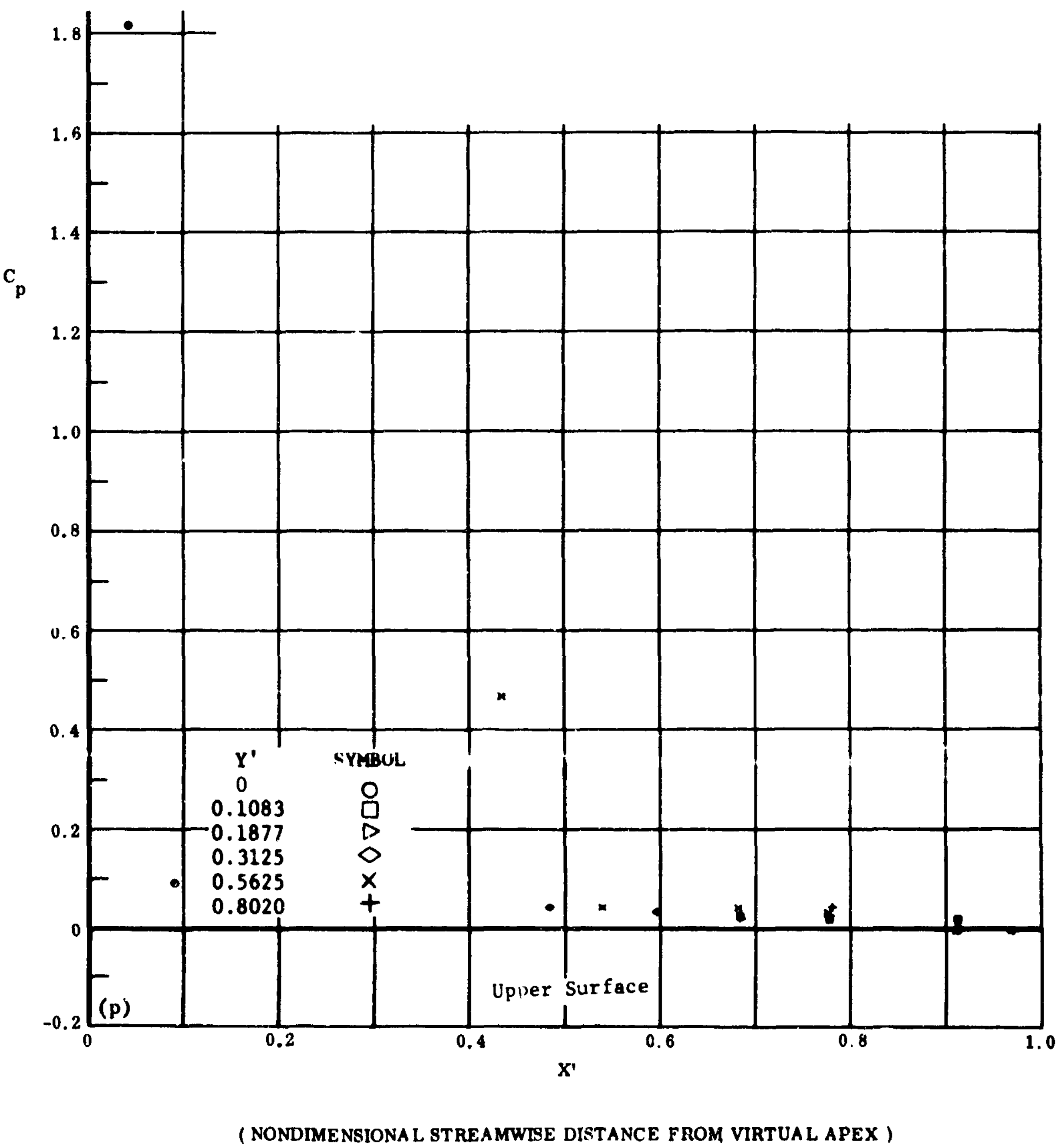

Fig. 29 Configuration IV, $\alpha = 0$, $\delta_2 = \delta_3 = +30$

o) C_p vs. Y', upper surface

p) C_p vs. X', upper surface

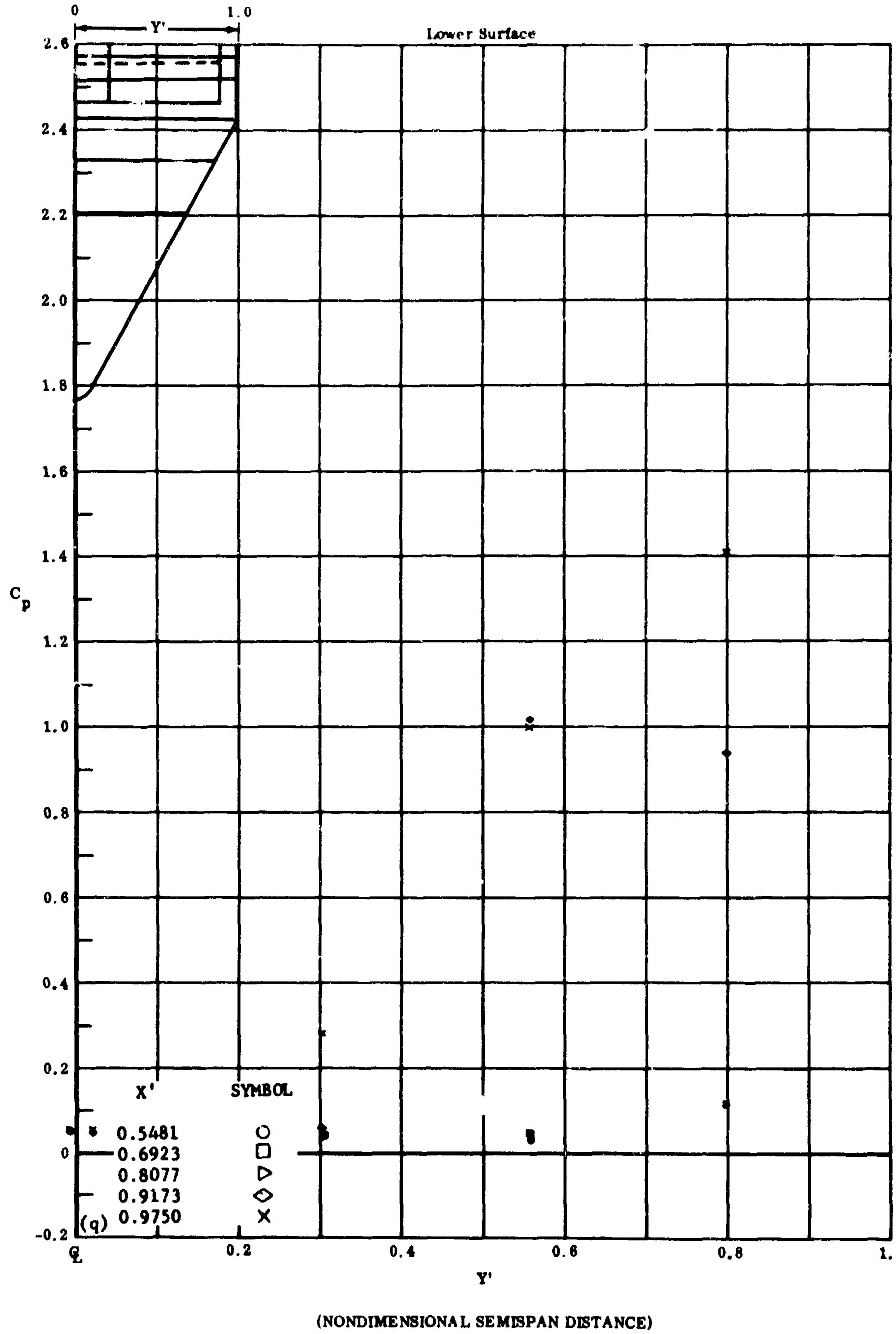

Fig. 29q Configuration IV, $\alpha = 0$, $\delta_2 = \delta_3 = +39$

C_p vs. Y', lower surface

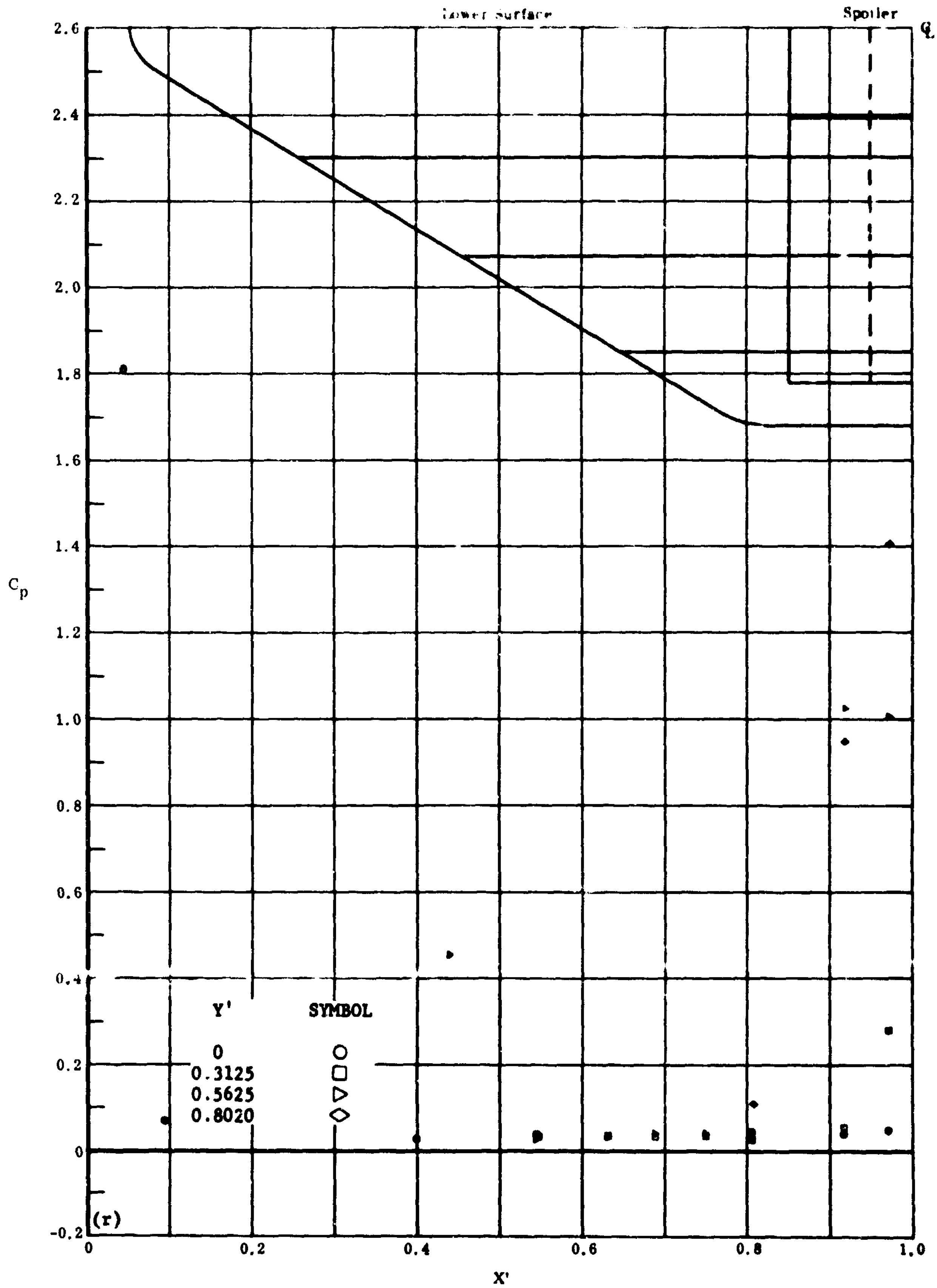

Fig. 29r Configuration IV, $\alpha = 0$, $\delta_2 = \delta_3 = +39$

C_p vs. X', lower surface

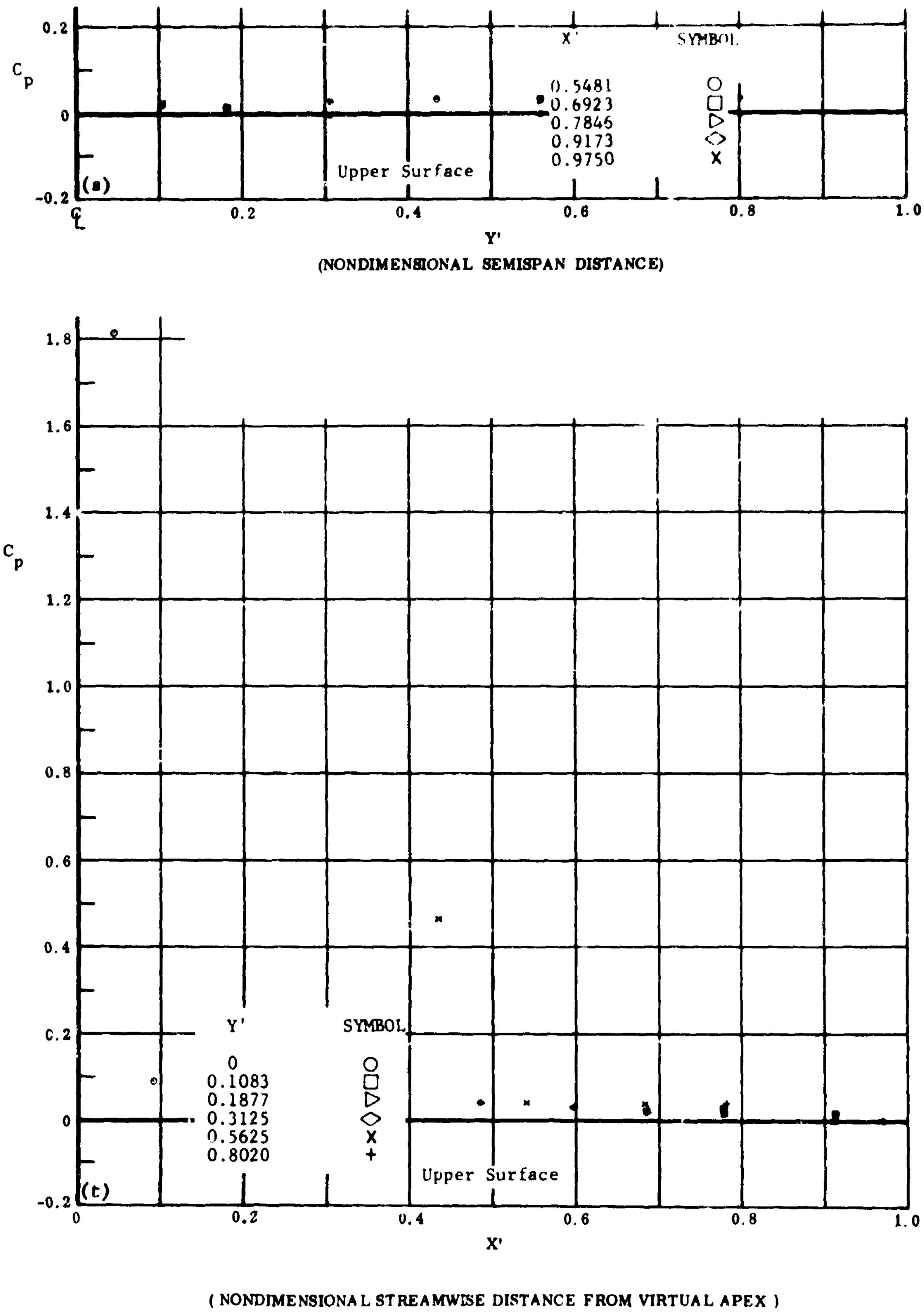

Fig. 29 Configuration IV, $\alpha = 0$, $\delta_2 = \delta_3 = +39$

s) C_p vs. Y', upper surface

t) C_p vs. X', upper surface

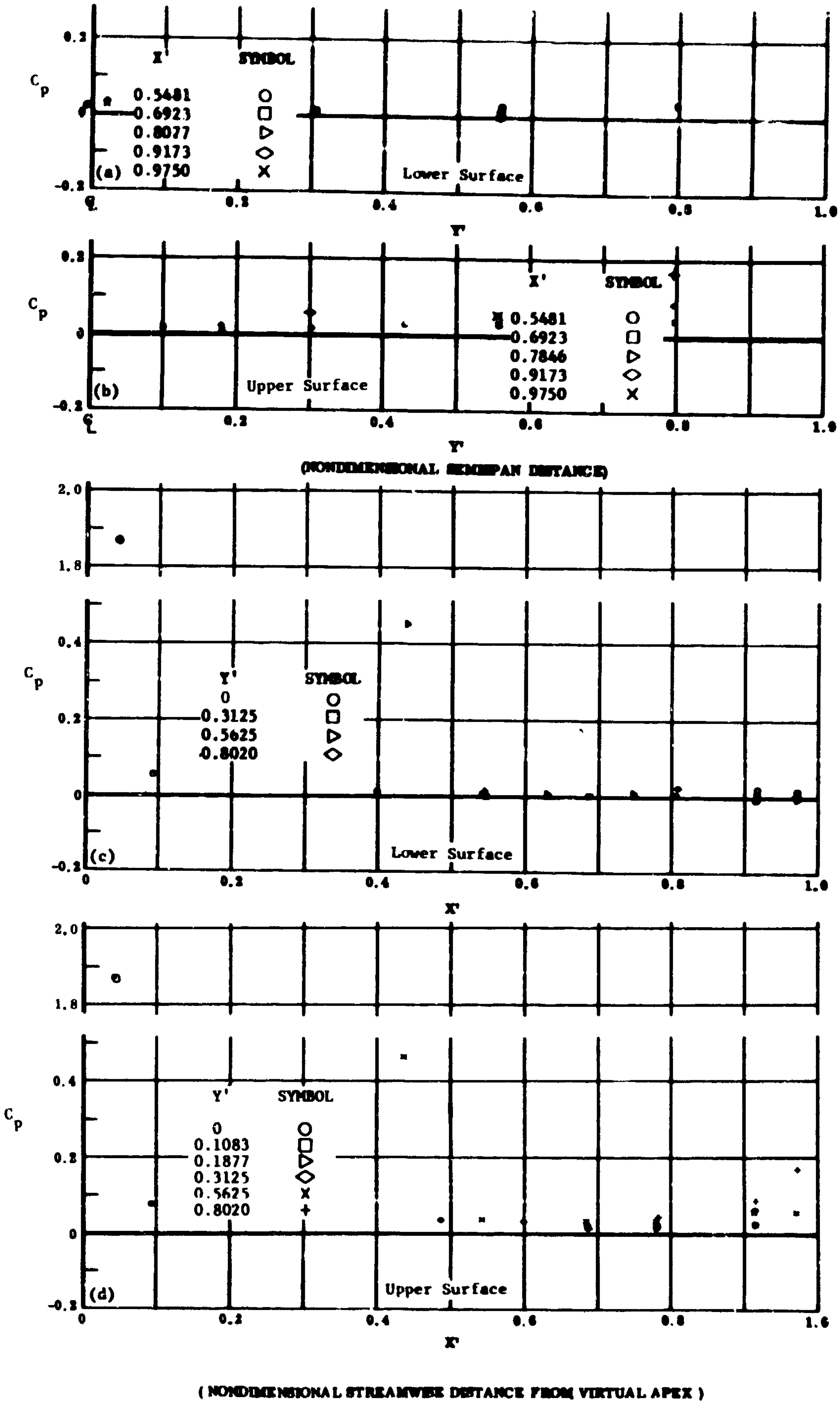

Fig. 30 Configuration IV, $\alpha = 0$, $\delta_2 = \delta_3 = -10$

a) C_p vs. Y', lower surface

b) C_p vs. Y', upper surface

c) C_p vs. X', lower surface

d) C_p vs. X', upper surface

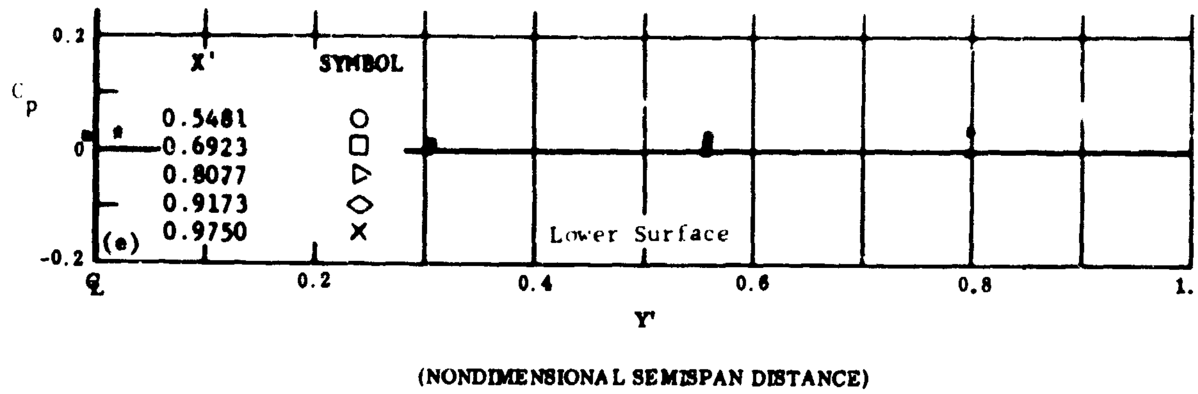

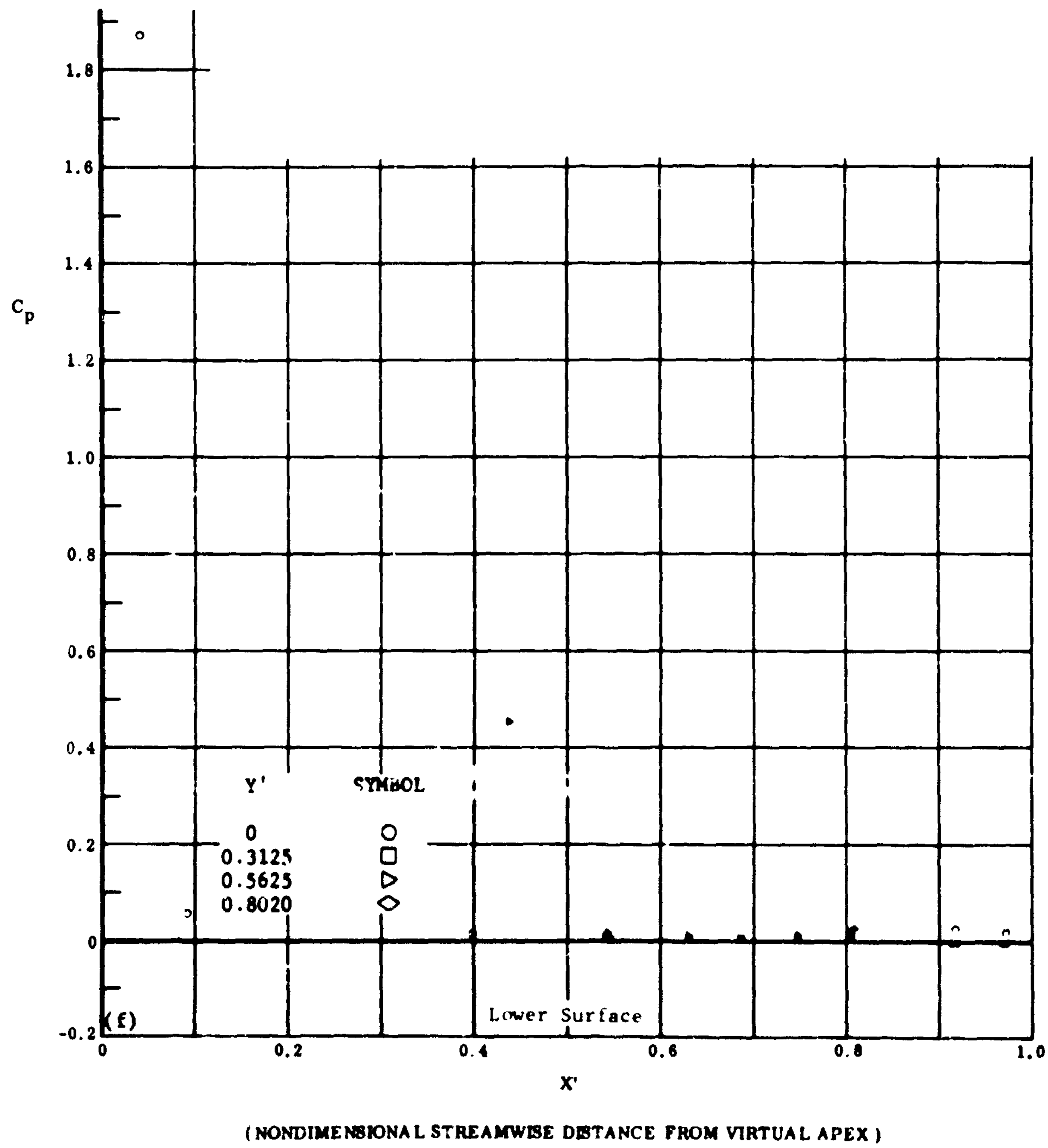

Fig. 30 Configuration IV, $\alpha = 0$, $\delta_2 = \delta_3 = -20$

e) C_p vs. Y', lower surface

f) C_p vs. X', lower surface

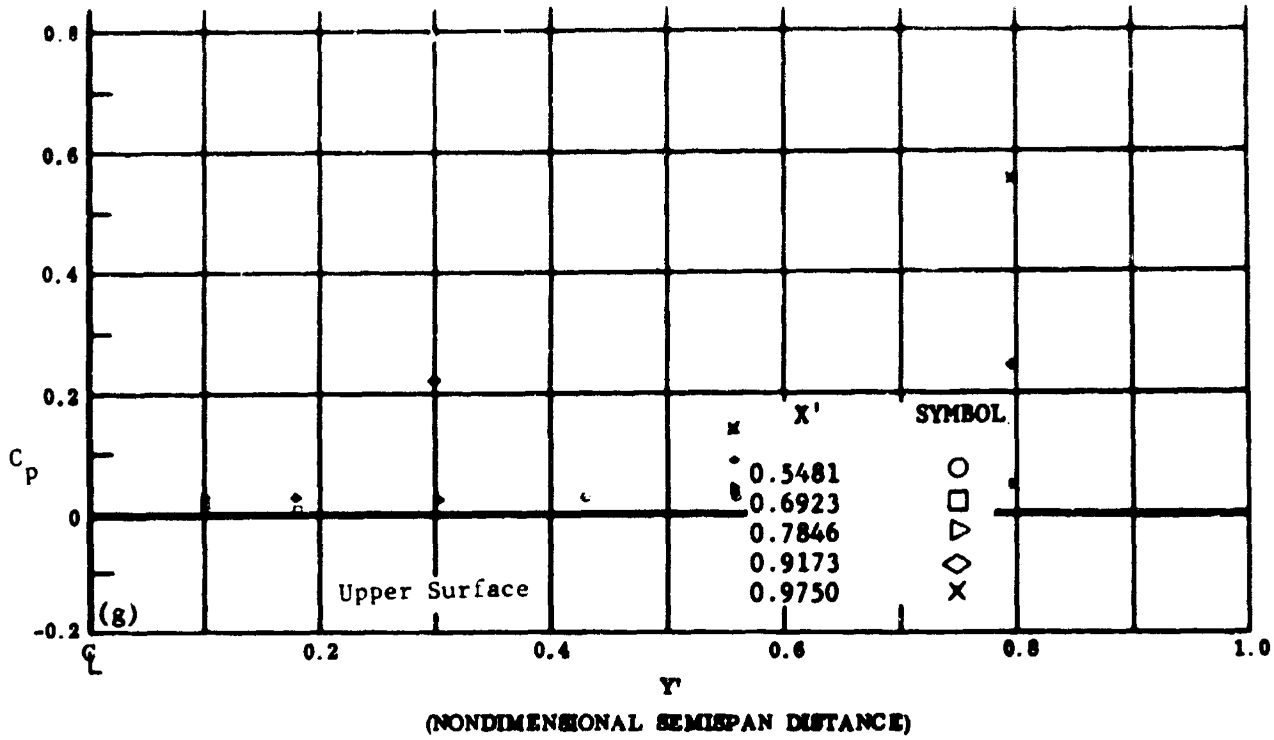

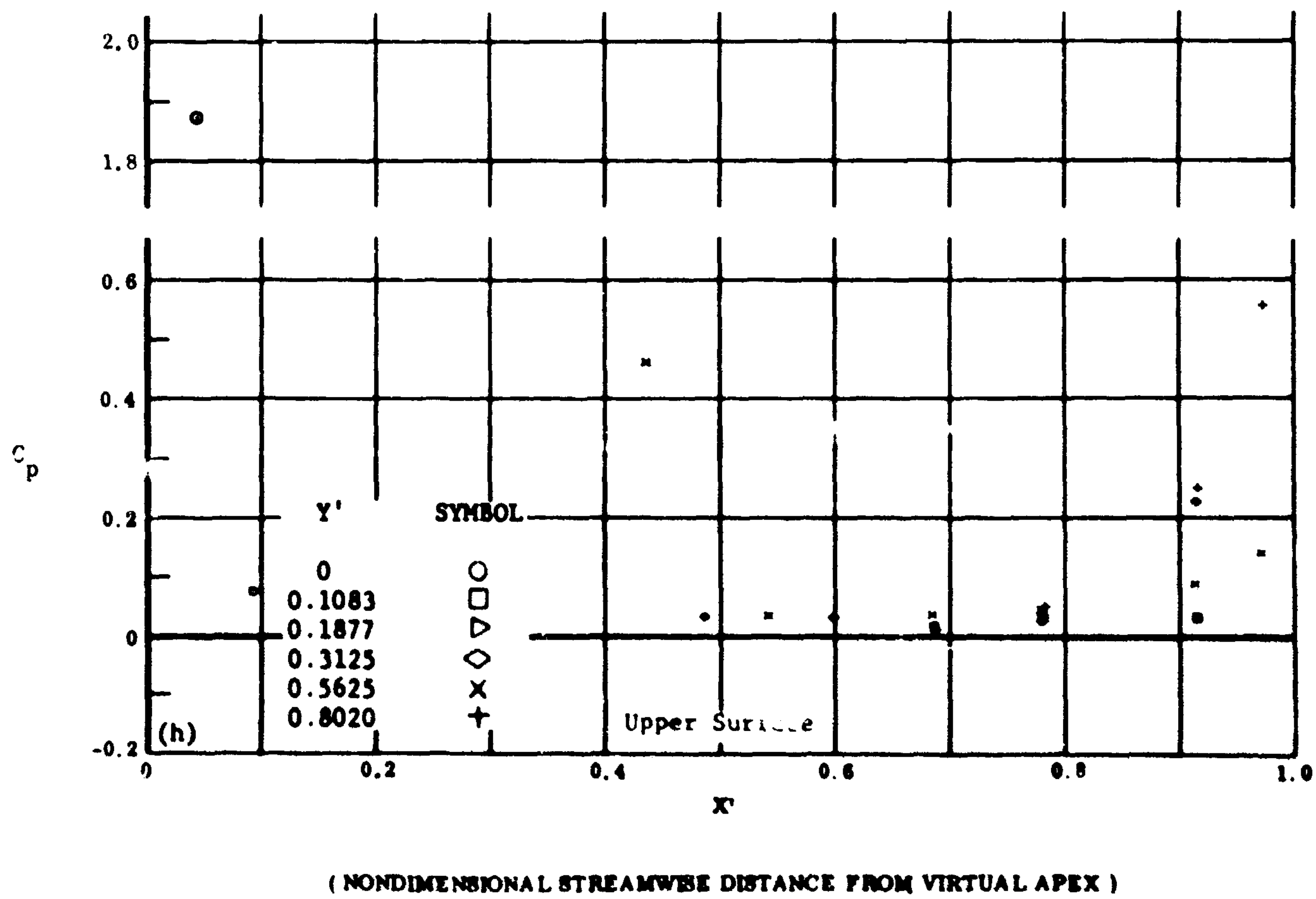

Fig. 30 Configuration IV, $\alpha = 0$, $\delta_2 = \delta_3 = -20$

g) C_p vs. Y', upper surface

h) C_p vs. X', upper surface

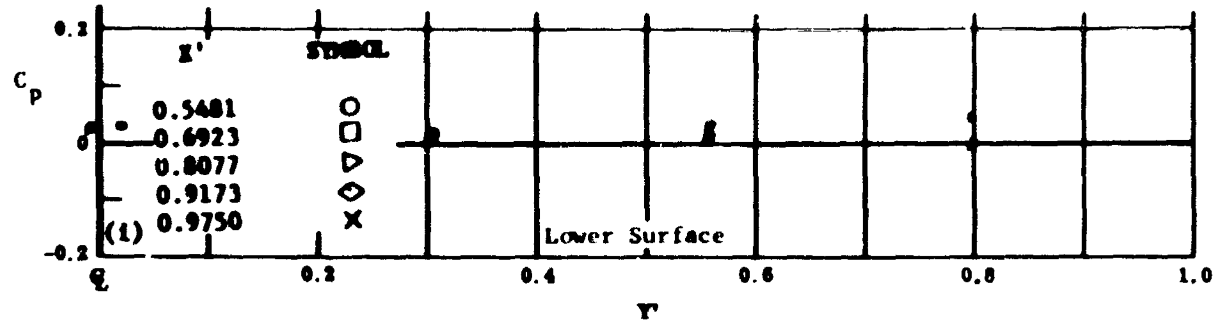

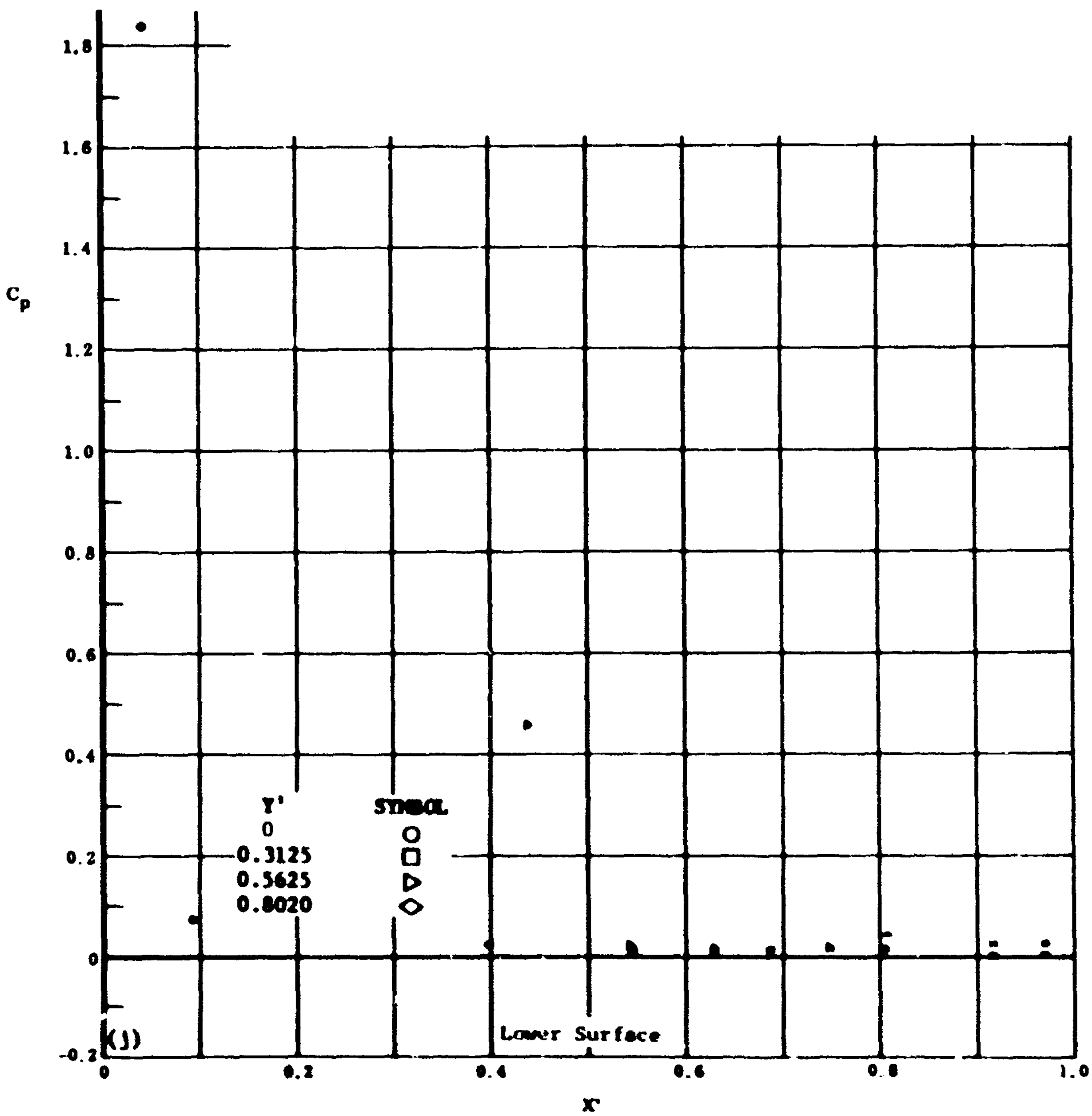

Fig. 30 Configuration IV, $\alpha = 0$, $\delta_2 = \delta_3 = -30$

i) C_p vs. Y', lower surface

j) C_p vs. X', lower surface

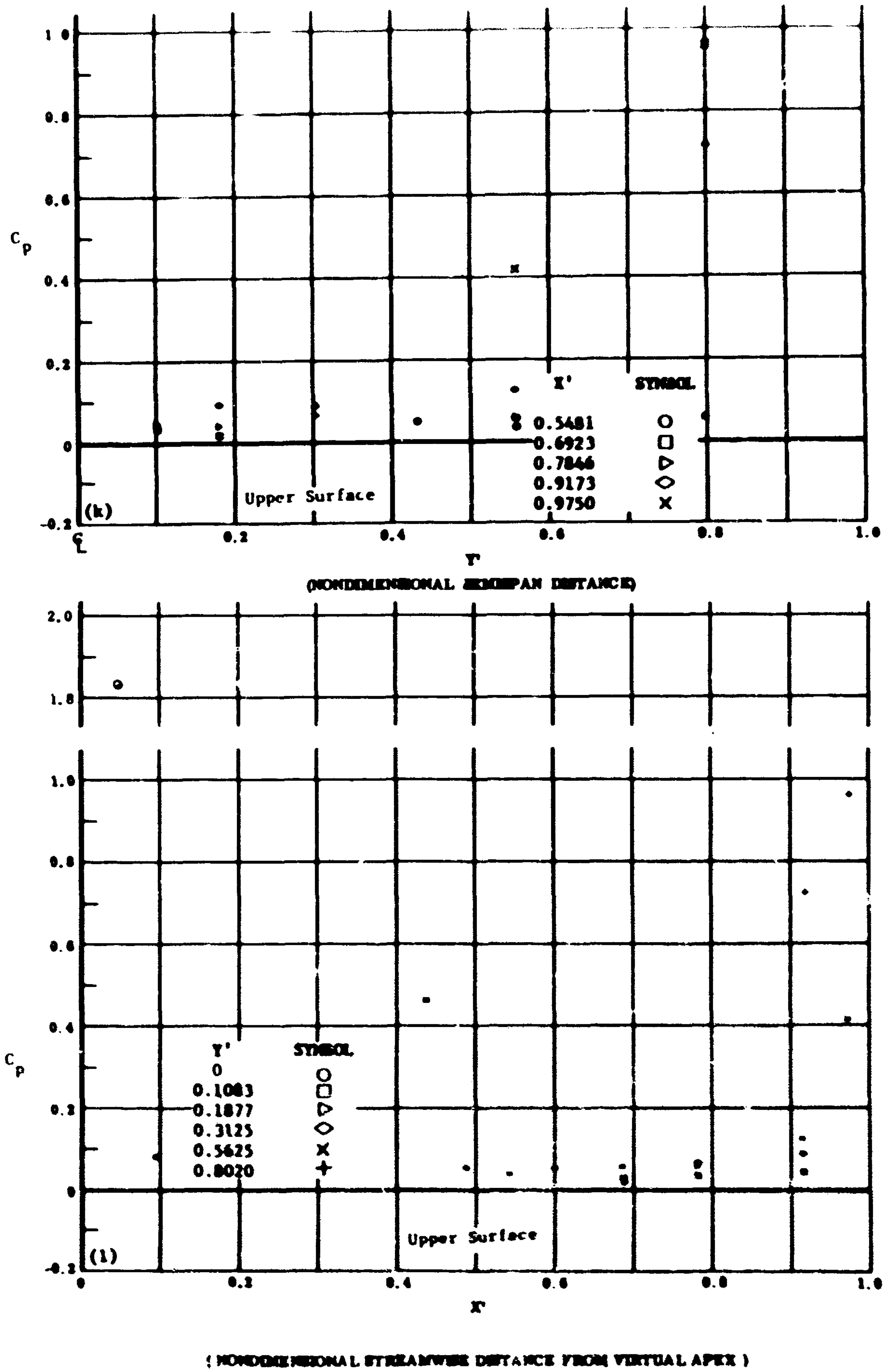

Fig. 20 Configuration IV, $\alpha = 0$, $\delta_2 = \delta_3 = -30$

k) C_p vs. Y', upper surface

l) C_p vs. X', upper surface

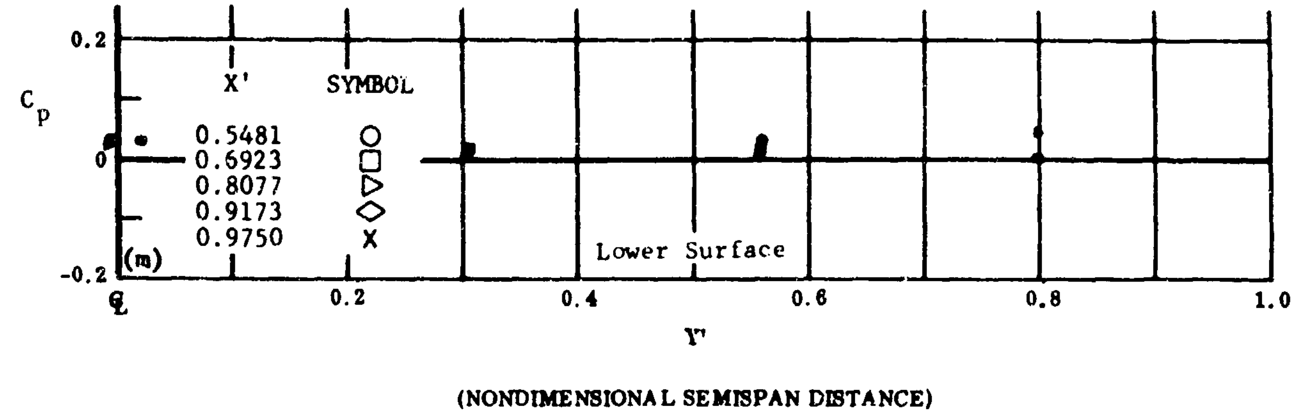

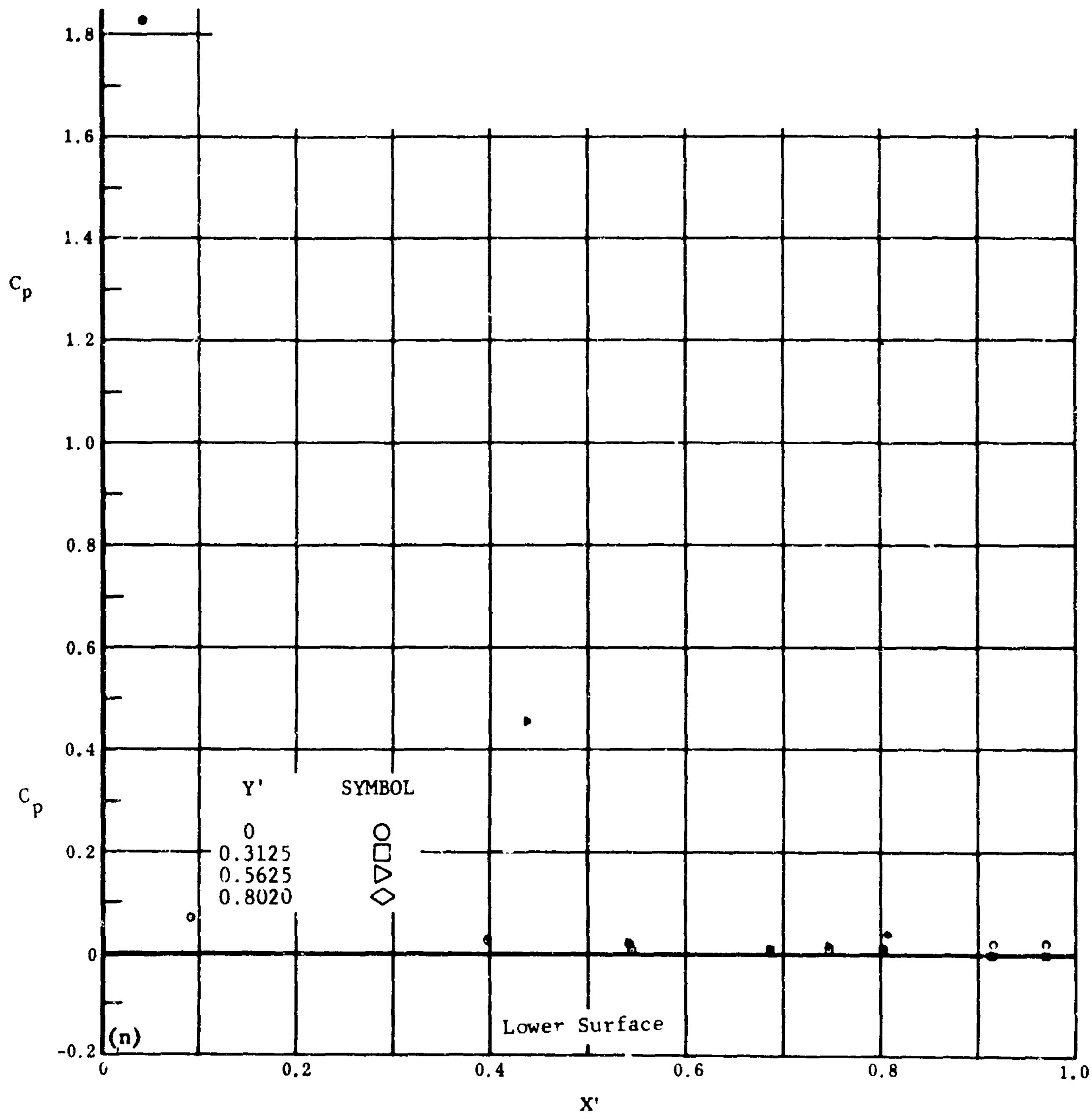

Fig. 30 Configuration IV, $\alpha = 0$, $\delta_2 = \delta_3 = -39$

m) C_p vs. Y', lower surface

n) C_p vs. X', lower surface

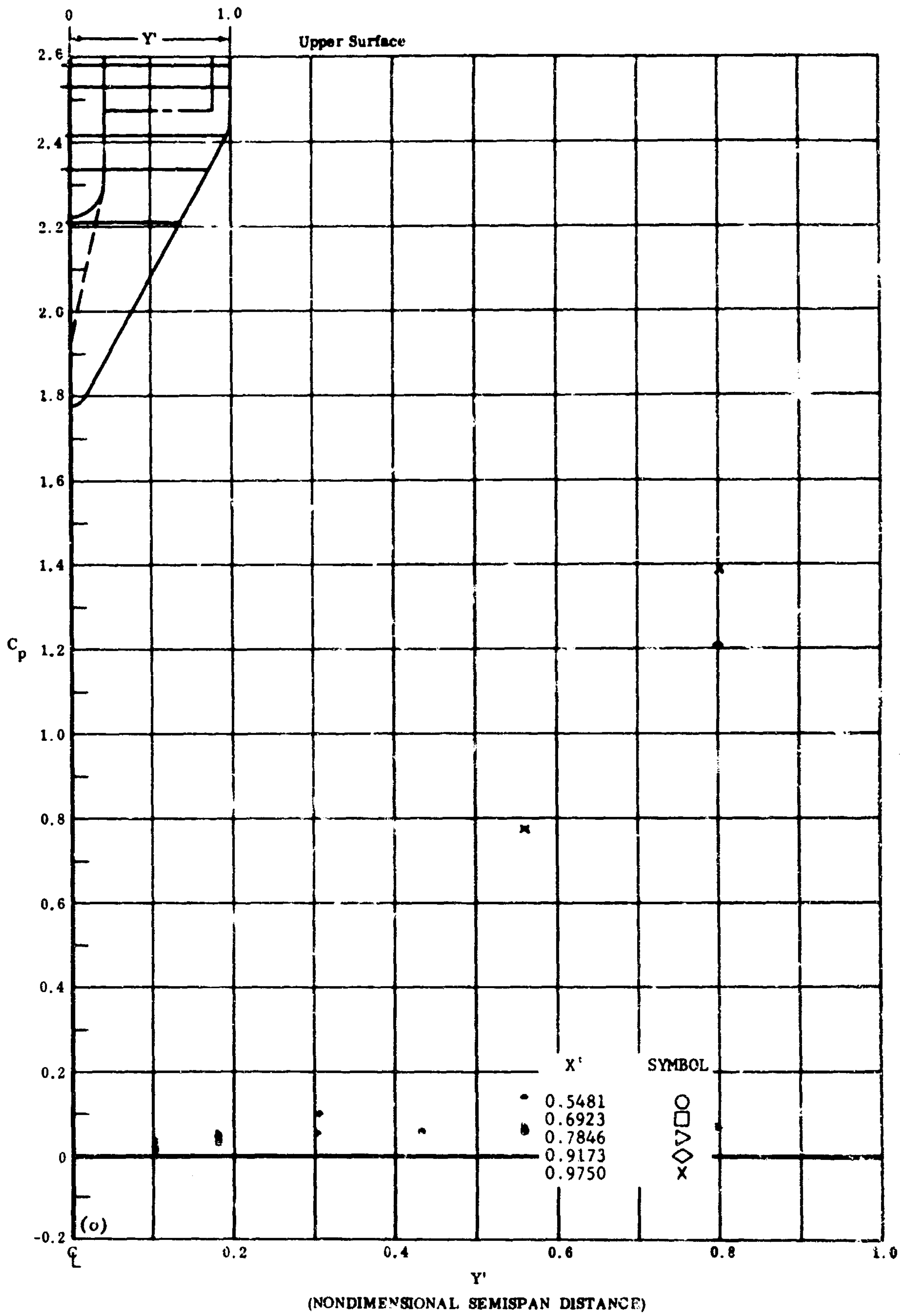

Fig. 30 Configuration IV, $\alpha = 0$, $\delta_2 = \delta_3 = -39$

o) C_p vs. Y', upper surface

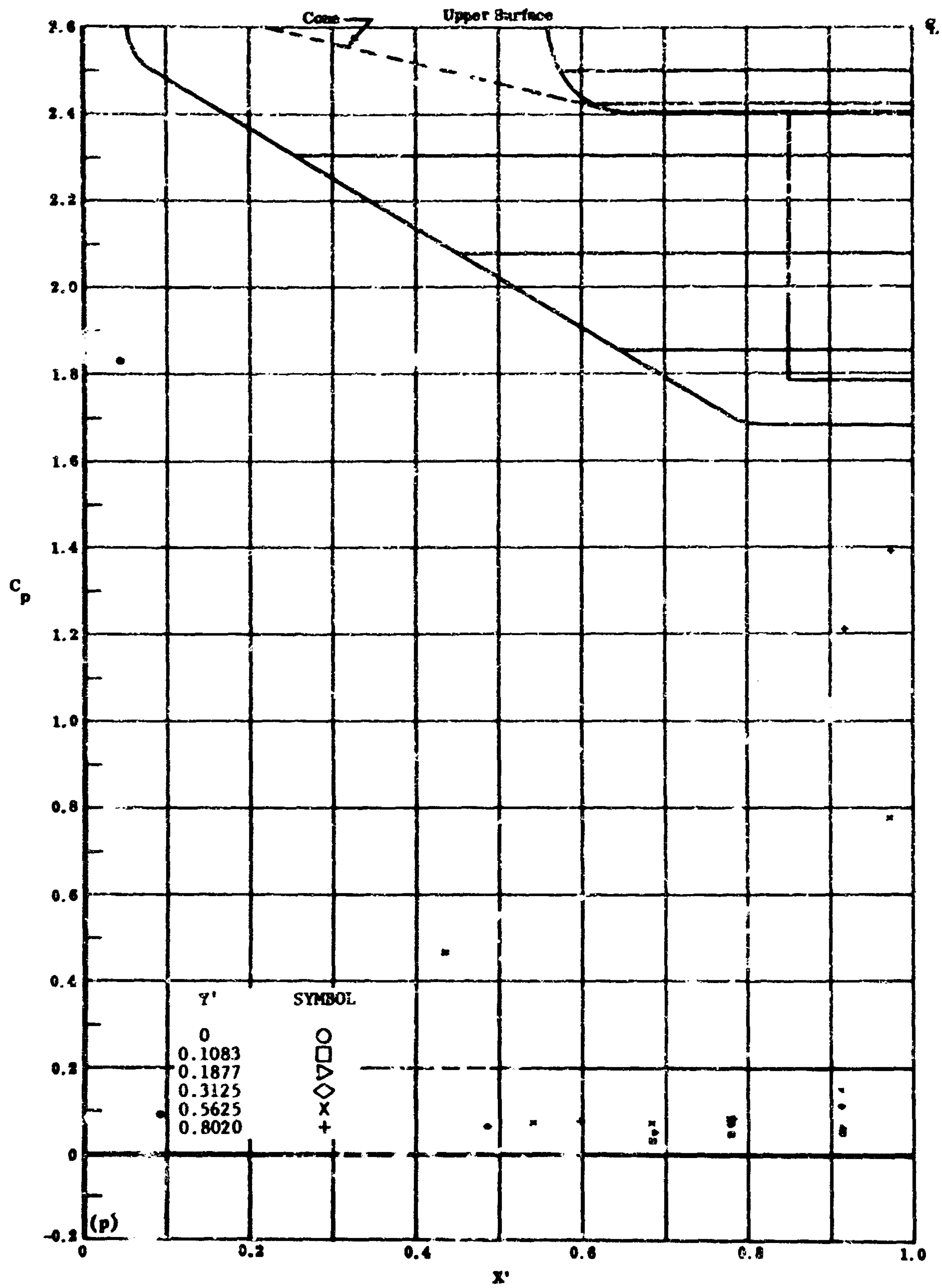

(NONDIMENSIONAL STREAMWISE DISTANCE FROM VIRTUAL APEX)

Fig 30 Configuration IV, $a = o$, $\delta_2 = \delta_3 = -39$

p) C_p vs. X', upper surface

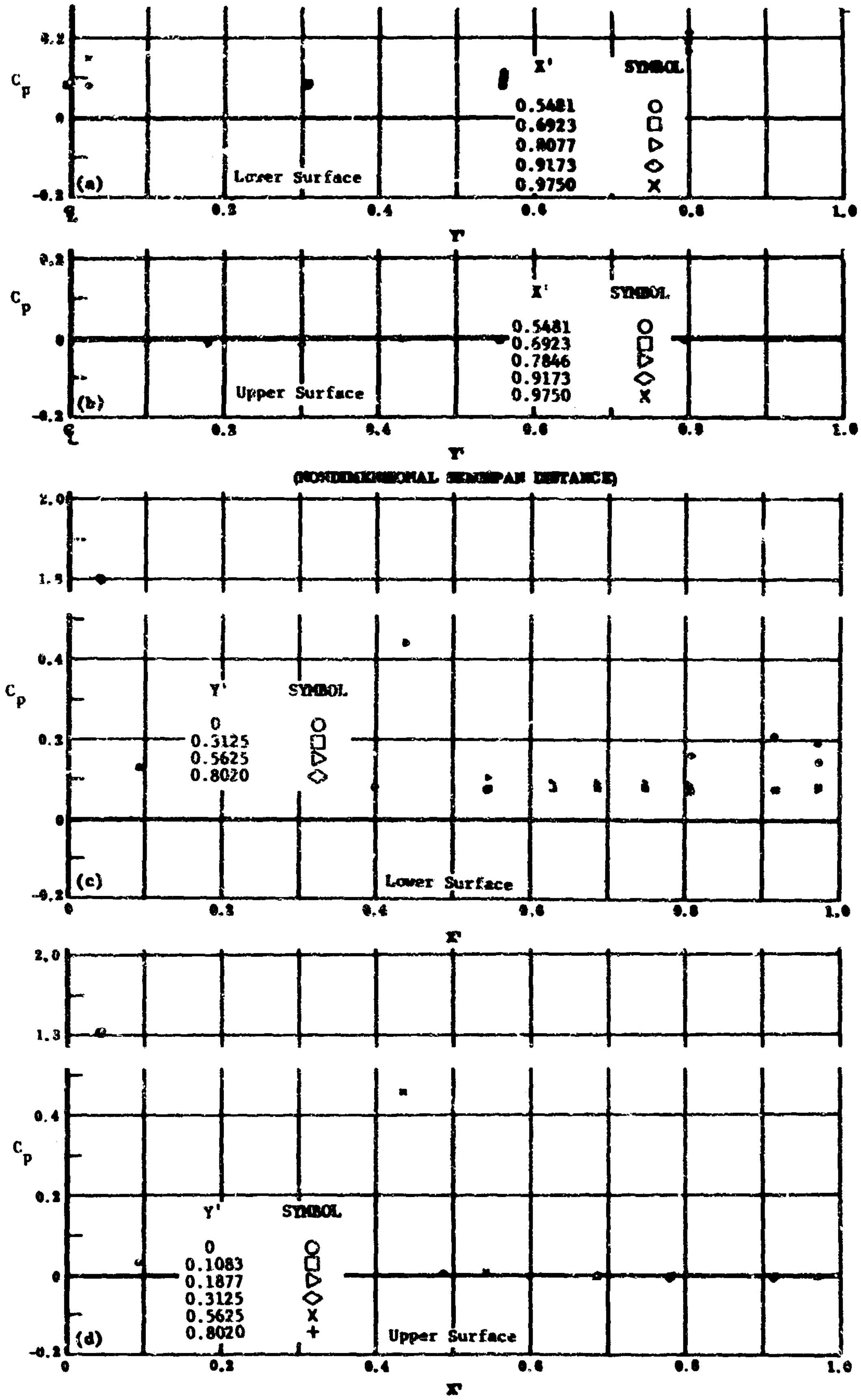

Fig. 31 Configuration IV, $\alpha = +10$, $\delta_2 = \delta_3 = 0$

a) C_p vs. Y', lower surface

b) C_p vs. Y', upper surface

c) C_p vs. X', lower surface

d) C_p vs. X', upper surface

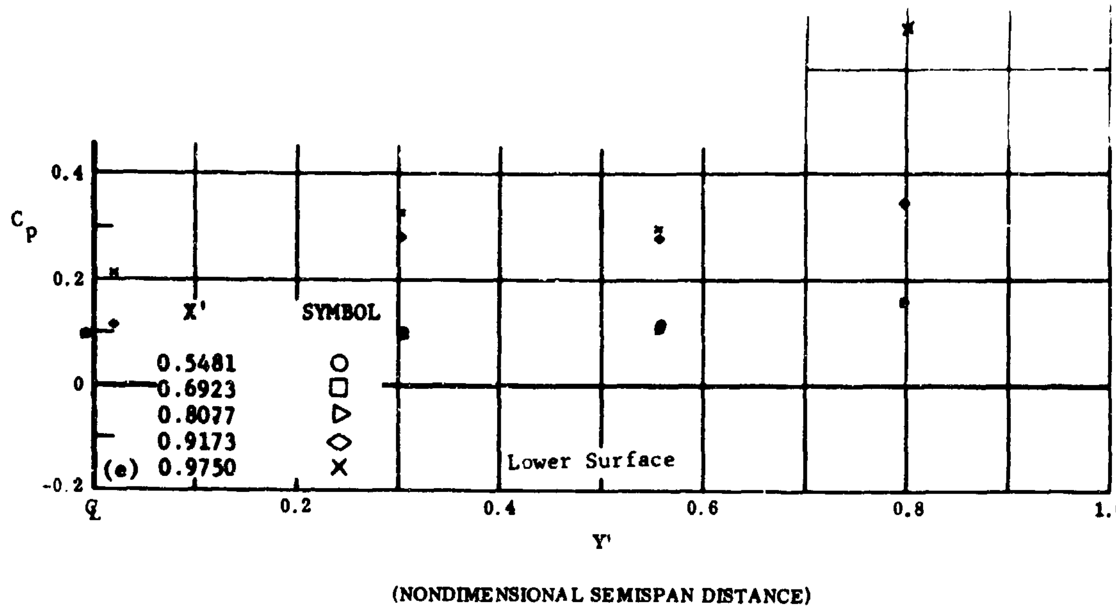

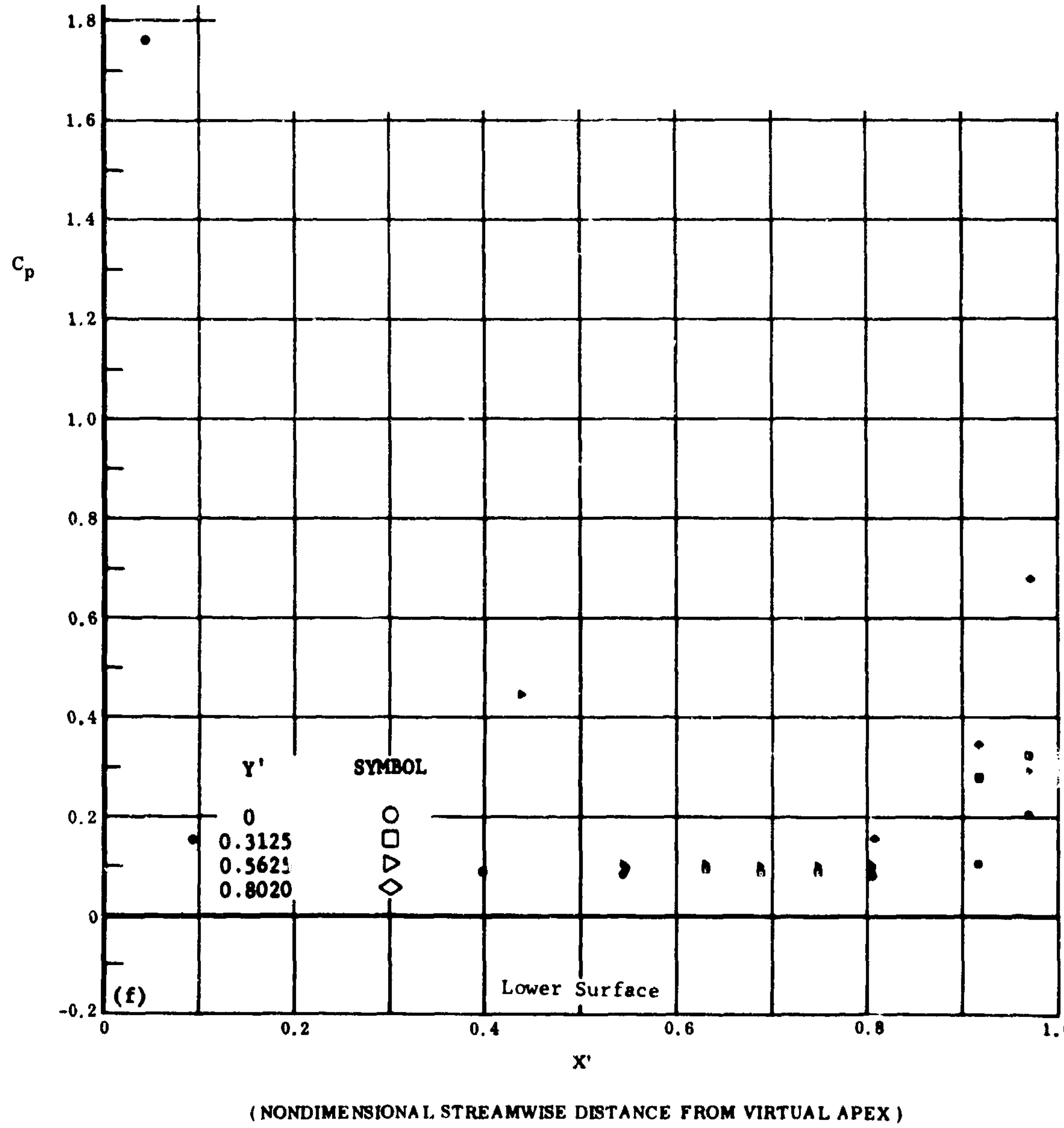

Fig. 31 Configuration IV, α = +10 , $\delta_2 = \delta_3$ = +10

e) C_p vs. Y', lower surface

f) C_p vs. X', lower surface

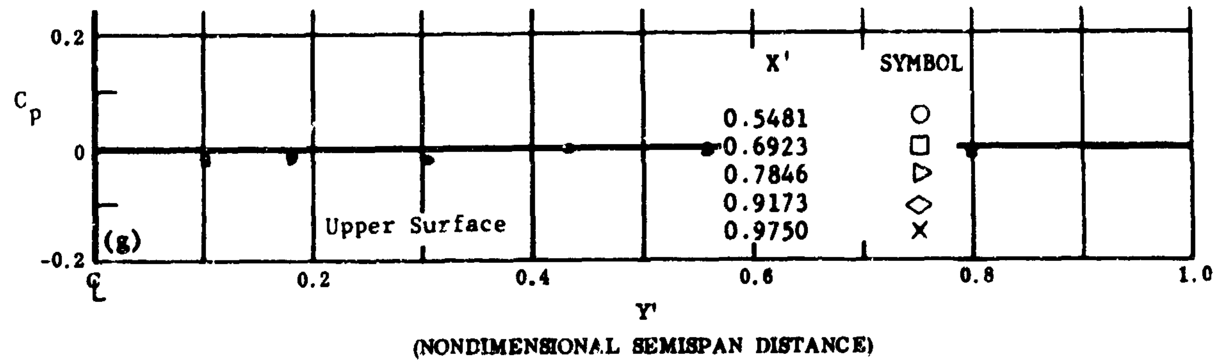

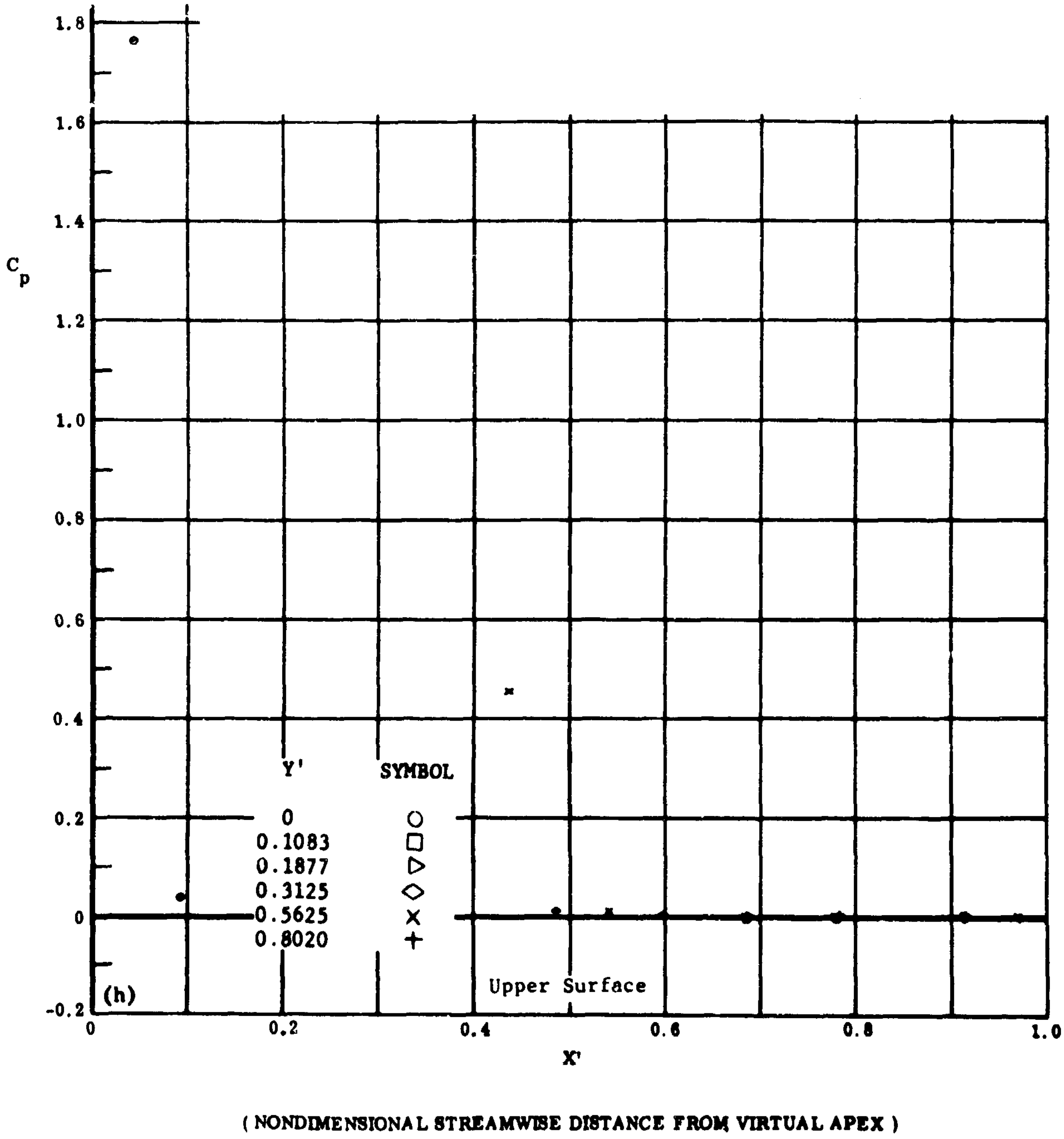

Fig. 31 Configuration IV, $\alpha = +10$, $\delta_2 = \delta_3 = +10$

g) C_p vs. Y', upper surface

h) C_p vs. X', upper surface

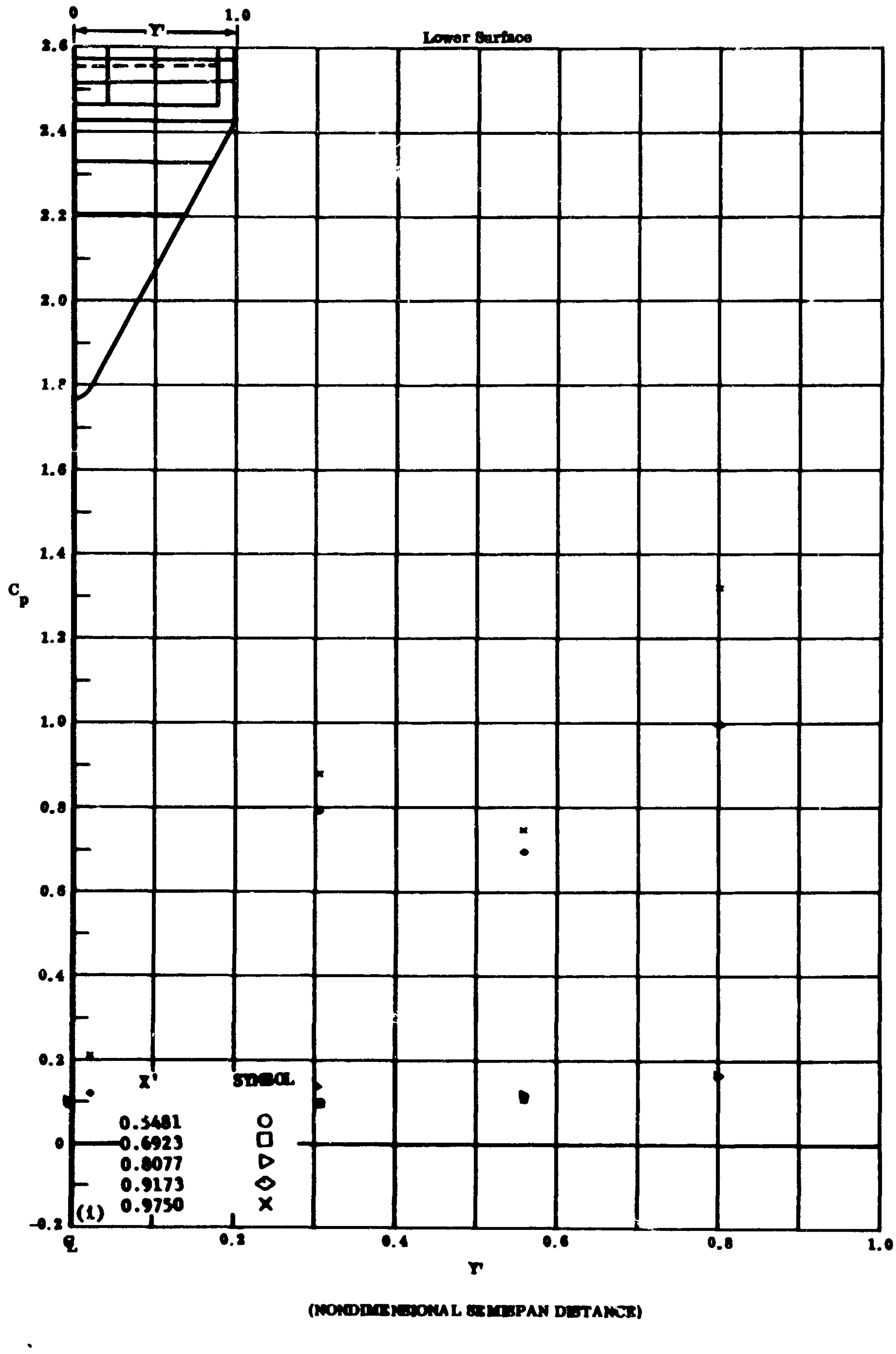

Fig. 311 Configuration IV, α = +10 , $\delta_2 = \delta_3$ = +20

C_p vs. Y', lower surface

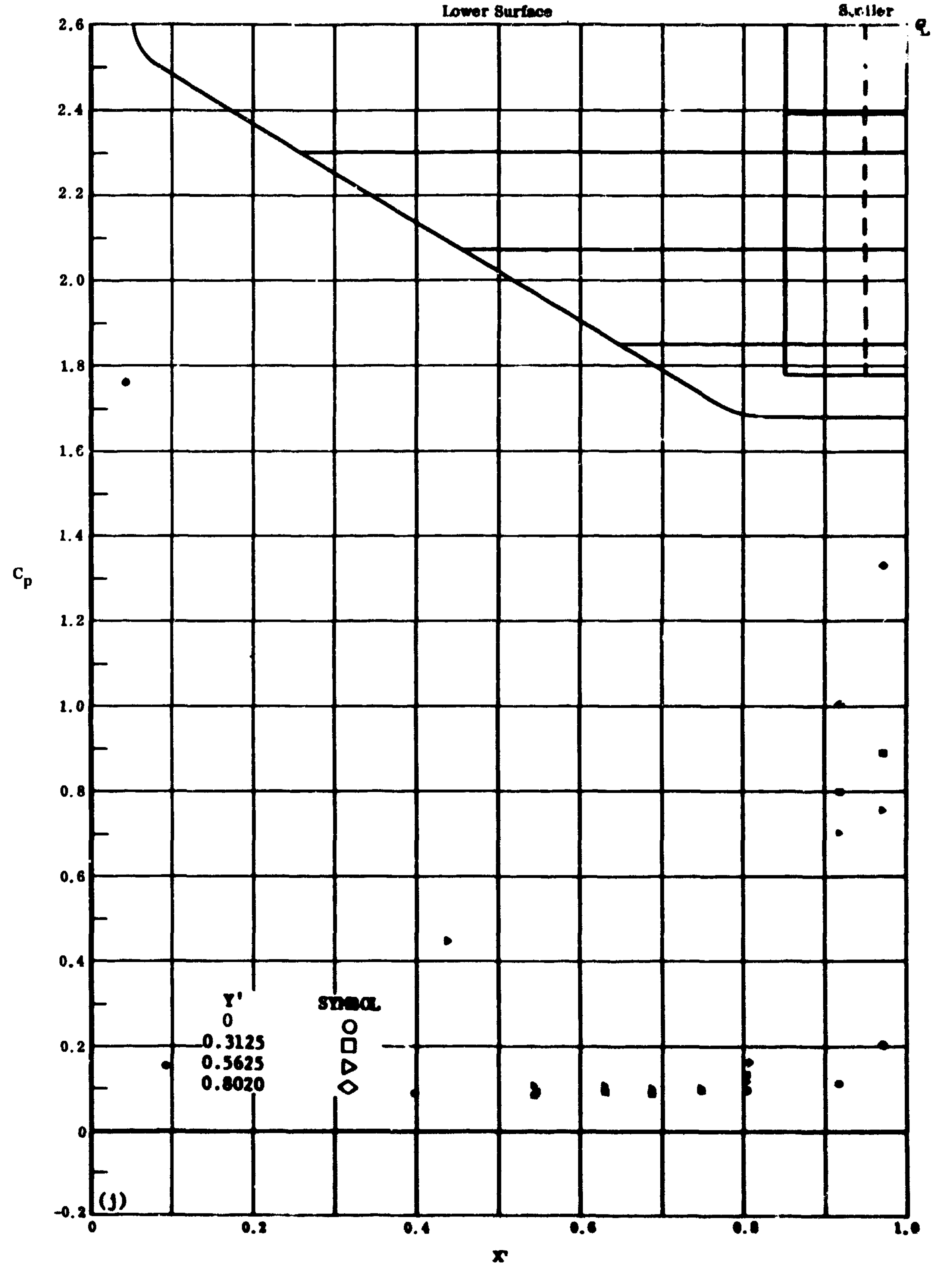

Fig. 31j Configuration IV, $\alpha = +10$, $\delta_2 = \delta_3 = +20$

C_p vs. X', lower surface

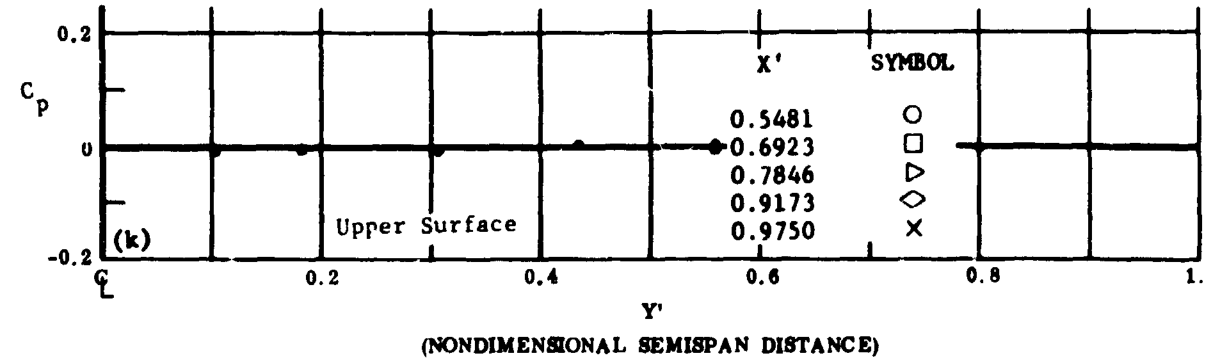

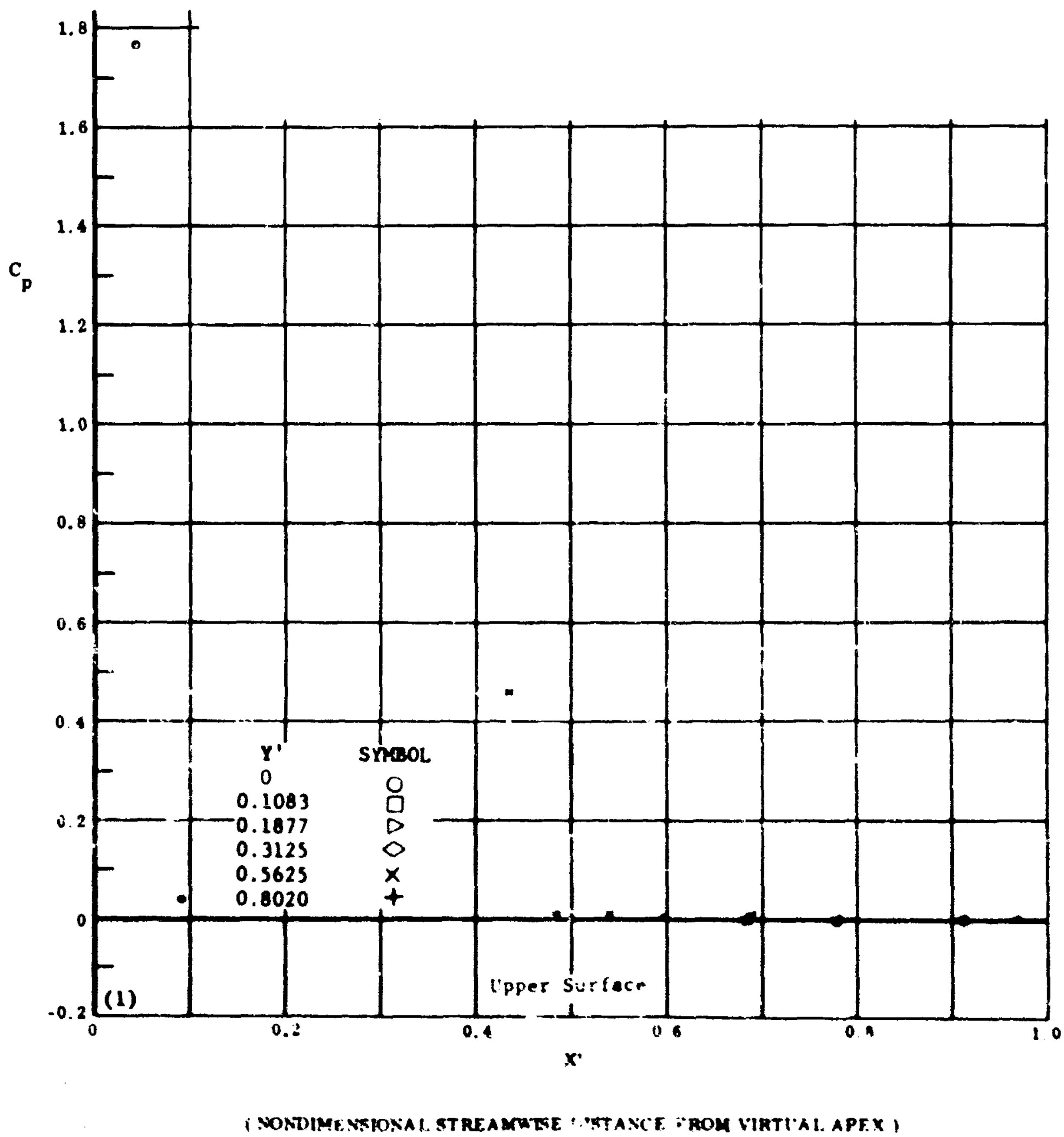

Fig. ... Configuration IV, α = +10 , $\delta_2 = \delta_3$ = +20

k) C_p vs. Y', upper surface

l) C_p vs. X', upper surface

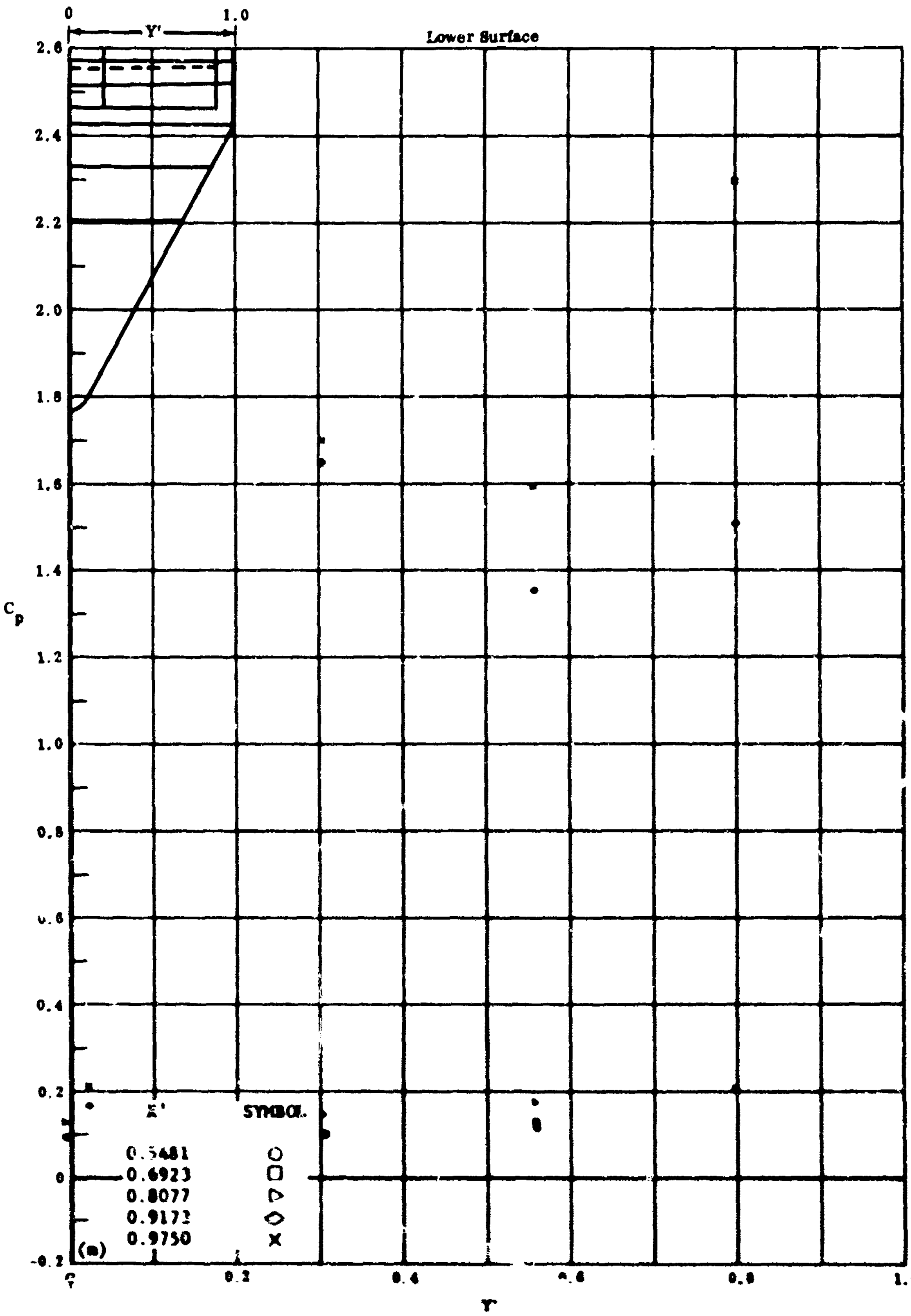

Fig. 31m Configuration IV, α = +10 , $\delta_2 = \delta_3$ = +30

C_p vs. Y', lower surface

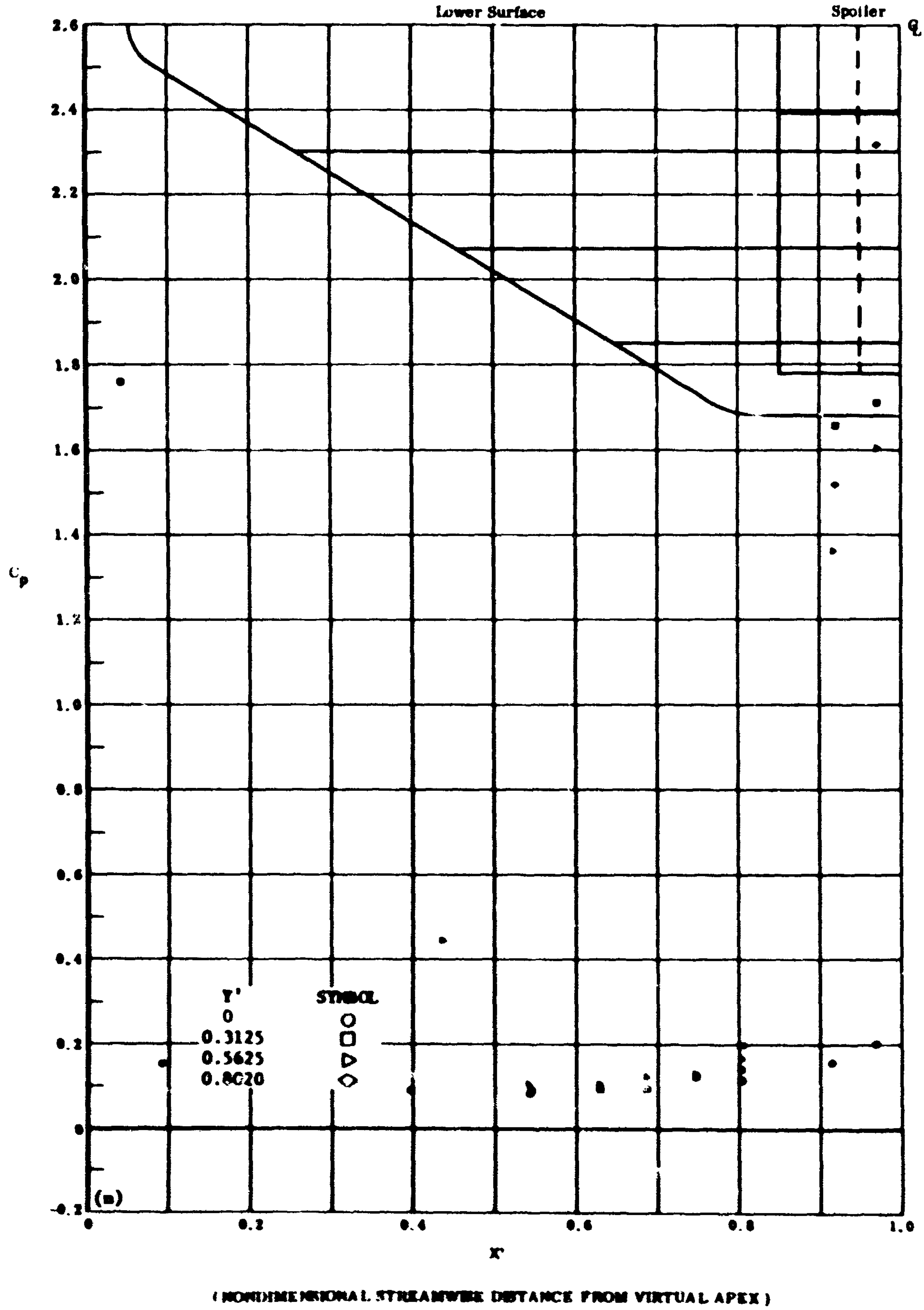

Fig. 31m Configuration IV, $\alpha = +10$, $\delta_2 = \delta_3 = +30$

C_p vs. X', lower surface

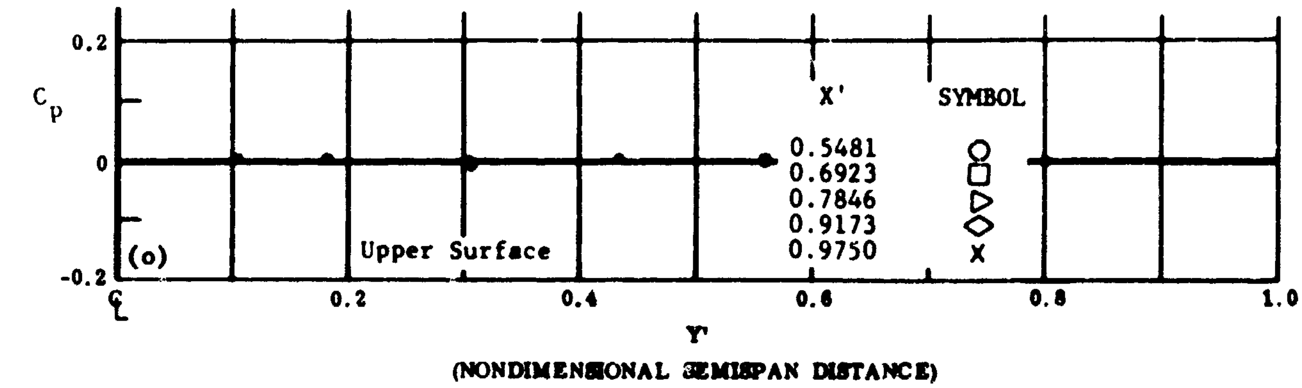

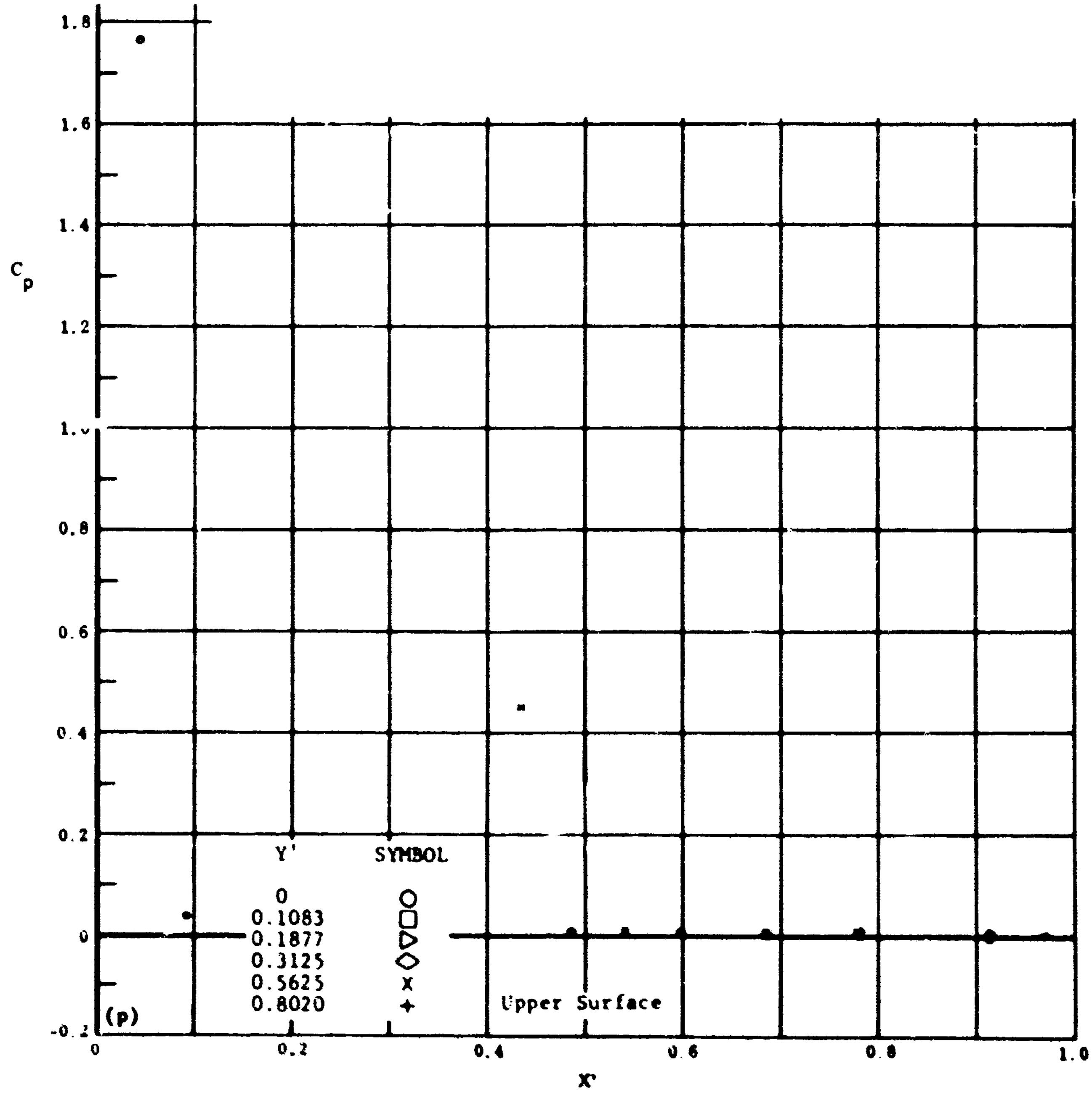

Fig. 3?. Configuration IV, $\alpha = +10$, $\delta_2 = \delta_3 = +30$

o) C_p vs. Y', upper surface

p) C_p vs. X', upper surface

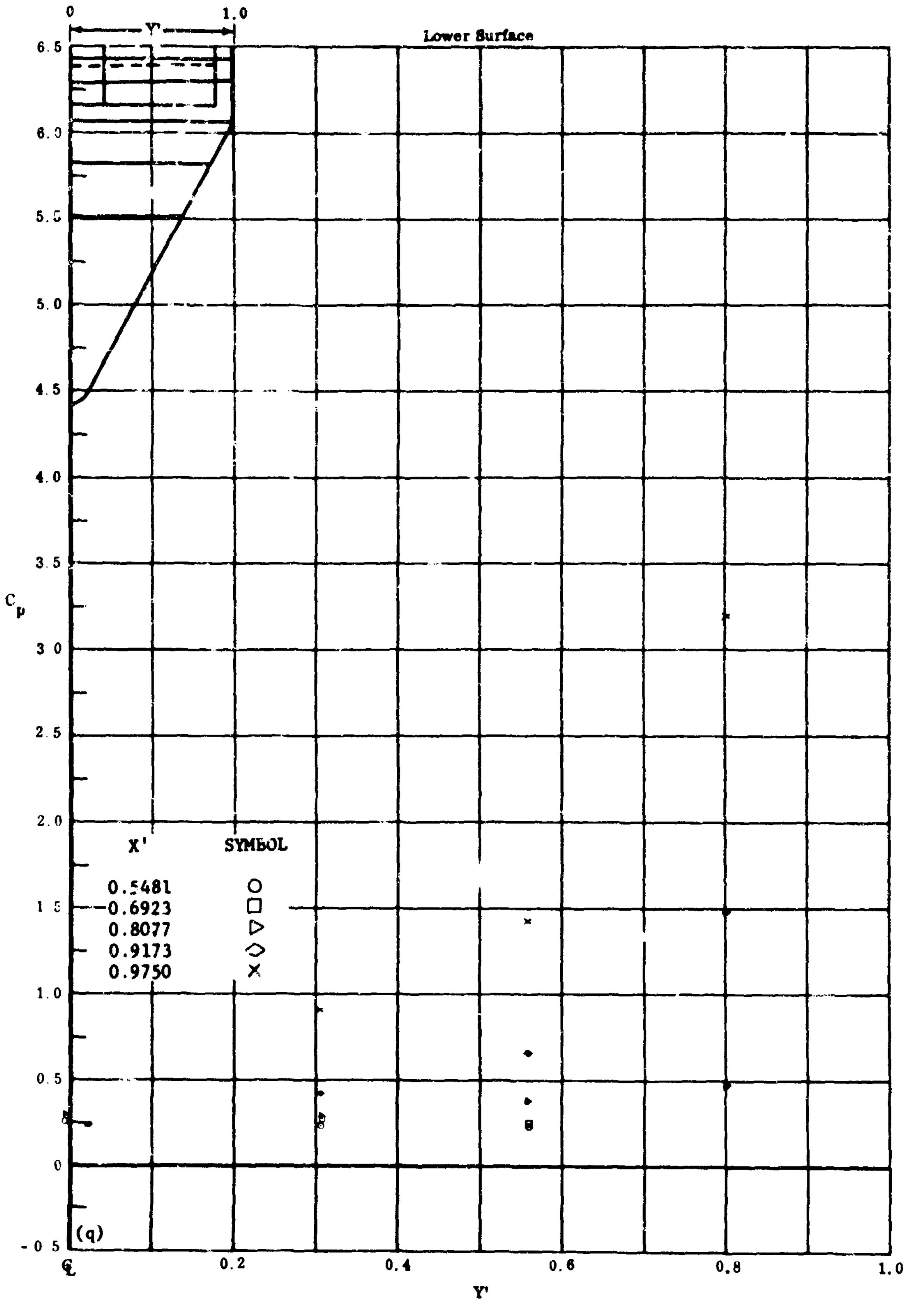

Fig. 31q Configuration IV, α = +10 , $\delta_2 = \delta_3$ = +39
C_p vs. Y', lower surface

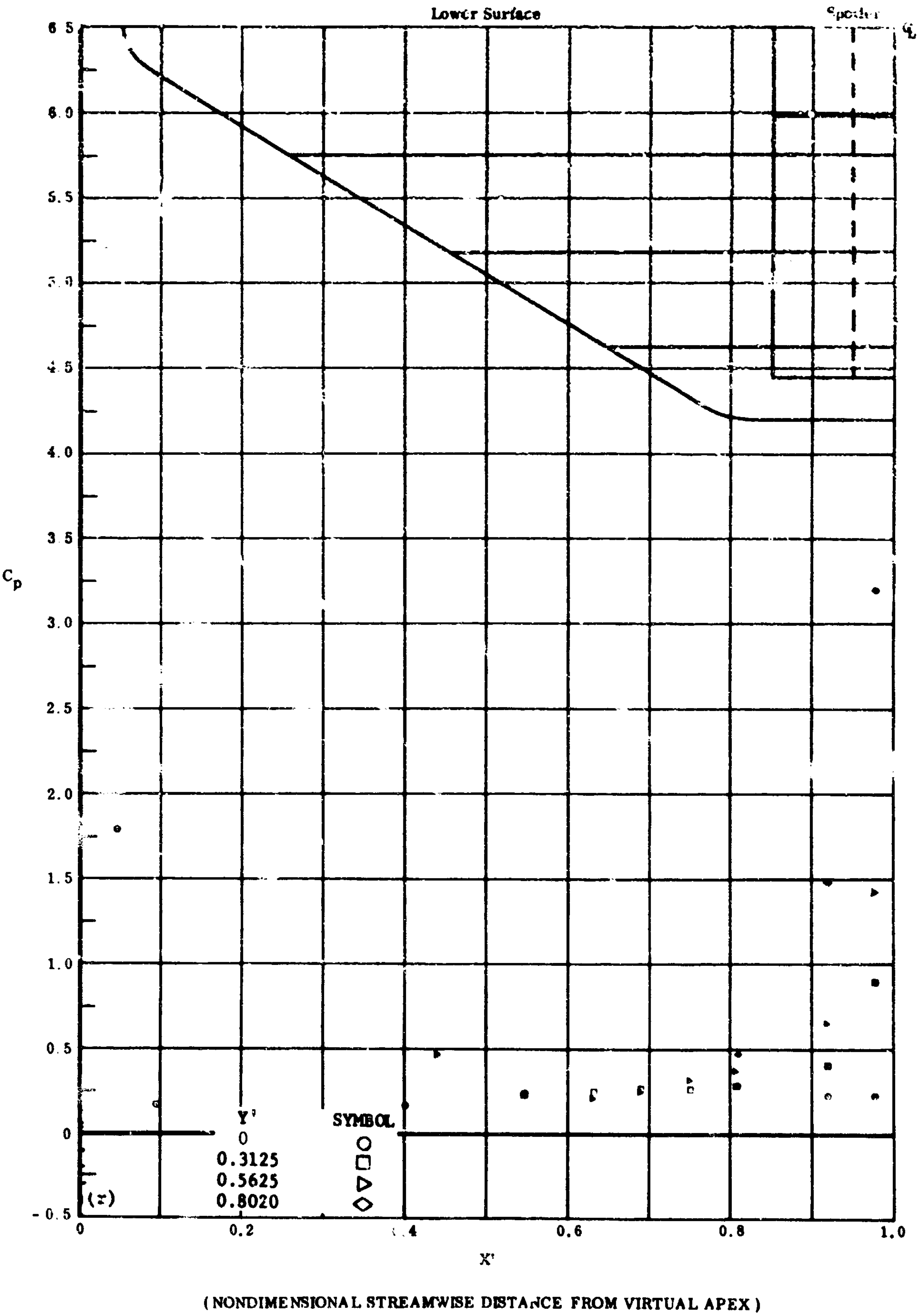

Fig. 31r Configuration IV, $\alpha = +10$, $\delta_2 = \delta_3 = +39$

C_p vs. X', lower surface

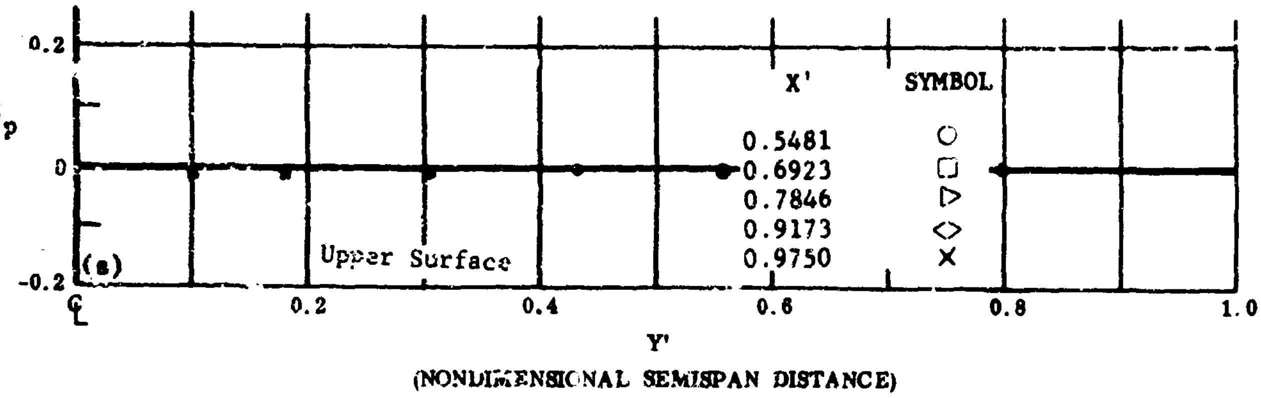

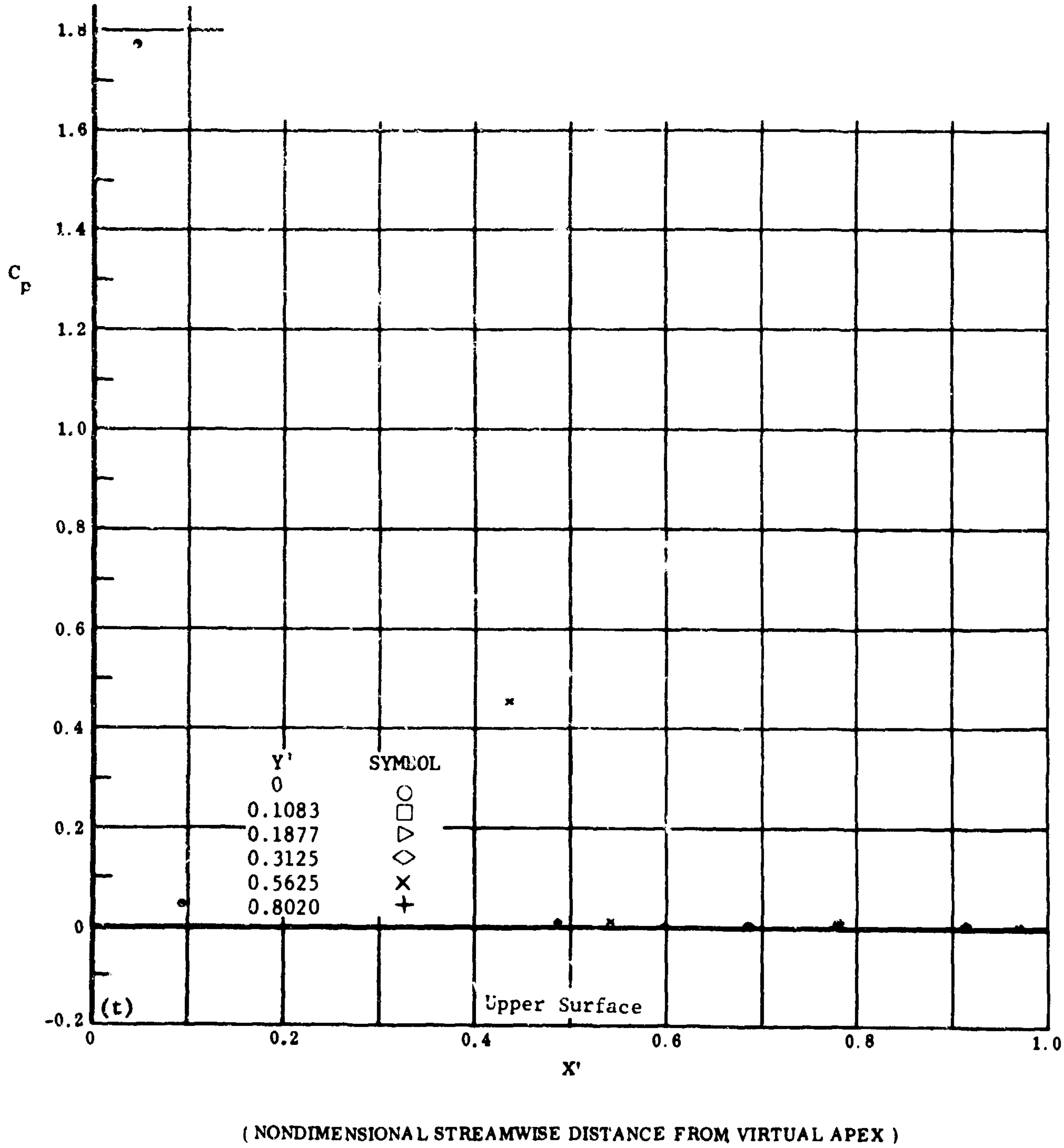

Fig. 31 Configuration IV, $\alpha = +10$, $\delta_2 = \delta_3 = +39$

s) C_p vs. Y', upper surface

t) C_p vs. X', upper surface

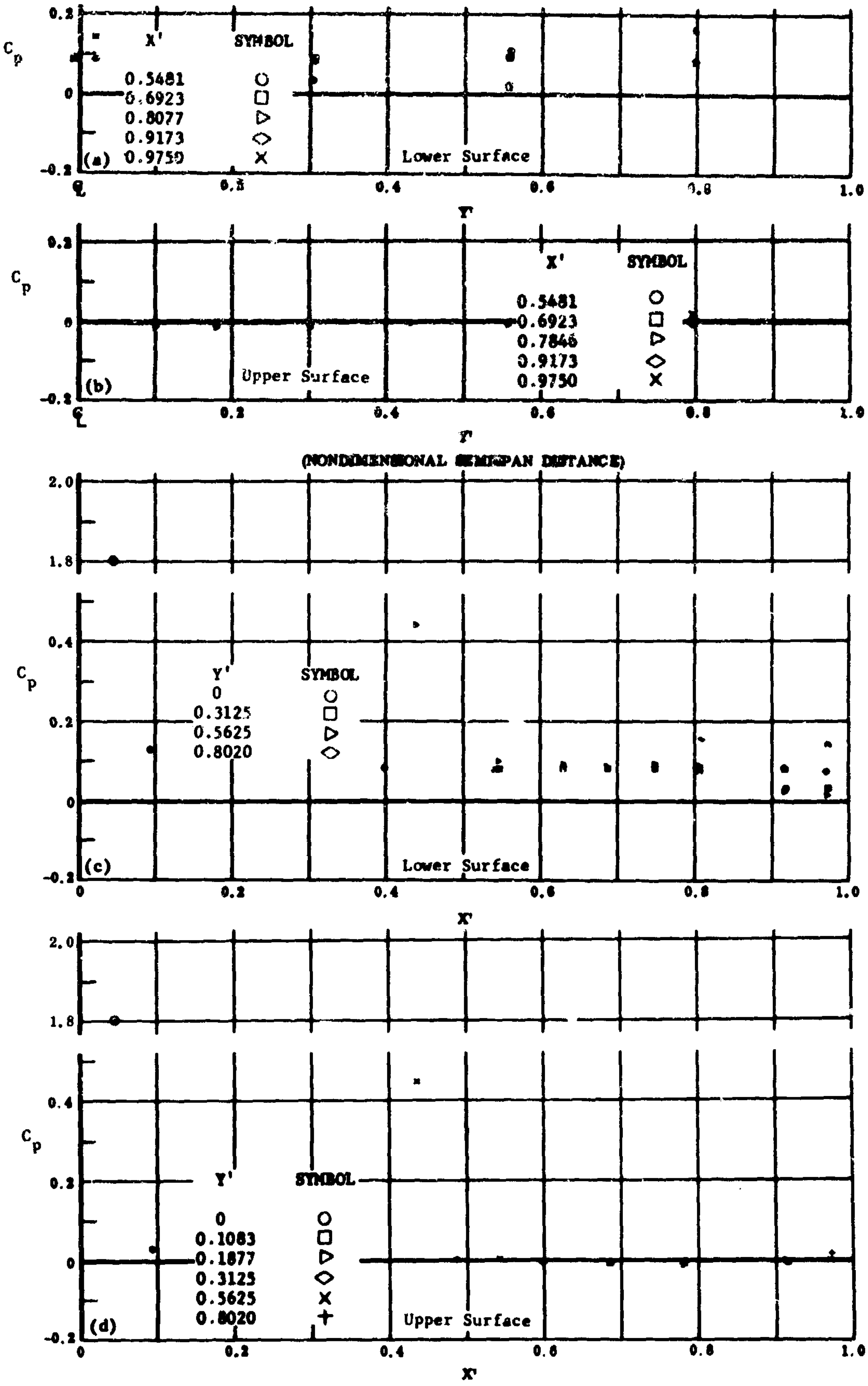

(NONDIMENSIONAL STREAMWISE DISTANCE FROM VIRTUAL APEX)

Fig. 32 Configuration IV, $\alpha = +10$, $\delta_2 = \delta_3 = -10$

a) C_p vs. Y', lower surface

b) C_p vs. Y', upper surface

c) C_p vs. X', lower surface

d) C_p vs. X', upper surface

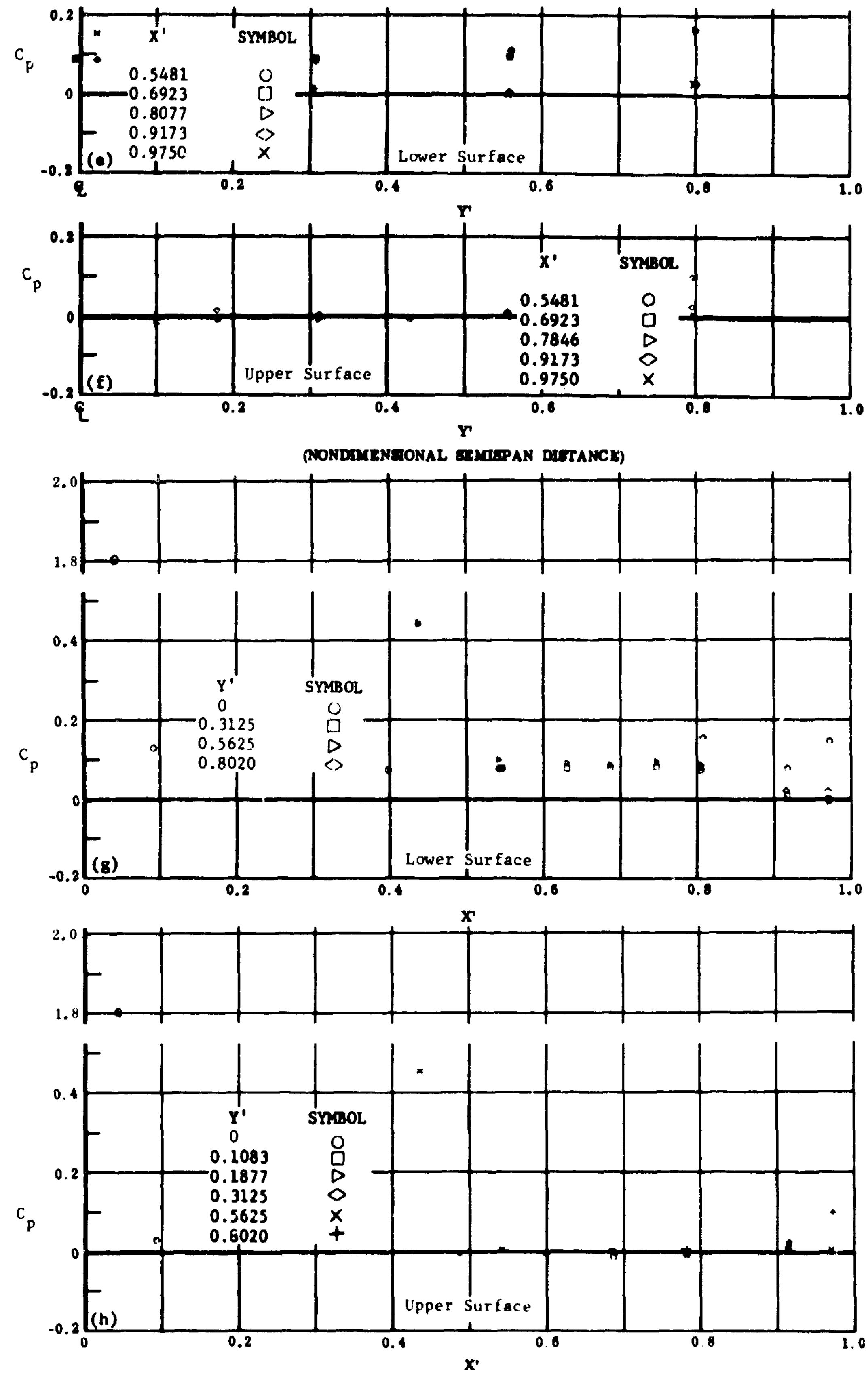

Fig. 32 Configuration IV, α = +10 , $\delta_2 = \delta_3$ = -20

e) C_p vs. Y', lower surface

f) C_p vs. Y', upper surface

g) C_p vs. X', lower surface

h) C_p vs. X', upper surface

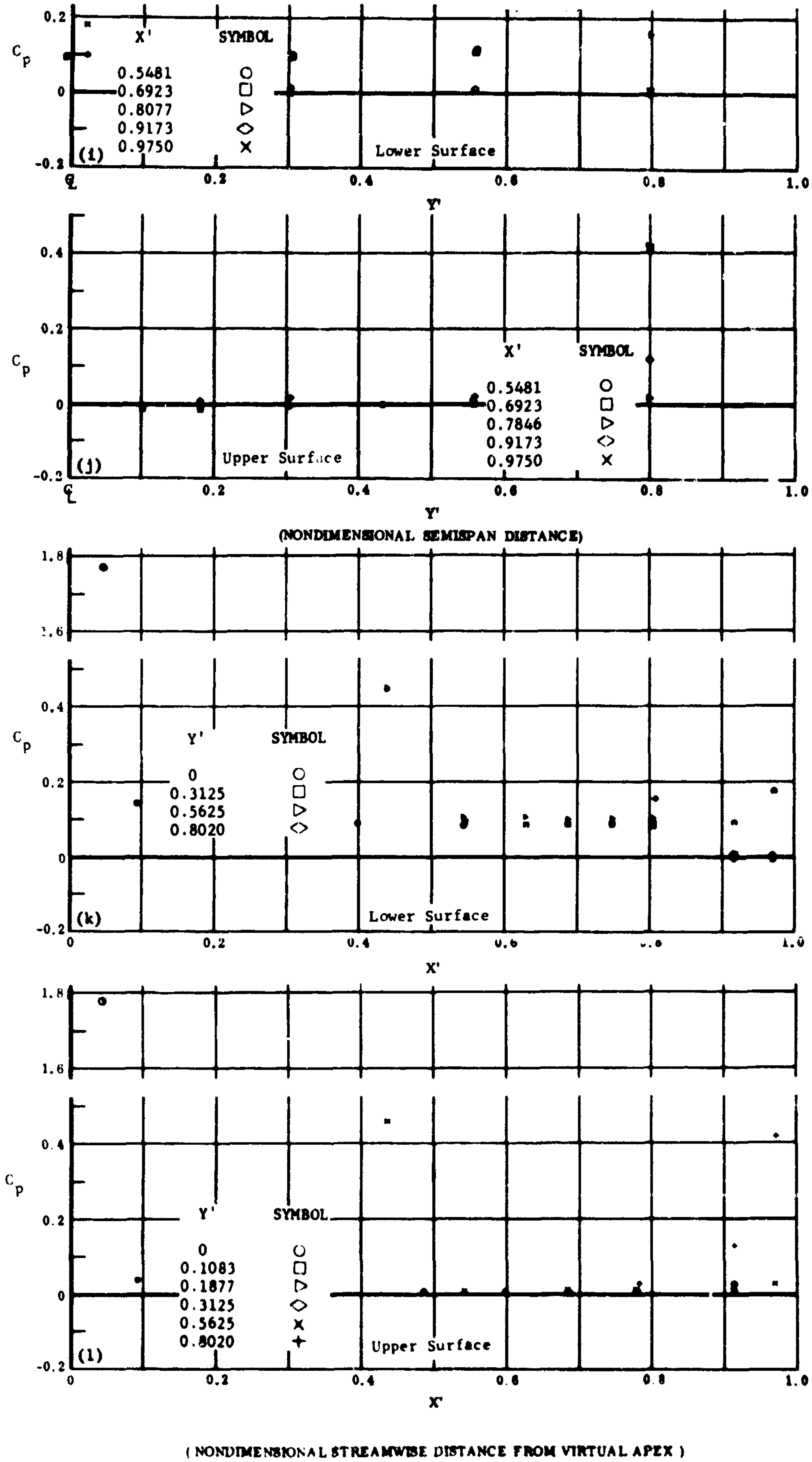

Fig. 32 Configuration IV, α = +10, $\delta_2 = \delta_3$ = -30

i) C_p vs. Y', lower surface

j) C_p vs. Y', upper surface

k) C_p vs. X', lower surface

l) C_p vs. X', upper surface

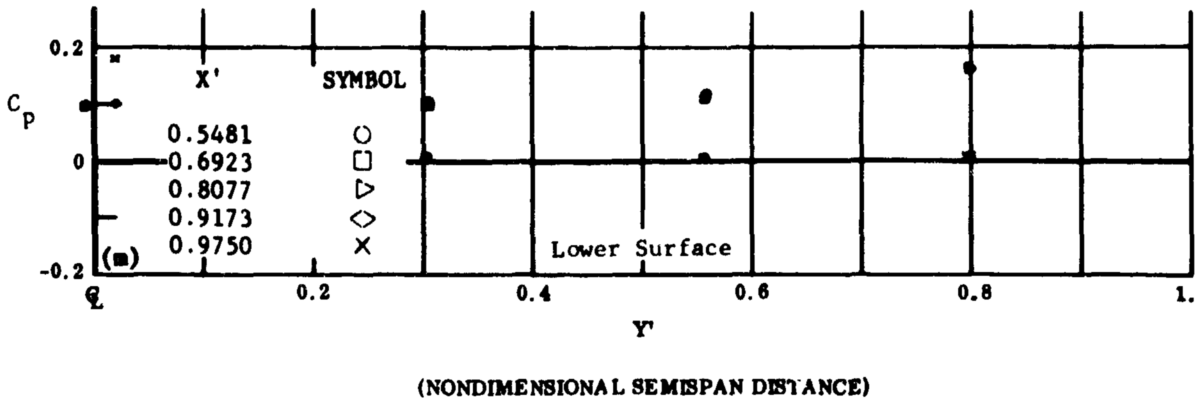

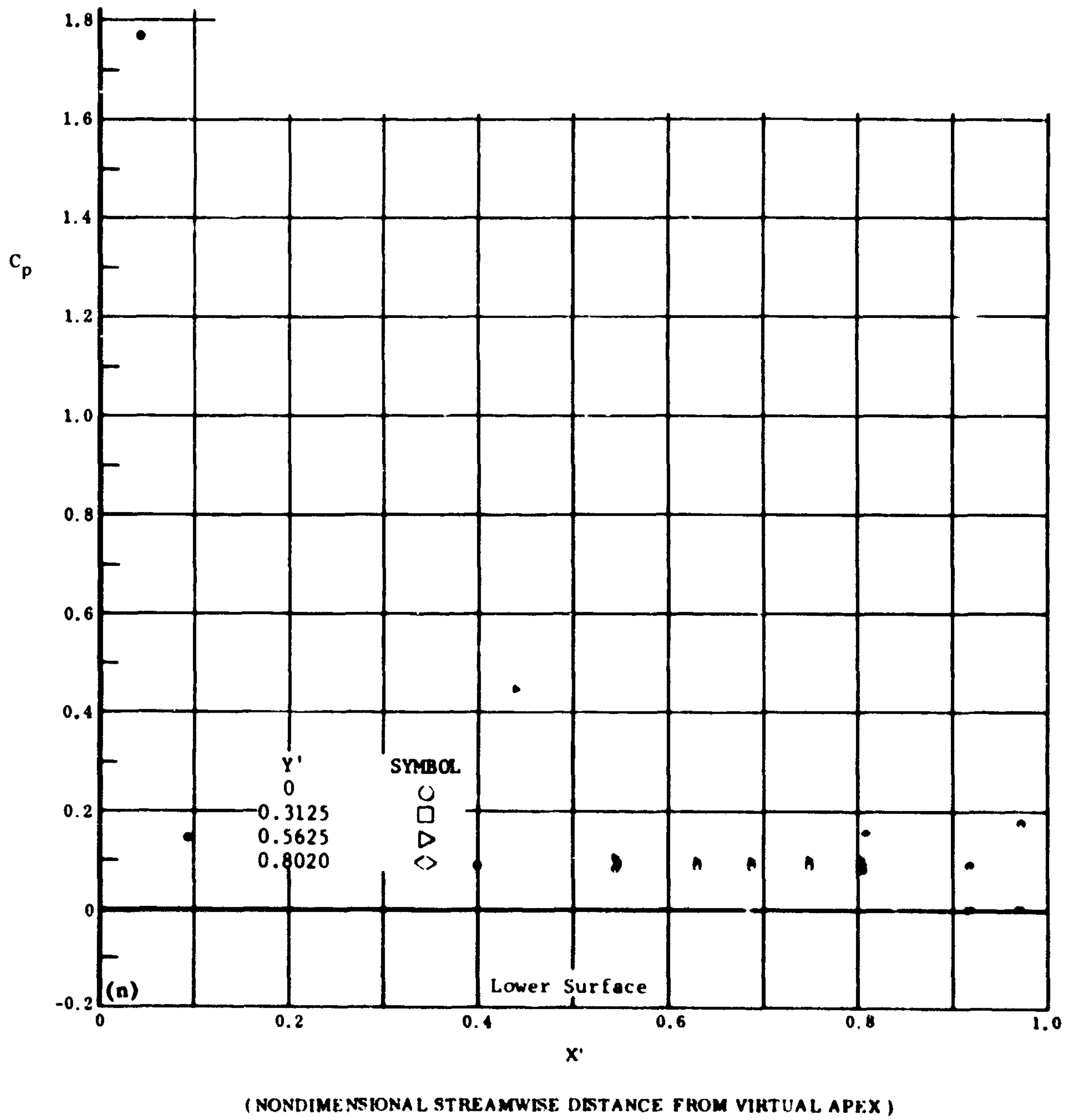

Fig. 32 Configuration IV, $\alpha = +10$, $\delta_2 = \delta_3 = -39$

m) C_p vs. Y', lower surface

n) C_p vs. X', lower surface

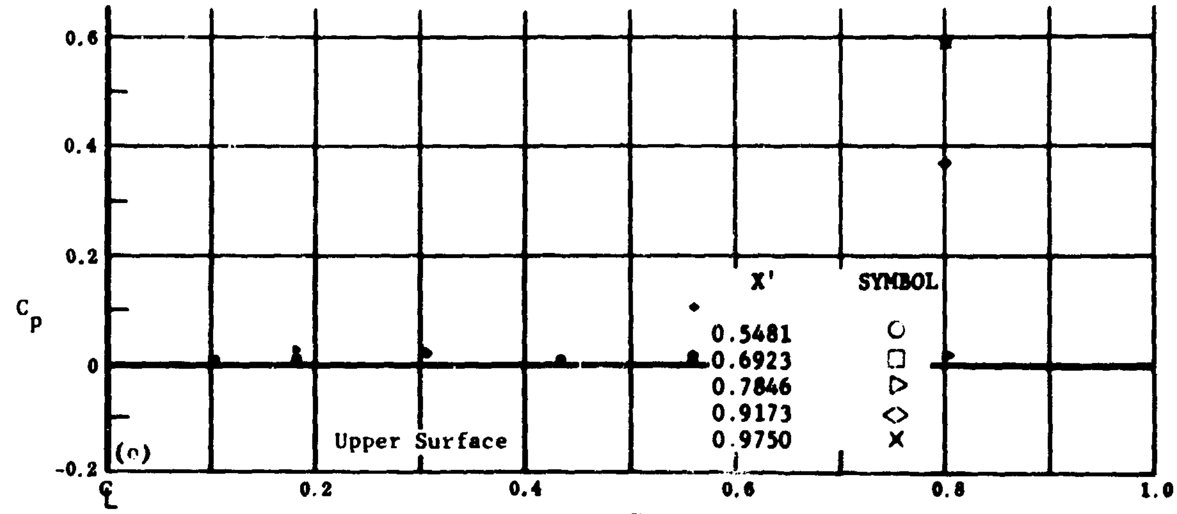

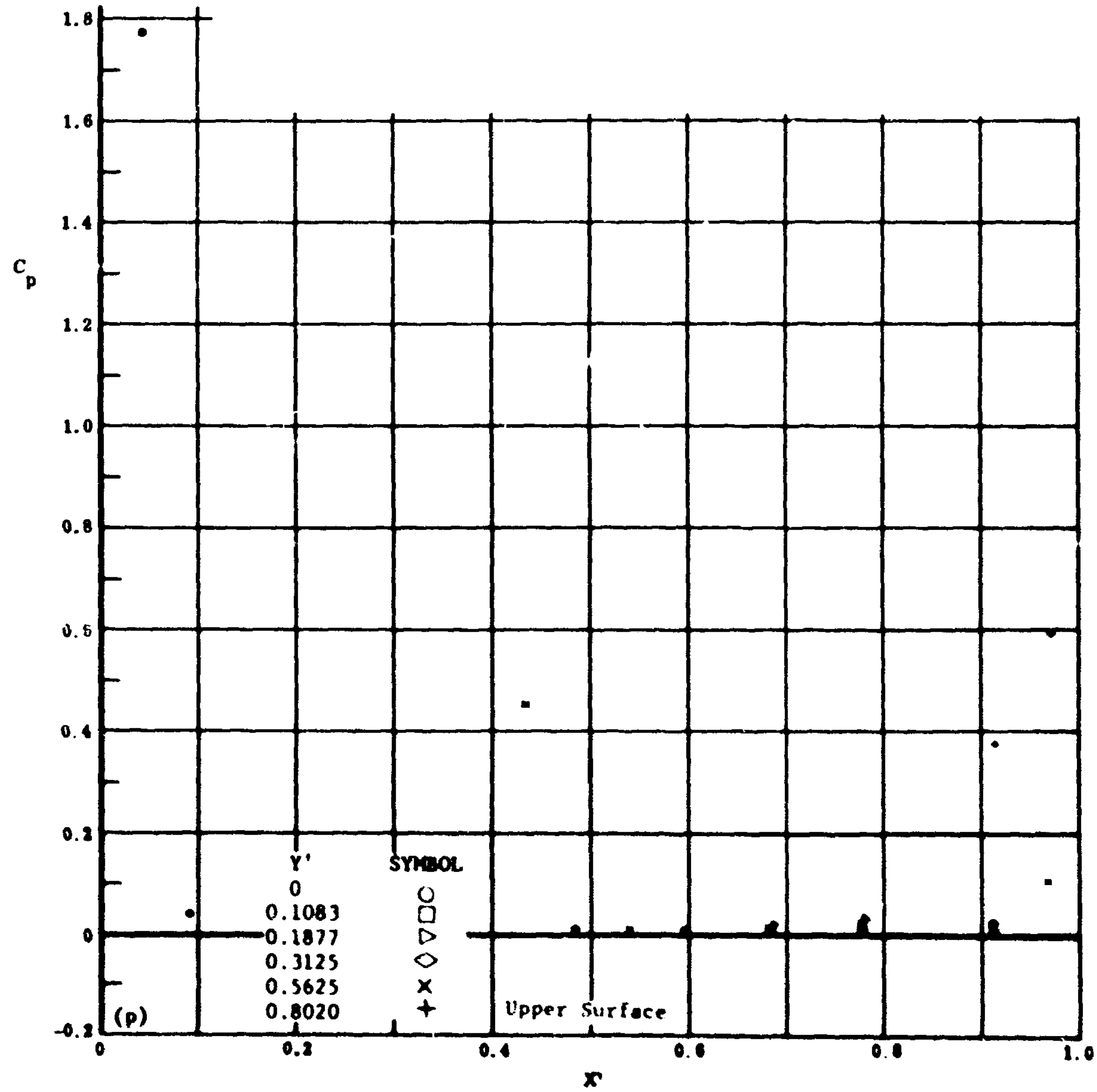

(NONDIMENSIONAL STREAMWISE DISTANCE FROM VIRTUAL APEX)

Fig. 32 Configuration IV, $\alpha = +10$, $\delta_2 = \delta_3 = -39$

o) C_p vs. Y', upper surface

p) C_p vs. X', upper surface

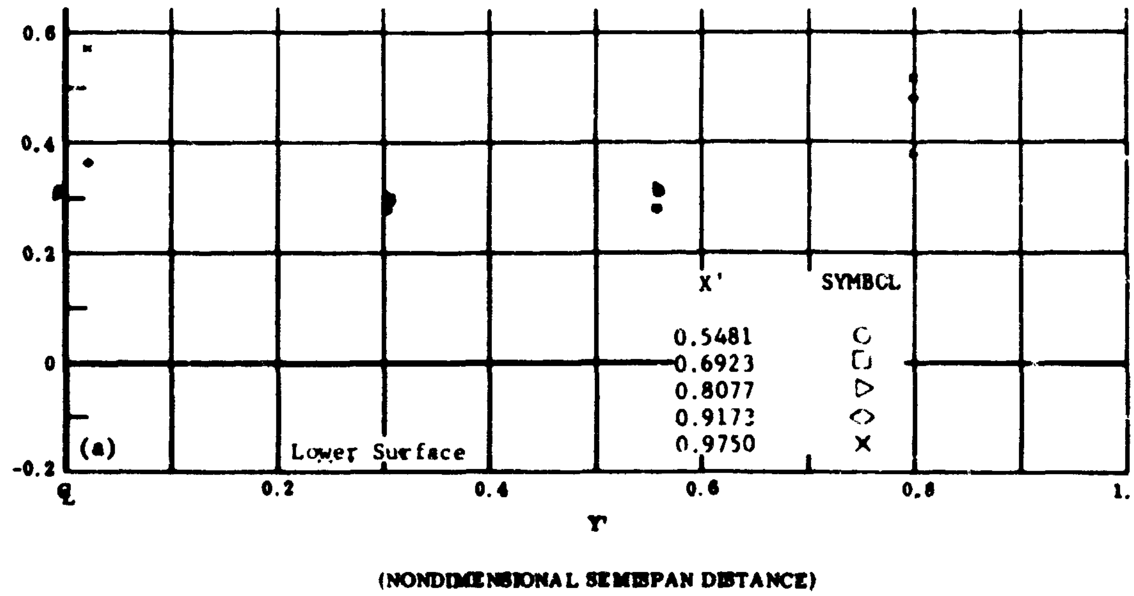

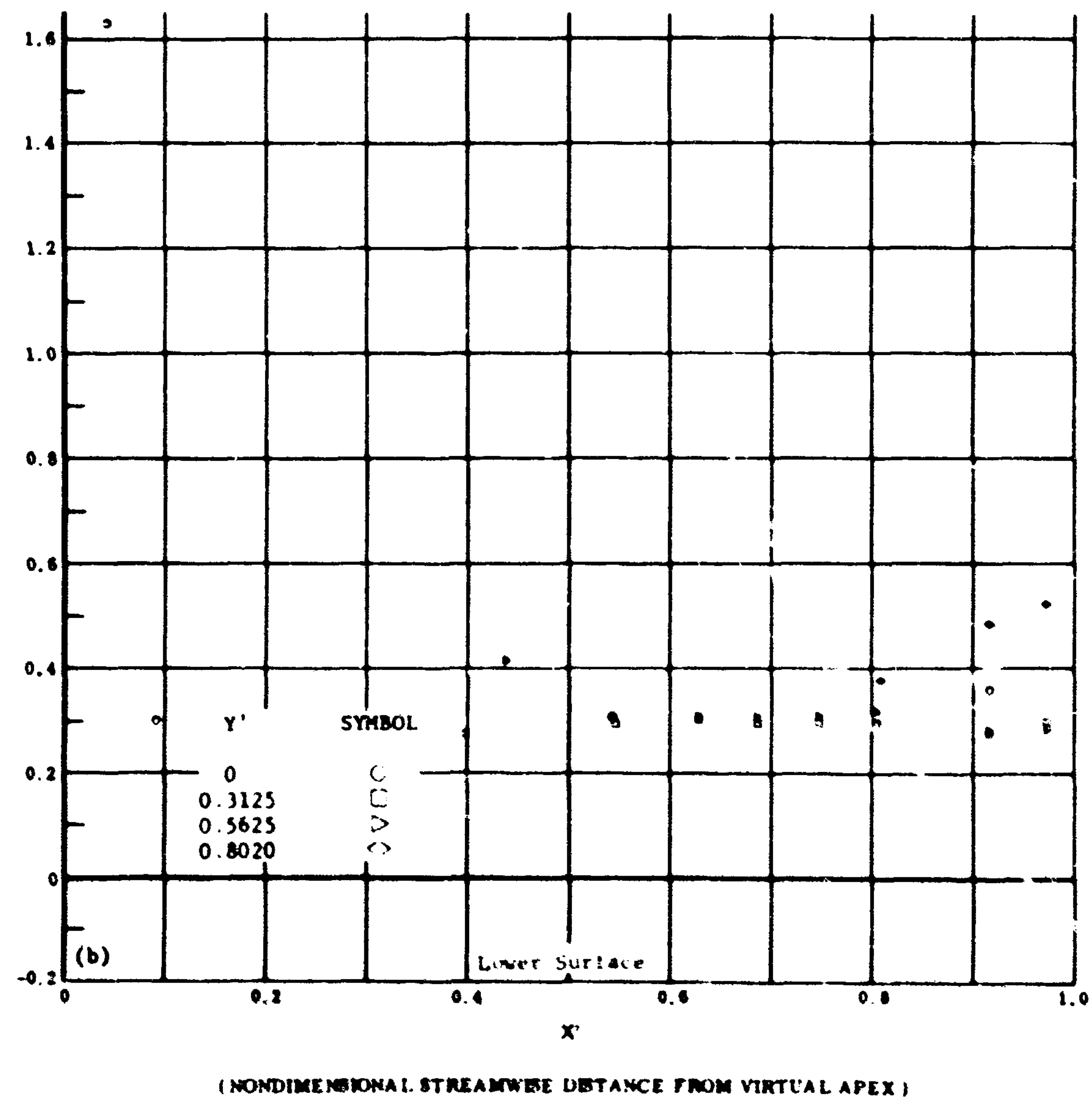

Fig. 33 Configuration IV, $\alpha = +20$, $\delta_2 = \delta_3 = 0$

a) C_p vs. Y', lower surface

b) C_p vs. X', lower surface

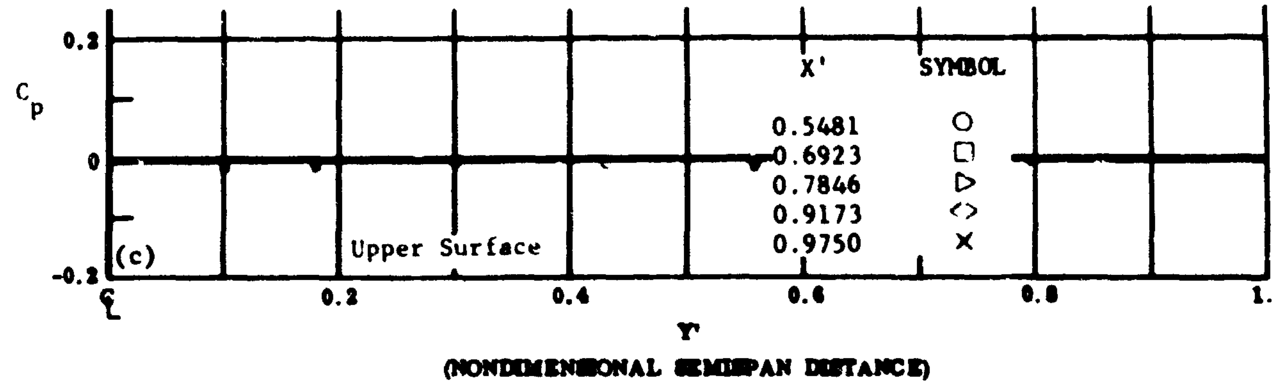

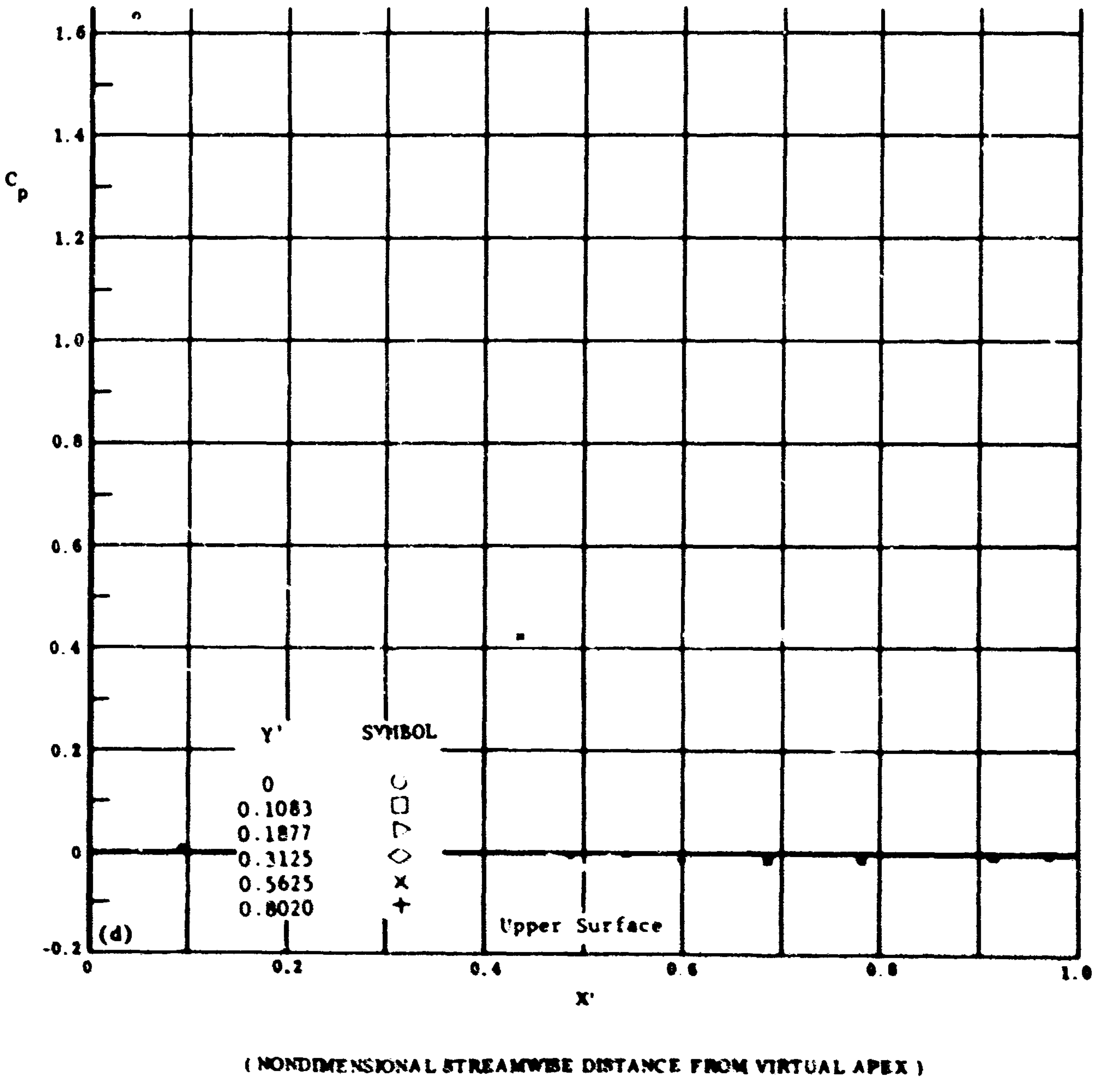

Fig. 33 Configuration IV, α = +20 , $\delta_2 = \delta_3 = 0$

c) C_p vs. Y', upper surface

d) C_p vs. X', upper surface

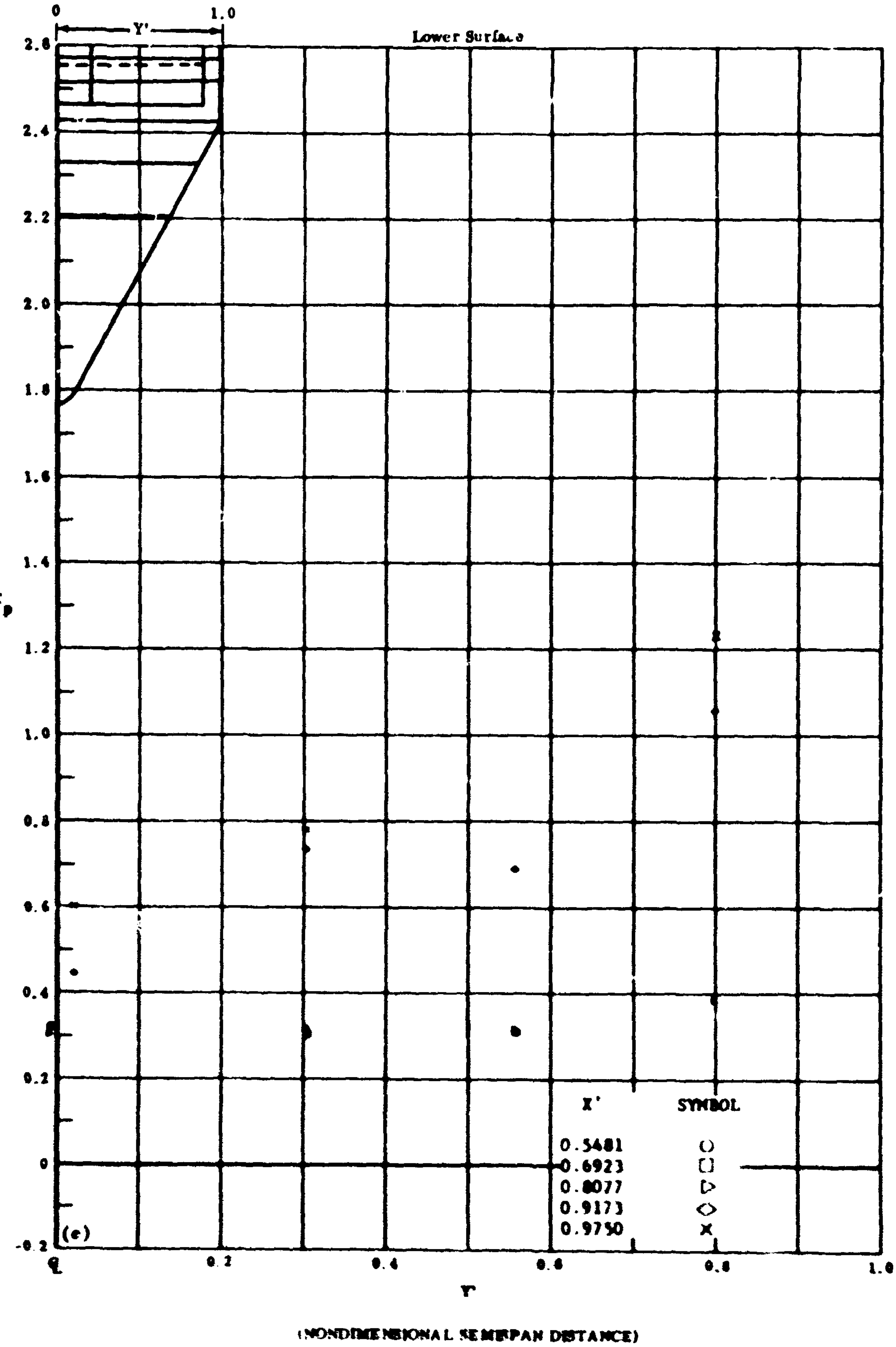

Fig. 33e Configuration IV, α = +20 , $\delta_2 = \delta_3$ = +10

C_p vs. Y', lower surface

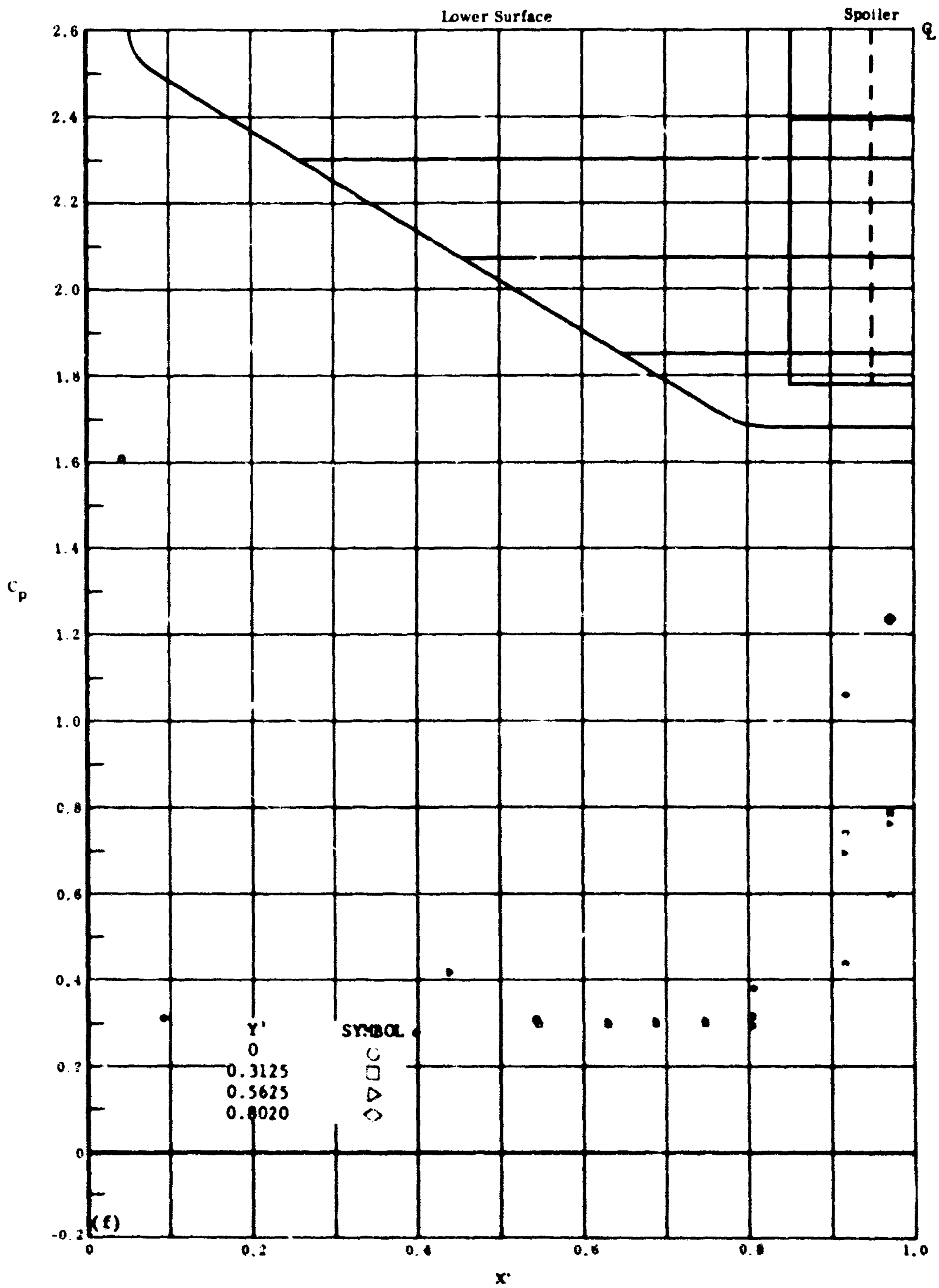

Fig. 33f Configuration IV, α = +20 , δ_2 = δ_3 = +10
C_p vs. X', lower surface

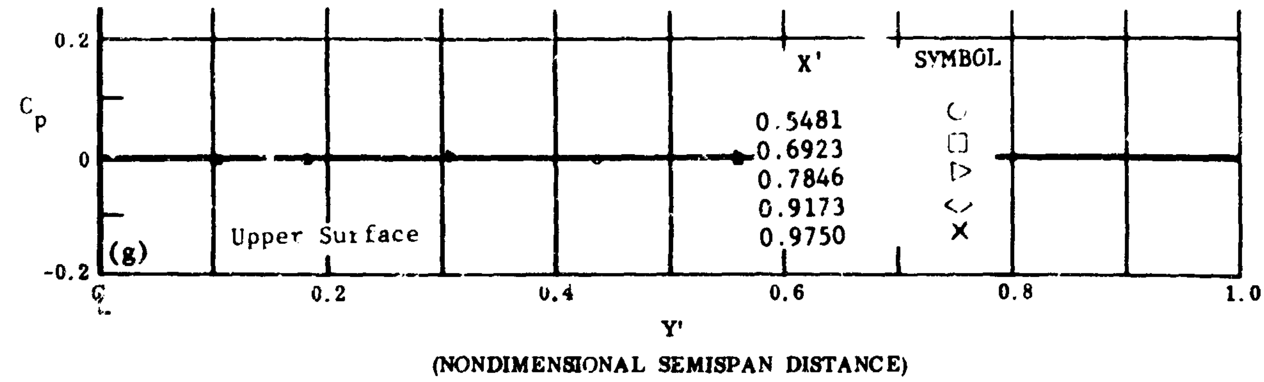

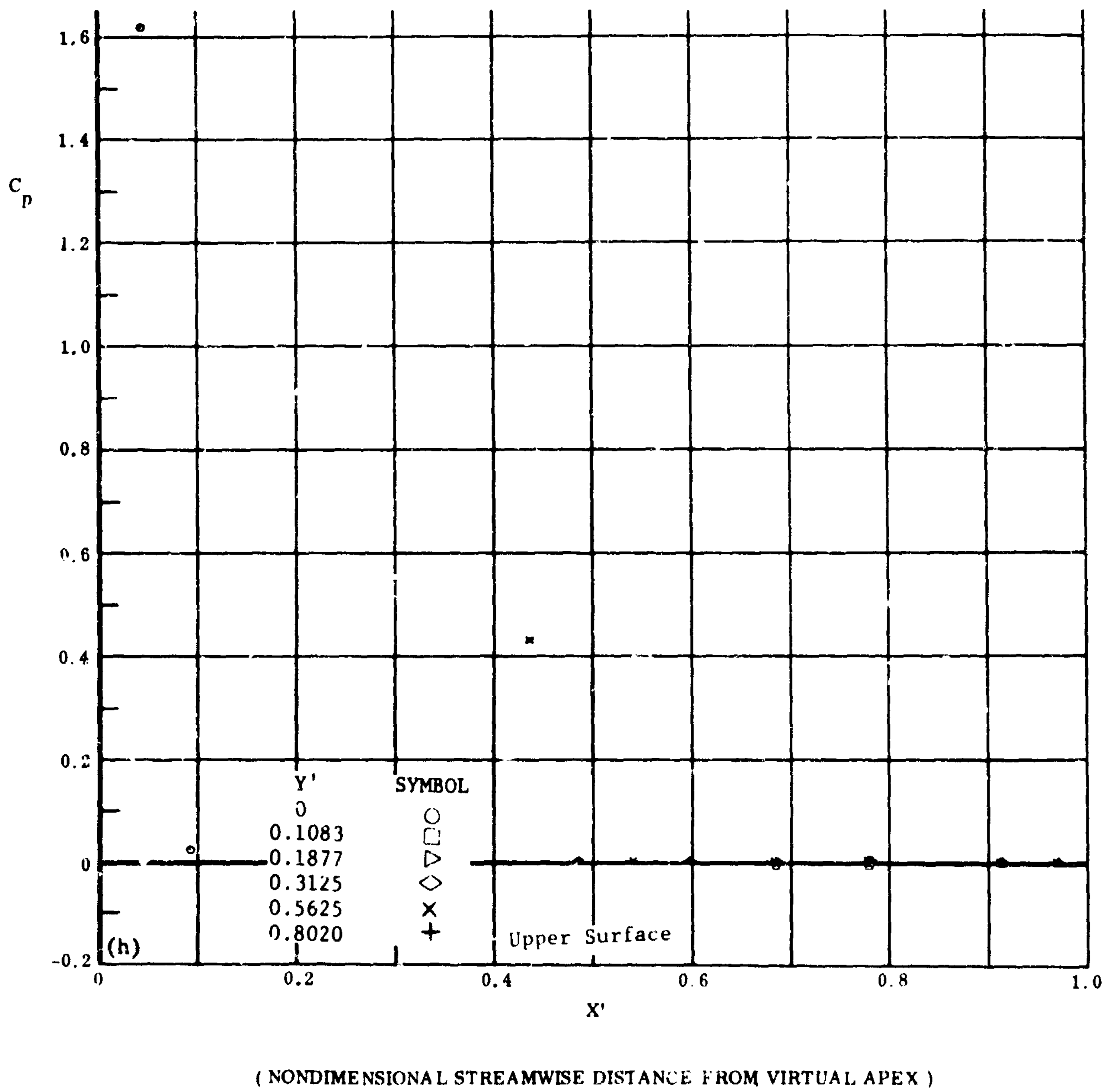

Fig. 33 Configuration IV, $\alpha = +20$, $\delta_2 = \delta_3 = +10$

g) C_p vs. Y', upper surface

h) C_p vs. X', upper surface

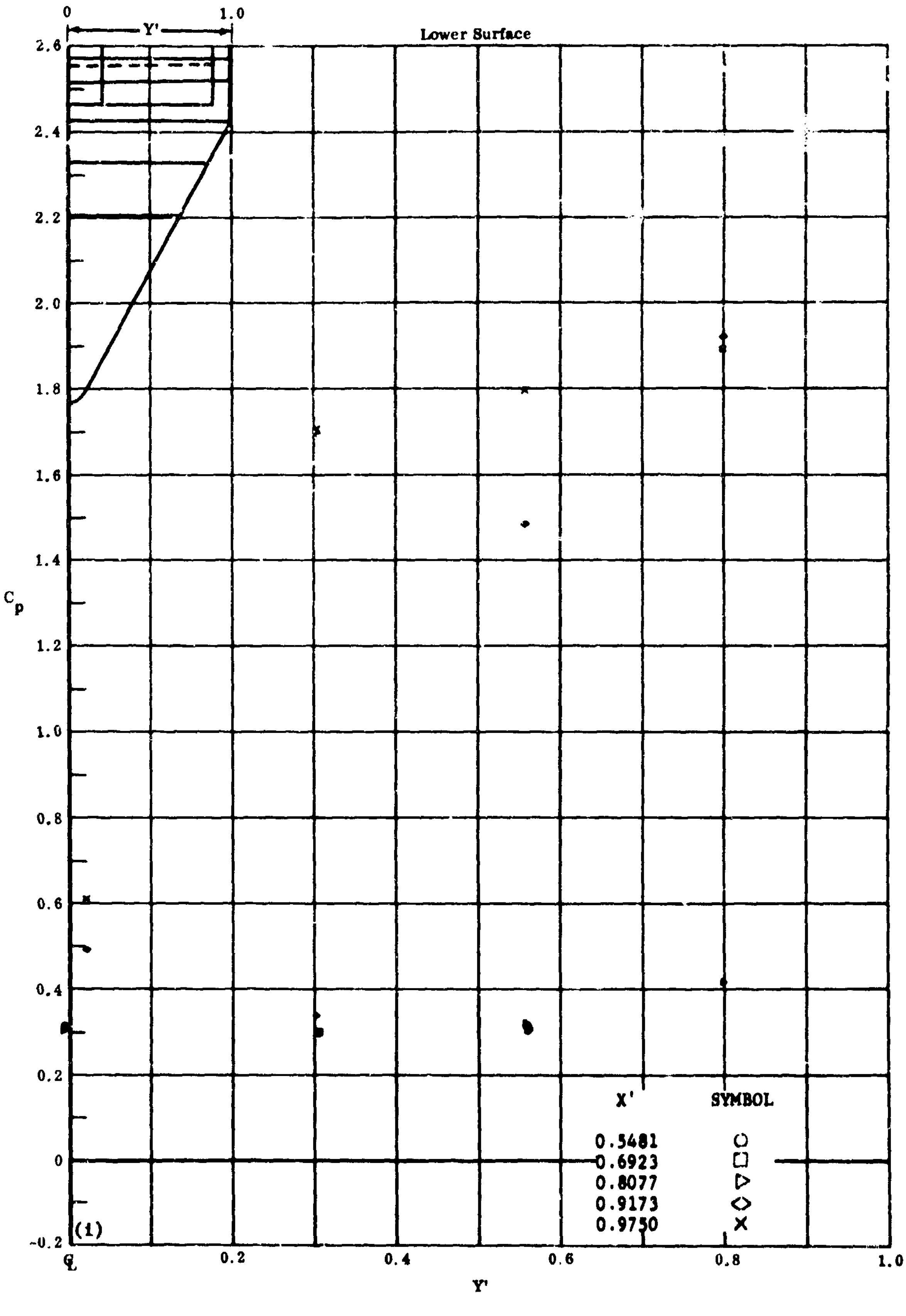

Fig. 33i Configuration IV, $\alpha = +20$, $\delta_2 = \delta_3 = +20$

C_p vs. Y', lower surface

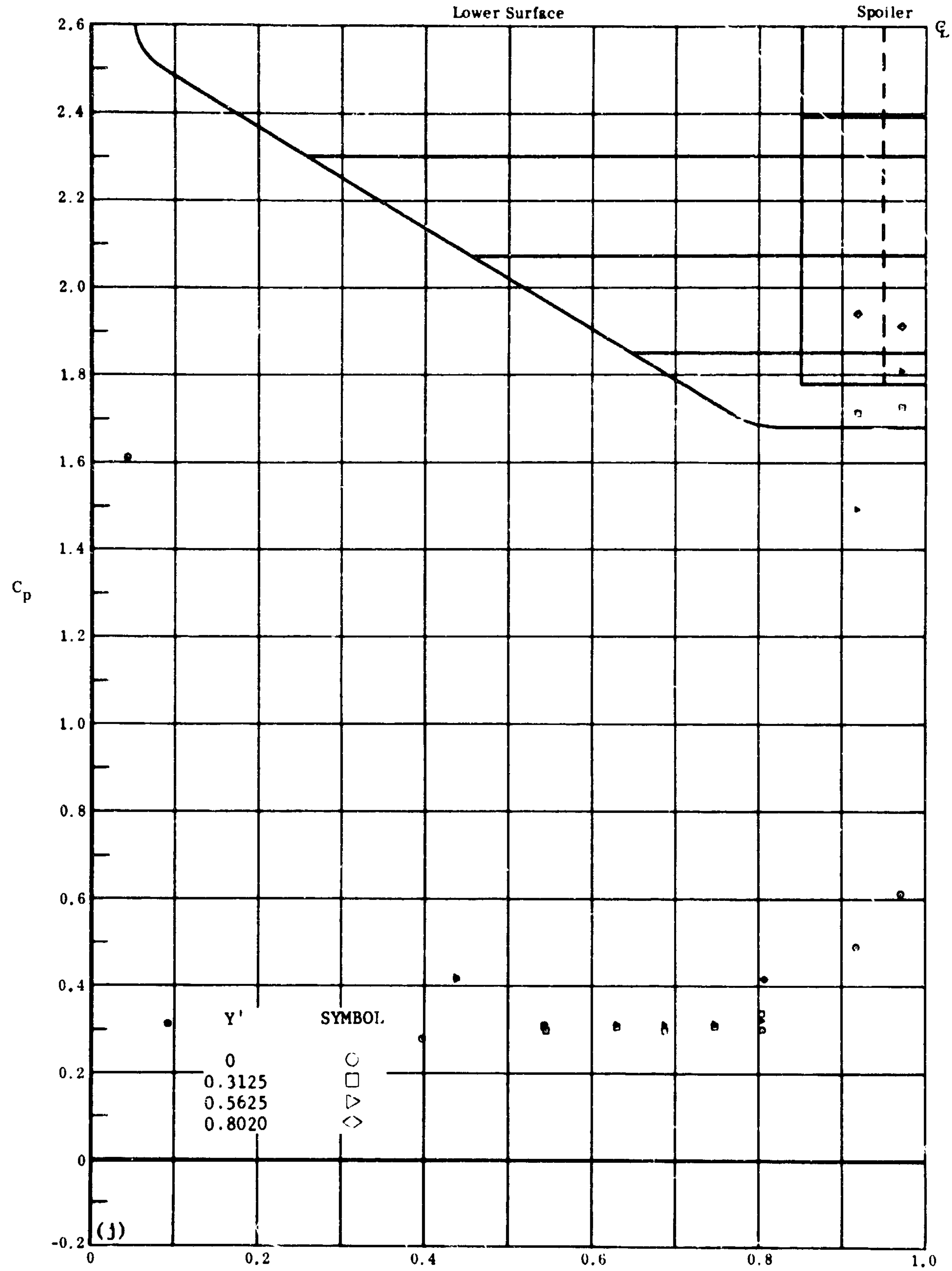

(NONDIMENSIONAL STREAMWISE DISTANCE FROM VIRTUAL APEX)

Fig. 33j Configuration IV, $\alpha = +20$, $\delta_2 = \delta_3 = +20$

C_p vs. X', lower surface

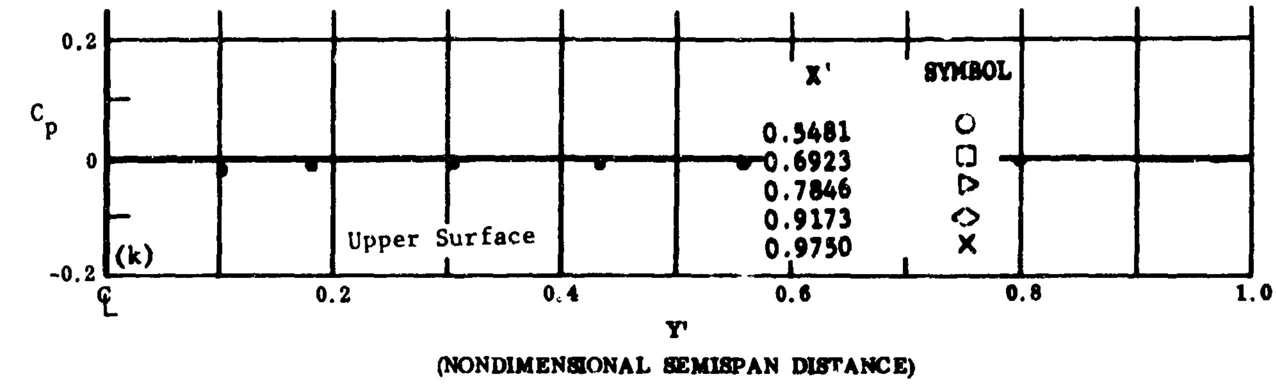

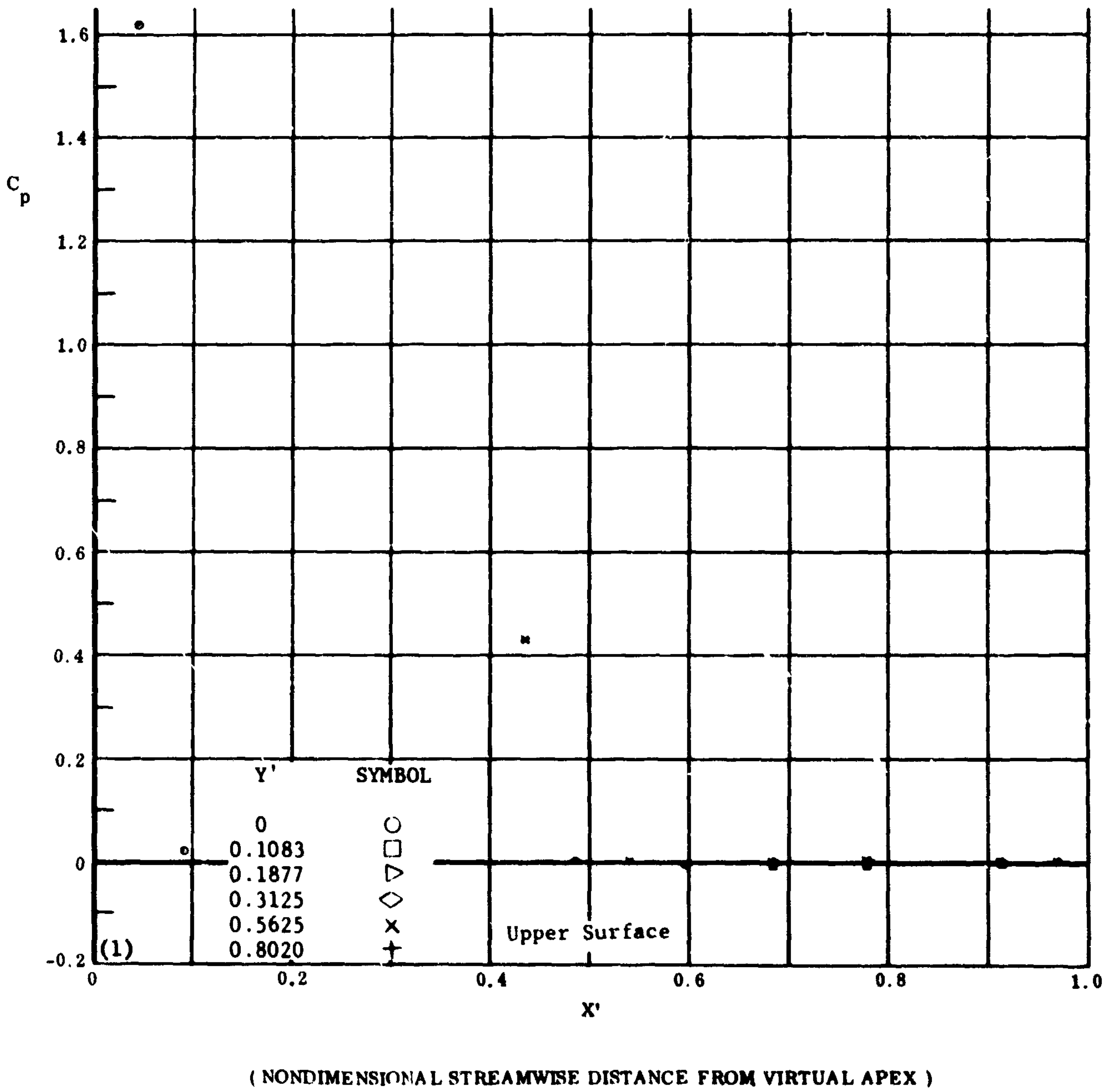

Fig. 33 Configuration IV, $\alpha = +20$, $\delta_2 = \delta_3 = +20$

k) C_p vs. Y', upper surface

1) C_p vs. X', upper surface

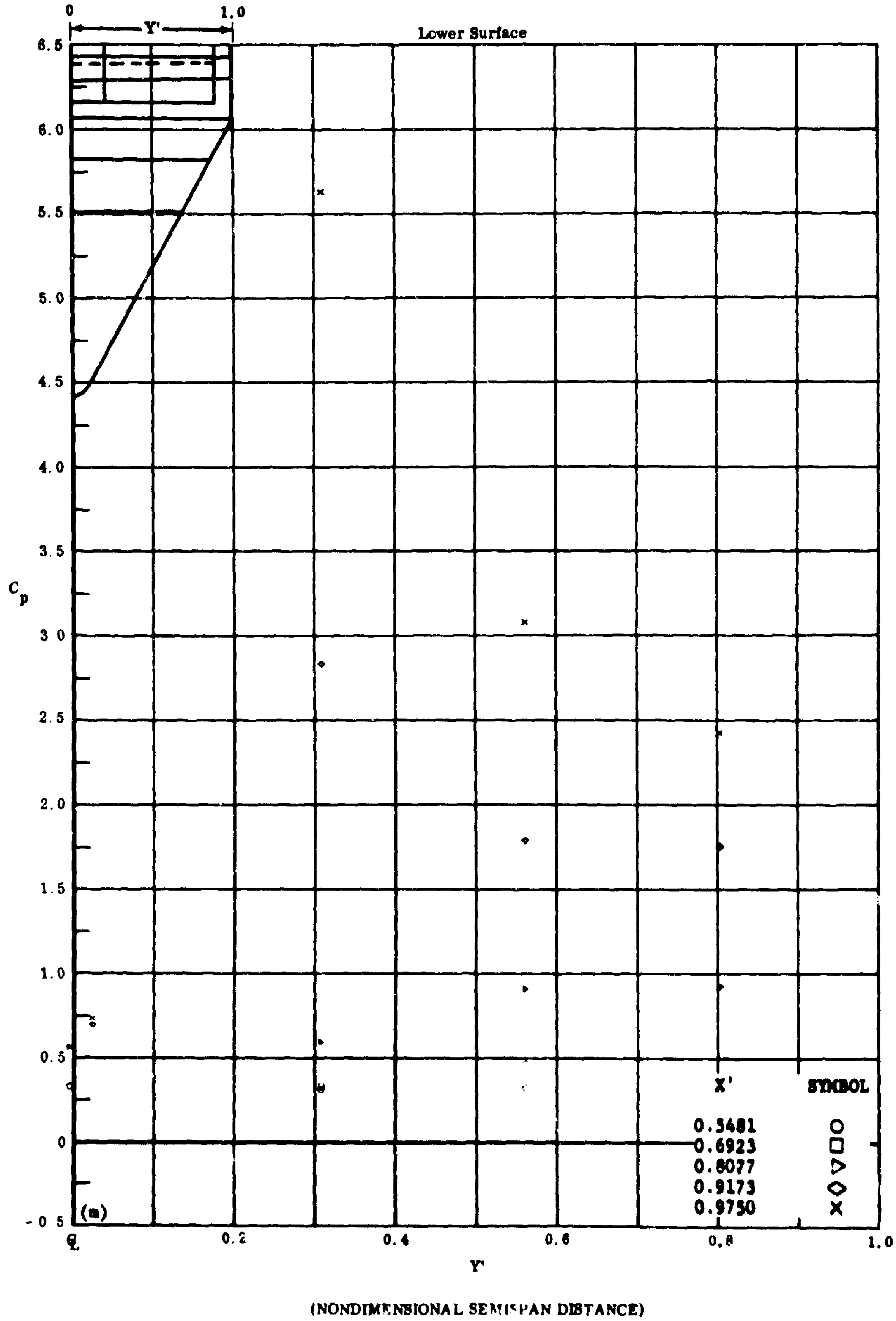

Fig. 33m Configuration IV, α = +20 , $\delta_2 = \delta_3$ = +30

C_p vs. Y', lower surface

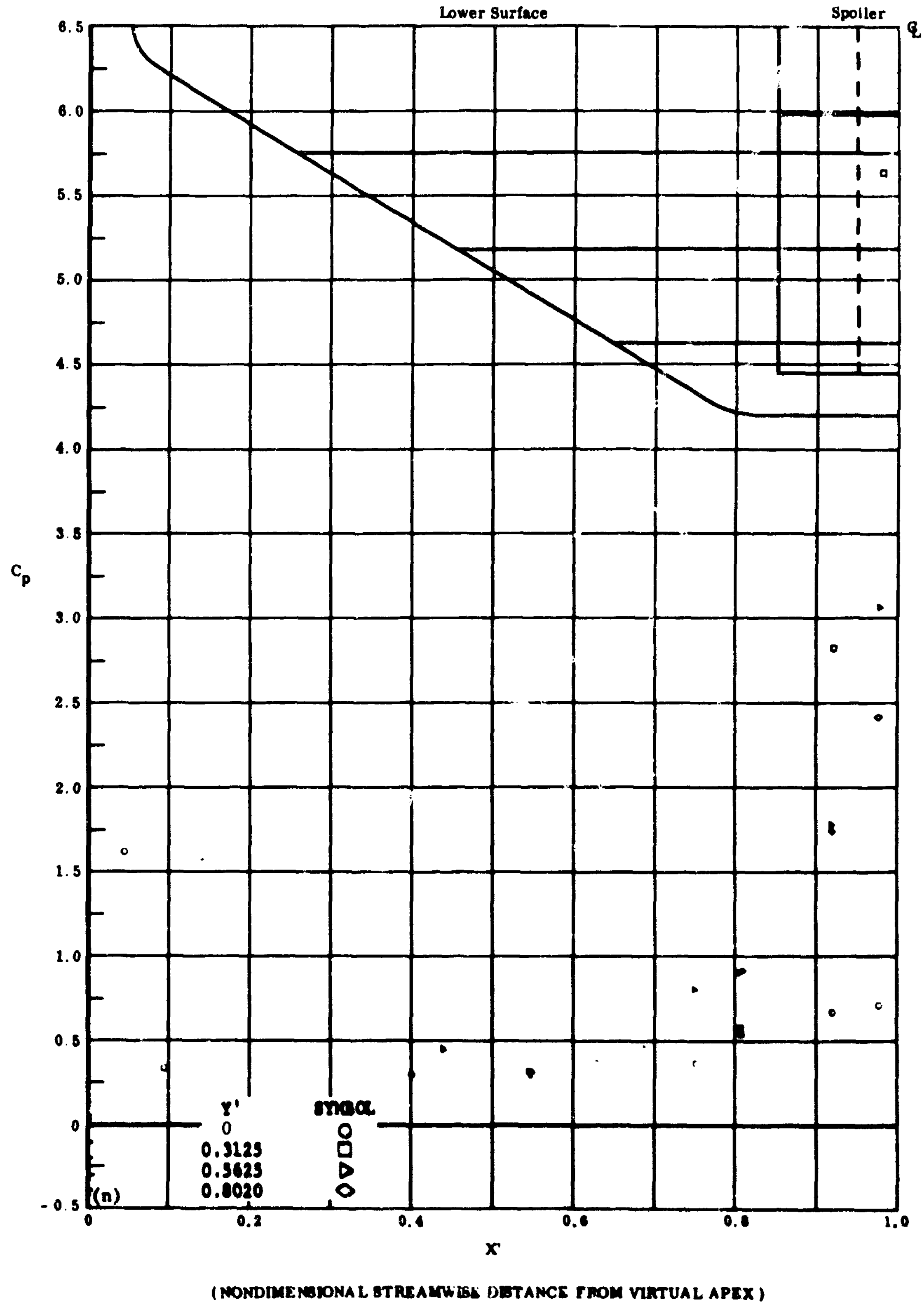

Fig. 33n Configuration IV, $\alpha = +20$, $\delta_2 = \delta_3 = +30$

C_p vs. X', lower surface

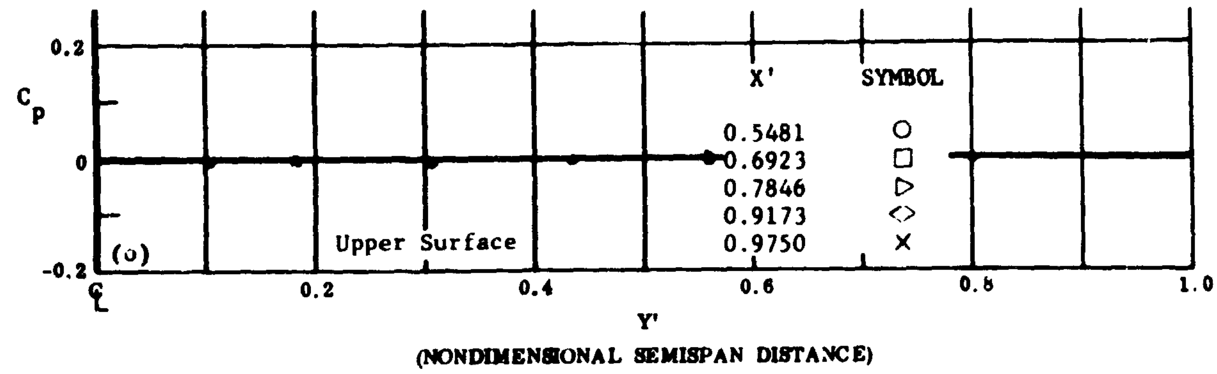

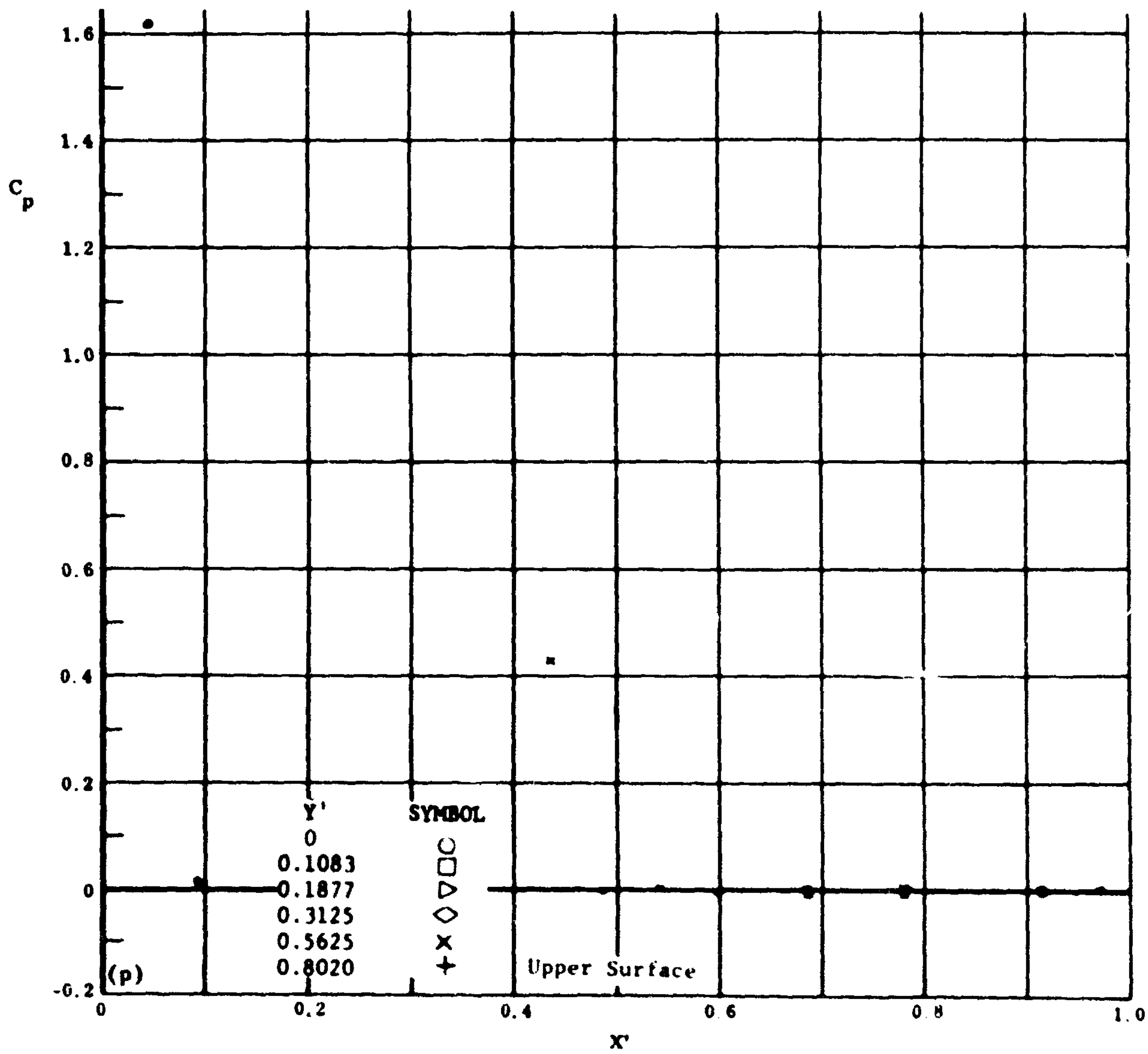

(NONDIMENSIONAL STREAMWISE DISTANCE FROM VIRTUAL APEX)

Fig. 33 Configuration IV, $\alpha = +20$, $\delta_2 = \delta_3 = +30$

o) C_p vs. Y', upper surface

p) C_p vs. X', upper surface

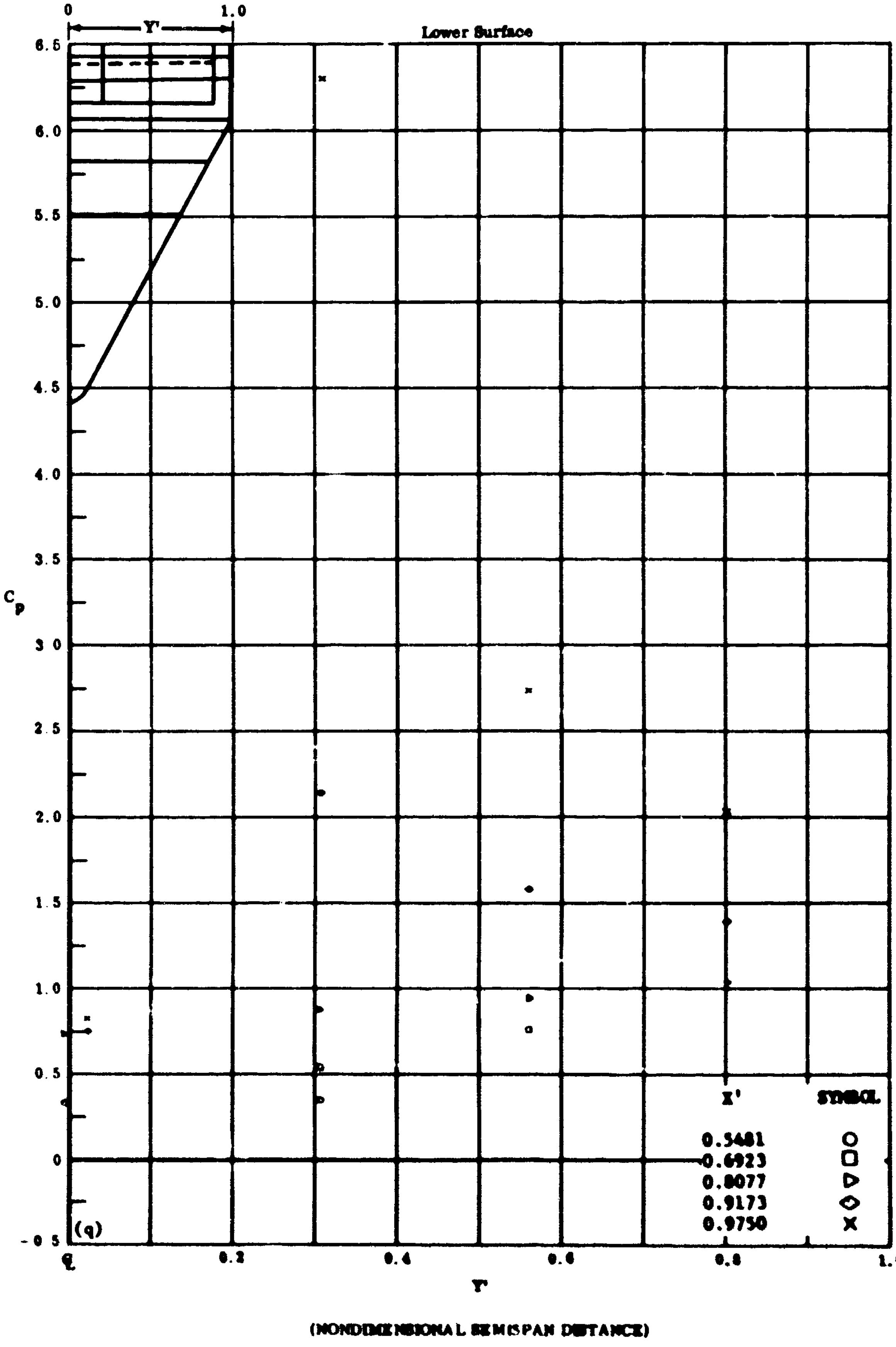

Fig. 33q Configuration IV, $\alpha = +20$, $\delta_2 = \delta_3 = +39$

C_p vs. Y', lower surface

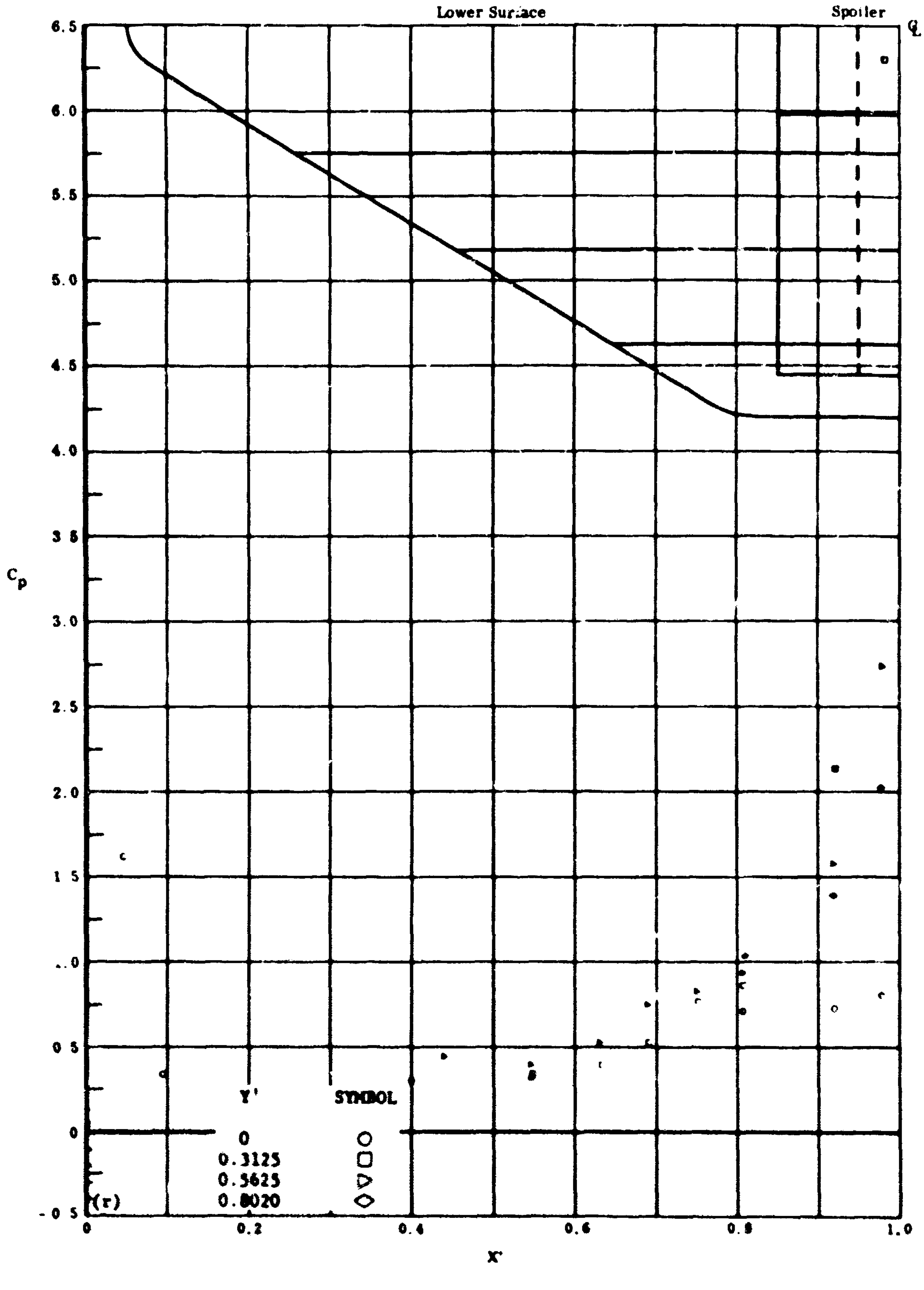

Fig. 33r Configuration IV, $\delta_1 = +20$, $\delta_2 = \delta_3 = +39$

C_p vs. X', lower surface

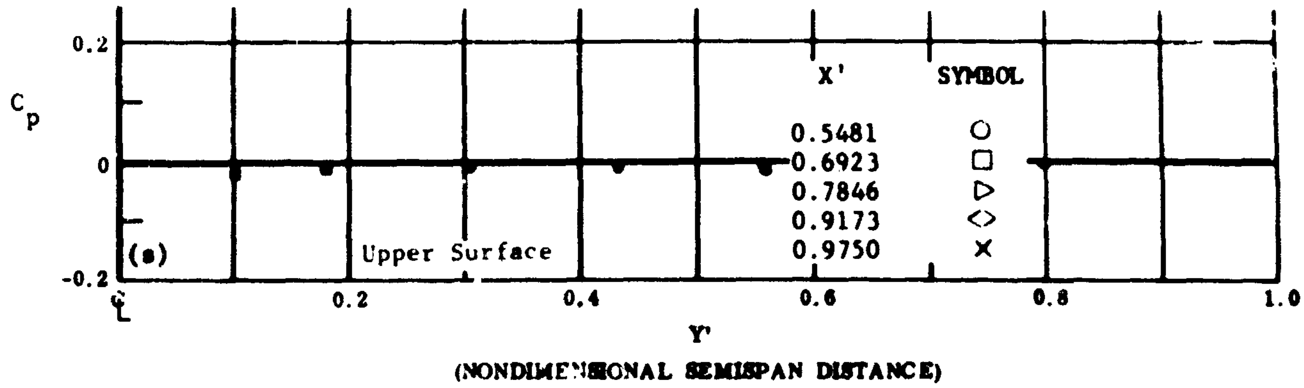

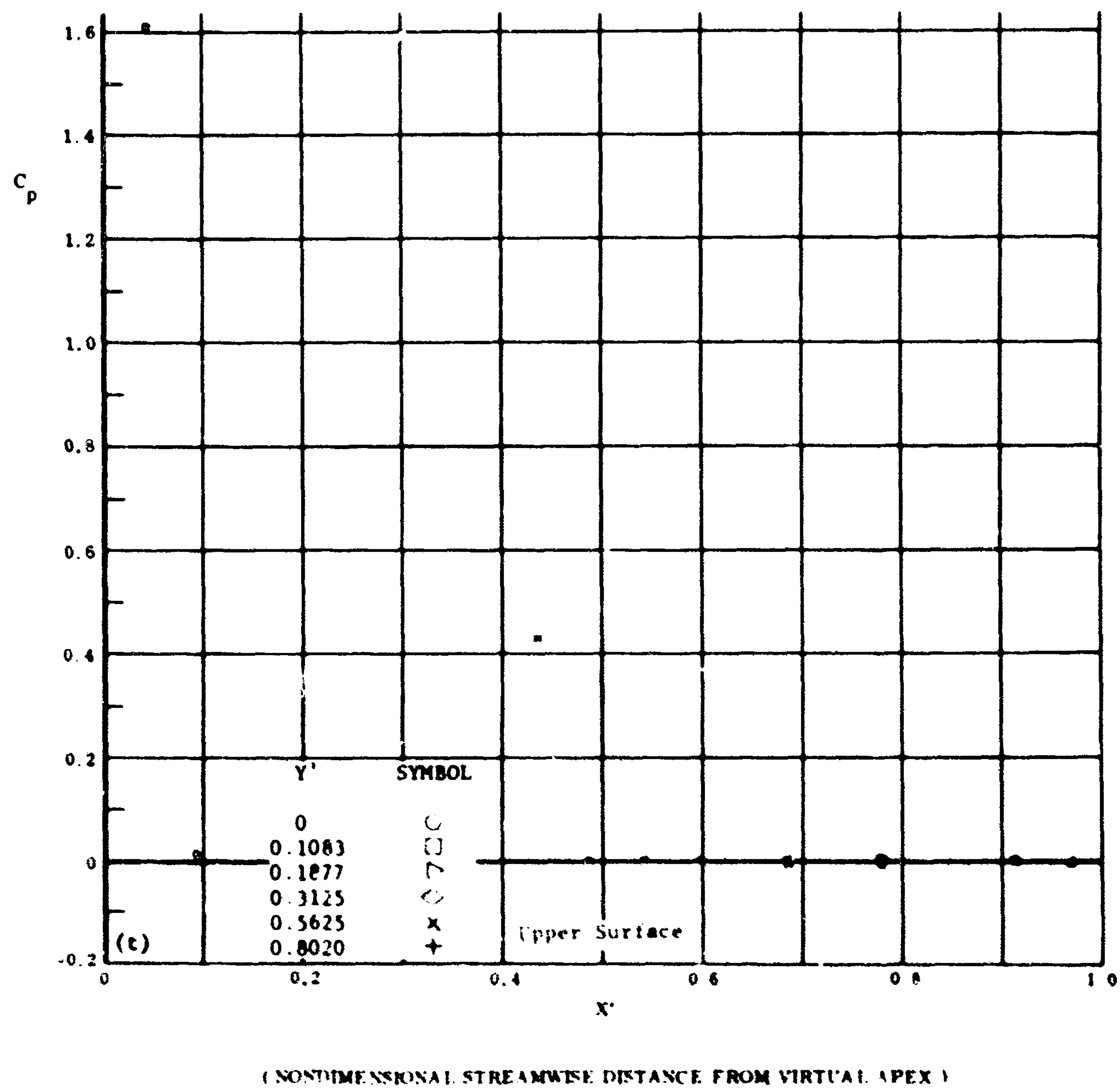

Fig. 33 Configuration IV, $\varepsilon_1 = +20$, $\varepsilon_2 = \varepsilon_3 = +39$

s) C_p vs. Y', upper surface

t) C_p vs. X', upper surface

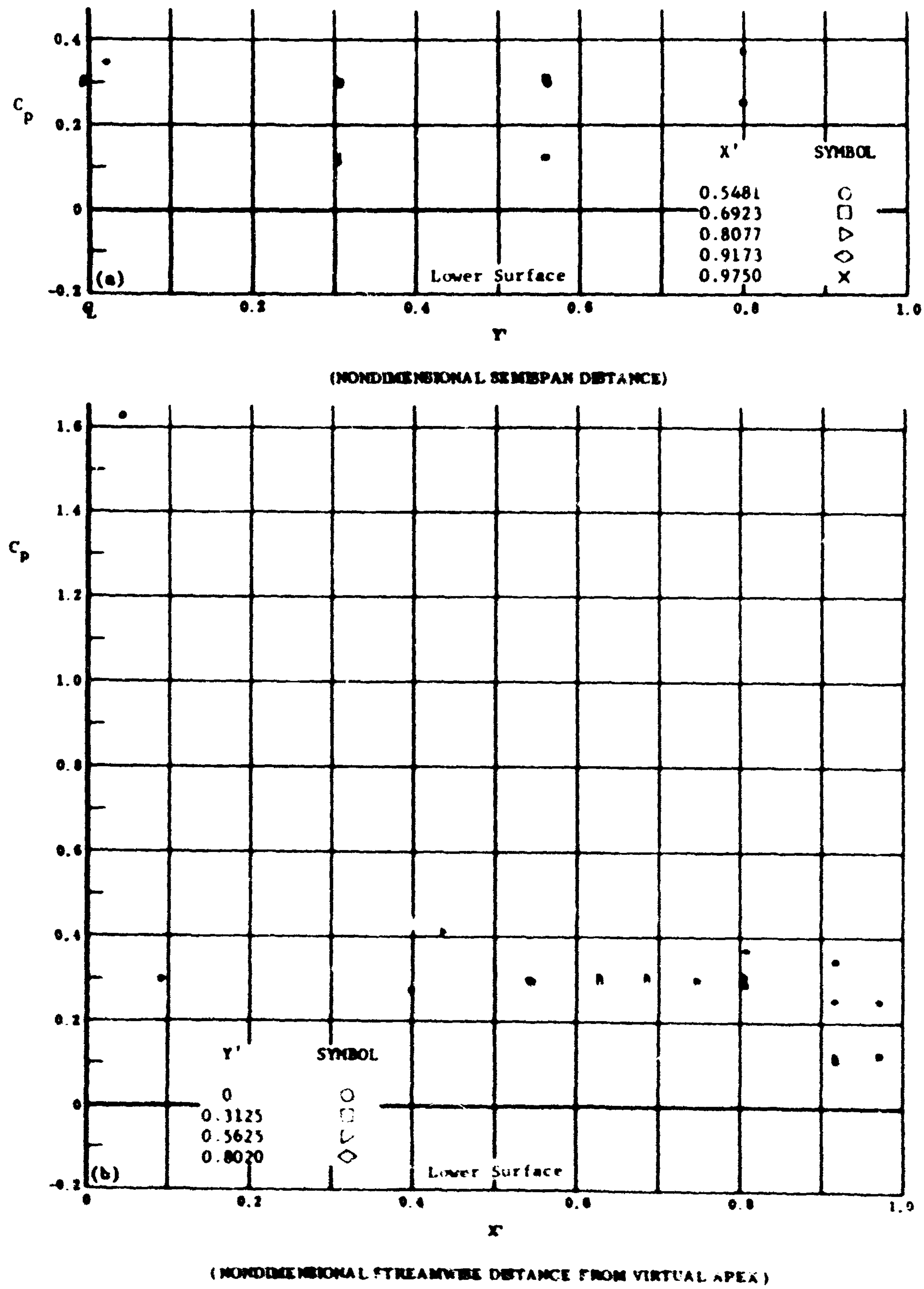

Fig. 34 Configuration IV, α = +20 , $\delta_2 = \delta_3$ = -10

a) C_p vs. Y', lower surface

b) C_p vs. X', lower surface

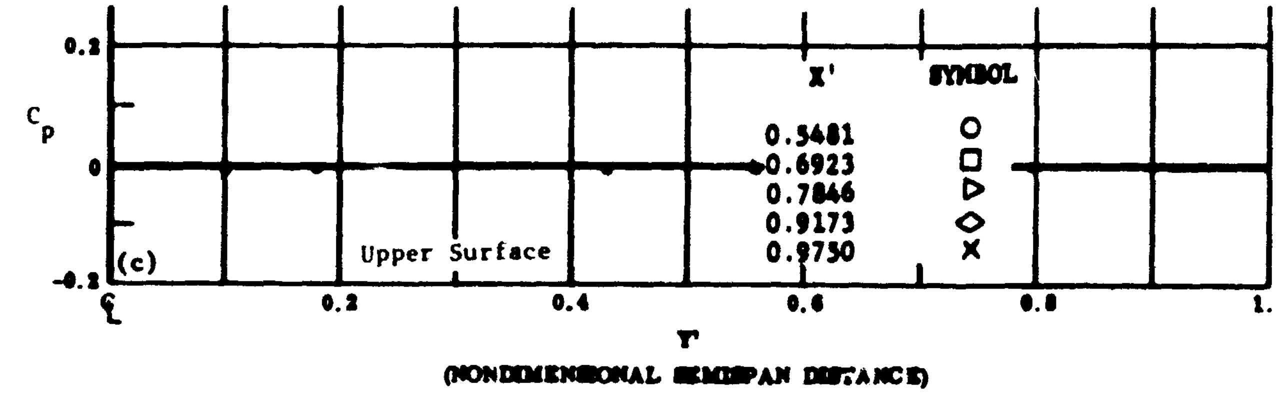

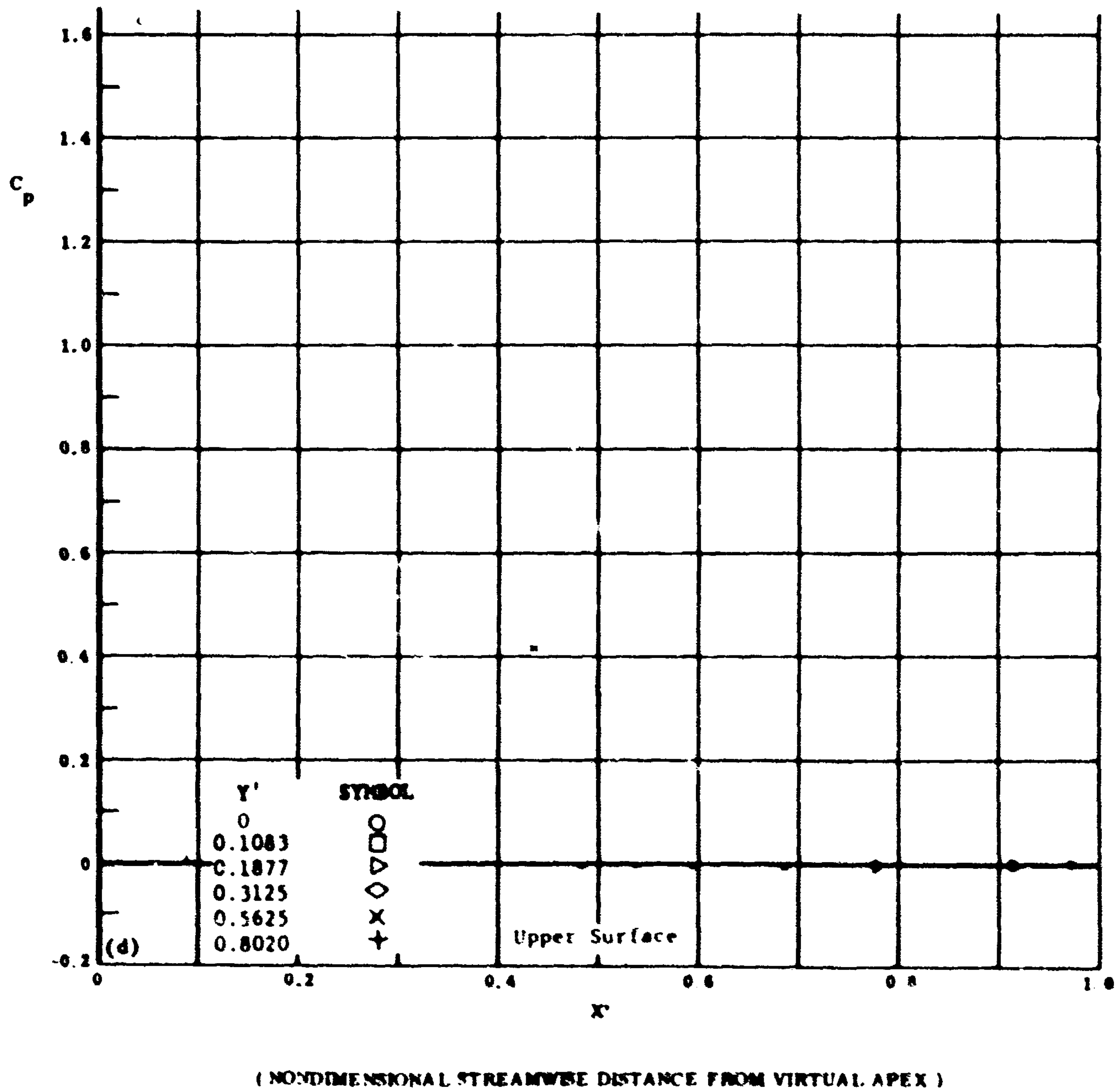

Fig. 34 Configuration IV, $\alpha = +20$, $\delta_2 = \delta_3 = -10$

c) C_p vs. Y', upper surface

d) C_p vs. X', upper surface

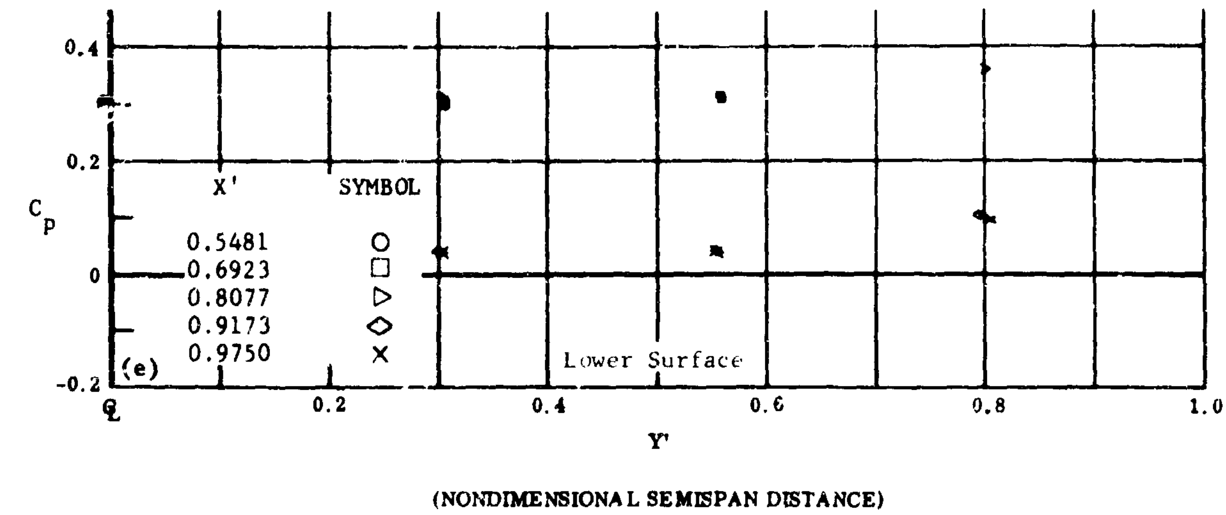

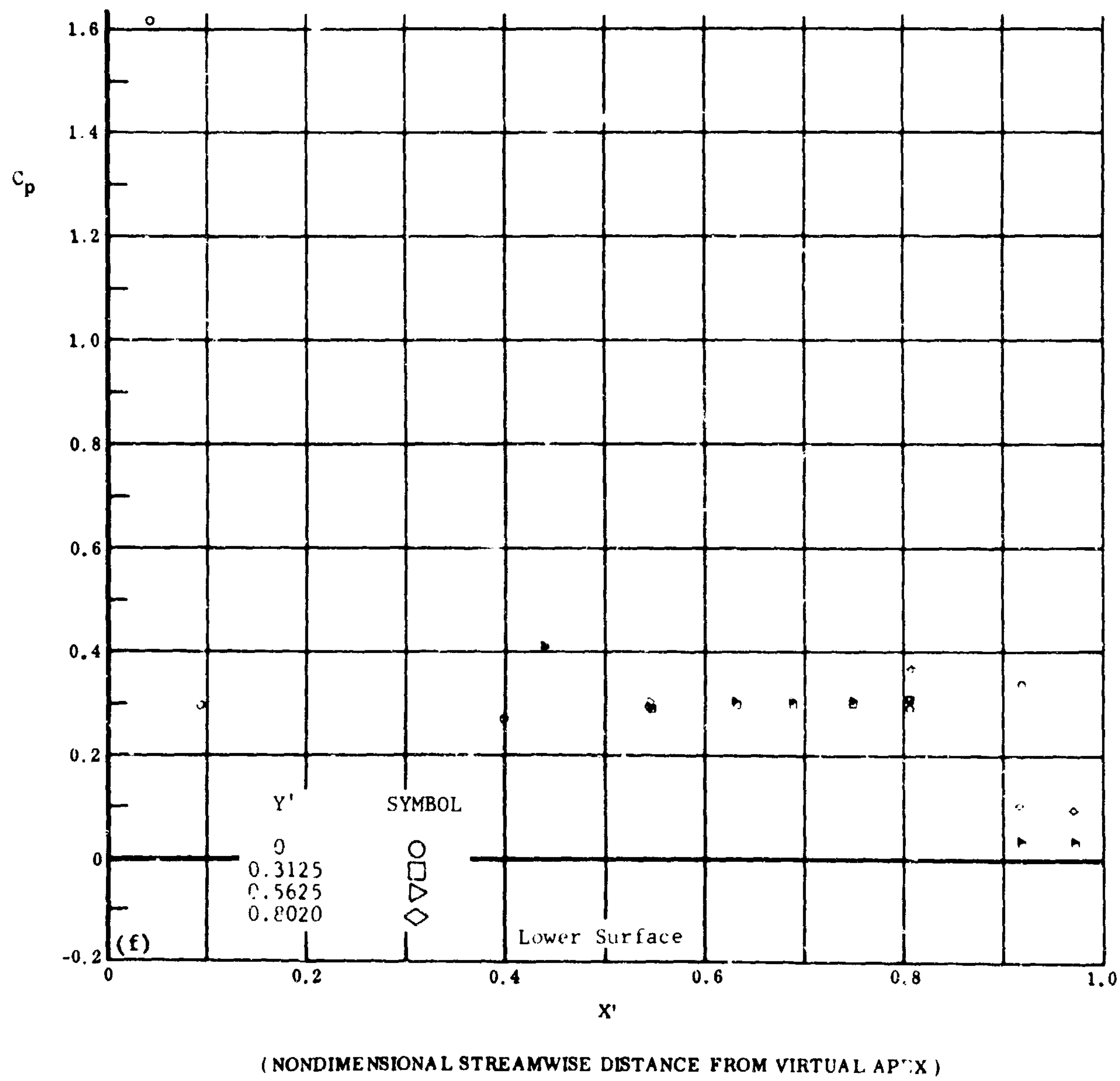

Fig. 34 Configuration IV, $\alpha = +20$, $\delta_2 = \delta_3 = -20$

e) C_p vs. Y', lower surface

f) C_p vs. X', lower surface

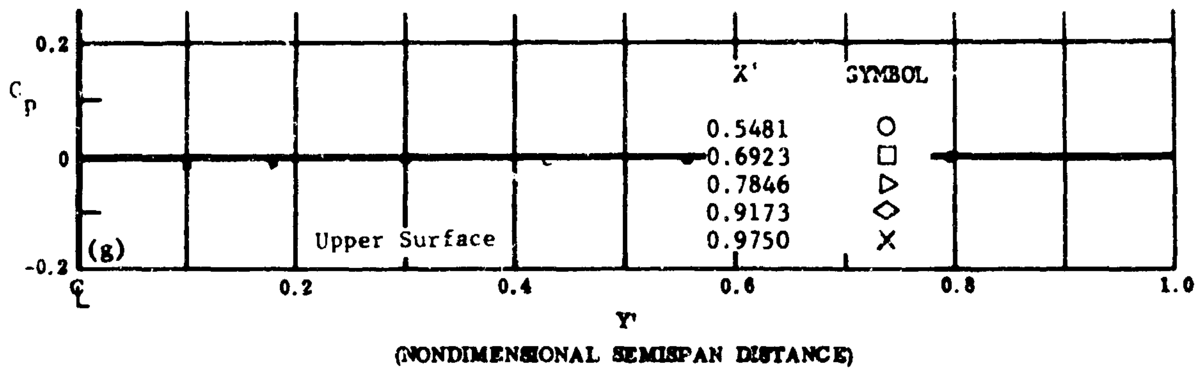

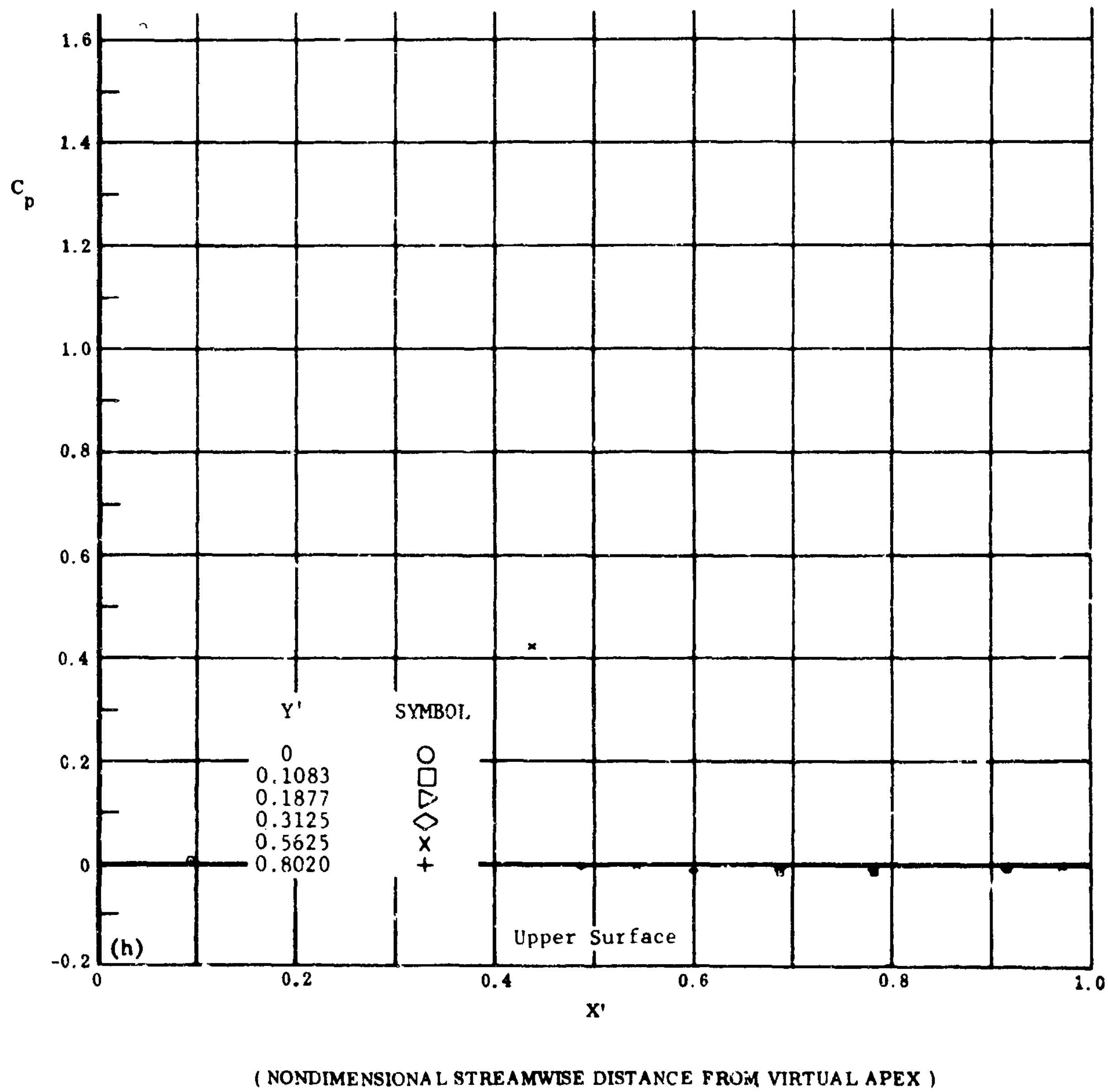

Fig. 34 Configuration IV, $\alpha = +20$, $\delta_2 = \delta_3 = -20$

g) C_p vs. Y', upper surface

h) C_p vs. X', upper surface

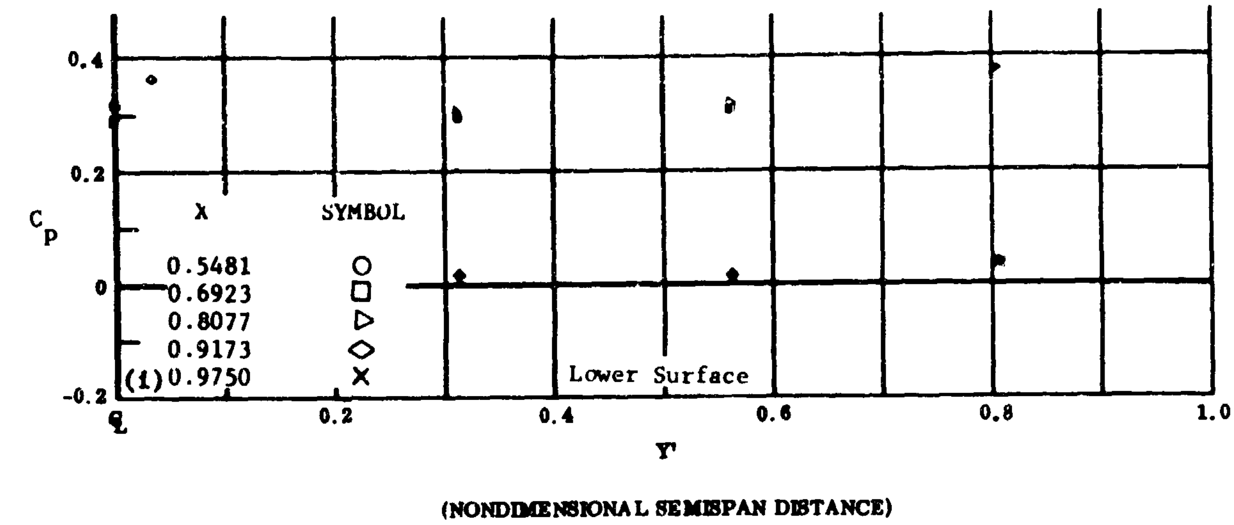

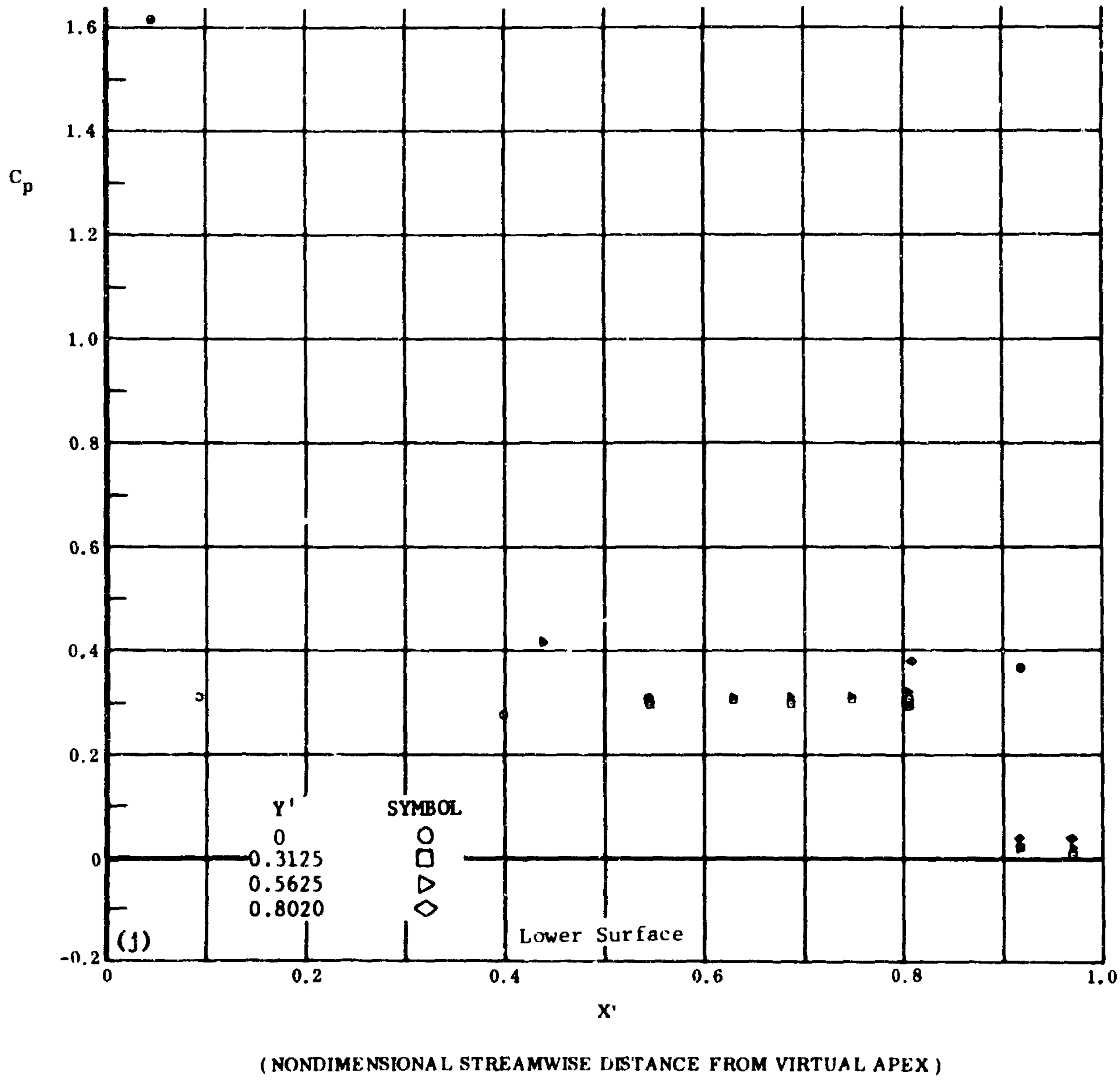

Fig. 34 Configuration IV, $\alpha = +20$, $\delta_2 = \delta_3 = -30$

i) C_p vs. Y', lower surface

j) C_p vs. X', lower surface

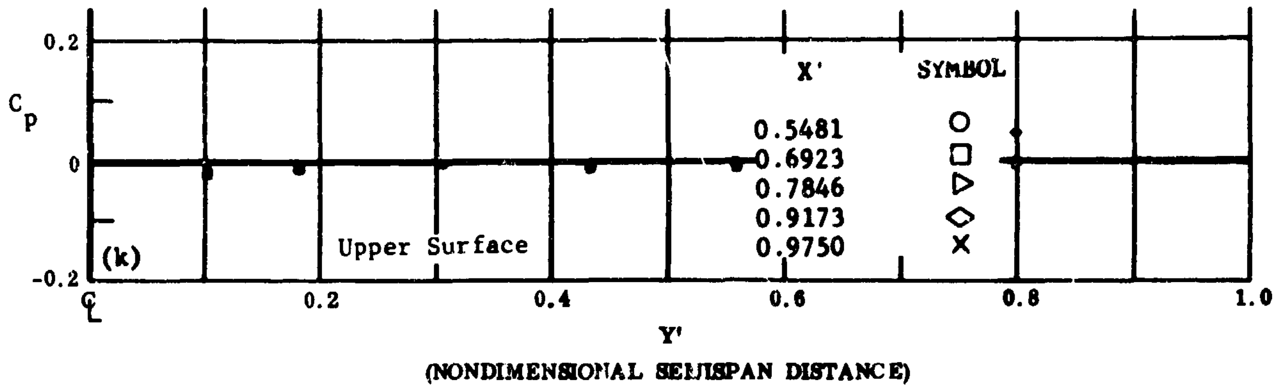

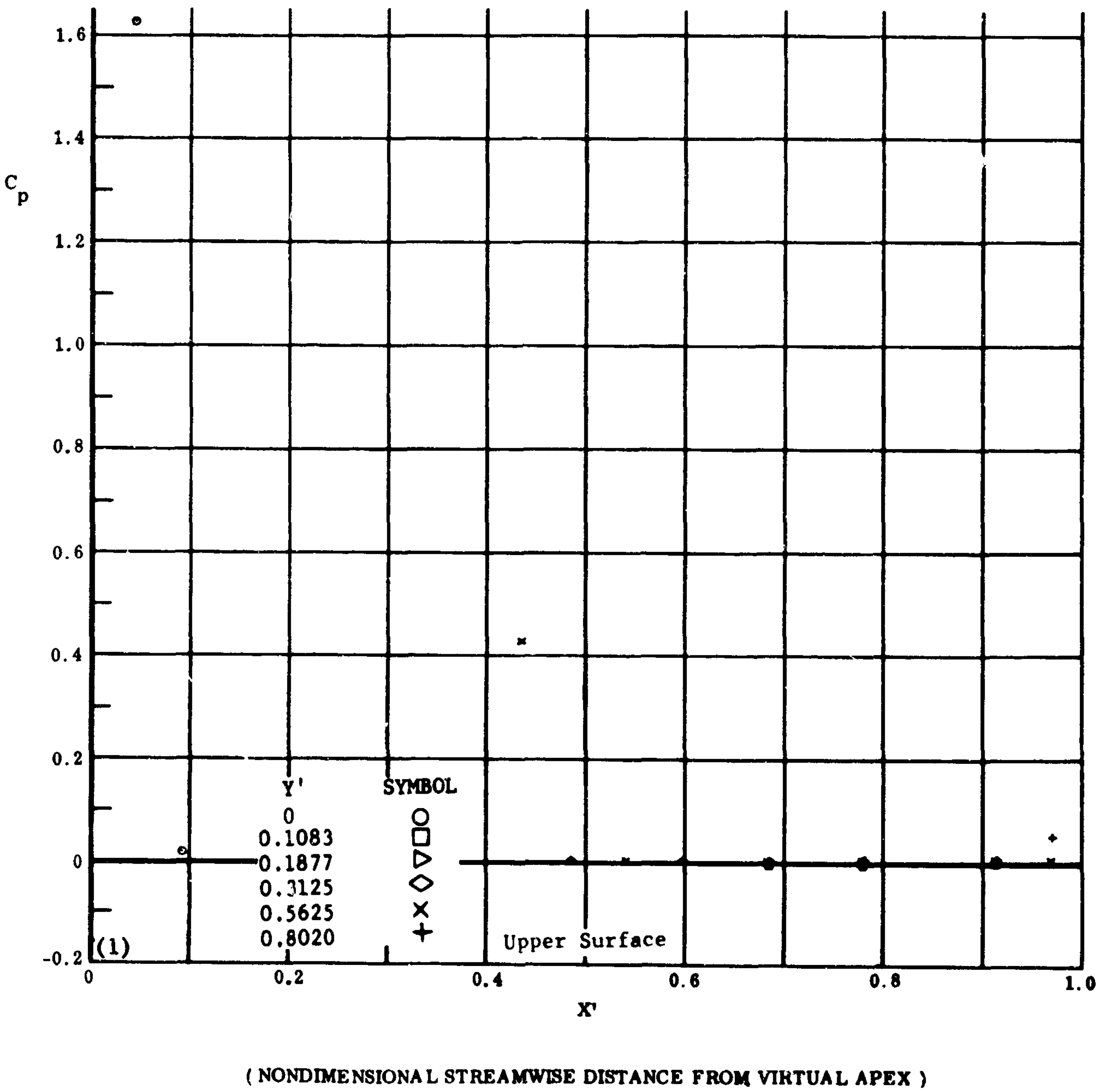

Fig. 34 Configuration IV, $\alpha = +20$, $\delta_2 = \delta_3 = -30$

k) C_p vs. Y', upper surface

1) C_p vs. X', upper surface

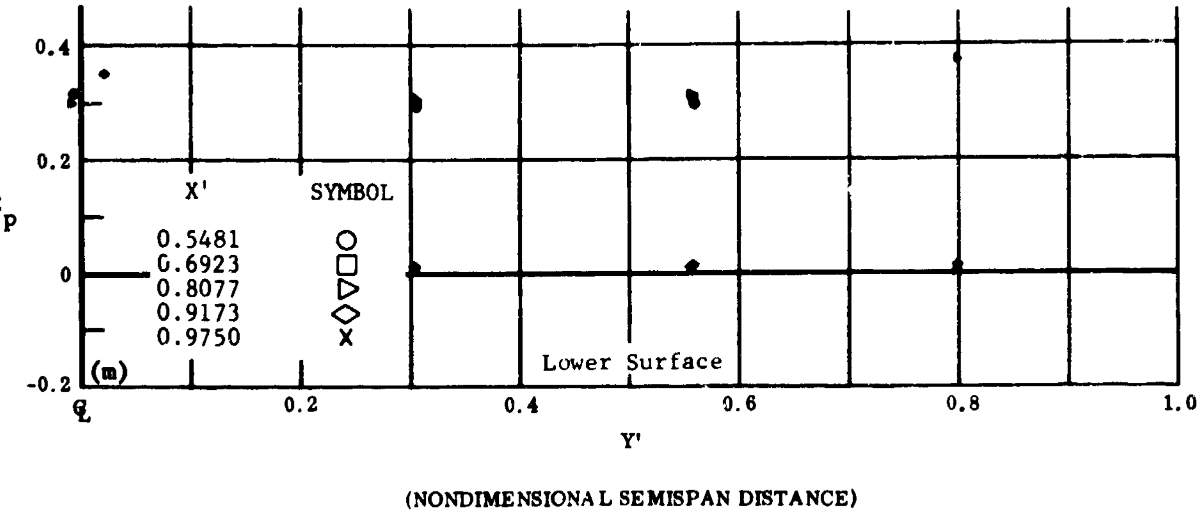

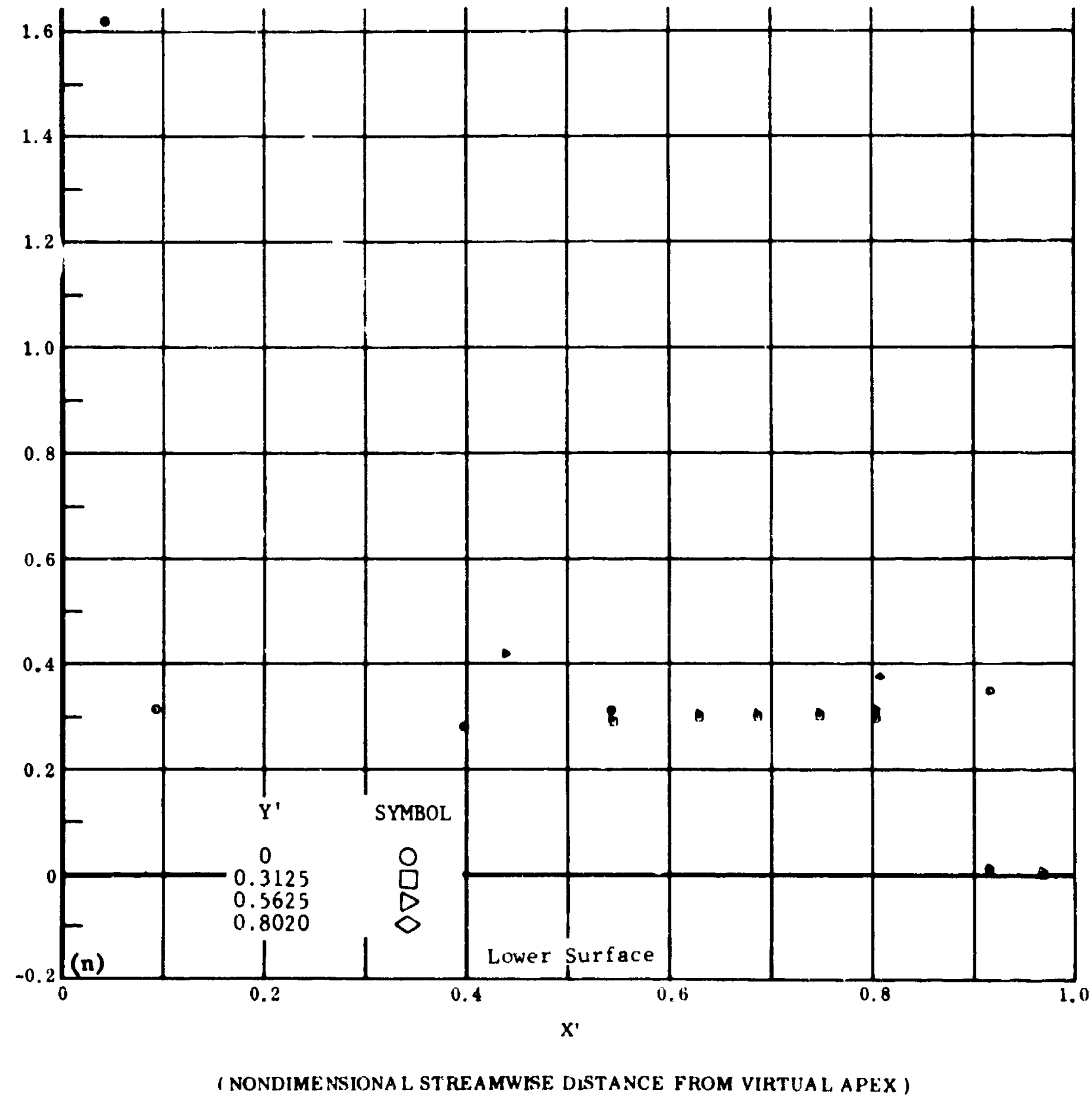

Fig. 34 Configuration IV, α = +20 , $\delta_2 = \delta_3$ = -39

m) C_p vs. Y', lower surface

n) C_p vs. X', lower surface

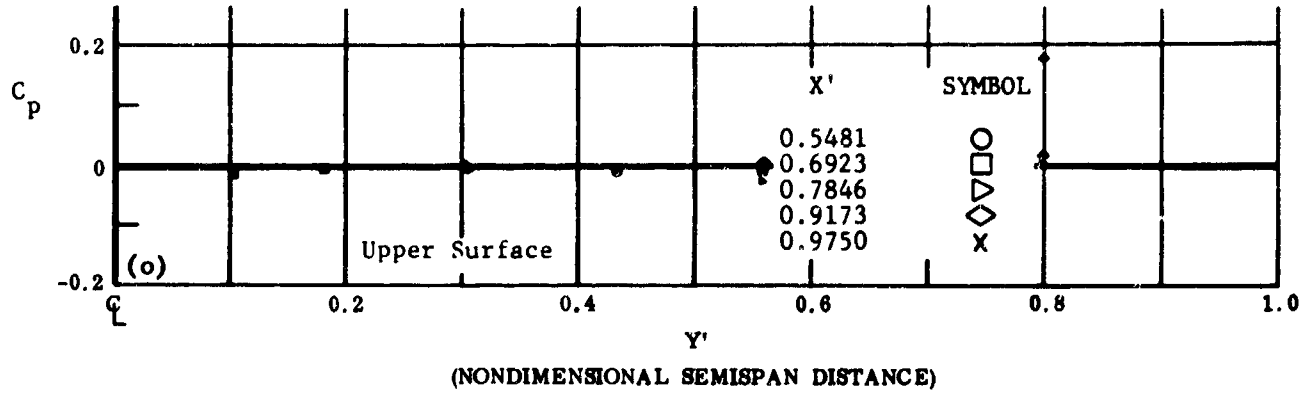

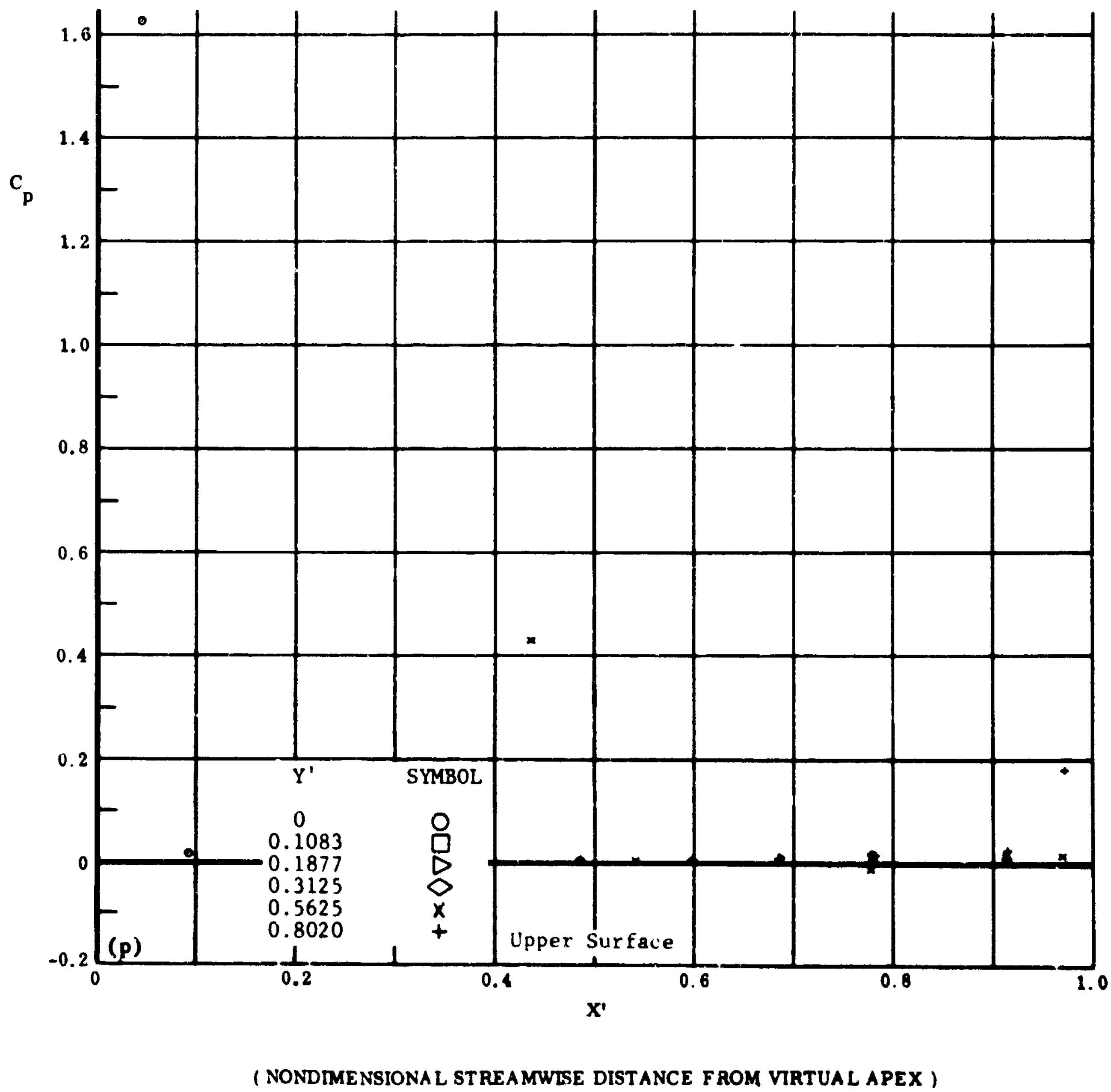

Fig. 34 Configuration IV, $\alpha = +20$, $\delta_2 = \delta_3 = -39$

o) C_p vs. Y', upper surface

p) C_p vs. X', upper surface

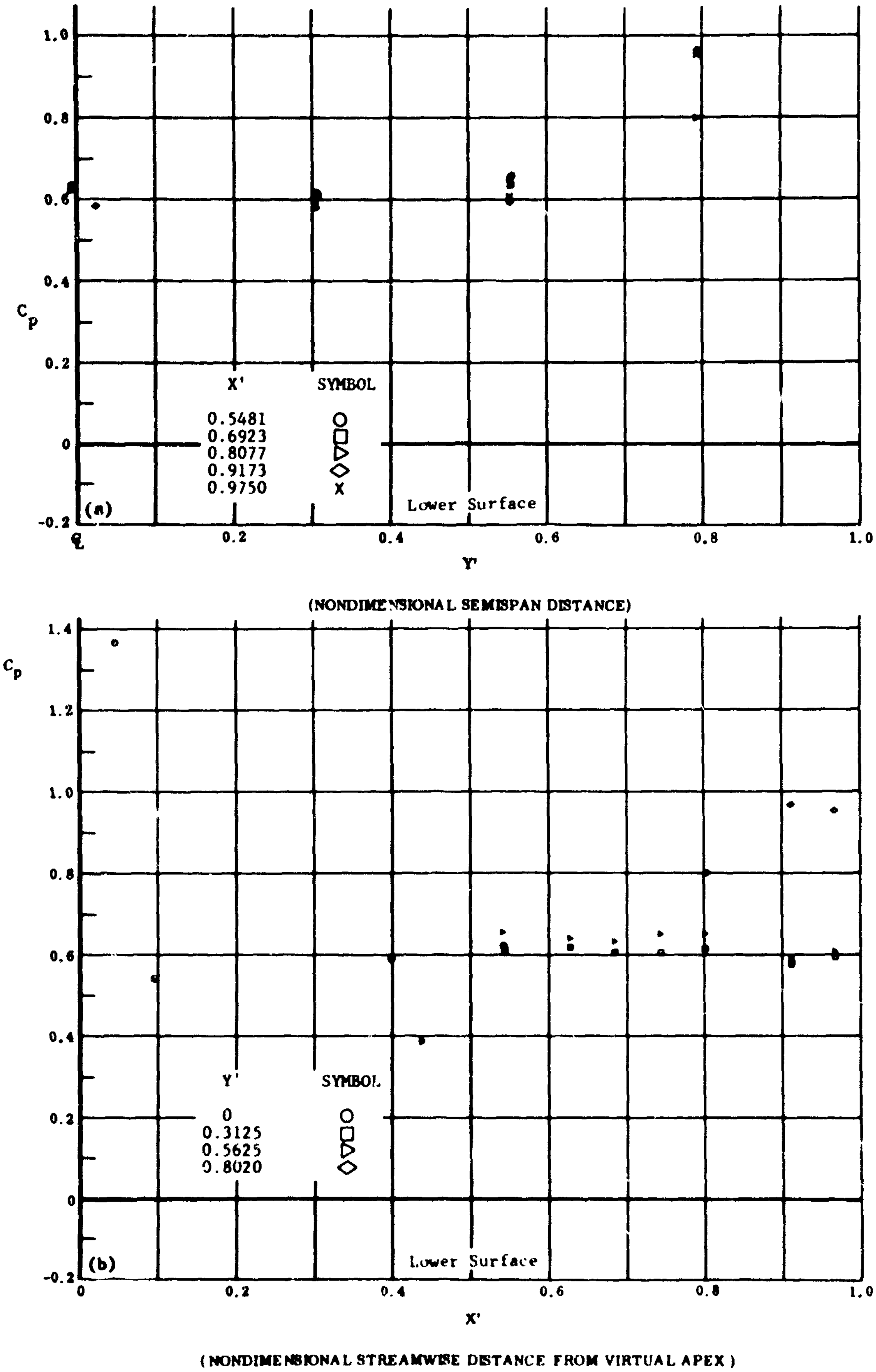

Fig. 35 Configuration IV, $\alpha = +30$, $\delta_2 = \delta_3 = 0$

a) C_p vs. Y', lower surface

b) C_p vs. X', lower surface

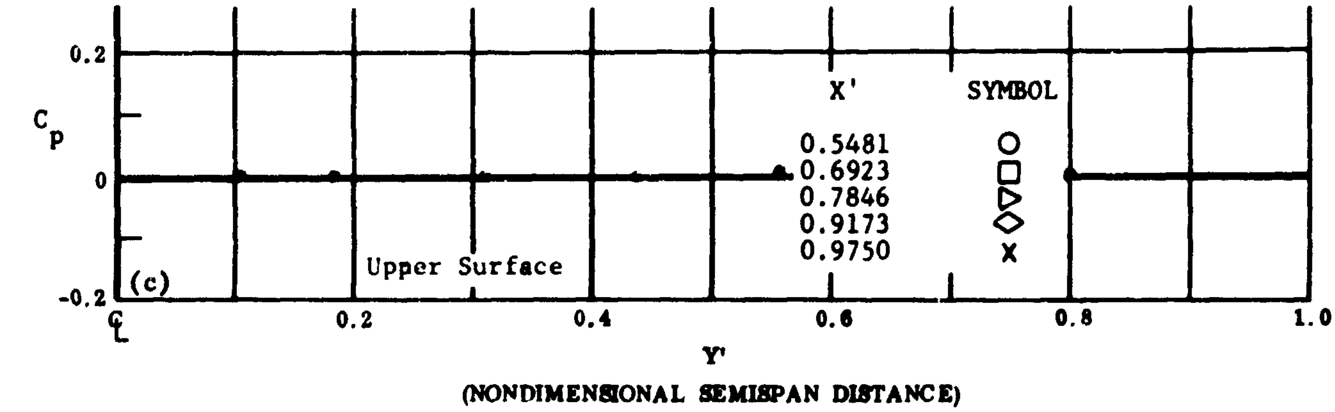

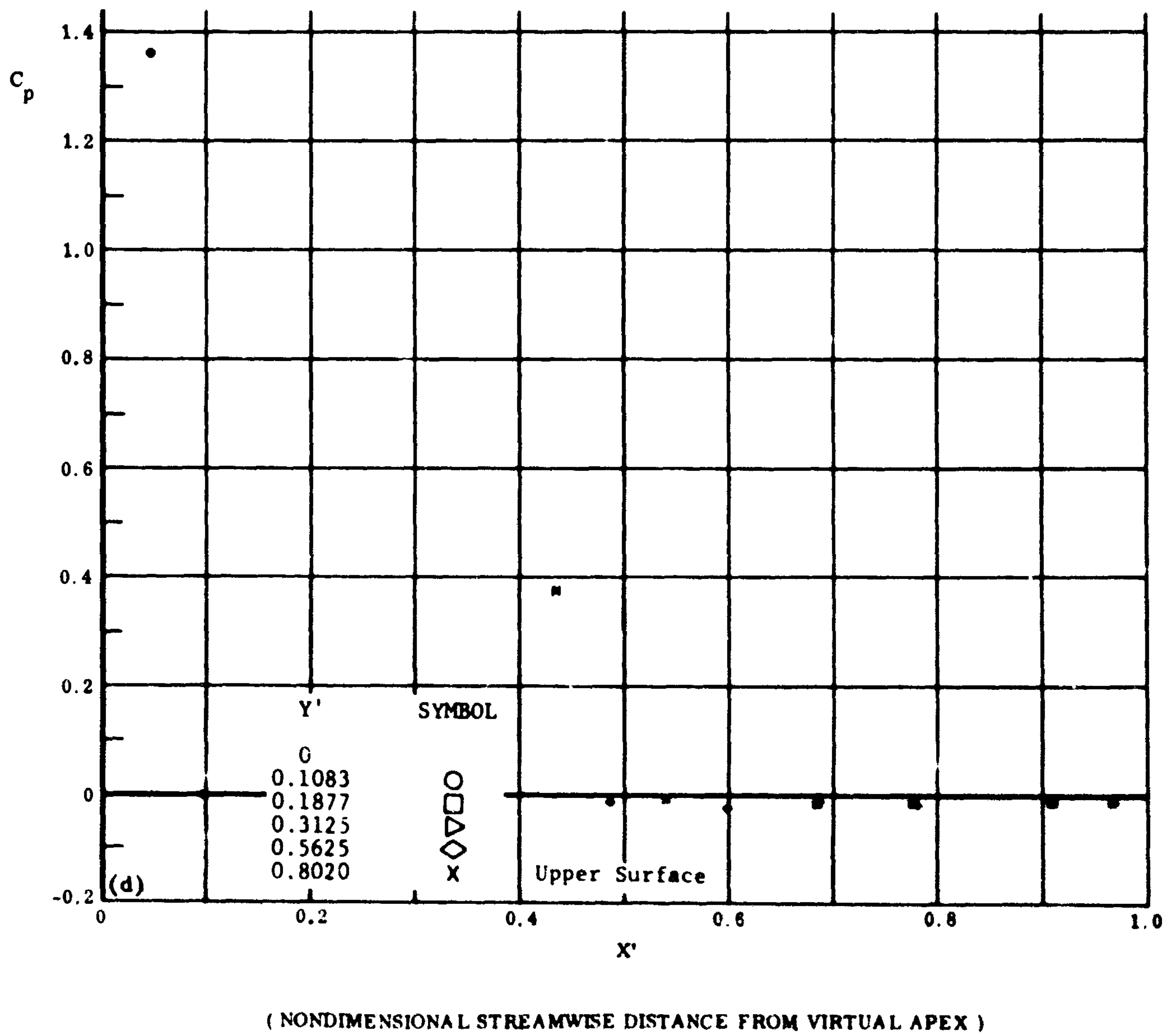

Fig. 35 Configuration IV, $\alpha = +30$, $\delta_2 = \delta_3 = 0$

c) C_p vs. Y', upper surface

d) C_p vs. X', upper surface

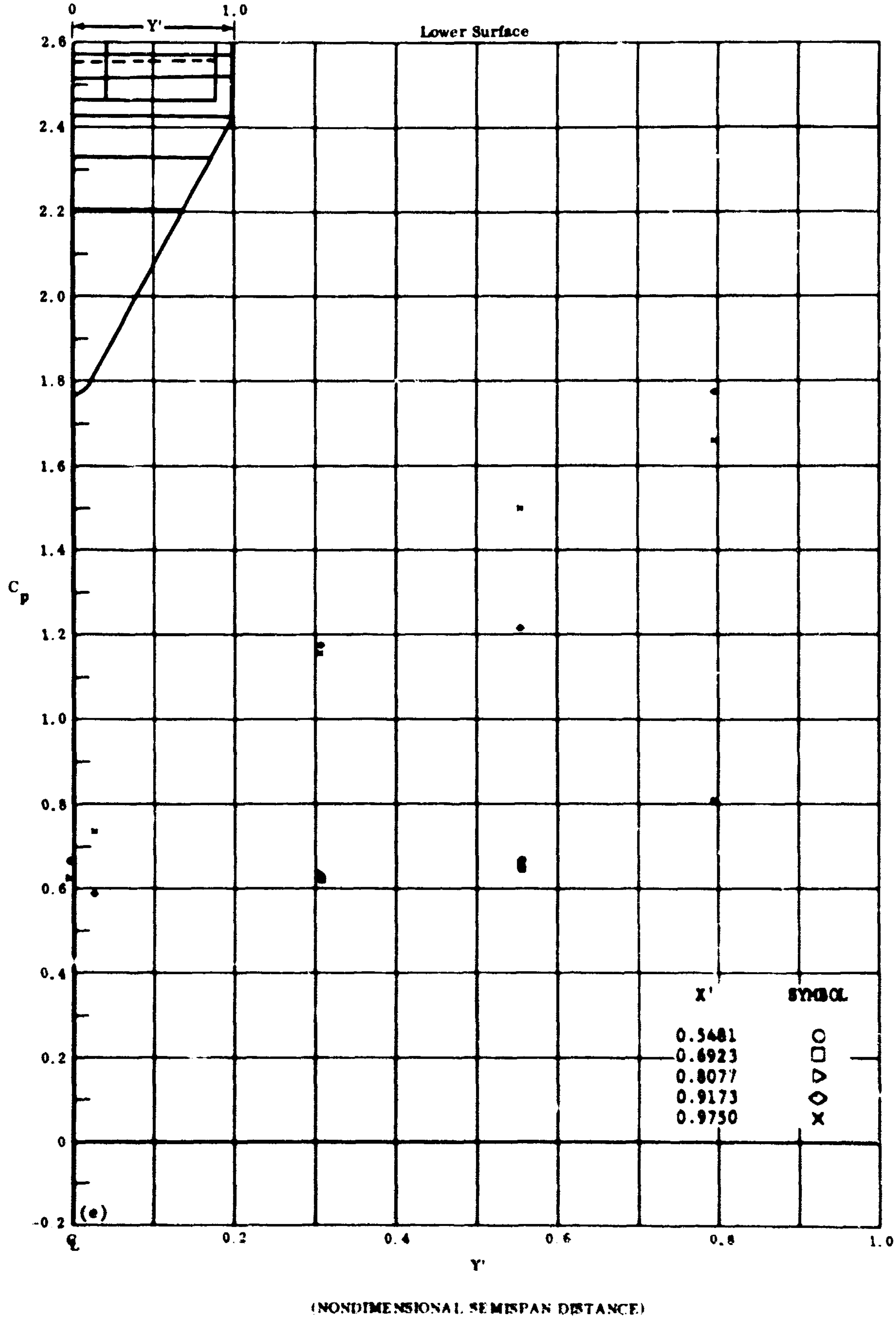

Fig. 35e Configuration IV, $_1$ = +30 , $_2$ = $_3$ = +10

C_p vs. Y', lower surface

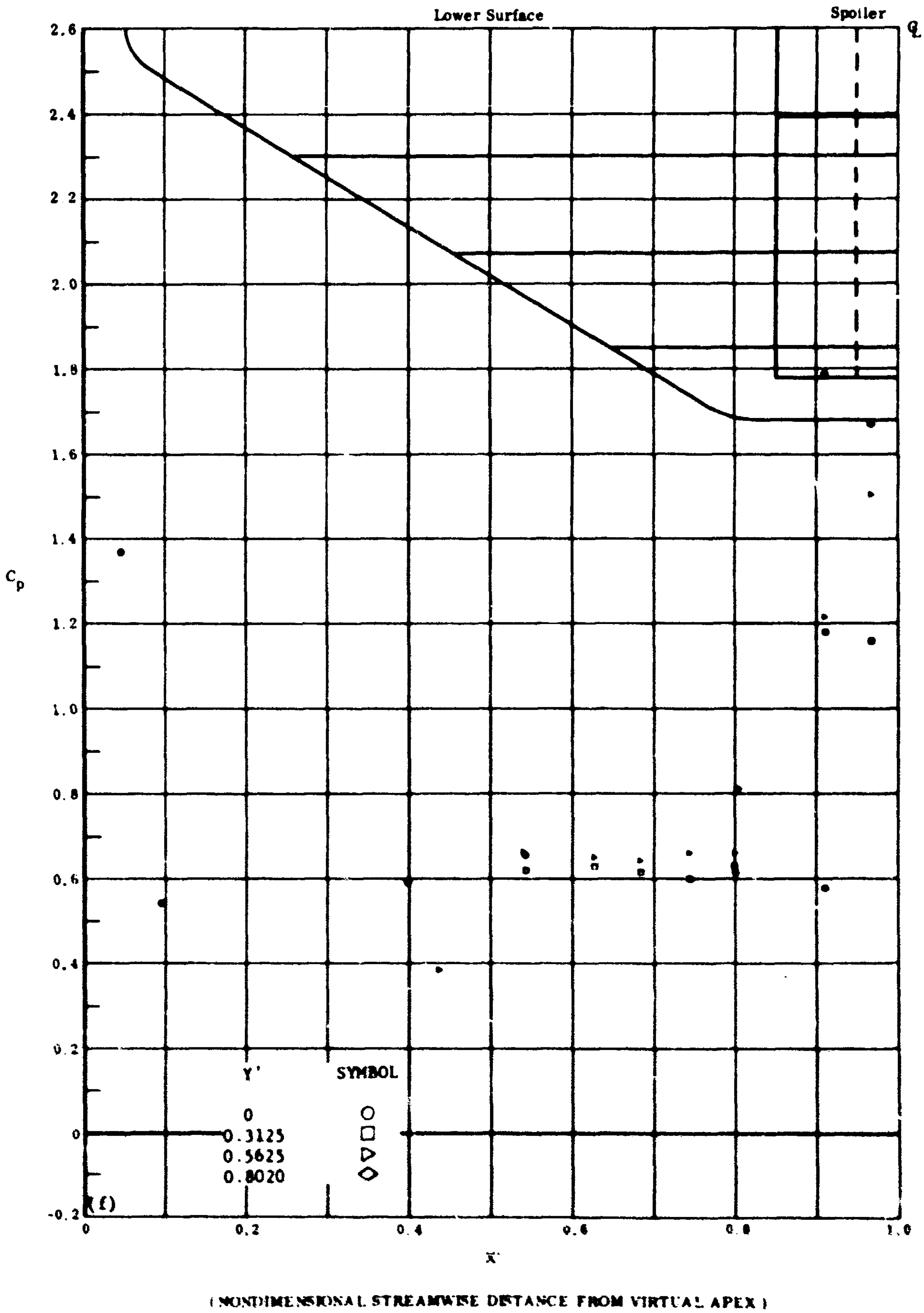

Fig. 35f Configuration IV, $\alpha = +30$, $\delta_2 = \delta_3 = +10$

C_p vs. X', lower surface

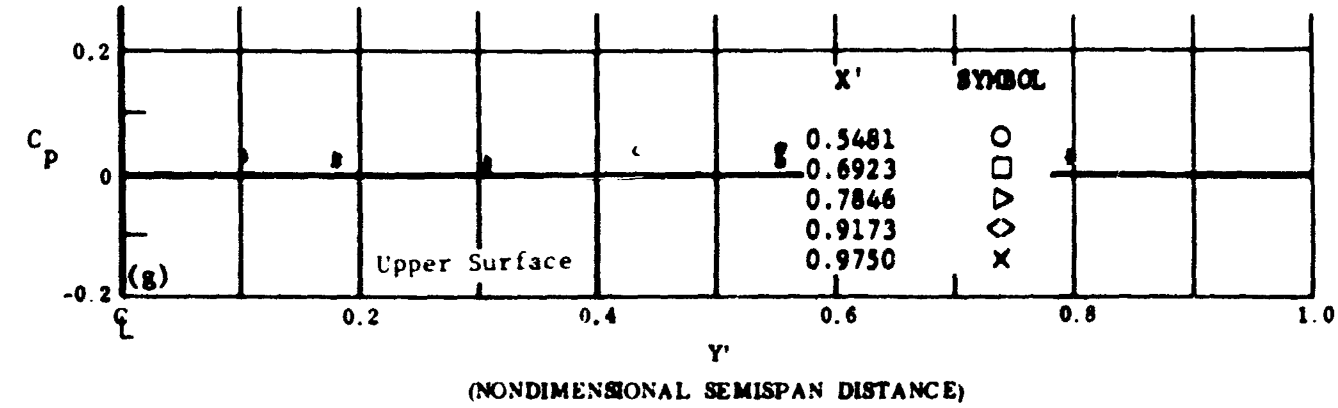

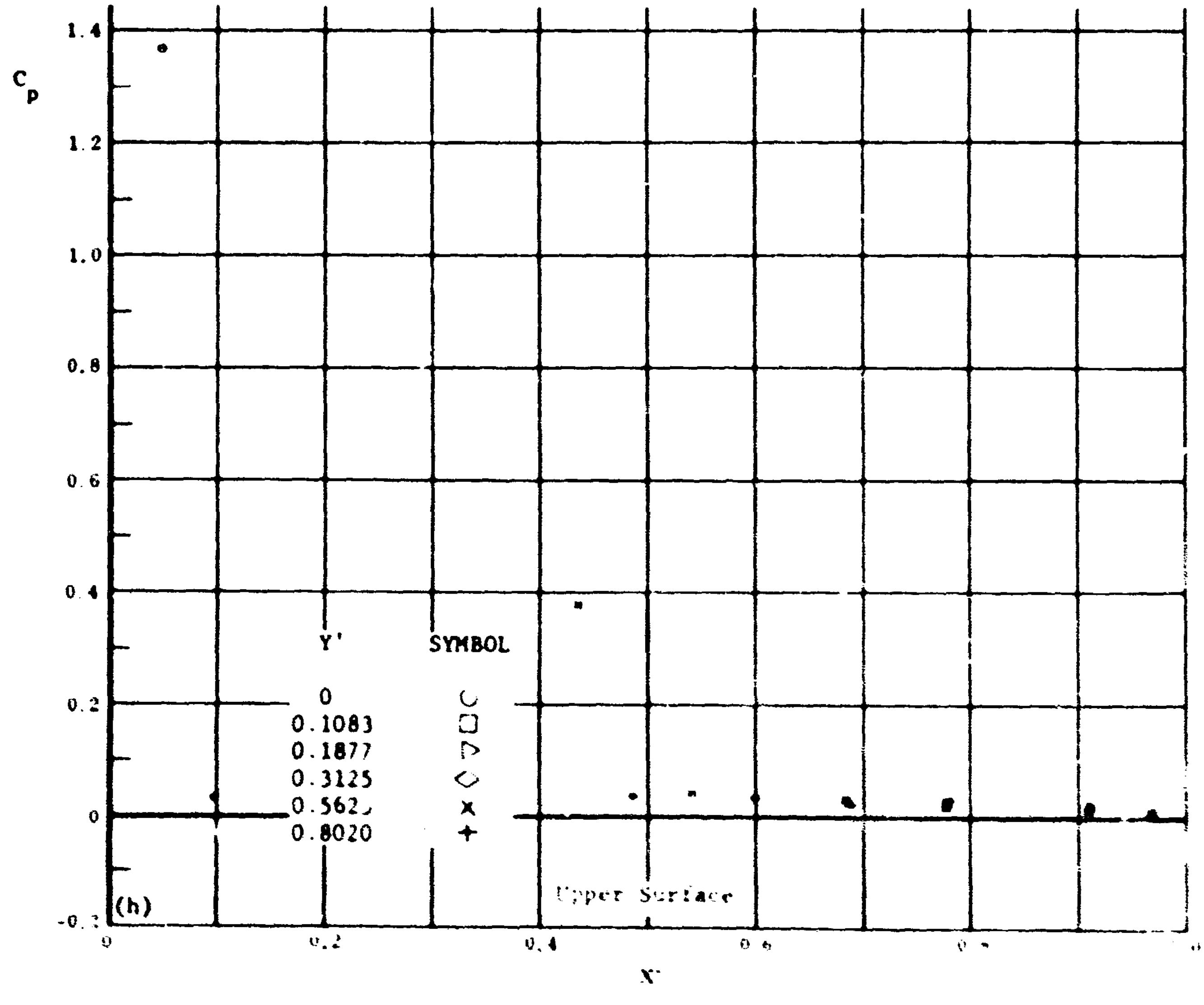

(NONDIMENSIONAL STREAMWISE DISTANCE FROM VIRTUAL APEX)

Fig. 35 Configuration IV, $\alpha = +30°$, $\delta_2 = \delta_3 = +10°$

g) C_p vs. Y', upper surface

h) C_p vs. X', upper surface

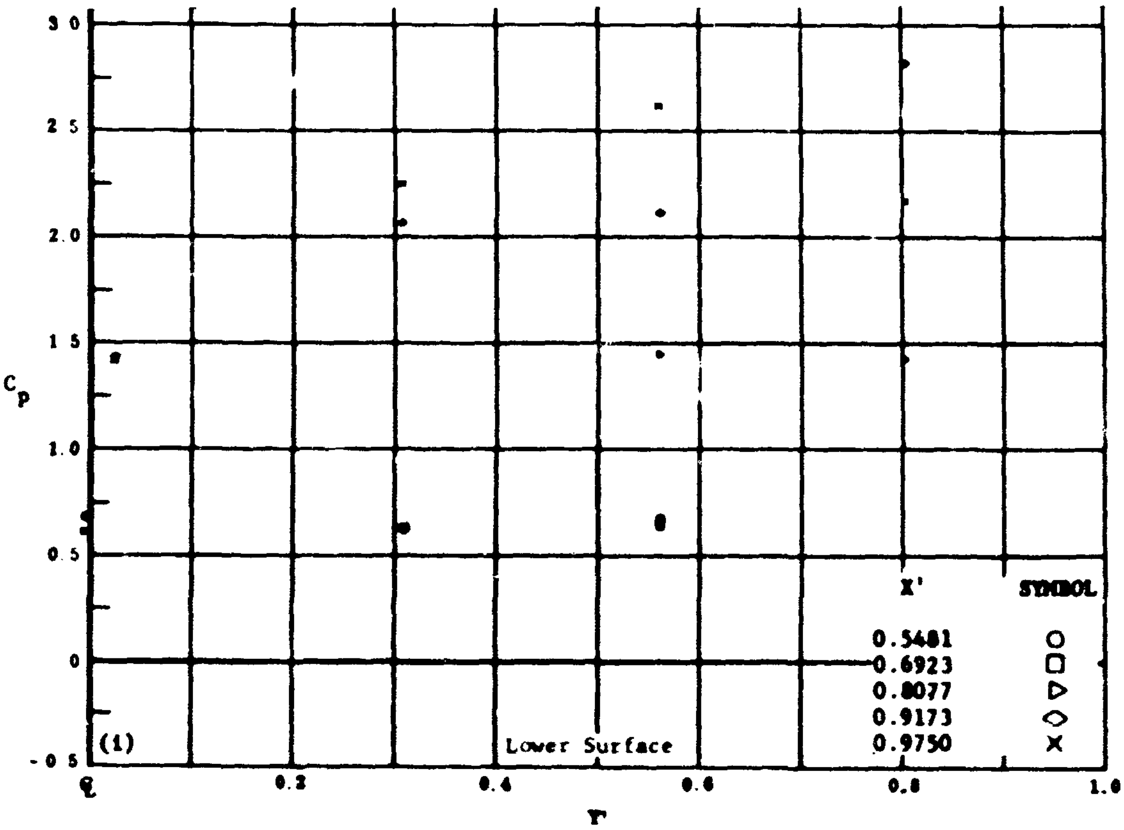

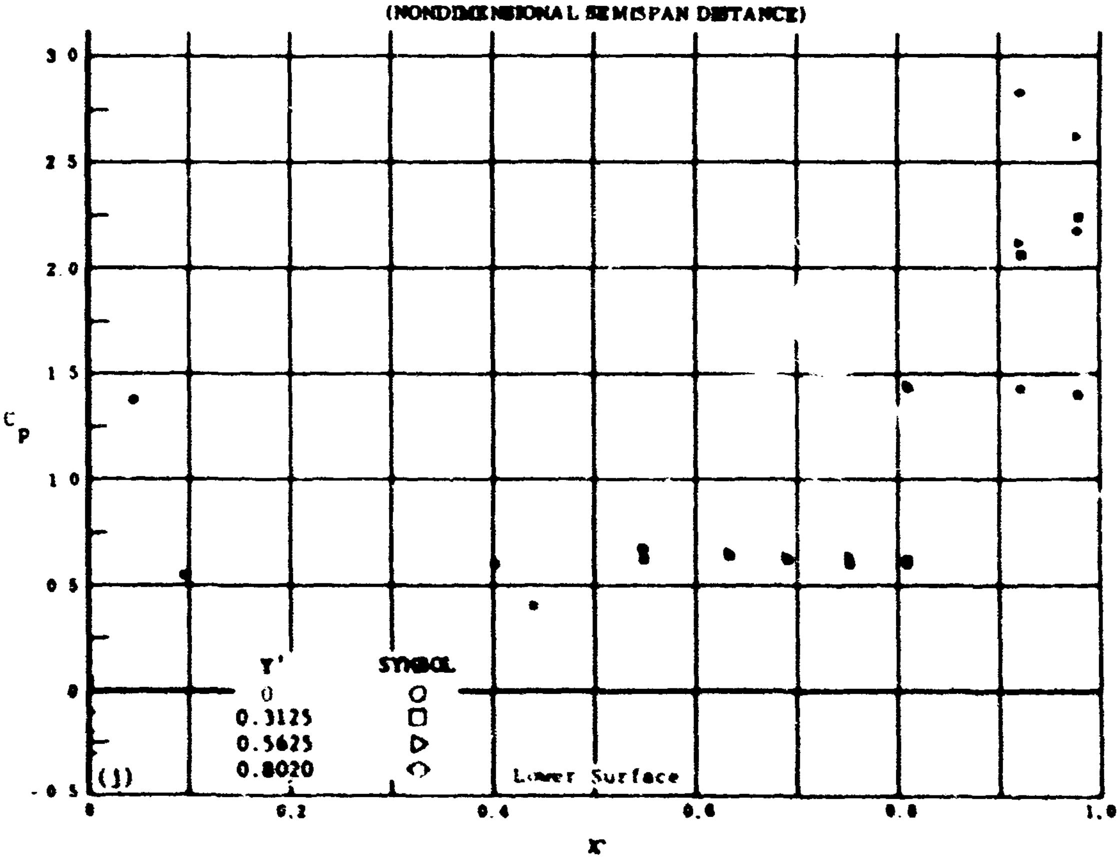

Fig. 35 Configuration IV, $\delta = +30$, $\delta_2 = \delta_3 = +20$

i) C_p vs. Y', lower surface

j) C_p vs. X', lower surface

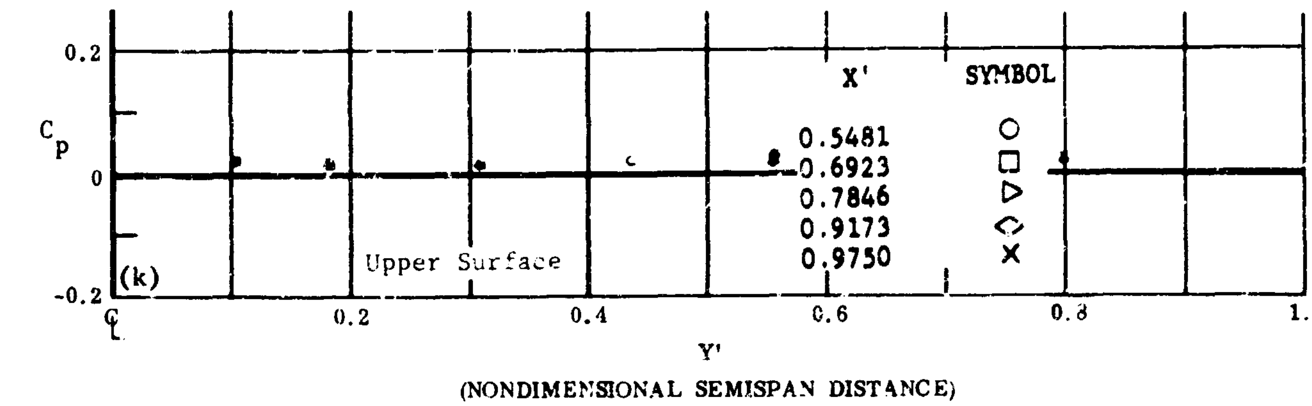

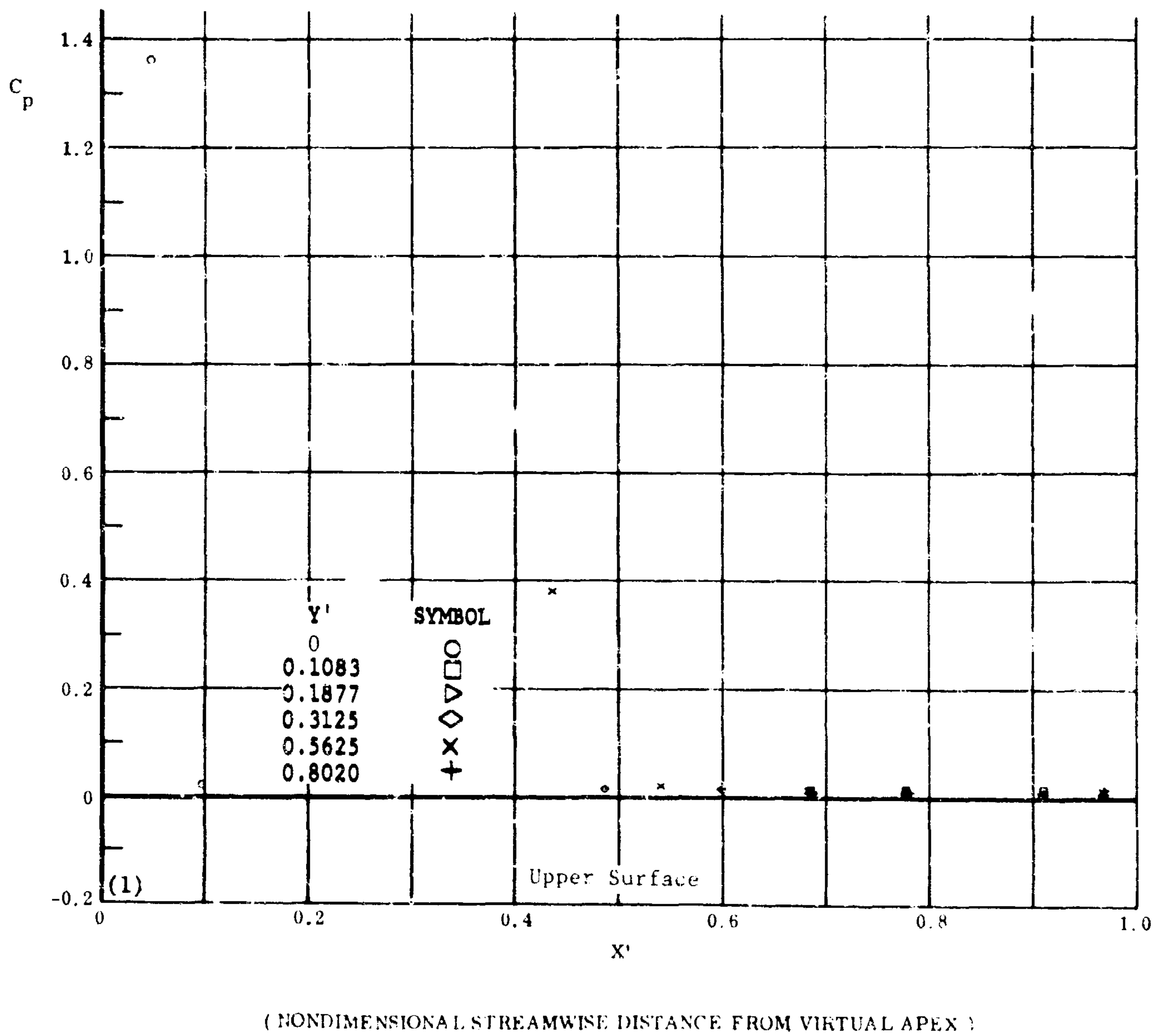

Fig. 35 Configuration IV, α = +30 , $\delta_2 = \delta_3$ +20

k) C_p vs. Y', upper surface

l) C_p vs. X', upper surface

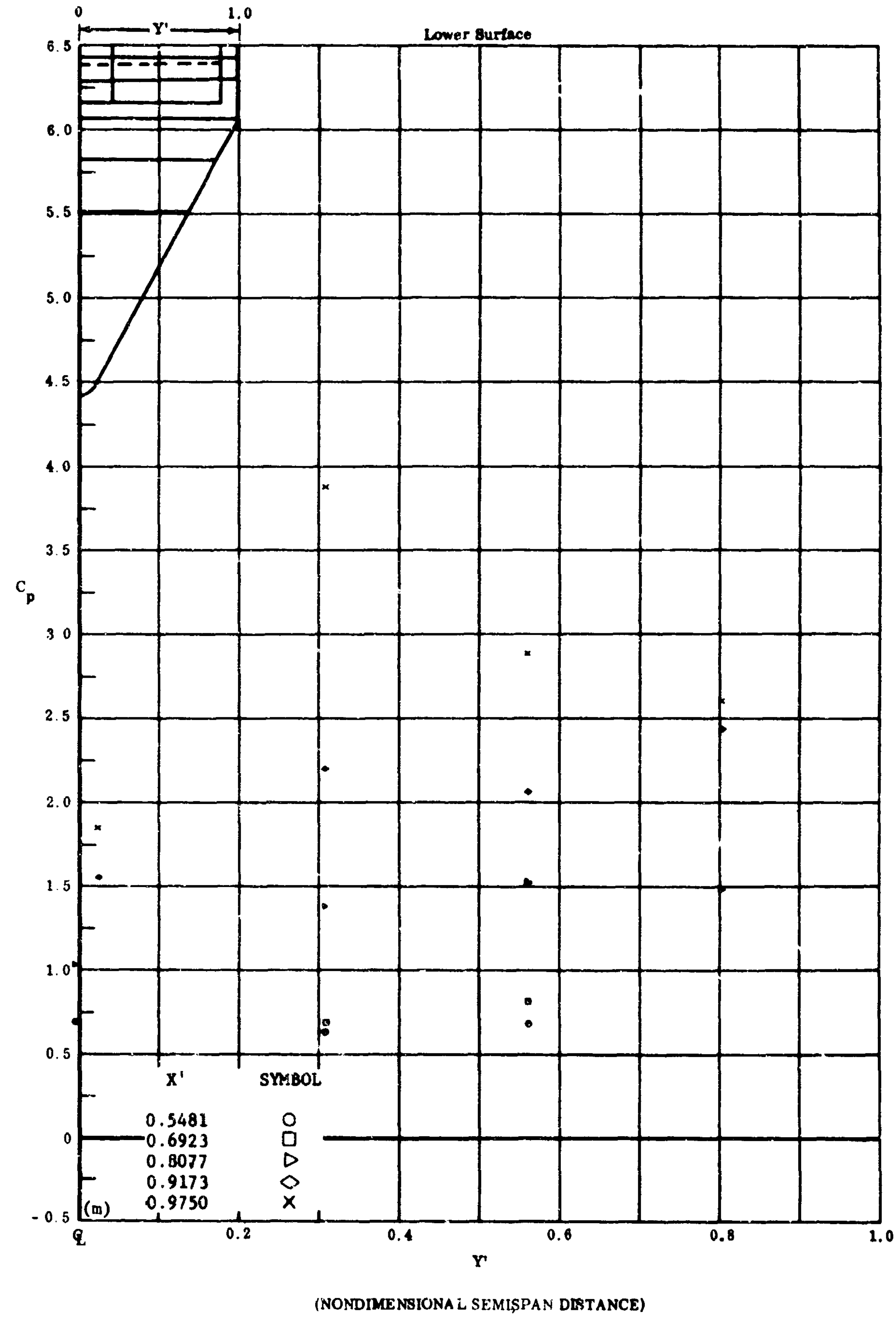

Fig. 35m Configuration IV, $\alpha = +30$, $\delta_2 = \delta_3 = +30$

C_p vs. Y', lower surface

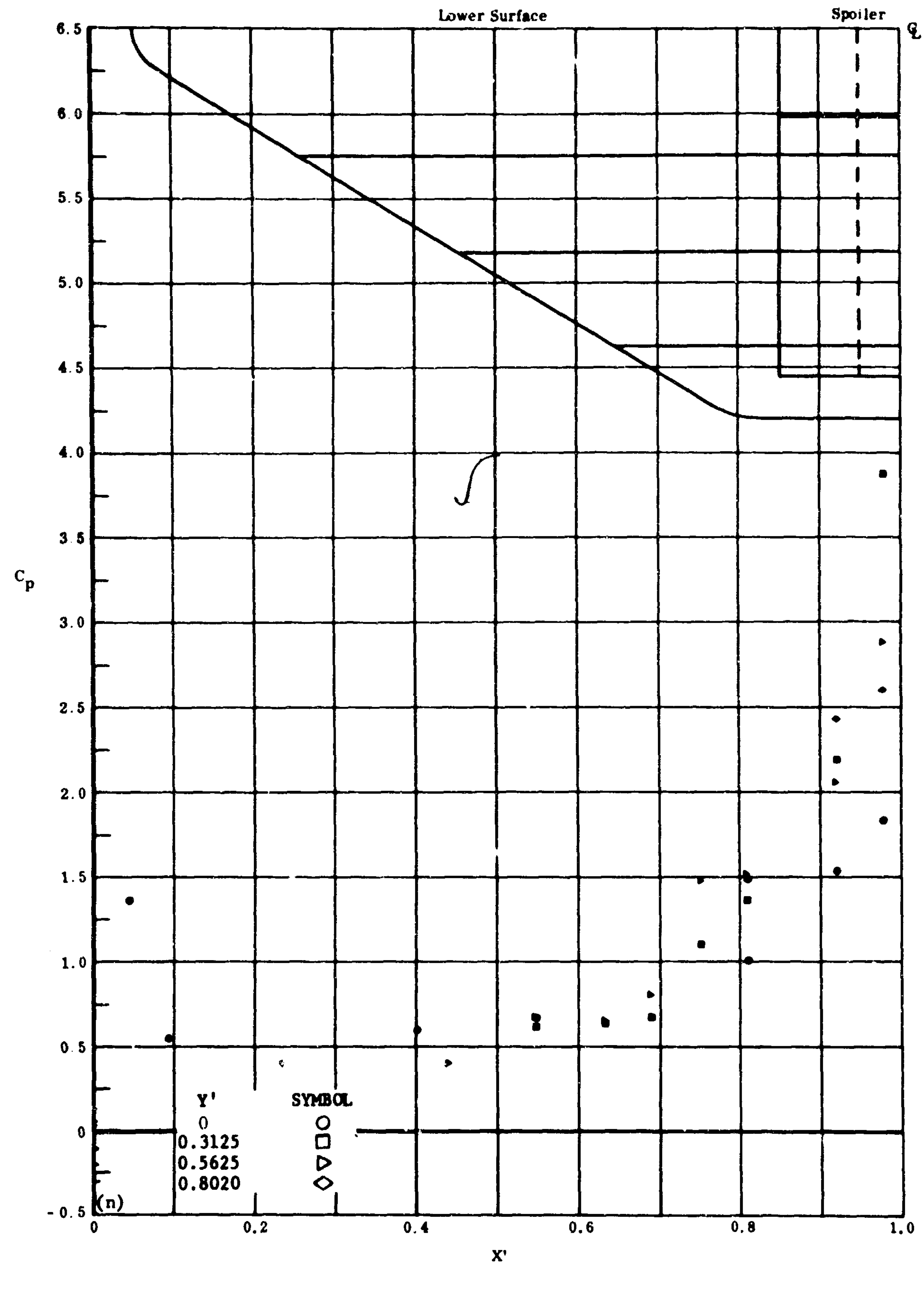

Fig. 35n Configuration IV, $\alpha = +30$, $\delta_2 = \delta_3 = +30$

C_p vs. X', lower surface

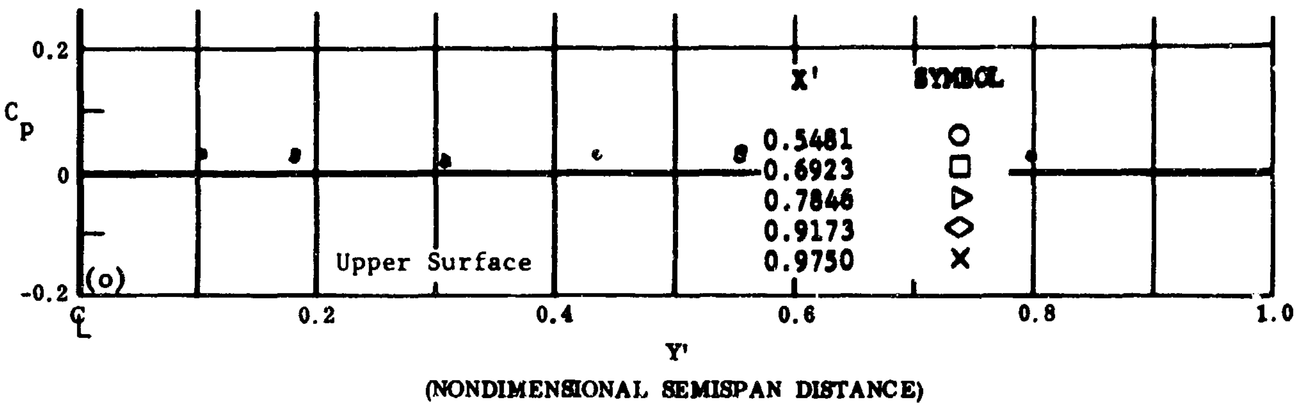

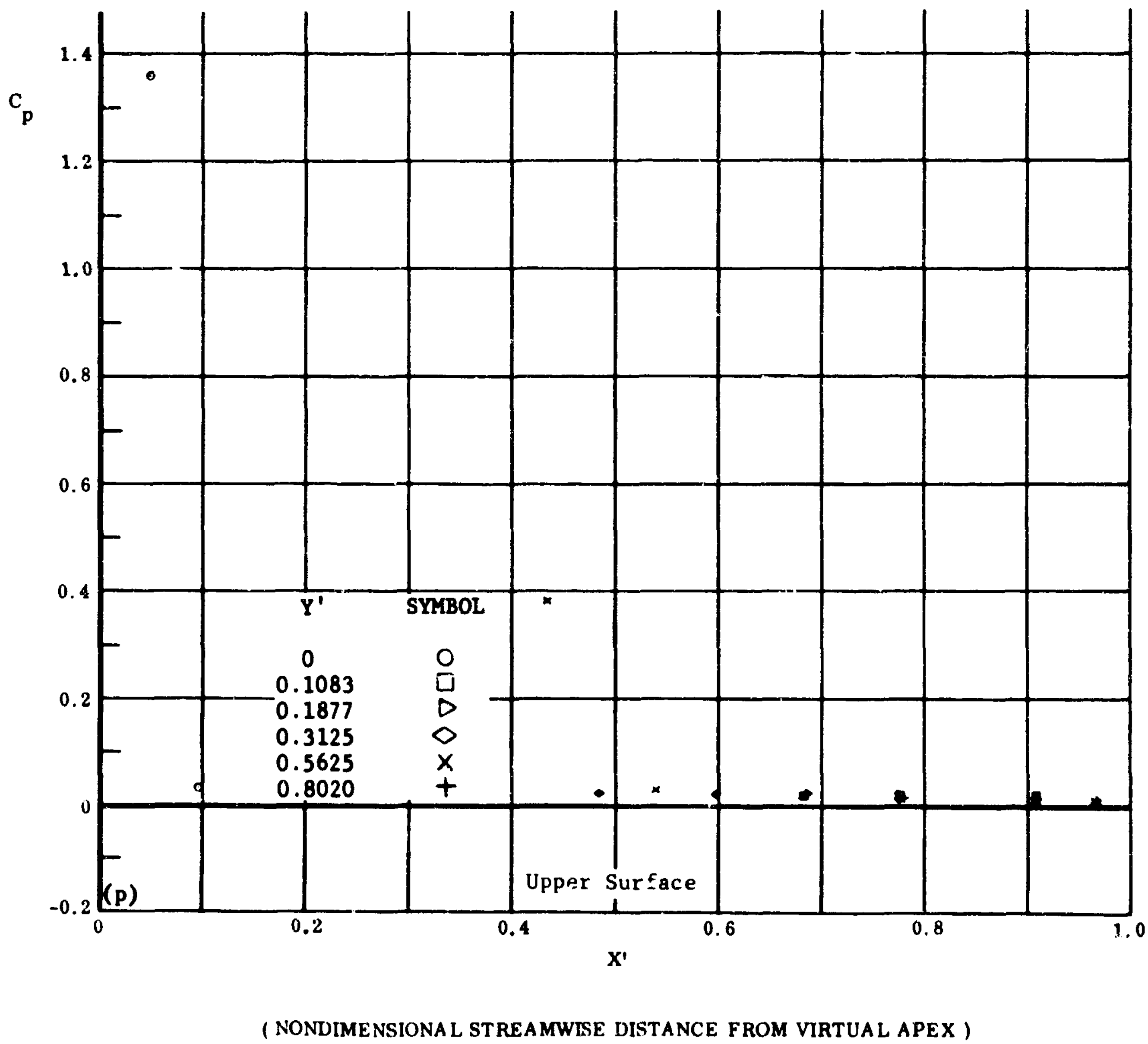

Fig. 35 Configuration IV, $\alpha = +30$, $\delta_2 = \delta_3 = +30$

o) C_p vs. Y', upper surface

p) C_p vs. X', upper surface

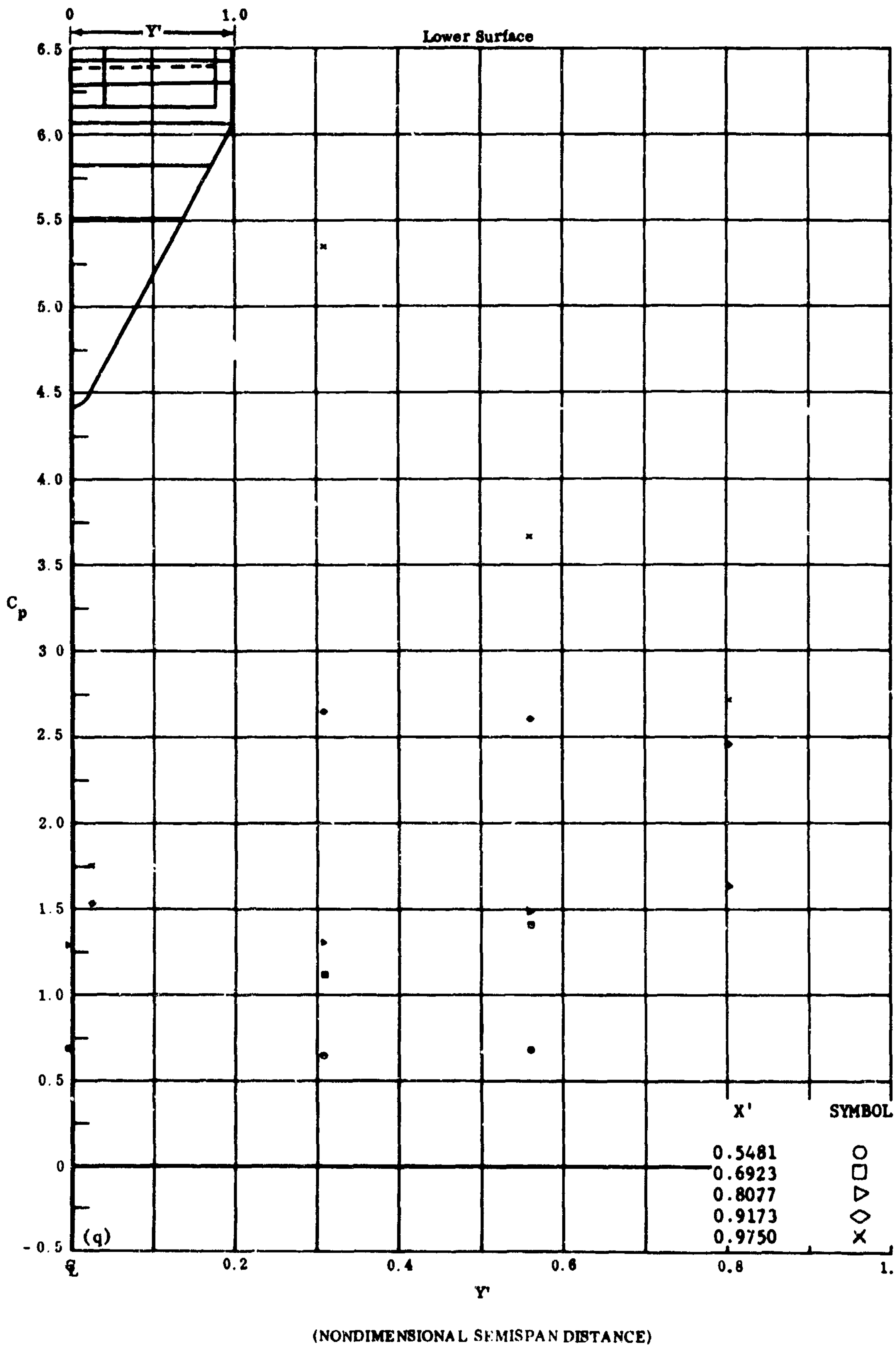

Fig. 35q Configuration IV, α = +30 , $\delta_2 = \delta_3$ = +39

C_p vs. Y', lower surface

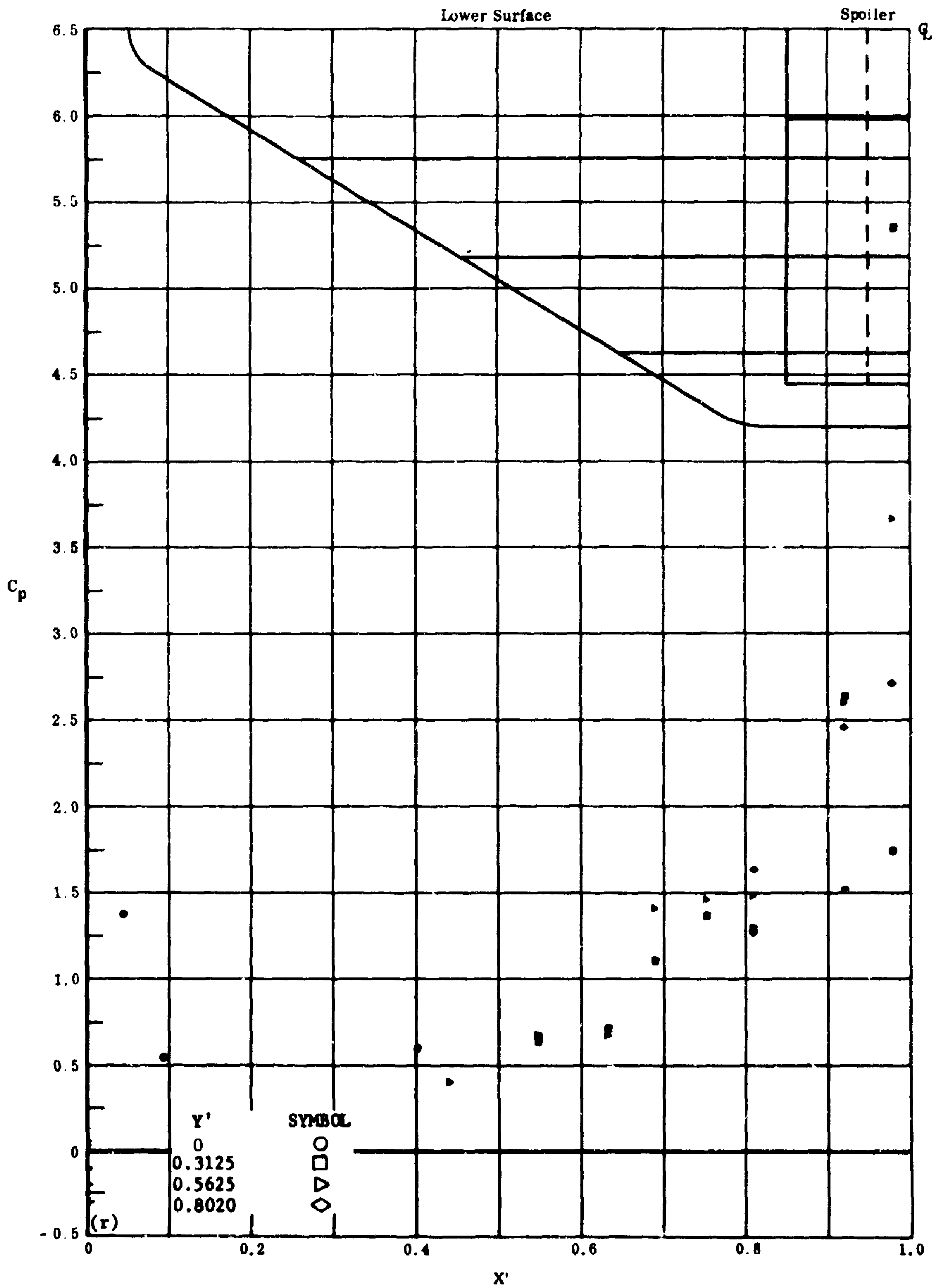

(NONDIMENSIONAL STREAMWISE DISTANCE FROM VIRTUAL APEX)

Fig. 35r Configuration IV, $\alpha = +30$, $\delta_2 = \delta_3 = +39$

C_p vs. X', lower surface

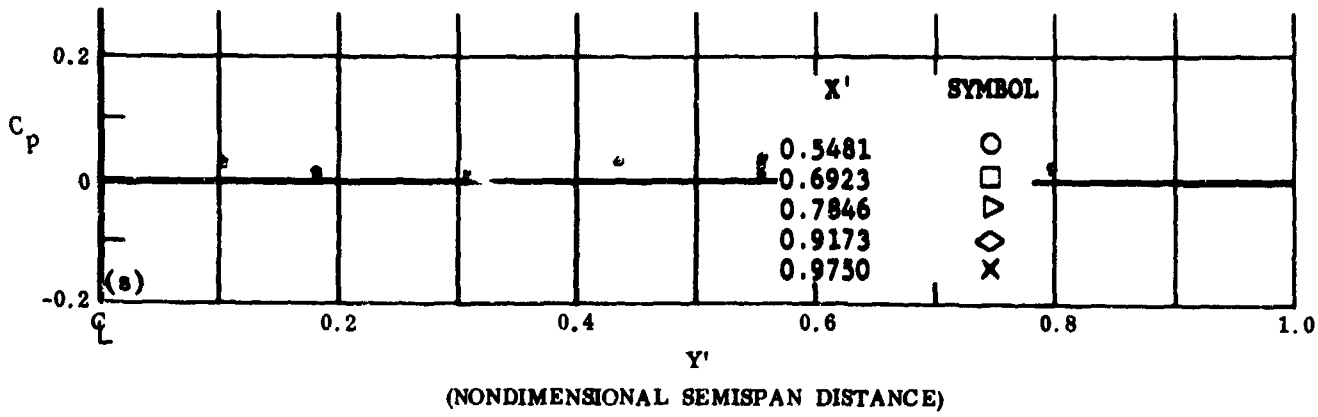

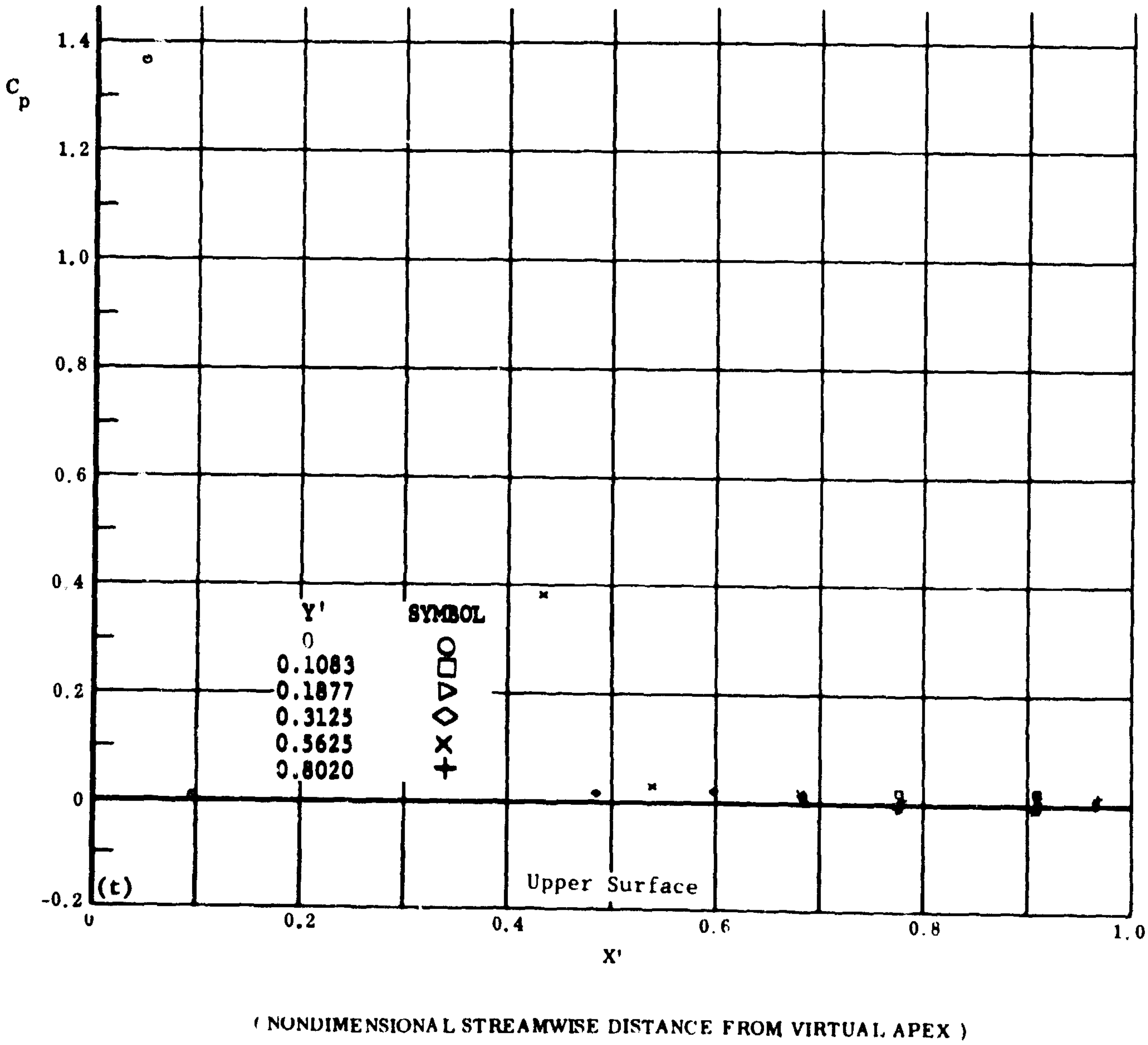

Fig. 35 Configuration IV, $\sigma = +30$, $\delta_2 = \delta_3 = +39$

s) C_p vs. Y', upper surface

t) C_p vs. X', upper surface

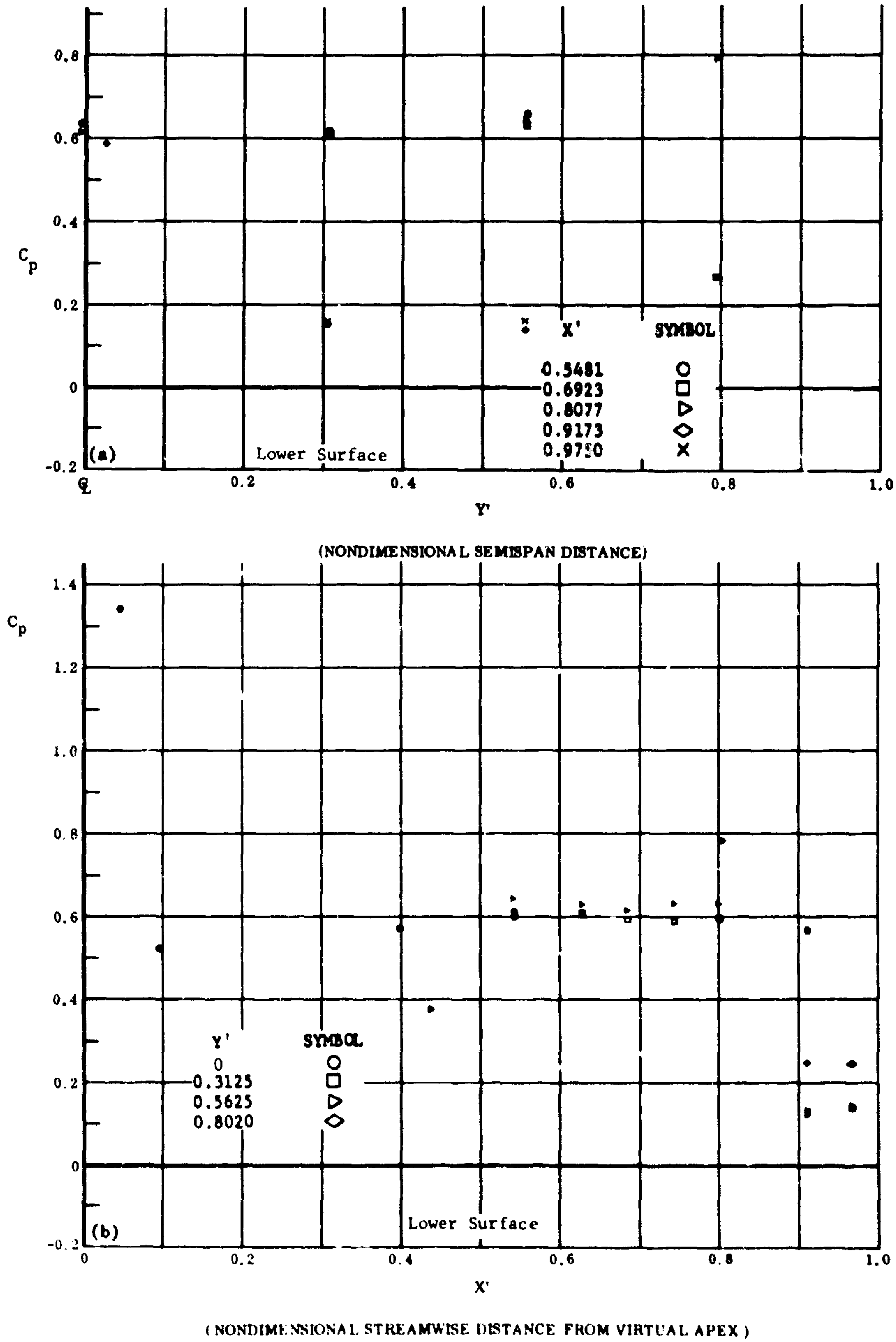

Fig. 36 Configuration IV, $\alpha = +30$, $\delta_2 = \delta_3 = -20$

a) C_p vs. Y', lower surface

b) C_p vs. X', lower surface

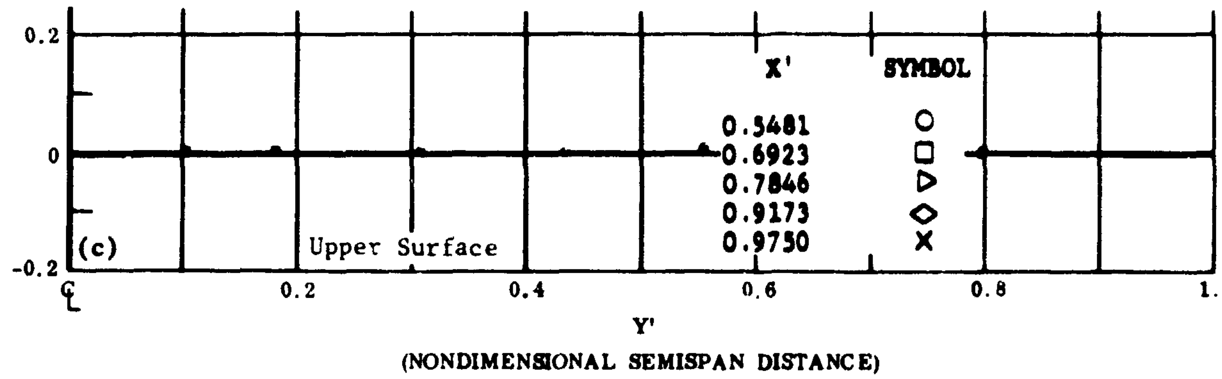

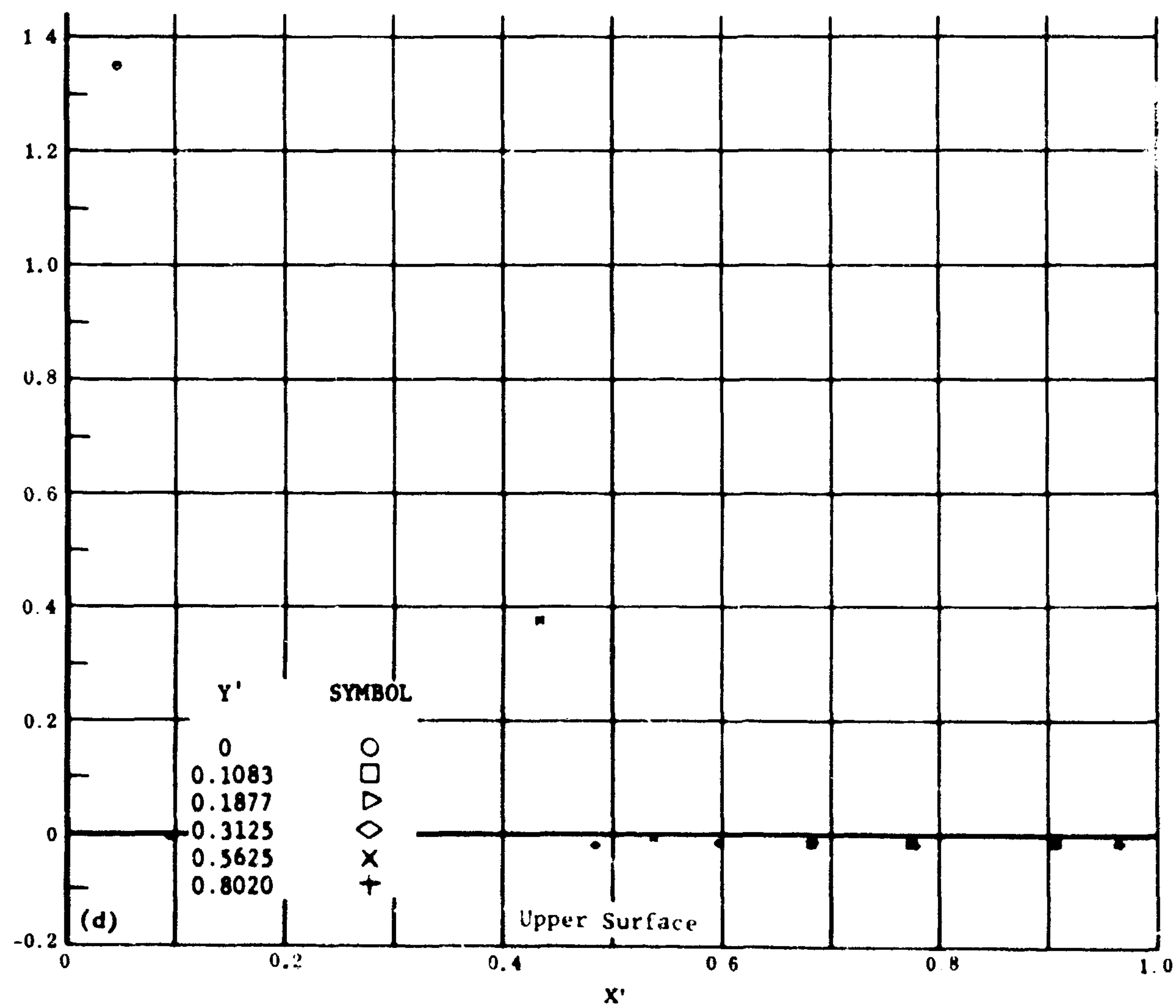

(NONDI... TREAMWISE DISTANCE FROM VIRTUAL APEX)

Fi... onfiguration IV, α = +30 , $\delta_2 = \delta_3$ = -20

... C_p vs. Y', upper surface

... C_p vs. X', upper surface

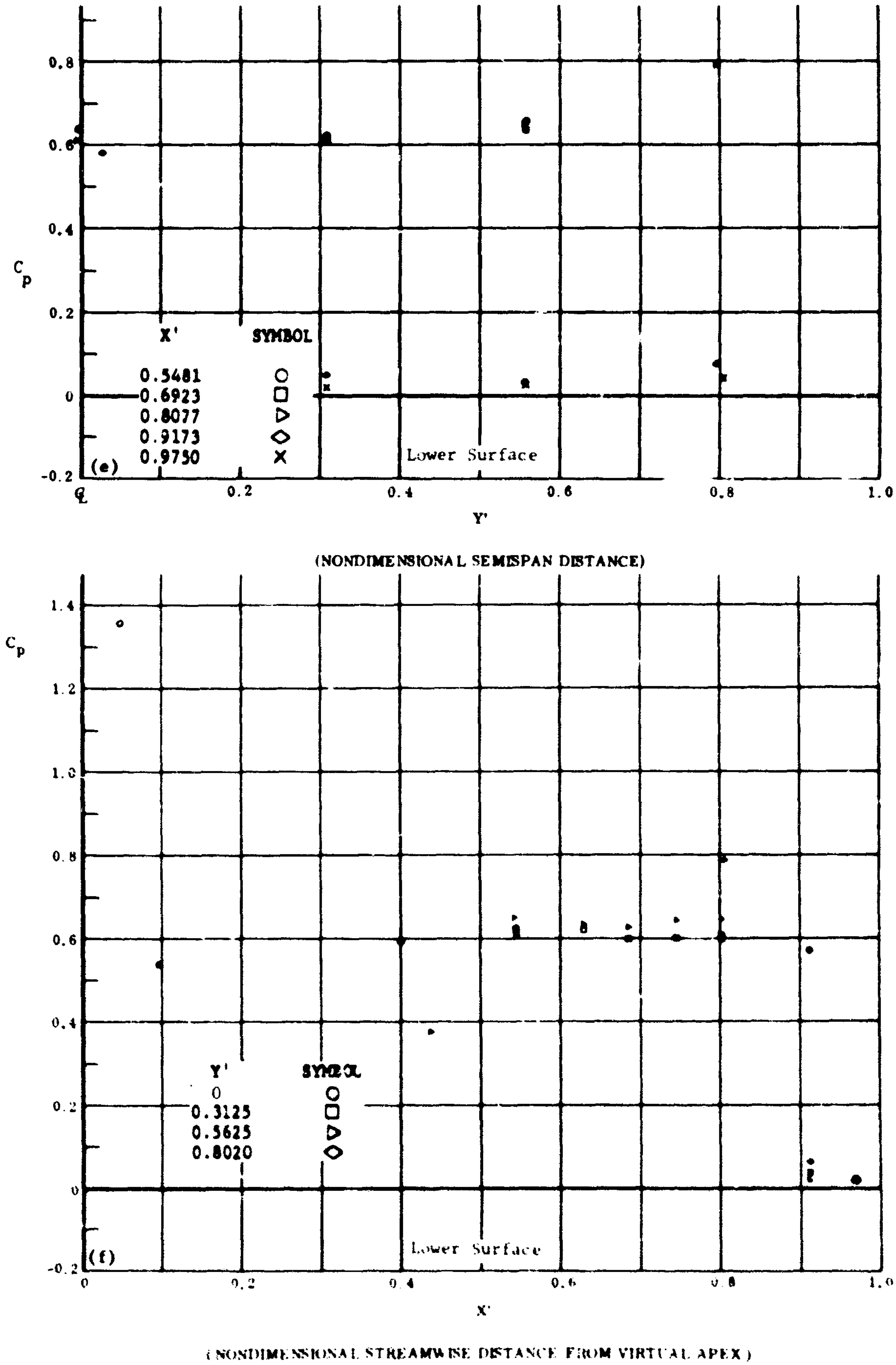

Fig. 36 Configuration IV, α = +30 , δ_2 = δ_3 = -39

e) C_p vs. Y', lower surface

f) C_p vs. X', lower surface

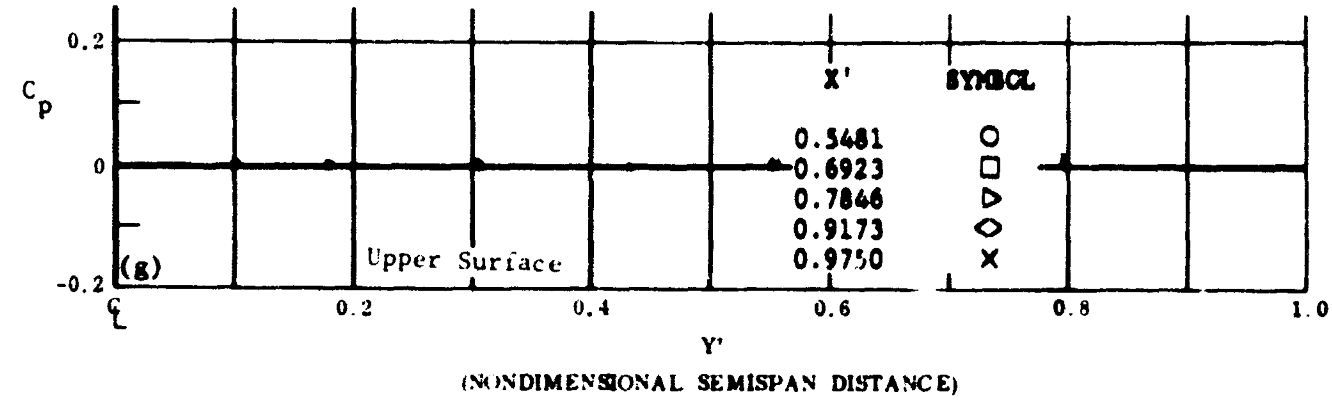

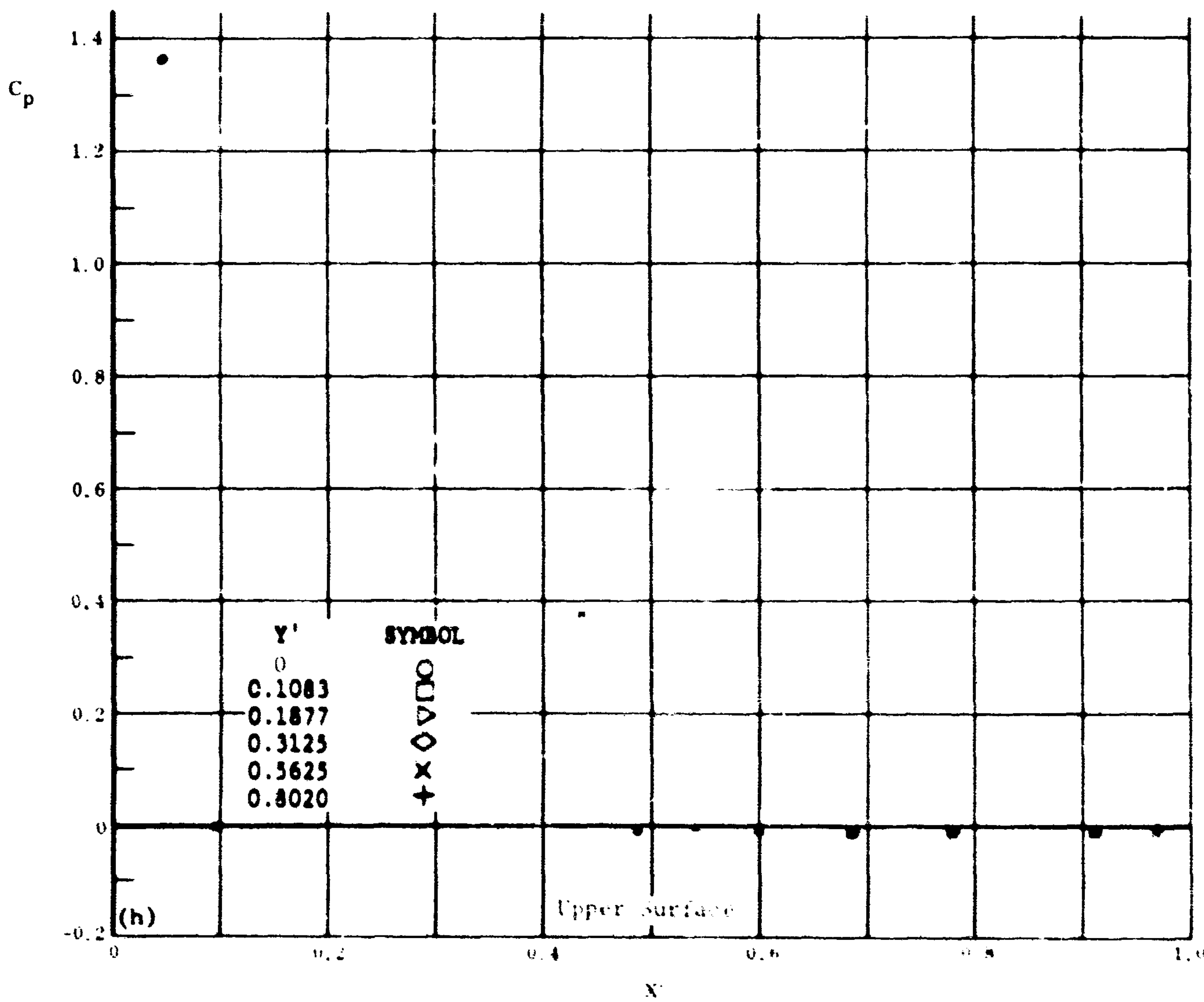

(NONDIMENSIONAL STREAMWISE DISTANCE FROM VIRTUAL APEX)

Fig. 36 Configuration IV, = +30 , $_2$ = $_3$ = -39

g) C_p vs. Y', upper surface

h) C_p vs. X', upper surface

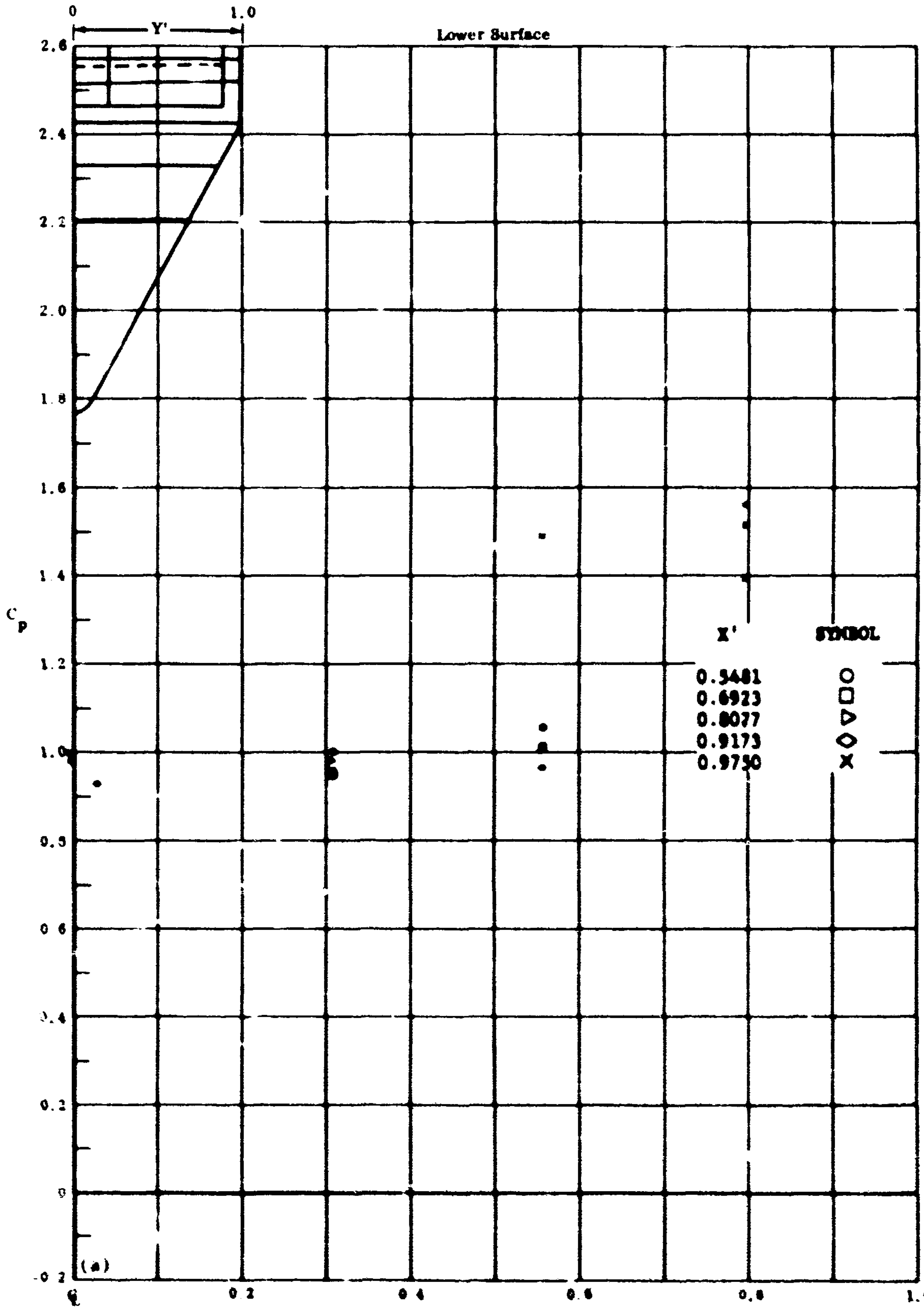

Fig. 37a Configuration IV, α = +40 . $\delta_2 = \delta_3 = 0$

C_p vs. Y', lower surface

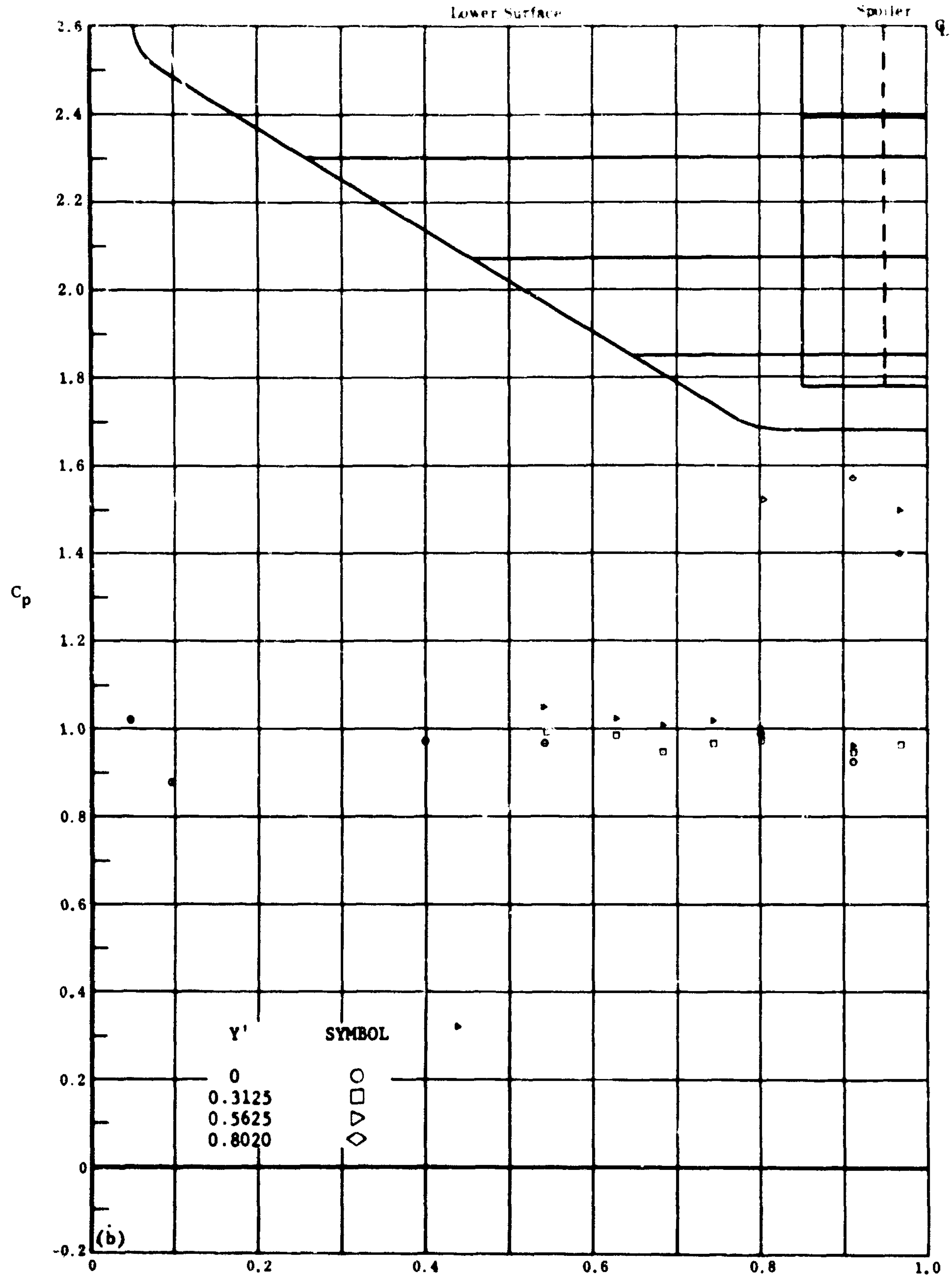

(NONDIMENSIONAL STREAMWISE DISTANCE FROM VIRTUAL APEX)

Fig. 37b Configuration IV, α = +40 , $\delta_2 = \delta_3 = 0$

C_p vs. X', lower surface

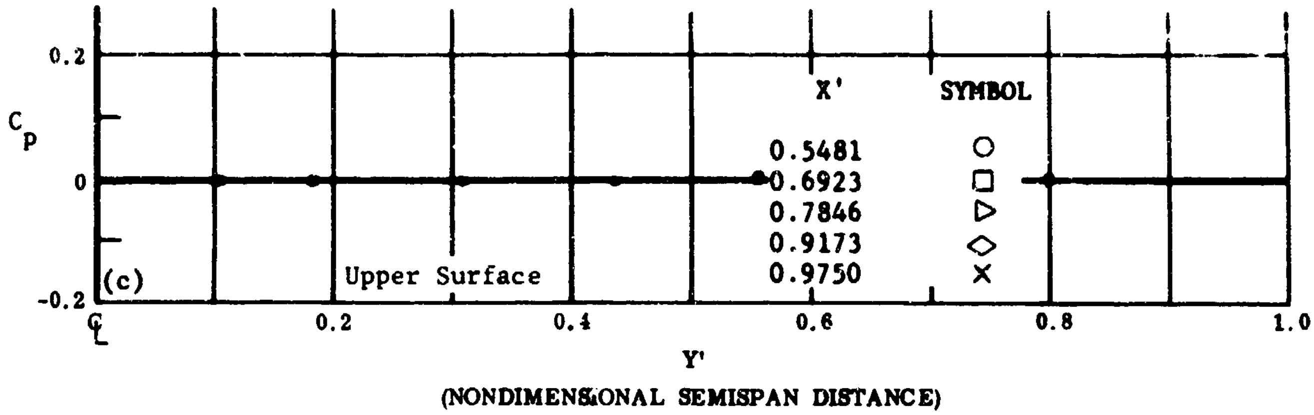

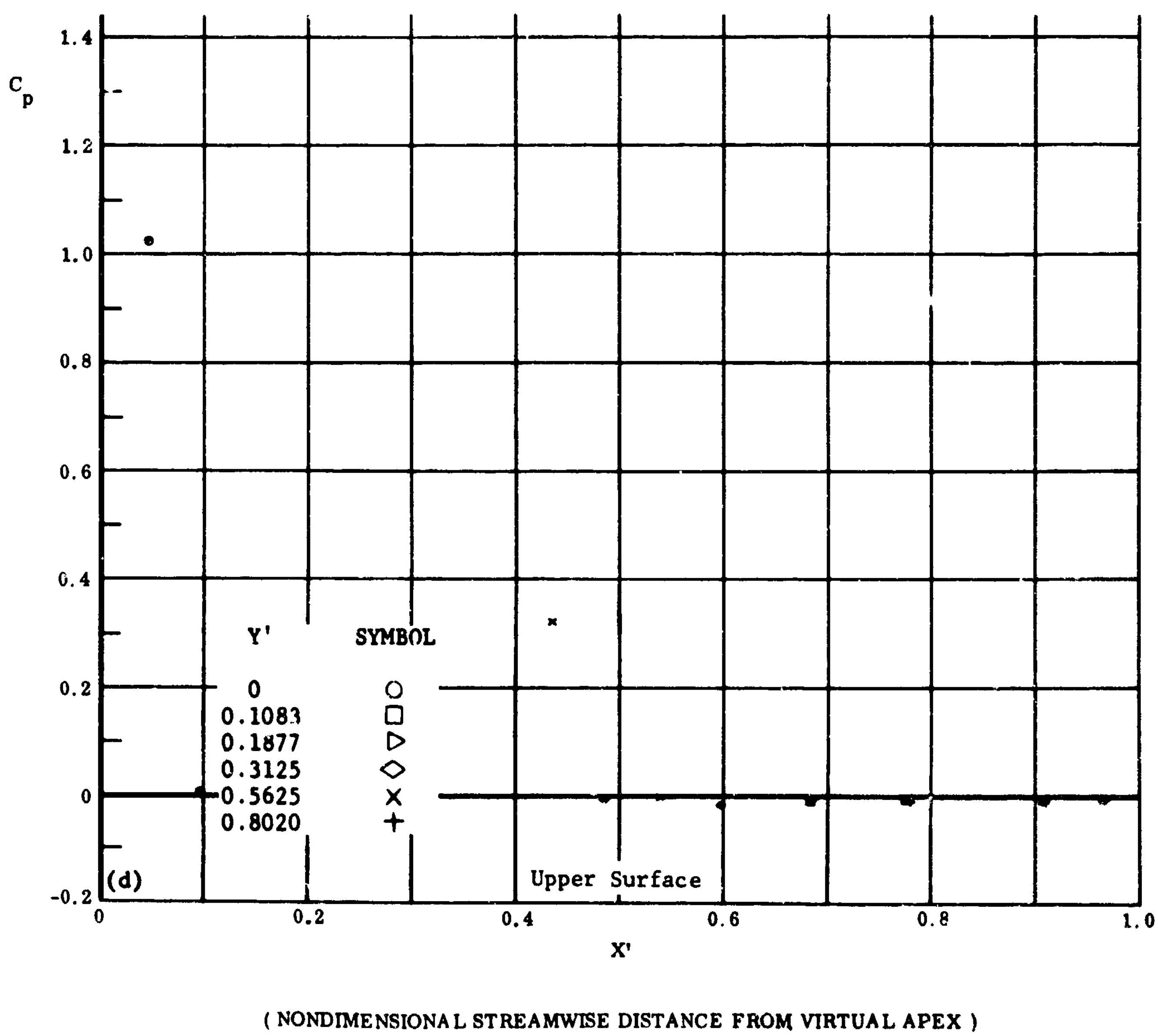

Fig. 37 Configuration IV, $\alpha = +40$, $\delta_2 = \delta_3 = 0$

c) C_p vs. Y', upper surface

d) C_p vs. X', upper surface

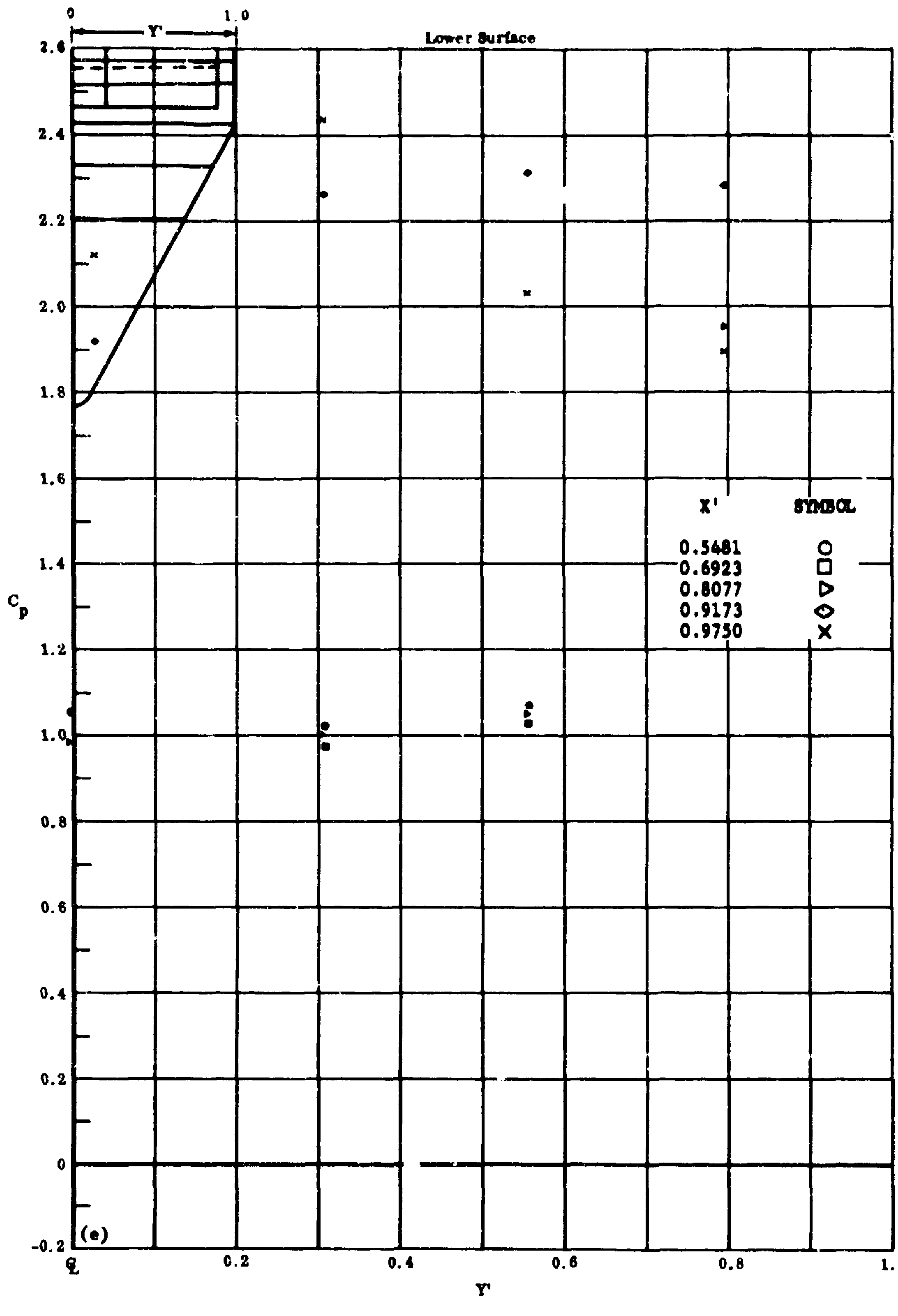

Fig. 37e Configuration IV, $\alpha = +40$, $\delta_2 = \delta_3 = +10$

C_p vs. Y', lower surface

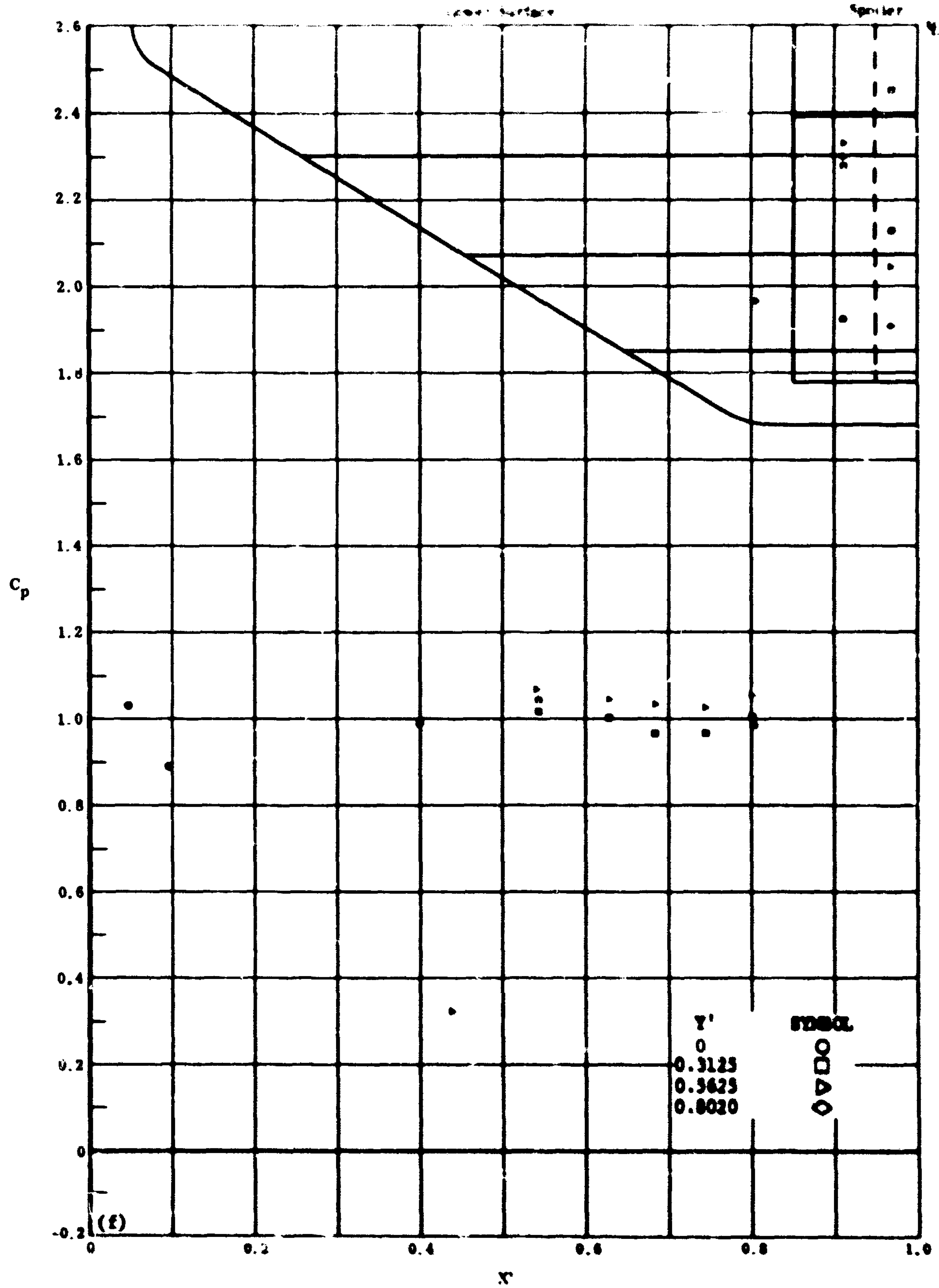

Fig. 37f Configuration IV, $\alpha = +40$, $\delta_2 = \delta_3 = +10$

C_p vs. X', lower surface

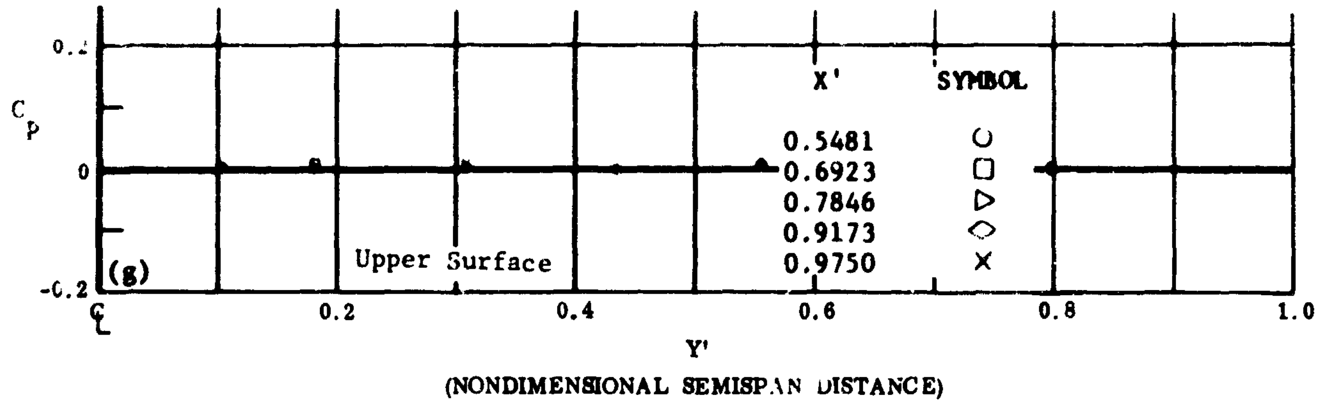

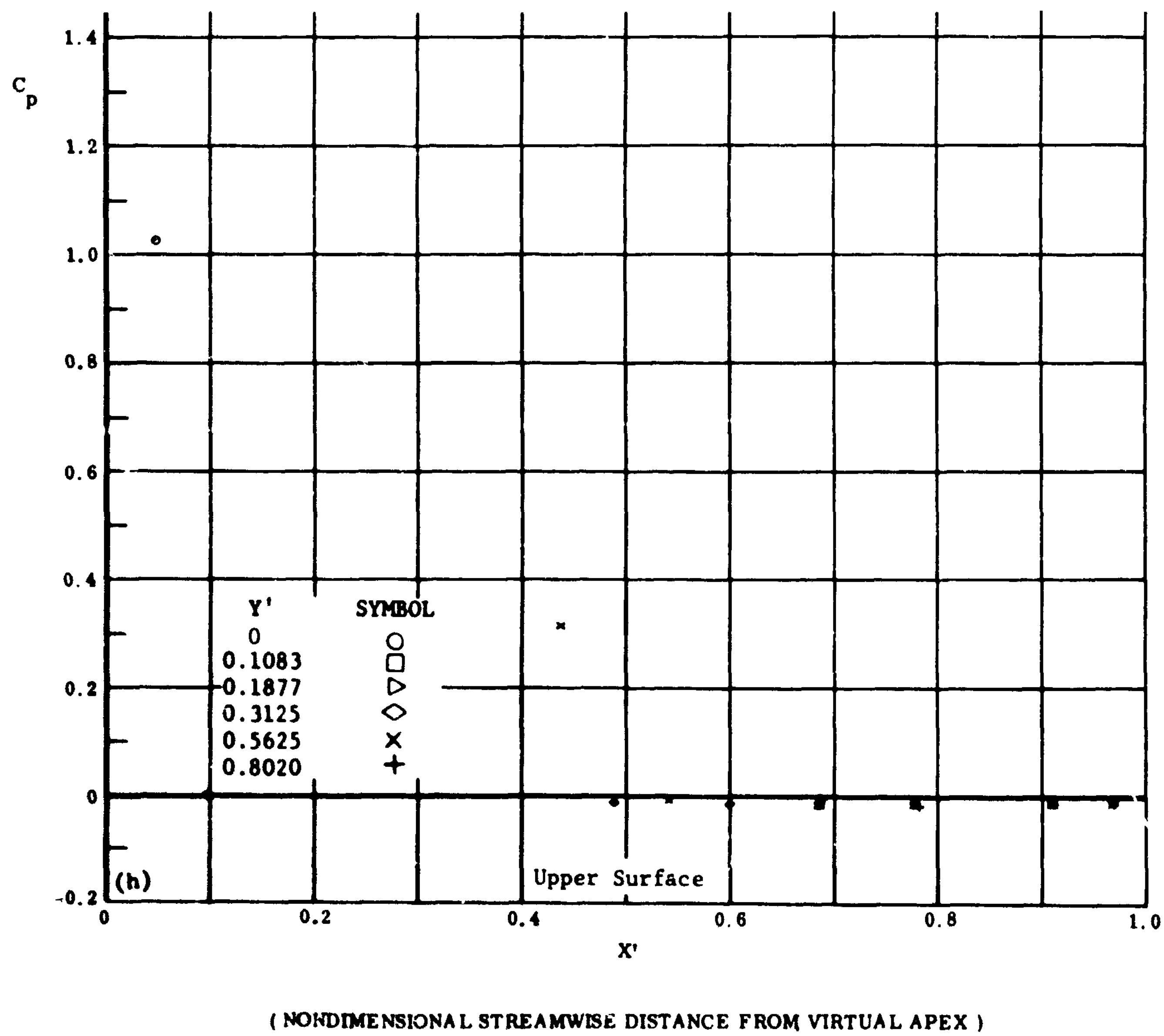

Fig. 37 Configuration IV, $\alpha = +40$, $\delta_2 = \delta_3 = +10$

g) C_p vs. Y', upper surface

h) C_p vs. X', upper surface

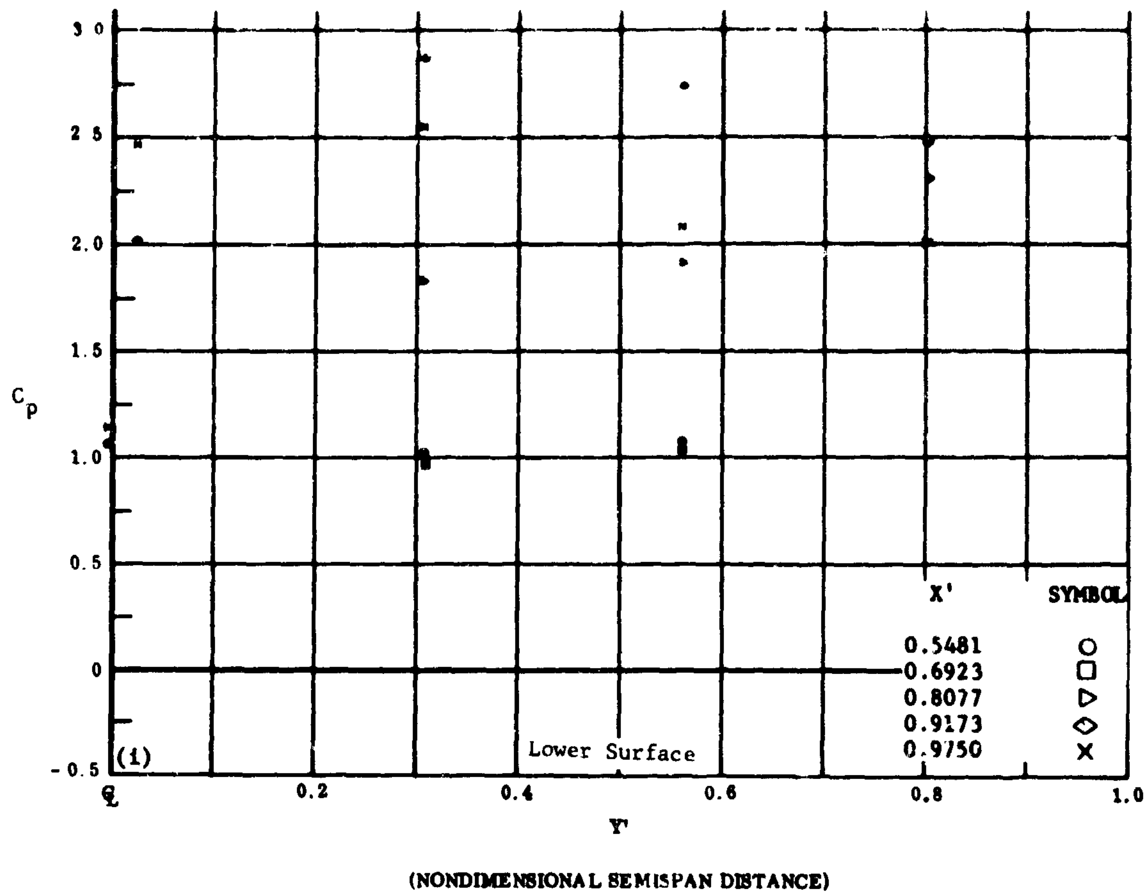

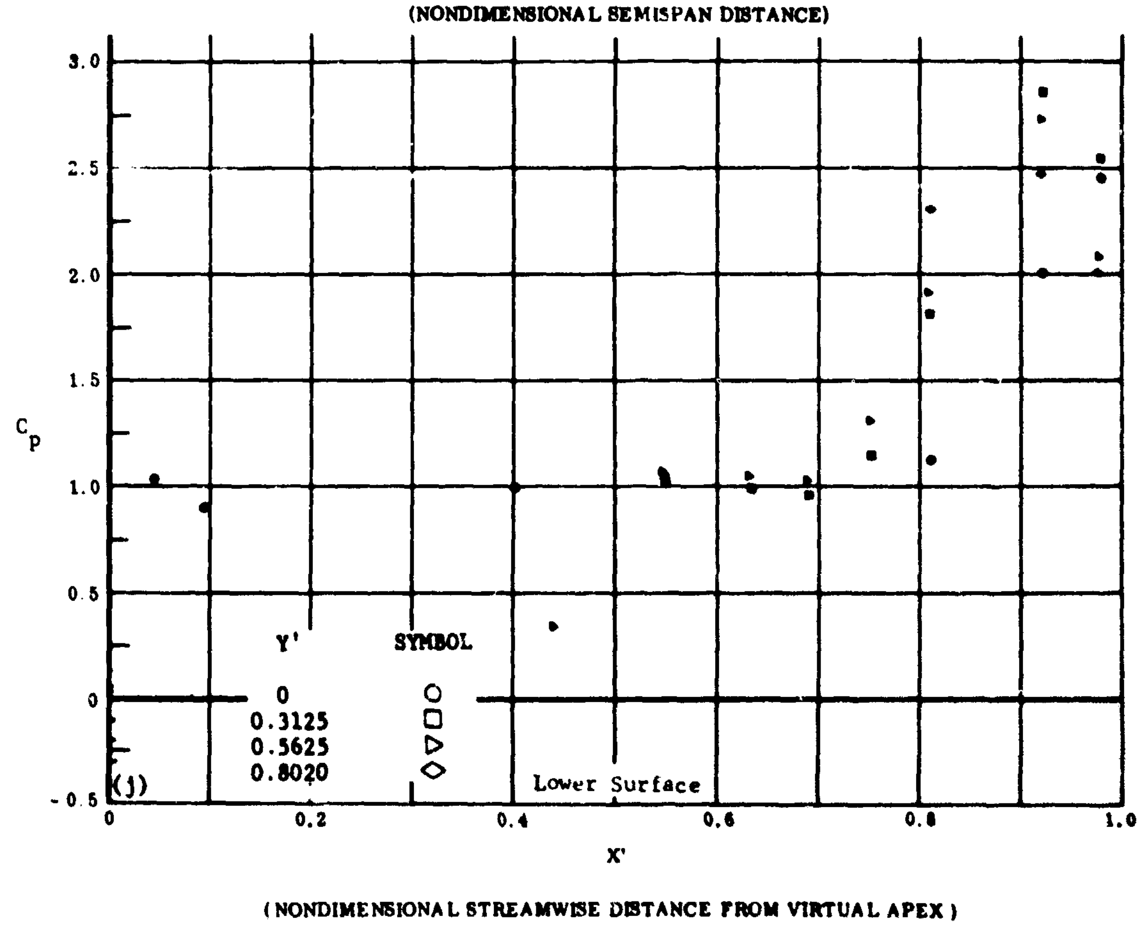

Fig. 37 Configuration IV, $\alpha = +40$, $\delta_2 = \delta_3 = +20$

i) C_p vs. Y', lower surface

j) C_p vs. X', lower surface

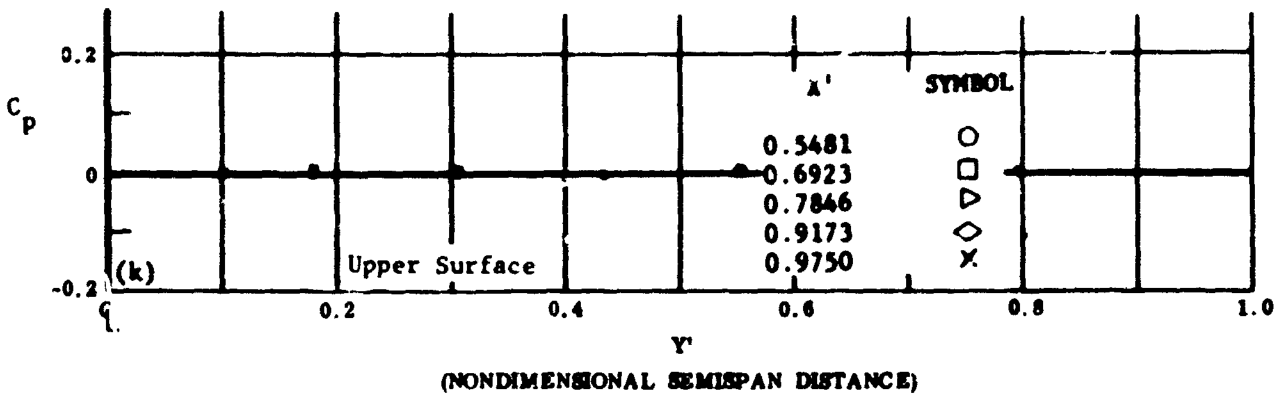

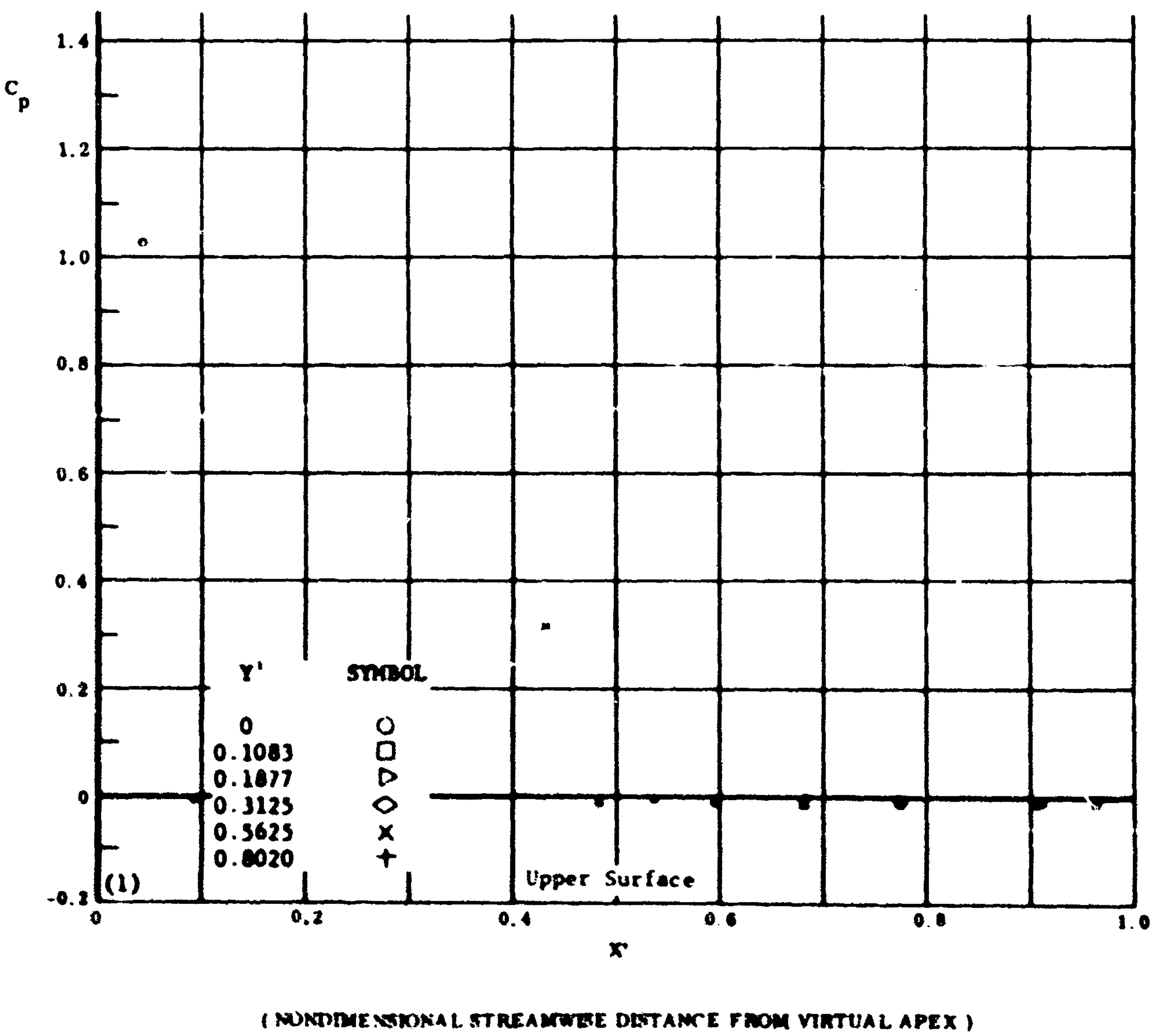

Fig. 37 Configuration IV, $\alpha = +40$, $\delta_2 = \delta_3 = +20$

k) C_p vs. Y', upper surface

l) C_p vs. X', upper surface

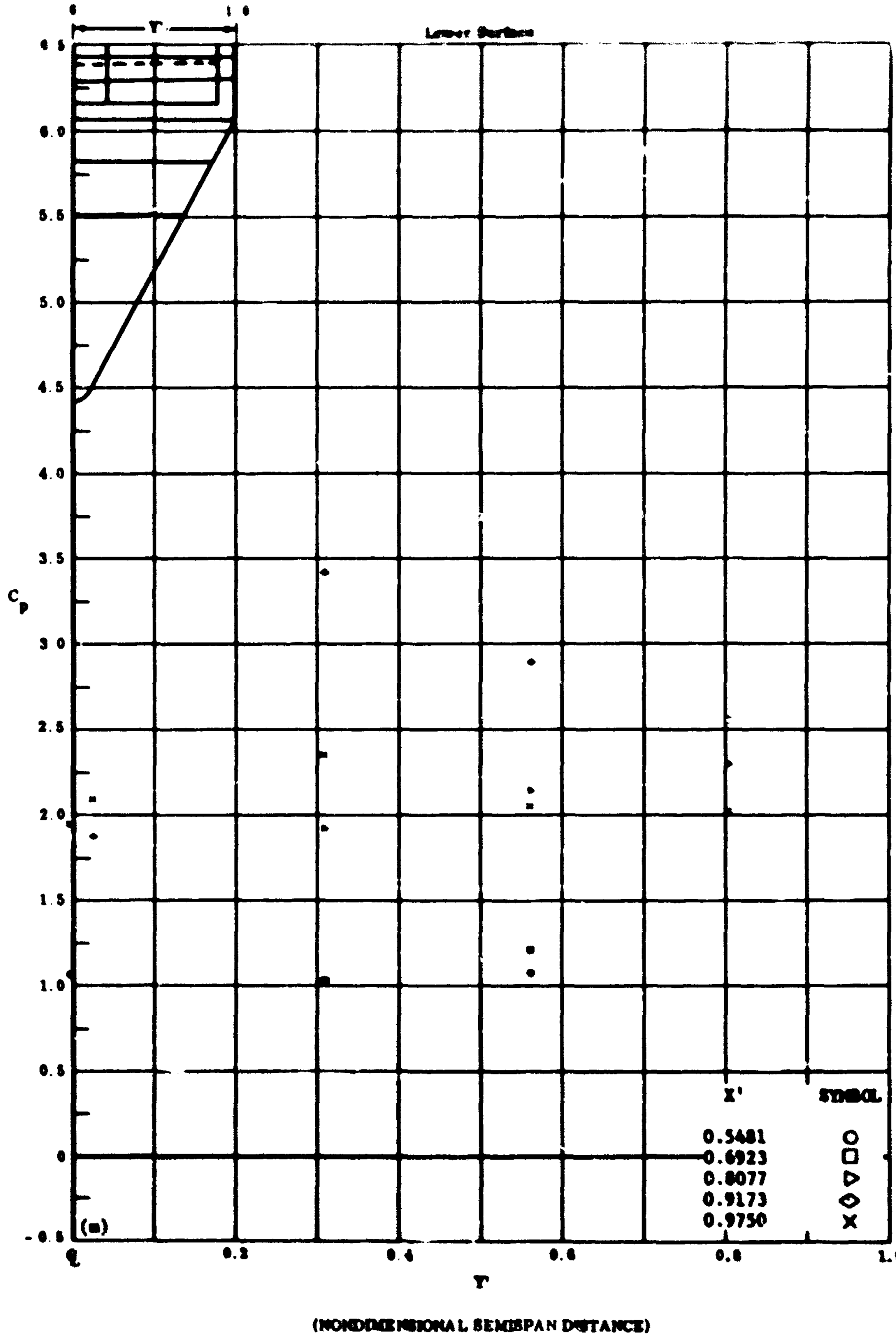

Fig. 37m Configuration IV, $\alpha = +40$, $\delta_2 = \delta_3 = +30$

C_p vs. Y', lower surface

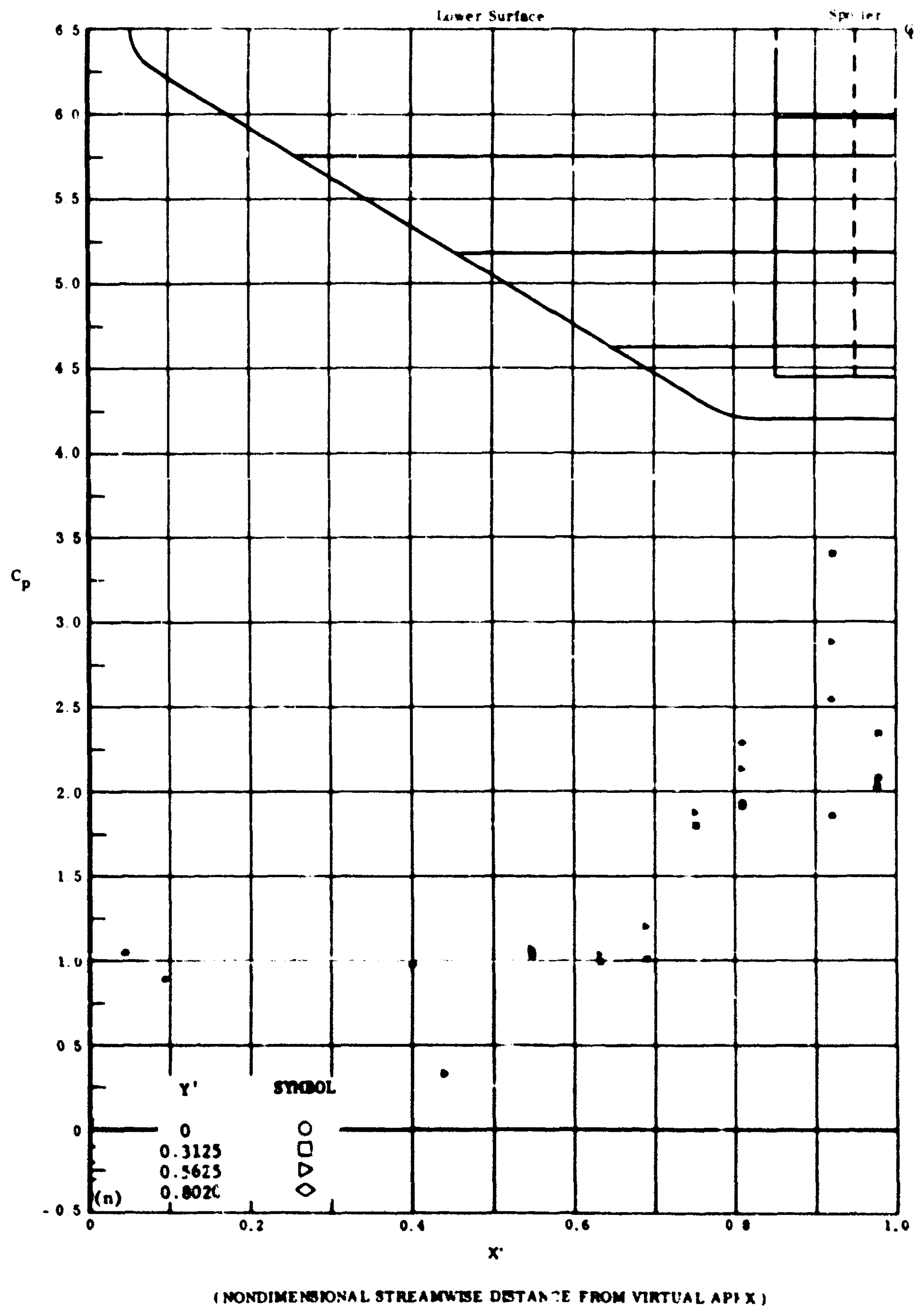

Fig. 37n Configuration IV, $\alpha = +40$, $\delta_2 = \delta_3 = +30$

C_p vs. X', lower surface

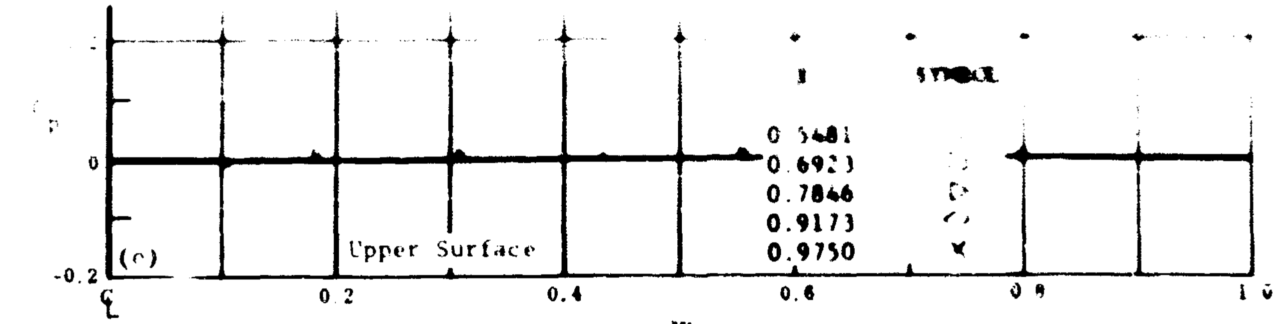

Y'

(NONDIMENSIONAL SEMISPAN DISTANCE)

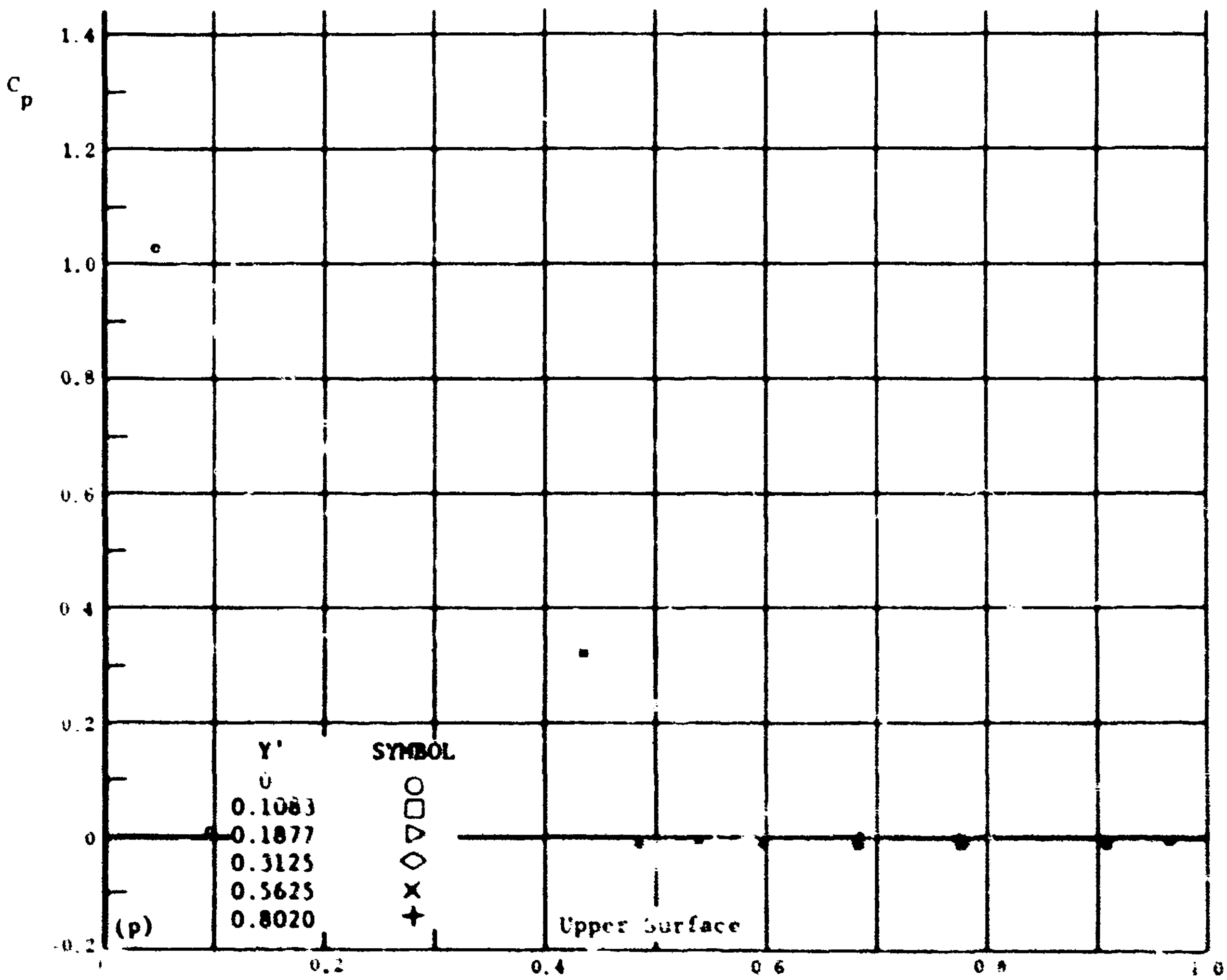

X'

(NONDIMENSIONAL STREAMWISE DISTANCE FROM VIRTUAL APEX)

Fig. 37 Configuration IV, α = +40, $\delta_2 = \delta_3$ = +30

o) C_p vs. Y', upper surface

p) C_p vs. X', upper surface

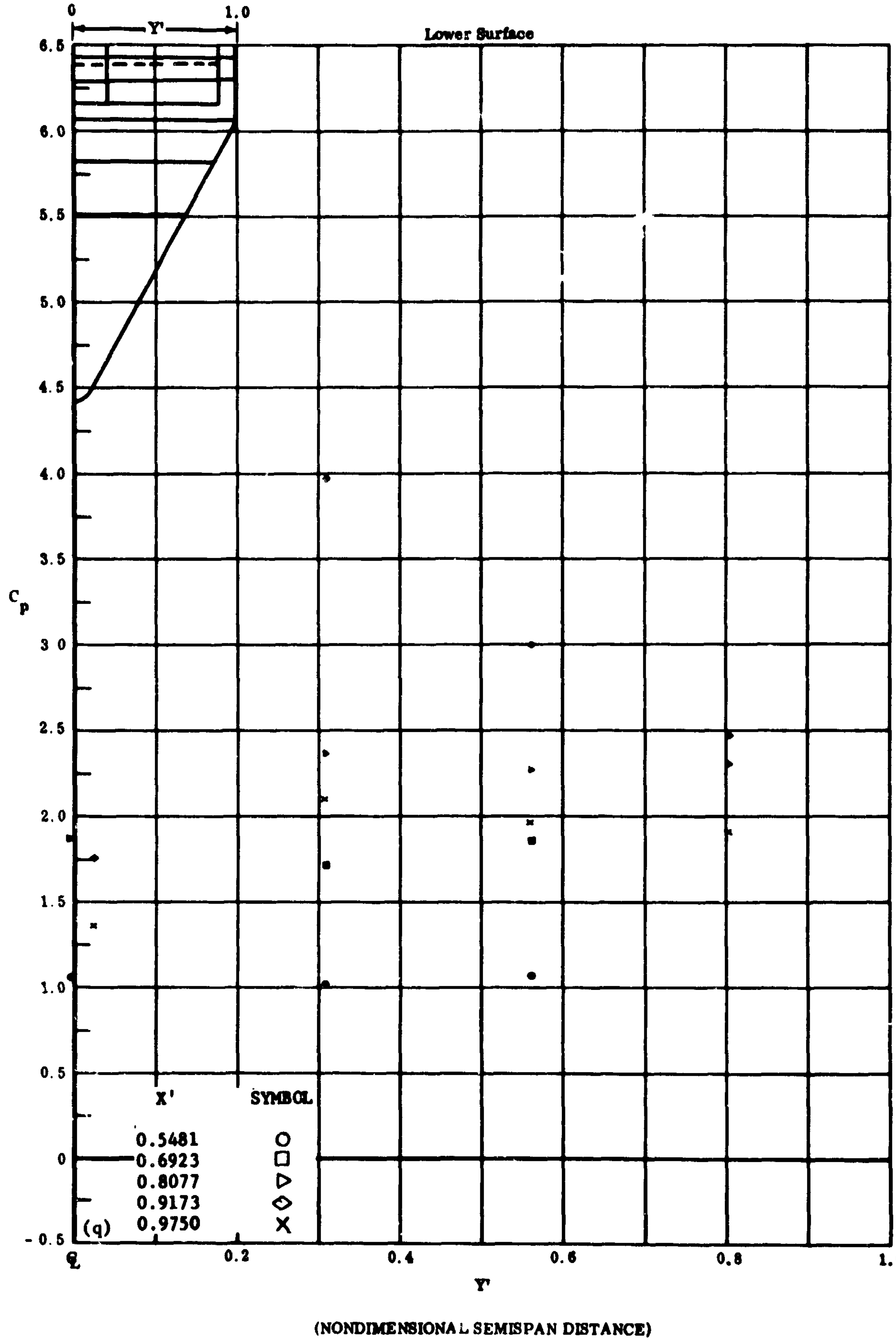

Fig. 37q Configuration IV, α = +40 , $\delta_2 = \delta_3$ = +39

C_p vs. Y', lower surface

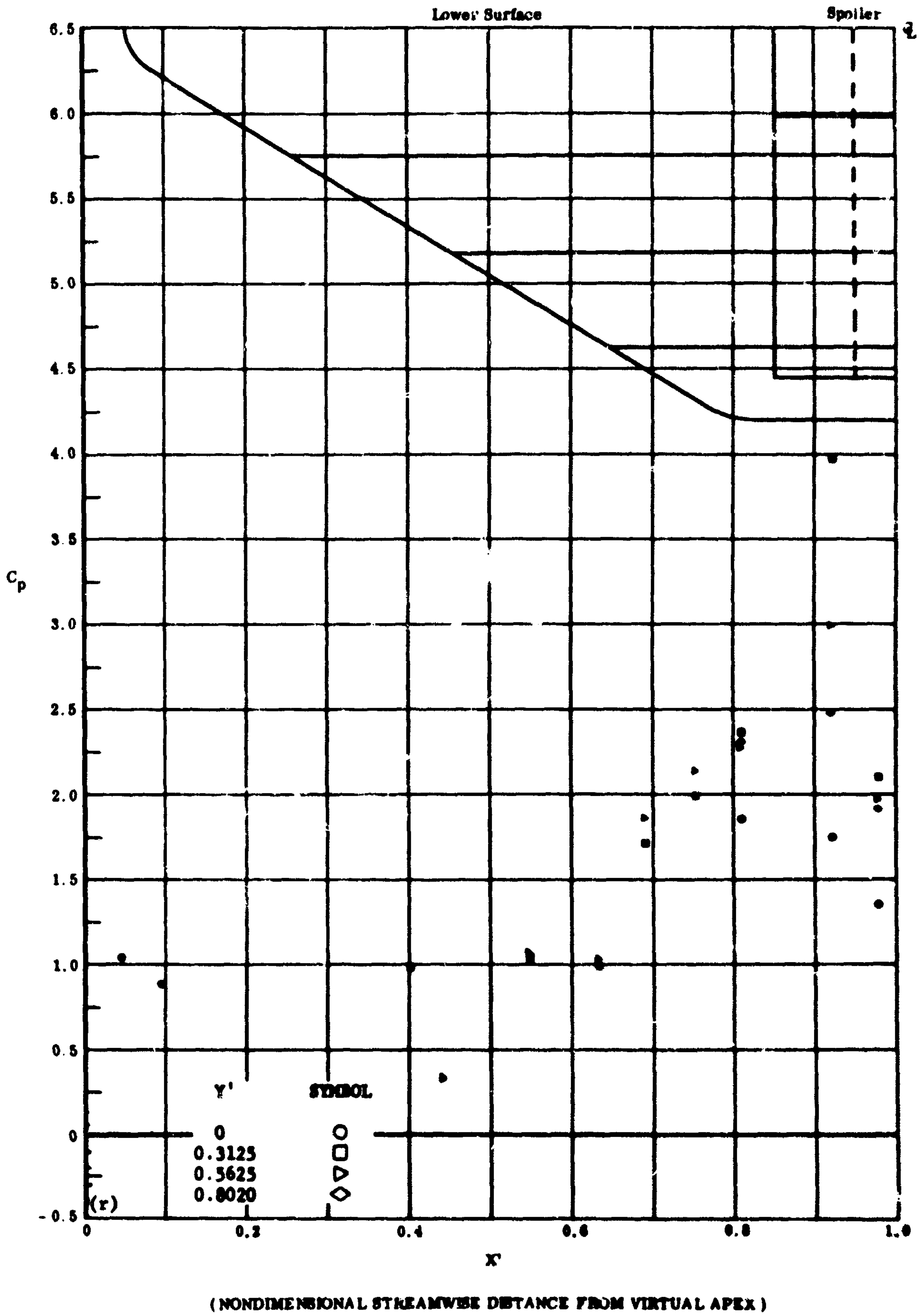

Fig. 37r Configuration IV, $\alpha = +40$, $\delta_2 = \delta_3 = +39$

C_p vs. X', lower surface

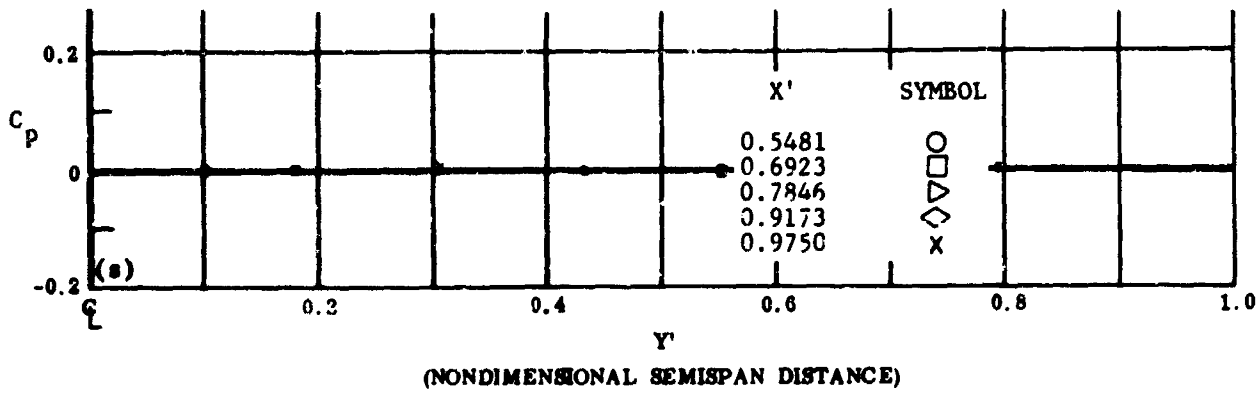

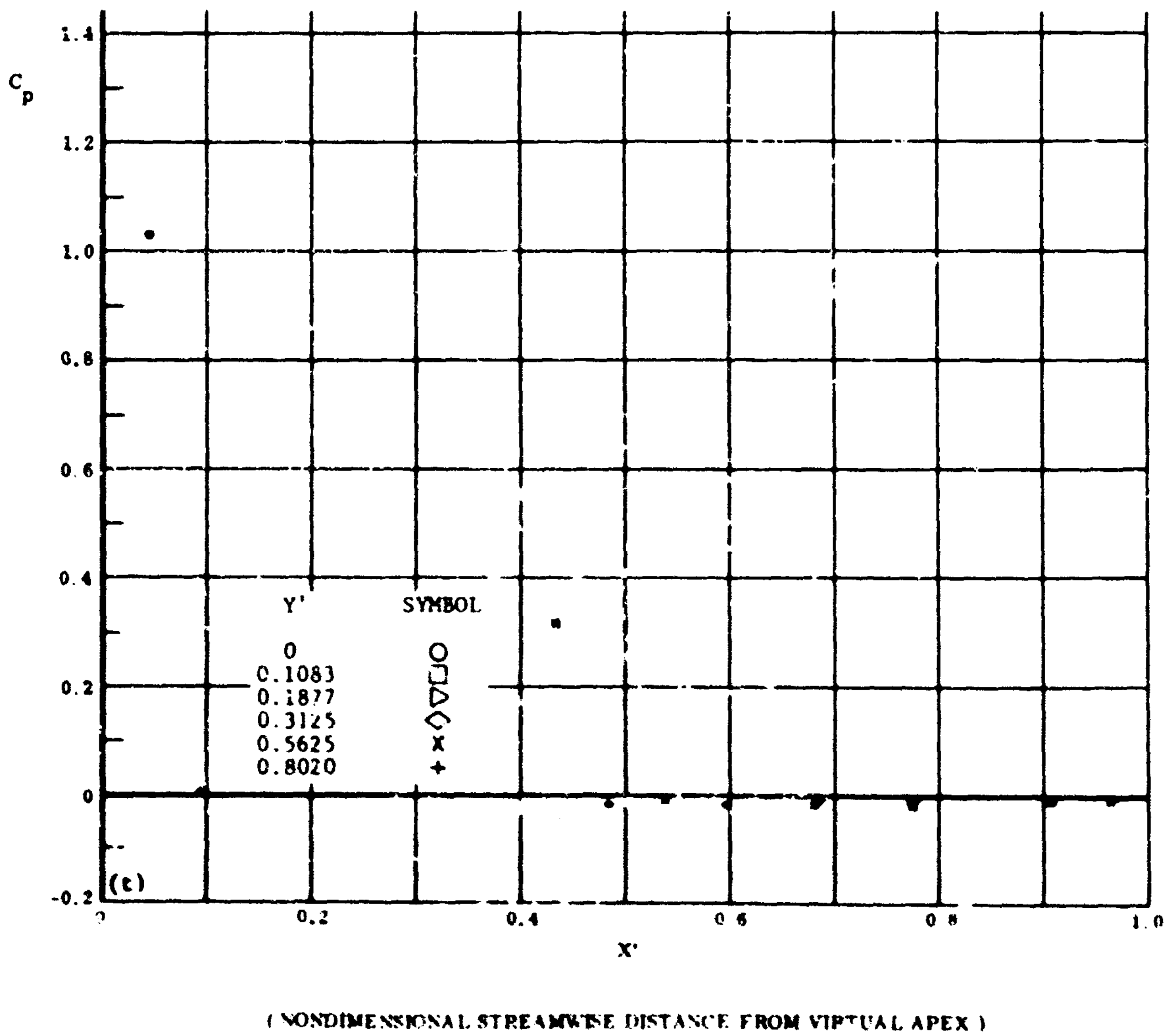

Fig. 37 Configuration IV, $\delta = +40$, $\delta_2 = \delta_3 = +39$

s) C_p vs. Y', upper surface

t) C_p vs. X', upper surface

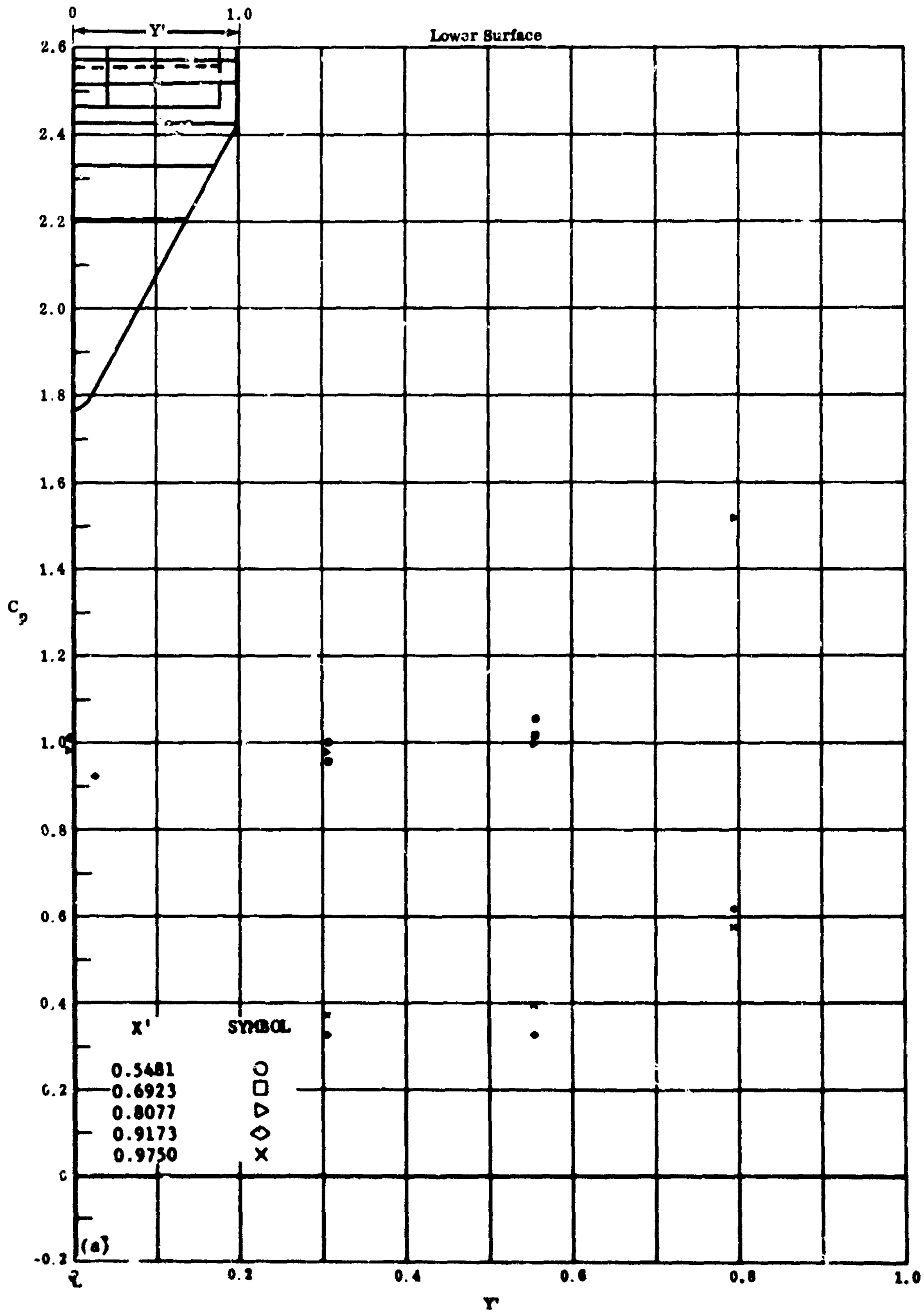

(NONDIMENSIONAL SEMISPAN DISTANCE)

Fig. 38a Configuration IV, $\alpha = +40$, $\delta_2 = \delta_3 = -20$

C_p vs. Y', lower surface

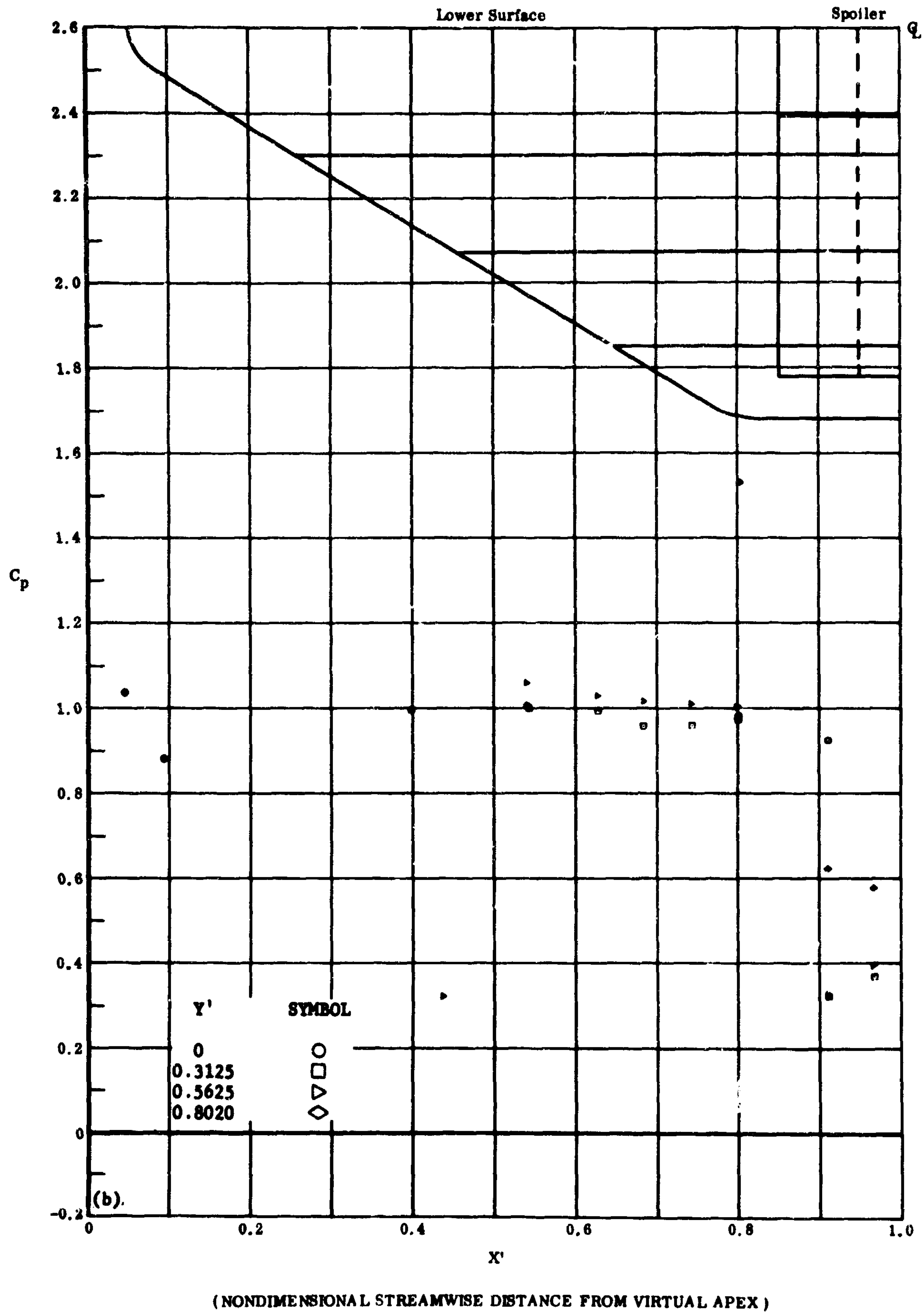

Fig. 38b Configuration IV, $\alpha = +40$, $\delta_2 = \delta_3 = -20$

C_p vs. X', lower surface

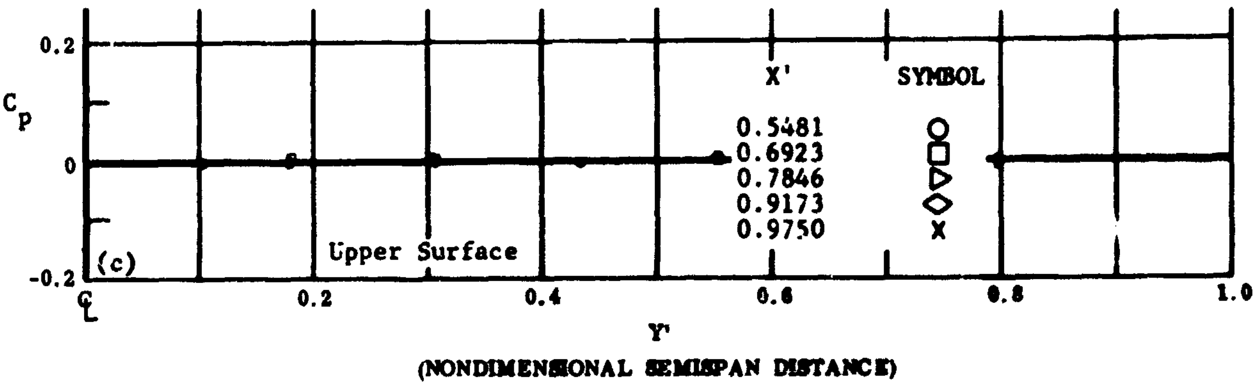

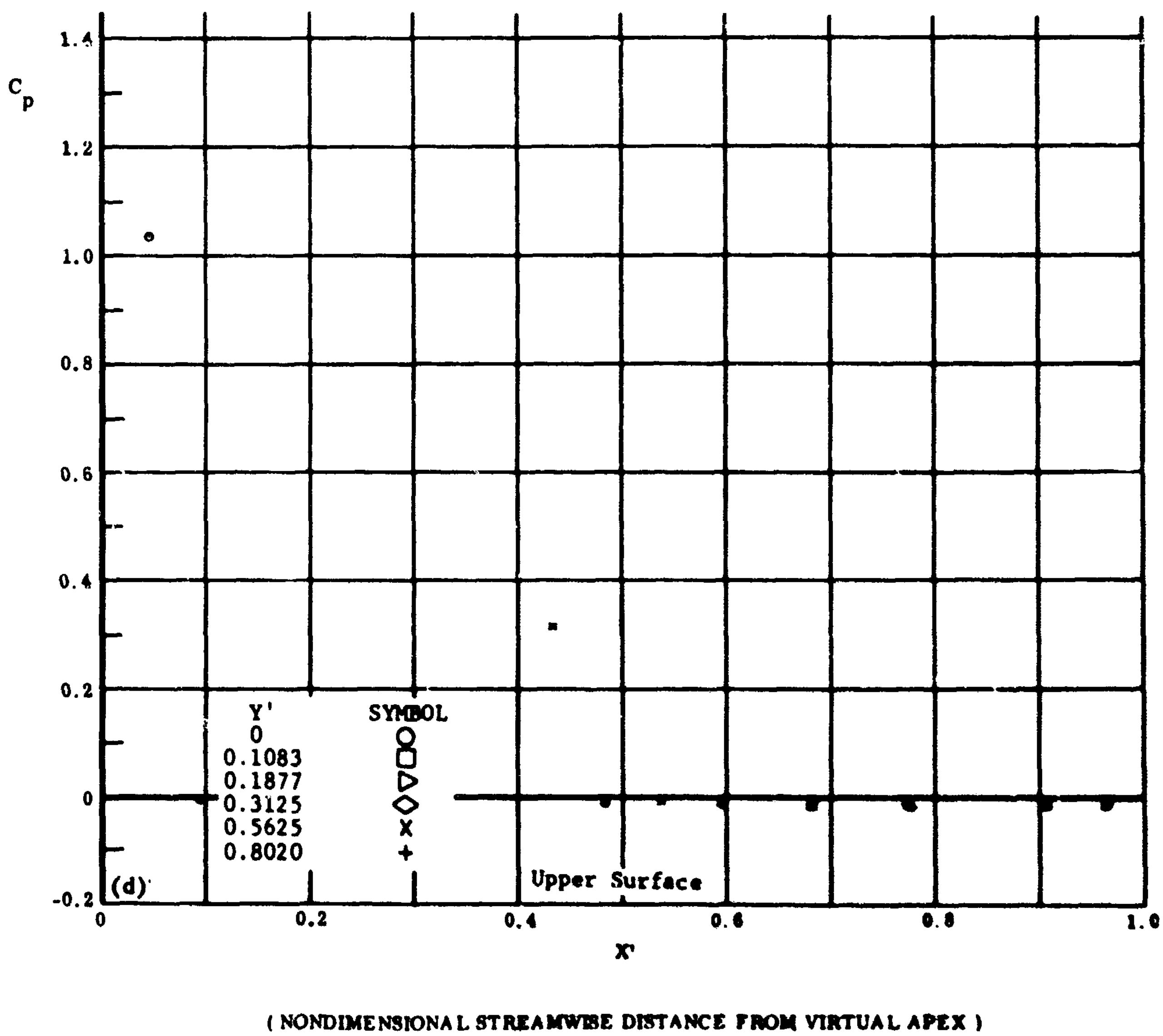

Fig. 38 Configuration IV, $\alpha = +40$, $\delta_2 = \delta_3 = -20$

c) C_p vs. Y', upper surface

d) C_p vs. X', upper surface

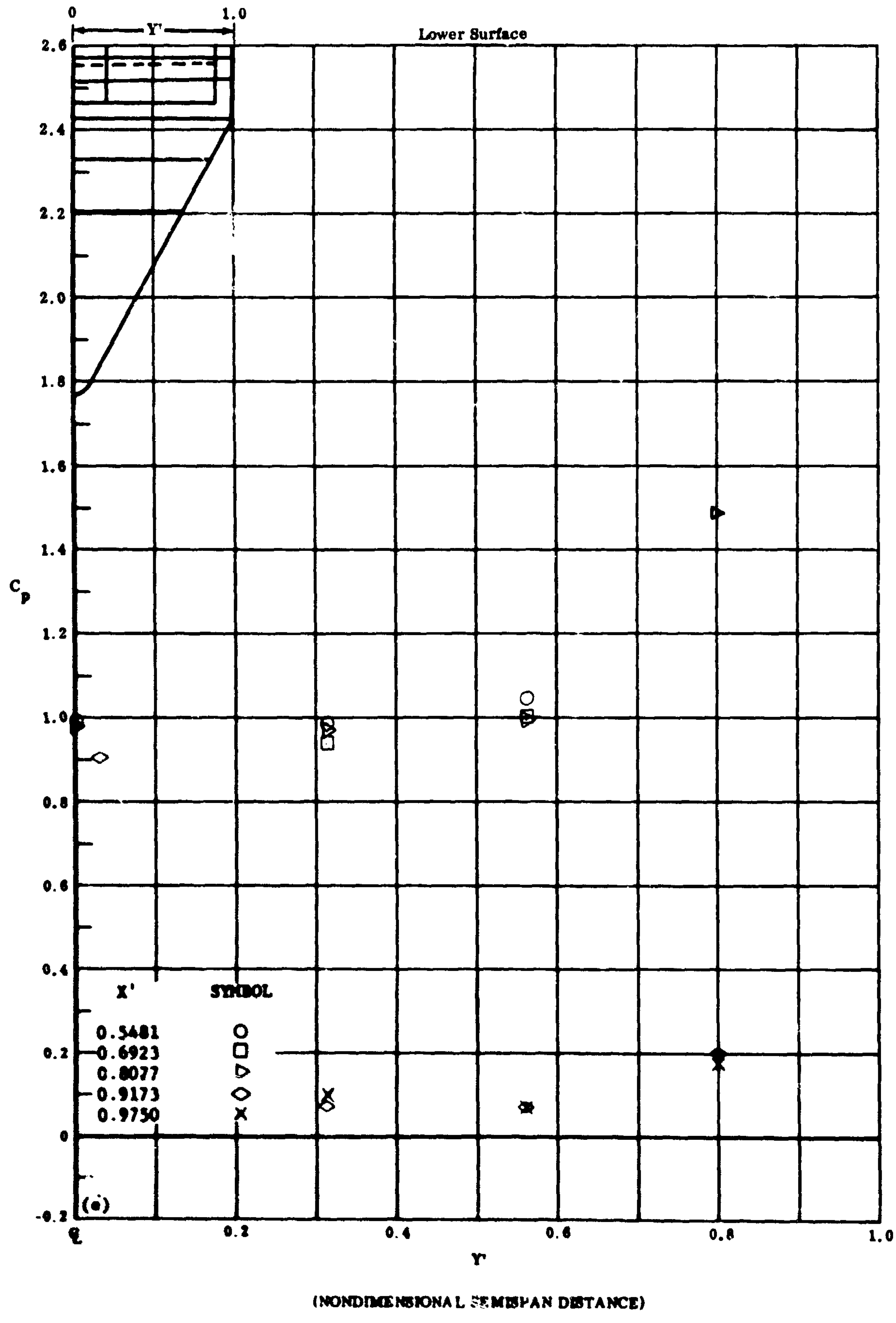

Fig. 38e Configuration IV, $\alpha = +40$, $\delta_2 = \delta_3 = -39$

C_p vs. Y', lower surface

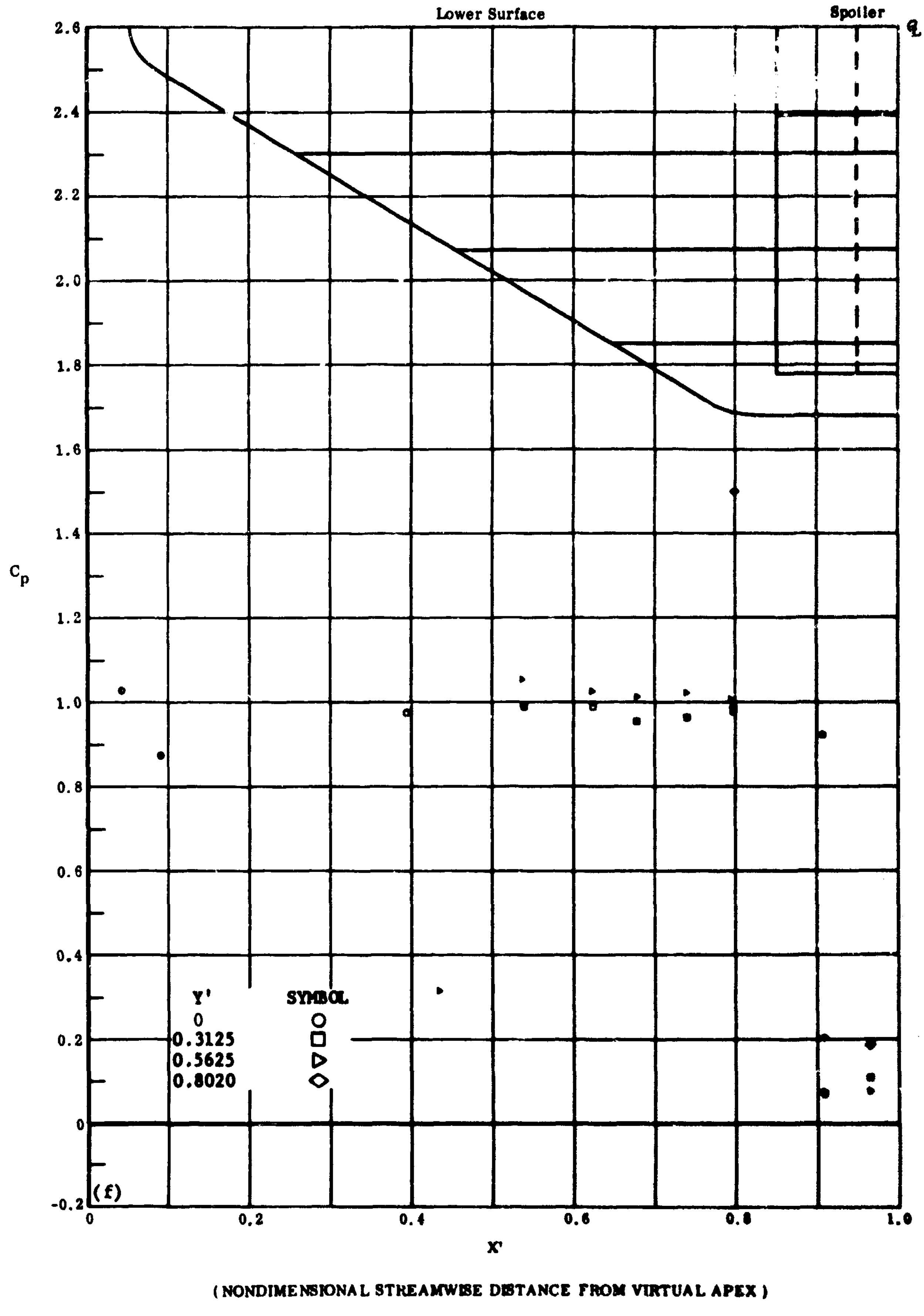

Fig. 38f Configuration IV, $\alpha = +40$, $\delta_2 = \delta_3 = -39$

C_p vs. X', lower surface

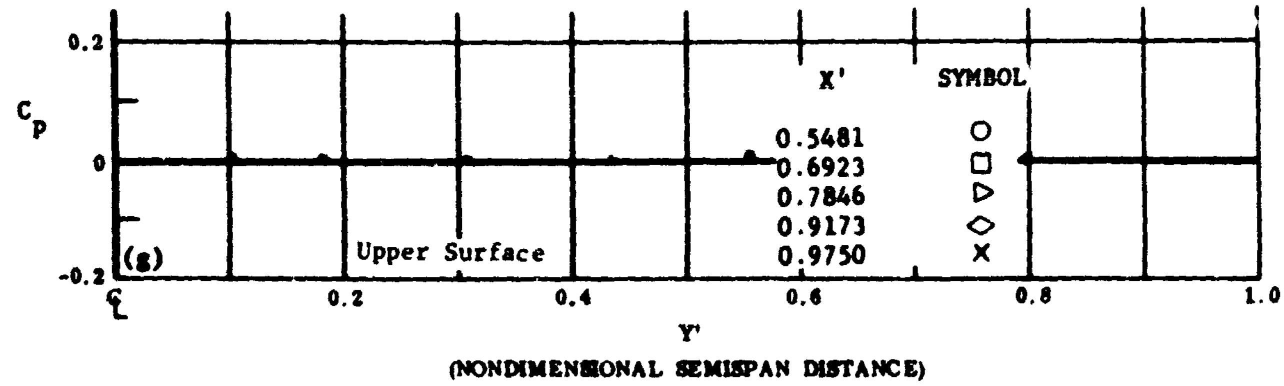

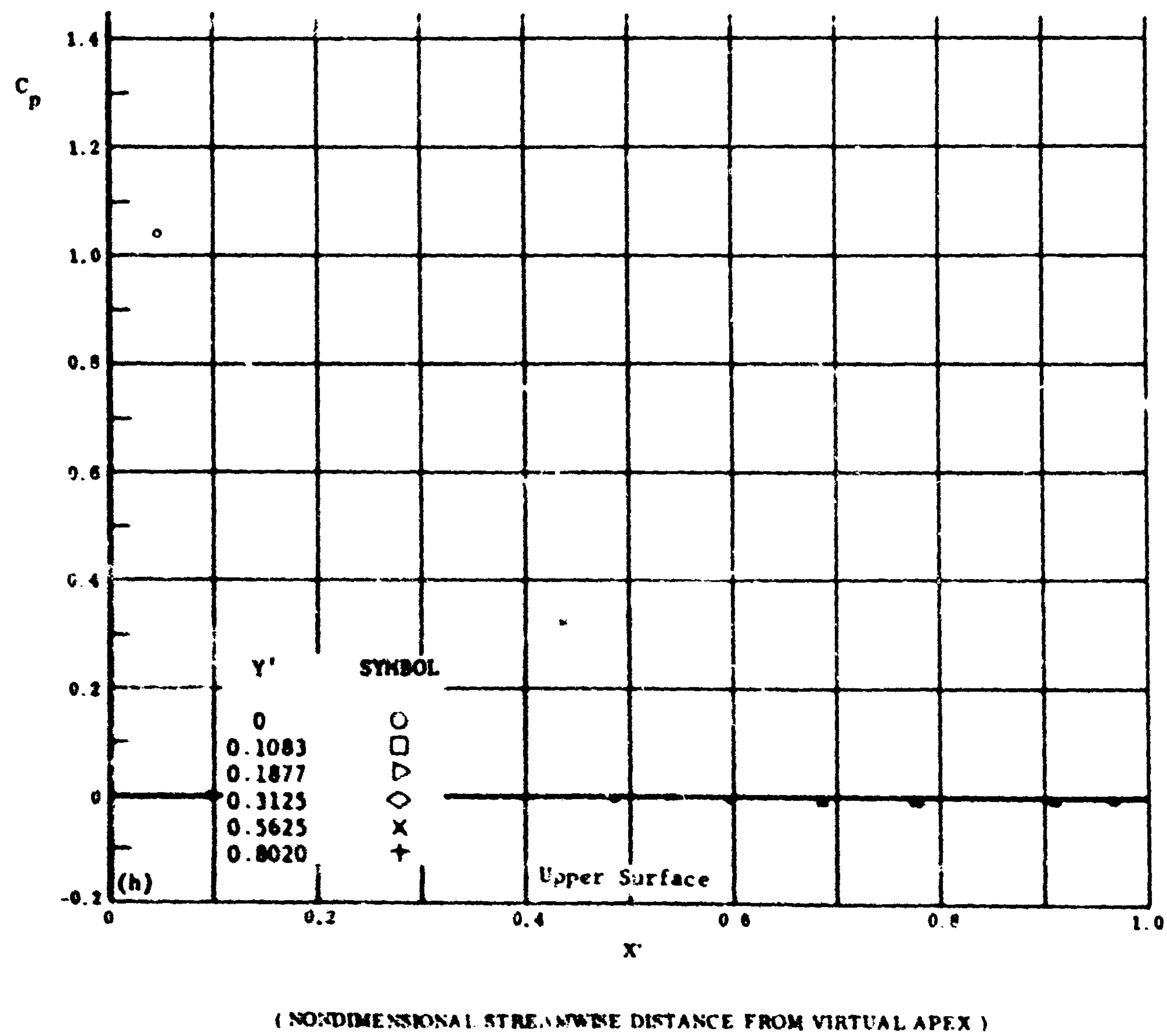

Fig. [illegible] Configuration IV, $\alpha = +40$, $\delta_2 = \delta_3 = -39$

(g) C_p vs. Y', upper surface

(h) C_p vs. X', upper surface

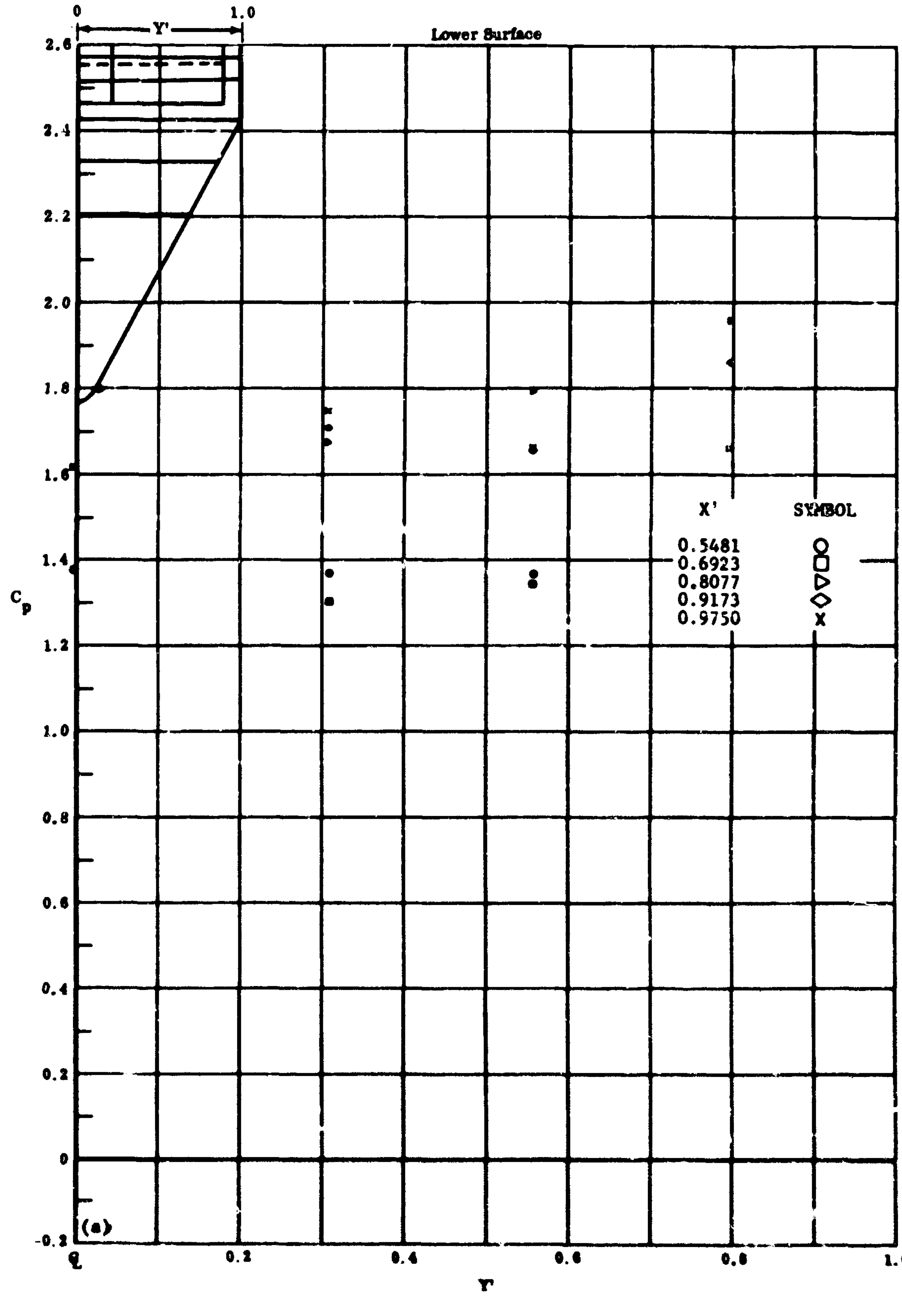

Fig. 39a Configuration 1?, α = +50 , $\delta_2 = \delta_3 = 0$

C_p vs. Y', lower surface

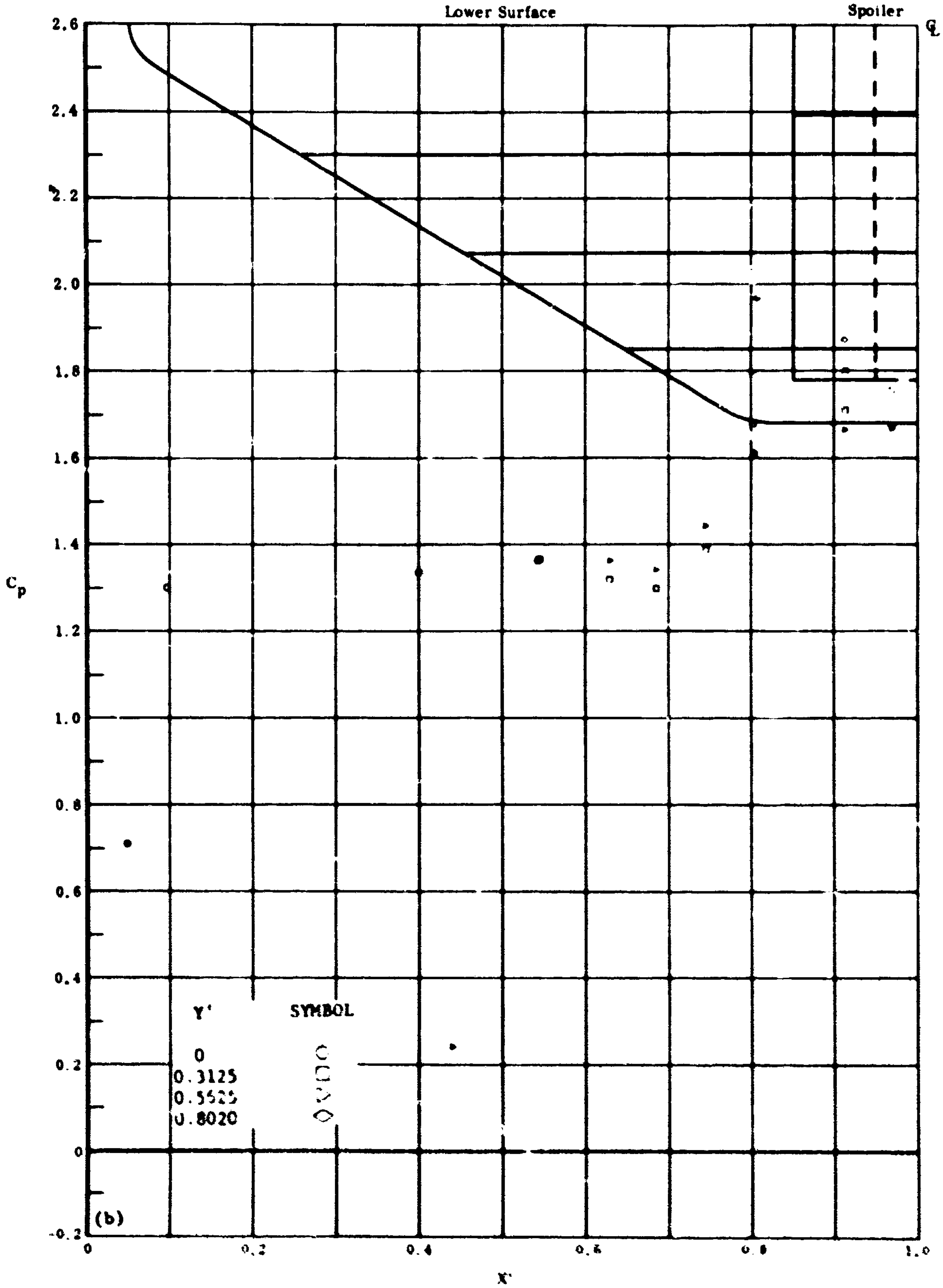

Fig. 39b Configuration IV, $\delta_1 = +50$, $\delta_2 = \delta_3 = 0$

C_p vs. X', lower surface

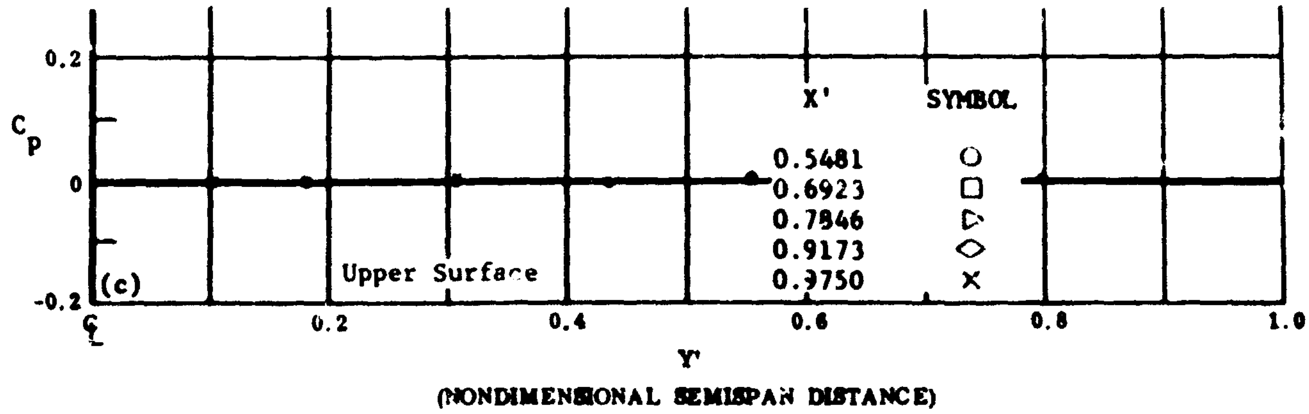

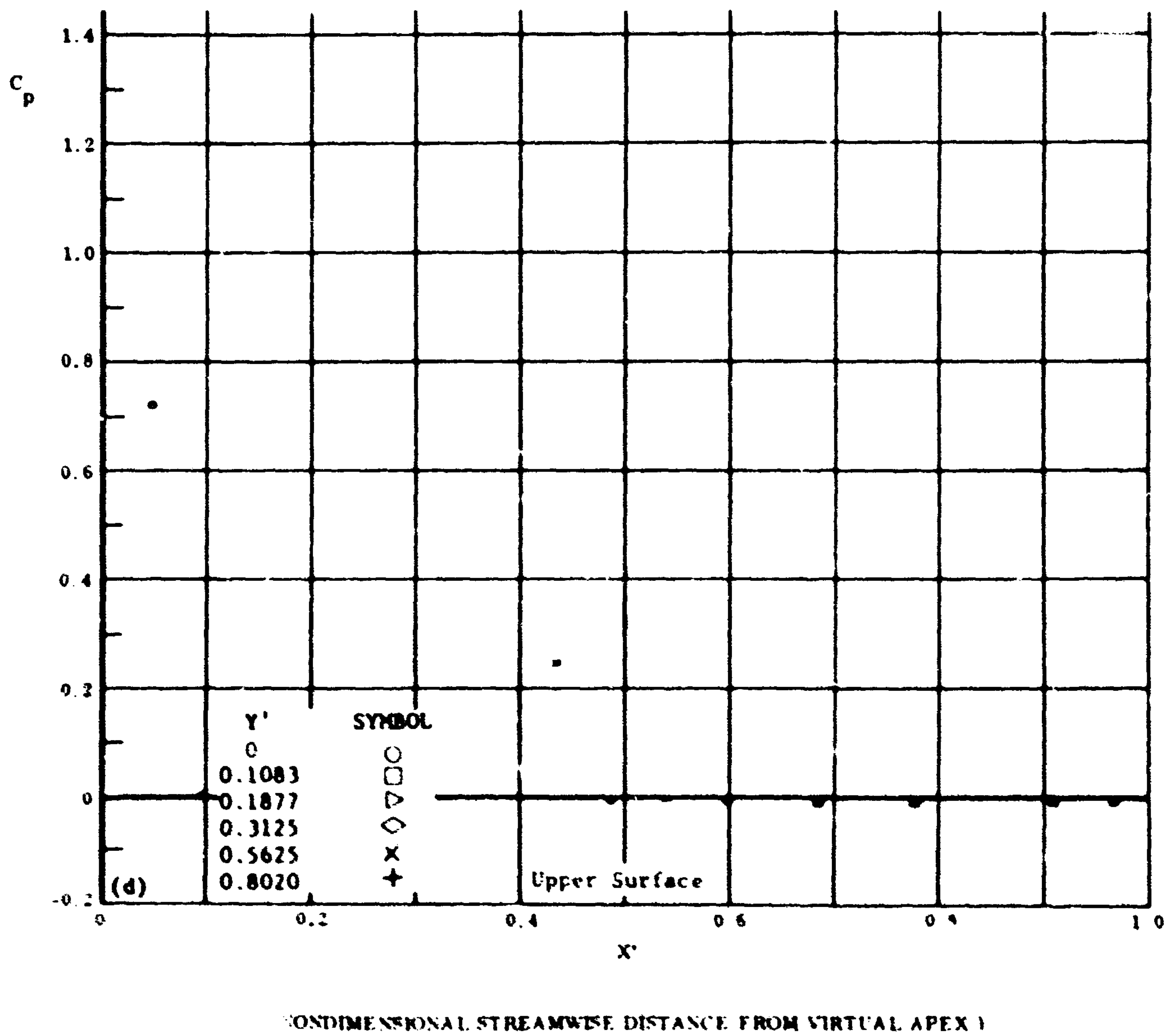

Fig. 39 Configuration IV, $\delta_1 = +50$, $\delta_2 = \delta_3 = 0$

c) C_p vs. Y', upper surface

d) C_p vs. X', upper surface

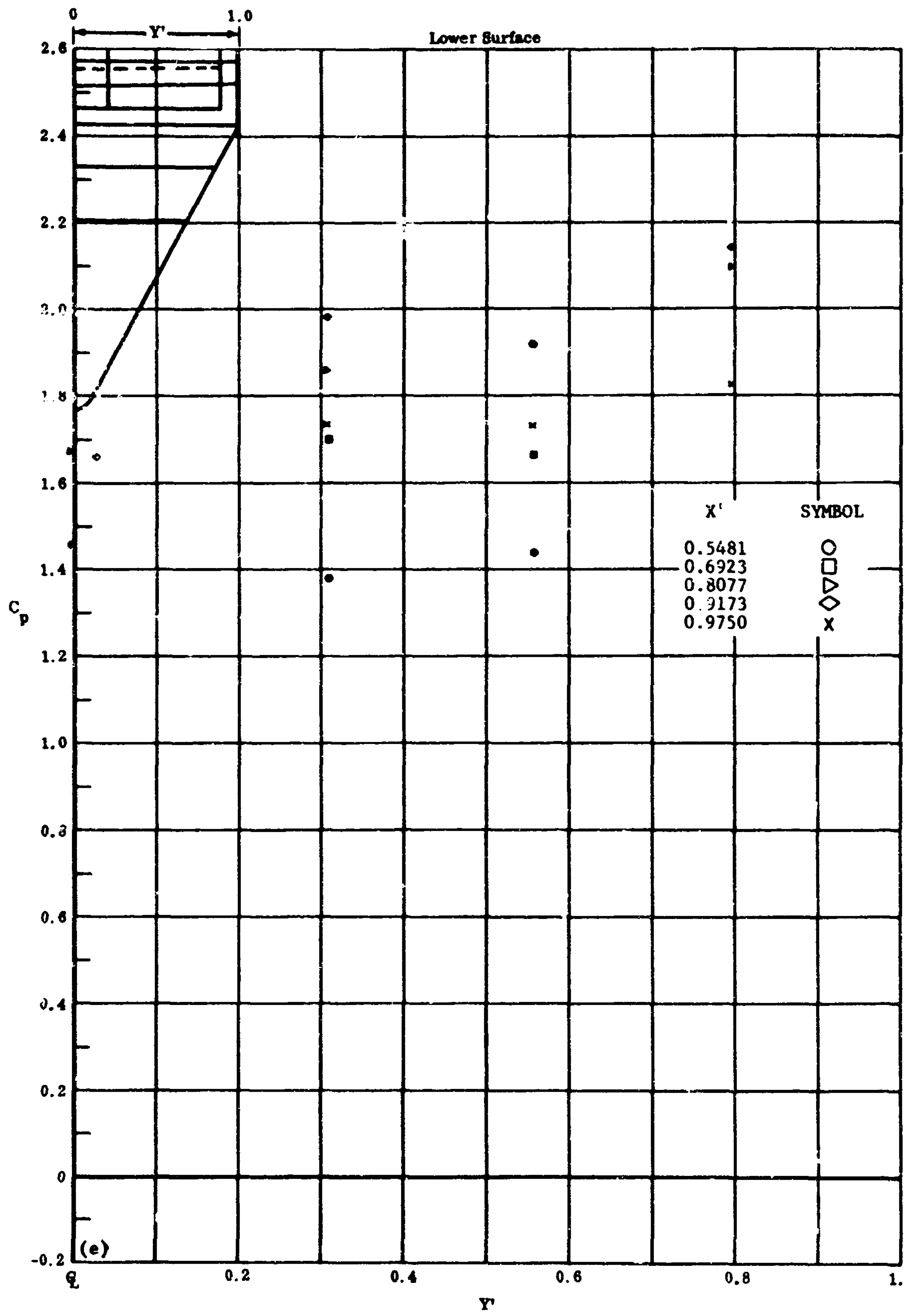

Fig. 39e Configuration IV, α = +50 , $\delta_2 = \delta_3$ = +20

C_p vs. Y', lower surface

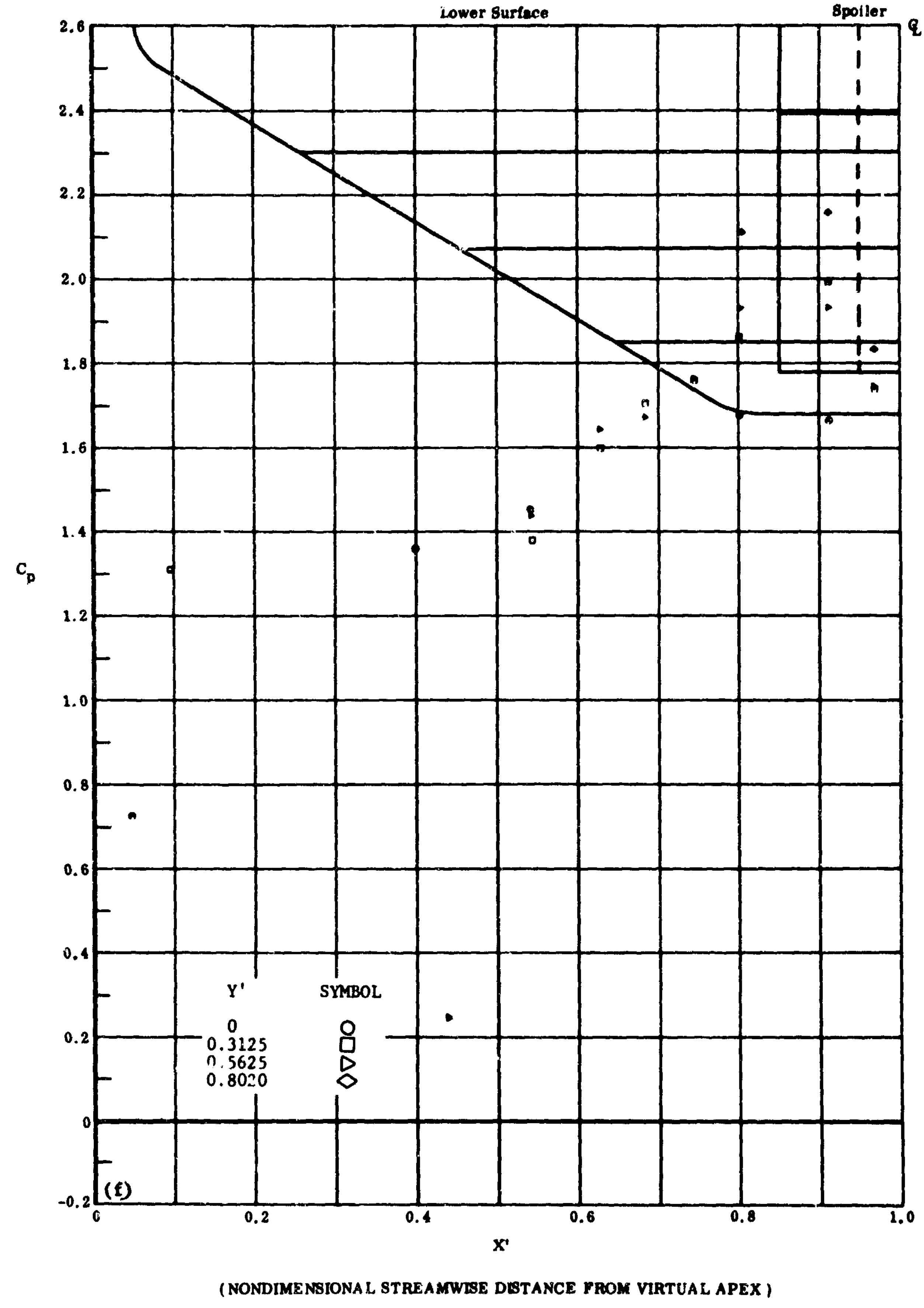

Fig. 39f Configuration IV, $\alpha = +50$, $\delta_2 = \delta_3 = +20$

C_p vs. X', lower surface

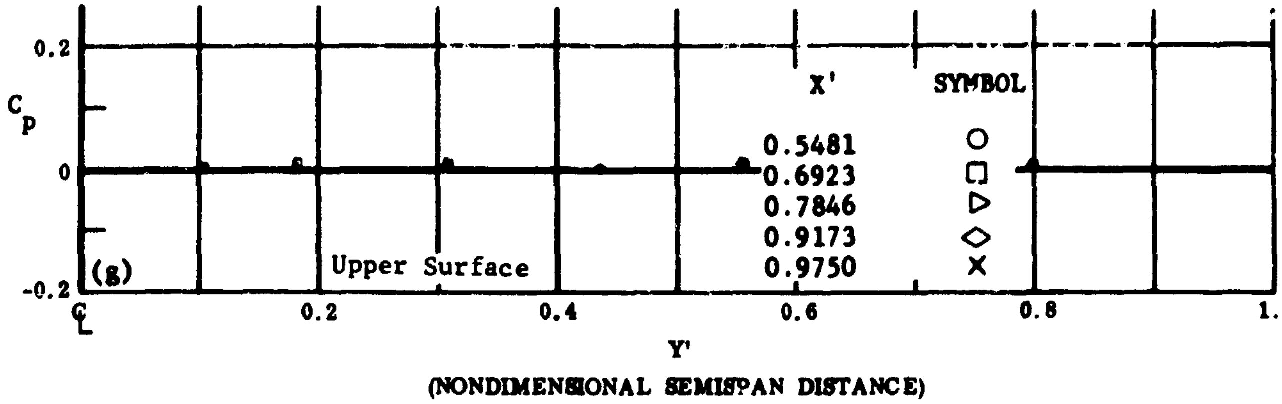

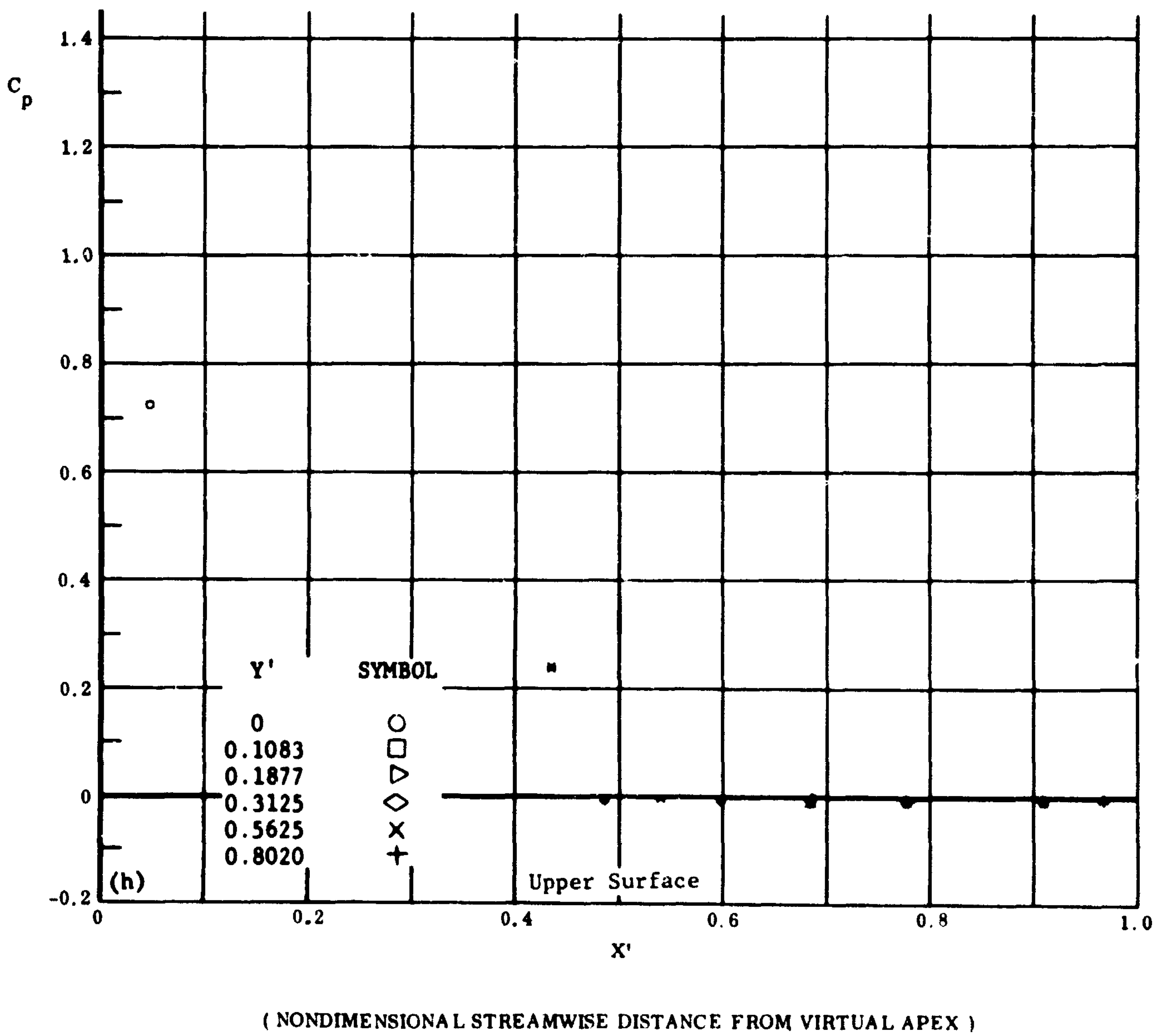

Fig. 39 Configuration IV, α = +50, δ_2 = δ_3 = +20

g) C_p vs. Y', upper surface

h) C_p vs. X', upper surface

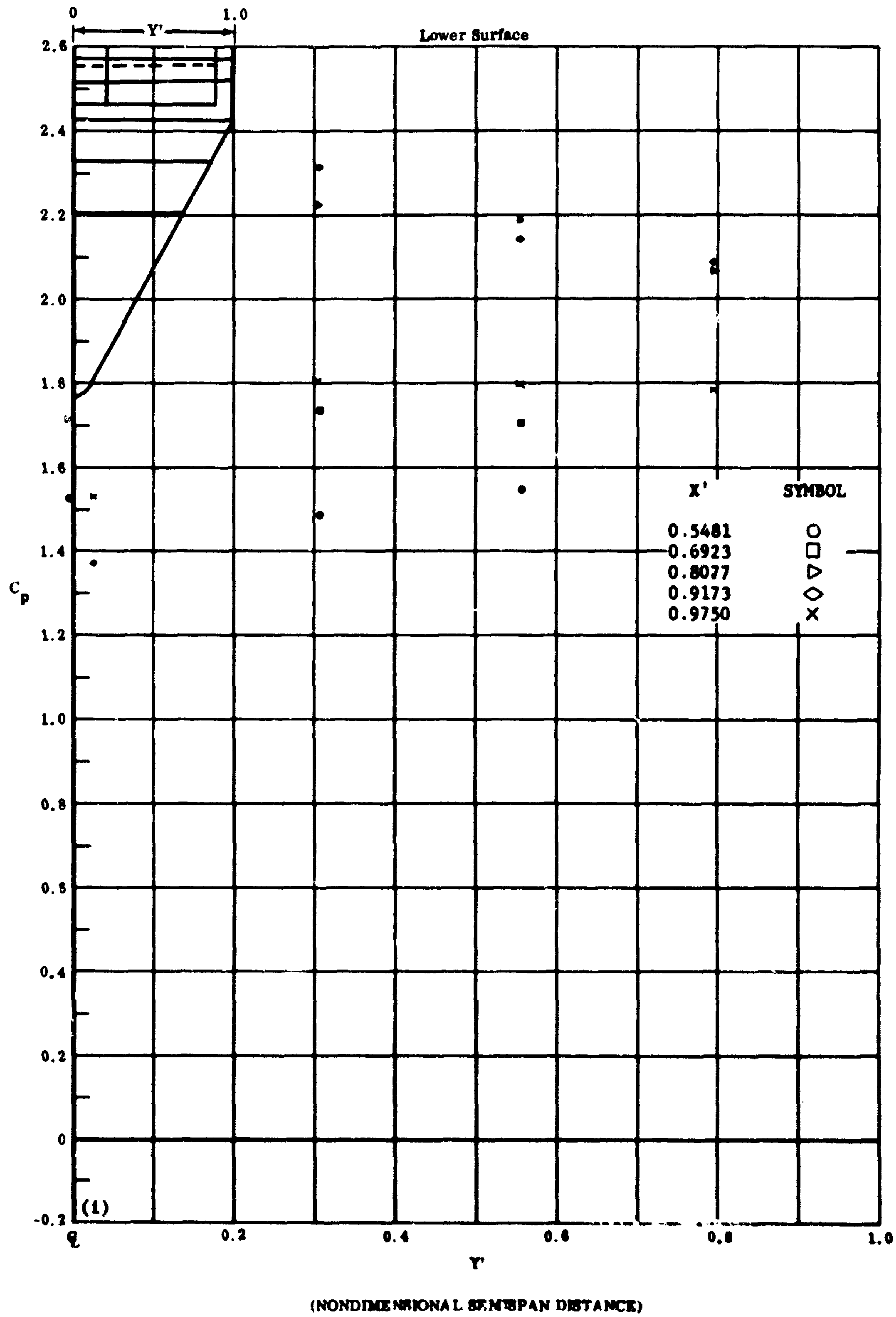

Fig. 391 Configuration IV, $\alpha = +50$, $\delta_2 = \delta_3 = +39$

C_p vs. Y', lower surface

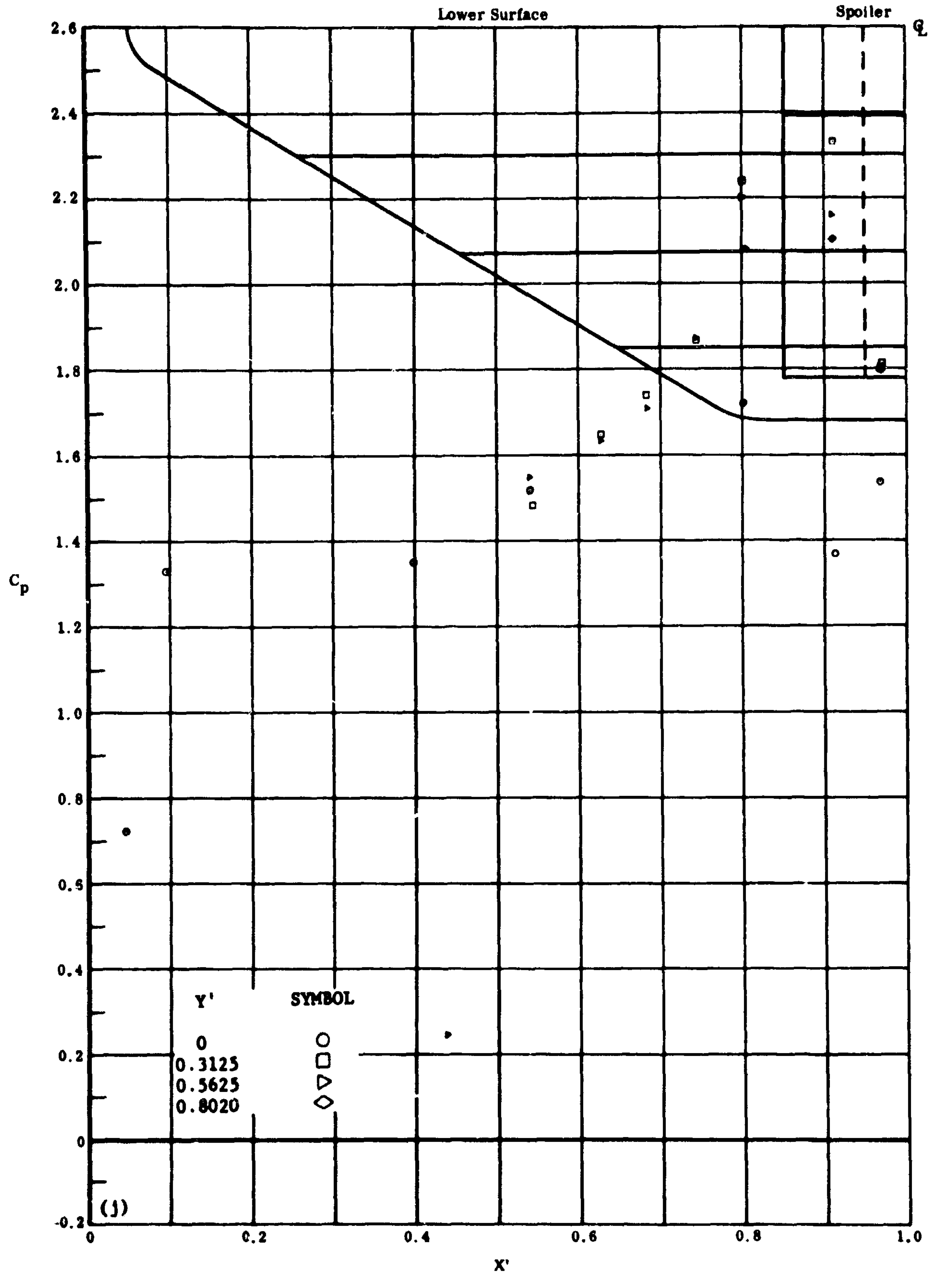

Fig. 39j Configuration IV, $\alpha = +50$, $\delta_2 = \delta_3 = +39$

C_p vs. X', lower surface

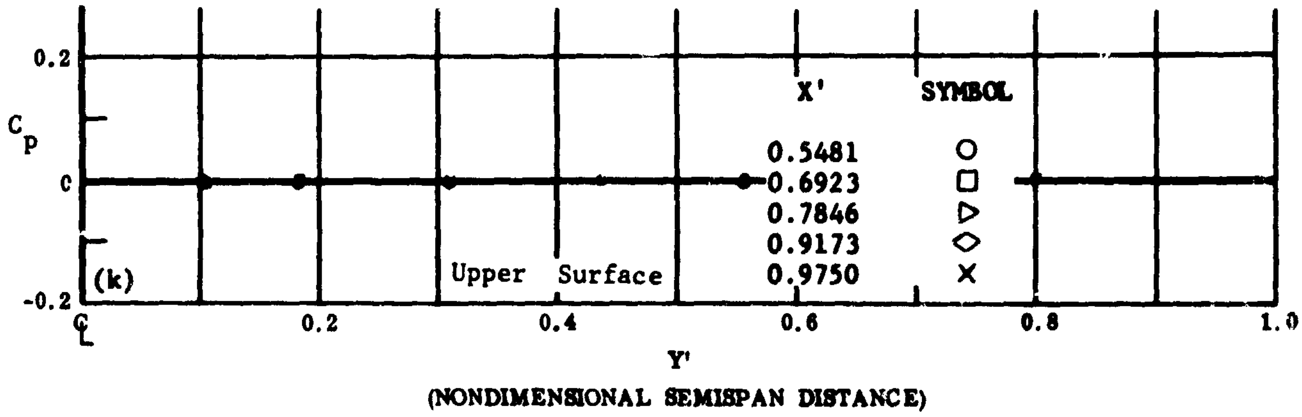

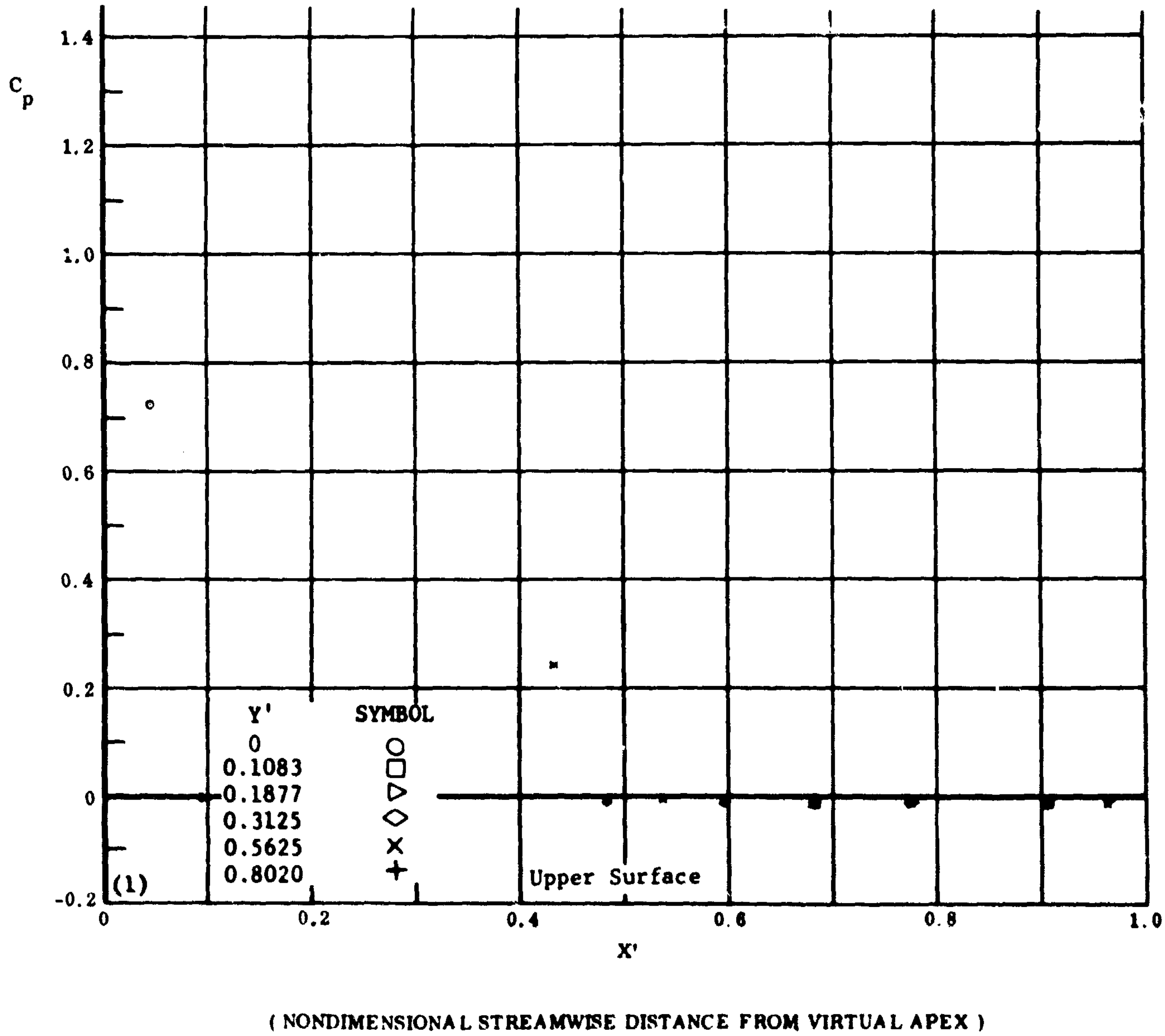

Fig. 39 Configuration IV, $\alpha = +50$, $\delta_2 = \delta_3 = +39$

k) C_p vs. Y', upper surface

l) C_p vs. X', upper surface

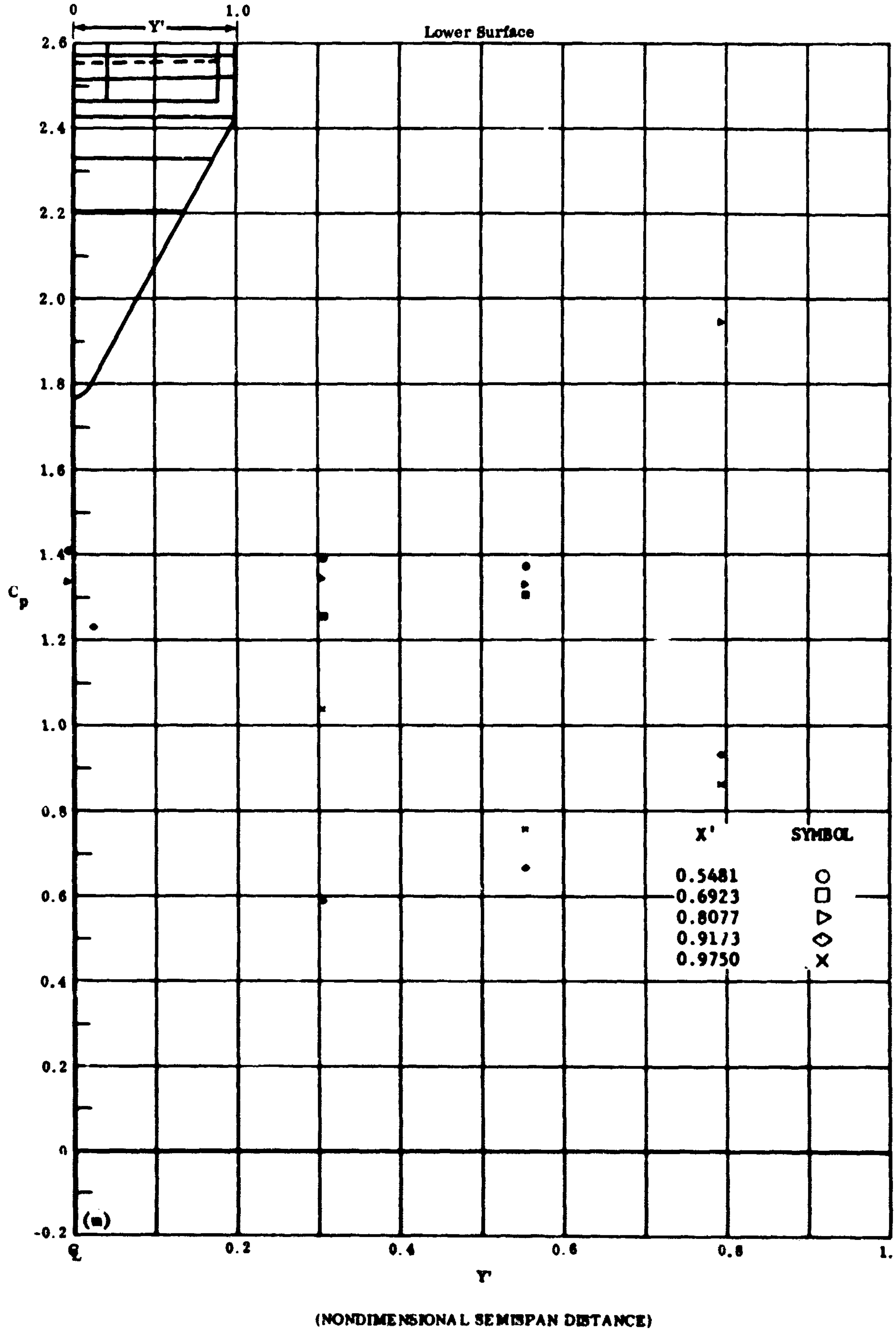

Fig. 39m Configuration IV, $\alpha = +50$, $\delta_2 = \delta_3 = -20$

C_p vs. Y', lower surface

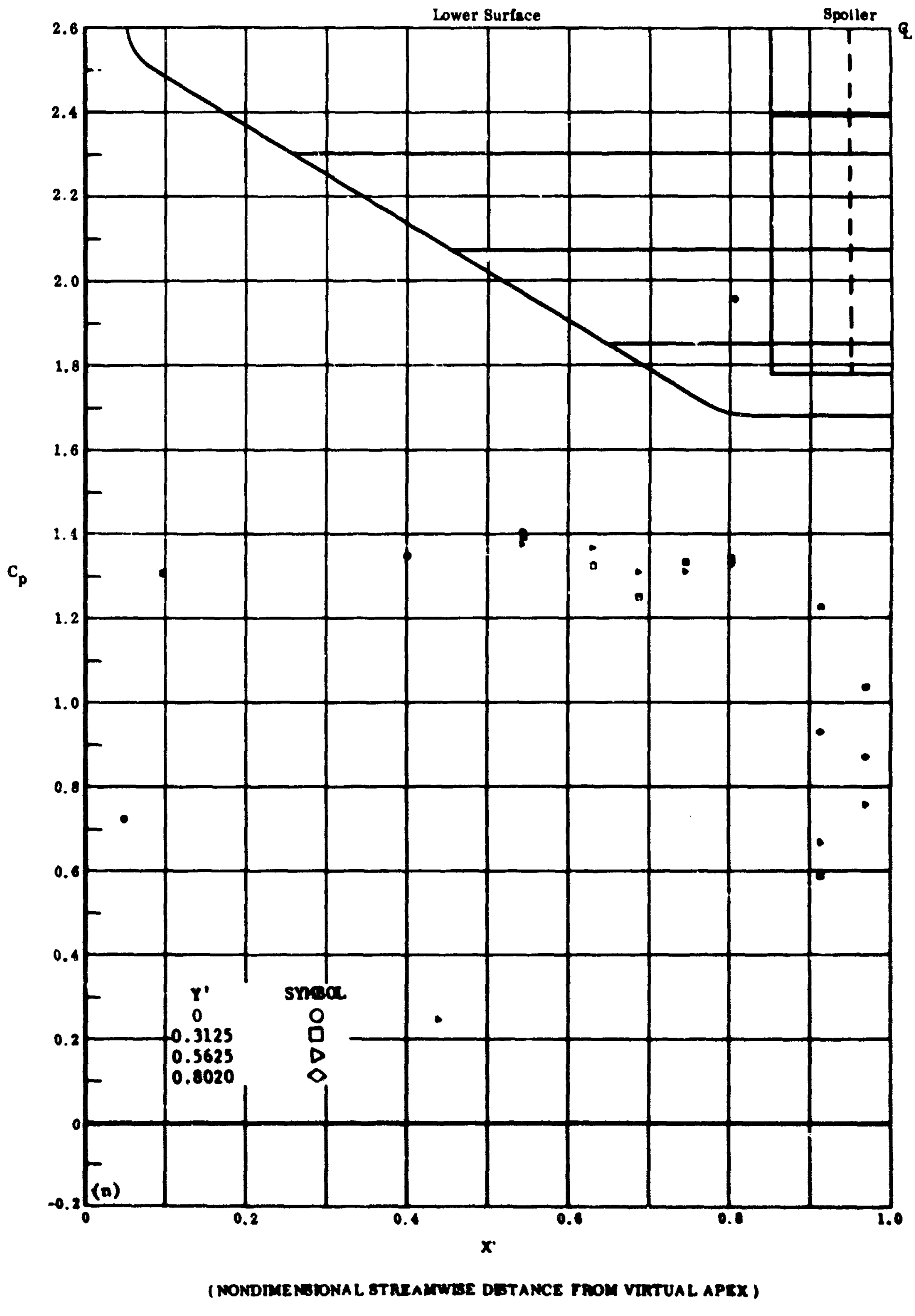

Fig. 39n Configuration IV, $\alpha = +50$, $\delta_2 = \delta_3 = -20$

C_p vs. X', lower surface

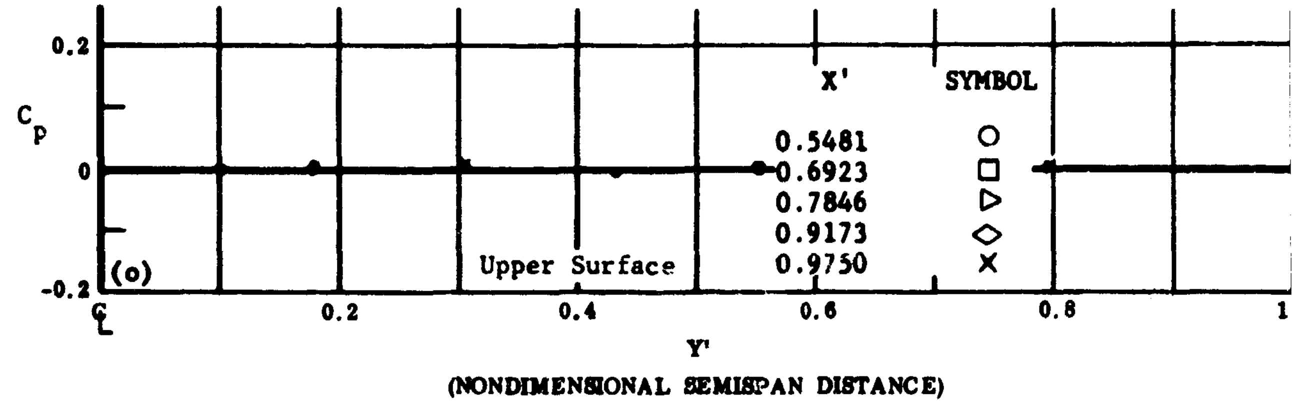

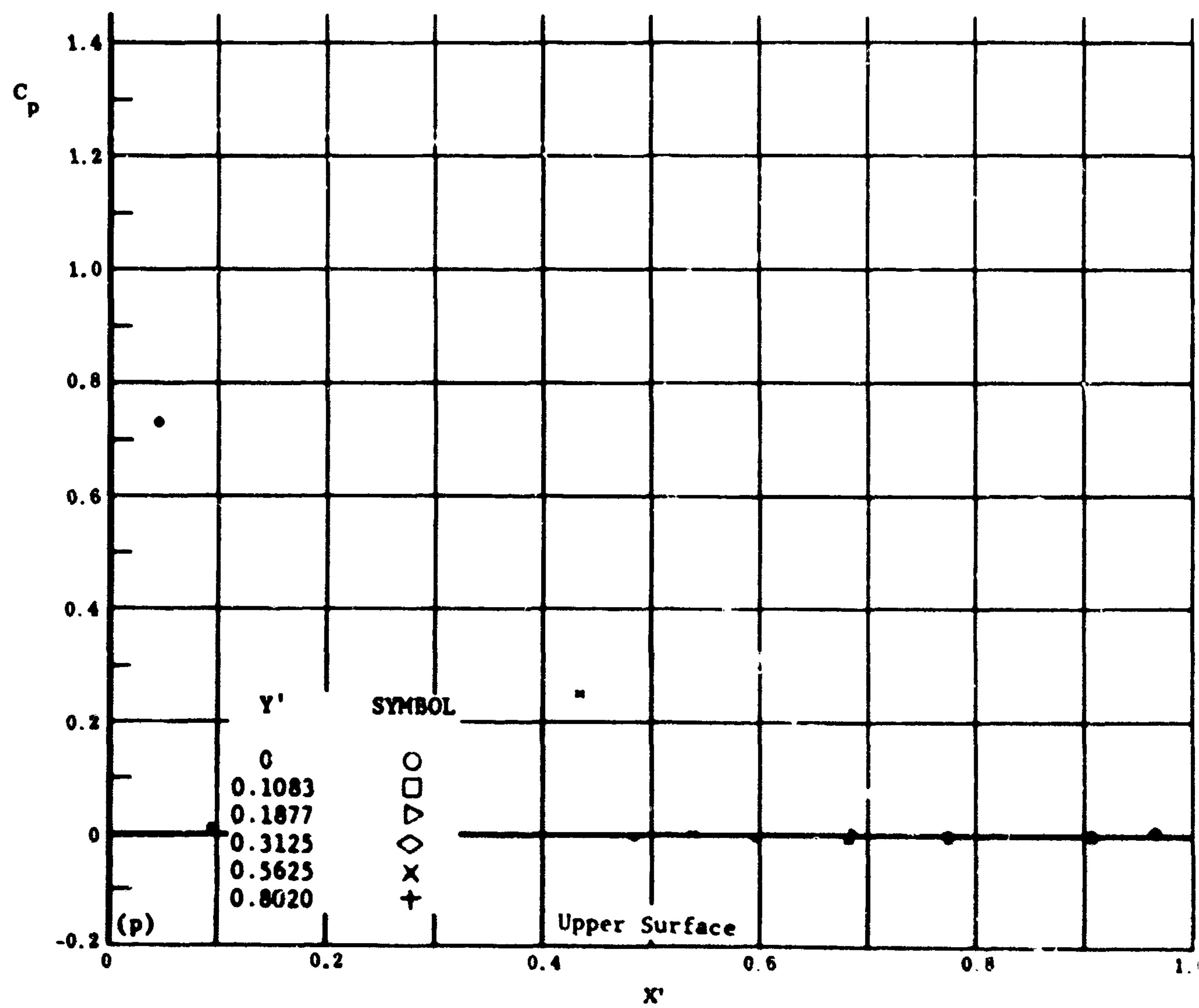

(NONDIMENSIONAL STREAMWISE DISTANCE FROM VIRTUAL APEX)

Fig. 39 Configuration IV, α = +50 , $\delta_2 = \delta_3$ = -20

o) C_p vs. Y', upper surface

p) C_p vs. X', upper surface

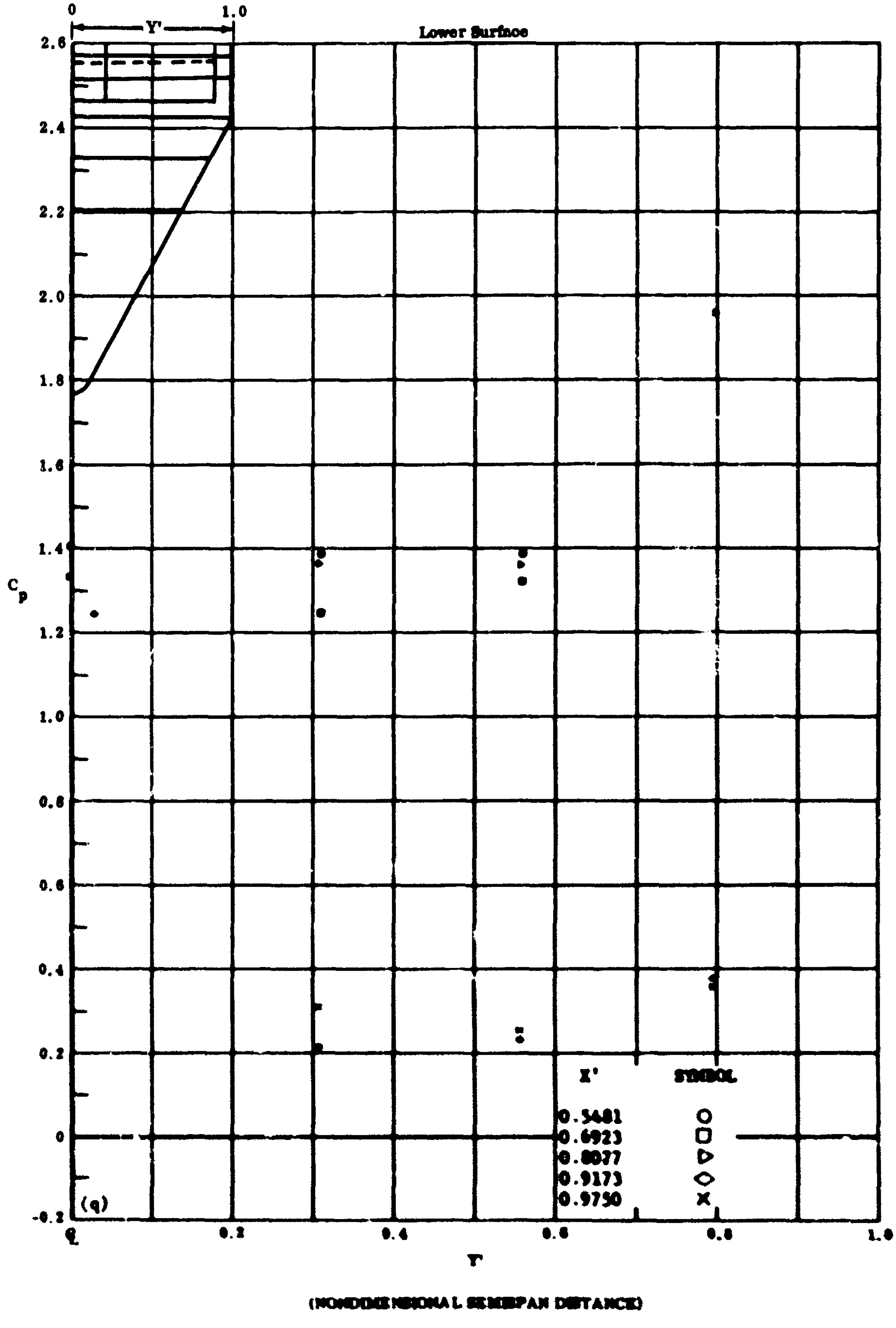

Fig. 39q Configuration IV, α = +50, $\delta_2 = \delta_3$ = -39

C_p vs. Y', lower surface

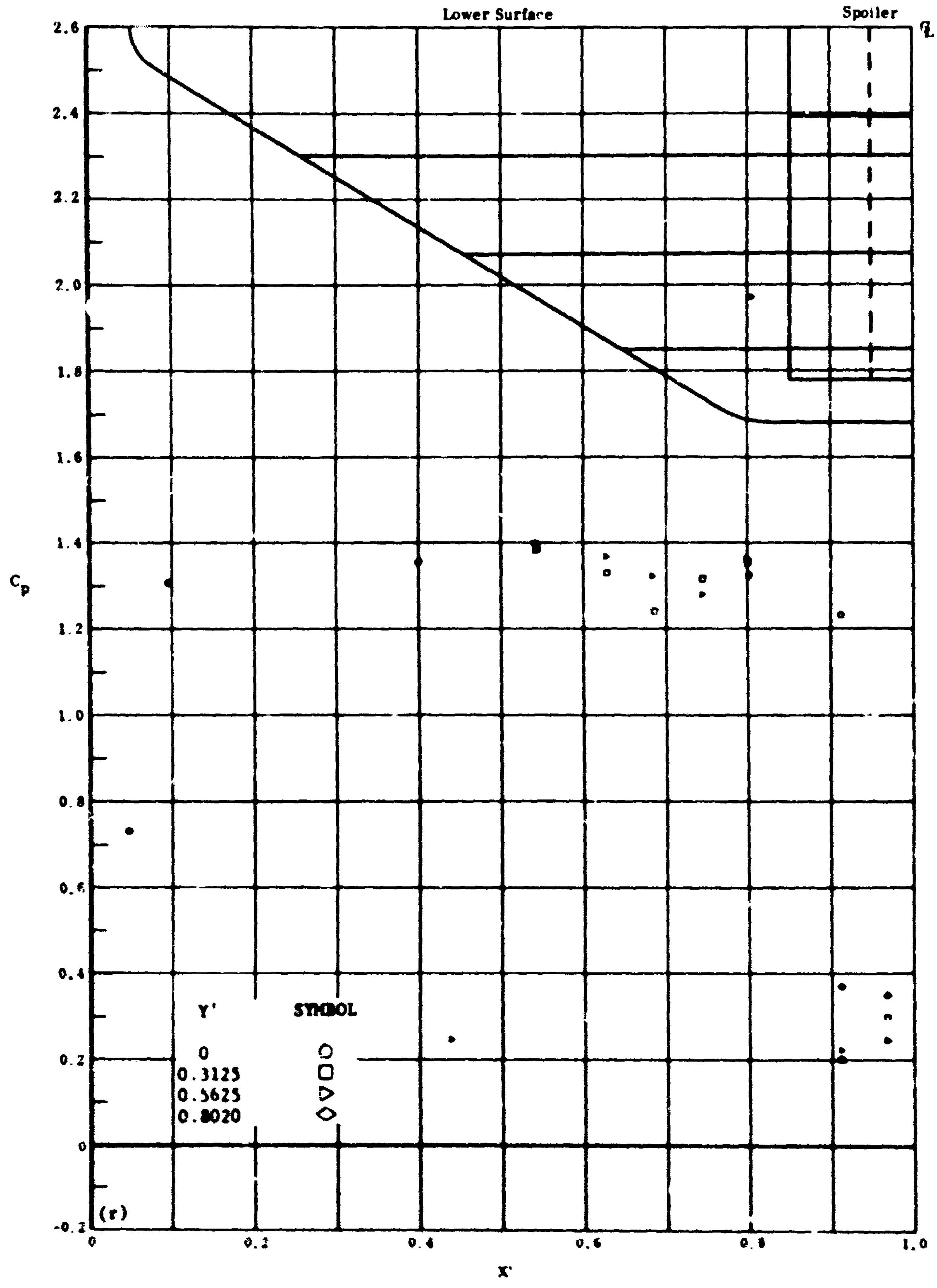

(NONDIMENSIONAL STREAMWISE DISTANCE FROM VIRTUAL APEX)

Fig. 39r Configuration IV, α = -50 , $\delta_2 = \delta_3$ = -39

C_p vs. X', lower surface

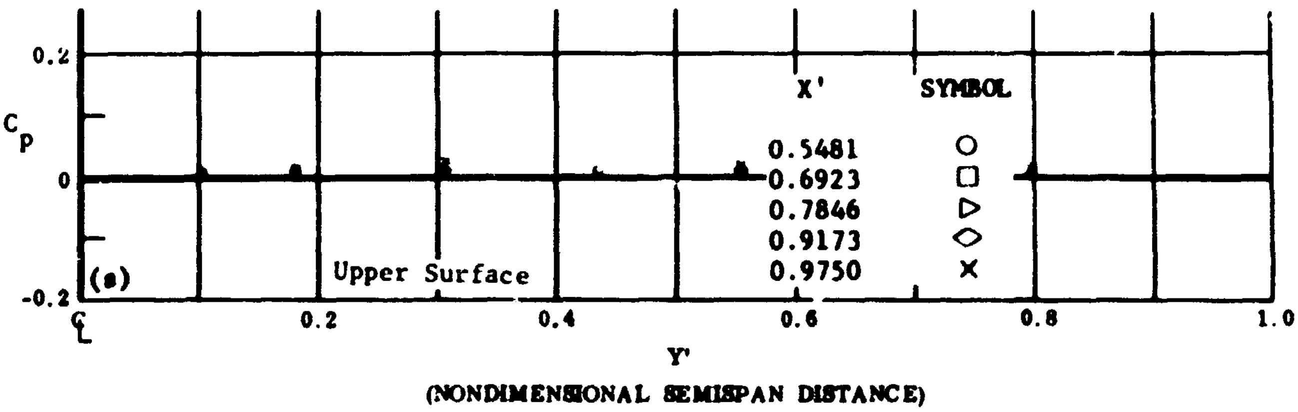

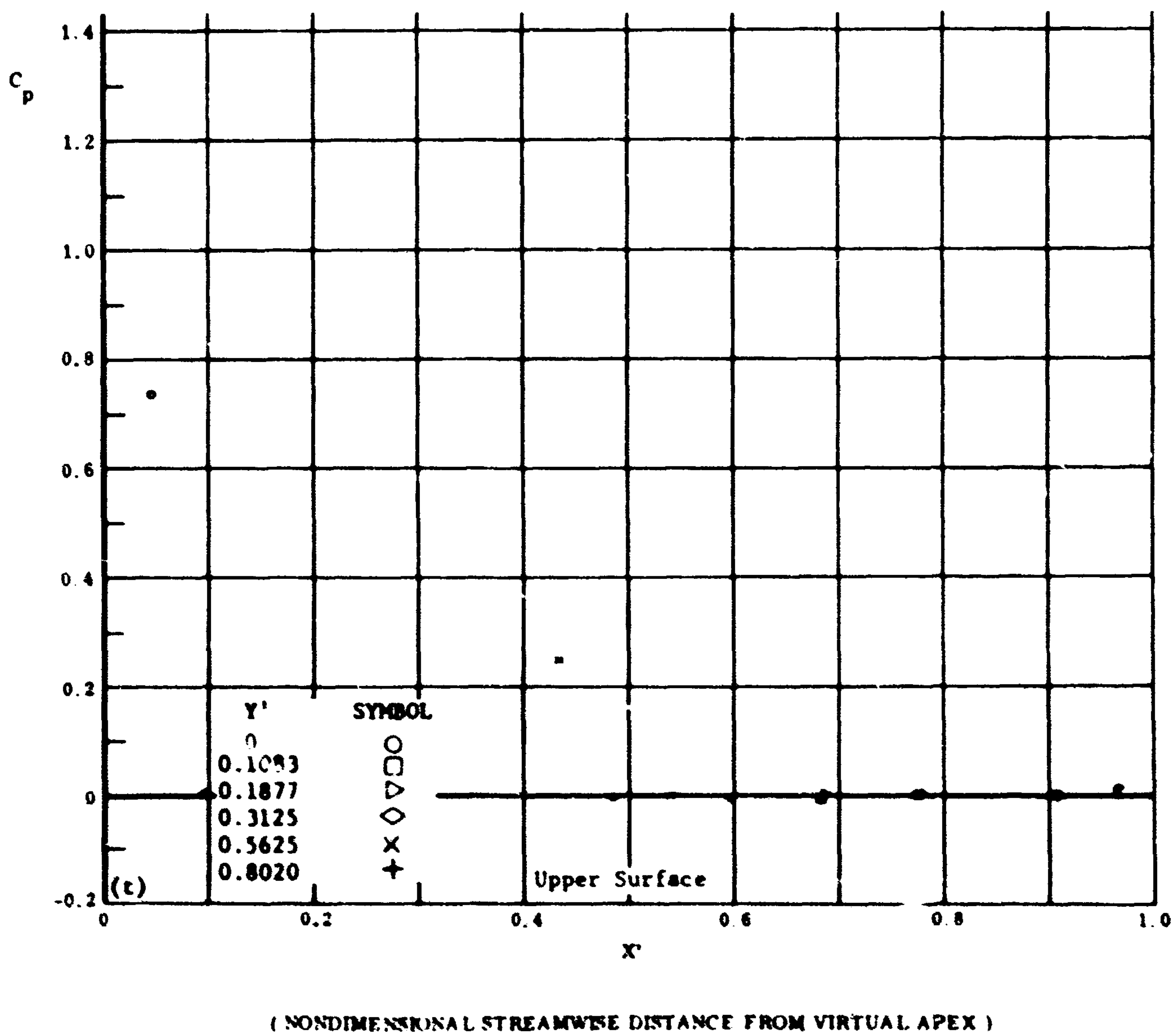

Fig. 39 Configuration IV, α = +50, $\delta_2 = \delta_3$ = -39

s) C_p vs. Y', upper surface

t) C_p vs. X', upper surface

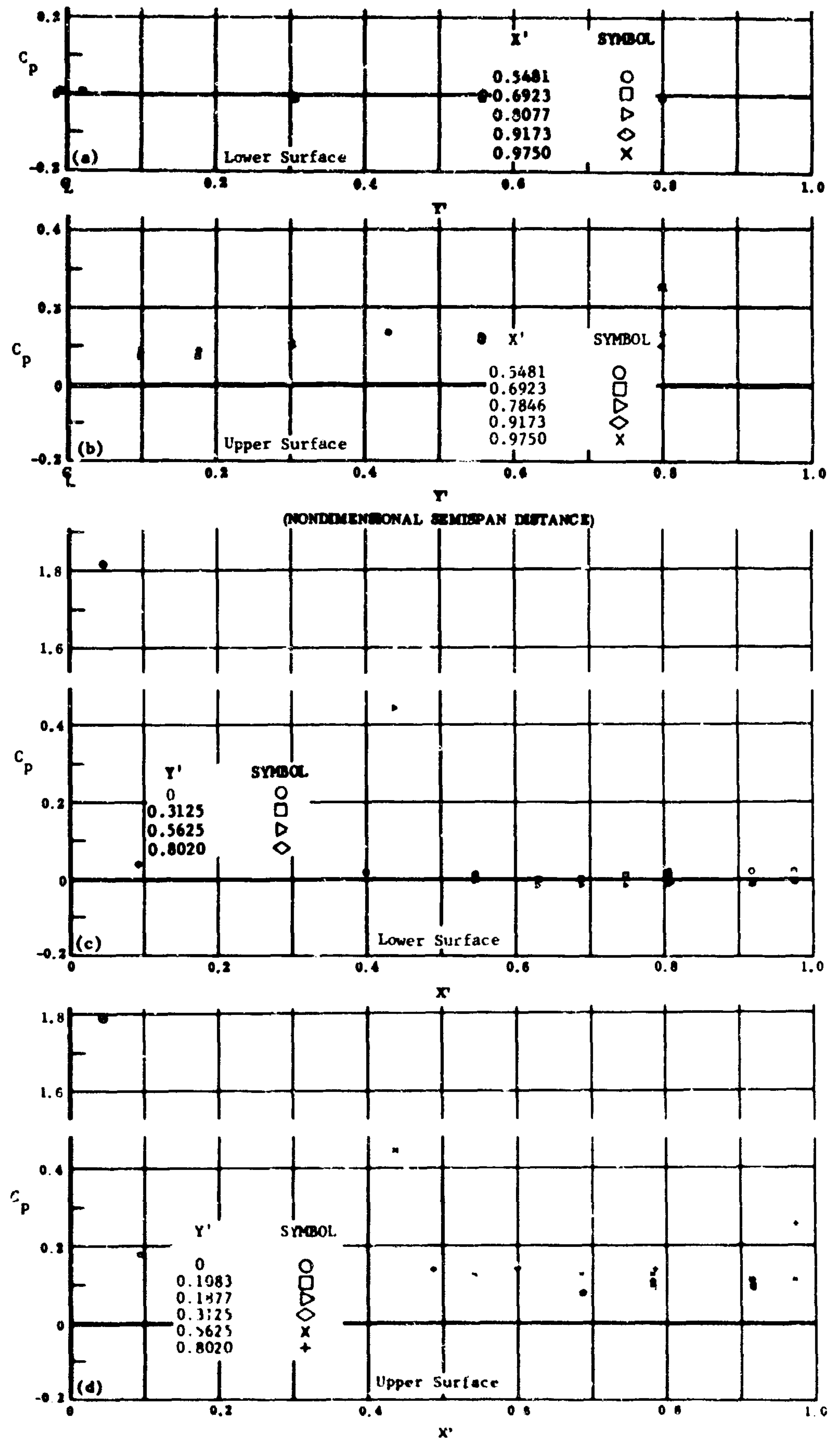

Fig. 40 Configuration IV, $\alpha = -10$, $\delta_2 = \delta_3 = 0$

a) C_p vs. Y', lower surface

b) C_p vs. Y', upper surface

c) C_p vs. X', lower surface

d) C_p vs. X', upper surface

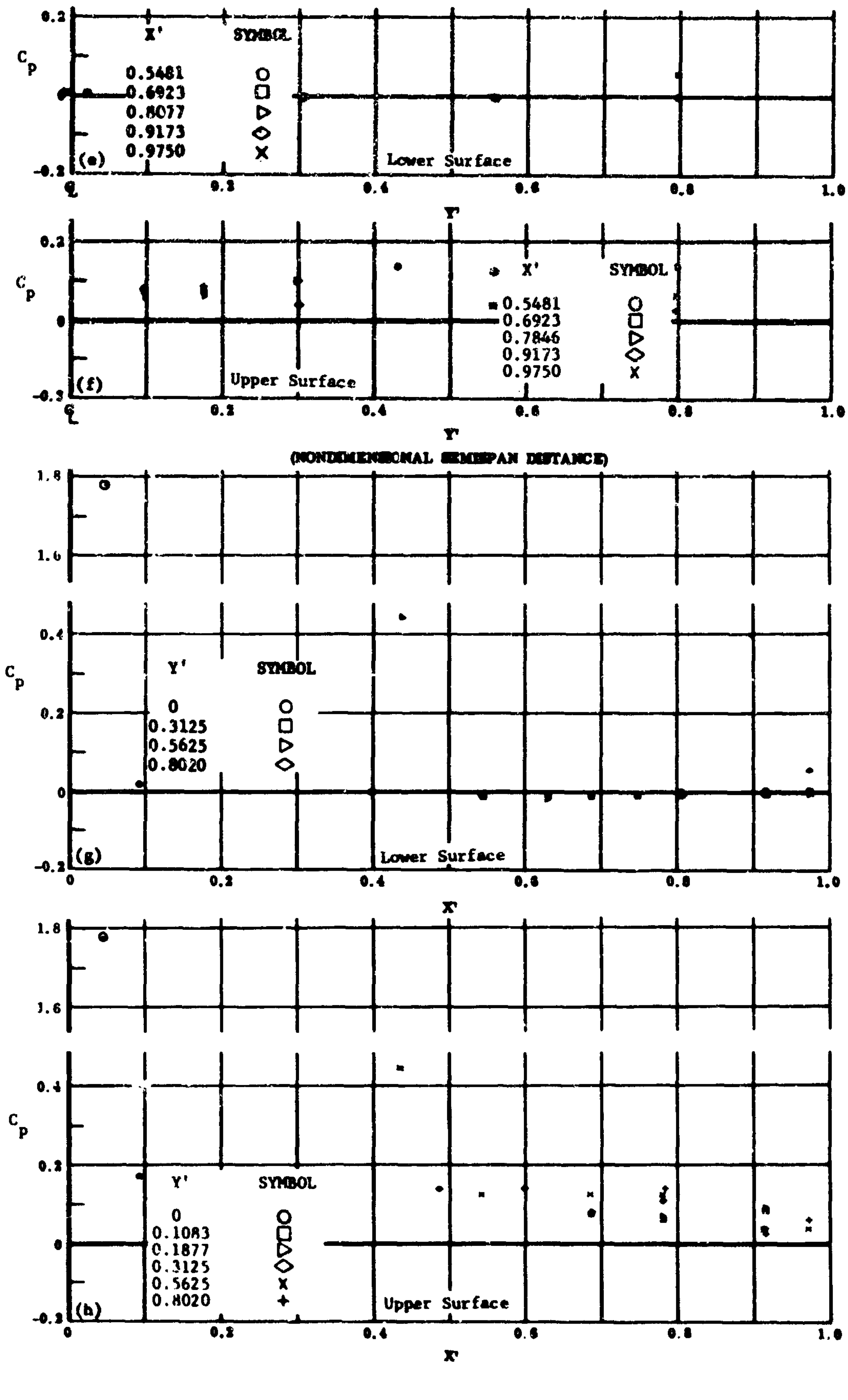

Fig. 40 Configuration XV, α = -10 , $\delta_2 = \delta_3$ = +10

e) C_p vs. Y', lower surface

f) C_p vs. Y', upper surface

g) C_p vs. X', lower surface

h) C_p vs. X', upper surface

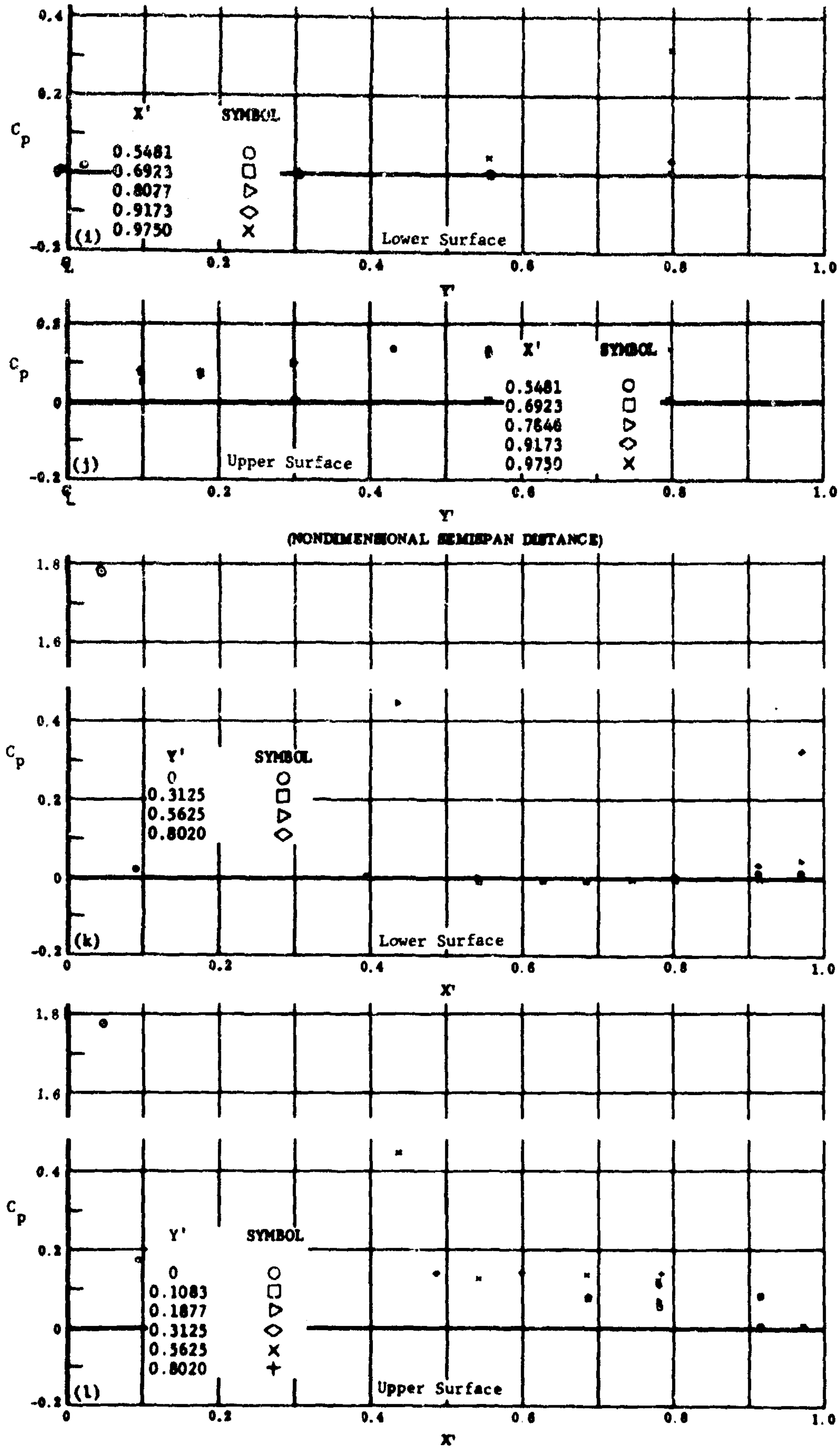

(NONDIMENSIONAL STREAMWISE DISTANCE FROM VIRTUAL APEX)

Fig. 40 Configuration IV, $\alpha = -10$, $\delta_2 = \delta_3 = +20$

i) C_p vs. Y', lower surface

j) C_p vs. Y', upper surface

k) C_p vs. X', lower surface

l) C_p vs. X', upper surface

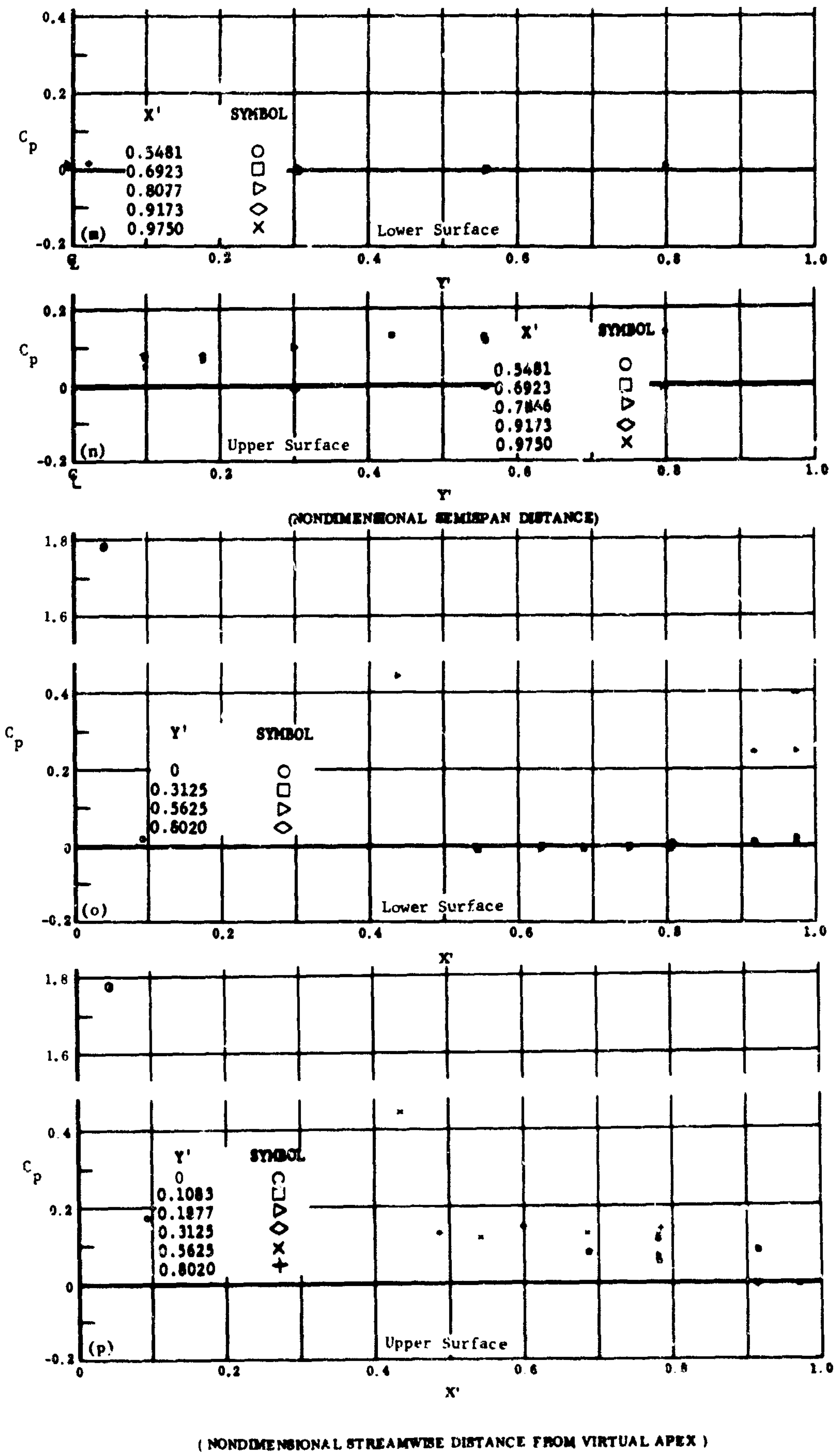

Fig. 40 Configuration IV, $\alpha = -10$, $\delta_2 = \delta_3 = +30$

m) C_p vs. Y', lower surface

n) C_p vs. Y', upper surface

o) C_p vs. X', lower surface

p) C_p vs. X', upper surface

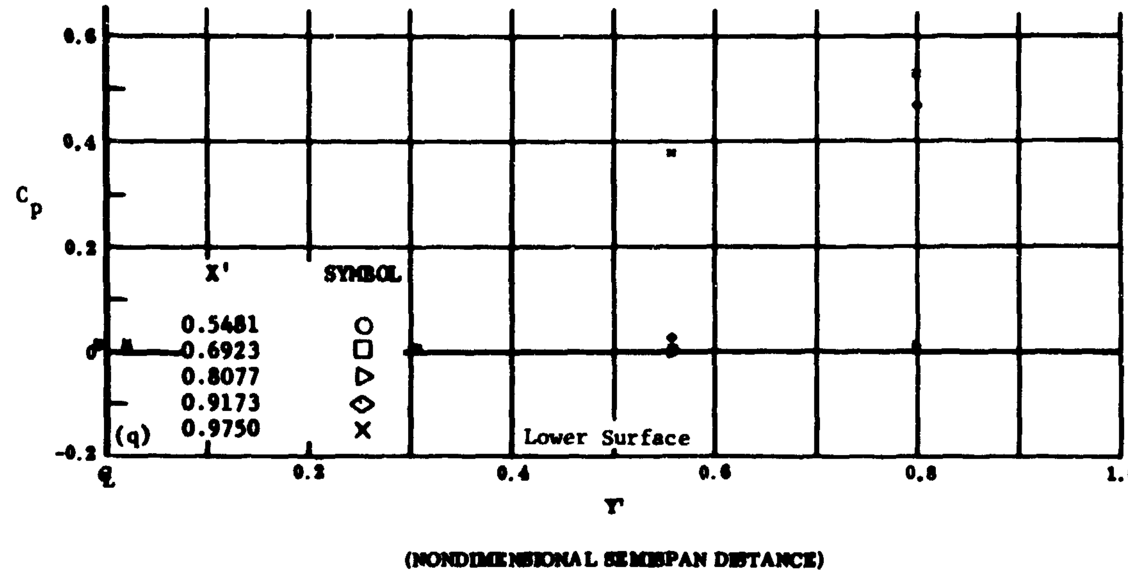

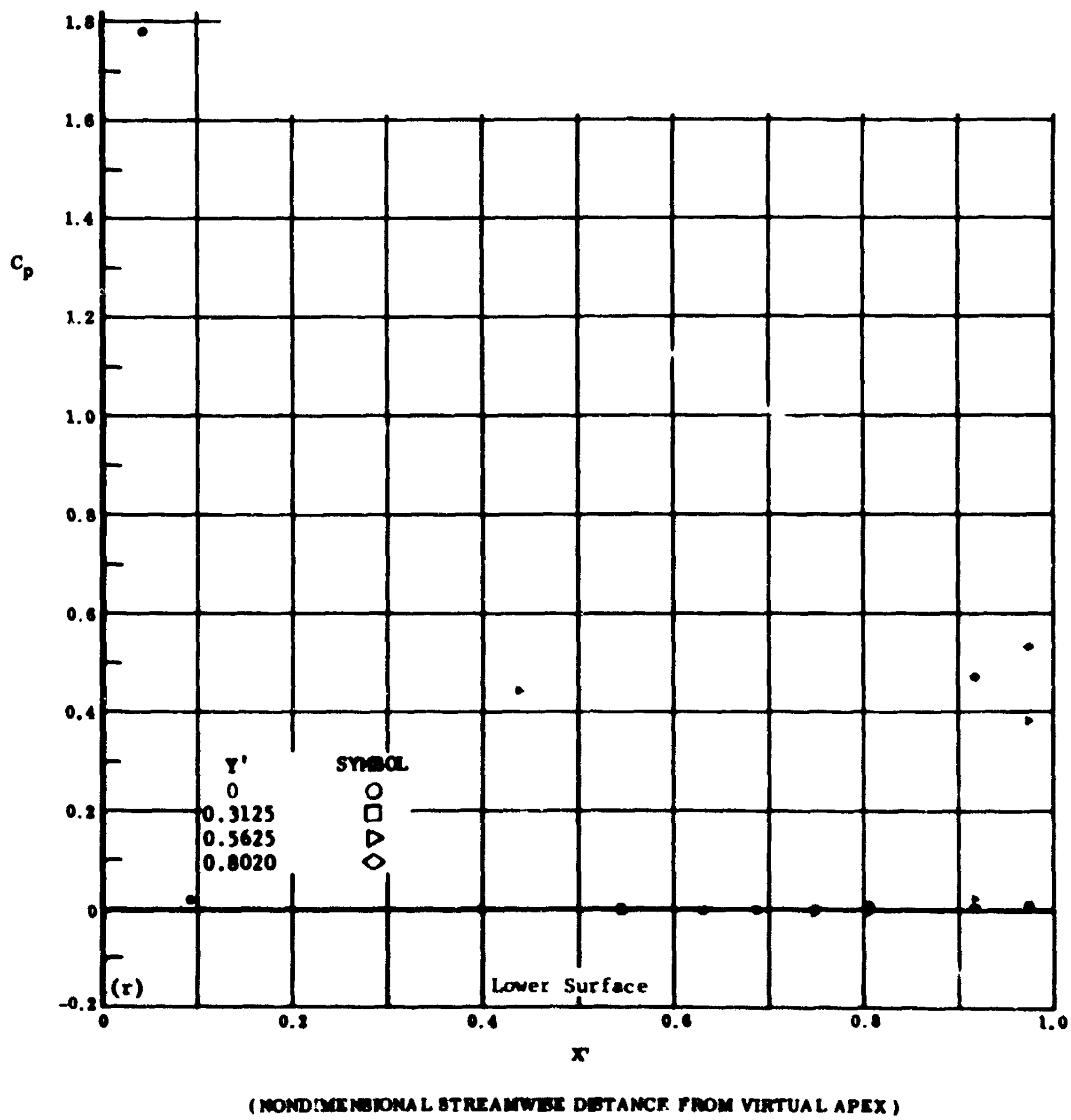

Fig. 40 Configuration IV, $\alpha = -10$, $\delta_2 = \delta_3 = +39$

q) C_p vs. Y', lower surface

r) C_p vs. X', lower surface

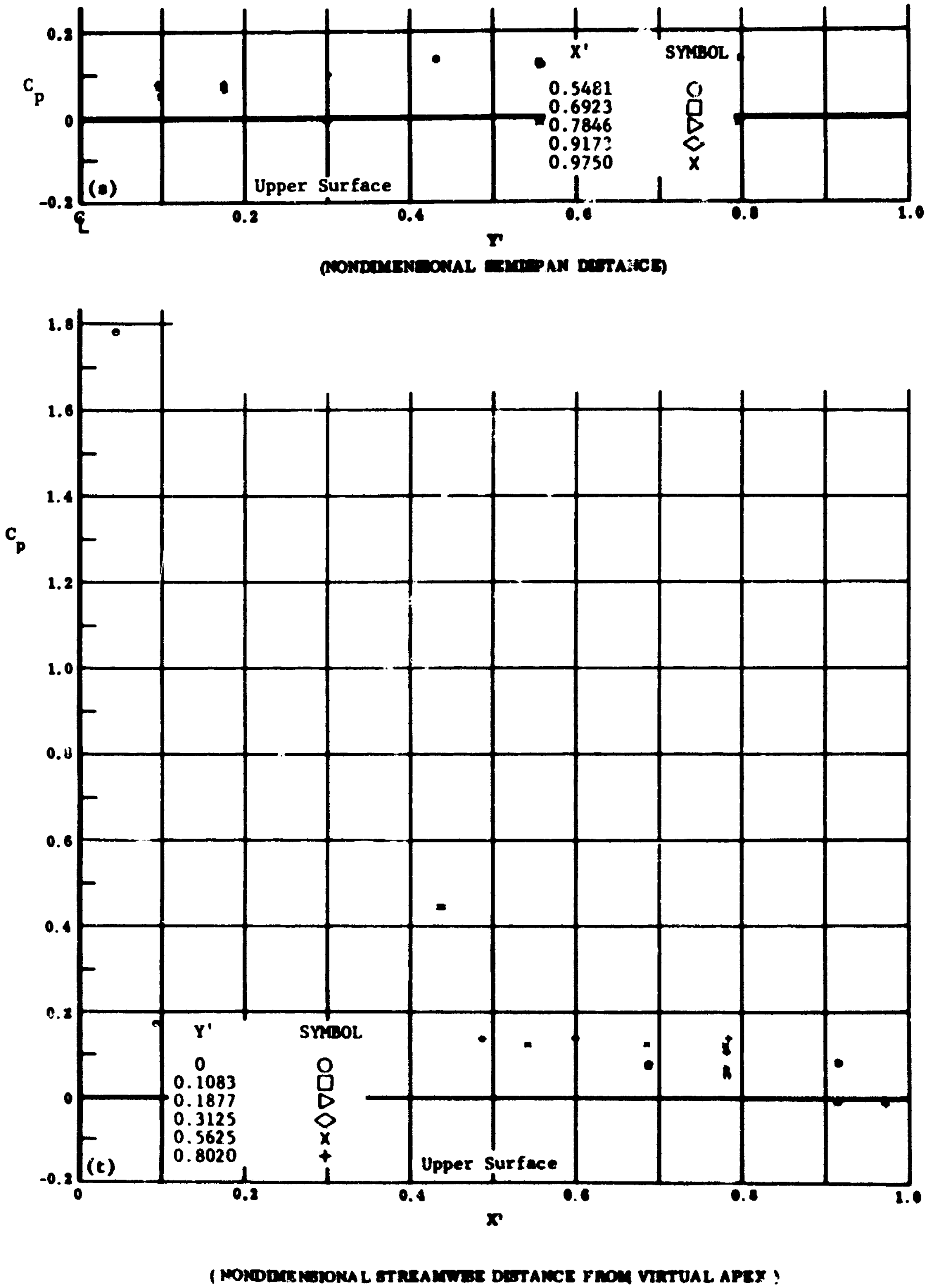

Fig. 40 Configuration IV, $\alpha = -10$, $\delta_2 = \delta_3 = +39$

s) C_p vs. Y', upper surface

t) C_p vs. X', upper surface

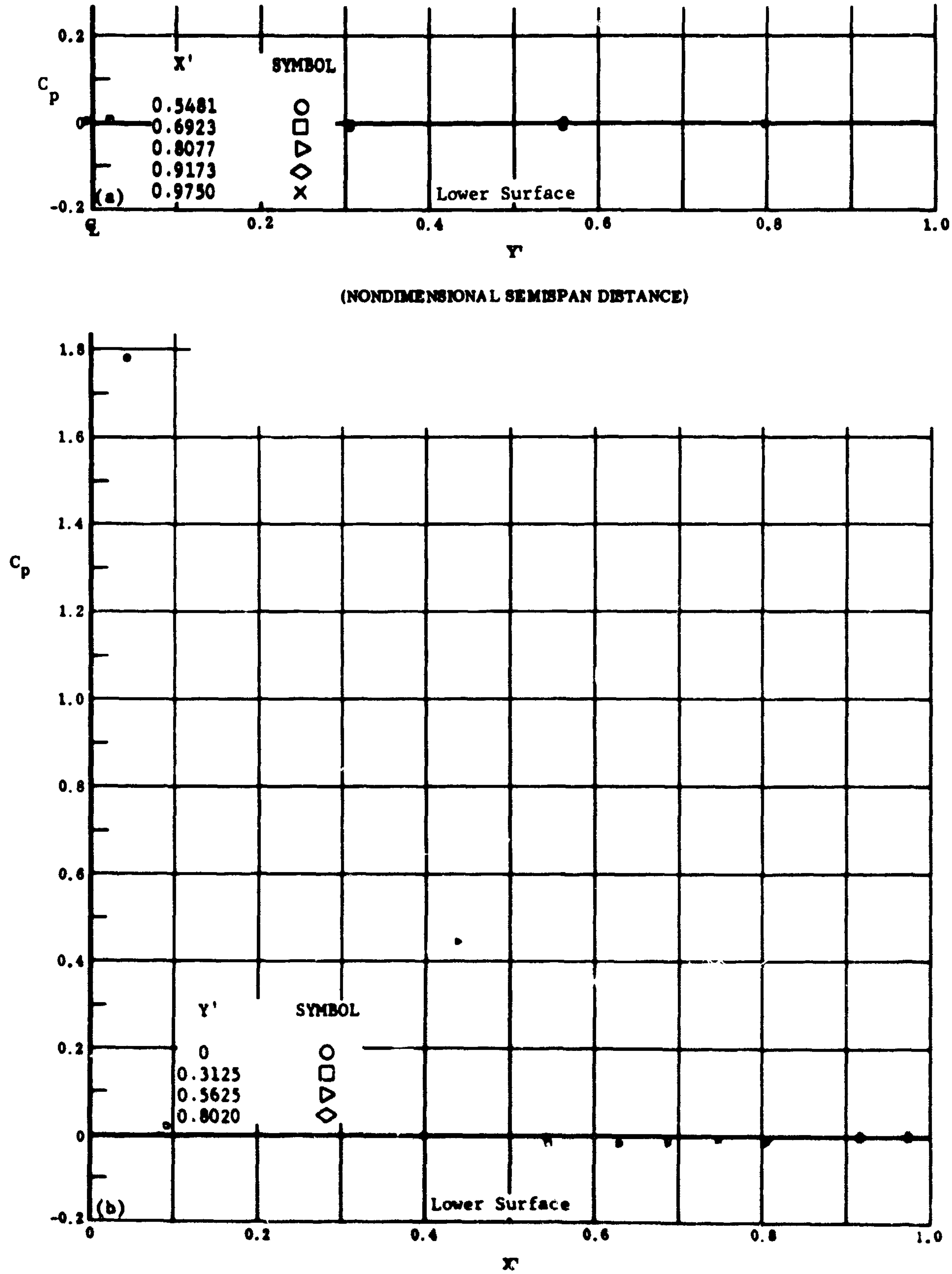

(NONDIMENSIONAL SEMISPAN DISTANCE)

(NONDIMENSIONAL STREAMWISE DISTANCE FROM VIRTUAL APEX)

Fig. 41 Configuration IV, $\alpha = -10$, $\delta_2 = \delta_3 = -10$

a) C_p vs. Y', lower surface

b) C_p vs. X', lower surface

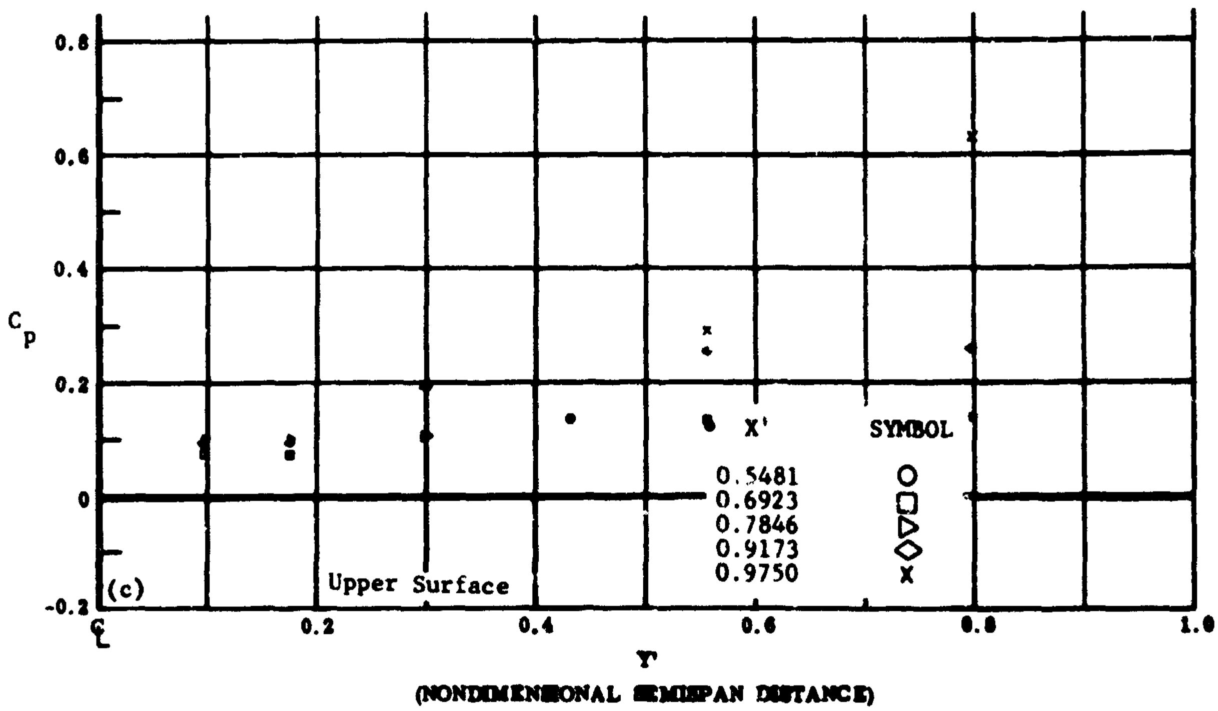

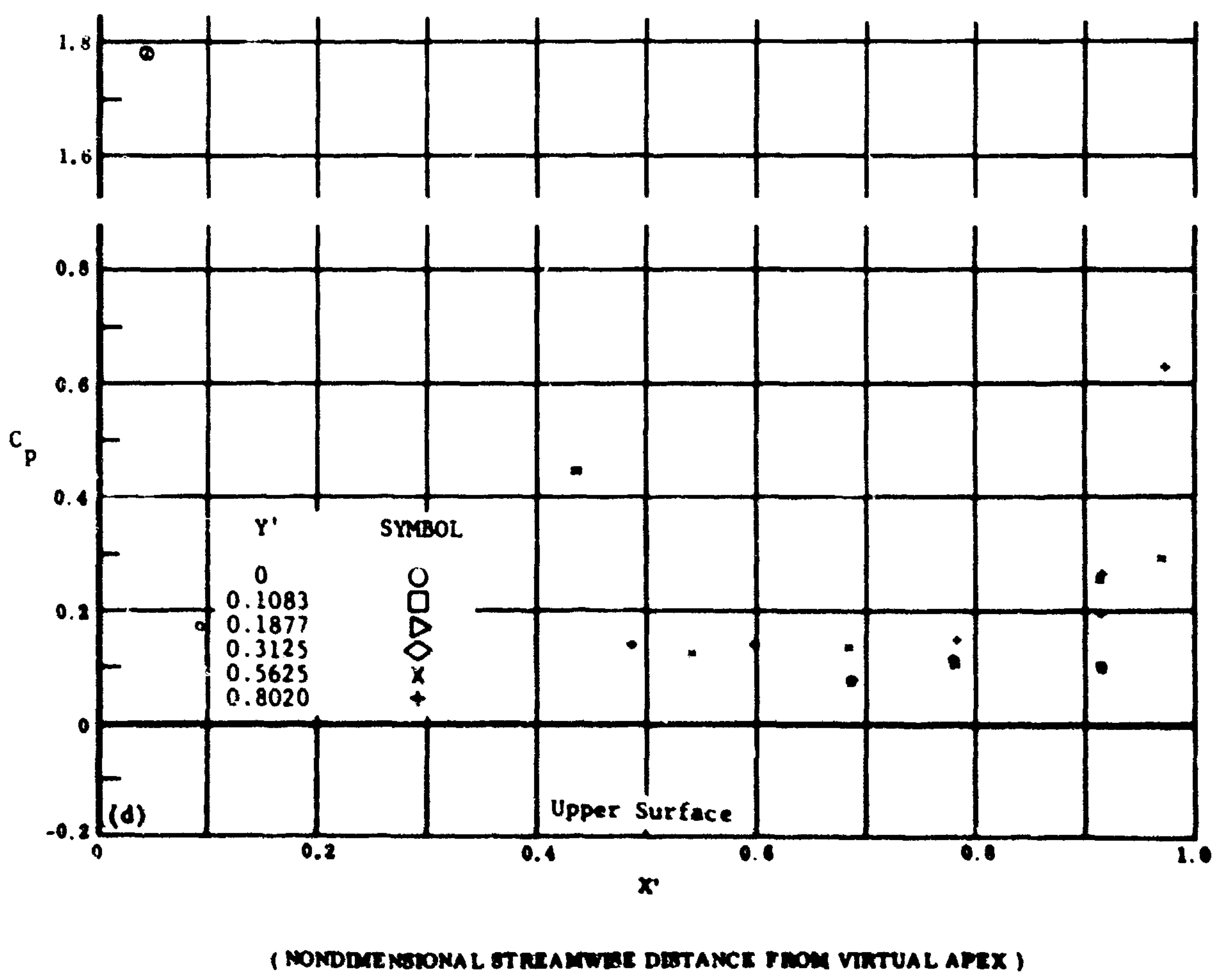

Fig. 41 Configuration IV, α = -10, $\delta_2 = \delta_3$ = -10

c) C_p vs. Y', upper surface

d) C_p vs. X', upper surface

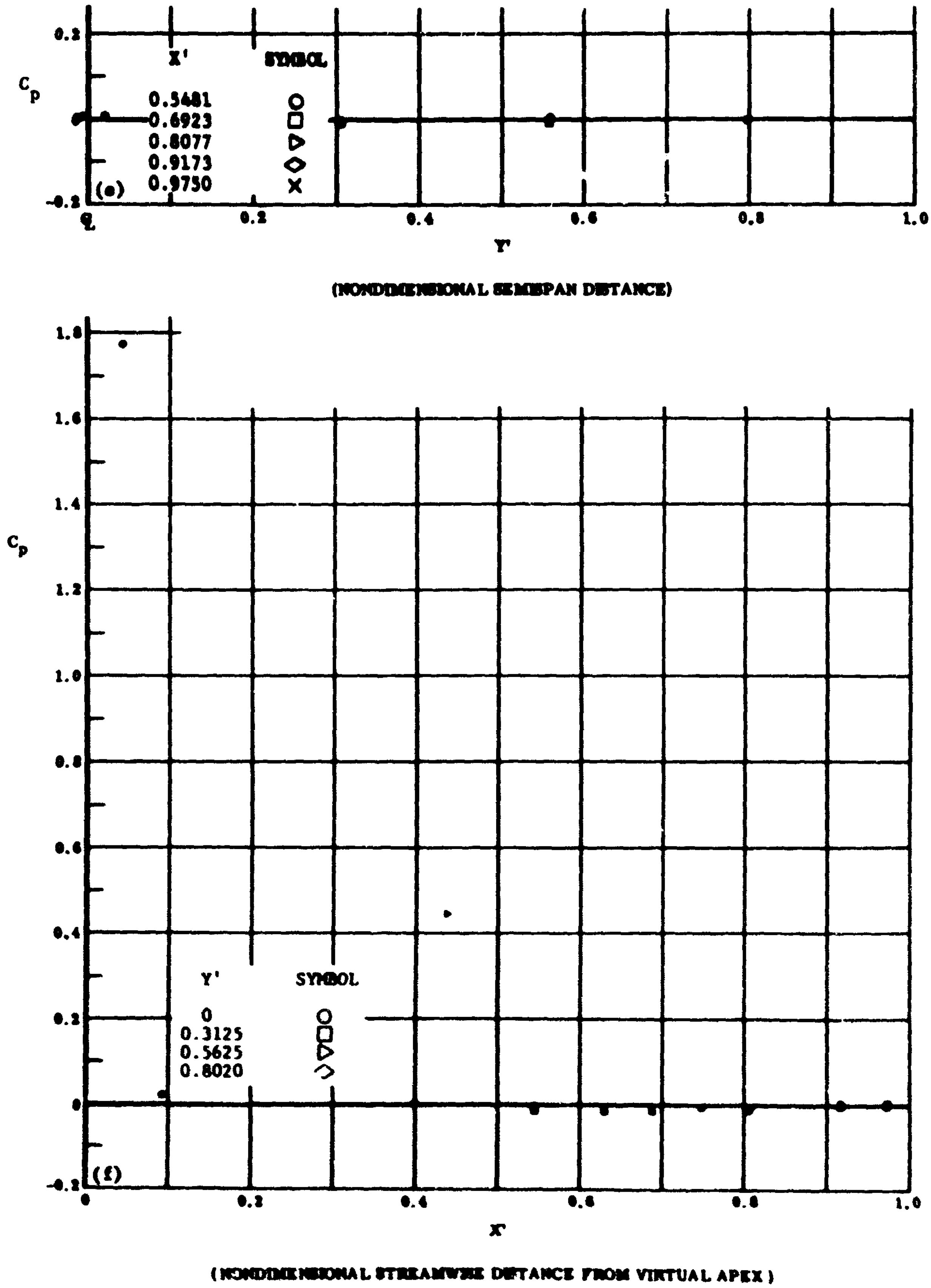

Fig. 41 Configuration IV, α = -10 , $\delta_2 = \delta_3$ = -20

e) C_p vs. Y', lower surface

f) C_p vs. X', lower surface

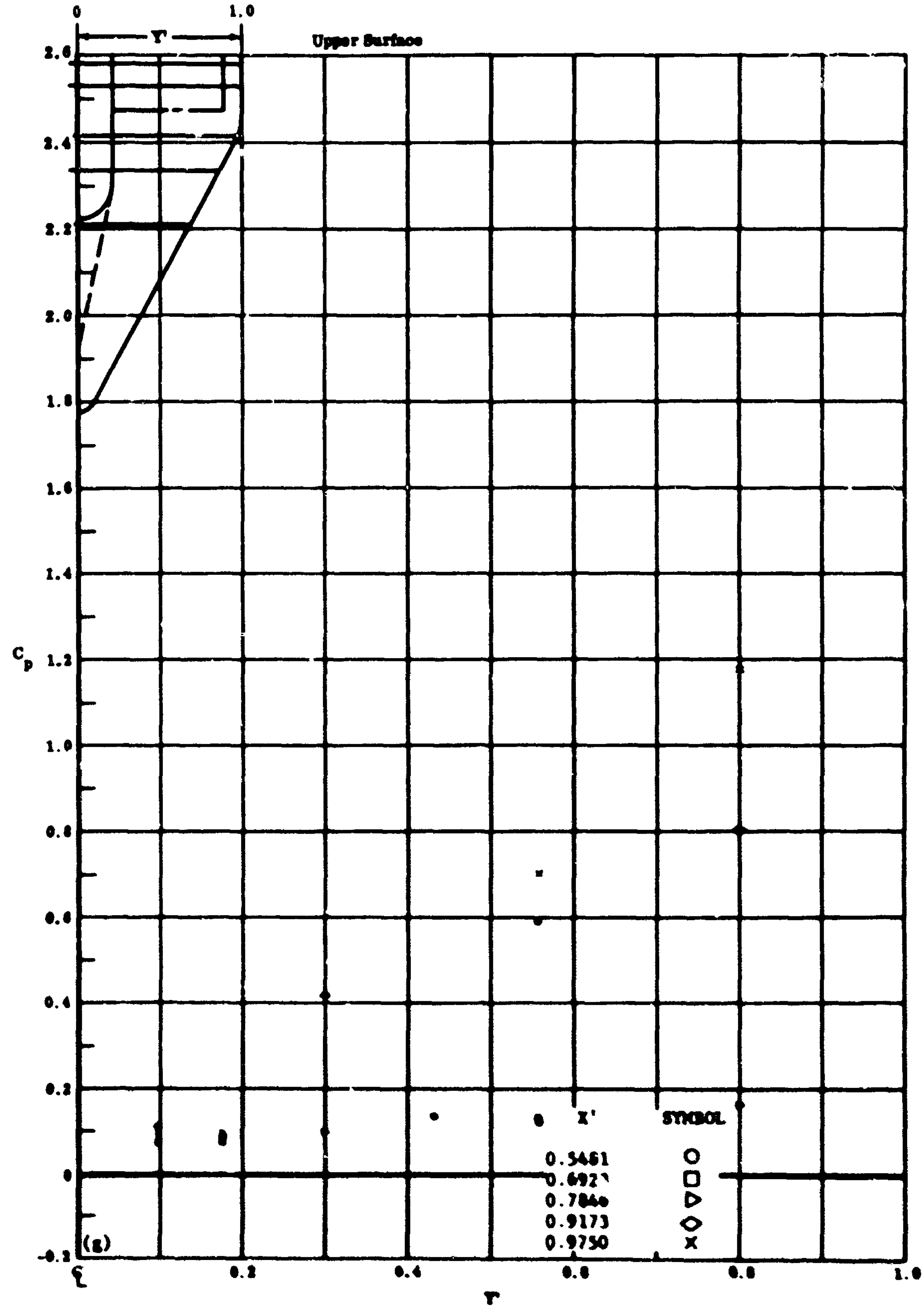

Fig. 41g Configuration IV, α = -10, $\delta_2 = \delta_3$ = -20

C_p vs. Y', upper surface

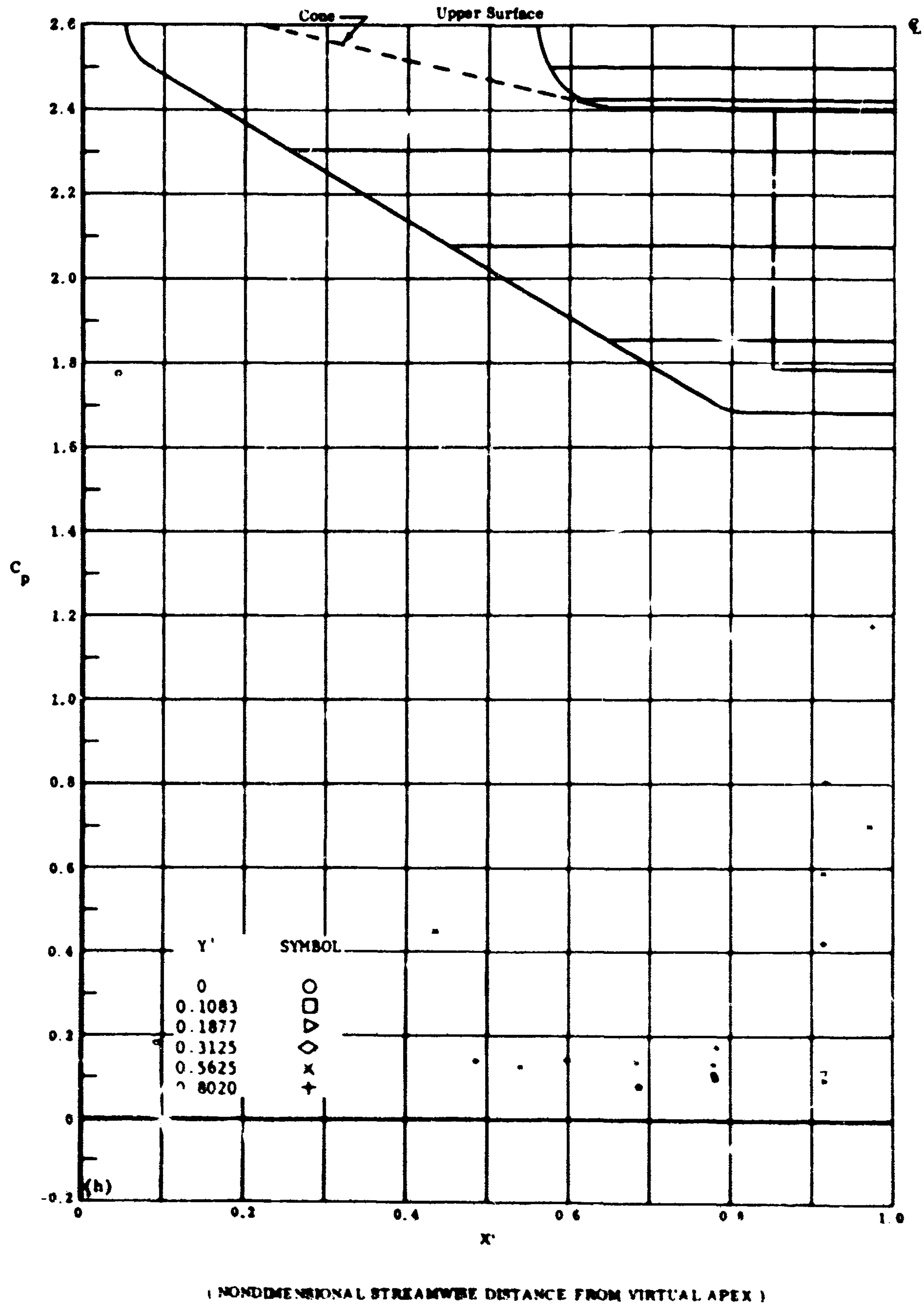

Fig. 41h Configuration IV, $\alpha = -10$, $\delta_2 = \delta_3 = -20$

C_p vs. X', upper surface

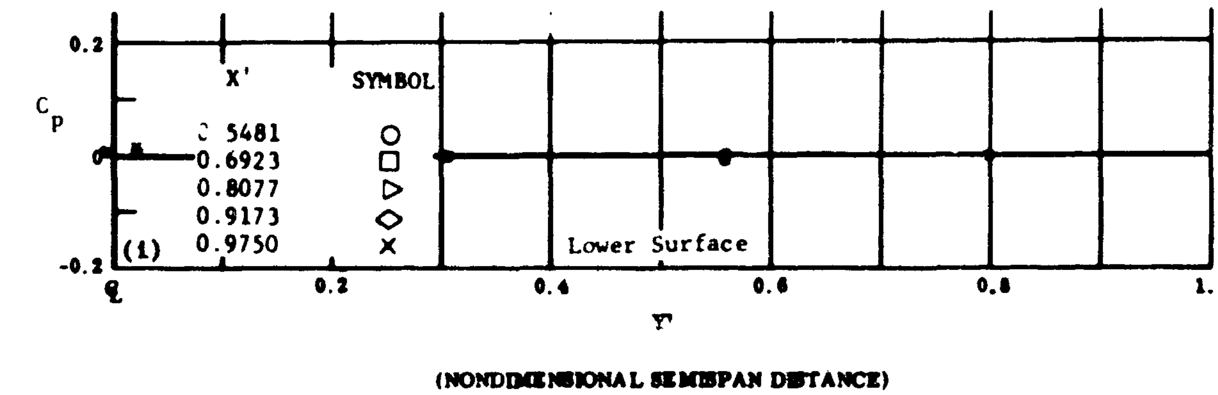

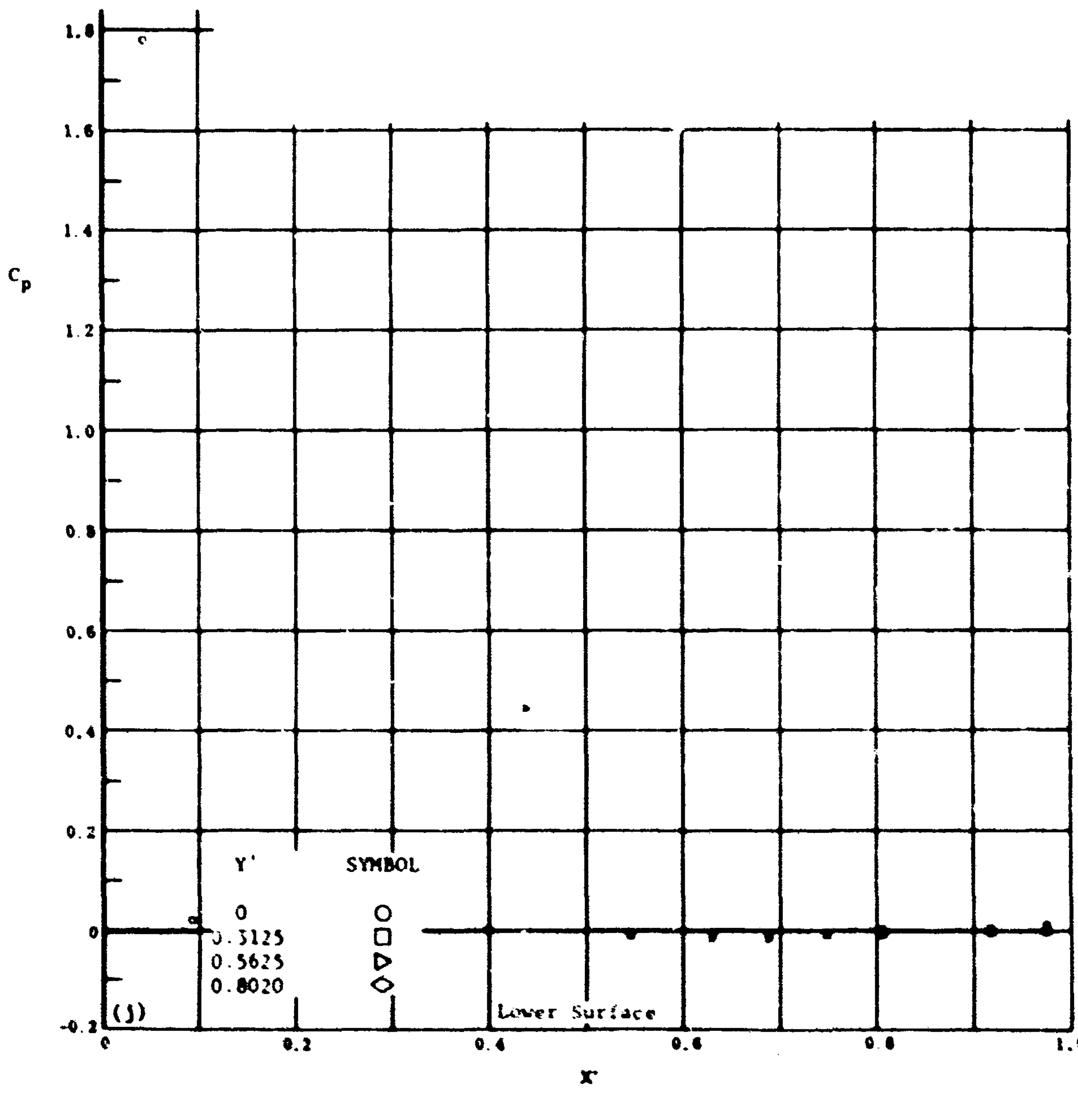

Fig. 41 Configuration IV, $\delta_1 = -10$, $\delta_2 = \delta_3 = -30$

i) C_p vs. Y', lower surface

j) C_p vs. X', lower surface

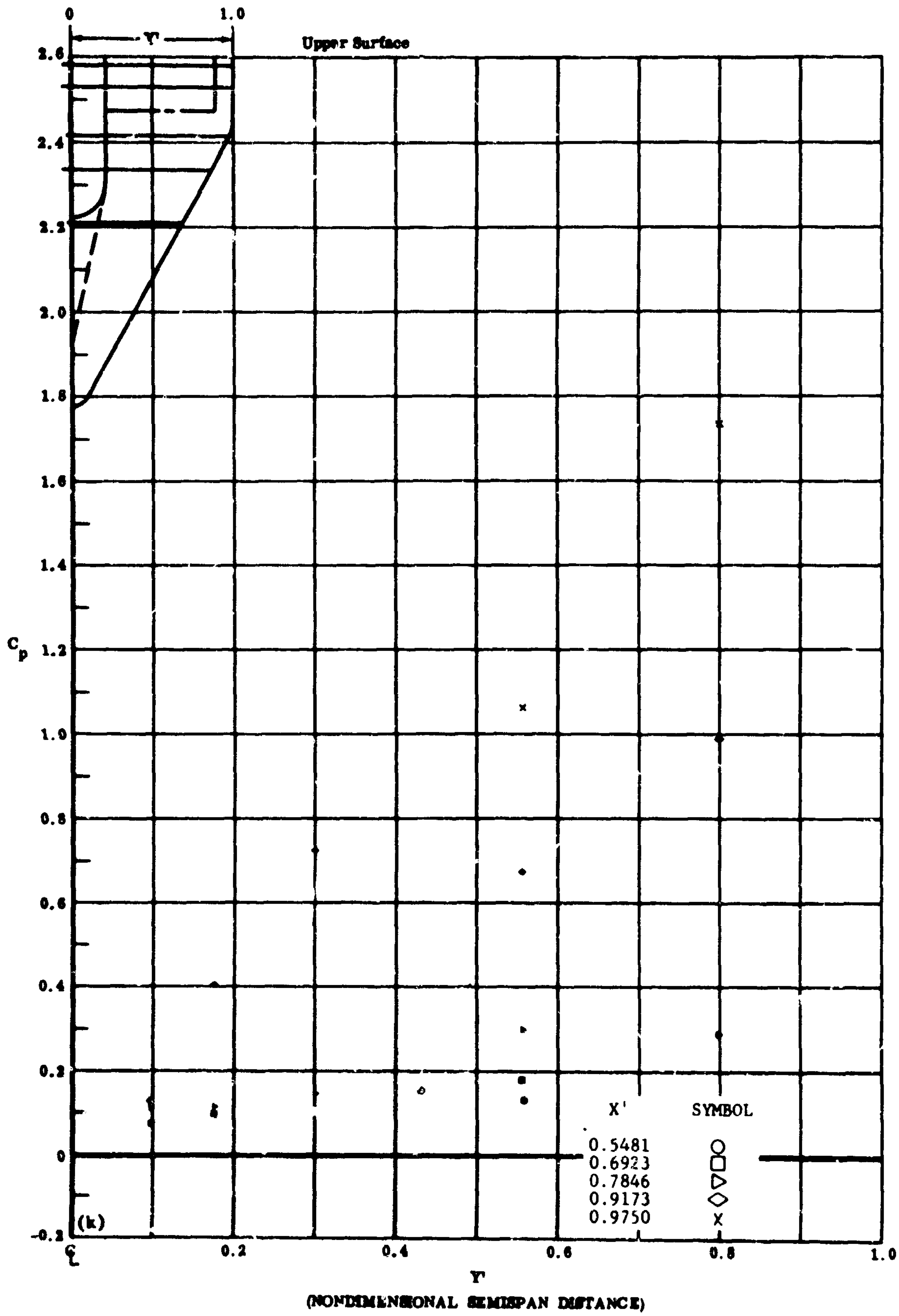

Fig. 41k Configuration IV, $\alpha = -10$, $\delta_2 = \delta_3 = -30$

C_p vs. Y', upper surface

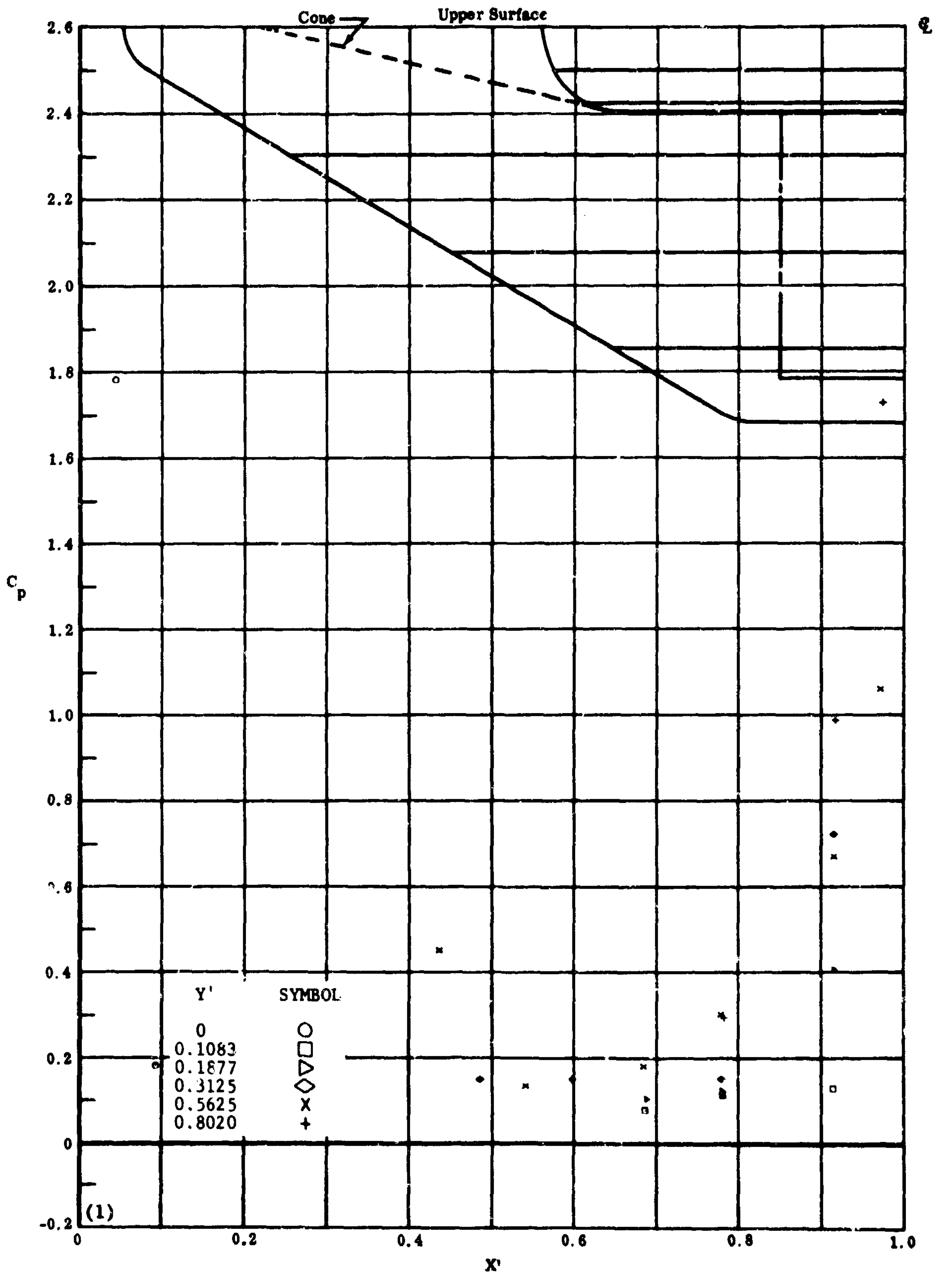

Fig. 411 Configuration IV, $\alpha = -10$, $\delta_2 = \delta_3 = -30$

C_p vs. X', upper surface

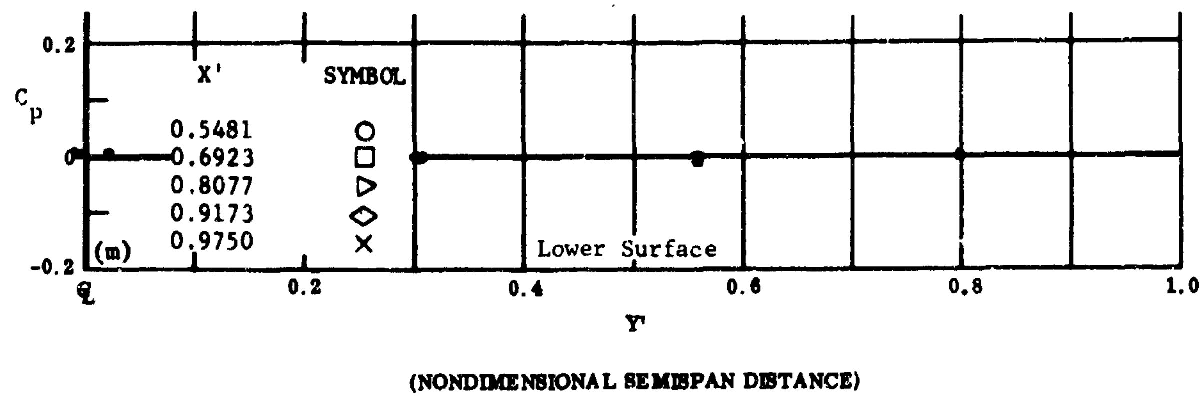

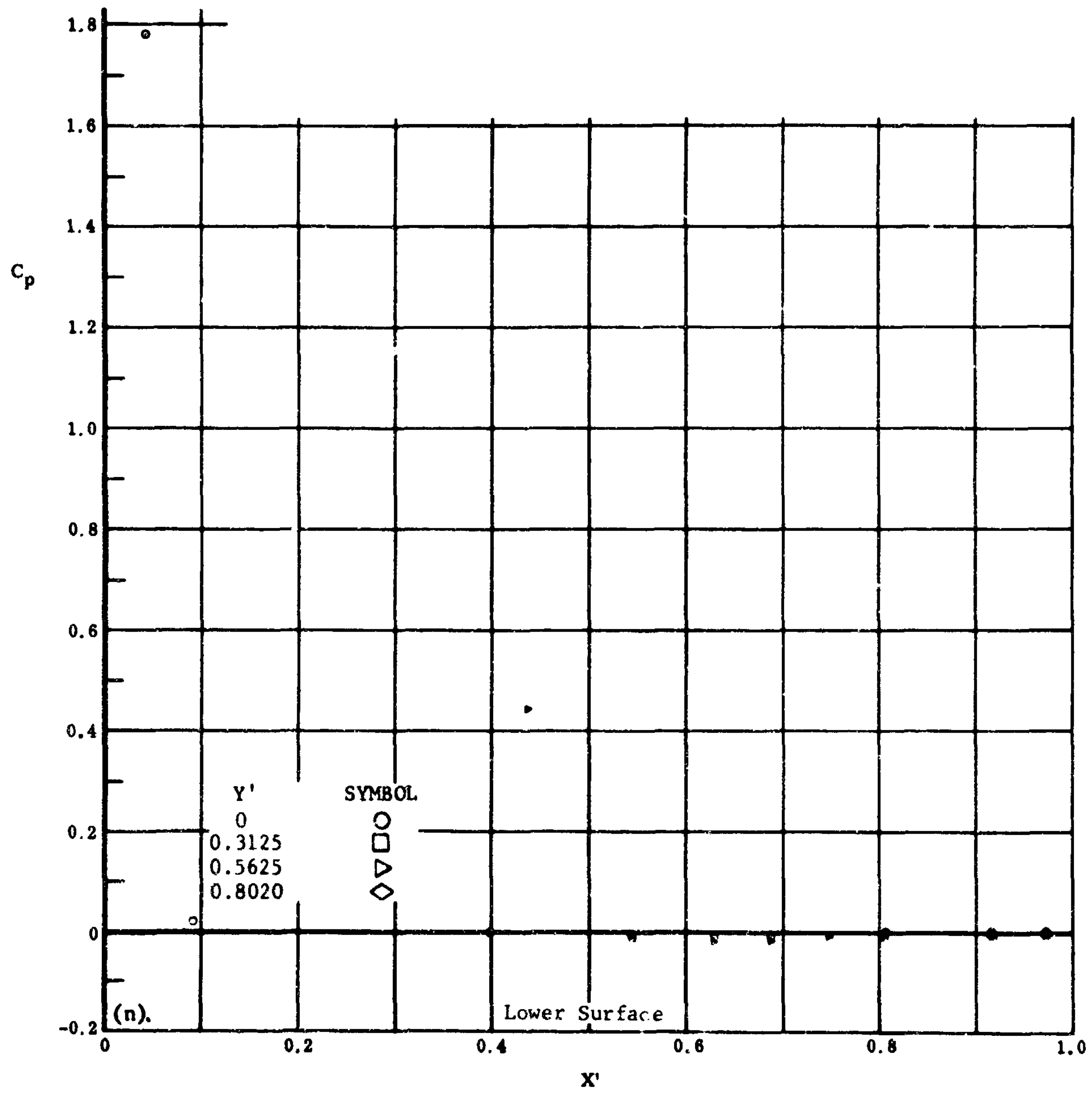

Fig. 41 Configuration IV, α = -10 , $\delta_2 = \delta_3$ = -39

m) C_p vs. Y', lower surface

n) C_p vs. X', lower surface

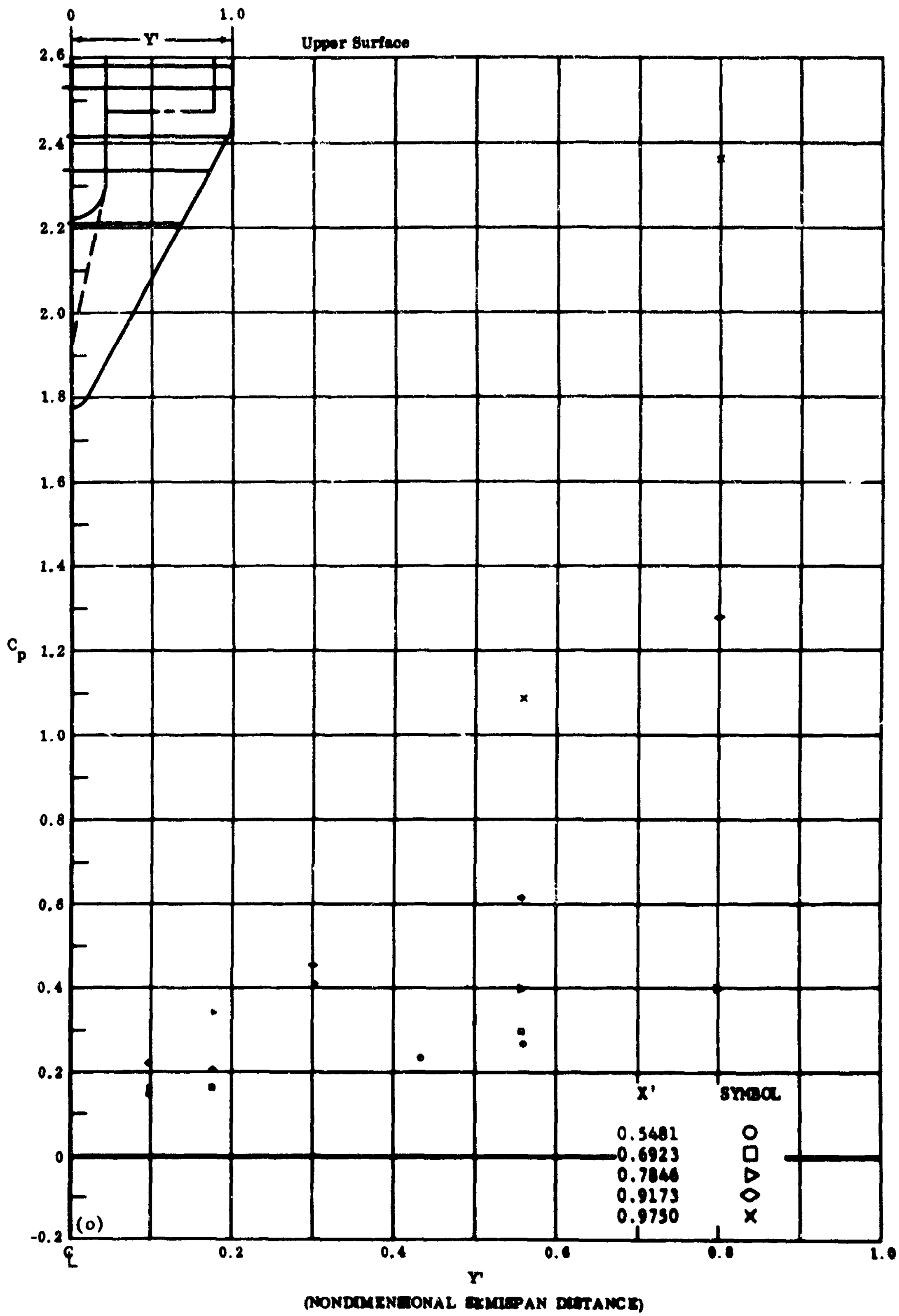

Fig. 41o Configuration IV, α = -10 , $\delta_2 = \delta_3$ = -39

C_p vs. Y', upper surface

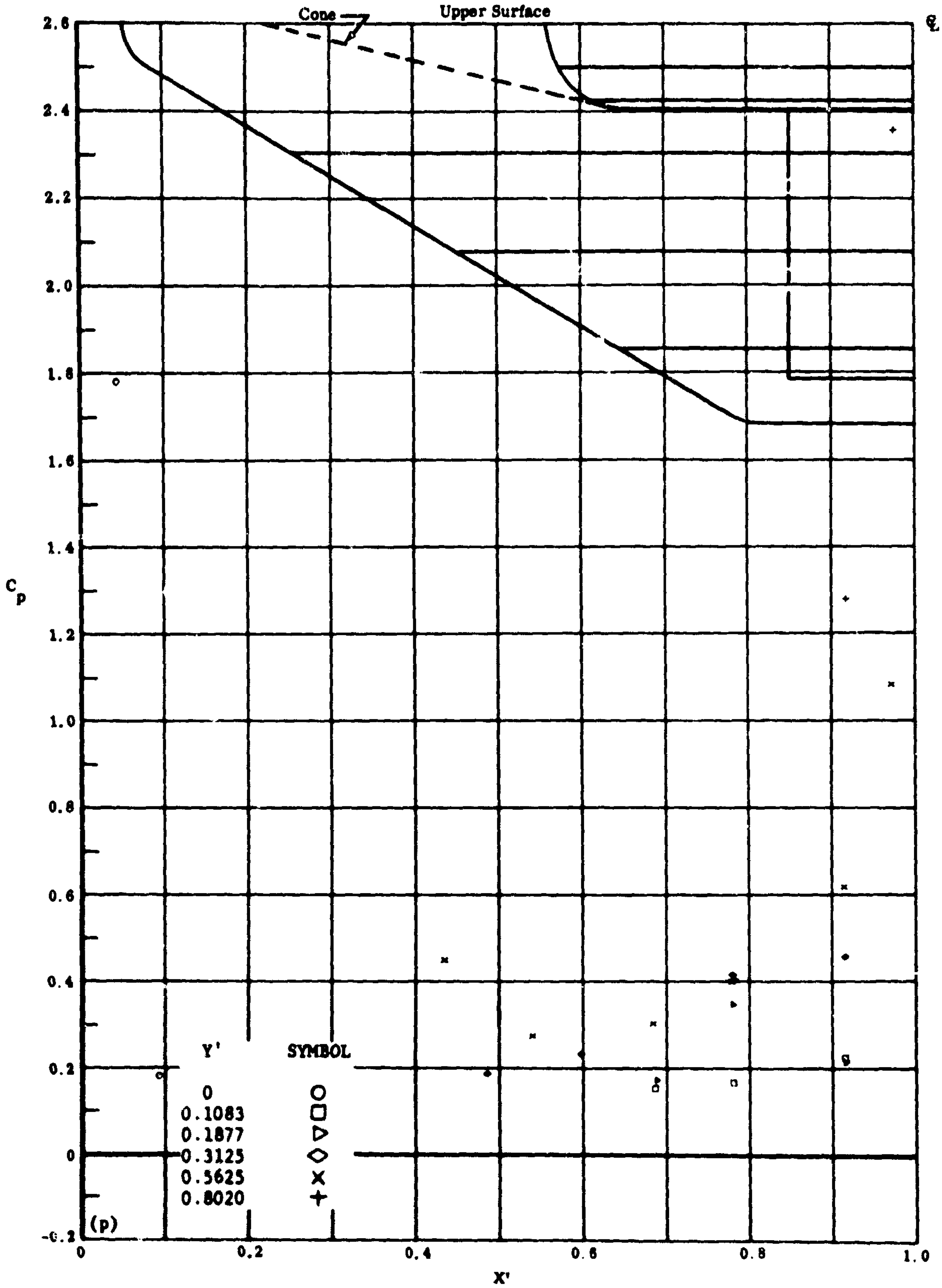

(NONDIMENSIONAL STREAMWISE DISTANCE FROM VIRTUAL APEX)

Fig. 41p Configuration IV, $\alpha = -10$, $\delta_2 = \delta_3 = -39$

C_p vs. X', upper surface

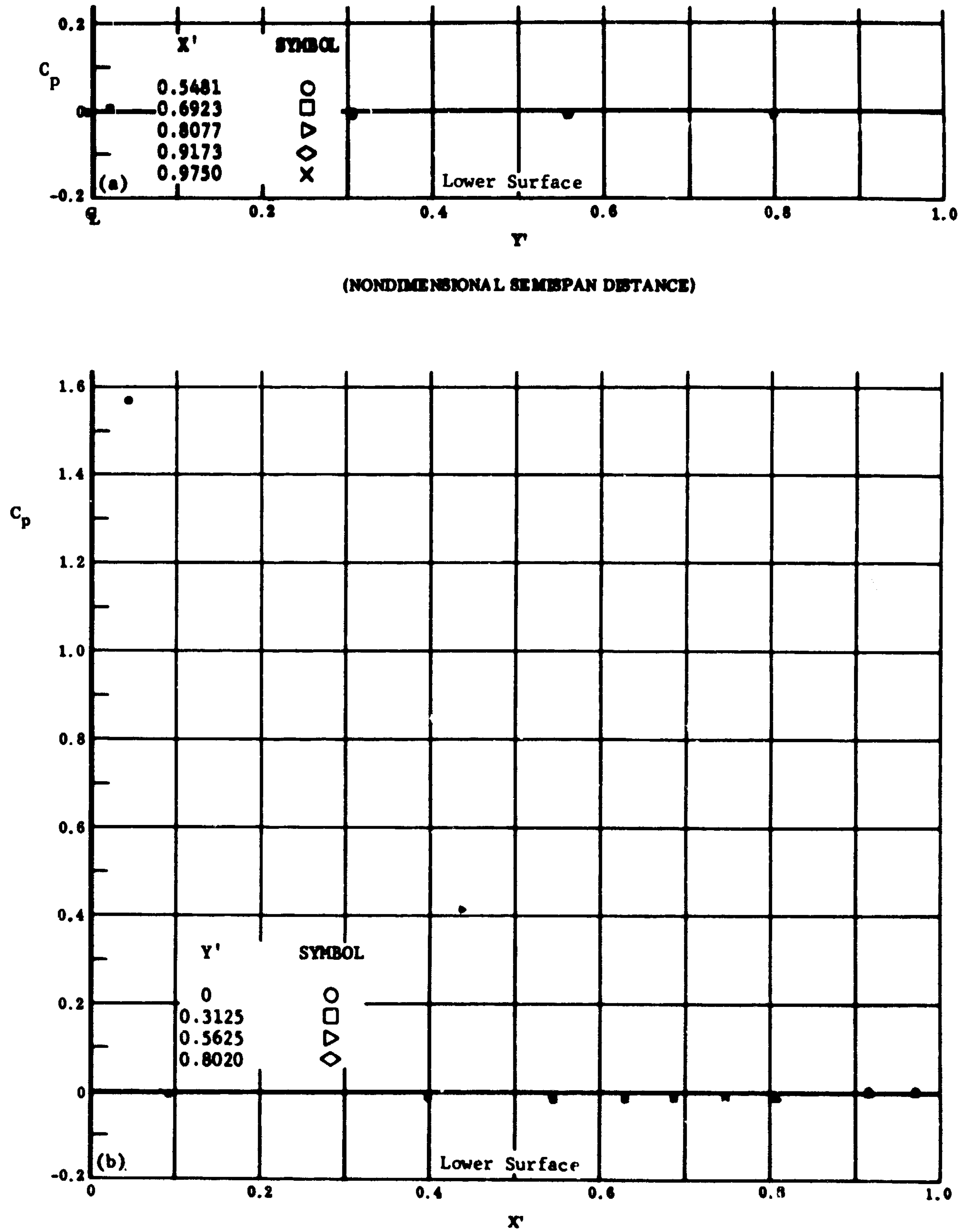

Fig. 42 Configuration IV, $\alpha = -20$, $\delta_2 = \delta_3 = 0$

a) C_p vs. Y', lower surface

b) C_p vs. X', lower surface

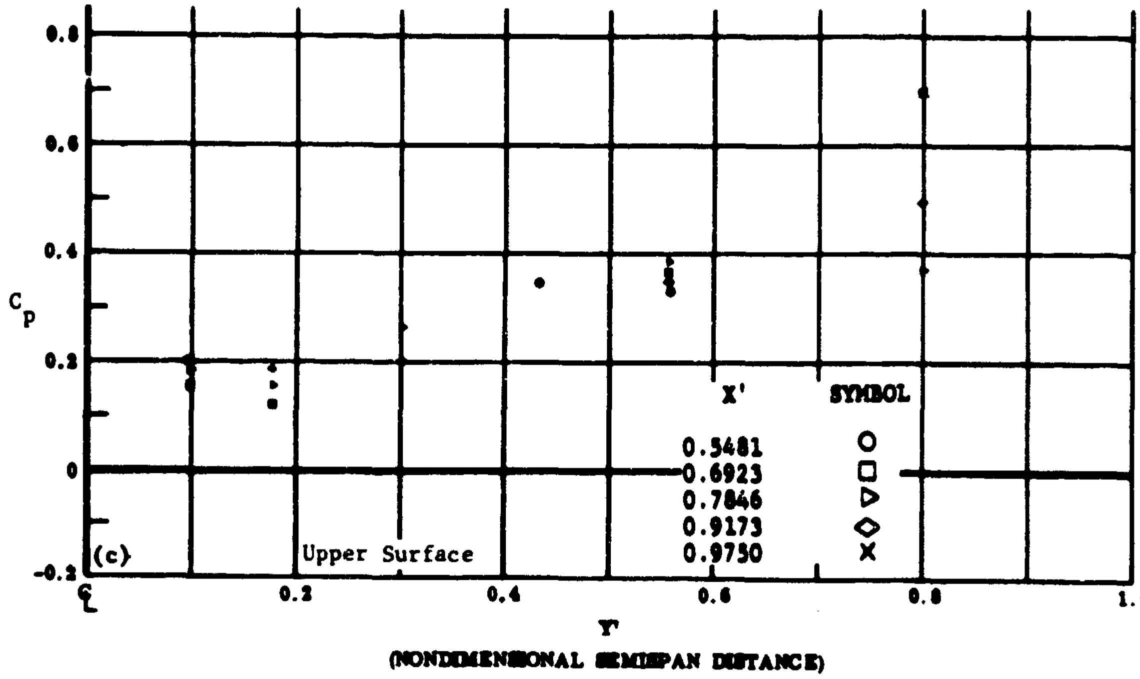

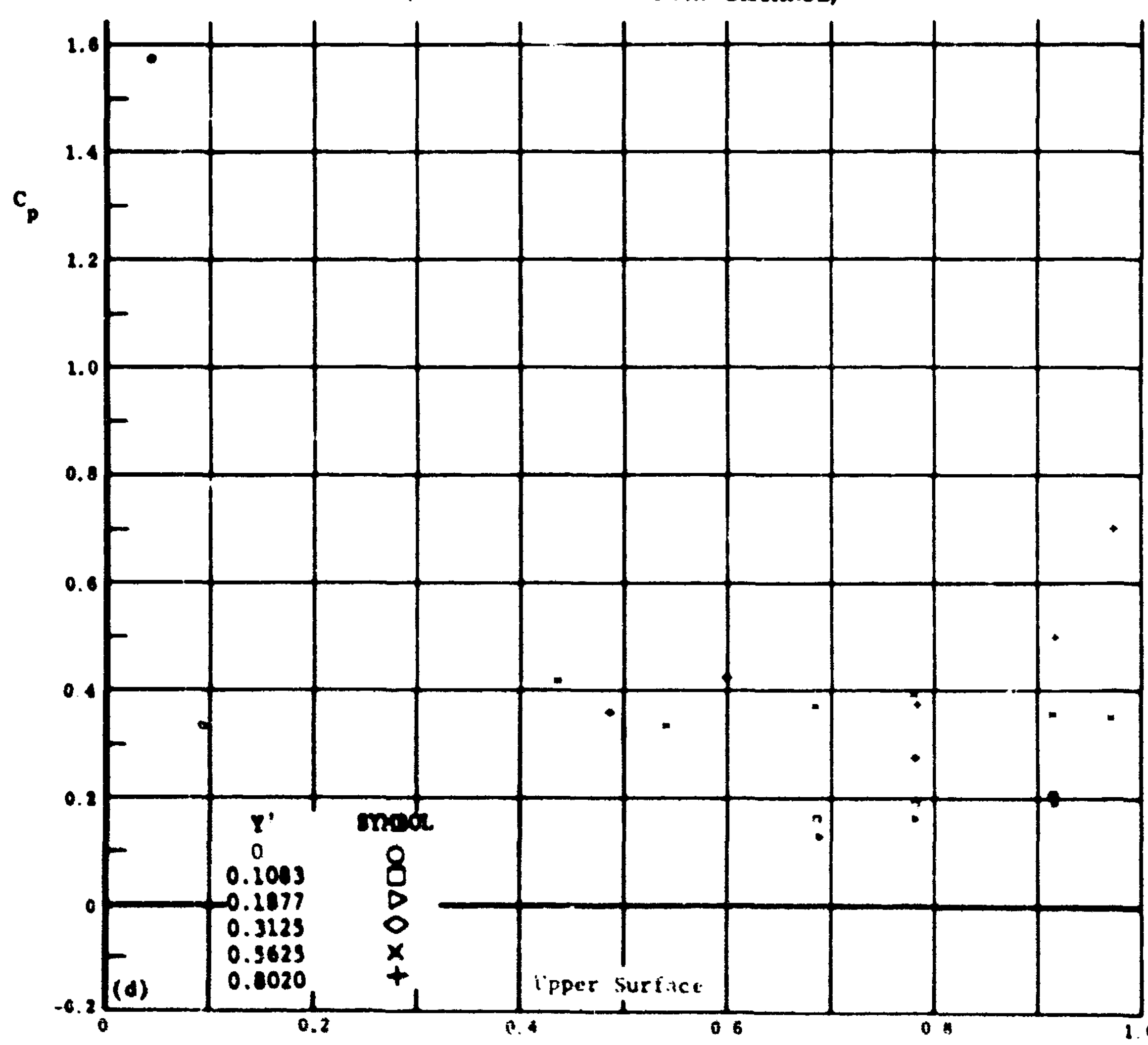

(NONDIMENSIONAL STREAMWISE DISTANCE FROM VIRTUAL APEX)

Fig. 42 Configuration IV, $\alpha = -20$, $\delta_2 = \delta_3 = 0$

c) C_p vs. Y', upper surface

d) C_p vs. X', upper surface

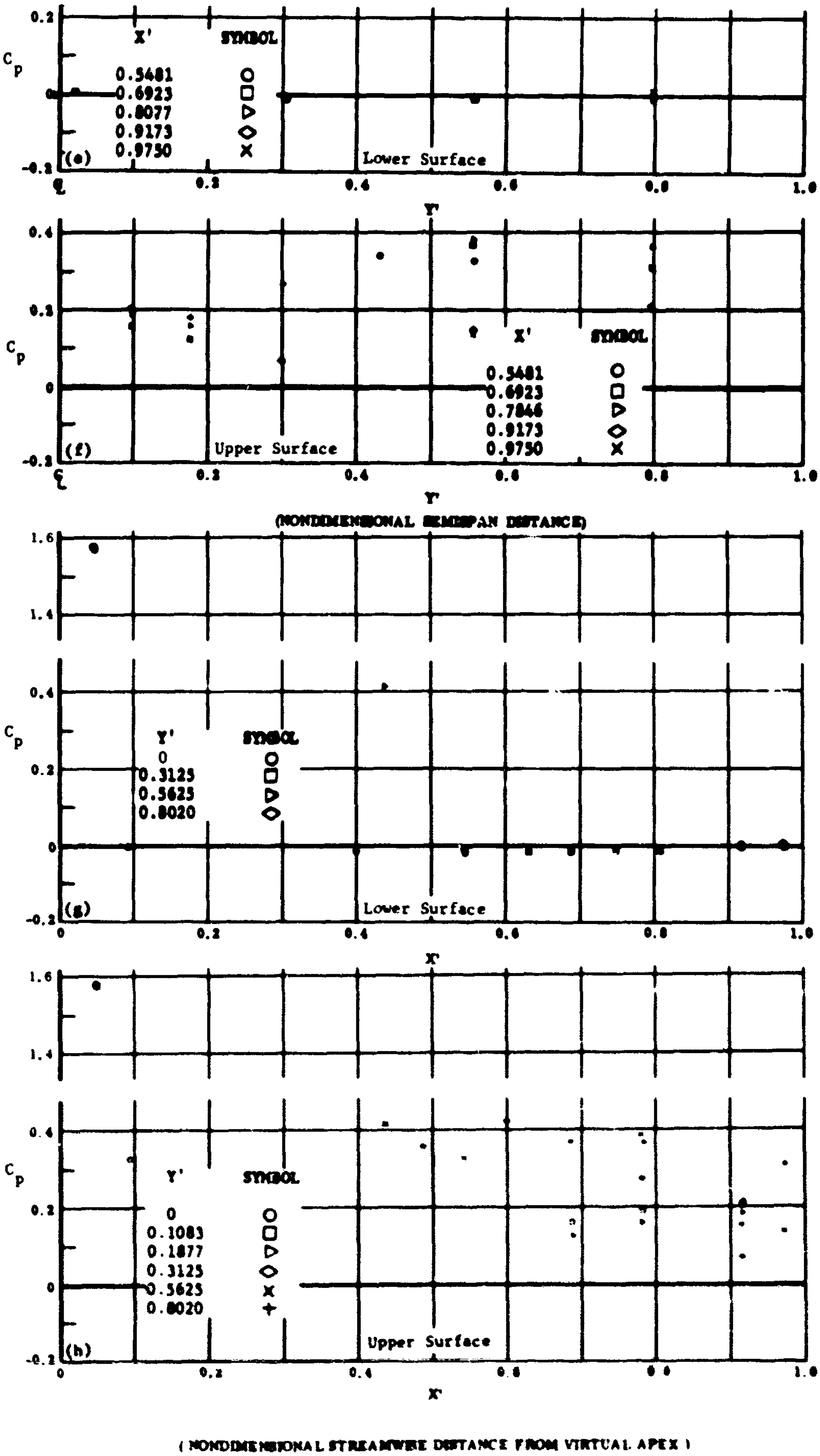

Fig. 42 Configuration IV, $\alpha = -20$, $\delta_2 = \delta_3 = +10$

e) C_p vs. Y', lower surface

f) C_p vs. Y', upper surface

g) C_p vs. X', lower surface

h) C_p vs. X', upper surface

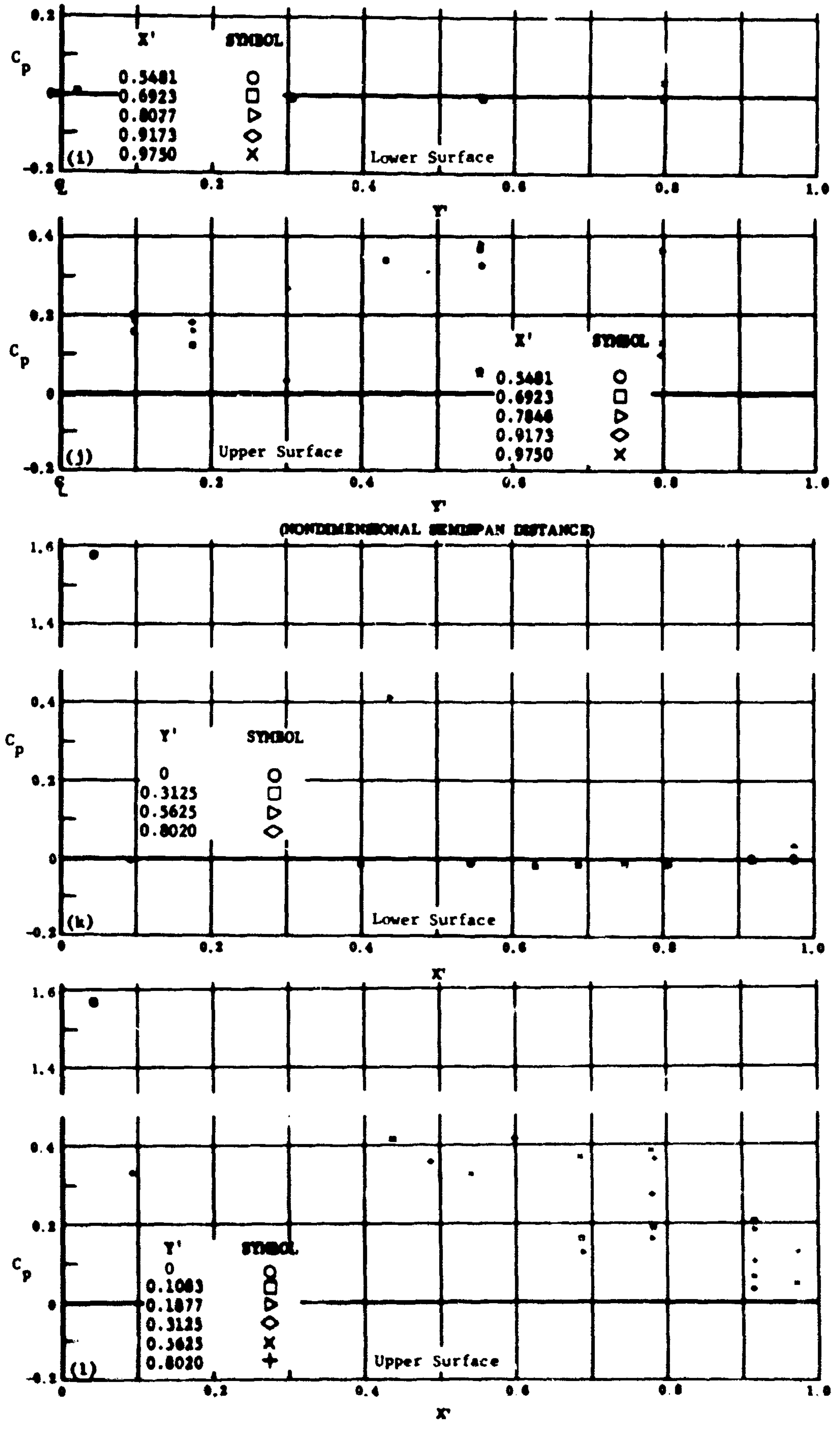

Fig. 42 Configuration IV, $\alpha = -20$, $\delta_2 = \delta_3 = +20$

i) C_p vs. Y', lower surface

j) C_p vs. Y', upper surface

k) C_p vs. X', lower surface

l) C_p vs. X', upper surface

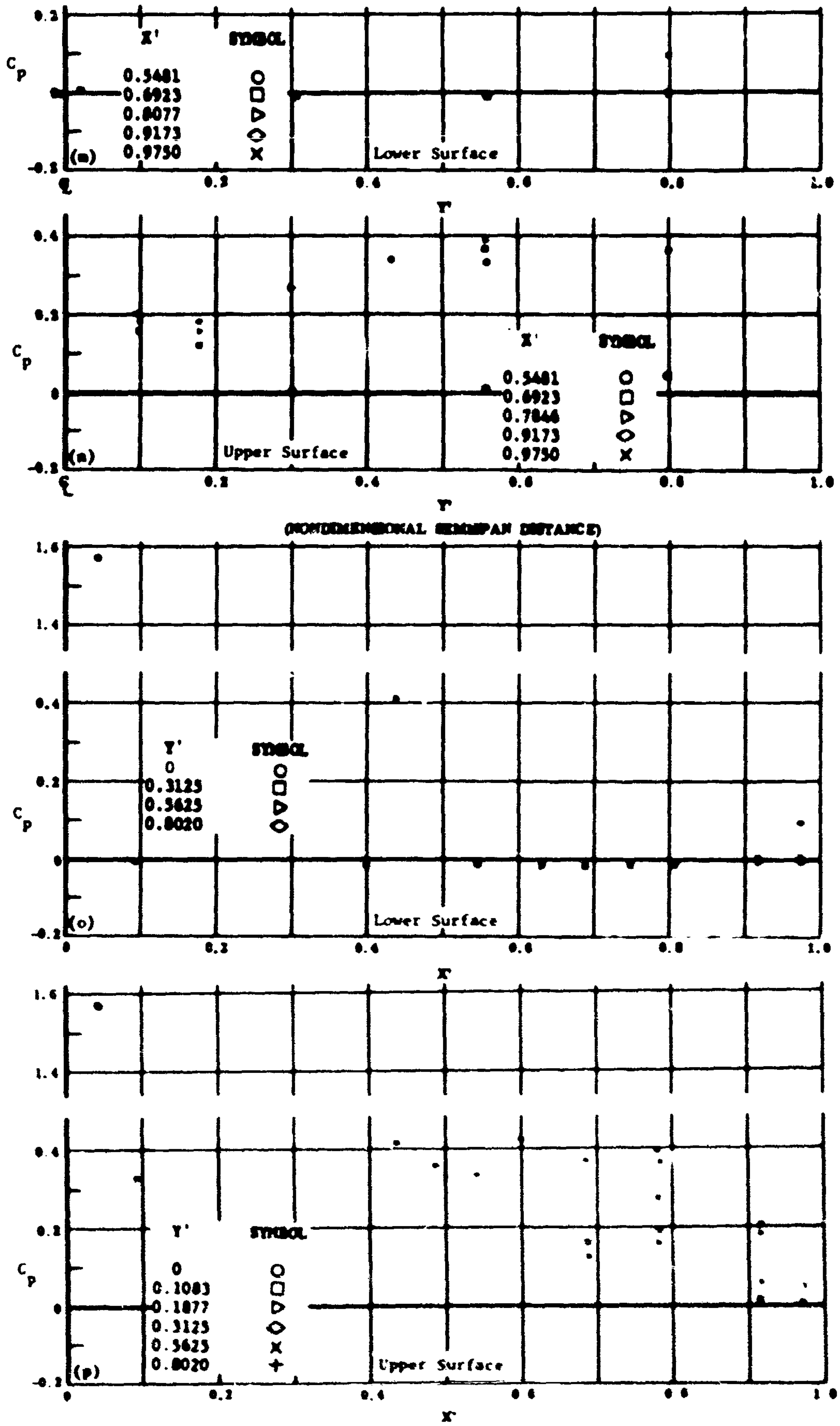

(NONDIMENSIONAL STREAMWISE DISTANCE FROM VIRTUAL APEX)

Fig. 42 Configuration IV, $\alpha = -20$, $\delta_2 = \delta_3 = +30$

m) C_p vs. Y', lower surface

n) C_p vs. Y', upper surface

o) C_p vs. X', lower surface

p) C_p vs. X', upper surface

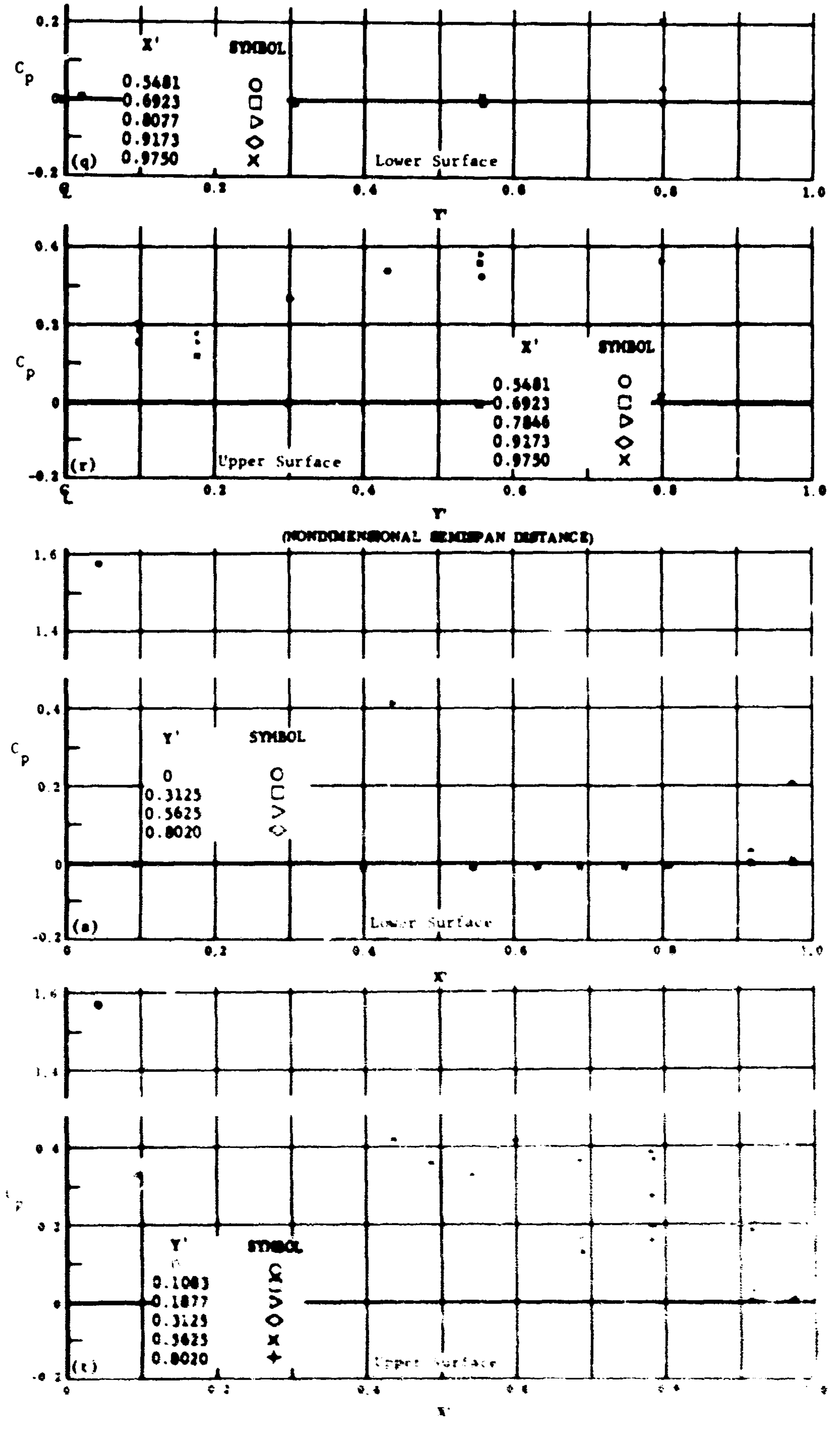

Fig. 42 Configuration IV, [illegible] = -20°, $\delta_2 = \delta_3$ = +39

q) C_p vs. Y', lower surface

r) C_p vs. Y', upper surface

s) C_p vs. X', lower surface

t) C_p vs. X', upper surface

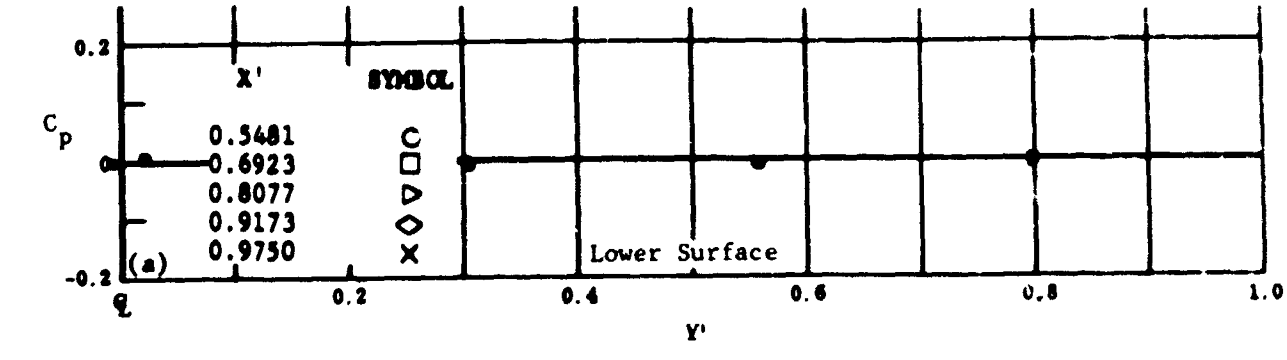

(NONDIMENSIONAL SEMISPAN DISTANCE)

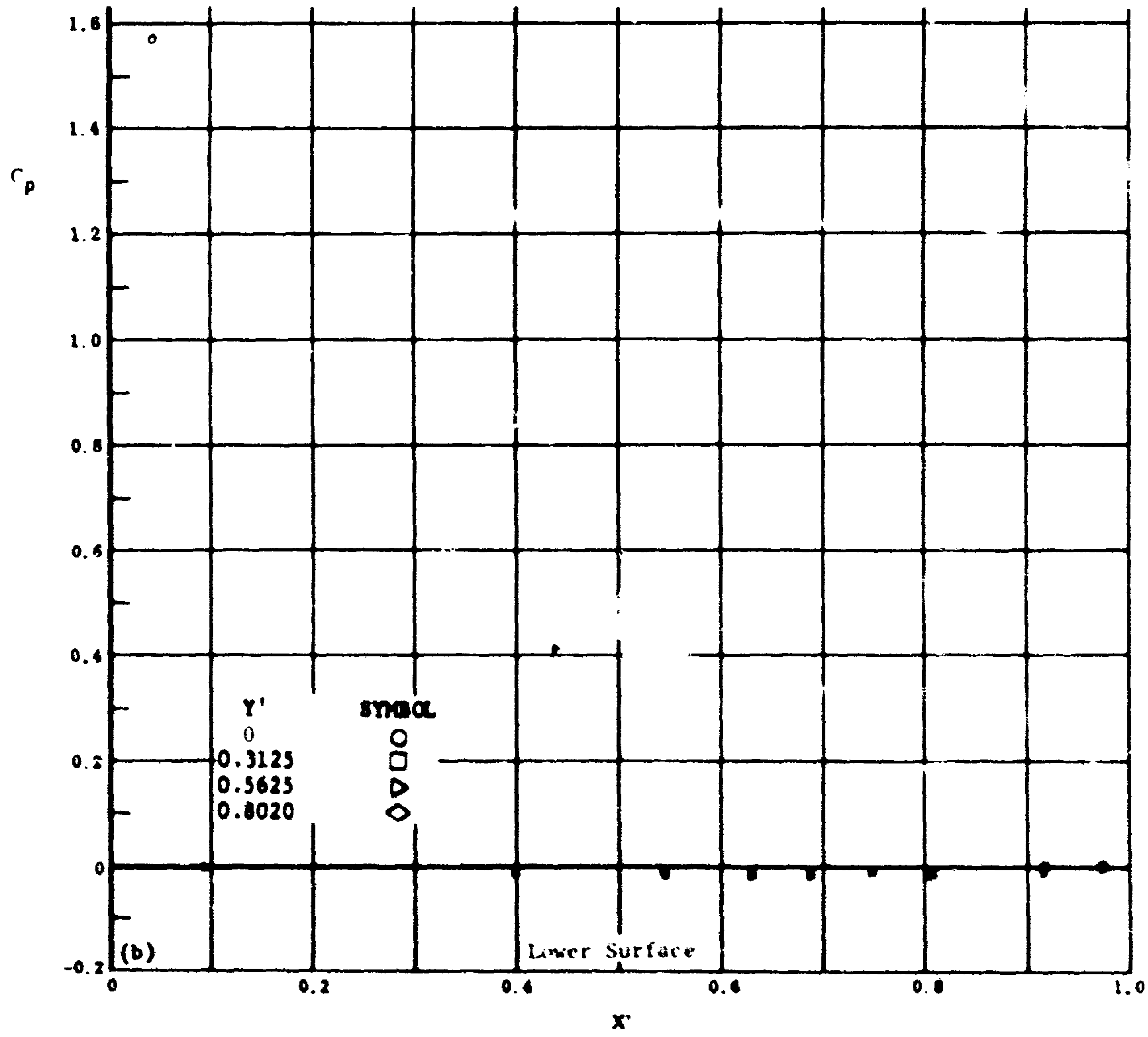

(NONDIMENSIONAL STREAMWISE DISTANCE FROM VIRTUAL APEX)

Fig. 43 Configuration IV, $\delta_1 = -20$, $\delta_2 = \delta_3 = -10$

a) C_p vs. Y', lower surface

b) C_p vs. X', lower surface

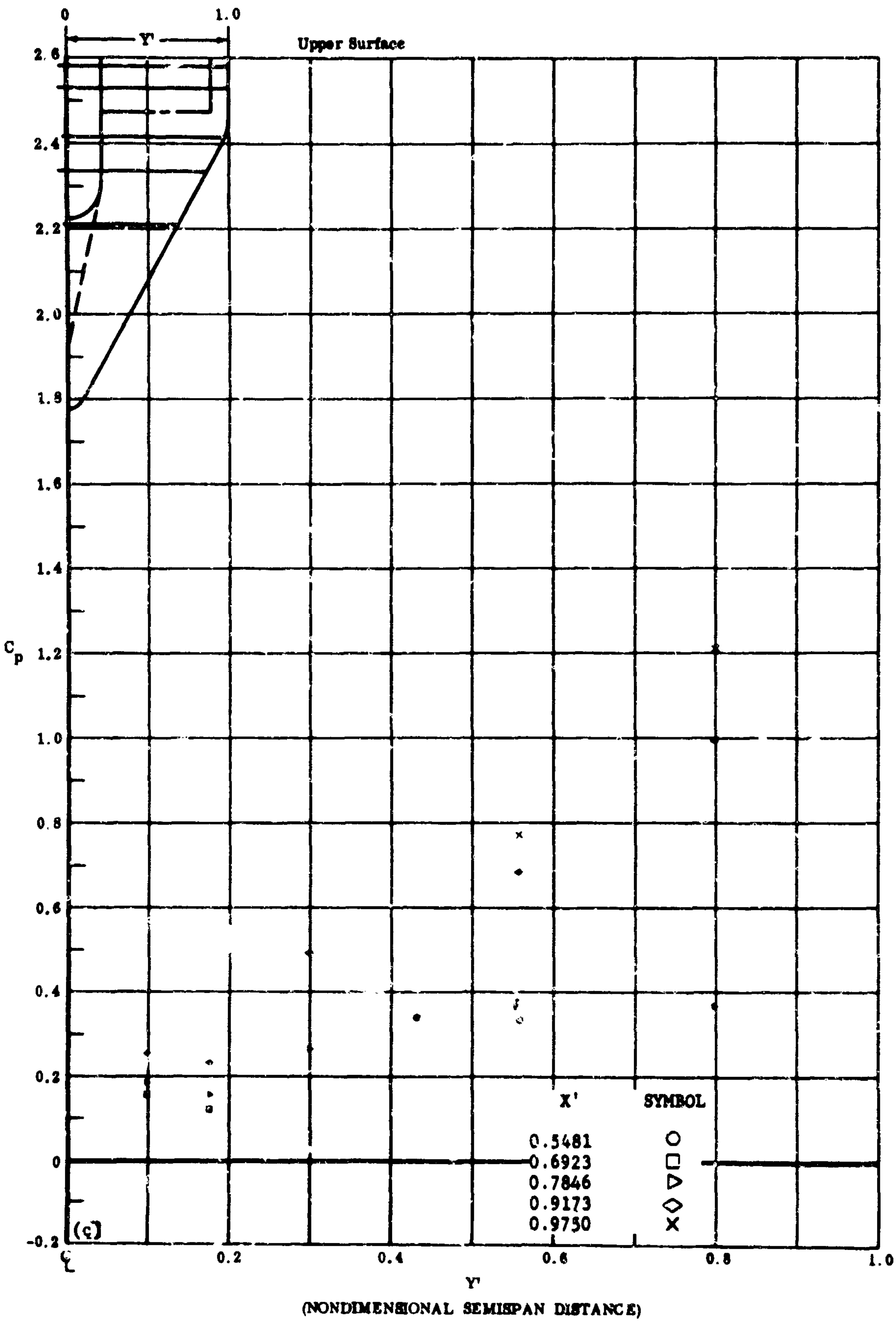

Fig. 43c Configuration IV, $\alpha = -20$, $\delta_2 = \delta_3 = -10$

C_p vs. Y', upper surface

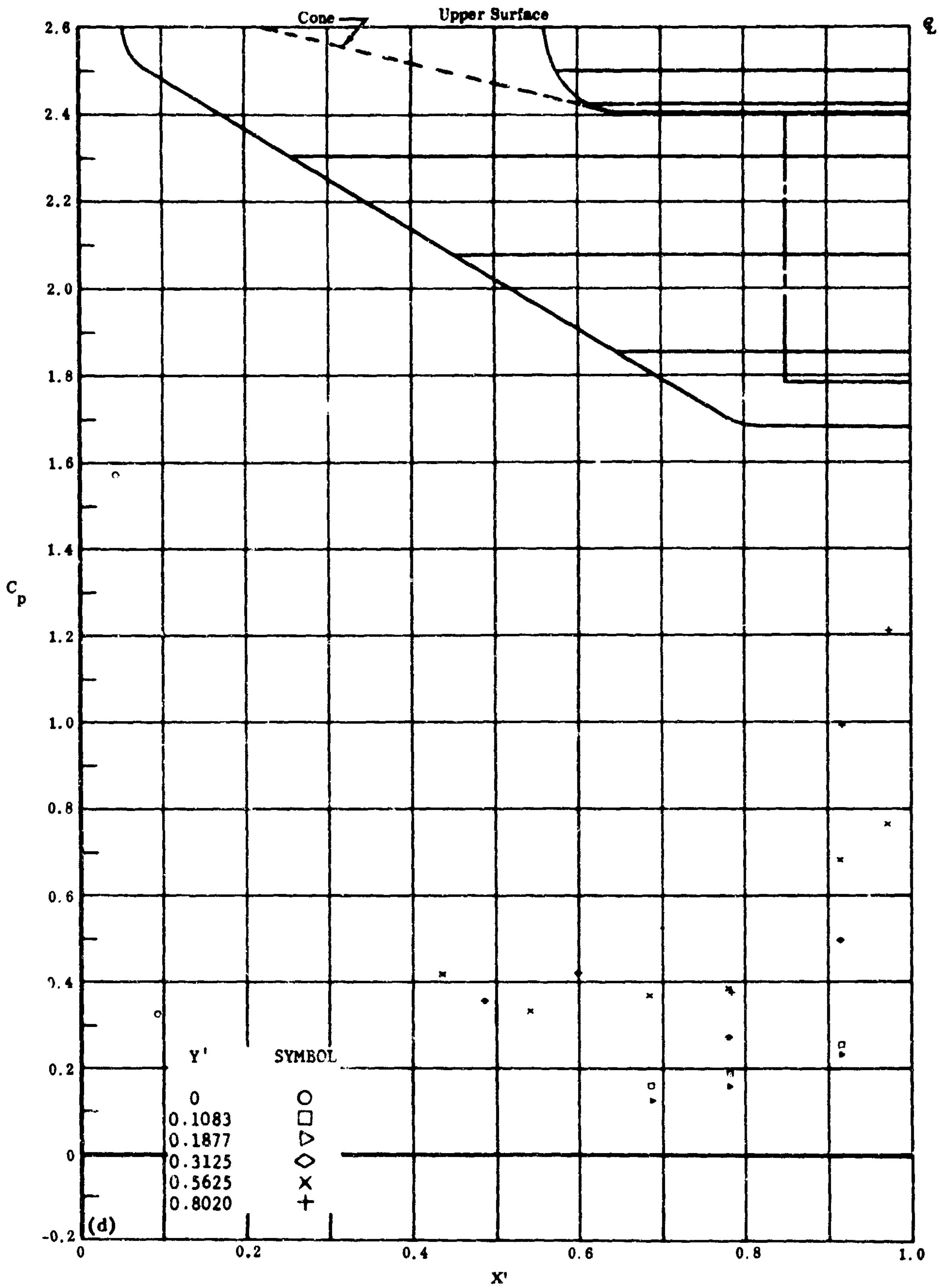

(NONDIMENSIONAL STREAMWISE DISTANCE FROM VIRTUAL APEX)

Fig. 43d Configuration IV, $\alpha = -20$, $\delta_2 = \delta_3 = -10$

C_p vs. X', upper surface

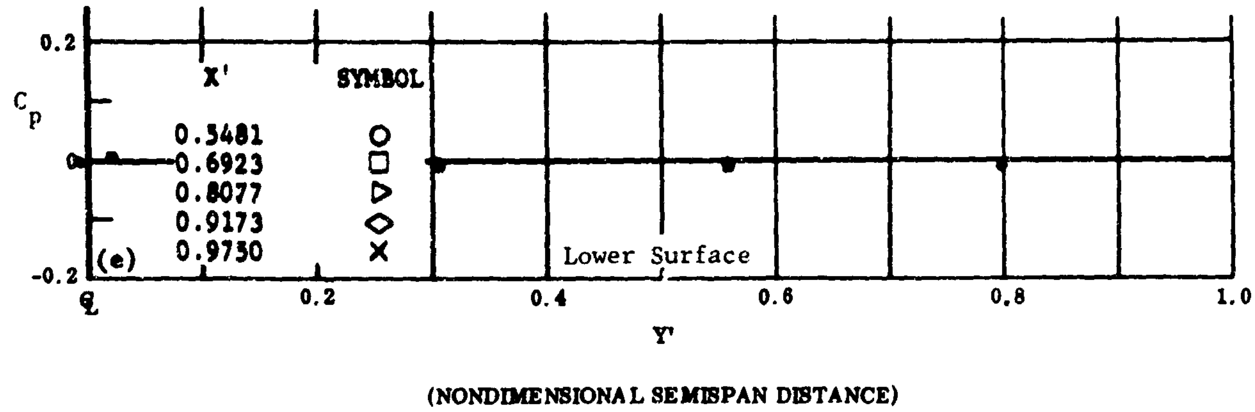

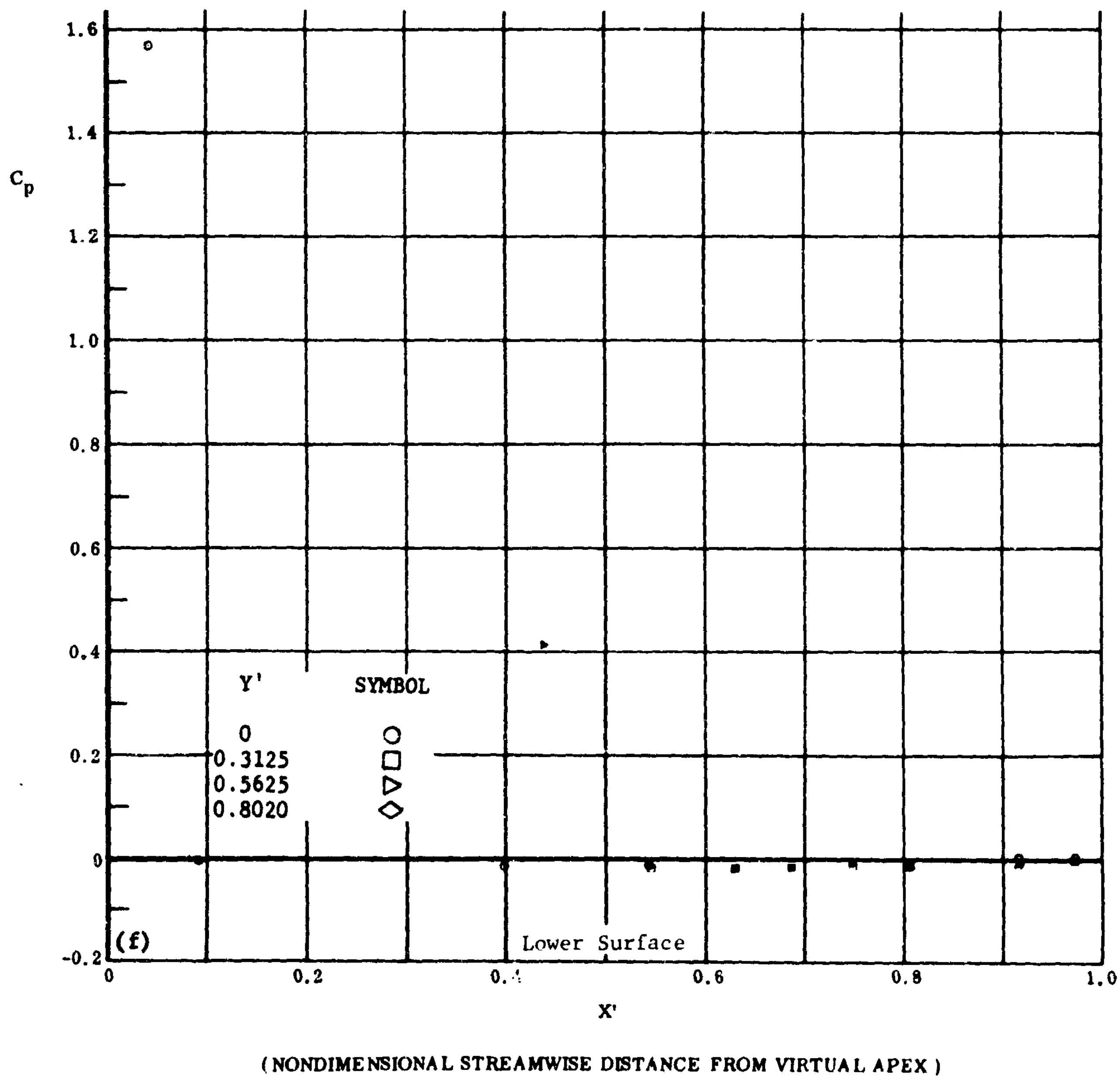

Fig. 43 Configuration IV, $\alpha = -20$, $\delta_2 = \delta_3 = -20$

e) C_p vs. Y', lower surface

f) C_p vs. X', lower surface

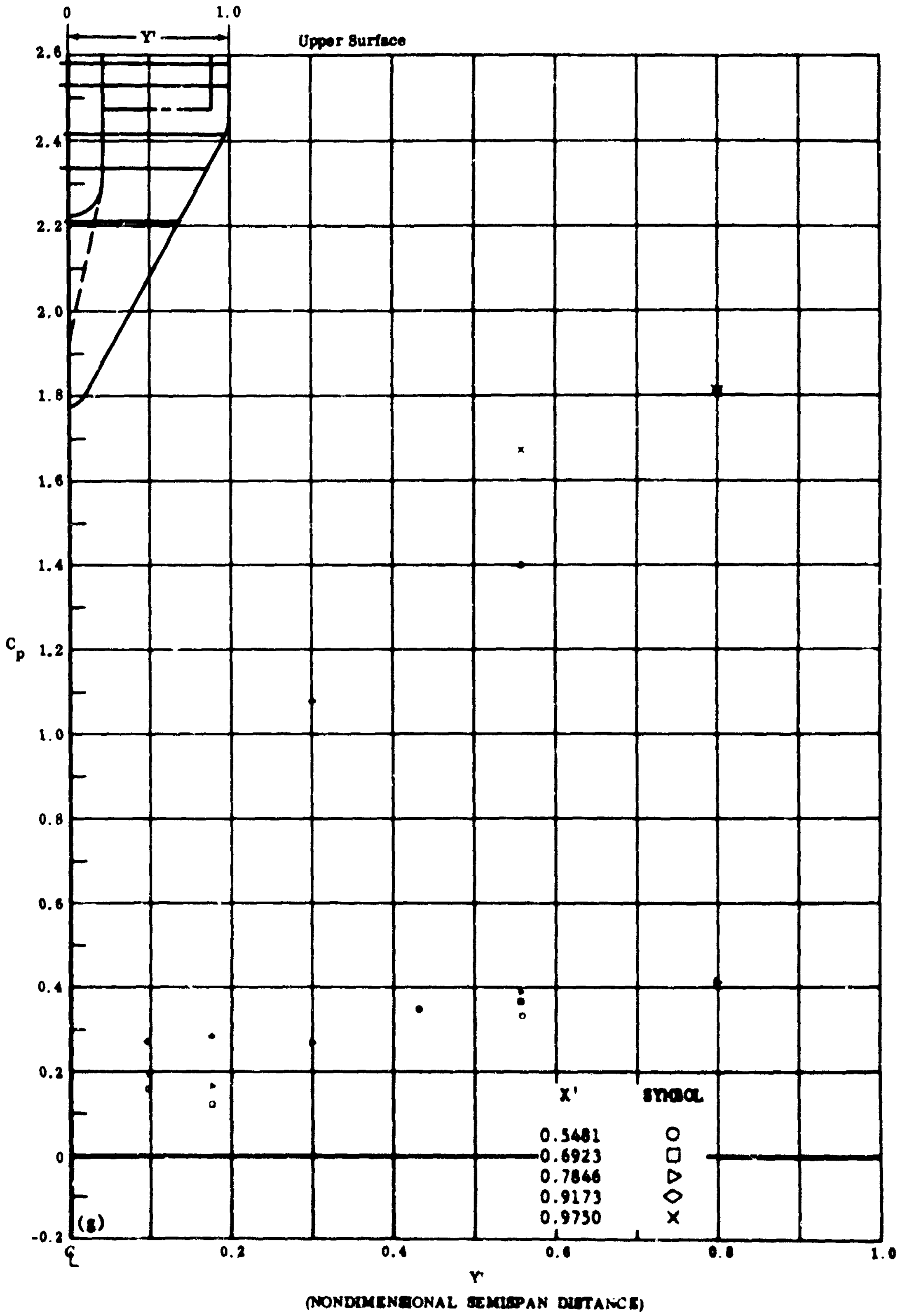

Fig. 43g Configuration IV, α = -20, $\delta_2 = \delta_3$ = -20

C_p vs. Y', upper surface

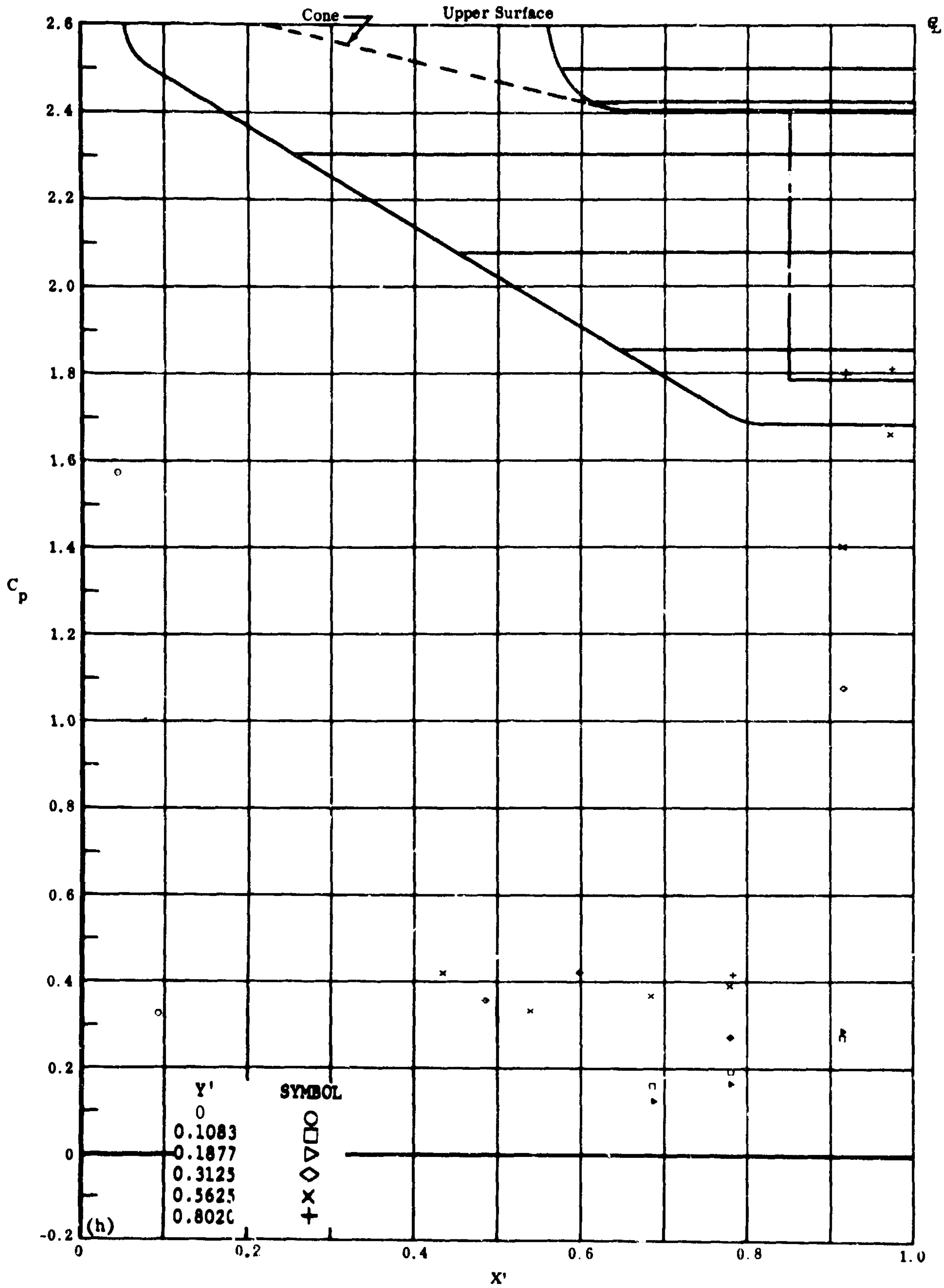

(NONDIMENSIONAL STREAMWISE DISTANCE FROM VIRTUAL APEX)

Fig. 43h Configuration IV, $\alpha = -20$, $\delta_2 = \delta_3 = -20$

C_p vs. X', upper surface

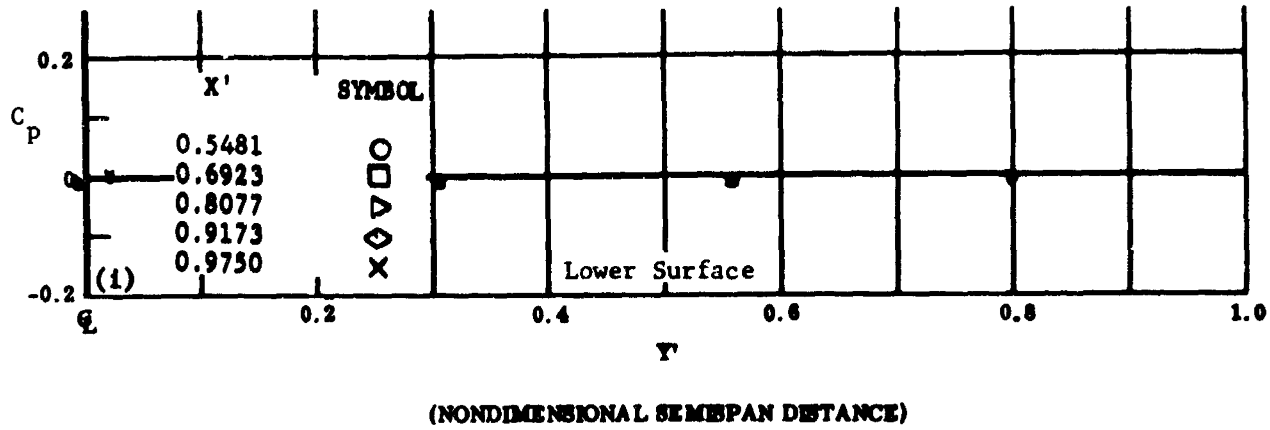

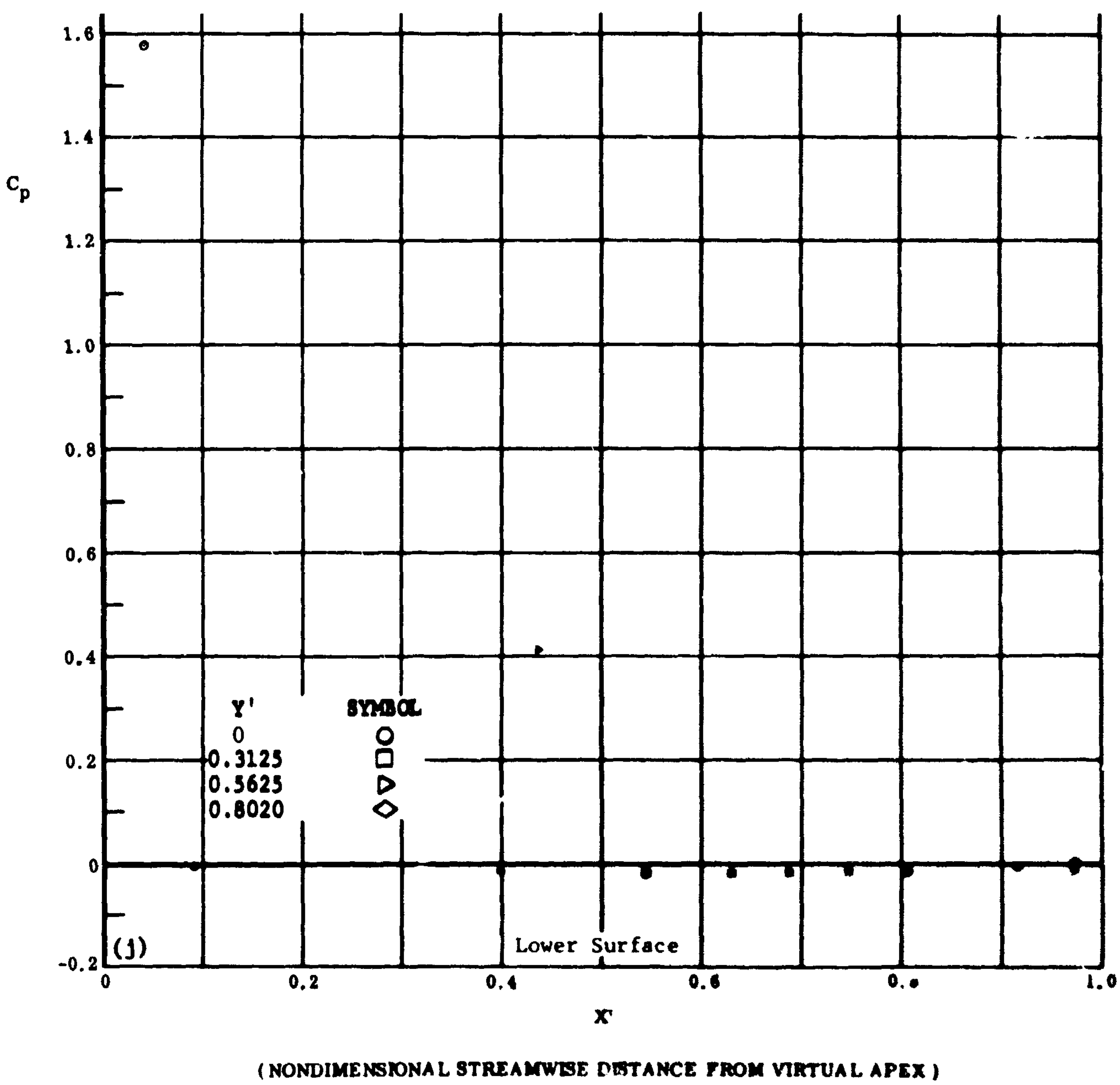

Fig. 43 Configuration IV, $\alpha = -20$, $\delta_2 = \delta_3 = -30$

i) C_p vs. Y', lower surface

j) C_p vs. X', lower surface

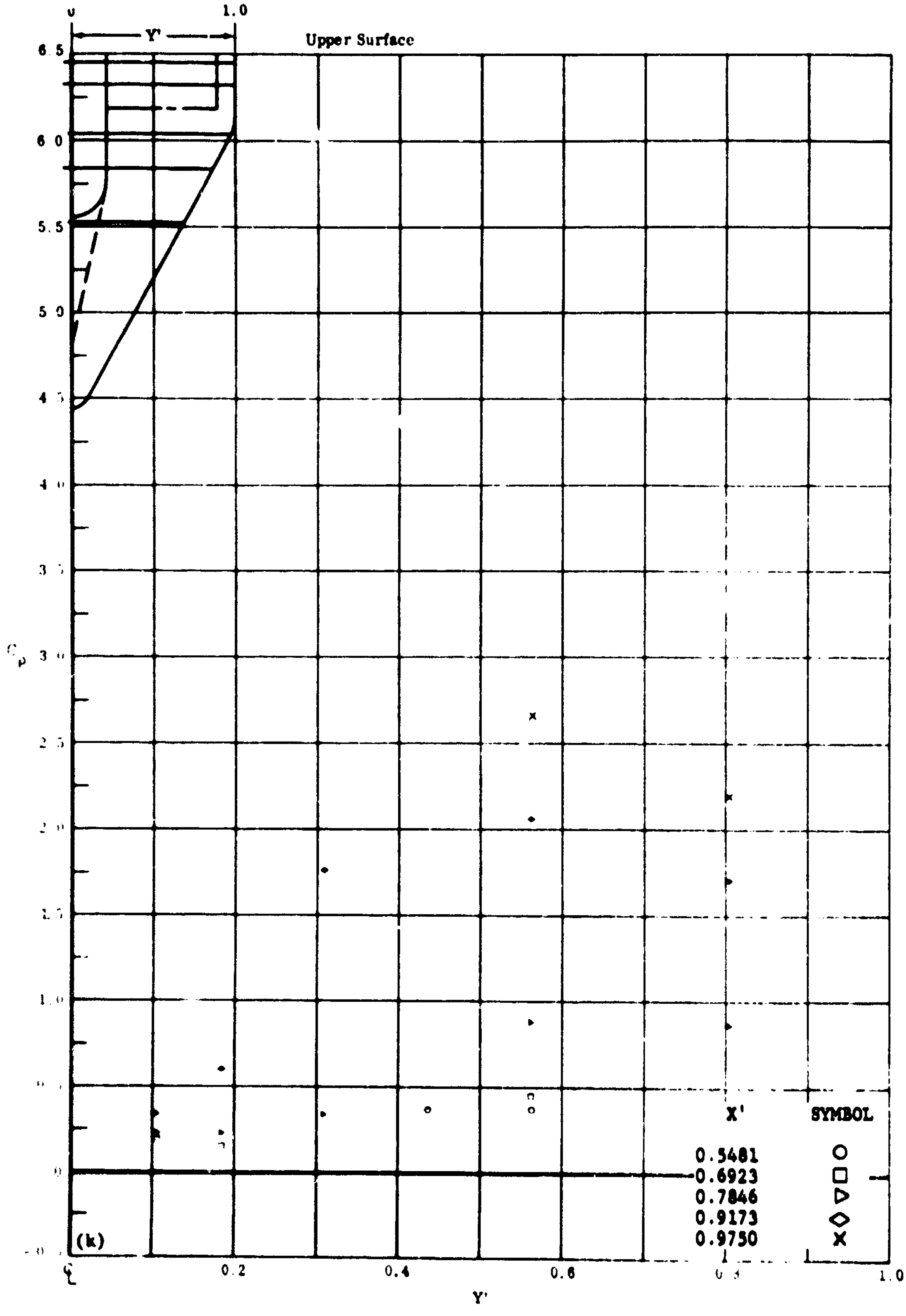

Fig. 43k Configuration IV, $\alpha = -20$, $\delta_2 = \delta_3 = -30$

C_p vs. Y', upper surface

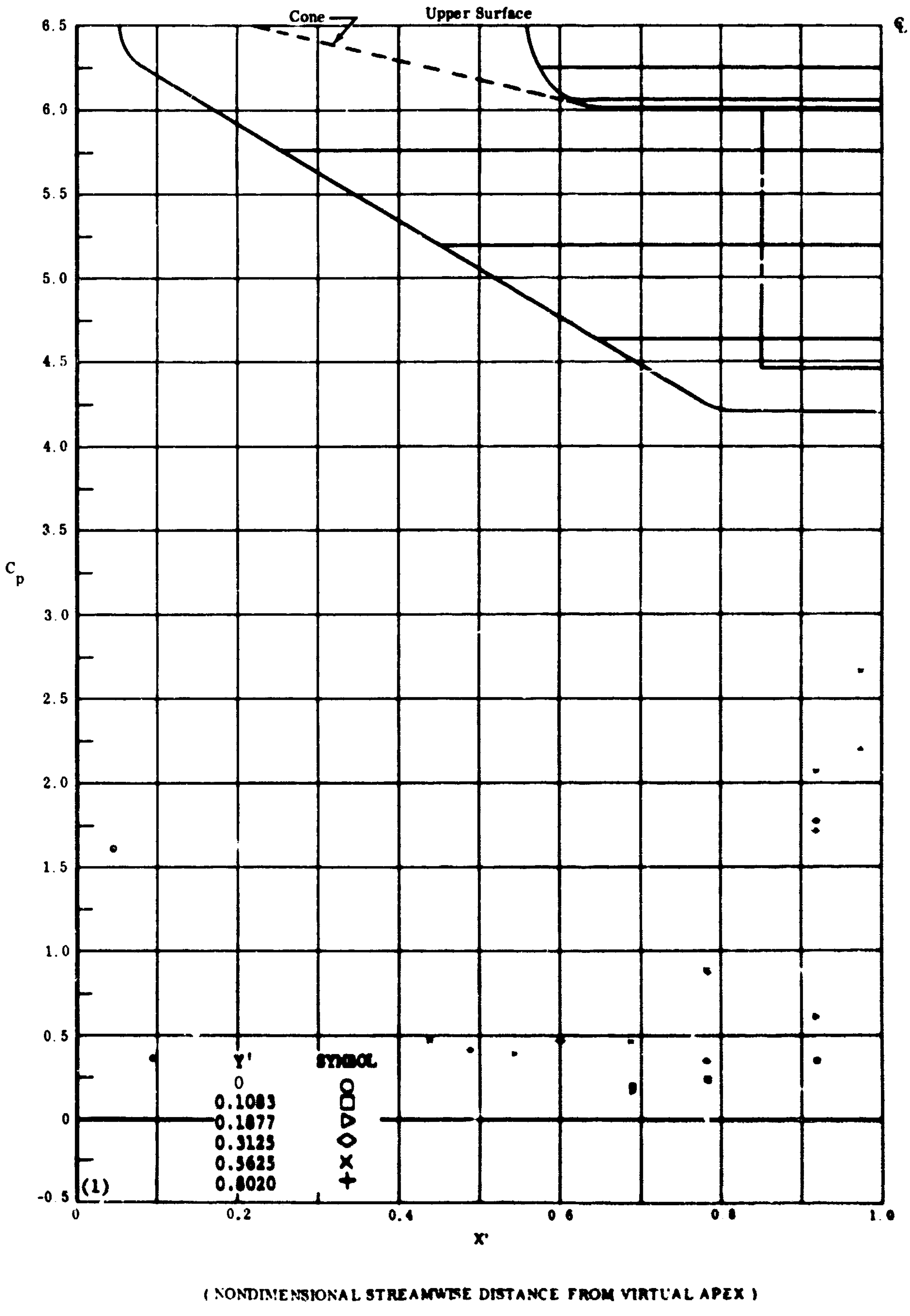

Fig. 431 Configuration IV, $\alpha = -20$, $\delta_2 = \delta_3 = -30$

C_p vs. X', upper surface

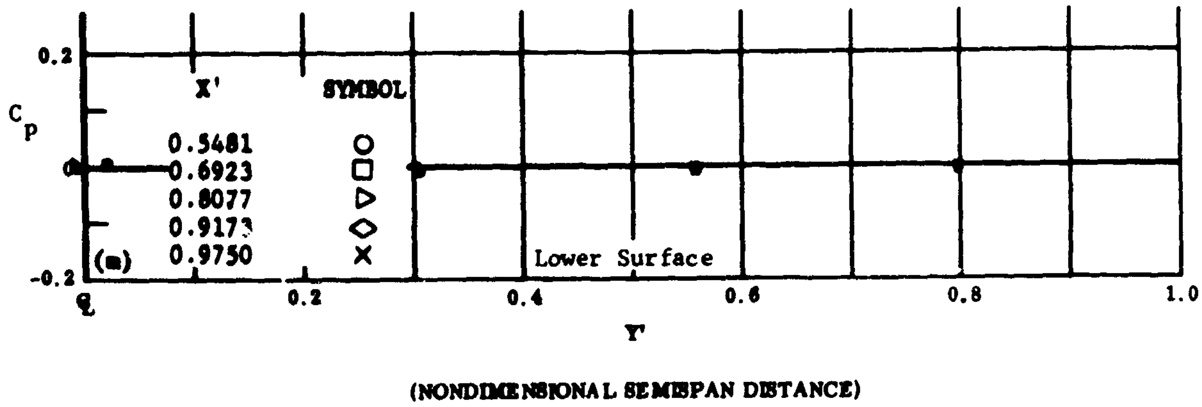

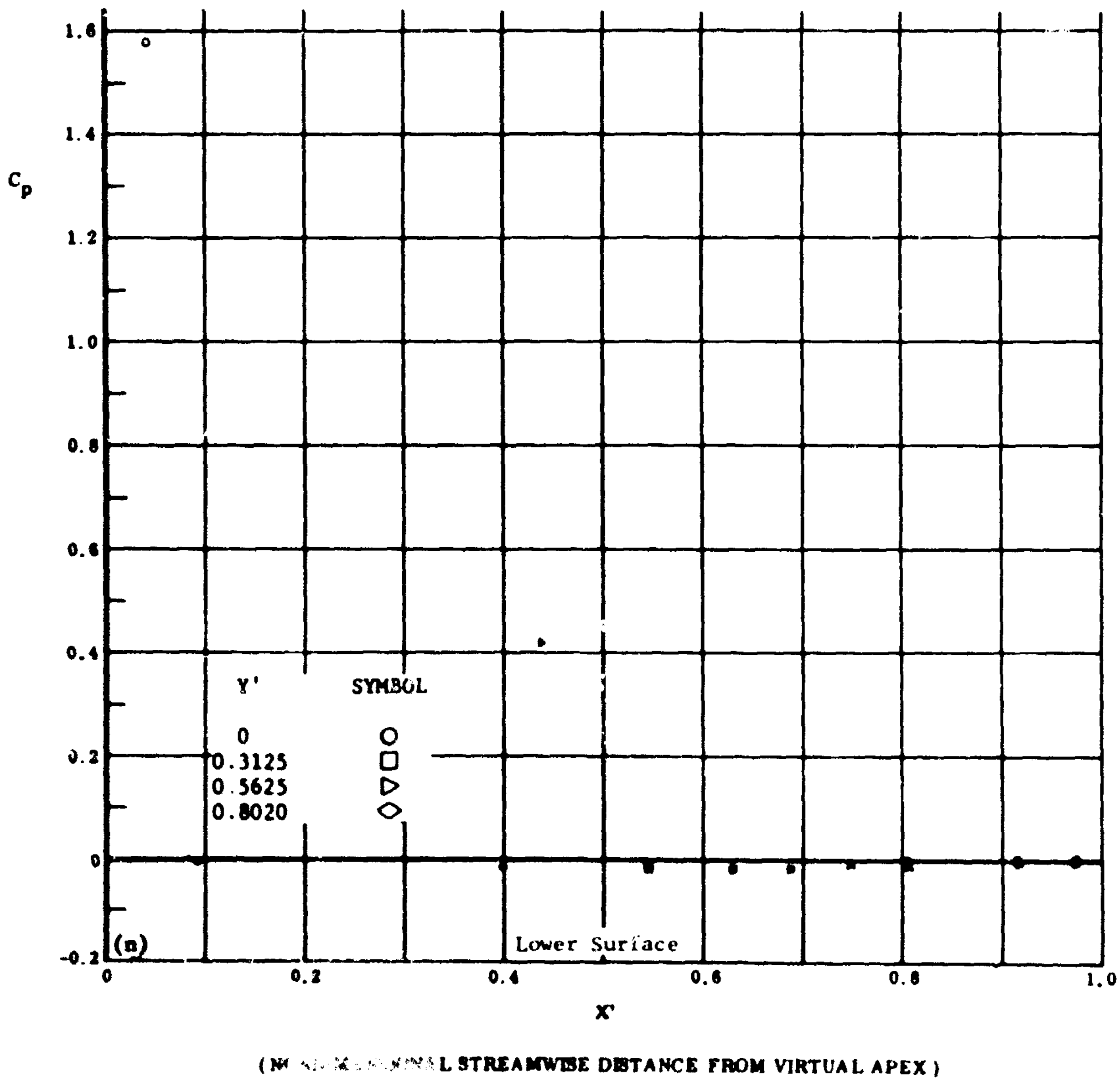

Configuration IV, [illegible] = -20, $\delta_2 = \delta_3 =$ -39

[illegible] C_p vs. Y', lower surface

[illegible] C_p vs. X', lower surface

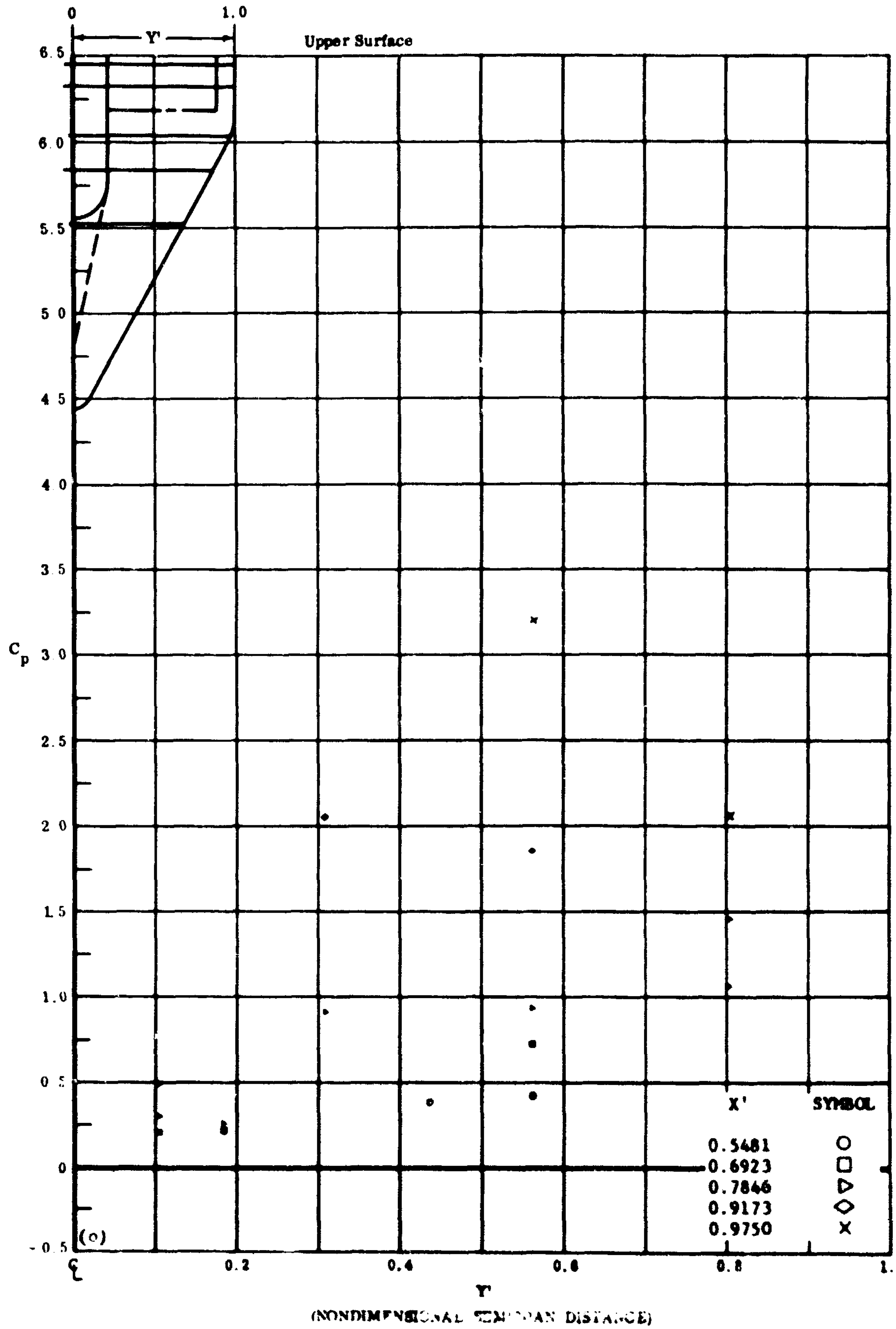

Fig. 43o Configuration IV, α = -20, δ_2 = δ_3 = -39

C_p vs. Y', upper surface

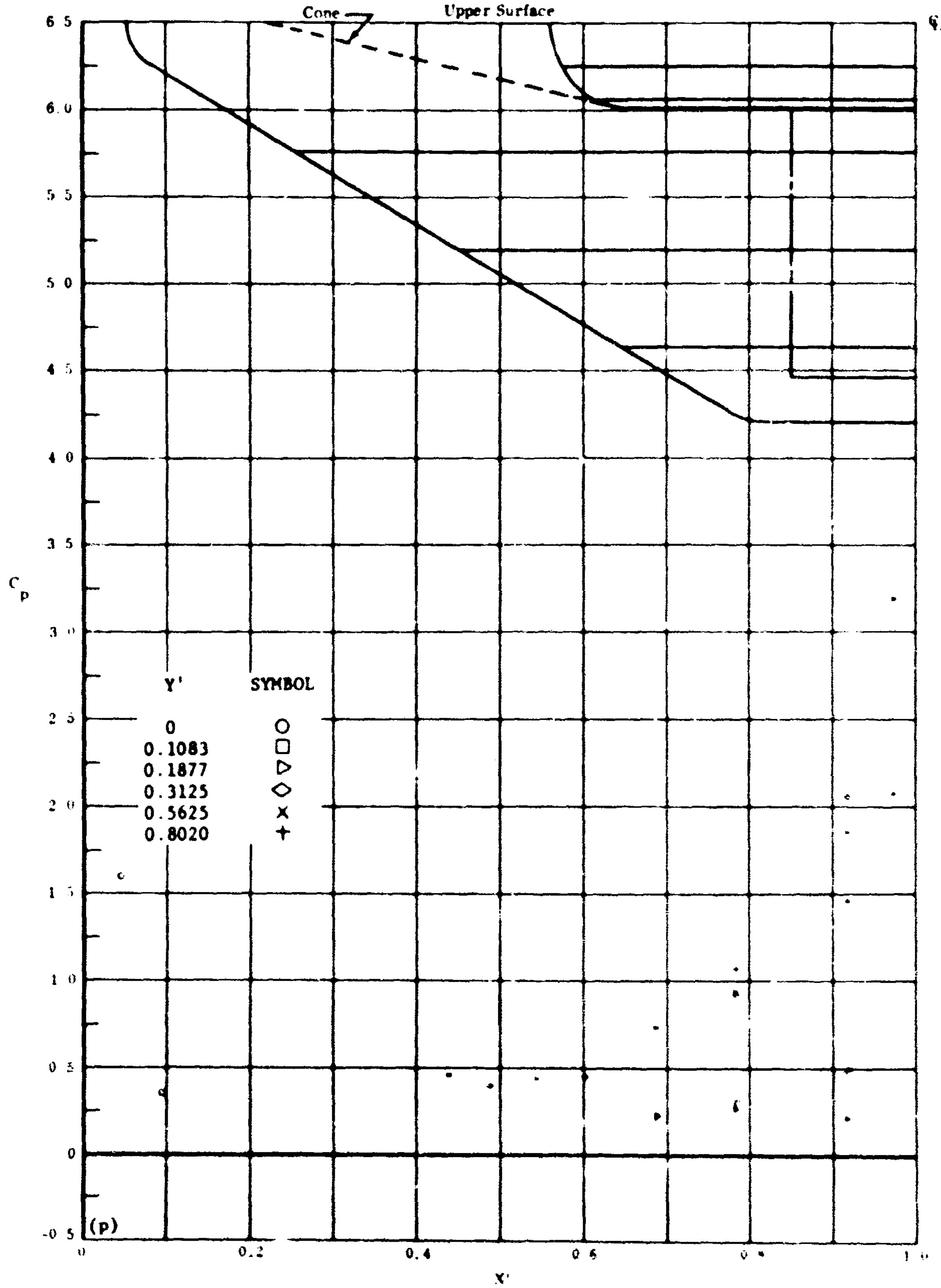

(NONDIMENSIONAL STREAMWISE DISTANCE FROM VIRTUAL APEX)

Fig. 43p Configuration IV, $\delta_1 = -20$, $\delta_2 = \delta_3 = -39$

C_p vs. X', upper surface

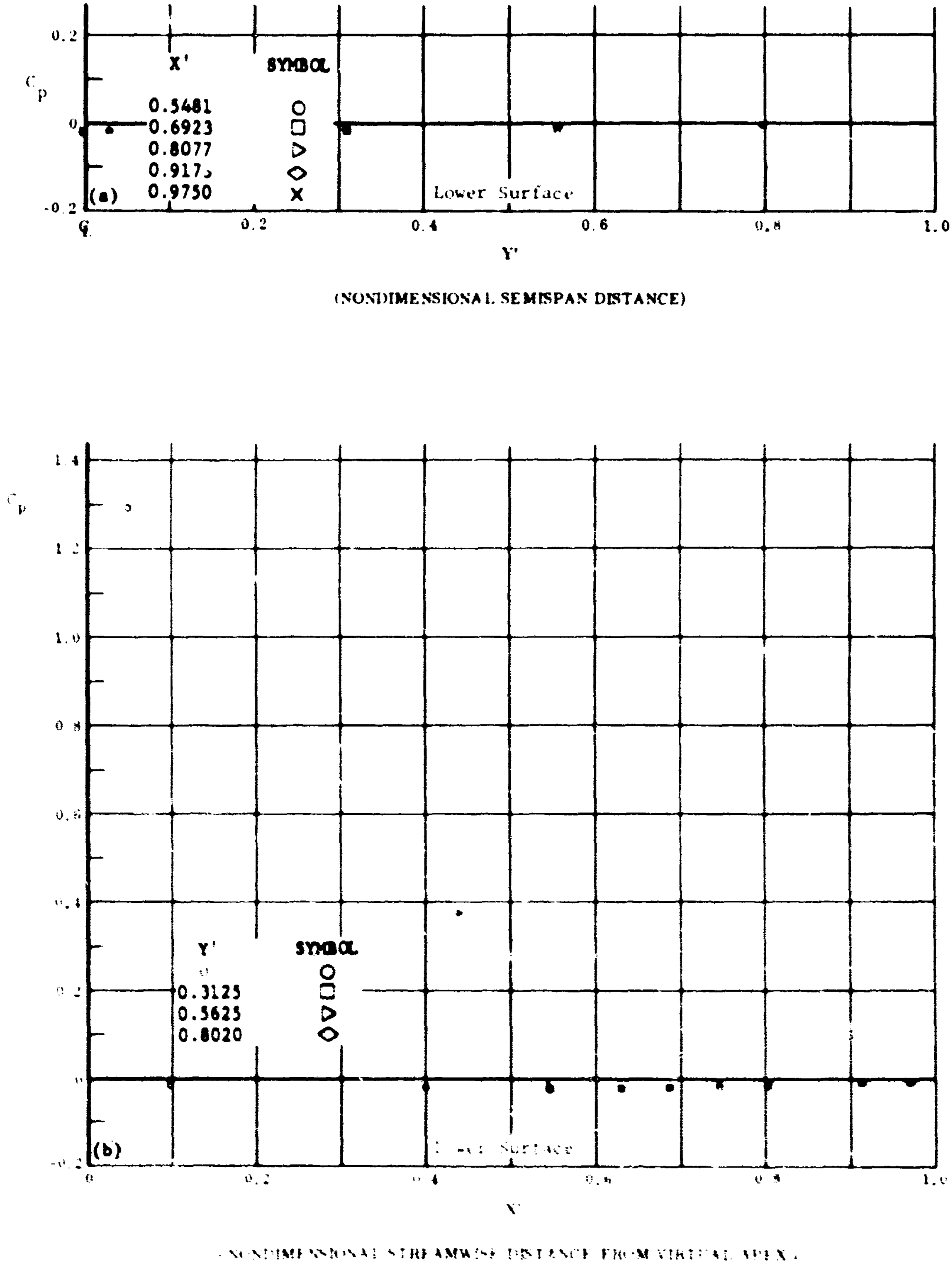

Fig. 44   Configuration IV, = -30 , $_2$ = $_3$ = 0

a) C_p vs. Y', lower surface

b) C_p vs. X', lower surface

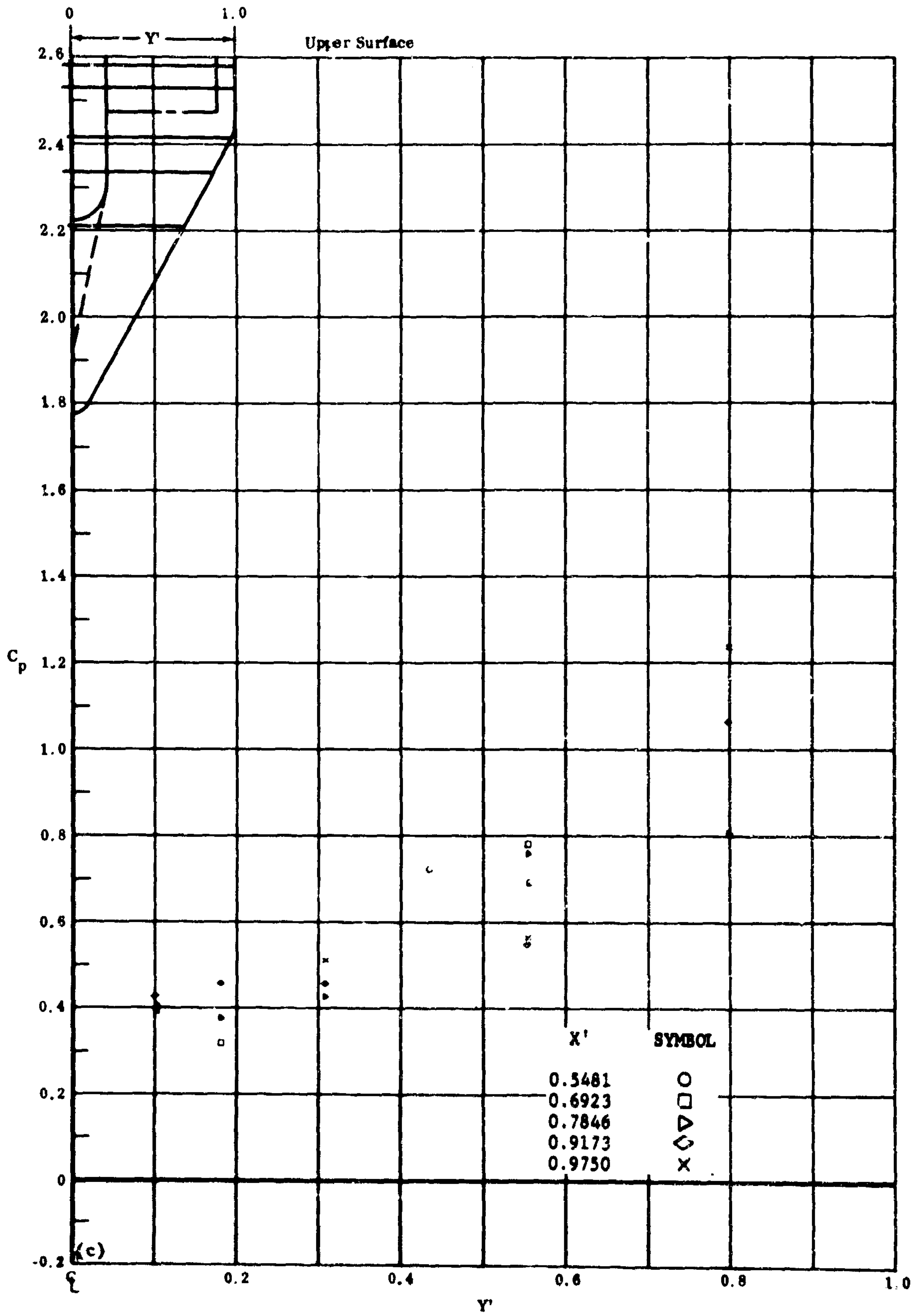

Fig. 44c Configuration IV, $\alpha = -30$, $\delta_2 = \delta_3 = 0$

C_p vs. Y', upper surface

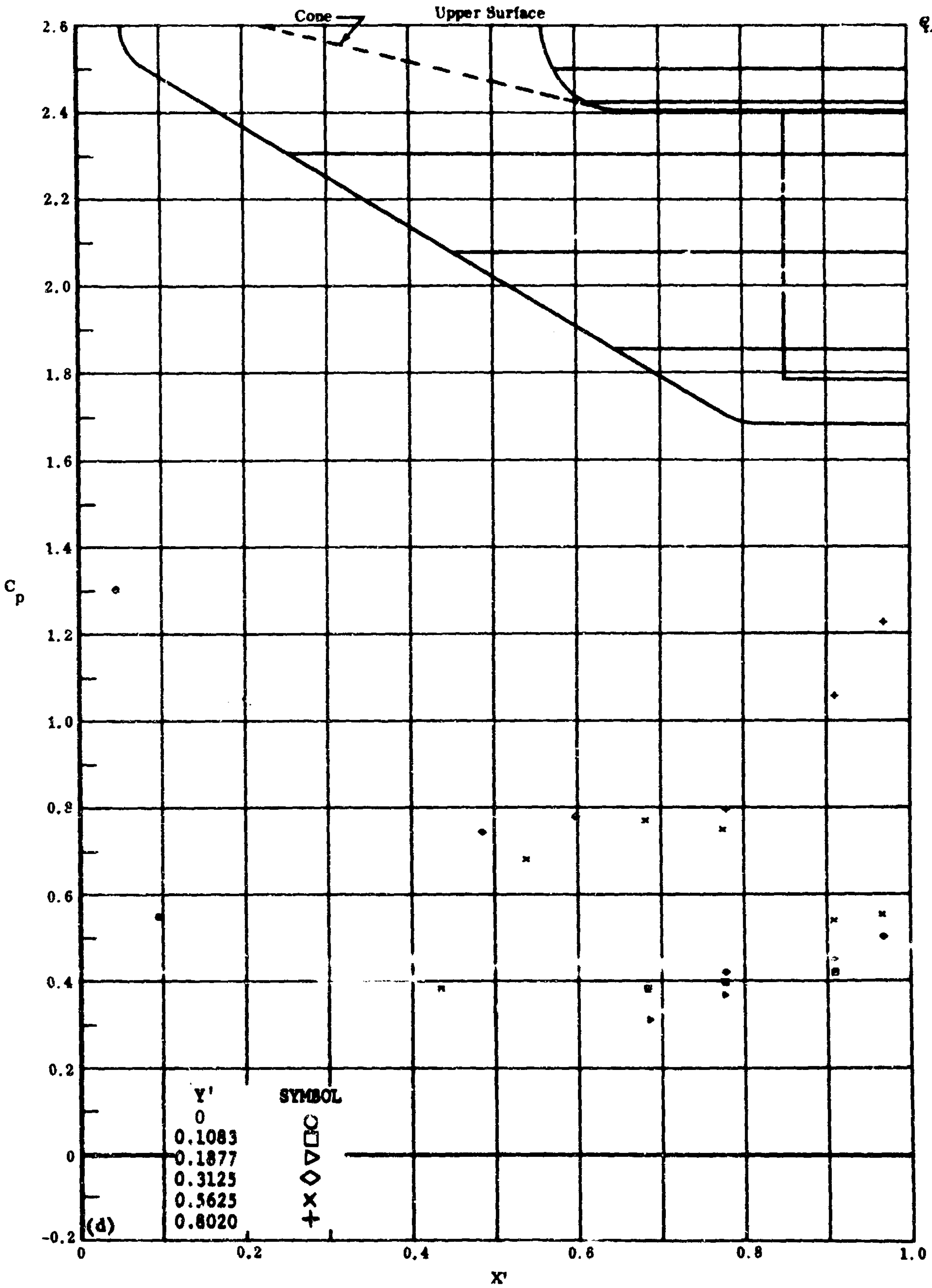

(NONDIMENSIONAL STREAMWISE DISTANCE FROM VIRTUAL APEX)

Fig. 44d Configuration IV, $\alpha = -30$, $\delta_2 = \delta_3 = 0$

C_p vs. X', upper surface

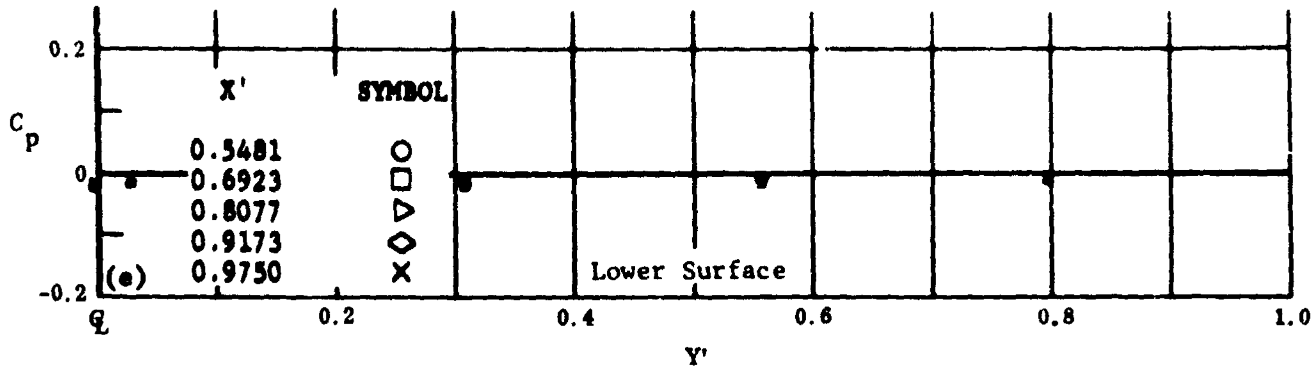

(NONDIMENSIONAL SEMISPAN DISTANCE)

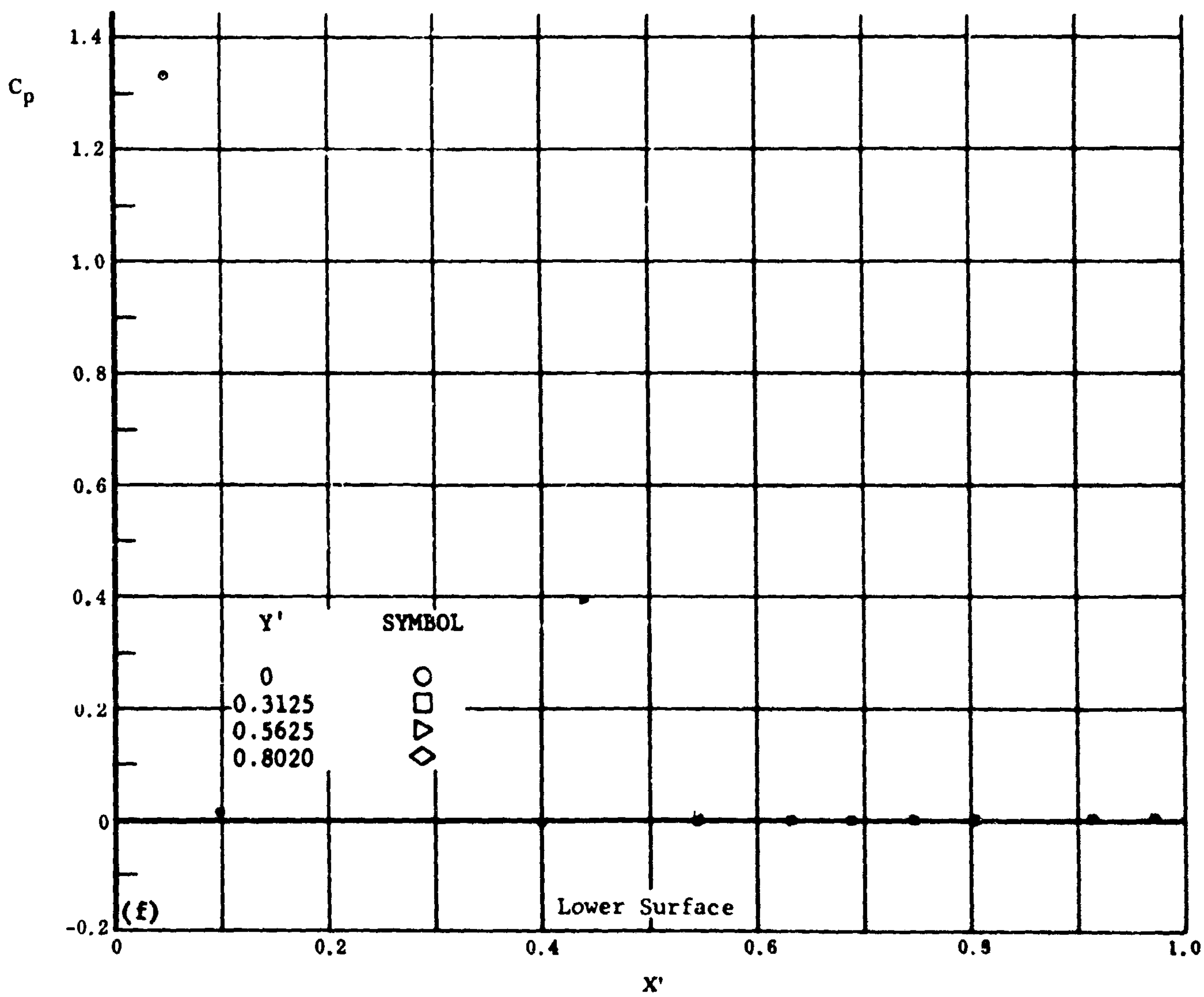

(NONDIMENSIONAL STREAMWISE DISTANCE FROM VIRTUAL APEX)

Fig. 44 Configuration IV, $\alpha = -30$, $\delta_2 = \delta_3 = +20$

e) C_p vs. Y', lower surface

f) C_p vs. X', lower surface

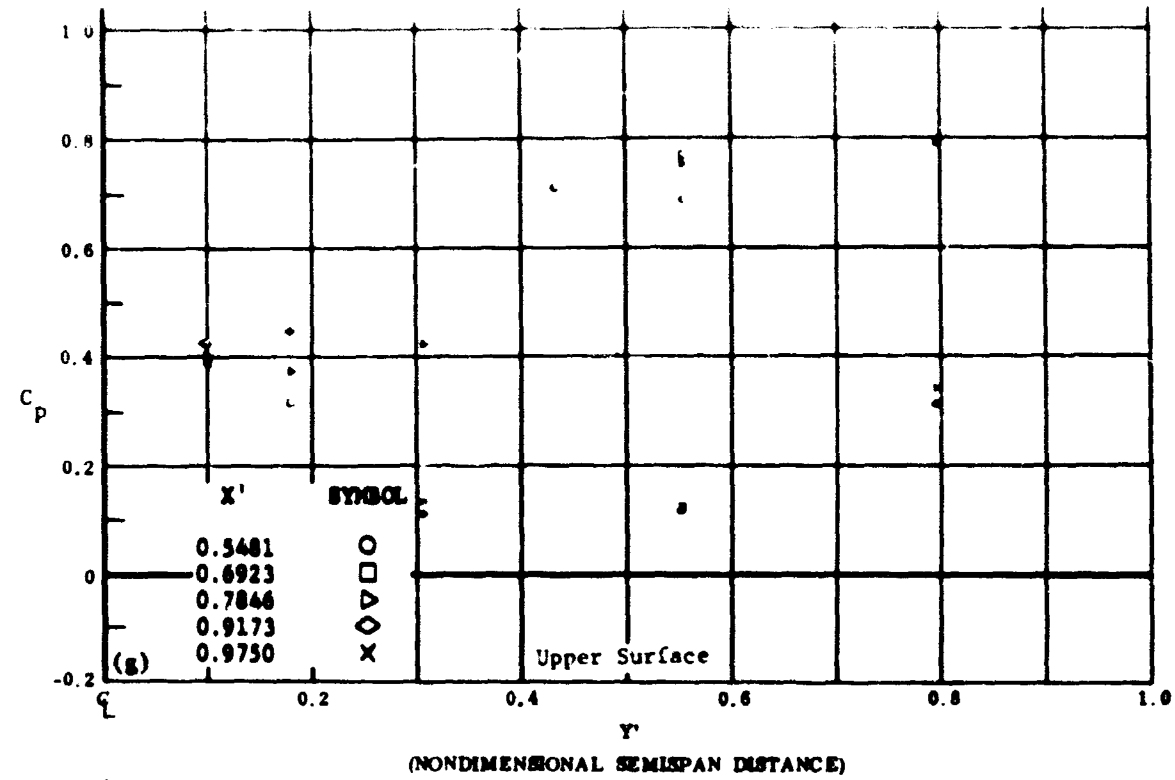

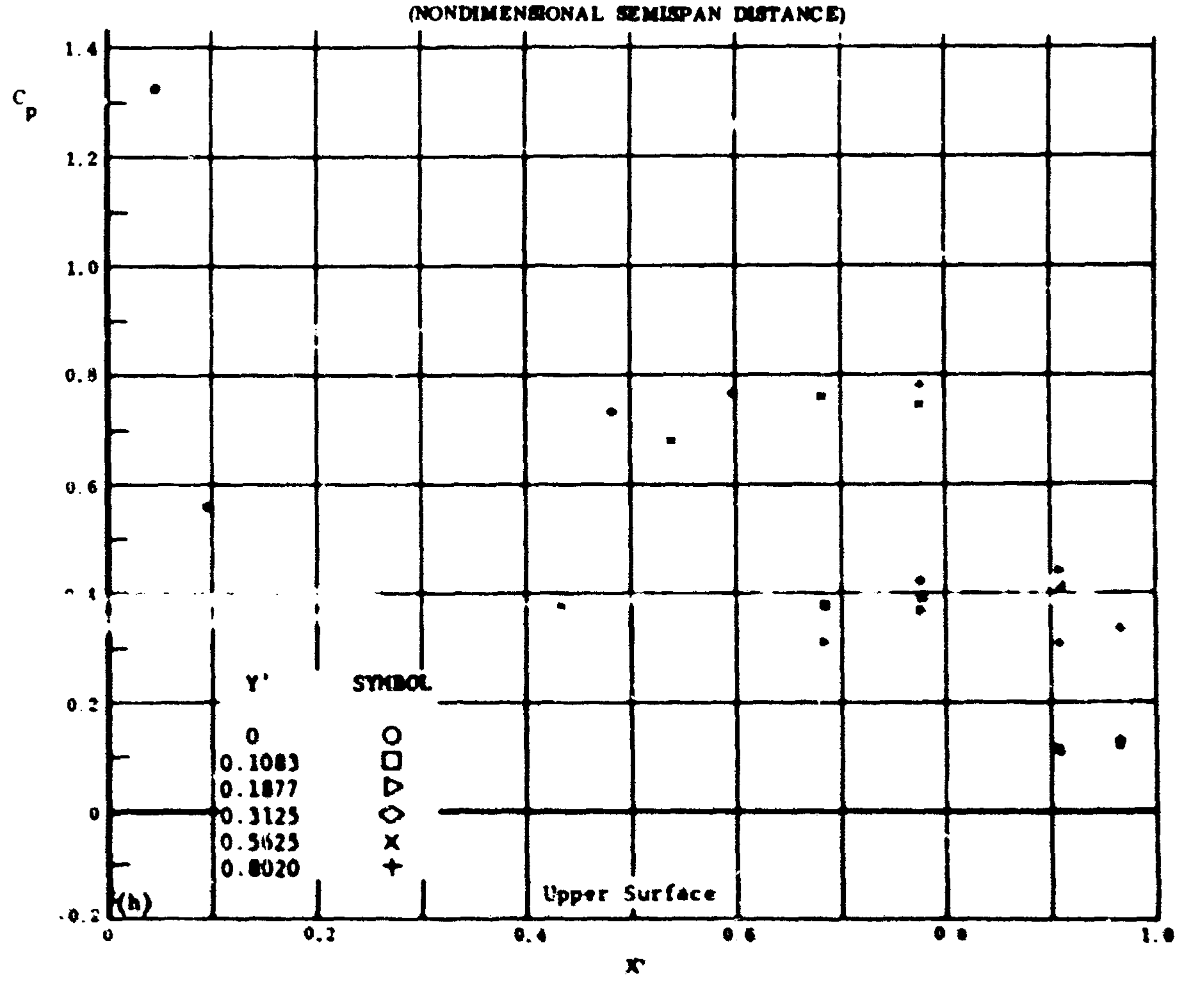

Fig. 44 Configuration IV, $\alpha = -30$, $\delta_2 = \delta_3 = +20$

g) C_p vs. Y', upper surface

h) C_p vs. X', upper surface

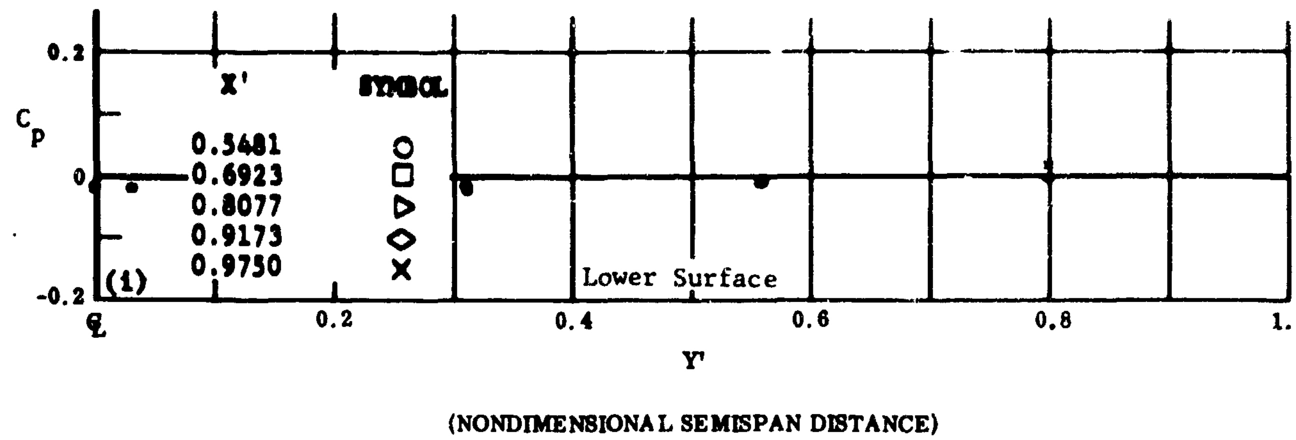

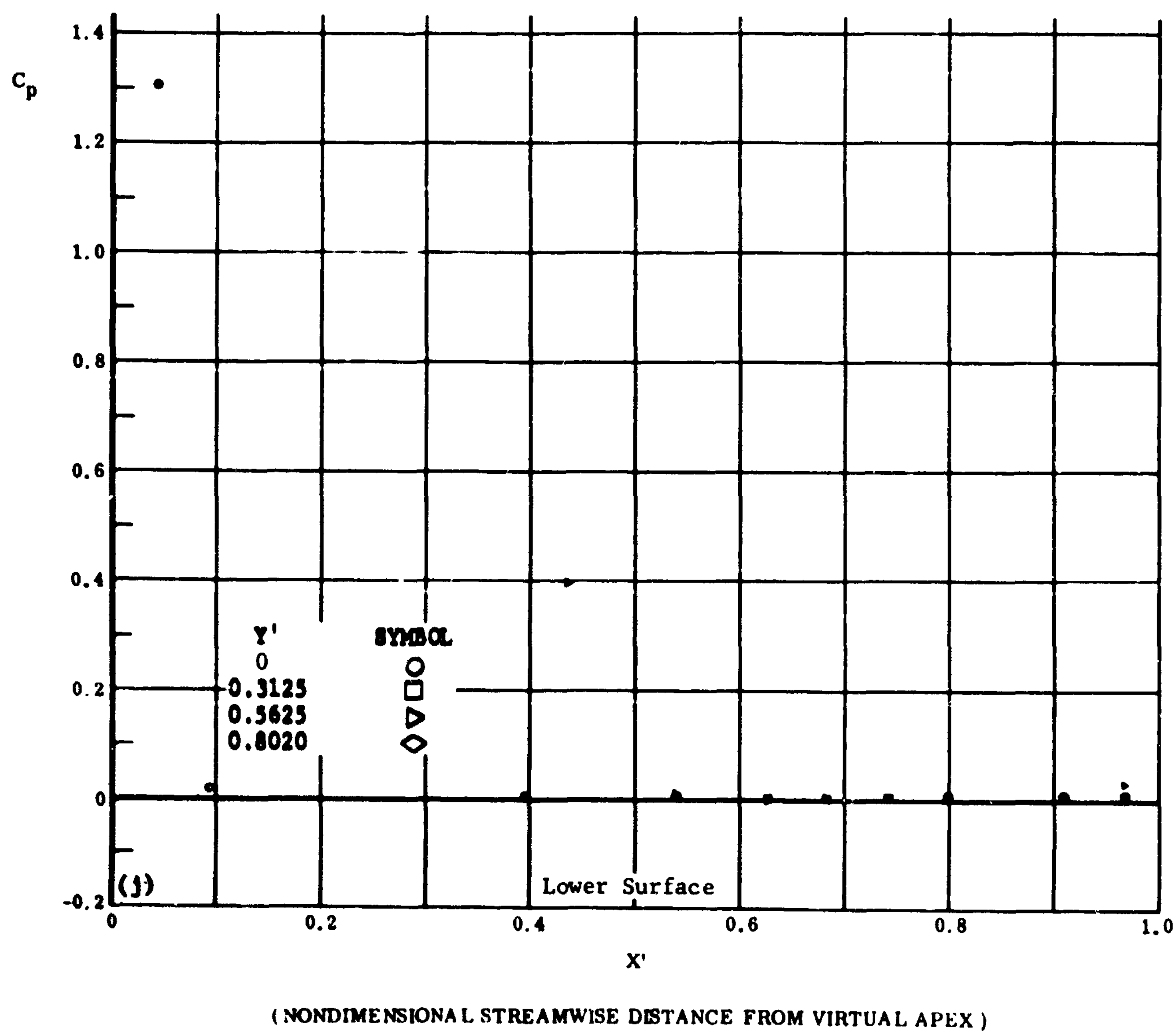

Fig. 44 Configuration IV, $\alpha = -30$, $\delta_2 = \delta_3 = +39$

i) C_p vs. Y', lower surface

j) C_p vs. X', lower surface

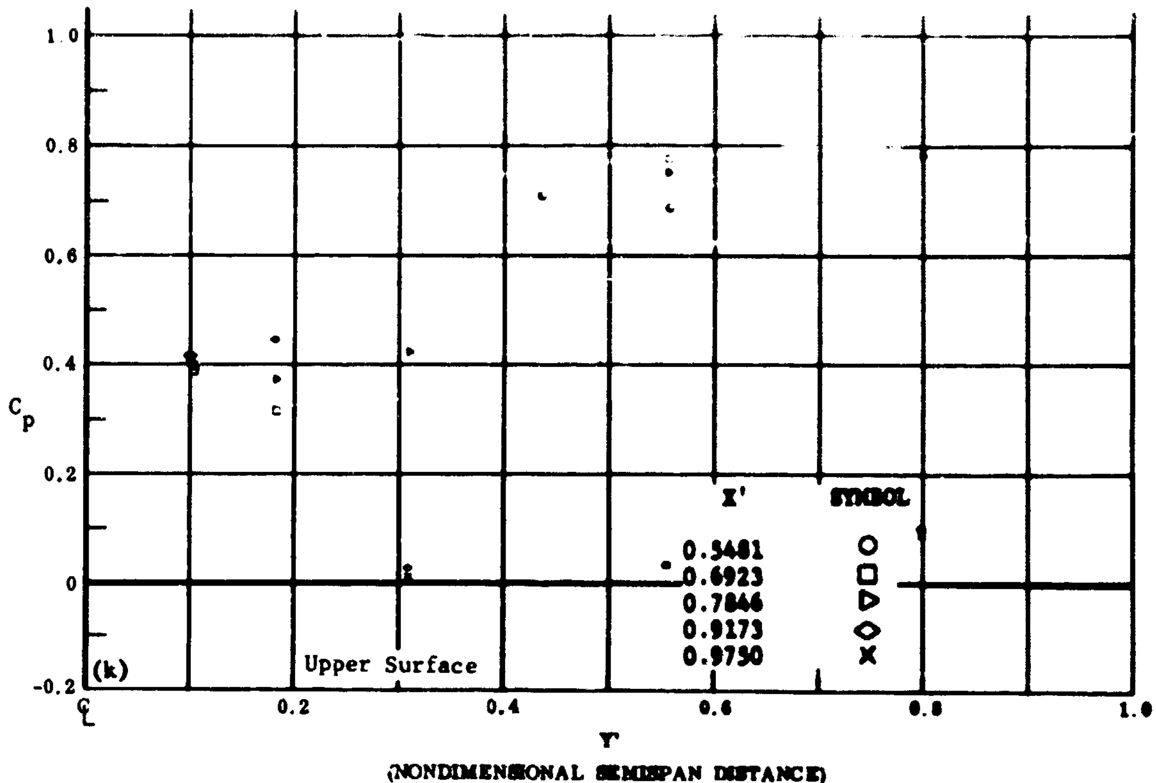

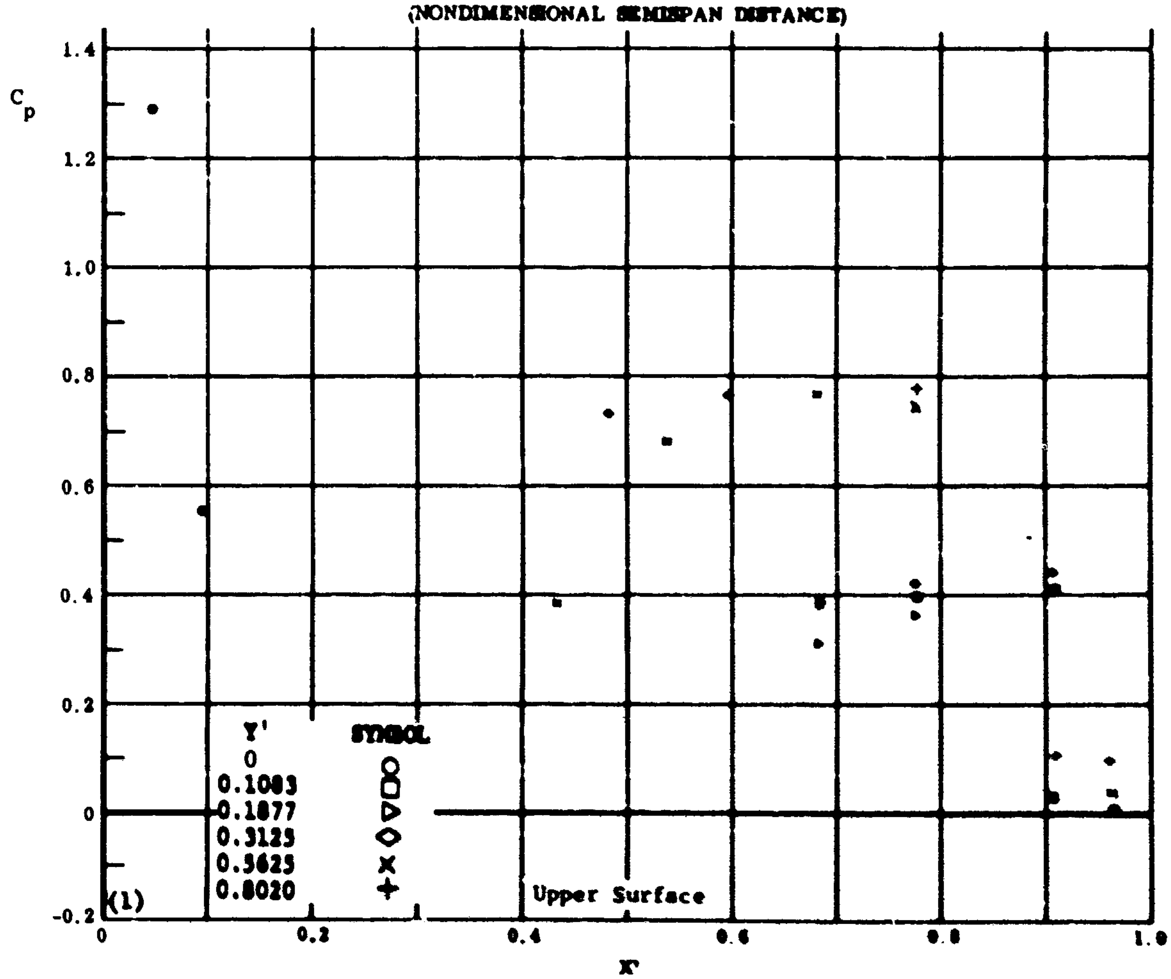

(NONDIMENSIONAL STREAMWISE DISTANCE FROM VIRTUAL APEX)

Fig. 44 Configuration IV, $\alpha = -30$, $\delta_2 = \delta_3 = +39$

k) C_p vs. Y', upper surface

l) C_p vs. X', upper surface

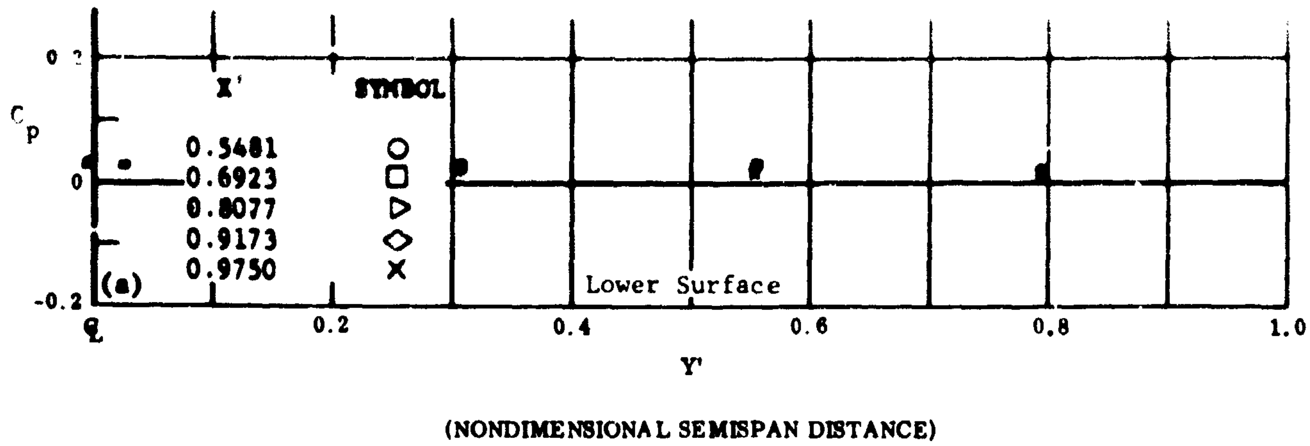

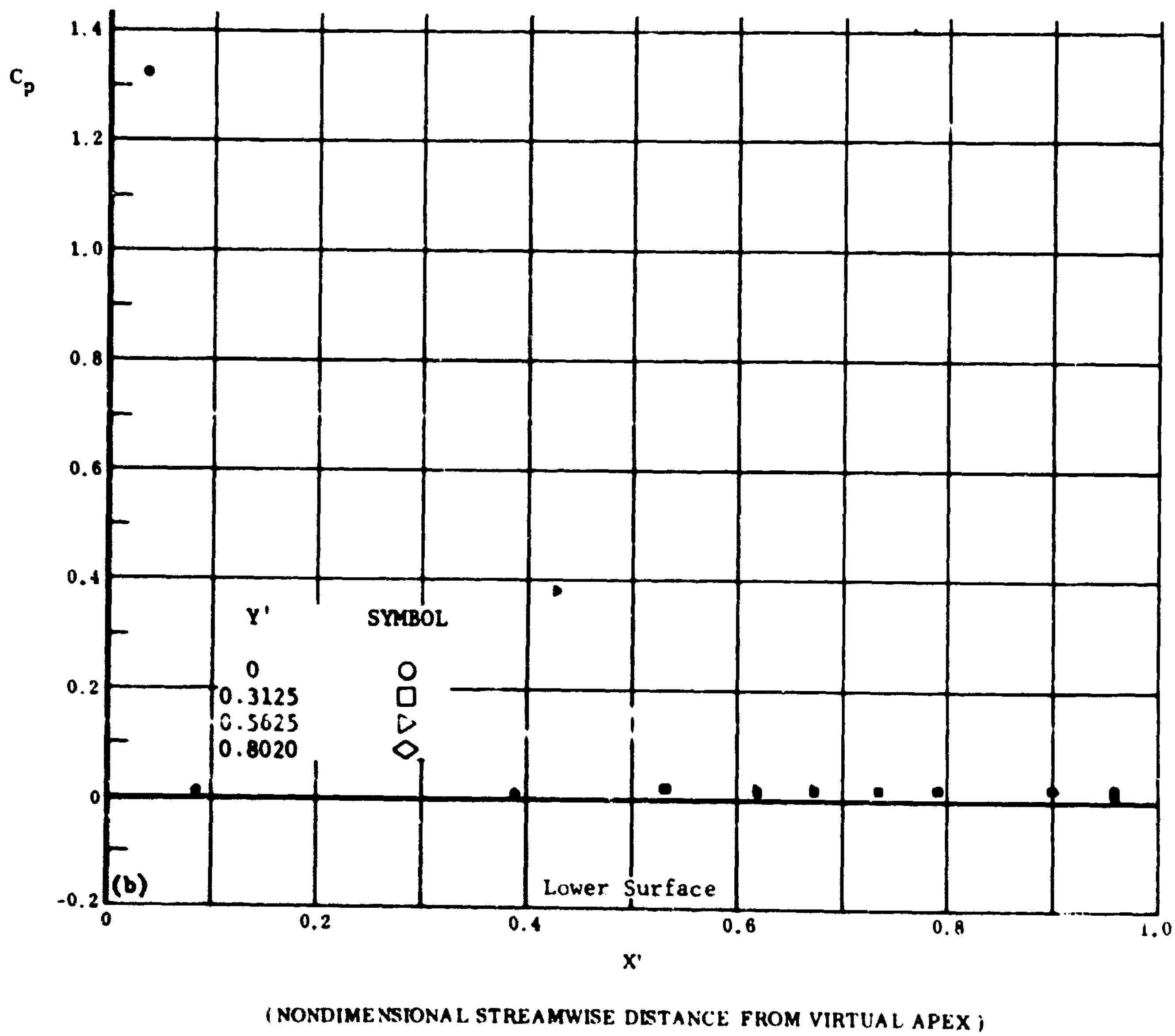

Fig. 45 Configuration IV, α = -30 , $\delta_2 = \delta_3$ = -10

a) C_p vs. Y', lower surface

b) C_p vs. X', lower surface

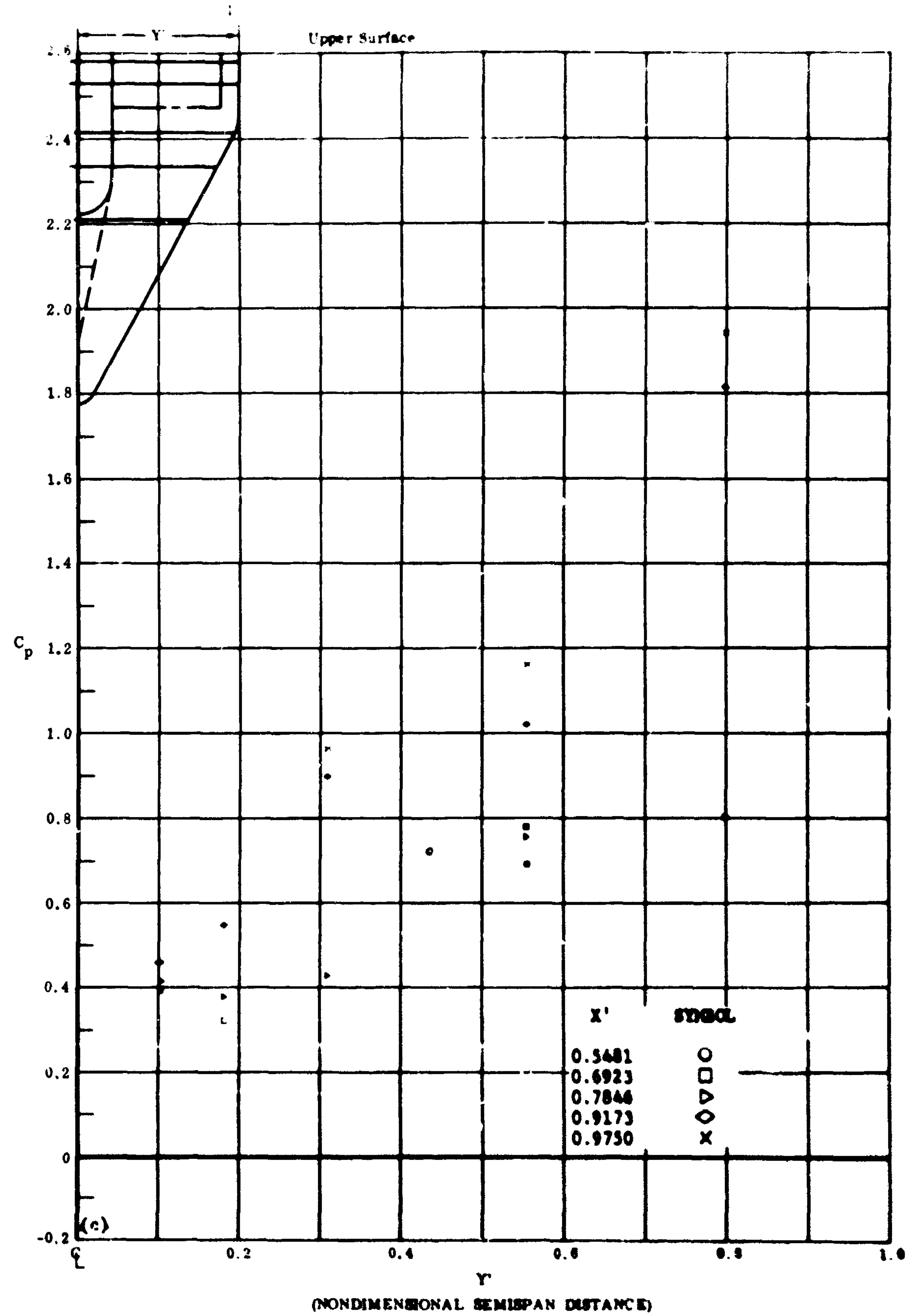

Fig. 45c Configuration IV, α = -30 , $\delta_2 = \delta_3$ = -10

C_p vs. Y', upper surface

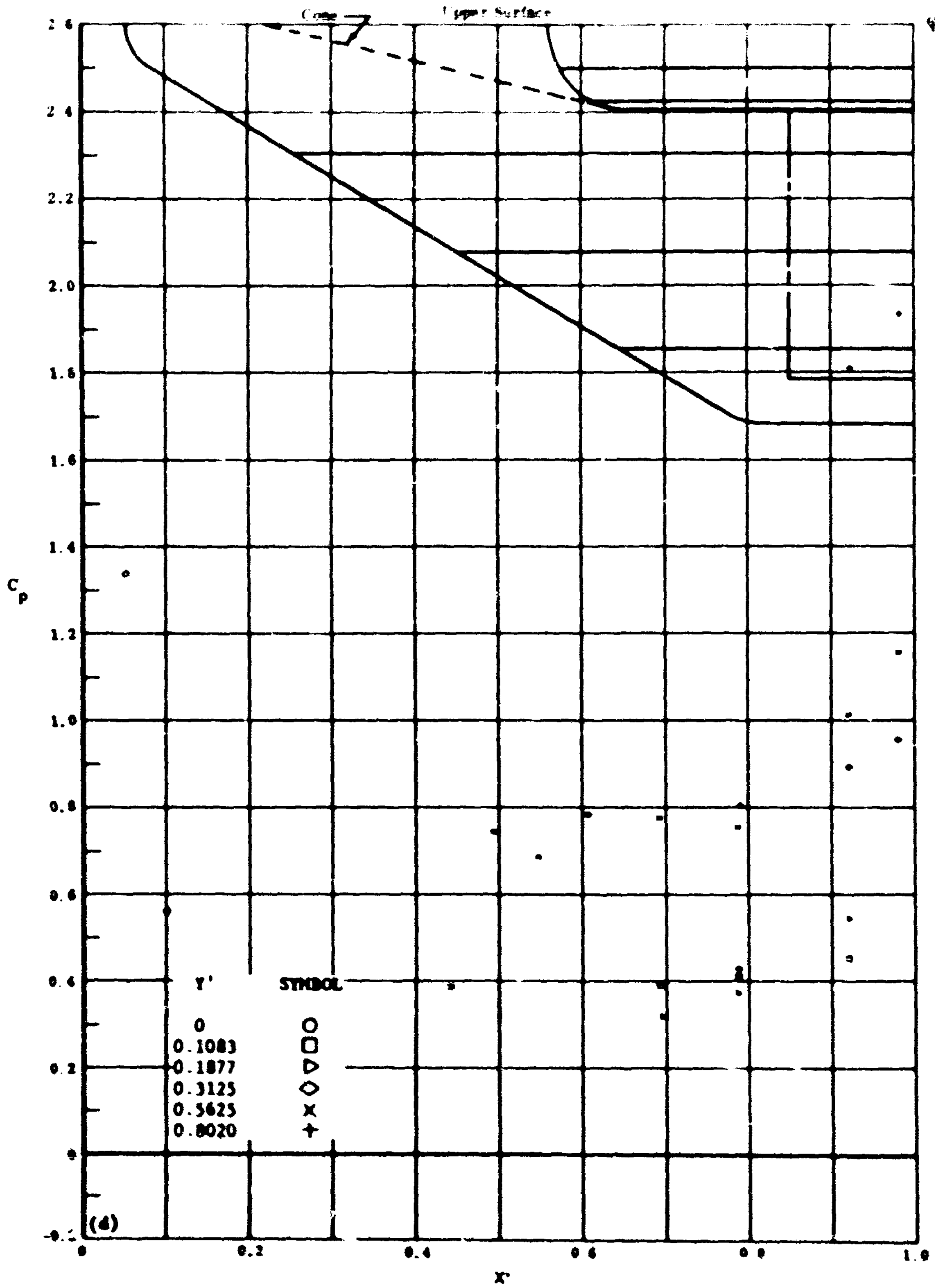

(NONDIMENSIONAL STREAMWISE DISTANCE FROM VIRTUAL APEX)

Fig. 45d Configuration IV, $\alpha = -30$, $\delta_2 = \delta_3 = -10$

C_p vs. X', upper surface

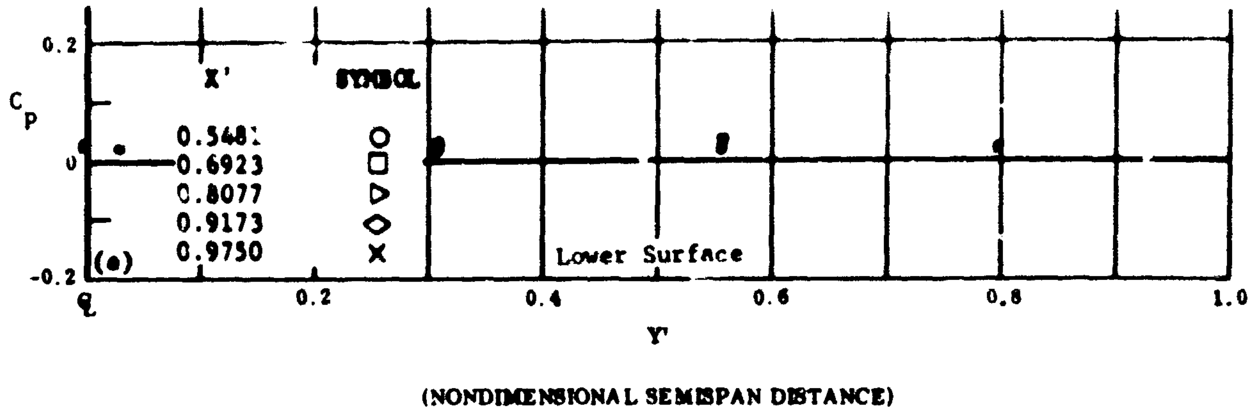

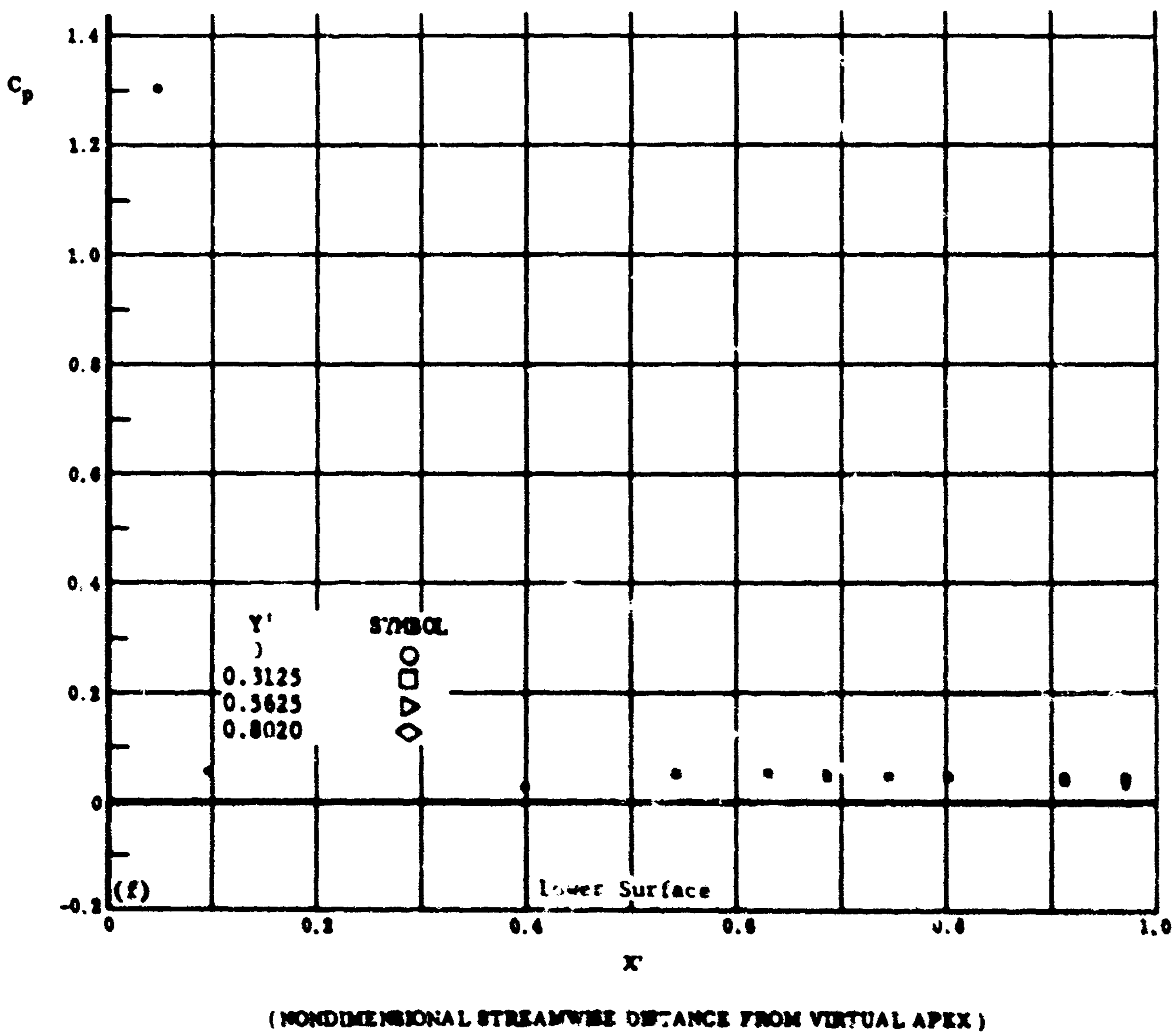

Fig. 45 Configuration IV, $\alpha = -30$, $\delta_2 = \delta_3 = -20$

e) C_p vs. Y', lower surface

f) C_p vs. X', lower surface

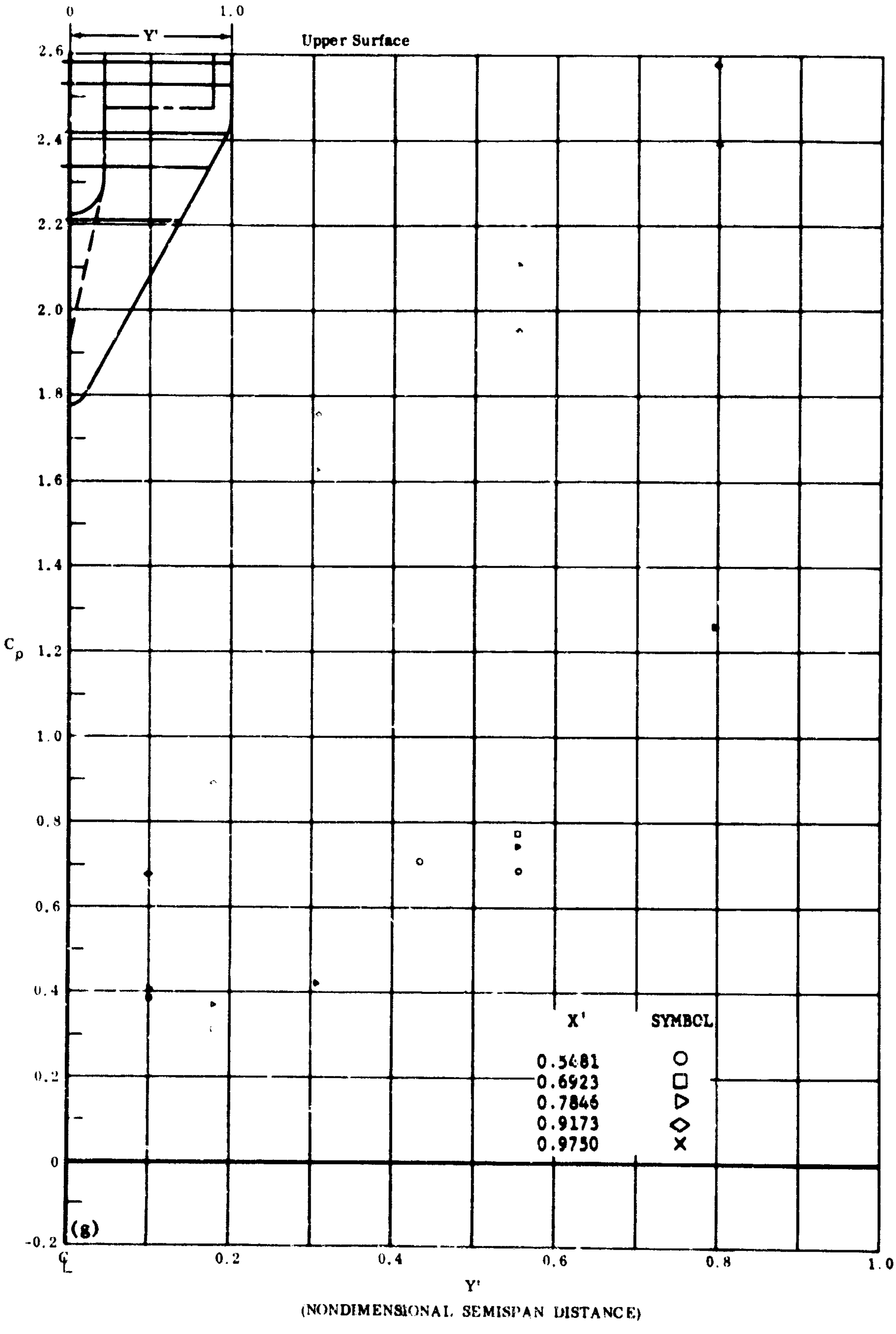

Fig. 45g Configuration IV, α = -30, $\delta_2 = \delta_3$ = -20

C_p vs. Y', upper surface

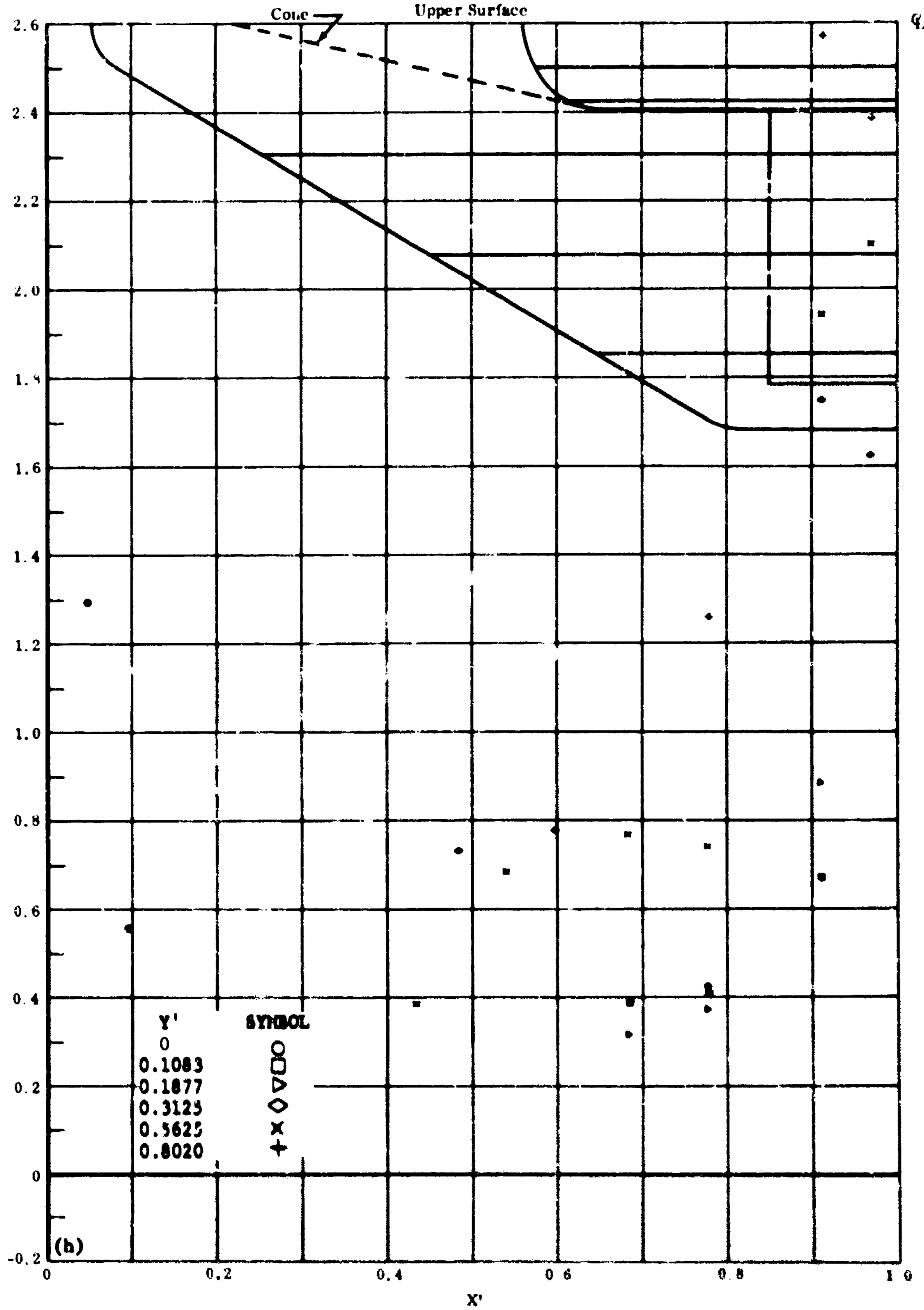

(NONDIMENSIONAL STREAMWISE DISTANCE FROM VIRTUAL APEX)

Fig. 45h Configuration IV, $\alpha = -30$, $\delta_2 = \delta_3 = -20$

C_p vs. X', upper surface

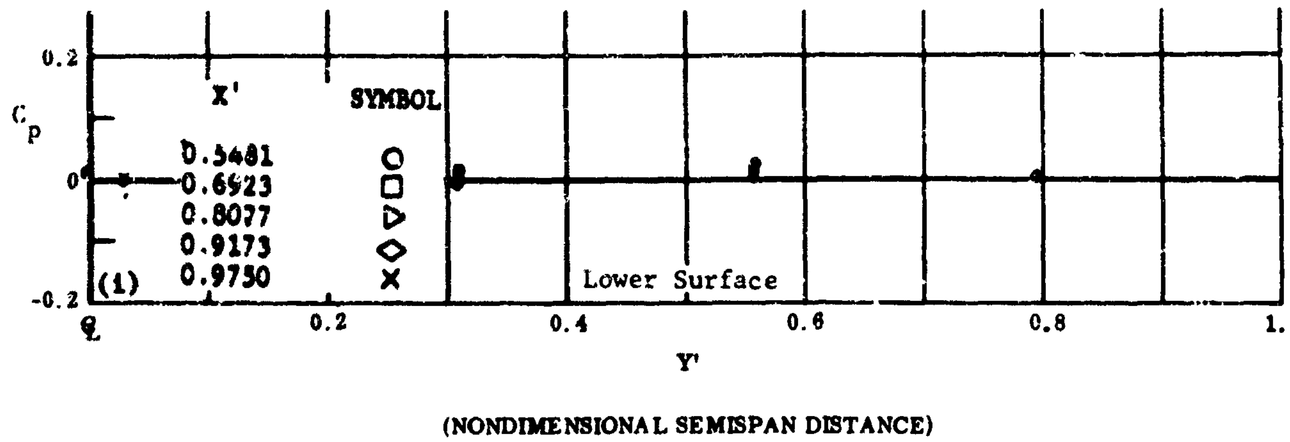

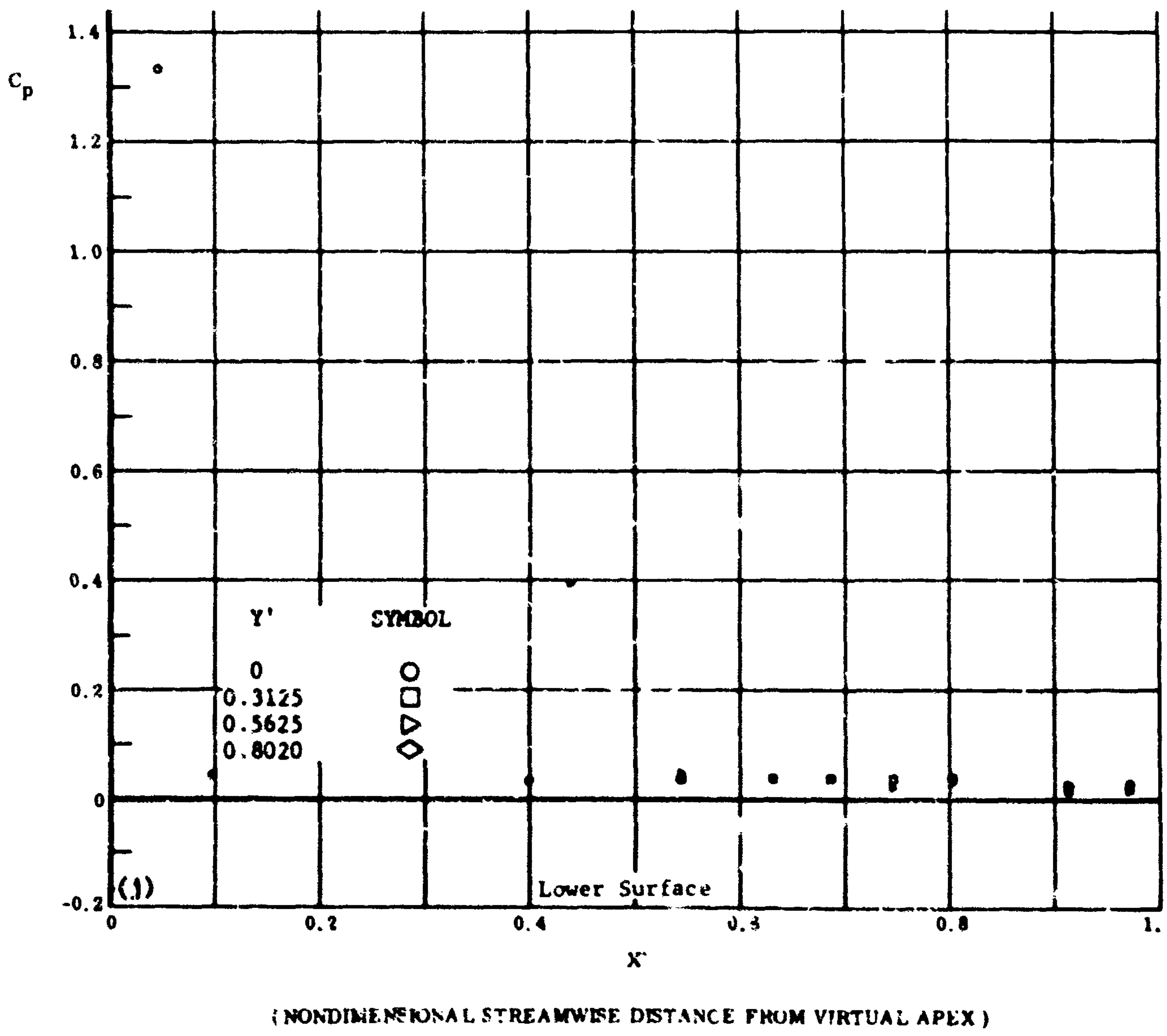

Fig. 45 Configuration IV, $\alpha = -30$, $\delta_2 = \delta_3 = -30$

i) C_p vs. Y', lower surface

j) C_p vs. X', lower surface

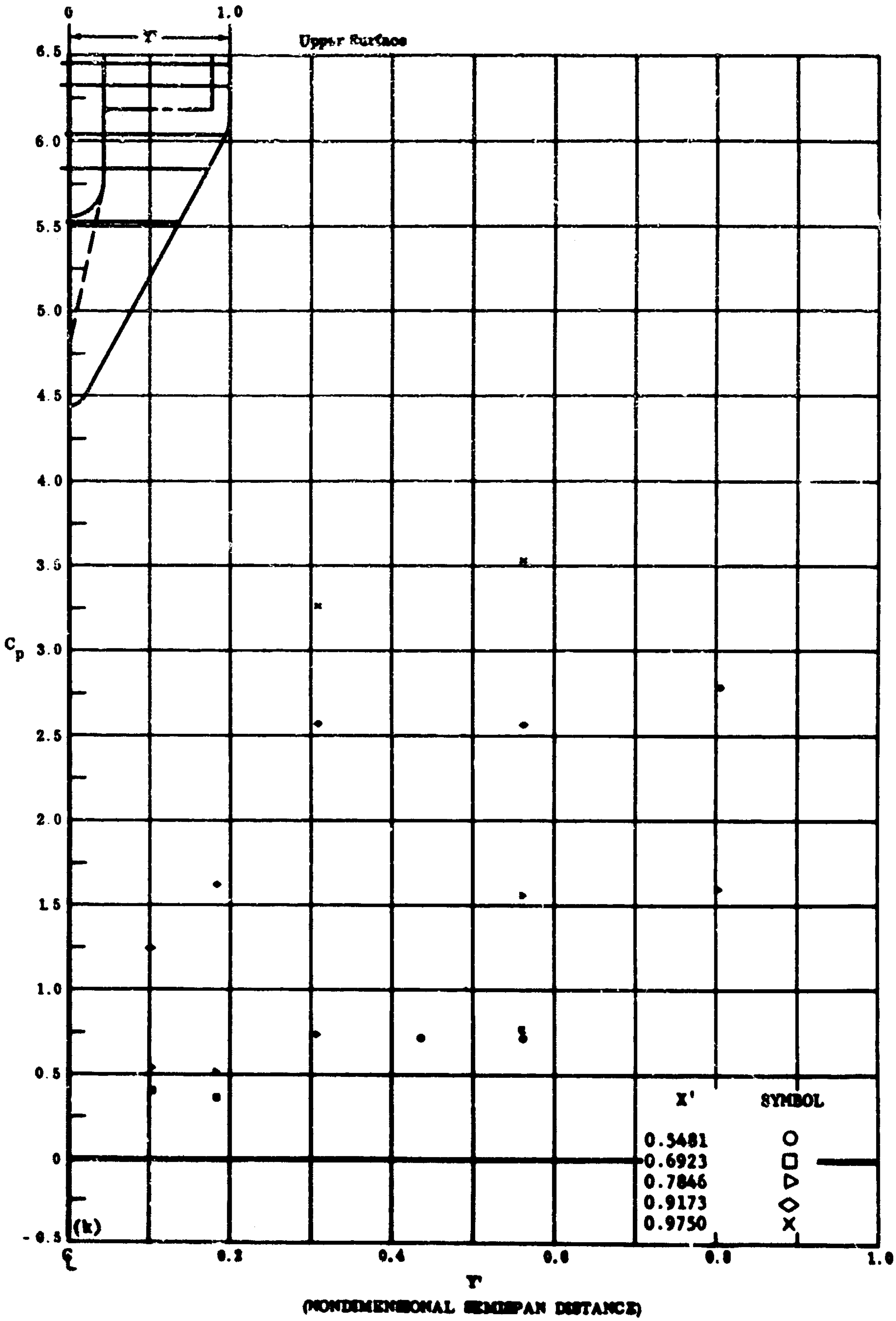

Fig. 45k Configuration IV, $\alpha = -30$, $\delta_2 = \delta_3 = -30$

C_p vs. Y', upper surface

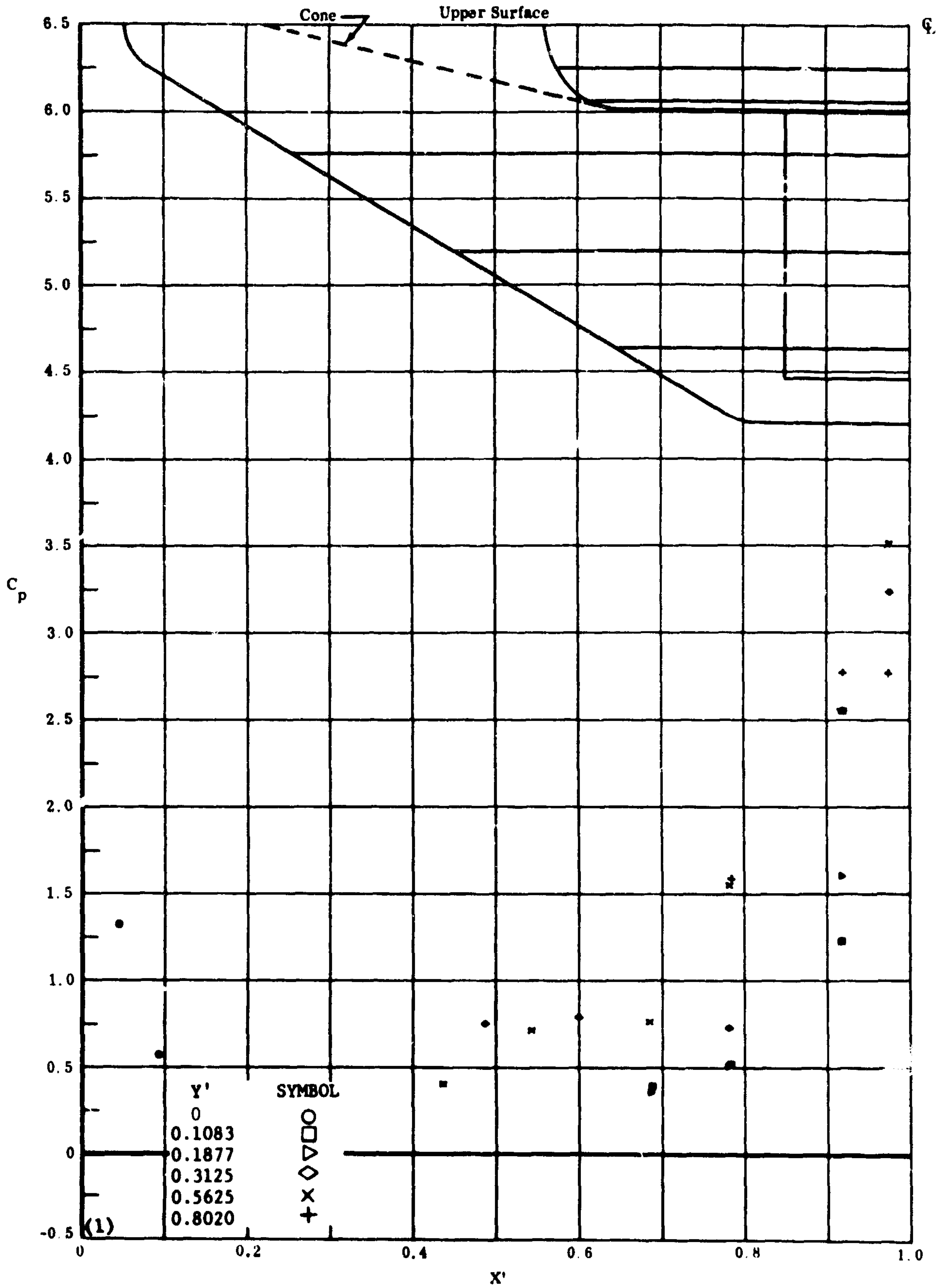

(NONDIMENSIONAL STREAMWISE DISTANCE FROM VIRTUAL APEX)

Fig. 451 Configuration IV, $\alpha = -30$, $\delta_2 = \delta_3 = -30$

C_p vs. X', upper surface

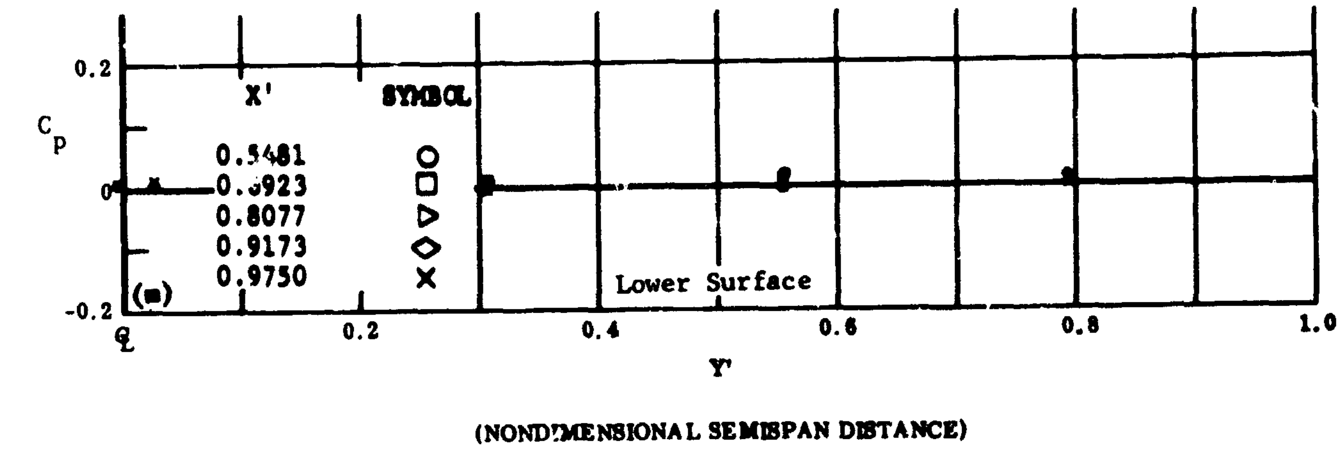

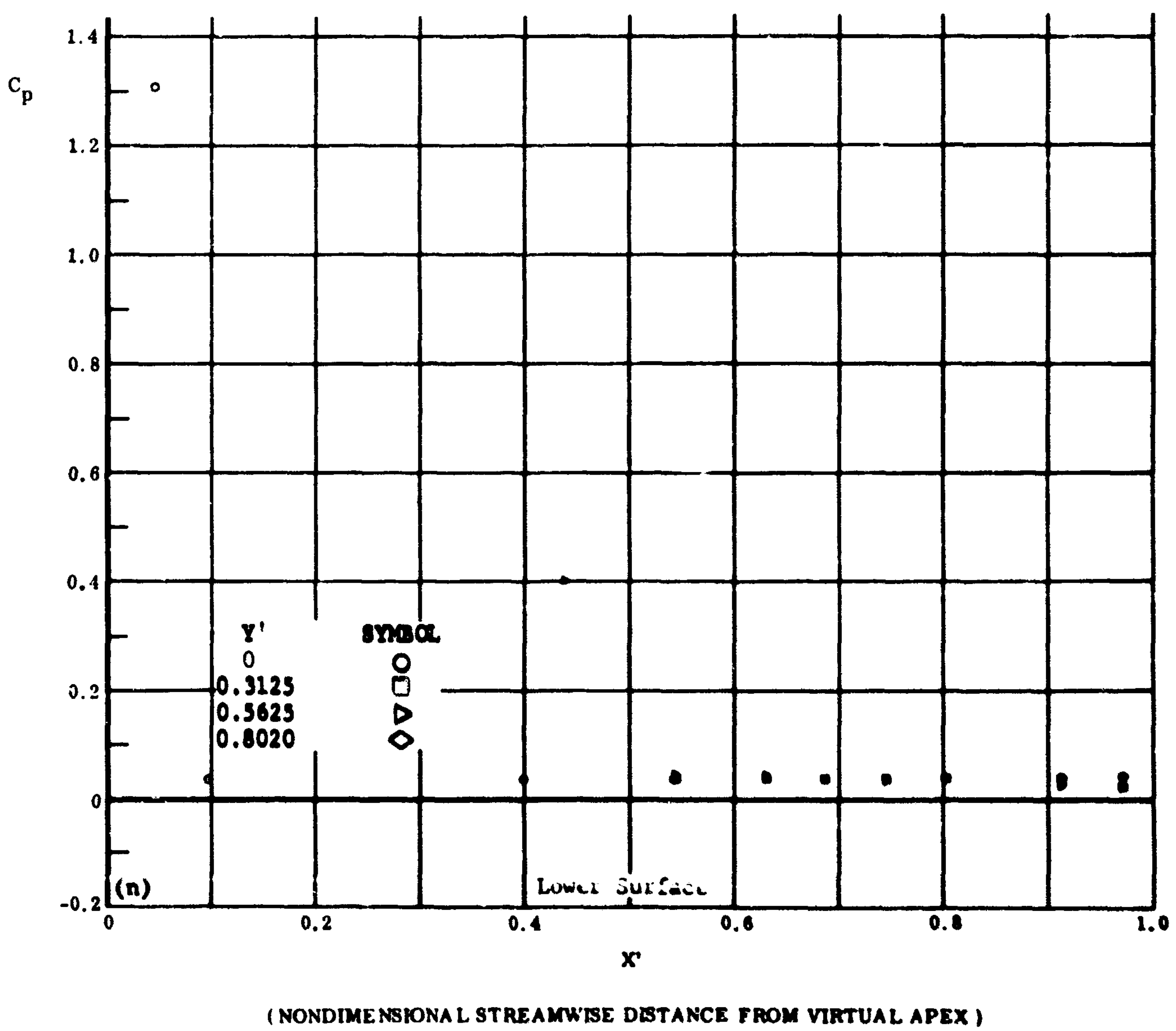

Fig. 45 Configuration IV, $\alpha = -30$, $\delta_2 = \delta_3 = -39$

m) C_p vs. Y', lower surface

n) C_p vs. X', lower surface

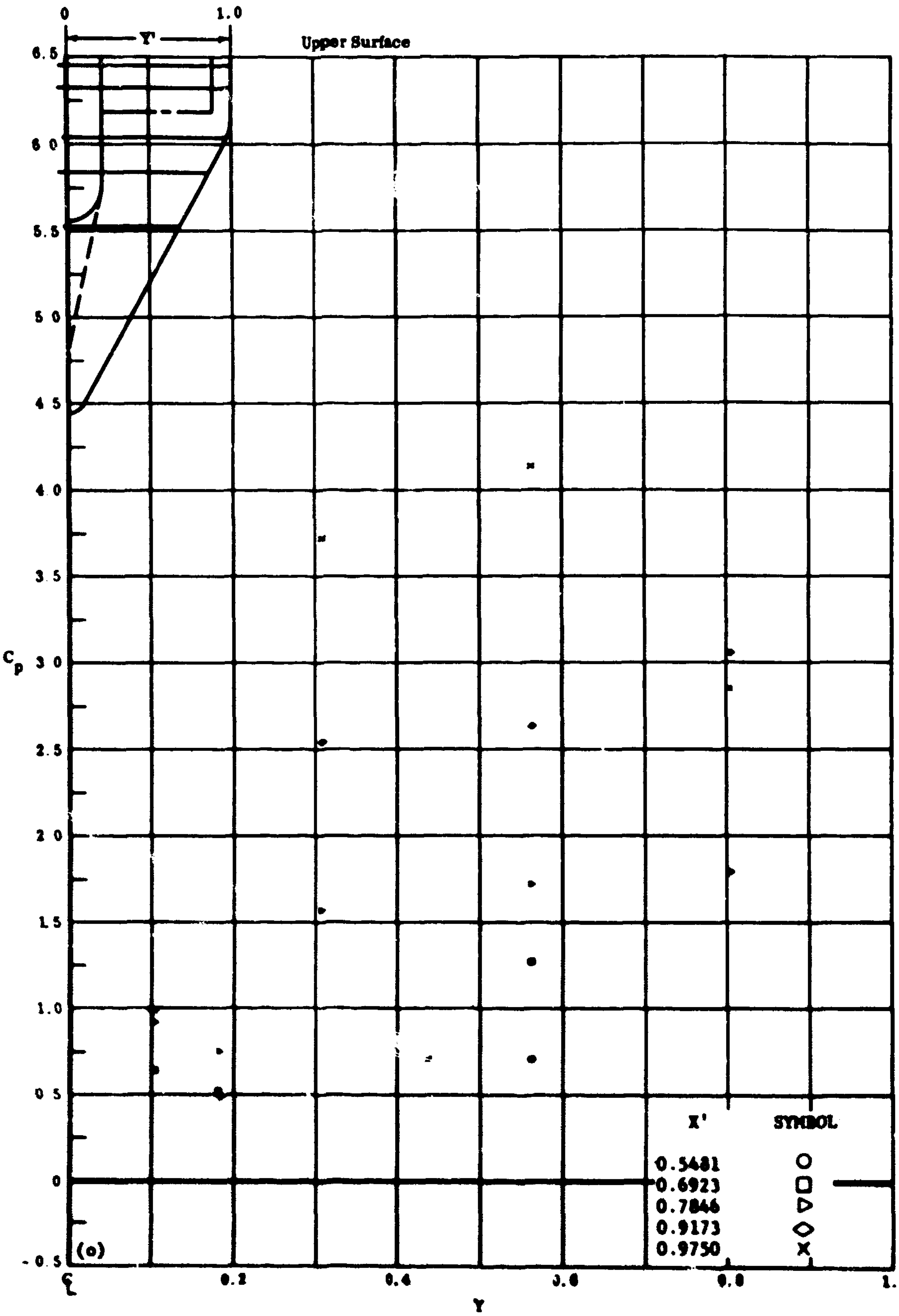

Fig. 45o Configuration IV, α = -30, $\delta_2 = \delta_3$ = -39

C_p vs. Y', upper surface

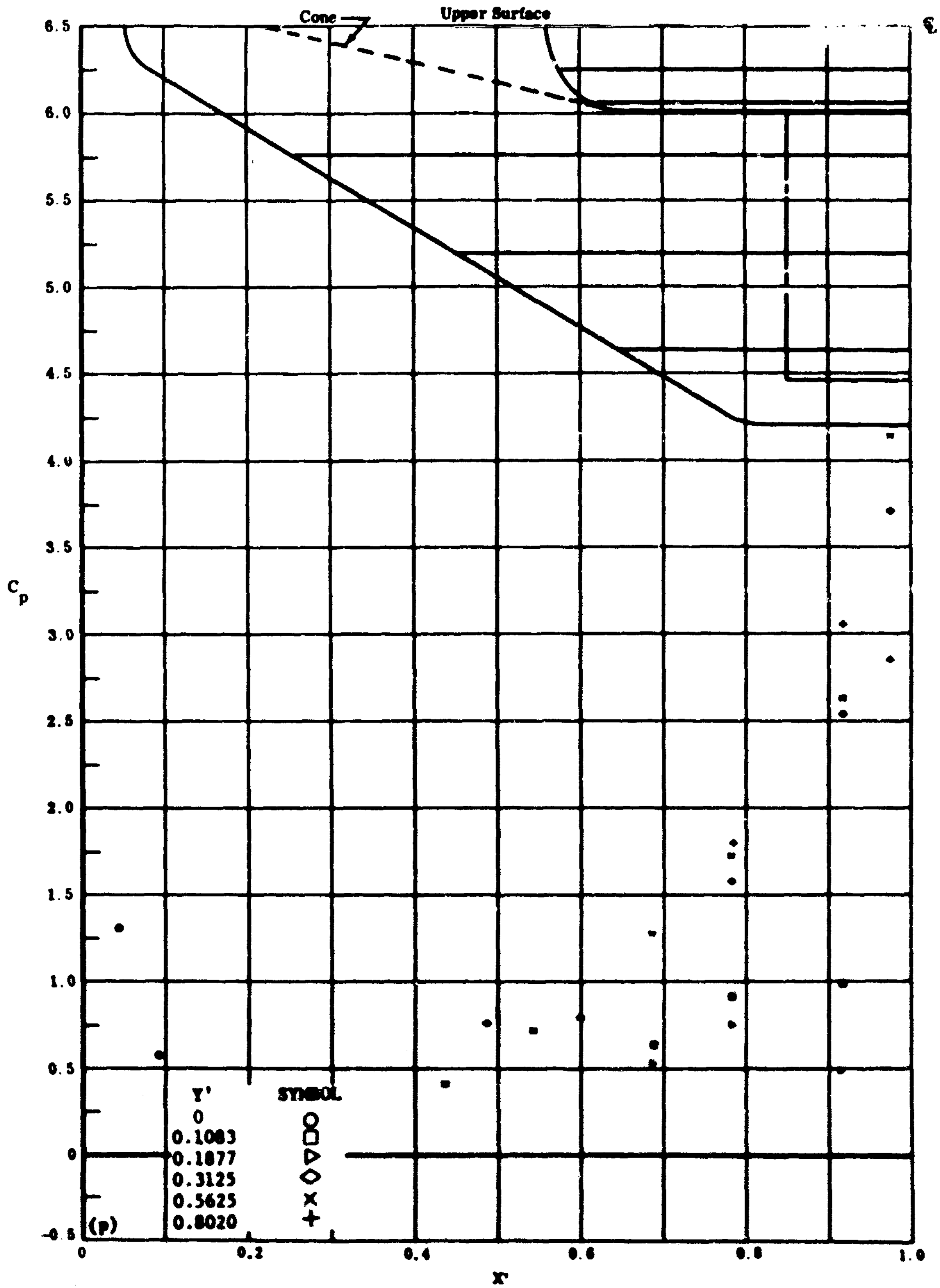

(NONDIMENSIONAL STREAMWISE DISTANCE FROM VIRTUAL APEX)

Fig. 45p Configuration IV, $\alpha = -30$, $\delta_2 = \delta_3 = -39$

C_p vs. X', upper surface

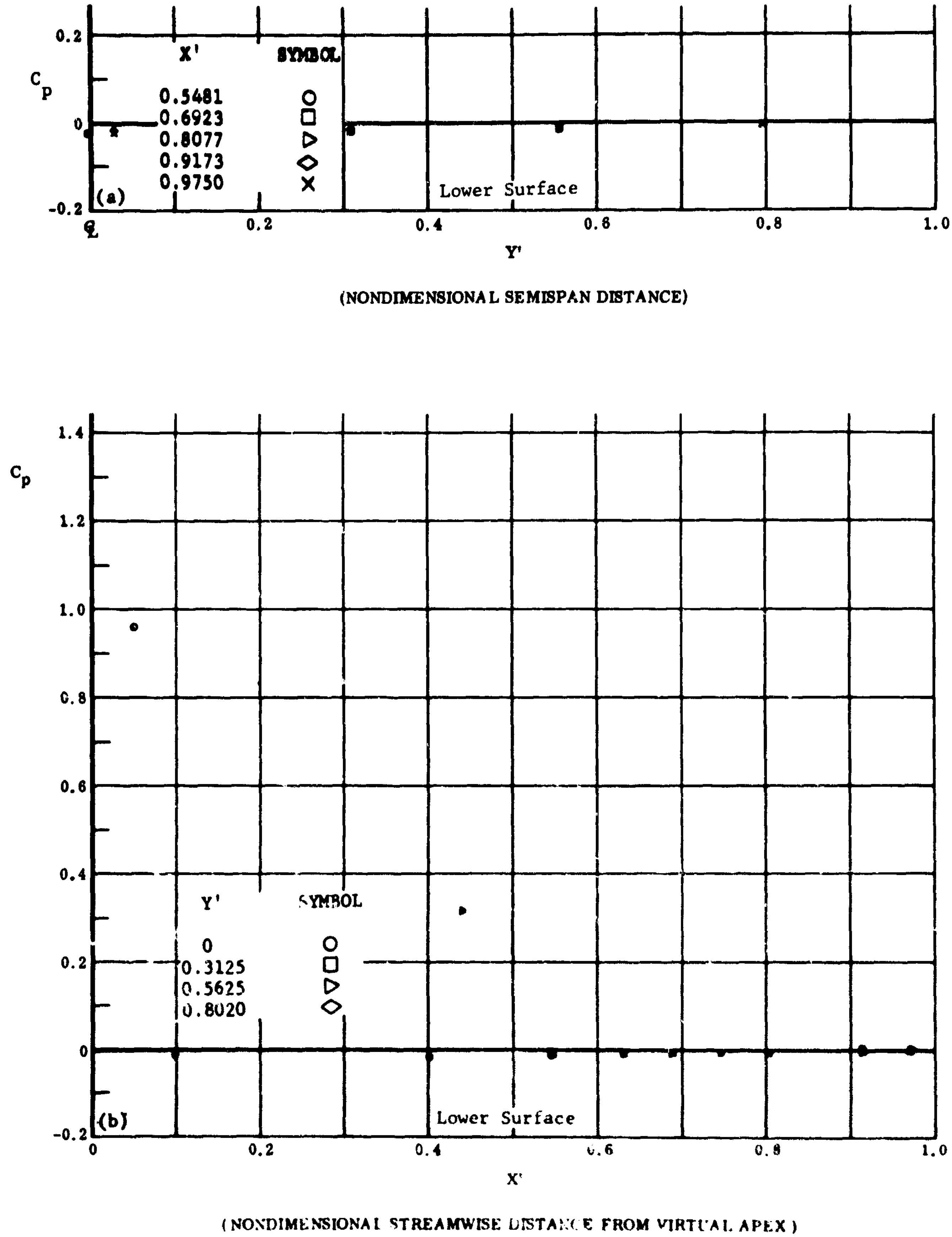

Fig. 46 ration IV, $\alpha = -40$, $\delta_2 = \delta_3 = 0$

a) C_p vs. Y', lower surface

b) C_p vs. X', lower surface

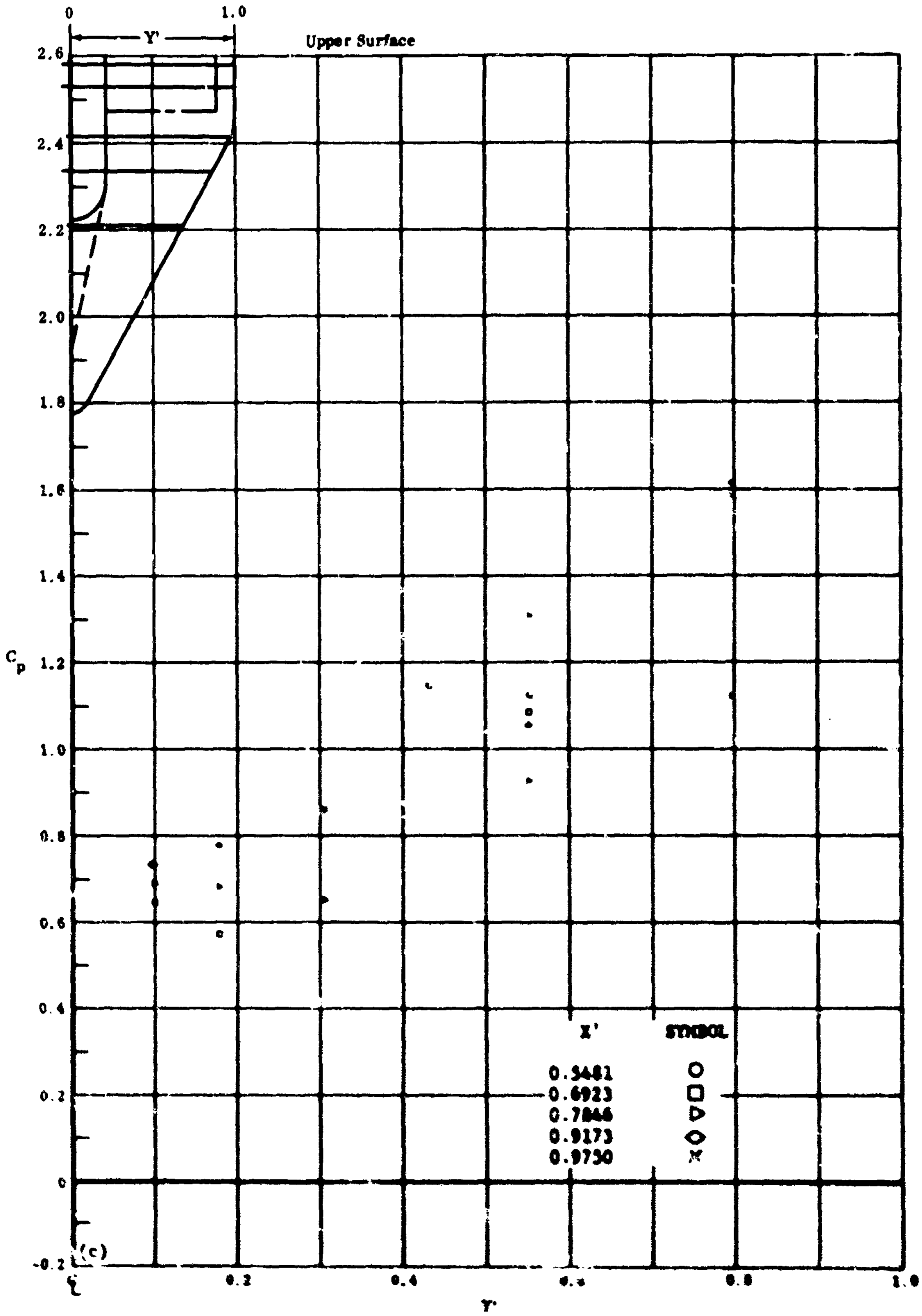

Fig. 46c Configuration IV, $\alpha = -40$, $\delta_2 = \delta_3 = 0$

C_p vs. Y', upper surface

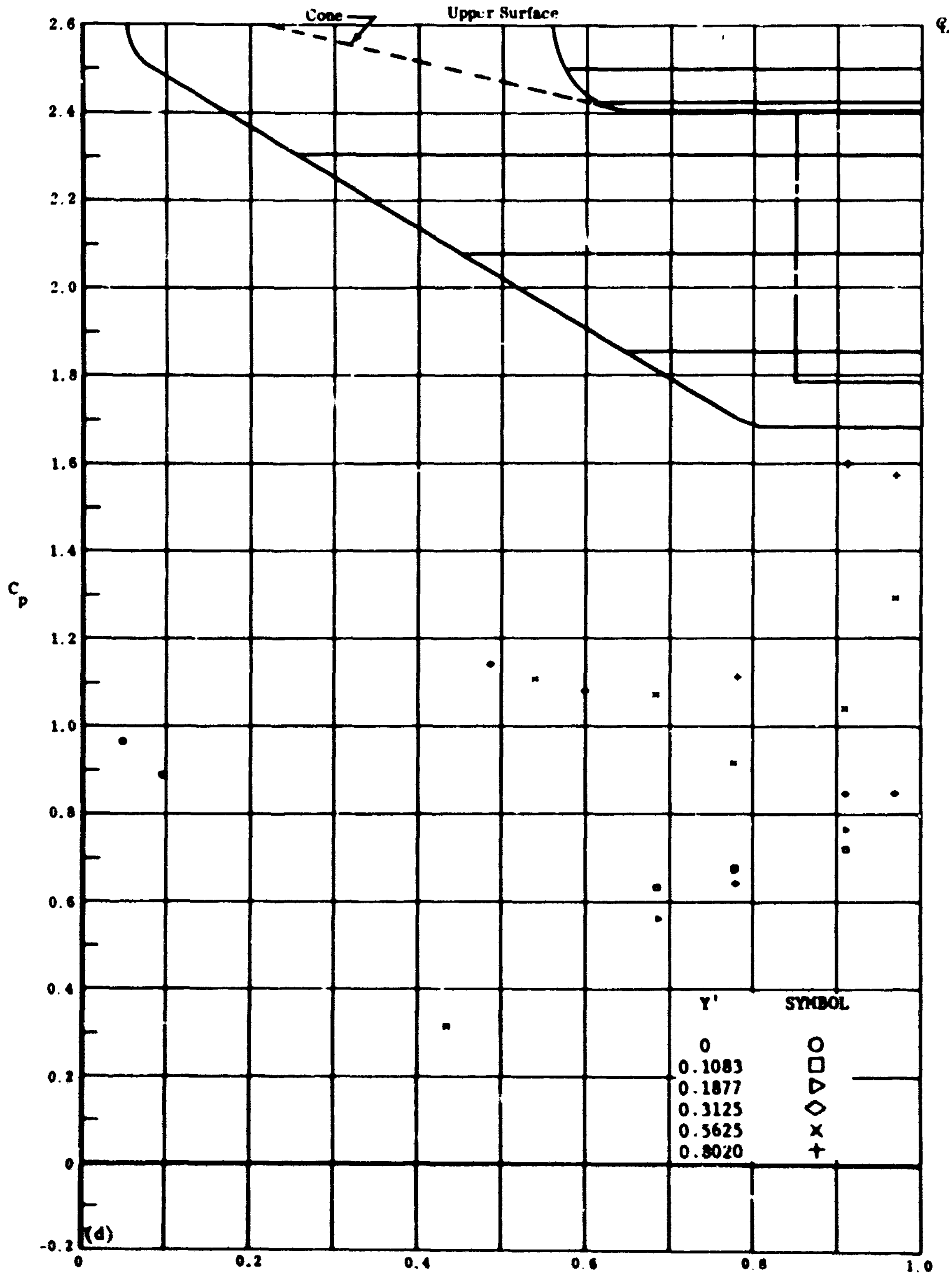

(NONDIMENSIONAL STREAMWISE DISTANCE FROM VIRTUAL APEX)

Fig. 46d Configuration IV, $\alpha = -40$, $\delta_2 = \delta_3 = 0$

C_p vs. X', upper surface

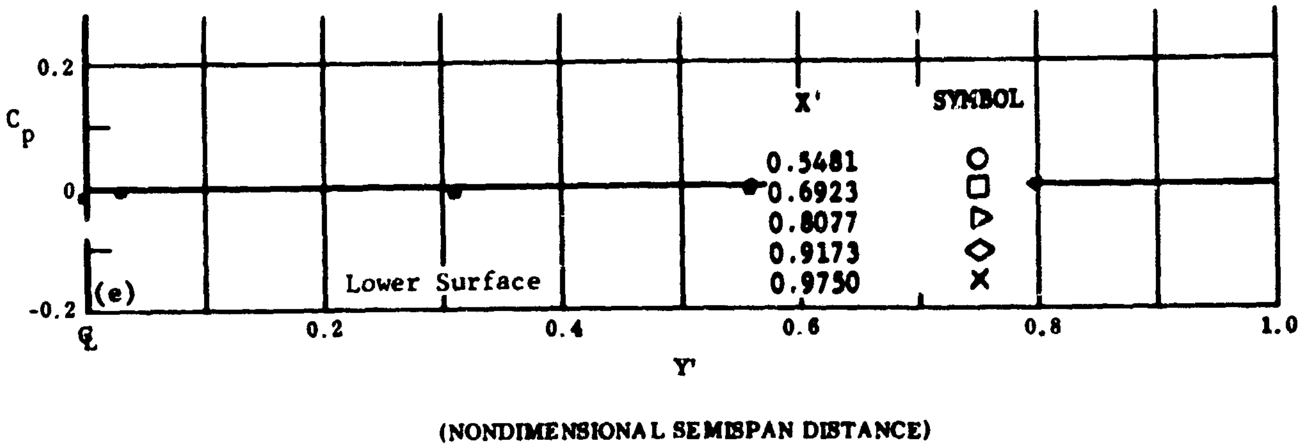

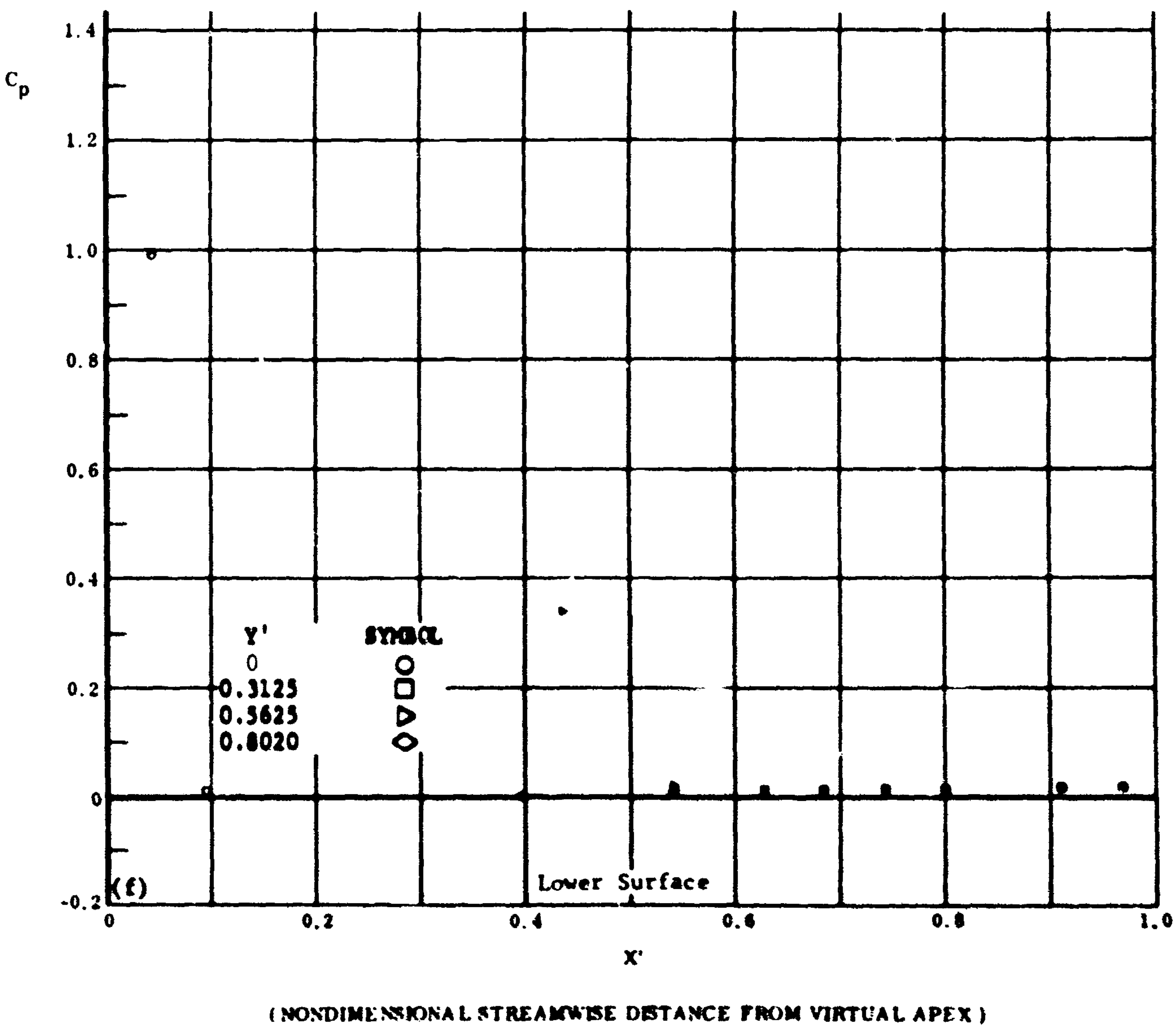

Fig. 46 Configuration IV, $\alpha = -40$, $\delta_2 = \delta_3 = +20$

e) C_p vs. Y', lower surface

f) C_p vs. X', lower surface

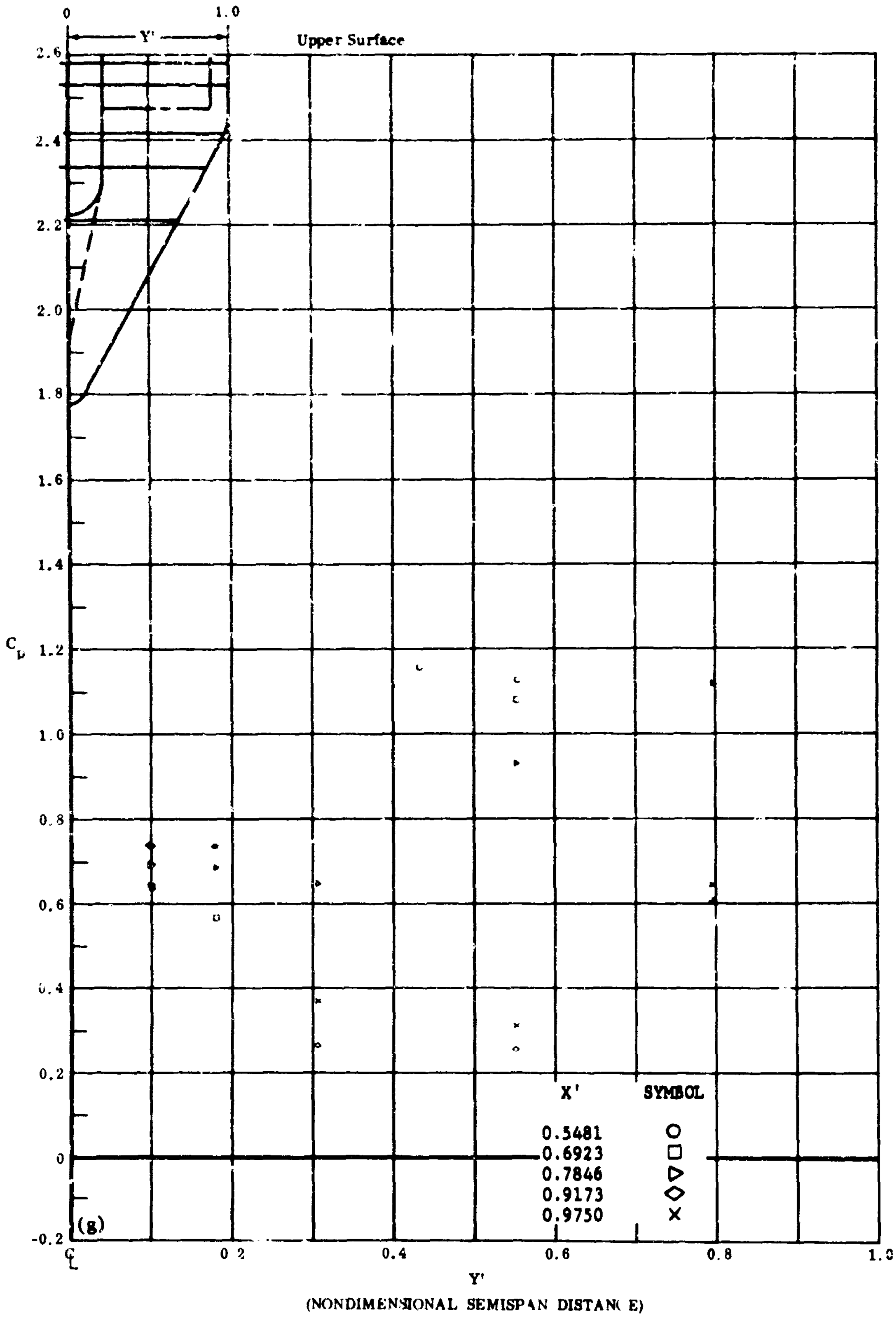

Fig. 46g Configuration IV, α = -40 , $\delta_2 = \delta_3$ =+20

C_p vs. Y', upper surface

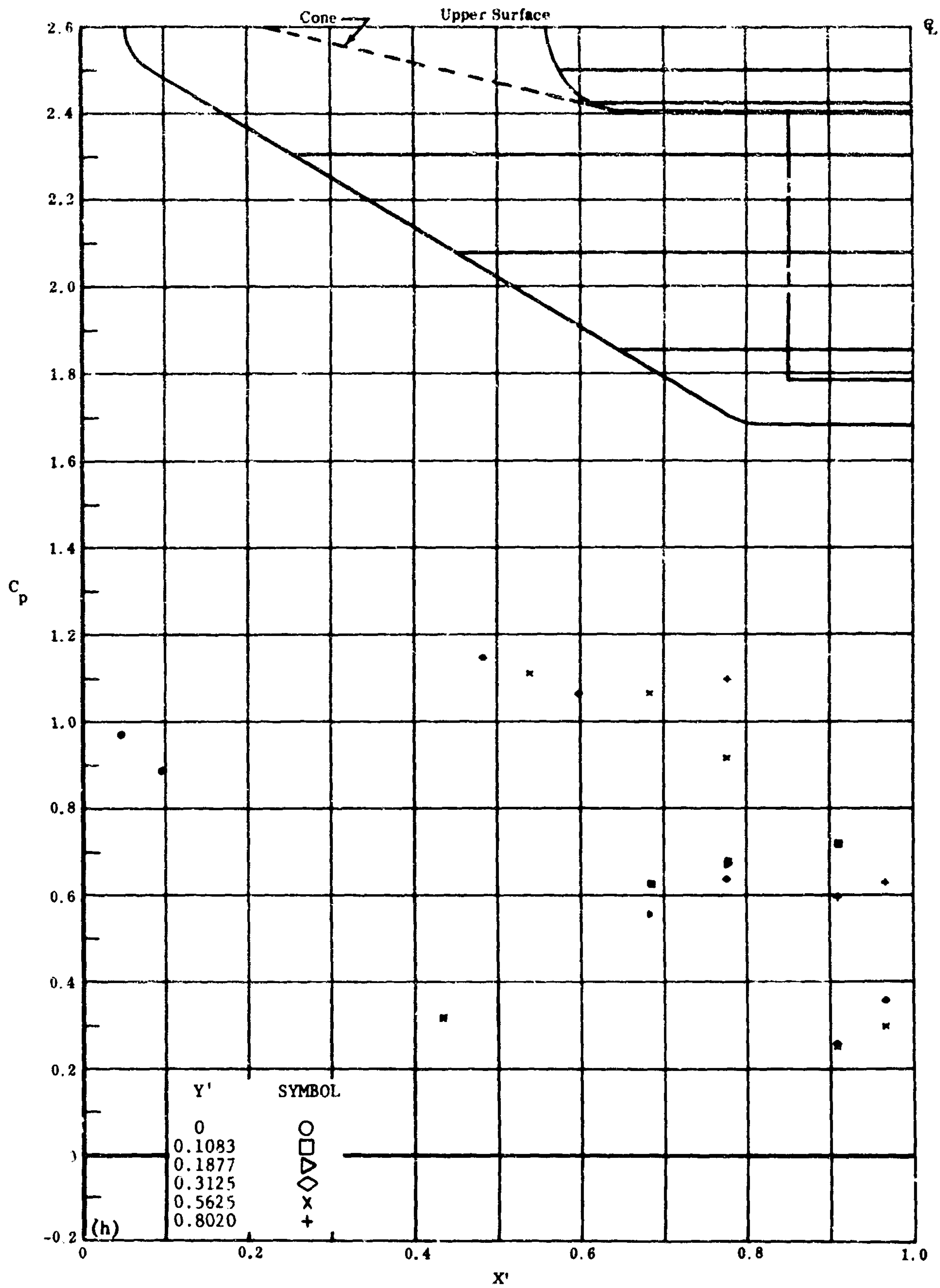

(NONDIMENSIONAL STREAMWISE DISTANCE FROM VIRTUAL APEX)

Fig. 46h Configuration IV, $\alpha = -40$, $\delta_2 = \delta_3 = +20$

C_p vs. X', upper surface

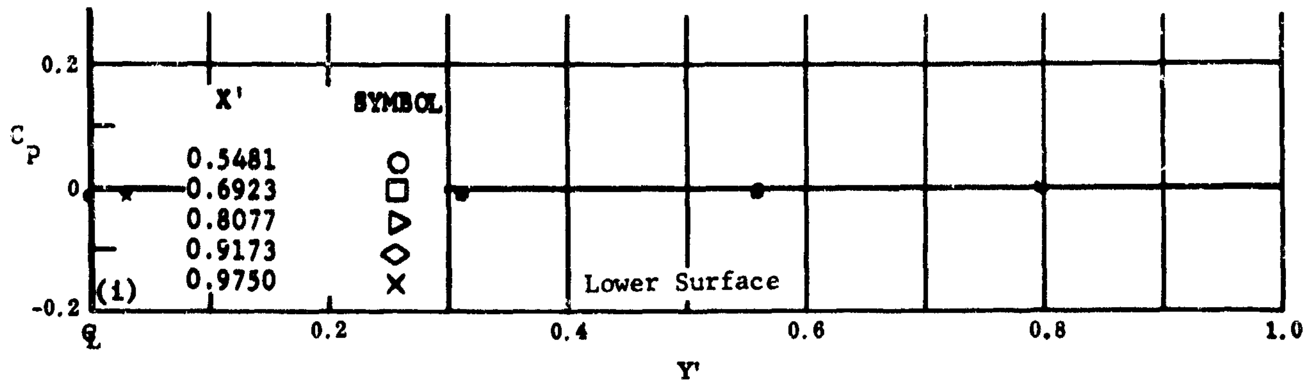

(NONDIMENSIONAL SEMISPAN DISTANCE)

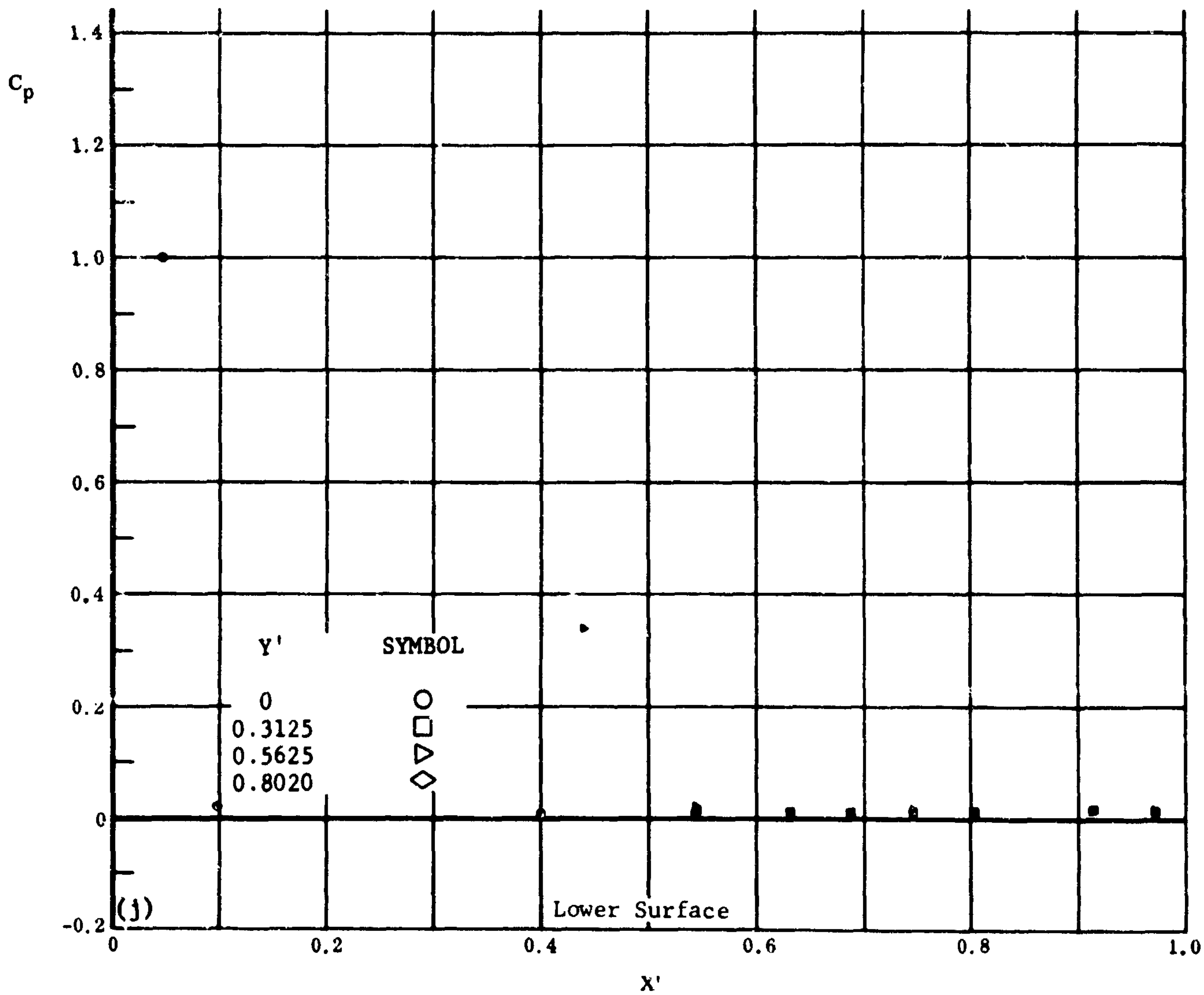

(NONDIMENSIONAL STREAMWISE DISTANCE FROM VIRTUAL APEX)

Fig. 46 Configuration IV, $\alpha = -40$, $\delta_2 = \delta_3 = +39$

i) C_p vs. Y', lower surface

j) C_p vs. X', lower surface

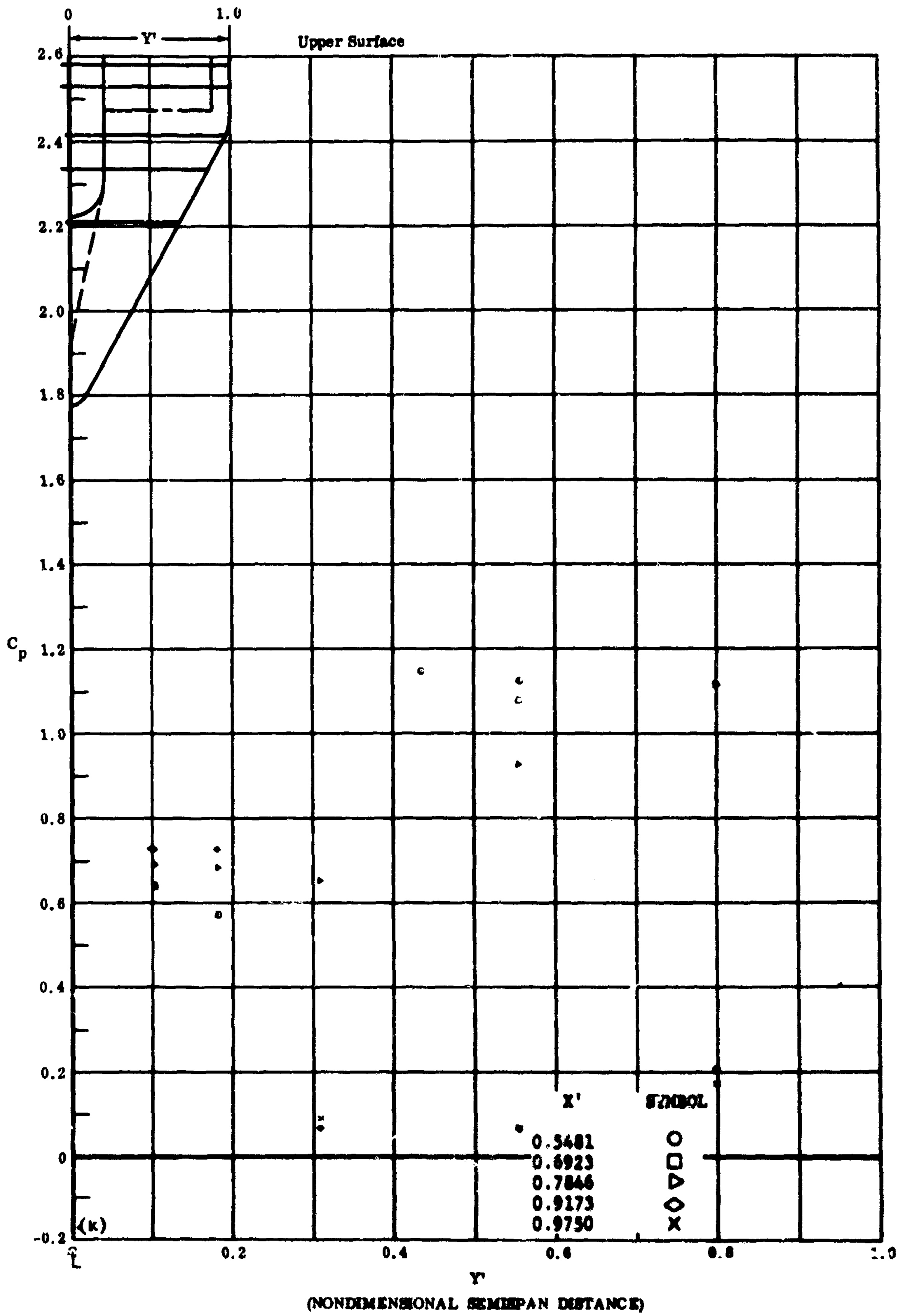

Fig. 46k Configuration IV, $\alpha = -40$, $\delta_2 = \delta_3 = +39$

C_p vs. Y', upper surface

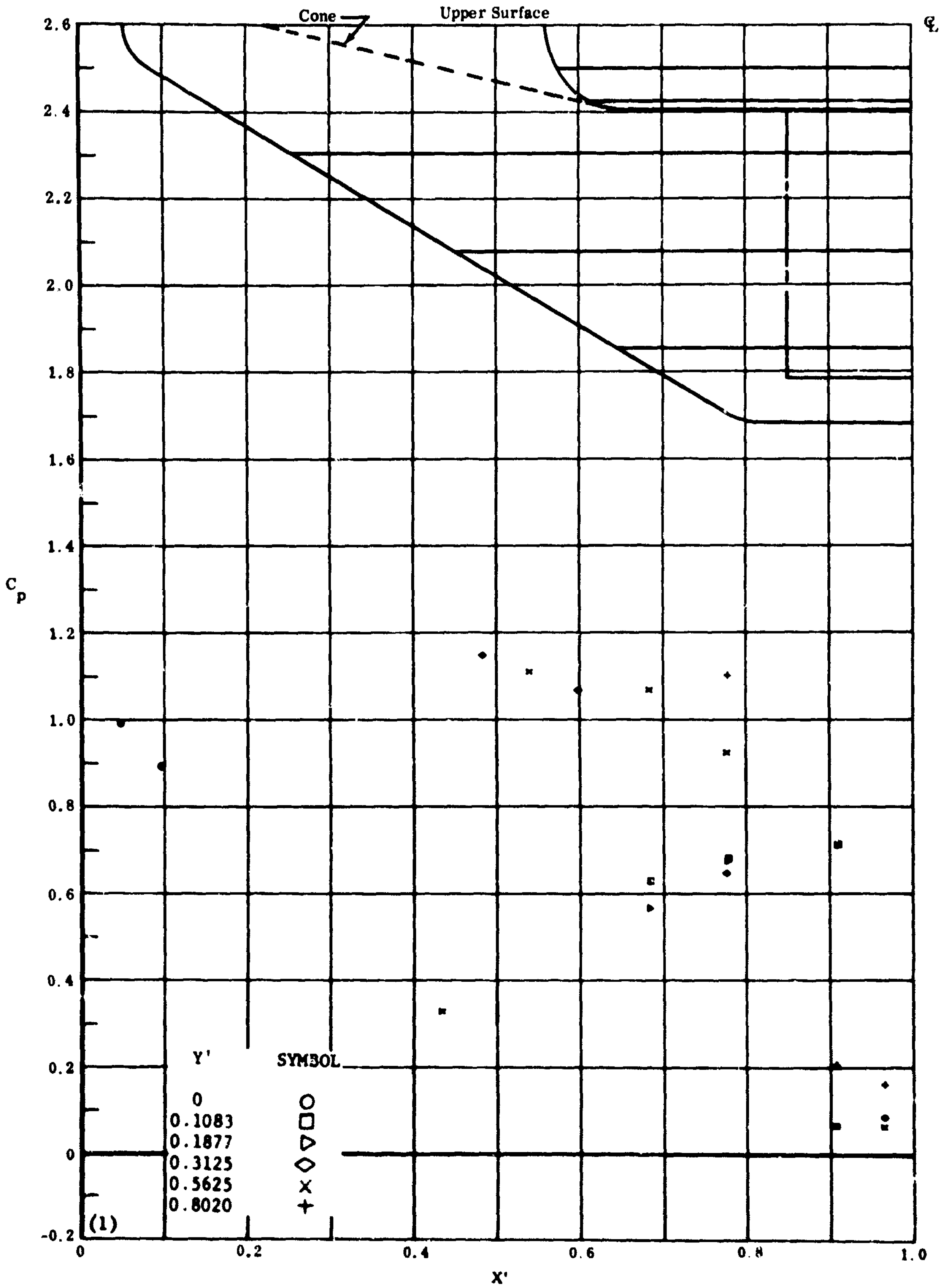

(NONDIMENSIONAL STREAMWISE DISTANCE FROM VIRTUAL APEX)

Fig. 461 Configuration IV, α = -40 , $\delta_2 = \delta_3$ = +39

C_p vs. X', upper surface

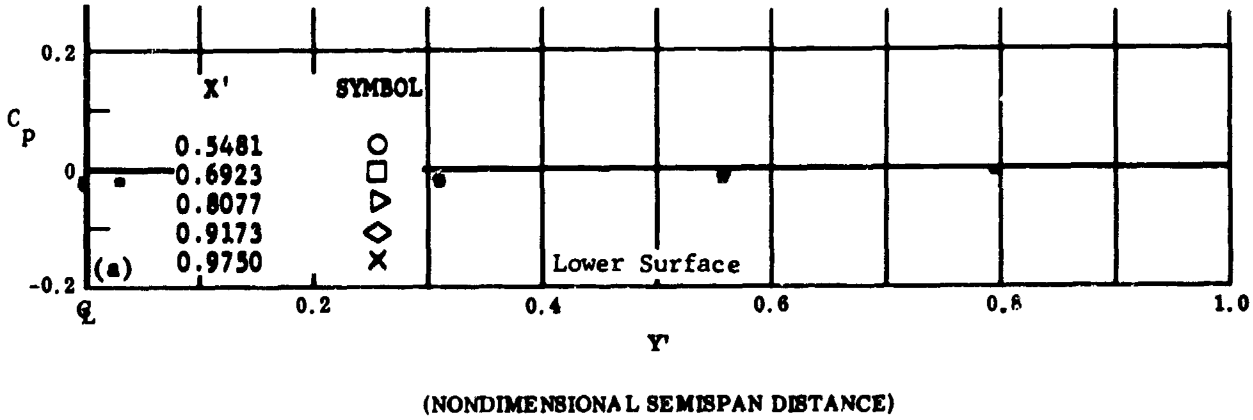

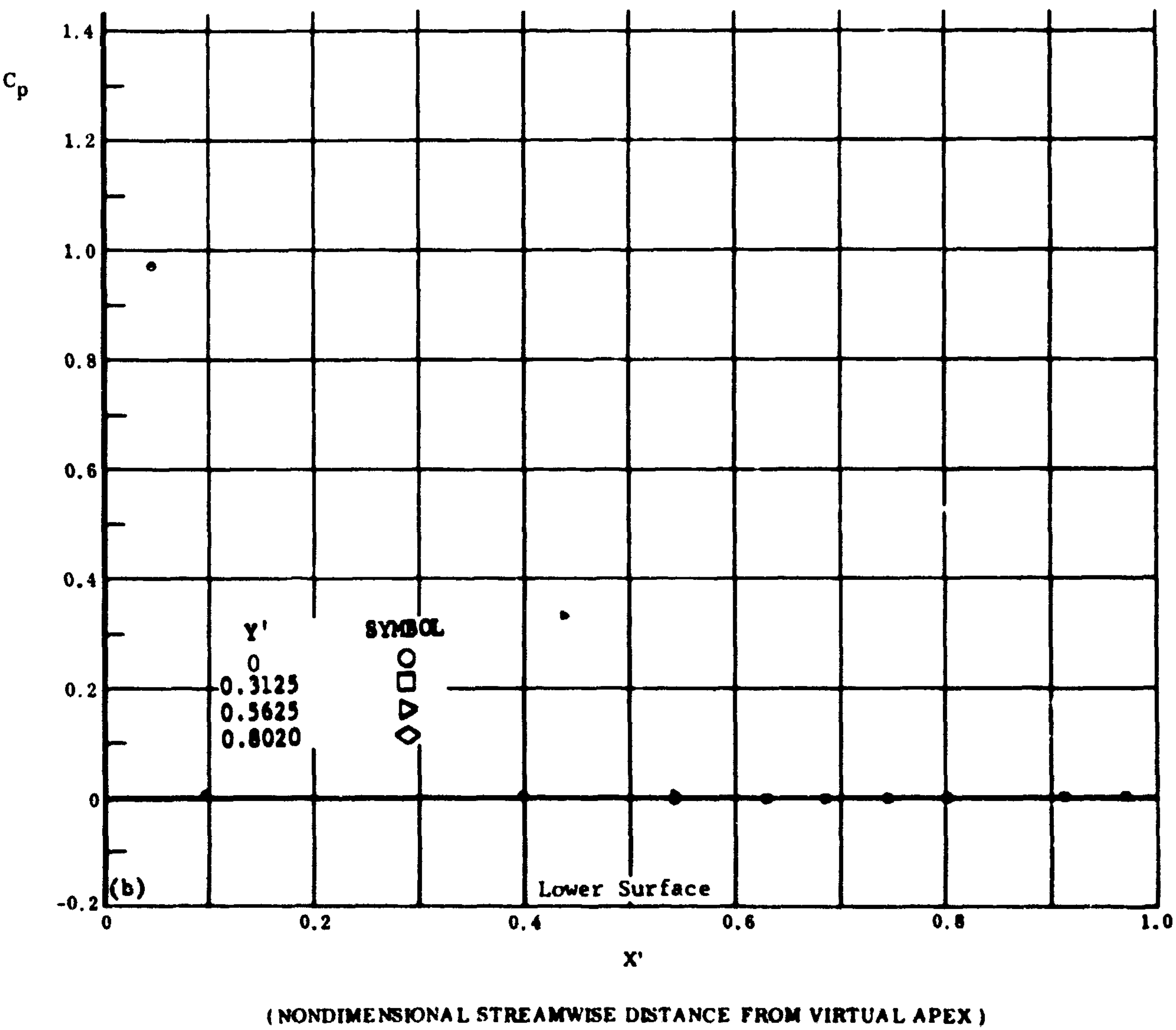

Fig. 47 Configuration IV, α = -40 , $\delta_2 = \delta_3$ = -10

a) C_p vs. Y', lower surface

b) C_p vs. X', lower surface

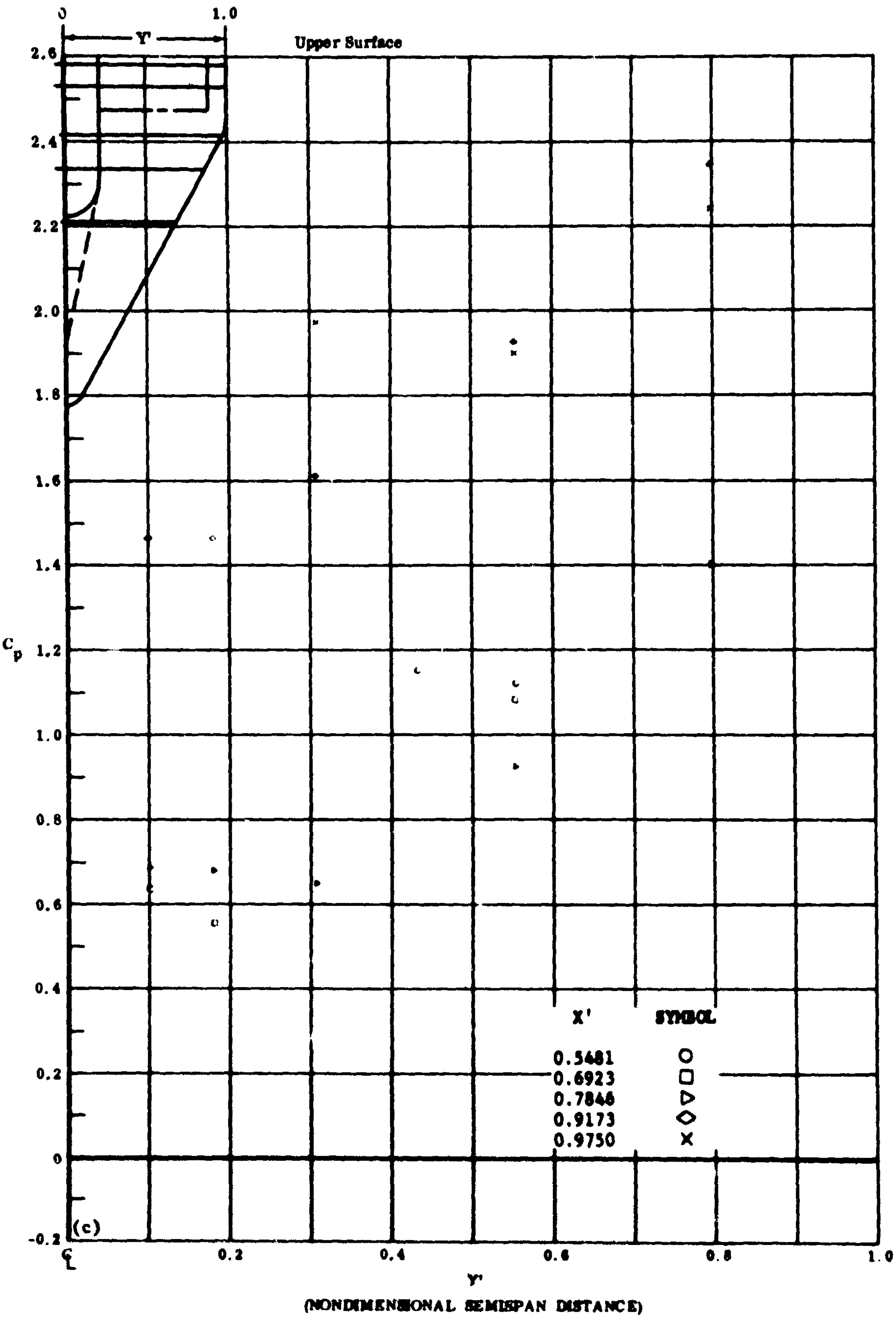

Fig. 47c Configuration IV, α = -40 , $\delta_2 = \delta_3$ =-10

C_p vs. Y', upper surface

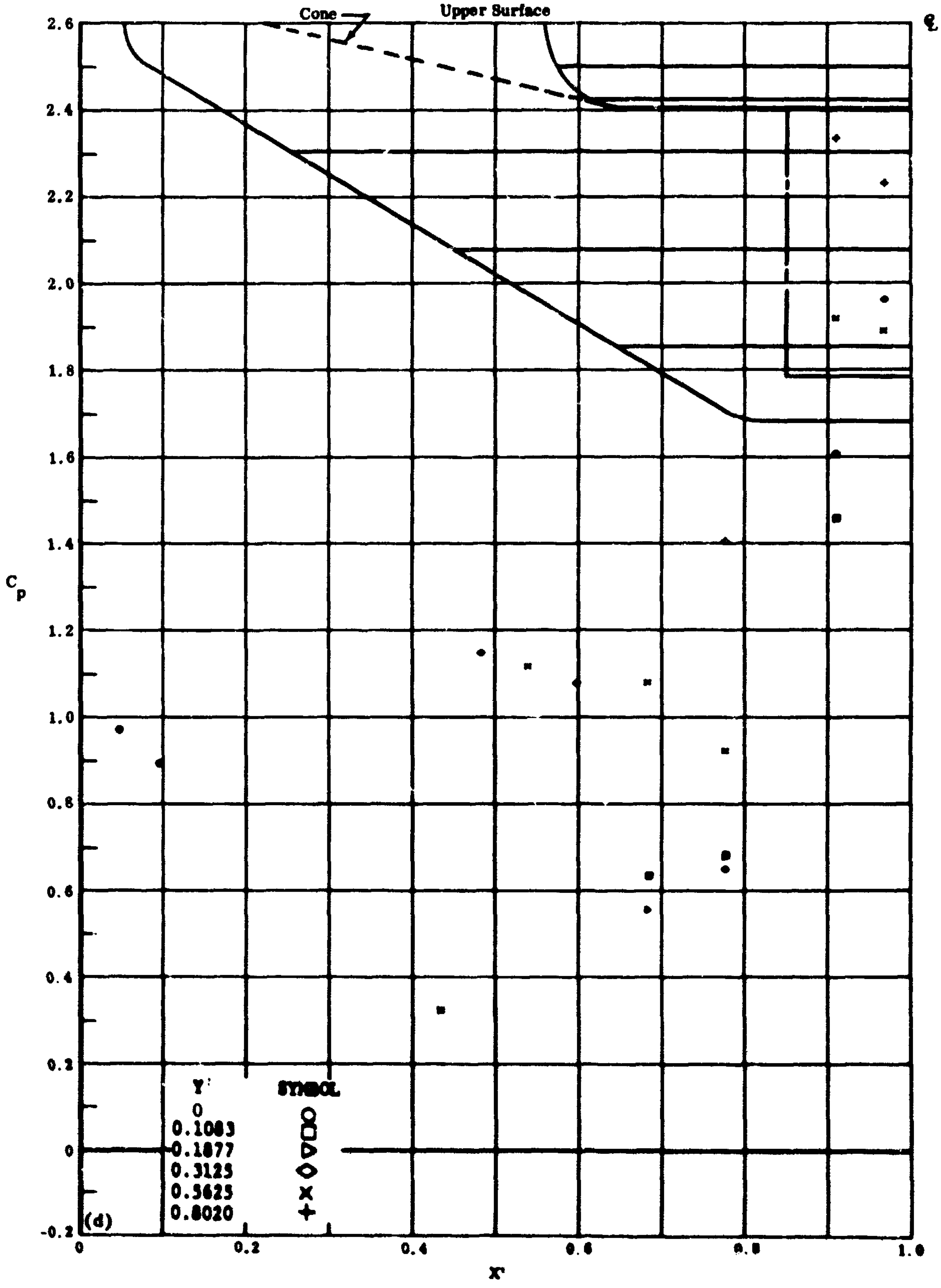

(NONDIMENSIONAL STREAMWISE DISTANCE FROM VIRTUAL APEX)

Fig. 47d Configuration IV, $\alpha = -40$, $\delta_2 = \delta_3 = -10$

C_p vs. X', upper surface

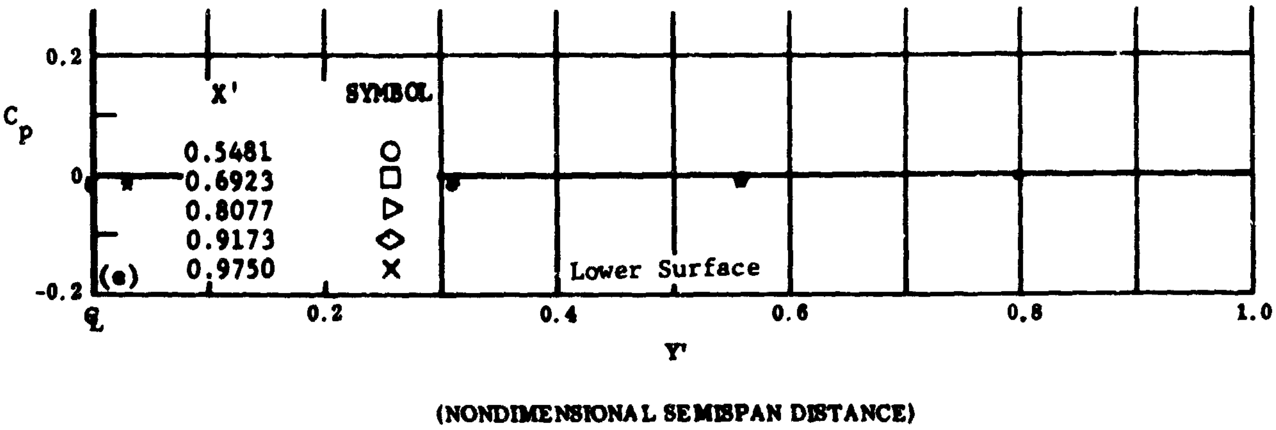

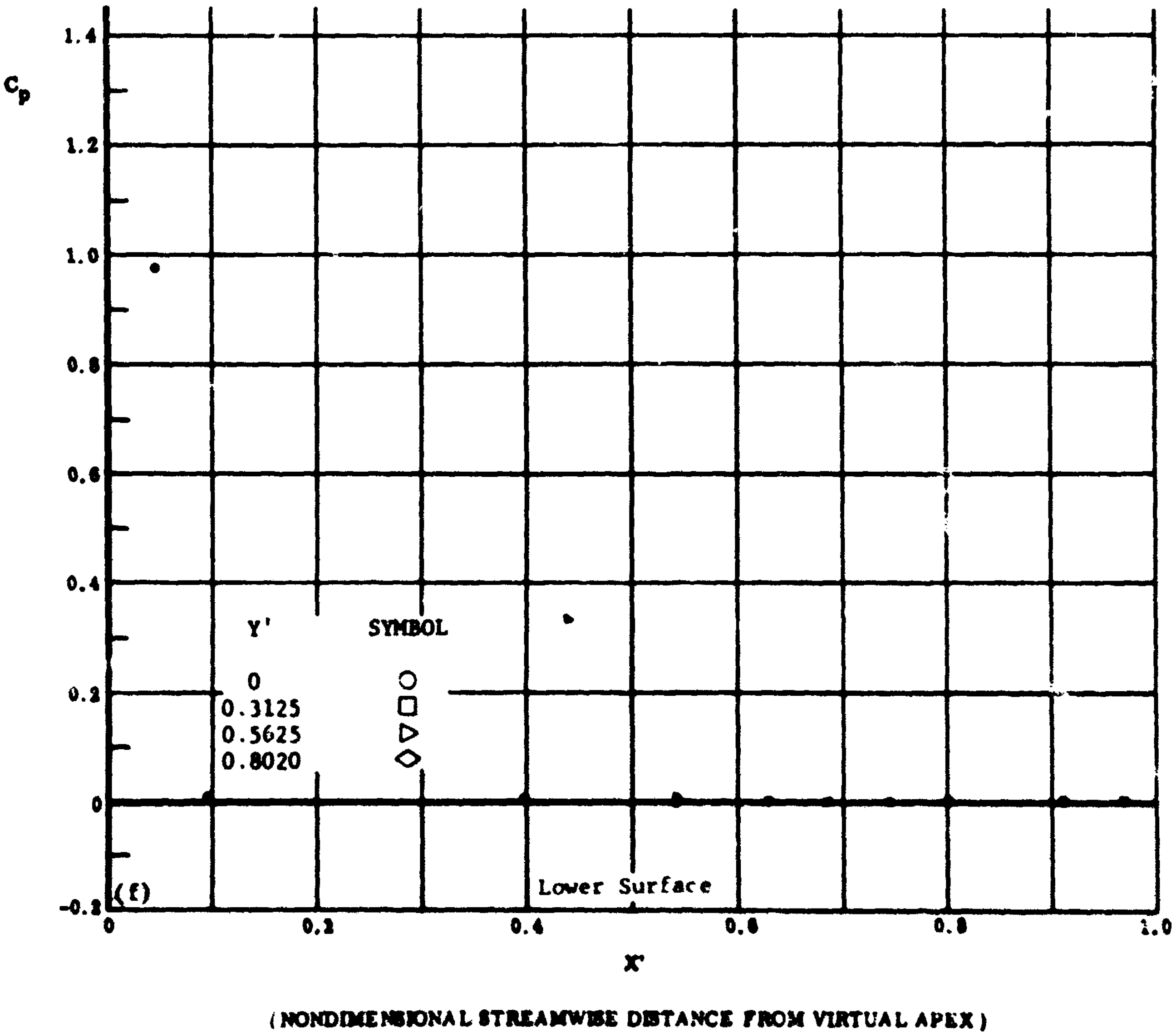

Fig. 47 Configuration IV, $\alpha = -40$, $\delta_2 = \delta_3 = -20$

e) C_p vs. Y', lower surface

f) C_p vs. X', lower surface

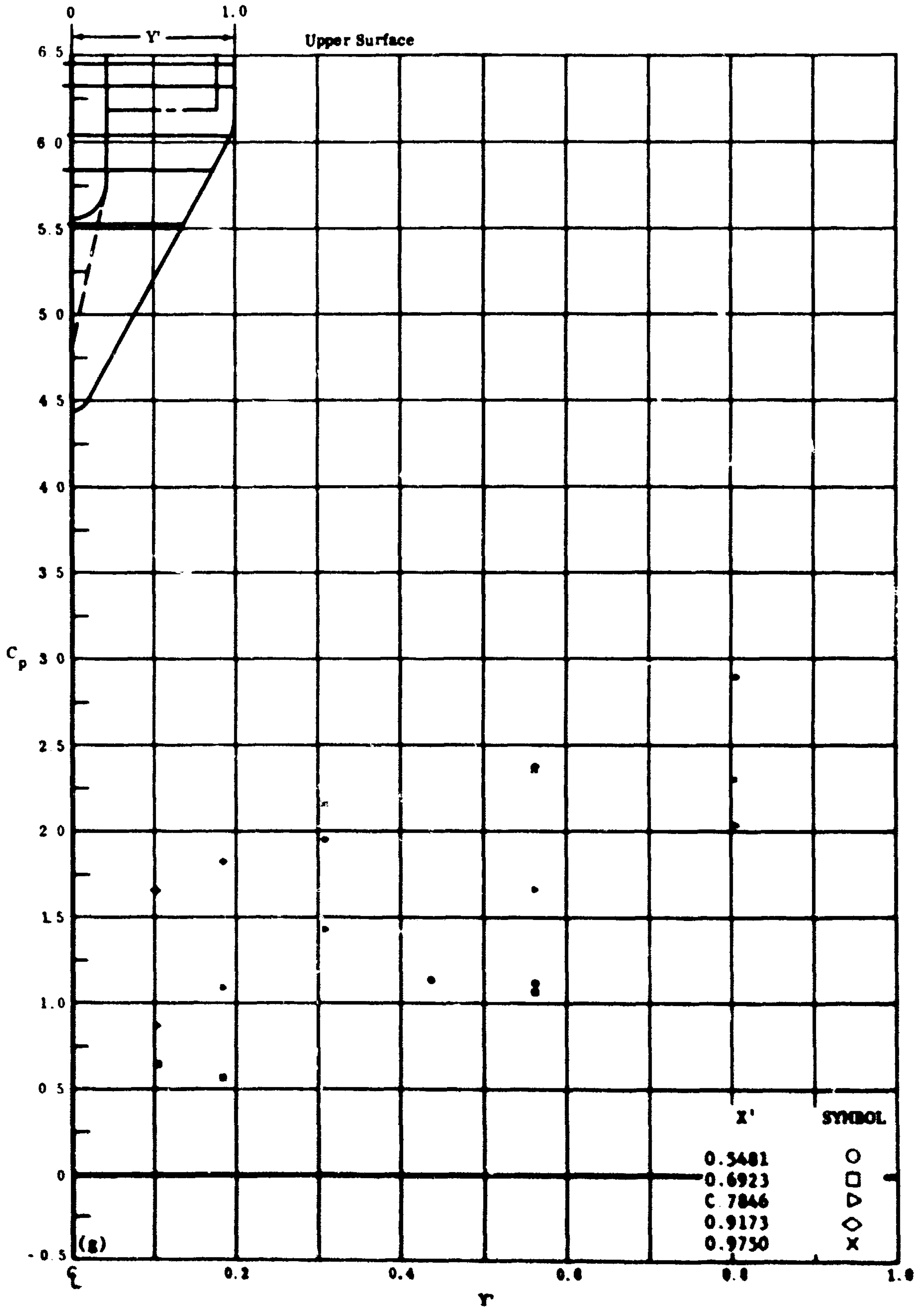

Fig. 47g Configuration IV, $\alpha = -40$, $\delta_2 = \delta_3 = -20$

C_p vs. Y', upper surface

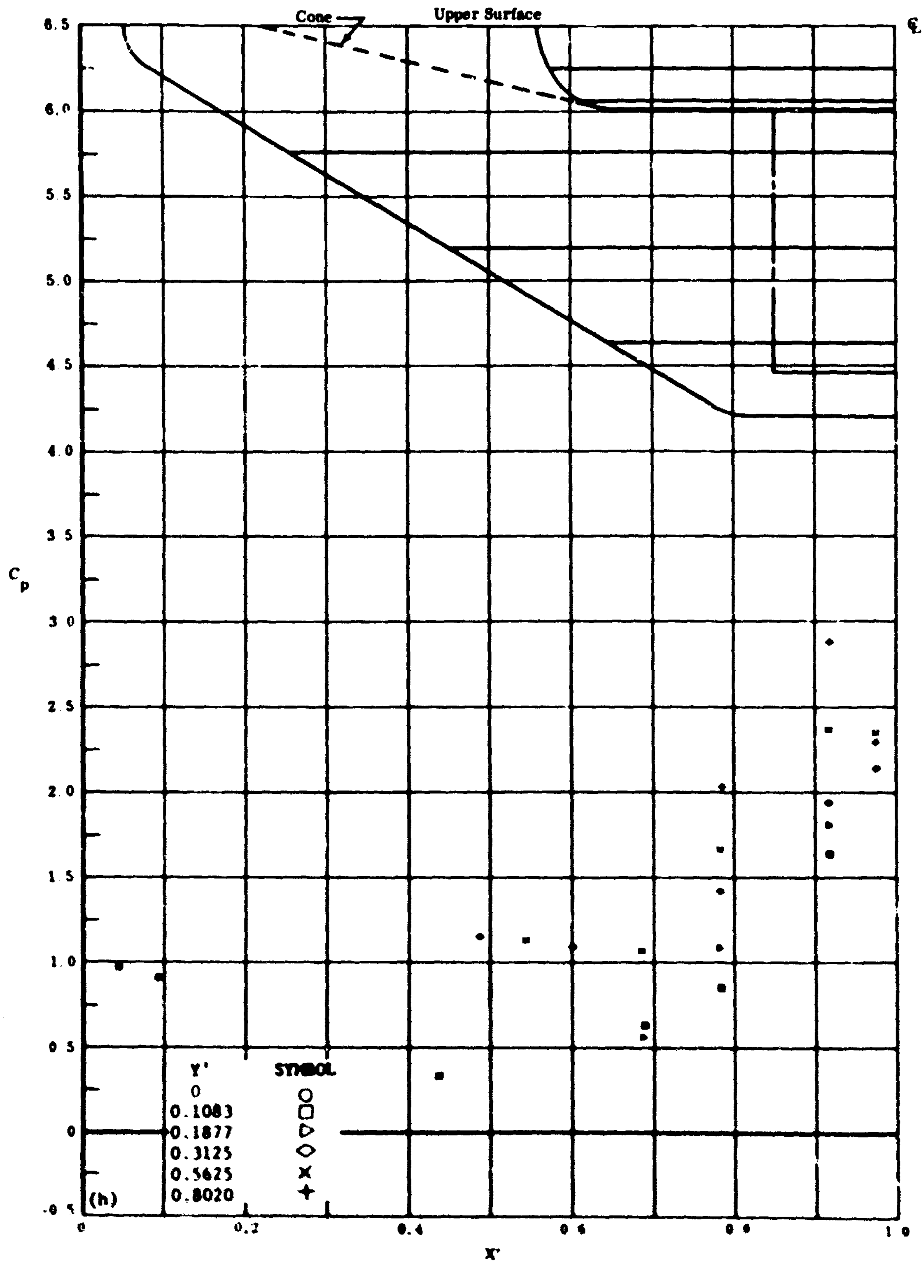

(NONDIMENSIONAL STREAMWISE DISTANCE FROM VIRTUAL APEX)

Fig. 47h Configuration IV, $\alpha = -40$, $\delta_2 = \delta_3 = -20$

C_p vs. X', upper surface

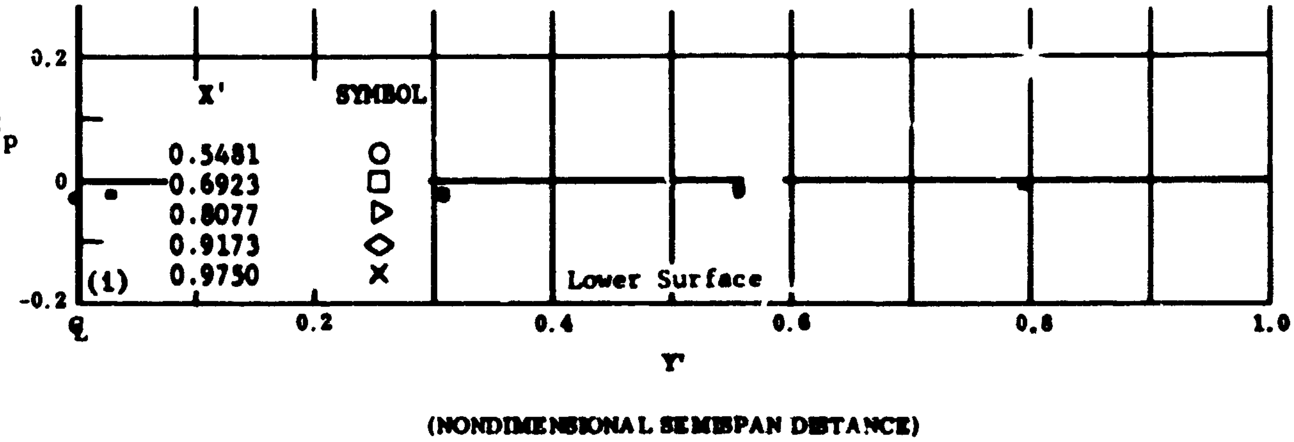

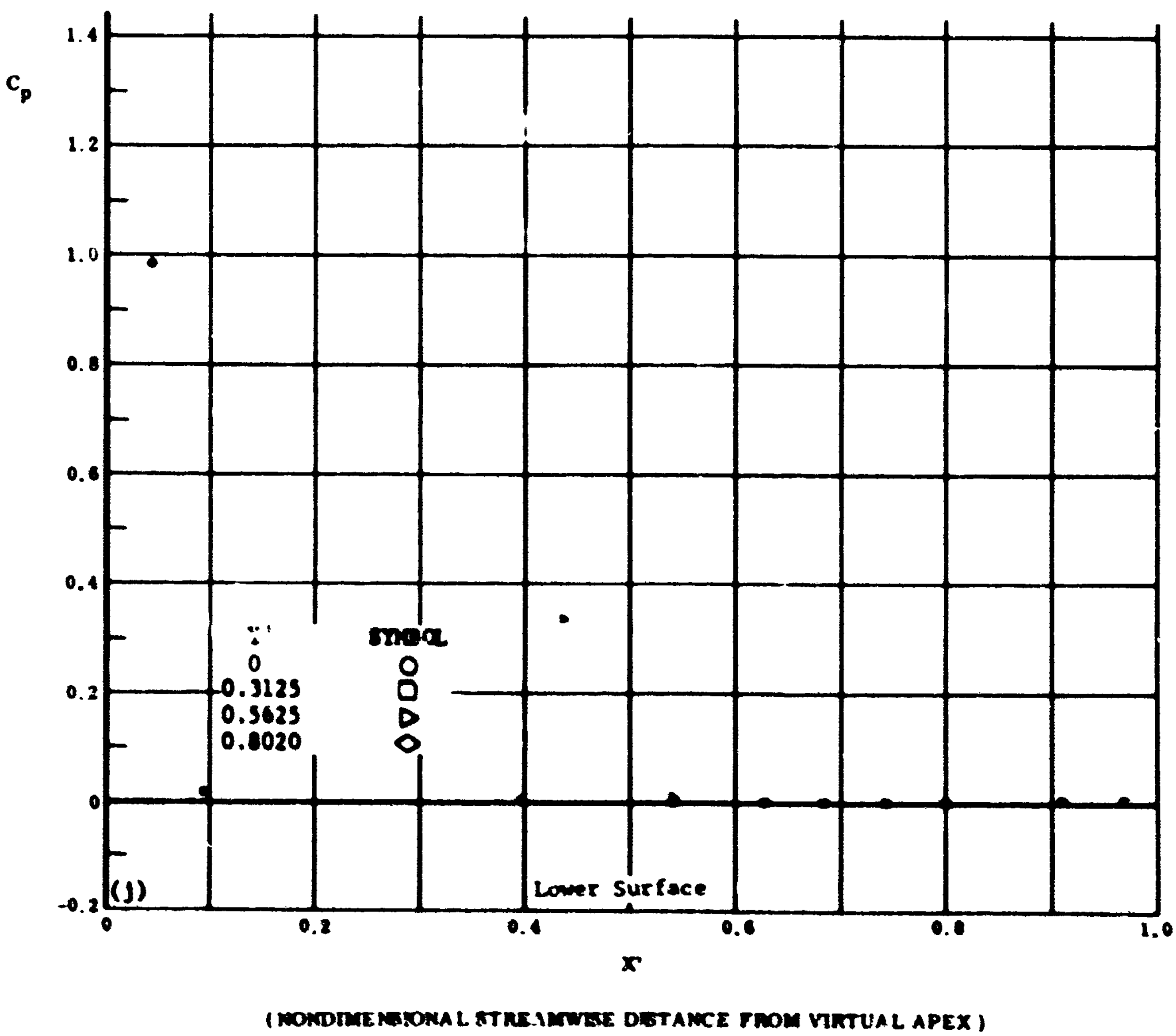

Fig. 47 Configuration IV, $\alpha = -40$, $\delta_2 = \delta_3 = -30$

i) C_p vs. Y', lower surface

j) C_p vs. X', lower surface

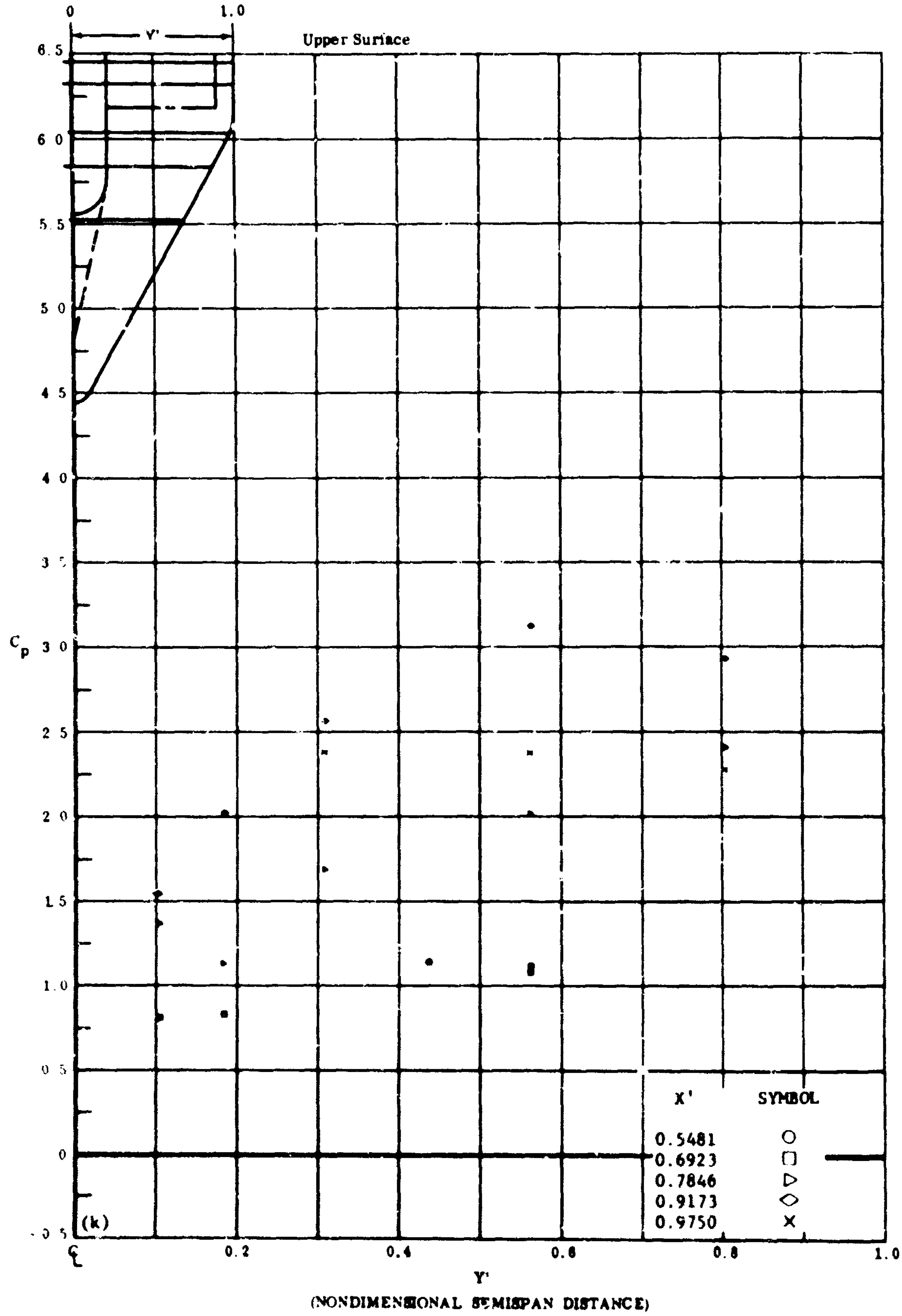

Fig. 47k Configuration IV, $\alpha = -40$, $\delta_2 = \delta_3 = -30$

C_p vs. Y', upper surface

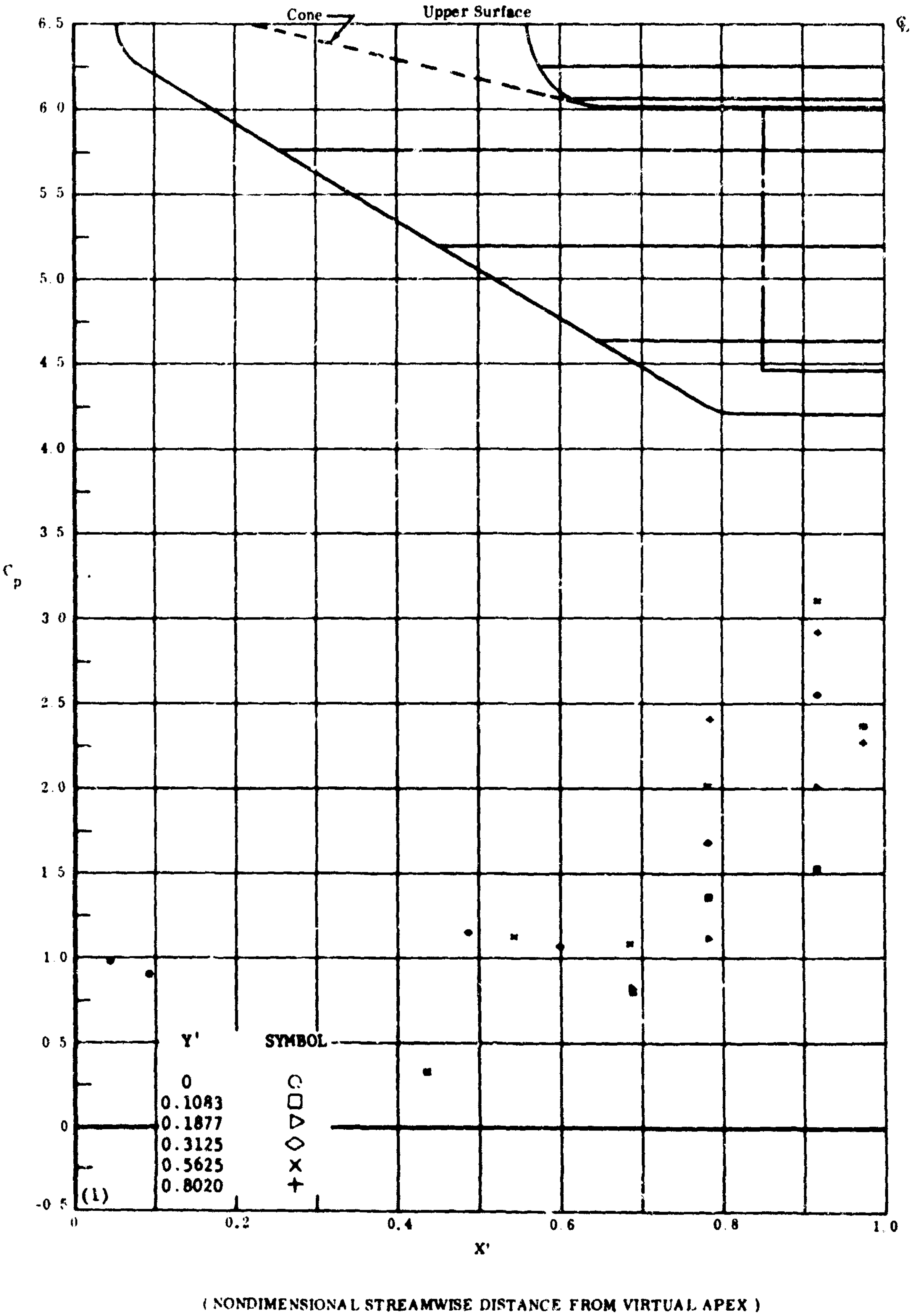

Fig. 471 Configuration IV, $\alpha = -40$, $\delta_2 = \delta_3 = -30$

C_p vs. X', upper surface

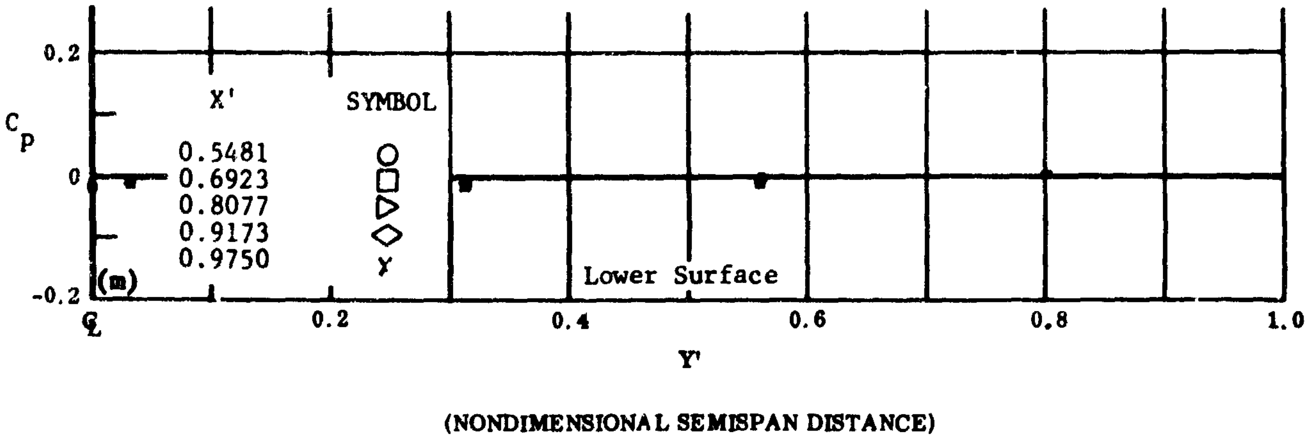

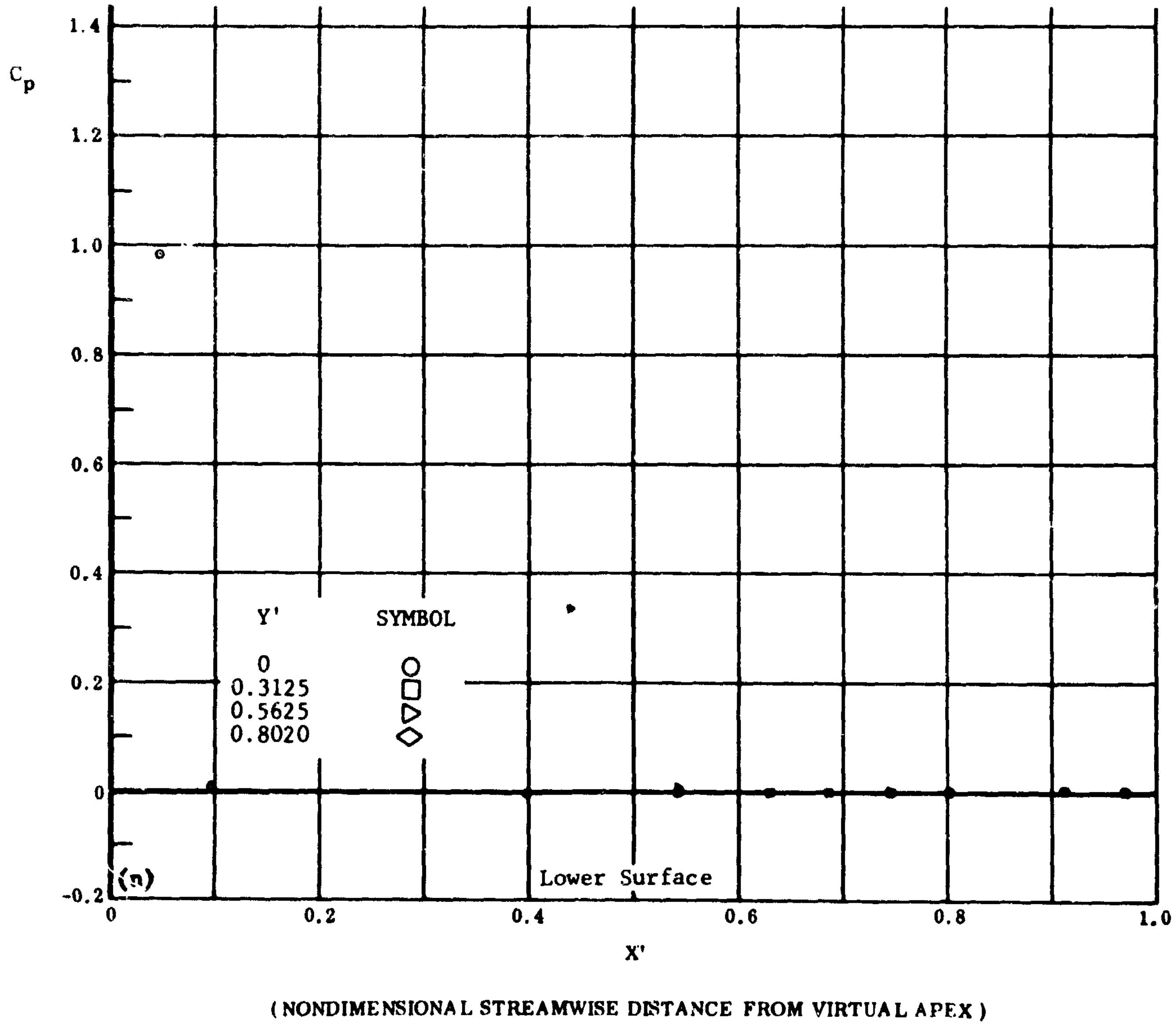

Fig. 47 Configuration IV, $\alpha = -40$, $\delta_2 = \delta_3 = -39$

m) C_p vs. Y', lower surface

n) C_p vs. X', lower surface

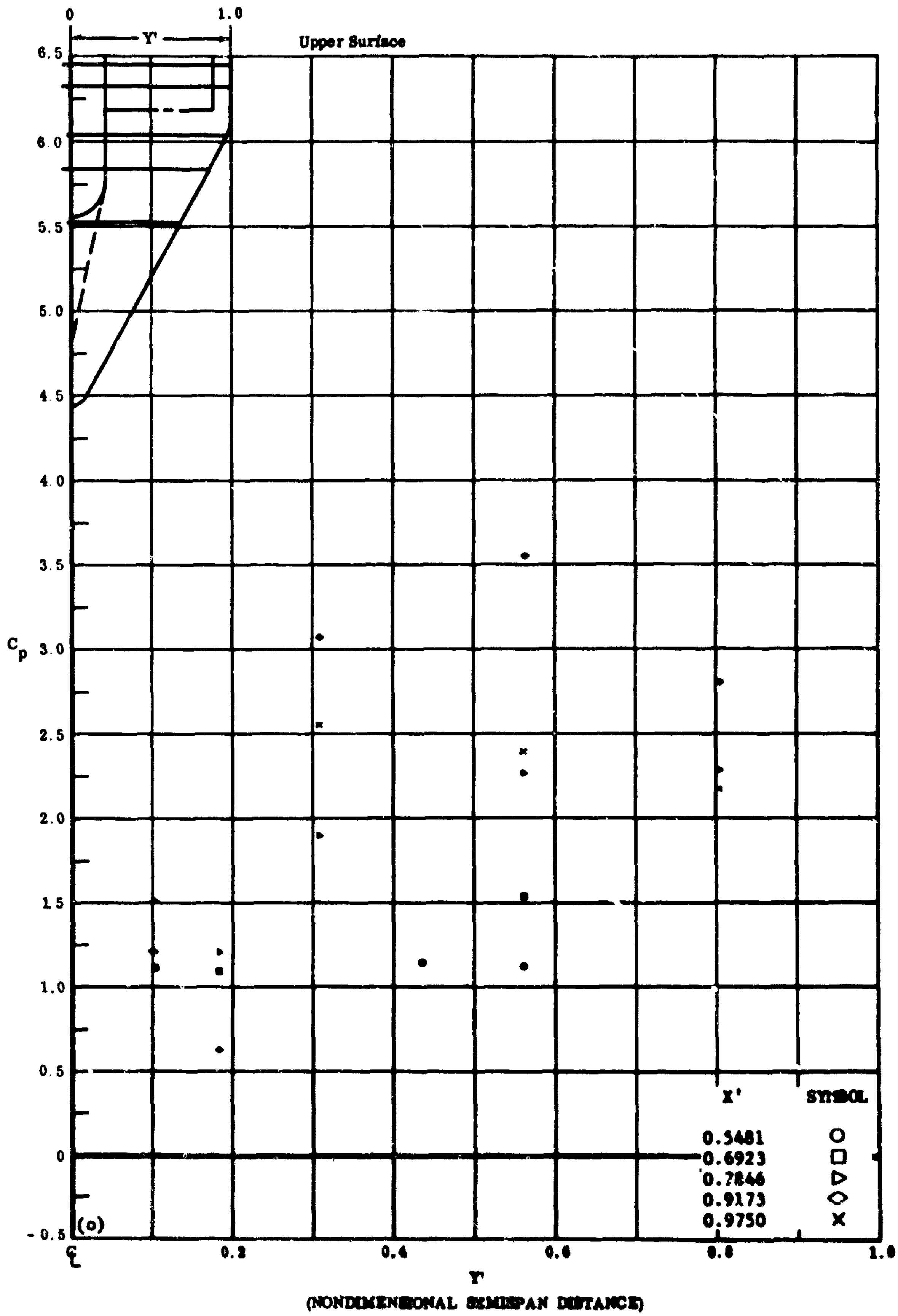

Fig. 47o Configuration IV, $\alpha = -40$, $\delta_2 = \delta_3 = -39$

C_p vs. Y', upper surface

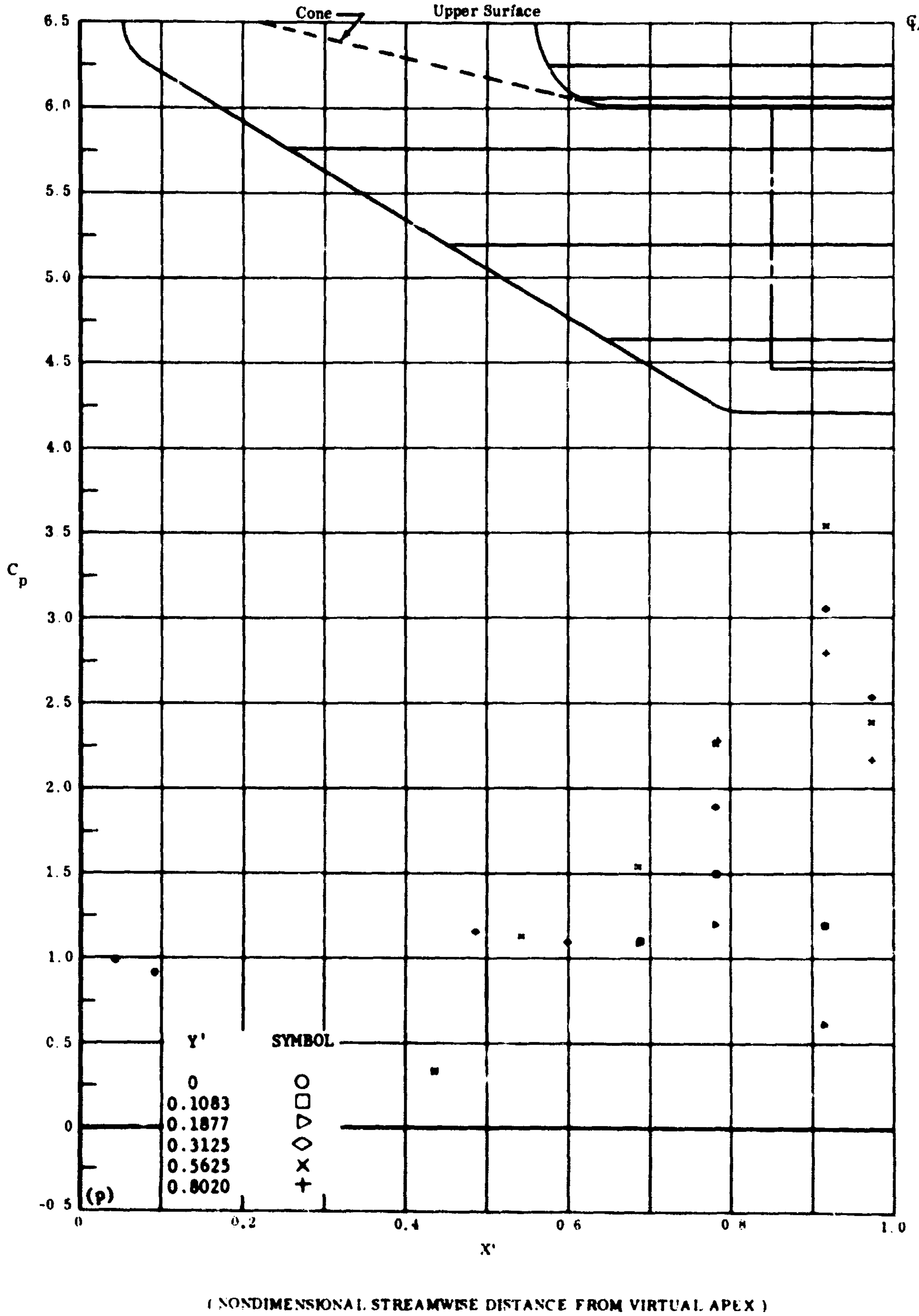

Fig. 47p Configuration IV, $\alpha = -40$, $\delta_2 = \delta_3 = -39$

C_p vs. X', upper surface

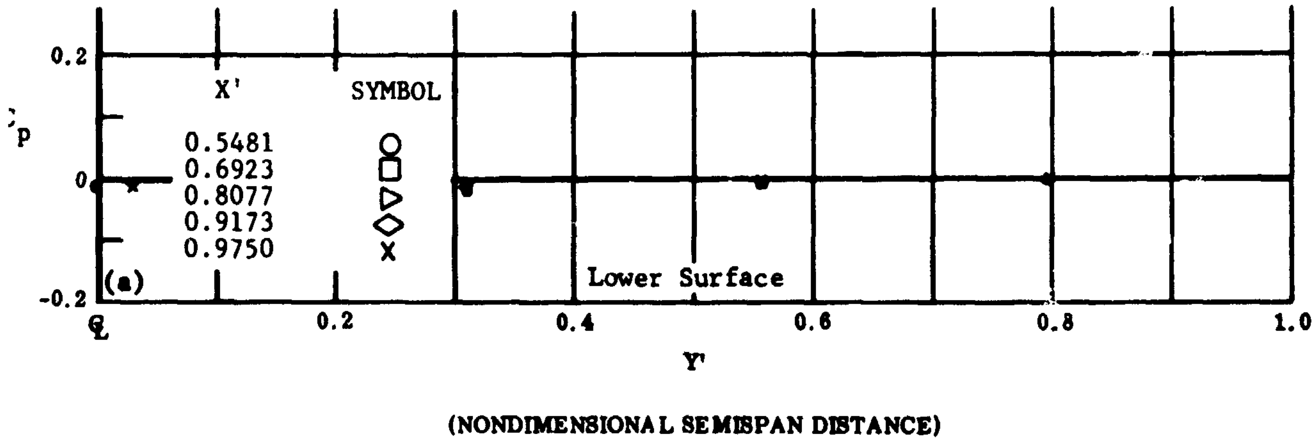

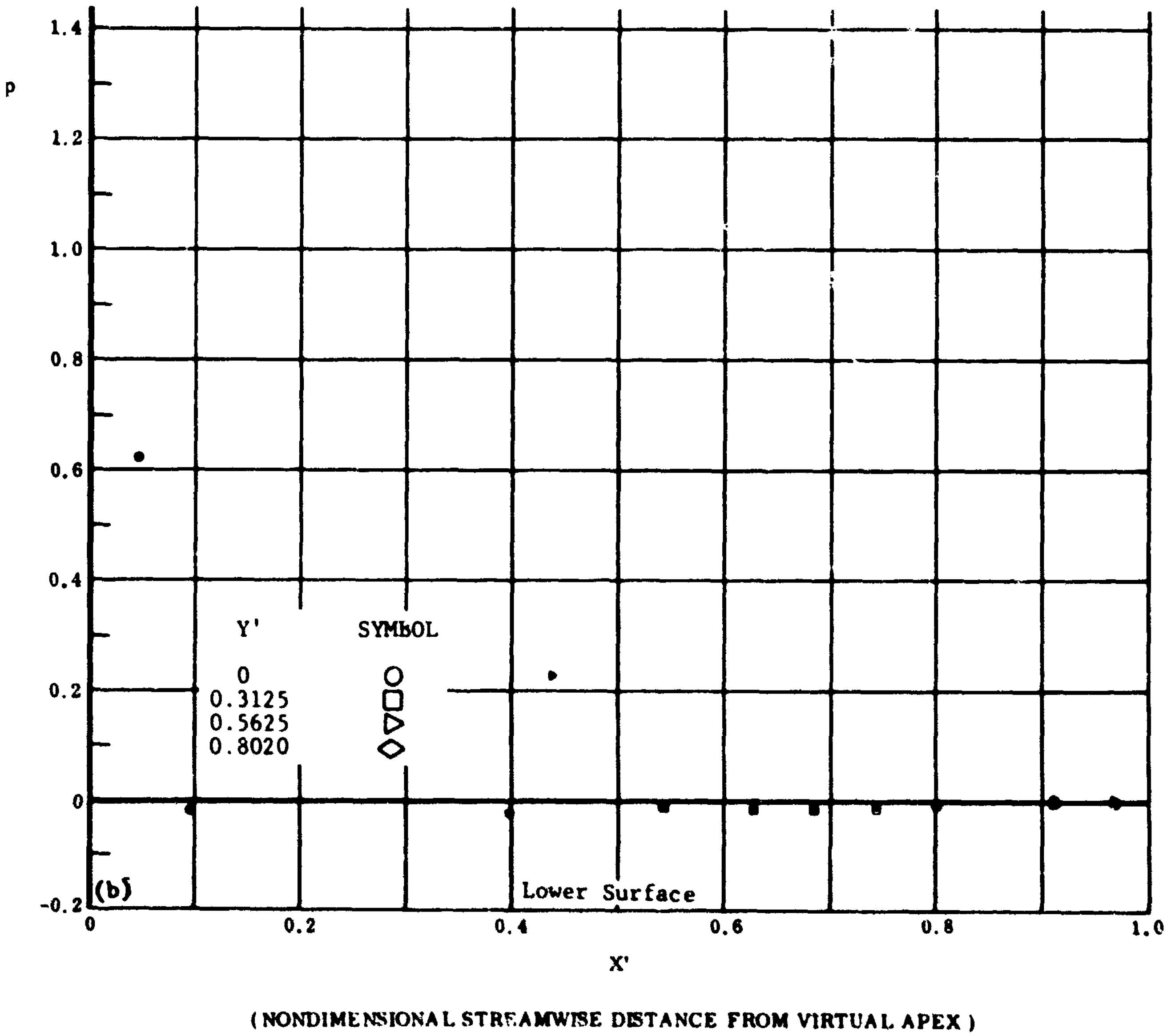

Fig. 48 Configuration IV, $\alpha = -50$, $\delta_2 = \delta_3 = 0$

a) C_p vs. Y', lower surface

b) C_p vs. X', lower surface

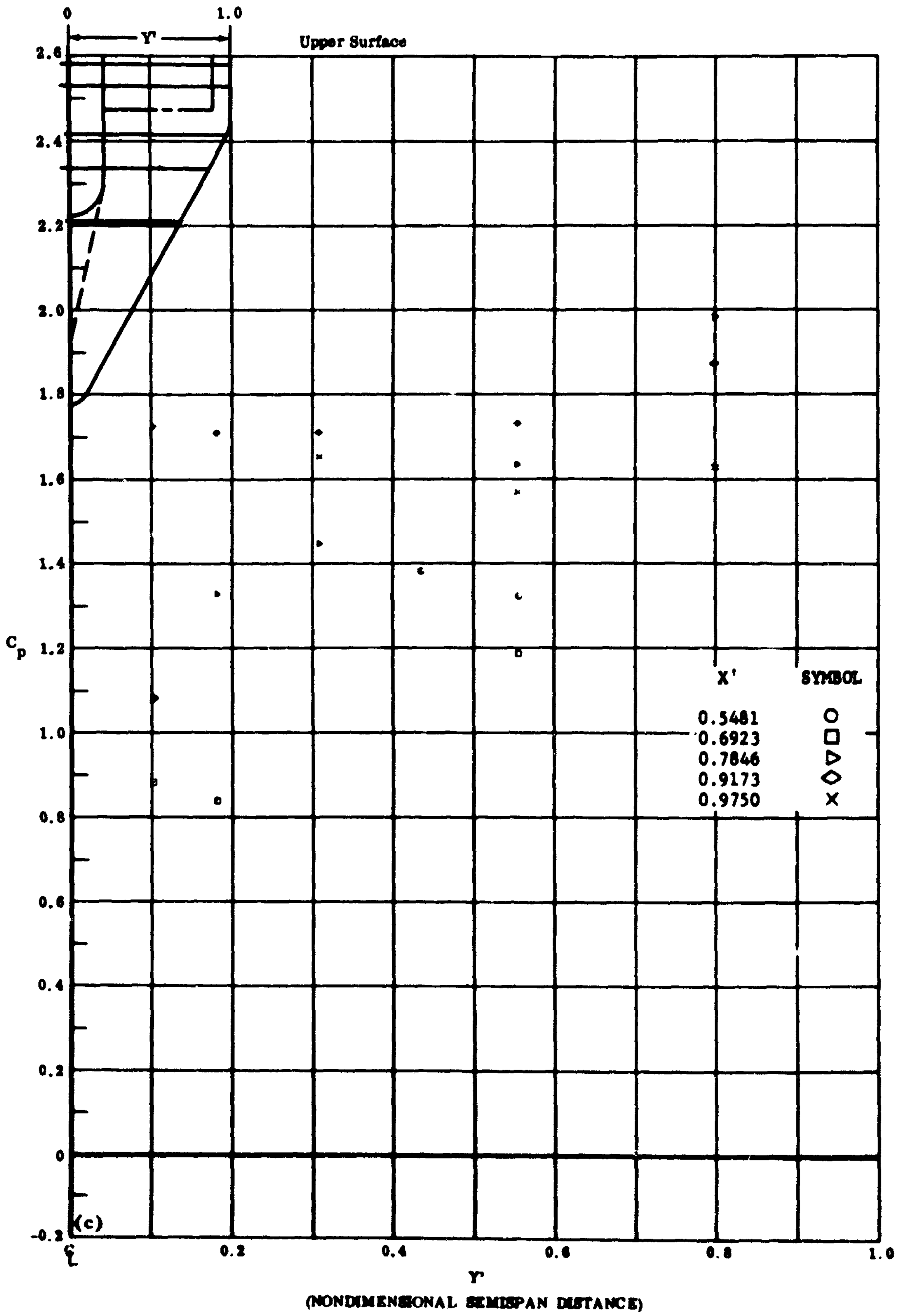

Fig. 48c Configuration IV, $\alpha = -50$, $\delta_2 = \delta_3 = 0$

C_p vs. Y', upper surface

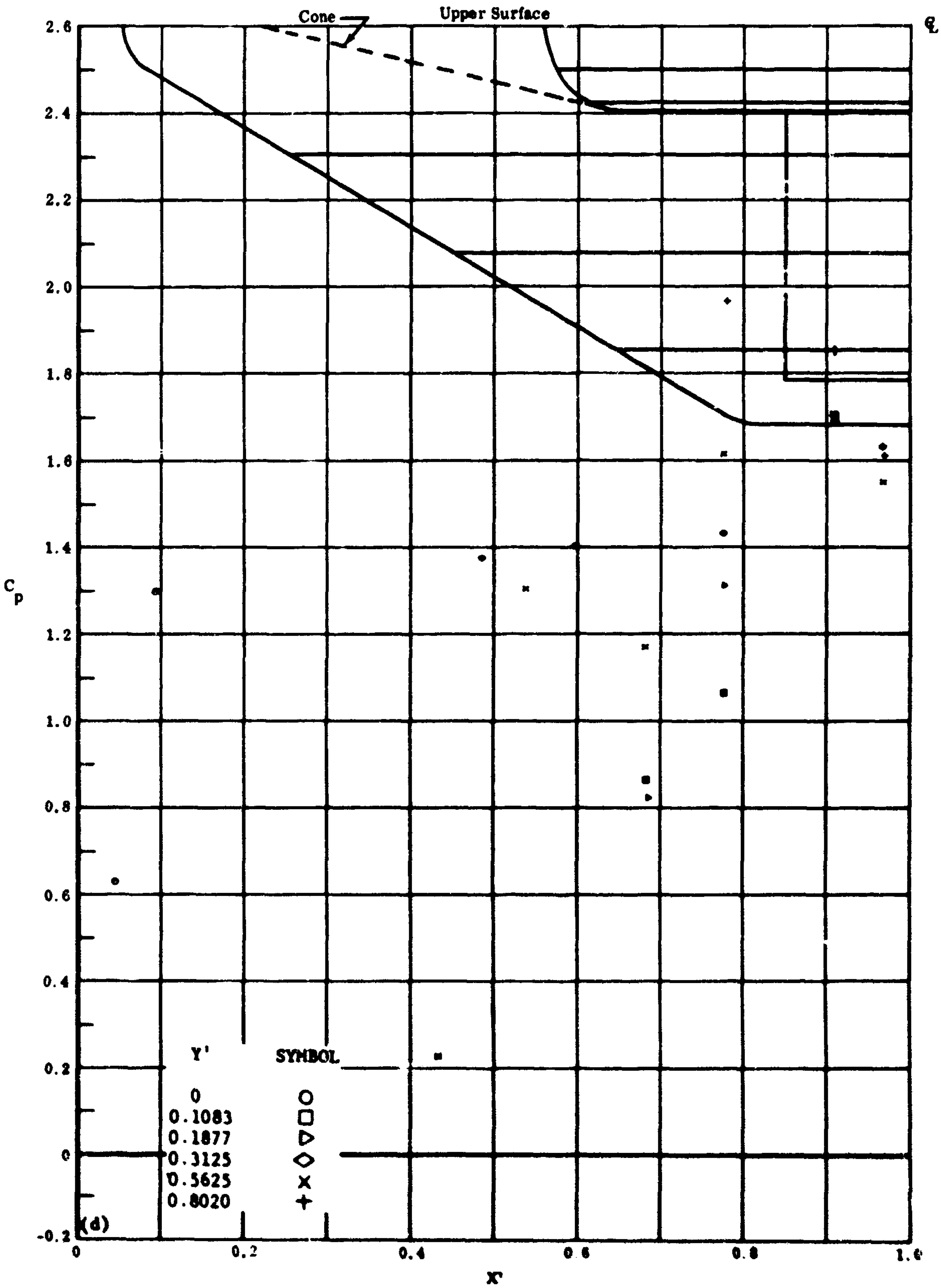

(NONDIMENSIONAL STREAMWISE DISTANCE FROM VIRTUAL APEX)

Fig. 48d Configuration IV, $\alpha = -50$, $\delta_2 = \delta_3 = 0$

C_p vs. X', upper surface

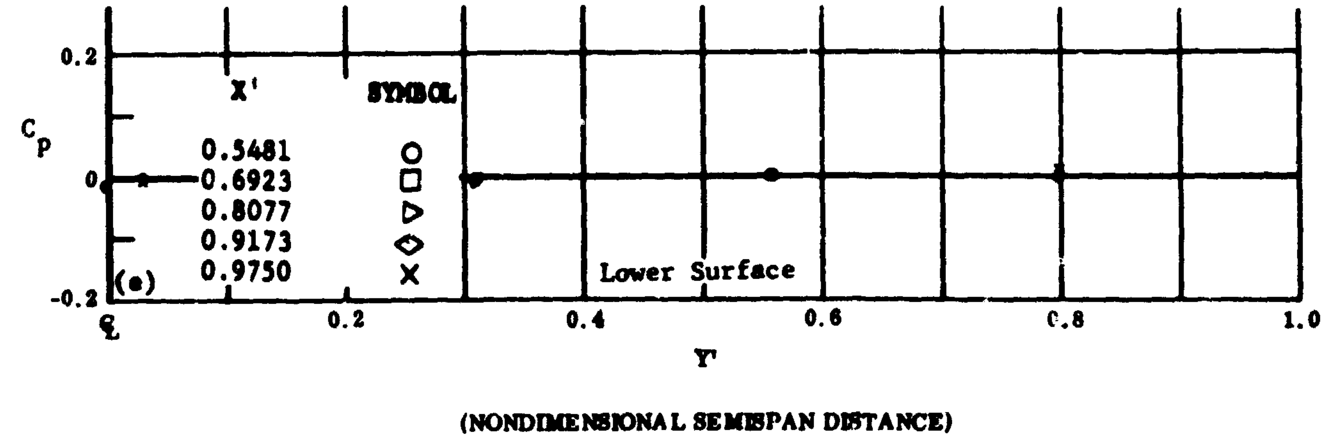

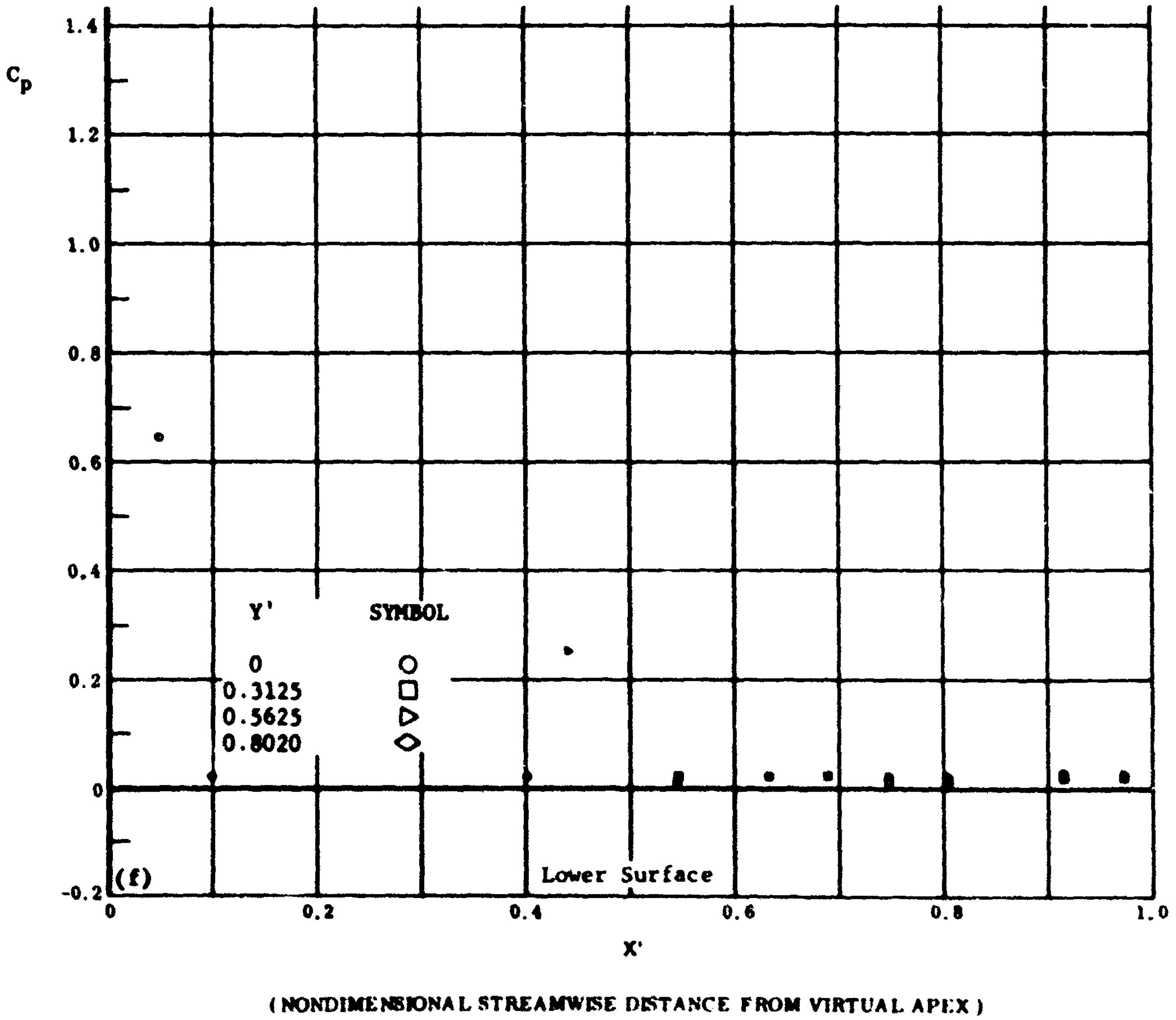

Fig. 48 Configuration IV, $\alpha = -50$, $\delta_2 = \delta_3 = +20$

e) C_p vs. Y', lower surface

f) C_p vs. X', lower surface

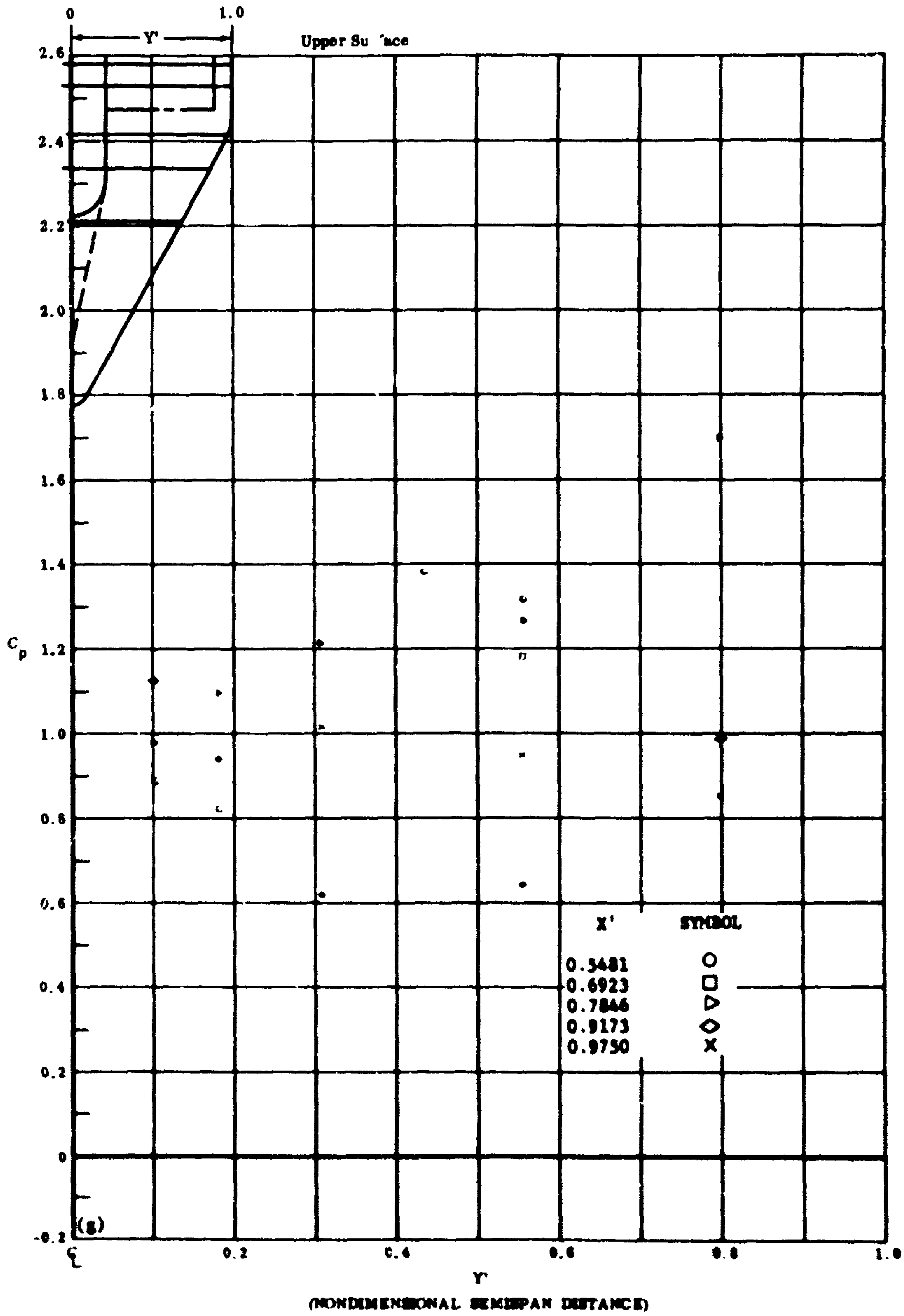

Fig. 48g Configuration IV, $\alpha = -50$, $\delta_2 = \delta_3 = +20$

C_p vs. Y', upper surface

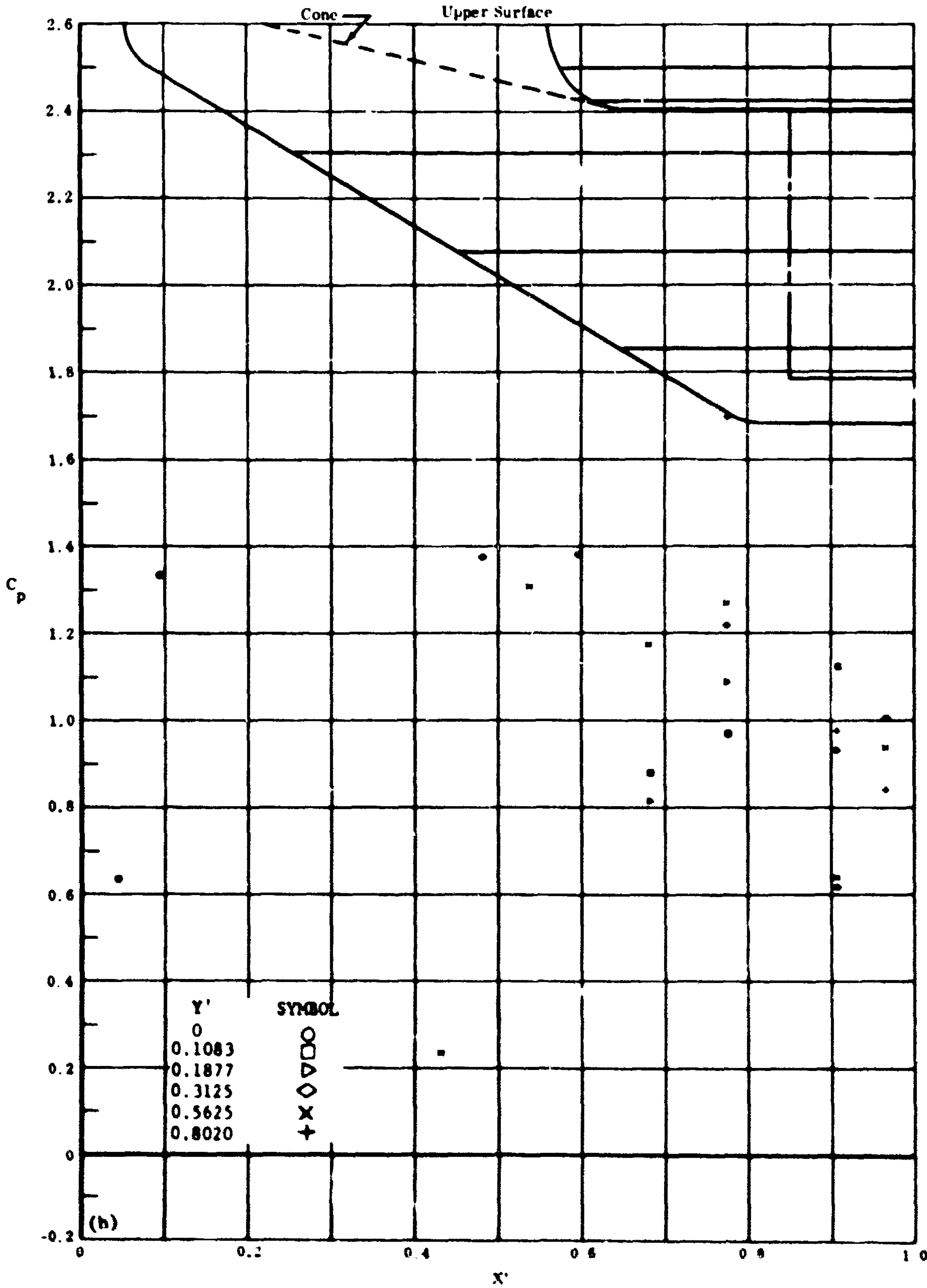

(NONDIMENSIONAL STREAMWISE DISTANCE FROM VIRTUAL APEX)

Fig. 48h Configuration IV, $\iota = -50$, $\delta_2 = \delta_3 = +20$

C_p vs. X', upper surface

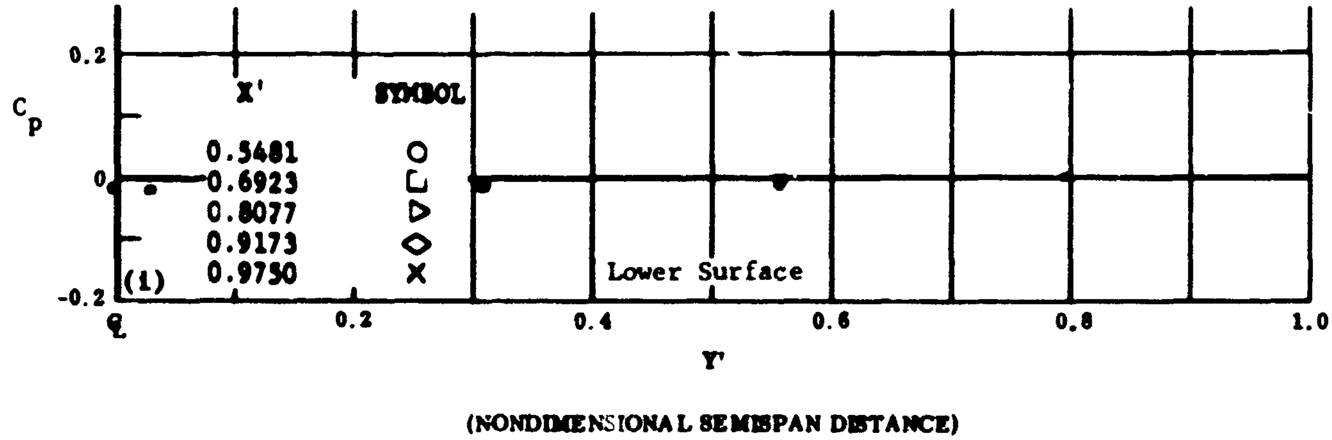

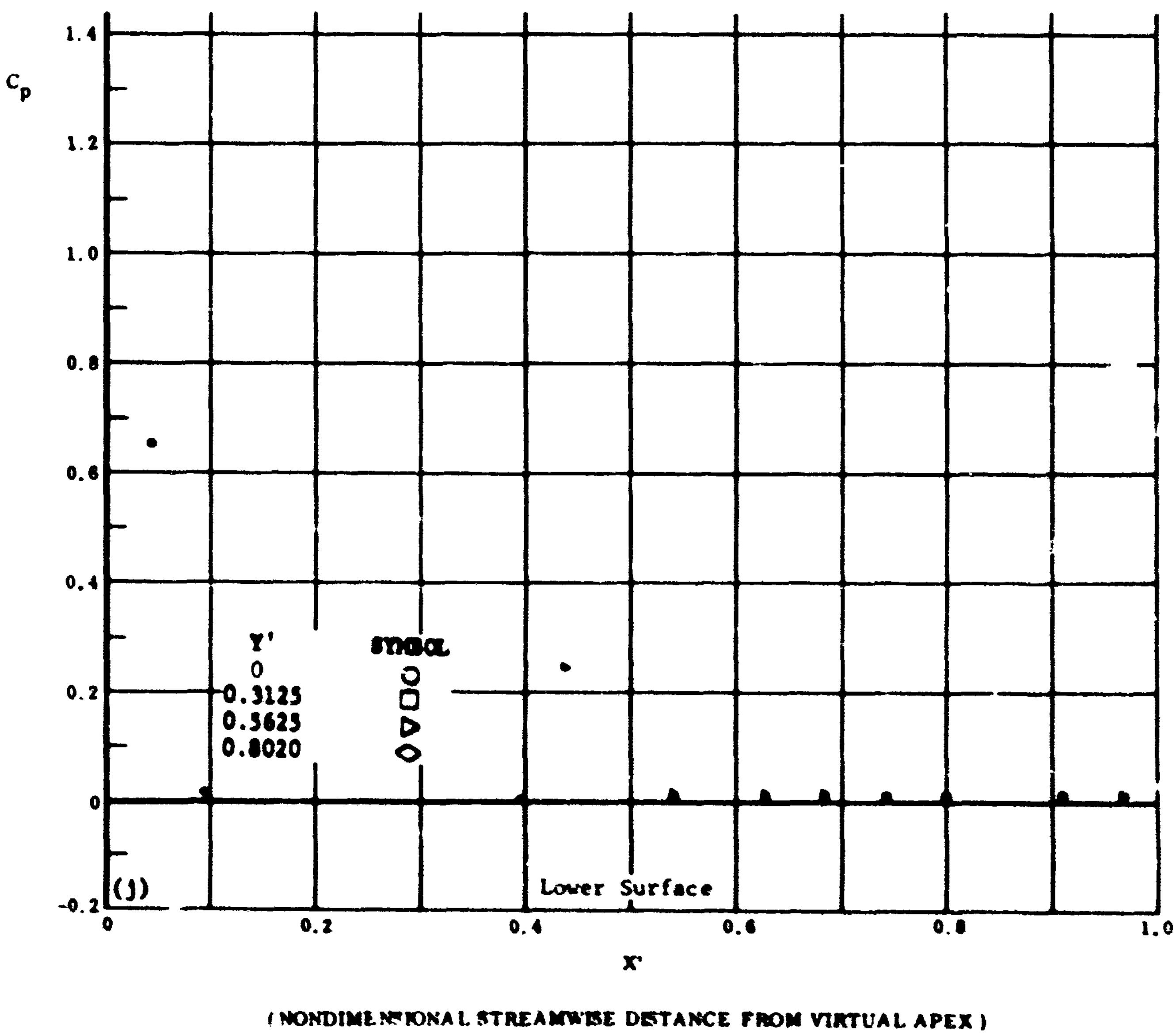

Fig. 48 Configuration IV, α = -50 , $\delta_2 = \delta_3$ = +39

i) C_p vs. Y', lower surface

j) C_p vs. X', lower surface

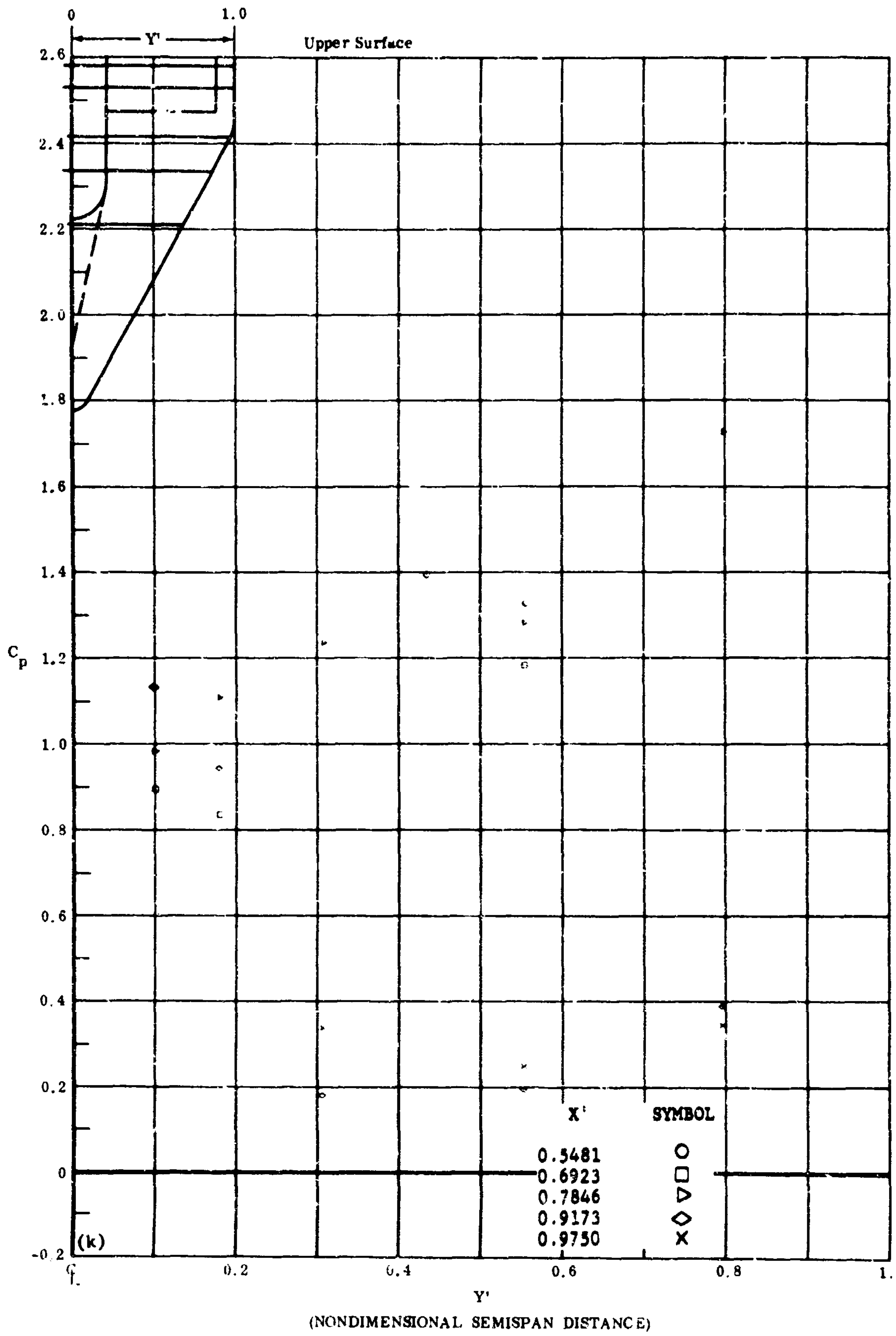

Fig. 48k Configuration IV, α = -50 , $\delta_2 = \delta_3$ = +39

C_p vs. Y', upper surface

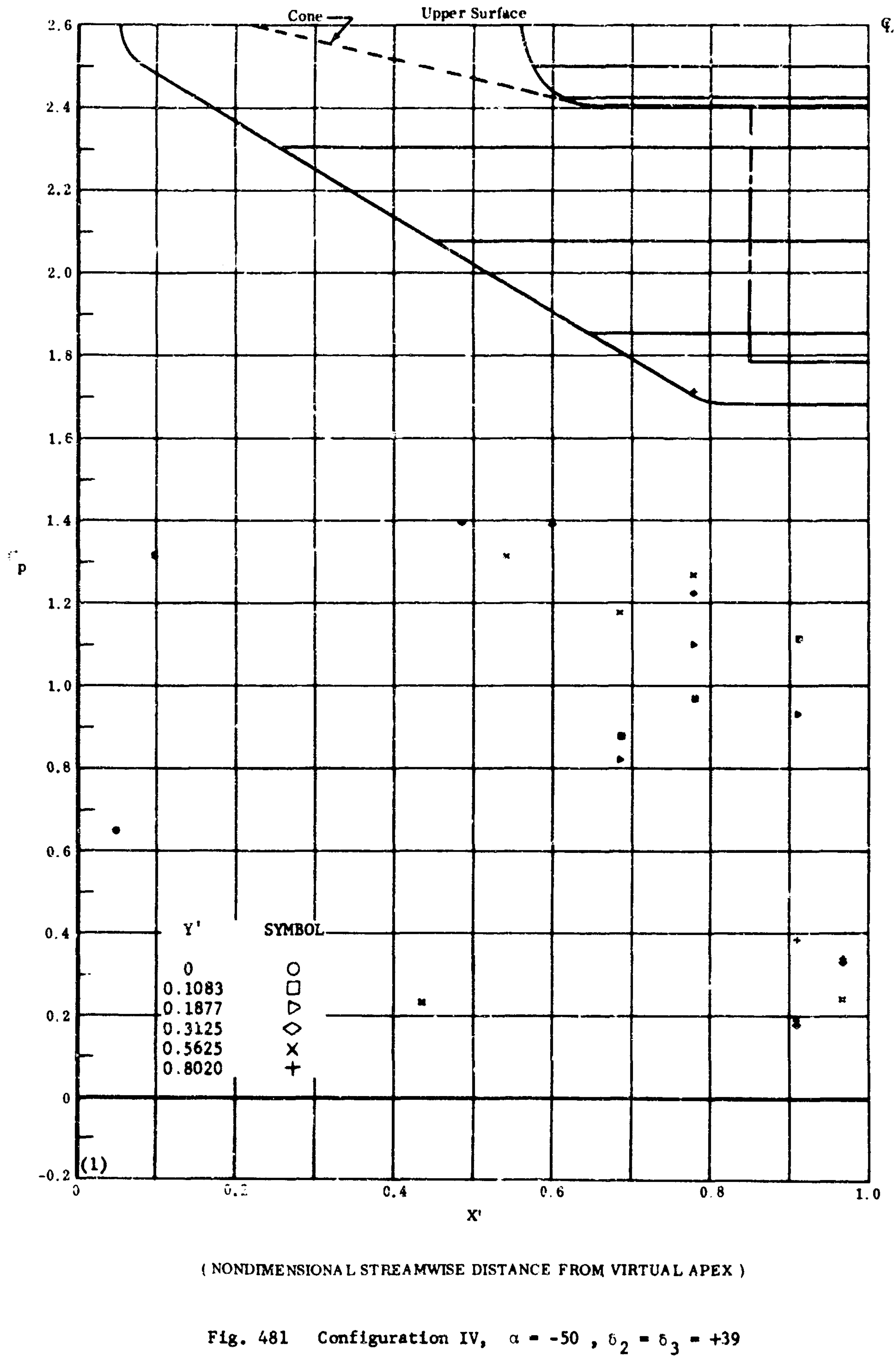

Fig. 481 Configuration IV, α = -50 , $\delta_2 = \delta_3$ = +39

C_p vs. X', upper surface

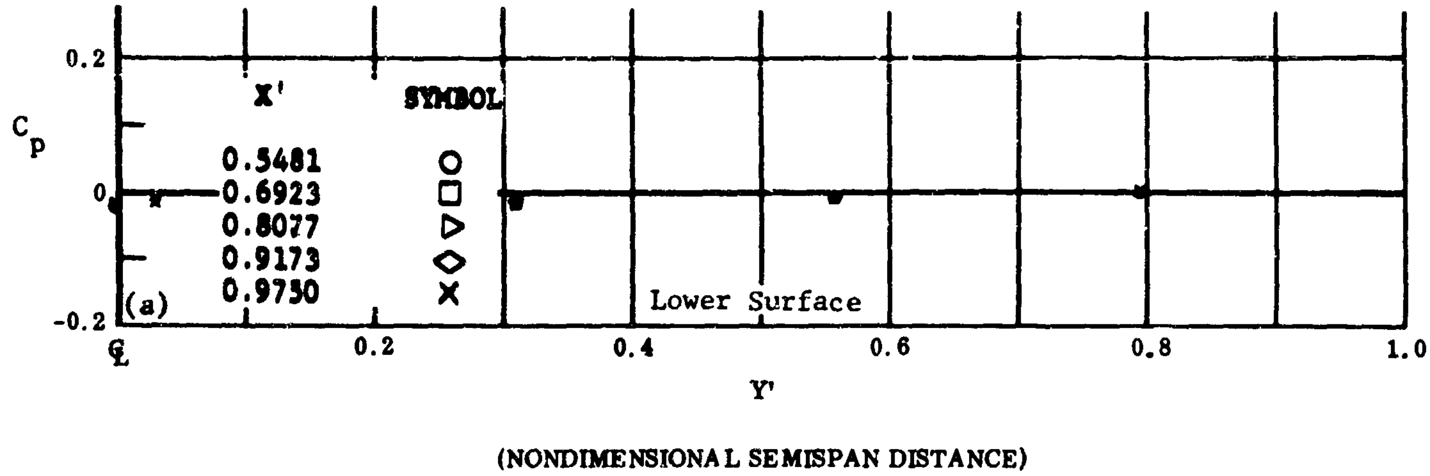

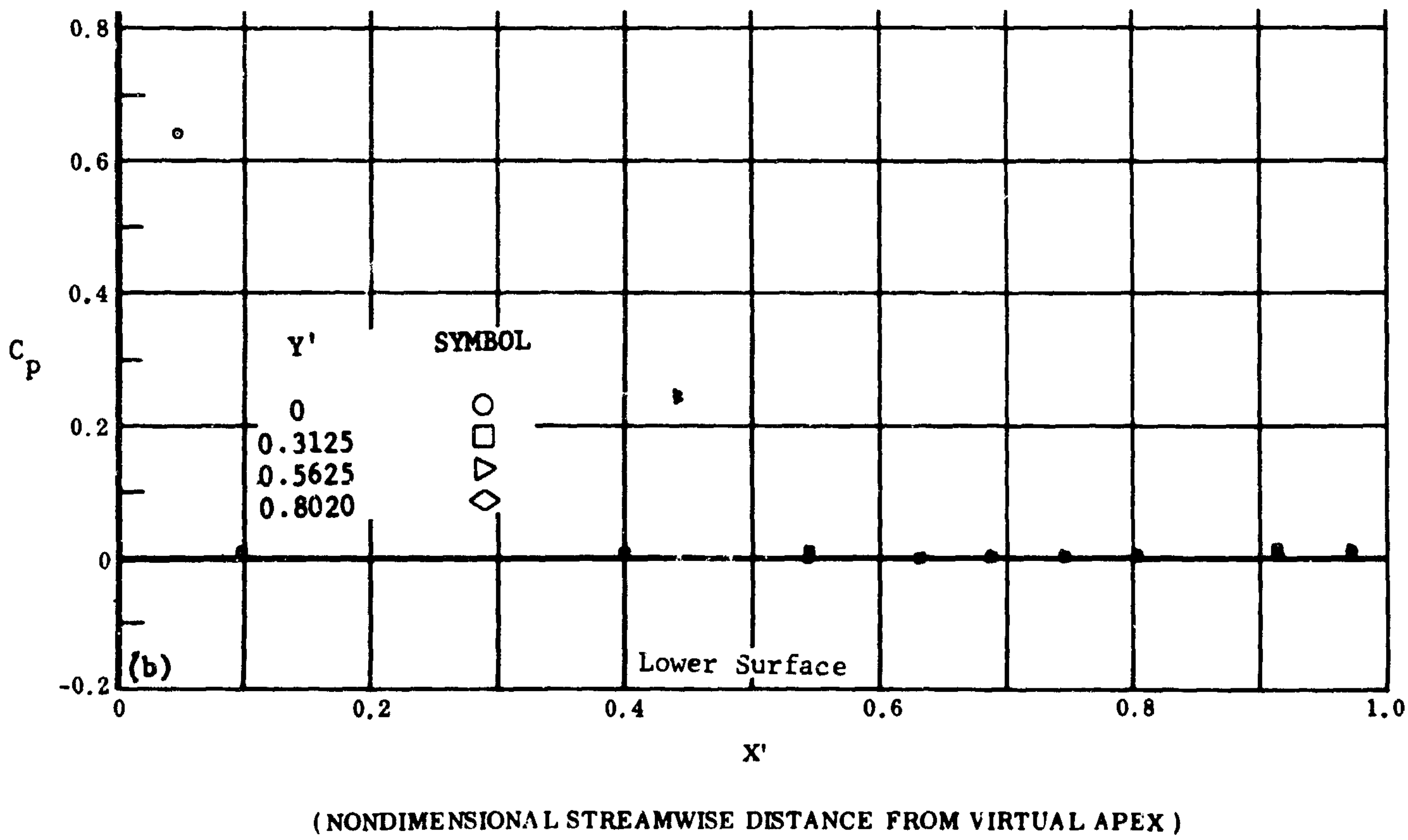

Fig. 49 Configuration IV, α = -50 , δ_2 = δ_3 = -10

a) C_p vs. Y', lower surface

b) C_p vs. X', lower surface

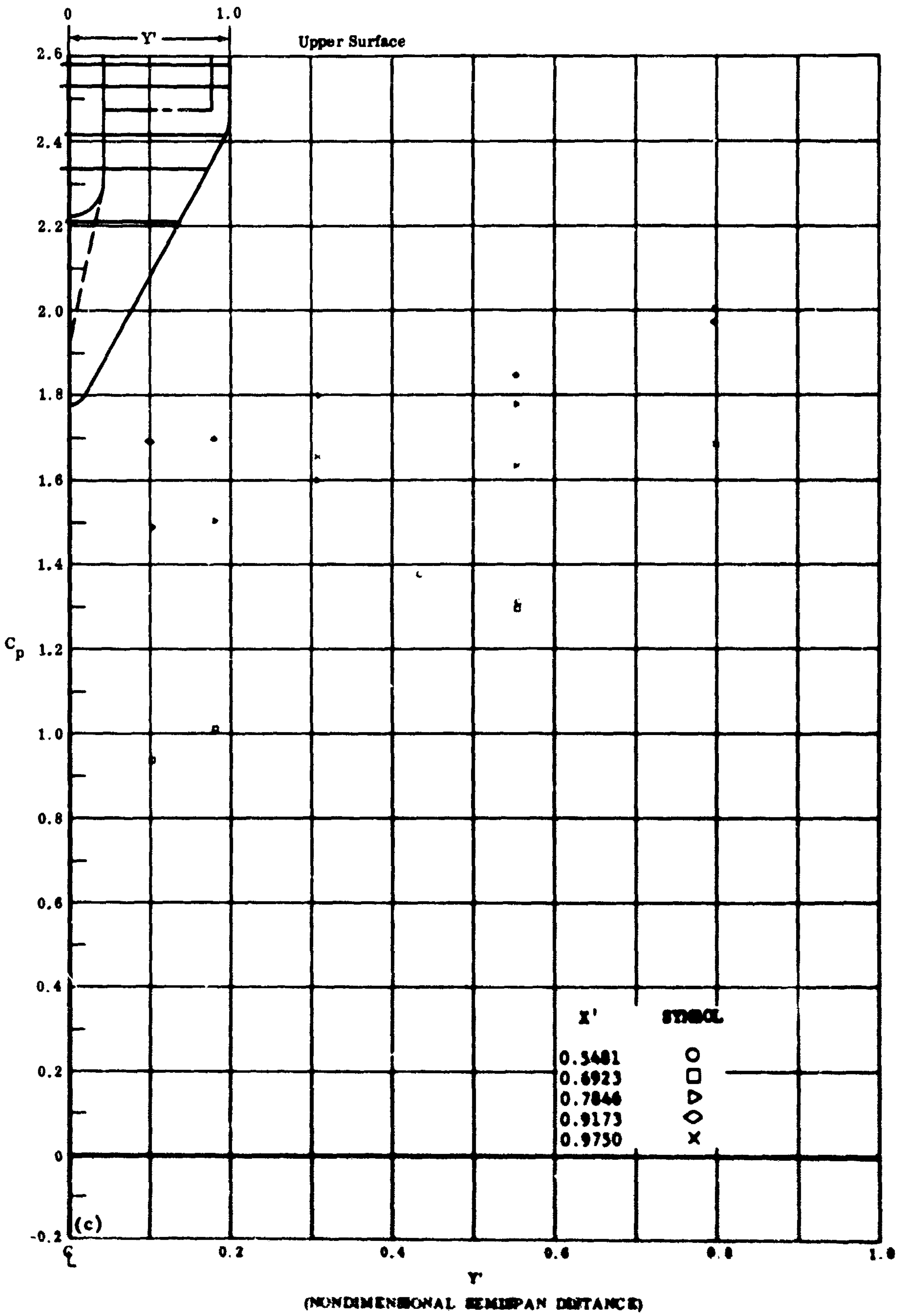

Fig. 49c Configuration IV, $\alpha = -50$, $\delta_2 = \delta_3 = -10$

C_p vs. Y', upper surface

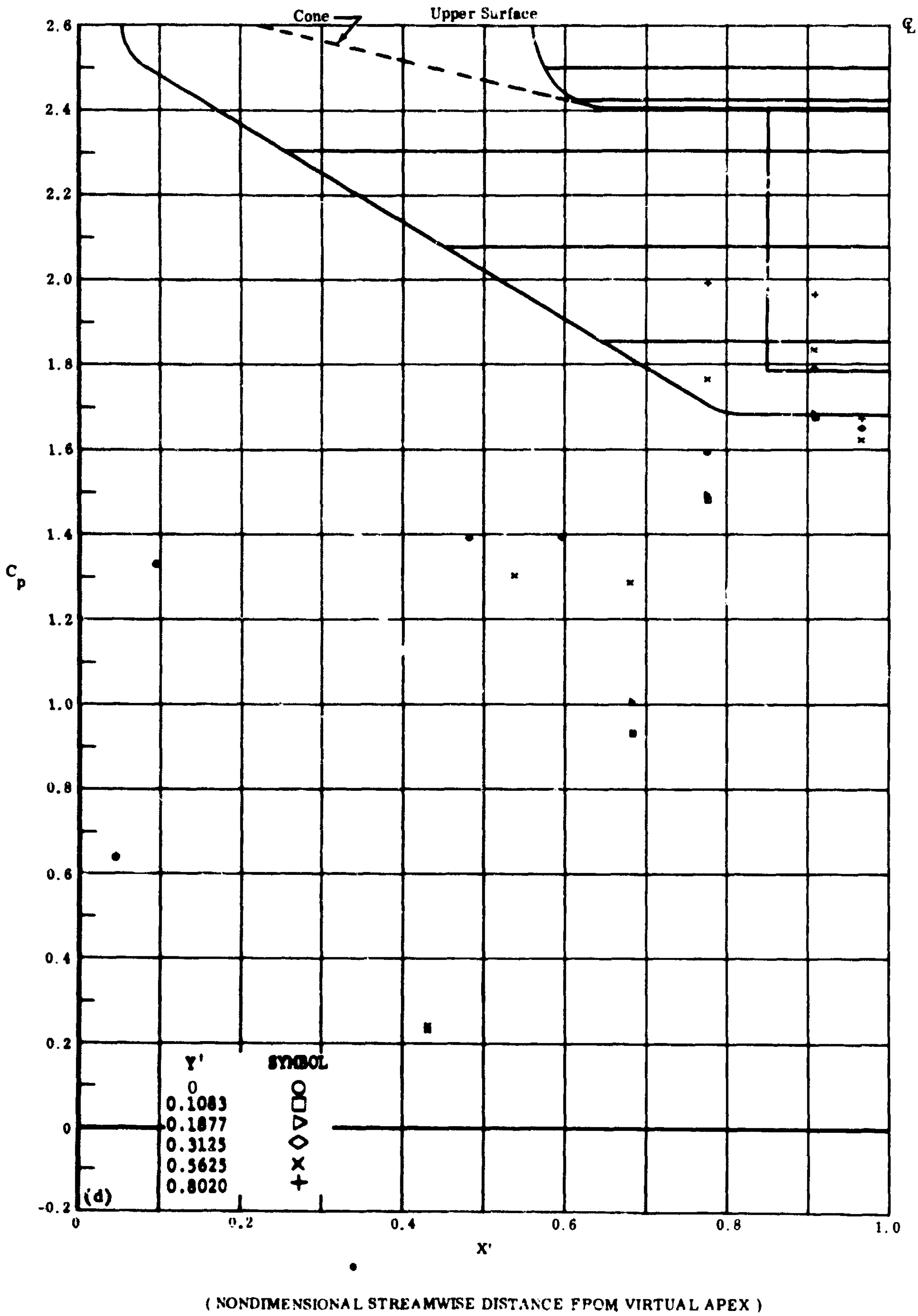

Fig. 49d Configuration IV, α = -50 , δ_2 = δ_3 = -10

C_p vs. X', upper surface

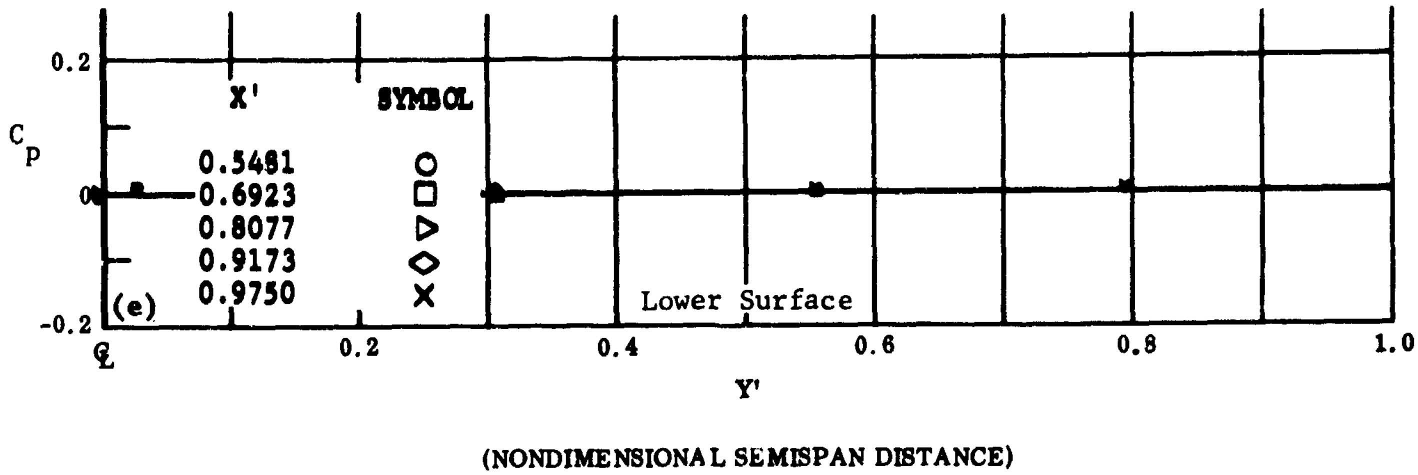

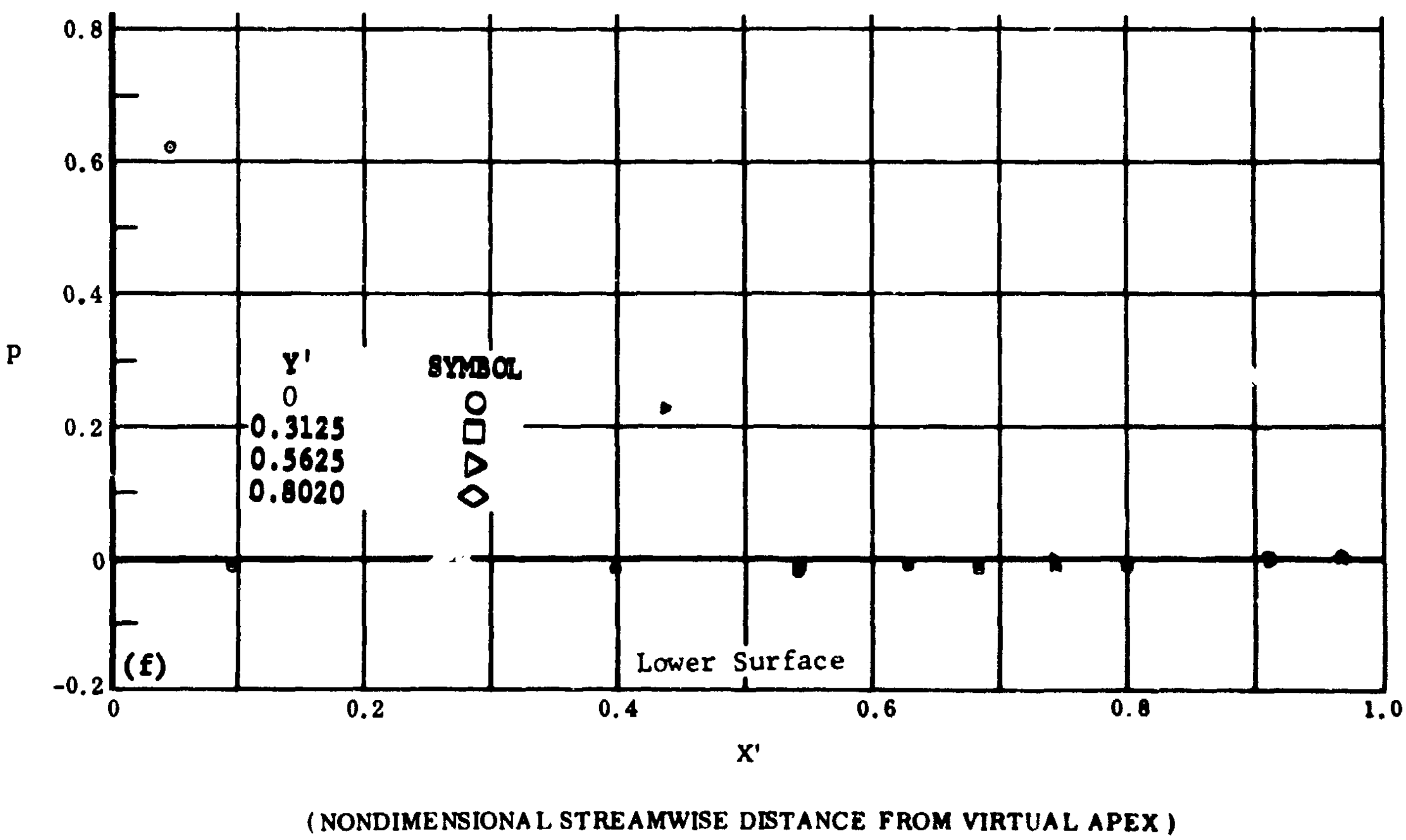

Fig. 49 Configuration IV, $\alpha = -50$, $\delta_2 = \delta_3 = -20$

e) C_p vs. Y', lower surface

f) C_p vs. X', lower surface

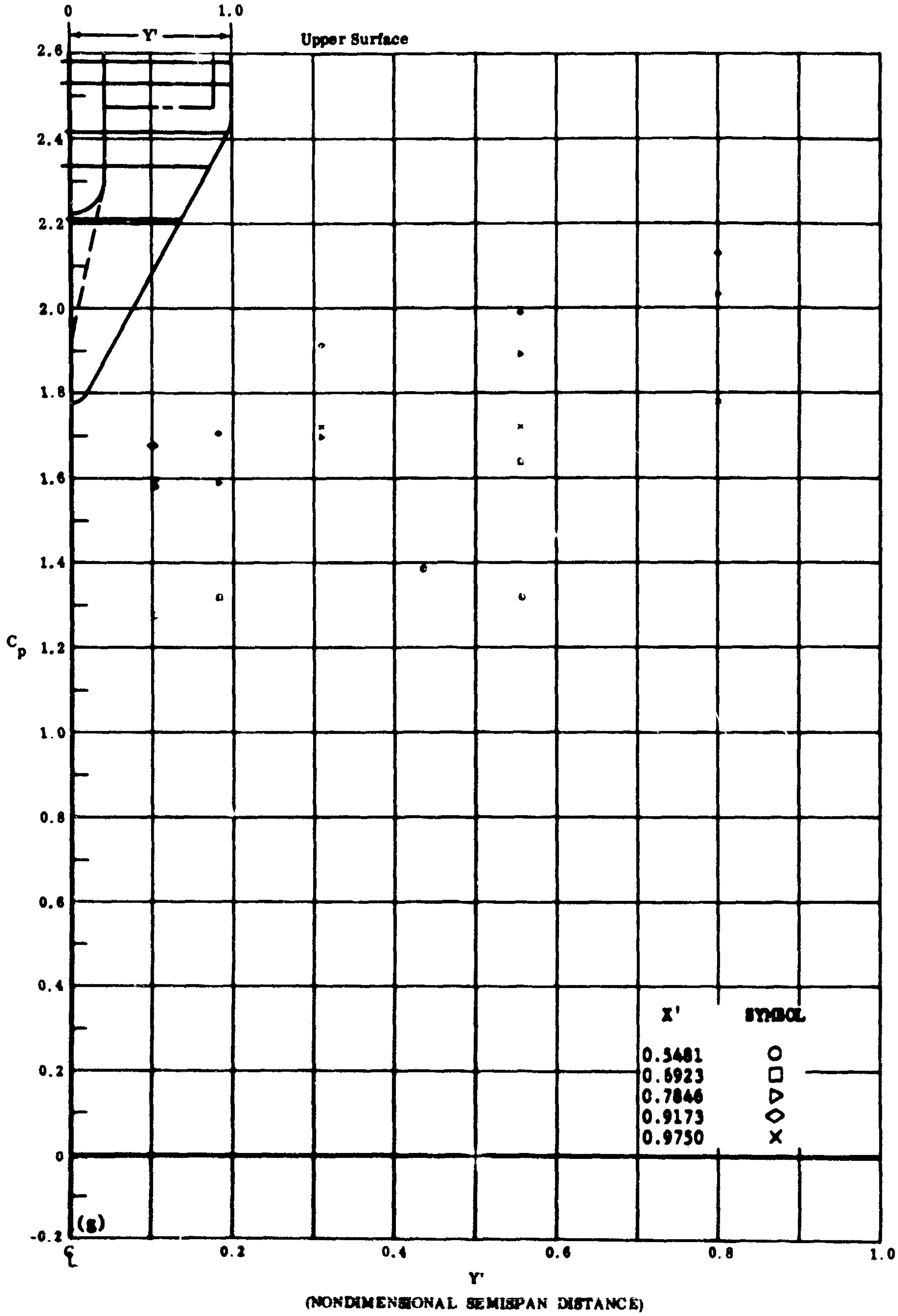

Fig. 49g Configuration IV, $\alpha = -50$, $\delta_2 = \delta_3 = -20$

C_p vs. Y', upper surface

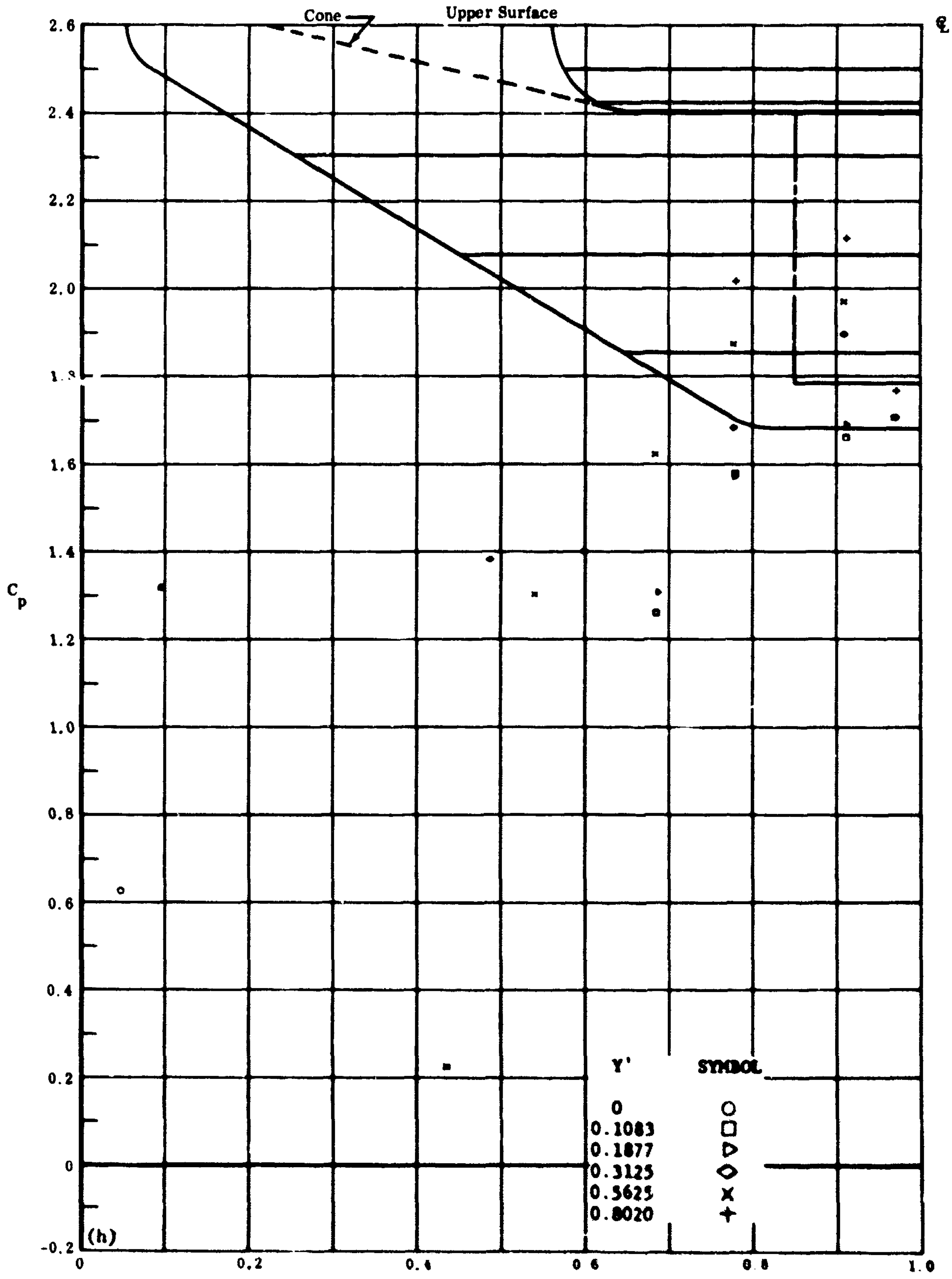

(NONDIMENSIONAL STREAMWISE DISTANCE FROM VIRTUAL APEX)

Fig. 49h Configuration IV, α = -50, $\delta_2 = \delta_3$ = -20

C_p vs. X', upper surface

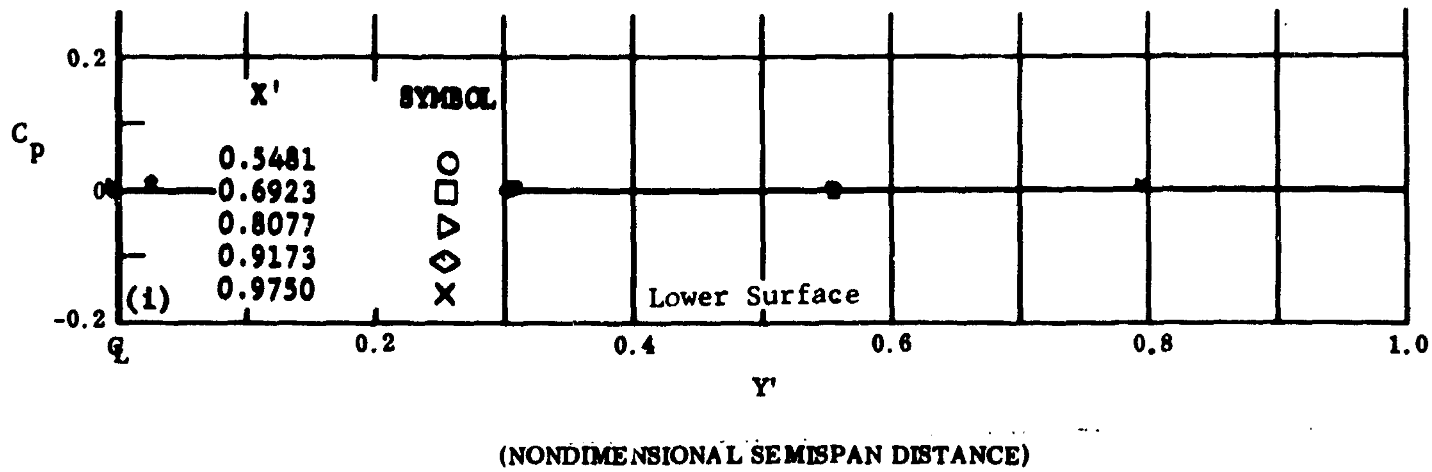

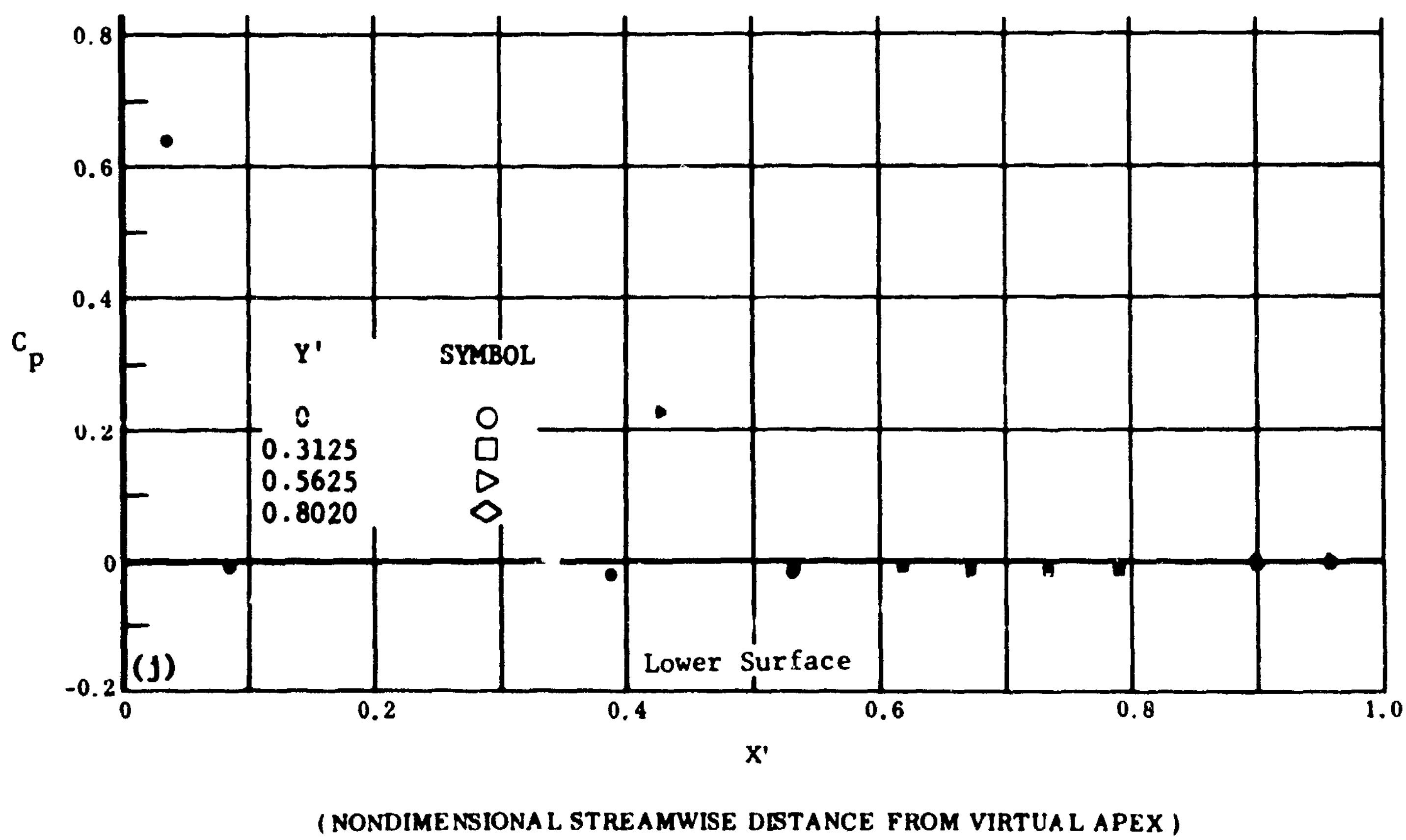

Fig. 49 Configuration IV, $\alpha = -50$, $\delta_2 = \delta_3 = -30$

i) C_p vs. Y', lower surface

j) C_p vs. X', lower surface

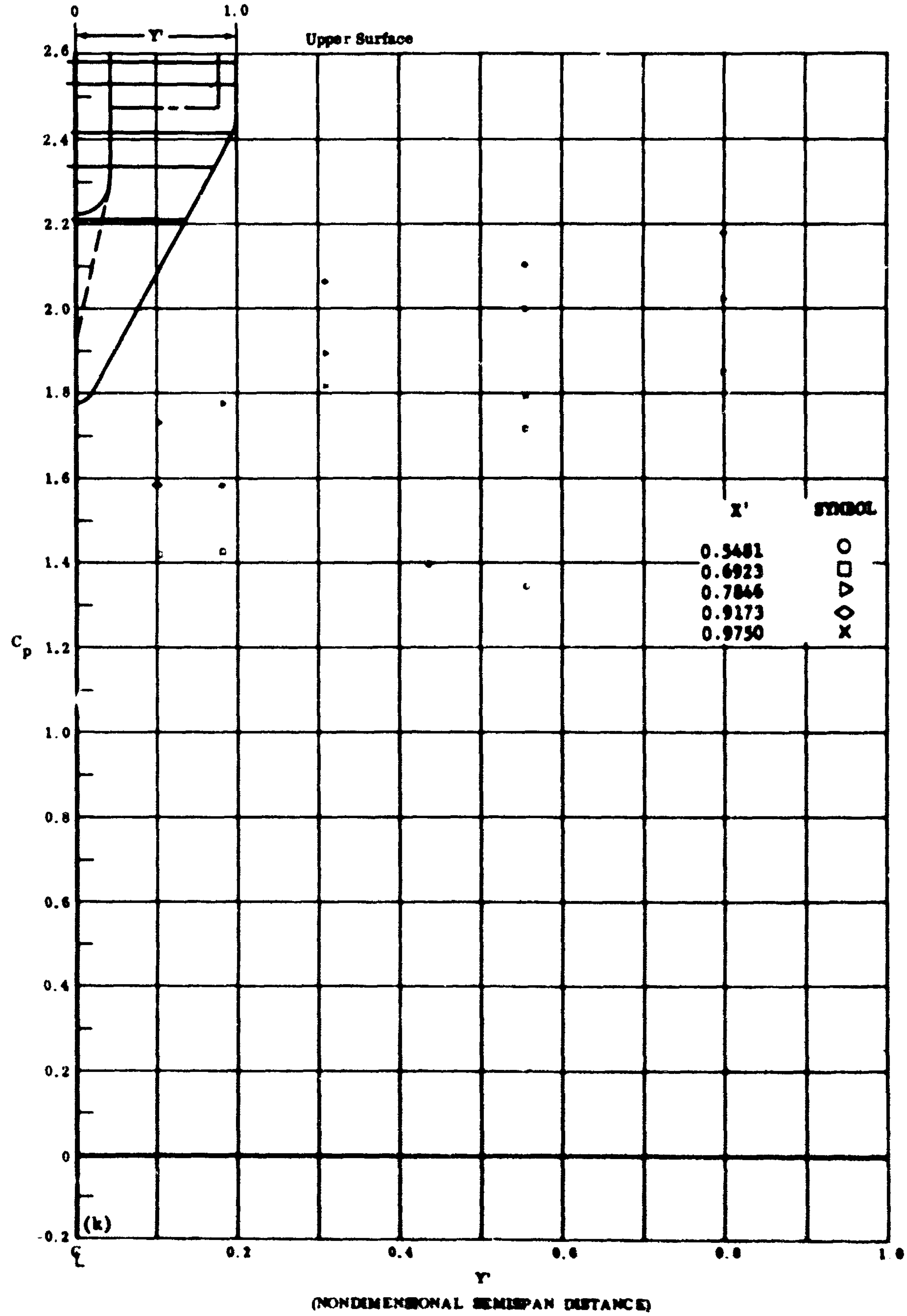

Fig. 49k Configuration IV, $\alpha = -50$, $\delta_2 = \delta_3 = -30$

C_p vs. Y', upper surface

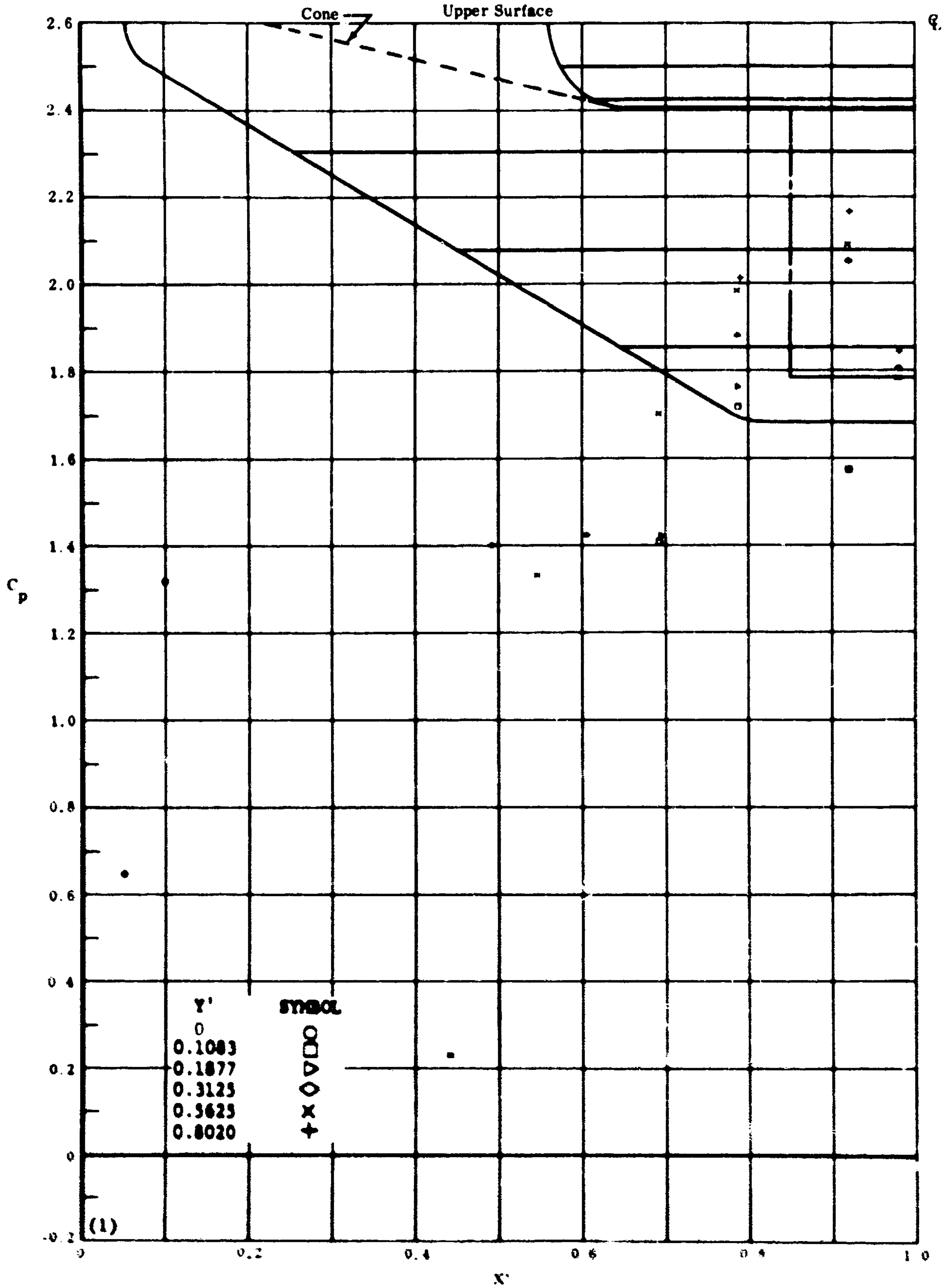

(NONDIMENSIONAL STREAMWISE DISTANCE FROM VIRTUAL APEX)

Fig. 491 Configuration IV, $\delta = -50°$, $\delta_2 = \delta_3 = -30°$

C_p vs. X', upper surface

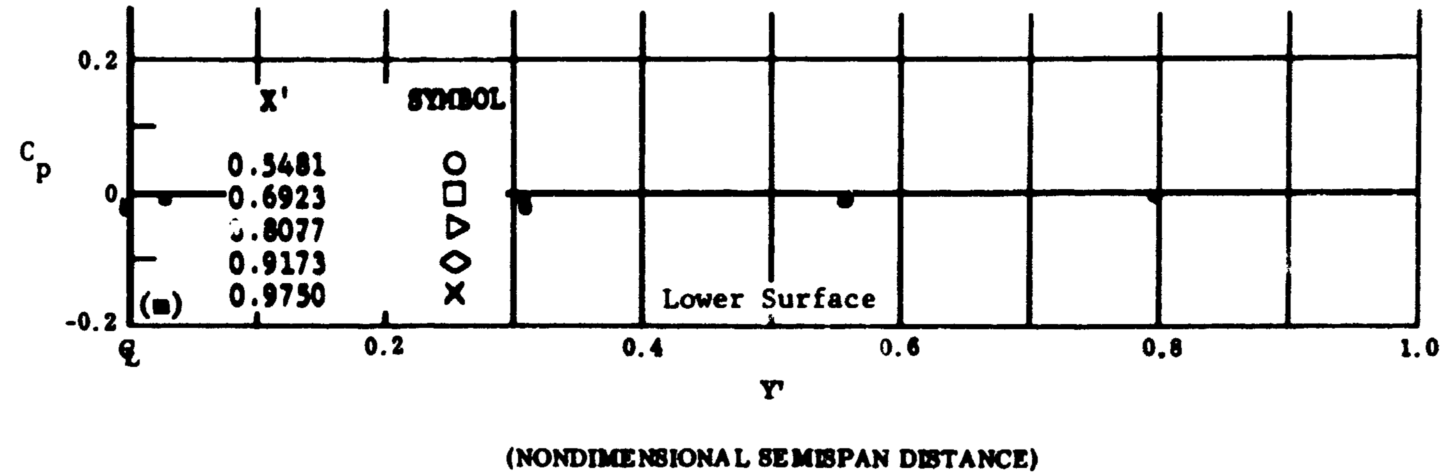

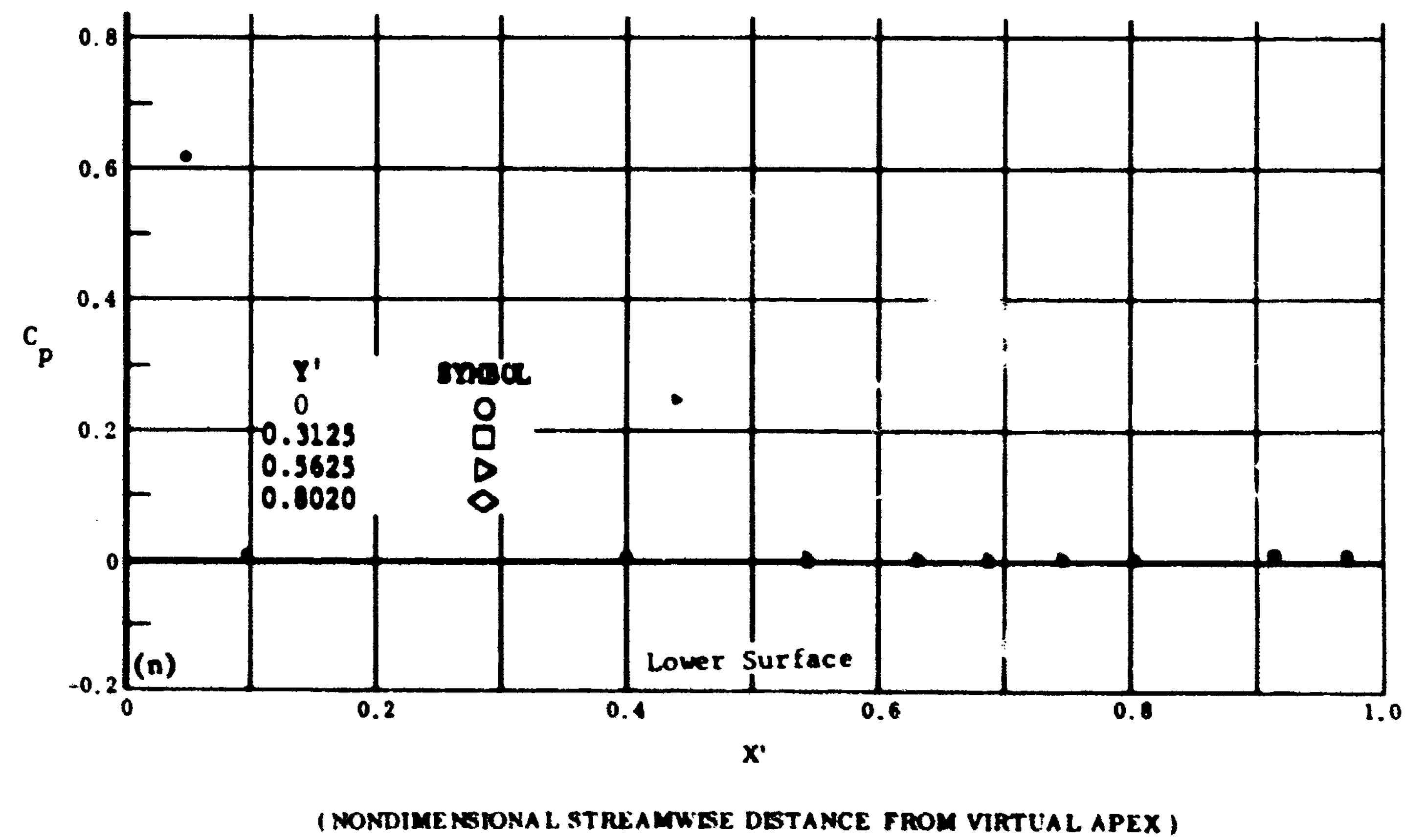

Fig. 49 Configuration IV, α = -50, $\delta_2 = \delta_3$ = -39

m) C_p vs. Y', lower surface

n) C_p vs. X', lower surface

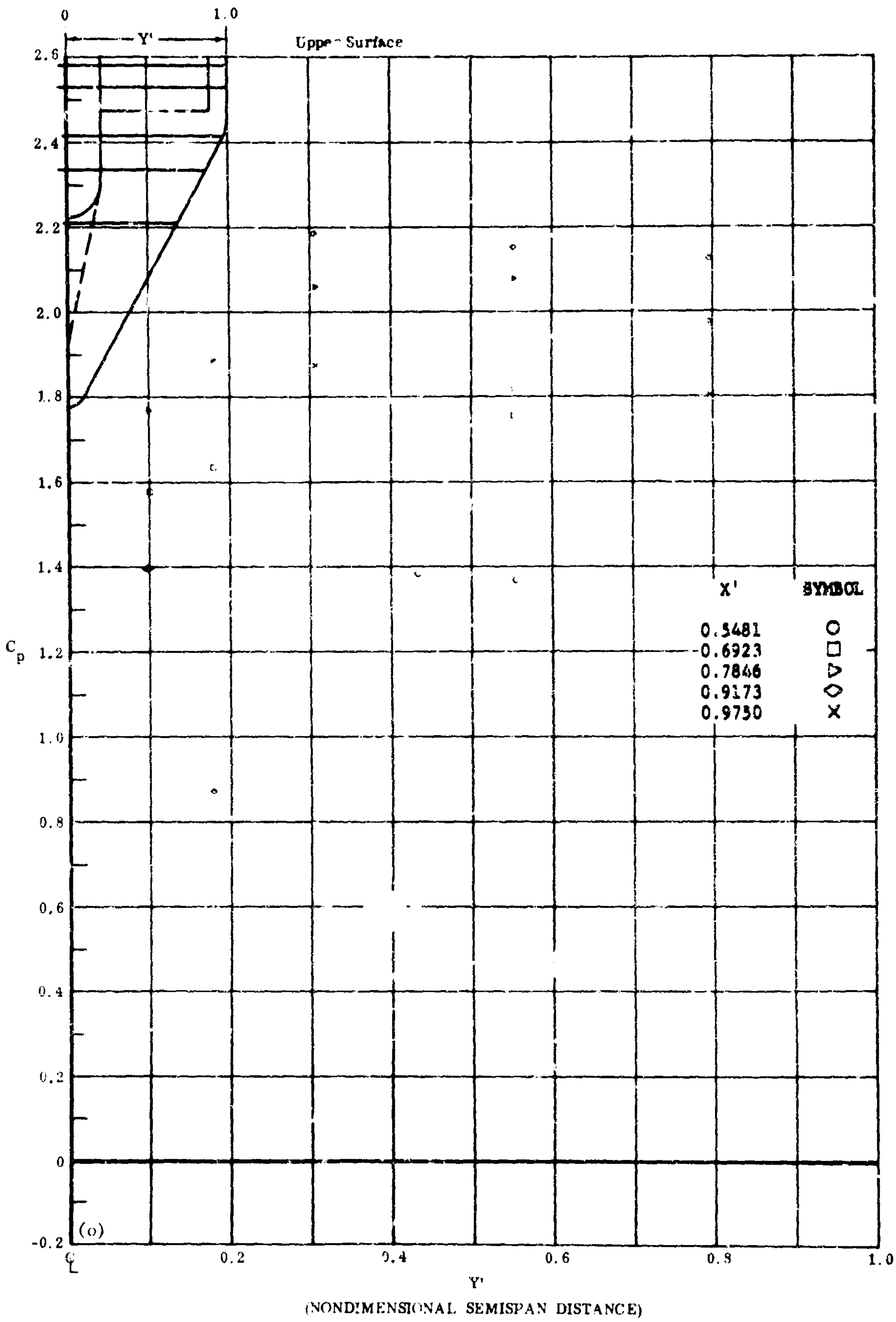

Fig. 49o Configuration IV, α = -50 , $\delta_2 = \delta_3$ = -39

C_p vs. Y', upper surface

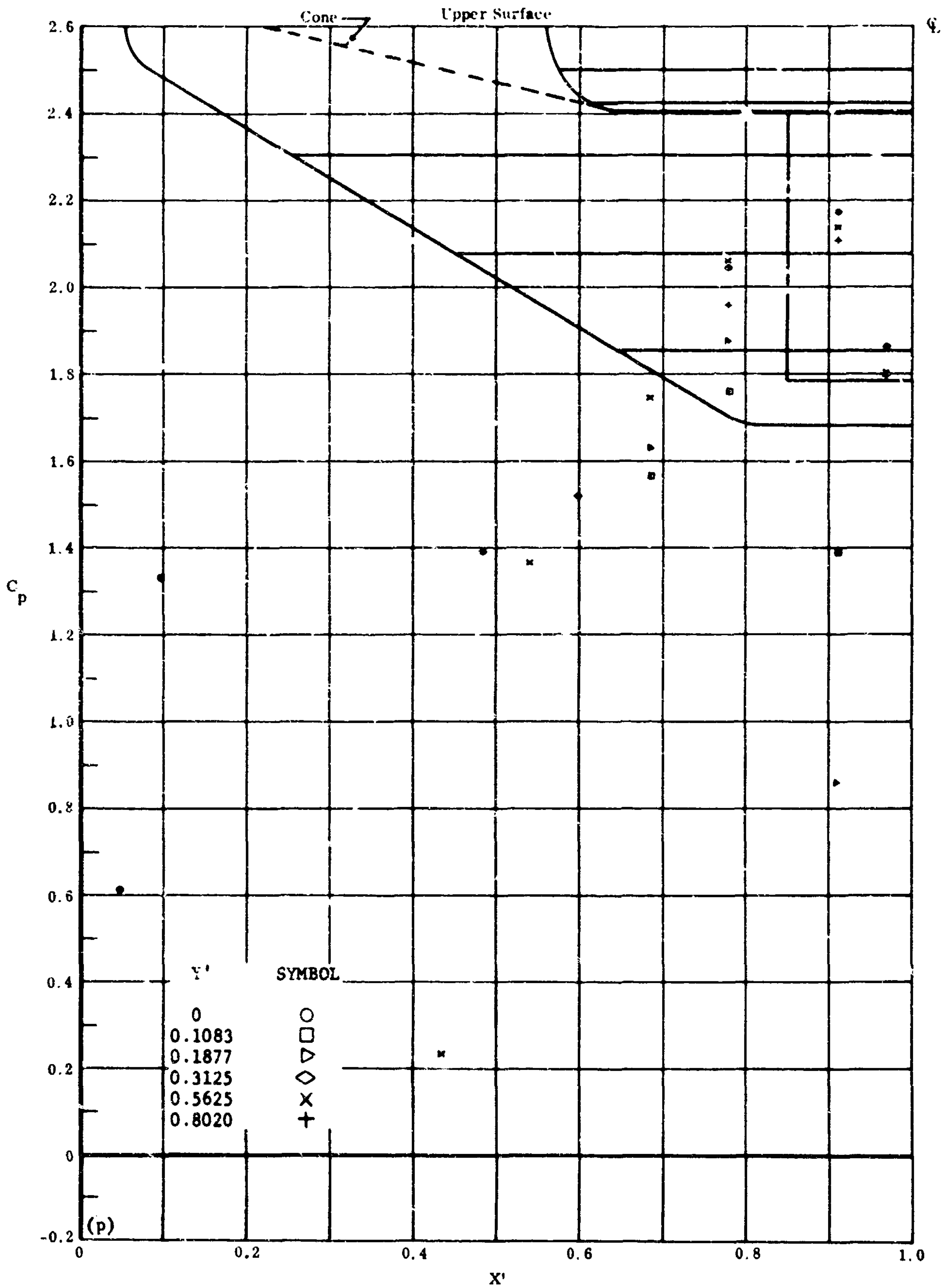

(NONDIMENSIONAL STREAMWISE DISTANCE FROM VIRTUAL APEX)

Fig. 49p Configuration IV, $\alpha = -50$, $\delta_2 = \delta_3 = -39$

C_p vs. X', upper surface

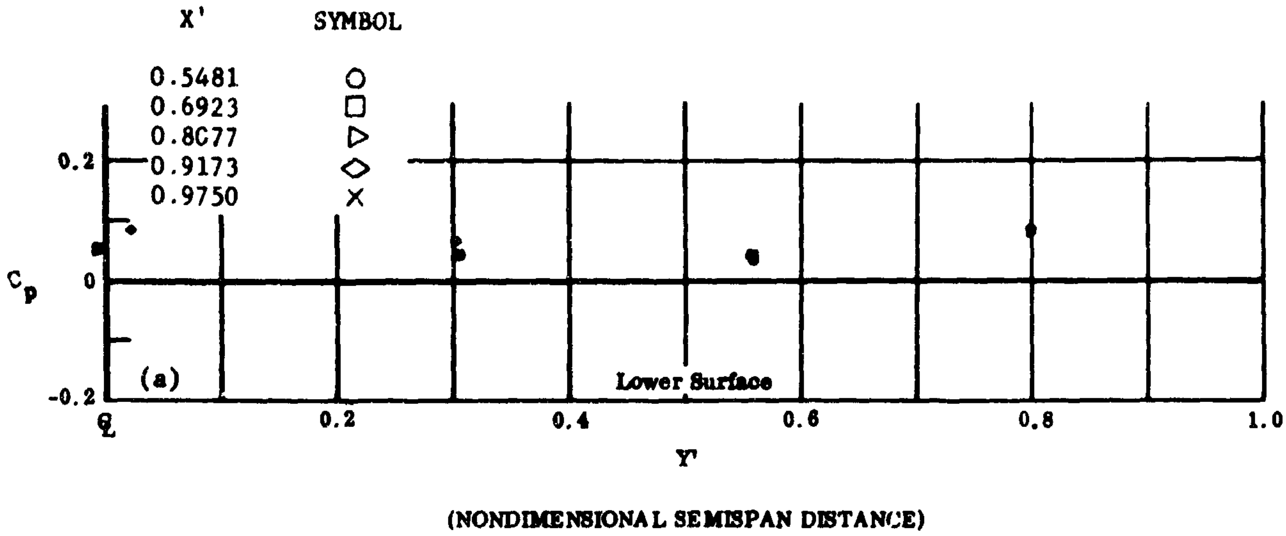

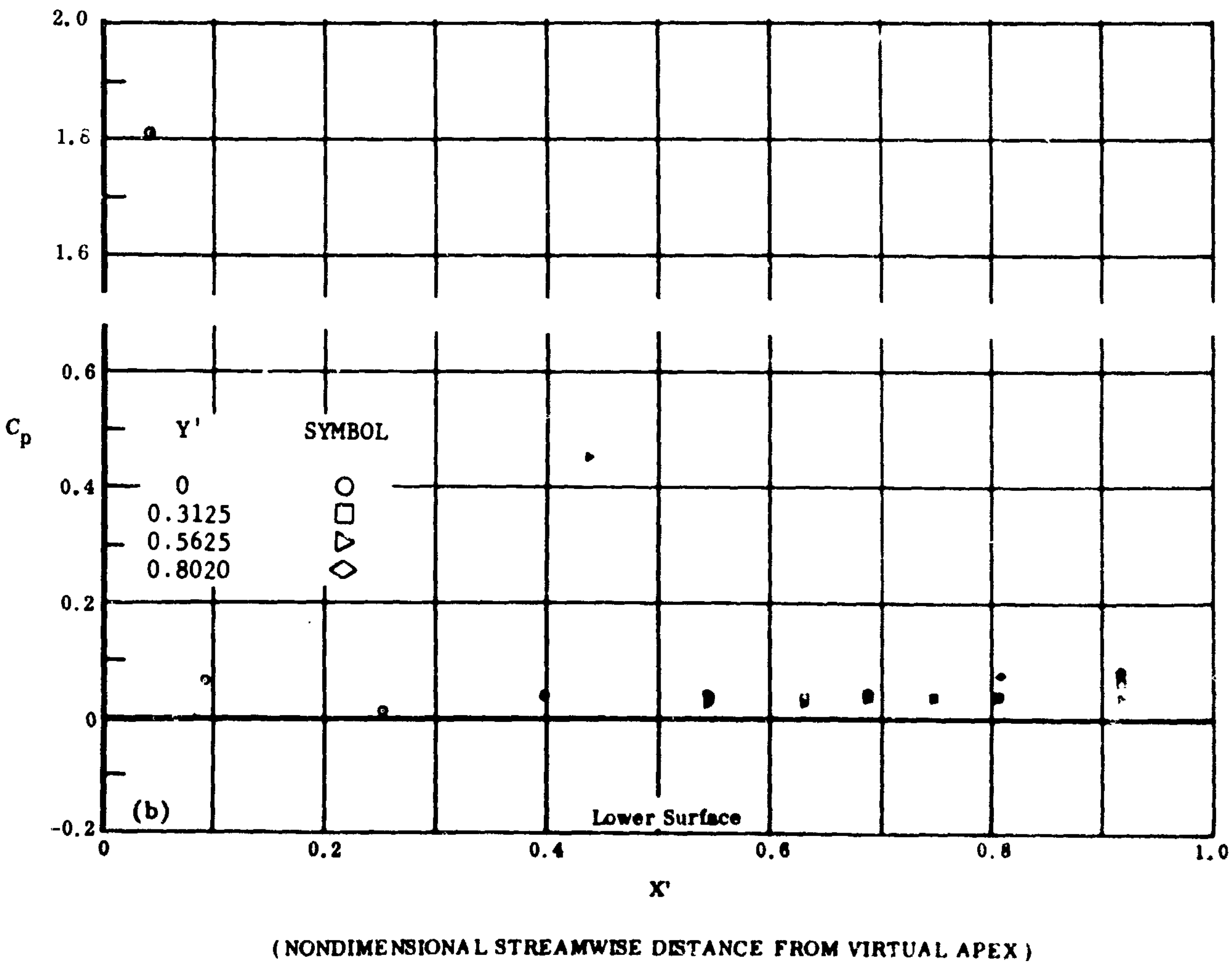

Fig. 50 Configuration VII, Spoiler On

a) C_p vs. Y', $\alpha = 0$, $Re_\infty/ft \times 10^{-6} = 3.3$, lower surface

b) C_p vs. X', $\alpha = 0$, $Re_\infty/ft \times 10^{-6} = 3.3$, lower surface

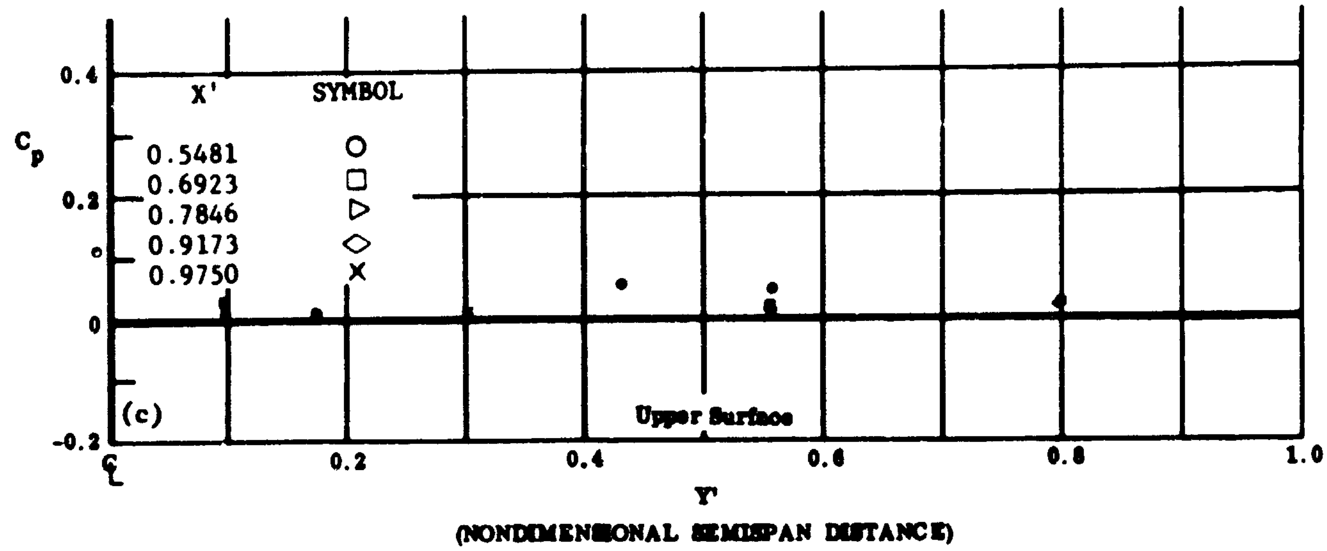

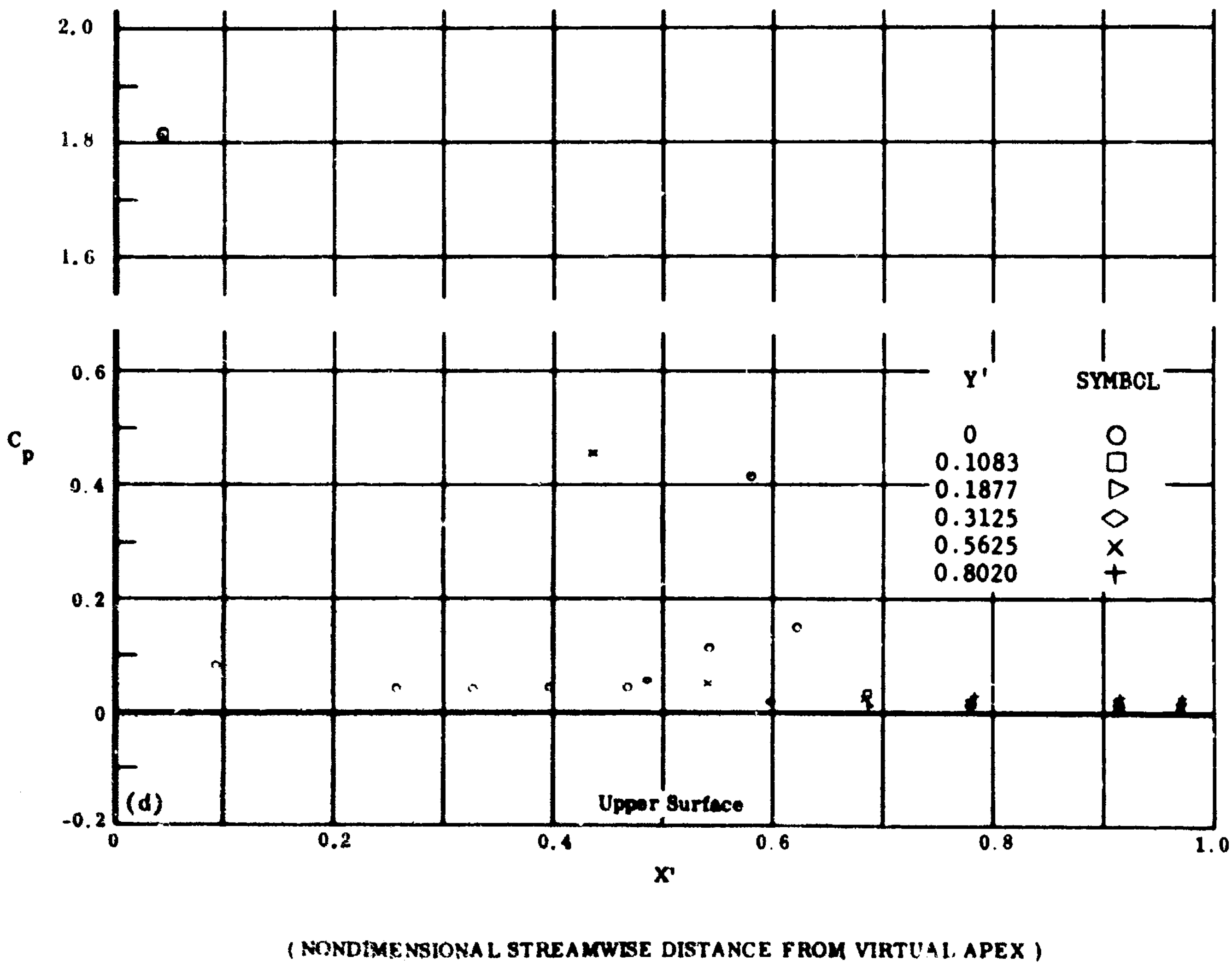

Fig. 50 Configuration VII, Spoiler On

c) C_p vs. Y', $\alpha = 0$, $Re_\infty/ft \times 10^{-6} = 3.3$, upper surface

d) C_p vs. X', $\alpha = 0$, $Re_\infty/ft \times 10^{-6} = 3.3$, upper surface

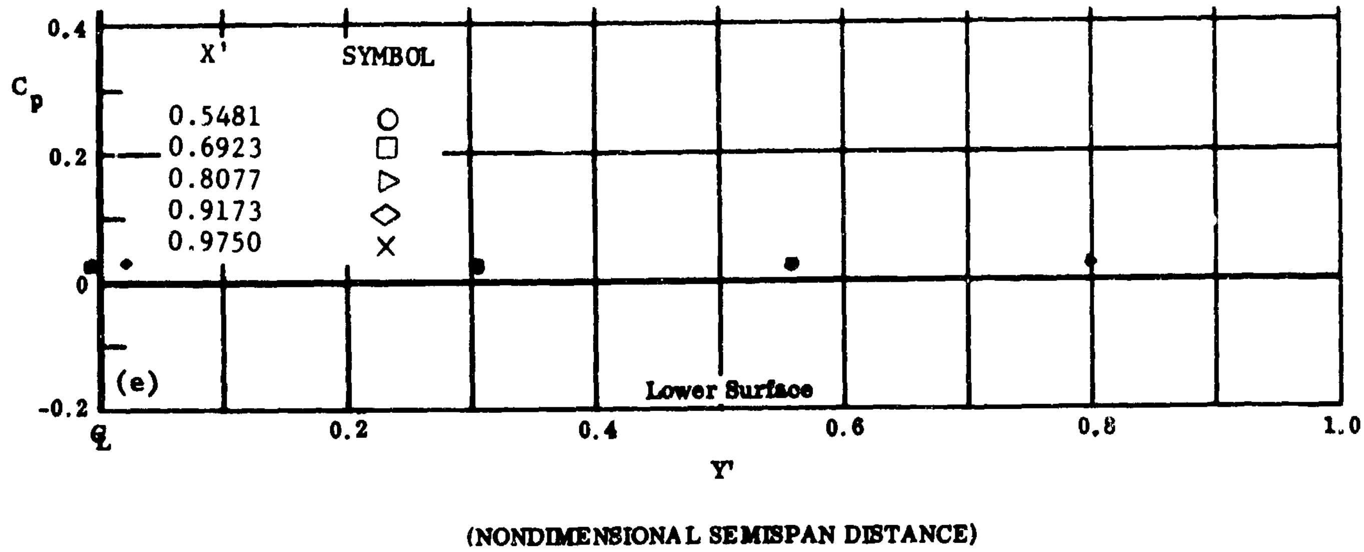

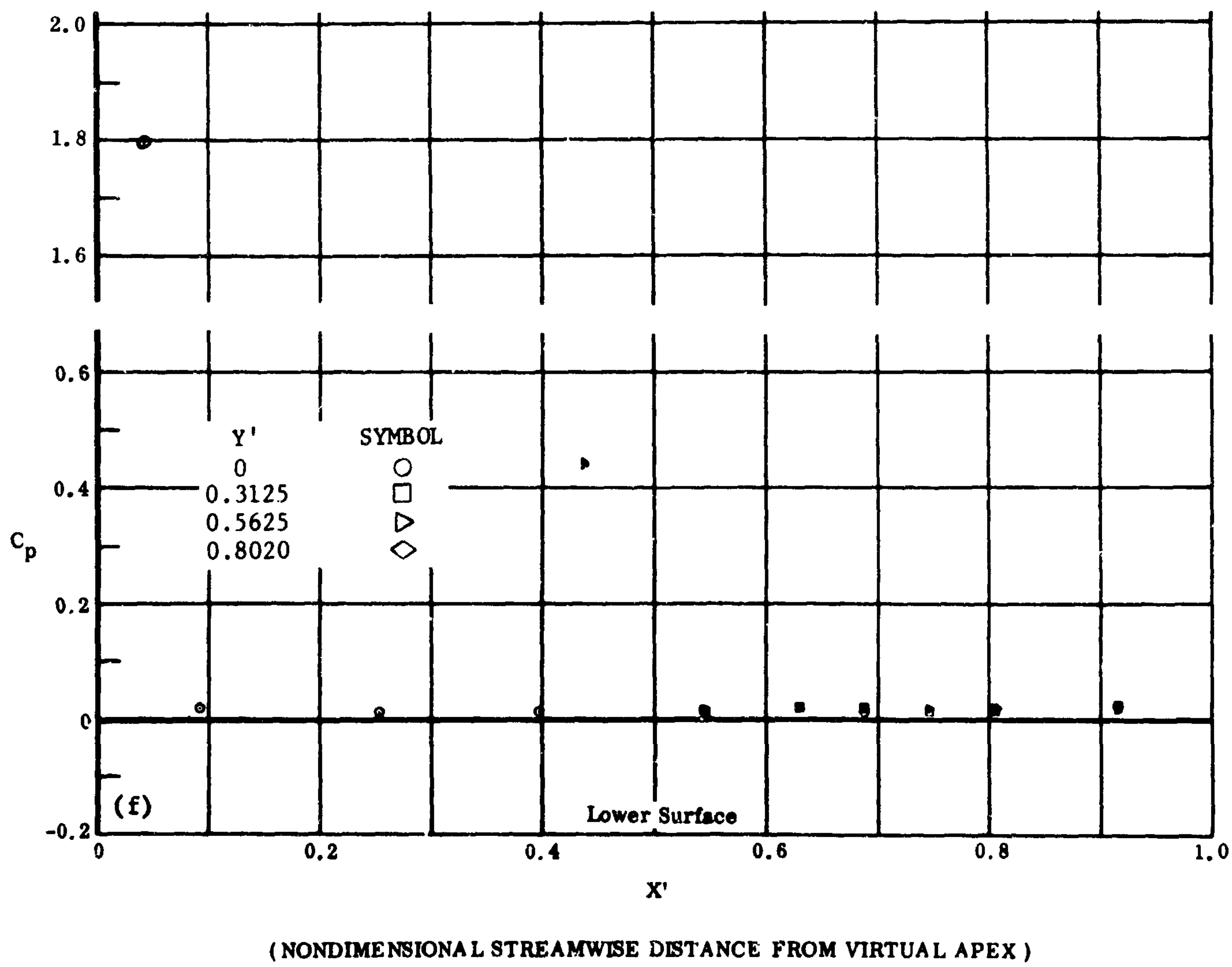

Fig. 50 Configuration VII, Spoiler On

e) C_p vs. Y', α = -10 , $Re_\infty/ft \times 10^{-6}$ = 3.3, lower surface

f) C_p vs. X', α = -10, $Re_\infty/ft \times 10^{-6}$ = 3.3, lower surface

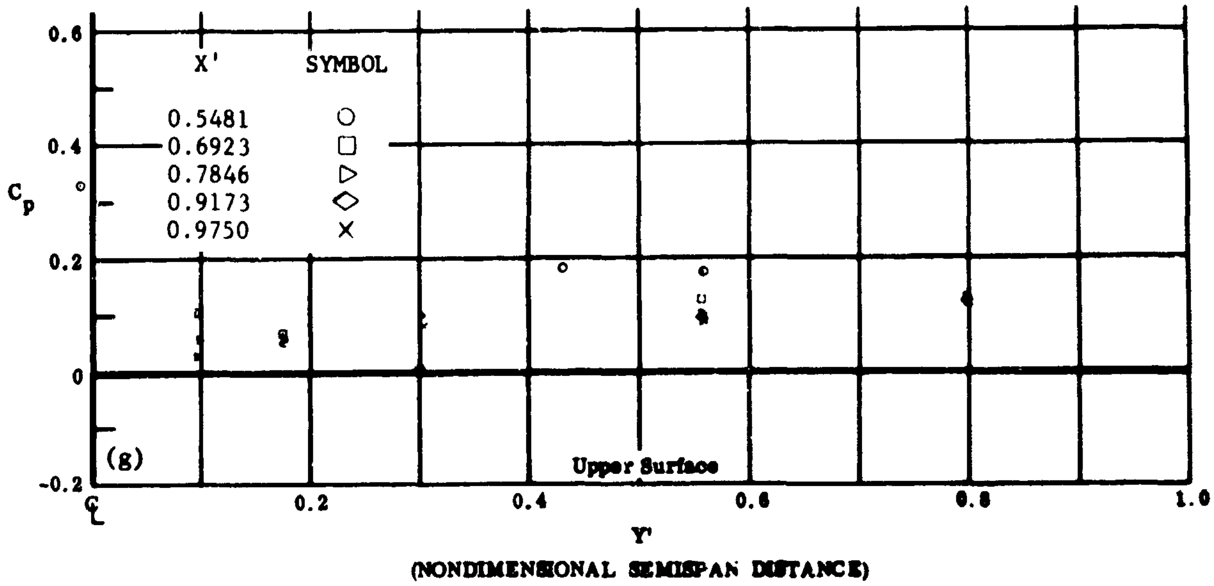

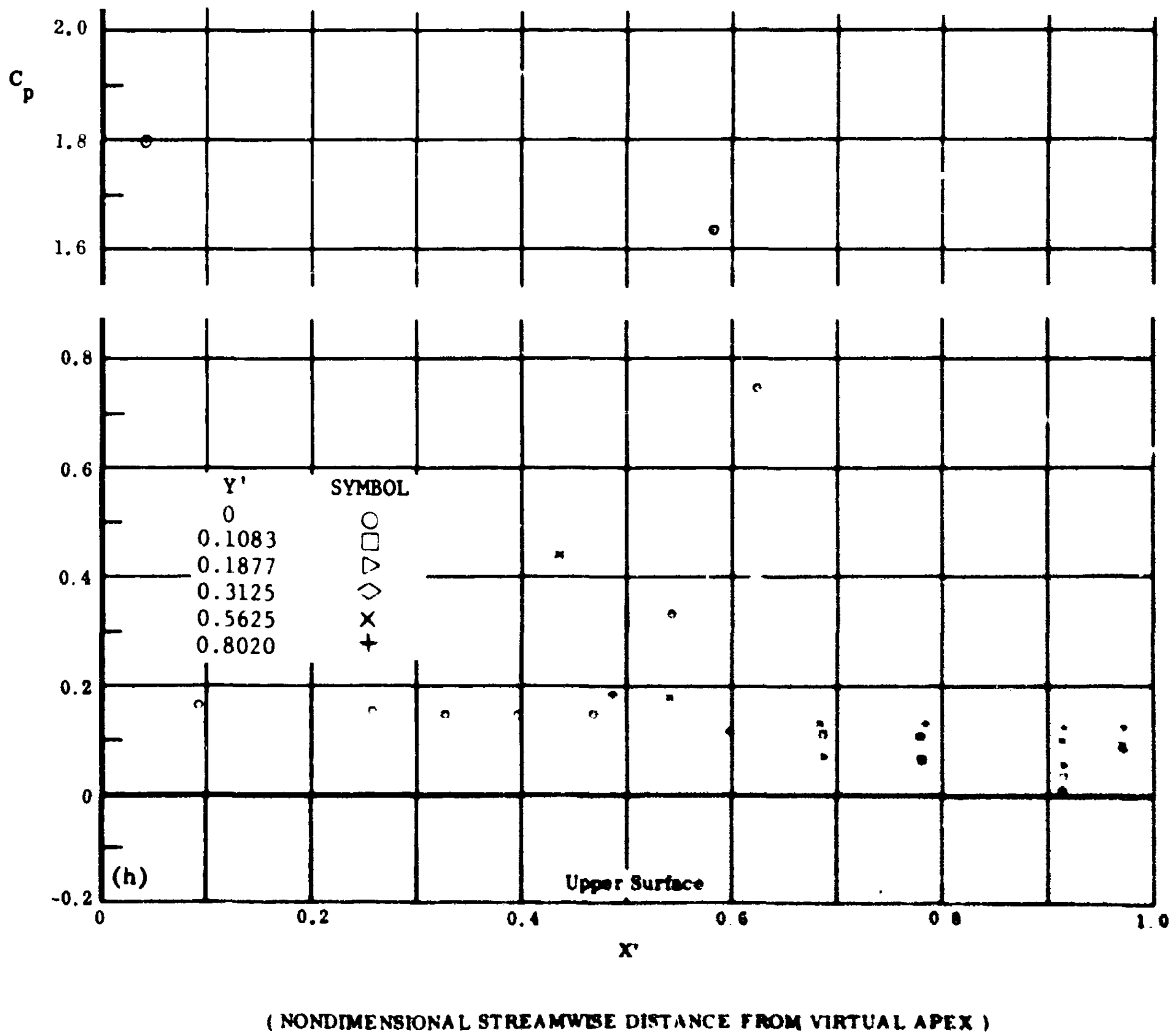

Fig. 50 Configuration VII, Spoiler On

g) C_p vs. Y', α = -10 , $Re_\infty/ft \times 10^{-6}$ = 3.3, upper surface

h) C_p vs. X', α = -10 , $Re_\infty/ft \times 10^{-6}$ = 3.3, upper surface

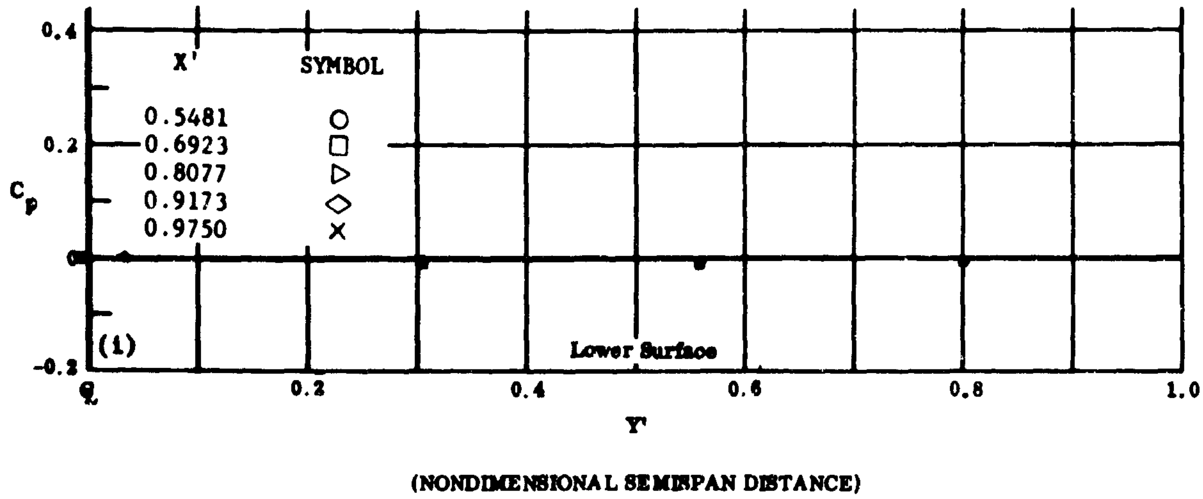

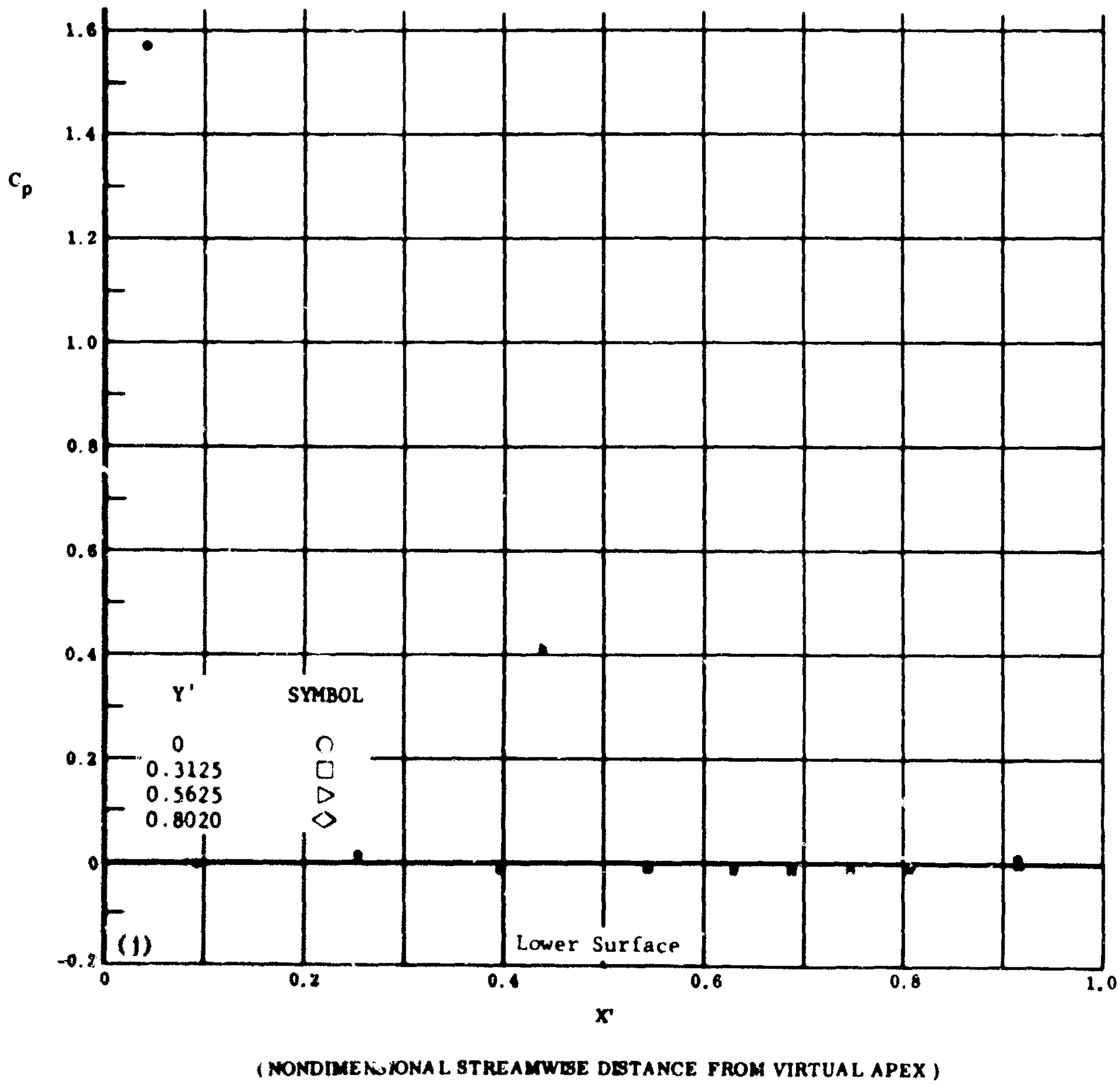

Fig. 50 Configuration VII, Spoiler On

i) C_p vs. Y', α = -20 , $Re_\infty/ft \times 10^{-6}$ = 3.3, lower surface

j) C_p vs. X', α = -20 , $Re_\infty/ft \times 10^{-6}$ = 3.3, lower surface

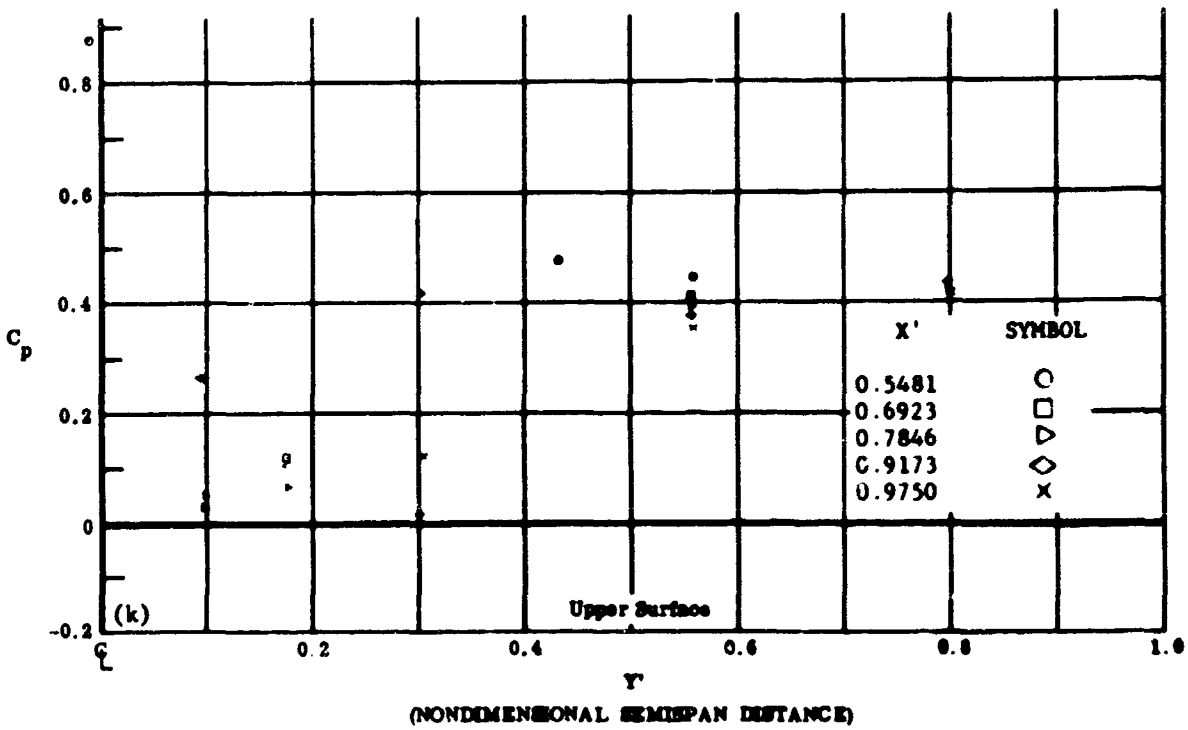

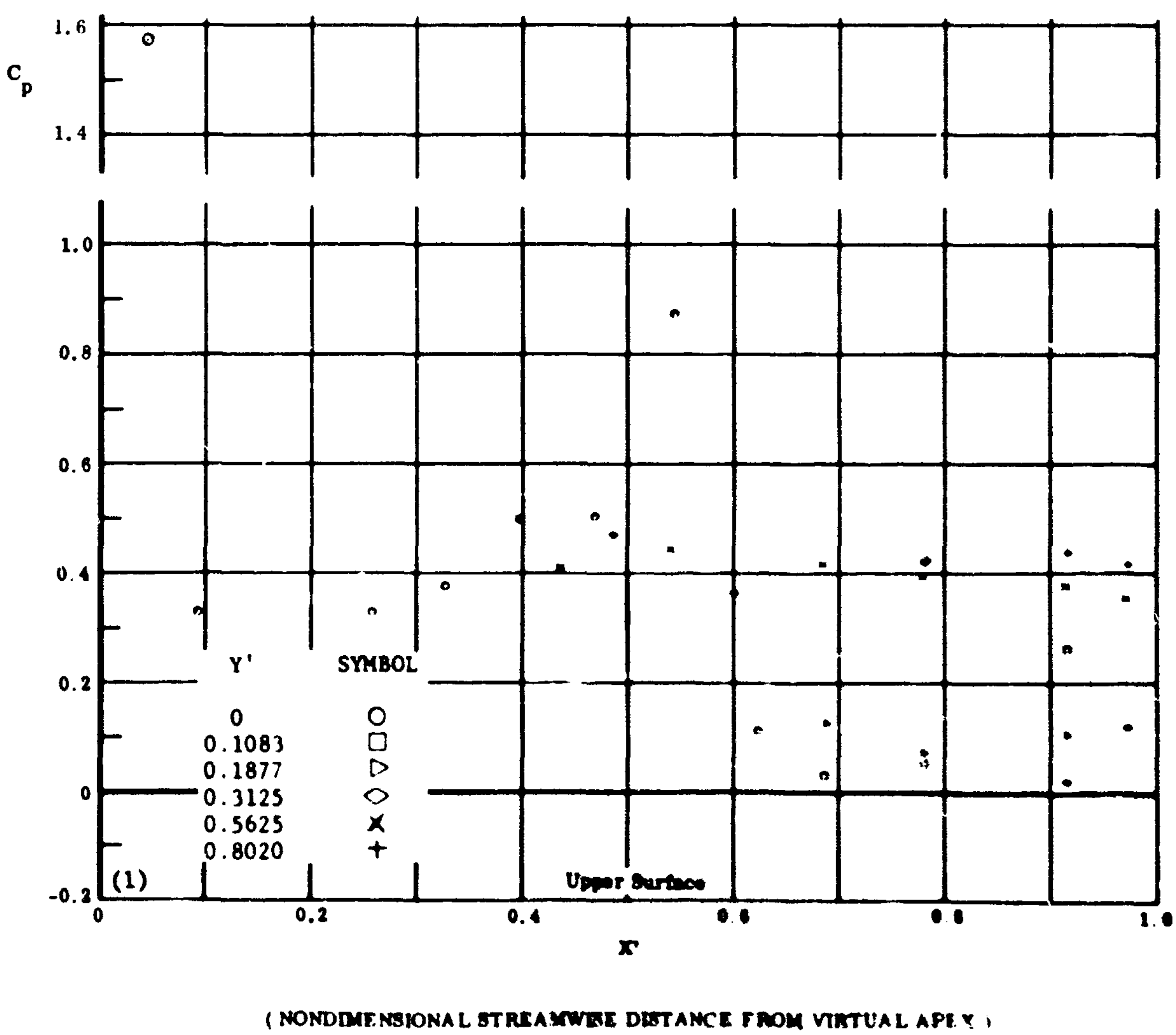

Fig. 50 Configuration VII, Spoiler On

k) C_p vs. Y', α = -20 , $Re_\infty/ft \times 10^{-6}$ = 3.3, upper surface

1) C_p vs. X', α = -20 , $Re_\infty/ft \times 10^{-6}$ = 3.3, upper surface

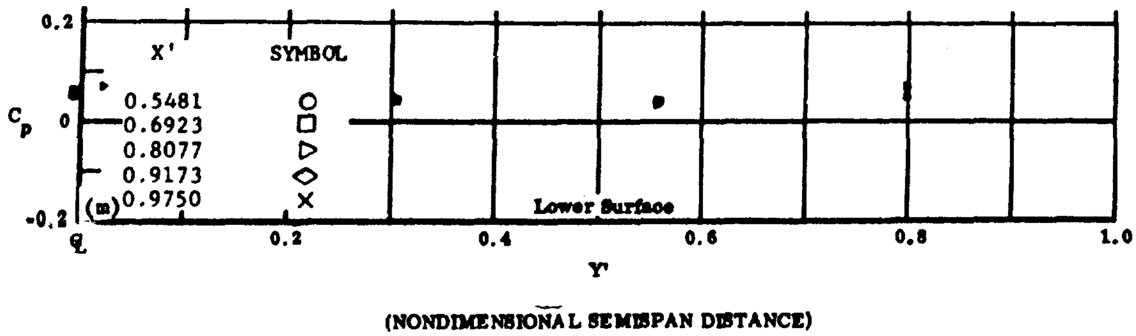

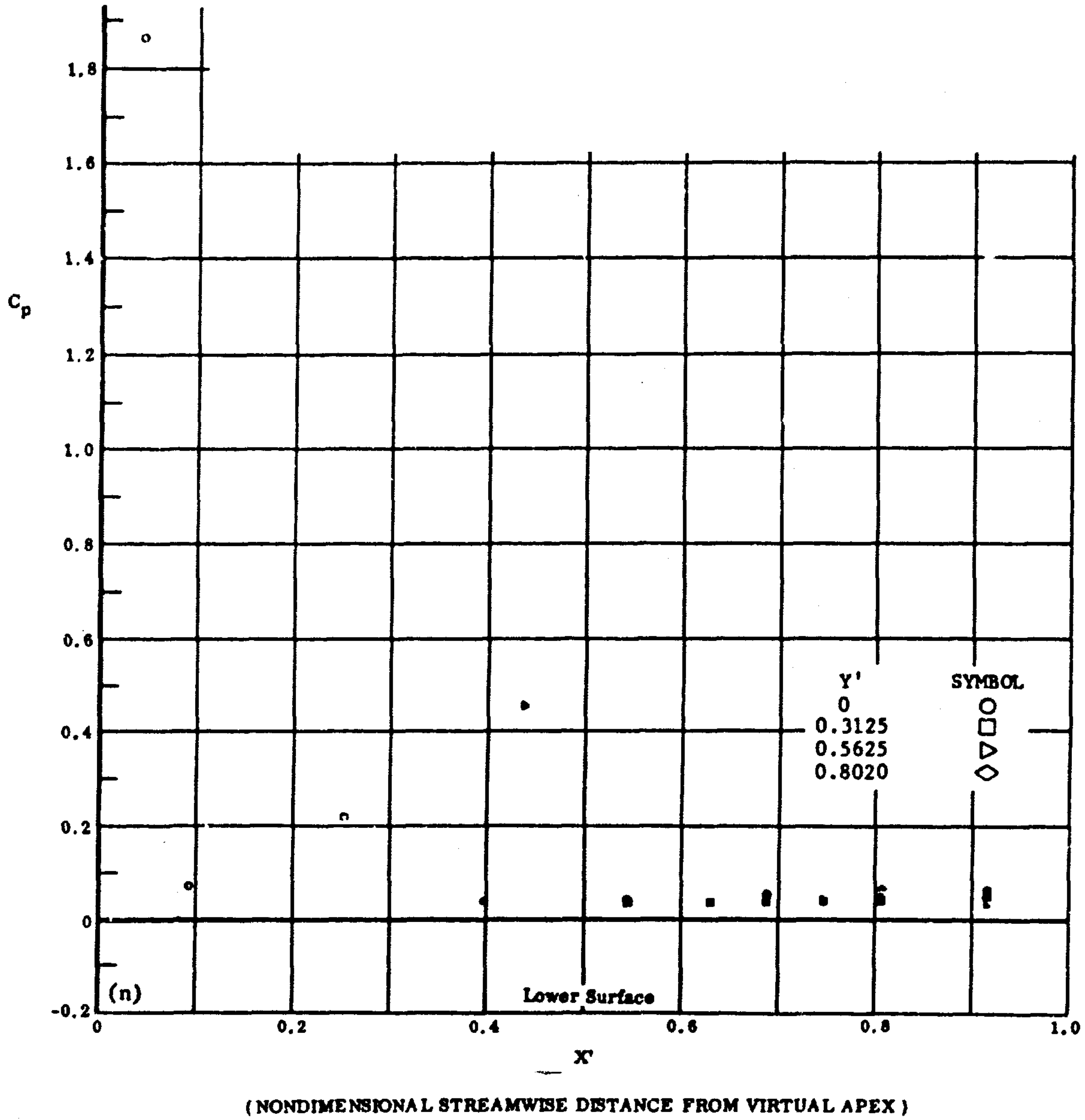

Fig. 50 Configuration VII, Spoiler On

m) C_p vs. Y', $\alpha = 0$, $Re_\infty/ft \times 10^{-6} = 1.1$, lower surface

n) C_p vs. X', $\alpha = 0$, $Re_\infty/ft \times 10^{-6} = 1.1$, lower surface

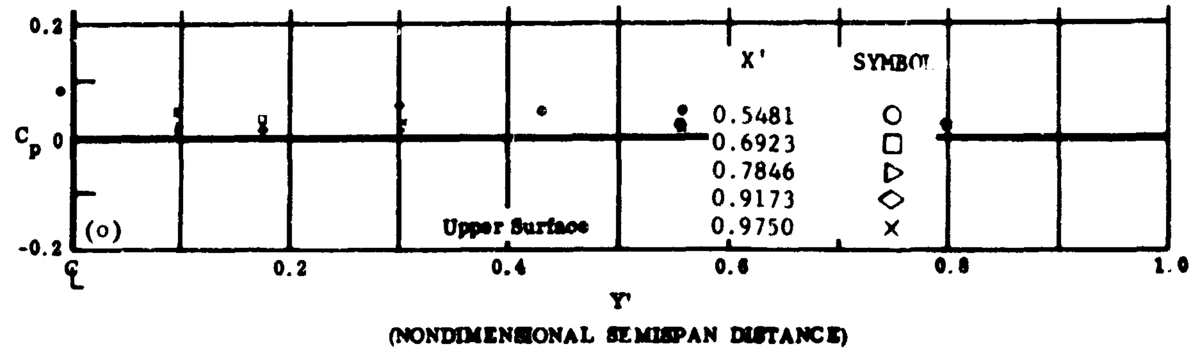

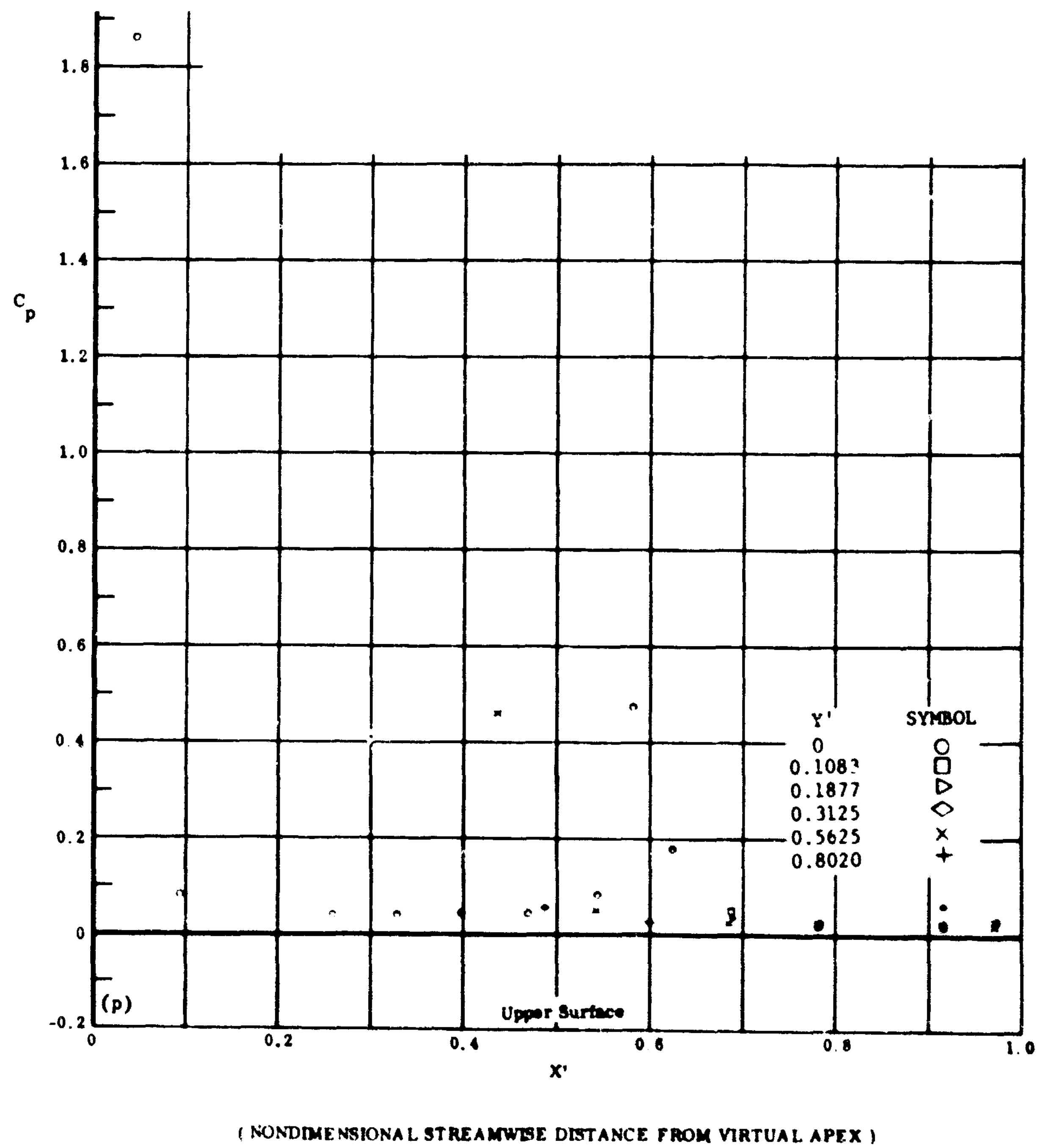

Fig. 50 Configuration VII, Spoiler On

o) C_p vs. Y', $\imath = 0$, $Re_\infty/ft \times 10^{-6} = 1.1$, upper surface

p) C_p vs. X', $\imath = 0$, $Re_\infty/ft \times 10^{-6} = 1.1$, upper surface

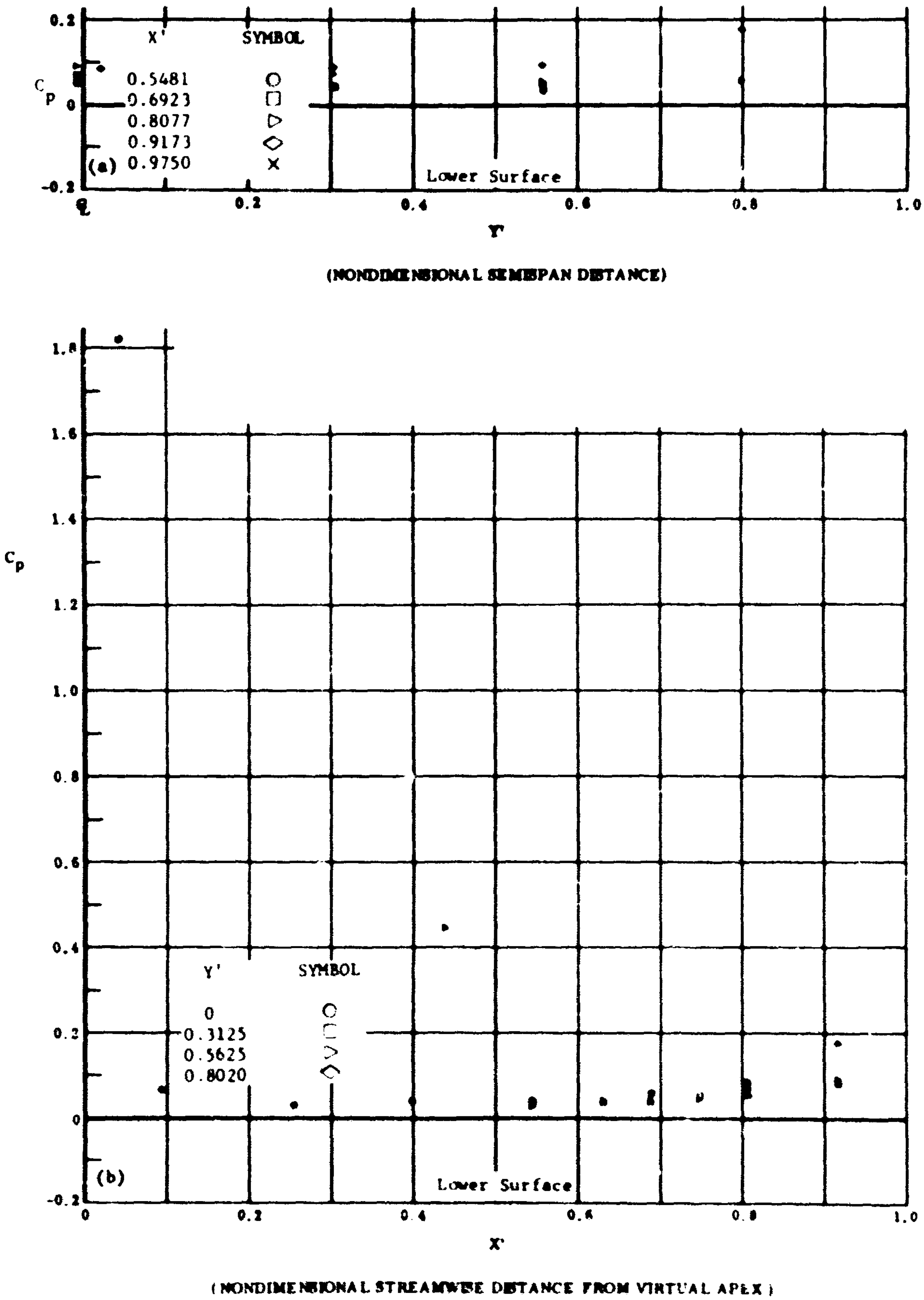

Fig. 51 Configuration VIII, Spoiler on, $Re_x/ft \times 10^{-6} = 3.3$

a) C_p vs. Y', $\alpha = 0$, lower surface

b) C_p vs. X', $\alpha = 0$, lower surface

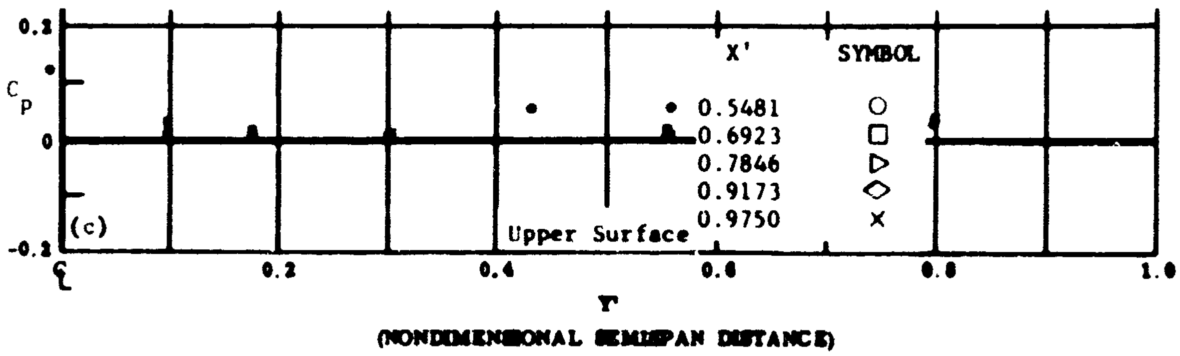

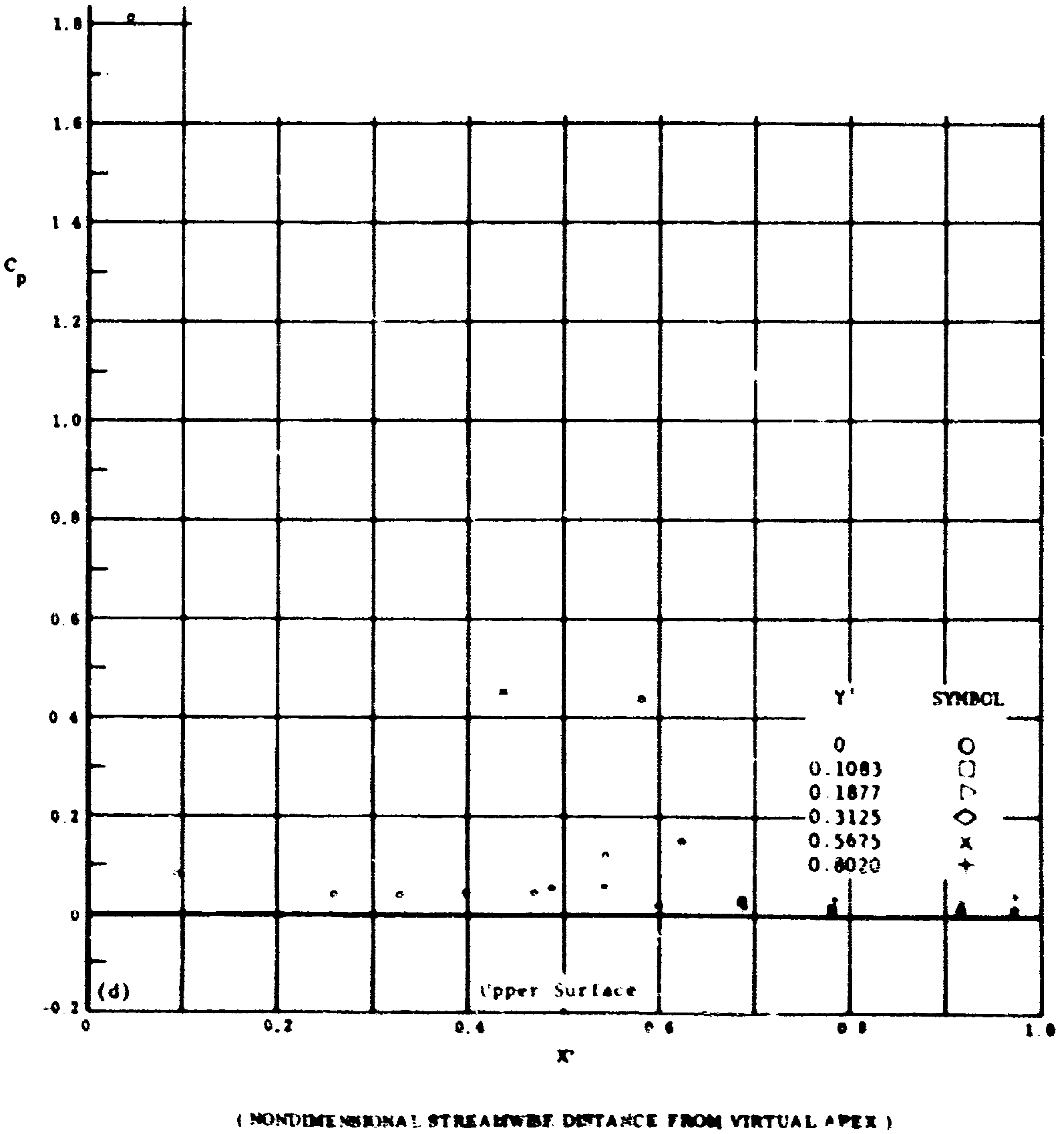

Fig. 51 Configuration VIII, Spoiler on, $Re_\infty/ft \times 10^{-6} = 3.3$

c) C_p vs. Y', $\alpha = 0$, upper surface

d) C_p vs. X', $\alpha = 0$, upper surface

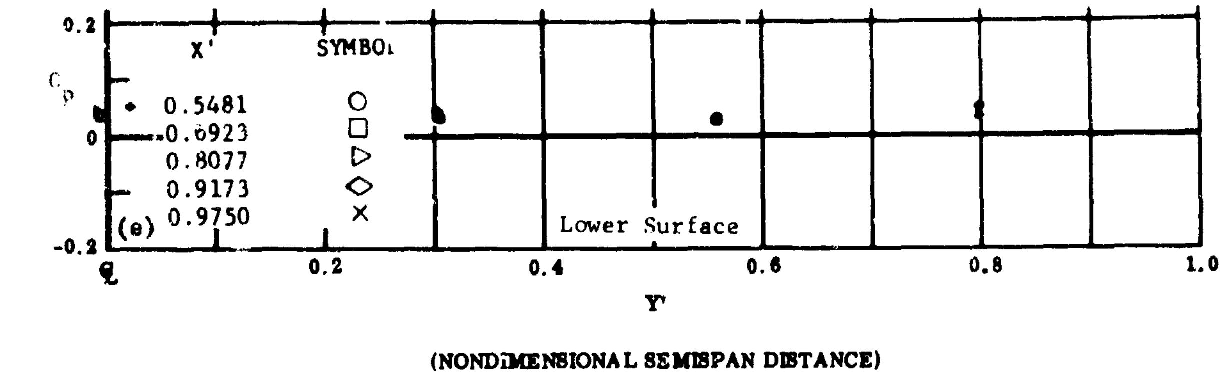

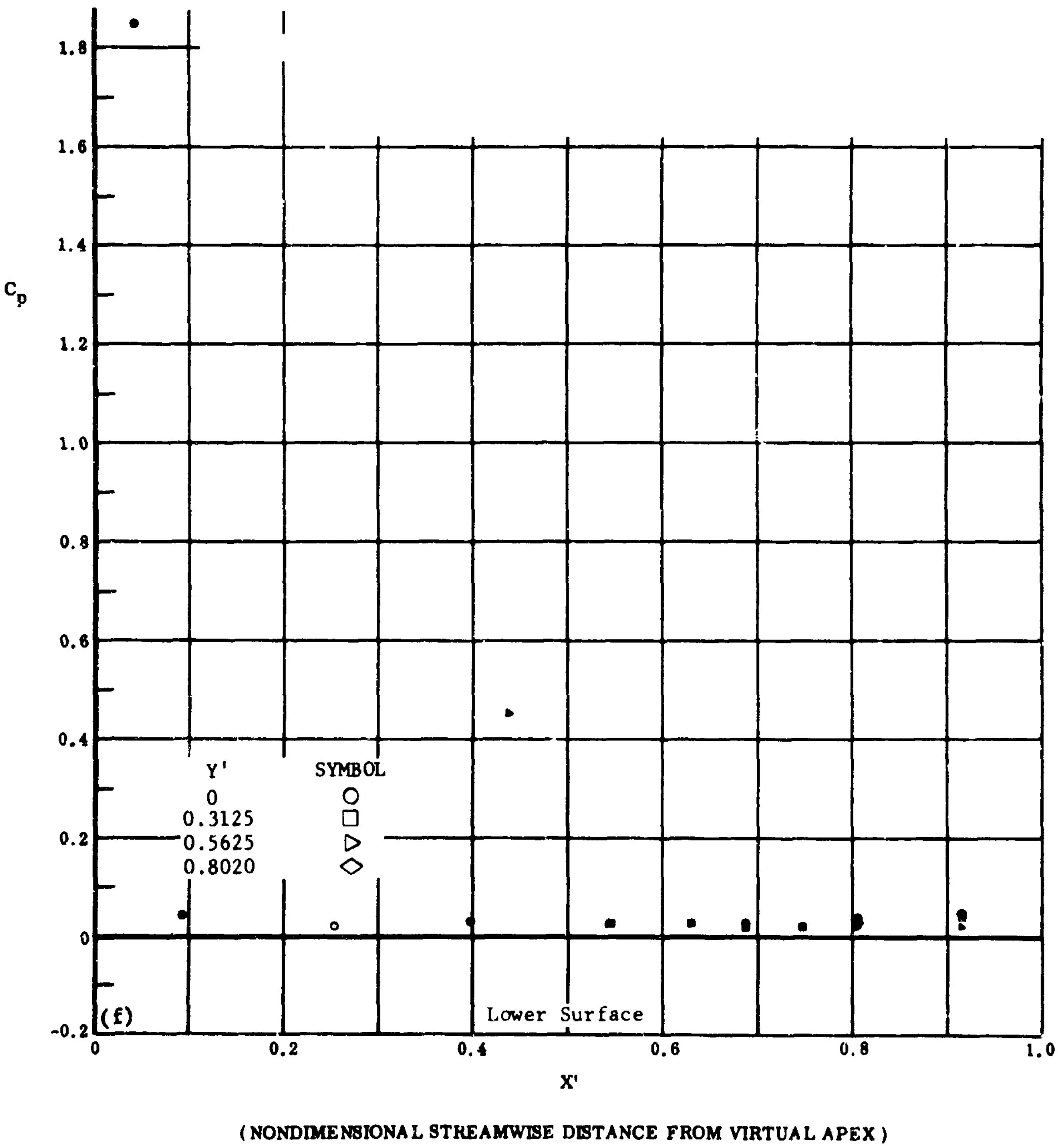

Fig. 51 Configuration VIII, Spoiler on, $Re_\infty/ft \times 10^{-6} = 3.3$

e) C_p vs. Y', $\alpha = -5$, lower surface

f) C_p vs. X', $\alpha = -5$, lower surface

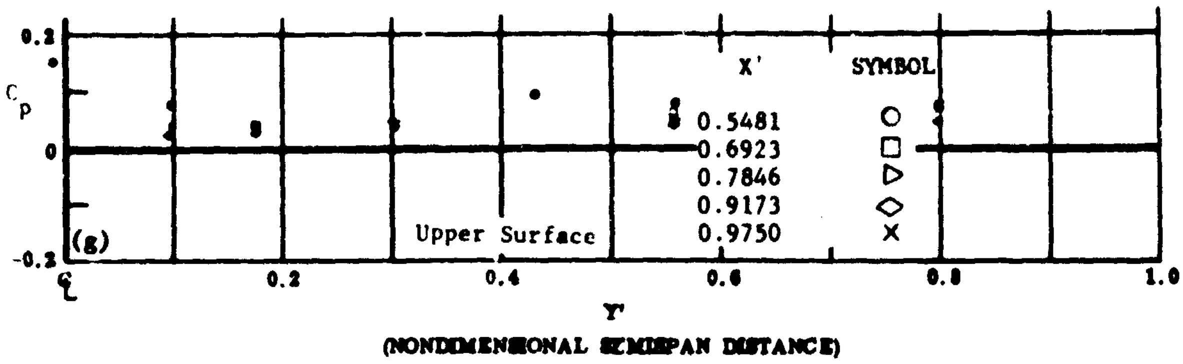

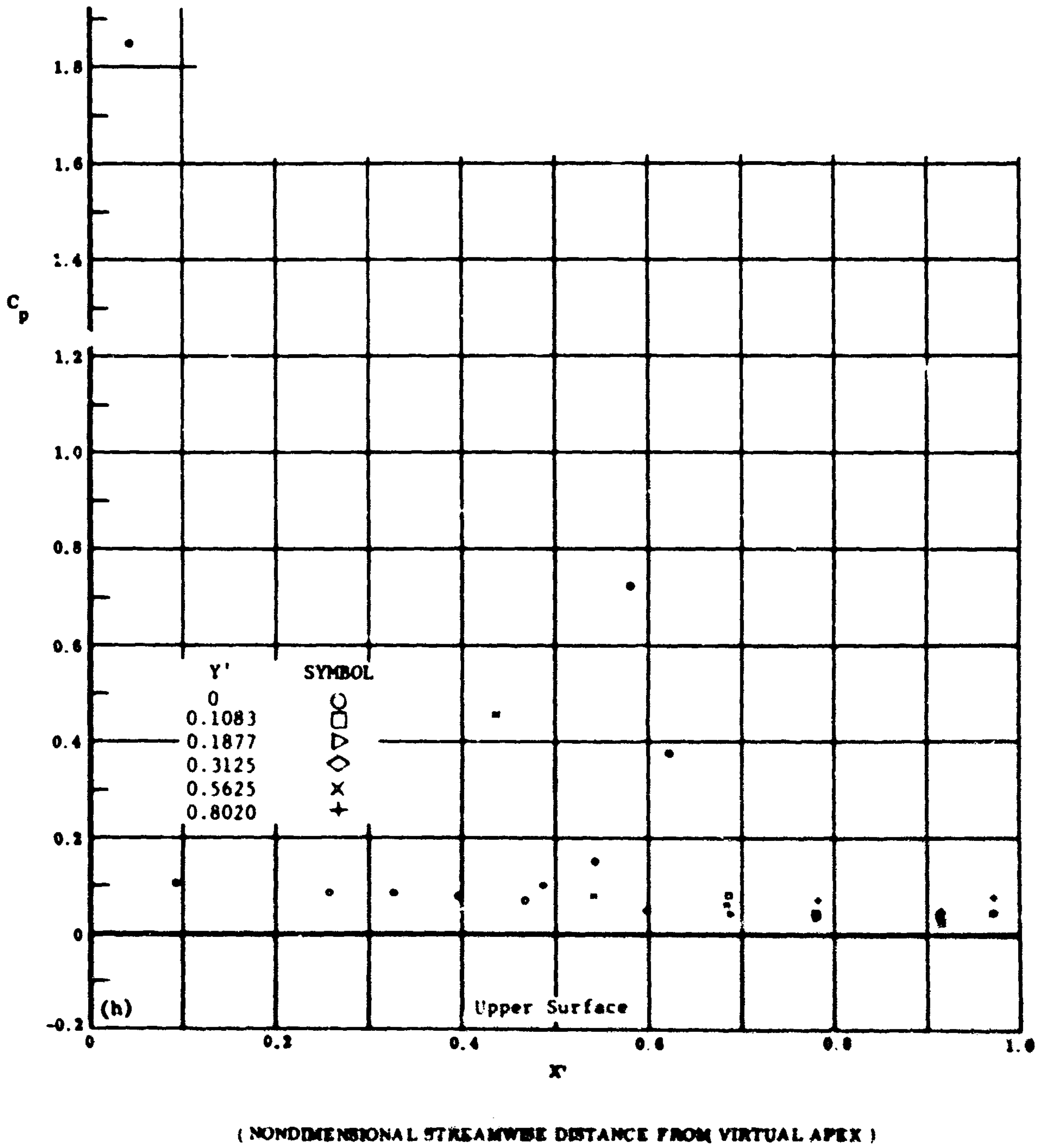

Fig. 51 Configuration VIII, Spoiler on, $Re_\infty/ft \times 10^{-6} = 3.3$

g) C_p vs. Y', $\alpha = -5$, upper surface

h) C_p vs. X', $\alpha = -5$, upper surface

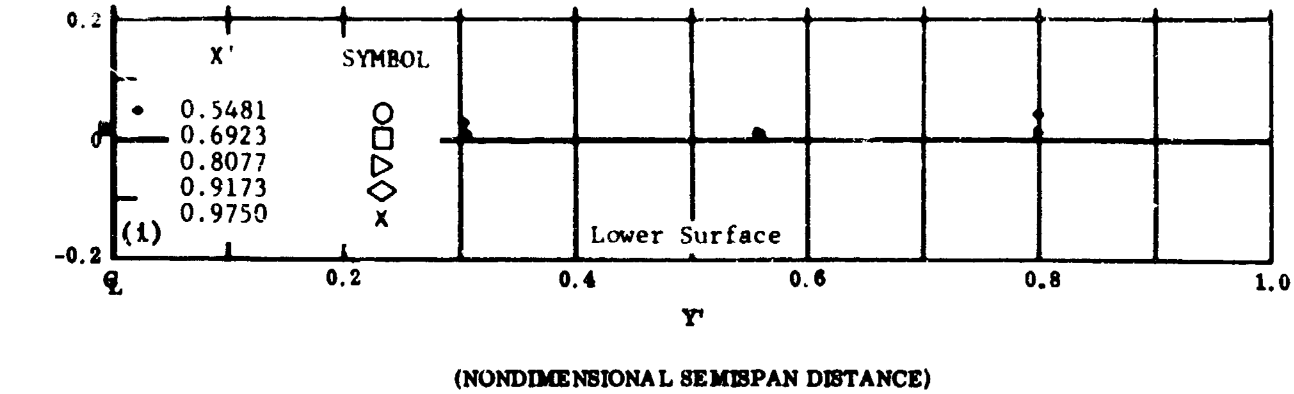

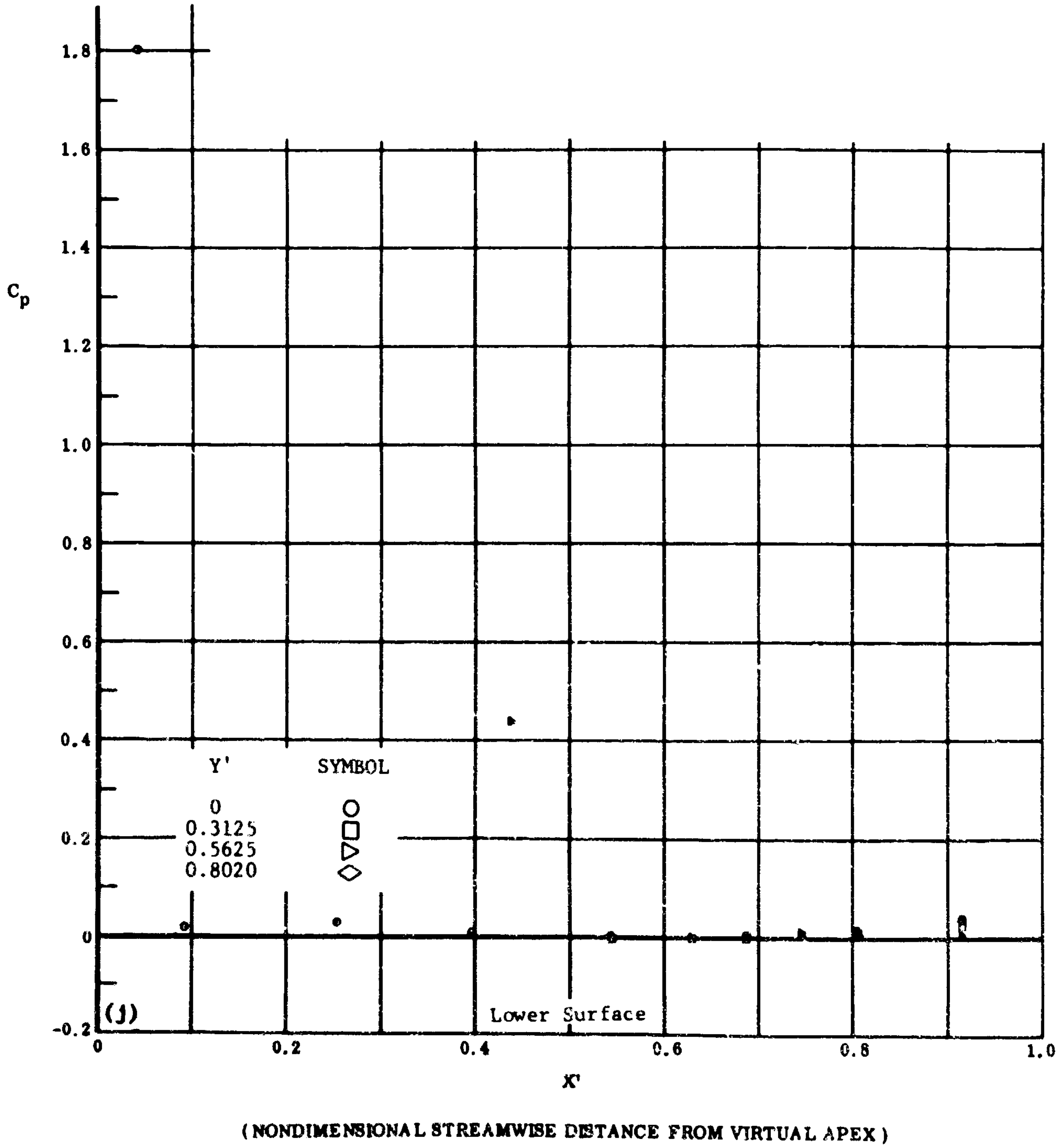

Fig. 51 Configuration VIII, Spoiler on, $Re_\infty/ft \times 10^{-6} = 3.3$

i) C_p vs. Y', $\alpha = -10$, lower surface

j) C_p vs. X', $\alpha = -10$, lower surface

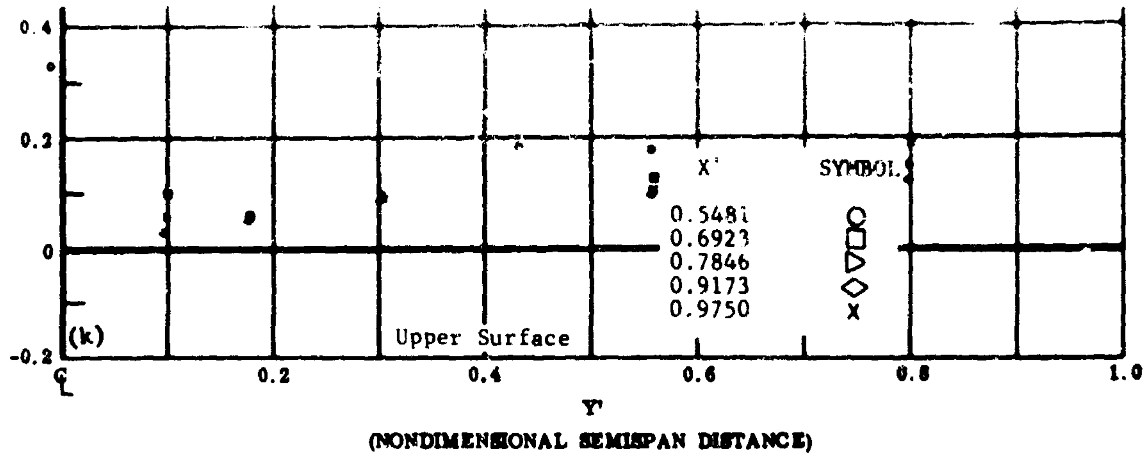

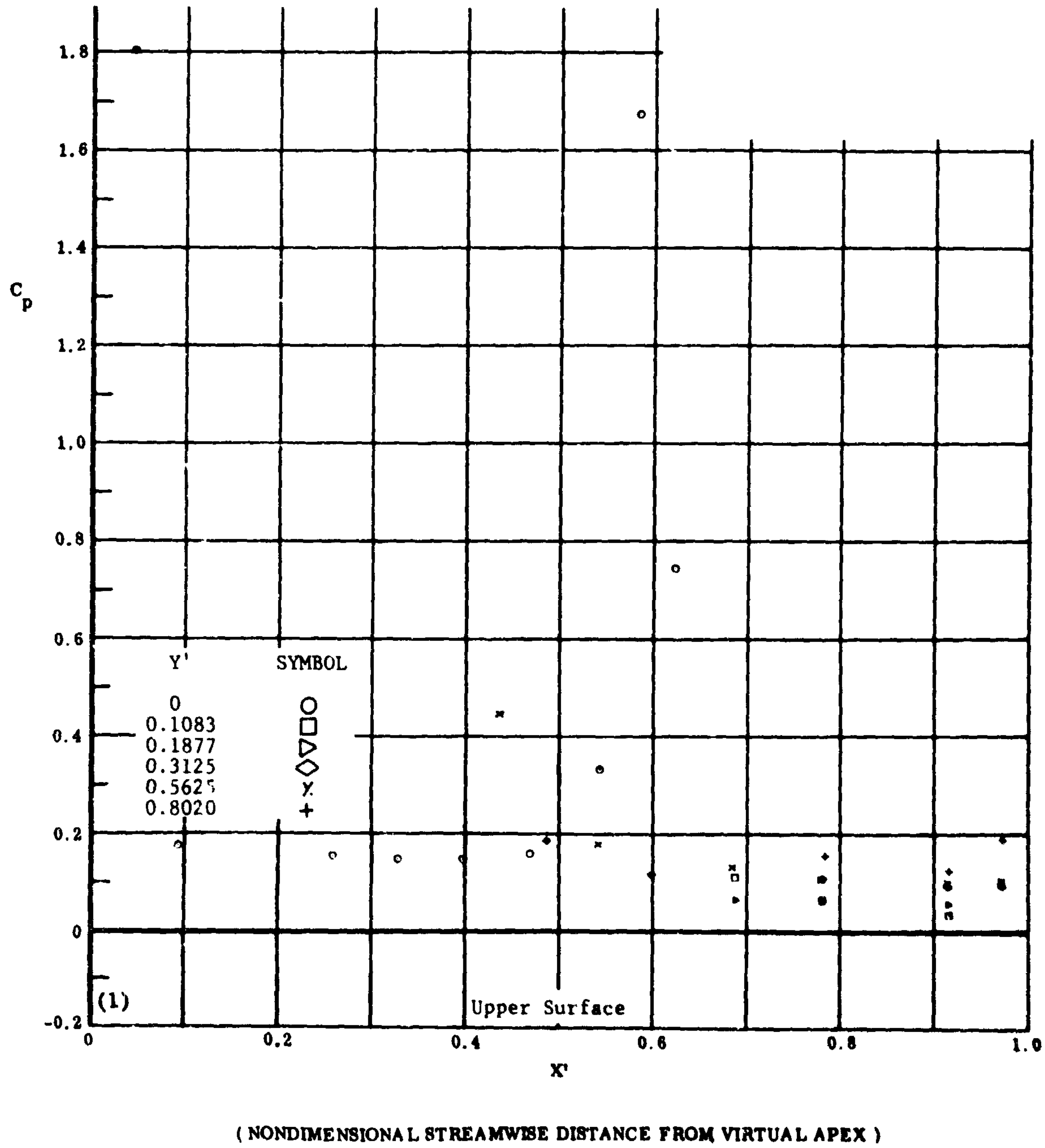

Fig. 51 Configuration VIII, Spoiler on, $Re_{\infty}/ft \times 10^{-6} = 3.3$

k) C_p vs. Y', $\alpha = -10$, upper surface

l) C_p vs. X', $\alpha = -10$, upper surface

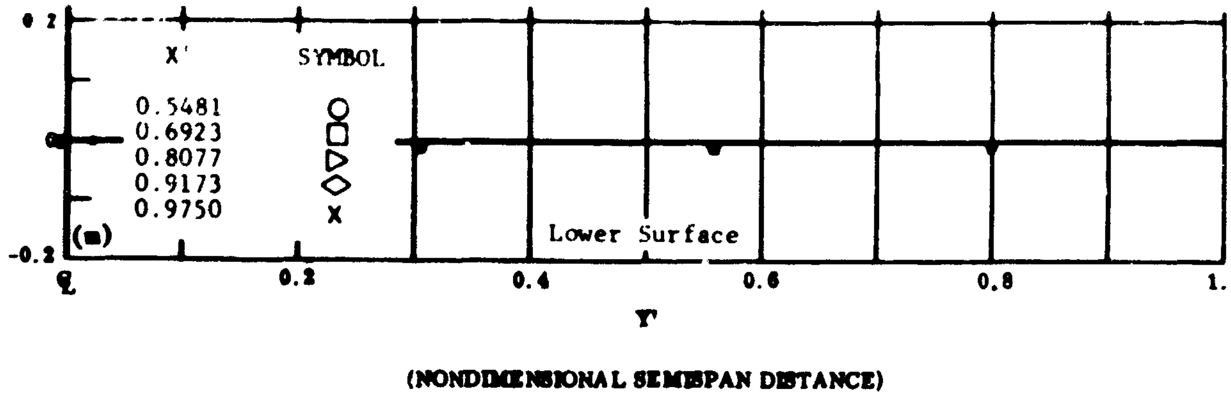

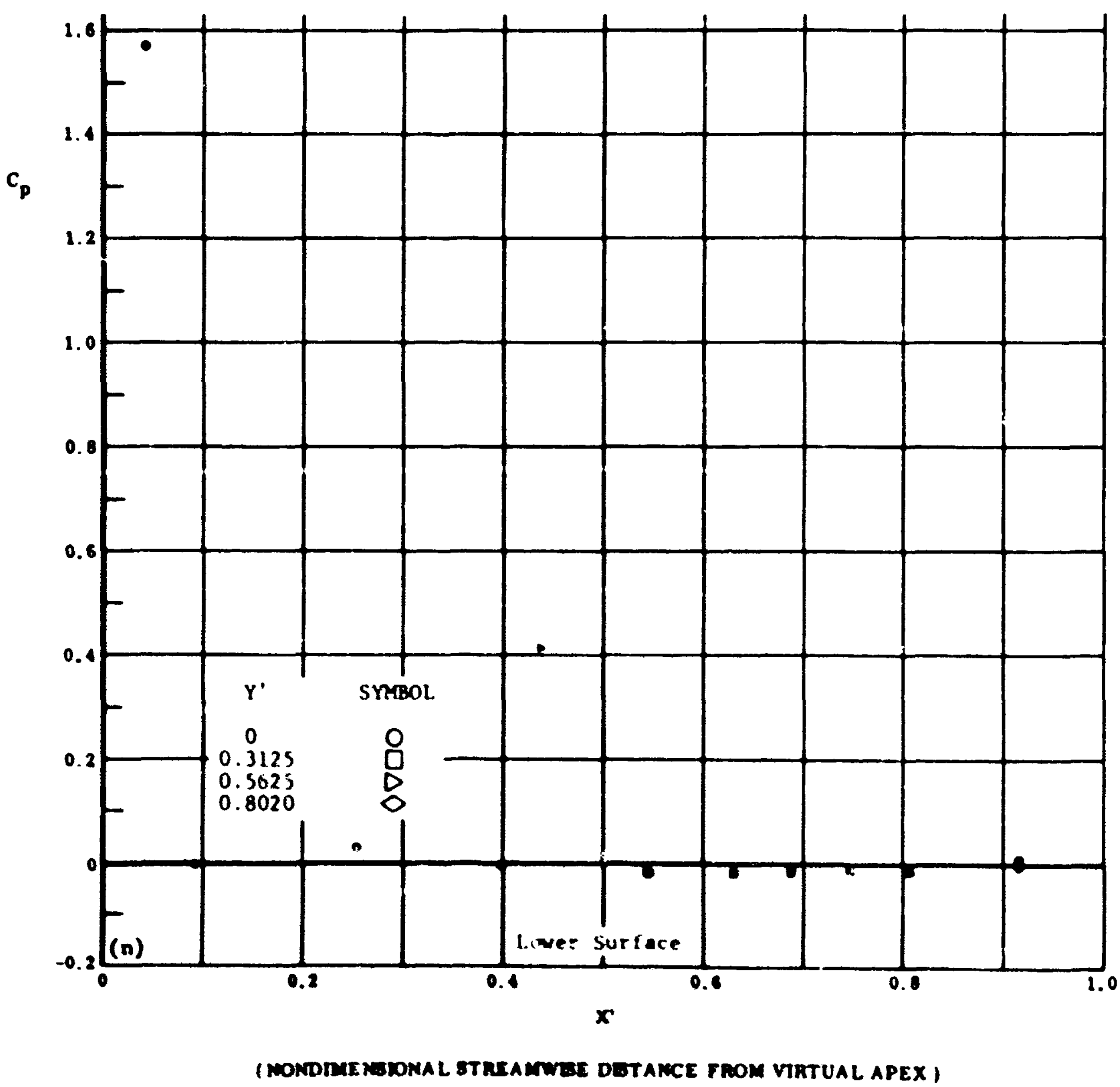

Fig. 51 Configuration VIII, Spoiler on, $Re_\infty/ft \times 10^{-6} = 3.3$

m) C_p vs. Y', $\alpha = -20$, lower surface

n) C_p vs. X', $\alpha = -20$, lower surface

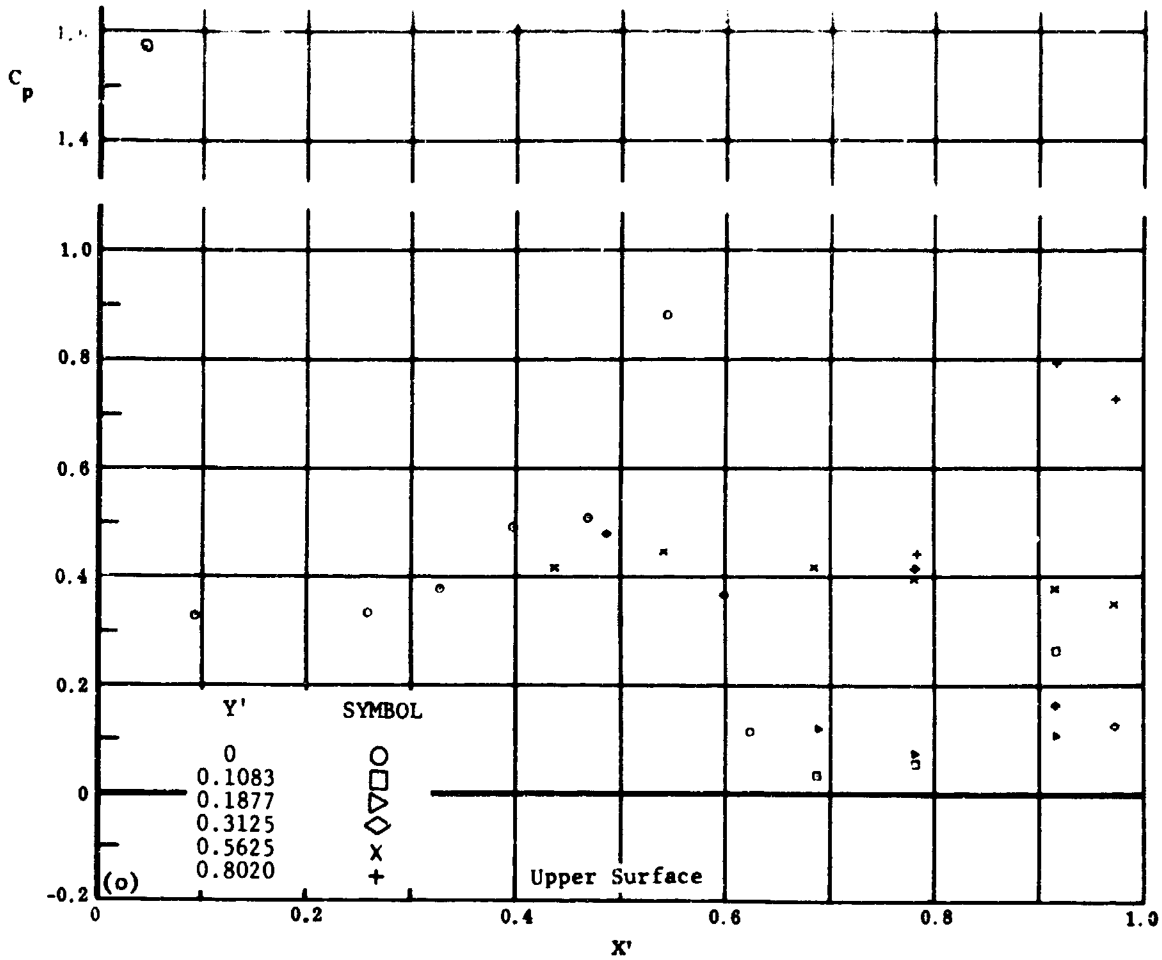

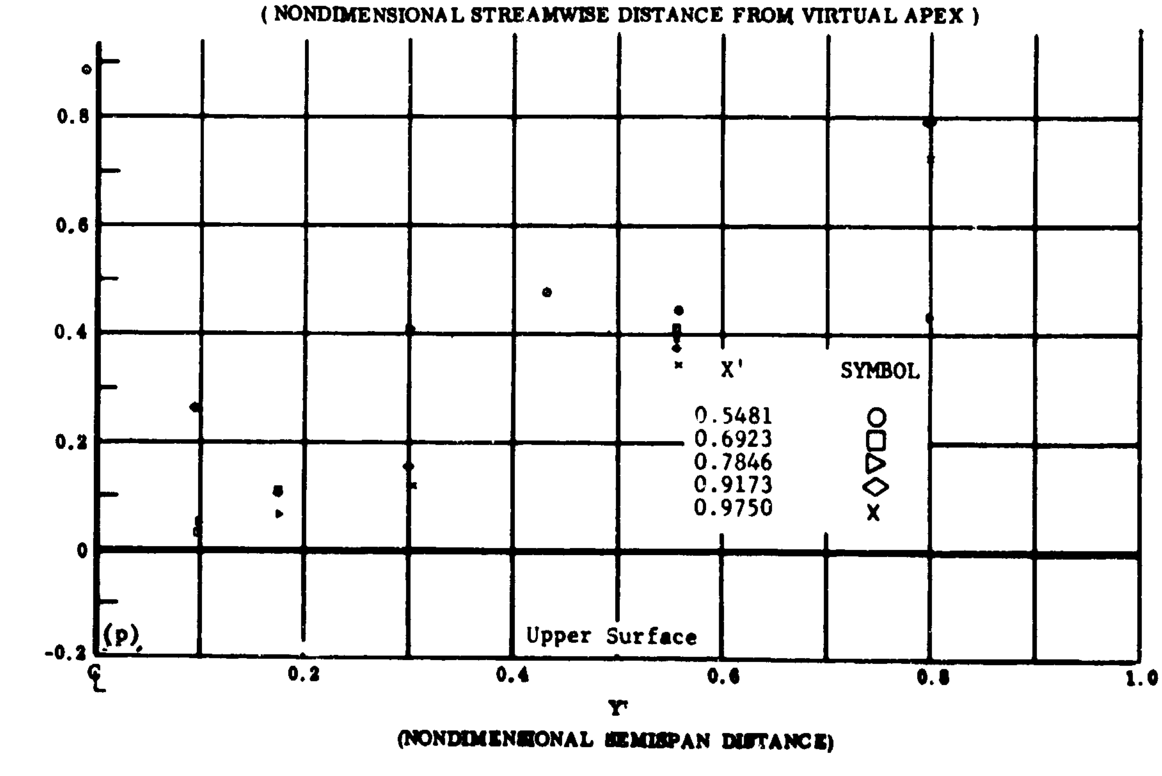

Fig. 51 Configuration VIII, Spoiler on, $Re_\infty/ft \times 10^{-6} = 3.3$

o) C_p vs. X', $\alpha = -20$, upper surface

p) C_p vs. Y', $\alpha = -20$, upper surface

UNCLASSIFIED
Security Classification

DOCUMENT CONTROL DATA - R&D

(Security classification of title, body of abstract and indexing annotation must be entered when the overall report is classified)

1 ORIGINATING ACTIVITY (Corporate author) Grumman Aircraft Engineering Corporation Bethpage, L.I., New York	2a REPORT SECURITY CLASSIFICATION UNCLASSIFIED; 2b GROUP N/A
3 REPORT TITLE Pressure Measurements at Mach 8 On An Aerodynamically Controllable Winged Re-entry Configuration	
4 DESCRIPTIVE NOTES (Type of report and inclusive dates) N/A	
5 AUTHOR(S) (Last name, first name, initial) Meckler, Lawrence	
6 REPORT DATE June 1965	7a TOTAL NO OF PAGES 453; 7b NO OF REFS 5
8a CONTRACT OR GRANT NO AF33(616)-8130; b PROJECT NO 8219-821902; c; d	9a ORIGINATOR'S REPORT NUMBER(S) FDL TDR 64-124; 9b OTHER REPORT NO(S) (Any other numbers that may be assigned this report) N/A
10 AVAILABILITY LIMITATION NOTICES N/A	
11 SUPPLEMENTARY NOTES N/A	12 SPONSORING MILITARY ACTIVITY AFFDL (FDCC) Wright-Patterson AFB, Ohio 45433

13 ABSTRACT

Pressure data were obtained at Mach 8 for a winged re-entry configuration having aerodynamic controls. The basic model consisted of a clipped delta wing with an overslung cone-cylinder body. The main controls tested were partial span trailing edge flaps. Data were also obtained on the effect of tip fins, hemisphere-cylinder body and a trailing edge spoiler. The data were obtained over an angle of attack range of -50° to +50°. Due to load limitations on the controls the unit test section Reynolds number varied from 3.3×10^6 at low angle of attack to 2.5×10^6 at high angle of attack.

DD FORM 1 JAN 64 1473

UNCLASSIFIED
Security Classification

UNCLASSIFIED

Security Classification

14. KEY WORDS	LINK A		LINK B		LINK C	
	ROLE	WT	ROLE	WT	ROLE	WT
hypersonic control						
pressure measurements						
winged re-entry						
flow separation						
control characteristics						

INSTRUCTIONS

1. ORIGINATING ACTIVITY: Enter the name and address of the contractor, subcontractor, grantee, Department of Defense activity or other organization *(corporate author)* issuing the report.

2a. REPORT SECURITY CLASSIFICATION: Enter the overall security classification of the report. Indicate whether "Restricted Data" is included. Marking is to be in accordance with appropriate security regulations.

2b. GROUP: Automatic downgrading is specified in DoD Directive 5200.10 and Armed Forces Industrial Manual. Enter the group number. Also, when applicable, show that optional markings have been used for Group 3 and Group 4 as authorized.

3. REPORT TITLE: Enter the complete report title in all capital letters. Titles in all cases should be unclassified. If a meaningful title cannot be selected without classification, show title classification in all capitals in parenthesis immediately following the title.

4. DESCRIPTIVE NOTES: If appropriate, enter the type of report, e.g., interim, progress, summary, annual, or final. Give the inclusive dates when a specific reporting period is covered.

5. AUTHOR(S): Enter the name(s) of author(s) as shown on or in the report. Enter last name, first name, middle initial. If military, show rank and branch of service. The name of the principal author is an absolute minimum requirement.

6. REPORT DATE: Enter the date of the report as day, month, year, or month, year. If more than one date appears on the report, use date of publication.

7a. TOTAL NUMBER OF PAGES: The total page count should follow normal pagination procedures, i.e., enter the number of pages containing information.

7b. NUMBER OF REFERENCES: Enter the total number of references cited in the report.

8a. CONTRACT OR GRANT NUMBER: If appropriate, enter the applicable number of the contract or grant under which the report was written.

8b, 8c, & 8d. PROJECT NUMBER: Enter the appropriate military department identification, such as project number, subproject number, system numbers, task number, etc.

9a. ORIGINATOR'S REPORT NUMBER(S): Enter the official report number by which the document will be identified and controlled by the originating activity. This number must be unique to this report.

9b. OTHER REPORT NUMBER(S): If the report has been assigned any other report numbers *(either by the originator or by the sponsor)*, also enter this number(s).

10. AVAILABILITY/LIMITATION NOTICES: Enter any limitations on further dissemination of the report, other than those imposed by security classification, using standard statements such as:

(1) "Qualified requesters may obtain copies of this report from DDC."

(2) "Foreign announcement and dissemination of this report by DDC is not authorized."

(3) "U. S. Government agencies may obtain copies of this report directly from DDC. Other qualified DDC users shall request through ____________."

(4) "U. S. military agencies may obtain copies of this report directly from DDC. Other qualified users shall request through ____________."

(5) "All distribution of this report is controlled. Qualified DDC users shall request through ____________."

If the report has been furnished to the Office of Technical Services, Department of Commerce, for sale to the public, indicate this fact and enter the price, if known.

11. SUPPLEMENTARY NOTES: Use for additional explanatory notes.

12. SPONSORING MILITARY ACTIVITY: Enter the name of the departmental project office or laboratory sponsoring *(paying for)* the research and development. Include address.

13. ABSTRACT: Enter an abstract giving a brief and factual summary of the document indicative of the report, even though it may also appear elsewhere in the body of the technical report. If additional space is required, a continuation sheet shall be attached.

It is highly desirable that the abstract of classified reports be unclassified. Each paragraph of the abstract shall end with an indication of the military security classification of the information in the paragraph, represented as *(TS), (S), (C), or (U)*.

There is no limitation on the length of the abstract. However, the suggested length is from 150 to 225 words.

14. KEY WORDS: Key words are technically meaningful terms or short phrases that characterize a report and may be used as index entries for cataloging the report. Key words must be selected so that no security classification is required. Identifiers, such as equipment model designation, trade name, military project code name, geographic location, may be used as key words but will be followed by an indication of technical context. The assignment of links, rules, and weights is optional.

UNCLASSIFIED

Security Classification